ISBN : 978-602-17221-9-0

HIMPUNAN AHLI TEKNIK TANAH INDONESIA
INDONESIAN SOCIETY FOR GEOTECHNICAL ENGINEERING (ISGE)
MEMBER OF INTERNATIONAL SOCIETY FOR SOIL MECHANICS
AND GEOTECHNICAL ENGINEERING (ISSMGE)

SIMSG ISSMGE

Proceedings

25th Annual National Conference on Geotechnical Engineering

"Geotechnical Diversity : Past, Present and Future"

Jakarta, 9 - 10 November 2021

Supported by :

Proceeding

25th Annual National Conference on Geotechnical Engineering

Jakarta, 9-10 November 2021

Theme :

"Geotechnical Diversity : Past, Present & Future"

HIMPUNAN AHLI TEKNIK TANAH INDONESIA
INDONESIAN SOCIETY FOR GEOTECHNICAL ENGINEERING (ISGE)
GRAHA HATTI, JOR TB Simatupang, Jalan Asmin No. 45
Jakarta Timur 13750 – INDONESIA

HIMPUNAN AHLI TEKNIK TANAH INDONESIA
INDONESIAN SOCIETY FOR GEOTECHNICAL ENGINEERING (ISGE)
GRAHA HATTI, JOR TB Simatupang, Jalan Asmin No. 45
Jakarta Timur 13750 – INDONESIA

WORDS FROM CHAIRMAN

Dear our honorable guest,

Mr. Basuki Hadimuljono – Minister of Public Works and Housing, Mr. Satryo S. Brodjonegoro – Chairman of AIPI, all Speakers, Sponsors, and Participants; Welcome to our 25th Annual National Conference – the silver anniversary ANC. It's an honour to have you all together, not only because your kindness to spare your valuable time, but also for your kindness to share your great experience in geotechnical engineering.

The conference, "Geotechnical Diversity: Past, Present, and Future" as our theme, raise from a thought how geotechnical evolve in this years. From a simple soil mechanics, to a computer modelling and with a less notice, we intersect with so many other major fields, Statistics, Mining, Earthquake, Tunneling, Bio-geotechnical, to legal aspect of Law.

We hope 9 keynote speakers, 1 special lecture, 80 speakers, 700 participants and 150 sponsors could see a new and bright future after this (2) years of pandemic. It's not slowing us down, but instead, it give all of us time to learn more, to understand more, to communicate, research, share more and in a much easier way like today. There is no more country boundary to share, there is only us. Long live Geotechnical Engineering.

Last but not least, allow me to express our gratitude to everyone, not only as speakers or sponsors or participants, but as our friends (.. of course I need to mention our Platinum sponsor Promisco, Geotekindo, FKNK, Daehan, Artha Geo Integritas, Hutama Karya Infrastruktur and Bauer Pratama Indonesia, also all sponsors), we made it together today.

I wish the conference a success and everyone can enjoy for the next two days. Thank you.

Jakarta, 9 November 2021

Dr. Aksan Kawanda
Chairman

PRESIDENT OF ISGE ADDRESS

Assalamu'alaikum Wr. Wb. Salam Sejahtera bagi kita semua.

The Minister of Public Works and Housing, the Chairman of the Indonesian Academy of Science, Keynote Speakers, Ladies and Gentlemen, the XXV Annual National Conference on Geotechnical Engineering, on behalf of the National Board of Indonesian Society for Geotechnical Engineering (ISGE / HATTI), we would like to welcome you all to this great conference. In particular, to the Minister of Public Works and Housing, we would like to express our sincere gratitude and highest appreciation for your willingness once again to address our conference.

Ladies and Gentlemen, this year conference is a special one as it is our 25th Annual National Conference. It is time to remember the great visions of the founding fathers and seniors of ISGE/HATTI. We still have our annual conference online for the second time due to the COVID-19 pandemic, but we are all optimistic that we will survive these challenges soon. In this spirit, we need to ready ourselves to support the economic development of Indonesia.

Dear Indonesian Society members, the theme of this conference is "Geotechnical Diversity: Past, Present, and Future". In this conference, we have a range of different topics from prominent geotechnical experts, as well as a number of technical paper contributors. We are grateful that two reputable journals are willing to publish some of the technical papers presented. We have also a number of interesting technical presentations from the geotechnical engineering companies. In addition, we would like also to report that ISGE/HATTI is establishing a *lembaga sertifikasi profesi*, an important step to ensure a further contribution to good geotechnical engineering practices in Indonesia.

We extend my sincere gratitude to all participants and all sponsors, particularly the Platinum Sponsors: PT. Promisco Sinergi Indonesia, PT. Bauer Pratama Indonesia, PT. Hutama Karya Infrastruktur, PT. Artha Geo Integritas, PT. Geotekindo, Daehan IM Co., Ltd., and FKNK Law Firm. We wish you a very enlightening and successful conference. Thank you very much.

Wassalamu'alaikum Wr. Wb.
Jakarta, 9 November 2021

Prof. Ir. Widjojo A. Prakoso, MSc., Ph.D
President of ISGE

Theme :

"Geotechnical Diversity : Past, Present & Future"

ORGANIZING COMMITTEE

Steering Committee	:	Prof. Ir. Widjojo Adi Prakoso, MSc, Ph.D Ir. Pintor Tua Simatupang, MT. Dr-Eng
Chairman	:	Dr. Aksan Kawanda, S.T., M.T.
Secretary	:	Ali Iskandar, S.T., M.T. Dr. Fahmi Aldiamar, S.T., M.T.
Treasurer	:	Ir. Idrus M. Alatas. M.Sc. Ph.D
Team Reviewer	:	Prof. Ir. Teuku Faisal Fathani, S.T., M.T., Ph.D., IPU Prof. Ir. Agus Setyo Muntohar, S.T., M.Eng.Sc., Ph.D. Ir. Dr. Eng. Ardy Arsyad, S.T., M.Eng.Sc Aswin Lim, S.T., M.T., Ph.D. Endra Susila, S.T., M.T., Ph.D. Erly Bahsan, S.T., M.Kom. Dr. Yudhi Lastiasih, S.T., M.T. Dr. Yustian Heri Suprapto, S.T., M.Sc Dr. James Jatmiko Oetomo S.T., M.T., MSc. Anthony Gunawan, Ph.D.
Editing	:	Yunan Halim, S.T., M.T. Stephen G. Handoko, S.T., M.T. Dwi Nandya, S.T., M.T. Rara Dwi Noviarti, S.T., M.T Fathiyah Hakim Sagitaningrum, S.T, M.T. Tatag Yufitra Rus, S.T., M.Sc
Events	:	Edwin Laurencis, S.T., M.T. Ir. Wawan Kuswaya, M.T. Ir. Fauzie Buldan Y. Nadya Ayu Anindita, S.T. (MC)
Sponsorship & equipment	:	Marcello Djunaedy, S.T., M.T. Yasin Widodo, S.T., M.T. Sugino
Secretariat	:	Sugino Budi Suryanto, S.,T. Sya'bani Wahyu Septiandi

Publisher	:	Himpunan Ahli Teknik Tanah Indonesia *(Indonesian Society for Geotechnical Engineering)*
Address	:	Graha HATTI JOR TB Simatupang, Jalan Asmin No. 45 RT.008 RW. 03 Susukan, Ciracas - Jakarta 13750 Telp. : 021 - 220900009 Email : sekretariat@hatti.or.id; hattipusat@yahoo.com Website : http://www.hatti.or.id
ISBN No.	:	978-602-17221-9-0

TABLE OF CONTENTS

Preface Committee Chairman …….. i

Message From President Of Indonesian Society For Geotechnical Engineering (ISGE) ii

Organizing Committee iii

Table of Contents v

Keynote Speakers :

1. Kok-Kwang Phoon, Jianye Ching - *Exploring "Data" in Data-centric Geotechnics*..... 1-6
2. Youssef M. A. Hashash - *Seismic Interaction Adjacent Tall Buildings with Underground Structures* …….. 7-8
3. I Wayan Sengara, Rachman Suhanda, Eyrton C. Silaban, Jamaluddin, Imam Sadisun - *Geotechnical Aspect on Tunnel Engineering Construction of Jakarta-Bandung High-Speed-Rail*..... 9-10
4. Susumu Iai, Masyhur Irsyam - *Analysis of void redistribution and delayed flow failure associated with liquefaction during earthquakes*..... 11-18
5. Keh-Jian (Albert) Shou - *Trenchless Technologies for Urban Development*…….. 19-20
6. Hendra Jitno - *Recent development on the tailings dam design in seismic active regions* ……. 21-32
7. Ilhan Chang - *Biopolymer-based Soil Treatment (BPST) - A Bio-Geotechnical Implementation for Sustainable Development*…….. 33-34
8. Nick Alexander, Masyhur Irsyam - *Promoting Widespread Application of Seismic Ground Motion for Evaluation and Retrofit of Existing Buildings in Indonesia* 35-40
9. Abdul Hakam, Deni Irda Mazni, Hendri Warman - *Desain Tidak Umum Dinding Penahan Tanah* …….. 41-46
10. Martin Patrick Nagel - *Resolution of Construction Legal Matters Due to Covid-19 Pandemic* …….. 47-54

Session I : R.A1

1. Heaving Behavior Of Road Embankment That Reinforced With Hybrid Pile – PVD *(Ahmad)*…… 55-60

2. Comparison Between Analytical Method And Finite Element Method (FEM) With Three-Dimensional (3D) For Road Embankment On Soft Soils Supported By Vibro Stone Columns *(Zaky Prawira, William Chong)*…… 61-66

3. Performance Of Axial Bearing Capacity For Cement-Fly Ash-Gravel (CFG) Piles From Static Loading Test Results *(Eyrton Crismartua Silaban, I Wayan Sengara, Dwi Ari Hidayat)* …… 67-70

4. Numerical Modeling Of Soil Improvement Using Vacuum Preloading Method With Finite Element Program *(Utama Nusanegara, Endra Susila, Hartanto Legowo)* …… 71-78

5. Pengaruh Energi Rapid Impact Compaction Terhadap Tingkat Kepadatan Tanah Timbunan *(Rokhman, Tri Harianto, Muhammad Akbar Walenna)*.. 79-86

6. Konstruksi Jalan Terapung Di Atas Tanah Lunak *(Juni Gultom, H. Pratikso, Abdul Rochim)* …… 87-94

7. Visual Observation Against Reaction Cumulation Using Ureolytic Bacteria Oceanobacillus Isolate P3BG41 And Isolate P3BG43 *(Yustian Heri Suprapto, Puspita Lisdiyanti, Budi Susilo Soepandji, Wiwik Rahayu)* …… 95-96

Session II : R.A2

8. Performance And Back Analysis Of Soil Improvement With Vertical Drains With Vacuums Preloading In Bandung Basin Area With Finite Element Analysis *(Eyrton Crismartua Silaban, I Wayan Sengara)* ……. 97-102

9. Determination Of Downhole Dynamic Compaction Parameters Based On Finite Element Analysis *(Martin Wijaya, Ahmad Kemal Arsyad, Aswin Lim, Paulus Pramono Rahardjo)* …… 103-104

10. Analysis Of Alternative Methods Of Soft Soil Improvement On Tailing Dam *(Yogina Lestari Ayu Situmorang, Eulis Karmila, Abdurahman Hafizudin)* …… 105-110

11. Perbaikan Tanah Lunak Dengan Metode Preloading Menggunakan Prefabricated Vertical Drain (Pvd) Pada Pembangunan Jalan Tol Padang – Lubuk Alung – Sicincin *(Indriani Lewinsky, Eva Rita, Robby Permata, Hendri Warman)* …… 111-116

12. Penurunan Tanah Dasar Akibat Beban Timbunan Dengan Penerapan Prefabricated Vertical Drain *(Dyah Pratiwi Kusumastuti, Indah Handayasari, Irma Sepriyanna)* 117-122

13. Settlement Analysis On Soft Soils Due To Box Traffic And Embankment Construction On Toll Road *(Liliwarti, Lukman Murdiansyah, Nayung Dhiya Almassyah)* 123-128

14. Vacuum Preloading: Consolidation Degree Determination Using Analytical Vs Graphical Method *(Roberto Renaldi Yona, Kumbara Kamajaya Cahya Hermawan)* 129-134

Session III : R.B1

15. Sustainable Retaining Structure Incorporating Recycled Concrete Aggregate *(Nurly Gofar, Alfrendo Satyanaga)* 135-136

16. Desain Konstruksi Dinding Penahan Tanah Pasangan Batu-Kali Dengan Metode Memotong Kaki-Lereng *(Mochammad Aswanto)* 137-144

17. Parametric Study Of Tunnel Analysis In Clayshale On Short-Term And Long-Term Condition Using Finite Element Method *(Danang Setiya Raharja, I Wayan Sengara, Imam A. Sadisun)* 145-146

18. Flotation Check In Underground Structure Based On JSCE, LTA, And Eurocode *(Justin Limoris, Masrur Abdull Hamid Ghani, Ito Kenichi)* 147-152

19. Glass Fiber Reinforced Polymer As Temporary Replacement For D-Wall Steel Reinforcement *(Christopher Gilbert)* 153-160

20. Dewatering On Tunnel Excavation Work Near Vulnerable Historical Building *(Jefry Rory Paath, Ihsan Riza, Jo Lian Huat)* 161-168

21. Dinding Dan Tiang Untuk Menahan Pergerakan Pipa Hidrokarbon Di Tanah Lunak Di Daerah Lereng *(Mutadi, Pratikso, Abdul Rochim)* 169-176

Session IV : R.B2

22. Study On Efficiency Of Negative Skin Friction On End Bearing Pile Groups Using 3D Finite Element Method (*Stefanus Diaz Alvi, Paulus Pramono Rahardjo)* 177-182

23. Diagnostic and Prediction of PC Spun Pile Lateral Capacity using Logistic Regression and Support Vector Regression (SVR) *(James J. Oetomo, Dimas Rakha Ammar)* 183-192

24. Analisis Tekanan Air Pori Ekses Akibat Pemancangan Dengan Metode Numerik Untuk Prediksi Soil Setup Pada Tanah Lempung *(David Wibisono Setiabudi, Paulus Pramono Rahardjo, Budijanto Widjaja)* ……. 193-202

25. Study On Soil Spring Parameter For Rectangular Underground Structures *(Indah Sri Wahyuningtyas, Masrur Abdull Hamid Ghani, Kenichi Ito)* …. 203-208

26. Displacement Ratio Untuk Mengestimasi Pergerakan Tanah Akibat Pekerjaan Pemancangan -– Studi Kasus Di Bekasi Dan Jakarta Utara *(Kirana Rongsadi, Prieschila C. Tamsir, Bondan W. Anggoto, Paulus P. Rahardjo)* …… 209-214

27. Dynamic Bearing Capacity Exclusivity Of Driven Pile With The Danish, Navy-Mckay And Eytelwein Empirical Formulas By Using The Final Set Value *(Munirwansyah, Reza P. Munirwan, Fauzan Mufid)* …… 215-220

28. Influence Of Pile Spacing To Immediate Settlement Of Short Pile Raft Foundation System On Peat Soil Under Static Load *(Sajiharjo Marto Suro, Dyah Pratiwi Kusumastuty, Kasbi Basri, Adnan Zainorabidin)* …… 221-226

Session V : R.C1

29. Kajian Penentuan Parameter Viskositas Material Pasir Kelanauan Pada Kondisi Terlikuifaksi dengan Menggunakan Shake Table dan Melalui Tahanan Friksi dari Hasil Pembacaan CPTu *(Albert Johan, Paulus P. Rahardjo, Budijanto Widjaja)* …… 227-234

30. Liquefaction Potential In Padang City Using Empirical Method *(Hendri Warman, Indra Farni, Monica Trinandi, Zufrimar)* …… 235-242

31. Bund Wall Stability Analysis In Open-Pit Coal Mines Affected By Soft Soil Layers *(Faizal Amru, Rangga Adiprima Sudisman)* …… 243-248

32. Studi Perbandingan Hasil Perambatan Percepatan Gempa Terhadap Hasil Penyusunan Modified Motion Permukaan Tanah Di Kota Bandung Berdasarkan Standar Nasional Indonesia (SNI) 1726 Tahun 2012 Dan 2019 *(Bayu Wintoro, Muhammad Asrurifak, Masyhur Irsyam)* …… 249-256

33. Evaluasi Stabilitas Sandaran Bendungan Bener Berdasarkan Korelasi Geomekanik Bawah Permukaan *(Daru Jaka Sasangka, Pranu Arisanto, Wahyu Prasetyo, Dian Insani)* …… 257-264

34. Proposed Ground Motion Selection And Modification For Jakarta Site Based On SNI 1726-2019 And ASCE 7-16 *(Det Komerdevi, I Wayan Sengara)* …… 265-272

Session VI : R.C2

35. Flexible Rockfall Barriers: Proposed Design Method And Indonesian Case Study *(Rivai Sargawi, Matteo Lelli, David Saputra)* ……..... 273-278

36. Analysis Of Wedge Failure Characteristic And Early Warning System In Open-Pit Mining From The Point Of View Of Slope Stability Radar Data *(Irvan Rahmawan, La Ode M. Shaleh, Rachmat Hamid Musa)* ……..... 279-284

37. Comparison Of Material Point Method And Finite Element Method For Post-Failure Large Deformation Geotechnical Analysis *(Arif Yunando Soen, Ezra Y. S. Tjung, Aswin Lim)* …… 285-286

38. Stability Design Of Coal Mine Dumping Based On Analysis Of Limit Equilibrium Method And Finite Element Method *(Nuzulridha Rizki Ramadhani, Rangga Adiprima Sudisman)* …… 287-294

39. Analysis Of Interface Slope Stability Using Thin Soil Materials In Finite Element Software *(Fathiyah Hakim Sagitaningrum, Samira Albati Kamaruddin, Idrus Muhammad Alatas)* …….. 295-300

40. Perencanaan Perbaikan Kelongsoran Lereng Pada TPA Melonguane, Kabupaten Kepulauan Talaud *(Musta'in Arif, Herman Wahyudi, Yudhi Lastiasih)* …… 301-308

41. Efek Cracks Lereng Tanah Terhadap Design Bore Pile Beton Untuk Penanggulangan Gejala Longsor Pada Fasilitas Dermaga Penyeberangan Sei. Kapitan Tebing Sungai Kumai, Kabupaten Kotawaringin Barat *(Stephanus Alexsander)* …… 309-314

Session VII : R.D1

42. Linear Shrinkage and its Correlation to the Shrinkage Limit and Index Properties of Kaolinite, Bentonite, and Eight Bandung Fine-Grained Soils *(Ignatius Tommy Pratama, Ana Yelina Arif, Budijanto Widjaja)* ……. 315-320

43. Evaluasi Korelasi Indeks Kompresi Tanah Lempung Indonesia *(Erza Rismantojo, Rizal Maulana, Fadlli Ash-Shidiqqy)* 321-330

44. Effect Of Variation In Concentration Of Dispersing Agent Solution On Atterberg Limits And Soil Gradation *(Budijanto Widjaja, Fendy)* …….. 331-336

45. Effectiveness Of Using Cellulolytic And Lignocellulolytic Bacteria In Decomposing Fibers Of Fibrous Peat. *(Noor Endah Mochtar, Enny Zulaika, Dwiaji Ari Yogyanta)* …… 337-338

46. Shear Strength Ratio Of Marine Siltation *(Hanif Audina Rahmawati, Mifrokhah Haniffa, Syukri Fitrialdi)* …… 339-342

47. Interface Shear Strength Progressive Between Weathered And Fresh Clay Shale *(Idrus M. Alatas, Pintor T. Simatupang)* …… 343-344

48. Effect Of Diatomaceous Earth Addition To CBR Values Of Glee Geunteng Soil Aceh Besar *(Banta Chairullah, Munira Sungkar, Muhammad Ghiffari Ritonga)* …… 345-346

Session VIII : R.D2

49. Consolidation Parameters Of Marine Siltation *(Nina Yuliana, Eko Sumanto Putro, Safrijhon Bastanta Tarigan)*…… 347-350

50. Compaction Characteristics Of Fine-Grained Soil From Several Locations In Indonesia Controlled By Degree Of Saturation And Plasticity Index *(Hasbullah Nawir, Laras Dipa Pramudita, Tita Kartika Dewi)* …… 351-352

51. Compressive Strength Characteristics Of Trass Stabilizied Dredged Soil *(Komang Arya Utama, Tri Harianto, Achmad Bakri Muhiddin, Ardy Arsyad)* …… 353-354

52. Studi Pengaruh Pecampuran Senyawa Synthetic Polyacrylamide (Pam) Pada Tanah Kohesif *(Reza Rahman Syafei, Masyhur Irsyam, Km Abuhuroyroh)* …… 355-360

53. Mapping Expansive Soil Characteristics On The National Road Segment In Java Island *(Diah Affandi)* …… 361-372

54. The Performance Of $Ca(OH)_2$ To Reduce The Plasticity Index And Increase The Shear Strength Parameter For Expansive Soil *(Mila K. Wardani, Putu Tantri K. Sari, Mafrita Refionasari)* …… 373-374

Session IX : R.E1

55. Large Penetration Test (LPT) In Gravelly Soils *(Syukri Fitrialdi, Sigit Prasetyo, Nina Yuliana)* …… 375-382

56. Good Practice Of Instrumentation And Monitoring Of Deep Excavations *(Agus Setianto Samingan, Kenneth Phua, Yudha Adi, Andreas Putra)* …… 383-390

57. Bearing Capacity Of Land As Main Factor Of Environmental Carrying Capacity In Regional Spatial Planning (A Study In Semarang) *(Pribadi Agung Wahyudi)* …… 391-398

58. Determining Yield Stress Ratio And Constrained Modulu Of Volcanic Soil In Kediri By Using SPT *(Prayoga Jeremia Pangaribuan, Martin Wijaya, Siska Rustiani, Paulus Pramono Rahardjo)* …… 399-404

59. Evaluasi Penurunan Akhir Akibat Jeda Penimbunan Dengan Pendekatan Analisis Balik Data Settlement Plate *(Yogina Lestari Ayu, Josua Adrianov, Benny Beckham Marbun)* …… 405-408

60. CPT-SPT Correlation Of Volcanic Soils In Kediri, East Java *(Aflizal Arafianto, Gregorius Rayhan, Martin Wijaya)* …… 409-418

61. SPT And CPT Correlation Of Expansive Clay In Indonesia *(Eddy Triyanto Sudjatmiko)* …… 419-420

Session X : R.E2

62. Duck Feet System Foundation (DFSF) For Building On Soft Soils (*Syahirman Suriadi, Prabandiyani R. W., Endra Susila, Windu Partono*)…… 421-428

63. Three-Dimensional Effects Of Deep Excavation In Soft Soils *(Ferawati Hariyanto, Keng Hwa Lee, Airlingga Putra, Irawan Tani)* …… 429-436

64. Seismic Finite Element Response Of Soil-Pile Kinematic Interaction Behavior On Interface Of Soft And Medium Clay Soil *(Dedi Apriadi, Zaitun Andarwan, Suched Likitlersuang, Thirapong Pipatpongsa)* …… 437-438

65. CMC Application And Performance Under High Rise Building With Combined Raft Footing System *(Yudhistira Rian, KM Abuhuroyroh, Masyhur Irsyam)* …… 439-440

66. Perencanaan Dan Pelaksanaan Konstruksi Geoteknik Di Mandalika International Street Circuit Lombok *(Hari Nugraha Nurjaman, Dwianto Winaryo)* …… 441-448

67. Shear Strength And Durability Behaviors Of Compacted Mixing Weathred Clay Shale With Portland Cement *(Pintor T. Simatupang, Idrus M. Alatas, Ayu Kartika Redyananda, Eko Arif Purnomo)* …… 449-450

Session XI : R.F1

68. Analysis Of The Axial Foundation Bearing Capacity For Bridge Construction In The Mantuil Region, Muara Harus District, Tabalong 451-456

Regency, South Kalimantan Province *(Muhammad Tobiby Pratama Pohan, Bekti Djatmiko, Nur Khoirullah)* ……

69. Pengaruh Getaran Akibat Proses Pemancangan Pada Tanah Terhadap Bangunan Sekitar *(Mochammad Rahadian Yunush, Aksan Kawanda)* …… 457-462

70. Perancangan Secant Pile Dengan Perkuatan Ground Anchor *(Farhan Azfiansyah Yazid, Aksan Kawanda)* …… 463-468

71. Embankment Dam Design And Parametric Study Based On Static And Dynamic Analysis Using Operating Basis And Maximum Design Earthquake *(Alvin Tjahjadi, Wirman Hidayat, Jevania Simanjuntak)* ……. 469-478

72. Laboratory Study Of Compressibility Characteristics Of Compacted Volcanic Soils (AMM) *(Charles Maxwelliem, Stefanus Diaz Alvi, Paulus P. Rahardjo)* …… 479-486

73. Studi Numerik Distribusi Beban Dan Penurunan Pada Fondasi Tiang-Rakit (Studi Kasus: Proyek Pembangunan Apartemen Di Fatmawati, Jakarta Selatan) *(Angela Dewi Maharani Susiyanti, Ignatius Tommy Pratama, Aswin Lim)* …… 487-492

74. The Geological and Geotechnical Studies for Road Construction Site Planning by Spatial Analysis and Slope Stability Modeling (Case Study: Penggaron-Mluweh Road, Semarang Regency, Central Java) *(M. Hajjrol Dava, Lia Suryani)* …… 493-498

75. Studi Parametrik Kondisi Batas Melalui Simulasi Numerik Uji Pembebanan Tiang Tunggal *(Kyrie Eleisia, Ignatius Tommy Pratama, Aswin Lim)* …… 499-506

Session XII : R.F2

76. Analisis Efektivitas Penggunaan Geotekstil Untuk Perkerasan Lentur Jalan Pada Tanah Lempung Lunak *(Rangga Wishnu Wardhana, Aksan Kawanda)* …… 507-514

77. Upaya Stabilisasi Tanah Berpotensi Likuifaksi Menggunakan Stone Column *(Mardianti Alvionita, Aksan Kawanda)* …… 515-522

78. Shear Strength Characteristics Of Volcanic Soils Mixed With Cement (AMM) *(Richo Brian, Stefanus Diaz Alvi, Paulus P. Rahardjo)* …… 523-528

79. Raft Pile Foundation Application For A 20-Story Building On Dense Sand Soil *(Alvin Tjahjadi, Jeffry Arnold Panggabean, Rangga Adiprima Sudisman, Arif Salman Dabigi)* …… 529-534

80. Korelasi Hasil Uji Lapangan Dengan Parameter Kuat Geser Undrained Pada Tanah Lunak Kendal *(Salma Aulia Andari, Nastiti Tiasundari)* 535-540

81. The Use Of Jack Bean As A Biocatalyst In Enzyme Mediated Calcite Precipitation For Soil Improvement Technique *(Alfaris Baqir Arrazzaq, Zayyaan Nabiila Khairunnisa, Heriansyah Putra)* 541-546

82. Analisis Ledakan Pada Struktur Basement Dengan Dinding Diafragma *(Kenny Erick, Alfred Jonathan Susilo, Aniek Prihatiningsih, Gregorius Sandjaja Sentosa)* 547-556

Exploring "Data" in Data-centric Geotechnics

Kok-Kwang Phoon
Singapore University of Technology and Design
Jianye Ching
National Taiwan University

ABSTRACT: The purpose of this keynote paper is to present a conceptualization of data-centric geotechnics, an emerging field that attempts to prepare geotechnical engineering for digital transformation. The agenda must include development of methods that make sense of all real-world data (not selective input data for a physical model) and offer insights of value to real-world decisions (not decisions for an ideal world). Given that a knowledge of the site is central to any geotechnical engineering project, data-driven site characterization (DDSC) must constitute one key domain in data-centric geotechnics, although other infrastructure lifecycle phases such as project conceptualization, design, construction, operation, and decommission/reuse would benefit from data-informed decision making as well. Ultimately, geotechnical structures need to be a part of a completely smart infrastructure that fits the circular economy and need to focus on delivering service to end-users and community from project conceptualization to decommission/reuse with full integration to smart city and smart society. It should go beyond constructing safe and economical infrastructure as an end goal.

Keywords: data-centric geotechnics, data-driven site characterization (DDSC), project DeepGeo, ugly data, site recognition challenge

1 INTRODUCTION

We are celebrating the silver anniversary of the prestigious annual conference of the Indonesian Society for Geotechnical Engineers (ISGE). In the current era of digital transformation that is sweeping across all industries, it is timely to talk about the role of data in decision making in geotechnical engineering and how far we have progressed as an industry over the past 25 years.

The purpose of this keynote paper is to present a conceptualization of data-centric geotechnics, an emerging field that attempts to prepare geotechnical engineering for digital transformation. Current practice in the form of allowable stress design or reliability-based design (RBD) is discussed to illustrate the gaps in making better data-informed decisions that are of value to a specific project at a specific site. Data-centric geotechnics is in its infancy, but some key elements of its agenda are clear given the goal is to transform practice to meet the needs of end-users and the community such as sustainability and resilience engineering. The future of our geotechnical engineering profession is surely as exciting as we can imagine, but there is little doubt that data-centric geotechnics will be part of this future.

2 ALLOWABLE (WORKING) STRESS DESIGN

The allowable (working) stress design remains the most familiar and popular method in geotechnical engineering to this day, but it has evolved into the current form:

$$F_n \leq Q_n/FS \quad (1)$$

in which F_n is the nominal load, Q_n is the nominal capacity and FS is the factor of safety. The nominal capacity is typically determined by a physics-based model such as the finite element method. Eqn. (1) is connected to site-specific data through the calculation of Q_n, but there is no rational method that can adjust FS based on the quality of the calculation model

and/or the quality of the input data. The values for FS have effectively remained unchanged since they were recommended by Terzaghi and Peck (1948) (Table 1).

Table 1. Factor of Safety for Various Structures, Terzaghi and Peck (1948).

Type of structures	Factor of safety	Remarks
Retaining structure	1.5	Against sliding
	1.5	Base heave
	2.0	Strut buckling
Slope stability	1.3-1.5	
Embankments	1.5	
	1.1-1.2	With monitoring
Footings and rafts	2.0-3.2	
Single piles	2.5-3.0	With load testing
	6.0	With Engineering News formula
Floating pile groups	2.0-3.0	w.r.t. base failure

While Q_n can be improved by collecting better data and developing better physics-based models, Eqn. (1) is conservative because the model factor is typically conservative and FS is always conservative (FS > 1). The model factor is defined as the ratio of the measured to the calculated response. Current practice is arguably highly successful, because significant failures are rare. Nonetheless, it is debatable if current practice that favors a large factor of safety is compatible with sustainable development goals. Geotechnical designs must be very safe, because there is no rational basis to optimize designs. The observational approach is a possible basis, but it is not applied to all projects. Current practice is also heavily reliant on precedents. It is unclear how external shocks arising from climate change and resiliency could be considered systematically.

3 RELIABILITY-BASED DESIGN

The most well-known implementation of reliability-based design (RBD) in practice is the Load and Resistance Factor Design (LRFD):

$$\eta F_n \leq \Psi Q_n \quad (2)$$

in which η is the load factor and Ψ is the resistance factor. The key ideas behind RBD are: (1) load F and capacity Q are random variables described by probability distribution functions and the (2) design goal is to ensure the probability of failure (Q < F) is less than a target value. LRFD is a simplified form of RBD. As shown in Fig. 1, the purpose of LRFD is to use η and Ψ to create sufficient spacing between two probability distribution functions (describing the uncertainties in F and Q) so that the probability of failure is sufficiently low. LRFD has been adopted in the 2014 edition of the Canadian Highway Bridge Design Code (CAN/CSA 2014) and others e.g., Bathurst et al. (2017).

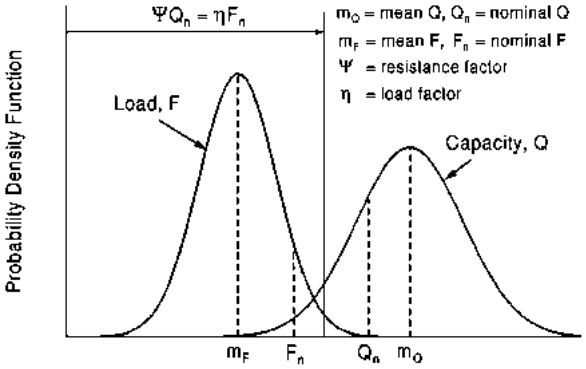

Fig. 1. Load and Resistance Factor Design (LRFD).

There is limited appreciation that RBD can optimize designs, because it is sensitive to the quality of site information and knowledge of the structure. In contrast to allowable stress design, it offers a rational pathway to achieve more sustainable designs. A simple example of design optimization using LRFD is shown in Table 2. The resistance factor depends on the "degree of understanding" (low, typical, high). Site understanding refers to how well the ground providing the geotechnical resistance is known and model understanding refers to the degree of confidence that a designer has in the model used to predict the geotechnical resistance. There is a growing awareness that data is an asset that has not been fully exploited in geotechnical practice and there is significant potential for digital technologies to transform geotechnical decision making in even more fundamental ways beyond RBD.

4 DATA-CENTRIC GEOTECHNICS

The intent of data-centric geotechnics is to create a platform for geotechnical practice to leverage on emerging digital technologies such as BIM, digital twin, machine learning, AI, and blockchains to deliver services that meet the need of the end-users and the community rather

than to build infrastructure as an end goal. By definition, data-centric geotechnics must adopt a "digital first" agenda. This agenda must include development of methods that make sense of all real-world data (not selective input data for a physical model) and offer insights of value to real-world decisions (not decisions for an ideal world). Real-world decisions refer to those made by engineers for a specific project at a specific site. In addition, any data-centric methodology must be applicable to all projects, including routine projects where data is frequently sparse and incomplete.

Table 2. Geotechnical Resistance Factors for the Ultimate Limit State (ULS) and Serviceability Limit State (SLS) Appearing in Table 6.2 of the 2014 Canadian Highway Bridge Design Code (CHBDC) (CAN/CSA 2014). Numbers Are for Illustration Only – The 2014 CHBDC Must Be Consulted for The Actual Factors, Source: Table 4, Fenton et al. (2016).

Application	Limit State	Test Method/Model	Degree of understanding		
			Low	Typical	High
Shallow foundations	Bearing, φ_{gu}	Analysis	0.45	0.50	0.60
		Scale model test	0.50	0.55	0.65
	Sliding, φ_{gu}	Analysis	0.70	0.80	0.90
	Frictional	Scale model test	0.75	0.85	0.95
	Sliding, φ_{gu}	Analysis	0.55	0.60	0.65
	Cohesive	Scale model test	0.60	0.65	0.70
	Passive resistance, φ_{gu}	Analysis	0.40	0.50	0.55
	Settlement or lateral movement, φ_{gs}	Analysis	0.70	0.80	0.90
		Scale model test	0.80	0.90	1.00
Deep foundations	Compression, φ_{gu}	Static analysis	0.35	0.40	0.45
		Static test	0.50	0.60	0.70
		Dynamic analysis	0.35	0.40	0.45
		Dynamic test	0.45	0.50	0.55
	Tension, φ_{gu}	Static analysis	0.20	0.30	0.40
		Static test	0.40	0.50	0.60
	Lateral, φ_{gu}	Static analysis	0.45	0.50	0.55
		Static test	0.45	0.50	0.55
	Settlement or lateral deflection, φ_{gs}	Static analysis	0.70	0.80	0.90

Table 3. Site Data for a Taipei Site, Ou and Liao (1987).

Depth (m)	s_u (kN/m^2)		s_u(mob) (kN/m^2)	Test results						
				LL	PI	LI	s'_v/P_a	s'_p/P_a	$s_u(mob)/s'_v$	q_{t1}
12.8	UU	55.2	46.9	30.1	9.1	1.20	1.26	1.71	0.37	3.35
14.8	VST	50.7	52.9	32.8	12.8	1.43	1.43		0.36	3.34
16.1	UU	61.9	51.7	36.4	14.5	1.24	1.54		0.33	3.15
17.8	UU	54.2	42.8	41.9	18.9	0.90	1.68	1.79	0.25	2.74
18.3	VST	59.5	59.3				1.72		0.34	2.76
20.2	UU	73.1	60.5	38.1	17.3	0.70	1.88		0.32	2.73
22.7	VST	63.3	64.4	37.0	16.0	0.58	2.08		0.31	2.97
24.0	UU	82.2	67.5	38.0	16.2	0.75	2.19	2.19	0.30	2.80
26.6	UU	98.1	82.1	34.8	13.8	0.80	2.41		0.34	3.92

Phoon and Ching (2021) presented an initiative called Project DeepGeo that is inspired by the above data-centric agenda. The purpose of Project DeepGeo is to produce a 3D stratigraphic map of the subsurface volume below a full-scale project site and to estimate relevant engineering properties at each spatial point based on site investigation data and other relevant Big Indirect Data (BID). Phoon et al. (2019) referred to big data as indirect to

emphasize the point that big data exists in geotechnical engineering, but it is not directly relevant to one specific project at one specific site. Generic soil property databases, Phoon et al. (2016), Ching et al. (2016) and load test databases, Tang and Phoon (2021) are examples of BID. Uncertainty quantification is necessary, as data is insufficient, incomplete, and/or not directly relevant to derive a deterministic map. This is a major challenge for at least five reasons: (1) inputs are restricted to actual real-world site investigation data such as those shown in Tables 3 and 4, (2) data from other sites are routinely used to supplement limited site-specific data in practice based in large part on engineering judgment and appreciation of regional geology, but there is no theoretically satisfactory method to do this for BID, (3) human experience cannot be incorporated in any learning algorithm thus far to produce continuous improvement in the algorithm, i.e. there is no virtuous machine-human decision cycle, Phoon et al. (2021), (4) machine learning algorithms remain "black-box" and the lack of "explainability" of the outputs may not inspire sufficient confidence in an engineer who takes responsibility for the decision, and (5) "bad" data that lead to wrong decisions should exist for a sufficiently large BID, but standard outlier analysis may not be applicable to spatially varying datasets.

Table 4. Site Data for the İzmir Subway Site, Turkey (Kıncal and Koca 2019).

No.	RQD	RMR*	Q	GSI	E_m (GPa)	E_{em} (GPa)	E_{dm} (GPa)	E_i (GPa)	σ_{ci} (MPa)
1	5	25.5			0.11			4.2	26.0
2	18	35			0.238			7.0	39.5
3	32	41.5			0.83			10.8	72.0
4	35	41			0.564			9.0	62.0
5	37.4	41			0.72			10.7	65.2
6	24	36			0.46			10.0	50.0
7	40	39			0.51			8.0	61.0
8	18	35			0.47			8.5	48.5
9	34	35			0.39			7.5	51.2
10	42.5	44.5			1.17			12.3	86.4
11	45	45			1.46			13.0	90.0
12	42	43			1.09			14.4	81.3
13	27.5	36			0.366			7.5	57.3
14	20	36			0.439			8.7	54.0
15	25	37			0.464			10.0	60.0
16	23	35			0.336			9.3	53.7
17	20	34			0.322			9.0	53.0
18	20	33			0.36			9.25	53.4
19	11	37			0.384			9.66	58.1
20	21.5	27			0.278			6.5	37.1
21	10	20			0.112			4.33	14.3
22	4	19.5			0.11			4.0	23.0
23	32	26			0.29			6.8	27.4
24	30	34			0.36			6.4	37.0
25	16	32			0.32			8.0	40.2
26	12	29			0.228			6.0	30.2
27	28	30.5			0.25			7.33	37.2
28	14	31			0.168			4.4	29.0
29	43	45			1.32			11.5	85.6
30	41.5	38			0.98			9.58	70.5
31	26	43			0.768			10.5	71.2
32	13	33.5			0.17			5.33	35.0

* Average of the lower and upper bounds of RMRs reported in Kıncal and Koca (2019)

The first challenge is fundamental to data-centric geotechnics. The spirit is not to "make perfect" the imperfections of real-world data, such as sparsity and incompleteness, using ad-hoc approaches. It is also clearly uneconomical to throw away data simply because the physical model cannot make sense of "extraneous" data. In Tables 3 and 4, sparsity is illustrated by the small number of rows and incompleteness is illustrated by the greyed-out boxes. Phoon et al. (2019) presented a useful mnemonic, MUSIC-X (Multivariate, Uncertain and Unique, Sparse, Incomplete, and potentially Corrupted with "X" denoting the spatial/temporal dimension) to highlight seven common ugly attributes in real site data.

It can be seen that the "ugly" data challenge is much harder than the "curse of small sample size" that has impeded the adoption of RBD in geotechnical engineering, Phoon (2017). Given that the feasibility of a data-centric agenda pivots on an acceptable solution to this challenge, it is natural to ask what is the state of research progress on this front. Surprisingly, despite an initial impression that the ugly data challenge is near intractable, a site-specific multivariate probability distribution for MUSIC data can be constructed in a reasonable way using a Bayesian machine learning method called GPR-MUSIC, Ching and Phoon (2019). It has since been developed to process MUSIC-X for 1D spatially varying datasets, Ching and Phoon (2020) and MUSIC-3X for 3D spatially varying datasets, Ching et al. (2021b). The learning behaviour of GPR-MUSIC is illustrated in Fig. 3 using simulated data. However, it is noteworthy that GPR-MUSIC

and improved versions have been shown to be effective for real-world datasets. The bivariate distribution is "flat" (or uninformative) when there are only two observations available to learn from, but it becomes increasingly "peaky" when more observations are included.

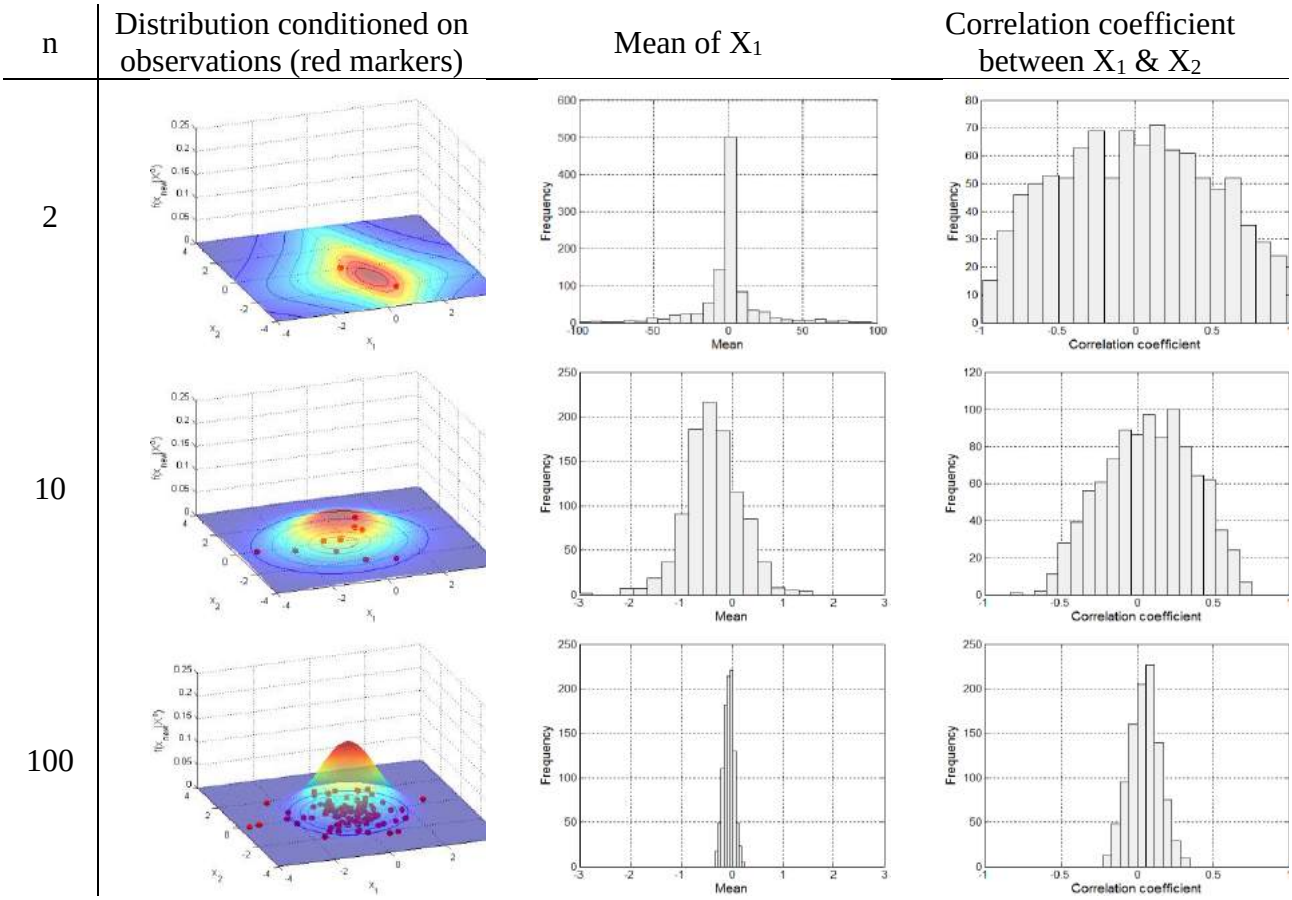

Fig. 3. "Site-Specific" Bivariate Distribution Conditioned on Observations and the Histogram of the Correlation Coefficient "Learnt" from Two, Ten, and One Hundred Observations (Red Markers) Simulated from A Bivariate Normal Distribution (X1, X2) with Mean = 0 and Covariance Matrix = Identity, Source: Fig. 6, Phoon et al. (2019).

Table 5. Incomplete List of Topics in Data-Driven Site Characterization, Source: Table 2, Phoon et al. (2021).

State of DDSC research	Some literature	Limited literature	None?	
Geomaterials	Soil	Rock	Improved ground	
Data types	Geotechnical investigation	Geophysical	Emerging: laser scanning, drone photogrammetry, etc.	
Ugly data challenge	MUSIC-3X (Multivariate, Uncertain and Unique, Sparse, Incomplete, potentially Corrupted, 3D spatially varying)	Truncated/censored data, mixed numerical and categorical data, etc.	Anonymized data, falsified data	
Site recognition challenge	Transformation models	Performance data: proof/load tests, observations, etc.	Health monitoring	Remote sensing
Stratification/mapping challenge	CPT-based soil behavior type	Discontinuities	Anomalies, voids, etc.	

Phoon et al. (2021) coined the term "data-driven site characterization" (DDSC) to refer to any site characterization methodology that relies solely on measured data, both site-specific data collected for the current project and existing data of any type collected from

past projects at the same site, neighboring sites, or beyond. The site uniqueness problem, or more formally the "site recognition challenge", is an intrinsic part of DDSC. A preliminary solution based on the hierarchical Bayesian model (HBM) is being studied, Ching et al. (2021a, b, c). In principle, the source of data can also go beyond site investigation and the type of data can go beyond numerical such as categorical, text, and expert opinion. Project DeepGeo only addresses one part of DDSC that pertains to numerical soil data in a site investigation report and soil property databases. To the knowledge of the authors, other possibilities have not been studied (Table 5). Given that a knowledge of the site is central to any geotechnical engineering project, DDSC must constitute one key domain in data-centric geotechnics, although other infrastructure lifecycle phases such as project conceptualization, design, construction, operation, and decommission/reuse would benefit from data-informed decision making as well.

5 CONCLUSIONS

There is little doubt that decision making in geotechnical engineering would be transformed in the future, as digital technologies become more pervasive and more powerful. This paper presents a brief overview of data-centric geotechnics and some key elements of its agenda. Data-driven site characterization (DDSC) is fundamental to data-centric geotechnics. One part of DDSC that addresses numerical soil data in a site investigation report and soil property databases is pursued under Project DeepGeo.

REFERENCES

Bathurst, R.J., S. Javankhoshdel, & T.M. Allen. 2017. LRFD Calibration of Simple Soil-Structure Limit States Considering Method Bias and Design Parameter Variability. *Journal of Geotechnical and Geoenvironmental Engineering* 143(9): 04017053.

CAN/CSA. 2014. *CAN/CSAS614: Canadian Highway Bridge Design Code*. Canadian Standards Organization, Mississauga, Ontario, Canada.

Ching, J., Li, D.Q., & Phoon, K.K. 2016. Statistical Characterization of Multivariate Geotechnical Data. *Chapter 4, Reliability of Geotechnical Structures in ISO2394*: 89-126. CRC Press/Balkema.

Ching, J., & Phoon, K.K. 2019. Constructing Site-Specific Multivariate Probability Distribution Model Using Bayesian Machine Learning. *Journal of Engineering Mechanics ASCE* 145(1): 04018126.

Ching, J., & Phoon, K.K. 2020. Constructing A Site-Specific Multivariate Probability Distribution Using Sparse, Incomplete, and Spatially Variable (MUSIC-X) data. *Journal of Engineering Mechanics ASCE* 146(7): 04020061.

Ching, J., Wu, S., & Phoon, K.K. 2021a. Constructing Quasi-Site-Specific Multivariate Probability Distribution Using Hierarchical Bayesian Model. *Journal of Engineering Mechanics ASCE* 147 (10): 04021069.

Ching, J., Phoon, K.K., Yang, Z.Y., & Stuedlein, A.W. 2021b. Quasi-Site-Specific Multivariate Probability Distribution Model for Sparse, Incomplete, and Three-Dimensional Spatially Varying Soil Data. *Georisk*.https://doi.org/10.1080/17499518.2021.1971256.

Ching, J., Phoon, K.K., Ho, Y.H., & Weng, M.C. 2021c. Quasi-Site-Specific Prediction for Deformation Modulus of Rock Mass. *Canadian Geotechnical Journal* 58(7): 936–951.

Fenton, G.A., Naghibi, F., Dundas, D., Bathurst, R.J., & Griffiths, D.V. 2016. Reliability-Based Geotechnical Design in the 2014 Canadian Highway Bridge Design Code. *Canadian Geotechnical Journal* 53(2): 236-251.

Kıncal, C., & Koca, M.Y. 2019. Correlations of In Situ Modulus of Deformation with Elastic Modulus of Intact Core Specimens and RMR Values of Andesitic Rocks: A Case Study of the İzmir Subway Line. *Bulletin of Engineering Geology and the Environment* 78: 5281-5299.

Ou, C.Y. & Liao, J.T. 1987. *Geotechnical Engineering Research Report*. GT96008, National Taiwan University of Science and Technology, Taipei.

Phoon, K.K. 2017. Role of reliability calculations in geotechnical design. *Georisk* 11(1): 4-21.

Phoon, K.K., Prakoso, W.A., Wang, Y., & Ching, J.Y. 2016. Uncertainty Representation of Geotechnical Design Parameters. *Chapter 3. Reliability of Geotechnical Structures in ISO2394:* 49-87 CRC Press /Balkema.

Phoon, K.K., Cao, Z. J., & Wang, Y. 2019. ISSMGE TC304/309/210 Machine Learning Dialogue for Geotechnics 2019. *7th International Symposium on Geotechnical Safety and Risk (ISGSR 2019)*: 905-911. Taiwan.

Phoon, K.K. & Ching, J.Y. 2021. Project DeepGeo - Data-Driven 3D Subsurface Mapping. *Journal of GeoEngineering* 16(2): 47-59.

Phoon, K.K., Ching, J.Y., & Shuku, T. 2021. Challenges in Data-Driven Site Characterization. *Georisk*. https://doi.org/10.1080/17499518.2021.1896005.

Tang, C. & Phoon, K.K. 2021. *Model Uncertainties in Foundation Design*. CRC Press.

Terzaghi, K. & Peck, R.B. 1948. *Soil Mechanics in Engineering Practice*. John Wiley.

Seismic Interaction Adjacent Tall Buildings with Underground Structures

Youssef M. A. Hashash
Professor of Civil and Environmental Engineering – University of Illinois

ABSTRACT: Underground structures are commonly constructed near existing or new tall buildings in dense urban areas worldwide. Tall buildings, during earthquake shaking, generate lateral forces carried by the building foundations and into surrounding soils. These lateral forces may be transmitted to adjacent underground structures. This presentation will describe a combined experimental and numerical study focused on the evaluation of the impact of tall buildings on the seismic response of underground structures with a focus on box structures representing underground transit stations. A series of dynamic centrifuge tests were employed in the evaluation of numerical simulations to evaluate the impact of highly idealized adjacent tall buildings on the seismic response of underground structures. The numerical models successfully reproduce the seismic behavior observed in the centrifuge experiments including the additional loading demands imposed by adjacent building on underground structures in addition to deformations. A large-scale parametric study, with nearly 11,000 simulations, using three-dimensional (3-D) nonlinear finite element analysis with more realistic soil-structure-underground structure (SSUS) representation is performed and presented to evaluate the impact of variability in the SSUS system on the seismic response of underground structures. The effects of different building heights, building foundations, underground structure configurations, and soil profiles are evaluated using a suite of ground motions. These configurations represent the range of conditions that are likely to be present in dense urban environments. The results show that (a) as the adjacent building became taller and hence the base shear increased, greater dynamic earth pressures were transmitted to the underground structure, (b) the dynamic earth pressures were reduced with increasing building to underground structure distance, and (c) the racking displacements of underground structures were strongly dependent on building foundation and underground structure configurations such as basement depth, pile length, and the depth of the underground structure. For design purposes, these interactions need to be considered by modeling a realistic building and underground structure representation in SSUS system to evaluate the added demands that a given building will impose on underground structures including cut-and-cover boxes and bored tunnels. Moreover, the presentation highlights the significant advances in 3D numerical modeling of seismic soil-structure interactions whereby detailed reliable analyses can now be readily used in seismic design application.

Geotechnical Aspect on Tunnel Engineering Construction of Jakarta-Bandung High-Speed-Rail

I Wayan Sengara
Professor, Faculty of Civil and Environmental Engineering – Institute Technology Bandung
Sr. Geotechnical Engineer – PT WSP Engineering
Sr. Engineer – CARS-DARDELA Joint Operation

Rachman Suhanda
General Manager Technical Design Management – Kereta Cepat Indonesia-China (KCIC)

Eyrton C. Silaban
Sr. Geotechnical Engineer – PT WSP Engineering
Sr. Engineer – CARS-DARDELA Joint Operation

Jamaluddin
Sr. Engineer – CARS-DARDELA Joint Operation

ABSTRACT: Jakarta – Bandung High-Speed-Rail Project (JB-HSR) project consist of 13 single-tunnels for its double-tracked main line, with overall length of 17 km out of the JB_HSR line total-length of 142.3 km. The longest tunnel is with overall length of 4478 m. In general, two methods are applied in the JB-HSR, namely TBM and NATM, with main the consideration of geological-geotechnical subsurface conditions, surrounding locations, and cost effectiveness of construction. Geological-geotechnical subsurface conditions along the JB-HSR varies significantly form soft to hard clay, clay-shale, to rock layers. TBM has been applied on soft alluvium to hard clay. TBM construction with slurry type is applied in Tunnel #1 of low-land Jakarta urban area with partially crossing underneath Jakarta-Cikampek toll-road. NATM sequence excavation construction method is applied in mountain hard rock to tertiary soft rock and clay-shale. Twelve tunnels were constructed using this NATM method with various excavation benching and blasting methods. Several benching of NATM methods have been applied considering type of geological-geotechnical sub-surface and surrounding conditions. Seven NATM tunnel construction on clay-shale is of particular interest due to some h=geotechnical stability issues during construction. Clay-shale layers of various weathering were encountered along the tunnel and various benching methods have been applied. JB-HSR applied strict deformation monitoring controls both inside and outside of the tunnel for safety during construction. Dynamic tunnel construction process and accurate analysis as well as decision on suitable methods were experienced, with feedback in tome, guiding construction and ensuring safety. Geotechnical aspect related to stability issues with deformation monitoring is an essential part on the HSR-JB tunnel construction.

Keywords: Jakarta-Bandung, high-speed-rail, tunnel, TBM, NATM, soft-clay, clay-shale, rock, deformation, instrumentation-monitoring

Analysis of Void Redistribution and Delayed Flow Failure Associated with Liquefaction during Earthquakes

Susumu Iai
Professor Emeritus – Kyoto University
President – FLIP Consortium

Masyhur Irsyam
Professor, Faculty of Civil and Environmental Engineering – Institute Technology Bandung

ABSTRACT: Ground deformation associated with void redistribution in a ground with low permeable surface crust is evaluated through nonlinear dynamic analyses by referring to case histories of delayed sand boil in level ground in Japan and delayed flow failure in gently sloping land in Indonesia with a slope angle of 2°, sliding over a range of 3 km with a displacement of 500 m. The results of the analyses conducted in this study are consistent with those of the case histories. Therefore, the analytical method can be applied to accurately evaluate essential engineering parameters governing delayed flow, including the degree of localization of volumetric strain in the inflow zone of pore water below the less permeable surface crust, extent of reduction of the residual strength from its initial value, and the effect of permeability. In particular, the analysis suggests that the reduction factor for the residual strength in the inflow zone is 1/40 or less in the referred case history.

Keywords: flow failure, localization, residual strength, steady state line, void redistribution

1 INTRODUCTION

Ground deformation induced by earthquake motion may be put into a general perspective relative to the steady state line (SSL) as shown in Fig. 1. The SSL represents the steady state condition where sand deforms continually, keeping the volume constant, under a constant shear stress and confining stress.

Considering the SSL in Fig. 1, the ground deformation during earthquakes is associated with lateral spread (path a) through settlement (path a*) corresponding to generation (path a) and dissipation (path a*) of excess pore water pressure during earthquakes. Transition point A in the figure represents cyclic mobility.

The figure also shows that the failure of a slope consisting of saturated soils with low permeability is associated with path b, which does not involve volume change and thus assumes an undrained condition. Path b eventually reaches the point B on the SSL, which represents the onset condition of flow failure if the residual strength of the soil defined by point B is less than the initial static shear stress induced in the slope by gravity.

Aside from the ground deformation briefly discussed above, a less-explored type of ground deformation in the discipline of earthquake geotechnics is that associated with the path d or d*, in which volumetric expansion occurs along the approach to the SSL. This type of ground deformation is typically represented as delayed flow failure, which is initiated when the path reaches and extends past point D on the SSL.

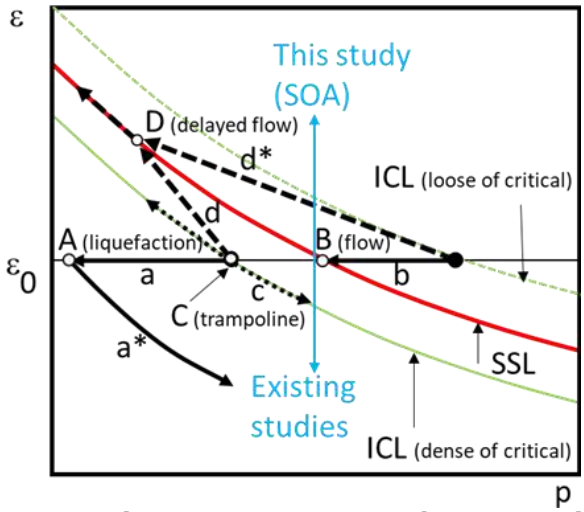

Fig. 1. Volumetric Stress-Strain Paths Associated with Four Types of Seismic Ground Deformation (A Through D) Relative to the Steady State Line (SSL).

Point D corresponds to the initial static shear stress induced in the slope by gravity. As schematically shown in Fig. 2, the cause of volumetric expansion is associated typically with void redistribution, in which mildly sloping ground is capped by a layer of low permeability, and the pore water flowing upward from the lower layer is trapped in the shallower layer just below the cap layer, Whitman (1985); Boulanger & Truman (1996); Kokusho (2000); Malvick et al. (2006); Seid-Karbasi & Byrne (2007); Kamai & Boulanger (2013). Because a certain amount of time is required for sufficient accumulation of pore water to arrive at point D from the point of the initial state through the process of void redistribution, this process is typically delayed.

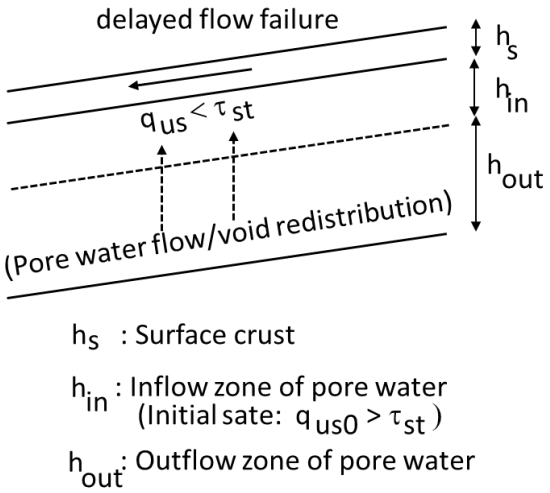

Fig. 2. Delayed Flow Failure (Modified after Iai (2019)).

The residual strength corresponding to point D is often significantly reduced from that corresponding to point B at the initial state. The residual strength at point B is typically measured and evaluated in a laboratory test performed under undrained conditions. In the present study, this is referred to as the initial residual strength.

This study addresses these parameters by conducting nonlinear dynamic analysis in reference to a recent case history of delayed flow failure associated with the 2018 Palu earthquake, Indonesia (M 7.4). The strain space multiple mechanism model previously proposed by the authors implemented in a computer code FLIP is used for the analysis, Iai et al. (2011). As a prelude to this discussion, preliminary analysis is performed to confirm the accuracy of the nonlinear dynamic analysis on void redistribution by referring to a case history of delayed sand boil occurring in level ground in the Tokyo Bay area during the 2011 off the Pacific coast of Tohoku earthquake, Japan (Mw 9.0).

2 RESIDUAL STRENGTH REDUCTION BY VOID RATIO CHANGE

Fig. 3 shows the relationship between the void ratio and the effective confining pressure at the steady state based on triaxial tests of Toyoura sand with a DL clay mixture performed by the author and his colleagues at the FLIP consortium. The residual strength is given by

$$q_{us} = p_{us} \sin \phi_f \tag{1}$$

The solid straight lines in Fig. 3 are drawn to show the general trend of these data based on the following back-fitting equation.

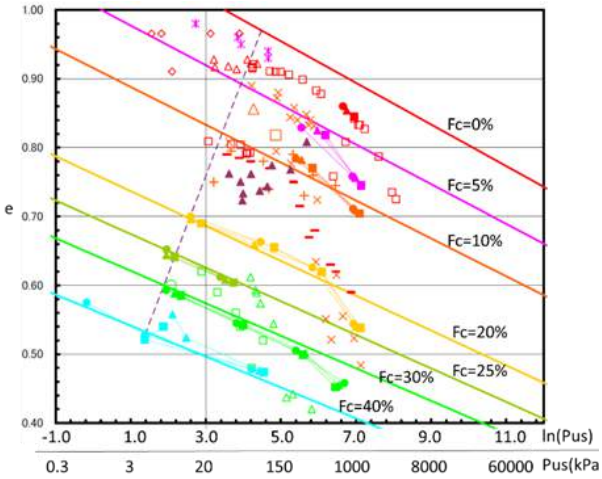

Fig. 3. Void Ratio and Confining Pressure at Steady State of Sand with Various Fines Content (Fc).

$$\ln\left(\frac{p_{us}}{p_a}\right) = -\left(\frac{e-e_a}{1+e_a}\right) / \varepsilon_{mus} \tag{2}$$

where the reference confining pressure is $p_a = 20$ kPa and the reference void ratio e_a at $p = p_a$ reflecting the effect of fines content F_c (%) is given as

$$e_a = 0.000174F_c^2 - 0.01992F_c + 1.015 \tag{3}$$

The factor governing the sensitivity of p_{us} to the void ratio in Eqn. (2) is given as $\varepsilon_{mus} = 0.015$, where ε_{mus} is related to the parameter λ in the classic soil mechanics as $\varepsilon_{mus} = \lambda/(1+e_a)$ with $\lambda \approx 0.03$.

By interpreting the changes in void ratio

from the reference state in Eqn. (2) and Fig.3 in terms of volumetric strain induced from the initial state and substituting Eqn. (1), this equation is rewritten as the degree of reduction in the residual strength owing to void ratio change as

$$\Delta \ln q_{us} = -\Delta\varepsilon / \varepsilon_{mus} \tag{4}$$

Where:

$$\Delta \ln q_{us} = \ln q_{us} - \ln q_{us0} = \ln\left(\frac{q_{us}}{q_{us0}}\right),\ \Delta\varepsilon = \varepsilon - \varepsilon_0 \tag{5}$$

The steady state after reduction in residual strength given by these equations is indicated by an open circle on the SSL on the $\varepsilon - p$ plane with the associated volumetric strain change in Fig. 4. In particular, the degree of reduction in residual strength is inferred by the reduction from the initial state p_{us0} to the current state p_{us}.

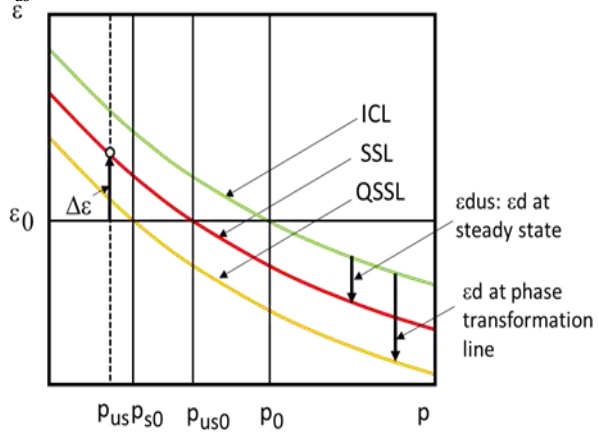

Fig. 4. Initial Consolidation Line (ICL), Steady State Line (SSL), and Quasi Steady State Line (QSSL) Implicitly Incorporated in the Strain Space Mechanism Model.

The volume expansion associated with pore water inflow to the zone with a thickness of h_{in} below the surface crust must be in balance with the volume compression associated with pore water outflow from the lower liquefiable zone with a thickness of h_{out} to keep the total mass of pore water preserved (Fig. 2). Thus, the volumetric strain change in the inflow zone is given by

$$\Delta\varepsilon = -r_{\Delta\varepsilon}\varepsilon_{out}\left(\frac{h_{out}}{h_{in}}\right) \tag{6}$$

where the reduction factor $r_{\Delta\varepsilon}$ accounts for the effect of partial drainage through the surface crust layer, with $r_{\Delta\varepsilon} = 1$ and $r_{\Delta\varepsilon} = 0$ representing no drainage and full drainage, respectively.

A simple equation is derived to estimate the degree of reduction in residual strength owing to void redistribution:

$$\ln\left(\frac{q_{us}}{q_{us0}}\right) = -r_L\left(\frac{\varepsilon_{out}}{\varepsilon_{mus}}\right) \tag{7}$$

where r_L denotes a localization factor and is given by

$$r_L = r_{\Delta\varepsilon}\left(\frac{h_{out}}{h_{in}}\right) \tag{8}$$

The solid line in Fig. 5 indicates the degree of reduction in residual strength expected to occur based on Eqn. (7) for the localization factor r_L up to 5. The value of $\varepsilon_{out} = -3\%$ is adopted on the basis of the post-liquefaction volumetric strain proposed by Ishihara & Yoshimine (1992). The broken line in the figure is plotted to indicate the sensitivity of ε_{mus}. The exact value of r_L depends on the degree of localization of the inflow zone associated with the void redistribution and the effect of partial drainage through the surface crust layer and must be evaluated through nonlinear dynamic analysis, as discussed subsequently.

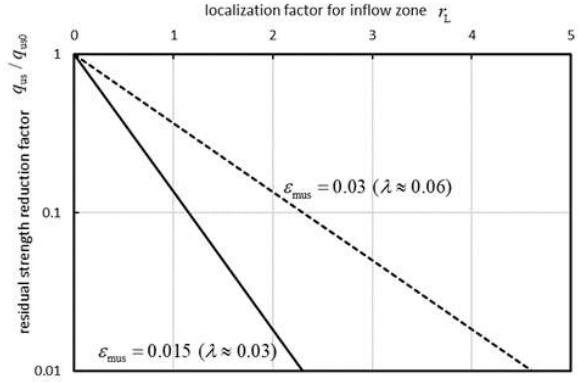

Fig. 5. Reduced Residual Strength Ratio Due to Void Redistribution for Sand with Post-Liquefaction Volumetric Strain of $\varepsilon_{out} = -3\%$.

3 VOID REDISTRIBUTION IN LEVEL GROUND

As previously mentioned, a case history of liquefaction occurring in level ground in the Tokyo Bay area during the 2011 off the Pacific coast of Tohoku earthquake (Mw 9.0) was selected in this study to demonstrate the applicability of the nonlinear dynamic analysis model in determining the void redistribution as a prelude to the analysis of delayed flow failure. In this case history, the Tokyo Bay area was shaken by earthquake motion of a long duration, longer than 2 min at the mainshock—followed by the aftershock (Mw 7.7) about 30 min later. In particular, no sand boil occurred during the mainshock but after the aftershock, a

considerable amount of time later, sand boil was monitored by a security camera at a site in Urayasu city.

Fig. 6 shows a soil profile of the liquefiable layers and finite element mesh used for the nonlinear dynamic analysis. In the analysis, the boundary condition of the pore water pressure is specified at an elevation of 0 m just below the surface crust layer (Layer B), as shown by water mark represented by the solid line. This condition is specified to represent the initial ground water table for initial gravity analysis for setting up the static pore water pressures and effective stress in the deposit prior. The static pore pressure in the surface crust was kept as $p = 0$ for simplicity.

The constraint condition of $p = 0$ at an elevation of 0 m was relaxed during the nonlinear dynamic analysis phase to enable the excess pore water pressure to increase just below the surface crust layer and, as a minimum requirement of the constraint condition of the pore water pressure, the boundary condition of $p = 0$ in terms of excess pore water pressure was imposed on the ground surface, as shown by water mark indicated by the broken line.

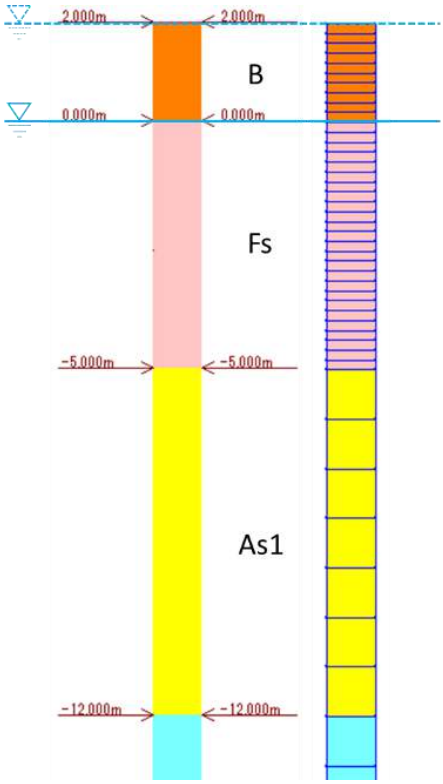

Fig. 6. Simplified Soil Profile and Finite Element Mesh Adopted for This Study (Urayasu City in The Tokyo Bay Area).

Among the parameter study, Case 1 represents the condition of the permeable surface crust with a permeability ratio of 5 over the permeability of liquefiable layer Fs. Case 2 represents the condition of the less permeable surface crust with a permeability ratio of 0.05.

Computed results in terms of excess pore water pressure distribution are shown in Fig. 7, where the broken lines represent the earlier phase up to 3,000 s, and the solid lines indicate the later phase from 3,000 to 250,000 s. For the refence case of permeable surface crust, Case 1, the excess pore water pressure at an elevation of 0 m just below the surface crust remained close to $p = 0$ throughout the process and thus represents the conventional distribution pattern of excess pore water pressure in the ground.

For the less permeable surface crust in Case 2, excess pore water pressure at an elevation of 0 m just below the surface crust increased and reached the initial effective vertical stress level at approximately 3,000s - 10,000 s. At that time, the excess pore water pressure in the surface crust layer (Layer B) at elevations of 2 – 0 m reached the initial effective vertical stress level throughout the layer, which cause the delayed sand boil at the ground surface.

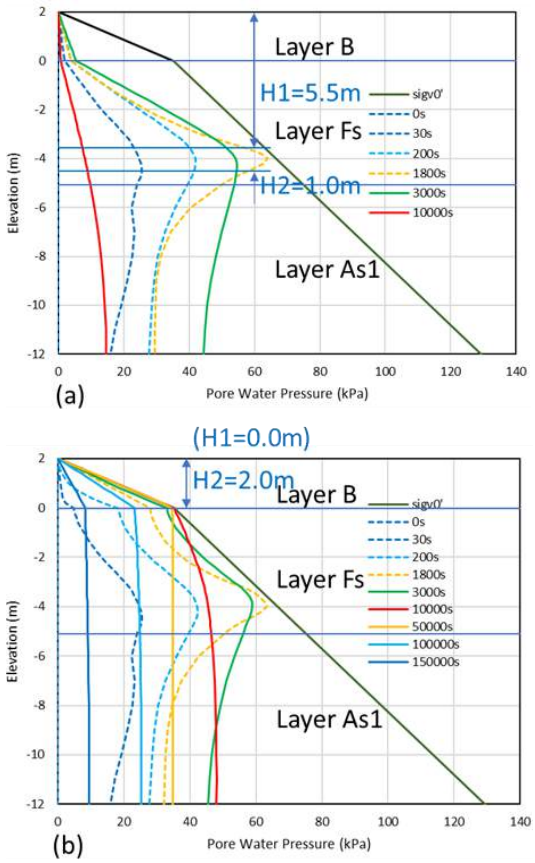

Fig. 7. Computed Distributions of Excess Pore Water Pressure: (a) Case 1, (b) Case 2.

The computed volumetric strain distributions are shown in Fig. 8. The reference case of permeable surface crust, Case 1, indicates that compressive volumetric strain of 7% was induced at an elevation of -4 m after the dissipation of excess pore water pressure at 10,000 s. With the less permeable surface crust, Case 2, experienced expansive volumetric strain of $\Delta\varepsilon \approx 5\%$, which was induced at an elevation of 0 m below the less permeable crust layer with a localized zone of 0.2 m in thickness. In contrast, the compressive volumetric strain of $\varepsilon_{out} \approx -5\%$ was induced at an elevation of -4 m in outflow zone of 0.5 m in thickness at 10,000 s. These void ratio changes are considered as evidence of void redistribution induced at the Urayasu city site during 2011 off the Pacific coast of Tohoku earthquake.

Based on the known values of volumetric strain and thickness of pore water inflow and outflow zones, the back-calculated reduction factor owing to dissipation from the surface crust layer in Eqn. (6) is estimated as $r_{\Delta\varepsilon} = 0.4$, with a thickness ratio of $h_{out} / h_{in} = 2.5$. Considering these values representing the void redistribution at the Urayasu city site together with $\varepsilon_{out} \approx -5\%$, the reduction factor in residual strength is $q_{us} / q_{us0} \approx 1/30$ in the order of magnitude given by Eqn. (7). Alternatively, direct substitution of $\Delta\varepsilon \approx 5\%$ into Eqn. (4) will result in the same reduction factor. However, these reduction factors depend on a gross change in permeability in the surface crust by the eruption of sand boils and opening of tension cracks toward the full stage of void redistribution. Thus, the numbers discussed above are considered as the conservative end of a credible scenario.

To summarize, the nonlinear dynamic analysis of the case histories of delayed sand boil in the Tokyo Bay area during the 2011 earthquake confirms the capability of the analysis model used in this study in simulating the void redistribution phenomenon beneath the less permeable surface crust.

4 DELAYED FLOW FAILURE INDUCED BY EARTHQUAKES

As mentioned previously, a recent case history of delayed flow failure during the 2018 Palu earthquake in Indonesia (M 7.4) was selected as a reference for discussing the ground deformation associated with path d or d* in Fig. 1. In this case history, the Palu area in the vicinity of the seismic fault was shaken with an earthquake motion for 80 s with a PGA of 0.3 g. In particular, the delayed flow failure of a gentle slope with an angle of 2°, occurring about 1 min after from the end of shaking or earlier, resulted in lateral displacement ranging of 400 – 700 m at Petobo city, Sahadewa et al. (2019); Kiyota et al. (2020); Okamura et al. (2020). An aerial photograph and schematic cross section of the gentle slope are shown in Fig. 9.

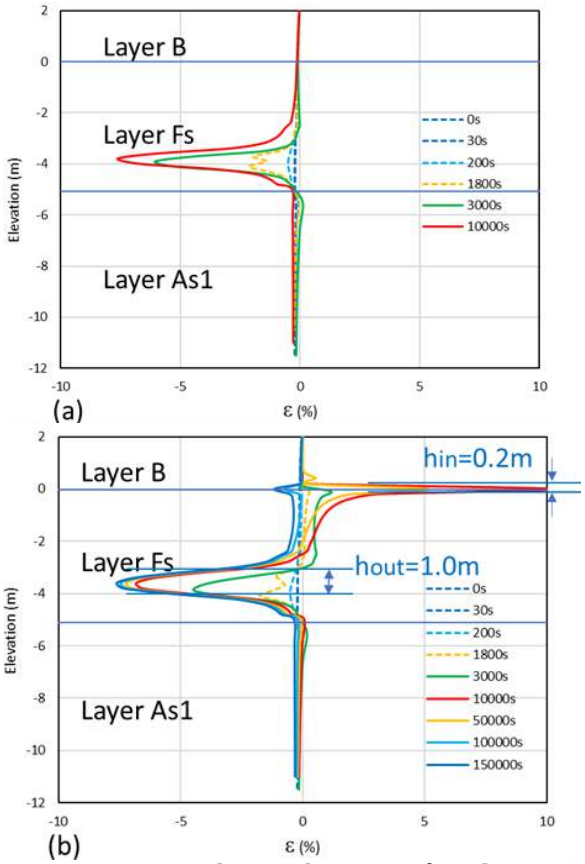

Fig. 8. Computed Distributions of Volumetric Strain; (a) Case 1, (b) Case 2.

In this study, a series of nonlinear dynamic analysis was performed with a focus on the ground deformation associated with void redistribution. The soil profile was simplified in the analysis for the sake of generality; analysis of the site-specific details is beyond the scope of this study.

Fig. 10 shows a soil profile of the liquefiable layers and finite element mesh used for this analysis. The boundary condition of the pore water pressure $p = 0$ was specified at an elevation of 0 m just below the surface crust layer (Layer S0) to represent the initial ground water table for initial gravity analysis for setting up the static pore water pressures and effective stress in the deposit prior to the earthquake. Static pore pressure in the surface crust over a

thickness of 2 m was kept as $p=0$ for simplicity. The constraint condition of $p=0$ at an elevation of 0 m was relaxed during the nonlinear dynamic analysis phase to enable the excess pore water pressure to increase just below the surface crust layer. In addition, as a minimum requirement of the constraint condition, a boundary condition of $p=0$ in terms of excess pore water pressure was imposed on the ground surface.

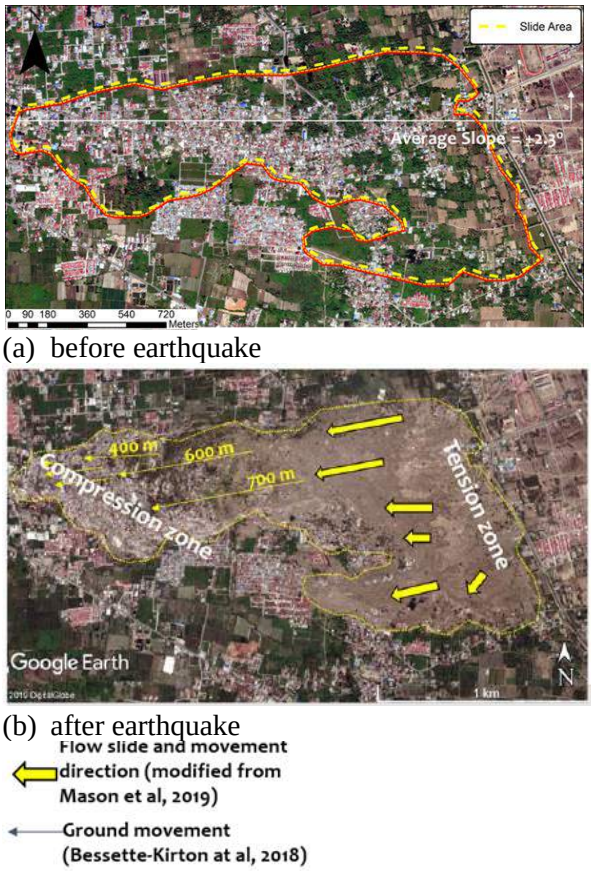

Fig. 9. Arial View and Deformation of Sloping Ground at Petobo, Indonesia (Sahadewa et al. (2019).

The computed excess pore water pressure distributions in the reference case of permeable surface crust, Case I, with a permeability ratio of 5 and initial residual strength of 20kPa, shown in Fig. 11(a), indicates that the excess pore water pressure at an elevation of 0 m just below the surface crust remained close to throughout the process and thus represents the conventional distribution pattern of excess pore water pressure in the ground. Fig. 11(b) shows Cases II, which had the less permeable surface crust with a permeability ratio of 0.005 indicates that excess pore water pressure at an elevation of 0 m just below the surface crust continued to increase and reached at the initial effective vertical stress level at about 150 s. At that time, the delayed flow slide was initiated, although the excess pore water pressure in the surface crust layer S0 at elevations of 2 – 0 m remained slightly lower than the initial effective vertical stress level throughout the layer.

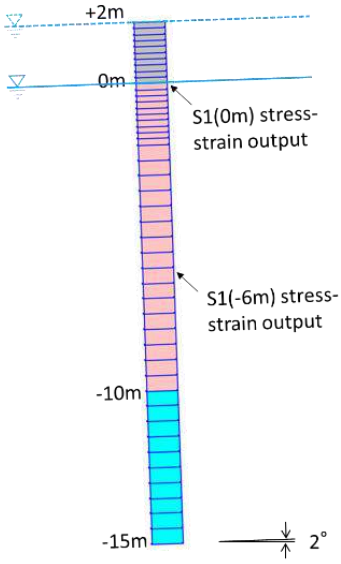

Fig. 10. Finite Element Mesh for 1D Analysis of Delayed Flow Failure.

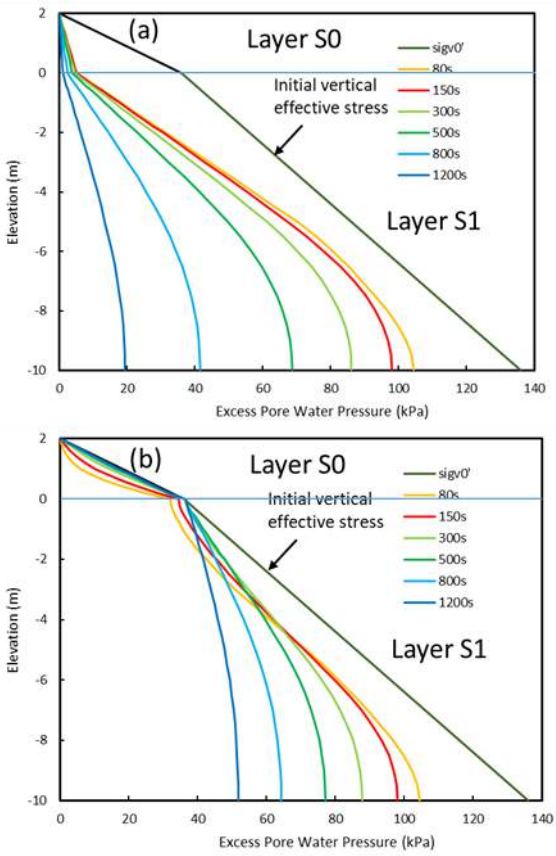

Fig. 11. Computed Distribution of Excess Pore Water Pressures; (a) Case-I, (b) Cases-II.

The computed volumetric strain distributions associated with the excess pore water pressures are shown in Fig. 12. In the reference case of

permeable surface crust, Case I, shown in Fig. 12(a), a compressive volumetric strain of -2% was induced below -5 m elevation after dissipation of excess pore water pressure at 1,200 s. With the less permeable surface crust, in Cases II, shown in Fig. 12(b), expansive volumetric strain of $\Delta\varepsilon > 2.5\%$ was induced in the inflow zone at an elevation of 0 m below the less permeable crust layer with a localized zone of 0.2 m in thickness. In contrast, a compressive volumetric strain of $\varepsilon_{out} = -1.5\%$ was induced below -5 m elevation in an outflow zone of 5 m in thickness at 1,200 s. This void redistribution is considered to have been induced at Petobo city during the 2018 Palu earthquake.

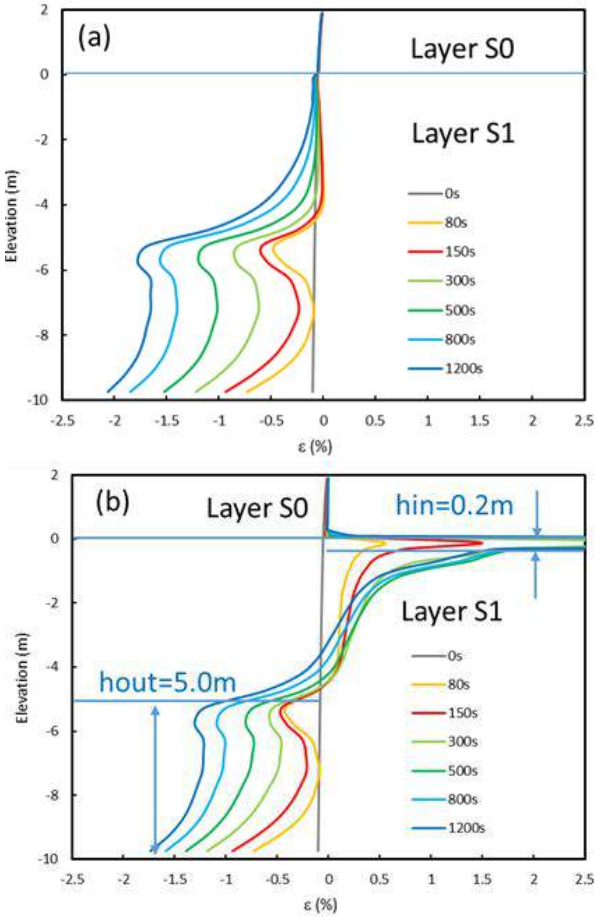

Fig. 12. Computed Distribution of Volumetric Strain; (a) Case-I, (b) Cases-II.

With the known values of volumetric strain and thickness of pore water inflow and outflow zones, the back-calculated reduction factor owing to dissipation from the surface crust layer in Eqn. (6) was estimated to be $r_{\Delta\varepsilon} > 0.17$ with a thickness ratio of $h_{out} / h_{in} = 10$ in this particular case. These values represent the void redistribution at the Petobo city site with a localization factor of $r_L > 1.7$. The reduction factor in the residual strength q_{us} / q_{us0} corresponding to the expansive volumetric strain of $\Delta\varepsilon > 2.5\%$ at inflow zone was less than 1/50, and was thus less than the threshold limit reduction factor of 1/16 for initiating delayed flow failure at the residual strength of 1.2 kPa decreased from the initial value of $q_{us0} = 20$ kPa .

As a parameter study, a case with an initial residual strength of $q_{us0} = 50$ kPa was also perform. The computed results suggest the reduction factor of 1/40 for initiating delayed flow failure at the residual strength of 1.2 kPa.

The computed residual strength values associated with void redistribution are shown in Fig. 13 for Case II. The reference case of permeable surface crust, Case I, is not shown in this figure because this case induces only compressive volumetric strain in the lower outflow zone, as shown in Fig. 12. With the less permeable surface crust, the residual strength in Case II, shown in Fig. 13, decreased from the initial value of 20 kPa to a value lower than the static shear stress induced by the slope at 150 s, when the delayed flow slide is initiated. These results are consistent with those observed at Palu, Indonesia, area.

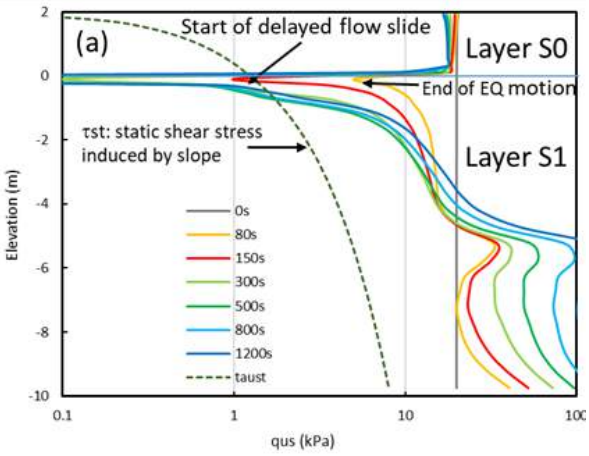

Fig. 13. Computed Distribution of Residual Strength for Case-II.

5 CONCLUSIONS

The major findings from this study are summarized below.

1. A case history of delayed sand boil, which occurred in level ground at 30 min after the mainshock and coincided with the aftershock, supports the applicability of the nonlinear dynamic analysis performed in this study for evaluating void redistribution and degree of localization of the inflow zone under the less permeable surface crust.
2. A recent case history of delayed flow,

which occurred at a slope angle of 2° and induced a lateral displacement of 500 m over a slope length of 3 km, supports the applicability of the nonlinear dynamic analysis for evaluating ground deformation owing to void redistribution.

3. The reduction factor of residual strength over its initial value owing to void redistribution is 1/40 or smaller. Unlike the flow under the undrained condition, the initial residual strength, if evaluated in the appropriate range of uncertainty, is not sensitive to the onset condition of delayed flow. The soil initially in the dense of critical state can be brought to a point on the SSL owing to void redistribution, resulting in delayed flow slide. The permeability of the liquefiable soil affects the delay time but not the rate of the flow slide.
4. Nonlinear dynamic analysis such as that performed in this study is appropriate for evaluating essential engineering parameters governing the ground deformation owing to delayed flow. These parameters include degree of localization of the inflow zone owing to void redistribution, the effect of permeability in the surface crust, and the reduction factor of residual strength.
5. Permeable surface crust does not induce void redistribution or delayed flow failure. As a mitigation measure for delayed flow failure, increased permeability in the surface crust layer can be effective.

REFERENCES

Bessette-Kirton, E., Allstadt, K., Hansen, M. 2018. USGS *Summary report on Analysis on Palu Large Landslide*. Preliminary report to Indonesia Society of Geotechnical Engineering.

Boulanger, R.W., Truman, S.P. 1996. Void redistribution in sand under post-earthquake loading. *Canadian Geotechnical Journal* 33: 829-834.

Iai, S. 2019. Evaluation of performance of port structures during earthquakes. *Soil Dynamics and Earthquake Engineering:* 126 (November).

Iai, S., Tobita, T., Ozutsumi, O., Ueda, K. 2011. Dilatancy of granular materials in a strain space multiple mechanism model. *International Journal for Numerical and Analytical Methods in Geomechanics* 35(3): 360-392.

Idriss, I.M., Boulanger, R.W. 2008. *Soil liquefaction during earthquakes*. Monograph MNO-12 Earthquake Engineering Research Institute, Oakland, CA.

Ishihara, K., Yoshimine, M. 1992. Evaluation of settlements in sand deposits following liquefaction during earthquakes. *Soils and Foundations* 32(1): 173-188.

Kamai, R., Boulanger, R.W. 2013. Simulations of a centrifuge test with lateral spreading and void redistribution effects. *Journal of Geotechnical and Geoenvironmental Engineering ASCE* 139(8): 1250-1261.

Kiyota, T., Furuichi, H., Hidayat, R.F., Tada, N., Nawir, H. 2020. Overview of long-distance flow-slide caused by the 2018 Sulawesi earthquake, Indonesia. *Soils and Foundations* 60(3): 722-735.

Kokusho, T. 2000. Mechanism for water film generation and lateral flow in liquefied sand layer. *Soils and Foundations* 40(5): 99-111.

Malvick, E., Kutter, B., Boulanger, R., Kulasingam., R. 2006. Shear localization due to liquefaction-induced void redistribution in a layered infinite slope. *Journal of Geotechnical and Geoenvironmental Engineering ASCE* 132(10): 1293-1303.

Mason, H.B., Irsyam, M., Gallant, A.P., Hutabarat, D., Montgomery, J., Reed, A.N., et al. 2019. Geotechnical Reconnissance: The 28 September 2018 M7.5 Palu-Donggala, Indonesia Earthquake.

Okamura, M., Ono, K., Arsyad, A., Minaka, U.S., Nurdin, S. 2020. Large-scale flowslide in Sibalaya caused by the 2018 Sulawesi Earthquake. *Soils and Foundations* 60(4): 1050-1063.

Sahadewa, A., Irsyam, M., Hanifa, R., Mikhail, R., Pamumpuni, A., Nazir, R., et al. 2019. Overview of the 2018 Palu Earthquake. *VII International Conference on Earthquake Geotechnical Engineering*: 857-869. Rome.

Seed, H.B. 1987. Design problems in soil liquefaction. *Journal of Geotechnical Engineering ASCE* 113(8): 827-845.

Seid-Karbasi, M., Byrne, P.M. 2007. Seismic liquefaction, lateral spreading, and flow slides: a numerical investigation into void redistribution. *Canadian Geotechnical Journal* 44(7): 873-890.

Whitman, R.V. 1985. On liquefaction. *Proc 11th International Conference on Soil Mechanics and Foundation Engineering*: 1923-1926.

Trenchless Technologies for Urban Development

Keh-Jian (Albert) Shou
Distinguished Professor, Department of Civil Engineering – National Chung-Hsing University
Vice President (Asia) elected – ISSMGE

ABSTRACT: The demand and the deterioration of municipal underground infrastructures have been increasing the necessity for better, i.e., efficient and economic methods of installation, rehabilitation, and inspection of underground utility pipelines. Taking environmental factors into account, open-cut methods have adverse impacts on the community and business due to traffic disruptions and undesirable pollution. Trenchless technologies used to rehabilitate, including repair, replace, and renovate, newly install underground pipelines with minimum surface disruption offer a feasible alternative to the open-cut methods.

The objective of this paper is to explore the most updated trenchless methodologies for underground pipelines, with discussions on their advantages and disadvantages. Moreover, the adopted typical methods, including the pipejacking installation method and the Cured In Place Pipe (CIPP) rehabilitation method were explored in more details with discussions on their key issues.

Keywords: trenchless technologies, underground infrastructure, pipejacking, CIPP, utility pipelines

Recent Development in Tailings Dam Design in Seismic Active Regions

Hendra Jitno
Rio Tinto Copper
Institut Teknologi Nasional

ABSTRAK: Makalah ini menyajikan gambaran umum tentang berbagai jenis tailing dari segi konsistensi, fasilitas penyimpanan tailing yang sesuai untuk masing tipe tailings, dan desain bendungan tailing yang biasa dipakai saat ini di daerah aktif gempa. Makalah ini juga menyajikan beberapa kasus kegagalan bendungan tailing akibat likuifaksi statis dan seismik dengan tujuan untuk memahami akar penyebab kegagalan tersebut. Makalah ini selanjutnya membahas evolusi kode seismik untuk desain tailing di negara aktif gempa seperti Chili dan Jepang. Relevansi penyebab kegagalan bendungan dengan iklim dan kegempaan Indonesia, dan evolusi kode di kedua negara tersebut akan didiskusikan.

Kata Kunci: tailings dam, static liquefaction, seismic, upstream construction.

ABSTRACT: The paper presents an overview on different types of tailings in terms of consistency, their corresponding suitable storage facilities and the current tailings dam design practice in seismic active region. It also presents several cases of tailings dam failures due to static and seismic liquefaction to understand the root causes of the failures. The paper further discusses the evolution of the seismic codes for tailings design in seismic active region of Chile and Japan. The relevance of the causes of dam failures with the Indonesian climate and seismicity, and the evolution of the codes in those two countries are highlighted.

Keywords: tailings dam, static liquefaction, seismic, upstream construction

1 INTRODUCTION

Tailings is by product of mining process during extraction of valuable metals or minerals from the rock's ores. Tailings are usually defined as crushed rock particles that are either produced or deposited in slurry form. This definition encompasses the vast majority of finely ground mill or mineral processing wastes remaining after extraction of mineral values, Vick (1983).

In the early days of the mining industry, the tailings storage facilities did not receive appropriate attention from the mining operators. Tailings were considered as cost center and they generally thought that it should be discarded at the lowest possible cost. Therefore, only minimum attention and cost were provided to properly design the tailings storage facilities.

With the increase number of tailings dam failures all over the world and their adverse impact on the population and environment, mining operators are more aware on the importance of the proper tailings storage design to ensure the safety of the people and environment downstream of the storage facilities.

In addition to high seismic load, there are some more stringent design criteria that need to be met for design tailings storage facilities in Indonesia. Unlike other seismic active region in other part of the world such as Iran, Turkey, and South American countries which are generally dry with low rainfall rate, Indonesia is also a country with high rainfall rate with up to 4000 mm per year, depending on the locations. Thus, combination of high seismic loads and high precipitation significantly increases the risk of

instability under both static and earthquake loading conditions.

This paper discusses different type of tailing dam design in other seismic active region, provides few case histories of tailings dam failures to understand the root causes of such failures, and discuss evolution of the seismic codes for tailings dam design.

2 CURRENT STATE OF PRACTICE

The optimum design of tailings storage facilities generally depends on the tailings solid content or tailings density (w/w). Fig. 1 shows the relationship between the tailings solid density with tailings yield strength and tailings consistency. As can be seen in Fig. 1, the higher the tailings solid content, the higher the yield strength/consistency and the higher the expected long-term tailings strength. Fig. 1 also shows that conventional tailings storage facilities are suitable for unthickened and thickened slurry tailings with solid density from 15% to about 60%. For tailings solid density higher than 60%, different method of storage can be utilized as seen in the Figure.

2.1 *Conventional Tailings Dam*

The conventional tailings dams are generally constructed using four methods:

1. Water Retaining Dam Construction
2. Downstream Construction Method.
3. Centerline Construction method, and
4. Upstream Construction method.

Characteristics of different construction methods in terms of suitability, requirements, restriction and cost of the above methods are shown in Table 1.

From the four methods mentioned above, the upstream-raised construction method is not recommended to use in a highly active seismic region such as Indonesia. The high rainfall rate also increases its likelihood for failure under seismic loading condition due to potential increase in phreatic levels in the tailings facilities. Other conventional methods are acceptable if all design criteria are met.

2.2 *Thickened Tailings Discharge Method*

For paste tailings with solid content between 60% to 70%, smaller dams can be used to contain the tailings if the steeper beach angle can be achieved during operation. Different deposition plan can also be used such as using centrally discharged tailings deposition. The principal advantages of the method are as follows:

1. Impoundment dams or embankments are largely eliminated, and return-water pumping is reduced.
2. Reclamation of the tailings pile may be simplified by the flatter and more uniformly graded pile slopes.
3. Seepage may be reduced by essentially eliminating the decant pond.
4. There is negligible or very low risk of embankment failure under static loading conditions.

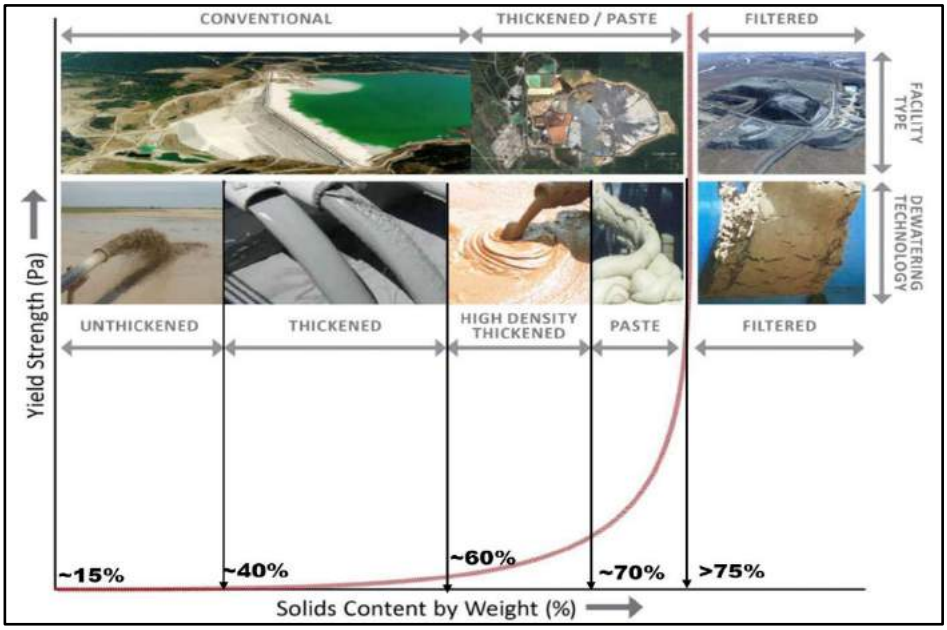

Fig. 1. Range of Tailings Density with Suitable Types of Storage Facilities, Modified from Mend (2017).

Table 1. Comparison of Conventional Tailings Storage Facilities, Vick (1983).

Embankment Type	Mill Tailings Requirements	Discharge Requirements	Water Storage Suitability	Seismic Resistance	Raising Rate Resistance	Embankment Fill Requirements	Relative Embankment Cost
Water retention	Suitable for any type of tailings	Any discharge procedure suitable	Good	Good	Entire embankment constructed initially or in stages	Earthfill, rockfill, (mine waste, filter)	High
Upstream	At least 40-60% sand in whole tailings. Low discharge solids content desirable to promote grain-size segregation	Peripheral spigotted discharge and well controlled beach necessary	Not suitable for significant water storage	Potentially poor in high seismic areas Unless specifically designed for seismic loads	Less than 5 – 10 m/yr most desirable	Natural soil, sand tailings or mine waste	Low
Downstream	Suitable for any type of tailings	Varies according to design details	Good	Good	None. Often built-in stages if rockfill is used	Sand tailings or mine waste if production rates are sufficient, or earthfill, rockfill	High
Centreline	Sand or low-plasticity slimes	Peripheral spigotted discharge of at least nominal beach necessary	Not recommended for permanent storage. Temporary flood storage acceptable with proper design details	Acceptable	Height restrictions for individual raises may apply	Sand tailings or mine waste if production rates are sufficient, or earthfill, rockfill	Moderate

2.3 *Dry-Stack Method*

For tailings with solid content more than 75%, the water contents of the tailing "cake" are generally close to its optimum moisture content and can be placed under dry condition and sometimes it is called "dry-stack". Due to its "dry" condition, the tailings need to be transported to the storage facilities either using conveyor or by trucks. The tailing "cake" can be placed without compaction or compacted just by dozer. However, for the dry-stack structural zone, which is located at the perimeter of the dry-stack, adequate compaction must be carried out to provide sufficient stability of the tailings stack.

Some of the benefits of this method are as follows:

1. Suitable at the sites where water is expensive.
2. Reduce footprint.
3. Eliminate groundwater contamination.
4. Progressive rehabilitation.
5. High seismic stability.

However, there are some remaining considerable challenges of this technology which includes:

1. The capex and opex are very high.
2. Factors such as ore grind and gypsum content affect the efficiency of the filtration process.
3. For some ores of high clay content, the process may not work at all.

Despite these challenges, this technology has gained more acceptance in the mining industry as one of the preferable methods for tailings management in seismic active regions. To the author knowledge, at least there are currently three mine sites in Indonesia are in the process to adopt this technology.

3 STATIC AND CYCLIC LIQUEFACTION

Liquefaction is a process by which sediments below the water table temporarily lose strength and behave as a viscous liquid rather than a solid. Liquefaction has generally been considered to occur due to earthquake shaking. The procedures to predict liquefaction are developed for seismic-induced liquefaction such as those discussed in Youd et al. (2001), Robertson and Wride (1998). However, liquefaction can also occur under static loading condition due to combination of many factors including brittle soil behaviour, increase in phreatic levels, and creep movement due to high stresses.

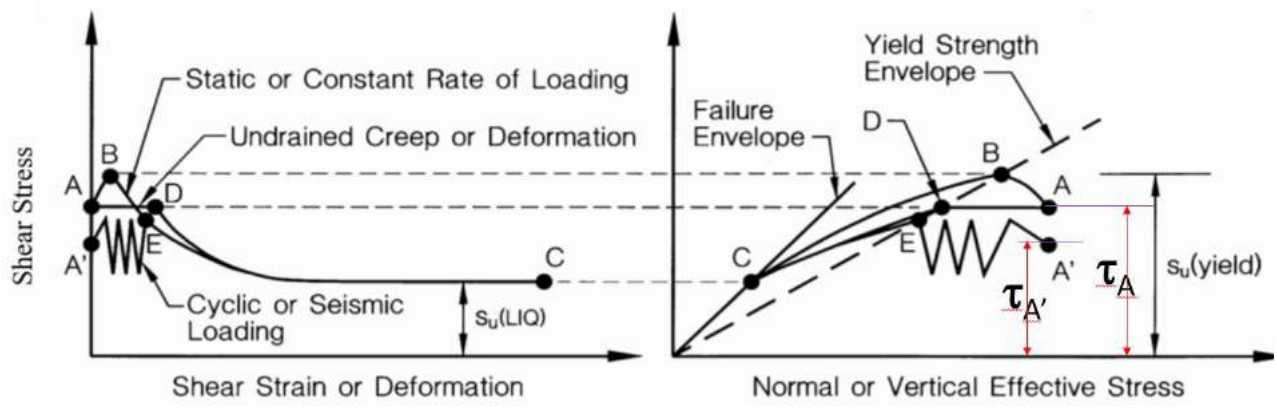

Fig.2. Mechanism of Static and Cyclic Liquefaction (a) Shear Stress Versus Strain, (b) Effective Stress Path.

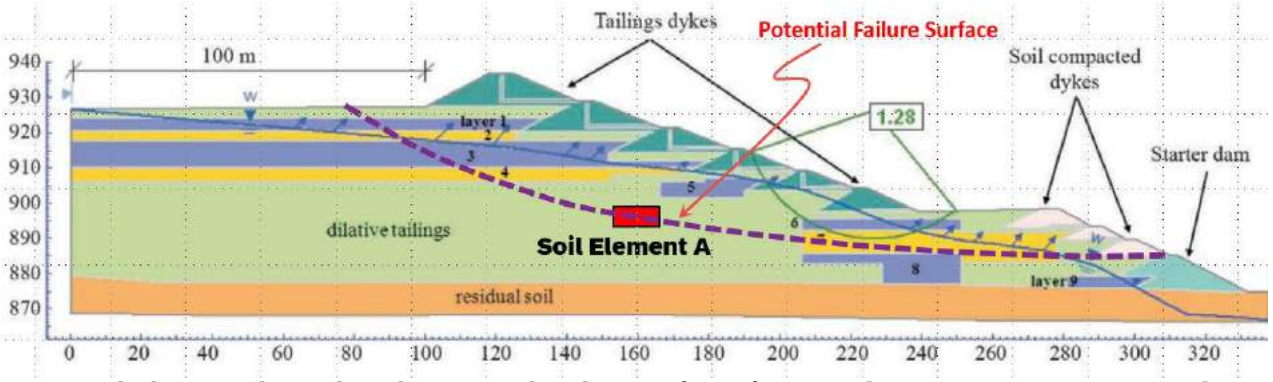

Fig.3. Soil Element a located at The Potential Failure Surface of a Typical Upstream Construction Tailings Dam.

In general, there are two types of liquefactions:

1. Flow Liquefaction:
   This occurs when the static driving stress is higher than the post-liquefaction strength of the soils. Flow liquefaction due to static loading is called Static Liquefaction.
2. Cyclic Mobility:
   Occurs when the static shear stress is smaller than the shear strength of the liquefied soil. In this case, incremental deformations are caused by both cyclic and static shear stresses.

Fig.2 depicts the mechanism of liquefaction under both static and cyclic loadings for a soil element A located under embankment shown in Fig.3. Fig.2a. shows the shear stress change with increasing strains under both static and seismic loadings for a soil susceptible to liquefaction or strain softening. Fig. 2b. illustrates the effective stress path for this soil element. Yield strength envelope is the line when the soil element starts to yield, reduces its strength and rapidly develop large deformation. This envelope is also called Flow Liquefaction Surface (FLS) and first proposed by Vaid and Chern (1985).

For example, Point A in this figure depicts the initial static shear stress (τ_A) of soil element **A** in the tailings dam, as shown in Fig. 3. Point C is the static condition after the failure and the soil reaches residual strength, $S_{u(LIQ)}$. The factor of safety at point A is given by:

$$FS = S_{u\,(yield)} / \tau_A \qquad (1)$$

If the shear stress at point A is increased due to any additional static load (eg. additional fill) and occurs under undrained condition, the stress at point A will move to point B (due to pore pressure increase) located at yield strength envelope. When the shear stress reaches point B, the factor of safety of the system becomes 1.0 (driving stress, τ_A = yield strength, $S_{u\,(yield)}$) and the tailings dam system starts to yield. In terms of deformation, the system starts to experience large plastic deformation and eventually reaches its residual strength at point C, as shown in the Figure 2a.

If there is an increase in phreatic levels due to rainfall or wetting related to tailings deposition without significant change in the static shear stress, then point A will move to point D (reduction in effective stress) and reaches yield strength envelope under constant static shear stress. Similarly, when it reaches yield envelope, large deformation will occur until it reaches its residual strength at point C. When this happens, the tailings will experience flow failure due to static liquefaction. When designing tailings dams, the design engineer must ensure that the stability requirements against static and seismic liquefaction failures must be met. Unfortunately, due to combination of many factors, this mechanism has happened in the previous tailings dam case histories in the last few decades.

4 RECENT TAILINGS DAM FAILURES

For the last 120 years, at least 170 conventional tailings dams have failed due to many different causes. The data does not include the unrecorded tailings failures which were not reported due to many different reasons. The statistics of these failures have been plotted in Fig. 4.

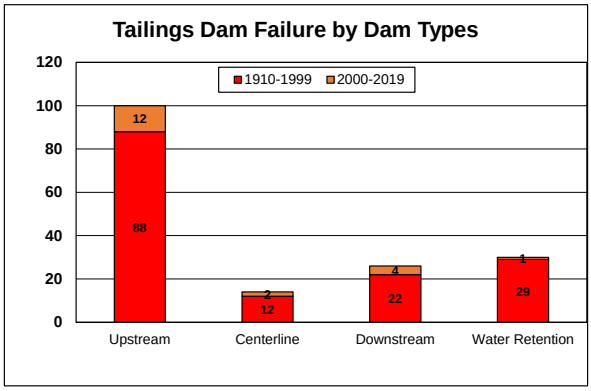

Fig. 4. Tailings Dam Failures by Types of Dam Construction Method, Data from Lyu et al. (2019).

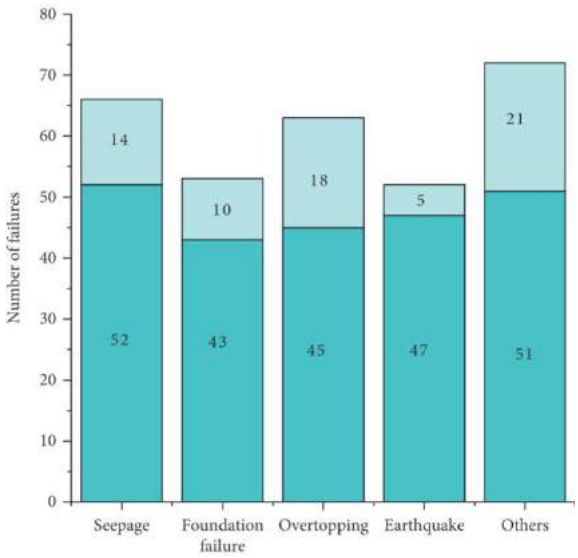

Fig 5. Tailings Dam Failures by Causes, Lyu et al. (2019).

Due to inherent marginal stability, one hundred of these failures occurred on the upstream-raised tailings dams, or almost one failure per year for the last 120 years.

The main causes of failures on these dams are shown in Fig. 5, which are seepage related problems, foundation bearing capacity failure, overtopping, earthquake loadings and others.

The majority of the upstream tailings dam failure are due to instability issues, either related to the properties of the tailings, poor water management, or high rainfall rate leading to high phreatic levels within the tailings. Examples of tailings dam failures due to static loading are Feijao (Brumadinho) and Fundao tailings dams in Brazil. Examples of failures due to seismic loading are El-Cobre, Barahona in Chile and Mochikoshi and Kayakari tailings dam in Japan.

The causes of downstream or centerline construction tailings dam failures are mainly due to bearing capacity failure. The root cause of the failures includes lack of understanding of the foundation soils due to limited data or insufficient understanding on the soil mechanics principles. Example of tailings dam failure due to inadequate foundation bearing capacity are Aznalcollar (Spain), Cadia (Australia) and Mt Polley (Canada) tailing dams.

4.1 *Feijao Tailings Dam Failure*

The most recent catastrophic tailings dam failure is the Feijao tailings dam, located in the municipality of Brumadinho, about 300km

north of Rio de Janeiro, Brazil. The dam failed at approximately 12:28 p.m. local time on January 25, 2019 due to static liquefaction. The dam released a mudflow that rapidly traveled through the mine's canteen and offices, as well as houses, farms, inns, bridges, and roads downstream, reaching the Paraopeba River. The failure caused a mud wave up to a height of about 30 m, which first washed up the downstream face of the adjacent Dam VI, then swept through the canteen and office complex downstream before coming to a stop in the Paraopeba River on the edge of Brumadinho border. The dam failure was captured by a camera and is shown in Fig.6.

Some of the contributing factors for the failure are:

1. the brittle behaviour of the iron-ore tailings and,
2. the increase of phreatic levels due to rain fall few months prior to failure.

The mechanism of failure can be explained by looking soil element A in Fig. 3, which experience effective stress reduction from point A to D at relatively constant static shear stress. It starts to experience loss of strength when it reaches point D at the yield envelope and then rapidly develop large deformation which lead to catastrophic failure.

Fig. 6. Failure of the Feijao Tailings Dam due to Static Liquefaction in 2019, Robertson et al. (2019).

Fig. 7. Failure of the Fundao Tailings Dam due to Static Liquefaction in 2015, Morgenstern et al. (2016).

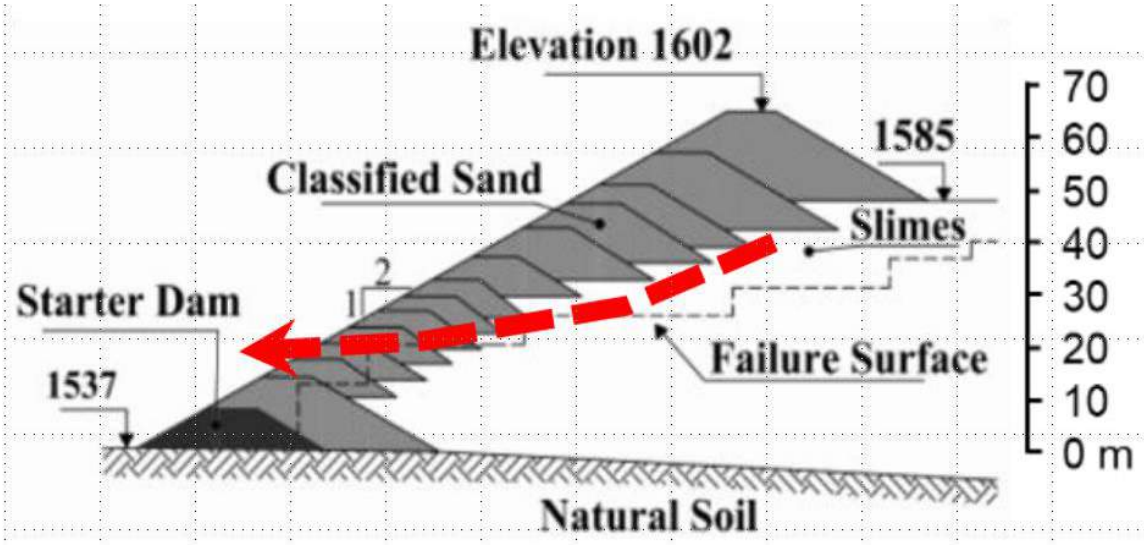

Fig. 8. Pre and Post-Failure Geometry (Black Dashed Line) of the Barahona Tailings Dam due to Earthquake-Induced Liquefaction, Troncosso et al. (1993). Red-Dashed Line Indicates the Direction of Flow Failure.

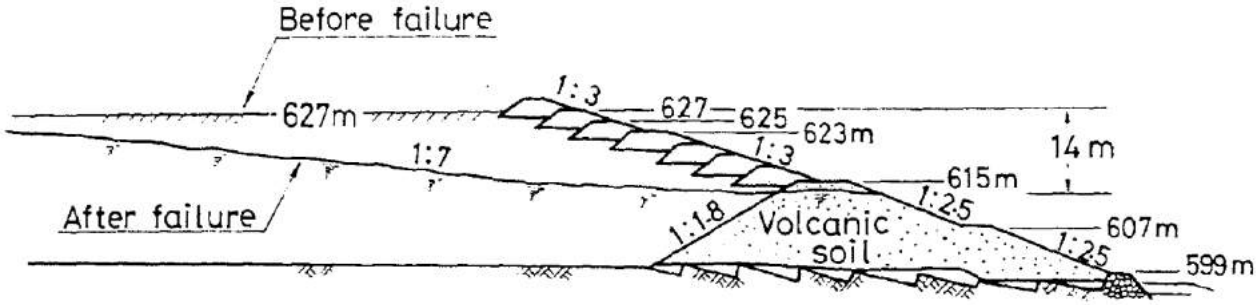

Fig. 9. Cross Section of Mochikoshi Tailings Dam No 1 Before and After the Failure, Ishihara (1984).

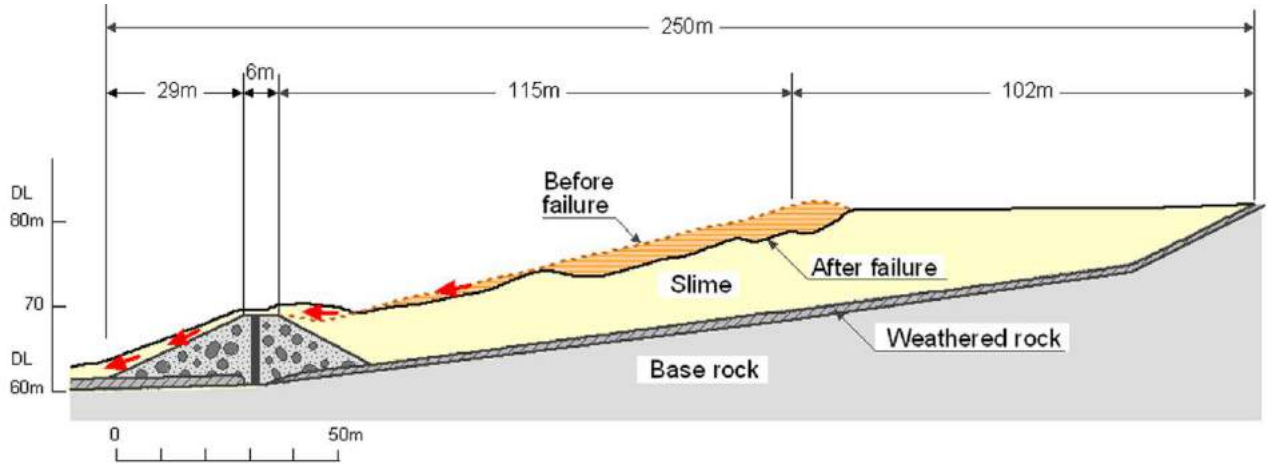

Fig. 10. Cross Section of Kayakari Tailings at Ohya Mine Before and After the Failure, Ishihara (2015).

4.2 *Fundao Tailings Dam Failure*

The 110m high Fundão Tailings Dam failed at about 3:45 pm local time on 5 November 2015 also due to static flow liquefaction. Similar to Feijao tailings dam, Fundao tailings dam is also raised using upstream construction method. The cause of the dam failure is combination of many contributing factors as follows, Morgenstern et al. (2016):

1. A change in design which caused an increase in saturation due to new drains, which eventually introduced the potential for liquefaction.
2. A reduction in lateral confining stress due to lateral extrusion of the slimes within the tailings and pulling apart of the sands as the embankment height increased. This mechanism has caused the soil elements in the tailings to move to the yield envelope.
3. Due to brittle behaviour of the tailings, once the yield envelope is reached, deformation develop very rapidly which lead to catastrophic failure.
4. Due to series of small shocks occurred about 90 minutes prior to the failure which cause small deformation which initiate the failure.

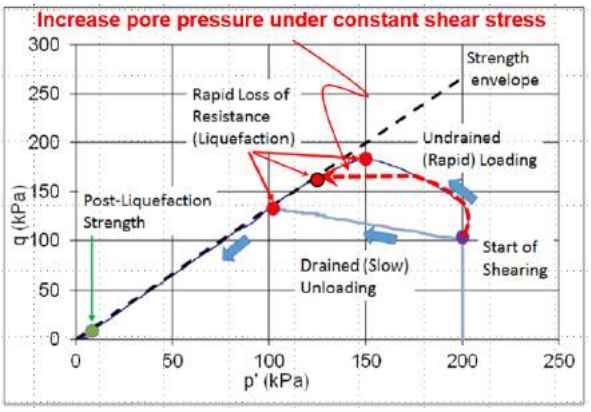

Fig. 11. Stress paths for undrained and drained loading of sand from Fundao tailings dam (modified from Morgenstern et al, 2016).

The failure can be explained in similar way to that for Feijao tailings dam. The results of lab test on sand sample from the site is shown in Fig. 11 under rapid loading and slow unloading. Both loads result in the failure of the sample due to static liquefaction when the sample reach the failure envelope.

As results of this failure, the Brazilian regulatory body now prohibit the use of upstream construction method in 2019.

4.3 *Barahona and El-Cobre Tailings Dam Failure*

Barahona tailings dam failed on 1st December 1928, when a M_L 8.2 earthquake struck the central zone of Chile. As can be seen in Fig. 8, Barahona is an upstream-raised tailings dam. Despite it is relatively far or about 180 km away from the epicenter, the dam failed due to liquefaction of the tailing slimes (fine fraction) under the embankment. The embankment was constructed from cyclone sands obtained from coarse portion of the tailings. The collapse of the dam resulted in flow liquefaction which destroyed towns and villages located downstream and killed 54 people.

This is the first case of failure due to liquefaction, which at that time, was not well understood. The failure of Barahona tailings dam did not change the practice of tailings dam construction in Chile as many more dams were constructed using upstream construction method after the failure. Many more tailings dam failure still occurred many more years after that due to earthquakes.

One notable failure event is El-Cobre tailings dam which failed in 1965 also due to liquefaction during the M7.4 earthquake in central Chile with epicenter only about 40km from the dam site. The failure caused more than 200 people dead, and widespread contamination of an agricultural valley.

4.4 *Mochikoshi Tailings Dam Failure*

The failure of Mochikoshi tailings dam No.1 was due to liquefaction triggered by the main shock of the M7.0 Izu-Ohshima-Kinkai earthquake on 14 January 1978, Ishihara (1984). The epicenter of the earthquake was located about 40km from the site. The 28-m high dike and 73 m wide at crest level collapsed almost at the same time during the main shaking of the earthquake. According to the guardian who witnessed the failure, within a matter of 10 seconds after the main shock, the front wall of the dike swelled, and the breach took place at the upper part in proximity to the left abutment. This was followed by a huge mass of slime rushing down the valley causing significant environmental damage.

The tailings flowed down the Mochikoshi river and deposited in the riverbed to a thickness of 1.0 to 1.9 m through the distance of about 800 m from the point of con-fluence. The flowing slime further travelled into the

Kano River and contaminated the river through a distance of about 10 km down to the mouth of the river.

4.5 *Kayakari Tailings Dam Failure*

On 11 March 2011, liquefaction occurred in the tailings deposit at Kayakari dam due to the strong shaking of the M_w 9 Tohoku earthquake which led to the breach of the dam. The tailings covering the area 100 m - 120 m with a depth of about 5 m flowed down the valley for about 2 km from the site. The peak ground acceleration at the site was about 0.3g and the duration was about 120 seconds.

The tailings dam has been closed since 1966 and the dam seismic stability has been verified in 1974 and 1981 and confirmed that the factors of safety under seismic loading was 1.38 (1974) and 1.28 (1981). The factors of safety against liquefaction were computed to be 1.8 to 3.4. Despite adequate seismic stability according to the code, the dam liquefied and failed due to 0.3g ground acceleration from the earthquake. This failure triggers the evaluation of the tailings design code applicable at that time.

5 RECENT TREND IN TAILINGS DAM DESIGN IN SEISMIC ACTIVE REGION

Based on the previous discussions, the main cause of tailings dam failure in seismic active region is liquefaction under seismic shaking. The liquefaction occurs if the sand is saturated, and the seismic load is high enough to reach the yield envelope as discussed previously. If these two conditions are not met, liquefaction will not occur.

Below is the evolution of the seismic design code for tailings dam design in Chile and Japan with time, in an effort to reduce the number of tailings dam failure in those countries.

5.1 *Chile*

As results of many tailings dam failure during the 1965 M_L7.5 earthquake, the government changed the seismic design code by discouraging the use of upstream-raised construction method in 1970, although not strictly prohibit it. Among other requirements from the Chilean Supreme Decree No. 86 of 1970 are as follows, Barrera et al. (2011):

1. The upstream method in general is not allowed. It can only be approved by special resolution.
2. A minimum construction density is required for the sand.
3. Prevent saturation of the sand by providing a base drainage system, permeable sand, to control the piezometric levels in the dam.
4. Management of the tailings pond far from the dam and with an appropriate freeboard.
5. A minimum factor of safety of 1.20 is established for the pseudo-static analysis that considers a seismic coefficient determined based on the population located downstream of the impoundment and within something called the dangerous distance.
6. It is recommended to construct the tailings dam using the borrow materials from outside the tailings dam, and not using the cyclone sand processed from the tailings.

With additional liquefaction-induced upstream tailings dam failures after this decree was implemented, this decree was replaced on 29 December 2006 by Supreme Decree No. 248 to prevent more failure, Barrera et al. (2011). Among other important points are:

1. The upstream method is now strictly prohibited.
2. Downstream and centerline construction methods are allowed.
3. Geotechnical design parameters associated with tailings sands to be used for the construction of the retaining dyke are to be
4. defined (including shear strength, compressibility, permeability, grain size, unit weight, specific gravity, and plasticity).
5. A freeboard (>2 m) and crest width (>1 m) must be ensured.
6. The retaining dyke must have an underlying drainage system to ensure that saturation is prevented.

5.2 *Japan*

Yasuda et al. (2017) reported the evolution of seismic design of tailings dams in Japan. Japan developed the first code for the tailings dam and waste soils in 1954 and revised the code in 1973 to include drainage facilities.

After the Mochikoshi tailings dam in 1978, Japan started to study the behaviour of tailings under cyclic loading led by Prof Ishihara at the University of Tokyo. Many cyclic triaxial tests and seismic response analyses were conducted

by Ishihara et al. (1981). Based on this work, the code was revised in 1980 to include the effect of liquefaction on the relevant structures. However, the code still adopts pseudo-static analysis to assess the seismic stability of the tailings dam. Reduction of tailings strength due to pore pressure increase caused by earthquake loading is incorporated in the analysis.

Following the 2011 M_w9 Tohoku earthquake which caused extensive damage in a wide area, the Japanese authority revised the seismic design code requirements for tailings dams. The new code requires the tailings dam to be designed to withstand Level 2 earthquake motion, which is extremely strong and have very low annual exceedance probability. Level 2 earthquake is similar to the Design Basis Earthquake with 10% chance probability of exceedance in 50 years, Becker et al. (2010). In Japan, the peak ground acceleration for Level 2 may exceed 1.0g.

5.3 *Indonesia*

With government regulation in prohibiting the export of raw materials from January 2014, many more mine companies process the ore in the country. As results, many more processing plants were constructed and therefore many more new tailings dams are in the process of getting the design and construction permit from the Indonesian regulatory body for tailings dam.

In Indonesia, in addition to high seismic region, the country has also high rainfall rate which may cause high phreatic level and high saturation zones within the tailings embankment. Therefore, the potential dam failure due to liquefaction in Indonesia are much higher than those in Chile (seismic active, but dry) or Brazil (high rainfall but not seismic active). The challenges do not stop there, as Indonesia has also many problematic soils such as clay-shale, expansive soils, peat and soft clay which provide different levels of challenges for designing stable tailings dams. Because of this, for example, some of the mining companies prefers to use different approach to manage their tailings such as deep-sea tailings disposal (Batu Hijau), or riverine tailings disposal (Grasberg), with their own challenges.

At the moment, there is no specific design code available for tailings dam design in Indonesia. Tailings dam design in Indonesia currently follows acceptable international standards such as ANCOLD, ICOLD and GISTM, which is newly introduced by ICMM and UNEP.

Most of the tailings dam currently built in Indonesia were designed using downstream construction method, which is more expensive, but it is much safer. The use of upstream construction method, while it is tempting due to low cost, it will pose very high risk of failure due to combination of high rainfall rate and high seismic loads.

6 SUMMARY AND CONCLUSIONS

This paper provided an overview on different types of tailings in terms of consistency, their corresponding suitable tailings storage facilities and the current tailings dam design in seismic active region. The slurry type tailings are usually stored using conventional tailings dam design, which uses downstream, centreline and upstream construction method.

Two cases of tailings dam failures in Brazil have been discussed. The root cause of the failure for both Feijao and Fundao tailings dam is static liquefaction due to high phreatic levels and the brittle behavior of the tailings. Several cases of dam failures due to seismic liquefaction have also been presented. The cause of the failures is liquefaction related to high phreatic levels and the levels of seismic shaking. All tailings dam failures above were constructed using upstream construction method. The method is prohibited in Chile since 2006 and no longer use in Japan as well.

Due to high rainfall rate and high seismicity in Indonesia, the use of upstream-raised tailings dam is very risky and has high probability of failure and therefore it is highly not recommended. The use of centreline and downstream construction method is acceptable if all design criteria are satisfied. The use of dry-stack method using tailings filtration technology is preferable if it is not costly prohibitive.

REFERENCES

ANCOLD. 2019. Guidelines on Tailings Dams – Planning, Design, Construction, Operation and Closure.

Barrera, S., Valenzuela, L., and Campaña, J. 2011. Sand Tailings Dams: Design, Construction, and Operation. *In Proceedings of Tailings and Mine Waste*. Vancouver, B.C.

Becker, T.C., Furukawa, S. Mahin, S.A and Nakashima, M. 2010. Comparison of US and Japanese Codes and Practices for Seismically Isolated Buildings. *Structures Congress*.

Dobry, R.; Alvarez, L. 1967. Seismic Failures of Chilean Tailings Dams. *J. Soil Mech. Found*. Div., 93: 237–260.

GISTM. 2020. Global Industry Standard on Tailings Management. UNEP-ICMM.

ICOLD – International Committee on Large Dams.

Ishihara, K. 1984. Post-Earthquake Failure of a Tailings Dam Due to Liquefaction of Pond Deposit. *1st International Conf. on Case Histories in Geotechnical Engineering*.

Ishihara, K, Yasuda, S and Yokota, K. 1981. Cyclic Strength of Undisturbed Mine Tailings. *Proc. International Conference on Recent Advances in Geotechnical Earthquake Engineering and Soil Dynamics* 1: 53-58.

Morgenstern N, Vick SG, Viotti CB, Watts BD. 2016. *Report on the Immediate Causes of the Failure of the Funda˜o Dam*. New York: Gottlieb Steen and Hamilton LLP.

Olson, S.M. and Stark, T.D. 2003. Yield Strength Ratio and Liquefaction Analysis of Slopes and Embankments. *Journal of Geotechnical and Geoenvironmental Engineering* Vol. 129, No. 8.

Robertson, P.K, de Melo,L, Williams, D.J and Wilson, G. Ward. 2019. *Report of the Expert Panel on the Technical Causes of the Failure of Feijão Dam I*.

Troncoso, J.H.; Avendaño, A.; Vergara, A. 1993. The Seismic Failure of Barahona Tailings Dam. *In Proceedings of the Third International Conference on Case Histories in Geotechnical Engineering* Paper No. 2.56: 1473–1479. St. Louis, MO, USA.

Vaid, Y. P. and Chern, J. C. 1985. Cyclic and Monotonic Undrained Response of Saturated Sands. *Proc. Advances in the Art of Testing Soils under Cyclic Conditions* ASCE Covention: 120 - 147. Detroit, Mich.

Vick, S.G. 1983. *Planning, Design, and Analysis of Tailings Dams.* New York: Wiley.

Yasuda, S, Fukui, K,Kunimatsu, D,Okamura, M, Kiyota, T, Koguchi, K. 2017. Revised Seismic Design Code for Tailings Dam and its Application to Existing Dam. *16th World Conference on Earthquake* 16 WCEE.

Youd, T.L., I.M. Idriss, R.D. Andrus, I. Arango, G. Castro, J.T. Christian, R. Dobry, W.D.L. Finn, L.F. Harder, M.E. Hynes, K. Ishihara, J.P. Koester, S.C.C. Liao, W.F. Marcuson, III., G.R. Martin, J.K. Mitchell, Y. Moriwaki, M.S. Power, P.K. Robertson, R.B. Seed, and K.H. Stokoe, II. 2001. Liquefaction Resistance of Soils. Summary report from the 1996 NCEER and 1998 NCEER/NSF. Workshops on Evaluation of Liquefaction Resistance of Soils. *Journal of Geotechnical and Geoenvironmental Engineering* 127:817–833.

Zongjie Lyu, Junrui Chai,Zengguang Xu,Yuan Qin, and Jing Cao. 2019. A Comprehensive Review on Reasons for Tailings Dam Failures Based on Case History. *Hindawi Advances in Civil Engineering* Volume 2019, Article ID 4159306, 18 pages https://doi.org/10.1155/2019/4159306.

Biopolymer-based Soil Treatment (BPST): a Bio-Geotechnical Implementation for Sustainable Development

Ilhan Chang
Associate Professor, Department of Civil Systems Engineering – Ajou University

ABSTRACT: The current climate change and accompanying natural hazards increase are increasing the socio-economic demands for safe and sustainable construction materials and their implementation. Worldwide sustainable development strategy has promoted various material and methodology developments in civil and construction engineering. Among others, the use of microbial biopolymers in the geotechnical engineering field has gained attention due to its competitive soil strength improvement and low carbon footprint characteristics. Biopolymer-based soil treatment (BPST) has been considered to be a new construction and building material for eco-friendly and sustainable development in recent years. BPST shows sufficient engineering performances in terms of soil strengthening, hydraulic conductivity control, erosion mitigation, vegetation growth promotion, and durability. This keynote provides a state-of-the-art overview of BPST technology including the geotechnical engineering behavior induced by BPST and the possible in-situ implementation forms of BPST for sustainable construction and development.

Keywords: biopolymer, soil, ground improvement, erosion, climate change, sustainability

Promoting Widespread Application of Seismic Ground Motion for Evaluation and Retrofit of Existing Buildings in Indonesia

Nick Alexander
Bandung Institute of Technology

Masyhur Irsyam
Bandung Institute of Technology

ABSTRACT: Situated in a high seismically active region, major cities in Indonesia are at risk of experiencing damaging earthquake events from various earthquake source mechanisms. The authors are currently involved in development of Indonesian code for seismic evaluation and retrofitting for existing building, which will mainly be adopting the widely accepted ASCE 41-17 standard. Referring to this standard, ground motion input for analysis will be required for performance-based evaluation of majority of existing buildings. Heavy reliance on local experts to manage all these cases is not realistic and may impede the effort of promoting seismic safety through evaluation and retrofitting of existing buildings. Thus, it will be of great use to develop a strategic tool that can facilitate proper widespread use of relevant ground motion time series for structural evaluation and retrofitting of majority of existing buildings. This system will serve as a valuable tool in supporting practical implementation of this national code.

Keywords: earthquake ground motion, time history analysis, seismic evaluation and retrofit of existing buildings

1 INTRODUCTION

Situated in a high seismically active region, major cities in Indonesia are at risk of experiencing damaging earthquake events from various earthquake source mechanisms (Fig. 1). Referring to the Indonesian seismic code, for the design of most new buildings, the availability of national seismic risk maps already facilitates the widespread use of linear response spectrum procedure without the need for earthquake ground motion as analysis input. Ground motion time series is required for performance-based approach, mandatory for design of a very small percentage of new buildings, specifically those with non-prescriptive system, base isolation, or damping system.

For these few cases, development of ground motion input can still be managed by knowledgeable local experts. The authors are currently involved in development of Indonesian code for seismic evaluation and retrofitting for existing building, which will mainly be adopting the widely accepted ASCE 41-17 standard. Referring to this standard, ground motion input for analysis will be required for performance-based evaluation of majority of existing buildings. Heavy reliance on local experts to manage all these cases is not realistic and may impede the effort of promoting seismic safety through evaluation and retrofitting of existing buildings. On the other hand, expecting practicing engineers to suddenly grasp such in-depth and highly specialized knowledge is also not realistic and can lead to improper application of the procedure practiced throughout the country.

Thus, it will be of great use to develop a strategic tool that can facilitate proper widespread use of relevant ground motion time series for practical engineering application in Indonesia, particularly for structural evaluation and retrofitting of majority of existing buildings. This system will serve as a valuable tool in supporting practical implementation of this national code.

2 CURRENT GMSM PRACTICE

2.1 *Code Requirements*

The currently developed Indonesian code for seismic evaluation and retrofitting of existing buildings will be adopting the ASCE 41-17 standards, which refers to the ASCE 7-16 requirements chapter 16 for requirements on ground motion selection and modification (GMSM) procedure. As a matter of convenience, the ASCE 7-16 seismic design provisions have also been adopted in the SNI 1726: 2019. This means that the framework for implementing GMSM procedure in Indonesia is already in place through SNI 1726: 2019.

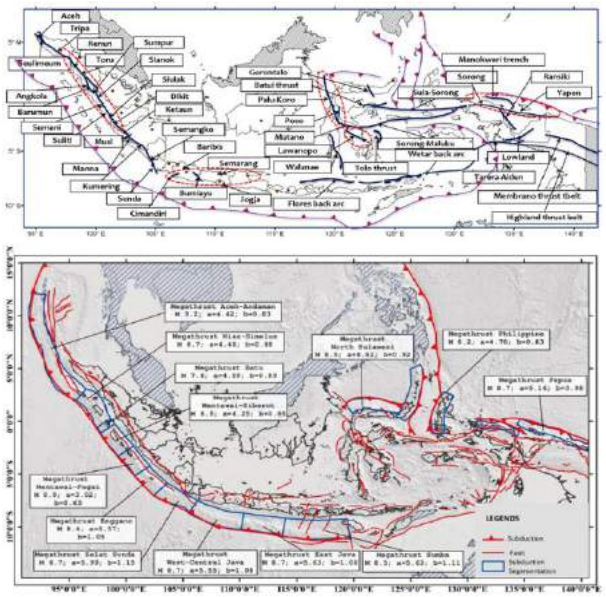

Fig. 1. Identified Earthquake Sources for Crustal Zone (Top) and Subduction Zone (Bottom) in Indonesia, Irsyam et al. (2017).

Referring to SNI 1726: 2019, the standard GMSM procedure starts with the development of one target spectrum or multiple target spectra, then followed by selection of seed ground motions from real earthquake recordings and modification of the seed motion time series to match the target spectrum within the period range that corresponds with significant dynamic response of the structure of interest.

The requirements for GMSM procedure in the latest standards are already well established, clearly stipulated, and much more specific compared with the previous version. However, several clauses can still be subject to multiple interpretations, particularly for practitioners without strong knowledge on earthquake engineering and structural dynamics. Currently, dissemination of knowledge in earthquake engineering field in Indonesia is still a work in progress with the goal of improving overall engineering practice in Indonesia. Until this goal is achieved, there is risk of improper application of the GMSM procedure unless an interventive and strategic tool is established to assist proper implementation of GMSM during the transition process.

2.2 *Target Spectrum*

The code permits the use of single Uniform Risk Spectrum (URS) response spectrum or multiple Conditional Mean Spectra (CMS). It is well-known that there is conservatism inherent in analysis using URS as a target for GMSM. This is one of the reasons the code provides the alternative use of CMS.

For practice in the US, development of CMS can be obtained using publicly available online hazard tools. However, in Indonesia this tool is not yet available and in the meantime development of CMS as target spectrum for GMSM can only be facilitated by a handful of knowledgeable experts. The use of multiple CMS as target also means multifold analysis effort - leading to significant increase in analysis time, which can cause issue if computing resources is limited.

Regardless, the URS code spectrum that can be generated using mapped spectral acceleration values at period of 0.2 and 1 second has been widely used by practitioners throughout Indonesia. Thus, development of target spectrum is not an issue for proper implementation of GMSM procedure in Indonesia.

2.3 *Modification of Ground Motion Time Series*

When seed ground motions for a suite have been selected, the code permits the use of amplitude scaling and spectral matching to modify the ground motion time series such that the average of the response amplitudes for the suite can resemble the target spectrum for the period range of interest.

Amplitude scaling consists of applying a single scaling factor to the pair of ground motion time series while spectral matching consists of modifying the frequency content of the time series. Various spectral matching technique have been developed and can be used to achieve compliance with code requirements.

Amplitude scaling is a much straight forward method compared to spectral matching. Ideally, spectral matching should be conducted with proper validation steps to ensure that the modified time series could still preserve important nonstationary characteristics inherent to the original ground motion time series, which requires understanding on characteristics of real ground motion records.

For the general GMSM practice in Indonesia, the use of amplitude scaling method is much more practical and will pose much less risk of inappropriate implementation of ground motion modification technique. Spectral matching is recommended to be used only for cases where amplitude scaling cannot result in reasonable suite of ground motions.

2.4 *Selection of Seed Ground Motion*

Among various main aspects of GMSM procedure, selection of the seed ground motion is one aspect that is most prone to misconduct when applied. This situation is particularly true for engineering practice in Indonesia where multi-source earthquake mechanism contributes to seismic hazard and where dissemination of earthquake engineering knowledge is still in progress. Presence of multi-source earthquake mechanism means that a practitioner will need to search ground motion data from more than one regional database, further complicating the selection process.

Selection of seed ground motions typically occurs in two steps. The first step is to initially screen ground motion candidates on the basis of tectonic regime, magnitude, distance, which can be determined based on disaggregation of probabilistic seismic hazard analysis (PSHA) and site soil conditions. Other important selection criteria for initial screening that are often overlooked are useable frequency and sampling frequency, which are properties closely related to structural dynamic characteristics. Once ground motion candidates have been selected, the next step is to finalize the selection process using spectral shape within period range of interest as a primary consideration. It is also preferrable to impose limit on scale factor and maximum motions obtained from a single event.

Based on the applicable selection criteria, it is clear that GMSM procedure is a multi-disciplinary effort requiring proper understanding on specialized subjects in the field of seismology, geotechnical earthquake engineering, and structural dynamics. Unfortunately, the common misconception in Indonesian practice is that selection of ground motion for analysis input is independent of knowledge on the structural dynamic properties of the building under evaluation.

2.5 *Current Database Availability and Condition*

Worldwide strong motion time series can be retrieved from various data source networks including but not limited to CESMD, COSMOS, K-NET, KIK-NET, JMA and PARI. Pacific Earthquake Engineering Research (PEER) Center has developed several ground motion database compiling metadata that contains useful information that can facilitate selection of ground motions. PEER database that are relevant for engineering practice in Indonesia are NGA-West2, which consists of more than 20,000 ground motion data from active shallow crustal zone and NGA-Sub, which consists of more than 60,000 ground motion data from subduction regions (Fig. 2).

NGA-West2 database are already equipped with an online digital ground motion library, containing processed acceleration time series suitable for use by engineering practitioners that can be chosen based on various relevant selection criteria. For engineering application in Indonesia, ground motion data from subduction zones are also important since subduction earthquakes contribute significantly to seismic hazards in cities in Indonesia.

Therefore, the NGA-Sub database serves an important role. Unfortunately, even though useful metadata for subduction zone earthquakes are available in the NGA-Sub database, currently accelerogram time series for subduction zones are still scattered in various data source network in unprocessed format - making them not readily usable for engineering application, particularly for dynamic time history analysis purposes. The procedure to process accelerograms is well-known to be very time-consuming and requires specialized knowledge in signal-processing, which is not commonly practiced by engineering offices in Indonesia.

Assessment of the current ground motion database condition shows that one of the main contributing factors that hinders proper and wide-spread implementation of GMSM in Indonesia is the unavailability of processed

ground motion time series from subduction zones. Another factor is the unavailability of metadata that can represent spectral shape for each record of ground motion horizontal component pair that is consistent with the maximum direction ground motion as defined by the code. In order to facilitate enforcement of existing building retrofitting code in Indonesia, it is of high strategic value to develop a database with organized relevant ground motion data, specifically intended for practical engineering application.

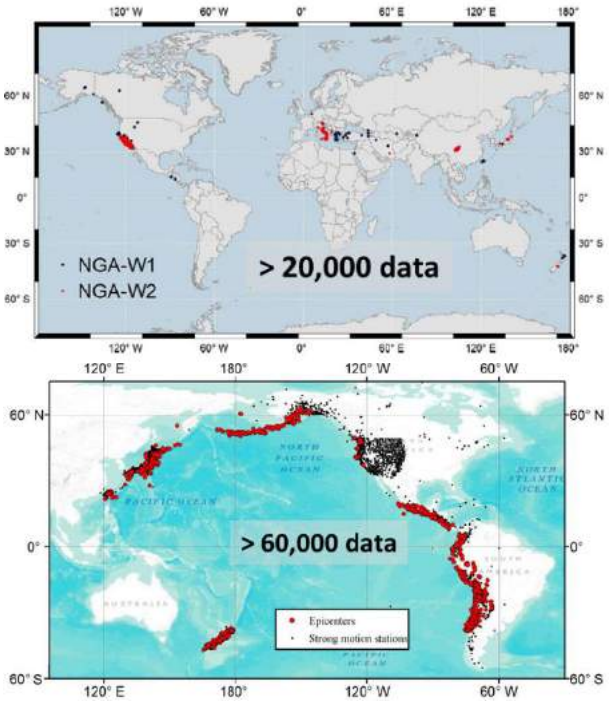

Fig. 2. Distribution of Earthquake Epicenters Included in NGA-West2 Database (Top) and NGA-Sub (Bottom) (PEER Center).

3 GROUND MOTION DATABASE FOR ENGINEERING APPLICATION

3.1 *Advantage and Strategic Role*

With a total of more than 80,000 ground motion data worldwide, NGA-West2 and NGA-Sub database are actively being used for research and engineering applications. These databases also contain information that are significantly useful for ground motion initial screening purposes. While the value of these database are recognized, the majority of data are actually not relevant for the purpose of engineering practice in Indonesia. Reducing the size of the data to include only ground motion data that are relevant will bring advantage from a practicality point of view and it will reduce the likelihood of inappropriate data being selected. The database must be reasonably sized to account a variety of design conditions.

If such database is equipped with similar capability as the NGA-West2 online tool, a strategic system that can facilitate wide-spread and practical application of GMSM will be in place. Implementation of such system will have some limitations valid for specific design conditions that best be undertaken by local experts. Examples where use of such system may no longer be effective include the use of CMS as target, spectral matching, and near-fault sites where pulse characteristics can have significant impact to response. Regardless, this system can be strategically implemented for the majority of seismic retrofit needs, encompassing various period range of buildings with various site soil conditions and various seismic hazard levels (Fig. 3).

It is also apparent that such system has inherently sustainable characteristics in its design. This system will have no difficulties in accommodating continual updates of the national seismic risk map. More ground motion data from next occurrences of large earthquakes can be added to expand the database as they become available. Ground motion data from earthquake events within Indonesia region can also be included when they become available.

3.2 *Organization and Data Processing*

Reduction of the ground motion database can be achieved by applying data filters on the basis of several parameters specifically accustomed to seismicity condition of cities throughout Indonesia combined with consideration on common structural dynamic characteristic range of buildings relevant to engineering practice.

Several examples excluding ground motion data with earthquake magnitude less than M_w6.0, source-to-site distance outside a certain range considering applicable conditions to cities in Indonesia, and representative site soil conditions to cities in Indonesia. It can also be considered to exclude ground motion data with maximum lowest usable frequency value in which use is outside common structural frequency range in engineering practice.

Although all ground motion data from the active crustal region contain accessible processed ground motion time series, processed ground motion time series from subduction

zones are not yet available. Therefore, signal-processing effort will be required to make processed ground motion time series from subduction zones available for use in engineering application in Indonesia. For engineering application, the use of baseline correction and acausal filtering (Fig. 4) is considered to be most appropriate, Boore & Bommer (2005).

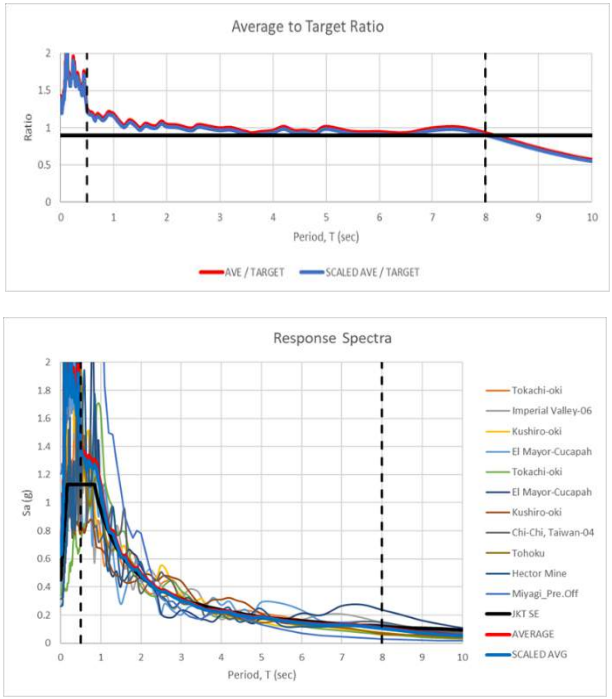

Fig. 3. Output Sample of Proposed GMSM Practical Engineering Tool to be Applied in Indonesia.

For more accurate selection process, spectral shape of each horizontal component pair of ground motion time series must be incorporated into the database. This can be represented by maximum direction (RotD100) response spectral values consistent with the ground motion intensity defined in the building code provided for structural periods relevant to engineering practice (Fig. 5). Inclusion of this metadata can initially be time-consuming but will be highly beneficial in the long run.

4 CONCLUDING REMARKS

With the upcoming plan to enforce Indonesian seismic retrofit code, proper implementation of GMSM procedure will be required. Currently, the dissemination of earthquake engineering knowledge in Indonesia is still underway and it will take time for practitioners to grasp the required knowledge within GMSM subject. Considering current limitation on local availability of expert resources, an interventive tool will be required to assist wide-spread and proper implementation of the GMSM procedure specifically aimed for common practical engineering cases. Without such strategic tool, the code enforcement effort to promote seismic safety in Indonesia will be impeded. This tool needs to be developed accustomed to seismicity condition of cities throughout Indonesia and is practically suitable for common engineering practice.

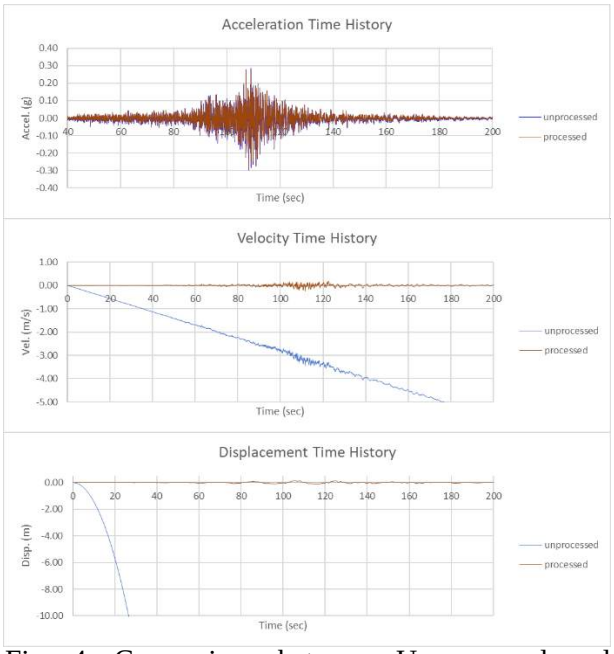

Fig. 4. Comparison between Unprocessed and Processed Time Series.

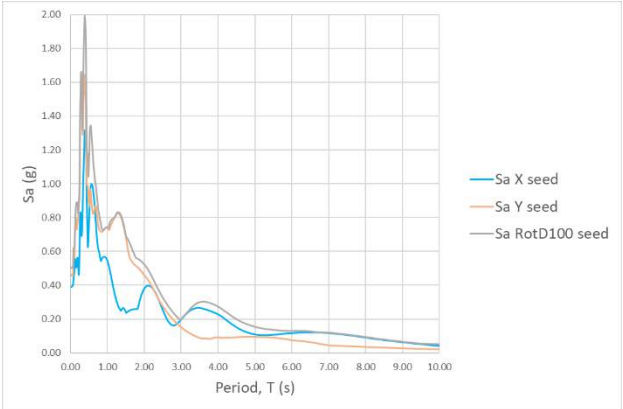

Fig. 5. Maximum Direction Spectrum from Horizontal Component Pair of a Ground Motion Time Series.

DAFTAR PUSTAKA - REFERENCES

Alexander, N., Sukamta, D., & Irsyam, M. 2019. Ground Motion Selection and Modification Procedure for Nonlinear Response History Analysis In Accordance with SNI 1726: 2019. *XXIII HATTI Annual Scientific Meeting*.

Ancheta, T. D., Darragh, R. B., Stewart, J. P., Seyhan, E., Silva, W. J., Chiou, B. S. J., Wooddell, K. E., Graves, R. W., Kottke, A. R., Boore, D. M., Kishida, T., & Donahue, J. L. 2014. *NGA-West2 Database*. *Earthquake Spectra* 30(3): 989–1005.

ASCE. 2016. Minimum Design Loads ad Associated Criteria for Buildings and Other Structures. *ASCE:* 7-16. American Society of Civil Engineers. Washington, D.C.

ASCE. 2017. Seismic Evaluation and Retrofit of Existing Buildings. *ASCE:* 41-17. American Society of Civil Engineers. Washington, D.C.

Boore, D. M., & Bommer, J. J. 2005. Processing of Strong-Motion Accelerograms: Needs, Options And Consequences. *Soil Dynamics and Earthquake Engineering* 25(2): 93–115.

Irsyam, M., Cummins, P. R., Asrurifak, M., Faizal, L., Natawidjaja, D. H., Widiyantoro, S., Meilano, I., Triyoso, W., Rudiyanto, A., Hidayati, S., Ridwan, M., Hanifa, N. R., & Syahbana, A. J. 2020. Development of the 2017 National Seismic Hazard Maps of Indonesia. *Earthquake Spectra* 36(1_suppl): 112–136.

Kishida, T., Bozorgnia, Y., & Abrahamson, N. A. 2017. *Development of the NGA-Subduction Database*. January.

Puslitbang PUPR. 2017. *Peta Sumber dan Bahaya Gempa Indonesia Tahun 2017*. Bandung, Indonesia: Pusat Penelitian dan Pengembangan Kementerian Pekerjaan Umum dan Perumahan Rakyat.

SIN. 2019. *Tata Cara Perencanaan Ketahanan Gempa Untuk Struktur Bangunan Gedung dan Nongedung*. SNI 1726:2019. Jakarta, Indonesia: Badan Standardisasi Nasional.

Desain Tidak Umum Dinding Penahan Tanah

Abdul Hakam
Universitas Andalas
HATTI Sumbar

Deni Irda Mazni
Universitas Andalas
Universitas Dharma Andalas

Hendri Warman
Universitas Andalas
HATTI Sumbar

ABSTRAK: Analisis stabilitas dinding penahan tanah yang ada umumnya dikembangkan berdasarkan tekanan tanah di belakang dinding. Tekanan tanah akibat berat sendiri diturunkan dengan asumsi pengurukan di belakang dinding cukup panjang, sehingga bentuk keruntuhan dapat digambarkan secara lengkap. Dalam kasus di mana timbunan di belakang dinding cukup sempit, metode yang ada harus diperbaiki atau dimodifikasi. Pada kasus praktis di daerah pegunungan sering dijumpai adanya konstruksi jalan yang dibangun pada lereng yang relatif curam, sehingga lokasi konstruksi menjadi sempit. Untuk membuat jalan tersebut stabil dan tidak longsor, maka diperlukan konstruksi dinding penahan tanah yang disesuaikan berdasarkan keadaan setempat. Dalam makalah ini disajikan prosedur perencanaan dinding penahan tanah untuk daerah yang relatif sempit, yang didasarkan pada bentuk keruntuhan timbunan sempit di belakang dinding penahan tanah. Prosedur ini sangat berguna untuk mengembangkan metode analisis dinding penahan tanah yang dibangun di lahan sempit akibat keterbatasan lokasi.

Kata Kunci: dinding penahan tanah, analisis kestabilan, timbunan sempit

ABSTRACT: The current methods of retaining walls stability analysis are generally developed based on the soil pressure behind the wall. The earth pressure due to self-weight is generated by assuming the backfill behind the wall is long enough, so that the failure plane can be plotted completely. In special cases where the embankment behind the wall are quite narrow, the existing method must be improved or modified. In the mountainous area, it is often found that roads are built on relatively steep slopes, so the construction site becomes limited. In the order to make the road stable, it is necessary to construct a retaining wall that is adapted to the local conditions. This paper presents the procedure for designing a retaining wall for a relatively narrow area, which is based on the failure shape of the narrow embankment behind the retaining wall. This procedure is very useful for developing a stability analysis of retaining walls constructed in narrow areas due to local condition.

Keywords: retaining wall, stability analysis, narrow backfill

1 PENDAHULUAN

Dinding penahan tanah merupakan konstruksi yang dibuat untuk menahan tanah sehingga terhindar dari kejadian longsor. Dinding penahan tanah merupakan konstruksi penambat buatan sebagai cara penanggulangan yang bersifat mengikat atau menahan massa tanah yang bergerak. Jenis konstruksi dinding penahan tanah yang dibuat harus disesuaikan dengan tujuan dari penambatan. Selain itu, bentuk dan geometri konstruksi dinding penahan tanah harus disesuaikan dengan keadaan lokasi, antara lain geometri lereng, kondisi hidrologi dan parameter tanah. Sebagai contoh, dinding penahan tanah yang dibangun yang berdekatan dengan suatu dinding eksterior basement, maka perlu dipelajari pengujian teori dan model untuk keruntuhan dan tekanan tanah aktif, Weidong et al. (2020).

Dinding penahan tanah yang dibuat, umumnya merupakan tipe kantilever yang terbuat dari beton bertulang. Jenis lain yang sangat sering digunakan adalah tipe gravity

yang terbuat dari pasangan batu atau juga beton. Kedua jenis dinding penahan tanah tersebut sangat jamak digunakan untuk menahan tanah, sehingga ukuran umum dinding tersebut secara konvensional telah banyak disebutkan dalam berbagai literatur sejak zaman dahulu, Bowless (1997), Das and Shoban (2014). Pada Gbr. 1 ditampilkan dinding penahan tanah konvensional yang digambarkan kembali dari Bowless (1997).

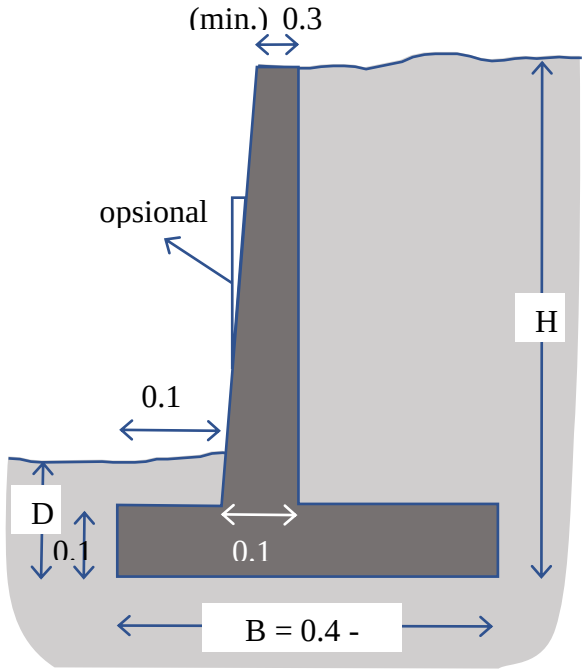

Gbr. 1. Dimensi Konvensional Dinding Kantilever.

Keputusan dalam mengambil nilai-nilai gaya atau tekanan yang bekerja merupakan tahap awal dalam analisis kestabilan. Hal tersebut merupakan faktor yang sangat penting dalam mendapatkan stabilitas dinding penahan tanah pada kondisi sebenarnya. Laporan tentang keruntuhan dinding penahan tanah telah disampaikan oleh Sharma (2011). Uraian kasus tersebut menjelaskan mekanisme kegagalan dinding penahan tanah. Dari pengalaman yang lalu, kegagalan dinding penahan tanah adalah diakibatkan oleh desain sistem penahan dan pendukung yang tidak tepat sebagaimana dilaporkan Lim (2018).

Kasus-kasus kegagalan lainnya juga telah dibahas oleh berbagai peneliti seperti Olson (1993), dimana dinding penahan tanah kantilever yang dirancang sesuai dengan prosedur dalam buku pegangan teknik sipil, ternyata mengalami gagal sesaat setelah pelaksanaan konstruksi selesai.

2 PENDEKATAN TEORI

2.1 *Teori Tekanan Tanah*

Tekanan tanah lateral yang disebabkan oleh berat sendiri tanah dibedakan menurut arah dan cara kerjanya. Prosedur umum dalam mengestimasi stabilitas dinding penahan tanah, diawali dengan tahapan menentukan gaya-gaya utama yang bekerja di belakang dinding. Hal ini disebabkan fungsi utama dari dinding penahan tanah adalah menahan tanah akibat gaya-gaya yang melongsorkan tanah di belakang dinding.

Teori tentang perhitungan tekanan lateral tanah akibat berat sendiri mulanya diperkenalkan oleh Coulomb (1776). Selanjutnya Rankine (1857) mengusulkan prosedur perhitungan yang relatif lebih sederhana. Teori Rankine didasarkan pada keadaan tegangan di massa tanah timbunan yang mencapai kondisi batas keseimbangan plastis di mana semua titik dalam massa tanah berada di ambang keruntuhan geser. Teori ini mengasumsikan bahwa tekanan lateral berada pada sudut yang sejajar dengan kemiringan urugan di belakang dinding penahan tanah. Dengan menggunakan lingkaran Mohr dapat ditunjukkan deformasi lateral yang menghasilkan kondisi batas untuk menentukan tegangan dengan parameter kekuatan geser tanah timbunan, c dan ϕ.

Teori Rankine ini terdapat hampir di semua buku referensi tentang tekanan tanah lateral dan mudah dipahami serta sering digunakan dalam analisis stabilitas dinding penahan tanah pada bagian berikut. Teori Rankine menunjukkan bahwa tekanan aktif lateral akibat berat tanah (γ)meningkat secara linier sebagai fungsi kedalaman (z), dan dapat dinyatakan dengan persamaan:

$$\sigma_a = (\gamma\, z)\ \tan^2 (45 - \phi/2) \qquad (1)$$

dimana bagian terakhir pada persamaan di atas dikenal sebagai nilai koefisien tekanan tanah aktif, K_a, yaitu:

$$K_a = \tan^2 (45 - \phi/2) \qquad (2)$$

2.2 *Uji model*

Dalam mendesain dinding penahan tanah, biasanya digunakan teori-teori tekanan tanah yang ada dengan tekanan tanah dihitung berdasarkan nilai koefisien tekanan tanah. Sebagai contoh dalam mendesain dinding

penahan tanah akibat gaya seismic, maka secara konvensional dilakukan dengan menggunakan teori Mononobe-Okabe. Teori ini merupakan adaptasi kondisi dinamis dari solusi klasik Coulomb untuk evaluasi tekanan tanah dalam kondisi statis.

Berdasarkan teori Mononobe-Okabe, efek goncangan gempa pada tekanan lateral yang bekerja di dinding dapat dimodelkan dengan memasukkan dalam persamaan keseimbangan batas dari massa tanah yang runtuh. Selanjutnya gaya inersia yang ada pada tanah karena percepatan seismik diasumsikan konstan dalam satu arah sesuai dengan arah gempa yang dipertimbangkan.

Nimbalkar et al. (2019) menjelaskan bahwa pendekatan teori konvensional Coulomb dan Monoobe-Okabe memberikan distribusi tekanan tanah seismik linear di belakang dinding penahan. Selanjutnya, metode pseudo-dinamis dapat digunakan untuk menghitung distribusi tekanan tanah aktif seismik dengan cara yang lebih realistis. Dalam analisis akibat seismik, pengaruh inersia pada massa dinding dan tanah harus dipertimbangkan dalam desain dinding penahan tanah.

Meskipun teori-teori yang ada juga dapat memberikan hasil yang cukup baik, namun kebutuhan terhadap bukti visual melalui eksperimental dan nantinya pada kasus nyata perlu juga dilakukan. Dengan demikian visualisasi tersebut akan menjadi yang bukti yang terdokumentasi. Beberapa pengujian untuk mempelajari perilaku sistem dinding penahan tanah dengan skala laboratorium telah dipublikasikan. Salah satu contoh adalah pengujian meja getar yang dilakukan terhadap dinding penahan tanah berbentuk L dengan urugan pasir kering oleh Cascone et al. (2000) dan (2001). Eksperimen dilakukan dengan kotak transparan dengan pencatatan terhadap percepatan dan perpindahan selama pengujian berlangsung. Hasil eksperimen dilaporkan dengan tujuan untuk memberikan gambaran visual dan kualitatif sehingga menambah pemahaman terhadap aspek penting dari perilaku dinding penahan tanah terutama akibat beban dinamis. Sistem dinding penahan tanah dengan timbunan horizontal dan timbunan miring telah dilakukan dengan hasil ditampilkan pada Gbr. 2.

Dari hasil tersebut terlihat bahwa garis keruntuhan pada tanah urugan di belakang dinding berbentuk bidang datar dengan membentuk sudut tertentu terhadap sumbu horizontal. Gbr. 2b di atas menunjukkan pola keruntuhan awal di mana pola keruntuhan masih membentuk satu garis saja. Untuk getaran selanjutnya, pola keruntuhan membentuk sudut lain dengan melibatkan massa tanah yang lebih besar namun bentuk bidang runtuh masih datar.

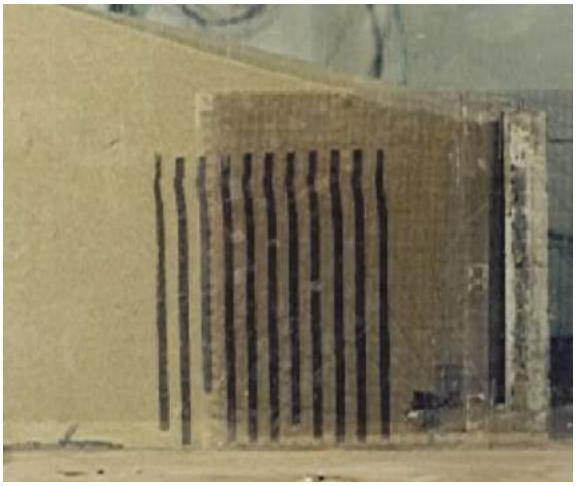

a. Sebelum pengujian

b. Setelah pengujian

Gbr. 2. Keruntuhan Dinding L dari Cascone (2000).

Hasil pengujian serupa telah disampaikan oleh Hakam (2010) bahwa bidang longsor di belakang dinding akibat beban dinamis sama atau lebih besar dari pada pembebanan aktif dengan sudut $\theta > 45+\phi/2$. Bila beban dinamis terus ditingkatkan, maka bidang runtuh bergerak secara perlahan dari keadaan statis akibat tekanan aktif (mengikuti bidang longsor Rankine) hingga keadaan keruntuhan pasif dengan sudut $\theta = 45-\phi/2$. Dalam keadaan ini kelongsoran total dari sistem dinding dinding sudah terjadi.

Bentuk keruntuhan massa tanah di belakang dinding penahan tanah yang dilaporkan umumnya merujuk pada keruntuhan dengan

urugan yang relatif jauh dari dinding sehingga mempunyai panjang yang cukup untuk membentuk bidang runtuh yang sempurna. Untuk melihat bentuk bidang runtuh dengan area urugan yang sempit, maka telah dilakukan eksperimen model dinding penahan tanah dengan hasil seperti pada Gbr. 3.

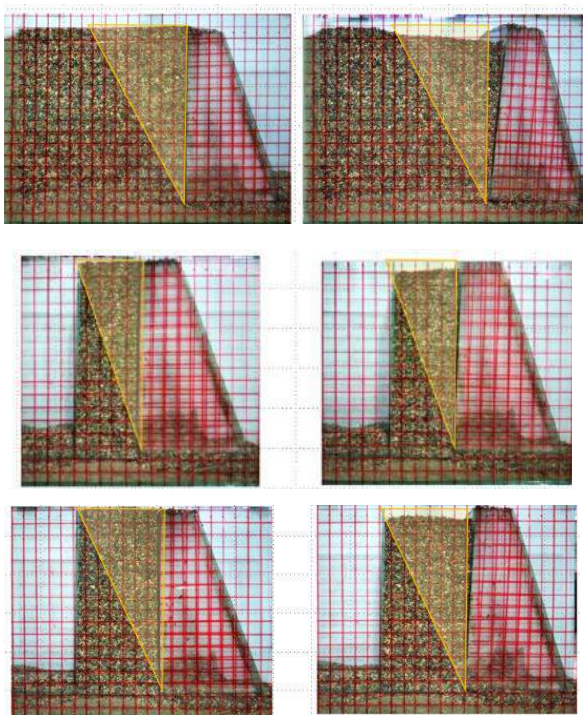

Gbr. 3. Keruntuhan Dinding pada Timbunan Sempit.

Hal serupa juga dilaporkan bahwa terbatasnya penggunaan teori keruntuhan klasik untuk dinding penahan tanah dengan tanah urugan yang sempit dikarenakan teori keruntuhan klasik dikembangkan dengan dasar asumsi tersedianya ruang yang besar dibelakang dinding, Chen et al. (2019). Studi silumasi elemen hingga menunjukkan bahwa ketika dinding penahan tanah bergerak secara translasi, satu sampai tiga permukaan slip akan terbentuk di tumit dinding, dan akhirnya berkembang ke permukaan sepanjang dinding.

2.3 *Gaya-gaya yang bekerja*

Berdasarkan uraian pada bagian di atas, selanjutnya dapat diturunkan gaya-gaya dominan yang bekerja pada sistem dinding penahan tanah (Gbr. 4). Gaya-gaya tersebut selanjutnya ditentukan nilainya dalam analisis kestabilan sistem dinding penahan tanah. Besaran gaya yang bekerja dipertimbangkan terhadap dimensi dari massa yang ikut bergerak, baik dalam kondisi pembebanan statis maupun akibat pengaruh seismik.

Kestabilan sistem dinding penahan tanah terhadap guling dan geser selanjutnya dapat dituliskan sebagai:

$$SF = \frac{M_R}{M_O} \quad \text{dan} \quad SF = \frac{\sum T_R}{\sum H_s} \tag{3}$$

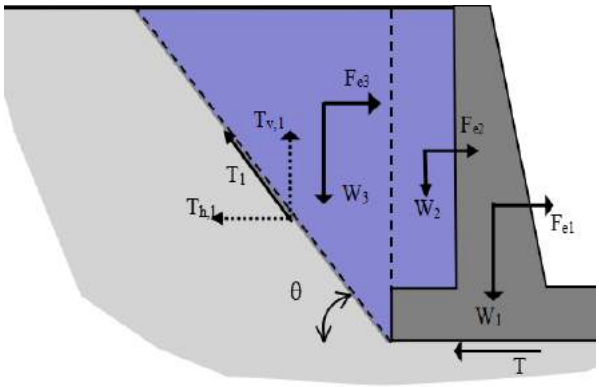

Gbr 4. Gaya-Gaya Dominan yang Bekerja.

dimana:

W_j = Gaya akibat berat (gravitasi)
F_{ij} = Gaya-gaya akibat percepatan gempa
T_{ij} = Gaya-gaya akibat pergeseran dua bidang
ΣT_R = Gaya-gaya penahan geser
ΣH_s = Gaya-gaya penyebab pergerakan geser
M_R = Momen penahan guling di ujung (tumit) dinding
M_O = Momen pengguling di ujung (tumit) dinding

3 APLIKASI KASUS

Aplikasi dari formulasi di atas pertama dilakukan dalam perencanaan dinding penahan tanah untuk kebutuhan pelebaran jalan. Jalan yang ada sebelumnya, mempunyai segmen-segmen sempit dengan lebar kurang dari 4m. Keadaan tersebut mengakibatkan lalulintas kendaraan tidak lancar. Untuk kelancaran lintas lalu kendaraan yang berselisih saat ini, salah satu kendaraan dari arus yang berselisih harus bergiliran dalam melintasi segmen yang sempit tersebut.

Kondisi topografi yang ada tergolong sangat curam. Lokasi rencana untuk pelebaran jalan juga yang sempit sehingga memerlukan alternatif dibuat konstruksi khusus. Sementara

itu keterbatasan sumber daya lokal dan pola penganggaran yang ada, mengakibatkan keterbatasan opsi yaitu tidak dimungkinkan membuat konstruksi yang relatif rumit. Sehingga konstruksi dinding penahan tanah konvensional berbahan beton bertulang tetap menjadi opsi utama.

Berdasarkan hasil pengujian lapangan (Gbr. 5) dengan menggunakan penetrasi standar (SPT), diestimasi bahwa konstruksi dinding penahan tanah masih dapat dibuat dengan daya dukung yang cukup. Analisis kestabilan dinding penahan tanah dengan menggunakan metoda yang dijelaskan pada bagian sebelumnya, memberikan faktor keamanan untuk beban dinamis 1,29 terhadap guling dan 1,04 terhadap geser. Sedangkan daya dukung pondasi mempunyai faktor keamanan sebesar 2,71 sudah termasuk beban dinamis. Dinding penahan tanah kantilever beton bertulang yang direncanakan mempunyai tinggi beragam mulai dari 3 m hingga mencapai 9 m dan lebar tapak 3,5 m, dengan ketebalan minimum 25 cm dan maksimum 40 cm. Dalam pelaksanaannya, ketinggian dinding bertambah karena menyesuaikan terhadap kondisi tanah yang ada. Konstruksi ini berhasil dibangun dan mampu memberikan kepuasan terhadap tujuan semula, yaitu memperlancar arus lalu lintas. Badan jalan yang semula sempit, dapat diperlebar bahkan melebihi dua kali lipat ukuran semula (Gbr. 6).

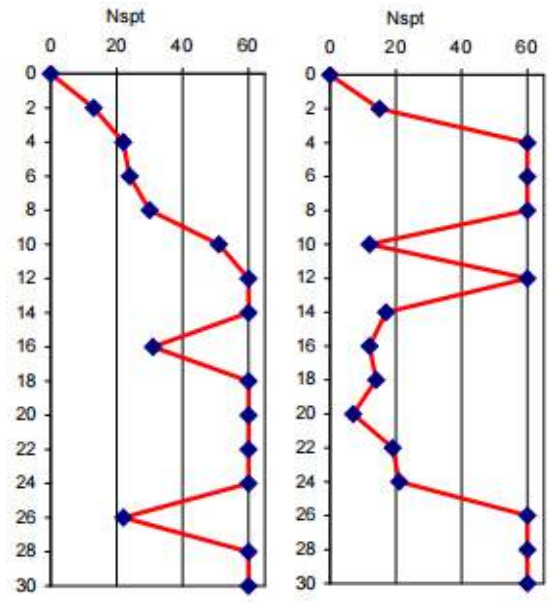

Gbr. 5. Hasil Pengujian Lapangan dengan SPT.

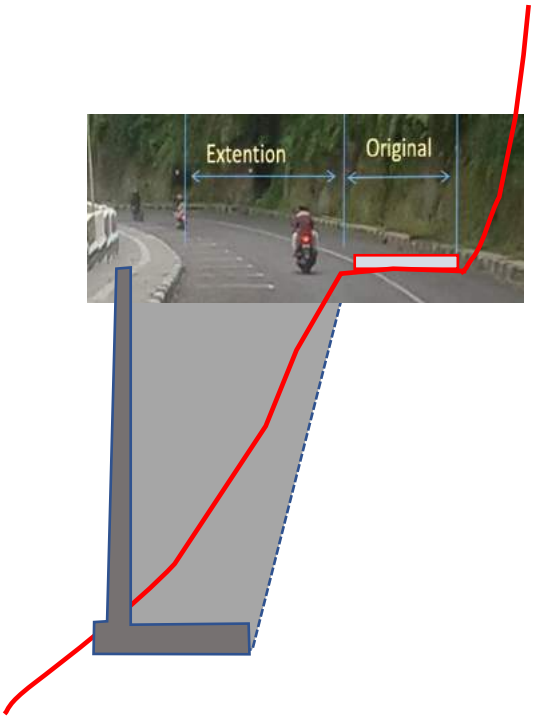

Gbr. 6. Pelebaran Jalan Lubuk Mato Kuciang.

4 DISKUSI

Dalam aplikasi pekerjaan nyata di lapangan, praktik rekayasa sipil terkadang dihadapkan pada permasalahan pada kasus dengan berbagai keterbatasan. Keterbatasan-keterbatasan yang dihadapi dapat berupa keterbatasan lokasi, yaitu lahan yang sempit untuk membuat konstruksi, topografi yang sangat curam dan terkadang kondisi tanah yang tidak menguntungkan. Selain itu terdapat juga keterbatasan local yaitu berupa kemampuan sumber daya manusia untuk membuat konstruksi, bahan local yang tersedia dan terkadang juga pola dan nilai anggaran yang disediakan. Untuk itu dalam menyelesaikan kasus khusus tersebut, diperlukan penyelesaian masalah dengan mempertimbangkan teori-teori yang sudah berkembang, kajian-kajian yang telah dilakukan, simulasi-simulasi baik dalam bentuk model numerik maupun model fisik berskala.

Dalam tulisan ini telah digambarkan secara ringkas mengenai pengalaman dalam menyelesaikan permasalahan perencanaan dinding penahan tanah untuk keperluan pelebaran jalan dengan melibatkan keterbatasan-keterbatasan yang dihadapi. Solusi dilakukan dengan cara merumuskan permasalahan serta mempertimbangkan prosedur perencanaan berdasarkan kajian-

kajian yang dilakukan dengan tetap memperhatikan kriteria kestabilan yang berlaku umum. Beberapa hal yang berlaku secara konvensional harus mengalami pergeseran sehingga perencanaan konstruksi yang diharapkan dapat diselesaikan dengan keamanan yang meyakinkan.

DAFTAR PUSTAKA

Bowles, Joseph E. 1997. *Foundation Analysis and Design* 5th Ed. McGraw Hill Inc.

Cascone, E., Lo Grasso, A.S., and Maugeri, M. 2000. Dynamic Model Tests On L-Shaped Gravity Retaining Walls. *Proc. WCEE 12th*, paper no. 2445.

Cascone, E; Lo Grasso, A.S., and M Maugeri. 2001. Dynamic Model Tests on Gravity Retaining Walls with Various Surcharge Conditions. *International Conferences on Recent Advances in Geotechnical Earthquake Engineering and Soil Dynamics*. 9. https://scholarsmine.mst.edu/icrageesd/04icrageesd/session07/9.

Chen, F., Yang, J. and Lin,Y. 2019. Active Earth Pressure of Narrow Granular Backfill against Rigid Retaining Wall Near Rock Face under Translation Mode. *Int. J. Geomech* Vol. 19 No. 12: 04019133.

Coulomb, C.A. 1776. Essai Sur Une Application DesRegles De Maximis Et Minimis a Quelques Problemes De Statique Relatifs a L'Architecture (Essay on Maximums and Minimums Of Rules To Some Static Problems Relating To Architecture). Mem. Acad. Roy,pres. Divers Savants, 7: 38. Paris.

Das, BM. and Sobhan, K. 2014. *Principles of Geotechnical Engineering* 8th ed. Cengage Learning

Hakam, A. 2010. *Stabilitas Lereng dan Dinding Penahan Tanah*. Universitas Andalas, Padang.

Lim, A. 2018. Lesson Learned from Retaining Wall Failures: a Geotechnical Disaster. *MATEC Web Conf* Vol. 229.

Nimbalkar, S., Pain, A., Mohd Ahmad, S., and Chen, Q. 2019. Stability Assessment of Earth Retaining Structures Under Static and Seismic Conditions. *Infrastructures* Vol. 4, No. 2.

Olson, R.E., 1993. Failure of a Twenty-FootHigh Retaining Wall. *Proceedings Missouri University of Science and Technology, Third International Conference on Case Histories in Geotechnical Engineering* Vol. 2, 1993: 791-797

Rankine, W.J.M. 1857. On the Stability of Loose Earth, Philosophical Transactions of the Royal Society of London (1776-1886). 1857-01-01. 147: 9–27.

Sharma, S. 2011. Teaching Retaining Wall Design with Case Histories. *Geo-Frontiers ASCE*: 2877-2886.

Weidong, H., Xinnian, Z., Xiaohong, L., Yongqing, Z. and Xiyu,Z. 2020. Active Earth Pressure against Cantilever Retaining Wall Adjacent to Existing Basement Exterior Wall. *Int. J. Geomech* Vol. 20, No. 11: 04020207.

Penyelesaian Permasalahan Hukum dalam Sektor Konstruksi Akibat Pandemi Covid-19

Martin Patrick Nagel
Managing Partner – FKNK Law Firm

Maynanda Aulia
Senior Associate – FKNK Law Firm

Ramos R. Sidjabat
Junior Associate – FKNK Law Firm

1 PENDAHULUAN

Kegiatan konstruksi di Indonesia adalah salah satu sektor yang memberi konstribusi bagi perekonomian Indonesia. Hal ini dapat dilihat melalui hasil survei perusahaan konstruksi triwulanan terhadap perusahaan konstruksi skala menengah dan besar di Indonesia yang dikeluarkan Badan Pusat Statistik.

Pada tahun 2019, peran sektor konstruksi untuk Produk Domestik Bruto Indonesia pada triwulan III adalah sebesar 10,60%, Badan Pusat Statistik, *Konstruksi Dalam Angka 2019*, BPS RI Jakarta (2019) Hlm. 1. Namun, setelah terjadinya Pandemi Covid-19, index laju pertumbuhan antar tahun untuk Produk Domestik Bruto pada sektor konstruksi di tahun 2020 turun menjadi -4,52%, Badan Pusat Statistik, *Konstruksi Dalam Angka 2020*, BPS RI, Jakarta (2020), Hlm. 30.

Badan Pusat Statistik juga menyediakan data atas Nilai Konstruksi yang Diselesaikan berupa realisasi penyelesaian pekerjaan konstruksi dalam satu triwulan pada suatu wilayah, Badan Pusat Statistik, *Indikator Konstruksi Triwulan I-2021,* BPS RI, Jakarta, (2021) Hlm. 13. Berdasarkan data atas Nilai Konstruksi yang Diselesaikan tersebut, terjadi penurunan penyelesaian kegiatan konstruksi di Indonesia pada tahun periode terjadinya pandemi Covid-19 (2020-2021).

Perlu diperhatikan bahwa pertumbuhan Nilai Konstruksi yang Diselesaikan pada periode triwulan IV-2019 adalah sebesar 2,92%, Badan Pusat Statistik, *Indikator Konstruksi Triwulan IV-2020,* BPS RI, Jakarta (2020) Hlm. 17. Namun demikian melalui data Badan Pusat Statistik atas Nilai Konstruksi yang Diselesaikan di atas, pada tahun 2020 ketika mulai merebaknya Covid-19, pertumbuhan Nilai Konstruksi yang Diselesaikan pada triwulan I-2020 menurun drastis hingga -20,29% (minus dua puluh koma dua puluh sembilan persen). Meskipun sempat terjadi kenaikan pada periode triwulan II-2020 hingga triwulan IV-2020, tetapi berdasarkan data Badan Pusat Statistik, *Indikator Konstruksi Triwulan I-2021,* Nilai Konstruksi yang Diselesaikan pada periode triwulan I-2021 kembali mengalami penurunan menjadi -2,10%.

Permasalahan hukum dalam sektor konstruksi memang sering terjadi, bahkan sebelum adanya Pandemi Covid-19. Hal ini sejalan dengan pernyataan yang pernah disampaikan oleh M. Husseyn Umar dalam Seminar Nasional Penyelesaian Sengketa di Bidang Infrastruktur Melalui Arbitrase, di Universitas Tanjungpura, Pontianak pada tahun 2019 bahwa sengketa hukum yang paling banyak diproses pada Badan Arbitrase Nasional Indonesia pada tahun 2018 adalah terkait sektor konstruksi yaitu sebanyak 27,09% (www.beritasatu.com/nasional/551730/sengketa-bidang-konstruksi-karena-pembangunan-infrastruktur-berkembang).

Penurunan pertumbuhan Nilai Konstruksi Yang Diselesaikan sebagaimana disampaikan dalam data Badan Pusat Statistik pada tahun 2020-2021 atau sejak adanya Pandemi Covid-19, dapat mengakibatkan potensi peningkatan permasalahan hukum atas pelaksanaan penyelesaian pekerjaan konstruksi. Permasalahan hukum dapat dihadapi oleh para pelaku usaha sebagai akibat adanya pihak yang hendak menuntut hak atau kewajiban dari pihak lain sebagaimana diatur di dalam kontrak kontruksi.

Selain itu, hambatan yang terjadi dalam pelaksanaan hak dan kewajiban pada kontrak

konstruksi tentunya mengakibatkan permasalahan keuangan bagi para pelaku usaha. Permasalahan keuangan ini tentunya juga akan berdampak untuk pembiayaan pelaksanaan proyek konstruksi yang sedang berjalan.

2 KONTRAK KONSTRUKSI

Pemerintah menilai perlunya kepastian hukum atas penyelenggaraan jasa konstruksi dengan mengeluarkan Undang-Undang No. 2 Tahun 2017 tentang Jasa Konstruksi. Dalam Pasal 1 angka 8 Undang-Undang No. 2 Tahun 2017 tentang Jasa Konstruksi mengatur bahwa "*Kontrak kerja konstruksi adalah keseluruhan dokumen kontrak yang mengatur hubungan hukum antara Pengguna Jasa dan Penyedia Jasa dalam penyelenggaraan Jasa Konstruksi*". Mengacu pada ketentuan pada Pasal 1 angka 8 Undang-Undang No. 2 Tahun 2017 tentang Jasa Konstruksi, maka setiap hak dan kewajiban antara para pihak dalam proses pelaksanaan pekerjaan konstruksi tentunya harus diatur di dalam kontrak.

Namun demikian, agar suatu kontrak menjadi mengikat para pihak harus memenuhi ketentuan Pasal 1320 Kitab Undang-Undang Hukum Perdata, yang mengatur mengenai 4 syarat sahnya perjanjian/kontrak, yaitu kesepakatan, kecakapan, hal tertentu dan sebab yang halal. Berdasarkan ketentuan tersebut, maka kontrak baru wajib dilaksanakan oleh para pihak apabila terjadi persetujuan/kesepakatan antara para pihak atas seluruh hal yang dimuat dalam suatu kontrak konstruksi. Kesepakatan ini dilakukan dengan cara para pihak menandatangani kontrak tertulis sebagaimana diatur di dalam Pasal 76 Peraturan Pemerintah Nomor 22 Tahun 2020 tentang Peraturan Pelaksanaan Undang-Undang Nomor 2 tahun 2017 tentang Jasa Konstruksi.

Undang-Undang No. 2 Tahun 2017 tentang Jasa Konstruksi mengatur bahwa kontrak konstruksi paling sedikit meliputi hal-hal sebagai berikut:

a. para pihak,
b. rumusan pekerjaan, lingkup kerja, nilai pekerjaan, harga satuan, lumpsum, dan batasan waktu pelaksanaan,
c. masa pertanggungan, jangka waktu pelaksanaan dan pemeliharaan,
d. hak dan kewajiban termasuk hak pengguna jasa memperoleh hasil pekerjaan dan kewajibannya untuk memenuhi ketentuan yang diperjanjikan, serta hak penyedia jasa untuk memperoleh informasi dan imbalan jasa serta kewajibannya melaksanakan pekerjaan konstruksi,
e. penggunaan tenaga kerja konstruksi bersertifikat,
f. cara pembayaran, termasuk di dalamnya jaminan atas pembayaran,
g. wanprestasi, memuat ketentuan tentang tanggung jawab dalam hal salah satu pihak tidak melaksanakan kewajiban sebagaimana diperjanjikan,
h. penyelesaian perselisihan, memuat ketentuan tentang tata cara penyelesaian perselisihan akibat wanprestasi,
i. pemutusan kontrak konstruksi,
j. keadaan memaksa, memuat ketentuan tentang kejadian yang timbul di luar kemauan dan kemampuan para pihak yang menimbulkan kerugian bagi salah satu pihak,
k. kegagalan bangunan, memuat ketentuan tentang kewajiban penyedia jasa dan/atau pengguna jasa atas kegagalan bangunan, serta pertanggungjawaban kegagalan bangunan,
l. perlindungan pekerja, memuat ketentuan tentang kewajiban para pihak dalam pelaksanaan keselamatan, dan kesehatan kerja serta jaminan sosial,
m. perlindungan terhadap pihak ketiga selain para pihak dan pekerja, memuat kewajiban para pihak dalam hal terjadi suatu peristiwa yang menimbulkan kerugian atau menyebabkan kecelakaan dan/atau kematian,
n. aspek lingkungan, memuat kewajiban para pihak dalam pemenuhan ketentuan tentang lingkungan,
o. jaminan atas risiko yang timbul dan tanggung jawab hukum kepada pihak lain dalam pelaksanaan Pekerjaan Konstruksi atau akibat dari Kegagalan Bangunan;
p. pilihan penyelesaian sengketa konstruksi.

Kesepakatan para pihak atas klausul kontrak konstruksi tentunya terlebih dahulu diawali dengan proses penawaran dan negosiasi antara pengguna jasa dan penyedia jasa. Karenanya, kata dan kalimat yang memuat ketentuan, syarat, hak, dan kewajiban dalam kontrak konstruksi harus jelas untuk menghindari terjadinya perbedaan penafsiran yang dapat

menjadi perselisihan (*dispute*) antara para pihak di kemudian hari.

Permasalahan hukum yang sering terjadi terkait kontrak konstruksi adalah mengenai pelaksanaan pembayaran dan pelaksanaan pekerjaan. Pelaksanaan pembayaran dan pelaksanaan pekerjaan bagai dua sisi mata uang yang tidak dapat dipisahkan satu dengan lainnya. Hal ini karena penyedia jasa memperoleh pembayaran dengan melaksanakan pekerjaan, dan pengguna jasa memperoleh hasil pekerjaan dengan melaksanakan pembayaran.

Pelaksanaan pekerjaan dalam kontrak konstruksi diikuti dengan penyerahan pekerjaan dari penyedia jasa kepada pengguna jasa. Penyerahan pelaksanaan pekerjaan pada suatu kontrak konstruksi pada umumnya dilakukan dengan mekanisme sebagai berikut:

a. Waktu Penyerahan Pekerjaan
   Para pihak dalam kontrak konstruksi tentunya mengatur ketentuan mengenai jangka waktu penyelesaian pelaksanaan pekerjaan. Penyerahan hasil pekerjaan konstruksi merupakan suatu proses yang membuktikan bahwa pengguna jasa telah menyerahkan pekerjaan kepada penyedia jasa, dan penyedia jasa telah melakukan pekerjaan berdasarkan kontrak baik berdasarkan progress yang telah disepakati maupun secara menyeluruh. Proses penyerahan pekerjaan terdiri dari:
   1. Serah Terima Lokasi Pekerjaan adalah proses pemberian lahan lokasi pelaksanaan pekerjaan oleh Pengguna Jasa kepada Penyedia Jasa. Serah Terima Lahan Pekerjaan ini dapat disepakati oleh para pihak sebagai jangka waktu dimulainya pelaksanaan pekerjaan konstruksi.
   2. Serah Terima Pekerjaan Tahap Pertama merupakan suatu kegiatan serah terima atas selesainya pekerjaan oleh Penyedia Jasa kepada Pengguna Jasa. Serah Terima Tahap Pertama ini bertujuan untuk memastikan Penyedia Jasa telah melaksanakan pekerjaan sesuai dengan persyaratan dan ketentuan kualitas, kuantitas, serta jadwal waktu yang disepakati dalam Kontrak Konstruksi. Perlu diperhatikan bahwa sangat penting untuk menentukan syarat dan batas waktu agar Serah Terima Pekerjaan Tahap Pertama dianggap telah dilaksanakan atau tidak.
   3. Serah Terima Akhir Pekerjaan adalah suatu kegiatan serah terima akhir pekerjaan dari Penyedia Jasa kepada Pengguna Jasa setelah Penyedia Jasa menyelesaikan semua kewajibannya selama masa pemeliharaan, hal mana bertujuan untuk (i) memastikan bahwa seluruh hasil pekerjaan penyedia jasa baik secara fisik maupun administrasi telah dapat diterima oleh Pengguna Jasa, (ii) sebagai tanggal waktu efektif selesainya kewajiban Penyedia Jasa, dan (iii) sebagai pernyataan berakhirnya tanggung-jawab Penyedia Jasa secara keseluruhan.

b. Perhitungan Progress Pekerjaan dan Sertifikasi Pembayaran
   Pelaksanaan perhitungan atas *progress* pelaksanaan pekerjaan konstruksi dilakukan untuk mengetahui sejauh mana proses pelaksanaan pekerjaan telah dilaksanakan. Pekerjaan konstruksi dapat menemui kendala dalam progress pelaksanaannya. Penyebab terjadinya permasalahan *progress* pekerjaan konstruksi adalah karena hal-hal sebagai berikut:
   1. Faktor ekonomi yaitu terkait anggaran (*cost*),
   2. Faktor teknis terkait jumlah (quantity) dan mutu (*quality*), dan
   3. Faktor waktu (*time*).

Perhitungan terhadap ketiga faktor tersebut menentukan terbitnya sertifikat pembayaran yang menjadi dasar bagi Penyedia Jasa untuk meminta Pengguna Jasa melaksanakan proses pembayaran. Pada tahun 2020 hingga saat ini, pandemi Covid-19 merupakan kendala yang menjadi penyebab tertundanya penyelesaian proyek konstruksi karena mempengaruhi ketiga faktor di atas.

Di dalam praktik, ketentuan mengenai nilai uang dalam suatu kontrak konstruksi antara lain meliputi nilai kontrak (*contract amount*), cara pembayaran (*method of payment*), jaminan-jaminan (*guarantee*/*bonds*). Jaminan-jaminan yang biasanya terdapat pada suatu kontrak konstruksi antara lain mengenai jaminan uang muka (*advance payment bond*), jaminan pelaksanaan (*performance bond*), jaminan perawatan atas cacat (*defect liability bond*), jaminan pembayaran (*payment guarantee*).

Klausul yang memuat cara pembayaran harus diatur secara komprehensif karena akan berpengaruh pada penyelesaian konstruksi.

Para pihak perlu mengatur secara tegas mengenai syarat pelaksanaan cara pembayaran, serta batas waktu untuk pemenuhan syarat tersebut, sehingga terdapat pemahaman yang sama bagi para pihak mengenai sejak kapan mulai timbul kewajiban pelaksanaan pembayaran oleh Pengguna Jasa.

Bahwa agar tidak terdapat perbedaan pemahaman atas prestasi-prestasi dalam kontrak konstruksi memang perlu terdapat standarisasi bentuk kontrak konstruksi. Di Indonesia tidak terdapat standarisasi bentuk kontrak dalam sektor konstruksi sehingga pemilihan bentuk kontrak lebih didasarkan dari karakteristik dan kondisi proyek itu sendiri sebagaimana hal ini sesuai dengan Pasal 46 Undang-Undang No. 2 Tahun 2017 tentang Jasa Konstruksi. Namun demikian, terdapat berbagai bentuk kontrak konstruksi yang digunakan para pelaku usaha di Indonesia, hal mana salah satunya adalah FIDIC yang merupakan model kontrak konstruksi yang digunakan di dunia internasional.

Terdapat proyek-proyek konstruksi di Indonesia yang ketentuannya mengacu pada klausul yang terdapat dalam kontrak FIDIC khususnya *Condition of Contract* (*Red Book*) dan *Design Build* (*Yellow Book*). Berikut adalah bentuk kontrak FIDIC yang dikenal dan dipakai untuk proyek konstruksi yaitu (Michael D. Robinson, *A Contractor's Guide to the FIDIC Conditions of Contract, First Edition*, United Kingdom, John Wiley & Sons, Ltd):

a. *Condition of Contract for Construction* "*Red Book*"
   FIDIC-*Condition of Contract for Construction* (*Red Book*) dikenal juga sebagai FIDIC *tradition contract* untuk pekerjaan sipil dan bangunan, atau juga dikenal sebagai *remeasurement contract* atau *design-bid-build*. Bentuk kontrak ini dipergunakan dalam hampir keseluruhan desain yang disiapkan oleh pengguna jasa atau konsultan perencana yang ditunjuk oleh pengguna jasa. Pada FIDIC-*Red Book*, pihak kontraktor bertanggung jawab untuk pelaksanaan pekerjaan sesuai dengan apa yang sudah disepakati di dalam kontrak.
b. *Condition of contract for Plant and Design-Build* "*Yellow Book*"
   FIDIC *Conditions of Contract for Plant and Design Build, for Electrical and Mechanical Plant, and for Building and Engineering Works, Designed by the Contractor* (*Yellow Book*) digunakan pada pekerjaan dimana mayoritas desain dilakukan oleh kontraktor, dalam hal ini untuk pekerjaan elektromekanikal termasuk biaya pemasangan di lapangan, yang didasari oleh spesifikasi dari pengguna jasa. *Engineer* akan melakukan administrasi kontrak, menyiapkan berita acara pembayaran sesuai dengan progress prestasi pekerjaan yang diselesaikan, misalnya dibayar setiap 20% dan seterusnya.

   Pada FIDIC-*Yellow Book*, pihak kontraktor bertanggung jawab dari mulai tahap perancangan dan tahap pelaksanaan. Dasar dari perancangan yang dilakukan oleh pihak Kontraktor berdasarkan *Employer Requirement* dan *Site Data* yang disiapkan oleh pihak Pemilik Proyek sebelum dilaksanakan tender.

   Apabila pihak pemilik proyek belum dapat menyelesaikan pekerjaan perancangan untuk proyek tersebut, maka pihak Pemilik proyek tidak dapat untuk melanjutkan ke tahap tender untuk proyek tersebut. Pemakaian FIDIC-*Yellow Book* sebagai standar kontrak proyek konstruksi di Indonesia dapat dipakai pada proyek-proyek yang memiliki masalah pada waktu yang terbatas tersebut. Melalui klausul dalam FIDIC-*Yellow Book*, pihak pemilik proyek dapat menyerahkan pekerjaan desain kepada kontraktor untuk dapat meneruskan pelaksanaan proyek sehingga pekerjaan perancangan menjadi satu kesatuan dengan pekerjaan pelaksaan.

   Namun demikian, klaim konstruksi pada penggunaan model kontrak FIDIC-*Yellow Book* dapat timbul karena kesalahpahaman pada klausula model kontrak FIDIC-*Yellow Book* dikarenakan pemilihan model kontrak FIDIC-*Yellow Book* dapat menimbulkan konsekuensi kontraktor melaksanakan pekerjaan yang menjadi satu kesatuan dengan pekerjaan perancangan, maka dapat terjadi kesalahan dan perbedaan pemahaman antara pemilik proyek dan kontraktor yang berujung pada suatu sengketa konstruksi.
c. *Condition of contract for Engineering Purchase Construction (EPC)/Turnkey Projects* "*Silver Book*"

FIDIC *Condition of Contract for Engineering Purchase Construction (EPC) (Silver Book)* digunakan pada pekerjaan dalam hal pihak kontraktor berencana untuk menyerahkan proyek yang telah diselesaikan dalam kondisi siap beroperasi. Pada umumnya, bentuk kontrak bangunan sebagaimana dimaksud digunakan untuk proyek besar atau kompleks di mana pembangun (kontraktor EPC) akan menyerahkan proyek yang telah selesai tersebut. FIDIC-*Silver Book* adalah panduan praktis bagi pihak yang terlibat dalam mempersiapkan, mengelola, atau berkontribusi pada rangkaian kontrak FIDIC.

FIDIC-*Silver Book* mengatur rincian dan penjelasan sehubungan dengan komunikasi dan pemberitahuan, perlakuan terhadap Kontraktor dan Pekerja, serta mekanisme penyelesaian sengketa dan kualitas manajemen yang sesuai dengan ketentuan kontrak. Dalam FIDIC-*Silver Book*, terdapat panduan secara khusus yang berjudul *"General Conditions of Dispute Avoidance/Adjudication Agreement"* yang dalam praktiknya menjadi suatu penyelesaian sengketa.

d. *Short Form of Contract* "*Green book*"
FIDIC *Short Form of Contract* (*Green Book)* ditujukan untuk pekerjaan sederhana yang dapat dilakukan berulang kali tanpa keterlibatan dari ahli atau sub-kontraktor. Ketentuan dalam FIDIC-*Green Book* dapat digunakan untuk pekerjaan konstruksi apapun termasuk pekerjaan desain pembangunan konstruksi sipil, bangunan, mekanikal dan/atau elektrikal.

3 PERMASALAHAN HUKUM DALAM KONTRAK KONSTRUKSI

Prestasi yang harus dilaksanakan oleh subyek hukum berasal dari suatu perikatan yang lahir dari suatu perjanjian/kontrak dan perundang-undangan sebagaimana diatur dalam Pasal 1233 Kitab Undang-Undang Hukum Perdata. Lebih lanjut, Pasal 1234 Kitab Undang-Undang Hukum Perdata mengatur 3 (tiga) macam prestasi, yaitu sebagai berikut:

a. memberikan/menyerahkan suatu barang,
b. berbuat sesuatu, dan
c. tidak berbuat sesuatu.

Pihak yang tidak melaksanakan prestasi dalam suatu perikatan dapat menimbulkan konsekuensi hukum terhadap pihak tersebut. Berikut adalah konsekuensi hukum yang dapat timbul akibat dari tidak dilaksanakannya prestasi oleh pelaku usaha dalam sektor konstruksi:

a. Cidera Janji Terhadap Klausul Dalam Kontrak Konstruksi
Dalam Kontrak Konstruksi, terdapat berbagai macam klausul yang dituangkan ke dalam berbagai pasal dalam mewujudkan maksud dari Kontrak Konstruksi tersebut. Para pihak yang bersepakat dalam suatu kontrak konstruksi sangat perlu mengetahui prestasi apa saja yang harus dilaksanakan sehingga klausul dalam kontrak konstruksi terlaksana sesuai dengan yang diperjanjikan.

Salah satu pihak yang tidak melaksanakan ketentuan-ketentuan yang diatur dalam kontrak dikatakan sebagai pihak yang cidera janji. Pihak yang melakukan cidera janji dapat menghadapi akibat hukum atas kelalaiannya, yang menurut pendapat Prof. R. Soebekti adalah sebagai berikut:

1. membayar kerugian yang diderita oleh kreditur atau dengan singkat dinamakan ganti-rugi,
2. pembatalan perjanjian atau juga dinamakan pemecahan perjanjian,
3. peralihan risiko, dan
4. membayar biaya perkara kalau sampai diperkarakan di depan pengadilan.

Pihak dapat dikatakan telah cidera janji atas kewajibannya dalam suatu kontrak apabila terhadap pihak tersebut telah menerima peringatan dari pihak lain atas kelalaiannya tersebut, sebagaimana ketentuan ini diatur dalam Pasal 1243 Kitab Undang-Undang Hukum Perdata, yang menyatakan sebagai berikut:
"*Penggantian biaya, kerugian, dan bunga karena tak dipenuhinya suatu perikatan mulai diwajibkan, bila debitur, walaupun telah dinyatakan lalai, tetap lalai untuk memenuhi perikatan itu, atau jika sesuatu yang harus diberikan atau dilakukannya hanya dapat diberikan atau dilakukannya dalam waktu yang melampaui waktu yang ditentukan."*

Mengacu kepada ketentuan dalam Pasal 1243 Kitab Undang-undang Hukum Perdata, pihak dalam suatu kontrak yang telah memberikan peringatan kepada pihak yang lalai, dapat menuntut ganti rugi, yaitu (Prof. Subekti, S.H., Hukum Perjanjian, Jakarta, Intermasa, Hlm. 47):

1. Biaya berupa segala pengeluaran atau perongkosan yang nyata-nyata sudah dikeluarkan oleh satu pihak,
2. Rugi berupa kerusakan barang-barang kepunyaan kreditur yang diakibatkan oleh kelalaian si kreditur, dan
3. Bunga berupa kelihangan keuntungan (winstderving) yang sudah dibayangkan atau dihitung oleh kreditur.

Selain itu, para pihak yang telah bersepakat atas kerugian, denda, dan bunga dalam suatu kontrak konstruksi dapat menuntut pembayaran atas kerugian, denda, dan bunga yang telah diatur pada klausul kontrak. Tuntutan terhadap pembayaran kerugian, denda, dan bunga oleh salah satu pihak terhadap pihak lain dalam kontrak konstruksi tidak menghilangkan kewajiban pihak lain untuk tetap melaksanakan prestasinya selama kontrak konstruksi tersebut masih berlaku, belum selesai, dan tidak dibatalkan.

b. Tanggung Jawab Berdasarkan Peraturan Perundang-Undangan

Para pihak yang terlibat dalam sektor konstruksi tentu perlu mengetahui batasan-batasan yang diatur dalam peraturan perundang-undangan dalam sektor konstruksi. Berikut adalah peraturan perundang-undangan yang mengatur mengenai sektor konstruksi antara lain yaitu Undang-Undang Nomor 2 Tahun 2017 tentang Jasa Konstruksi, Undang-Undang Republik Indonesia Nomor 11 Tahun 2020 tentang Cipta Kerja, Peraturan Pemerintah Republik Indonesia Nomor 22 Tahun 2020 tentang Peraturan Pelaksanaan Undang-Undang Nomor 2 Tahun 2017 tentang Jasa Konstruksi, dan Peraturan Pemerintah Republik Indonesia Nomor 14 Tahun 2021 tentang Perubahan Atas Peraturan Pemerintah Nomor 22 Tahun 2020 tentang Peraturan Pelaksanaan Undang-Undang Nomor 2 Tahun 2017 tentang Jasa Konstruksi.

Kesepakatan para pihak dalam kontrak konstruksi dapat saja bersinggungan dengan ketentuan peraturan perundang-undangan yang mengatur mengenai kesepakatan tersebut. Oleh karena itu, selain kewajiban yang telah disepakati dalam suatu kontrak konstruksi, para pihak wajib melaksanakan tanggung jawab yang diatur dalam peraturan perundang-undangan.

Sebagai contoh, seperti halnya mengenai tanggung jawab atas kegagalan bangunan yang diatur dalam Bagian Kedua Undang-Undang No. 2 Tahun 2017 tentang Jasa Konstruksi. Pasal 63 Undang-Undang No. 2 Tahun 2017 tentang Jasa Konstruksi mengatur keharusan bagi penyedia jasa untuk mengganti atau memperbaiki kegagalan bangunan yang disebabkan kesalahan penyedia jasa.

Sebagaimana telah disampaikan di awal, nilai penyelesaian proyek konstruksi pada masa Pandemi Covid-19 tidaklah baik. Berbagai larangan-larangan berkegiatan usaha dan pembatasan-pembatasan selama Pandemi Covid-19 menimbulkan konsekuensi adanya pihak yang tidak dapat melaksanakan prestasi yang diperjanjikan termasuk prestasi memberikan/menyerahkan suatu barang, berbuat sesuatu, dan/atau tidak berbuat sesuatu sebagaimana diatur dalam kontrak konstruksi. Pandemi Covid-19 juga seringkali digunakan menjadi suatu alasan bagi pihak mengenai adanya keadaan memaksa yang membuat salah satu pihak tidak dapat melaksanakan prestasi berupa pelaksanaan pekerjaan atau pelaksanaan pembayaran.

Keadaan memaksa memang diatur di dalam Pasal 1245 Kitab Undang-Undang Hukum Perdata, yaitu sebagai berikut:

"Tidaklah biaya, rugi, dan bunga harus digantinya, apabila karena keadaan memaksa atau karena suatu kejadian yang tak disengaja, si berutang berhalangan memberikan atau berbuat sesuatu yang diwajibkan, atau karena hal-hal yang sama telah melakukan perbuatan yang terlarang."

Ketentuan tersebut mengatur bahwa pihak yang tidak melaksanakan kewajibannya dibebaskan untuk memenuhi kewajibannya berdasarkan kontrak apabila terdapat keadaan memaksa. Namun demikian, perlu diperhatikan bahwa salah satu unsur agar berlakunya suatu keadaan memaksa adalah tidak ada itikad buruk

sebagaimana hal ini diatur dalam Pasal 1244 Kitab Undang-Undang Hukum Perdata. Dalam hukum Indonesia, doktrin keadaan memaksa dilaksanakan demi hukum, bukan pelaksanaan karena kesepakatan dalam kontrak. Artinya walaupun para pihak tidak secara spesifik mengatur keberlakukan doktrin keadaan memaksa dalam kontraknya, tetap saja demi hukum doktrin keadaan memaksa dapat berlaku, Ricardo M. Simanjuntak, *Teknik Perancangan Kontrak Bisnis*, Jakarta, PT Gramedia, Hlm. 203.

Tetapi dalam sektor konstruksi perlu diperhatikan ketentuan pada Pasal 47 huruf (f) Undang-Undang No. 2 Tahun 2017 tentang Jasa Konstruksi, yang menyatakan bahwa keadaan memaksa, memuat ketentuan tentang kejadian yang timbul di luar kemauan dan kemampuan para pihak yang menimbulkan kerugian bagi salah satu pihak, yang mencakup:

a. keadaan memaksa yang bersifat mutlak (absolut) yakni bahwa para pihak tidak, mungkin melaksanakan hak dan kewajibannya, dan
b. keadaan memaksa yang bersifat tidak mutlak (relatif), yakni bahwa para pihak masih dimungkinkan untuk melaksanakan hak dan kewajibannya.

Dalam penjelasan Pasal 47 huruf (f) Undang-Undang No. 2 Tahun 2017 tentang Jasa Konstruksi mengatur bahwa risiko yang diakibatkan oleh keadaan memaksa dalam sektor konstruksi dapat diperjanjikan oleh para pihak, antara lain melalui lembaga pertanggungan (asuransi). Dengan kata lain, ketentuan peraturan perundang-undangan terkait jasa konstruksi memberikan kebebasan para pihak untuk memperjanjikan siapa yang bertanggungjawab atas beban risiko yang timbul akibat keadaan memaksa, yang sejalan dengan asas kebebasan berkontrak yang dianut hukum perjanjian/kontrak di Indonesia.

Oleh karena adanya ketentuan ini, penting bagi para pihak untuk mengetahui apakah telah diatur klausul di dalam suatu perjanjian yang menyatakan pada pokoknya bahwa pandemi merupakan salah satu keadaan memaksa. Apabila telah diatur di dalam perjanjian, maka terdapat kewajiban bagi pihak yang lalai dengan menggunakan alasan Pandemi Covid-19, untuk membuktikan secara nyata akibat dari Pandemi Covid-19 tersebut. Permasalahan hukum yang timbul sejak adanya Pandemi Covid-19 dapat diselesaikan melalui forum-forum yang akan diuraikan lebih lanjut.

4 PENYELESAINA SENGKETA HUKUM KONSTRUKSI

Pasal 88 ayat 2 Undang-Undang No. 2 Tahun 2017 tentang Jasa Konstruksi mengatur bahwa para pihak dapat mengadakan kesepakatan untuk memilih tahapan upaya penyelesaian sengketa kontrak konstruksi. Pihak yang tidak dapat melaksanakan prestasinya karena keadaan Pandemi Covid-19 dapat melihat upaya-upaya yang dapat ditempuh dalam kontrak.

Para pihak dalam kontrak konstruksi penting untuk mengetahui forum dan hukum apa yang disepakati para pihak untuk digunakan dalam melakukan upaya hukum terhadap pihak yang melakukan kelalaian dalam kontrak konstruksi, seperti tidak melanjutkan pekerjaan atau tidak melaksanakan pembayaran. Pasal 88 ayat (3) Undang-Undang No. 2 Tahun 2017 tentang Jasa Konstruksi mengatur mengenai beberapa tahapan upaya penyelesaian sengketa Kontrak Kerja Konstruksi yang dapat disepakati oleh para pihak yang bersengketa, yaitu mediasi, konsiliasi, dan arbitrase, dengan rincian sebagai berikut:

a. Negosiasi
   Negosiasi sebagai sarana bagi para pihak yang bersengketa untuk mendiskusikan penyelesaiannya tanpa keterlibatan pihak ketiga sebagai penengah. Tidak terdapat prosedur baku yang harus dijalankan dalam proses penyelesaian sengketa melalui negosiasi.

   Namun demikian, kesepakatan yang dibuat dalam proses negosiasi ini tidak memiliki kekuatan memaksa untuk dilaksanakan oleh para pihak yang bersepakat di dalamnya. Karenanya, untuk kepentingan pembuktian terhadap hal-hal yang telah dibicarakan dan disepakati, para pihak yang bersengketa perlu menuangkan hal-hal yang dibicarakan dan/atau disepakati dalam suatu minuta tertulis.
b. Mediasi
   Mediasi adalah penyelesaian sengketa dengan dibantu oleh pihak ketiga (mediator) yang netral/tidak memihak. Peranan mediator adalah sebagai penengah (yang pasif) yang memberikan bantuan berupa alternatif-alternatif penyelesaian sengketa untuk selanjutnya ditetapkan sendiri oleh pihak yang bersengketa.

Prosedur penyelesaian melalui mediasi dapat dituangkan secara rinci di dalam kontrak konstruksi, termasuk mengenai jumlah mediator, pemilihan mediator, dan jangka waktu mediasi. Sama halnya dengan negosiasi, kesepakatan di hadapan mediator tidak memiliki kekuatan mengikat secara hukum.

c. Arbitrase

Para pihak perlu mengadakan kesepakatan secara tertulis apabila hendak memilih arbitrase sebagai forum penyelesaian sengketa kontrak konstruksi di Indonesia, sebagaimana hal ini diatur dalam Undang - Undang Nomor 30 Tahun 1999 Tentang Arbitrase dan Alternatif Penyelesaian Sengketa. Apabila para pihak telah mengadakan kesepakatan untuk memilih arbitrase sebagai forum penyelesaian sengketa konstruksi, maka pihak tersebut tidak dapat mengajukan tuntutan melalui forum pengadilan negeri dengan dasar gugatan cidera janji sebagaimana diatur dalam Pasal 11 ayat (2) Undang - Undang Nomor 30 Tahun 1999 Tentang Arbitrase dan Alternatif Penyelesaian Sengketa.

Pada saat para pihak mengajukan permohonan arbitrase terhadap sengketa konstruksi, maka para pihak dapat memilih arbiter untuk menyelesaikan sengketa kontrak konstruksi yang sedang dihadapinya. Putusan yang dikeluarkan yang memeriksa sengketa kontrak konstruksi bersifat *final and binding*, artinya putusan tersebut telah berkekuatan hukum tetap untuk dilaksanakan oleh para pihak.

Selain ketiga upaya penyelesaian di atas, para pihak yang hendak menuntut prestasi dalam sektor konstruksi selama masa pandemi Covid-19 ini, dapat juga melakukan upaya hukum lain, yaitu sebagai berikut:

a. Gugatan ke Pengadilan Negeri

Gugatan dapat diajukan dengan dasar adanya cidera janji atau perbuatan melawan hukum yang dilakukan oleh salah satu pihak dalam kontrak konstruksi. Namun demikian, penting bagi para pihak untuk mengetahui bahwa gugatan diajukan ke pengadilan negeri berdasarkan kompetensi relatifnya yaitu tempat tinggal tergugat (pihak yang dituntut dalam perkara) atau berdomisili hukum yang ditunjuk dalam perjanjian, sebagaimana diatur dalam Pasal 118 ayat (1) HIR. Putusan Majelis Hakim pada Pengadilan Negeri dapat dilakukan upaya hukum biasa dan upaya hukum luar biasa, yaitu banding ke Pengadilan Tinggi, kasasi dan peninjauan kembali ke Mahkamah Agung.

b. Permohonan Penundaan Kewajiban Pembayaran Utang/PKPU dan Pailit ke Pengadilan Niaga

Tentunya dengan hambatan penyelesaian atas proyek kontruksi dapat mengganggu *cash* terhadap para pihak itu sendiri, baik Pengguna Jasa maupun Penyedia Jasa. Permasalahan cash flow ini tentunya dapat berdampak juga secara sistemik kepada para pihak ketiga lainnya yang memiliki hubungan bisnis dengan salah satu pihak.

Salah satu upaya yang dapat ditempuh untuk membahas penyelesaian pembayaran adalah dengan mengajukan permohonan Penundaan Kewajiban Pembayaran Utang/PKPU ke Pengadilan Niaga. Permohonan PKPU dapat diajukan oleh pihak kreditor (pihak yang belum menerima pembayaran) maupun debitor (pihak yang harus melakukan pembayaran).

Dalam proses PKPU ini, pihak debitor dapat memberikan gambaran atas akibat pandemi Covid-19 melalui proposal perdamaian yang disusun atau melalui audit oleh ahli, untuk dapat meyakinkan kreditor menerima skema penyelesaian yang ditawarkan dalam proses PKPU. Dalam proses PKPU ini akan dibicarakan dan disepakati (atau tidak) mekanisme pembayaran yang diajukan oleh Debitor, dengan tunduk pada proses yang diatur dalam Undang-Undang Nomor 37 tahun 2004 tentang Penundaan Kewajiban Pembayaran Utang dan Kepailitan.

Pihak kreditor dan debitor juga dapat melakukan upaya hukum kepailitan. Upaya hukum kepailitan ini bertujuan agar kreditor nantinya memperoleh pembayaran melalui proses pemberesan atas harta debitor yang dilakukan oleh kurator.

Heaving Behavior of Road Embankment that Reinforced with Hybrid Pile – PVD

Ahmad
BPJN Papua Barat – Kementerian Pekerjaan Umum dan Perumahan Rakyat

ABSTRACT: Utilization of timber pile which in combination with PVD (Prefabricated Vertical Drain) – "Hybrid Pile - PVD" – is an innovation of soil reinforcement technology to increase bearing capacity at a time can be accelerate the consolidation rate. This research has showing heaving behavior at toe road embankment on soft soil that reinforced with hybrid pile -PVD. Heaving behavior is the result of numerical simulation. Subsurface soil and embankment were modeled as elastic-plastic solid materials, timber pile was modeled as spring. Geotechnical profile and sub soil properties based on soil investigation. The construction of embankment was planned on 20 m length, 30 m width, slope of 1.5 horizontal: 1 vertical, and 4.5 m of embankment high. Heaving behavior compared to variation of hybrid pile – PVD length and each stage construction. Simulation result showed that heave at toe embankment almost not occur that hybrid pile - PVD 8 meters.

Keywords: embankment, heaving, hybrid pile-PVD, numeric

1 INTRODUCTION

Along with the times, road development continues to face extraordinary challenges. This is triggered by high traffic growth, the increasing of demands society, availability of the budget that is more limited than the necessity, limited construction area, overloading and misapplication the utilization of the road. This issue demands an innovative mindset and creative action in utilizing technological developments for the sustainability of the road network. Over this issue, the road network continuous to be developed even though on soft ground area. Construction on soft ground area will be faced low bearing capacity and long process of consolidation. The fact is found in lowland area of Indonesia, is shown in Fig. 1, Atlas (2019).

Embankment construction is one method to adjust the elevation of the ground surface. The material used required to have well engineering properties so that it can be as a base layer. Applied embankment on compressible soft soil definitely consist surface settlement and consolidation as a result increased.

Recently, various technique was developed to overcome the problem of construction embankment on soft soil. Bearing capacity can be increased by stage construction, inserted pile to the soft soil, reinforced by geotextile, and other methods. Prefabricated Vertical Drain (PVD) has received recognition to overcome the problem of very thick compressible soft soil. Hybrid pile – PVD is present as an innovative technology to overcome the soft soil problem at a time.

2 LITERATURE REVIEW

The performance of embankment on soft soil it has been extensively researched through physical testing in the laboratory as well as in full-scale test. Instrumentation and observation were conducted to determine deformation behavior. Settlement plat used to monitor vertical deformation, and horizontal displacement monitored by inclinometer. In addition, embankment stability monitored by piezometer to measure pore water pressure.

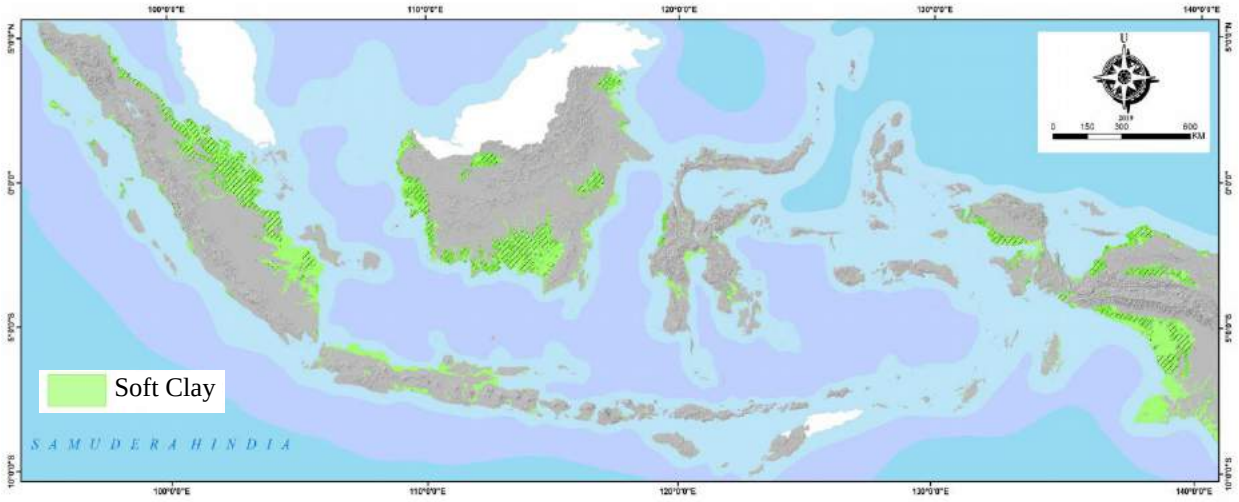

Fig. 1. Soft Clay Map, Indonesia.

Some studies reported using various type of technique to overcome conductivity (e.g. Mitchell et al. (1977); Bergado et al. (2000); Saowapakpiboon et al. (2009). Ma et al. (2009) reported that a case history of the performance of highly sensitive Ariake clay under stage constructed embankment. Practical application of the piled raft to normally consolidated clay was performed in Malaysia, Tan et al. (2004), (2005). Han et al. (2012) reported that the construction of a long railway embankment supported by the piled raft on clay deposits. Miki and Nozu (2004) conducted a design and numerical analysis of road embankment with low improvement ratio deep mixing method and showed that reduce settlement on soft ground surface more than 60% when using floating piles compared to without piles.

Sandyutama et al. (2015) was conducted three full scale trial embankments on soft soil. The first trial embankment reinforced with geosynthetics. The second trial embankment reinforced with conventional timber pile 6 m length. A reinforcement innovative was constructed the third embankment, called hybrid pile-PVD. Observation of trial embankment by using settlement plate, piezometer and inclinometer was conducted continuously for a period of 97 day. The results of study reported that trial embankment with reinforced hybrid – Pile PVD significant improvement on soft ground surface settlement and at the time can be accelerate the consolidation rate. Unfortunately, heaving at toe embankment during construction not observed.

3 METHODOLOGY

3.1 *Hybrid Pile – PVD Construction*

Road embankment planned on 20 m length, 30 m width, slope of 1.5 horizontal: 1.0 vertical, and 4.5 m of embankment high. Timber pile integrated PVD with 6 m length driven to the soft soil with square pattern a spacing 1.0 m by 1.0 m. Timber pile actually have 10 cm dia, composed of 3 timber pile fastened each other. The center part of timber pile arrangement installed PVD 10 cm width that has been rolled. There are 2-layer geotextile with Tensile Strength 52 kN/m inserted as separator between embankment and soft soil. Embankment was planned for 3 stages construction. The 1st stage constructed on 1.5 m heigh implement on geotextile layer, and the next stage added 1.5 m up to 4.5 m. Each stage construction carries out for 7 days and consolidated for 14 days. Configuration of embankment reinforced with hybrid pile – PVD shown in Fig. 2.

3.2 *Material Properties*

The properties of soil and reinforcement materials in analysis refer to result of Soil Investigation Toll Road Balikpapan – Samarinda Section 4, East Kalimantan. Hard soil is found 30 m depth underground surface. The result of borehole with Standard Penetration Test (SPT) and Cone Penetration Test (CPT) show that Fig. 3 and Fig. 4, respectively. Subsoil properties from laboratory test show that Table 1. Timber pile used have a compressive strength 23.34 kN, 10 cm dia.

Between embankment and subsoil separated by geotextile with tensile strength 52 kN/m. Soil permeability coefficient for improvement zone is used equivalent permeability coefficient.

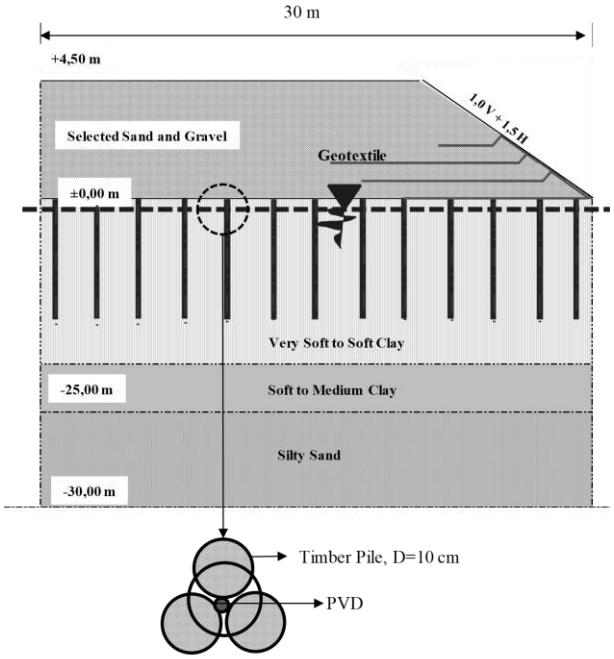

Fig. 2. Configuration of Embankment Reinforced with Hybrid Pile – PVD.

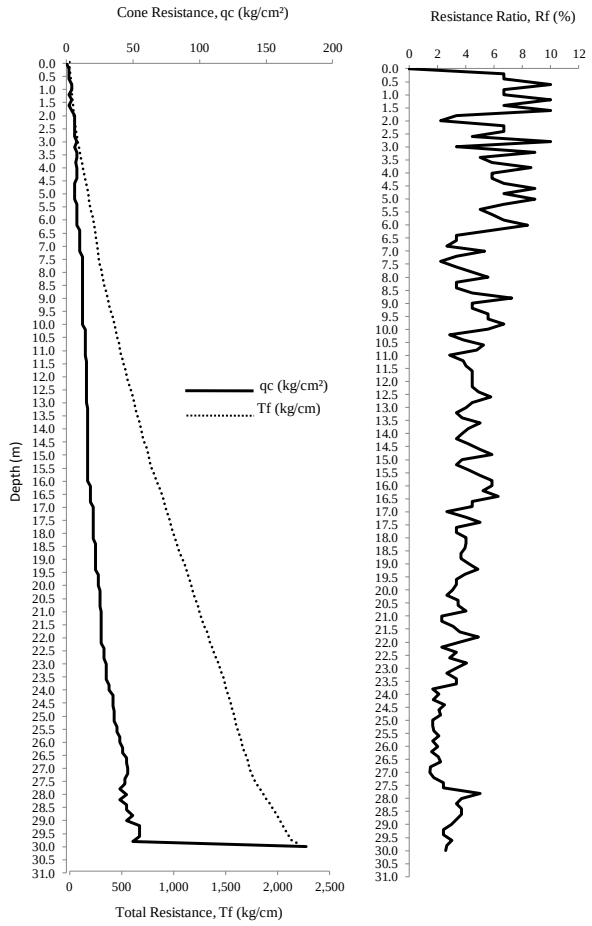

Fig. 3. The Result of Cone Penetration Test (CPT).

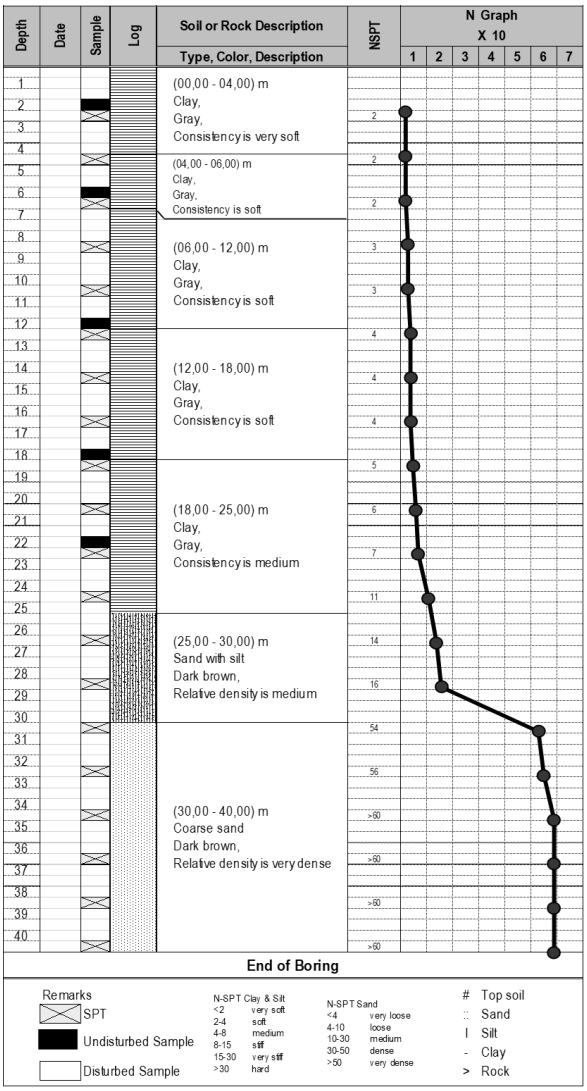

Fig. 4. The Result of Borehole with Standard Penetration Test (SPT).

3.3 *Numerical Design*

Analysis of surface settlement by numerically method based on finite element. In settlement analysis, subsoil and embankment soil was modeled as solid materials, timber pile modeled as spring, whereas behavior of solid material to embankment and subsoil modeled with elastic - plastic material. Geotextile modeled as tensile element. Failure criteria for embankment was modeled by Mohr-Coulomb with shear strength parameter (cohesion and internal angel friction), where as deformation behavior of the soil modeled using stiffness properties. Spring model for timber pile using elastic-plastic model. Elastic spring is calculated from the ultimate bearing capacity a timber pile. Constant a spring calculated by ultimate bearing capacity a timber pile divided by required settlement to mobilize pile capacity.

Table 1. Material Properties.

a. Soil Properties								
Constitutive Models		Soft Soil					Mohr Coulomb	
Soil Type		Layer 1 (00.00 – 04.00) m	Layer 2 (04.00 – 06.00) m	Layer 3 (6.00 – 12.00) m	Layer 4 (12.00 – 18.00) m	Layer 5 (18.00 – 25.00) m	Layer 6 (25.00 – 30.00) m	Fill
		Clay					Sand	Slected Sand and Gravel
γ_{unsat}	(kN/m³)	12.0	12.0	13.0	15.0	16.0	16.5	19.0
γ_{sat}	(kN/m³)	14.5	14.5	15.0	16.0	18.0	20.0	20.0
k_x	(m/day)	1.38×10^{-3}	1.38×10^{-3}	1.38×10^{-3}	1.38×10^{-3}	1.38×10^{-3}	2	2
k_y	(m/day)	6.89×10^{-4}	6.89×10^{-4}	6.89×10^{-4}	6.89×10^{-4}	6.89×10^{-4}	1	1
k_{xeq}	(m/day)	2.72×10^{-4}	7.82×10^{-3}	5.94×10^{-2}	5.94×10^{-2}	8.03×10^{-2}	-	-
k_{yeq}	(m/day)	1.36×10^{-2}	3.91×10^{-2}	2.97×10^{-2}	2.97×10^{-2}	4.02×10^{-2}	-	-
E	(kN/m²)	-	-	-	-	-	8,000	10,000
v	(-)	-	-	-	-	-	0.35	0.35
Cc	(kN/m²)	0.9	0.9	0.85	0.6	`	-	-
Cs	(kN/m²)	0.13	0.11	0.13	0.09	0.09	-	-
e_0	(-)	2.2	2.2	2.0	1.8	1.5	-	-
ϕ	(°)	5.0	8.0	12.0	14.0	16.5	30.0	33.0
c	(kN/m²)	10	12	20	25	30	1	1
b. Pile Properties								
E	(kN/m²)	948.07						
D	cm	10.00						
F_{comp}	kN	23.34						
F_{tens}	kN	0.00						
c. Geotextile Properties								
TS	(N/m)	52						
thick	mm	5						
ε_{max}	%	20						

4 HEAVING BEHAVIOR OF ROAD EMBANKMENT

Analysis by numerical methods used to observe the effect of hybrid pile - PVD length to heave as the impact of vertical settlement and lateral displacement at a certain of consolidation rate of the embankment over soft soil. Hybrid pile – PVD used have a variety of the depth 4 m, 6 m, 8 m, 12 m, 10 m, 12 m, 15 m, and 20 m. The result of analysis show that rate settlement was low if hybrid pile – PVD used the deeper and rate consolidation relatively faster (Fig. 5). Effect of the depth hybrid pile - PVD to rate consolidations compared to length various hybrid pile and relatively degree consolidations U_{R60}, U_{R80}, and U_{R90}. The U_R value defined as settlement at t time (δ_t) compared to settlement after final consolidations ($\delta_{\sim}$).

$$U_R = \frac{\delta_t}{\delta_{\sim}} \quad (1)$$

Furthermore, the result of total settlement and time consolidations is summarized in Table 2, then plotted on the graph (Fig. 6). Hybrid pile – PVD is effectively as subgrade reinforcement with length 8 m to over soft soil (25 – 30 m). The reduction of surface settlement is not significant for hybrid pile -PVD deeper than 8 m, because influence factor of embankment was low on the depth of more than 8 m.

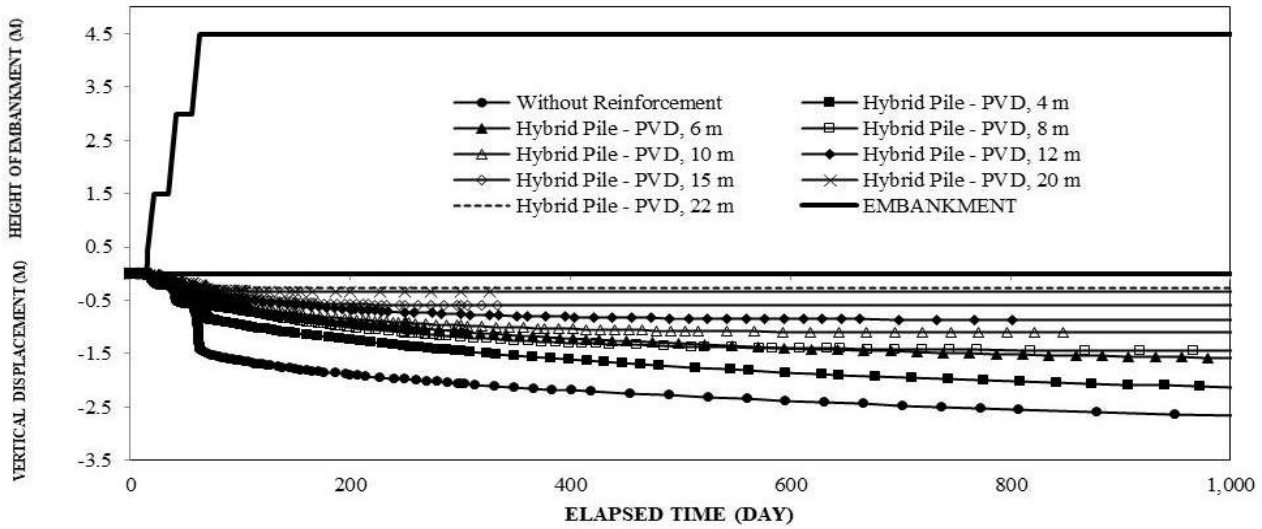

Fig. 5. Relationship Vertical Displacement vs Elapsed Time.

Table 2. Effect of the Depth Hybrid Pile - PVD to Rate Consolidations.

Reinforcement type	Total Settlement (m)			Time Consolidation (day)		
	(U_{R60})	(U_{R80})	(U_{R90})	(U_{R60})	(U_{R80})	(U_{R90})
Without Reinforcement	-1.87	-2.5	-3.12	650	737	4200
Hybrid Pile - PVD, 4 m	-1.15	-1.77	-2.33	232	513	2614
Hybrid Pile - PVD, 6 m	-1	-1.32	-1.67	200	498	2038
Hybrid Pile - PVD, 8 m	-0.86	-1.16	-1.45	145	281	1065
Hybrid Pile - PVD, 10 m	-0.65	-0.89	-1.11	114	227	848
Hybrid Pile - PVD, 12 m	-0.49	-0.69	-0.86	106	216	802
Hybrid Pile - PVD, 15 m	-0.36	-0.48	-0.6	69	113	333
Hybrid Pile - PVD, 20 m	-0.22	-0.27	-0.33	62	65	200
Hybrid Pile - PVD, 22 m	-0.19	-0.21	-0.27	43	59	128

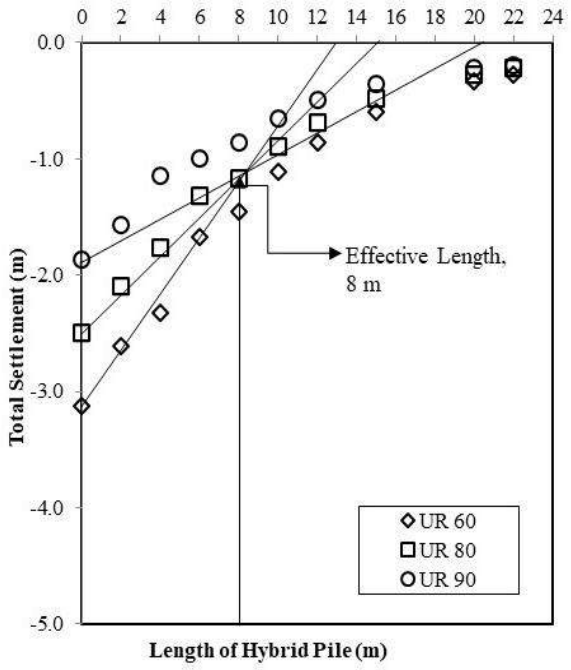

Fig. 6. Relationship Length of Hybrid pile – PVD vs Total Settlement.

Embankment without reinforcement and 4.5 m of embankment high obtained surface settlement of 3.12 m and times consolidations 4,200 days. Settlement reduction by hybrid pile – PVD occurs because the embankment load distributed by a pile and transferred to deeper layers. Load transfer is continued through skin and tip resistance pile at a time process of pore water dissipation become faster because the length of pore water flow horizontal direction become shorter and transmitted through the vertical drain (PVD).

Heaving behavior at various degrees of consolidation is presented in Fig. 7. Heaving behavior almost not occur on embankment with reinforcement hybrid pile – PVD 8 m length. Hybrid pile – PVD 8 m length able to mobilize vertical movement at the toe embankment so that the vertical settlement becomes uniform. The biggest heaving was found at embankment without reinforcement. Extreme heaving occurs at distance 2 - 5 m from toe embankment, and continues to occur at a distance of 30 m.

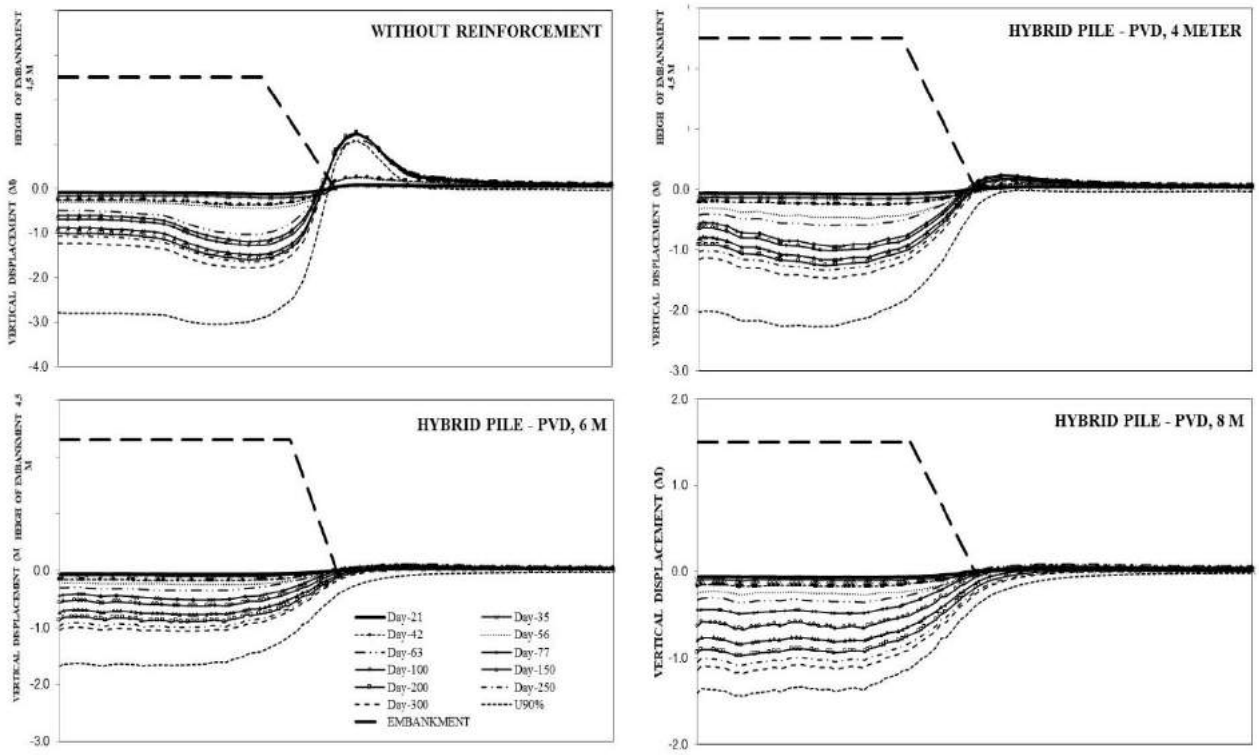

Fig. 7 Heaving Behavior at Various Hybrid Pile – PVD Length.

5 CONCLUSIONS

The bearing capacity of reinforced soil with hybrid pile - PVD are sufficient to support the 4.5 m embankment. Hybrid pile -PVD able to reduce surface settlement at a time can be accelerate the consolidation rate. The very lower of heaving for near toe embankment is indicated stability of embankment sufficient with 8.0 m hybrid pile – PVD.

REFERENCES

Atlas Sebaran Tanah Lunak Indonesia. 2019. *Badan Geologi, Kementerian Energi dan Sumber Daya Mineral*. ISBN: 978-602-9105-80-3. Jakarta.

Bergado D. T., Sasanakul I. & Lin D. G. 2000. Electro-Osmotic Consolidation of Bangkok Clay Using Coper and Carbon Electrode with Prefabricated Vertical Drain (PVD). *Proc. of Intl. Symp. on Lowland Technology*: 221-228. Japan.

Han S. GT., Song S. O. & Kim S. K. 2012. Construction of a Long Railway Embankment Supported by the Piled Raft on Clay Deposits. *Proc. of Int. Symp. on Lowland Technology*: 227-232. Japan.

Ma L., Shen S. L. & Tang X. W. 2009. Strength Increases of PVD-Improved Soft Clay Under Staged Embankment Loading. *Geosynthetics in Civil and Environmental Engineering*: 456-459.

Miki H. & Nozu M. 2004. Design And Numerical Analysis of Road Embankment with Low Improvement Ratio Deep Mixing Method. *Geo-Trans 2004. ASCE* 126(2): 1395-1402.

Mitchell J. K. & Wan T. K. 1977. Electro-Osmosis Consolidation-Its Effect on Soft Soils. *Proc. 9th Intl. Conf. of Soil Mechanics and Foundation Eng* (1): 219-224. Japan.

Sandyutama, Y., Samang, L., Imran, A.M. & Harianto, T. 2015. Study of Soft Soil Reinforcement Using Hybrid Pile - PVD. 2. ARPN *Journal of Engineering and Applied Sciences* Vol. 10: 23 – 28.

Saowapakpiboon J., Bergado D. T., Chai J. C., Kovittayanon N. & de Zwart T. P. 2009. Vacuum-PVD Combination with Embankment Loading Consolidation in Soft Bangkok Clay: A Case Study of the Suvarnabhumi Airport Project. *Geosynthetics in Civil and Environmental Engineering*: 440-449.

Suheriyatna, Samang, L., Tjaronge, M.W. & Harianto, T. 2015. Model Test of Road Embankment Reinforced by Inclined Pile on Soft Soil. ARPN *Journal of Engineering and Applied Sciences* Vol. 10 (8).

Tan Y. C., Chow C. M. & Gue S. S. 2005. Piled Raft with Different Pile Length for Medium Rise Buildings on Very Soft Clay. *Proc. Int. Conf. Soil Mech. Found. Eng* 3: 2045-2048. Osaka.

Tan Y. C., Chow C. M. & Gue S. S. 2004. A Design Approach for Piled Raft with Short Friction Piles for Low Rise Buildings on Very Soft Clay. *Proceeding of 15th Southeast Asian Geotech. Soc. Conf., Bangkok* 1: 171-176.

Comparison between Analytical Method and Finite Element Method (FEM) with three-dimensional (3D) for Road Embankment on Soft Soils Supported by Vibro Stone Columns

Zaky Prawira
PT Keller Franki Indonesia

William Chong
Keller Foundations (S E Asia) Pte Ltd

ABSTRAK: Jalan Tol Serang – Panimbang adalah proyek infrastruktur nasional yang menghubungkan Provinsi Jakarta dengan Provinsi Banten. Ditemukan 17m kedalaman tanah lunak dengan qc (CPT tahanan ujung) sekitar 0,25 MPa hingga 1 MPa di beberapa lokasi di sepanjang rencana jalan. Untuk memenuhi waktu konstruksi yang sangat ketat, dibutuhkan jenis perbaikan tanah yang telah terbukti pada proyek yang serupa, dengan demikian Vibro Stone Column dipilih sebagai metode perbaikan tanah pada proyek ini. Dalam mendisain Vibro Stone Column, metode Priebe dan Finite Element Method (FEM) merupakan metode yang sering digunakan. Jika dibutuhkan analisis sederhana untuk mengetahui penurunan terhadap waktu, maka dapat menggunakan metode Balaam – Booker. Alat instrumentasi penurunan dengan menggunakan batang pengukur dan penanda penurunan telah dipasang pada proyek ini untuk mengetahui dan memonitor performa penurunan dari perbaikan tanah dengan menggunakan Vibro Stone Column. Pada *paper* ini akan membahas mengenai perbandingan antara hasil prediksi penurunan dengan hasil pengamatan dilapangan.

ABSTRACT: Serang – Panimbang Expressway is a strategic national infrastructure project that connecting the region in Jakarta Province with Banten Province. 17m thick of Soft soils with qc (CPT tip resistance) in the range of 0,25 MPa to 1 MPa are found in several locations along the road. In order to meet the tight schedule, a historical proven technique, Vibro Stone Column has been adopted as the ground improvement solution. There are many design methods available for Vibro Stone Column design and the most used are Priebe's method and Finite Element Method (FEM). When time-dependent settlement analysis is required, Balaam-Booker method is adopted. Rod settlement gauges and settlement markers were installed in Vibro Stone Column area to monitor the performance of the treatment. This paper will discuss and compare the settlement prediction using both design method against monitored settlement results.

Keywords: Expressway, toll road, vibro stone column, soft soils, analytical method, Priebe, Balaam-booker, FEM 3D, settlement instrumentation.

1 INTRODUCTION

Serang – Panimbang Toll Road is an expressway that connects Serang and the Tanjung Lesung Tourism Special Economic Zone, Banten. The Serang–Panimbang Toll Road will also be connected to the Jakarta-Merak Toll Road.

During the construction of the 26km Serang Panimbang Toll Road, up-to 17m thick of soft clay with organic content was found at STA 20+400 to STA 20+700 chainage. Therefore, the soil improvement is needed to support the 2m to 4m height road embankment. The layout plan of the treatment area is shown in Fig. 1.

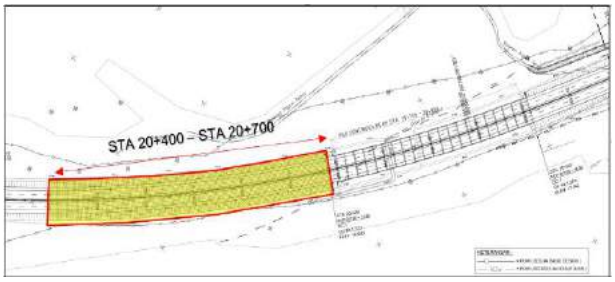

Fig. 1. Treatment Area.

To increase the bearing capacity of the soil and reduce long-term settlement with a tight

construction schedule, Vibro Stone Column (VSC) has been selected. and 19,000 linear meters of stone column had been installed in this project. Rod settlement gauge and settlement markers had been installed to monitor the performance of the ground improvement works.

There are varies design methods for ground improvement using stone column. The most commonly method are Priebe (1995) method and modelling discrete column using FEM 3D. The analytical results using Priebe's method and FEM 3D are compare with monitored results.

2 SOIL CONDITIONS

There are 2 numbers of boreholes with Standard Penetration Test (SPT) and 24 numbers of Cone Penetration Test (CPT) had been conducted in this area. The soft organic clay can be found below 1m to 2.5m below current ground level. The 6m to 18m thick of soft organic clay is having a CPT qc value of 0.25 MPa to 0.8MPa. This qc value can translate into Su of 12kPa to 40kPa. The stable soil layer is found underneath the soft organic clay with qc > 2MPa. The typical soil profile is shown in Fig. 2.

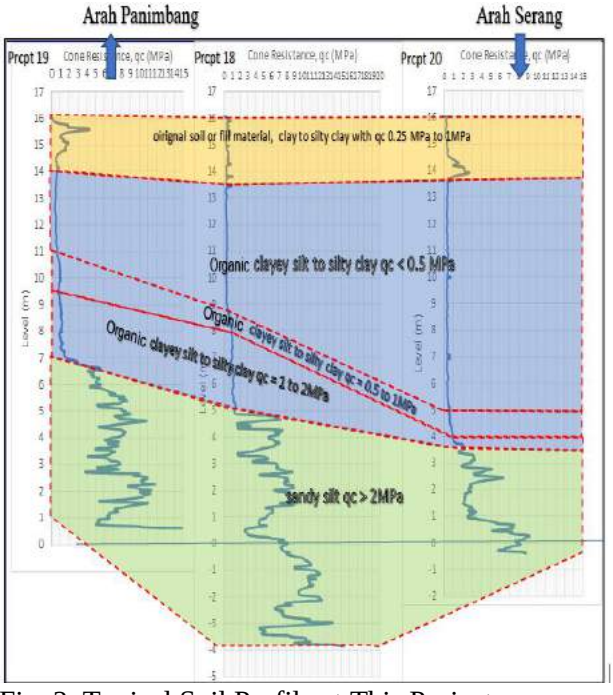

Fig. 2. Typical Soil Profile at This Project.

Table 1. shows the soil properties obtained from the CPT and soil lab samples used for design.

Table 1. Physical and Mechanical Soil Properties.

Soil Name	Fill Material Soft	Organic Soft Clay	Organic Firm Clay	Very Stiff Clay
Depth (m)	0 - 2	2 - 10.5	10.5 - 12	12 -20
Density (kN/m^3)	15	15	16	19
E_{50} (kPa)	1583	1888	9882	93724
E_{oed} (kPa)	1267	1510	7906	74979
E_{ur} (kPa)	3800	4531	23717	224937
m	1	1	1	1
S_u(kPA)	12.5	15	50.0	250.0
K (m/s)	$1x10^{-10}$	$1x10^{-10}$	$1x10^{-10}$	$1x10^{-10}$

3 GROUND IMPROVEMENT DESIGN

Road embankment design typically require to checks the road embankment settlement and slope stability. The cross section of the vibro stone column at the instrumentation location is as shown in Fig. 3. The in-plane vibro stone column spacing is in the range of 2.2m to 2.8m. The stone column diameter in the soft clay is 1.0m diameter. For design optimization, long stone column is installed at the main carriageway for settlement reduction while short stone column is installed beyond the slope stability slip circle to enhance the shear strength of the soil.

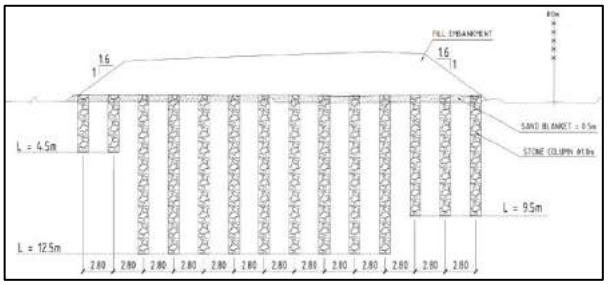

Fig. 3. Cross Section of Installed Vibro Stone Column.

Finite Element Method (FEM) 3D is carried out by using Plaxis 3D software. The stone column is modeled as individual columns, as shown in Fig. 3 to predict the slope stability and the settlement vs time behavior.

Limit Equilibrium Method (LEM) analysis is done using SlopeW for slope stability. Total settlement of the embankment is done using 1-Dimensional Consolidation settlement with Boussines stress distribution. The improved ground parameters are adopting Priebe's composite properties. The time-dependent behaviour due to consolidation is using Balaam and Booker (1981) approach.

The Priebe's composite properties are derived from Priebe's improvement factor. Priebe introduces n_1 and n_2 improvement factor where n_1 improvement factor is recommended for slope stability analysis while n_2 for settlement analysis. The reinforcing soil with VSC will have an increment of the soil properties compare with ground without ground improvement.

3.1 *Vibro Stone Column dry bottom feed method*

Within the high water level at site, dry bottom feed method is used for this project. Dry bottom feed Vibro Stone Column (VSC) is a technique to construct underground columns which using rough materials in form of stone as a filler. VSC construction which is used is bottom feed method (dry method) where the stones are distributed through the stone tube to and flowed out through the probe tip to surrounding soil layers. This method is called bottom-feed method. Work illustration scheme is shown in Figure 4.

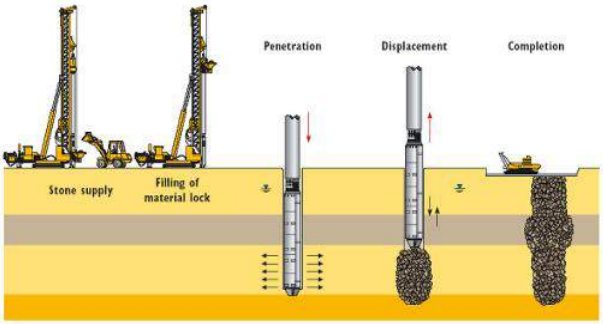

Fig. 4. Dry Bottom Feed Installation Method.

With using the dry bottom feed method, individual stone column for FEM 3D analysis, can use the density = 19 kN/m^3, friction angle (Ø) = 42^0, Young Modulus = 120 MPa and permeability, K = 0.864 m/day.

For LEM analysis, Priebe's composite properties are tabulated in Table 2**.**

Table 2. Composite Parameter.

Depth	Composite Parameter, n_1			Composite Parameter, n_2		
	phi_1	c_1	E_{oed1}	phi_2	c_2	E_{oed2}
m	[°]	kPa	mPa	[°]	kPa	mPa
0.0-2.0	20.8	7.2	2.0	22.5	6.8	2.1
2.0-10.5	20.8	8.7	2.4	30.8	5.1	4.0
10.5-12.0	24.2	27.5	13.0	31.8	19.1	18.7

Refering to Ng and Tan (2015), composite permeability can be determined from the area replacement. For this project is used composite permeability, $K_{composite}$ = 0.02 m/day.

Keller had developed own equipment to carry out dry bottom feed installation method in a faster and safe manner. Figure 5 is showing Keller's equipment working in this expressway construction site.

Fig. 5. Keller Installing Stone Column in Paddy Field.

3.2 *Embankment Settlement and Time Rate Consolidation Comparison*

The total settlement prediction using FEM 3D predict a higher settlement than using Priebe's composite parameters. The comparison of these two methods are shown in Fig. 6.

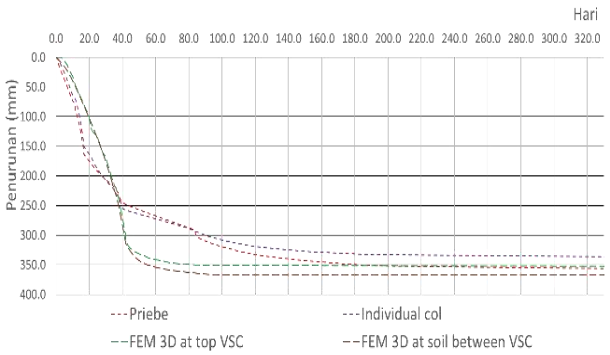

Fig. 6. Settlement Analysis Results Priebe vs FEM 3D.

The result of analyses predicted a maximum total settlement using Priebe ranges between 335mm at the top of the stone column (individual column) and 356mm at the topsoil between the stone column (Priebe). FEM 3D gives the settlement results at the top of the stone column at 351mm, and the soil between the stone column is 366mm. Thus, the

settlement magnitude is given a close result between Priebe and FEM 3D.

The major different between these two methods is predicting the time rate settlement. Consolidation settlement is faster in FEM 3D model. This is probably due to FEM 3D is based on ideal situation while Balaam-Booker method is derived from field test results.

3.3 *Embankment Stability Comparison*

Slope stability analysis were carried out using Morgenstern-Price's equilibrium included in SlopeW. Plaxis 3D using Phi-C reduction method for slope stability. The results of slope stability using LEM and FEM 3D are presented in Fig. 7 and Fig. 8, respectively.

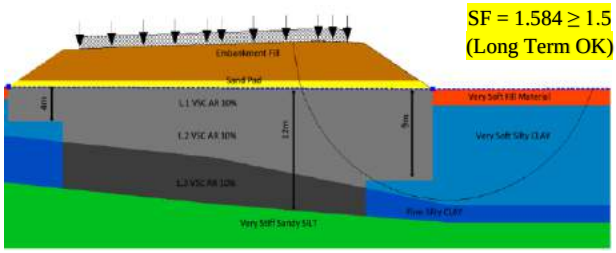

Fig. 7. Embankment Stability by SlopeW.

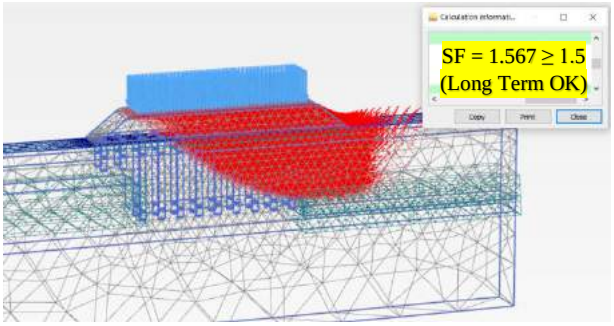

Fig. 8. Embankment Stability by FEM 3D.

Both modelling predict similar factor of safety for long term slope stability. The slip circle shape is different. This is probably due to the untreated soil drainage type used in FEM 3D. The drainage type for the untreated soil is adopting Undrained B. This drainage type is using undrained shear strength as their shear parameter. Therefore, there will be no gain of strength is considered.

4 SETTLEMENT MONITORING

There are four numbers of rod settlement gauges and two settlement markers installed in this project. The position of the instrument is shown in Fig. 9. Unfortunately, there are two gauges being damage during embankment construction. This instrumentation monitoring monitored the settlement performance within around 350 days from first day of embankment filling works.

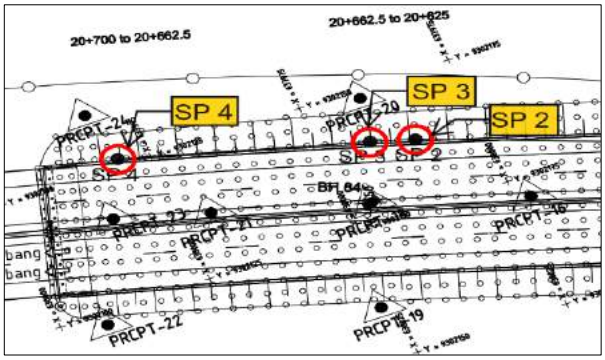

Fig. 9. Settlement Plate Location.

The monitored settlement was lower than predicted settlement.

Taylor's square root of time fitting method is adopted to assess the in-situ degree of consolidation. Fig. 10 showing the plots for SP-3 with square root of time on the x axis and settlement on the y axis.

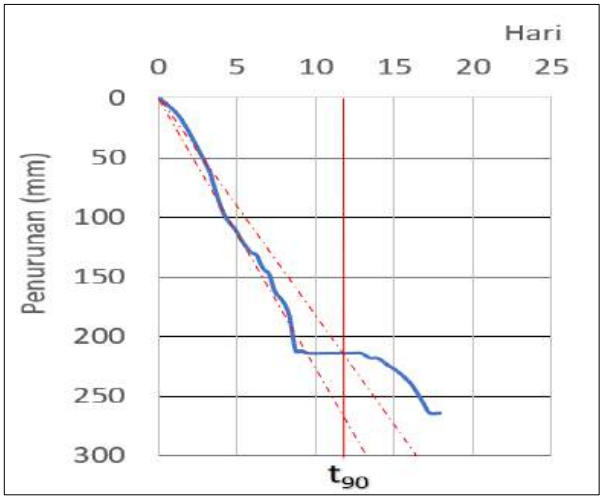

Fig. 10. Estimate of 90% consolidation time using Tylor square root of time fitting method

From the plots it can be inferred 90% degree of consolidation has taken place 60 days after completion of embankment construction. The settlement results comparison between monitoring data and prediction are presented in Fig. 11.

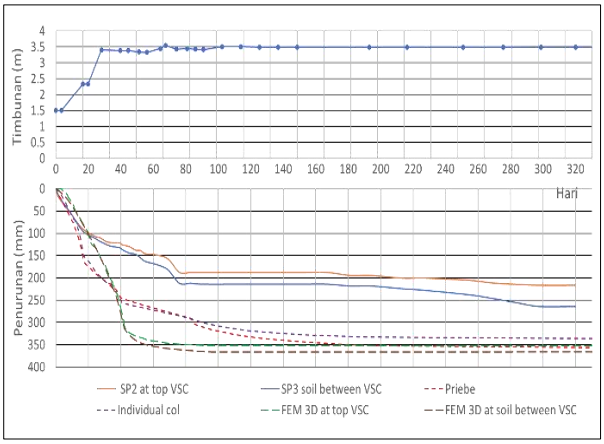

Fig. 11. Embankment Height and Settlement versus Time Plot.

When the embankment fill reaches the maximum height of 3.5m, the settlement measured is in the range of 217mm to 264mm. Most settlement took place during embankment construction and pavement construction works.

After 300 days, the rate of settlement is stabilized. The time rate settlement using Balaam-Booker and total settlement prediction using Priebe's composite parameter and FEM.

3D methods are generally larger than the monitored data. However, the time rate settlement prediction using Balaam-Booker have the closest gradient with the monitored data.

5 DISCUSSION & CONCLUSION

Vibro Stone Column has proven to be an effective method of treating the deep soft soil. Where technically feasible, it has proven to be an economical alternative to conventional solutions such as piling.

Both FEM 3D and LEM using Priebe's composite parameters are proven design method for vibro stone column design. Balaam-booker method can be adopted for time rate settlement prediction. Both methods give a safe design approach to vibro stone column design. The biggest advantage of using Priebe's composite parameter are the speed of analysis comparing with FEM 3D due to no meshing and not a FEM analysis.

Due to the difference of analysis results between modeling with monitored data, it is possibly caused by many factors. One of the factors that may be subjected to the soil properties input is slightly conservative. Further study needs to be detailed in determining the soil parameter.

The expressway is already completed. Fig. 12 is showing the completed road embankment.

Fig. 12. Completed Expressway.

REFERENCES

Balaam, N.P. and Booker, J.R. 1981. Analysis of Rigid Rafts Supported by Granular Piles. *International Journal for Numerical and Analyitical Method in Geomechanics* Vol 5: 379-403.

Ng, K.S., Tan, S.A. 2015. Simpified Homogenization Method in Stone Column Designs. *Soil and Foundations* 55(1): 154-165.

Priebe, H.J. 1995. The Design of Vibro Replacement. *Ground Engineering*: 31-37.

Raju, V.R., Masud, A. and Ha, P. 1997. Vibro Replacement – A Technique for Extensive Ground Improvement works in Very Soft Cohesive soils at the Shah Alam Expressway. *4th Geotechnique Colloquium*. Darmstadt, Germany.

Raju, V.R., Yee, Y.W., Sreenivas P., and Tam, E. 2004. Vibro Replacemet for the construction of a 15m high Highway Embankment over a Mining Pond. *Malaysian Geotechnical Conference*. Kuala Lumpur, Malaysia.

Znamenskii, V.V., Sayed, D.A. 2019. Comparison Between Analytical Method and Numerical Model for Footings on Soft Clay Supported by Stone Colom.

Performance of Axial Bearing Capacity for Cement-Fly Ash-Gravel (CFG) Piles from Static Loading Test Results

Eyrton Crismartua Silaban
Sr. Geotechnical Engineer – PT WSP Engineering

I Wayan Sengara
Professor, Faculty of Civil and Environmental Engineering – Institute Technology Bandung

Dwi Ari Hidayat
Subgrade Engineeer – CARS-Dardela Joint Operation

ABSTRAK: Tanah lempung lunak adalah masalah yang sering ditemukan di Indonesia. Sudah banyak metode perbaikan tanah yang ditemukan akhir-akhir ini. Solusi metode perbaikan tanah yang tergolong baru di Indonesia adalah dengan tiang CFG. Kontraktor memilih metode ini karena pemasangannya yang praktis dan mampu mengontrol kualitas material beton secara real-time. Selain kualitas material beton, performa tiang CFG biasanya dikontrol dari hasil static loading test (SLT) berupa kapasitas daya dukung aksial. Paper ini bertujuan untuk membandingkan hasil static loading test terhadap panjang dan jenis tanah yang diperbaiki. Meskipun konsultan desain biasanya sudah menentukan kapasitas melalui rumus empiris, maka perlu suatu tinjauan untuk memverifikasi hasil hitungan tersebut karena karakteristik tanah yang unik dan bervariasi. Di akhir makalah, disajikan suatu *best practice* penentuan kapasitas aksial tiang CFG dengan variabel panjang tiang, jenis tanah, dan nilai NSPT tanah yang diperbaiki. Kajian ini diharapkan menyempurnakan perhitungan daya dukung dan efisiensi panjang tiang CFG di masa mendatang.

Kata Kunci: lempung lunak, tiang CFG, kapasitas daya dukung aksial, static loading test

ABSTRACT: Soft clay is a common problem in Indonesia. Recently there have been relatively new soil improvement methods; one of them is CFG piles. The contractor chooses this method because of practical installation and real-time quality control of the concrete material. In addition to the quality of the concrete material, the performance of CFG piles is usually controlled from the results of the static loading test (SLT) in the form of axial bearing capacity. This paper aims to compare the results of the static loading test on length and type of improved soil. Although design consultants usually determine capacity through empirical formulas, a review is needed to verify the calculation results due to the unique and various characteristics of the soil. At the end of the paper, the paper will present a best practice for determining the axial capacity of CFG piles with variable pile length, soil type, and the NSPT value of the improved soil. This study is expected to improve the calculation of bearing capacity and efficiency of the CFG pile length in the future.

Keywords: soft clay, CFG pile, axial bearing capacity, static loading test

1 INTRODUCTION

The total length of the Jakarta-Bandung High-Speed Railways (Jakarta-Bandung HSR) project is 142.273 kilometers. The length of the subgrade is 44.722 kilometers (accounting for 31.43%). Embankment slope protection, cutting slope protection, soft soil, loose soil subgrade, and pile wall are some of the most common types of special subgrade. Soft soil is almost spread evenly over the subgrade embankment along this subgrade.

Recently there have been relatively new soil improvement methods named CFG piles. The contractor chooses this method because of practical installation and real-time quality control of the concrete material.

Application of Cement-Fly Ash-Gravel Pile technology as soil improvement is the first to be implemented in Indonesia through the Jakarta-Bandung High-Speed Railways project. The Chinese introduce this method/technology as the designer consultant and contractor. Cement-Fly Ash-Gravel Pile was developed based on

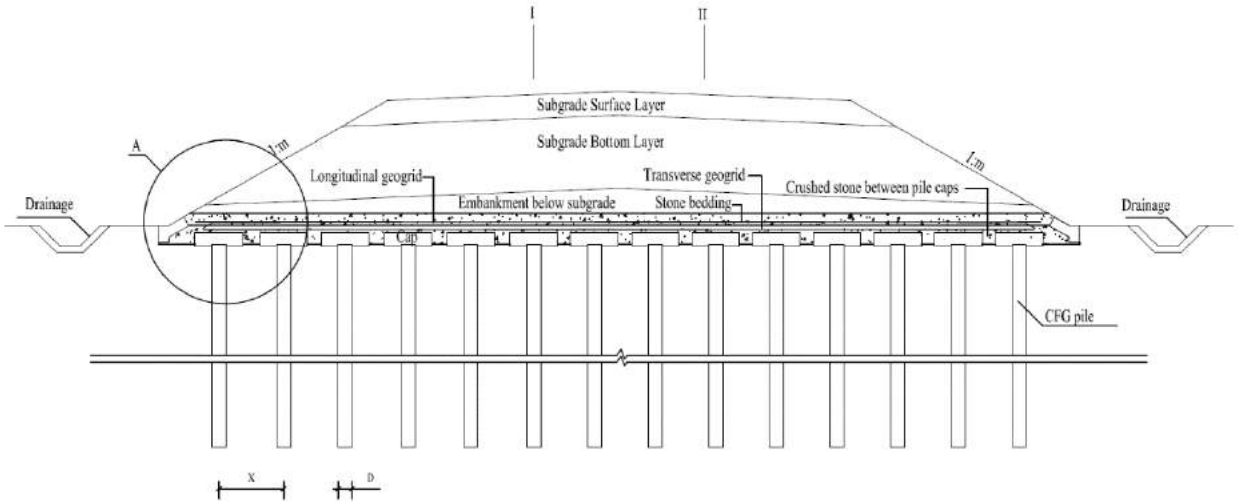

Fig. 1. Standard Cross-Section of CFG Pile.

the stone column method as rigid inclusion in soil improvement methods.

2 GEOLOGICAL CONDITIONS ALONG JAKARTA-BANDUNG

Lacustrine, alluvial, alluvial-diluvial, and residual loose accumulation formations cover the intermountain basins, plains, and mild slopes before the hills. The lithologic characters are cohesive soil, silt, sludge, mucky soil, sand, and gravel soil. Volcanic sediment covers much of the hilly and low mountain areas, with alluvial-diluvial, drift-diluvial, drift, and residual deposits revealed somewhere.

The lithologic characters are mainly composed of cohesive soil, silt, gravel soil, and sandy soil featured with deep and various thicknesses of overburden layer and exhibit expansibility, semi-diagenesis, and semi-cementation somewhere.

Underlying strata are Cenozoic Tertiary intermediate-basic volcanic and sedimentary rocks with the relative complexity of rock types and bedrock emerging somewhere. The volcanic rock varies significantly due to the different eruption results. The sedimentary rocks are dominated by Tertiary sandstone, mudstone, shale, tuff, marlstone, tuffaceous sandstone, tuffaceous conglomerate, limestone, volcanic breccia; the volcanic rocks include andesite and basalt, which are locally distributed only.

Along HSR mainline, much soil is not classified as soft soil in the alluvium and Volcanic deposit. But the basic bearing capacity of the soil is so low that its subsidence can't meet the engineering requirements. The soil should be surveyed and designed as loose soil.

3 DESIGN CRITERIA

It is necessary to test the CFG once it has been completed. The test includes the low strain on the pile body quality and the static load test to test the bearing capacity of the single pile:

1. After 28 days of pile formation, the static loading test of the single pile of composite foundation shall be carried out; the number is 2% of the total number of the pile and not less than 3.
2. Low strain detection is carried out within seven days after pile formation; the number is 10% of the total number of piles and not less than 3. For the unqualified, it is necessary to do a core inspection.

Based on TB 10106-2010 about Technical Code for Ground Treatment of Railway Engineering stated that the check and calculation of the single pile bearing capacity of the foundation treatment structure should meet the below requirement:

1. The allowable vertical bearing capacity of a single pile [P] should meet the requirements of the following formula:

$$P_0 \leq 1/\varphi\,[P] \qquad (1)$$

Where:

P_0 = The subgrade, track structure, and trainload within the range of single pile reinforcement (kN).

[P] = allowable vertical bearing capacity of a single pile (kN).
φ = The utilization factor of single pile bearing capacity, which is 0.9~1.0.

2. The single pile load test data can be used to value the allowable vertical bearing capacity of a single pile [P]. The value of a single pile's vertical ultimate bearing capacity is divided by the **safety factor 2**.

4 SITE CONDITION

The project site mainly consists of alluvium and volcanic deposits with a soft consistency. This study found that some sites have a soft consistency from the borlog. This condition needs to be treated to increase the bearing capacity. The soil investigation results showed that the NSPT range of improved soil with CFG piles is from 1-20, as shown in Fig. 2.

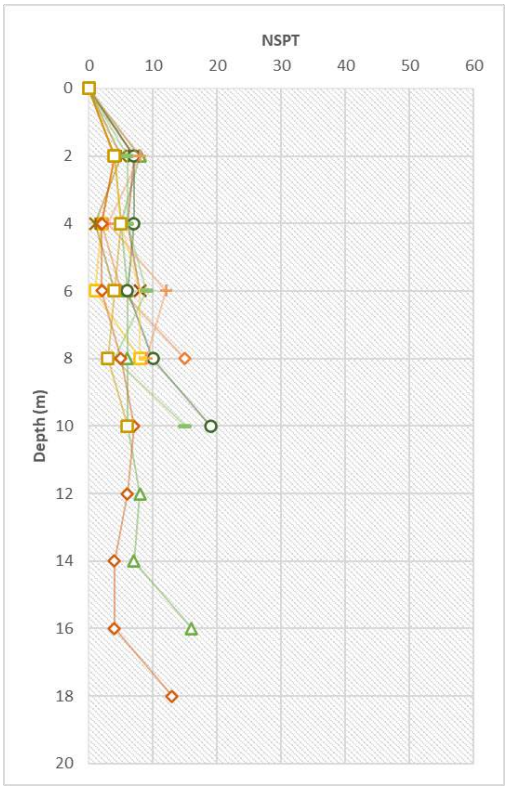

Fig. 2. NSPT Value vs. Depth from Improvement Area of CFG Pile.

5 RESULTS AND DISCUSSIONS

Based on Technical Code for Ground Treatment of Buildings (JG 79-2012), the composite ground bearing capability of cement-fly ash-gravel pile and plain concrete pile shall be determined by on-site composite ground load test. In design, it can be calculated:

$$R_a = u_p \sum_{i=1}^{n} q_{si} l_i + q_p A_p \quad (2)$$

where R_a is the vertical bearing capacity eigenvalue of the single pile, kN; u_p is the pile perimeter, m; n is the soil layers divided along with the pile; q_p and q_{si} are the shaft resistance eigenvalue of the i layer in lateral pile-soil and tip resistance eigenvalue of pile respectively, kPa; l_i is the thickness of the i-layer soil, m.

This calculation is based on the parameters of the shear strength parameters of sand or clay. Based on Chinese Standard, JG 79-2012, the qsi and qp values are only based on the empirical relationship between the physical index properties of the soil and the basic bearing capacity parameter ((0). There is no additional section on how to determine the values of q_{si} and q_p. As a result, the results of the static load test with ultimate bearing capacity data will be used to evaluate the performance of the CFG pile in this study.

Fig. 3 shows an overview of analysis performance of different locations in Jakarta-Bandung HSR subgrade based on several pile capacity analyses and the results of static load testing of CFG piles with 500 mm diameter. Each axial pile load test result is analyzed using three (3) methods: Chin, Davisson, and Mazurkiewicz.

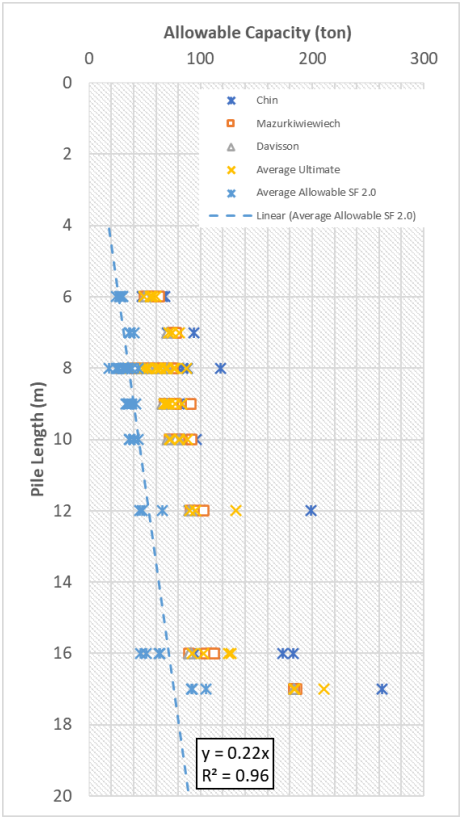

Fig. 3. Analysis and Performances Consist of Several Sites in Jakarta-Bandung HSR Subgrade for CFG Pile with 500 mm Diameter.

Fig. 4 shows the proposed coefficients as the best practice for calculating the CFG pile bearing capacity with variable shear strength, diameter, and pile length. As an assumption that is calculated assuming only the friction bearing capacity works. The friction bearing capacity equation adopted from the calculation of the bearing capacity of the bored pile is as follows:

$$Q_s = \alpha . C_u . L_i . p \quad \text{(kPa)} \qquad (3)$$

Where α is the proposed coefficient of friction bearing capacity of CFG pile; Cu is the undrained cohesion; Li is the length of improved soil layer; p = pile perimeter. Then, the correlation implemented for the value of undrained cohesion in the above equation adopts C_u = 6 x N-SPT$_{average}$ (kPa).

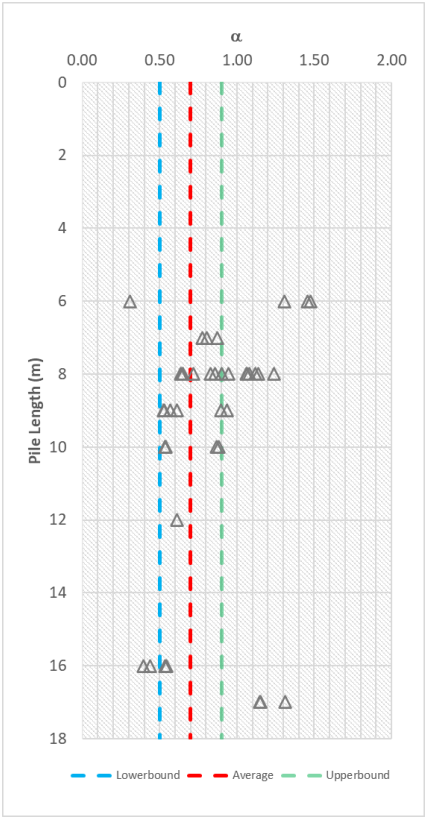

Fig. 4. Proposed Coefficient of Friction Bearing Capacity of CFG Pile vs. Depth.

6 CONCULDING REMARKS

Based on the soil investigation data collection for subgrade embankment area project, the CFG pile improvement was implemented for the NSPT value within the range of 1-20 to increase the subgrade bearing capacity.

Based on the analysis on performance review of the CFG pile system, this study proposed prediction formula for the bearing capacity of the CFG pile depth with the following equation:

$$Q_a = 0.22 * L \qquad (4)$$

where Q_a is the allowable bearing capacity and L is the length of the CFG pile.

Furthermore, by considering the shear strength of clay, this study likewise has provided new findings on the proposed coefficient of unit skin frictions (α) of the soft clay layer improved by the CFG pile. The proposed range value of α value is 0.5-0.9.

7 ACKNOWLEDGEMENTS

The authors are thankful to Mr. Suryanto Supardi and Prof. Adang Surahman from CDJO for moral and technical support until the paper is completed. Special thanks to Mr. Rachman Suhanda as General Manager Technical/Design Management of KCIC for sharing geotechnical data testing and reports related to this paper. Lastly, the authors would like to express their gratitude to KCIC and HSRCC for sharing some geotechnical data and preliminary information.

DAFTAR PUSTAKA - REFERENCES

Chen, Q., Zhao, M., Zhou, G., Zhang, Z. 2008. Bearing Capacity and Mechanical Behavior of CFG Pile Composite Foundation. *J. Cent. South Univ. Technol* 15(S2): 045−049.

Silaban E.C., Sahadewa A., Aprilianti. 2019. Bearing Capacity Calculation of Cement-Fly Ash-Gravel Pile in HSR Jakarta-Bandung. *Proceeding Annual National Conference on Geotechnical Engineering HATTI XXXIII*. Jakarta.

SNI 8460:2017. 2017. *Persyaratan Perancangan Geoteknik*. Badan Standardisasi Nasional.

TB 10106-2010. 2010. *Technical Code for Ground Treatment of Railway Engineering*. Beijing: China Railway Press.

Terzaghi, K. dan R. B. Peck. 1967. *Soil Mechanics in Engineering Practice*. John Wiley and Sons.

Tomlinson, M.J. 1970. Adhesion of Piles in Stiff Clay. *CIRIA Report* 26. London.

Wang, W., Feng., Li. 2013. Analysis on Bearing Capacity of CFG Pile Composite Foundation in Baotou. *Applied Mechanics and Materials* Vols 353-356:337-340. Switzerland: © Trans Tech Publications.

Sengara, I.W. 2015. *Keynote Speaker Annual National Conference on Geotechnical Engineering HATTI XIX*. Jakarta.

Numerical Modeling of Soil Improvement Using Vacuum-Preloading Method with Finite Element Program: A Case Study of Vacuum System Utilization in Kendal, Central Java, Indonesia

Utama Nusanegara
Bandung Institute of Technology

Endra Susila
Bandung Institute of Technology

Hartanto Legowo
PT Geostructure Dynamics

ABSTRACT: This paper discussed about soil improvement modeling using finite element program (ABAQUS) for vacuum-preloading method. Field monitoring data that was used as a review is Kendal Industrial District Vacuum Project, Central Java. Modeling was done in three conditions such as axisymmetric, single drain plane strain, and multi drain plane strain. Result from modeling was compared with field monitoring data (settlement plate, vacuum gauge, and SPT). Soft clay is modeled using Modified Cam Clay. Soil behavior analysis in this paper consists of settlement, pore water pressure, and gained strength after soil improvement using vacuum-preloading method. Furthermore, analysis of vacuum pressure distribution in PVD and relationship between vacuum duration with the increased in soil effective stress was carried out in this paper. The modeling results from ABAQUS produced predictions that was close to field measurements.

Keywords: ABAQUS, vacuum, PVD, soft clay, soil behavior.

1 INTRODUCTION

Urbanization in the current era makes infrastructure development increases rapidly. Construction is carried out on various types of soil. Soft soil is one of the most frequently encountered soils in Indonesia. Problem that often arises in construction on soft soil is large settlement because it has low bearing capacity and high compressibility.

It is necessary to improve the soil to prevent problems during construction and after the infrastructure has been built. Soft soils tend to have low permeability, so it takes a very long time to reach the desired degree of consolidation.

There are several techniques used to speed up the consolidation process such as sand drains, stone column, sand compaction piles, and PVD (Prefabricated Vertical Drain). The consolidation process will occur if there is a load on the soil. Vacuum method, Kjellman (1952) is an alternative solution that can be used to improve soft clay soils.

Vacuum preloading method is used in soil improvement project of Smart Ecoland Company. Vacuum method modeling that combined with pre-load embankment will be performed using finite element program (ABAQUS). Result from modeling will be compared with the monitoring data obtained in the field such as settlement plate and SPT. Comparison is used as a verification of soil improvement modeling using ABAQUS.

Sources for analysis were obtained from Geostructure Dynamics Company. The data consists of soil investigation and monitoring data. In addition, vacuum pressure distribution in PVD and relationship between vacuum duration with the increase of soil effective stress was carried out in this paper.

2 TWO-DIMENSIONAL VERTICAL DRAIN MODELING

Multi drain modeling often uses two-dimensional plane strain to simplify the model. It is necessary to have plane strain equivalence with axisymmetric values to obtain realistic results in two-dimensional modeling. Vertical drain is axisymmetric in shape which has a symmetrical shape about an axis.

Indraratna and Redana (1997) stated several ways to achieve the equivalence, (1) geometric matching-the drain spacing is matched while maintaining the same permeability coefficient; (2) permeability matching-the coefficient of permeability is matched while keeping the same drain spacing; and (3) a combination of (1) and (2) with the plane strain permeability calculated for a convenient drain spacing.

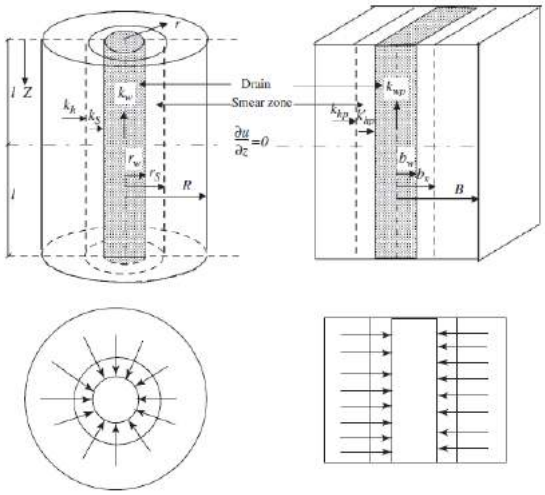

Fig. 1. Conversion of an Axisymmetric Unit Cell into Plane Strain Condition, Indraratna and Redana (1997).

Indraratna and Redana (1997) converted the vertical drainage system with permeability matching. Permeability equivalence of the model can be determined from the following equation.

$$k_{hp} = \frac{k_h\left[\alpha+\beta\times\frac{k_{hp}}{k'_{hp}}+\theta\left(2lz-z^2\right)\right]}{\left[\ln\left(\frac{n}{s}\right)+\left(\frac{k_h}{k'_h}\right)\ln(s)-\frac{3}{4}+\frac{\pi(2lz-z^2)k_h}{q_w}\right]} \quad (1)$$

The geometric parameters α, β, θ are defined as follow.

$$\alpha = \frac{2(n-s)^3}{3(n-1)\,n^2} \quad (2)$$

$$\beta = \frac{2(s-1)\times\left[3n(n-s-1)+\left(s^2+s+1\right)\right]}{3(n-1)n^2} \quad (3)$$

$$\theta = \frac{\pi\, k_{hp}}{q_w}\left(1-\frac{1}{n}\right) \quad (4)$$

A new equation is obtained by substituting Eqn. (2), Eqn. (3), Eqn. (4) into Eqn. (1), which is the ratio between the permeability coefficient of the undisturbed area under plane strain conditions and the permeability coefficient of the smear zone area under plane strain conditions.

$$\frac{k_{hp}}{k'_{hp}} = \frac{\frac{k_{hp}}{k_h}\left[\ln\left(\frac{n}{s}\right)+\frac{k_h}{k'_h}\ln(s)-0.75\right]-\alpha}{\beta} \quad (5)$$

The definition for each variable, k_{hp} = permeability of the undisturbed area under plane strain condition, k'_{hp}= permeability of the smear zone area under plane strain condition, k_h= permeability of the undisturbed area under axisymmetric condition, k'_h = permeability of the smear zone area under axisymmetric condition.

Formula proposed by Indraratna (2005) for undisturbed soil is as follow.

$$\frac{k_{hp}}{k_h} = \frac{0.67\times\frac{(n-1)^2}{n^2}}{\ln(n)-0.75} \quad (6)$$

3 DEGREE OF CONSOLIDATION

Degree of consolidation as an important parameter in evaluating the effectiveness of soil improvement especially for vacuum method. It is a ratio between settlement at a period compared to the total settlement. For soil improvement project, the total settlement is not known yet, so it needs to be predicted. There are two methods commonly used in determining the degree of consolidation.

3.1 *Interpretation based on pore pressure*

An alternative way to determine the degree of consolidation based on pore water pressure is the idea proposed by Chu and Yan (2005). Pore water dissipation ratio can be calculated by comparing the initial pore water pressure with the pore water pressure at a certain time. The formula for calculating the average degree of consolidation as follows.

$$U_{avg} = 1 - \frac{\int [u_f(z) - u_s]\, dz}{\int [u_o(z) + \Delta\sigma - u_s]\, dz} \quad (7)$$

The definition for each variable, $u_o(z)$ = initial pore water pressure, $u_r(z)$ = final pore water pressure, $u_s(z)$ = suction line.

3.2 *Interpretation based on settlement*

Estimation of total settlement by graphical method was proposed by Asaoka in 1978. It helps to predict the possibility of future settlement. The equation for the Asaoka method as follows.

$$p_i = \beta_o + \beta_1 \times p_{i-1} \quad (8)$$

$$p_f = \beta_o/(1 - \beta_1) \quad (9)$$

The definition for each variable, p_i = settlement at t_i, p_f = total settlement, β_o and β_1 are constants that depend on the observed data.

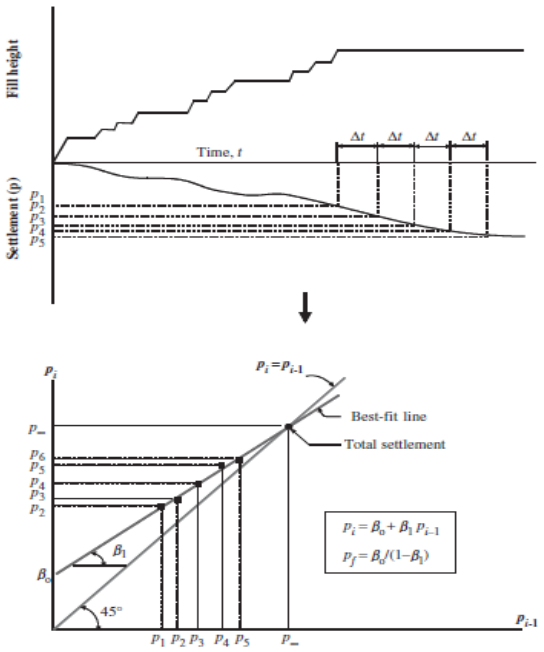

Fig. 2. Asaoka Graphical Method, Asaoka (1978).

The horizontal axis on the graph represents the observations in the previous time and the vertical axis represents settlement in present. Intersection between the linear line and the dots is the result of the ultimate settlement.

4 CASE STUDY

4.1 *Project Description*

The vacuum project is located at Kendal Industrial Park, Central Java. The project was conducted in August 2018 and ended in April 2019. Composition of subsoil is dominated by normally consolidated soft clay. The project used vacuum preloading with geomembrane system and PVD below the geomembrane. PVD were installed in square pattern with 1 meter spacing.

Table 1. Soil Parameters from Geostructure Dynamics Soil Investigation.

Depth (m)	0-2	2-5	5-8	8-20	20-25
Soil Type	Clayey Sand	Clay	Sandy Silt	Clay	Clay
N-SPT	13	7	7	2	8
e_o	0.8	2.37	2.35	3.71	1.4
γ_{sat}	15.5	14.7	13.79	13.43	18
Cc	-	0.63	0.772	0.445	1.299

Several instrumentations were placed in the improvement area to monitor the project for 238 days. Instruments that were used in this project are settlement plate and vacuum gauge. SPT is also conducted before and after the improvement to check the gained strength.

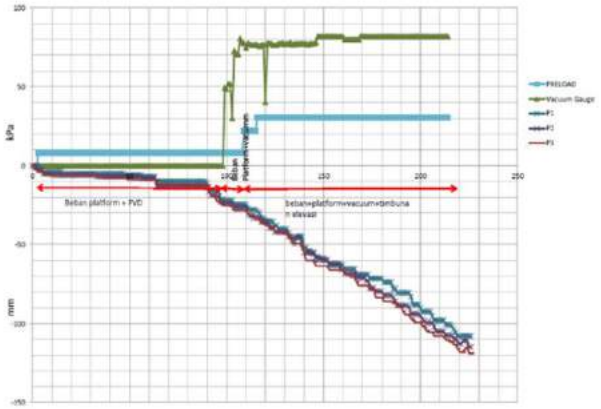

Fig. 3. Vacuum Project Monitoring Data from Geostructure Dynamics.

4.2 *Modeling Parameters*

Modeling parameters consist of soil and PVD parameters that were used in ABAQUS. Modified Cam Clay (MCC) was used as constitutive soil model for modeling soft clay. It has additional parameters such as critical

state line (M), log bulk modulus (κ), and log plastic bulk modulus (λ).

Table 2. Modified Cam Clay Design Parameters in ABAQUS.

Depth(m)	0-2	2-5	5-8	8-20	20-25
Soil Type	Clayey Sand	Clay	Sandy Silt	Clay	Clay
λ	0	0.217	0.336	0.194	0.565
κ	0	0.054	0.067	0.038	0.113
M	1.287	0.651	0.621	0.783	0.772
$0.5p_c'$ (kPa)	7.75	22.13	29.37	43.21	64.31

Furthermore, there are additional design parameters in the form of permeability coefficients for soil and PVD under axisymmetric and plane strain conditions. PVD modeled with a width of 98 mm and 4 mm thickness.

Table 3. Parameters of PVD.

Properties		Installation	
Width	0.098 m	Pattern	Square
Thickness	0.004 m	Spacing	1 m
d_w	0.0518 m	n	21.815
r_w	0.0259 m	s	1.6
d_s	0.0828 m	d_e	1.13 m
r_s	0.0414 m	r_e	0.565 m

Calculation of the permeability coefficient for PVD is based on the discharge capacity. The PVD discharge capacity is in accordance with the minimum requirement of SNI 8460:2017. The value for the discharge capacity is 200 m^3/year.

Table 4. Permeability Coefficient of Soil and PVD.

Depth (m)	0-2	2-5	5-8	8-20	20-25
k_h (m/day)	$8.64x10^{-2}$	$8.64x10^{-5}$	$8.64x10^{-3}$	$8.64x10^{-5}$	$8.64x10^{-5}$
k'_h (m/day)	$2.88x10^{-2}$	$2.88x10^{-5}$	$2.88x10^{-3}$	$2.88x10^{-5}$	$2.88x10^{-5}$
k_{hp} (m/day)	$2.26x10^{-2}$	$2.26x10^{-5}$	$2.26x10^{-3}$	$2.26x10^{-5}$	$2.26x10^{-5}$
k'_{hp} (m/day)	$3.84x10^{-3}$	$3.84x10^{-6}$	$3.84x10^{-4}$	$3.84x10^{-6}$	$3.84x10^{-6}$
k_{pvd} (m/day)	260	260	260	260	260

5 MODELING AND ANALYSIS RESULT

5.1 *Modeling Result*

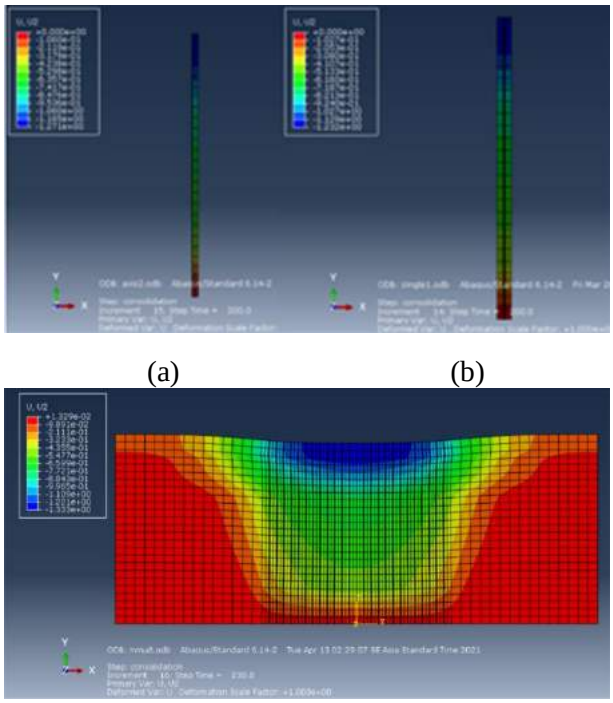

(a) (b)

(c)

Fig. 4. (a) Axisymmetric Model (b) Single Drain-Plane Strain Model (c) Multi Drain-Plane Strain Model.

The first model is axisymmetric, the model is rotationally symmetric about an axis. PVD is modeled with the equivalent radius, using the equation proposed by Long and Covo (1994). The second model is single drain plane strain. Permeability coefficient for PVD and soil under plane strain condition is the result of conversion from the axisymmetric form. The last model is multi drain plane strain. This model represents PVD working concurrently in the field.

5.2 *Comparison between Modeling Result with Monitoring Data*

There are two monitoring data that will be compared with the model result, settlement plate which represents settlement of soil during the improvement and SPT for soil gained strength.

Settlement during improvement is caused by the load from the platform, embankment, and vacuum system. The settlement trend of the model is close to the monitoring data trend. Settlement value for axisymmetric, single drain plane strain, and multi drain plane strain consecutively are 119.37 cm, 112.77 cm, and

123.6 cm. Meanwhile, the amount of settlement from monitoring data are 119.6 cm, 123.2 cm, and 129.03 cm. Axisymmetric model can represent the decreasing value of settlement plate 1 with a difference of 0.19% and multi drain model can represent the value of settlement plate 2 with a difference of 0.32%.

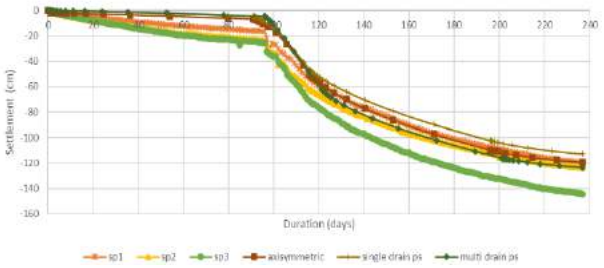

Fig. 5. Settlement from Model vs Monitoring Data.

Gained strength started to occur since the platform was given to the ground, but the increase was not significant.

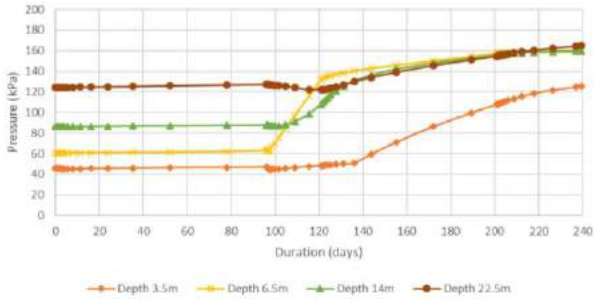

Fig. 6. Effective Pressure at Each Layer after Improvement.

The increase in effective stress in each layer affects the shear stress of the soil. The increase in the effective stress value in the soil is due to the reduction of pore water pressure from the vacuum system.

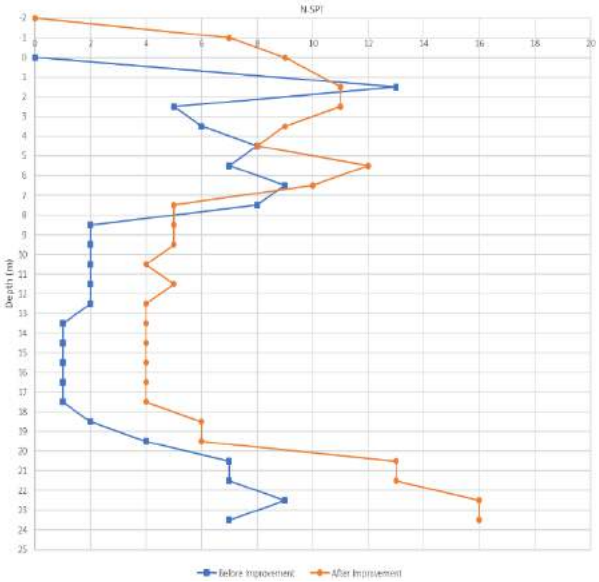

Fig.. 7. N-SPT after Improvement.

From Fig 7, the increase of N-SPT value is around 2 to 3 N-SPT. This value is equivalent to Cu (undrained cohesion) which is 12-18 kPa. An estimation of the increase in Cu value from the modeling results will be carried out using Mesri (1988) equation.

$$\Delta C_u = 0.22 \times \Delta\sigma \times U$$

$$\Delta C_u = 16.6\ kPa$$

The average increment of Cu in soft clay is 16.6 kPa. These results are close to the field test, the increase in cohesion that occurs is around 12 to 18 kPa. In addition, vacuum project is terminated based on the degree of consolidation. If the degree of consolidation reaches 90%, then the project can be stopped. Asaoka method is used to determine the degree of consolidation in the field.

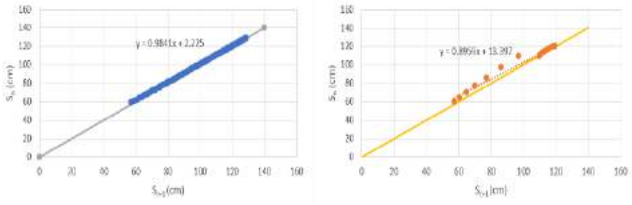

(a) (b)

Fig. 8. (a) Degree of Consolidation from Monitoring Data (b) Degree of Consolidation from Model.

Based on Asaoka method, the ultimate settlement that may occur in the field is 139.94 cm with 92.21% degree of consolidation and for modeling is 128.69 cm with 92.75% degree of consolidation. Degree of consolidation has exceeded 90%, so the vacuum system in the field can be stopped.

5.3 *Sensitivity Analysis*

Sensitivity analysis was done by changing the parameters on the model such as permeability coefficient of soil, permeability coefficient of PVD, unit weight, compression index, and void ratio. The amount of change for each parameter is 36%. The smallest change was in the soil permeability coefficient and the largest change was in the unit weight parameter. This result shows that unit weight is very sensitive to the model and the permeability coefficient is less sensitive to the model.

Table 5. Sensitivity Analysis.

Parameter	Value	Analysis Value	Model Settlement (cm)	Analysis Settlement (cm)	Deviation (cm)
Soil Permeability (m/s)	10^{-9}	$1.4x10^{-9}$	-119.37	-119.37	0.00
PVD Permeability (m/day)	260	166	-119.37	-118.97	-0.40
γ soil (kN/m^3)	15.5	21	-119.37	-106.71	-12.66
Cc	1.299	0.832	-119.37	-112.03	-7.34
e_0	1.4	0.9	-119.37	-109.70	-9.67

5.4 *Vacuum Duration*

The duration of the vacuum system will affect the increase of soil effective stress. The relationship is modeled in Abaqus by changing the duration of vacuum and observing the change of stress. An analysis will be carried out from 100 days to 331 days and the effective stress is reviewed at a depth of 14 meters where the soft soil is located.

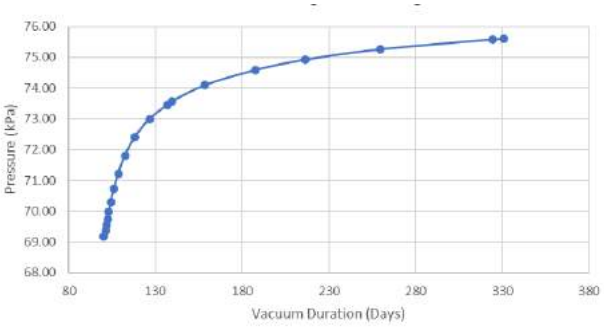

Fig. 9. Vacuum Duration vs Effective Stress.

Fig. 9 shows a linear relationship between vacuum duration and the increase of effective stress when the duration was 100 days to 112 days. But after 112 days, the increment was not significant, so the graph began to move asymptotically with a value of 76 kPa. There is an optimum vacuum duration for soil improvement in the field so that the vacuum system doesn't need to activate for a long duration if the effective stress increment is not significant.

5.5 *Vacuum Pressure Distribution in PVD*

Based on the journal "Analytical and Numerical Modeling of Soft Soil Stabilized by Prefabricated Vertical Drains Incorporating Vacuum Preloading", Indraratna et al. (2005), stated that the vacuum pressure received by the soil will be channeled through PVD and its value will decrease linearly with soil depth.

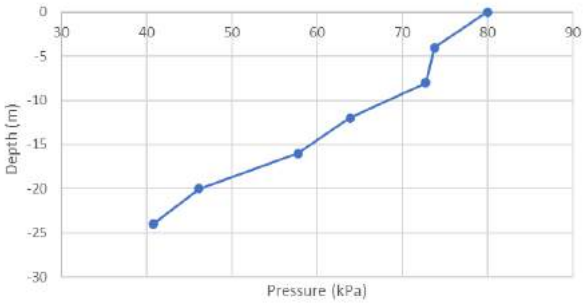

Fig. 10. Vacuum Pressure Distribution in PVD

There is a decrease in vacuum pressure as the soil depth increases. The distribution obtained is quite linear except for depth between 4 to 8 meters. The distribution of vacuum pressure in PVD is in accordance with the existing theory and the decrease rate of vacuum pressure is 1.63 kPa/meter.

6 CONCLUSION

Based on the result of analyses, the following conclusions can be made:

1. The modeling result is compatible to the monitoring data (settlement plate and degree of consolidation) especially for Axisymmetric and Multi Drain Plane Strain model. Permeability conversion that was used in this paper is an equation proposed by Indraratna and Redana (1997), the equation based on permeability matching.
2. The parameters of unit weight, void ratio, and compression index are quite sensitive to the model, while the soil permeability coefficient parameters are less sensitive.
3. There is an optimum vacuum duration in the field, so the vacuum system does not need to be activated if stress increment is not significant.
4. Vacuum pressure in PVD decreases linearly with the increasing depth of PVD. In this case, the decrease rate of vacuum pressure is 1.63 kPa/meter.

ACKNOWLEDGEMENTS

The authors are grateful to Geostructure Dynamics Company whose data on Vacuum System Project has been shared. The data was also used for the first author's undergraduate final project in Bandung Institute of Technology (ITB).

REFERENCES

Ameratunga, Jay., Sivakungan, Nagaratnam., Das, Braja. 2016. *Correlations of Soil and Rock Properties in Geotechnical Engineering.* India: Springer.

Das, Braja., Sobhan, K. 2014. *Principles of Geotechnical Engineering.* USA: Cengage Learning.

Han, Jie. 2015. *Principles and Practice of Ground Improvement*. New Jersey: John Wiley & Sons, Inc.

Helwany, Sam. 2007. *Applied Soil Mechanics with ABAQUS Applications.* New Jersey: John Wiley & Sons, Inc.

Indraratna, B., Chu, J., Rujikiatkamjorn, C. 2015. *Embankments with Special Reference to Consolidation and Other Physical Methods.* UK: Elsevier Ltd.

Indraratna, B., Chu, J., Hudson, J. 2005. *Ground Improvement-Case Histories.* UK: Elsevier Ltd.

Indraratna, B., Sathananthan, I., Rujikiatkamjorn, C., Balasubramaniam, A. 2005. *Analytical and Numerical Modeling of Soft Soil Stabilized by Prefabricated Vertical Drains Incorporating Vacuum Preloading:* 1-2.

Kenandio. 2020. *Studi Perilaku Tanah Pada Metode Perbaikan Tanah Vacuum dan Timbunan Prabeban dengan Program Elemen Hingga:* 94.

Mesri, G. 1988. *A Reevalution of* $s_{u(mob)} = 0.22\sigma'_p$ *Using Laboratory Shear Tests:* 162-164.

Ti, Kok., Huat, Bujang., Noorzaei, Jamaloddin., Jaafar, Moh'd., Sew, Gue. 2009. *A Review of Basic Soil Constitutive Models for Geotechnical Application:* 5-6.

Pengaruh Energi *Rapid Impact Compaction* terhadap Tingkat Kepadatan Tanah Timbunan

Rokhman
Mahasiswa Program Doktoral Jurusan Teknik Sipil – Universitas Hasanuddin

Tri Harianto
Associate Professor, Departemen Teknik Sipil – Universitas Hasanuddin

Muhammad Akbar Walenna
Dosen, Departemen Teknik Sipil – Universitas Hasanuddin

ABSTRAK: Penelitian ini karakteristik untuk menganalisis pengaruh energi pemadatan Metode Rapid Impact Compact (RIC) terhadap tanah. Metode ini menggunakan model alat RIC yang dikendalikan secara elektro-mekanis dengan frekuensi 40-60 tumbukan per menit. Pemadatan dilakukan dengan variasi jumlah tumbukan, berat penumbuk 70 kg dan tinggi jatuh 15 cm. Elemen uji menggunakan cetakan berdiameter 15 cm dan tinggi 25 cm. Model uji menggunakan bak silinder berdiameter 80 cm dan tinggi 120 cm. Tingkat kepadatan tanah diuji dengan DCP Test, CBR Test dan Sandcone Test. Hasil pengujian menunjukkan bahwa energi pemadatan RIC terhadap nilai CBR, berat kering dan kuat tekan bebas memenuhi persamaan d RIC = 0,0864 (ESP) + 1,052 dimana titik optimumnya adalah 3,05. Pada jumlah tumbukan 90 kali tanah tidak mengalami penurunan. Nilai CBR tertinggi terletak di lapisan atas tanah. Evaluasi kinerja pemadatan RIC menggunakan nilai Relatif Compaction (Rc) adalah 95,46% ini berarti kinerja pemadatan RIC baik untuk digunakan.

Kata kunci: rapid impact compaction, energi pemadatan, kepadatan tanah

ABSTRACT: This study aims to analyze the effect of compaction energy using the Rapid Impact Compact (RIC) method on the embankment soil. This method uses an electro-mechanically controlled RIC model with a frequency of 40-60 collisions per minute. Compaction was carried out with variations in the number of collisions, the weight of the pounder is 70 kg and the height of the fall is 15 cm. The test element used a mold with a diameter of 15 cm and a height of 25 cm. The test model used a cylindrical tub with a diameter of 80 cm and a height of 120 cm. Soil density was examined through DCP Test, CBR Test and Sandcone Test. The test results indicated that the compaction energy of RIC on the value of CBR, dry weight and free compressive strength produced the equation d RIC = 0.0864 (ESP) + 1.052 with the optimum point is 3.05. At the number of collisions 90 times the soil did not experience any settlement. The highest CBR value is located in the topsoil. The percentage of the RIC compaction performance evaluation using the Relative Compaction (Rc) value was 95.46%, this means that the compaction performance of RIC was categorized as appropriate to use.

Keywords: rapid impact compaction, compaction energy, soil density

1 PENDAHULUAN

Salah satu metode pemadatan dinamis lapisan timbunan tebal yang dikenal saat ini diantaranya adalah Rapid Impact Compaction. Metode ini adalah pemadatan tanah secara dinamis dengan konsep Low Energi Dynamic Compaction,. Peralatan utama Rapid Impact Compaction berupa massa penumbuk yang di jatuhkan dari ketinggian tertentu. Hal yang membedakan metode ini dengan Dynamic Compaction adalah penggunaan massa penumbuk yang lebih ringan, tinggi jatuh yang lebih rendah namun dengan frekuensi tumbukan yang lebih tinggi, sehingga total kumulatif energi yang dihasilkan pada metode RIC lebih besar daripada metode Dynamic Compaction (DC) dalam satuan waktu yang sama, Adam and Paulmichl (2007), Mohammed et al. (2013).

Dilaboratorium pengaruh usaha pemadatan umumnya di uji menggunakan standar proctor maupun modified proctor dengan mengacu pada kurva hasil pemadatan. Telah umum di ketahui bahwa jika energi usaha pemadatan persatuan volume tanah berubah maka kecenderungannya adalah kurva pemadatan juga akan berubah dengan meningkatnya usaha pemadatan dengan parameter utamanya adalah berat volume kering dan kadar air, Das (2010).

Menurut Proctor, ada hubungan yang pasti antara kadar air dan berat volume kering yang dipadatkan sebagaimana Pers. (1) dalam hal ini w (%) persentase kadar air; γ = berat volume tanah. Untuk berbagai jenis tanah pada umumnya terdapat suatu nilai kadar air optimum tertentu untuk mencapai berat volume kering maksimumnya, kepadatan kering pada kadar air optimum didefinisikan sebagai kepadatan kering maksimum. Berdasarkan Pers. (1) setiap peningkatan kadar air yang melebihi kadar air optimum cenderung mengurangi kepadatan kering, Das (2010).

$$\gamma d = \frac{\gamma}{1+\frac{w(\%)}{100}} \tag{1}$$

Selain kadar air dan jenis tanah, faktor penting lainnya yang mempengaruhi pemadatan adalah energi per satuan volume. Energi pemadatan per satuan volume yang digunakan untuk uji Proctor dintentukan oleh jumlah tumbukan perlapisan (N); jumlah lapisan per mould (l); berat penumbuk (W) dan tinggi jatuh penumbuk (h) persatuan volume mould (V) yang dapat dinyatakan dengan Pers. (2) Das (2010).

$$E = \frac{N \cdot l \cdot W \cdot h}{V} \tag{2}$$

Meningkatkan usaha pemadatan akan meningkatkan kepadatan maksimum namun akan mengurangi kadar air optimum. Kurva pemadatan secara umum memperlihatkan bahwa rasio void udara tetap sama pada kepadatan maksimum, sehingga pada kadar air yang tinggi, hanya ada sedikit pertambahan kepadatan yang diperoleh dengan meningkatkan usaha pemadatan. Tanah lempung memiliki kandungan air optimum yang jauh lebih tinggi, akibatnya menurunkan kepadatan kering maksimum. Efek meningkatkan upaya pemadatan juga jauh lebih besar dalam kasus tanah lempung, Rajasekhar et al. (2016).

Peralatan Rapid Impact Compaction, RIC terdiri atas tiga komponen utama yaitu alas penumbuk; alur penumbuk, dan penumbuk, Bedu et al. (2017). Pada metode pemadatan rapid impact compaction, penumbuk dijatuhkan secara tetap pada alas penumbuk yang ditempatkan diatas permukaan tanah dengan frekuensi tumbukan antara 30-60/menit sebagai ciri metode rapid compaction, Bedu et al. (2017). Parameter energi pemadatan metode, RIC ditentukan oleh berat penumbuk (Compactor); berat dan luas geometri landasan penumbuk (anvil); frekuensi tumbukan dan kumulatif total tumbukan dalam satu siklus pemadatan pada titik tumbukan yang sama.

Peralatan *Rapid Impact Compaction*, RIC terdiri atas tiga komponen utama yaitu alas penumbuk; alur penumbuk dan penumbuk. Peralatan penumbuk ditautkankan ke hydraulic excavator sebagai perangkat penopang mekanik yang dapat mengatur frekuensi tumbukan antara 40-60/menit sebagai ciri metode rapid compaction, Adam and Paulmichl (2007). Pada metode dynamic compactioan, maka total energi E tumbukan per luas bidang kontak alas penumbuk (kJ/m^2), dihitung dengan Pers. (3), dalam hal ini E adalah kumulatif total energi yang dikenakan kN.m (kJ), A adalah luas bidang tumbuk dari alas penumbuk (m^2), dan N adalah jumlah tumbukan, Falkner et al. (2010).

$$E = \frac{1}{2}\left(W_H + W_F\right) \cdot V_F{}^2 \left(\frac{N}{A}\right) \tag{3}$$

2 METODE PENELITIAN

2.1 *Material*

Contoh tanah yang digunakan masuk klasifikasi sebagai tanah lanau plastisitas tinggi (MH) sesuai dengan sistem klasifikasi tanah USCS. Adapun sifat fisik contoh tanah yang di gunakan dalm penelitian ini dirangkum dalam Tabel 1.

Tabel 1. Sifat fisik material tanah pengujian

Sifat fisik	Nilai
Berat Volume Basah, γ	1,03 gr/cm^3
Kadar air rata-rata, ω	38,36 %
Spesific gravity, G	2,73
Batas Cair, *LL*	55,89 %
Batas Plastis, *PL*	47,48 %
Indeks Plastisitas, *IP*	8,41 %

2.2 *Peralatan Pengujian*

Dalam penelitian ini digunakan peralatan pengujian repetead load impak berbasis air pneumatik pressure sebagaimana diperlihatkan dalam Gbr. 1. Adapun komponen utama peralatan tersebut terdiri dari kompressor udara; piston double acting; valve selenoid, panel kendali kontroller, massa penumbuk dan landasan tumbukan, alat ini sebagaimana di uraikan secara rinci dalam, Bedu et al. (2017).

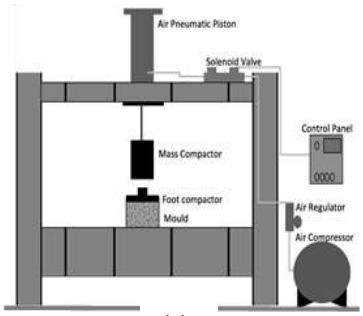

(a)

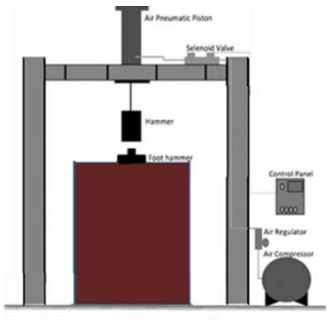

(b)

Gbr. 1. *Set-Up* Peralatan: a. Uji RIC Elemen; b. Uji RIC Model.

Digunakan massa penumbuk yang terbuat dari material baja seberat 70 kg yang ditautkan pada ujung batang piston yang berfungsi sebagai kait beban. Beban tersebut dapat di jatuhkan pada ketinggian sesuai dengan setting ketinggian pada panel kontrol. Untuk pengujian di gunakan mould dengan ukuran diameter dalam 15 cm, tigggi 25 cm, volume cetakan 0,0044 m^3. Untuk proses pemadatan, mold di lengkapi dengan alas pemadat yang ukurannya disesuaikan dengan diameter cetakan. Alas tumbukan terbuat dari pelat baja diameter 15 cm.

2.3 *Rancangan Pengujian*

- Persiapan Sampel Tanah.
  Tanah dalam tabung silinder untuk kompaksi diperoleh dari sampel yang dibentuk kembali. Untuk menyiapkan sampel ini, sejumlah berat tanah yang sebelumnya telah kering oven dicampur dengan sejumlah air mendapatkan kadar air yang sesuai dengan target kadar air rencana pengujian yaitu 15%-35%, dimana rentang kadar air ini sebelumnya telah di uji menggunakan pemadatan proctor. Tanah yang telah di atur kadar air diambil seberat 4,6 kg dan di isikan dalam tabung silinder tanpa dilakukan pemadatan dengan mengontrol kepadatan gemburnya sebesar 1,03 gr/cm^3.

- Proses Pemadatan RIC elemen
  Upaya pemadatan dengan *Rapid Impact Compaction* dilakukan pada mould berukuran diameter 15 cm dan tinggi 25 cm. Untuk mengetahui pencapaian nilai kepadatan dilakukan uji DCP dan CBR. Pemadatan dilakukan menggunakan berbagai tingkat energi dengan menerapkan berbagai usaha impak yang digunakan. Penumbuk yang berbentuk persegi dengan berat 70 kg dijatuhkan dari ketinggian 15 cm dengan variasi jumlah pukulan 5, 15, 25 dan 35 m lihat Gbr. 1(a).

- Proses Pemadatan RIC Uji Model
  Upaya pemadatan dengan *Rapid Impact Compaction* pada bak uji silinder dengan ukuran diameter 80 cm dan tinggi 120 cm. yang diisi tanah sampai penuh sebanyak 621 kg. Pemadatan dilakukan menggunakan peralatan RIC dengan berat penumbuk 70 kg, tinggi jatuh 15 cm dna geometri alas tumbukan berdiameter 30 cm. Proses pemadatan dilakukan sampai dengan tanah tidak mengalami penurunan lagi. Untuk mengetahui pencapaian nilai kepadatan dilakukan uji CBR, uji DCP dan uji Sandcone lihat Gbr. 1(b).

3 HASIL DAN PEMBAHASAN

3.1 *Energy Proctor Compaction dan Rapid Impact Compaction*

Hasil perhitungan *Energy Proctor Compaction* dan *Rapid Impact Compaction* serta rasio perbandingannya dapat dilihat pada tabel berikut ini:

Tabel 2. *Energy Proctor Compaction* dan *Rapid Impact Compaction* serta Rasio Perbandingannya.

Type Pemada-tan	Berat Penum-buk (kg)	Jumlah Tumbu-kan Per Lapis	Energi Pemada - tan (kJ/m^3)	Rasio Energi Standar
Standar Proctor	2,5	25	592	1,00
Modified Proctor	4,54	25	2695	4,54
RIC-01	70	5	117	0,20
RIC-02	70	15	351	0,59
RIC-03	70	25	585	0,98
RIC-04	70	35	819	1,38

Energy pemadatan baik metode standar proctor maupun modified di dasarkan pada usaha pemadatan yang dilakukan dalam sebuah mould pemadatan berdiamater 101,6 mm dan tinggi 116,43 mm yang memiliki volume 944 cm^3. Pada pengujian standar proctor besarnya energi pemadatan adalah 592 kJ/m^3, sementara untuk modified proctor adalah 2.695 kJ/m^3. Sementara untuk model *Rapid Impact Compaction* besarnya didapatkan dengan memvariasikan jumlah tumbukan 5 kali, 15 kali, 25 kali dan 35 kali dengan berat beban penumbuk yang digunakan sebesar 70 kg, tinggi jatuh 15 cm dan 1 lapis tanah. Semua proses pemadatan dilakukan hanya menggunakan 1 lapisan pada mould berdiameter 15 cm dan tinggi 25 cm dengan volume 0,0044 m^3. Sehingga dari proses pemadatan RIC ini besarnya energi usaha pemadatan bervariasi antara 111 kJ/m^3 untuk yang terkecil dan 1.365 kJ/m^3 untuk energi yang terbesar atau jika bandingkan terhadap energi standar proctor bervariasi antara 0,20-1,38 kali.

3.2 *Kepadatan Kering dan Kadar Air Optimum pada Tingkat Energi Berbeda*

Untuk menjelaskan hubungan variabel kepadatan kering, kadar air optimum pemadatan dan tingkat energi dari usaha pemadatan, maka dilakukan pengamatan dengan hubungan ketiga variabel tersebut, dalam hal ini hubungan tersebut dinyatakan sebagai perbandingan terhadap energi metode standar proctor yaitu 592 kJ/m^3 terhadap perubahan kadar air setiap mould pemadatan sesuai besarnya energi *Rapid Impact Compaction* yang diberikan lihat Gbr. 2.

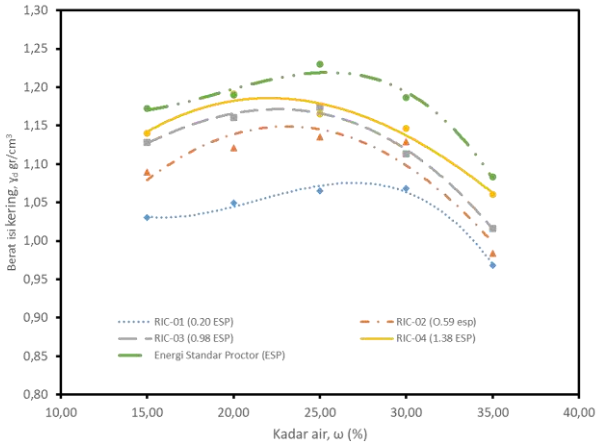

Gbr. 2. Hubungan antara Energi RIC dan Kadar Air terhadap Berat Isi Kering (Ɣd).

Kecenderungan berat isi kering dipengaruhi oleh tingkat energi usaha pemadatan dan kadar air seperti yang terlihat pada Gbr. 2. Terlihat bahwa setiap tingkat energi yang diberikan akan menghasilkan kadar air optimum untuk menghasilkan berat isi kering tanah maksimum. Dimana hasilnya memperlihatkan bahwa penambahan energi cenderung mengurangi besarnya nilai kadar air optimum. Untuk energi terbesar pada RIC ini kadar air optimum didapat 20 %. Bila di bandingkan hasil pemadatan Standar proctor maka berat isi kering yang dihasilkan masih dibawah standar proctor. Untuk mencapainya tentunya harus menaikan energi RIC menyamai bahkan lebih dari energi standar proctor.

3.3. *Hubungan Energi Pemadatan RIC dan Energi Pemadatan Proctor terhadap Berat Isi Kering*

Untuk energi yang sama dengan standar proctor (1,00 ESP = 592 kJ/m^3) dihasilkan berat isi kering sebesar 1,14 gr/cm^3 atau sebesar 92,68% terhadap berat isi kering hasil pemadatan standar proctor (1,23 gr/cm^3). Agar berat isi kering hasil pemadatan RIC sama dengan berat isi kering tanah Standar Proctor maka energi

RIC harus ditingkatkan sampai dengan 2,01 ESP atau sebesar 1.190 kJ/m^3 lihat Gambar 3.

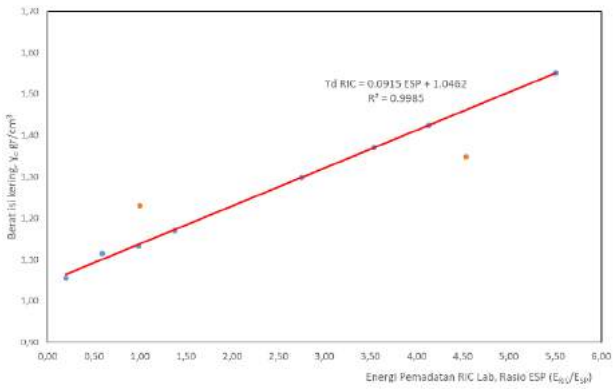

Gbr. 3. Hubungan antara Energi Pemadatan RIC, Standar Proctor dan Modified Proctor terhadap Berat Kering.

Dari Gbr. 3 diperoleh persamaan berat isi kering tanah hasil pemadatan RIC yaitu:

$$\Upsilon d_{RIC} = 0.0915\ ESP + 1.0462 \quad (4)$$

Dimana:

Υd_{RIC} = berat isi kering tanah hasil pemadatan *Rapid Impact Compaction* (RIC)

ESP = rasio perbandingan antara Energi RIC terhadap Energi Standar Proctor (E_{RIC}/E_{SP})

Kadar air optimum untuk mendapatkan berat isi kering maksimum untuk energi pemadatan standar proctor adalah sebesar 25% Sedangkan kadar air optimum untuk mendapatkan berat isi kering maksimum pada pemadatan RIC adalah sebesar 20% sesuai hasil pengujian pada sejumlah tingkat energi yang berbeda.

Hubungan antara garis berat isi kering hasil pemadatan RIC (Υd_{RIC}) dan berat isi kering hasil pemadatan standar proctor ($\Upsilon d_{Standar\ Proctor}$) terjadi perpotongan di titik 2,01 ESP, artinya dengan energi RIC dinaikan sampai dengan 2,01 kali energi Standar Proctor (2,01 x 592 kJ/m^3 = 1.190 kJ/m^3) maka berat isi kering yang dihasilkan bisa mencapai 1,23 gr/cm^3 sama dengan berat isi kering hasil pemadatan standar proctor lihat Gbr. 3. Untuk menghasilkan energi sebesari 1.190 kJ/m^3 bila menggunakan alat RIC dengan berat penumbuk 70 kg, tinggi jatuh 15 cm dan diameter alas tumbukan 15 cm maka dibutuhkan jumlah tumbukan sebanyak 51 kali.

Hubungan antara garis berat isi kering hasil pemadatan RIC (Υd_{RIC}) dan berat isi kering hasil pemadatan Modified Proctor ($\Upsilon d_{Modifed\ Proctor}$) terjadi perpotongan di titik 3,32 ESP, artinya dengan energi RIC dinaikan sampai dengan 3,32 kali energi Standar Proctor (3,32 x 592 kJ/m^3 = 1.965 kJ/m^3) maka berat isi kering yang dihasilkan bisa mencapai 1,35 gr/cm^3 sama dengan berat isi kering hasil pemadatan Modified Proctor lihat Gbr. 3. Untuk menghasilkan energi sebesari 1.965 kJ/m^3 bila menggunakan alat RIC dengan berat penumbuk 70 kg, tinggi jatuh 15 cm dan diameter alas tumbukan 15 cm maka dibutuhkan jumlah tumbukan sebanyak 85 kali.

Titik perpotongan garis hubungan antara berat isi kering hasil pemadatan RIC dan Standar Proctor maupun Modified Proctor adalah sebagai acuan untuk mendapatkan energi optimum agar hasil pemadatannya (berat isi kering tanah) yang diperoleh sama dengan kepadatan tanah hasil pemadatan Standar Proctor maupun Modified Proctor.

Dari hasil penelitian Gbr. 3 dapat dilihat bahwa dibutuhkan energy RIC yang lebih besar untuk mencapai kepadatan yang sama pada pemadatan standar proctor. Hal ini disebabkan pada pemadatan standar proctor metode pemadatan lapis demi lapis sehingga energi yang diterima tanah merata pada keseluruhan volume tanah tersebut. Sebaliknya pada pemadatan RIC metode pemadatan hanya satu lapis saja. Sesuai dengan teori distribusi tegangan tanah energi besar hanya diterima di permukaan tanah saja, semakin jauh dari permukaan energy yang diterima tanah semakin kecil.

3.4 *Hubungan antara Jumlah Tumbukan (Energi Pemadatan RIC Uji Model) terhadap Penurunan*

Hasil pemadatan RIC uji model dapat diketahui bahwa pada awal penumbukan terjadi penurunan yang cukup dalam. Namun pada penumbukan selanjutnya penurunannya berkurang dan akhirnya pada kumulatif jumlah pukulan 90 kali tanah tidak mengalami penurunan lagi. Hal ini sejalan dengan teori yang mengatakan bahwa salah satu syarat dihentikan penumbukan pada pemadatan RIC salah satunya adalah bila kumulatif jumlah tumbukkan sudah mencapai 90 kali.

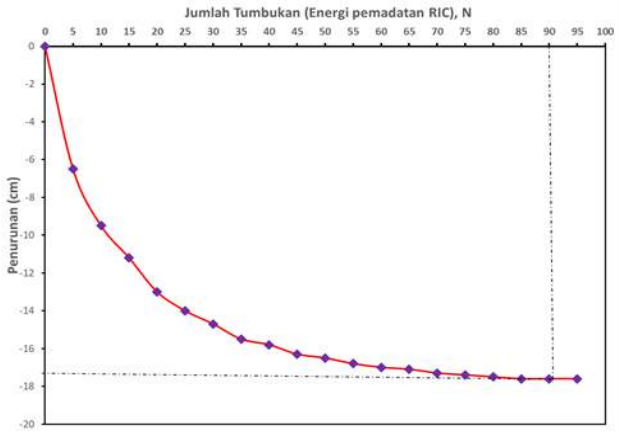

Gbr. 4. Hubungan antara Nilai CBR dan Kedalaman Tanah.

3.5 Evaluasi kinerja pemadatan RIC dengan Analisa Relatif Compaction, RC

Untuk mengevaluasi hasil pemadatan RIC di lapangan maka dilakukan uji model. Pengujian ini dilakukan pada bak uji berbentuk silinder dengan ukuran diameter 80 cm dan tinggi 120 cm. Seingga volume drum tersebut adalah 0,603 m^3 kemudian diisi tanah dengan berat isi 1,03 gr/cm^3 sampai penuh atau sebanyak 621 kg. Berat penumbuk *Rapid Impact Compaction* yang digunakan adalah 70 kg dengan tinggi jatuh 15 cm dan diameter alas 30 cm serta jumlah tumbukan sebanyak 90 kali. Setelah proses pemadatan selesai maka dilakukan pengujian tingkat kepadatan menggunakan Sandcone test untuk mendapatkan berat isi kering tanah (ϒd) dan juga dilakukan pengujian Dynamic Cone Penetrometer (DCP) Test untuk mendapatkan nilai CBR lapangan.

Untuk kriteria kinerja hasil pemadatan tersebut diukur dengan nilai *Relatif Compaction* (R_c) yaitu membandingkan hasil pencapaian kepadatan kering hasil pemadata RIC terhadap kepadatan kering hasil pemadatan standar proctor, sesuai Pers. (5) yang dinyatakan dalam prosentase. Nilai ini menyatakan pencapaian kepadatan tanah hasil pemadatan RIC terhadap kepadatan tanah hail pemadatan standar proctor.

$$Rc = \frac{\gamma d \text{ RIC Model}}{\gamma d \text{ Standar Proctor}} \qquad (5)$$

Dari hasil pengujian pemadatan RIC pada uji model dengan sandcone test maka diperoleh berat isi kering (ϒd) = 1,174 gr/cm^3. Sehingga nilai Relatif Compaction (R_c) dapat diperoleh sebesar 95,46%.

Dengan demikian dari hasil pengujian ini dapat diketahui bahwa pemadatan RIC dapat menghasilkan kinerja pemadatan yang baik, sehingga pemadatan *Rapid Impact Compation (RIC)* dapat diterapkan di lapangan.

4 KESIMPULAN

Dari hasil penelitian ini dapat diambil kesimpulan sebagai berikut:

1. Adanya hubungan antara besarnya energi pemadatan *Rapid Impact Compaction (RIC)* dan kadar air terhadap besarnya berat isi kering tanah. Semakin besar energi pemadatan maka berat isi kering tanah juga akan meningkat, yang dibarengi dengan kadar optimum kecenderungannya semakin berkurang.
2. Besarnya energi pemadatan *Rapid Impact Compaction (RIC)* mempengaruhi karateristik pemadatan tanah yaitu berat isi kering. Semakin besar energi pemadatan RIC kecenderungannya akan menghasilkan berat isi kering tanah yang lebih besar.
3. Besarnya energi pemadatan *Rapid Impact Compaction (RIC)* berdasarkan kumulatif jumlah tumbukan berpengaruh terhadap penurunan tanah. Penurunan tanah awalnya cukup besar tetapi lama kelamaan berkurang dan sampai tidak terjadi penurunan lagi. Penurunan tidak terjadi pada jumlah kumulatif pukulan mencapai 90 kali. Artinya pemadatan RIC dapat dihentikan jika kumulati jumlah tumbukan sudah mencapai 90 kali.
4. Untuk mengevaluasi kinerja pemadatan *Rapid Impact Compaction (RIC)* di lapangan maka dapat digunakan Analisa *Relatif Compaction* yaitu perbandingan antara berat isi kering hasil pemadatan RIC terhadap berat isi kering hasil pemadatan standar proctor. Dimana dari hasil pengujian didapat nilai Rc sebesar 95% ini berarti pemadatan RIC dapat digunakan di lapangan.

DAFTAR PUSTAKA

Adam D. and I. Paulmichl. 2007. Rapid Impact Compactor − An Innovative Dynamic Compaction Device for Soil Improvement. *Improvement of Soil Properties*: 183–193.

Bedu, A. et al. 2017. Pengembangan Alat Uji Pneumatic Rapid Impact Compaction. *Prosiding Konferensi Nasional Teknik Sipil 11*: 75–80. Universitas Tarumanagara, Jakarta.

Becker, P.J. 2011. *Assessment of Rapid Impact Compaction for Transportation Infrastructure Applications.* Graduate Theses and Dissertations. Paper 10261, Iowa State University.

Das, B.M. 2010. *Principles of Geotechnical Engineering, 7 th*. Cengage Learning 200 First Stamford Place, Suite 400 Stamford, CT 06902 USA.

Falkner, F. et al. 2010. *Rapid Impact Compaction for Middle-Deep Improvement of the Ground – Numerical and Experimental Investigations*. From Res. to Des. Eur. Pract., no. June: 2–11.

Mohammed, M.M. et al. 2013. Assessment of rapid impact compaction in ground improvement from in-situ testing. *Journal of Central South University* Vol. 20: 786–790.

Rajasekhar C. et al. 2016. To Develop a Correlation Between CBR and Dynamic Cone Penetration Value. *Int. J. Technol. Res. Eng*., Vol. 4, No. 1: 11–16.

Konstruksi Jalan Terapung di Atas Tanah Lunak

Juni Gultom
Departemen Teknik Sipil – Universitas Islam Sultan Agung

Pratikso
Departemen Teknik Sipil – Universitas Islam Sultan Agung

Abdul Rochim
Departemen Teknik Sipil – Universitas Islam Sultan Agung

ABSTRAK: Pembangunan konstruksi jalan di atas tanah lunak dewasa ini selalu menjadi diskusi yang menarik. Permasalahan tanah lunak sebagai tanah problematik memiliki daya dukung yang rendah, *settlement* yang besar, dan kemampatan yang besar. Riset ini bertujuan menemukan sebuah konstruksi alternative di atas tanah lunak yang selalu terendam air. Metoda eksperimental yang dilaksanakan di laboratorium dengan memodelkan konstruksi *raft pile foundation* dengan bantalan *geofoam* diuji dalam sebuah bak uji berisi air. Pembebanan variatif dari 0 kN sampai dengan 20 kN. Dalam percobaan laboratorium tebal *geofoam* 50 cm memiliki daya apung 6.86 kN dengan reduksi *settement* 0.61 cm, tebal *geofoam* 90 cm memiliki daya apung 10.78 kN reduksi *settlement* 0.45 cm. Dengan memanfaatkan daya dukung tanah lunak dan daya apung air konstuksi mampu mereduksi penurunan dan dinamakan konstruksi terapung. Berdasarkan percobaan tersebut persamaan *Katzenbacth* tentang daya dukung *raft pile foundation* $R_{tot} = R_{raft} + \sum_{i=1}^{n} R_{pile}$ dengan bantalan *geofoam* mendapatkan persamaan baru yaitu $R_{tot} = R_{raft} + \sum_{i=1}^{n} R_{pile} + R_{uplift\ g}$

Kata Kunci: pondasi tiang rakit, geofoam, settlement, tanah lunak, PLAXIS

ABSTRACT: Road construction on soft soil nowadays has always been an interesting discussion. The problem of soft soil as problematic soil has a low carrying capacity, large settlements, and high compressibility. This research aims to find an alternative construction on soft soil that is always submerged in water. The experimental method carried out in the laboratory by modeling the construction of pile foundations with geofoam bearings was tested in test bath. Loading varies from 0 kN to 20 kN. In laboratory experiments, 50 cm thick geofoam has a buoyancy of 6.86 kN with a reduction of 0.61 cm, while 90 cm thick geofoam has a buoyancy of 10.78 kN with a reduction of 0.45 cm. By utilizing the bearing capacity of soft soil and the buoyancy of construction water, it is able to reduce subsidence and build floating. Based on this experiment, Katzenbacth on the bearing capacity of the raft pile $R_{tot} = R_{raft} + \sum_{i=1}^{n} R_{pile}$ with geofoam bearings got a new equation, namely $R_{tot} = R_{raft} + \sum_{i=1}^{n} R_{pile} + R_{uplift\ g}$

Keywords: raft pile foundation, geofoam, settlement, soft soil, PLAXIS

1 PENDAHULUAN

Berbagai literatur mencatat bahwa tanah lunak diindikasikan sebagai bagian dari tanah problematik. Permasalahan utama konstruksi jalan di atas lahan lunak adalah terbatasnya daya dukung sehingga biaya pembangunan, pemeliharaan maupun peningkatan memerlukan biaya tinggi dan secara teknis tidak jarang mengalami kegagalan.

Salah satu konstruksi yang sering diaplikasikan sebagai kelengkapan jalan yang dibangun adalah *box culvert*. Konstruksi *box culvert multicell* yang dimodelkan menjadi *raft pile foundation* dengan bantalan *geofoam* akan menjadi salah satu alternative.

2 METODOLOGI PENELITIAN

Dalam pelaksanaan penelitian ini menggunakan pendekatan eksperimental model

prototipe skalatik di laboratorium. Model dibuat konstruksi mengapung di atas tanah lunak menggunakan *geofoam* divakum dalam sebuah ruang tertutup sehingga dapat mengapung.

Tahapan pelaksanaan pembuatan model *Prototype* antara lain:

1. Penyediaan bak uji ukuran 300 cm x 200 cm x 200 cm.
2. Pembuatan model *Raft-Pile-Geofoam Foundation* dari beton bertulang,
3. Pemasangan *Dial Gauge* dan *Hydraulik Jack*.
4. Tanah lunak yang sudah ditest, dimasukkan ke dalam bak uji sampai pada batasan tertentu.
5. Benda uji dimasukkan ke dalam bak uji.
6. Pembebanan dengan *hydraulic jack*.

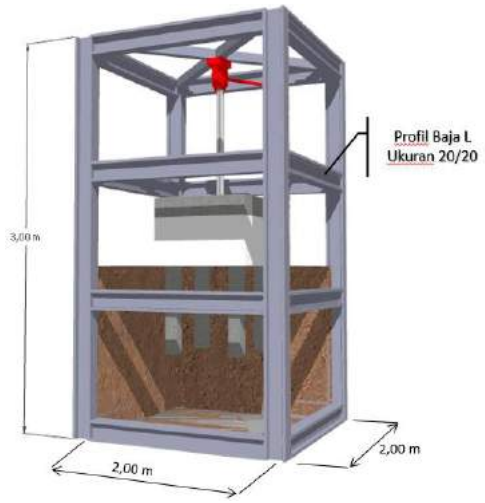

Gbr. 1. Bak Uji.

Adapun ruang lingkup penelitian ini adalah sebagai berikut:

1. Uji model pondasi rakit bantalan *geofoam* dengan skala kecil di laboratorium
2. *Prototype* pondasi rakit kombinasi *geofoam* terlebih dahulu dianalisis melalui analisa numeris Plaxis dan divalidasi dengan hasil laboratorium.
3. Data tanah lunak yang digunakan dalam uji model di laboratorium adalah data tanah lunak.
4. Beban Vertikal dalam model uji laboratorium secara manual dapat ditambah sesuai kebutuhan.
5. Material beton yang digunakan merupakan beton dengan f'c=20 Mpa setara dengan K-250.
6. Material *geofoam* yang digunakan adalah EPS40 dengan spesifikasi densitas blok 16 kg/m^3, tegangan elastisitas batas 40 kPa dengan modulus Young 4 Mpa.

Adapun model penelitian yang diangkat adalah model pondasi tiang rakit dengan bantalan *geofoam* di atas tanah lunak.

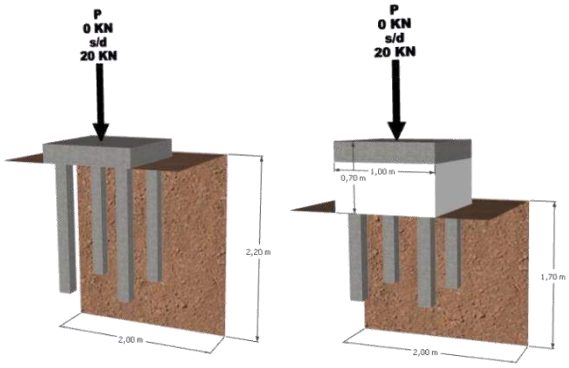

Gbr. 2. Model Benda Uji Dalam 3 Dimensi Tanpa Bantalan *Geofoam* dan Dengan Bentalan *Geofoam.*

3 HASIL DAN PEMBAHASAN

Settlement yang terjadi dengan menggunakan bantalan *geofoam* atau tanpa bantalan *geofoam* dari hasil Laboratorium dengan output Plaxis. Dari hasil analisa dengan menggunakan Plaxis tersebut kemudian dibandingkan dengan hasil Laboratorium, hasilnya memiliki kecenderungan yang sama.

3.1 *Uji Tanah di Laboratorium*

Tanah yang sudah diambil akan digunakan sebagai media dalam bak uji terlebih dahulu dilakukan pengujian untuk mendapatkan klasifikasi sebagai tanah lunak, Tabel. 1.

3.2 *Uji Eksperimen*

Analisis *settlement* eksperimental diuraian sebagai fungsi dimensi *geofoam* (tg), beban (P) dan level muka air (w) yaitu s = f (tg,P,w) dapat dilihat pada grafik Gbr. 3 dan Gbr.4.

Tabel 1. *Summary of Soil Data.*

Sampel	Gs	w	γ_m	γ_d	e	n	Atterberg Limits			Gravel	Sand	Silt	Clay
		(%)	(gr/cm^3)	(gr/cm^3)		(%)	LL	PL	PI	%	%	%	%
1	2.665	50.978	1.713	1.135	1.349	0.574	73.00	40.43	32.57	0.75	30.25	30.65	38.36
2	2.674	54.664	1.680	1.086	1.462	0.065	71.00	35.33	35.67	1.19	23.81	21.66	53.34

Tabel 1. *Summary of Soil Data (lanjutan).*

Sampel	c	ϕ	Triaxial UU		Triaxial CU		Consolidation
	(kg/cm^2)	(°)	c	ϕ	c	ϕ	cc
1	0.101	14.45	0.122	14.412	0.113	13.712	0.335
2	0.064	14.45	0.058	13.630	0.042	13.380	0.361

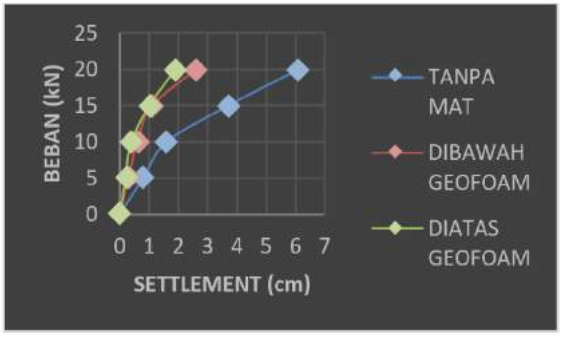

Gbr. 3. Grafik Penurunan Vs Pembebanan Tebal *Geofoam* 0.5 m (Hasil Permodelan Komputasi FEM).

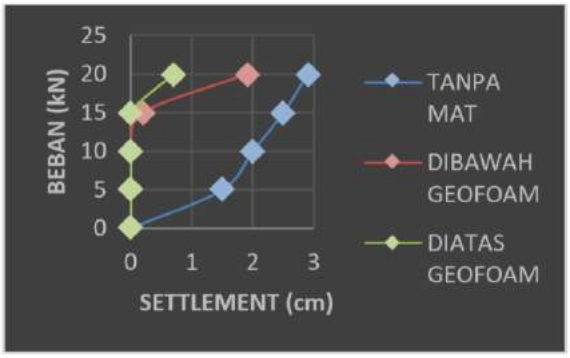

Gbr. 4. Grafik Penurunan Vs Pembebanan Tebal *Geofoam* 0.9 m (Hasil Pengujian Laboratorium).

Hubungan Ketebalan *Geofoam* dengan Berat Sendiri Beton

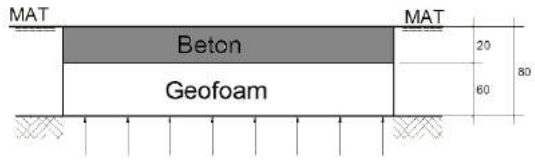

Gbr. 5. Plat Beton dan *Geofoam* di Atas Tanah Lunak Terendam Air.

Perbandingan antara tebal *geofoam* dengan berat sendiri beton, dapat dilihat pada tabel berikut:

Tabel 2. Perbandingan Ketebalan *Geofoam* dengan Berat Sendiri Beton (Sumber Hasil Analisis).

Tebal *Geofoam*	Gaya Berat *Geofoam*	Gaya Berat Plat Beton	Gaya Apung	*Safety Factor*
(m)	(N)	(N)	(N)	
	Fo = m x g	F l = p x l x t x γ_{beton} x g	F2 = ρ x g x v	SF = F2/ (Fo+F1)
0	0	4704	0	0
0.5	140.728	4704	6,860	1.4
0.9	258.132	4704	10,780	2.1

Ketebalan minimal *geofoam* dengan *safety factor* 1.5 didapat tinggi air = 0.253 di atas permukaan tanah dan tebal *geofoam* 0.5 m sebagaimana hitungan berikut.

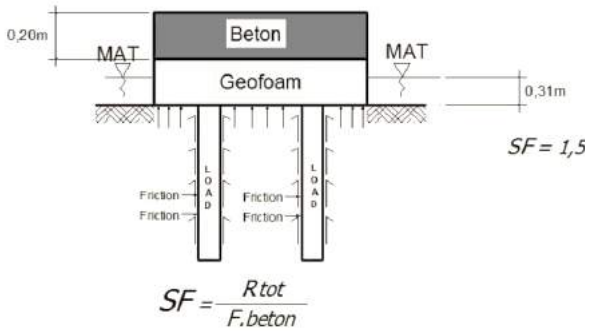

Gbr. 6. Ilustrasi Berat Beton dan Tinggi Muka Air Dengan SF =1.5.

Hubungan Penurunan dan Daya Apung

Percobaan laboratorium menunjukan terdapat hubungan antara daya apung dengan besaran penurunan sebagaimana terlihat pada tabel berikut:

Tabel 3**.** Reduksi Penurunan oleh Daya Apung Hasil Eksperimental Laboratorium.

Tebal *Geofoam*	Beban	Kondisi MAT	Penurunan	Daya Apung	Perbedaan Penurunan Delta S	Reduksi Penurunan per satuan Daya (6/5)
(m)	(kN)		(cm)	(kN)	(cm)	(cm/kN)
1	2	3	4	5	6	7
0.5	20	Tanpa MAT	6.1	0	4.2	0.61
		Di bawah Geofoam	2.6	0		
		Di atas Geofoam	1.9	6.86		
0.9	20	Tanpa MAT	2.9	0	2.2	0.45
		Di bawah Geofoam	1.9	0		
		Di atas Geofoam	0.7	10.78		

Secara rata rata dalam eksperimen laboratorium gaya *uplift* mereduksi 0.53 cm *settlement.*

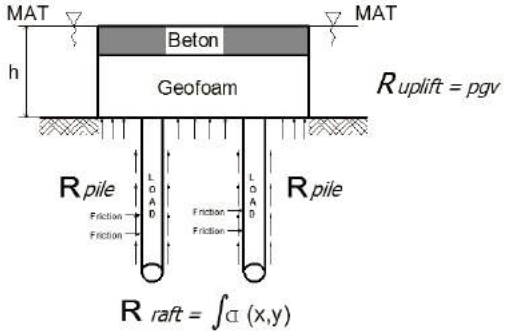

Gbr. 7. Reduksi Gaya *Uplift* terhadap Penurunan Benda Uji.

3.3 *Perbandingan Settlement Struktur Floating dengan Metode Model Skala Laboratorium dan Pemodelan Komputasi FEM*

Nilai penurunan struktur *floating* dengan Metode Model Skala Laboratorium dan Permodelan Komputasi FEM telah diperhitungkan sebagaimana terlihat pada grafik perbandingan penurunan seperti pada grafik di bawah ini:

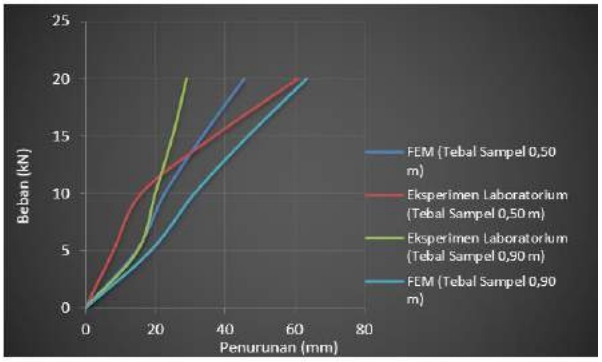

Gbr. 8. Grafik Penurunan vs Pembebanan Tebal *Geofoam* 0.5 m dan 0.9 m Kondisi Tanpa MAT (Hasil Pengujian Laboratorium dan Permodelan Komputasi FEM).

Pada kondisi *protype* uji coba laboratorium dan hasil analisis FEM pada kondisi uji coba tanpa muka air beban diatas 10 kN, semakin tebal *geofoam* semakin kecil penurunan.

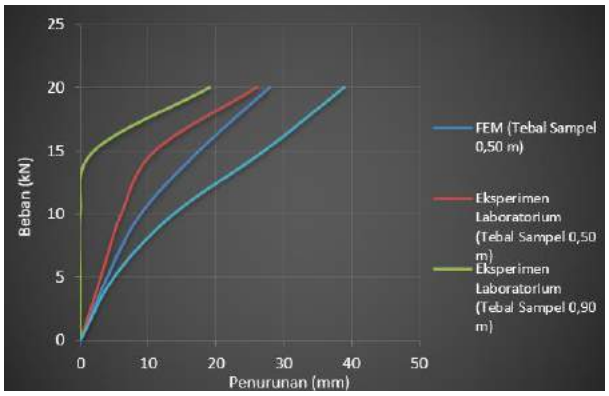

Gbr. 9. Grafik Penurunan vs Pembebanan Tebal *Geofoam* 0.5 m dan 0.9 m Kondisi Air di Bawah *Geofoam* (Hasil Pengujian Permodelan Laboratorium dan Komputasi FEM).

Pada kondisi protype uji coba laboratorium dan hasil analisis FEM pada kondisi uji coba dengan muka air dibawah *geofoam*, pada semua kondisi pembebanan 0 sampai dengan 20 kN, semakin tebal *geofoam* semakin kecil penurunan.

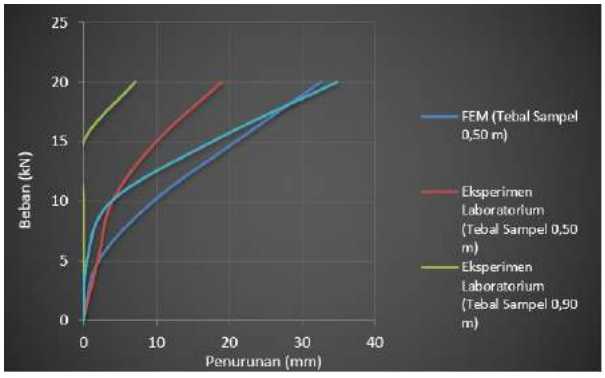

Gbr. 10. Grafik Penurunan vs Pembebanan Tebal *Geofoam* 0.5 m dan 0.9 m Kondisi Air di Atas Geofoam (Hasil Pengujian Laboratorium dan Permodelan Komputasi FEM).

Pada kondisi protype uji coba laboratorium dan hasil analisis FEM pada kondisi uji coba dengan muka air diatas *geofoam*, pada semua kondisi pembebanan 0 sampai dengan 20 kN, semakin tebal *geofoam* dan semakin tinggi permukaan air menghasilkan penurunan yang semakin kecil.

3.4 *Rumusan Daya Dukung Total* Raft Pile Foundation dengan Geofoam

a. Perhitungan Gaya Apung *Geofoam*

Besar gaya apung yang terjadi pada *geofoam* dan struktur *raft pile foundation* pada ketebalan *geofoam* 0.5 m gaya apung sebesar 6,860 N dan ketebalan *geofoam* 0.9 m gaya apung sebesar 10,780 N. Sebagaimana terlihat dalam table berikut:

Tabel 4. Tabel Tebal *Geofoam* dan Gaya Apung, Sumber: Hasil Analisis.

Tebal *Geofoam*	Gaya Apung (N) F = ρ x g x v
0.5	6,860
0.9	10,780

b. Perhitungan Daya Dukung Fondasi Rakit
Diketahui dari data percobaan:

c = 0,122 kg/cm²`
θ = 14,412°

Maka, nilai N_c, N_q , N_γ diperoleh dari tabel Faktor Daya Dukung Terzaghi sebagaimana terlihat pada tabel daya dukung Terzaghi untuk kondisi general *shear failure* di bawah ini, melalui interpolasi nilai sudut geser tanah yang di dapat dari hasil eksperimen laboratorium.

N_c = 12.46
N_q = 4.13
N_γ = 1.29

Tabel 5. Faktor Daya Dukung Terzaghi untuk Kondisi *General Shear Failure.*

ϕ	Nc	Nq	Nγ	ϕ	Nc	Nq	Nγ
0	5.70	1.00	0.00				
1	6.00	1.10	0.01	26	27.09	14.21	9.84
2	6.30	1.22	0.04	27	29.24	15.90	11.60
3	6.62	1.35	0.06	28	31.61	17.81	13.70
4	6.97	1.49	0.10	29	34.24	19.98	16.18
5	7.34	1.64	0.14	30	37.16	22.46	19.13
6	7.73	1.81	0.20	31	40.41	25.28	22.65
7	8.15	2.00	0.27	32	44.04	28.52	26.87
8	8.60	2.21	0.35	33	48.09	32.23	31.94
9	9.09	2.44	0.44	34	52.64	36.50	38.04
10	9.61	2.69	0.56	35	57.75	41.44	45.41
11	10.16	2.98	0.69	36	63.53	47.16	54.36
12	10.76	3.29	0.85	37	70.01	53.80	65.27
13	11.41	3.63	1.04	38	77.50	61.55	78.61
14	12.11	4.02	1.26	39	85.97	70.61	95.03
15	12.86	4.45	1.52	40	95.66	81.27	115.31
16	13.68	4.92	1.82	41	106.81	93.85	140.51
17	14.60	5.45	2.18	42	119.67	108.75	171.99
18	15.12	6.04	2.59	43	134.58	126.50	211.56
19	16.56	6.70	3.07	44	151.95	147.74	261.60
20	17.69	7.44	3.64	45	172.28	173.28	325.34
21	18.92	8.26	4.31	46	196.22	204.19	407.11
22	20.27	9.19	5.09	47	224.55	241.80	512.84
23	21.75	10.23	6.00	48	258.28	287.85	650.67
24	23.36	11.4	7.08	49	298.71	344.63	831.99
25	25.13	12.72	8.34	50	347.50	415.14	1072.80

$$q_u = c^*N_c + q^*N_q + \gamma^*N_\gamma \quad (1)$$

= (11.96 x 12.46) + (11.35 x 1 x 4.13) + (0.5 x 0.2 x 1.29)

= 3.91 kN

c. Perhitungan Daya Dukung Fondasi Tiang Rakit

1. Tanpa *Geofoam*

$$K_r = \frac{4*E_r*t_r^3*B*(1-v_s^2)}{3*\pi*E_s*L^4} \quad (2)$$

$$= \frac{4*21409*0.2^3*0.2\ (1-0.34^2)}{3*3.14*1.8*1.4^4}$$

= 1.86

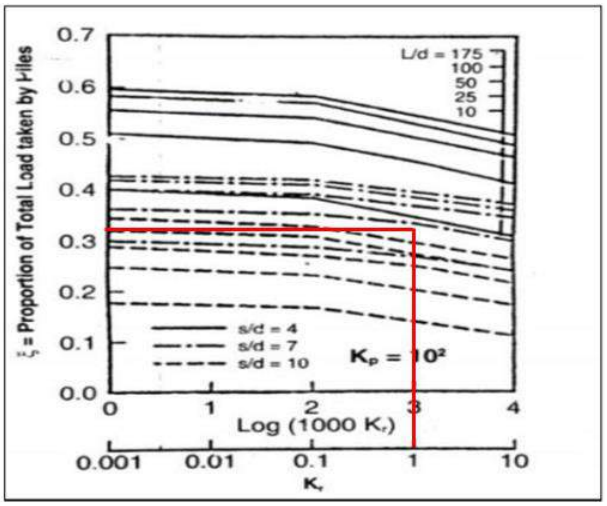

Gbr. 11. Grafik Relatively Compressible Piles (Kp = 102), Lee (1993).
L/d = 1.4m/0.2m = 7

Berdasarkan grafik, didapat nilai δ = 0.34 kN. Maka daya dukung yang terjadi adalah:

$$P = \frac{\delta*P*FS}{Nt*\eta} \quad (3)$$

$= \frac{0.34*4{,}704\ kN*2}{4*1.1}$

= 0.72 kN

2. Dengan *Geofoam* 0.5 m

$$K_r = \frac{4*E_r*t_r^3*B*(1-v_s^2)}{3*\pi*E_s*L^4} \quad (4)$$

$= \frac{4*21409*0.2^3*0.2\ (1-0.34^2)}{3*3.14*1.8*0.9^4}$

= 10.89

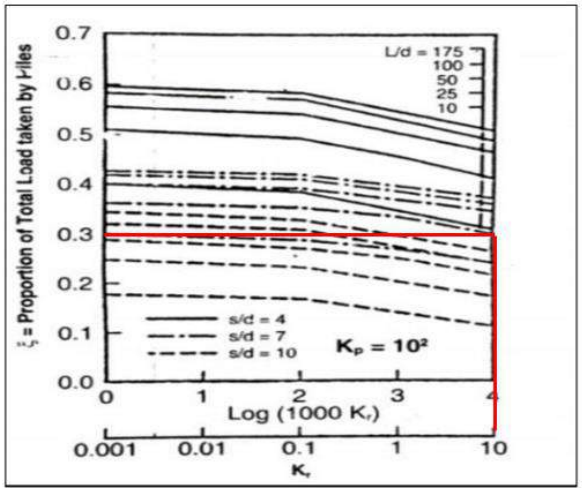

Gbr. 12. Grafik Relatively Compressible Piles (Kp = 102) (Lee, 1993).
L/d = 0.9m/0.2m = 4.5

Berdasarkan grafik, didapat nilai δ = 0.31 kN. Maka daya dukung yang terjadi adalah:

$$P = \frac{\delta*P*FS}{Nt*\eta} \quad (5)$$

$= \frac{0.31*4.704\ kN*2}{4*1.1}$

= 0.66 kN

3. Dengan *Geofoam* 0.9 m

Daya dukung pondasi tiang rakit yang terjadi pada *geofoam* 0.9 m bernilai 0. Karena perbandingan antara panjang pile dengan diameter pile (L/d = 0.5/0.2 = 2.5) lebih kecil dari 4, sesuai dengan grafik 5.1. (*Relatively Compressible Pile*, Kp = 10²), Lee (1993). Nilai daya dukung tiang tidak diperhitungkan.

Maka, dari hasil perhitungan di atas, dapat di akumulasikan bahwa daya dukung total akibat *uplift*, raft pondasi dan *raft pile* pondasi dalam berbagai kondisi sebagaimana terlihat pada penjelasan berikut:

a. Daya Dukung Total Tanpa *Geofoam*
= Gaya uplift + Daya Dukung Pondasi Rakit + Daya Dukung Pondasi Tiang Rakit
= 0 kN + 3.91 kN + 0.72 kN
= 4.63 kN
Dengan *safety factor* = (4.63 kN/4.704 kN)
= 0.98

b. Daya Dukung Total Dengan *Geofoam* 0,5 m
1. Tanpa Muka Air Tanah
= Gaya uplift + Daya Dukung Pondasi Rakit + Daya Dukung Pondasi Tiang Rakit
= 0 kN + 3.91 kN + 0.66 kN
= 4.57kN
Dengan *safety factor* = (4.57 kN/4.704 kN)
= 0.971

2. Di bawah Muka Air Tanah
= Gaya uplift + Daya Dukung Pondasi Rakit + Daya Dukung Pondasi Tiang Rakit
= 0 kN + 3.91 kN + 0.66 kN
= 4.57 kN
Dengan *safety factor* = (4.57 kN/4.704 kN)
= 0.971

3. Di atas Muka Air Tanah
= Gaya uplift + Daya Dukung Pondasi Rakit + Daya Dukung Pondasi Tiang Rakit
= 6.86 kN + 3.91 kN + 0.66 kN
= 11.43 kN
Dengan safety factor = (11.43 kN/4.704 kN)
= 2.42

c. Daya Dukung Total Dengan *Geofoam* 0.9 m
1. Tanpa Muka Air Tanah
= Gaya uplift + Daya Dukung Pondasi Rakit + Daya Dukung Pondasi Tiang Rakit
= 0 kN + 3.91 kN + 0 kN
= 3.91 kN
Dengan *safety factor* = (3.91 kN/4.704 kN)
= 0.83

2. Di bawah Muka Air Tanah
   = Gaya uplift + Daya Dukung Pondasi Rakit + Daya Dukung Pondasi Tiang Rakit
   = 0 kN + 3.91 kN + 0 kN
   = 3.91 kN

   Dengan *safety factor* = (3.91 kN/4.704 kN) = 0.83

3. Di atas Muka Air Tanah
   = Gaya uplift + Daya Dukung Pondasi Rakit + Daya Dukung Pondasi Tiang Rakit
   = 10.78 kN + 3.91 kN + 0 kN
   = 14.69 kN

   Dengan *safety factor* = (14.69 kN/4.704 kN) = 3.12

4. KESIMPULAN

Ketebalan *geofoam* dan tinggi MAT berpengaruh terhadap settlement yang terjadi. Semakin tebal *geofoam* dengan MAT yang tinggi, maka *settlement* yang terjadi semakin kecil. Hal tersebut terjadi karena masa *geofoam* lebih kecil daripada air, dimana jika *geofoam* di tekan maka air akan memberikan perlawanan dalam bentuk gaya ke atas.

DAFTAR PUSTAKA

Diana, W., Hardiyatmo, H. C. & Suhendro, B. 2016. Small-Scale Experimental Investigation on the Behaviour of Nailed Slab System in Expansive Soil. *AIP Conf. Proc.* 1755.

Ekanayake, S.D., Liyanapathirana, D.S.. and Leo, C.J. 2015. Numerical Simulation of EPSGeofoam Behaviour in Triaxial Tests. *Engineering Computations* Vol. 32 (5):1372-1390.

Tom A. and Sindhu A.R. 2016. Model Study on the Behavior of Piled Raft Foundation. *International Journal of Science Technology & Engineering* Volume 3, Issue 02: 324-328.

Wong I.H., et al. 2000. Raft Foundations with Disconnected Settlement Reducing Piles. *In: Design application of Raft Foundations and Ground Slabs*: 469-486. London: Thomas Telford.

Visual Observation Against Reaction Cumulation Using Ureolytic Bacteria Oceanobacillus Isolate P3BG41 and Isolate P3BG43

Yustian Heri Suprapto
Departement of Civil Engineering, Faculty of Engineering – University of Indonesia

Puspita Lisdiyanti
Departement of Civil Engineering, Faculty of Engineering – University of Indonesia

Budi Susilo Soepandji
Departement of Civil Engineering, Faculty of Engineering – University of Indonesia

Wiwik Rahayu
Departement of Civil Engineering, Faculty of Engineering – University of Indonesia

ABSTRACT: Bacteria from Bacilla genus could produce urease enzymes that able to use in to catalyze the calcium chloride and urea into calcite particles. Specific isolate of Oceanobacillus P3BG41 and P3BG43 are used in this research due to their capability of urease production. The bacteria are grown under specific medium and mixed with cementation solution with comparison of 1:3. This composition is then injected to the sand and observe the reaction of calcite production, which expected to fill the soil pores. This process will take effect on the soil's particle binding. The observation was done in five days and found that the highest urease activity was occurred in 48 hours after injection. The samples then visually observed using scanning electron microscope (SEM) and energy dispersive x-ray (EDX). The composition of calcium (Ca) and oxygen (O) were dominated all over the samples with concentration above 30%.

Keywords: bacilla, cementation, oceanobacillus, urease enzyme

Performance and Back Analysis of Soil Improvement with Vertical Drains with Vacuums Preloading in Bandung Basin Area with Finite Element Analysis

Eyrton Crismartua Silaban
Sr. Geotechnical Engineer – PT WSP Engineering

I Wayan Sengara
Professor, Faculty of Civil and Environmental Engineering – Institute Technology Bandung

ABSTRAK: Wilayah Cekungan Bandung memiliki tantangan khusus untuk menangani masalah daya dukung dan settlement tanah sangat lunak. Lapisan tanah lunak memiliki karakteristik kadar air yang tinggi, kompresibilitas yang tinggi, permeabilitas air yang rendah, dan kuat geser yang relatif rendah Salah satu metode perbaikan tanah di wilayah ini adalah dengan memasang PVD dengan *vacuum preloading* yang dilakukan di lapangan. Makalah ini akan menyajikan hasil analisis balik dengan pemodelan elemen PLAXIS 2D hingga penurunan dari data lab (kuat geser dan kompresibilitas) dibandingkan dengan monitoring penurunan untuk memastikan parameter input yang paling cocok. Hasil performa ini juga diharapkan dapat memprediksi besaran dan laju waktu penurunan residual di mana tanah lunak dimodelkan sebagai model *modified* Cam-clay. Hasil studi menunjukkan bahwa penurunan selama 235hari di lapangan sesuai dengan penurunan model PLAXIS 2D dengan rentang parameter tertentu. Kemudian model juga sudah mampu memprediksi besarnya penurunan residual pasca konstruksi yang harus dipertimbangkan struktur atas.

Kata Kunci: cekungan bandung, tanah lunak, pvd, vacuum preloading, plaxis 2d, monitoring penurunan, elemen hingga, penurunan residual

ABSTRACT: Bandung Basin Area has challenges to deal with bearing capacity and settlement of very soft soil issues. The soft soil layer is characterized by high moisture content, high compressibility, poor water permeability, and low shear strength. So, the consolidation settlement and bearing capacity should be determined, and the appropriate design measures applied. One method to improve the soil in the Bandung Basin Area is installing vertical drains with vacuums preloading conducted in the field. This paper will present back-analysis results by modeling the PLAXIS 2D finite element decrement from the lab data (shear strength and compressibility) compared to the settlement monitoring to ensure the most suitable input parameters. The performance result is also expected to be able to predict the magnitude and rate of residual settlement time where the soft soil is modeled as a modified Cam-clay model. The results of the study show that the settlement for 235 days in the field corresponds to the settlement in the PLAXIS 2D model with a specific parameter range. The model is also able to predict the increase in post-construction settlement that must be considered the upper structure.

Keywords: bandung basin, soft soil, vertical drains, vacuum preloading, plaxis 2d, settlement monitoring, finite element, residual settlement

1 INTRODUCTION

The Indonesian Jakarta-Bandung high-speed railway project connects Jakarta, the capital of Indonesia, with Bandung, the capital of West Java Province. The end of this HSR project station is in Cileunyi, known as the Bandung Basin Area.

Bandung Basin Area has an intense soft clay thickness characteristic that can reach 70-100 meters, Tohari et al. (2015). The soft clay layer is included in classifying clay with high plasticity, which is easier to consolidate according to depth. Other characteristics include high moisture content, high

compressibility, poor water permeability, and low shear strength.

In Indonesia, one quite familiar method to improve soft soil, such as in the Bandung Basin Area, is the preloading and prefabricated vertical drain (PVD). This method aims to accelerate the magnitude and time rate consolidation settlement.

2 GEOLOGICAL CONDITION

The area is in the mountain basin with gentle terrain. The surface is mainly woods, rice fields, and villages. There is primarily the Quaternary Holocene artificial fill layer (Qml) fill soil, plain fill, and miscellaneous fill; the Quaternary Holocene lacustrine layer (Ql) silt, clay, silty clay, silt, silt, fine sand, medium sand, Quaternary Pleistocene volcanic accumulation layer (Qyu) clay, fine sand, fine round gravel, fine breccia, mudstone (semi-diagenesis), sandstone (semi-diagenesis), breccia (semi-diagenesis/diagenesis).

Based on the Geological Map of Bandung Quadrangle, Java, published by the Geological Survey of Indonesia (Fig. 1), this location is currently on Lake Deposits (Ql) map unit. This map unit has Quaternary age and can reach a depth of about 0-125m with lithology descriptions of tuffaceous clay, sandstone, gravel, and conglomerate. Locally forms horizontal layers, and it contains limestone concretions, plant remains, freshwater mollusks, and bones of vertebrates. Locally also intercalated by breccia, Silitonga (1973).

Based on shallow and deep drilling results, the geological and engineering geology sections are obtained as presented in Fig. 2 for the North-South direction. The density level of the layer gradually gets more profound and denser because the layer below is compacted due to the loading of the layer above it (overburden). Based on the N-SPT value, the subsurface profile shows the consistency of a low (soft) soil layer getting thicker towards the basin's center. The north-south cross-section shows that the medium to very dense sand layer has thickened in the middle of the basin, while the clay underneath is getting thicker to the north. This dense sand layer results in an increase in the consistency of the underlying clay layer from being stiff to very stiff, Tohari et al. (2015).

The previous study indicates that the thick, soft soil layers are an issue that must be considered in the development of the Bandung Basin Area. Consolidation settlement requires quite a long time, and therefore settlement during construction and operation must be considered in this area.

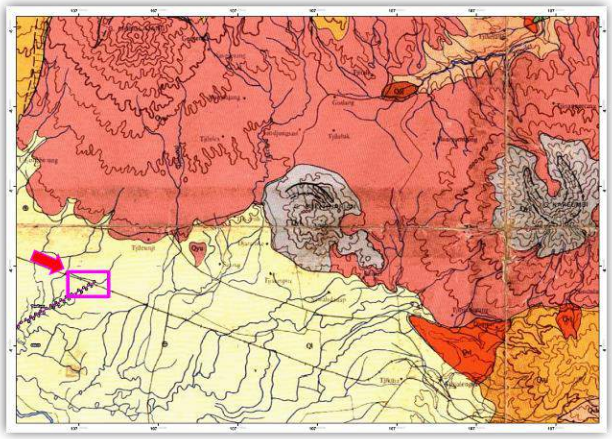

Fig. 1. Location of Tegal Luar Station based on Geological Map of Bandung Quadrangle, Java, Silitonga (1973).

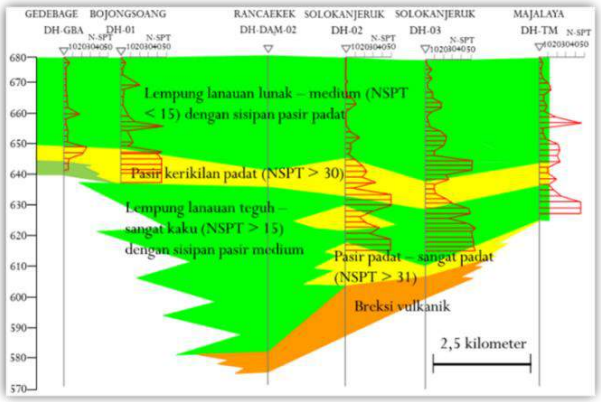

Fig. 2. Geological Cross Section of The Gedebage - Bojongsoang - Solokanjeruk – Majalaya, Tohari et al. (2015).

3 SITE CONDITION

The study area has conducted several deep borings to provide NSPT and undisturbed samples (UDS) distributed at several points. The cross-section of the soil is shown in Figure 3 in the form of a soil stratigraphy along with annotations.

Based on the soil collected in this area, six main layers are simplified for further analysis. The soil profile as stratigraphy layer is shown in Fig. 3. Layer 1 from depth 0 - 5 m is the gravelly silt/clay as fill material with medium dense consistency and N-SPT of 7-9. Layer 2 from 5 - 22 m is clay with a very soft consistency and N- SPT of 0. Layer 3 at a 22-

39 m is clay with medium-stiff to a stiff consistency and N- SPT of 4-17. Layer 4 at a depth of 39 - 41 m is gravelly sand medium dens consistency with N-SPT of 19. Layer 5 at a depth of 41 - 46 m is clay with medium stiff and stiff consistency with N-SPT of 14-16, and Layer 6 at a depth of 46-60 m is a breccia with very hard consistency with N-SPT varies more than 60.

The soft clay layer underneath the fill material has a thickness of 17 meters. Then there are two compressibility layers with a thickness of 22 meters, which can undergo settlement consolidation.

According to the triaxial test (UU and CU), the mud and Holocene clays' undrained and adequate cohesion shear strength varies between 7-36 kPa and 6-23 kPa, respectively. Cc is a compression index ranging from 0.39 to 1.22 with a compression ratio (CR) for the mud layer. Based on the consolidation test, the vertical coefficient of consolidation (Cv) is around $2x10^{-3}$ cm2/sec. The corresponding soil properties at a depth of 60 meters are shown in Fig. 4 to Fig. 6.

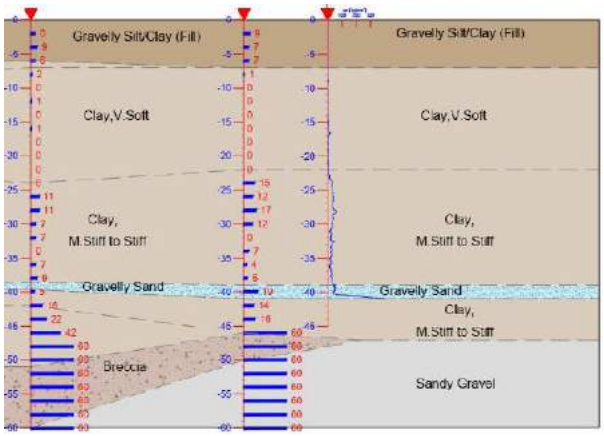

Fig. 3. Cross-Section of The Soil profile.

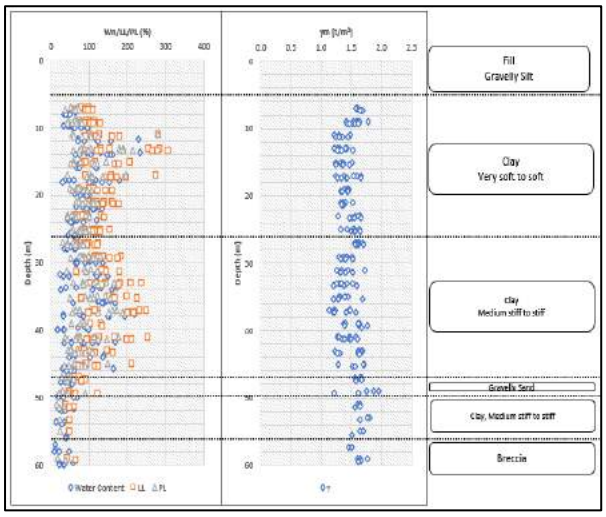

Fig. 4. The Variations of Water Content, LL, PL, and Unit Weight vs. Depth.

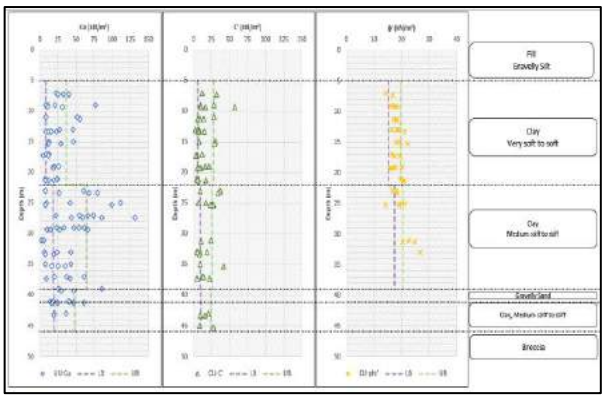

Fig. 5. The Variations and Boundary of Shear Strength Parameters vs. Depth.

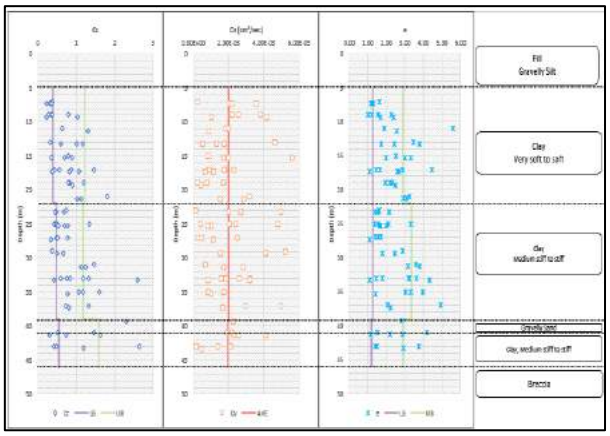

Fig. 6. The Variations and Boundary of Compressibility Parameters vs. Depth.

4 MONITORING RESULT

During the construction of a vacuum combined with preloading soil, observations are strengthened, and the settlement monitoring data is conducted every day. The monitoring includes the location of the monitoring point and the construction progress (vacuum pressure, preloading soil height, and pore pressure). Fig. 7 shows the instrumentation plan and site layout. According to the design requirements, nine settlement points, five vacuum dial observation points, 1 set of piezometer points, one water level observation point, and one inclinometer point.

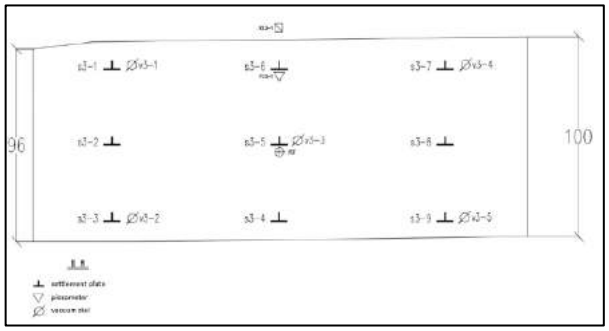

Fig. 7. The Layout of the Monitoring Point.

From the monitoring result, the maximal total settlement in this area is 4.526 meters with a 7.0-meter backfill thickness for 235 days. After inserting the vertical drain, pore water pressure probes were installed in the vacuum preloading area. The summary graph between soil preloading height, vacuum preloading (assumed γ_w=18 kN/m^3), and the settlement that occurs with time are shown in Fig. 8.

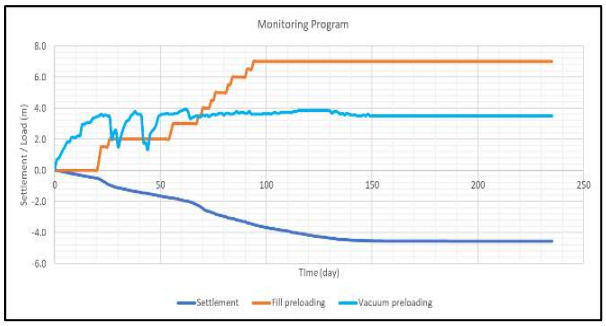

Fig. 8. Summarize Time against Vacuum Pressure, Preloading Soil Height, and Settlement.

5 NUMERICAL MODELING

The finite element approach was used for numerical modeling PLAXIS 2D. The soil layer was separated into 6 (six) layers based on the soil profile in this study (Figure 9). The soft soil is modeled using a modified Cam-clay model.

It's important to note that the adjusted indices κ^* and λ^* with the original Cam-Clay parameters are different. Instead of the volumetric strain ε_v, the void ratio e describes the latter characteristics.

Apart from the isotropic compression test, the parameters κ and λ can be obtained from a one-dimensional compression test. Here a relationship exists with the internationally recognized parameters for one-dimensional compression and swelling, C_c and C_s.

$$\lambda^* = C_c/(1+e) \quad (1)$$

$$\kappa^* = 2C_s/2.3(1+e) \quad (2)$$

Where Cc is compression index, Cs is swelling index, and e_0 is the initial void ratio. Table 1 shows the input soil parameters in the numerical analysis in PLAXIS 2D include shear strength and compressibility parameters.

To accurately verify the performance of vacuum combined surcharge preload as ground improvement and soil design parameters, this study will conduct several simulations of permeability parameters from field monitoring results.

The study area of the vacuum preloading is 100m wide and 120m long. The vertical drain properties include penetration length 22 meters, spacing 1.0m, configuration is the square layout, and the bottom of the vertical drain should penetrate the mud layer approximately 1m.

The simulation input data of the vacuum pressure value is assumed to be the vacuum reading divided by 10 (γ_w=10 kN/m^3) in the negative direction. It means that the vacuum will provide an additional load which will be adjusted numerically along with the preloading height in analysis.

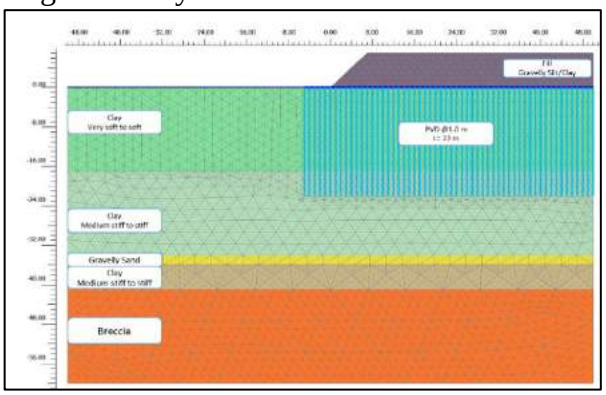

Fig. 9. Model Geometry and Mesh Generation of Project Study.

Installation of PVD causes water to tend to escape in a horizontal direction. So, this study will consider the range of permeability coefficients in the horizontal direction of the field for soft soils based on Rixner et al., 1986 can be seen in Table 2.

Table 1. Range Ratio k_h/k_v Soft Clay Soil, after Rixner et al. (1986).

Nature Clay	Kh/kv
No or slightly developed macro fabric, essentially homogeneous deposits	1-1.5
From relatively well-developed macro fabric, e.g., sedimentary clays with discontinuous lenses and layers of more permeable material	2-4
Varved clays and other deposits containing embedded and more or less continuous permeable layers	3-15

Soil permeability coefficient classification refers to Craig 2004 in this study, as shown in Fig. 10. Based on the soil permeability test, the permeability value is 7x10^{-9} m/s, categorized as unfissured clays and clay-silts.

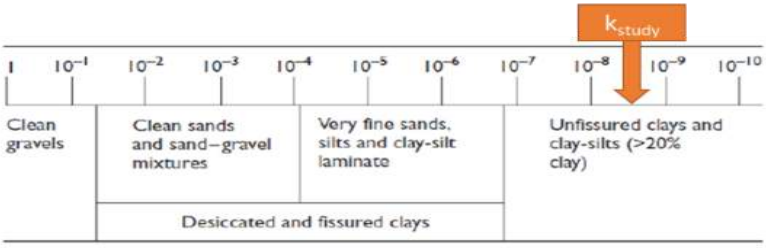

Fig. 10. Soil Permeability Range in m/s.

Table 1. Input Soil Parameters in The Numerical Analysis PLAXIS 2D.

Layer	Depth			Soil Description	NSPT Range	Shear Strength Parameter		Compressibility Parameter					
	From	-	To			C' (kPa)	ϕ' (kPa)	Cc	Cs	Cvx10^{-4} (cm^2/sec)	e	OCR	CR
1	0	-	5	Fill, Gravelly Silt/Clay	7-9	-	30	-					
2	5	-	22	Clay, V.Soft to Soft	0	6-23	15-19	0.39-1.22	0.04-0.1	6-30	1.23-2.89	1-2.76	0.14-0.32
3	22	-	39	Clay, M.Stiff to Stiff	4-17	9-25	17-20	0.49-1.18	0.05-0.12	6-30	1.41-3.53	1-1.74	0.18-0.32
4	39	-	41	Gravelly Sand	19	-	25	-					
5	41	-	46	Clay, M.Stiff to Stiff	14-16	10-22	22-26	0.55-1.59	0.05-0.16	8-30	1.17-2.88	1.14	0.15-0.33
6	46	-	60	Breccia	60	-	36	-					

6 RESULTS AND DISCUSSIONS

This study simulated the shear strength and compressibility parameters of very soft soil layer with three conditions: average, lower bound, and upper bound parameters. It can be seen from the simulation results that, there are some deviations from the monitoring data because the soil data parameters are limited However, on the other hand, the range of consolidation settlement is included in the boundary graph area, meaning that the parameters range of the justification results of this study is in accordance with field conditions

Fig. 11 shows the comparison of monitoring of land surface settlement in the middle of the embankment and the simulation results using the PLAXIS 2D numerical method. After 235th day, the differences between the of average, lower-bound, and upper bound parameters were compared to and the settlement monitoring results are about 1.5%, 7.8%, and 8.2%, respectively. After 235 days of settlement analysis, the Soft Clay model of PLAXIS 2D can predict long-term settlement fairly well.

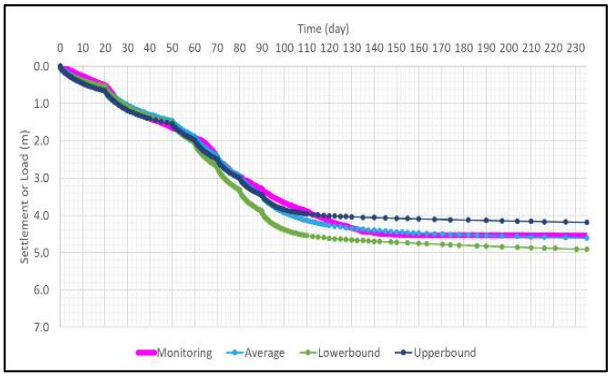

Fig. 11. Comparison between Monitoring and Simulated Settlements from PLAXIS 2D.

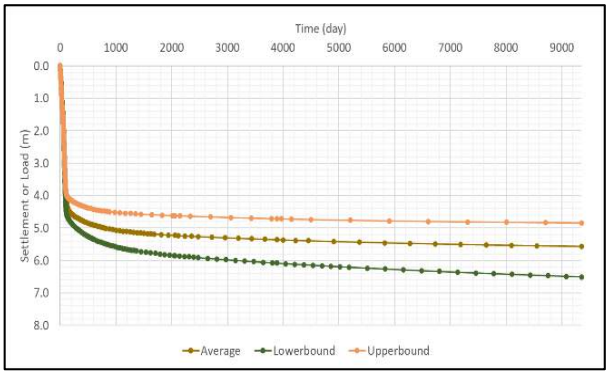

Fig. 12. Long-Term Settlement Prediction up to 25 Years after Improvement.

7 CONCLUSION

1. The analysis and prediction of settlement using PLAXIS 2D adopting Soft Clay constitutive model parameters are considered to be reliable enough to simulate the settlement and gain the strength of the soil during stage construction process. The parameter uncertainty can still be covered with boundary parameters so that the settlement is within the range, and it is following ground improvement performance (PVD + vacuum preloading).
2. From the analysis of long-term conditions, there are indications of subsidence after the soil is repaired. The compressible layer under the improvement layer contributes to the cause of residual settlement. From the analysis of long-term conditions, there are indications of subsidence after the soil is repaired. The compressible layer under the improvement layer contributes to the cause of residual settlement. This settlement value must be mitigated properly so that it does not adversely affect the upper structure.

ACKNOWLEDGEMENTS

The authors are thankful to Mr. Suryanto Supardi, and Prof. Adang Surahman from CDJO for moral and technical support until the paper is finished. Special thanks to Rachman Suhanda as General Manager Technical/Design Management of KCIC for sharing geotechnical data testing and reports related to this paper.

REFERENCES

Brinkgreve R.B.J. 2017. *PLAXIS Tutorial Manual.* Plaxis bv. Delft.

Deng Y. et al. 2017. Finite Element Analysis of Vacuum Consolidation with Modified Compressibility and Permeability Parameters. *International Journal of Geosynthetics and Ground Engineering* 3:15. Switzerland: © Springer International Publishing.

Gumilar I. et al. 2013. Land subsidence in Bandung Basin and its possible caused factors. *ISEDM 2013 3rd International Symposium on Earthquake and Disaster Mitigation*. Bandung.

Indraratna, B. et al. 2011. Performance and Prediction of Vacuum Combined Surcharge Consolidation at Port of Brisbane. *Journal of Geotechnical and Geoenvironmental Engineering*. Virginia:© American Society of Civil Engineers.

SNI 8460:2017. 2017. *Persyaratan Perancangan Geoteknik*. Badan Standardisasi Nasional.

Tjie-Liong, D. G. 2014. Common Mistakes on the Application of Plaxis 2D in Analyzing Excavation Problems. *International Journal of Applied Engineering* Research ISSN 0973-4562 Volume 9, Number 21 (2014): 8291-8311, 8291-8312.

Rixner, J.J., K. S.R. dan A.D. Smith. 1986. Prefabricated Vertical Drains. *Vol. I: Summary of Research Report Final Report*. Washington D.C: Federal Highway Admin.

Saputro S.A. et al. 2018. Ground settlement prediction of embankment treated with prefabricated vertical drains in soft soil. *The 4th International Conference on Rehabilitation and Maintenance in Civil Engineering*. EDP Sciences.

Tohari A. et al. 2015. Kondisi Geologi Teknik Bawah Permukaan Wilayah Cekungan Bandung (Lintas Gedebage-Bojongsoang-Solokanjeruk-Majalaya). *Prosiding Pemaparan Hasil Penelitian Puslit Geoteknologi LIPI Tahun 2015*. Bandung.

Determination of Downhole Dynamic Compaction Parameters Based on Finite Element Analysis

Martin Wijaya
Lecturer – Universitas Katolik Parahyangan

Ahmad Kemal Arsyad
Geotechnical Engineer – PT Geotechnical Engineering Consultant

Aswin Lim
Lecturer – Universitas Katolik Parahyangan

Paulus Pramono Rahardjo
Professor of Geotechnical Engineering – Universitas Katolik Parahyangan

ABSTRAK: Tanah-tanah yang *collapsible* sangat umum ditemukan di Cina dan telah menyebabkan banyak kerusakan terhadap bangunan dan infrastruktur. Untuk mengatasi hal tersebut, perbaikan tanah menjadi kebutuhan agar dapat menstabilkan tanah-tanah yang *collapsible*. *Downhole dynamic compaction* (DDC) bersama dengan buangan material pembongkaran konstruksi telah umum dipergunakan di Cina untuk menstabilkan tanah yang *collapsible*. DDC akhir-akhir ini dipergunakan untuk perbaikan tanah di proyek bandara di Indonesia. Di proyek ini, material DDC didapatkan dari tanah sekitar yang banyak mengandung butir dengan ukuran besar. Akibatnya, sulit untuk menenetukan parameter DDC berdasarkan uji laboratorium. Oleh karena itu, uji pembebanan statis di lakukan untuk mendapatkan kurva beban dan penurunan dari tiang DDC dan kurva beban dan penurunan dari tiang DDC akan di analisa balik mempergunakan metode elemen hingga agar parameter DDC dapat ditentukan.

Kata Kunci: DDC, tanah vulkanik, metode elemen hingga, analisa balik, uji pembebanan statis

ABSTRACT: Collapsible soil are commonly encountered in China and has caused significant damage to building and infrastructure. As a result, ground improvement has become necessity in order to stabilize the collapsible soil. Downhole dynamic compaction (DDC) together with construction and demolition waste material (CDW) has been commonly used in China to stabilize collapsible soil. DDC has just been recently used as one of the ground improvement methods for airport project in Indonesia. In this project, DDC material is from the in-situ soil which contains a lot of oversize particle size. As a result, it is difficult to determine DDC parameters based on laboratory test. Hence, static load test is conducted in order to obtain load deformation curve from the DDC pile the load deformation curve from the DDC pile will be back analysis by using Finite element method in order to determine DDC parameter.

Keywords: DDC, volcanic soil, finite element method, back analysis, static load test

Analisis Alternatif Metode Perbaikan Tanah Lunak pada Pembangunaan Tailing Dam

Yogina Lestari Ayu Situmorang
Departemen Teknik Pertanian dan Biosistem – Universitas Padjadjaran

Eulis Karmila
PT Ika Adya Perkasa

Abdurahman Hafizudin
PT Ika Adya Perkasa

ABSTRAK: Bauksit merupakan salah satu komoditi tambang utama di Indonesia. Untuk menunjang proses penambangan dibutuhkan tailing dam. Salah satu tailing dam dikonstruksi di Kalimantan barat dimana terletak pada tanah lunak terkompresibel. *Starter Dam* terletak pada tanah lunak dengan kedalaman hingga 16 meter, sehingga diperlukan penanganan terlebih dahulu. Penangan tanah lunak direncanakan dengan 3 (tiga) alternatif penanganan, yaitu PVD (*Prefabricated Vertical Drain*) dan *Preloading*, PVD – *Vacuum Preloading*, dan DCM (*Deep Cement Mixing*). Ketiga alternatif tersebut dibandingkan dalam hal performa perbaikan kekuatan tanah meliputi Angka Keamanan, besar penurunan tanah, dan metode pelaksanaan. Secara analitikal, ketiga alternatif memiliki performa yang memenuhi kriteria desain. Penggunaan PVD – *Preloading* dan PVD – *Vacuum Preloading* memerlukan tinggi preloading yang sangat besar, sehingga memerlukan penambahan lahan dan juga berpengaruh pada stabilitas penimbunan. Penggunaan DCM tidak memerlukan preloading sehingga lebih efisien untuk timbunan tinggi seperti tailing dam.

Kata Kunci: tailing dam, pvd, preloading, dcm

ABSTRACT: Bauksit is one of the major mining commodities in Indonesia. To support the mining process, a tailings dam is needed. One of the tailing dams constructed in West Kalimantan is located on compressible soft soil. Starter Dam has 16 meters compressible soft soil, therefore soil improvement needed. Soil Improvement is designed with 3 alternatives methods, PVD (Prefabricated Vertical Drain) dan Preloading, PVD – Vacuum Preloading, and DCM (Deep Cement Mixing). The alternatives are compared in terms of performance such as shear strength improvements, settlements, and constructability. Analytically, the alternatives meet the design criteria. PVD – Preloading and PVD – Vacuum Preloading requires a high preloading embankment, so it requires additional land and affects the stability of the embankments. DCM does not require preloading, so it is more efficient for high embankment such as tailings dams.

Keywords: tailing dam, pvd, preloading, dcm

1 PENDAHULUAN

Saat ini merupakan kewajiban bagi setiap perusahaan tambang di Indonesia untuk memiliki fasilitas pengolahan bijih mineral atau *smelter*. Pada pertambangan Bauksit *smelter* bertujuan mengolah bijih bauksit menjadi alumina maupun aluminium. Pembangunan pabrik *Smelter Grade Alumina Refinery* (SGAR) kemudian mulai proses pembangunannya yang terletak di kabupaten Mempawah, Kalimantan Barat. Sebagai penunjang proses pengolahan, maka diperlukan Tailing Dam yang terintegrasi pada *smelter*. Tailing Dam tipe *earthfill* dengan starter dam setinggi 25 meter direncanakan sebagai penampungan limbah tambang. Volume limbah tambang pada umumnya sangat besar, oleh karena itu diperlukan kolam yang sangat besar pula dalam menampung limbah agar tidak menimbulkan dampak merugikan pada lingkungan. Menurut Fitriyanto & Taruko (2014), residu bauksit yang masuk ke dalam *tailing storage facility* nantinya adalah berupa *redmud* dengan *moisture content* sekitar 32% setelah proses *press filtration*. Dari segi

perencanaan awal, perencanaan Tailing dam sama dengan perencanaan pada bendungan penampung air. Perbedaannya terletak pada teknik pelaksanaan konstruksi dan operasinya serta pada material yang ditampung, baik secara fisik maupun kandungan kimia.

Bagaimana meningkatkan stabilitas dan keamanan bendungan tailing menjadi tantangan bagi para perencana terutama jika bendungan berada di atas tanah lunak yang tebal. Dalam makalah ini, dilakukan analisis terhadap alternatif metode perbaikan tanah lunak menggunakan PVD dengan *Preloading*, PVD-*Vacuum Preloading* dan *Deep Cement Mixing*. Ketiga alternatif tersebut di analisis secara performa dalam meningkatkan stabilitas Tailing dam meliputi *Safety Factor*, besar penurunan tanah, dan metode pelaksanaan.

2 PERTIMBANGAN ALTERNATIF PENANGANAN TANAH

Tailing Dam tipe *earthfill* homogen direncanakan dengan starter dam setinggi 25 meter di rencanakan untuk menampung limbah tambang berupa *redmud*. Dengan tinggi demikian, tentu menjadi perhatian jika dibangun di atas *soft ground*. Tanah Lunak daya dukung tanah dasar yang relatif rendah. Tanah tersebut juga menghadapi penurunan yang relatif besar yang berlangsung relatif lama. Untuk memastikan keamanan pada bendungan maka perlu upaya penanganan dalam mengurangi besar penurunan.

Di antara banyak metode perbaikan tanah lunak telah dikembangkan dan diterapkan di seluruh dunia, menurut Gouw & Gunawan (2020) *vacuum* PVD merupakan skema perbaikan tanah yang ramah lingkungan jika dibandingkan dengan kombinasi penggunaan *Preloading*. Hal ini didasari *preloading* membutuhkan material urugan dalam jumlah besar sehingga biasa dilakukan pemotongan bukit dalam mendapatkan material urugan. Meskipun performa kedua metode tersebut baik PVD *Preloading* dan PVD-*Vacuum Preloading* menunjukkan terjadi perbaikan *strength* pada tanah.

Metode lainnya adalah *Deep Cement Mixing* (DCM). Seperti dijelaskan dalam buku oleh Kitazume & Terashi (2013), DCM merupakan metode perbaikan tanah dengan cara mencampurkan tanah in situ dengan semen sebagai bahan pengikat. Manfaat metode DCM antara lain memperbaiki lempung lunak dan tanah organik untuk berbagai keperluan seperti stabilitas, pengurangan penurunan/ deformasi dan pengontrol rembesan. DCM menjadi pertimbangan solusi karena tidak memerlukan *preloading*, mengingat tubuh tailing dam sangat tinggi.

Belakangan ini, Nguyen et al. (2020) meneliti terhadap performa penggunaan *deep cement mixing* yang digunakan sebagai metode perbaikan tanah pondasi pada pembangunan tanggul penutup Wonogiri multi-purpose dam, di Jawa Tengah. Tanggul berupa timbunan setinggi 7 meter dibangun dengan tujuan mengurangi sedimentasi pada pengambilan bendungan. Tanah dasar di bawah tanggul terdiri dari *very soft* ke *soft clay*. Ketebalan tanah yang di-*improve* bervariasi, dari 6 meter hingga 24 meter. Perbaikan tanah dengan metode *deep cement mixing* diterapkan untuk mengatasi stabilitas lereng dan konsolidasi. Evaluasi performa DCM menunjukkan, sebagian besar area yang perbaikan tanah menunjukkan nilai N-SPT meningkat. Namun demikian, ada beberapa area yang tidak terjadi perbaikan, diakibatkan sulitnya monitoring pada saat pelaksaanaan berlangsung.

3 KONDISI UMUM LOKASI *TAILING DAM*

Tailing Dam pada Alumina *Refinery* di Mempawah, Kalimantan Barat berada di area pesisir pantai. Seperti terlihat pada Gbr. 1, tanah didominasi oleh *soft* ke *medium silt* hingga kedalaman 16 m.

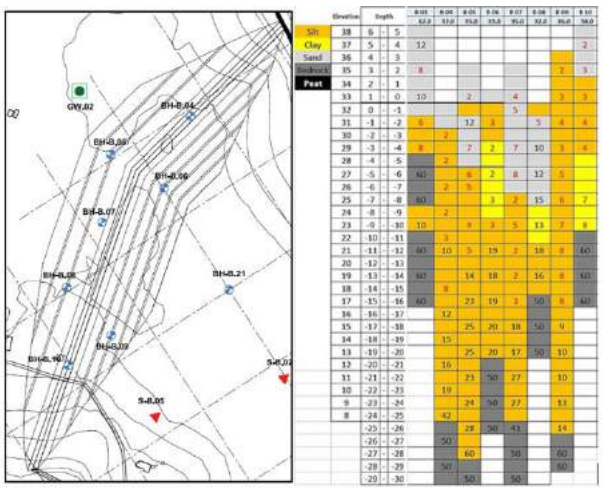

Gbr. 1. Penyelidikan Tanah Area Starter Dam.

Perlapisan tanah di bawah permukaan starter dam terdiri dari lapisan gambut tipis, *soft clay* ke *medium stiff silty clay* dengan ketebalan 5 m. Kemudian dibawah lapisan ini terdapat lapisan

soft ke *very stiff silty clay* dengan ketebalan 8 m. Dibagian bawah lapisan ini terdapat *medium stiff* ke *hard silty clay* setebal 9 m dan batuan dasar berupa batuan granit keras ditemukan di kedalaman 22 m dari permukaan tanah.

4 METHODOLOGY

Dalam studi ini, analisis dilakukan dengan metode elemen hingga dibantu *software* Plaxis 2D. Adapun data input yang digunakan dalam Plaxis seperti disajikan pada Tabel 1. Dalam memodelkan *PVD* ke dalam program, maka perlu dilakukan ekuivalensi dari *axysimetris* ke *plane strain*. Ekuivalen yang digunakan adalah dengan metode oleh Chai et al. (2013) seperti pada Gbr. 2. PVD dimodelkan dengan pola segitiga dengan spasi 1 m serta ditanam hingga kedalaman 16 m.

Pada Plaxis, DCM dimodelkan sebagai *cluster* tanah dengan rata-rata undrained shear strength (Su). Konfigurasi dari DCM bergantung pada Su ekuivalen dan *improvement area ratio*, Bruce et al. (2013). Ekuivalen dari Su adalah rata-rata kuat dari kolom DCM dengan tanah in situ antar kolom DCM. Konfigurasi DCM pada studi ini seperti pada Gbr. 2.

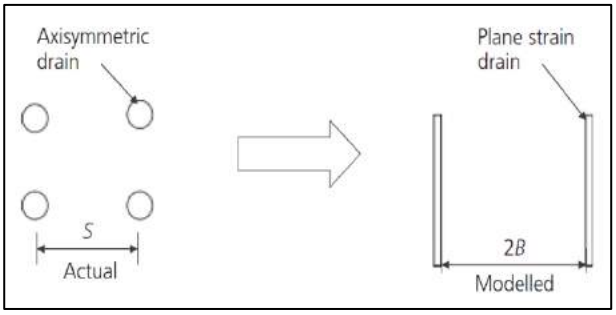

Gbr. 2a. Model Ilustrasi Ekuivalen PVD pada Plaxis (Chai et al. 2013).

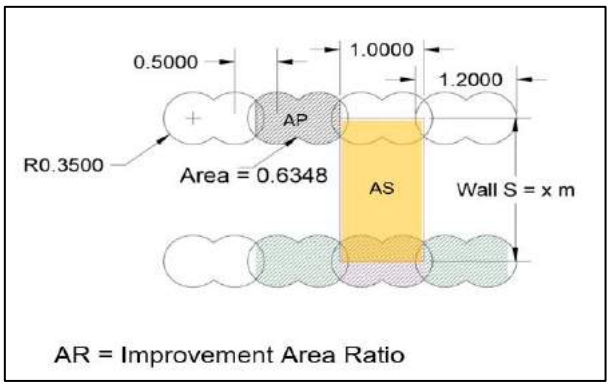

Gbr. 2b. Konfigurasi DCM.

Improvement area ratio (AR) merupakan besarnya area kolom DCM dibanding dengan besarnya area tanah in situ.

Tabel 1. Parameter Geoteknik yang digunakan dalam Analisis.

Material	γsat (kN/m³)	E' (kN/m²)	v	c (kPa)		ϕ (°)		Permeabilitas (cm/s)	
				Efektif	Total	Efektif	Total	Kh	Kv
Material Timbunan									
Fill Material	19,52	30.000	0,35	15	16	25	23	4,41 x 10-4	8,82 x 10-5
Rocktoe (Rockfill)	22	70.000	0,3	0	0	39	39	Lulus Air	Lulus Air
Horizontal Drain	20,81	70.000	0,3	0	0	32,12	32,12	1,0 x 10-3	1,0 x 10-3
Tanah Pondasi									
Loose Sand	17	8.400	0,35	1	-	30	-	1,0 x 10-6	1,0 x 10-6
Soft Silt	17	2.100	0,35	2	15	25	0	1,0 x 10-10	1,0 x 10-10
V. Stiff Silt 1	17	29.750	0,35	5	85	25	0	1,0 x 10-9	1,0 x 10-9
V. Stiff Silt 2	17	47.250	0,35	10	135	25	0	1,0 x 10-9	1,0 x 10-9
Bedrock	23	87.500	0,30	25	250	38	0	1,0 x 10-6	1,0 x 10-6
DCM *Properties*									
AR 32% (S=2m)	20	76.364	0,3	-	143,5	-	0	$1,0 \times 10^{-9}$	$1,0 \times 10^{-9}$
AR 42% (S=1.5m)	20	101.119	0,35	-	186,4	-	0	$1,0 \times 10^{-9}$	$1,0 \times 10^{-9}$

Sebelum dilakukan penanganan dengan DCM, tanah permukaan yang mengandung tanah organik di gali terlebih dulu, dan digantikan dengan tanah material timbunan. Kemudian, digunakan geogrid sebagai *Load Transfer Platform* (LTP). Kemudian dilanjutkan dengan penimbunan secara bertahap. Geometri pada pemodelan penanganan tanah dapat dilihat pada Gbr. 3.

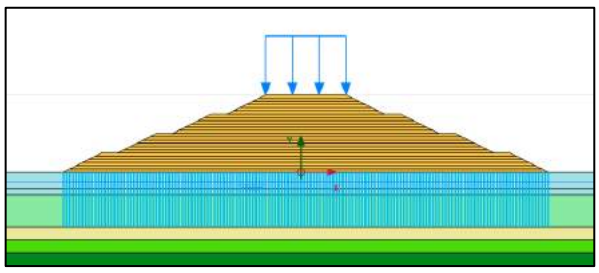

(a) Metode PVD *Preloading*

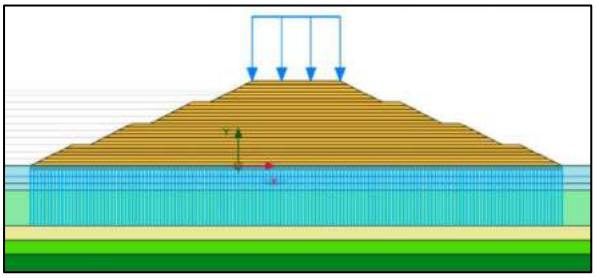

(b) Metode PVD - *Vacuum Preloading*

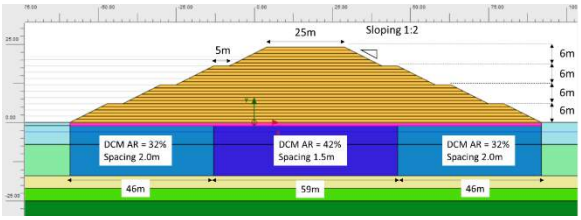

(c) Metode *Deep Cement Mixing*

Gbr. 3. Model Penanganan Tanah (a) Metode PVD *Preloading*, (b) Metode PVD-*Vacuum Preloading*, (c) Metode *Deep Cement Mixing*.

5 HASIL DAN PEMBAHASAN

Analisis penurunan alami menggunakan pendekatan penurunan 1D terzaghi berkisar 2,58 meter dan tercapai dalam waktu 33 tahun. Grafik penurunan terhadap waktu seperti terlihat pada Gbr. 4 berikut ini.

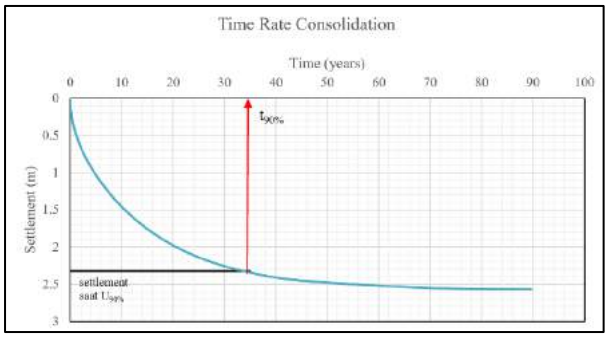

Gbr. 4. Penurunan Terhadap Waktu berdasarkan 1D-Terzaghi.

Analisis stabilitas dengan menggunakan *Prefabricated Vertical Drain - Preloading* diperoleh pola deformasi seperti Gbr. 5.

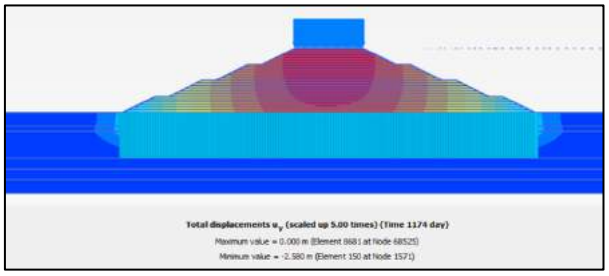

Gbr. 5. Pola Deformasi Penanganan PVD *Preloading.*

Pada penanganan ini penurunan konsolidasi sebesar 2,58 m. Nilai penurunan ini mendekati hasil perhitungan 1D-Terzaghi. Nilai angka keamanan dengan metode PVD-*Preloading* adalah 1,35.

Kemudian selanjutnya dilakukan analisis stabilitas dengan menggunakan *Prefabricated Vertical Drain – Vacuum Preloading*. Tinggi *preloading* sebesar 2,5 m digantikan menjadi beban *Vacuum* (setara 60 kPa). Gambar pola keruntuhan pada kondisi akhir dapat dilihat pada Gbr. 6.

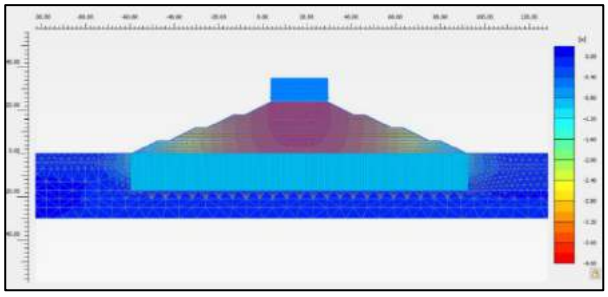

Gbr. 6. Pola Deformasi Penanganan PVD - *Vacuum Preloading.*

Pada penanganan ini penurunan konsolidasi terjadi sebesar 2,64 m. Nilai penurunan ini mendekati hasil perhitungan 1D-Terzaghi. Nilai angka keamanan dengan metode PVD-*Vacuum Preloading* adalah 1,41.

Analisis stabilitas kemudian dilakukan dengan menggunakan metode *Deep Cement Mixing*. Gambar pola keruntuhan pada kondisi akhir dapat dilihat pada Gbr. 7.

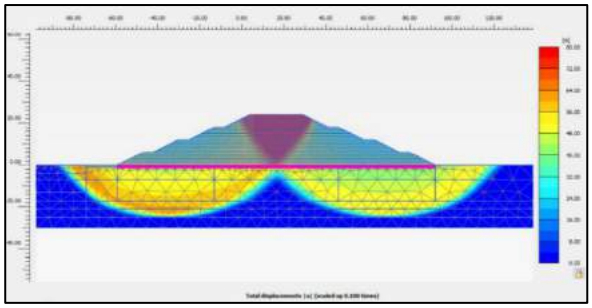

Gbr. 7 Pola Deformasi Penanganan *Deep Cement Mixing.*

Pada penanganan ini penurunan konsolidasi sudah tidak terjadi, besar penurunan seketika yang terjadi adalah 0,06 m. Nilai angka keamanan dengan metode DCM adalah 1,32. Pada penanganan ini penurunan konsolidasi sudah tidak terjadi, besar penurunan seketika yang terjadi adalah 0,06 m.

Dari hasil analisis maka dapat dibuat perbandingan seperti pada Tabel 2.

Tabel 2 Perbandingan Alternatif Penanganan.

Metode	Stabilitas Angka Keamanan	Penurunan	Kemudahan Pelaksanaan
Deep Cement Mixing	1,32	0,06	1
PVD - Preloading	1,35	2,50	2
PVD - Vacuum - Preloading	1,41	2,58	3

Pada performa kenaikan nilai Angka keamanan, Metode PVD Vacuum – Preloading memiliki kenaikan angka keamanan yang signifikan. Hal ini dimungkinkan karena penimbunan setara 60 kPa digantikan dengan *suction* menggunakan vacuum. Dari segi besar penurunan tanah yang terjadi, metode *Deep Cement Mixing* memiliki nilai penurunan paling kecil atau hampir tidak terjadi yaitu sebesar 0,06 m. Dari segi kemudahan pelaksanaan, metode *Deep Cement Mixing* lebih mudah untuk dikonstruksi. Mengingat tubuh dam adalah berupa timbunan yang dibuat sangat tinggi, maka dengan metode DCM tidak lagi diperlukan *surcharge*. Setelah membandingkan ketiga faktor diatas, maka penggunaan *Deep Cement Mixing* menjadi lebih baik untuk kasus ini.

6 KESIMPULAN

Pemilihan metode penanganan didasarkan pada stabilitas/ angka keamanan, risiko penurunan, waktu pelaksanaan dan kemudahan pelaksanaan. Ketiga alternatif penanganan memberikan nilai angka keamanan (stabilitas) yang hampir sama. PVD dengan *vacuum preloading* memberikan nilai angka kemanan lebih besar dibandingkan dengan PVD *preloading*, ini dimungkinkan karena penimbunan setara 60 kPa digantikan dengan *suction* menggunakan *vacuum*.

Pada alternatif PVD *Preloading* dan PVD-*Vacuum Preloading* memberikan penurunan sekitar 2,5 meter, sedangkan pada metode DCM penurunan konsolidasi nyaris tidak terjadi. Dengan demikian resiko perbedaan penurunan yang terjadi pada area tubuh *dam* setelah perbaikan tanah juga masih ada untuk penanganan selain DCM. Dari segi kemudahan pelaksanaan, metode *deep cement mixing* lebih mudah untuk dikonstruksi karena tidak memerlukan *surcharge* yang cukup tinggi. Dengan melihat ketiga faktor diatas, penggunaan *Deep Cement Mixing* menjadi lebih baik untuk kasus ini.

DAFTAR PUSTAKA

Bruce, C., Collin, J., Berg, R., Filz, G., Terashi, M., & Yang, D. 2013. Federal Highway Administration Design Manual: Deep Mixing for Embankment and Foundation Support , October 2013 - FHWA-HRT-13-046. october, 244. http://www.fhwa.dot.gov/publications/research/infrastructure/structures/bridge/13046/index.cfm

Chai, J., Bergado, D. T., & Shen, S. L. 2013. Modelling prefabricated vertical drain improved ground in plane strain analysis. *Proceedings of the Institution of Civil Engineers: Ground Improvement 166*(2): 65–77. https://doi.org/10.1680/grim.11.00007

Fitriyanto, A., & Taruko, W. 2014. Design Optimization of Bauxite Residue Dam in Connection with Environment and Land Acquisition in Mempawah SGA , Indonesia. *International Symposium of The 82nd Annual Meeting of International Commission on Large Dams (ICOLD)*.

Gouw, T. L., & Gunawan, A. 2020. Vacuum preloading, an alternative soft ground improvement technique for a sustainable development. *IOP Conference Series: Earth and Environmental Science 426*(1): 0–12. https://doi.org/10.1088/1755-1315/426/1/012003

Kitazume, M., & Terashi, M. (2013). *The Deep Mixing Method*. CRC Press.

Nguyen, H. S., Adachi, Y., Kizuki, T., Maeba, H., & Inazumi, S. 2020. Integration of Information and Communication Technology (ICT) Into Cement Deep Mixing Method. *International Journal of GEOMATE* 19(74): 194–200. https://doi.org/10.21660/2020.74.9329

Perbaikan Tanah Lunak dengan Metode *Preloading* Menggunakan *Prefabricated Vertical Drain* (PVD) pada Pembangunan Jalan Tol Padang – Lubuk Alung – Sicincin

Indirani Lewinsky
Program Studi Teknik Sipil, Fakultas Teknik Sipil dan Perencanaan – Universitas Bung Hatta

Eva Rita
Program Studi Teknik Sipil, Fakultas Teknik Sipil dan Perencanaan – Universitas Bung Hatta

Robby Permata
Program Studi Teknik Sipil, Fakultas Teknik Sipil dan Perencanaan – Universitas Bung Hatta

Hendri Warman
Program Studi Teknik Sipil, Fakultas Teknik Sipil dan Perencanaan – Universitas Bung Hatta

ABSTRAK: Kondisi tanah pada proyek pembangunan Jalan Tol Padang – Lubuk Alung – Sicincin STA 3+550 – STA 3+750 memiliki konsistensi tanah sangat lunak dengan nilai tahanan konus (qc) sebesar 0-10 kg/cm2. Tanah dengan kondisi tersebut mempunyai daya dukung rendah dan pemampatan tanah dasar yang relatif besar, sehingga dapat mengakibatkan keruntuhan struktur yang dibangun diatasnya. Untuk itu dilakukanlah perbaikan tanah menggunakan metode preloading dan Prefabricated Vertical Drain (PVD). Metoda penelitian ini menggunakan data sondir elektrik (CPTu) untuk menentukan paramater tanah dan menggunakan persamaan-persamaan untuk menghitung besarnya penurunan dan periode. Perencanaan PVD ini menggunakan pola segitiga dan bujur sangkar dengan jarak (s = 1;1,5;2 m). Hasil perencanaan diperoleh, Hr = 2 m, Hpreloading = 2,64 m, Htotal = 4,64 m dan Stotal = 71,329 cm. Pada derajat konsolidasi 90% tanpa PVD dibutuhkan waktu konsolidasi selama 13,27 tahun, sedangkan menggunakan PVD dengan jarak 1 m untuk pola segitiga didapat t=120 hari dan dengan pola bujur sangkar t = 150 hari.

Kata Kunci: tanah lunak, CPTU, prefabricated vertical drain (PVD), penurunan, waktu

ABSTRACT: The soil consistency of the STA 3+550 – STA 3+750 construction project Padang – Lubuk Alung – Sicincin Toll Road is very soft, with a cone resistance value (qc) of 0-10 kg/cm2. Because soil with these qualities has a limited bearing capacity and a considerable subgrade compression, it can cause the structure built on it to collapse. As a result, preloading and PVD (Prefabricated Vertical Drain) technologies are used to improve the soil. Electrical sondir (CPTu) data is used to identify soil characteristics, and equations are used to compute the amount of settlement and periode. This PVD layout employs a triangle and square pattern with a distance of (s = 1; 1,5; 2 m). Hr = 2 m, Hpreloading = 2.64 m, Htotal = 4.46 m and Stotal = 71.329 cm are the planning outcomes. With no PVD and a distance of 1 m, consolidation time is required for 13.27 years. With PVD and a distance of 1 m, t=120 days for triangular patterns and t=150 days for square patterns are produced.

Keywords: soft clay, CPTu, prefabricated vertical drain (PVD), settlement, periode

1 PENDAHULUAN

Keberadaan Jalan mempunyai peranan penting dalam bidang ekonomi, politik, sosial budaya, perdagangan dan sektor lainnya. Hal ini membuat Pemerintah Indonesia memfokuskan infrastruktur jalan menjadi prioritas utama khususnya jalan tol. Pulau sumatera juga merupakan bagian dari rencana pembangunan dan pengembangan kawasan, untuk itu dalam melaksanakan percepatan pembangunan dibutuhkan perencanaan dan pelaksanaan konstruksi yang tepat (Peraturan Presiden No. 100 Tahun 2014). Proyek yang saat ini sedang dalam pembangunannya ialah jalan tol Ruas Padang – Pekanbaru, pada pekerjaan jalan tol ini dijumpai permasalahan berupa tanah lunak, karena mempunyai sifat tanahnya yang berdaya dukung rendah, pemampatan tanah dasarnya yang relatif besar sehingga membutuhkan waktu konsolidasi yang lama, hal ini akan berpotensi mengalami penurunan (*settlement*)

serta kerusakan sebelum mencapai umur konstruksi jalan yang direncanakan. Maka dari itu untuk memperbaiki sifat tanah dasar tersebut agar dapat digunakan sebagai pendukung konstruksi diatasnya maka perlu diadakannya usaha perbaikan pada tanah lunak tersebut.

Salah satu metode yang digunakan untuk mengatasi masalah pada tanah lunak adalah metode prapembebanan (*preloading*). Metode ini digunakan untuk mengoptimalkan kinerja *Prefabricated Vertical Drain* (PVD) dengan cara memberikan tambahan beban pada konstruksi jalan yang di bangun hingga proses konsolidasi tercapai, Susiazti et al. (2020). PVD ialah sistem drainase buatan yang dipasang vertikal di dalam lapisan tanah lunak yang bertujuan untuk mempercepat proses pemampatan atau penurunan konsolidasi, sehingga lintasan drainase air pori menjadi lebih pendek, Hardiyatmo (2020).

2 METODE

Penelitian ini menggunakan data sekunder berupa data tanah dasar Piezocone (CPTu), data indeks properties tanah timbunan pada STA 3+550 – STA 3+750 dan spesifikasi PVD (jenis, ukuran dan kemampuan permeability), data tersebut diperoleh dari PT. Hutama Karya Infrasrtuktur.

Menentukan jenis perilaku tanah dan parameter-parameter tanah untuk melakukan perencanaan perbaikan tanah lunak dengan metode *Preloading* dan PVD sehingga didapatkan berapa besar penurunan dan waktu konsolidasi. Tahapan metodologi penelitian dapat diilihat pada Gbr. 1.

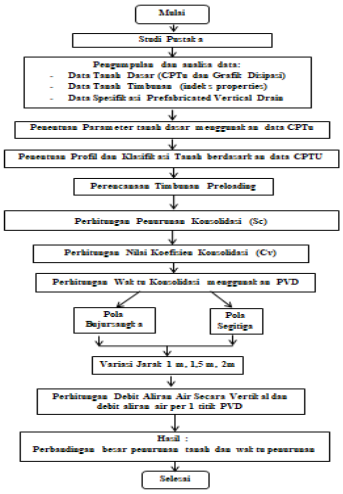

Gbr. 1. Bagan Alir Penelitian Perencanaan Perbaikan Tanah.

Terkait dengan perhitungan perencanan perbaikan tanah dapat digunakan persamaan-persamaan sebagai berikut:

1. Profil dan Klasifikasi Tanah

$$qt = qc + u_2 (1 – a) \quad (1)$$

2. Berat Isi Tanah

$$\gamma/\gamma_w = 0{,}27 [\text{Log Rf}] + 0{,}36 [qt / pa] + 1{,}236 \quad (2)$$

3. Over Consolidation Ratio (OCR)

$$OCR = k \left(\frac{qt - \sigma vo}{\sigma' vo} \right) \quad (3)$$

4. Constrained Modulus (M)

$$M = \alpha m (qt – \sigma_{vo}) \quad (4)$$

$$\alpha m = Qt, \quad Q_t = \frac{qt - \sigma vo}{\sigma vo'}$$

5. Tinggi Preloading

$$H_{beban} = \frac{q (\text{beban perkerasan+beban lalu lintas})}{\gamma \text{timbunan}} \quad (5)$$

6. Penurunan Konsolidasi
   Penurunan Konsolidasi Primer

$$Sc = (\Delta\sigma'v / M) H \quad (6)$$

   Penurunan Konsolidasi Sekunder

$$Ss = C\alpha \, \Delta z \log (t/tp) \quad (7)$$

7. Koefisien Konsolidasi Vertikal (Cv)

$$C_v = \frac{k \, . \, M}{\gamma w} \quad (8)$$

8. Waktu Konsolidasi

$$T = \frac{T90\% \, x \, H^2}{Cv} \quad (9)$$

9. Perencanaan PVD

Pola Segitiga 1,05 x S (10)

Pola Bujur Sangkar 1,13 x S (11)

3 METODE

3.1 *Menentukan Konsistensi Tanah*

Tabel 1. Konsistensi Tanah Lunak.

Konsistensi Tanah	Taksiran Harga Kekuatan Geser Undrained, Cu		Taksiran Harga SPT, Harga N	Taksiran Harga Tahanan Konus, qc	
	kPa	Ton/m^2		kg/cm^2	kPa
Sangat Lunak (Very Soft)	0 - 12,5	0 - 1,25	0 - 2,5	0 - 10	0 - 1000
Lunak (Soft)	12,5 - 25	1,25 - 2,5	2,5 - 5	10 - 20	1000 - 2000
Sedang (Medium)	25 - 50	2,5 - 5	5 - 10	20 - 40	2000 - 4000
Kaku (Stiff)	50 - 100	5 - 10	10 - 20	40 - 75	4000 - 7500
Sangat Kaku (Very Stiff)	100 - 200	10 - 20	20 - 40	75 - 150	7500 - 15000
Keras (Hard)	> 200	> 20	> 40	> 150	> 15000

Tanah kohesif yang berkemampatan tinggi adalah tanah yang dominan mengandung lanau (*silt*) dan lempung (*clay*) dengan konsistensi sangat lunak (*very soft*), lunak (*soft*) dan menengah (*medium*). Dalam praktek, biasanya ditentukan dengan nilai N-SPT ≤ 10 atau qc ≤ 20 kg/cm^2 , Kuswanda W.P (2015). Uji CPTu dilakukan pada tanah yang lunak dengan tujuan untuk mengetahui besarnya perlawanan tanah terhadap penetrasi konus serta besarnya tekanan air pori pada tanah lunak tersebut. Dari hasil uji CPTu dilapangan didapatkan nilai tahanan konus sebesar 0 – 5 kg/cm, maka sesuai Tabel 1 dapat diartikan bahwasanya nilai tahanan konus dengan rentang 0-10 kg/cm^2 dapat dikatakan bahwa konsistensi tanah pada STA 3+650 yaitu tanah sangat lunak (*very soft*).

3.2 *Menentukan Parameter Tanah*

Menurut Robertson dan Cabal (2015), Parameter tanah yang diperlukan untuk perbaikan tanah lunak dengan menggunakan data CPTu yaitu, profil dan klasifikasi tanah, berat isi tanah (ɣ), tegangan total dan tegangan efektif, *Over Consolidation Ratio* (OCR) dan *Constrained Modulus* (M).

Tabel 2. Properties Tanah.

Properties Tanah					
Kedalaman Tanah (cm)	(ɣ) (kg/cm^3)	Teg.total (kg/cm^2)	Teg. Efektif (kg/cm2)	(OCR)	(M) (kN/m2)
0	0	0,0000	0,0000	0,0000	0
50	0,00078658	0,0106	0,0393	27,4299	8748,3513
100	0,00078658	0,0286	0,0786	9,8018	3000,1341
150	0,00086786	0,0720	0,1220	2,1949	1085,2570
200	0,0008842	0,1162	0,1662	3,5576	1603,3637
250	0,0008030	0,1564	0,2064	2,5674	1123,3953
300	0,0008966	0,2012	0,2512	2,7857	1701,7383
350	0,0009436	0,2484	0,2984	2,1635	1267,0242
400	0,0009714	0,2970	0,3470	2,3566	1797,1797
450	0,0009870	0,3463	0,3963	1,9780	1476,5746
500	0,0010576	0,3992	0,4492	1,9505	1655,0643
550	0,001074	0,4529	0,5029	1,7234	1465,9059
600	0,0010851	0,5072	0,5572	2,1073	2454,2481
650	0,0011226	0,5633	0,6133	1,8754	2158,9704
700	0,0011413	0,6204	0,6704	2,1589	3150,7202
750	0,0011311	0,6769	0,7269	1,9535	2814,8028

3.3 *Jenis Perilaku Tanah*

Dalam mencari jenis perilaku tanah, ditentukan oleh garfik dan tabel berikut ini:

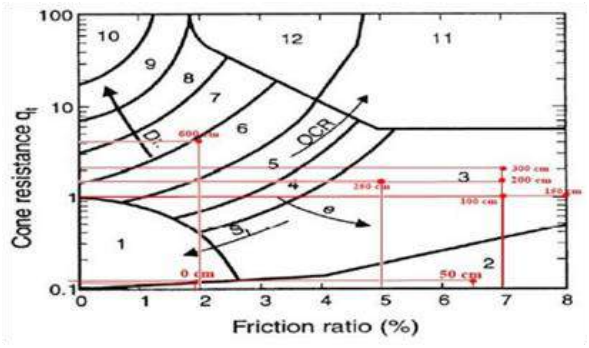

Gbr. 2. Grafik Menentukan Jenis Perilaku Tanah (SBT) CPTu Menurut (Robertson et al., 1986).

Tabel 3. Jenis Perilaku Tanah (SBT), Guide to In-Situ Testing Robertson et al. (1986).

Zona	Jenis Perilaku Tanah
1	Berbutir Halus Sensitif
2	Bahan Organik
3	Tanah Liat
4	Tanah Liat Berlumpur Menjadi Tanah Liat
5	Campuran Lumpur – Lanau Menjadi Lempung Berlumpur
6	Campuran Lumpur – Lanau Berpasir Hingga Lanau Berlempung
7	Campuran Pasir – Pasir Berlumpur Hingga Lanau Berpasir
8	Pasir Sampai Pasir Berlumpur
9	Pasir
10	Pasir Kerikil ke Pasir
11	Berbutir Halus Sangat Kaku
12	Pasir Sampai Pasir Liat

Dari hasil nilai resitensi kerucut (qt) dan nilai rasio gesekan (Fr) didapatkan jenis perilaku tanah berupa bahan organik, tanah liat, lanau liat menjadi lempung berlumpur dan lanau berpasir hingga lanau berlempung.

3.4 *Metode Preloading*

Adapun beban yang digunakan untuk metode preloading ini adalah beban lalu lintas sebesar 15 kPa (SNI 8460-2017), beban perkerasan 27,301 kN/m^2 dan tinggi timbunan rencana 2 m ditambah tinggi *preloading* 2,64 m dengan tinggi total 4,64 m sehingga berat total tanah timbunan didapat sebesar 74,24 kN/m^2, dengan nilai distribusi tegangan sebesar 171,107 kN/m^2.

3.5 *Penurunan Konsolidasi*

Penurunan konsolidasi merupakan keadaan dimana lapisan tanah mengalami penambahan beban sehingga tekanan air pori akan naik secara mendadak. Keluarnya air pori disertai dengan berkuranganya volume tanah yang menyebabkan penurunan lapisan tanah, Zhafirah dan Amalia (2019). Terdapat 2 jenis penurunan pada STA 3+570 – 3+750 yaitu penurunan primer 71,207 cm dan penurunan sekunder 0,122 cm, sehingga penurunan total 71,329 cm.

3.6 *Waktu Konsolidasi Tanpa PVD*

Untuk menentukan waktu konsolidasi tanpa PVD diperlukan nilai dari koefisien konsolidasi (C_v), tebal tanah mampat (H_{dr}) dan faktor waktu pada sistem drainase vertikal (T_v), yang didapat masing-masing sebesar C_v = 0,002461 m^2/hari, H_{dr} = 3,75 m dan T_v (90%) = 0,848, sehingga waktu konsolidasi yang diperoleh tanpa menggunakan PVD selama 13,27 tahun.

3.7 *Perencanaan Prefabricated Vertical Drain (PVD)*

Beberapa koefisien dan parameter tanah yang yang perlu dalam menentukan jarak antar vertical drain yaitu koefisien konsolidasi vertikal (C_v), horizontal (C_h), diameter ekivalen (de), faktor waktu vertikal (T_v), radial (T_h) dan diameter daerah tangkapan vertikal drain (D). Adapun perencanaan *Prefabricated Vertical Drain* menggunakan 2 pola yaitu pola segitiga dan pola bujur sangkar, dengan jarak pemasangan sebesar 1 m, 1,5 m dan 2 m.

Tabel 4. Perencanaan PVD.

Jarak	Pola Segitiga		Pola Bujur Sangkar	
	Waktu	Penurunan	Waktu	Penurunan
(m)	(hari)	(cm)	(hari)	(cm)
1	120	0,7140	150	0,7102
1,5	300	0,7264	360	0,7142
2	550	0,7087	650	0,7117

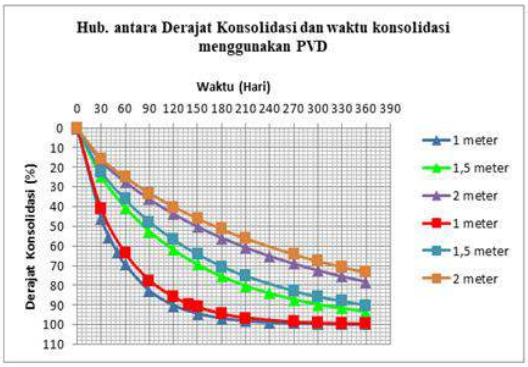

Gbr. 2. Hubungan antara derajat konsolidasi dan waktu konsolidasi menggunakan PVD.

Dari gambar 3 didapatkan hasil uji hubungan antara derajat konsolidasi dan waktu konsolidasi menggunakan PVD pola segitiga dengan jarak 1m, 1,5 sampai 2m mengalami waktu konsolidasi lebih cepat dibandingkan dengan pola bujur sangkar. Jarak antar PVD sangat berpengaruh terhadap waktu yang dibutuhkan untuk mencapai derajat konsolidasi 90%. PVD dengan pola segitiga dan bujur sangkar dengan spasi 1 m membutuhkan waktu untuk mencapai derajat konsolidasi 90% lebih cepat dibanding dengan PVD yang dipasang 1,5 m atau 2 m.

4 KESIMPULAN DAN SARAN

Tanah lunak pada area STA 3+550 – STA 3+750 dengan kedalaman 7,5 m didapatkan penurunan total 71,329. Pada derajat konsolidasi 90% tanpa PVD didapatkan waktu konsolidasi 13,27 tahun. Untuk konsolidasi menggunakan PVD pola pemasangan berbentuk segitiga dengan jarak 1 m diperlukan waktu konsolidasi selama 120 hari dan untuk PVD pola pemasangan berbentuk bujur sangkar dengan jarak 1m diperlukan waktu selama 150 hari. Maka pola segitiga membutuhkan waktu konsolidasi yang lebih singkat dan menghasilkan penurunan yang lebih seragam, sehingga pola ini lebih banyak digunakan.

DAFTAR PUSTAKA

Badan Standardisasi Nasional, 2017. *Persyaratan Perancangan Geoteknik (SNI 8460-2017)*. Jakarta.

Gunawan Tomy dkk. 2020. Analisis Penurunan Pada Timbunan Dengan Prefabrecated Drain (PVD) Menggunakan Data Hasil Uji CPTu. Program Studi Sarjana Teknik Sipil, Universitas Tarumanegara.

Gaol Lumban Berman, dkk. 2020. Analisa Preloading dengan Prefabricated Vertical Drain (PVD) Terhadap Perbaikan Tanah Lunak pada Pembangunan Jalan Tol Tebing Tinggi – Indrapura. Program Studi Teknik Sipil, Institut Teknologi Medan.

Hardiyatmo, H,C. 2020. *Perbaikan Tanah*. Yogyakarta: Gadjah Mada University Press.

Kuswanda. W. P. 2016. Perbaikan Tanah Lempung Lunak Metoda Preloading pada pembangunan infrastruktur transportasi di Pulau Kalimantan. Program Studi Teknik Sipil Uniam. Banjarmasin.

Kuswanda, P Wahyu. 2015. Problematika Pembangunan Infrastruktur pada Tanah Lempung Lunak dan Alternatif Metoda Penanganannya. ISBN 978-602-648-300-3. *Prosiding Seminar Nasional Teknik Sipil Universitas Lampung*.

Putra Herdian Ricky, dkk. 2018. Studi Efisiensi Konfigurasi Pemasangan PVD dari Segi Teknis dan Biaya Konstruksi. *Rekayasa Pratama Konsultan dan Univesitas Bung Hatta*. Padang Sumatera Barat.

Robertson, P.K. dan Cabal, K.L. 2015. *Guide to Cone Penetration for Geotechnical Engineering.* California: Signal Hill.

Susiazti Heny dkk. 2020. Analisis Penurunan Konsolidasi Metode Preloading dan Prefabrecated Vertical Drain (PVD). *Jurnal Ilmu Pengetahuan dan Teknologi Teknik Sipil.*

Zhafirah dan Amalia. 2019. *Perencanaan Preloading dengan Penggunaan Prefabrecated Vertical Drain untuk Perbaikan Tanah Lunak Pada Jalan Tol Pejagaan- Pemalang.* Laporan Penelitian. Jurusan Teknik Sipil Politeknik Negeri Bandung.

Penurunan Tanah Dasar Akibat Beban Timbunan dengan Penerapan *Prefabricated Vertical Drain*

Dyah Pratiwi Kusumastuti
Program S1 Teknik Sipil – Institut Teknologi PLN

Indah Handayasari
Program S1 Teknik Sipil – Institut Teknologi PLN

Irma Sepriyanna
Program S1 Teknik Sipil – Institut Teknologi PLN

ABSTRAK: Jalan dan jembatan yang dibangun diatas tanah lunak seringkali mengalami kegagalan seperti retak-retak, penurunan dan keruntuhan. Hal tersebut disebabkan karakteristik tanah lunak yang memiliki daya dukung rendah, kemampumampatan besar dan proses konsolidasi yang memakan waktu lama. Untuk mengatasi permasalahan tersebut dapat dilakukan dengan perbaikan yang tepat. Khususnya untuk mengatasi waktu konsolidasi yang lama dapat digunakan dengan menggunakan drainase vertikal yang dikombinasikan dengan timbunan baik yang bersifat permanen maupun prapembebanan. Pada penelitian menggunakan drainase vertikal pabrikan atau *prefabricated drain* (PVD) tipe CT-D822 dan variasi jarak atau spasi 0,8; 1; 1,1 dan 1,3 yang dikombinasikan dengan beban timbunan dengan variasi 16 t/m^2, 17 t/m^2, 18 t/m^2, 19 t/m^2, 20 t/m^2. Berdasarkan hasil penelitian dengan tinggi timbunan akhir rencana 8,50 m diperoleh pada derajat konsolidasi 90% , PVD dipasang dengan jarak 1 m selama 10 minggu menghasilkan penurunan 3,807 m.

Kata Kunci: waktu konsolidasi, drainase vertikal, timbunan

ABSTRACT: Roads and bridges built on soft soil often experience failures such as cracks, subsidence and collapse. This is due to the characteristics of soft soil which has low bearing capacity, high compressibility and the consolidation process that takes a long time. To overcome these problems can be done with appropriate repairs. In particular to overcome the long consolidation time can be used by using vertical drainage combined with embankment both permanent and pre-loading. In this study, using a factory vertical drainage or prefabricated drain (PVD) type CT-D822 and variations in distance or spacing of 0.8; 1; 1.1 and 1.3 combined with embankment loads with variations of 16 t/m^2, 17 t/m^2, 18 t/m2, 19 t/m^2, 20 t/m^2. Based on the results of the study with the final embankment height of 8.50 m obtained at 90% consolidation degree, PVD installed at a distance of 1 m for 10 weeks resulted in a decrease of 3.807 m.

Keywords: time of consolidation, vertical drainage, embankment

1 PENDAHULUAN

Pembangunan infrastruktur jalan atau jembatan memiliki peranan penting dalam meningkatkan perekonomian suatu wilayah. Namun pembangunannya tidak lepas dari berbagai permasalahan, salah satu permasalahan yang sering dijumpai adalah ketika konstruksi jalan atau jembatan berdiri diatas tanah lunak. Hal ini yang dapat menyebabkan kerusakan seperti retak-retak sampai keruntuhan karena tanah lunak memiliki daya dukung yang rendah dan penurunan yang besar, Kusumastuti et al. (2019) serta waktu konsolidasi yang cukup lama, Nooe et al. (2010) karena nilai koefisien permeabilitas yang rendah, Chairani (2020).

Untuk mengatasi permasalahan-permasalahan yang terjadi pada tanah lunak dapat dilakukan dengan perbaikan seperti stabilisasi mekanis dengan penambahan pasir, Pradita et al. (2019) dan penggunaan bahan sintetis seperti geotekstil dan *vertical drain* dan pra pembebanan, Putra et al. (2020) serta stabilisasi kimiawi, Kusumastuti et al. (2019). Namun pemilihan metode perbaikan harus tepat agar permasalahan dapat teratasi dengan baik. Salah satunya adalah pemasangan *vertical drain* yang dikombinasikan dengan pra

pembebanan yang memiliki tujuan tercapainya penurunan akhir tanah lunak dengan mempersingkat waktu konsolidasi, Chairani (2020). Penggunaan *vertical drain* sendiri dapat terjadinya aliran arah horisontal dan vertikal yang menyebabkan air pori pada lapisan tanah dapat keluar lebih cepat, Aspar et al. (2017).

Kasus yang terjadi pada penelitian ini adalah ditemuinya lapisan tanah lunak yang cukup tebal sehingga dapat mengancam stabilitas konstruksi diatasnya. Penerapan pra pembebanan yang dikombinasikan *vertical drain* dengan variasi jarak dipilih untuk mendapatkan penurunan dan waktu konsolidasi sesuai rencana.

2 METODE

Langkah awal penelitian adalah dengan mengumpulkan data tanah dari pengujian *Standar Penetration* (SPT) dan uji laboratorium karakteristik fisik serta mekanik. Data-data yang diperoleh kemudian diinterpretasikan, jika terdapat data yang tidak diperoleh dari hasil pengujian maka akan dilengkapi dengan menggunakan korelasi. Data tanah yang digunakan dalam analisis, tidak hanya data tanah dasar tetapi juga data tanah timbunan sebagai pra pembebanan yang diterapkan.

Setelah pengumpulan dan interpretasi data tanah, dilakukan penentuan atau perencanaan PVD yang digunakan. Pada penelitian ini digunakan PVD tipe CT-D822, dengan spesifikasi sebagai berikut:
Berat = 75 gr/m
Lebar = 100 mm
Tebal = 4 mm
Tensile Strength = 2,75 kN
PVD direncanakan terpasang dengan pola segitiga (Gbr. 1) dan variasi jarak 0,8 m; 1 m; 1,1 m dan 1,3 m.

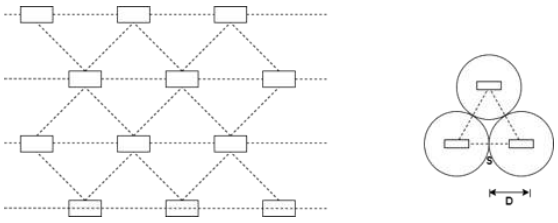

Gbr. 1. Pola Segitiga Pada Pemasangan PVD.

Untuk mengetahui efektifitas pemasangan PVD, maka dianalisis penurunan dan waktu konsolidasi kondisi eksisting dan kondisi dengan pemasangan PVD. Penurunan dan waktu konsolidasi dengan pemasangan PVD akan dipilih dengan derajat konsolidasi 90% pada jarak yang efisien.

3 HASIL DAN PEMBAHASAN

3.1 *Data Tanah*

Data tanah dasar yang digunakan dalam penelitian ini adalah dari uji SPT, uji di laboratorium dan korelasi. Diketahui dari hasil uji SPT pada titik A1 bahwa ketebalan tanah yang memiliki sifat kompresibel ditandai dengan nilai N-SPT ≤ 10 mencapai kedalaman 23 m dan letak muka air tanah pada kedalaman 2 m. Adanya lapisan tanah yang mudah mampat pada titik bor A1 yang cukup tebal, berpotensi menyebabkan terjadi penurunan yang tidak seragam sehingga mengakibatkan kerusakan pada struktur maupun pondasi.

Berdasarkan nilai N-SPT, untuk kebutuhan analisis maka parameter tanah didapatkan dengan menggunakan korelasi seperti pada Tabel 1.

Tabel 1. Parameter Tanah.

TITIK BOR		A1			
DLM (m)	N-SPT	Deskripsi	γ_{sat}	c_u	ϕ
			kN/m^3	kN/m^2	
0	0.0	Lanau lempung pasiran, very soft	14,7	5	
2	4.0				
4	5.0	Lanau lempung pasiran, soft	16,2	50	
6	6.0	Lempung lanau, medium	16,7	80	
8	8.0				
10	6.0				
12	7.0				
14	10.0				
16	8.0				
18	6.0				
20	7.0				
22	10.0				
24	5.0	Lanau lempung pasiran, soft	16,2	50	
26	22.5	Lanau lempung pasiran, medium - stiff	19,1	150	

TITIK BOR			A1		
DLM (m)	N-SPT	Deskripsi	γ_{sat}	c_u	ϕ
			kN/m^3	kN/m^2	
28	38.0	Kerikil pasiran, dense	17,5		33.7
30	38.5				
32	38.0	Lanau lempung pasiran, very hard	25,0	241	
34	30.0				
36	38.5				
38	38.0				
40	38.5				

Nilai parameter tanah berdasarkan korelasi dengan nilai N-SPT yang digunakan dalam perhitungan atau analisis penurunan hanya sampai kedalaman 23 m yang seluruhnya merupakan lapisan kompresibel atau mudah mampat. Sedangkan untuk data tanah timbunan yang digunakan dalam penelitian ini adalah sebagai berikut:

Berat volume timbunan, γ_t = 1,79 t/m^3
Kohesi, c = 0
Sudut geser, φ = 30^o
dengan rencana penampang timbunan (Gbr. 2).

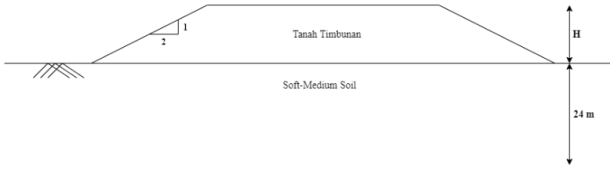

Gbr. 2. Desain Penampang Timbunan.

3.2 *Penurunan*

Analisis penurunan pada penelitian terdiri dari penurunan konsolidasi akibat beban timbunan (q_o) dan penurunan akibat beban perkerasan yang berada diatas tanah timbunan (q_{pav}). Beban timbunan yang diterapkan dalam perhitungan penurunan bervariasi mulai 16 t/m^2, 17 t/m^2, 18 t/m^2, 19 t/m^2, 20 t/m^2. Untuk beban perkerasan diatas tanah timbunan diasumsikan sebagai beban trapesium sebesar 1,2 t/m^2.

Perhitungan penurunan konsolidasi menggunakan persamaan sebagai berikut:

a. Jika $P'_o + 2\Delta P > P'_c$

$$S_c = \frac{C_s H}{1+e_o}\log\frac{\sigma'_c}{\sigma'_o} + \frac{C_c H}{1+e_o}\log\left(\frac{\sigma'_o+\Delta\sigma'}{\sigma'_c}\right) \quad (1)$$

b. Jika $P'_o + 2\Delta P < P'_c$

$$S_c = \frac{C_s H}{1+e_o}\log\left(\frac{\sigma'_o+\Delta\sigma'}{\sigma'_o}\right) \quad (2)$$

Penurunan dihitung pada lapisan tanah dengan interval 1 m sampai 23 m yang merupakan lapisan akhir tanah kompresibel. Hasil perhitungan penurunan akibat beban timbunan dan beban perkerasan dapat dilihat pada Tabel 2.

Tabel 2. Penurunan Konsolidasi Akibat Beban Timbunan dan Perkerasan.

Q_{timb} t/m^2	Sc_{timb} M	Sc_{pav} m	Sc_{tot} m
16	4,204	0,054	4,258
17	4,376	0,052	4,428
18	4,541	0,049	4,590
19	4,699	0,047	4,747
20	4,851	0,046	4,897

3.3 *Tinggi Timbunan*

Tinggi timbunan yang digunakan dalam perhitungan penurunan akan berbeda dengan tinggi timbunan saat pelaksanaan di lapangan. Tinggi timbunan saat pelaksanaan harus lebih tinggi dari tinggi rencana karena timbunan akan mengalami penurunan sehingga tinggi timbunan pelaksanaan akan memenuhi tinggi rencana. Untuk perhitungan tinggi timbunan terdiri dari tinggi pelaksanaan ($H_{initial}$), tinggi akhir (H_{final}) dan tinggi bongkar ($H_{bongkar}$).

Perhitungan tinggi timbunan juga menerapkan beban timbunan yang bervariasi seperti pada perhitungan sebelumnya. Hasil perhitungan tinggi timbunan dapat dilihat pada Tabel 3.

Tabel 3. Tinggi Timbunan dengan Penerapan Beban Timbunan.

Q_{timb} t/m^2	$H_{inisial}$ m	$H_{bongkar}$ m	H_{pav} m	H_{final} m
16	11,317	0,432	0,5	7,127
17	11,971	0,432	0,5	7,611
18	12,620	0,432	0,5	8,098
19	13,266	0,432	0,5	8,587
20	13,909	0,432	0,5	9,079

Berdasarkan hasil perhitungan penurunan dan tinggi timbunan, akan ditentukan tinggi pelaksanaan berdasarkan tinggi akhir rencana timbunan di lapangan (Gbr. 3). Untuk kemudian berdasarkan penentuan tinggi akhir akan didapatkan besarnya penurunan (Gbr. 4).

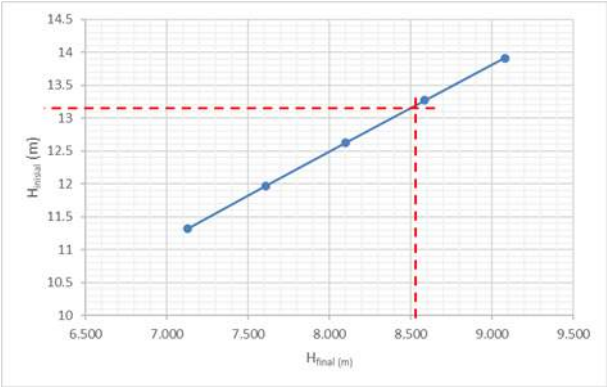

Gbr. 3. Hubungan Tinggi Timbunan Pelaksanaan ($H_{initial}$) dengan Tinggi Timbunan Akhir (H_{final}).

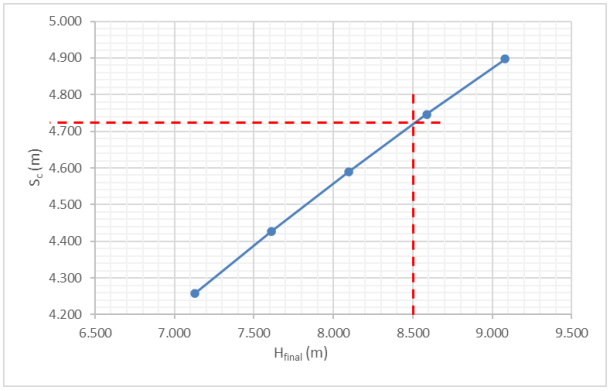

Gbr. 4. Hubungan Tinggi Timbunan Pelaksanaan ($H_{initial}$) dengan Total Penurunan ($S_{c\ total}$).

Dari Gbr. 3 yang merupakan grafik hubungan hasil perhitungan tinggi timbunan pelaksanaan dengan tinggi timbunan akhir, jika tinggi akhir yang diinginkan adalah 8,5 m maka tinggi timbunan pelaksanaan yang harus dikerjakan adalah 13,15 m. Sedangkan dari Grafik 4 yang merupakan grafik hubungan tinggi timbunan pelaksanaan dengan total penurunan, jika tinggi timbunan akhir yang direncanakan adalah 8,5 m akan didapatkan totalnya penurunan sebesar 4,720 m.

3.4 *Waktu Konsolidasi*

Perhitungan waktu konsolidasi pada penelitian ini dilakukan sebelum penggunaan PVD dan setelah penggunaan PVD. Hal tersebut untuk mengetahui efisiensi waktu konsolidasi dengan adanya penggunaaan PVD. Perhitungan waktu konsolidasi tanpa PVD dengan menggunakan data-data sebagai berikut:

T_v = 0,848 (U = 90%)
H_{dr} = 24 m
$C_{v\ rata\text{-}rata}$ = 1,222 m^2/tahun

Maka didapatkan 20.838,08 minggu atau 399,63 tahun.

Untuk perhitungan penurunan kumulatif setiap tahun dihitung dengan dua kondisi air pori tanah ($\overline{\overline{U_v}}$), yaitu:

a. U_v antara 0 s/d 60%
   Didapatkan $\overline{\overline{U_v}}$ = 5,199%
b. U_v > 60%
   Didapatkan $\overline{\overline{U_v}}$ = 19,35%

Sehingga untuk kondisi satu tahun dipilih nilai $\overline{\overline{U_v}}$ = 5,199% dengan besarnya penurunan selama satu tahun adalah 0,221 m.

Selanjutnya berdasarkan waktu, besarnya derajat konsolidasi dan penurunan didapatkan waktu untuk mencapai U 90% adalah 300 tahun dengan besarnya penurunan sebesar 3,825 m. Waktu yang dibutuhkan untuk mencapai U 90% cukup lama, sehingga dibutuhkan bantuan bahan lain agar proses pemampatan lebih cepat. Salah satu bahan yang sering digunakan adalah dengan menggunakan *prefabricated vertical drain* (PVD).

3.5 *Perencanaan PVD*

Hasil perhitungan tanpa menggunakan PVD, waktu yang dibutuhkan untuk konsolidasi yaitu 300 tahun, sehingga perlu penggunaan PVD untuk mempercepat waktu proses pemampatan. Pada penelitian direncanakan PVD dipasang dengan pola atau susunan segitiga menggunakan PVD tipe CT-D822.

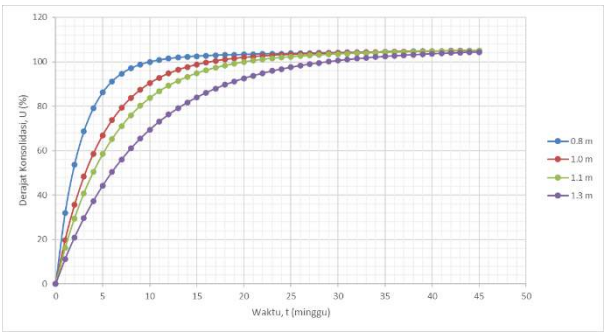

Gbr. 5. Waktu Konsolidasi dan Derajat Konsolidasi dengan Penggunaan PVD Pola Segitiga.

Berdasarkan hasil perhitungan waktu dan derajat konsolidasi seperti yang ditampilkan pada Gbr. 5, terlihat bahwa semakin jauh jarak pasang PVD dengan derajat konsolidasi yang sama maka waktu yang dibutuhkan untuk menyelesaikan proses konsolidasi semakin lama. Untuk derajat konsolidasi 90%, waktu yang dibutuhkan untuk jarak pasang PVD 0,8 m; 1,0 m; 1,1 m dan 1,3 m berturut-turut adalah

6 minggu, 10 minggu, 13 minggu dan 18 minggu. Sesuai dengan waktu pelaksanaan proyek sehingga dipilih jarak pasang PVD 1,0 m dengan waktu selesai proses konsolidasi 90% adalah 10 minggu.

KESIMPULAN

Berdasarkan hasil analisis penelitian dapat disimpulkan bahwa dengan tinggi akhir timbunan sesuai rencana pelaksanaan 8,5 m yang memiliki tebal lapisan tanah kompresibel 24 m akan mengalami penurunan total 4,720 sehingga tinggi awal timbunan yang diperlukan adalah 13,15 m. Waktu yang dibutuhkan untuk menyelesaikan proses konsolidasi dengan derajat konsolidasi 90% akan memakan waktu selama 300 tahun dengan penurunan 3,825 m.

Dengan waktu konsolidasi yang sangat lama, sehingga digunakan PVD untuk mempercepat waktu konsolidasi. Sesuai dengan kebutuhan pelaksanaan proyek maka waktu konsolidasi yang dibutuhkan dengan derajat konsolidasi 90% dan jarak pemasangan PVD 1,0 m adalah 10 minggu.

PENGHARGAAN

Ucapan terima kasih kepada Rektor dan Lembaga Penelitian dan Pengabdian Masyarakat (LPPM) dari Institut Teknologi PLN untuk bantuan dana Hibah Internal kegiatan Penelitian Dosen Pemula 2020/2021 dan semua pihak yang telah membantu kegiatan Penelitian ini.

DAFTAR PUSTAKA - REFERENCES

Aspar, W. A. N., Fitriani, E. N., & Arthono, A. 2017. Perhitungan Kembali Nilai Koefisien Konsolidasi Pada Perbaikan Tanah Lempung Lunak. *Teknologi 7*(1).

Chairani, P. A. 2020. Perancangan Efektivitas Perbaikan Tanah Dengan Menggunakan Metode Prefabricated Vertical Drain. I*ndonesian Journal of Construction Engineering and Sustainable Development* (Cesd), *3*(2): 110. https://doi.org/10.25105/cesd.v3i2.8553

Kusumastuti, D. P., & Sepriyanna, I. 2019. Soft Soil Stabilization with Rice Husk Ash and Glass Powder Based on Physical Characteristics. *IOP Conference Series: Materials Science and Engineering* 650(1). https://doi.org/10.1088/1757-899X/650/1/012025

Kusumastuti, Dyah Pratiwi, & Sepriyanna, I. S. 2019. Pengaruh Penambahan Serbuk Kaca Dan Abu Sekam Pada Tanah Lunak Berdasarkan Uji Konsolidasi. *Forum Mekanika* 8(2): 63–70. https://doi.org/10.33322/forummekanika.v8i2.882

Noor, A. A., & SH, P. 2010. Analisis Deformasi Vertikal dan Horisontal Tanah Lunak Di Bawah Piled-Geogrid Supported EMbankment (Analysis of Horizontal and Vertical Deformation of Soft Soil Below Piled- Geogrid Supported Embankment). *Dinamika Rekayasa* 6(2): 39–43.

Pradita, Y. A., & Putri, C. A. 2019. Analisis Penurunan Tanah Lunak Akibat Penimbunan Bertahap. *Prosiding Seminar Intelektual Muda*: 374–377.

Putra, C. E., & Makarim, C. A. 2020. Analisis Alternatif Perbaikan Tanah Lunak dan Sangat Lunak Pada Jalan Tol. *Jurnal Mitra Teknik Sipil 3*(4): 1137–1150.

Settlement Analysis on Soft Soils Due to Box Traffic and Embankment Construction on Toll Road

Liliwarti
Civil Engineering Department – Politeknik Negeri Padang

Lukman Murdiansyah
Civil Engineering Department – Politeknik Negeri Padang

Nayung Dhiya Almassyah
Civil Engineering Department – Politeknik Negeri Padang

ABSTRACT: Padang – Sicincin section is the first toll road development in West Sumatra. Besides its positive impact, the existence of the toll road cuts off the regency road that connects these subdistricts along with it, which will restrict public access to these areas. To overcome this problem, box traffic is constructed . Based on the SPT data, this location consists of deep soft soil, which can lead to settlements. This paper discusses the settlement that occurs due to box traffic construction on toll roads (Padang – Sicincin). The analysis is carried out on the load that works on box traffic. The analysis results show that the total settlement due to embankment is 0.43 m, and due to box traffic equal to 0.35 m, both of this condition are greater than the allowed settlement. Therefore, it is suggested that toll road construction at this location requires soil improvement so as to increase the bearing capacity of the soil.

Keywords: box traffic, settlement, soft soil, toll road

1 INTRODUCTION

Padang – Pekanbaru toll road is part of the Trans Sumatra toll road that will improve connectivity between Riau and West Sumatra, Badan Pengatur Jalan Tol (2020) along 254.8 km, Khristina et al. (2020). According to Toll Road Management Agency-Ministry of Public of Works and Housing, Indonesia (BPJT), this project is divided into 6 sections: Section I Padang – Sicincin, Section II Sicincin - Bukittinggi, Section III Bukittinggi - Payakumbuh, Section IV Payakumbuh - Pangkalan, Section V Pangkalan - Bangkinang, and Section VI Bangkinang – Pekanbaru, Badan Pengatur Jalan Tol (2020).

The first toll road development in West Sumatra is Padang – Sicincin section, Khristina et al. (2020), where the construction begins in February 2018, Badan Pengatur Jalan Tol (2020). The route will pass through several subdistricts, such as Batang Anai (Padang Pariaman regency) and Koto Tangah (Padang City). Besides its positive impact, the existence of the toll road cuts off the regency road that connects these subdistricts, which will restrict the public access to these both areas. In other way, we can say that it is possible to cut the local connections, or in splintering-urbanism terms, this phenomenon is called "local-dis-connections", Hoffman (2016). Therefore, additional structure constructions on the toll road to keep this connection are needed. One of the additional structures is box traffic. Box Traffic is an underground tunnel or underpass bridge that aims to connected the area cut off due to road construction above or below it. Box Traffic also serves to withstand lateral loads and gravity load, Sulardi et al. (2019).

Box traffic for the toll road project is constructed in Nagari Kasang, located in Batang Anai, Padang Pariaman. According to SPT (Standard Penetration Test) data, this location consists of deep soft soil. This soil condition is prone to settlement, Nissa Mat Said et al. (2019), Zhou et al. (2016), which can damage the road and box traffic construction. In addition, Sicincin ring road – Lubuk Alung, Padang Pariaman district has deformed, cracks on the road pavement, and settlement, caused by poor bearing capacity of the subgrade, Liliwarti (2019). Therefore, it is necessary to analyze the settlement that occurs with and without the box traffic construction.

This paper discusses the settlement that occurs due to the construction of box traffic on

the toll road. The analysis is carried out on the load that works on the box traffic, i.e., weight, traffic load, and road pavement, by using numerical modeling. Then, the settlement analysis is performed to obtain the total settlement, which consists of immediate settlement and consolidation settlement. This analysis is very important in order to find the right solution to solve the problem of the settlement on the highway or toll road.

2 RESEARCH METHOD

The research used secondary data that are collected from laboratory tests and filed data of Padang – Sicincin STA 2 + 175 Toll Road Construction Project. It consists of soil parameters and traffic box specifications. From these data, then the box traffic loads are calculated. Then, the settlement characteristics will be obtained based on the total settlement calculations.

2.1 *Soil Parameters*

Soil parameters are very necessary because it will show the properties and characteristics of the soil. In this paper, soil parameter data is in the form of bor log results and SPT, as shown in Table I. SPT is one type of soil test that is often used to determine the bearing capacity of the soil.).

To perform the settlement calculations, other soil parameters are needed, i.e., unit weight (ɣ), Poisson ratio (μ), and modulus of soil elasticity (E). ɣ values are obtained based on the results of the N-SPT correlation. For sandy soils, it used the correlation table according to Teng (1962), and for loam soils, it used Terzaghi and Peck (1943) correlation table. Furthermore, μ and E are obtained based on the correlation table, according to Bowless (1977).

2.2 *Box Traffic Load*

Load calculation on box traffic is carried out according to SNI 1725 (2016), where the regulation concerning loading for bridges includes own load, additional dead load, traffic load, brake load, ground pressure, wind load, and temperature effects.

2.3 *Settlement*

Settlement occurs due to the appearance of strain in the loaded soil layer, where the strain arises due to changes in soil composition and reduced pore cavities in the soil. The amount of strain that occurs in the entire soil layer is a decrease in the total soil, Hardiyatmo (2010), (2011).

The total settlement that occurs as a result of loading can be stated as follows:

$$S = S_i + S_c + S_s \quad (1)$$

where,
S : total settlement (m)
S_i : immediate settlement (m)
S_c : primary consolidation settlement (m)
S_s : secondary consolidation settlement (m)

in this paper, the total settlement are calculated from S_i and S_c, while S_S ignored ($S_S = 0$).

3 RESULTS AND DISCUSSION

From the correlations then it obtained others soil parameters, i.e., unit weight (ɣ), Poisson ratio (μ), and modulus elasticities (E) shown in Table 1.

Table 1. Soil Data Recapitulation.

Depth (m)	Type of Soil	N-SPT	ɣsat kN/m^3	ɣ kN/m^3	μ	E kN/m^2
0	Clay	0.0	-	18.0	0.3	1172.1
0.5	Clay	5.0	-	18.0	0.3	4481.6
2	Sand	12.7	19.6	-	0.3	9859.5
8	Silt	11.0	19.4	-	0.5	10243.5
9.4	Silt	10.0	19.3	-	0.5	9219.3
10.6	Sandy Silt	15.7	20.1	-	0.5	15297.2
16	Sand	13.5	19.7	-	0.4	106179.3
20.3	Sandy Silt	30.0	22.0	-	0.5	19925.9
22	Sand	21.0	20.3	-	0.4	159268.9
25	Sandy Silt	30.0	22.0	-	0.5	19925.9
30	Silent Sand	21.5	20.3	-	0.4	16685.3
35	Sandy Silt	24.3	21.2	-	0.5	22945.8
40	Sand	31.0	20.2	-	0.4	235111.2
42	Sandy Silt	39.5	22.0	-	0.5	23924.8

Two conditions of settlement are analyzed, i.e., settlement occurs due to embankment without box traffic, and the settlement that occurs after the construction of box traffic.

3.1 *Settlement due to Embankments*

Total settlement on of embankment consist of immediate settlement and consolidation settlement and load due to embankment comes from the construction of the toll road where the intensity of each load of elements of the toll road is shown in Table 2.

Table 2. The Intensity of Each Load of Elements of The Toll Road.

Load element	Intensity
Embankment soil weight	51 kN/m^2
The pavement weight	13.2 kN/m^2
Traffic load	15 kN/m^2
	(SNI 8460: 2017)

Total immediate settlement equals to 0.08-meter consist of multiple layers with a total depth of 8 meters, as shown in Table 3.

Table 3. Recapitulation of Immediate Settlement Due to The Embankment.

No.	Type of soil	H (m)	Depth (m)	E (kN/m²)	Si (m)
1	Clay	0.5	0.5	1172.11	0
2	Clay	1.5	2	4481.59	0.02
3	Sand	6	8	9859.5	0.03
4	Silt	1.4	9.4	10243.5	0
5	Silt	1.2	10.6	9219.26	0
6	Sandy Silt	5.4	16	15297.2	0.01
7	Sand	4.3	20.3	106179	0
8	Sandy Silt	1.7	22	19925.9	0
9	Sand	3	25	159269	0.0001
10	Sandy Silt	5	30	19925.9	0.002
11	Silent Sand	5	35	16685.3	0.002
12	Sandy Silt	5	40	22945.8	0
13	Sand	2	42	235111	0.000015
14	Sandy Silt	8	50	23924.8	0
				Total	0.08

Total consolidation settlement is equal 0.35 m, and the soil is over consolidation consist of multiple layers dominated by the silt-clay layer, shown in Table 4.

Table 4. Recapitulation of Primary Consolidation Settlement Due to The Embankment.

No.	Type of soil	H (m)	po' (kN/m²)	Sc (m)
1	Clay	0.5	9	0.014
2	Clay	1.5	36	0.014
3	Sand	-	-	-
	Dry	1.6	65.6	-
	Saturated	4.4	108.7	-
4	Silt	1.4	122.1	0.005
5	Silt	1.2	133.5	0.003
6	Sandy Silt	5.4	189.0	0.007
7	Sand	4.3	231.4	-
8	Sandy Silt	1.7	252.1	0.004
9	Sand	3	283.4	-
10	Sandy Silt	5	344.4	0.053
11	Silent Sand	5	397.0	-
12	Sandy Silt	5	453.9	0.082
13	Sand	2	474.7	-
14	Sandy Silt	8	572.2	0.166
			Total	0.35

The total settlement that occurs as a result of the embankment (S) as follows:

$$S = S_1 + S_c + S_s \quad (1)$$
$$= 0.08 \text{ m} + 0.35 \text{ m} + 0 \text{ m}$$
$$= 0.43 \text{ m}$$

The total settlement due to embankment is 0.43 m, This a large settlement.

3.2 *Settlement due to Box Traffic*

The amount of load due to box traffic is calculated in two conditions, i.e., Strong I, and Serviceability I.

Loads of box traffic consist of own weight, additional load, traffic load, brake load, ground pressure, and wind load, as well as temperature effects. Immediate Settlement value with the strong I condition is 0.03 m, each layer (Table 5).

Table 5. Recapitulation of Immediate Settlement Due to strong 1 of the box Traffic.

No.	Type of soil	H (m)	Depth (m)	E (kN/m²)	Si (m)
1	Clay	0.5	0	1172.1	0
2	Clay	1.5	2	4481.6	0.005
3	Sand	6	8	9859.5	0.013
4	Silt	1.4	9.4	10243.5	0.002
5	Silt	1.2	10.6	9219.3	0.001
6	Sandy Silt	5.4	16	15297.2	0.003
7	Sand	4.3	20.3	106179.3	0.002
8	Sandy Silt	1.7	22	19925.9	0.0002
9	Sand	3	25	159268.9	0.0001
10	Sandy Silt	5	30	19925.9	0.0008
11	Silent Sand	5	35	16685.3	0.0005
12	Sandy Silt	5	40	22945.8	0.0006
13	Sand	2	42	235111.2	0.0000
14	Sandy Silt	8	50	23924.8	0.0002
				Total	0.03

Immediate settlement with Serviceability I Condition is 0.021 m, as shown in Table 6.

Table 6. Recapitulation of Primary Consolidation Settlement Due to Serviceability 1 of Box Traffic.

No.	Type of soil	H (m)	Depth (m)	E (kN/m²)	Si (m)
1	Clay	0.5	0	1172.1	0
2	Clay	1.5	2	4481.6	0.004
3	Sand	6	8	9859.5	0.009
4	Silt	1.4	9.4	10243.5	0.001
5	Silt	1.2	10.6	9219.3	0.001
6	Sandy Silt	5.4	16	15297.2	0.002
7	Sand	4.3	20.3	106179.3	0.001
8	Sandy Silt	1.7	22	19925.9	0.0002
9	Sand	3	25	159268.9	0.0001
10	Sandy Silt	5	30	19925.9	0.0006
11	Silent Sand	5	35	16685.3	0.0003
12	Sandy Silt	5	40	22945.8	0.0004
13	Sand	2	42	235111.2	1.27E-05
14	Sandy Silt	8	50	23924.8	0.0001
				Total	0.021

Consolidation settlement value with a Strong I Condition is 0.32 m as in Table 7.

Table 7. Recapitulation of Primary Consolidation Settlement Due to Strong I of The Box Traffic.

No.	Type of soil	H (m)	po' (kN/m²)	Sc (m)
1	Clay	0.5	9	0.01
2	Clay	1.5	36	0.01
3	Sand	-	-	0.00
	Dry	1.6	65.6	-
	Saturated	4.4	108.7	-
4	Silt	1.4	122.1	0.00
5	Silt	1.2	133.5	0.00
6	Sandy Silt	5.4	189.0	0.00
7	Sand	4.3	231.4	-
8	Sandy Silt	1.7	252.1	0.00
9	Sand	3	283.4	-
10	Sandy Silt	5	344.4	0.05
11	Silent Sand	5	397.0	-
12	Sandy Silt	5	453.9	0.08
13	Sand	2	474.7	-
14	Sandy Silt	8	572.2	0.17
			Total	0.32

Total consolidation settlement with Serviceability I condition is 0.32 m, as shown in Table 8.

Table 8. Recapitulation of Primary Consolidation Settlement Due to Serviceability I of The Box Traffic.

No.	Type of soil	H (m)	po' (kN/m²)	Sc (m)
1	Clay	0.5	9	0.01
2	Clay	1.5	36	0.00
3	Sand			
	Dry	1.6	65.6	-
	Saturated	4.4	108.7	-
4	Silt	1.4	122.1	0.00
5	Silt	1.2	133.5	0.00
6	Sandy Silt	5.4	189.0	0.00
7	Sand	4.3	231.4	-
8	Sandy Silt	1.7	252.1	0.00
9	Sand	3	283.4	-
10	Sandy Silt	5	344.4	0.05
11	Silent Sand	5	397.0	-
12	Sandy Silt	5	453.9	0.08

No.	Type of soil	H (m)	po' (kN/m²)	Sc (m)
13	Sand	2	474.7	-
14	Sandy Silt	8	572.2	0.17
			Total	0.32

3.3 *Total Settlement*

The total settlement that occurs as a result of the traffic box load as follows:

$$S_{KI} = S_i + S_c + S_s \quad (2)$$
$$= 0.03 \text{ m} + 0.32 \text{ m} + 0 \text{ m}$$
$$= 0.35 \text{ m}$$

$$S_{DLI} = Si + S_c + S_s \quad (3)$$
$$= 0.02 \text{ m} + 0.32 \text{ m} + 0 \text{ m}$$
$$= 0.34 \text{ m}$$

Based on the settlement calculations, we can see that the settlement that occurs due to embankment, pavement load, and traffic load is 0.43 m.

This indicates that the subgrade at that location consists of soft soil, so that subgrade improvement is needed. The box traffic construction on the Padang – Sicincin toll road in a total Settlement of 0.35 m (Strong 1) and at serviceability of 0.34 m, as shown in Table 9.

Table 9. Settlement Calculations Result Due to Embankment and Due to Box Traffic.

Settlement due to embankment (m)		Settlement due to box traffic (m)		
Immediate	0.08	Immediate	Strong I	0.03
			Service ability I	0.021
Primary Consoli-dation	0.35	Primary Consolida-tion	Strong I	0.32
			Service ability I	0.32
Total	0.43	Total	Strong I	0.35
			Service ability I	0.34

The settlement of embankment (without box traffic) is 0.43 m, and in this case, 3 m of embankment height is used to reach the road elevation. This causes a significant settlement. It is suggested that road construction at this location requires soil improvement so as to increase the bearing capacity of the soil.

This research shows that the construction of box traffic will increase the soil's subgrade load; thus, the settlement is higher. Therefore, it is necessary to have an appropriate method of soil improvement of subgrade so that the construction of traffic boxes and toll roads can be used according to the planned age.

This research can be useful for construction implementers, consultants, contractors, especially for the construction of roads on soft soil.

ACKNOWLEDGMENT

This research are fully funded by DIPA Politeknik Negeri Padang.

REFERENCES

Badan Pengatur Jalan Tol. 2020. *Progres Fisik Capai 20,49%, Tol Padang – Sicincin Ditargetkan Beroperasi Desember 2021 07*.

Hardiyatmo, H. C. 2010. *Mekanika Tanah 2*. Gajah Mada University Press.

Hardiyatmo, H. C. 2011. *Analisis dan Perancangan Fondasi 1*. Gajah Mada University Press.

Hoffman, A. J. 2016. *the Impact of Toll Road Development: an Analysis Based on Public Administration Ecology*. 32(3): 255–272.

Khristina, D., Warman, K., & Andora, H. 2020. Deposit of Compensation in Land Acquisition for the Construction of the Padang-Pekanbaru Toll Road in Public Interest. *International Journal of Multicultural and Multireligious Understanding 7*(8): 285. https://doi.org/10.18415/ijmmu.v7i8.1877.

Liliwarti, L.-. 2019. Peningkatan Nilai CBR Tanah Dasar (Sub Grade) dengan Penambahan Kapur dan Abu Sekam Padi. *Jurnal Ilmiah Poli Rekayasa* 14(2): 24. https://doi.org/10.30630/jipr.14.2.124.

Nissa Mat Said, K., Safuan A Rashid, A., Osouli, A., Latifi, N., Zurairahetty Mohd Yunus, N., & Adekunle Ganiyu, A. 2019. Settlement Evaluation of Soft Soil Improved by Floating Soil Cement Column. *International Journal of Geomechanics* 19(1): 04018183. https://doi.org/10.1061/(asce)gm.1943-5622.0001323.

Sulardi, 1, Prasetyo, S. D., & 2. 2019. Perancangan Beban Dorong Pada Box Underpass. *Jurnal Desain Konstruksi Volume 13 No. 2 Desember 2014* 7(2): 28–35.

Zhou, S., Di, H., Xiao, J., & Wang, P. 2016. Differential Settlement and Induced Structural Damage in a Cut-and-Cover Subway Tunnel in a Soft Deposit. *Journal of Performance of Constructed Facilities* 30(5): 04016028. https://doi.org/10.1061/(asce)cf.1943-5509.0000880.

Vacuum Preloading: Consolidation Degree Determination using Analytical Solution vs Graphical Method

Roberto Renaldi Yona
PT Geotekindo

Kumbara Kamajaya Cahya Hermawan
PT Geotekindo

ABSTRAK: Dalam suatu pekerjaan pematangan lahan dengan menggunakan metode pra-pembebanan vakum, istilah derajat konsolidasi selalu dirujuk dalam justifikasi proses konsolidasi tanah. Beberapa metode grafis umum digunakan untuk melakukan analisis derajat konsolidasi, dimana persamaan matematika digunakan untuk mendapatkan suatu nilai penurunan akhir yang membutuhkan suatu kondisi berakhirnya penurunan tanah. Hal ini menjadi kontradiktif dengan mempertimbangkan faktor penurunan sekunder yang bersifat linear terhadap *logarithmic* waktu. Sebuah metode solusi analitis digunakan dalam penelitian ini sebagai bentuk pendekatan untuk menentukan derajat konsolidasi tanpa memaksakan penghentian terhadap penurunan kompresi sekunder. Hasil dari solusi analitis tersebut dibandingkan dengan hasil analisis derajat konsolidasi menggunakan metode grafis untuk menganalisis keterbatasan penggunaan metode grafis dalam penentuan derajat konsolidasi.

Kata Kunci: pra-pembebanan vakum, derajat konsolidasi, metode grafis, solusi analitis

ABSTRACT: In a soil improvement project using vacuum preloading method, the term consolidation degree is always referred in the soil consolidation process justification. Several graphical methods are commonly used to analyze consolidation degree, where mathematic equation is used to get an ultimate settlement value which need an end situation for soil settlement. This type of analysis become contradictive in regards of secondary compression factor which have linear relationship with logarithm of time. An analytical solution method is used in this research as an approach in consolidation degree determination without forcing an ending to secondary compression settlement. The result from this analytical solution is compared to the result from graphical method to analyze the limitation of graphical method in consolidation degree determination.

Keywords: vacuum preloading, consolidation degree, graphical method, analytical solution

1 INTRODUCTION

Vacuum preloading method have been developed significantly since its first proposed by Kjelmann in 1952, Chu et al. (2008). It has been proven to be successfully used in several soil improvement projects around the world, Chu et al. (2000), Ngoc et al. (2020), Khrisnapriya (2015). As in Indonesia's recent development, vacuum preloading method have been used in several project around Indonesia archipelago to prepare a suitable ground condition for further construction.

Advantages and disadvantages of this method have been summarized and discussed in previous research (Ngoc, et al, 2010), including the demand of good quality control of the system during the improvement period. Degree of consolidation (DOC) is an important parameter that always been referred to justify the success rate of the vacuum consolidation process and be used as the design specification in a soil improvement contract, Chu et al. (2005). Several graphical methods such as ASAOKA, 1/t, and FORE method is widely used to analyze settlement recording in several vacuum consolidation project to predict the ultimate settlement and followed by an estimation value of consolidation degree.

Conventional graphical method requires an end situation of settlement, which from that point onward there is no settlement happened

including the secondary compression settlement. This situation leads to a discussion about an ending point for secondary compression settlement which consider a constant secondary compression index is unacceptable, Mesri (2005). However, Mesri (2005) has described the limitation of 'first order rate equation" in describing secondary compression factor by presenting several examples of secondary compression settlement observed in oedometer test and conclude that secondary compression index may remain constant, decrease, or increase with time, and there is no rational requirement for $C\alpha$ comes to a complete stop, Mesri (2005).

This research aims to present an approach for consolidation degree justification in a vacuum consolidation process by performing an analytical solution using an isotache model to estimate consolidation degree value by not forcing an ending to the secondary compression settlement. Furthermore, the result of the analytical solution is compared to the consolidation degree value resulted from conventional graphical method to analyze the graphical method limitation.

2 ANALYTICAL SOLUTION

Volume loss by creep of soft soil (eg. peat and clay) is well known and a crucial part of settlement calculation caused by surcharge or embankment in road or residential construction, Kooi and Erkens (2020). Isotache model first proposed by Buisman (1934) and develop over many years up to this day as the fruit of insight in the creep behavior of soil. The first computer program that combined both consolidation process and isotache behavior developed by the school of Leroueil (1986), and in 1996 Grondmechanica Delft (now Deltares) make a commercially available isotache model for settlement calculation with M-Settle (now D-Settlement), Haan (2007).

Isotache model can be refered as the generalization or extension of Terzaghi's elasto-plastic model. The minor difference between the two is the the use of void ratio (e) in Terzaghi model that transates into strain (ε) in the isotache model, which also explain compression index (Cc) and recompression index (Cr) explained into Compression Ratio (CR) and Recompression Ration (RR) in the isotache model, Kooi and Erkens (2020).

D-Settlement provides the transient settlement calculation using one of the three predefined soil model such as NEN-Bjerrum, Isotache a/b/c, and NEN-Koppenjan. In this particular study NEN-Bjerrum soil model coupled with Darcy consolidation model are used as the basis of the settlement calculation.
NEN-Bjerrum model shared the same basic theory as Isotache a/b/c model, however supports common linear strain parameter CR, RR, and $C\alpha$ instead of a/b/c natural strain parameters. NEN Bjerrum model assumes that the creep rate will decrease along with the increasing overconsolidation ratio (OCR) and the overconsolidation ratio will increased by unloading and ageing, Deltares (2016).

3 GRAPHICAL METHOD

Graphical method used in this research take 3 common methods used for analyzing settlement recording data to determine consolidation degree in a vacuum consolidation project. The method used mathematical equation as an approach to determine a single ultimate settlement value that later used to calculate an estimation of consolidation degree achieved at a certain time during the improvement period.

3.1 *ASAOKA method*

In 1978, Asaoka published a journal titled "Observational Procedure of Settlement Prediction" which proposed an observational method to predict an ultimate settlement value from settlement recording.

Settlement value $\rho 1,\ \rho 2,\ \rho 3, \dots, \rho n$ plotted in y-axes and $\rho n{-}1$ value in x-axes. Predicted ultimate settlement (ρf) determined from intersection point between $\rho n = \rho n{-}1$ line which forms a 45 degree angle and linear trend line of $\rho n{-}1$ to ρn. Linear differential equation of Asaoka research shown in Eqn. (1).

$$\rho_n = \beta_0 + \beta_1 . \rho_{n-1} \tag{1}$$

Ultimate settlement value can be determine at a condition where $\rho n = \rho n{-}1$, therefore by substituting this condition to Eqn. (1), Eqn. (2) is formulated to calculate the ultimate settlement value.

$$\rho_f = \frac{\beta_o}{1-\beta_1} \tag{2}$$

3.2 *1/t method*

Rahardjo (1995) proposed a method that can be used to predict the ultimate settlement value (*Sult*) by taking a basic concept that an ultimate settlement condition will be fulfilled at infinite time (t = ∞), so that 1/t translated as 1/∞ that is 0 in value. Settlement recording data plotted in a graph with settlement value (S) as its y-axes, and 1/t data as its x-axes. The ultimate settlement value is derived from the point in which the trend line of the function crossed y-axes (1/t value is 0).

3.3 *FORE Method*

The journal "First Order Rate Equation in Geotechnical Engineering" published by Handy (2002) stated that the ultimate settlement value can be predicted by using a first order rate equation (FORE) which is a form of chemical kinetic equation to determine reaction rate of a reactan. The basic concept of this equation is presented in Eqn. (3). Linearization of Eqn. (3) by using its integral form is converted into logarhitmic form to achieve Eqn. (4).

$$\frac{d(s_n+s_u)}{dt_n} = -a(s_n - s_u) \quad (3)$$

$$\log(|s_u - s_n|) = -a.t_n + b) \quad (4)$$

Ultimate settlement value can be achieved by variating trial Su value in the Eqn. (4) until the best fit Su value is achieved and Eqn. (4) bring out a nearly ideal plot between log (|Su−Sn|) to tn that form a straight lain shown in Fig. 1. Coefficient determination value of the trendline is monitored to justify the goodness of fit of the trial Su value.

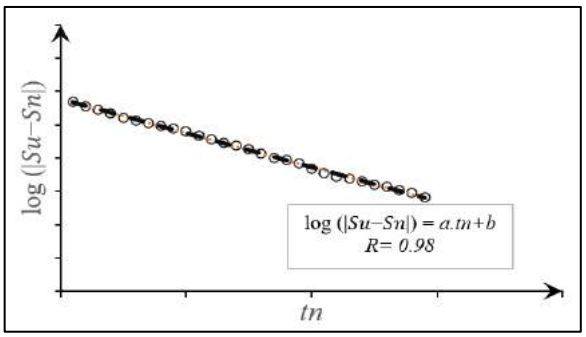

Fig. 1. log (|Su−Sn|) vs *tn* in FORE Method.

4 STUDY CASE

A road construction is planned to be built on a recently backfilled swamp area around Jakarta Bay in 2018. A soil improvement works is carried on to pre-consolidate the soft soil underlain the road area using a vacuum preloading method. For the improvement purpose the 3.4 kilometers long road section is divided into several vacuum preloading zone. The particular research area covered 7,400 m^2 that is 140 meters long and 54 meters wide.

Two meters thick backfill red clay is located on top of the original soil to provide a working platform for the improvement works and the road construction itself. Preliminary Cone Penetration Test (CPT) recording show the original soil underlaying the working platform is typically 9 meters thick in-situ soft soil deposit that made of 4 meters clay-organic soil and 5 meters clayey-silt that potentially imposed a geotechnical challenge for its settlement and stability during road construction and operational period.

Vacuum consolidation method is implemented on construction site before the road construction process began, to pre-consolidate the original soil to reduce the post construction settlement of the soft soil deposit. Prefabricated vertical drain is installed to the design depth to distribute vacuum pressure and provide a drainage path for excess porewater to dissipate. Vacuum pressure is implemented for 146 days, with 80 kPa pressure reached after 23 days from vacuum running and maintained for 124 days.

During the vacuum consolidation process a monitoring program is implemented to record soil settlement, porewater pressure changes, applied vacuum load, and lateral displacement. Instruments including vacuum gauge, settlement plate, piezometer, and inclinometer are installed on the improvement area according to the layout shown at Fig. 2.

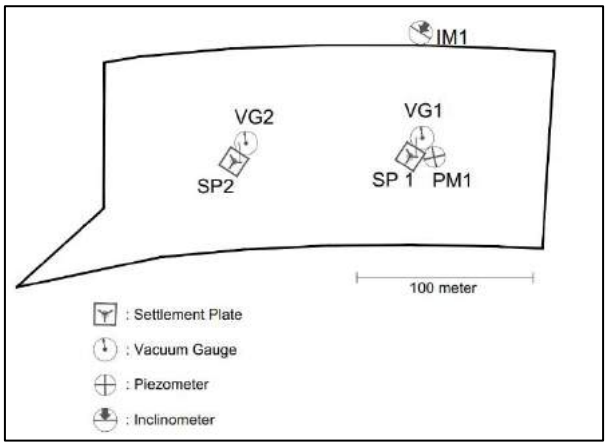

Fig. 2. Monitoring Instrument Layout.

Under 146 days of vacuum load application soil settlement data is recorded daily. As can be seen from Fig 3. an average of 674 mm soil settlement is recorded during the improvement period. Porewater pressure changes also monitored at 4 meters and 9 meters depth that recorded 75 – 78 kPa porewater pressure reduction during the vacuum consolidation process.

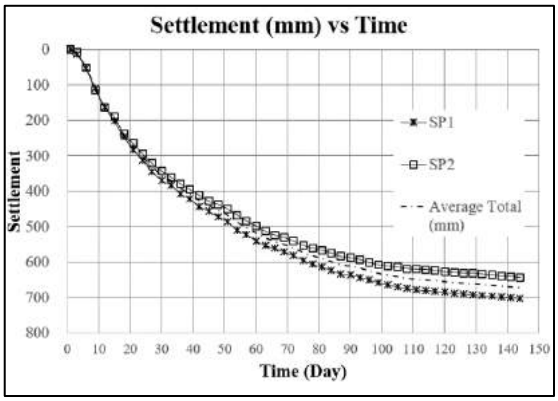

(a)

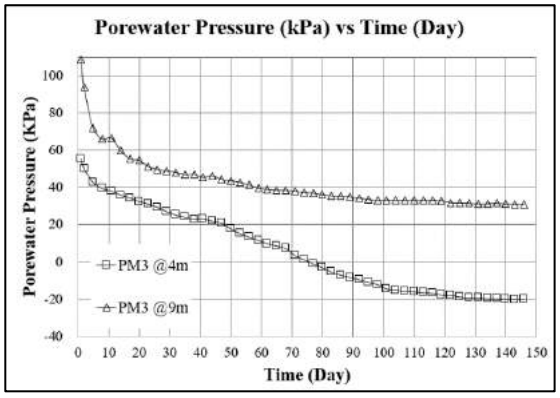

(b)

Fig. 3. (a) Settlement Recording vs Time Recording (b) Porewater Pressure vs Time.

5 RESULT AND COMPARISON

Analytical solution utilizes D-Settlement computer program to calculate settlement happen as soil response under improvement load. NEN-Bjerrum soil model and Darcy consolidation model is chosen to simulate the settlement as the form of soil responses.

Preliminary CPT data is used to determine soil profile on each settlement plate location, which later is used as the input data for the consolidation model. Soil stratification determined from CPT data is then grouped into several soil cluster with relatively similar properties where each soil cluster is given a set of initial soil parameter governing its behavior under a certain load.

Initial soil parameter is acquired from previously collected data from the laboratory and in-situ soil testing for the whole construction area to provide typical soil properties in the region. To check its accuracy a curve matching analysis is executed by comparing simulated settlement curve resulted from the calculation and actual settlement curve from field observation.

Initial soil parameter is then calibrated to provide a better fit soil parameter that is expected to represented actual soil response under improvement loading and later bring out a better fit settlement simulation compared to the actual settlement recorded.

Adjustments made to the soil parameter is limited to a certain degree, so that it does not violent the typical value range for each soil cluster. Fig. 4 show that after the fit soil parameter is defined and implemented to the calculation, the model produced a relatively well-fit settlement curve to the actual settlement measurement. It also implied that the fit soil parameter is expected to well represent the actual soil response on site under improvement load.

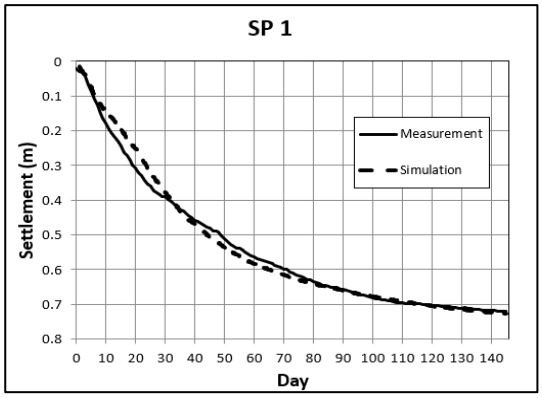

(a)

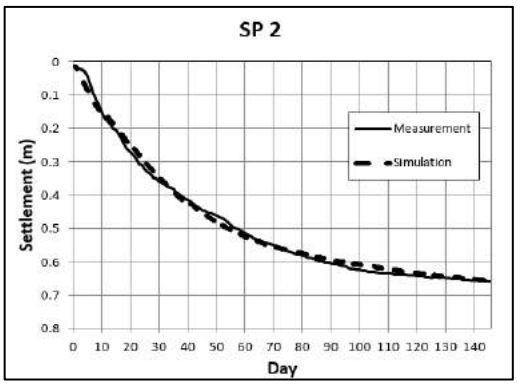

(b)

Fig. 4. Settlement Simulation Result for (a) Settlement Plate 1 (b) Settlement Plate 2.

For the consolidation degree determination purpose a modification is made to the model by taking out the secondary compression factor from calculation so that it only calculated primary consolidation settlement independently. Applying this modification, a comparison between primary and secondary settlement during consolidation period can be determined (Table 1).

Table 1. Primary and Secondary Settlement Comparison during Improvement Period.

Day			Primary Settle-ment	%	Secondary Settle-ment	%	Total
0	-	20	0.238	99%	0.002	1%	0.24
20	-	40	0.208	97%	0.007	3%	0.215
40	-	60	0.073	63%	0.043	37%	0.116
60	-	80	0.023	41%	0.033	59%	0.056
80	-	100	0.011	30%	0.026	70%	0.037
100	-	120	0.008	29%	0.02	71%	0.028
120	-	140	0.001	6%	0.017	94%	0.018
140	-	160	0	0%	0.012	100 %	0.012

(a)

Day			Primary Settlement	%	Secondary Settlement	%	Total
0	-	20	0.233	100%	0	0%	0.233
20	-	40	0.158	90%	0.017	10%	0.175
40	-	60	0.079	77%	0.024	23%	0.103
60	-	80	0.027	55%	0.022	45%	0.049
80	-	100	0.015	45%	0.018	55%	0.033
100	-	120	0.01	40%	0.015	60%	0.025
120	-	140	0.008	40%	0.011	55%	0.019
140	-	160	0	0%	0.01	100%	0.01

(b)

Table 1 clearly show that the calculated settlement both primary and secondary happen simultaneously during the improvement period. Settlement happened initially is subjected to the primary consolidation settlement by means of porewater dissipation, then it gradually decreases and come to stop at day 121 and 140 for both SP 1 and SP 2 respectively. On the other hands very small portion to none secondary compression settlement calculated during the early stages of vacuum consolidation process then it gradually rises and by the end of the improvement period all of the settlement happened is caused by secondary compression. With all that being said, an assumption is made that during the improvement period the primary consolidation of soil has finished considering the fact that there is no more primary settlement happened at the end of improvement period. To check this assumption another analysis is built by extending the improvement period to be 2 years long, and the result is still consistent that even during the extended period, there is no more primary settlement calculated. Another fact supporting this assumption is presented in the porewater pressure recording (Fig. 3) where from day 120 towards the end of improvement period there is little to relatively none porewater pressure changes recorded. No porewater pressure changes also indicate there is no primary consolidation happened in the end of the consolidation period.

Another consolidation analysis is prepared using three graphical methods (ASAOKA, 1/t method, and FORE) to compare the result of analytical solution and graphical method. For the comparison and analysis purposes several checkpoints are established every 10 days duration. Consolidation degree is calculated for every checkpoint as the last recorded settlement data. The result of this analysis is presented and compared to the analytical solution's result in Table 2.

Table 2. Analytical Solution and Graphical Method Consolidation Degree Comparison (a) Settlement Plate 1 (b) Settlement Plate 2.

Day	Settlement (mm)	DOC			
		Analytical	ASAOKA	FORE	1/t
60	543	77%	71%	80%	68%
80	614	87%	79%	85%	75%
100	663	94%	86%	90%	78%
120	687	98%	92%	93%	88%
130	695	100%	93%	95%	89%
146	704	100%	95%	96%	87%

(a)

Day	Settlement	DOC			
	(mm)	Analytical	ASAOKA	FORE	1/t
60	503	79%	69%	81%	75%
80	567	89%	80%	86%	75%
100	610	96%	86%	90%	79%
120	627	98%	92%	94%	88%
130	633	99%	94%	95%	90%
146	644	100%	95%	97%	89%

(b)

Table 2 show the degree of consolidation resulted from the analytical solution that exclusively calculated primary consolidation settlement while neglected the secondary compression factor compared to the degree of consolidation result from graphical method. As can be seen from Table. 2 FORE method gives the closest result to the analytical solution, however all 3 methods generally underestimated the achieved consolidation degree. The distinction between the analytical solution and graphical method become clearer towards the end of the consolidation period, where according to the analytical solution most of the settlement recorded is caused by the secondary compression.

The limitation of the graphical method compared to the analytical method is primarily due to the fact that every recorded settlement at the end of the consolidation process whether primary or secondary settlement resulted in a new and bigger ultimate settlement calculation as an end situation thus underestimated the achieved consolidation degree that is described in term of primary consolidation.

6 CONCLUSIONS

Comparison between analytical solution and graphical method for consolidation degree determination in a vacuum preloading project are presented in this research. Based on the methods review and study cases, several key points can be concluded:

1. Analytical solution offered an approach for consolidation degree determination without forcing an ending situation for secondary compression settlement.
2. The study case of consolidation degree determination in vacuum consolidation project show that conventional graphical method tends to underestimated achieved consolidation degree compared to the analytical solution.
3. Graphical method potentially produced a biases value of consolidation degree for soft soil that have significant secondary compression factor.

ACKNOWLEDGEMENTS

We thank you PT Geotekindo that provide data and the facility used for this research, and also its engineering team that help review and give meaningful suggestions in this research writing.

REFERENCES

Asaoka, A. 1978. Observational Procedure of Settlement Prediction. *Journal of Japanese Society of Soil Mechanics and Foundation Engineering* Vol.18 (4).

Chu, J. & Yan, W. 2005. Estimation of Degree of Consolidation for Vacuum Preloading Projects. *Journal of Geotechnical and Geoenvironmental Engineering ASCE*: 158.

Chu, J, Yan, SW and Indraratna, B. 2008. Vacuum Preloading Techniques-Recent Developments and Applications. *GeoCongress 2008, New Orleans, Geosustainability and Geohazard Mitigation GPS 178, Reddy, KR, Khire, MV, Alshawabkeh, AN (eds)*, 2008: 586-595.

Deltares. 2016. *D-Settlement User Manual*. Delft:Deltares.

Den Haan, E.J. 2007. A History of the Development of Isotache Model.

Handy, R.L. 2002. First Order Rate Equations in Geotechnical Engineering. *Journal of Geotechnical and Geoenvironmental Engineering* 128(5):416 – 425.

Khrisnapriya, P.B., Sandeep, M.N., Antony, J. 2016. Efficiency of Vacuum Preloading on Consolidation Behavior of Cochin Marine Clay. *Journal of International Conference on Emerging Trends in Engineering, Science, and Technology* 24: 256 – 262.

Kooi, H. & Erkens, G. 2020. Creep Consolidation in Land Subsidence Modelling; Integrating Geotechnical and Hydrological Approach in A New Modflow Package (SUB-CR). *Tenth International Symposium on Land Subsidence* 382:499 – 503.

Mesri, G. & Vardhanabhuti, B. 2005. Secondary Compression. *Journal of Geotechnical and Geoenvironmental Engineering ASCE* 131(3): 398.

Ngoc, V.B., Dung, N.T., Suneel,M. 2011. Vacuum Preloading Consolidation Method, A Case Study of Dinh Hu Polyester Plant.

Sustainable Retaining Structure Incorporating Recycled Concrete Aggregate

Nurfly Gofar
Associate Professor, Postgraduate – Program Universitas Bina Darma

Alfrendo Satyanaga
Assistant Professor, Postgraduate – Program Universitas Bina Darma

ABSTRACT: In tropical countries, slope failures are thought to be a typical disaster. Negative pore water pressure within the soils must be maintained on a stable slope so as to possess sufficient shear strength. If the drainage systems are ineffective, the water pressure build-up caused by rainwater flow will reduce shear strength, increasing the chance of slope failure. The objective of this study is to explore the possibility of a sustainable retaining structure, Geobarrier system (GBS), designed using recycled concrete aggregate (RCA) rather than natural aggregate. Consistent with the study's findings, the soundness of the GBS incorporating RCA is achieved through careful design and construction of sustainable GBS, as needed by EUROCODE. As a result, the development of the GBS may be aided by the utilization of RCAs, which may be easily obtained from demolition waste materials.

Desain Konstruksi Dinding Penahan Tanah Pasangan Batu-Kali dengan Metode Memotong Kaki-lereng

Moch. Aswanto
Teknik Sipil – Universitas Muhammadiyah Jakarta

ABSTRAK: Sistim dinding penahan tanah (DPT) dari pasangan batu-kali, termasuk golongan type gravitasi dimana stabilitasnya tergantung pada berat dinding itu sendiri dan sebagian tanah yang duduk diatas bagian dari dinding itu. DPT ini dibangun menerapkan metode memotong Kaki-Lereng, yaitu DPT dibangun menjorok masuk kearah dalam/diatas area lereng yang longsor, sehingga mendapatkan tambahan area lahan disisi depan DPT, dalam hal ini potensial lahan baru yang didapat sekitar 700 m^2. Ketinggian tanah yang ditahan DPT sekitar 8m, sepanjang 90m. Tebal dinding bagian bawah 1,36 m dan puncaknya 0,6 m. Jenis batu yang digunakan, diambil dari kuari Teluk Bayur, Berau, Kalimantan Timur. Analisa stabilitas lerengnya menggunakan metode kesetimbangan batas (*limit equilibrium*). Evaluasi meliputi Angka keamanan (SF) terhadap *Slope Stability* pada saat awal SF 3,18, penggalian dimasa kontruksi SF=2,38, kondisi DPT sudah berdiri SF=4,61 dan terhadap kegempaan SF=4,44.

Kata Kunci: dinding penahan tanah, batu-kali, stabilitas lereng, metode kesetimbangan batas

ABSTRACT: The retaining wall system of stone masonry (DPT), belongs to the gravity type where its stability depends on the weight of the wall itself and the part of the soil that sits on top of the wall. This DPT was built behind the slope of the landslide, thus obtaining additional land area on the front side of the DPT, in this case the potential for new land obtained was around 700 m2. The height of the soil retained by DPT is about 8m, 90m long. The bottom wall is 1.36m thick and the top is 0.6m. The type of stones used was taken from the Teluk Bayur quarry, Berau, East Kalimantan. The slope stability analysis uses the limit equilibrium method. The evaluation includes the safety factor (SF) on the slope stability at the initial condition SF= 3.18, excavation during construction SF = 2.38, the condition of the DPT already built SF = 4.61 and against seismicity SF = 4.44.

Keywords: gravity masonry retaining wall, stone masonry, slope stability, limit equilibrium method

1 PENDAHULUAN

Penanganan kelongsoran di Indonesia adalah pekerjaan yang relatif rutin di Indonesia. Dikarenakan hampir disemua pelosok kondisi kontur tanahnya terdapat perbukitan dan karena perkembangan pemanfaatan lahan diarea perbukitan yang tidak terelakan, maka pekerjaan *cut & fill* akan menyisakan pekerjaan perkuatan lereng.

Tidak semua pekerjaan perkuatan dapat bertahan lama, seringkali disebabkan karena pembiayaan pelaksanaan yang sangat terbatas diawal proyek.

Sebagai contoh dalam hal ini, perkuatan lereng dengan metode pemasangan *geotextile* disepanjang lereng, setelah beberapa tahun menunjukan performa yang kurang baik. Dengan terlihat melorotnya dan bergesernya lereng beserta konstruksi *geotextile*-nya sekaligus. Gbr. 1 menunjukan kondisi lereng dengan perkuatan *geotextile* yang mulai bergerak dan perlu diperbaiki dengan metode yang lebih sesuai keperluan pemilik.

Gbr. 1. Kondisi Lereng Mulai Bergerak.

Diatas sisi bukit terdapat menara BTS dan disisi bawah sudah dibangun Workshop alat berat untuk perawatan dan fasilitas pertambangan.

Gbr. 2. Denah Area Lereng dan Arah Kelongsoran.

Untuk mencegah kelongsoran yang membahayakan konstruksi BTS dan *Workshop*, maka alternatif perbaikan yang kami rencanakan adalah dengan memotong lereng kearah bukit sehingga kita mendapat tambahan area *stoking-yard* (Gbr. 9) dan membangun DPT dari Pasangan Batu-Mortar, pemilihan metode ini untuk meminimalisir biaya dan kemudahan pelaksanaan agar dapat dikerjakan *General Kontraktor* di lokal area. Lokasi Lereng di Tanjung Redeb, Berau.

2 METODOLOGI

2.1 *Kriteria Umum*

- Verifikasi kecukupan stabilitas global terhadap Pembebanan Gravitasi dan Gempa, masing-masing:
- *Slope Stability* SF >1,5 dan >1,1
- Verifikasi kecukupan stabilitas lokal DPT terhadap Pembebanan Gravitasi dan Gempa, masing-masing:
  - *Overturning* dengan SF >2 dan >1,1
  - *Slip* dengan SF >1,5 dan > 1,1
  - Daya Dukung Tanah SF > 3
- Analisa kegempaan *psedo* dengan metode *Mononobe-Akabe*.
- Perhitungan kontribusi tekanan tanah pasif dengan metode *Coulomb* dan tekanan aktif dengan *Caquot-Kerisel*. Tekanan aktif dikonsiderasi 2/3 dari kapasitas aktifnya.
- Analisa *slope-stability* global dengan metode *Bishop*.

2.2 *Properties Tanah*

Titik penyelidikan dan pengambilan sampel diambil di 3 lokasi, yaitu Puncak lereng, Tengah lereng dan Kaki lereng.

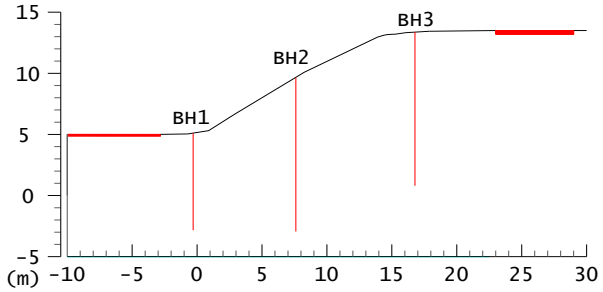

Gbr. 3. Posisi Titik-titik Penyelidikan Tanah.

Penyelidikan meliputi *in-situ* test SPT/BorLog, sampel untuk Laboratorium Test. Bagan Test dan elevasi pengambilan sampel dapat dilihat di Gbr. 3 dan Gbr. 4.

Penyelidikan Dapat dikategorisasi menjadi 4 lapis tanah, dengan deskripsi warna seperti di Gbr. 5, sebagai berikut:

1) Lapis I: Tanah Urugan dan Konstruksi *Geotextile* (Warna Kuning)bercampur dengan Lempung Silt Pasir - Kekuningan *Stiff*, CH (warna kuning kecoklatan).
2) Lapis II: 10 (warna kuning kecoklatan).
3) Lapis III: Lempung Silt Pasir - Coklat Abu-abu *hard*, bercampur lapisan tipis Batubara. (warna Merah-muda).
4) Silt pasir *cemented*-Coklat Abu-abu-*hard*, SPT diatas 50 (warna biru).

Tidak ditemukan muka air tanah sampai kedalaman 18 m.

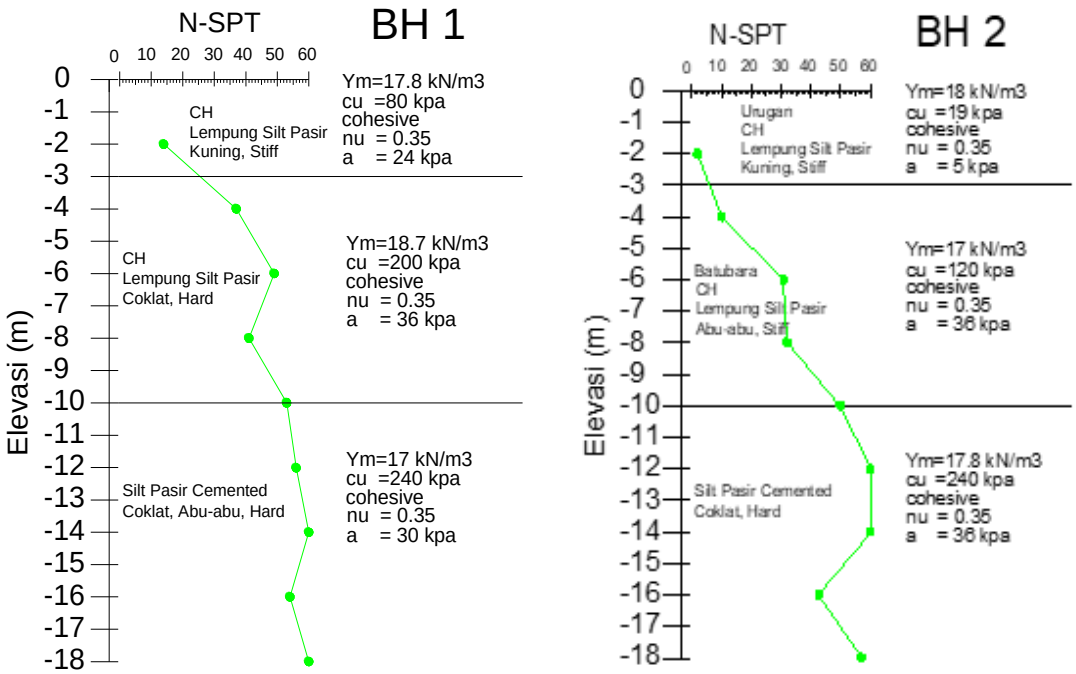

Gbr.4A. Plot N-SPT vs Elevasi, Profil dan Parameter Tanah Masing-masing BH1, BH2.

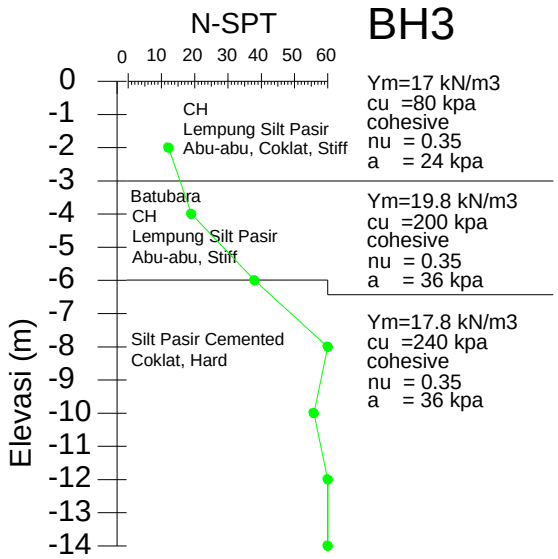

Gbr.4B. Plot N-SPT vs Elevasi, Profil dan Parameter Tanah di BH3.

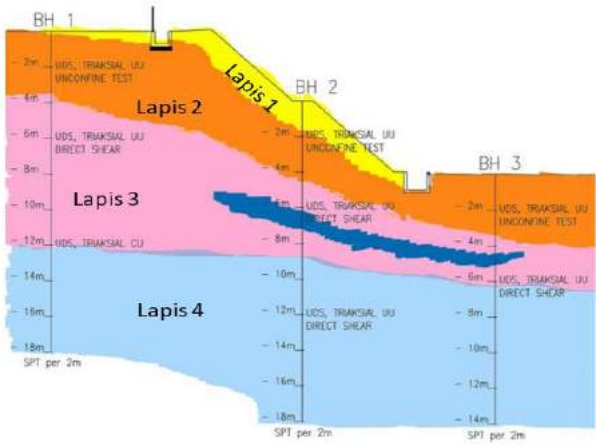

Gbr.5. Sketsa Lapis-lapis Tanah.

Sedangkan untuk analisa, agar lebih sederhana maka lapis Lapis 1 dan 2 dijadikan satu. Selanjutnya pengambilan nilai properties desain sebagai berikut:

1. Di Gbr. 5 diatas dideskripikan jenis pengujian dan elevasi dikedalaman berapa sampel diambil.
2. Penentuan koefisien *earth pressure at rest (K*o*)*, untuk tanah kohesif, program meminta input nilai nu (rasio *poisson v*) untuk menghitung Ko. Nilai *v* diambil 0,35 untuk Lempung kelanauan dikondisi *slow loading*, dari *Poulos & Small 2000*.
3. Penentuan *adhesion(*a*)* antara tanah dan struktur pasangan batu kali didekati dari Tabel 24,4 dari *Canadian Foundation Manual.*
4. Penentuan nilai cu desain yang diambil dari Uji *Unconfined* dan Uji Triaksial, terhadap korelasi-korelasi tipikal dipresentasikan di Tabel 1.

Tabel 1. Rangkuman Pengambilan Nilai Cu.

Layer	Jenis Tanah	N_{SPT}	Cu korelasi N_{SPT} Cu=0.6N (kPa)	Cu *Triaxial UU* (kPa)	Cu *Uncondifed* (kPa)	Cu *Typical* (kPa)	Cu diambil (kPa)
1 dan 2	Lempung Silt Pasir - Kekuningan, *Stiff*, CH	12	72	20	130	50-100	80
3	Lempung Silt Pasir - Coklat Abu-abu, *Hard*, CH	35	210	-	250	>200	200
4	Silt Pasir *Cemented* - Coklat Abu-abu, Hard	50	300	-	300	>200	240

2.3 *Metoda Analisa*

a) Analisa *slope-stability*, meliputi 3 kondisi sebagai berikut:

1) Kondisi I, awal yaitu kondisi eksisting sebelum pekerjaan konstruksi DPT dimulai.
2) Kondisi II, masa konstruksi, yaitu penggalian lereng dengan memotong kaki lereng kearah bukit sejauh 12-13m.
3) Kondisi III, pembangunan DPT.
4) Kondisi IV, setelah DPT terbangun.

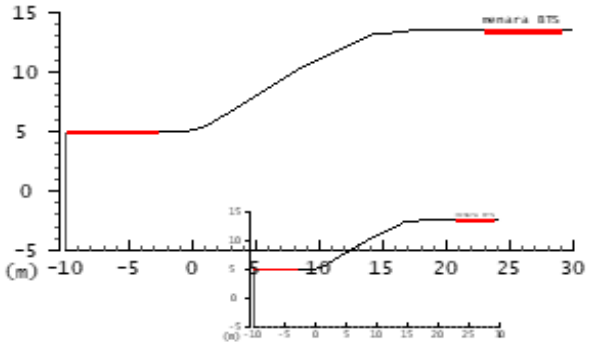

Gbr.6. Kondisi I: Awal Lereng.

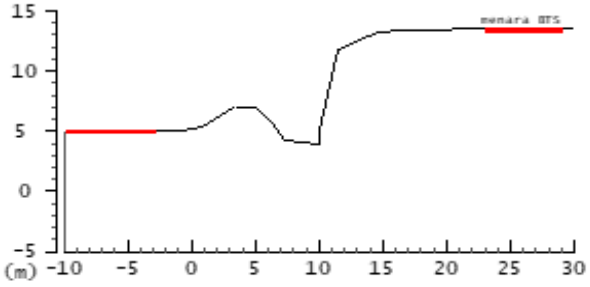

Gbr.7. Kondisi II: Penggalian.

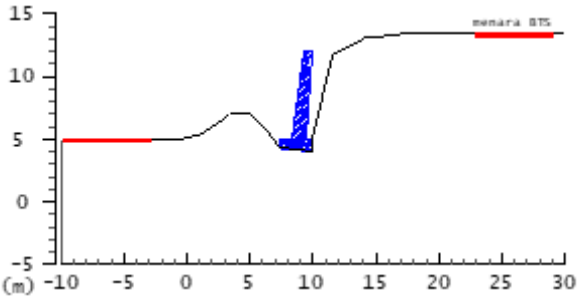

Gbr.8. Kondisi III: Masa Konstruksi DPT.

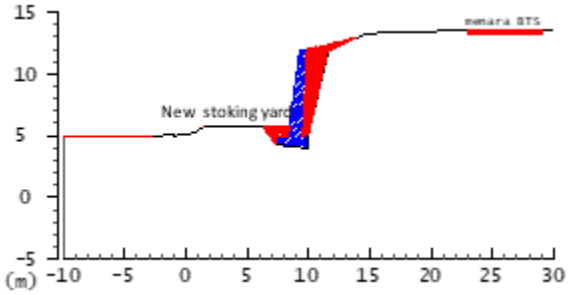

Gbr.9. Kondisi IV: Setelah DPT Terbangun.

b) Analisa terhadap DPT, meliputi verifikasi terhadap Dimensional DPT sebagai berikut:

1) Verifikasi *overturning*
2) Verifikasi *slip*
3) Verifikasi kecukupan *bearing capacity*
4) Verifikasi dimensi dinding / *wall-stem* terhadap Geser, Lentur dan Tekan, Lentur.
5) Verifikasi kecukupan kuat menahan Geser, Lentur dan Tekan, Lentur di pertemuan *wall-stem* dan pasangan batu di dasar DPT (*base-footing*) dielevasi 5m, lihat Gbr. 10.

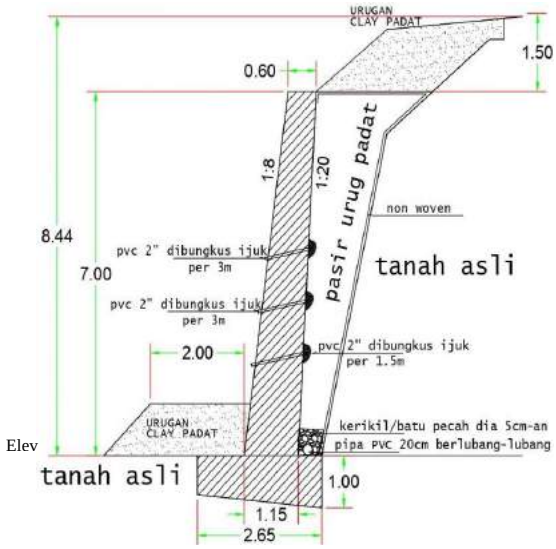

Gbr. 10. Dimensional DPT (m).

c) Kapasitas daya dukung tanah untuk dudukan *base-footing* dari DPT, diambil dari BH3 di elevasi -2 m (Gbr. 4). Menggunakan rumus *Terzaghi*, dan digunakan daya dukung Ijin 300 kpa/3 kg/cm^2.

2.4 *Pembebanan*

Ada 3 beban utama yaitu:

1) Beban gempa didekati dengan metode *pseudostatic* menggunakan *Mononabe-Okabe* (SNI-8460 2017, 12.2.5) dengan lokasi Tanjung Redeb:
   - PGA (1%-100Y) = 0,4 *g*
   - Faktor Keutamaan = 1,25
   - Percepatan *g* = 9,6 m/s2
   - Kh = 0,051

   Dimana Kh=koefisien gempa horizontal.

$$Kh = \frac{PGA \times Faktor\ Keutamaan}{g} \qquad (1)$$

2) Beban tower BTS dan pondasinya sebesar 1160 kN yang bekerja pada area 36m^2.
3) Beban *top-soil* diatas DPT sebagai q=10 kN/m^2/m.

2.5 *Urugan Belakang DPT*

Dibelakang DPT, diurug pasir-padat, yang berfungsi sebagai drainase. Air hujan yang meresap masuk dari belakang dan bagian atas DPT akan ditangkap pasir yang akan dialirkan keluar melewati saluran PVC dibawah kaki DPT. Air dibuang keluar menuju saluran utama kota. Adapun permodelan input material properties pasir padat sebagai berikut :

- γ = 18 kN/m^3
- ϕ = 35^0, c = 0
- δ= 17^0 (*angle of friction soil-structure*)

2.6 *Geotextile*

Digunakan *geotextile non-woven* sebagai separator, antara tanah asli dan pasir urug yang ada dibelakang DPT. (Lihat Gbr.10) Hal ini untuk mencegah bercampurnya tanah asli dengan pasir, diharapkan hanya aliran air yang dapat merembes menembus geotextile.
Spesifikasi yang digunakan:

- *Non woven* serat polymer.
- Permeabilitas 3 x 10^{-3} m/s
- Ukuran pori 110-90 micron
- Berat 238 gr/m^2

2.7 *Pemasangan Batu Kali*

Perhitungan kapasitas penampang DPT dianalisa berdasarkan dari estimasi kekuatan pasangan batu kali dan mortar sebagai berikut :

- Kuat Tekan = 12,5 Mpa
- Kuat Geser = 5 Mpa
- Kuat Lentur = 1,5 Mpa

Uji dan penelitian selanjutnya terhadap kapasitas tegangan terhadap tekan, geser dan lentur pasangan batu kali yang spesifik dari Tanjung Redeb perlu dikerjakan.

3 ANALISA & PERHITUNGAN

3.1 *Global Stability*

Perhitungan menggunakan perangkat-lunak Geo5 (*Slope-stability dan Gravity Wall*). Diawali dengan analisa Global *Slope-Stability* terhadap tahapan-tahapan pekerjaan:

1) Tahap pertama: Analisa Global *Slope-stability* **kondisi eksisting** sebelum konstruksi DPT dikerjakan (Kondisi Gbr. 6)

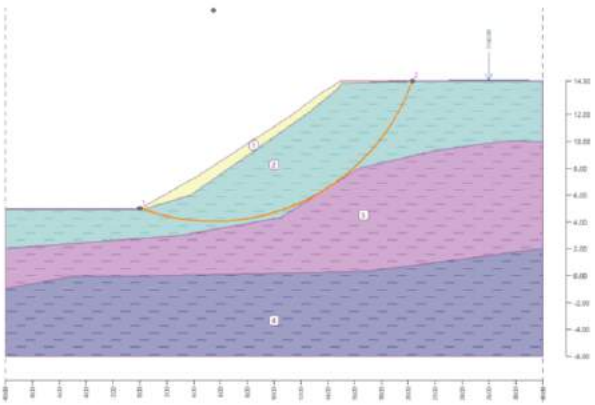

Gbr.11. Faktor Keamanan *Bishop* 3.18 > 1.5.

2) Tahap kedua: Analisa Global *Slope-stability* **kondisi galian** dikerjakan. (Kondisi Gbr.7 dan Gbr. 8) sebagai berikut:

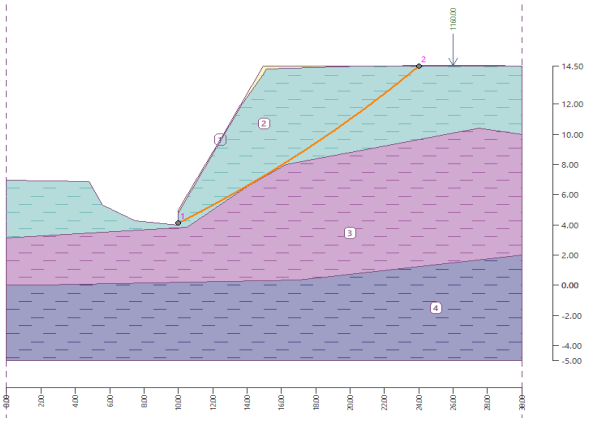

Gbr.12. Faktor Keamanan *Bishop* 2.38 > 1.5.

3) Tahap ketiga: Analisa Global *Slope-stability* saat DPT dan urugan dibelakangnya **kondisi terpasang** (Kondisi Gbr. 9) sebagai berikut:

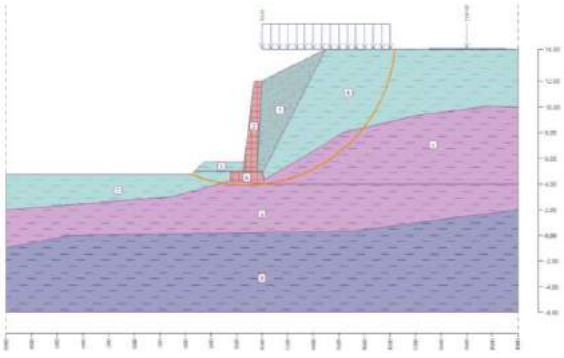

Gbr.13. Faktor Keamanan *Bishop* 4.61 > 1.5.

4) Pengaruh **kegempaan** terhadap kestabilan lereng dan DPT dianalisa dengan hasil sebagai berikut:

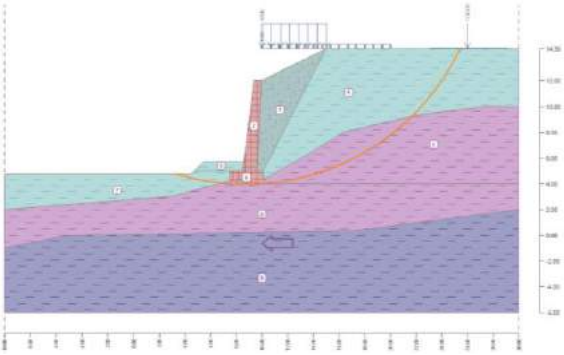

Gbr.14. Faktor Keamanan *Bishop* 4.44 > 1.1.

3.2 *Kapasotas Internal DPT*

Tahap selanjutnya pemeriksaan verifikasi terhadap *over-turning, slip, bearing capacity* dan kekuatan internal konstruksi DPT terhadap:

- Beban mati permanen yang diaplikasikan diatas DPT adalah beban merata mewakili kemungkinan timbunan tanah berlebih, q = 5kN/m^2/m.
- Beban *accidental* mewakili kemungkinan ada peralatan pekerjaan disekitar BTS, q = 2,5 kN/m^2/m.
- Tekanan pasif (Pp) didepan DPT, dalam analisa direduksi menjadi 2/3 Pp, sebagai asumsi kompatibilitas terhadap $P_{aktif.}$ Tahanan pasif ini selain dari tanah asli dikaki DPT, juga ditambahkan urugan clay yang dipadatkan setebal 1 meter.

Runutan analisa sebagai berikut:

1) Dihitung terlebih dahulu gaya-gaya yang bekerja terhadap DPT, yaitu gaya Aktif akibat beban Tanah dibelakang DPT, beban sendiri struktur DPT, hambatan tekanan Pasif dan beban-beban yang ada di puncak tanah. Sehingga didapatkan SF terhadap ***Over turning*** dengan beban gravitasi sebagai berikut (Gbr. 15). Verifikasi *overturning-stability* sebagai berikut: Momen *resisting* = 523,86 kNm/m > Momen *overturning* = 259,63 kN/m, maka SF = 2,02 > 2

   Verifikasi *Slip*

   Tahanan horizontal = 574,52 kN/m > Gaya Aktif horizontal = -154,35 kN/m, SF = 3,7 > 1.5.

2) **Kapasitas pondasi DPT**, diambil kapasitas ijin daya dukung tanah 300 kpa. Kapasitas daya dukung tanah dihitung dengan rumus *Terzaghi*.

Analisa terhadap beban yang bekerja dan gaya-gaya lainnya terhadap pondasi DPT menyebabkan Tegangan maksimum dibawah pondasi akibat kombinasi:

Momen = 10,8 kNm/m, Normal = 176,45kN/m dan Shear = 152,91 kN/m; sehingga Tegangan yang terjadi = 61,43 kpa < Tegangan Ijin = 300 kpa, maka SF =4,88 > 3.

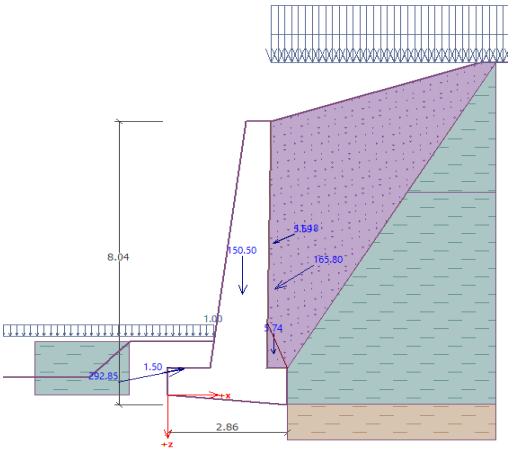

Gbr.15. Faktor Keamanan *Over turning* DPT 2.02 > 2 (Beban-beban Gravitasi).

3) Kapasitas **kekuatan penampang Dinding**/*Wall-stem* dengan penampang yang diperhitungkan 1.36m sebagai berikut:

- Kapasitas Geser (*ultimate*) = 3862,26 kN/m > Gaya Geser yang terjadi 3,51 kN/m
- Kapasitas *Compresive force* (*ultimate*) = 284,83 kN/m > 126,52 kN/m
- Kapasitas *Moment* (*ultimate*) = 489,72 kNm/m > *Moment* yang terjadi 233,44 kNm/m

Sehingga Kapasitas Penampang memenuhi syarat, dengan utilitas penampang yang digunakan sekitar 48%.

4) Selanjutnya dengan **memperhitungkan kegempaan**, hasil analisa sebagai berikut:
Verifikasi *overturning-stability* sebagai berikut: Momen *resisting* = 545,85 kNm/m > Momen *overturning* = 344,23 kN/m, maka SF = 1,59 > 1,1

Verifikasi *Slip*

Tahanan horizontal = 426,64 kN/m > Gaya aktif horizontal = -121,36 kN/m, maka SF = 3,5 > 1,1.

Kapasitas kekuatan penampang Dinding/*Wall-stem* dengan penampang yang diperhitungkan 1,36 m sebagai berikut:

- Kapasitas Geser (*ultimate*) = 3862,74 kN/m > Gaya Geser yang terjadi 30,38 kN/m.
- Kapasitas *Compresive force* (*ultimate*) = 284,95 kN/m > 132,11 kN/m.
- Kapasitas *Moment* (*ultimate*) = 489,82 kNm/m > *Moment* yang terjadi 296,03 kNm/m
- Kapasitas Penampang memenuhi syarat, dengan utilitas penampang sekitar 60%.

Resume tersaji sebagai berikut:

Tabel.2. Resume Pemeriksaan Angka Keamanan.

	Pemeriksaan	FK	
		DPT	Izin
	I. Global Stability		
a	Sebelum digali	3,18	1,5
b	Penggalian lereng	2,38	1,5
c	DPT selesai dibangun	4,61	1,5
d	Pengaruh gempa	4,44	1,1
	II. Internal DPT		
	Beban Gravitasi		
a	Over turning	2,02	2
b	Slip	3,70	1,5
c	Daya dukung tanah	4,88	3
	Pengaruh Kegempaan		
a	Over turning	1,59	1,1
b	Slip	3,50	1,1
c	Daya dukung tanah	3,39	1,1

Tabel 3. Resume Pemeriksaan Kapasitas Penampang Dasar Dinding/*Stem*.

Keterangan	Kapasitas	Gaya Luar
I. Beban Gravitasi		
Geser (V)	3862,26 kN/m'	3,51 kN/m'
Aksial (P)	284,83 kN/m'	126,52 kN/m'
Momen (M)	489,72 kN m/m'	233,44 kN m/m'
II. Beban Gempa		
Geser (V)	3862,26 kN/m'	30,38 kN.m'
Aksial (P)	284,83 kN/m'	132,11 kN/m'

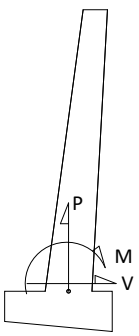

Keterangan	Kapasitas	Gaya Luar
Momen (M)	489.72 kN m/m'	296,03 kN m/m'

4 KESIMPULAN

Hasil analisa Pemeriksaan Angka Keamanan dan Pemeriksaan Kapasitas Penampang, dapat diyakinkan masih dalam koridor aman.

Saat ini, perencanaan DPT dengan menggunakan perangkat-lunak geoteknik yang mengaplikasikan metode *limit equilibrium*, dan dilengkapi dengan *user interface* yang baik, secara signifikan mempercepat proses *perencanaan.*

Rutin input bentuk struktur, pembebanan dan penampang-penampang DPT sudah tersedia dalam berbagai variasi *template*.

Apabila diinginkan komputasi lebih detail seperti mendapatkan pola deformasi, gradasi tegangan maka dapat dilanjutkan dengan analisa *Finite Element.*

DAFTAR PUSTAKA

Aswanto, M. 2015. Analisa Stabilitas Lereng Proyek Facility PAMA di Kalteng. PT Pamapersada Nusantara. Design Report PT MGU.

Aswanto, M. 2017. Perbaikan dan Analisa Resiko Terhadap Kelongsoran Lereng. PT United Tractors Berau. Design Report PT AWK.

Aswanto, M. 2019. Perencanaan Penahan Tanah 15m dengan Dinding Kantilever di Skyland Jayapura. *Jurnal Konstruksia*.

Badan Standarisasi Nasional. 2017. *SNI 8460 Persyaratan Perancangan Geoteknik*. BSN.

Badan Standarisasi Nasional. 2012. SNI *1726-2012 Tata Cara Perencanaan Ketahanan Gempa*. BSN.

Canadian Geotechnical Society. 2006. Foundation *Engineering Manual 4th Edition:* 382.

GEO5. 2018. *Engineering Manual Gravity Walls & Stability Analysis*.

Gouw Tjie-Liong. 2014. Sample of Derivation of Soil Parameters from a Soil Investigation Report. GTL.

Gouw Tjie-Liong. 2015. Kestabilan Lereng, Tekanan Tanah Lateral dan Galian Dalam. *Pelatihan Geoteknik GTL*.

Gouw Tjie-Liong. 2021. *Korelasi Parameter Tanah*. GTL.

Hardiyatmo, H.C. 2012. *Tanah Longsor & Erosi, Kejadian dan Penanganan:*237-239.

NAVFAC. 1986. Foundation *& Earth Structures Design Manual 7.02:* 63.

PUSGEN. 2017. Peta *Sumber dan Bahaya Gempa Indonesia 2017*.

Parametric Study of Tunnel Analysis in Clayshale on Short-Term and Long-Term Condition Using Finite Element Method

Danang Setiya Raharja
Research Student – Institute Technology Bandung

I Wayan Sengara
Professor, Geotechnical Engineering Research Group, Faculty of Civil and Environmental Engineering – Institute Technology Bandung

Imam Achmad Sadisun
Associate Professor, Department of Geological Engineering, Faculty of Earth Sciences and Technology – Institute Technology Bandung

ABSTRAK: Penelitian ini bertujuan untuk mengetahui karakteristik dan klasifikasi tanah clayshale di Jawa Barat serta implikasinya pada stabilitas terowongan dalam kondisi *short-term* dan *long-term* menggunakan *finite element method*. Data sekunder dari proyek di Jawa Barat yang terdapat clayshale dikumpulkan dan dianalisis. Clayshale tersebar pada 4 Formasi batuan yaitu Formasi Cihoe (Tpc), Formasi Subang (Tms), Formasi Cantayan (Mtts/Mttc), dan Formasi Jatiluhur (Tmj). Setiap formasi memiliki properti *mechanical* dan *engineering* yang cukup berbeda. Analisis menggunakan model Mohr Coulomb (MC) dan Hardening Soil (HS) dilakukan dengan software Plaxis. Ketebalan *overburden* divariasikan antara 3 kali diameter terowongan (3D), 6D, dan 9D. Model HS dipertimbangkan memberikan hasil yang lebih baik daripada model MC karena model HS memperhitungkan non-linearity. Ketebalan overburden yang semakin besar menghasilakn *surface deformation* yang lebih kecil. Kondisi jangka panjang memiliki stabilitas lebih rendah dibandingkan kondisi setelah konstruksi. Deformasi jangka panjang meningkat setelah konstruksi dan memberikan peningkatan tegangan pada tunnel lining yang perlu dipertimbangkan dalam desain terowongan.

Kata Kunci: clayshale, finite element, mohr coulomb, hardening soil

ABSTRACT: This study aims to determine the characteristics and classification of clayshale in West Java and their implications for tunnel stability under short-term and long-term conditions using the finite element method. Secondary data from projects in West Java containing clayshale were collected and analyzed. Clayshale is widespread over 4 rock formations, namely Cihoe Formation (Tpc), Subang Formation (Tms), Cantayan Formation (Mtts/Mttc) and Jatiluhur Formation (Tmj). Each formation has quite different mechanical and engineering properties. Analysis using Mohr Coulomb (MC) and Hardening Soil (HS) models was carried out using Plaxis software. While, the overburden thickness was varied between 3 times the tunnel diameter (3D), 6D and 9D. The HS model is considered to give better results than the MC model because the HS model takes into account non-linearity. The greater the overburden thickness will produce a minor surface deformation. Long-term conditions have lower stability than short-term conditions. Long-term deformations increase after construction and provide increase in tunnel lining stress that need to be considered in the tunnel design.

Keywords: clayshale, finite element, mohr coulomb, hardening soil

Flotation Check in Underground Structure Based on JSCE, LTA and Eurocode

Justin Limoris
Shimizu – Adhi Karya Joint Venture

Masrur Abdull Hamid Ghani
Shimizu – Adhi Karya Joint Venture

Ito Kenichi
Shimizu – Adhi Karya Joint Venture

ABSTRAK: Salah satu kegagalan pada struktur bawah tanah adalah pengapungan. Kondisi pengapungan biasanya terjadi ketika muka air banjir. Kondisi pengapungan ini biasanya dilakukan pada struktur yang keseluruhan strukturnya berada di bawah tanah dikarenakan tidak adanya beban struktur tambahan yang berada di atas permukaan tanah yang berguna untuk melawan gaya apung yang diberikan oleh air. Tulisan ini membandingkan pengecekan pengapungan berdasarkan standar dari *Japan Society of Civil Engineers* (JSCE), *Eurocode* dan *Land Transport Authority* (LTA) untuk bisa dijadikan sebagai referensi pada pengecekan pengapungan bangunan bawah tanah di Indonesia. Hasil dari pengecekan pengapungan pada contoh kasus menunjukkan bahwa perhitungan LTA lebih konservatif dari JSCE dan Eurocode.

Kata Kunci: pengecekan pengapungan, muka air banjir, tekanan air uplift, struktur bawah tanah

ABSTRACT: One of the failures on the stability of underground structure is flotation. The flotation usually happened at flood water level. Flotation needs to be checked on the structure that is buried under ground because there is no additional weight from the upper structure that will contribute against the buoyancy force from water. This paper will examine and compare flotation check based on the standard from Japan Society of Civil Engineers (JSCE), Eurocode, and Land Transport Authority (LTA) so it can be referred as reference for flotation check underground structures in Indonesia. The result of floatation checks on the sample case show that LTA calculation is more conservative that JSCE and Eurocode, respectively.

Keywords: flotation check, flood water level, uplift water pressure, underground structure

1 INTRODUCTION

In a developing city where land area is limited to build new structures, underground structures become a solution. With the increasing demand of this structure, the understanding of its design is also necessary. Underground structures such as metro stations usually have a shallow cover of soil over roof slab that provides minimum depth to accommodate pavement construction and small services. With that characteristics and location below ground water level, the structure must sustain uplift force or floatation to avoid stability failure.

This paper compares floatation check calculation from different code and standard which have been applied in underground station construction in overseas. Those referred code and standard are Japan Society of Civil Engineers (JSCE) from Japan, Land Transport Authority Civil Design Criteria (LTA CDC) from Singapore and Eurocode.

2 FLOTATION CHECK THEORIES

The flotation check is also known as stability against uplift. The flotation check compares resisting forces and the uplift force. Resisting forces mainly come from self-weight of structure, friction resistances of soil and soil with the structure. Uplift forces itself is the buoyancy from the water. The differences of formula in each code can be distinguished from the factors that modifying the value of the resisting forces and the uplift force.

The factors that used in every codes are detailed in the following sections.

3 FLOTATION CHECK BASED ON JSCE STANDARD SPECIFICATIONS FOR TUNNELING 2016: CUT AND COVER TUNNELS

The calculation for flotation check is based on Eqn. (1).

$$\gamma_i \frac{U_s}{W_s+W_B+2Q_s+2Q_B} \leq 1.0 \quad (1)$$

$$U_s = \gamma_f u_s B \quad (2)$$

$$W_B = f_{uw} w_B \quad (3)$$

$$W_s = f_{uw} p_v B \quad (4)$$

$$Q_s = f_{us} H' (c_s + K_0 \sigma'_{vs} \tan\phi_s) \quad (5)$$

$$Q_B = f_{us} H (c_B + K_0 \sigma'_{vB} \tan\phi_B) \quad (6)$$

Where:

U_s = Design value of hydrostatic uplift force on tunnel bottom
W_B = Design self-weight of cut-and-cover tunnel
W_s = Design value of vertical load
Q_s = Resistance of cover soil
Q_B = Friction drags on tunnel side
w_B = Characteristic value of self-weight of tunnel
p_v = Characteristic value of vertical earth pressure
K_0 = Coefficient of earth pressure at rest
σ_{vs},σ_{vB} = Effective overburden pressure of soil in center depth of cover soil and tunnel
H' = Thickness of cover soil
c_s, c_B = Cohesion of cover soil and tunnel side
ϕ_s = Angle of shear resistance of cover soil
H, B = Height and width of tunnel
ϕ_B = Angle of wall friction on tunnel side, where $\phi_B=2\phi/3$. (ϕ= internal friction angle of soil around tunnel)
u_s = Characteristic value of uplift pressure
γ_i, γ_f = Structure factor, action factor
f_{us}, f_{uW} = Ground resistance coefficient for uplift, where f_{us}= 0.3, f_{uw}= 0.9

4 FLOTATION CHECK BASED ON LTA E/GD/09/106/A2

Based on LTA, underground structures shall be checked for the possibility of flotation at all stages of the construction and throughout the service life of the structure. The calculation for flotation check based on LTA refers to Eqn. (7) and Eqn. (8). R/U must be at least 1.1.

$$U = \gamma_w h_t B \quad (7)$$

Where:

γ_w = Unit weight of water
h_t = Height of structure
B = Width of structure

$$R = \frac{\gamma' B(H-1,5)}{\gamma_{f1}} + \frac{(h_t+H-2)2S}{\gamma_{m1}} + \frac{W}{\gamma_{f2}} \quad (8)$$

Where :

γ' = Submerged weight of backfill material
S = Average shear resistance
W = Self weight of structure
H = Depth of backfill
B = Width of structure
γ_{f1} = Partial safety factor for weight of soil = 1.3
γ_{m1} = Partial safety factor for weight of structure = 1.1
γ_{f2} = Partial safety factor for shear resistance = 2.0

5 FLOTATION CHECK BASED ON EN 1997 – 1 EUROCODE 7

The calculation for flotation check based on Eurocode refers to Eqn. (9) and Eqn. (10).

$$V_{dst,d} \leq G_{stb;d} + R_d \quad (9)$$

$$V_{dst,d} = G_{dst;d} + Q_{dst;d} \quad (10)$$

Where :

$V_{dst;d}$ = Design value of the destabilising vertical action on a structure
$G_{dst;d}$ = Design value of the destabilising permanent actions for uplift verification
$G_{stb;d}$ = Design value of the stabilizing permanent vertical actions for uplift verification
R_d = Design value of the resistance to an action

$Q_{dst;d}$ = Design value of the destabilizing variable vertical actions for uplift verification.

Eurocode introduces partial factors on actions and partial factors for soil parameters and resistances. The factors can be seen in the Table 1 and Table 2.

Table 1. Partial Factors on Action.

Action	Symbol	Value
Permanent		
Unfavourable[a]	$\gamma_{G;dst}$	1.0
Favourable[b]	$\gamma_{G;stb}$	0.9
Variable		
Unfavourable[a]	$\gamma_{Q;dst}$	1.5

[a] Destabilising;
[b] Stabilising

Table 2. Partial Factors for Soil Parameter and Resistances.

Soil Parameter	Symbol	Value
Angle shearing resistance[a]	$\gamma_{\varphi'}$	1.25
Effective cohesion	$\gamma_{c'}$	1.25
Undrained shear strength	γ_{cu}	1.40
Tensile pile resistance	$\gamma_{s;i}$	1.40
Anchorage resistance	γ_a	1.40

[a] This factor applied to tan φ

6 COMPARISON

To exercise and compare the result of each code and standard, one example case of typical underground station cross section will be used. Please see Fig. 1 for the section.

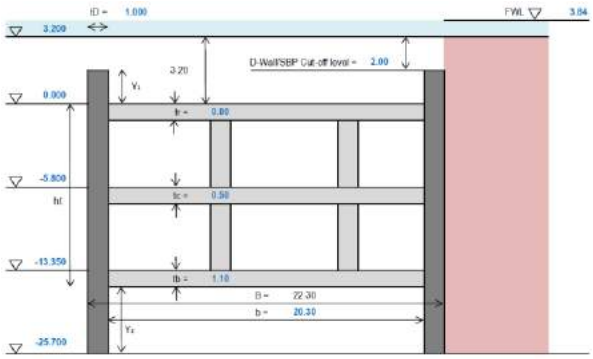

Fig. 1. Typical Underground Station Section.

The data that is used for this section can be seen below.

Ground level = +3.2 meters
Flood water level = +3.84 meters
Roof slab thickness, t_R = 0.8 meters
Concourse slab thickness, t_c = 0.5 meters
Base slab thickness, t_b = 1.1 meters
D-Wall thickness, t_D = 1.0 meters
Width of station box, b = 20.3 meters
Density of concrete, γ_c = 24.0 kN/m^3
Density of soil cover, γ_{soil} = 18.0 kN/m^3
Density of water, γ_w = 10.0 kN/m^3

For the geotechnical condition, the considered soil layer and parameter are shown in Fig. 2 and Table 3, respectively.

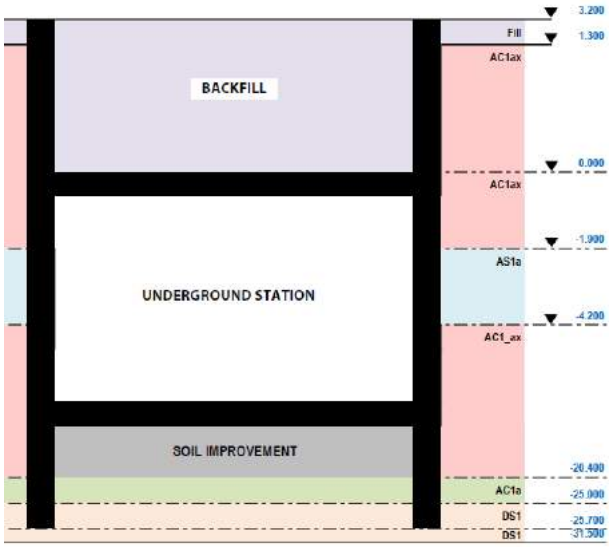

Fig. 2. Soil Elevation.

Table 3. Soil Properties.

Layer	Soil Type	γ kN/m^3	c' kN/m^2	Φ'	K_0
1	Fill	16.00	1	35	0.426
2	AC1ax	15.00	8	29	0.762
3	AS1a	15.00	0	30	0.500
4	AC1ax	15.00	8	29	0.647
5	AC1a	16.00	16	26	0.656
6	Backfill	18.00			
7	DS1	17.50	0	40	0.357

From the three codes, they have the same components, those are the self-weight, soil resistance, and uplift force. The structural self-weight is calculated from the cross-section. The structural self-weight consists of the slab, diaphragm walls, column, waterproofing, concrete finishing, and track. The formula used for calculating the self-weight can be seen in Eqn. (11).

$$W_{member} = b \times t \times \gamma \times pcs \quad (11)$$

The summary table for other members can be seen in Table 4.

Table 4. Member Self-weight.

No.	Member	Weight	
1)	Roof Slab	389,760	kN/m
2)	Concourse Slab	243,600	kN/m
3)	Base Slab	535,920	kN/m
4)	D-Wall	1329,600	kN/m
5)	Internal Column	38,400	kN/m
6)	Waterproofing	23,345	kN/m
7)	Conc. Finish slab (base)	21,505	kN/m
8)	Conc. Finish slab (conc)	43,010	kN/m
9)	Track	52,740	kN/m
	Total	2677,880	kN/m

The uplift force is calculated using the equation $U = (h_{stat}B + 2(h_{d\ wal\ l} - h_{stat})\ B_{d\ wall})\ \gamma_w$ (.

$$U = (h_{stat}B + 2(h_{d\ wal\ l} - h_{stat})\ B_{d\ wall})\ \gamma_w \quad (12)$$

$$U = (14.45\ \text{m} \times 20.3\ \text{m} + 2(27.7\ \text{m} - 14.45)1\ \text{m})10\frac{\text{kN}}{\text{m}^3}$$

$$U = 3198.35\frac{\text{kN}}{\text{m}}$$

6.1 *Floatation Check according to JSCE*

The first code that is used for comparison is JSCE. The other component for flotation check in JSCE is self-weight, the resistance of cover soil, friction drag on tunnel side, and uplift force.

For the structural self-weight, the value is calculated using Eqn. (13)$W_B = f_{uw}\ w_B$(.

$$W_B = f_{uw}\ w_B \quad (13)$$

$$W_B = 0.9 \times 2677.88\frac{\text{kN}}{\text{m}} = 2410.092\frac{\text{kN}}{\text{m}}$$

The other self-weight is the backfill located on the top of the structure. There are two types of soil height, those are 3.2 meters, that located on top of the roof slab, and 2 meters, that located on top of the diaphragm walls. The calculation is using Eqn. (4).

$$W_s = f_{uw} \sum(b_{soil} \times h_{soil} \times \gamma')$$

$$W_s = 0.9\left(\left(20.3\ m \times 3.2\ m \times 8\frac{kN}{m^3}\right) + \left(1\ m \times 2\ m \times 8\frac{kN}{m^3} \times 2\right)\right) = 496.512\frac{kN}{m}$$

The soil resistance on the tunnel side is calculated like in deep foundation, that is using the skin friction from the soil to the diaphragm walls. The calculation is using Eqn. (6)$Q_B = f_{us}\ H\ (c_B + K_0\ \sigma'_{vB}\ \tan\phi_B)$(.

Table 5. Skin Friction Based on JSCE.

No.	Soil Type	Q_B	
1)	Fill	0,569	kN/m
2)	AC1ax-1	12,659	kN/m
3)	AS1a	4,163	kN/m
4)	AC1ax-2	142,045	kN/m
5)	AC1a	59,856	kN/m
6)	DS1	5,652	kN/m
7)	Inner AC1ax-2	21,379	kN/m
8)	Inner AC1a	34,385	kN/m
9)	Inner DS1	2,258	kN/m
	Total	282,965	kN/m

The soil resistance from cover soil is calculated like in above calculation. The calculation is using Eqn. ($Q_s = f_{us}\ H'\ (c_s + K_0\ \sigma'_{vs}\ \tan\phi_s)$ ()$Q_s = f_{us}\ H'\ (c_s + K_0\ \sigma'_{vs}\ \tan\phi_s)$(.

$$Q_s = f_{us}\ H'(c_s + K_0\ \sigma'_{vs}\ tan\phi_s)$$

$$Q_s = 0.3 \times 1.2\ m \times (1\frac{kN}{m^2} + 0.426 \times 3.6\frac{kN}{m^2} \times tan(25°) = 0.75\frac{kN}{m}$$

The last component for flotation check in JSCE is the uplift force. Uplift force is calculated with Eqn. (7).

$$U_s = \gamma_f u_s\ B$$

$$U_s = \gamma_f U$$

$$U_s = 1 \times 3198.35\frac{kN}{m} = 3198.35\frac{kN}{m}$$

For flotation check based on JSCE, the structure is calculated using Eqn. (1)$\gamma_i \frac{U_s}{W_s+W_B+2Q_s+2Q_B} \leq 1.0 \gamma_i \frac{U_s}{W_s+W_B+2Q_s+2Q_B} \leq 1.0$.

$$\gamma_i \frac{U_s}{W_s+W_B+2Q_2+2Q_B} \leq 1.0$$

$$1\frac{3198.35\frac{\text{kN}}{\text{m}}}{496.512\frac{\text{kN}}{\text{m}}+2410.092\frac{\text{kN}}{\text{m}}+2\times0.75\frac{\text{kN}}{\text{m}}+2\times282.965\frac{\text{kN}}{\text{m}}} \leq 1.0$$

0.921≤1.0 (OK)

6.2 *Floatation Check according to LTA*

The second code is compared is from LTA Singapore. The shear resistance calculation is like in JSCE's calculation, but the shear resistance of 2 meters from the ground level is ignored and the weight of soil calculation is the same as in JSCE but the soil weight from 1.5 meters from ground level is ignored, LTA (2019). The resistance calculation is calculated using Eqn. (8).

$$R = \frac{\gamma' B(H-1.5)}{\gamma_{f1}} + \frac{(h_t+H-2)2S}{\gamma_{m1}} + \frac{W}{\gamma_{f2}}$$

$$R = \frac{20.3\ m \times 1.7\ m \times 8\frac{kN}{m^3}}{1.3} + \frac{2\times 940.208\ \frac{kN}{m}}{2} + \frac{2677.88\ \frac{kN}{m}}{1.1}$$

$$R = 3587.014\ \frac{kN}{m}$$

For the uplift calculation, the calculation is calculated with equation $U = \gamma_w\ h_t\ B$.

$$U = \gamma_w\ h_t\ B$$

$$U = 3198.35\ \frac{kN}{m}$$

For flotation check based on LTA, it is based on ratio from R/U with at least 11 to fulfill the requirement.

$$\frac{R}{U} = \frac{3587.014\frac{kN}{m}}{3198.35\frac{kN}{m}} = 1.122 < 1.1\ (OK)$$

6.3 *Floatation Check according to Eurocode*

The last code that to be compared is Eurocode. There are three components in Eurocode's flotation check, the first one is $V_{dst,d}$, the design of destabilizing vertical actions on the structure. On this case, the destabilizing vertical action is uplift force. The second component is $G_{stb;d}$, the design of stabilizing vertical actions on the structure. For this case, the stabilizing vertical actions are the self-weight of the structure and the weight of soil above the station. The last component is R_d, the design of the resistance to action. The calculation for $V_{dst;d}$ and $G_{stb;d}$ are using the calculation from the previous calculation with the factor from Eurocode.

$$V_{dst;d} = \gamma_{G;dst} U = 1 \times 3198.35\frac{kN}{m} = 3198.35\frac{kN}{m}$$

$$G_{stb;d} = \gamma_{G;stb}(W_{str}+W_{soil})$$

$$G_{stb;d} = 0.9 \times \left(2677.88\frac{kN}{m} + 551.68\frac{kN}{m}\right)$$

$$= 2906.604\frac{kN}{m}$$

The calculation for R_d is like the calculation from the previous code but there are factors that are used for cohesion and angle resistance parameters. For the factor, please see Table 2.

The calculation only showed for AC1ax-1.

$$R_d = \sum\left(H\left(\frac{c_B}{\gamma_c'} + \frac{K_0\ \sigma'_{vB}\ tan\phi_B}{\gamma'_\varphi}\right)\right)$$

$$R_{d\text{-}AC1ax\text{-}1} = 0.7\ m \times \left(\frac{8\frac{kN}{m}}{1.25} + 0.762 \times 19.4\frac{kN}{m^2} \times \frac{tan(\frac{2}{3}\times 29°)}{1.25}\right)$$

$$R_{d\text{-}AC1ax\text{-}1} = 33.757\frac{kN}{m}$$

The

Table

No.	Soil	R_d	
1)	Fill	1,517	kN/m
2)	AC1ax-	33,757	kN/m
3)	AS1a	11,100	kN/m
4)	AC1ax-	378,786	kN/m
5)	AC1a	159,615	kN/m
6)	DS1	15,073	kN/m
7)	Inner	57,009	kN/m
8)	Inner	91,692	kN/m
9)	Inner	6,022	kN/m
	Total	754,573	kN/m

After getting the three components, the flotation check is calculated with Eqn. ($V_{dst,d} \leq G_{stb;d} + R_d$).

$$V_{dst,d} \leq G_{stb;d} + R_d$$

$$3198.35\frac{kN}{m} \leq 2906.604\frac{kN}{m} + 754.573\frac{kN}{m}$$

$$3198.35\frac{kN}{m} \leq 3661.177\frac{kN}{m}\ (OK)$$

Based on the above results, the comparison is shown in U/C ratio for comparison as follows.

JSCE : 0.921
LTA : (1/1.122)/(1/1.1) = 0.980

Eurocode : 3198.35/3661.177 = 0.874

7 CONCLUSION

The components of flotation check from the three code and standards are the same with different multiplication factor for each components. The summary from each codes is in Table 7.

Table 7. Code's Factor Summary.

Code	Self-weight		Soil Resist-ance	Shear Resist-ance Angle	U/C
	Struc-ture	Soil			
JSCE	90%	90%	30%	-	92%
LTA	91%	77%[a]	50%[b]	-	98%
Euro-code	90%	90%	80%	80%	87%

[a]Top 1.5 meter soil is ignored

[b]Top 2 meter soil is ignored

The result of floatation check on the sample case show that LTA calculation is more conservative that JSCE and Eurocode, respectively.

REFERENCES

Building and Construction Standards Committee. 2010. *SS EN 1997 - 1 : 2010 - Eurocode 7 - Geotechnical Design - General Rules*. Singapore: Spring Singapore.

Frank, R. 2004. *Designers' guide to EN 1997-1 Eurocode 7: Geotechnical Design-General Rules* Vol. 17. Thomas Telford.

Japan Society of Civil Engineers (JSCE). 2018. *Standard Specifications for Tunneling – 2016 : Cut-and-Cover Tunnels*.

Land Transport Authority (LTA). 2019. *E/GD/09/106/A2 - Civil Design Criteria for Road and Rail Transit Systems*.

Glass Fiber Reinforced Polymer as Temporary Replacement for D-Wall Steel Reinforcement

Christopher Gilbert
Design Engineer – Shimizu Adhi Karya Joint Venture

Jakarta CP201 merupakan bagian dari proyek konstruksi MRT Jakarta Fase 2 yang terdiri dari pembangunan dua stasiun dan terowongan bawah tanah. Demi menunjang pengeboran tanah, diperlukan struktur khusus dalam stasiun sebagai *launching* dan *arriving shaft Tunnel Boring Machine (TBM).* Elemen struktur dari Launching Shaft adalah dinding diafragma beton bertulang. Perkuatan tulangan pada dinding diafragma yang akan dilewati oleh TBM memerlukan perkuatan khusus untuk memudahkan proses pengeboran beton bertulang. Selain menyesuaikan mutu beton, *Glass Fiber Reinforced Polymer (GFRP) juga dapat dimanfaatkan* sebagai pengganti sementara tulangan baja. Makalah ini secara garis besar membahas mengenai prosedur desain beton bertulang dinding diafragma dengan material (*GFRP*) beserta detail penulangan yang perlu diperhatikan.

Kata Kunci: dinding diafragma, Glass Fiber Reinforced Polymer

ABSTRACT: Jakarta CP201 is part of the second phase of Jakarta MRT Project that shall execute the design and constructionof two underground stations & bored tunnels. Within the soil boring procedures, a particular structure within the station is required to initiate the operation of tunnel boring machine, commonly known as the TBM Launching & Arriving Shaft. One of the structural elements of this launching shaft consist of reinforced concrete diaphragm wall. As a result, the D-Wall that is to be demolished by the TBM must be specially reinforced so that it enhances the constructability of concrete penetration. Other than adjusting the concrete grade, Glass Fiber Reinforced Polymer (GFRP*)* can also be utilized as a temporary replacement of steel reinforcement. Overall, the following paper covers the design procedure of D-Wall Reinforcement by GFRP as well as the reinforcement details required by the code.

Keywords: diaphragm wall, *Glass Fiber Reinforced Polymer*

1 INTRODUCTION

Jakarta CP201 MRT Project oversees the design & construction of two underground stations as well as bored tunnels. Within the south & north side of the station layout, TBM Shafts have been designed to accommodate the erection works, launching and arrival of Tunnel Boring Machine.

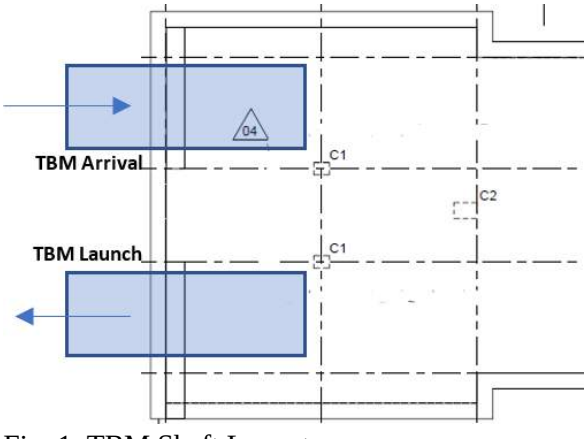

Fig. 1. TBM Shaft Layout.

The shaft itself consists of reinforced concrete diaphragm walls, which will eventually be penetrated by TBM during launching and arrival, as indicated in Fig. 1. Therefore, in order to ensure the penetration of concrete, a special reinforcement is provided within the tunnel eye by using GFRP.

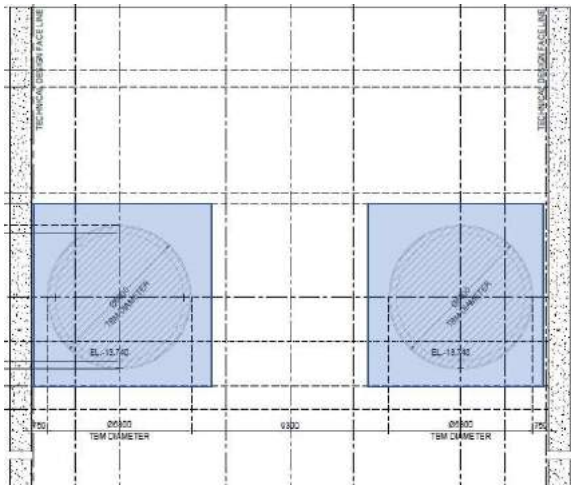

Fig. 2. GFRP Reinforcement within Tunnel Eye.

2 MATERIAL CHARACTERISTIC

2.1 *Tensile Strength & Ductility*

When loaded in tension, FRP bars exhibit no plastic behavior (yielding) before rupture. Unlike steel reinforced concrete sections, which are commonly designed to ensure a tension-controlled behavior by yielding of steel before crushing of concrete, FRP reinforcement can't provide the same level of ductility and warning of failure of the member. If FRP reinforcement ruptures, failure of the member is sudden and catastrophic.

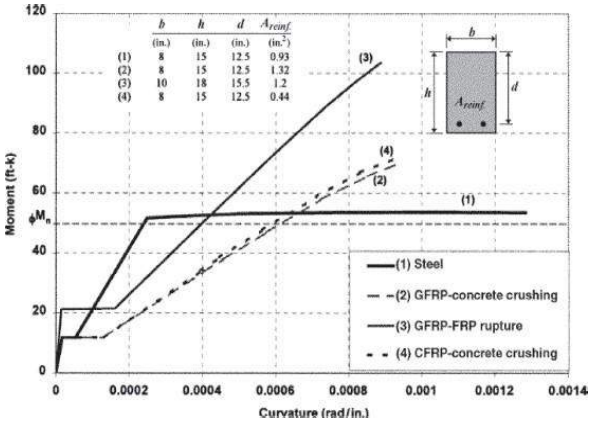

Fig. 3. Moment – Curvature Relationships.

2.2 *Compression Strength*

FRP reinforcement has a significantly lower compressive strength than tensile strength. Therefore, the strength of any FRP bar in compression should be ignored in design calculations.

2.3 *Design Properties*

Long-term exposure to various types of environments can reduce the tensile strength of FRP bars. Therefore, the material properties provided by the manufacturer should be considered as initial properties that hasn't included this exposure effect. The design tensile strength and rupture strain shall be determined by Eqn. (1) & (2) respectively.

$$f_{fu} = C_E f_{fu^*} \quad (1)$$

$$\varepsilon_{fu} = C_E \varepsilon_{fu^*} \quad (2)$$

However, since the application of GFRP withinthis project is temporary, such long-term effect may be ignored. The design material propertiesprovided by the manufacturer are as follows:

Table 1. Material Properties.

GFRP			Concrete		
Ø (mm)	f_{fu} (MPa)	E_f (GPa)	f_c (MPa)	E_c (MPa	ε_{cu}
20	1000	58			
45	800	58	30	$4700\sqrt{fc'}$	0.003
50	800	58			

2 DESIGN PROCEDURES

All design procedures refer to ACI 440.1R-15.

3.1 *Flexural Design*

Since FRP reinforcement bar is considered non-ductile compared to steel, compression-controlled behavior is marginally more desirable for the flexural design. The nominal flexural capacity shall be determined based on strain compatibility, internal force equilibrium, and the controlling limit state.

3.1.1 *Determination of Design Forces*

The D-Wall bending moment is determined based on 2D finite element analysis in PLAXIS that simulates the excavation phases during temporary stage. After multiplying the forces with a certain load factor, the design bending moment are summarized in Table 2.

Table 2. Design Bending Moment.

Elevation (m)	Location	M_u (kN.m/m)
-6.8 to -8	External	1482.1
	Internal	976.1
-8 to -11	External	0.0
	Internal	1947.1
-11 to 14.6	External	0.0
	Internal	1555.1

3.1.2 *Determination of Section Parameters*

Several section parameters that will be required within the design calculation are summarized in Table 3.

Table 3. Section Parameters.

Width (mm)	7800
Depth (mm)	950
Cover (mm)	50
β_1	$0.85 - 0.005 \frac{fc'-28}{7}$

3.1.3 *Determination of Failure Control*

If the reinforcement ratio is less than the balanced ratio (ρf < ρfb), the FRP rupture limit state controls. Otherwise, the concrete crushing limit state controls.

$$\rho_{fb} = 0.85\,\beta_1 \frac{fc^F}{f_{fu}} \frac{E_f S_{cu}}{E_f S_{cu} + f_{fu}} \quad (3)$$

If the design adopts 49D50 for the main vertical rebar and D20 for the horizontal rebar, then the controlling limit state shall be compression controlled, as summarized in Table 4.

3.1.4 Determination of Strain Compatibility

The strain compatibility shall be achieved by using a linear strain distribution curve in which the concrete ultimate strain is set at 0.003.

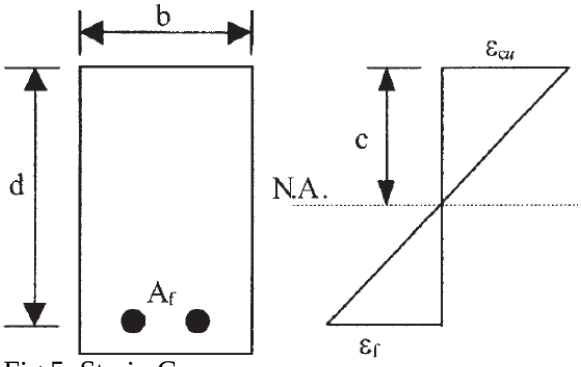

Fig 5. Strain Curve.

Table 4. Controlling Limit State.

Elevation	Location	Provided Reinforcement		Af design	Af bar	Failure Control
		Number n1	Diameter D1 (mm)			
6.8 – 8	Soil	49	50	96211	31736	Compression
	Excavation	49	50	96211	31736	Compression
8 – 11	Soil	49	50	96211	31736	Compression
	Excavation	49	50	96211	31736	Compression
11 – 14.6	Soil	49	50	96211	31736	Compression
	Excavation	49	50	96211	31736	Compression

Table 5. Calculate Rebar Strain.

Elevation	Location	Provided Reinforcement		Effective Depth	Rebar Strain
		Number n1	Diameter D1 (mm)	d (mm)	εf 1
6.8 – 8	Soil	49	50	855	0.0074
	Excavation	49	50	855	0.0074
8 – 11	Soil	49	50	855	0.0074
	Excavation	49	50	855	0.0074
11 – 14.6	Soil	49	50	855	0.0074
	Excavation	49	50	855	0.0074

Therefore, the rebar strain (εf) may be calculated with Eqn. (4).

$$\varepsilon = 0.003\ x\ \frac{d-c}{c} \quad (4)$$

The distance of neutral axis (c) is determined by iteration in Microsoft Excel. The results of rebar strain is summarized in Table 5.

3.1.5 *Detemination of Force Equilibrium*

Force equilibrium between concrete compression and rebar tensile force is achieved by iterating the neutral axis depth in Microsoft Excel. The results of are summarized in Table 6.

The concrete compression and the rebar tensile force are determined based on Eqn. (5) & (6) respectively.

$$C_c = 0.85 f c' (\beta_1\ c) b \quad (5)$$

$$T_f = A_f E_f \varepsilon_f \quad (6)$$

3.1.6 *Detemination of Moment Capacity*

The nominal moment capacity may be determined by Eqn. (7).

$$\Phi M_n = T_f \frac{(d-\beta_1 c)}{2} \quad (7)$$

Since FRP members do not exhibit a ductile behavior, a more conservative value of strength reduction factor (∅) shall be adopted based on Eqn. (8).

$$0.55\ for\ \rho_f \leq \rho_{fb}$$

$$\Phi = 0.3 + 0.25 \frac{\rho_f}{\rho_{fb}} \quad \text{for } \rho_{fb} \leq \rho_f \leq 1.4\ \rho_{fb} \quad (8)$$

$$0.65\ for\ \rho_f \geq 1.4\ \rho_{fb}$$

The results which are summarized in Table 7, indicate that the moment capacity have satisfied the temporary stage bending moment.

Table 6. Neutral Axis Depth & Force Equilibrium.

Elevation	Location	N.A	β1	Force Equilibrium		
		mm		Cc	Tf1	ΣF
				kN	kN	kN
6.8 – 8	Soil	247.4	0.84	41120	41120	0
	Excavation	247.4	0.84	41120	41120	0
8 – 11	Soil	247.4	0.84	41120	41120	0
	Excavation	247.4	0.84	41120	41120	0
11 – 14.6	Soil	247.4	0.84	41120	41120	0
	Excavation	247.4	0.84	41120	41120	0

Table 7. Flexural Capacity.

Elevation	Location	Mu	φ	φMn	Check
		kN.m/m		kN.m/m	
6.8 – 8	Soil	1482.1	0.65	2575.6	OK
	Excavation	976.1	0.65	2575.6	OK
8 – 11	Soil	0.0	0.65	2575.6	OK
	Excavation	1947.1	0.65	2575.6	OK
11 – 14.6	Soil	0.0	0.65	2575.6	OK
	Excavation	1555.1	0.65	2575.6	OK

3.2 *Shear Design*

The vertical shear force along the D-Wall is determined based on 2D finite element analysis in PLAXIS. After multiplying the forces with a certain load factor, the design shear force are summarized in Table 8.

Table 8. Design Shear Force.

Elevation (m)	Vu (kN/m)
-6.8 to -8	9051.9
-8 to -11	2131
-11 to -14.6	6207.9

3.2.2 *Concrete Shear Capacity*

Compared to steel reinforced concrete, a cross section using FRP reinforcement provides a lower axial stiffness due to much lowermodulus of elasticity. As a result, the generated shear resistance is smaller. Therefore, the formulation of concrete shear capacity is modified by parameter k, which accounts for the axial stiffness of FRP longitudinal reinforcement.

$$V_c = 0.4\sqrt{fc'}\, b_w(kd) \quad (9)$$

Value of k may be determined by equation 10, in which n_f represents the ratio of Ef / Ec.

$$k = \sqrt{2\rho_f n_f + (\rho_f n_f)^2} - \rho_f n_f \quad (10)$$

The results of concrete shear capacity is summarized in Table 9.

Table 9. Concrete Shear Capacity.

Elevation (m)	Af (mm^2)	ρf	k	Vc kN
-6.8 to -8	96211	0.014	0.225	3280.6
-8 to -11	96211	0.014	0.225	3280.6
-11 to -14.6	96211	0.014	0.225	3280.6

3.2.3 *Shear Capacity of FRP Stirrups*

The shear resistance provided by the FRP stirrups can be determined by Eqn. (11).

$$\text{Vf (provided)} = \frac{A_{fv} f_{fv} d}{s} \quad (11)$$

In order to maintain shear integrity of the concrete and avoid failure at the bent portion of the FRP stirrup, the stress level (f_{fv}) within the FRP shear rebar shall be limited by Eqn. (12).

$$f_{fv} = 0.004E_f \le f_{fb} \quad (12)$$

f_{fb} represents the tensile stress that occurs within the bent portion of the FRP stirrup. It may be determined by Eqn. (13).

$$f_{fb} = \left(0.05\frac{r_b}{d_b} + 0.3\right) f_{fu} \quad (13)$$

The required shear capacity of FRP stirrups to resist the remaining shear force after considering the concrete shear capacity, may bedetermined by Eqn. (14). The value of V_f shall be limited by Eqn. (15) which represents the maximum shear reinforcement in ACI 318.

$$v_{frequired} = \frac{Vu}{\Phi} - Vc \quad (14)$$

$$V_{fmax} = \frac{2}{3}\sqrt{fc'}\, b_w d \quad (15)$$

Table 10. Required Shear Capacity by FRP Stirrup.

Elevation (m)	Vc kN	Ffv MPa	Vf req kN	Vf max kN
-6.8 to -8	3281	232	8789	24352
-8 to -11	3281	232	-439	24352
-11 to -14.6	3281	232	4997	24352

Based on Eqn. (11) & (14), the results of required and final design spacing are summarized in Table 11.

Table 11. Required and Final Design Spacing.

Elevation	Provided Shear Rebar			S required	S design
(m)	n	D (mm)	Av (mm^2)	mm	mm
-6.8 to -8	25	20	7854	177	150
-8 to -11	25	20	7854	-3547	300
-11 to -14.6	25	20	7854	312	250

3.3 *Reinforcement Details*

3.3.1 *Lap Splices*

This refers to the lap splice of GFRP with the steel rebar beyond the tunnel eye. Several manufacturers might allow using the splice length of steel rebar, based on lab test results of bond-dependent coefficient (k_b). ACI 440.1R-06 states that k_b is a coefficient that accounts for the degree of bond between FRP bar and the surrounding concrete. For FRP bars having bond behavior similar to uncoated steel bars, Kb is assumed equal to 1.

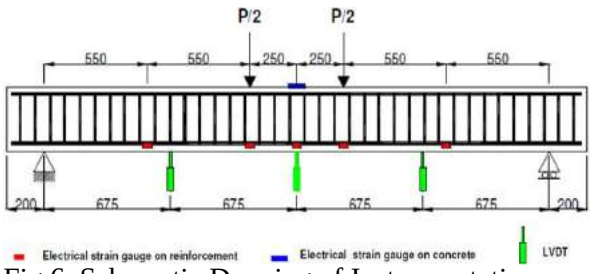

Fig 6. Schematic Drawing of Instrumentation.

The test procedure simply involves vertical loading of a simply supported FRP reinforced concrete beam, to observe the generated crack width and rebar strain until beam failure. Strain gauges may be used to measure the tensilestrain within the GFRP rebar while LVDT may be installed to measure the crack widths. By using equation 16, which refers to ACI 440.1R-06, section 8.3.1, the bond coefficient (k_b) is then determined based on the measured crack width (w) and rebar strain (ε_f) during testing, while all other variables are known.

$$w = 2\varepsilon_f \beta x k_b x \sqrt{(d_c)^2 + \frac{s^2}{2}} \quad (16)$$

If the test results indicate that the overall average value of kb is relatively close to 1, concluded that the FRP rebar has a similar bond behavior to steel and may adopt the steel splice length.

However, within this project, a more conservative approach is selected to determine the development length by using Eqn. (17), based on ACI 440.1R-15, Section 10.3.

$$l_d = \frac{\alpha \frac{f_{fr}}{0.083\sqrt{fcF}} - 340}{13.6 + \frac{c}{d_b}} d_b \quad (17)$$

The value of C is the lesser of the cover to rebarcenter or half of the rebar c/c spacing. f_{fr} refersto the stress within the GFRP rebar. Based on the rebar strain (ε_f) calculated in Table 5, f_{fr} can be determined by using Eqn. (18).

$$f_{fr} = E_f \times \varepsilon_f \leq f_{fu} \quad (18)$$

The result of GFRP development length is summarized in Table 13. The lap splice (l_{st}) is then determined by taking the maximum between Ld of GFRP and Lst of the steel rebar, based on SNI 2847-2019, Section 25.5.2.2. The result is summarized in Table 14.

Table 12. GFRP Development Length.

d_b	C	εf	Ffr	Ld	Ld final
mm	mm		MPa	mm	mm
50	75	0.0074	427.4	1987	2000

Table 13. Splice Length of GFRP & Steel.

	GFRV	Steel
d_b (mm)	50	40
Ld (mm)	2000	
Lst (mm)		1900
Lst final	2000	

3.3.2 Detail of Strrups

The maximum spacing of vertical steel stirrups given in ACI 318 as the smaller of d/2 or 600 mm may be used for vertical FRP shear reinforcement.

Table 14. Stirrup Maximum Spacing.

Elevation	S_{design}	S_{max}
(m)	(mm)	(mm)
-6.8 to -8	150	427.5
-8 to -11	300	427.5
-11 to -14.6	250	427.5

Furthermore, FRP stirrups should be closed with 90-degree hooks, with a minimum tail length of $12d_b$.

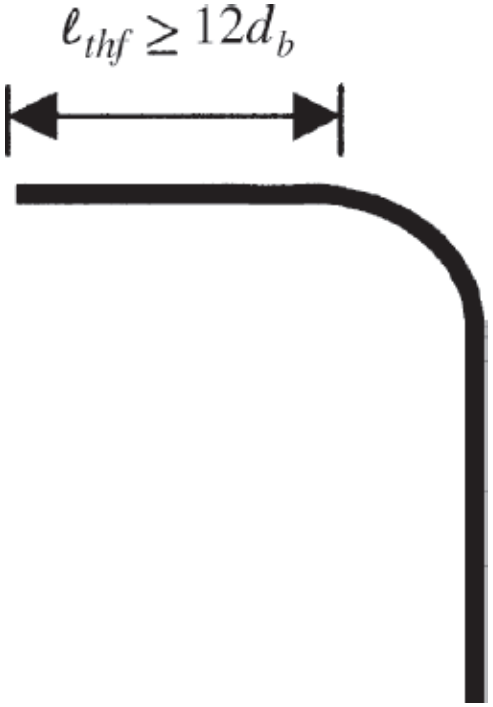

Fig 7. Required Tail Length for FRP Stirrups.

4 CLOSING REMARKS

For temporary works purposes, Glass Fibre Reinforced Polymer may be considered a viable alternative to replace steel reinforcement within the structural design of diaphragm wall. This is necessary to enable the penetration of concrete by Tunnel Boring Machine. However, in terms of permanent design, it is more reliable to adopt steel reinforcement rather than GFRP due to its brittle behavior.

REFERENCES

American Concrete Institute (ACI) 440.1R-15. 2015. *Guide for the Design and Construction of Structural Concrete Reinforced with Fiber – Reinforced Polymer (FRP) Bars*. Michigan : American Concrete Insititute.

Benmokrane et al. 2012. *Certification of FiReP Glass Fibre-Reinforced Polymer (GFRP) Rebars in Concrete: Bond – Dependent Coefficient (kb) of GFRP Bar*s: 1-27.

Dewatering on Tunnel Excavation Work Near Vulnerable Historical Building

Jefry Rory Paath
PT Tarumanegara Bumiyasa

Ihsan Riza
PT Tarumanegara Bumiyasa

Jo Lian Huat
PT Tarumanegara Bumiyasa

ABSTRACT: Dewatering in excavation work that is between buildings which have a high risk of damage, such as buildings with shallow foundations or very old buildings where the condition of the structure is possible to weaken. The design of dewatering plans and monitoring of work in the field are very important. This is to determine the seepage of water that enters the excavation, groundwater level subsidence, settlement risk, and the radius of the pumping effect. From this analysis, an early warning system will be created as a tolerance guideline during monitoring work for excavation and dewatering activities. From the results of the analysis, it was found that the seepage of water entering the excavation was 30 – 35 m^3/day, the decrease in groundwater level outside the excavation was 0.5 – 1.0 m, the land subsidence was 1.0 – 2.3 cm. Compared to the results of factual monitoring in the field, some monitoring results give a value greater than the specified tolerance. Several measures were taken to prevent damage to surrounding buildings so as not to cause damage to buildings around the excavation.

Keywords: dewatering, high risk building, early warning system

1 INTRODUCTION

For excavation work, where the elevation of the deepest excavation is below the groundwater level (GWL), it will definitely interfere with the structural work in the excavation. Dewatering work is one of the efforts that will be made to overcome these problems.

Besides being able to support an excavation work, this dewatering work can also pose a risk of a disadvantage to buildings around the excavation in the form of a decrease in the groundwater level outside the excavation where this thing can result in a ground level decrease in the building structure around the radius of the dewatering effect. Especially the excavation and dewatering work that is close to historical buildings which are a cultural heritages that are more than 50 years old and considered structurally to have experienced some weakness and also buildings that only use shallow foundations.

Through this paper, we will provide information regarding the implementation of dewatering work in tunnel excavation carried out near one of the cultural heritage buildings which are known based on information that this building uses shallow foundations. Fig. 1 is given the position illustration of the tunnel work and the historical building which is only about 28 meter.

Fig. 1. Tunnel and Historical Building Position, Source: Google Earth.

2 PROJECT DESCRIPTION

This tunnel will function as a pedestrian tunnel for visitor's access from the basement parking to the location of the cultural heritage building. This excavation work will be carried out using an open excavation method using diaphragm wall as a retaining wall with a 14.5 meter depth which will cut through one of the roads in Central Jakarta. The excavated area is about 433 m^2 with an average excavation depth of 7 meters where the tunnel excavation plan and the diaphragm wall plan are shown in Fig. 2 and the tunnel cross sections can be seen in Fig. 3.

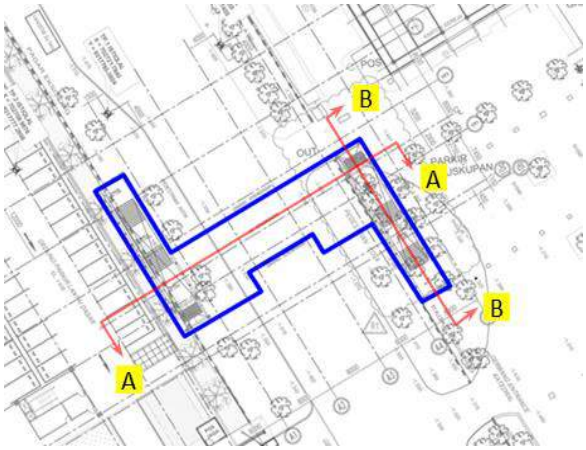

Fig. 2. Tunnel Excavation Plan & Diaphragm Wall Plan.

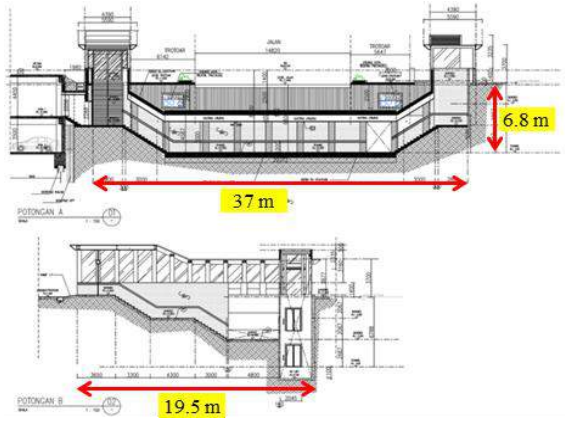

Fig. 3. Tunnel Cross Section, Architectural.

3 SOIL CONDITION OVERVIEW

At the project site, several soil tests were carried out in the form of sondir, deep drilling tests accompanied by standard penetration tests and sampling for laboratory tests. The position plan of the soil investigation test point can be seen in Fig. 4.

From Fig. 5 can be seen that the soil layers at the project site are very diverse, there are sand layers between the clay or silt layers. The depth of the hard soil layer from the results of deep drilling and also CPT was found at a depth of 10.0 meters in the form of a layer of dense sand. The impermeable layer was found from the surface to a depth of 10.0 meters and then the permeable layer was found at a depth of up to 14.0 meters. The next layer to a depth of 16.0 meters contains a layer of clay or silt. The next layer to a depth of 23.0 meters is a layer of sand. The next layer to a depth of 25.0 meters is a layer of clay or silt. The next layer to a depth of 34 meters consists of a layer of sand.

In addition to the above tests, a pumping test was also carried out to determine the hydraulic parameters. The pumping test results can be seen in Table 1 below.

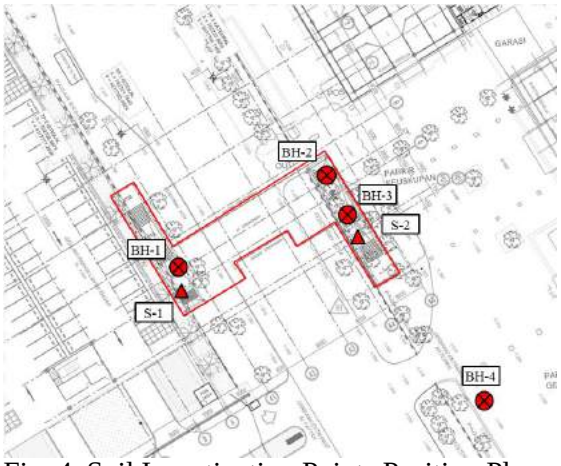

Fig. 4. Soil Investigation Points Position Plan.

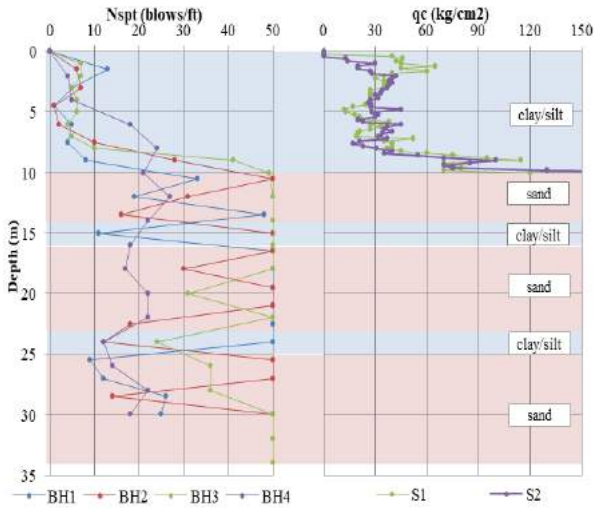

Fig. 5. Deep Drilling and CPT Results.

Table 1. Pumping Test Results.

No.	Hydraulic Parameter	Result
1	Pumping Discharge	302.40 m^3/day
2	Transmissibility (T)	97.275 m^2/day
3	Specific Yield (Cs)	69.35 m^3/day/m
4	Storage Coefficient (S)	2.01 x 10^{-2}
5	Influence Radius	> 50 m
6	Permeability, k	6.75 x 10^{-3} cm/sec

4 DEWATERING ANALYSIS

To support the excavation work, dewatering work is needed to help lowering the groundwater level when excavation work is carried out. To find out the total amount of flow that will enter the excavation and also to determine the decrease in groundwater level that will occur outside the excavation.

The analysis of this dewatering was carried out using the help of the Plaxis 8.6 program. Modeling of soil, soil layers, and retaining walls is presented in Fig. 6. In this program, the initial and final groundwater level to be achieved in the excavation are modeled, then pump modeling with a predetermined capacity is also carried out using the trial error method until the groundwater level is obtained as shown in Fig. 7.

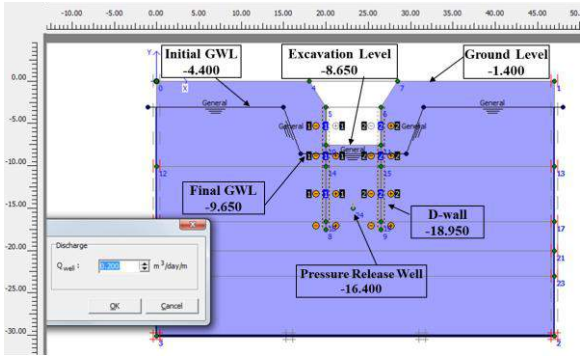

Fig. 6. Groundwater Level and Pump Modeling.

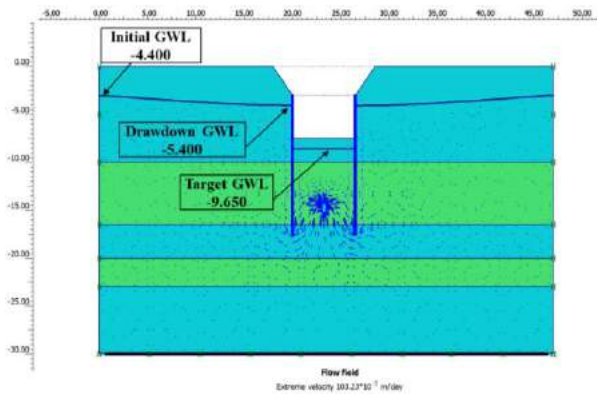

Fig. 7. Program Analysis Result for Excavation.

From the results of the program analysis, it can be seen that with a pumping capacity of 0.2 m^3/day/m can lowered groundwater level to 1 meter below the planned deepest excavation elevation. The decrease in groundwater level outside the excavation that will occur is 1 meter, from a depth of -4.400 meters to -5.400 meters. From these results, an analysis is then carried out to determine the risk of land subsidence due to a decrease in groundwater level using the equation :

$$s = \Delta H = \frac{H_{0} \cdot \Delta\sigma}{E} \quad (1)$$

Based on Hooke's law, Eqn. (1) is derived to determine the subsidence of the soil surface (ΔH) due to changes in the effective soil stress ($\Delta\sigma$). From the consolidation test results obtained soil modulus (E) is 3477.5 kPa. Then with Eqn. (1) above, it is obtained that the value of land subsidence is 1.0-2.3 cm.

5 DEWATERING METHOD

The dewatering work on this tunnel excavation was carried out with the aim of lowering the groundwater level at a depth of 3.00 meters (elevation -4.400) to 1.00 meter below the elevation of the deepest excavation at -9.650. The dewatering method that used is a passive dewatering, it is carry out by installing a pressure release well which functions as a guide to the flow of water from the ground, which then collects groundwater into a sump-pit. Inside the sump-pit is installed 2 units of surface pump with a pump capacity of 50-100 liters/minute each. On side of the the high-risk building, a recharging well is installed as an effort to restore the groundwater level around the excavation which has fallen due to dewatering in the excavated area. The recharging well is made of 3 points of 6" PVC pipe, with a wellbore diameter of about 10" with a depth of 15 meters. The plan of the dewatering points can be seen in Fig. 8.

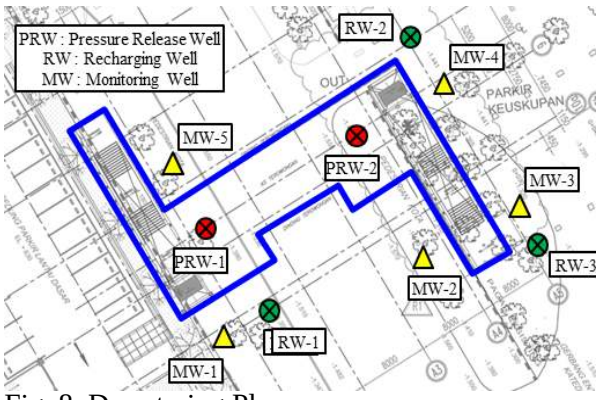

Fig. 8. Dewatering Plan.

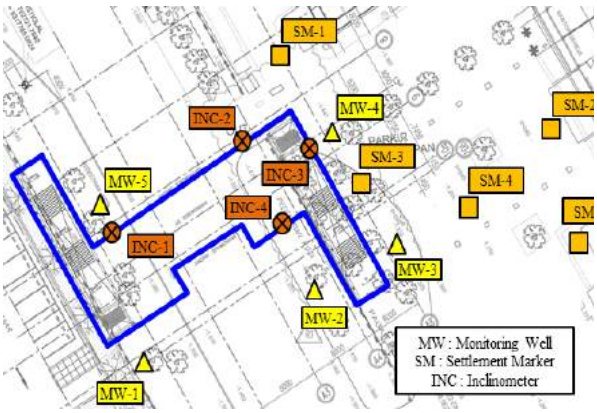

Fig. 9. Monitoring Points Plan.

6 DEWATERING AND EXCAVATION MONITORING PROGRAM

Groundwater level measurements were carried out using a water standpipe with a diameter of 2" of PVC casing which was measured with a diameter. Observation of the deflection on the retaining wall was carried out with an inclinometer measuring instrument (in addition to the inclinometer point, monitoring was also carried out on the capping beam to determine changes in position using a deflection marker). Land subsidence was measured with a conventional settlement marker using a total station. Cultural heritage buildings are also monitored in the form of measuring the verticality of cultural heritage buildings using a total station as a measuring instrument. Table 2 describes the monitoring readings for each instrumentation and Fig. 9 provides an overview of the position of the monitoring point.

Table 2. Frequency of Dewatering & Excavation Monitoring.

Monitoring Program	Frequency	Day – (In a Week) 1	2	3	4	5	6	7
Monitoring Well	Everyday	■	■	■	■	■	■	■
Inclinometer	3x/Week		■		■		■	
Deflection Marker	2x/Week			■			■	
Settlement Marker	4x/Week	■		■		■		■
Building Verticality	3x/Week		■		■		■	

Note: Monitoring is stared before the excavation work begins until the tunnel structure work finished

7 EARLY WARNING SYSTEM (EWS)

In monitoring work, it is very important to know the maximum tolerance limits. The maximum limit becomes a reference value to determine what actions will be taken when the maximum limit is reached. This is called an early warning system (EWS) that provides warnings to ensure that all work can still be carried out safely for stabilization of excavations and buildings around construction activities.

The maximum reference value is divided into several percentages. The percentage distribution before reaching 100% is at 50% and 75% of the maximum value. The percentage of achievement of this maximum value becomes a reference for the actions to be taken (contingency plan). The maximum value of this tolerance limit is obtained from the results of planning and also some references from books and standards commonly used in excavation planning or dewatering. An explanation of the early warning system and contingency plan implemented in this project can be seen in Table 3.

8 MONITORING RESULTS AND EVALUATION

Monitoring is carried out based on the planned frequency and carried out from the beginning of the work before excavation until the work is completed. In the process, there were several problems when the groundwater level and inclinometer measurements were carried out.

In monitoring wells around the cultural heritage buildings, namely at MW3 and MW4

there is a significant decrease in the groundwater level from March 13, 2021 to March 25, 2021 and continues until June 20, 2021. From these results, it can be seen that MW3 initial groundwater level is at an elevation of -2.60 m and the deepest groundwater level is at -3.80 m while at MW4, the initial groundwater level is at an elevation of -2.80 m and the deepest groundwater level is at an elevation of -3.80 m. Groundwater level fluctuations at MW 3 and MW4 can be seen in Fig. 11. On average, the drawdowns that occur are around 1.00 meters and 1.20 meters, where this measurement has passed the maximum value specified in the early warning system. Then the action is carried out in accordance with the contingency plan that was planned at the beginning, by adding a recharging well as can be seen in Fig. 10 and filling the wells with a larger discharge.

Table 3. Early Warning System and Contingency Plan.

Type of Monitoring	Excavation Stage	Maximum Value Reference	Maximum Value	Contingency Plan
Groundwater Level (GWL)	Stage 1 Depth 2.90 meter Stage 2 Depth 5.50 meter Stage 3 Depth 7.15 meter	Based on the analysis, the maximum groundwater level drawdown is 1 m	GWL Drawdown 1 meter (100%) 50% = 0.50 meter 75% = 0.75 meter	Increase Recharging Well Point Increase Discharge Water to Recharging Well
Inclinometer & Deflection Marker	Stage 1 Depth 2.90 meter	SNI 8460 : 2017 (0.5% from the depth of excavation)	50% Maximum 7.250 mm	Stop the Excavation work Increase Inclinometer Reading Frequency
			75% Maximum 10.875 mm	Stop the Excavation Work & Backfill Strutting Installation on D-wall
	Stage 2 Depth 5.50 meter		50% Maximum 13.875 mm	Stop the Excavation Work Increase Inclinometer Reading Frequency
			75% Maximum 20.813 mm	Stop the Excavation Work & Backfill Strutting Installation on D-wall
	Stage 3 Depth 7.15 meter		50% Maximum 17.875 mm	Stop the Excavation Work Increase Inclinometer Reading Frequency
			75% Maximum 26.813 mm	Stop the Excavation Work & Backfill Strutting Installation on D-wall
Settlement Marker	Stage 1 Depth 2.90 meter	Based on the analysis the maximum settlement is 2.3 cm; Chang Yu Ou, 2006 0.1125% from the depth of excavation	50% Maximum 1.631 mm	Stop the Excavation Work & Backfill Increase Monitoring Frequency
			75% Maximum 2.447 mm	Stop the Excavation Work & Backfill Soil Improvement
	Stage 2 Depth 5.50 meter		50% Maximum 3.094 mm	Stop the Excavation Work & Backfill Increase Monitoring Frequency
			75% Maximum 4.641 mm	Stop the Excavation Work & Backfill Soil Improvement
	Satge 3 Depth 7.15 meter		50% Maximum 4.022 mm	Stop the Excavation Work & Backfill Increase Monitoring Frequency
			75% Maximum 6.033 mm	Stop the Excavation Work & Backfill Soil Improvement

Type of Monitoring	Excavation Stage	Maximum Value Reference	Maximum Value	Contingency Plan
Building Verticality	Stage 1 Depth 2.90 meter Stage 2 Depth 5.5 meter Stage 3 Depth 7.15 meter	SNI 8460 : 2017 (Building inclination 1/500 = 0.2%)	Zero tolerance for inclination of cultural heritage buildings	If there is an inclination, the project activities will be completely stopped, backfill is carried out, and resumed if reinforcements has been made to the cultural heritage building

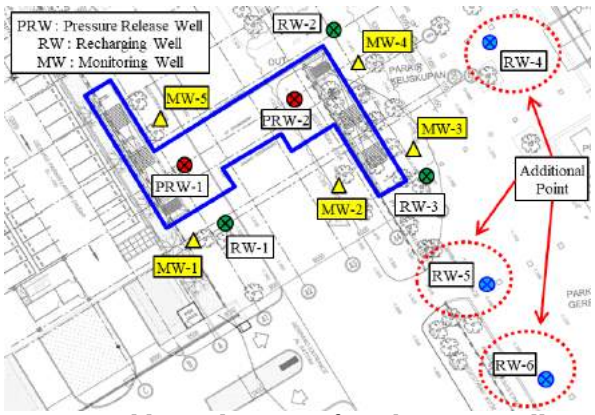

Fig. 10. Additional Points of Recharging Well.

For observation of the diaphragm wall, especially at the INC-3 point or on the side of the cultural heritage building, where at that point the maximum deflection value in the direction towards the excavation almost reaches 50% of the maximum value that has been determined in the early warning system for an excavation depth of 5.50 meters. On Fig. 12 shows the results of the inclinometer at the INC-3 point, from this figure, it can be seen that when excavation work starts from the ground level of 0.00 meters to -7.24 meters it only takes 2 days where at that time the deflection that occurs immediately reaches 6,336 mm. Then the inclinometer reading is carried out every day at that point and on March 15, 2021 it reaches 9,526 mm. From these results, by calculating the maximum reference limit is 0.5% (SNI 8460:2017) of the excavation depth, 50% of the maximum allowable value for wall deflection is 18.1 mm. Referring to the deflection value from the inclinometer monitoring results to the 50% limit of the maximum allowable value, it can be seen that the deflection is still within the safe limit. However, what must be noted is that there is a significant increase or deviation for each reading from March 11, 2021 to March 15, 2021. The daily deviation that occurs is 2,057 mm to 3,461 mm, based on this data the excavation was stopped and strutting was performed.

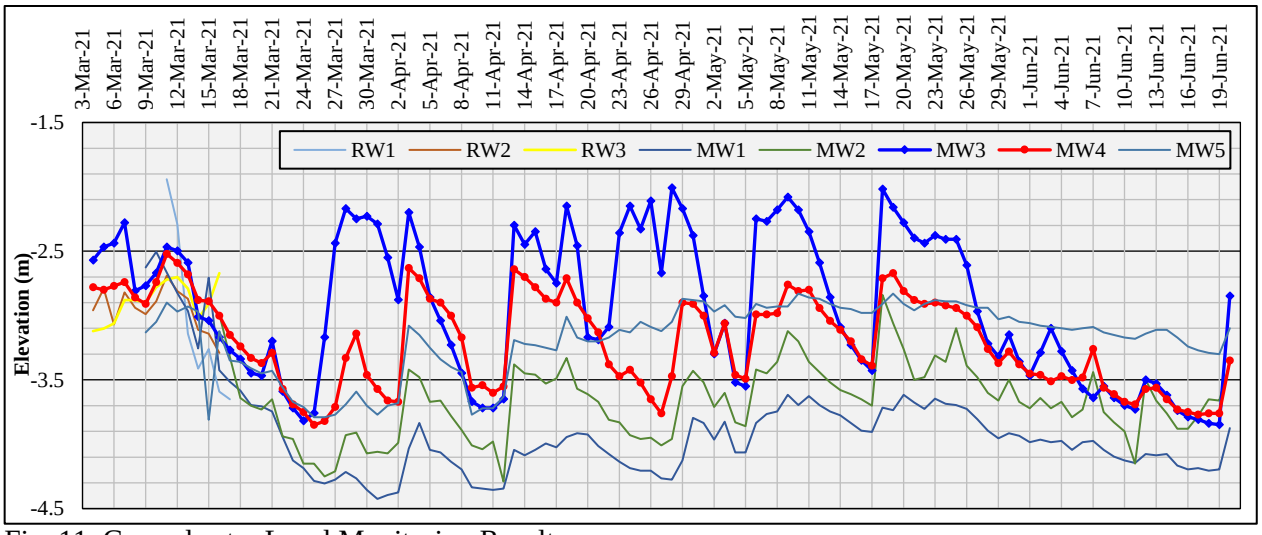

Fig. 11. Groundwater Level Monitoring Results.

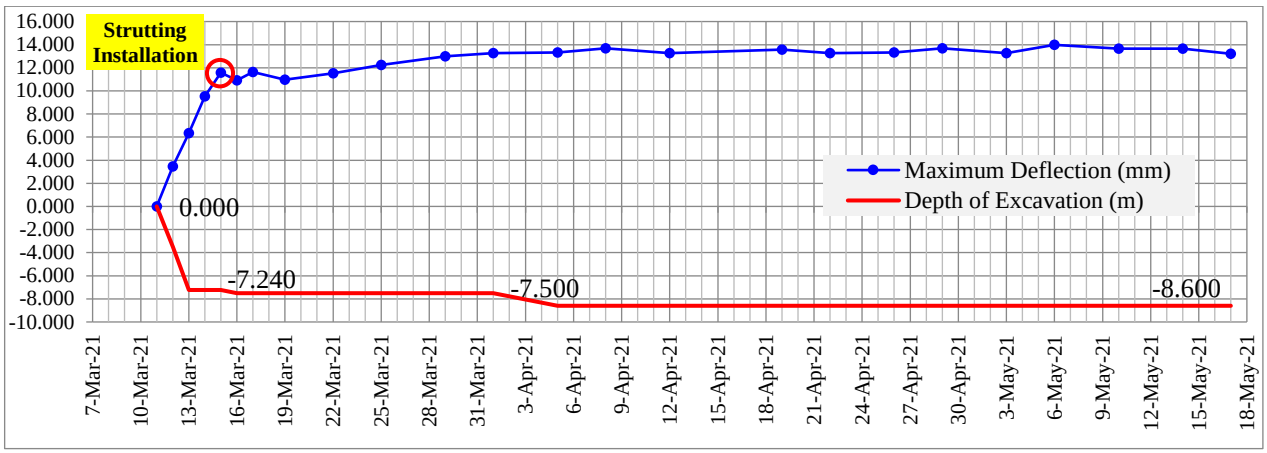

Fig. 12. Inclinometer Results on INC-3.

9 CONCLUSIONS AND SUGGESTIONS

Based on the results of planning and implementation of dewatering work on tunnel excavations adjacent to cultural heritage buildings. Conclusions and suggestions can be drawn in terms of planning and implementation.

At the time of planning, it is necessary to take into account in detail, the situation of the structural conditions of the buildings or infrastructure that are close to the excavation work. It is necessary to collect a complete and clear supporting data regarding soil conditions. So that in the analysis or design for this excavation work can get safer results when carried out. It is also very important to monitor, evaluate, and execute each type of work that being carried out. Monitoring data must also be given a maximum tolerance value for each type of monitoring. At the same time, also determining the work that must be done if the monitoring data is approaching the maximum value in an early warning system and contingency plan.

REFERENCE

Cedergren, H. R. 1967. *Seepage, Drainage, and Flownets.* New York : John Wiley and Sons: 489.

Department of the Army, The Navy and The Air Force 1983. *Dewatering and Groundwater Control*. NAVY NAVFAC: 418.

Holtz, R.D., and Kovacs, W.D., Sheahen, T.C. 2011. *An Introduction to Geotechnical Engineering*. Pearson Education Inc.

Ou, Chang-Yu. 2006. *Deep Excavation : Theory and Practice*. Taylor & Francis Group.

Powers, J. P. 1992. *Construction Dewatering and Groundwater Control*. New Jersey: John Wiley and Sons. Inc.

PT Tarumanegara Bumiyasa. 2021. Laporan-Laporan Monitoring Pekerjaan Dewatering dan Instrumentasi Proyek Terowongan.

PT Tarumanegara Bumiyasa. 2021. Metode Kerja Dewatering dan Instrumentasi Proyek Terowongan.

SNI. 2017. Persyaratan Perancangan Geoteknik. SNI : 8460-2017.

Dinding dan Tiang untuk Menahan Pergerakan Pipa Hidrokarbon di Tanah Lunak di Daerah Lereng

Mutadi
PhD Candidate, Civil Engineering Departement – Universitas Islam Sultan Agung
Lecturer in Engineering Faculty – Universitas Tujuh Belas Agustus 45

Praktiso
Civil Engineneering Departement – Universitas Islam Sultan Agung

Abdul Rochim
Civil Engineneering Departement – Universitas Islam Sultan Agung

ABSTRAK: Pipa hidrokarbon yang dipasang di lereng yang tidak stabil di tanah lunak rentan mengalami pergerakan. Jaringan pipa hidrokarbon yang ditanam didaerah lereng yang tidak setabil sering mengalami pergerakan akibat adanya gaya lateral dari pergerakan tanah yang mana dapat menyebabkan kerusakan pada pipa dan bias menimbulkan kebakaran dan ledakan. Penelitian pada sebuah model skala kecil laboratorium dari sistim perkuatan dinding dan tiang dilakukan untuk menyelidiki pengaruh beban lateral dan vertical pada sistim perkuatan untuk masalah tersebut. Pada percobaan ini digunakan gaya lateral sebesar 0,3 kN; 0.35 kN; dan 0,4 kN serta gaya vertikal sebesar 0,05 kN; 0,1 kN; dan 0,15 kN. Gaya lateral dari jack elektrik dan Jack manual dilengkapi dengan Load Cell sebagai pembaca beban dan gaya vertical semen box baja digunakan untuk percobaan ini. Untuk memvalidasi hasil eksperimen, program elemen hingga digunakan. Hasil percobaan menunjukkan bahwa peningkatan pembebanan lateral, mengakibatkan adanya peningkatan perpindahan atau regangan pada sistem perkuatan. Untuk Beban Vertikal 0,05 kN dan terhadap beban lateral 0,3 kN menyebabkan perpindahan horizontal sebesar 0,34 mm dan peningkatan sebesar 2,94 % untuk pembebanan sebesar 0,35 kN dan peningkatan sebesar 8,82% untuk pembebanan 0,4 kN. Pola yang sama pada analisis metode elemen hingga, dimana terjadi peningkatan sebesar 2.38% untuk pembebanan 0,35 kN dan meningkat menjadi 33,33 % untuk pembebanan 0,4 kN. Pada Beban yang sama, Sistem Perkuatan dapat diandalkan seperti yang ditunjukkan pada Faktor Keamanan pada tanah lunak di daerah lereng pada kondisi tanah kering atau kemaaru Faktor Keamanan adalah 3,33; 2,828 dan 2,476; dan pada kondisi tanah basah atau musim hujan nilai Faktor Keamanan adalah 2,99; 2,524 dan 2,237.

Kata Kunci: tanah lunak, perpindahan dinding, dinding-tiang, (untuk) pipa hidrokarbon

1 PENDAHULUAN

Kondisi tanah lunak di daerah lereng merupakan masalah tersendiri yang harus segera ditanggulangi jika pipa akan dipasang di daerah lereng, dan menurut Praktiso & Sudarno (2019) menyatakan bahwa sekitar 30% dari total tanah Indonesia merupakan tanah lunak, dengan daya dukung daya dukung. Beberapa solusi yang ditemukan dalam menangani permasalahan pergerakan pipa akibat pergerakan tanah lunak di daerah lereng adalah dengan membuat lereng dan penopang tiang kayu, dan hanya membuat dinding penahan tanah tanpa tiang pancang, namun solusi ini seringkali gagal. Namun pada penelitian ini solusi dari permasalahan pergerakan pipa pada tanah lunak akibat longsor adalah dengan membuat metode perkuatan dengan sistem tiang dan dinding.

Sistem dinding dan tiang merupakan salah satu solusi untuk tanah lunak di daerah lereng yang terdiri dari tiang dan dinding. Ini bekerja secara simultan untuk menahan gerakan pipa-tanah. Jika dibandingkan dengan dinding penahan tanah tanpa tiang, maka dinding penahan tanah dianggap lebih kuat dalam lentur akibat beban lateral yang mendorongnya, tetapi sangat lemah untuk stabilitas lereng, karena keruntuhan permukaan atau garis longsor berada di bawah bagian bawah dinding. Sistem dinding dan tiang itu dengan adanya tiang dapat menerima beban aksial, sehingga dapat meningkatkan kekuatan sistem pendukung interaksi pipa-

tanah sehingga diharapkan tidak terjadi longsor.

2 METODE PENELITIAN

Sistem dinding dan tiang untuk menahan pipa di tanah lunak di daerah lereng, Mutadi; Praktiso & Rochim (2021), dan interaksi pipa-tanah memainkan peran penting dalam analisis tegangan pipa yang mengalami pergerakan tanah karena ketidakstabilan lereng dan/atau kegagalan lereng. Ketika tanah/lereng mulai runtuh, maka jaringan pipa hidrokarbon yang diinstall atau dipasang atau dikubur di dalam tanah dalam zona runtuh akan menanggung beban tambahan yang sering menyebabkan tegangan berlebih berlebih pada pipa atau tekuk, Endra Susila (2018).

2.1 *Prototipe dan Instrumentasi*

LVDT digunakan untuk memantau perpindahan horizontal untuk dinding dan selain itu, alat pemantau dari strain gauge dipasang pada tiang pancang, dinding, dan pipa dihubungkan ke data logger dan dipantau langsung oleh komputer. Sistem dinding dan tiang pancang dari baja ASTM-A36, dipasang, dilas dan difabrikasi di bengkel. Setelah sistem tiang pancang dipasang pada wadah di laboratorium kemudian dipasang LVDT dan strain gauge pada sistem tiang pancang dan pipa. Soket listrik dilengkapi dengan sel beban yang dipasang pada platform kecil yang terpasang pada wadah untuk memberikan beban lateral. Load cell akan mengontrol beban lateral yang diberikan untuk percobaan. 3 buah dongkrak hidrolik atau jack hidrolik yang dilengkapi dengan load cell akan dipasang untuk percobaan ini. Jack hidrolik dan load cell pertama akan dipasang di platform atas dan dihubungkan ke dinding dengan Round Bar D19 mm untuk memberikan beban lateral, jack hidrolik dan load cell kedua akan dipasang di tengah platform dan dihubungkan dengan Round Bar D19 mm untuk memberikan beban lateral pada pipa, dan jack hidrolik dan load cell ke tiga dipasang di platform bawah dan dihubungkan ke tiang dengan Round Bar D19 mm untuk memberikan beban lateral. Tahapan sistem monitoring instalasi pada sistem tiang, dinding dan pipa, seperti terlihat pada Gbr. 1, Gbr. 2, Gbr. 3, Gbr. 4, Gbr. 5 dan Gbr. 6.

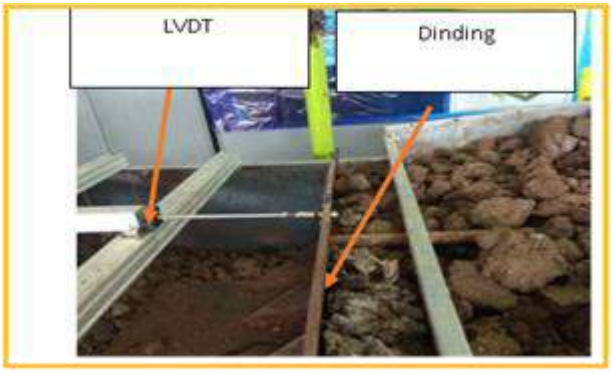

Gbr. 1. Sambungan LVDT ke Dinding.

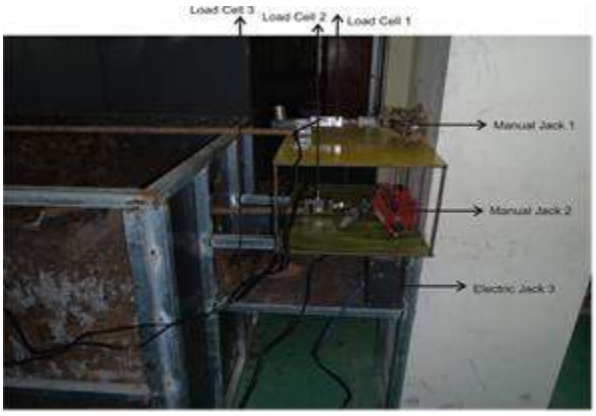

Gbr. 2. Jack 3 Buah dan Load Cell.

Gbr. 3. Kontainer, Jack, Strain Gauge dan Logger dan Komputer Terpasang.

Gbr. 4. Tampilan Lengkap.

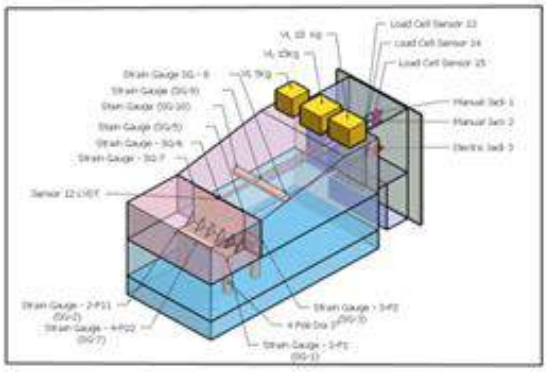

Gbr. 5. Bentuk 3D Skematik Laboratorium.

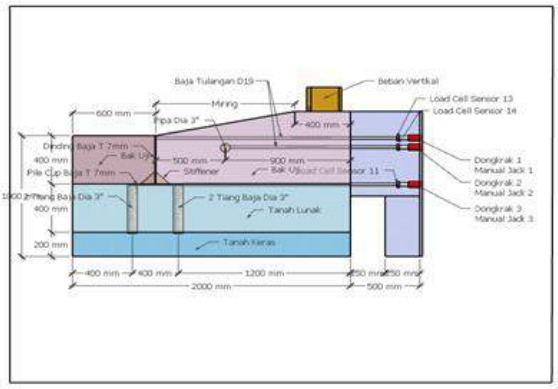

Gbr. 6. Tampak Samping Model.

2.2 *Sifat Tanah dan Persiapan Sampel*

Tanah lunak digunakan dalam bak uji dan hasil pengujian tanah dapat dilihat pada Tabel 1. Digunakan dalam bak uji dan dipadatkan sesuai dengan tingkat kepadatan di lapangan, tahapan pemadatan di bak uji adalah 20 cm per lapisan. Pemadatan dilakukan untuk mencapai konsolidasi yang diinginkan, Gouw (2017).

Tabel 1 Sifat Tanah Lunak.

No.	Parameter	Unit	Average
1	Spesific Gravity, GS	-	2.65
2	Consistency Limits Liquid Limit, LL Plastic Limit, PL Plasticity Index, PI	 % % %	 87.8 37.62 50.18
3	Water Content, w	%	53.22
4	Bulk Density, γ	kN/m^3	16.27
5	Dry Density, γd	kN/m^3	11.14
6	Triaxial UU Shear Test Cohession, c Friction Angle, ϕ	 kN/m^2 deg	 3.63 6.79
7	CBR	%	1.69
8	Soil Clasification AASHTHO ASTM D 4318, USCS		 A-7-6 CH

2.3 *Metode Elemen Hingga*

Analisis metode elemen hingga, Plaxis 2D digunakan untuk menentukan perubahan dan pergerakan sistem tiang dinding. Pengaturan umum untuk geometri disimulasikan dengan model regangan bidang. Pada kondisi awal untuk permukaan lereng tanah, Prosedur K0 dan pembebanan gravitasi harus diterapkan. Analisis undrained juga digunakan untuk tanah lunak. Antara dinding dan tanah, tiang dan tanah, dan pipa dan tanah akan menempatkan elemen antarmuka (interface). Batas-batas akan diletakkan cukup jauh untuk menghindari pengaruh kondisi batas. Gbr. 7 menunjukkan model dinding dan tiang

Input data plaxis untuk tanah dan baja: Modulus Young baja (E) = 2,10E+09kN/m^2, Rasio Poisson baja (μ) = 0,15, Berat satuan baja (γ_s) = 78 kN/m^3. Sifat-sifat lempung lunak diambil sebagai γ_{unsat} = 11,14 kN/m^3, γ_{sat} = 16,27 kN/m^3, E_{ref} = 15000 kN/m^2, R_{inter} = 0,5, kohesi tanah C = 2,63 kN/m^2, sudut geser tanah ϕ = 6,79^o, rasio Poisson tanah μ = 0,3. Masukkan data plaxis untuk tanah dan baja: Modulus Young baja (E) = 2,10E+09kN/m^2, Rasio Poisson baja (μ) = 0,15, Berat satuan baja (γ_s) = 78 kN/m^3. Sifat lempung lunak diambil sebagai γ_{unsat} = 11,14 kN/m^3, γ_{sat} = 16,27 kN/m^3, E_{ref} = 15000 kN/m^2, R_{inter} = 0,5 kohesi tanah C = 3,63 kN/m^2, sudut gesr tanah ϕ = 6,79^o, rasio Poisson tanah μ = 0,3.

3 METODE PENELITIAN

3.1 *Analisis Eksperimen vs Metode Elemen Hingga (FEM)*

Hasil perhitungan dengan metode elemen hingga pada Gbr. 8 menunjukkan bahwa perpindahan terbesar berada pada ujung atas Dinding. Untuk pembebanan lateral 40 kg atau 0,4 kN dan Beban Vertikal 15 kg atau 0,15 kN adalah 0,6 mm. Untuk pembebanan lateral sebesar 35 kg atau 0,35 kN dan Beban Vertikal sebesar 15 kg atau 0,15 kN sekitar 0,51 mm. Untuk pembebanan lateral 30 kg atau 0,3 kN dan Beban Vertikal 15 kg atau 0,15 kN adalah 0,50 mm. Untuk pembebanan lateral dan pembebanan vertikal lainnya yang lebih kecil, hasilnya dapat dilihat pada Tabel 2.

Pola hasil pengujian eksperimen mirip dengan perhitungan dengan analisis metode elemen hingga. Untuk beban lateral 40 kg atau 0,4 kN dan Beban Vertikal 15 kg atau 0,15 kN sekitar 0,43 mm. Untuk pembebanan lateral 35

kg atau 0,35 kN dan Beban Vertikal 15 kg atau 0,15kN sekitar 0,39 mm, untuk pembebanan lateral 30 kg atau 0,3 kN dan Beban Vertikal 15 kg atau 0,15 kN sekitar 0,37 mm.

Dari hasil di atas dapat dilihat dan dipastikan bahwa hasil uji eksperimen masih berada di bawah perpindahan horizontal yang diperbolehkan jika dibandingkan dari analisis metode elemen hingga sesuai dengan penelitian Mutadi, Praktiso & Rochim (2021).

Gbr. 8 menunjukkan perubahan deformasi, Gbr. 7 menggambarkan perpindahan Dinding di ujung atas dan tepi bawah Dinding ketika diterapkan beban lateral dari analisis metode elemen hingga.

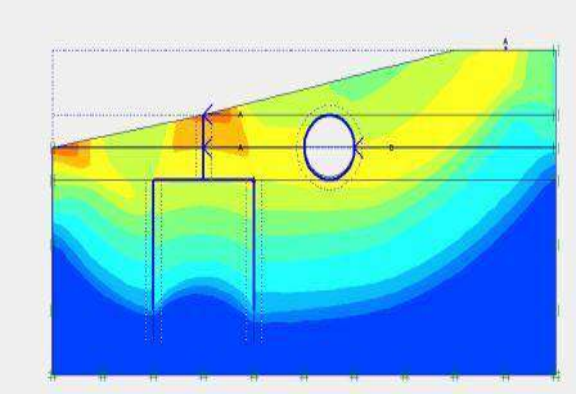

Gbr. 8. Perubahan Perpindahan Setelah Pembebanan Terapan.

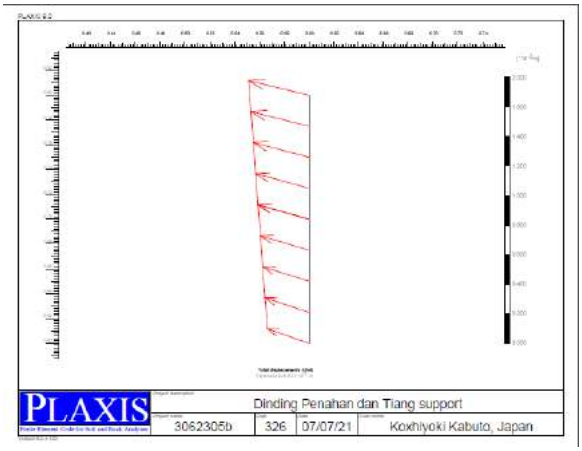

Gbr. 9. Perpindahan Dinding Horizontal Setelah Pemuatan Terapan.

3.2 *Lendutan Dinding*

Analisis perpindahan dinding dilakukan untuk mengetahui besarnya pengaruh pembebanan lateral terhadap perpindahan dinding, dan hasil ini akan dibandingkan dengan hasil analisis metode elemen hingga menggunakan plaxis. Hasil analisis dapat dilihat pada Tabel 2.

Tabel. 2. Akumulasi Lendutan Dinding.

	Measured LL			FEM LL		
	LL Kg	LL Kg	LL Kg	LL Kg	LL Kg	LL Kg
VL (Kg)	30	35	40	30	35	40
15	0,37	0,39	0,43	0,50	0,51	0,60
10	0,36	0,37	0,39	0,46	0,49	0,57
5	0,34	0,35	0,37	0,42	0,43	0,56

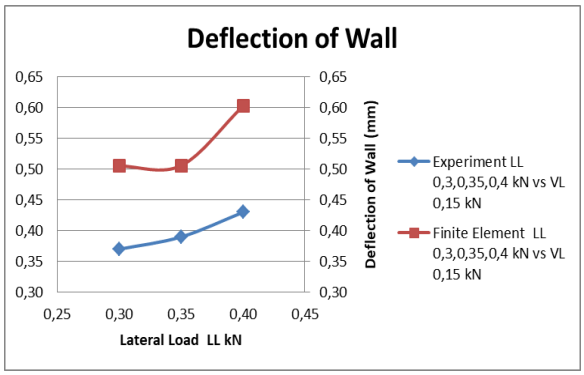

Gbr. 10. Lendutan Dinding Terukur vs Model FEM LL 30 Kg, 35 Kg, 40 Kg, VL 15 Kg.

Gbr. 10, Lendutan Dinding Ukur vs Model FEM LL 30 Kg, 35Kg, 40 Kg, VL 15 Kg membedakan analisis metode elemen hingga dan hasil pengujian eksperimen, dimana perpindahan dinding pada ujung atas dinding dari pengujian eksperimen adalah 0,43 mm sedangkan hasil analisis metode elemen hingga adalah 0,60 mm. Hasil tersebut menunjukkan bahwa hasil metode elemen hingga lebih besar jika dibandingkan dengan hasil eksperimen, hal ini menunjukkan bahwa hasil pengujian eksperimen masih dianggap aman.

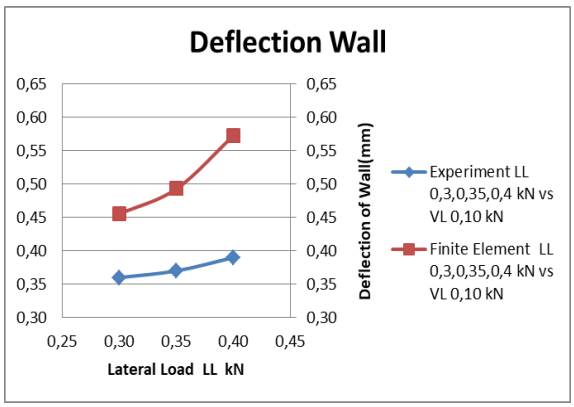

Gbr. 11. Lendutan Dinding Terukur vs Model FEM LL 30 Kg, 35Kg, 40 Kg, VL 10 Kg.

Gbr. 11 membedakan analisis metode elemen hingga dan hasil pengujian eksperimen, dimana defleksi dinding pada bagian atas dinding dari pengujian eksperimen adalah 0,39 mm sedangkan hasil analisis metode elemen hingga adalah 0,57 mm. Hasil tersebut menunjukkan bahwa hasil metode elemen hingga lebih besar jika dibandingkan dengan hasil eksperimen, hal ini menunjukkan bahwa hasil pengujian eksperimen masih dianggap aman.

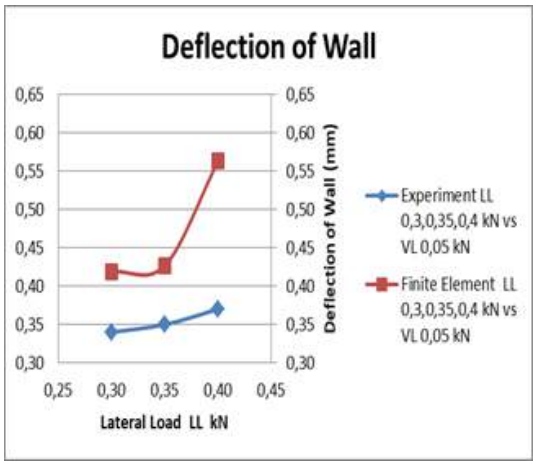

Gbr. 12. Lendutan Dinding Terukur vs Model FEM LL 30 Kg, 35Kg, 40 Kg, VL 5 Kg.

Gbr. 12 membedakan analisis metode elemen hingga dan hasil pengujian eksperimen, dimana defleksi dinding pada bagian atas dinding dari pengujian eksperimen adalah 0,37 mm sedangkan hasil analisis metode elemen hingga adalah 0,56 mm. Hasil tersebut menunjukkan bahwa hasil metode elemen hingga lebih baik jika dibandingkan dengan hasil pengujian eksperimen, hal ini menunjukkan bahwa hasil pengujian eksperimen masih dianggap aman.

3.3 *Pergeseran Horizontal Tiang*

Analisis defleksi tiang dilakukan untuk mengetahui sejauh mana pengaruh pembebanan lateral terhadap lendutan tiang, dan hasil ini akan dibandingkan dengan hasil analisis metode elemen hingga menggunakan plaxis.

Tabel. 3. Lendutan Akumulasi Tiang P1.

Acumulation Displacement of Pile 1						
	Measured			FEM LL		
	LL Kg			LL Kg		
VL (Kg)	30	35	40	30	35	40
15	0,33	0,35	0,37	0,38	0,39	0,41
10	0,28	0,32	0,34	0,29	0,34	0,35
5	0,27	0,29	0,32	0,28	0,31	0,34

Tabel. 4. Lendutan Akumulasi Tiang P2.

Acumulation Displacement of Pile 2						
	Measured			FEM LL		
	LL Kg			LL Kg		
VL (Kg)	30	35	40	30	35	40
15	0,37	0,38	0,43	0,47	0,48	0,51
10	0,34	0,35	0,39	0,37	0,42	0,43
5	0,33	0,34	0,37	0,36	0,39	0,42

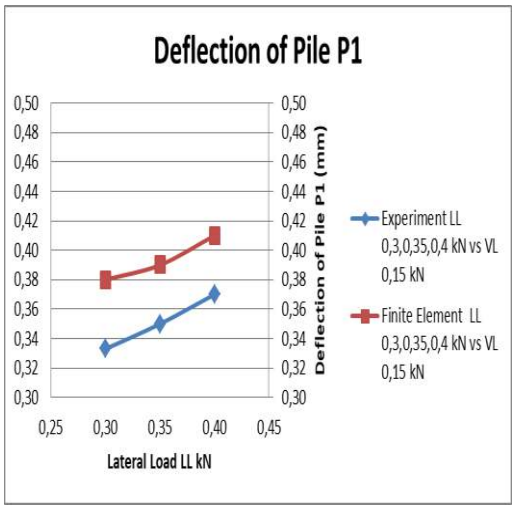

Gbr. 13. Lendutan Tiang P1 Terukur vs Model FEM LL 30 Kg, 35Kg, 40 Kg, VL 15 Kg.

Gbr. 13 membedakan analisis metode elemen hingga dan hasil uji eksperimen yang diterapkan untuk pembebanan lateral 30 Kg, 35 Kg, dan 40 Kg. Hasil ini menunjukkan bahwa terdapat kesamaan pola antara uji eksperimen dan analisis metode elemen hingga, untuk pembebanan lateral defleksi tiang atas sebesar 40 Kg adalah 0.37 mm untuk pengujian eksperimen dan 0.41 mm untuk analisis metode elemen hingga. Hasil ini untuk Pile P2 pada LL 40 Kg vs VL 15 Kg. Untuk hasil lainnya dapat dilihat pada tabel 4 dan untuk tiang P2 pada tabel 3. Namun semua

hasil dari percobaan lendutan masih dibawah lendutan yang diijinkan dari hasil analisis metode elemen hingga.

3.4 *Defleksi Pipa*

Analisis defleksi pipa dilakukan untuk mengetahui besarnya pengaruh pembebanan lateral terhadap defleksi pipa, dan hasil ini akan dibandingkan dengan hasil analisis metode elemen hingga menggunakan plaxis.

Tabel. 5. Akumulasi Lendutan Pipa.

Acumulation Displacement of Pipe						
	Measured			FEM LL		
	LL Kg			LL Kg		
VL (Kg)	30	35	40	30	35	40
15	0,38	0,40	0,46	0,42	0,51	0,60
10	0,36	0,38	0,44	0,37	0,42	0,49
5	0,35	0,36	0,39	0,36	0,38	0,42

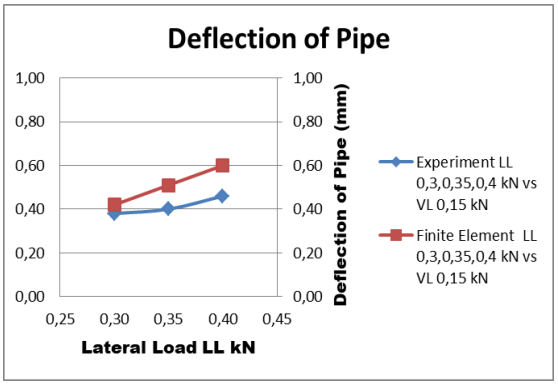

Gbr. 14. Lendutan Tiang P1 Terukur vs Model FEM LL 30 Kg, 35Kg, 40 Kg, VL 15 Kg.

Gbr. 14 membedakan analisis metode elemen hingga dan hasil uji eksperimen untuk pembebanan lateral terapan 30 Kg, 35Kg, dan 40Kg. Hasil ini menunjukkan bahwa terdapat kesamaan pola antara uji eksperimen dan analisis metode elemen hingga. Untuk pembebanan lateral defleksi pipa sebesar 40Kg adalah 0.56 mm untuk uji eksperimen dan 0.60 mm untuk analisis metode elemen hingga. Hasil ini untuk LL 40 Kg vs VL 15 Kg. Untuk hasil lainnya dapat dilihat pada tabel 5. Namun semua hasil dari percobaan defleksi masih dibawah defleksi yang diijinkan dari hasil analisis metode elemen hingga.

3.5 *Faktor Keamanan*

Analisis Faktor Keamanan dilakukan untuk membandingkan kondisi kering dengan kondisi basah. Hasilnya dapat dilihat pada Tabel 6.

Tabel. 6. Faktor Keamanan.

Safety Factor						
	Measured			FEM LL		
	LL kN			LL kN		
VL (kN)	0,3	0,35	0,4	0,3	0,35	0,4
0,15	3,329	2,821	2,472	2,97	2,521	2,229
0,10	3,330	2,824	2,474	2,98	2,522	2,235
0,05	3,330	2,828	2,476	2,99	2,524	2,237

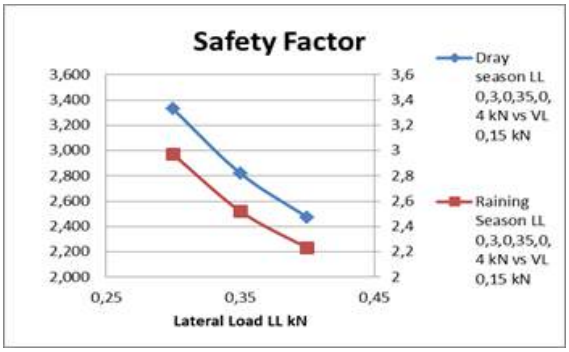

Gbr. 15. Faktor Keamanan Kering vs Hujan LL 30 Kg, 35Kg, 40 Kg, VL 15 Kg.

Gbr. 15 membedakan analisis metode elemen hingga pada kondisi kering dan kondisi hujan/basah dari hasil Faktor Keamanan untuk pembebanan lateral yang diterapkan 30 Kg, 35 Kg, dan 40 Kg versus beban vertikal 15 Kg. Hasil ini menunjukkan bahwa terdapat pola yang sama antara analisis metode elemen hingga kondisi Kering dan kondisi Basah. Untuk pembebanan lateral 40 Kg Safety Factor kestabilan lereng adalah 2,472 untuk kondisi kering, dan 2,229 untuk kondisi basah/hujan. Hasil ini untuk LL 40 Kg vs VL 15 Kg. Untuk hasil lainnya dapat dilihat pada Tabel 6. Namun semua hasil menunjukkan bahwa peningkatan beban lateral menurunkan Faktor Keamanan untuk kondisi kering dan basah.

4 KESIMPULAN

1. Dalam melaksanakan disain untuk pipa-pipa yang ditimbun di tanah lunak di daerah lereng, harus dipertimbangkan efek pembebanan lateral dan vertikal terhadap

stabilitas sistem tiang dinding, bila diterapkan di lapangan.

2. Semakin besar pembebanan lateral dan vertikal maka semakin besar pula defleksi dinding, tiang pancang dan pipa yang dihasilkan.
3. Untuk beban lateral maksimum hingga 40 Kg dan beban vertikal hingga 15 Kg, defleksi dinding, tiang pancang, dan pipa masih di bawah defleksi yang diizinkan.

DAFTAR PUSTAKA - REFERENCES

Susila, E. 2018. Perilaku Interaksi Pipa-Tanah pada Lereng Tidak Stabil dengan Simulasi Elemen Hingga. *Jurnal Teknik Sipil ITB.*

Gouw, Tjie-Liong. 2017. Pengaruh Gerakan Lateral Tiang, Jarak Tiang dan Jumlah Tiang pada Tiang Kelompok yang Dibebani Secara Lateral. Tumpukan *Konferensi Internasional*.

A, Praktikso. & S, Sudarno. 2019. Analisis Konsolidasi Tanah Sebagai Penyebab Utama Penurunan Tanah di Semarang - Indonesia. *Jurnal Internasional Teknik Sipil dan Teknologi (IJCIET)* 10(02): 793–802.

Situmorang, A. 2017. Lendutan Sistem Pelat Paku Perkerasan Kaku dengan Lateral Beban. *Prosiding Konferensi Internasional: Masalah, Solusi dan Pengembangan Wilayah Pesisir dan Delta Semarang, Indonesia.*

Mutadi, A. Praktiso. & Rochim, A. 2021. *Dinding dan Tiang untuk Pipa Hidrokarbon di Tanah Lunak di Daerah Lereng*.

Study on Efficiency of Negative Skin Friction on End Bearing Pile Groups Using 3D Finite Element Method

Stefanus Diaz Alvi
Deputy Head Division – PT Geotechnical Engineering Consultant

Paulus P. Rahardjo
Professor of Geotechnical Engineering – Universitas Katolik Parahyangan

ABSTRACT: For pile foundations embedded in the under-consolidating layer or liquefied sandy soil, the soil around the pile will settle. If the soil settlement around the pile is greater than the pile settlement, there will be friction between the pile sleeve and the soil which causes the pile to be pulled downwards. This frictional force is referred to as negative skin friction (NSF) or down-drag force which will reduce the compressive axial bearing capacity of the pile foundation. The down-drag force for the end bearing pile is generally greater than the friction pile. This paper contains 3D modeling with the Finite Element Method for end-bearing pile groups. The results showed that the NSF force of each pile in a group is not the same and smaller than that of a single pile. In a pile group configuration, the down-drag force for the pile in the middle of the pile group will be smaller than the pile at the edge. This large reduction in NSF is expressed as an "efficiency" value. The mechanism that causes the NSF efficiency in the pile group is the constraint effect on the soils between the piles. This paper presents a case study of pile groups embedded in soil under-consolidating layer with the degree of consolidation obtained from the CPTu, modeling the NSF in pile groups using the Finite Element Method, and the comparison of down-drag on the single pile and pile group.

Keywords: negative skin friction, down-drag force, efficiency, reduction factor, finite element method

1 PENDAHULUAN

One of the problems that need to be considered in the pile foundation is the possibility of a down-drag on the pile. The down-drag phenomenon or condition where the pile is pulled down is often referred to as Negative Skin Friction (NSF). NSF occurs if the pile is embedded in the under-consolidating layer where settlement occurs or in sandy soil during liquefaction.

This negative skin friction provides a reduction in the axial compression bearing capacity of the pile foundation. Several methods have been developed to estimate the NSF force that affects a reduction in the bearing capacity for a single pile. However, it is often assumed that the NSF force in a pile group system is equal to the NSF force for single pile times the number of piles in the group.

This paper contains a case study of a group of end-bearing piles embedded in an under-consolidating layer, where there is a down-drag force acting on the pile group. The discussion begins with information related to the down-drag phenomena and the CPTu test to investigate the degree of consolidation for the under-consolidating layer. After that, we discussed the modeling and analysis methods using the Three-Dimensional Finite Element Method using the MIDAS GTS NX Software to model the NSF on the end-bearing pile groups for a case study in Jakarta.

2 NEGATIVE SKIN FRICTION

2.1 *Mechanism of Negative Skin Friction (NSF)*

In a pile that is embedded in a layer of under-consolidating soil, either due to the load of the embankment above it or due to the self-weight of the soil from the sedimentation process, the soil around the pile will tend to move downwards. If the soil settlement around the pile is greater than the pile settlement, then the layer of soil that has decreased greater than the

settlement of the pile will drag the pile downwards, resulting in downward friction of the pile perimeter which is known as negative skin friction or down-drag. The pile shaft that receives the negative friction / NSF force is the pile shaft that is above the neutral point. The neutral point is the position or elevation where there is no shear between the pile blanket and the ground, or where the pile settlement and soil settlement around the pile are equal, as shown in Fig. 1.

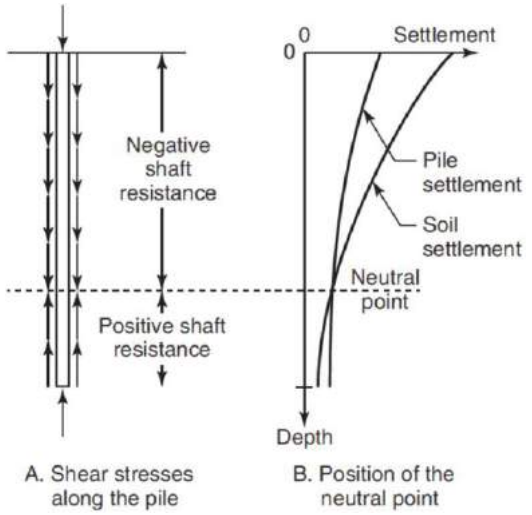

Fig. 1. Neutral Point, Briaud (2013).

2.2 *NSF on Single Pile*

The down-drag force can be obtained from the negative skin friction multiplied by the area of the pile shaft above the neutral point. The down-drag force on the friction pile and the end-bearing pile will be different because the end-bearing pile generally has a smaller pile settlement than the friction pile. Therefore, the NSF force in the end-bearing pile will be greater than the friction pile for the same soil condition. Briaud and Tucker (1977) provide some criteria which NSF needs to be taken into account in pile foundations:

1. The total settlement of the ground surface will be larger than 100 mm
2. The settlement of the ground surface after the piles are installed will be larger than 10 mm.
3. The height of the embankment to be placed on the ground surface exceeds 2 m.
4. The thickness of the soft compressible layer is larger than 10 m.
5. The water table will be drawn down by more than 4 m.
6. The piles are longer than 25 m.

Fig. 2 shows the load transfer curve under conditions with and without down drag. The load transfer in conditions without down drag shows that the load transfer curve will decrease from top to bottom or the cumulative mobilized bearing capacity increases from bottom to top. In the load transfer curve with down-drag conditions, the load transfer curve above the neutral point will decrease from the neutral point to the pile top because there is a reduction by NSF forces.

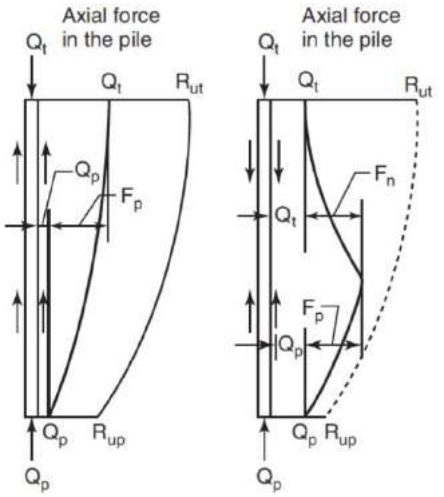

(a) Without down-drag (b) With down-drag

Fig. 2. Load Transfer without Down-Drag and with Down-Drag, Briaud (2013).

2.3 *NSF on Pile Group*

The NSF forces acting on a pile group will be less than the NSF force for single pile times the number of piles in the pile group. There is a reduction value or efficiency factor of the NSF force per pile in a pile group. This is because the soil between the piles will have a smaller settlement than the soil on the perimeter of the pile group, as shown in Fig. 3.

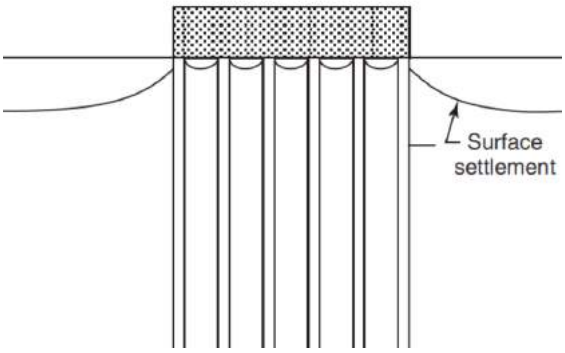

Fig. 3. Soil Settlement Pattern Around a Pile Group, Briaud (2013).

Briaud and Tucker (1997) recommend an NSF reduction factor for the pile group with a rigid pile cap as shown in the following figure.

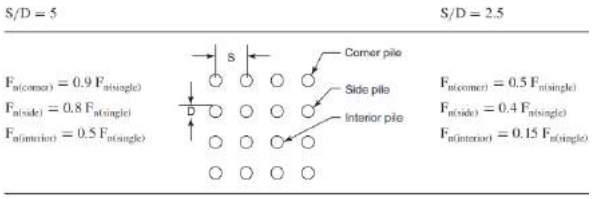

Fig. 4. Reduction Factor of Downdrag Force, Briaud and Tucker (1997).

3 DETERMINATION OF DEGREE OF CONSOLIDATION USING CPTU

Cone Penetration Test with pore pressure measurement (CPTu) or Piezocone Test can measure cone resistance (q_c), sleeve friction (f_s), and pore pressure (u_2). The pore pressure measured by pore pressure filter is very useful to obtain soft soil behavior such as soil permeability from dissipation tests, stress history (degree of consolidation and OCR), and the excess pressure that is still acting on the soil.

Several methods can be used to estimate the degree of consolidation from CPTu test. This paper will discuss the determination of the degree of consolidation (%U) based on the Bq value, Setionegoro (2012) and Rahardjo et al. (2013) and the Bq* value, Rahardjo (2016) and Setiawan (2017).

3.1 *Determination of The Degree of Consolidation from Bq, Setionegoro (2012) and Rahardjo et al. (2013)*

Pore pressure ratio (Bq) is the ratio between the excess pore water pressure measured during the penetration (u_2) to the hydrostatic water pressure (u_0) compared to the net end resistance value (q_t-σ_{v0}).

Based on the literature, there is a relationship between the value of the Bq and the value of the over-consolidation ratio (OCR). Setionegoro & Rahardjo (2013) published a publication regarding the relationship between %U and Bq for under-consolidating soils (Fig. 5).

From this research, it is found that under-consolidating soils generally have a Bq value above 0.7. The equation of the curve can be seen in the following formula.

$$OCR = \frac{1}{(1.2xBq)+0.1} \quad (1)$$

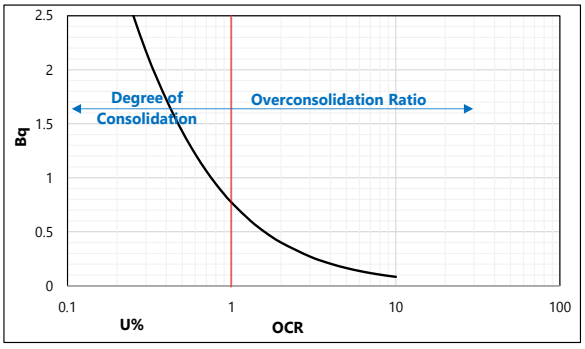

Fig. 5. OCR Interpretation based on Bq Value, Setionegoro (2012) & Rahardjo et al. (2013).

3.2 *Determination of The Degree of Consolidation from Bq*, Rahardjo (2016) dan Setiawan (2017)*

Determination of the degree of consolidation from Bq has a weakness because the value of Bq is very dependent on the density of the soil where the value is assumed. Rahardjo (2016) and Setiawan (2017) propose a new parameter, namely Bq*, to replace the Bq with the following formula.

$$Bq^* = \frac{u_2}{q_t} \quad (2)$$

where the OCR or %U can be obtained using the following formula.

$$OCR = 10^{1.002-1.57\ Bq^*} \quad (3)$$

4 STUDI KASUS DI JAKARTA UTARA

4.1 *Soil Condition*

In a project in North Jakarta, a building was constructed with driven pile groups embedded in soft soil with the tip of the pile in dense sand. Soil conditions from drilling data and SPT can be seen in Fig. 6. The top layer is the embankment. The second layer is very soft clay. This layer is marine clay. The third layer is a medium to stiff clay. The fourth layer is a very dense layer of sand. This layer is the supporting layer for the driven pile. The fifth layer under the sand lens is stiff to hard clay. The groundwater table is at a depth of 1 m from the ground surface.

With the embankment on soft soil, a CPTu test was conducted to obtain information on whether the soft soil was still consolidating due to the embankment load. The results of the CPTu test can be seen in Fig. 7.

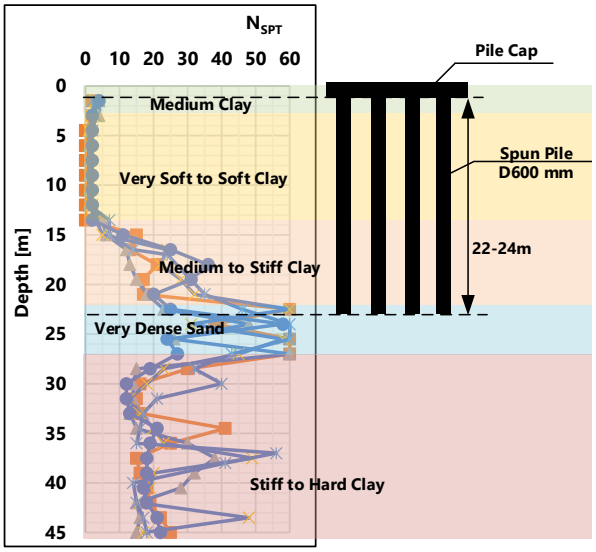

Fig.6. Soil Stratification and Pile Foundation.

Based on the results of the CPTu test, information can be obtained that the under-consolidating layer is found at a depth of 5 m to 14 m. The average degree of consolidation in this layer based on the values of Bq and Bq* ranges from 62% to d. 65%.

4.2 *Modeling and Analysis using 3D FEM*

The analysis is carried out using the 3D Finite Element Method (FEM) using the MIDAS GTS NX Program. The soil material is modeled as a cluster with Soft-Soil Model for clayey soils and Hardening Soil Model for sandy soils. The pile cap is modeled as an elastic cluster with concrete material and the pile is modeled as an embedded beam element. The thickness for each soil layer is modeled according to the drilling data.

The study was carried out in 3 stages:

1. The first stage is the determination of the final settlement due to the existing embankment.
2. The second stage is modeling pile construction when the degree of consolidation of 65% (from the CPTu test). As for the calculation, the degree of consolidation is translated in the form of a ratio between the estimated settlement that has occurred to the final settlement.
3. The third stage is to conduct an NSF study with the starting point of pile installation time when the 65% degree of consolidation is reached.

4.3 *Analysis Results and Discussion*

The results of the analysis are shown in the form of settlement contour due to the consolidation process in the soft clay layer (Fig. 10) and pile settlement due to the upper-structure load (Fig. 11).

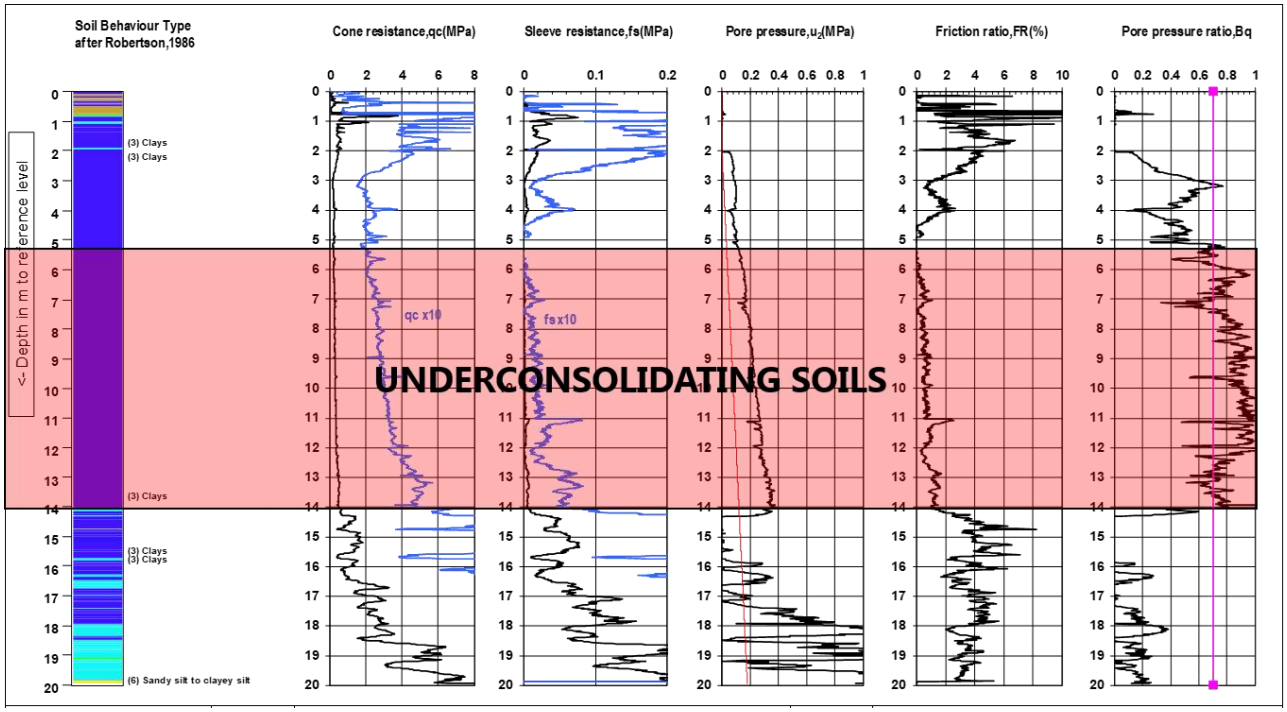

Fig. 7. CPTu Test Result.

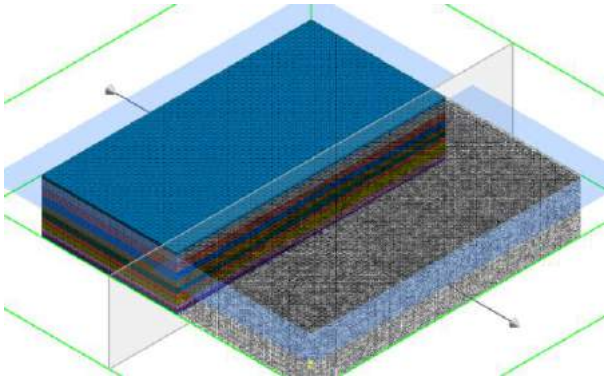

Fig. 8. Soil Stratification Modeling Using 3D MIDAS GTS NX.

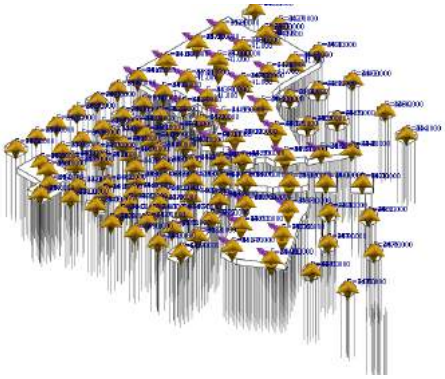

Fig. 9. Forces and Pile Foundation Modeling.

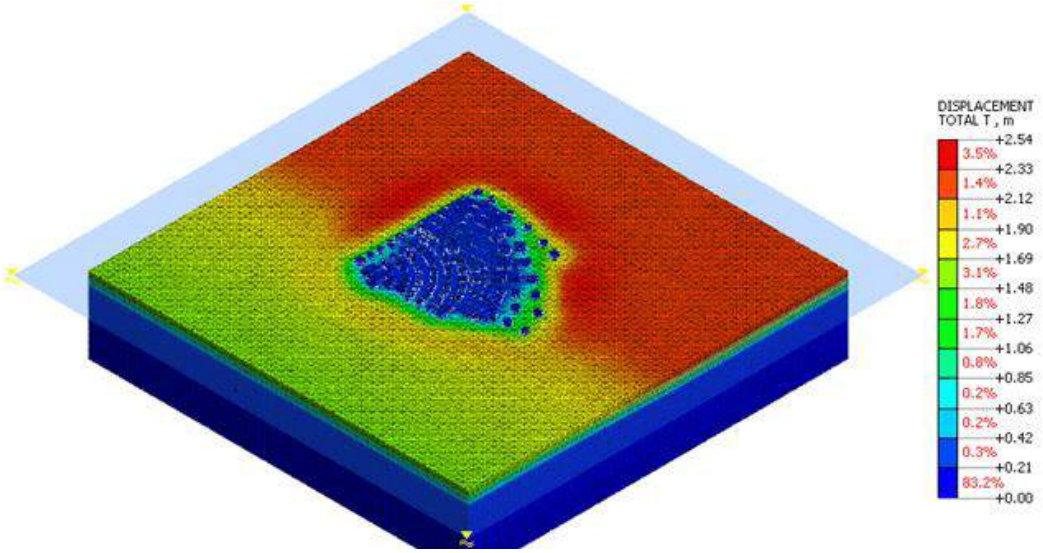

Fig. 10. Soil Settlement Contour from 3D FEM Using MIDAS GTS NX.

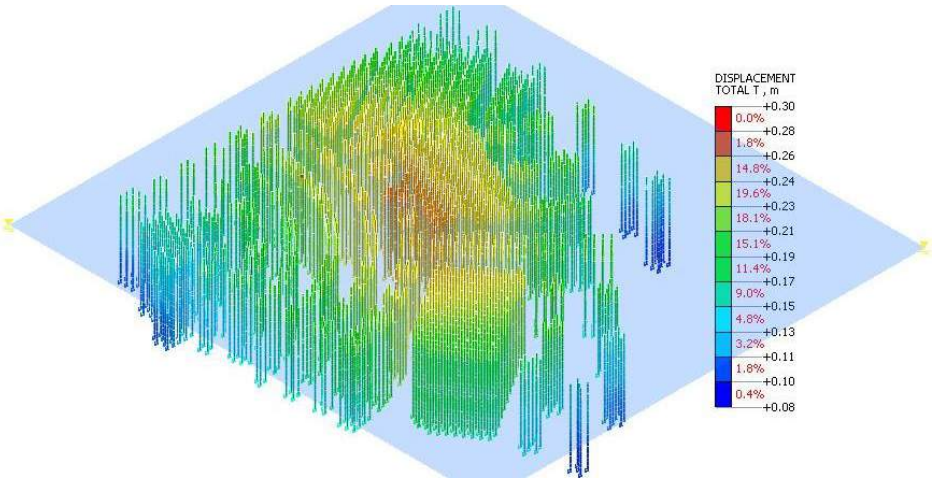

Fig. 11. Pile Settlement from 3D FEM Using MIDAS GTS NX.

Based on the results of the load transfer analysis for single piles and piles in groups, it can be obtained that the NSF force for piles in groups is smaller than single piles. In addition, it is also obtained that the pile positioned on the inner side of the pile group has a smaller NSF force than the outer side. This supports the literature presented previously by Briaud and Tucker, where there is a reduction in the down-drag force in a pile group.

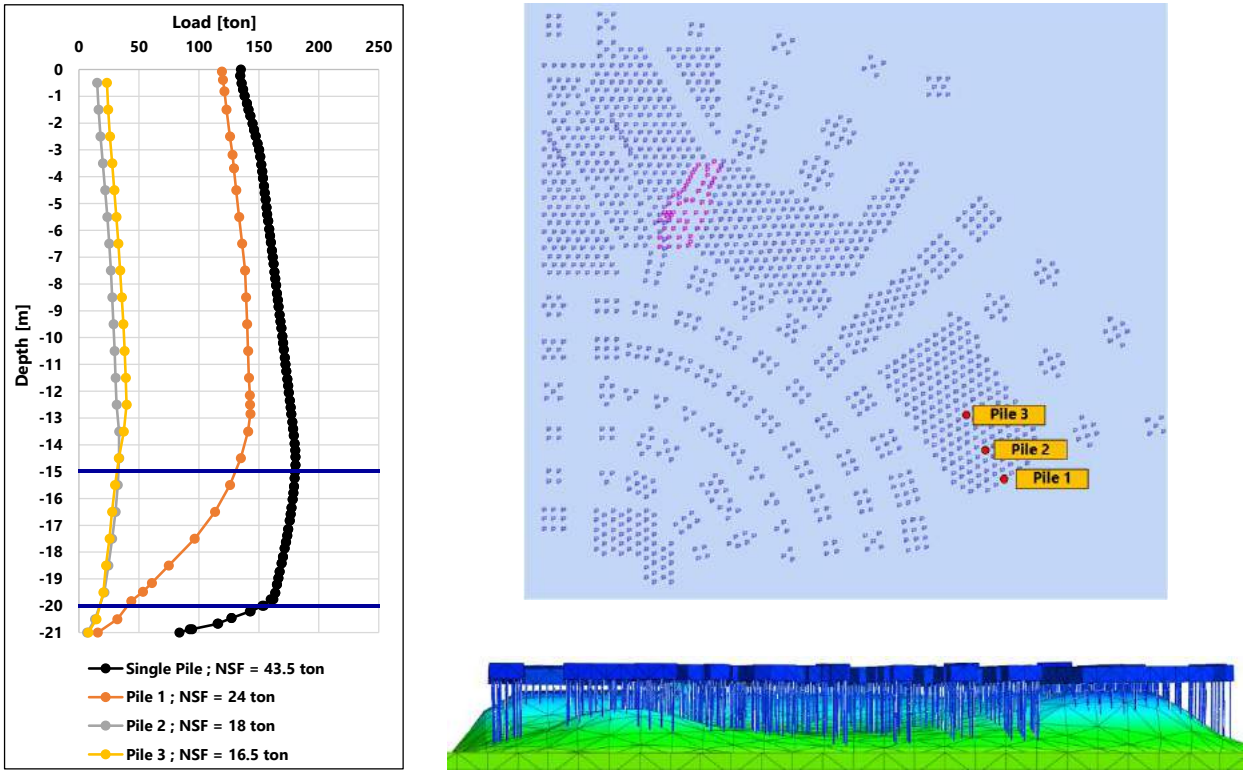

Fig. 12. Load Transfer Comparison between the Single Pile and Pile Groups.

Fig. 12 also shows that the soil between the piles in the pile group is constrained so that the pile settlement between the piles in the pile group is smaller than the pile settlement outside the pile group. This is consistent with the opinion of Briaud and Tucker (1997).

The amount of settlement that occurs in a pile group is greater than the settlement for a single pile. Because the soil settlement around the pile has a similar value, the position of the neutral point moved to a higher elevation. Therefore, the NSF in the pile group will be of less value than the NSF in the single pile.

5 CONCLUSIONS

The phenomenon of down-drag or negative skin friction (NSF) occurs in piles that are embedded in the under-consolidating soils. NSF can be modeled using 3D FEM for single piles and pile groups with the down-drag force obtained through load transfer from the neutral point to the top of the pile.

The case study is conducted on end-bearing driven pile groups for a building in North Jakarta. The piles are embedded in under-consolidating soils. The CPTu test can be used to investigate the degree of consolidation of the existing soft soils.

The results of the analysis using 3D FEM by MIDAS GTS NX show that the NSF of each pile in the group is smaller than the NSF of a single pile. In addition, the piles located on the inner side of the group gave a smaller NSF value than the piles on the edge.

The efficiency of NSF in pile groups occurs due to the soil confinement between piles. In addition, the settlement of the pile group is larger than the settlement of the single pile. It causes the neutral point to move to a higher position, resulting in a smaller NSF.

REFERENCES

PT Geotechnical Engineering Consultant. 2019. Laporan Faktual Penyelidikan Tanah No. 01/D190349/19-09/053. Bandung

PT Geotechnical Engineering Consultant. 2019. Laporan Desain dan Analisis Geoteknik No. 02/D190349/19-09/053. Bandung

Briaud J.-L., and L. M. Tucker. 1997. Design and Construction Guidelines for Downdrag on Uncoated and Bitumen-Coated Piles. *NCHRP Report*: 393. Washington, DC: Transportation Research Board, National Academy Press.

Okabe, T. 1977. Large Negative Friction and Friction-Free Pile Methods. *In Proceedings of the 9th International Conference on Soil Mechanics and Foundation Engineering*: 679–682. Tokyo.

Deep Foundation Research Institute. 2017. *Manual Pondasi Tiang Edisi 5*. Bandung: Universitas Katolik Parahyangan.

Diagnostic and Prediction of PC Spun Pile Lateral Capacity using Logistic Regression and Support Vector Regression (SVR)

James J. Oetomo
PT Inti Karya Persada Tehnik (IKPT)

Dimas Rakha Ammar
PT Inti Karya Persada Tehnik (IKPT)

ABSTRACT: Prediksi kapasitas lateral tiang merupakan salah satu tugas yang rutin dilakukan dalam pekerjaan rekayasa geoteknik praktis. Saat ini, prediksi tersebut lazim dilakukan dengan menggunakan metode p-y, dalam hal ini lapisan tanah dimodelkan sebagai material elastoplastik. Tulisan ini menawarkan pendekatan lanjutan untuk memprediksi kapasitas lateral tiang beton prategang dengan menggunakan pembelajaran mesin berdasarkan data simulasi p-y. Dua algoritma pembelajaran mesin akan digunakan: (1) Regresi logistik; (2) *Support Vector Regression* (SVR). Algoritma pertama adalah algoritma klasifikasi; ini digunakan untuk mendiagnosa fitur yang dipilih. Setelah itu, SVR (algoritma regresi) digunakan untuk memprediksi kapasitas lateral tiang. Dalam studi ini, simulasi pembelajaran mesin dilakukan dengan menggunakan GNU Octave. Variasi dari properti tanah dan ukuran tiang beton prategang telah dipertimbangkan didalam model. Akurasi dari hasil prediksi juga didiskusikan.

Kata Kunci: kapasitas lateral tiang, tiang beton prategang, metode p-y, pembelajaran mesin tersupervisi, regresi logistik, support vector regression

ABSTRACT: Predicting lateral pile capacity is one of the routine tasks in geotechnical engineering practice. It is now customary to predict it using p-y approach at which soil layers are modeled as elastoplastic material. This paper proposes an extended approach for predicting lateral pile capacity of Prestressed Concrete (PC) spun pile using machine learning based on p-y simulation data. Two machine learning algorithms are used: (1) Logistic Regression; (2) Support Vector Regression (SVR). The former is the classification algorithm; it is used for diagnosing the selected features. Thereafter, SVR (a regression algorithm) is used for predicting the lateral pile capacity. In this study, the machine learning simulation is performed with GNU Octave. Variation of soil properties and PC pile sizes have been considered; prediction accuracy is also discussed.

Keywords: lateral pile capacity, PC spun pile, p-y analysis, supervised machine learning, logistic regression, support vector regression

1 INTRODUCTION

Piles are structural elements in deep foundation that transfer loading from superstructure onto a firm or less-compressible soils and/or rocks. These piles must resist lateral load, either from wind and/or seismic load or from active earth pressure, hence predicting its capacity is one of the key tasks in geotechnical engineering practices. In comparison to the prediction of pile axial capacity; it is comparatively a complex task involving variables such as: Pile strength and rigidity, soil strength and stiffness, pile-foundation boundary conditions, and the nature of the loading itself.

Empirical approach might have been the preferred approach in the past, prediction was carried out by consulting lateral load test data from similar pile diameters and soil types (e.g. McNulty (1956)). Unfortunately, predicting the lateral pile capacity based on empirical data/anecdotal experiences would typically not yield an accurate prediction, except when applied in the same locality.

Some analytical approaches have been formulated in the past for predicting lateral pile

capacity. Chang (1937), idealizes soils as an elastic material and the laterally loaded pile problem is solved by using simple closed-form formula; details can be consulted in OCDI (2002). In 1960s, Hansen (1961) proposes a simple pile lateral capacity formula based on the premise that pile rotates as a rigid body at failure; then Broms (1964(a,b)) devises an analytical approach based on simplified lateral soil resistance distribution for both cohesive and cohesionless soils.

The following decade saw the rise of discretized soil layer approach. In its simplest form, soil layers are modeled as unconnected elastic springs, Poulos and Davis (1980) (Winkler's model). Following this approach, studies from Matlock (1970), Reese et al. (1974) have extended these springs into non-linear elastoplastic load-deformation curves (now known as p-y approach). Given the pile rigidity and pile-foundation boundary conditions, this problem can be formulated with series of differential equations, it is then very common to solve it with finite difference method, Wang and Reese (1993).

Even though soil layers are not continuum in the p-y approach, comparison with test results indicates that this method provides a good agreement, Reese and Van Impe (2011). In fact, commonly used commercial software for the analysis of laterally loaded piles such as LPILE, Isenhower et al. (2019) and AllPile, CivilTech (2009), they adopt this p-y approach.

By using p-y approach, one can obtain the predicted lateral deflection and maximum moment in pile, in function of the lateral load. Accordingly, the design of pile lateral capacity shall also conform to the following design criteria: (1) Pile shear strength; (2) Deflection limit, and (3) Cracking moment capacity. The data set in this study uses a deflection limit of 12 mm for free-head pile and 6 mm for fixed-head pile, SNI 8460 (2017), NAVFAC (1986)]. The cracking moment capacity of hollow Prestressed Concrete spun pile, hereafter called PC Pile, it follows the JIS A5335 (1987) requirements, a commonly referred standard by PC Pile manufacturer in Indonesia.

In this study, we propose an extended approach based on machine learning for predicting the PC Pile lateral capacity based on data set from p-y analyses; the data set used in this study is described more in details in Section 2. The machine learning method, coined in late 1950s, Samuel (1959), it uses a set of procedures, allowing a computer to learn. Essentially, it imitates the human/animal capability for learning from the experiences.

Fig. 1 shows the comparison of conventional process for predicting lateral pile capacities and the machine learning approach. By using a supervised machine learning algorithm, we let the machine to learn from training data. These training data consist of input data (with multiple features) and prediction data (also known as label). The data diagnostic will be discussed in Section 3.

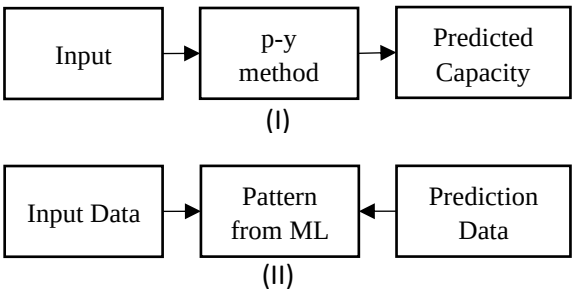

Fig. 1. Comparison of the Conventional Approach for Predicting Lateral Pile Capacity (I) and the Machine Learning Approach (II).

Machine learning gains lots of popularity in the last 15 years or so; it has now been applied to other fields outside the computer science. There have been several studies that apply machine learning approach for predicting pile lateral capacity in clay soil. Das and Basudhar (2006) uses an Artificial Neural Network (ANN). Samui (2008) implements Support Vector Machine (SVM). Muduli et al. (2013) adopt a relatively recent development of feedforward neural network algorithm known as Extreme Learning Machine. [Das and Suman (2015)] discusses the use of two machine learning algorithms: Multivariate Adaptive Regression Spline (MARS) and a variation of neural network concept called Functional Network (FN).

Stunningly, the above-mentioned studies, all of them, use the same data set from, Rao and Kumar (1996). It consists of 75 pile loading test data, but in total only 38-44 data records were used in the mentioned studies (for both training and testing). As far as the author aware, these machine learning models have not been generalized for sandy soil.

In contrast with the above-mentioned studies, in this study, the authors have compiled more than thousand data records (from p-y simulations) allowing the authors to perform in-depth diagnostic of the input features. Indeed, it is a synthetic data, but it covers broader soil

data variations; thus it is supposedly able to predict pile lateral capacity in broad range of soil conditions.

There are two machine learning algorithms that are used in this study. Firstly, we use the one-vs-all logistic regression algorithm for establishing the learning curve and diagnosing the selected features. This machine learning algorithm is a classification algorithm where the labels must be classified into classes.

Thereafter, a Support Vector Regression (SVR) algorithm, more precisely ε-SVR, Vapnik (1998), is used to predict the lateral pile capacity. We use the LIBSVM open-source library developed by Chang and Lin (2011). Iterative process is used to determine the parameters for the prediction purpose. Finally, prediction accuracies are presented and discussed. Both algorithms are implemented using GNU Octave, Eaton et al. (2020).

2 DATA COLLECTION

For performing machine learning study, data availability is necessary. In total, there are 1104 data from p-y analyses that have been accrued by the authors; it comprises of 154 unique (soil) SPT data variations. The p-y analyses have been performed with AllPile version 7. The data set labels have considered the design criteria mentioned previously.

There are 65 features that have been recorded; they are as follows:

- Ground water level.
- Soil type (clay/sand) of the top 10m.
- SPT N-value of the top 10m.
- Cohesion and friction angle of the top 10m.
- Soil modulus variation of the top 10m.
- Axial strain of soil corresponding to one-half of maximum principal stress (ε_{50}) of the top 10 m.
- Pile length and diameter.
- Pile fixity head (free/fixed).
- Pile axial load.

The authors have assumed that 10m of soil data, consisting of one data per meter, should be sufficient for predicting accurately the pile lateral capacity (this will be explored in Section 3). Consequently, the size of data set is uniform, then no further adjustment is required. For learning purpose, feature scaling using z-score normalization has been applied for all the features.

In addition to the SPT N-value, soil cohesion, and soil friction angle; the soil modulus variation k and soil strain at one-half of maximum principal stress ε_{50} are also added in the original feature matrix. These two parameters are used for the construction of p-y curves, Reese and Van Impe (2011). These data are primarily correlated from SPT N-values (see details in CivilTech (2009)).

Certain other parameters are set constant and not considered in the feature matrix, such as: (1) Pile class: Class A with concrete compressive strength $f_c' = 50$ MPa; (2) Pile thickness is tied to the pile diameter as per [JIS A5335 (1987)]; (3) Pile protrusion (eccentricity) is zero.

Fig. 2 shows the statistic of these features, it can be observed that most of the lateral capacity data is in the range of 1-9 ton. The following pile diameters have been represented in the data set: D300, D350, D400, D450, D500, and D600; these are standard pile diameters as regulated in [JIS A5335 (1987)].

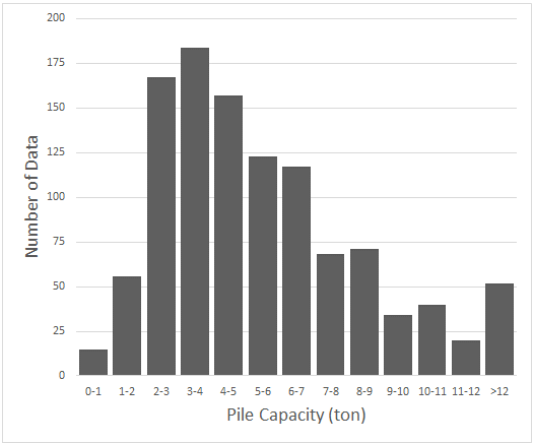

(a)

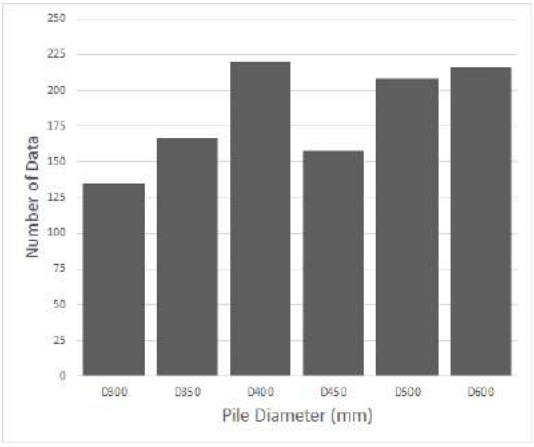

(b)

Fig. 2. Statistic of Lateral Capacity Data By: (a) Classes of Capacities; (2) PC Pile Diameters.

Within the data set, each record is unique. For a general outlook, if one look only the upper 3m of soil data (out of 10m), there are 670

records of clay soil, 216 records of sand soil, and 218 records of mixed soil. Among these, there are 508 data with GWL at surface (0 m).

It must be noted that we do use the actual lateral pile load test data, due to the following reasons:

1) Lateral pile load test data are relatively scarce and might not be well instrumented, while on the other hand, supervised learning requires enough data.
2) Standard Penetration Test (SPT) values in borehole data, it is rarely corrected to N_{60} in Indonesia. When using SPT as predictor, this deficiency would hugely impact the prediction accuracy.
3) There might be in-situ soil variations (e.g., re-compaction of surface layer for working platform) or pile variations (e.g., pile is far thicker); these in-situ variations would inflate the measured pile capacity.

For the purpose of machine learning, the data set will be divided into training data (80%) and cross validation data (20%). This is an important step for checking that the learning parameters can really be generalized. Samples of data set is given in the Appendix.

3 DATA DIAGNOSTIC WITH ONE-VS-ALL LOGISTIC REGRESSION

The authors use one-vs-all logistic regression algorithm for diagnosing the collected data. The logistic regression cost function $J(\theta)$ takes the following form:

$$J(\theta) = -\frac{1}{m}\sum_{i=1}^{m}\left[y^{(i)}\log\left(h_\theta\left(x^{(i)}\right)\right) + \left(1 - y^{(i)}\right)\log\left(1 - h_\theta\left(x^{(i)}\right)\right)\right] + \frac{\lambda}{m}\sum_{j=1}^{n}\left[\theta_j^2\right] \quad (1)$$

where: θ is the model parameters, $x^{(i)}$ is input the features for the $(i)^{th}$ training example, y is the output label, h_θ is the hypothesis function, m is the number of training examples, n is the number input features and λ is the regularization parameter. The regularization parameter is set to $\lambda = 0.1$ in this section.

The hypothesis function in the logistic regression model uses the sigmoid function (a.k.a. logistic function) as follows:

$$h_\theta(x) = \frac{1}{1+e^{-\theta^T x}} \quad (2)$$

In essence, this form of hypothesis function yields a value between 0 and 1; as it is a classification problem, we can take the following decision boundary: $y = 1$ if $h_\theta(x) \geq 0.5$ and $y = 0$ if $h_\theta(x) < 0.5$.

The objective of machine learning model is to minimize the cost function, in this case, the Eqn. (1). In this study, we use an optimization function based on conjugate gradient method called fmincg written by [Rasmussen (2013)]. The maximum iteration is set to 5000 iterations; this applies for each binary learning.

The one-vs-all logistic regression classification is essentially the generalization of binary logistic regression into multi-classes logistic regression. It is done by training the logistic regression classifier $h_\theta^{(i)}(x)$ for each class i; the selected prediction is the one that has the highest probability.

By observing Fig. 2a, we can immediately classify data labels into classes of 0-1, 1-2, …, 10-11, and >11 ton; twelve (12) classes in total. As there aren't many data with lateral capacity greater than 11 ton; for that, these data are consolidated into a single class of ">11 ton".

Having all that, the first question that should be answered is whether the machine learning prediction would be better with more data. This can be learnt by establishing the learning curve. Fig. 3 shows the learning curve of regularized one-vs-all logistic regression.

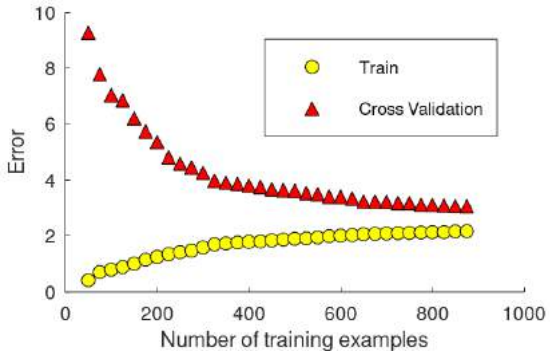

Fig. 3. Learning Curve of Regularized One-vs-All Logistic Regression.

The vertical axis in Fig. 3 shows the optimized cost function values. We can observe that the training and cross validation data slowly converge with more training data; this indicate that providing more data is beneficial. Conversely, we can also say that with limited data (say below 600 training data), the model would have a high variance issue.

Then, we have to justify that learning with 10 m of soil data is acceptable. In order to check this, we run three (3) series of simulations,

named Case X, Case Y, Case Z with soil data of 10 m, 7 m, and 4 m, respectively. Fig. 4 shows the training and cross-validation curves for these cases. It is clear that in Case Z, the training and cross-validation curves are fully closing their gap; meaning it has a bias issue caused by insufficient features. Hence, using only 4 m of soil data is not recommended. The error difference by using less features in Case Y), compared to Case X, is about 4%; Case X is better, as expected.

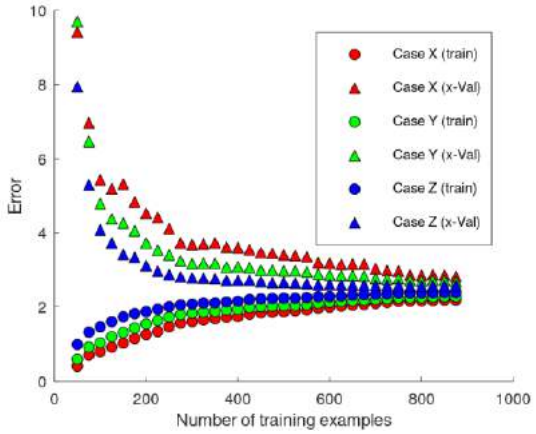

Fig. 4. Learning Curve Comparison of One-vs-All Regularized Logistic Regression: (Case X) Total 10 m of Soil Data; (Case Y) Total 7 m of Soil Data; (Case Z) Total 4 m of Soil Data.

For studying which features are more pertinent, four (4) different cases of soil data features are tested:

- Case 1 is the base case where we use all the mentioned features (see Section 2).
- Case 2 is the case where only SPT N-values are considered (for soil-related data).
- Case 3 is the case where only both cohesion and friction angle are considered.
- Lastly, Case 4 is the case where we exclude parameter k and ε_{50} in the feature matrix.

Fig. 5 shows the cost function of the four (4) mentioned cases. Case 1 produce the best result, as expected, with error of 2.15. Case 2 produce the worst result with error of 2.45 (about 14.0% larger than Case 1); it is not surprising as SPT N-values are only a rough representation of soil properties. Then, in Case 3 where we use soil cohesion and friction angle; it yields an error of 2.36 (about 9.8% larger than Case 1). Now by excluding only parameter k and ε_{50} (essentially using features from Case 2 and Case 3), it can be observed that the error reduces to 2.30 (about 6.9% larger than Case 1).

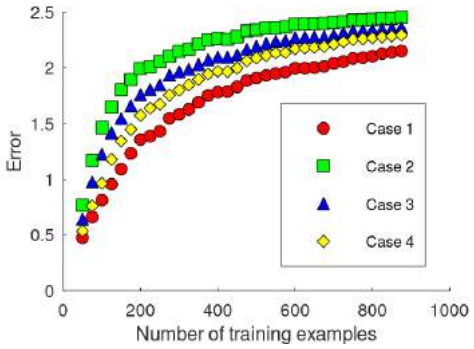

Fig. 5. Cost Function Comparison of One-vs-All Regularized Logistic Regression with Variation of Soil Data Features: (Case 1) Base Case with All Features; (Case 2) Only SPT N-value; (Case 3) Only Cohesion and Friction Angle; (Case 4) SPT N-Value, Cohesion, and Friction Angle, but Excluding k and ε_{50}.

Therefore, there are two (2) things that can be remarked: (1) Adding SPT N-value data to the model just reducing the cost function by 2.8% (Case 3 vs Case 4); focusing on tabulating the correct cohesion and friction angle data is certainly more important; (2) By comparing Case 2 vs Case 4 and Case 1 vs Case 4; we can observe that c, ϕ, k and ε_{50}, they are nearly equally good predictors and should be included in the feature matrix.

We can apply the same cost function comparison for certain auxiliary features, namely pile axial load and pile fixity head (fixed or free). As it can be observed in Fig. 6, these two parameters only marginally affect the overall model accuracy; the cost function increases by approximately 1% when these parameters are neglected.

Diagnostic summary can be seen in Table 1. Relative error is compared to the base case of each respective series. Positive relative error value means that such case would have less prediction accuracy, compared to the base case.

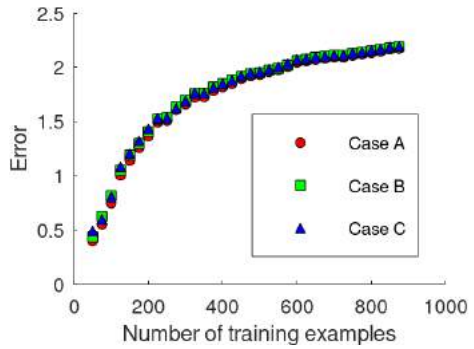

Fig. 6. Cost Function Comparison of One-vs-All Regularized Logistic Regression: (Case A) Base Case with All Features; (Case B) Without Axial Load Data; (Case C) Without Fixity Data.

Table 1. Diagnostic summary of Various Feature Set.

Case	Description	Relative Error
Series 1: Soil data quantity		
X	10m thick of soil data	Base Case
Y	7m thick of soil data	+4.1%
Z	4m thick of soil data	+9.3%
Series 2: Soil properties		
1	All soil features	Base Case
2	Use SPT only	+14.0%
3	Use c & ϕ only	+9.8%
4	Exclude k & ε_{50}	+6.9%
Series 3: Miscellaneous		
A	Base case (all features)	Base Case
B	Without axial data	≈ +1%
C	Without fixity data	≈ +1%

Finally, for an illustration purpose, if we consider that a prediction is accurate within +/- 1 (one) class; prediction accuracies using regularized logistic regression of cross validation set from three random shuffles are as follows 69.23%, 66.51%, and 72.85%. This prediction accuracy could still be improved by adding high-order features through feature mapping process; however, in general it is computationally expensive. In the next section, we use a kernelized SVR algorithm that can provide computationally effective high-order mapping for predicting lateral pile capacities.

4 PILE LATERAL CAPACITY PREDICTION USING SVR

Support Vector Machine (SVM) is a relatively new machine learning algorithm. Developed by Vapnik (1998) and his colleagues at AT&T Bell Laboratories; this algorithm is also known as the large margin classifier; the regression version is called Support Vector Regression (SVR). An overview of this approach is given here.

The cost function of SVR is as follows:

$$J(\theta) = \min_{w,b,\xi_i,\xi_i^*} \frac{1}{2}\|\bar{w}\|^2 + C\sum_{i=1}^{l}(\xi_i + \xi_i^*) \qquad (3)$$

The penalty parameter C is inversely proportional to the regularization parameter λ; it is used to control the slack variable ξ. The slack variable provides a soft margin tolerance. When C is large, the solution tends to be low bias-high variance, it will be prone to overfitting, and vice-versa. The best penalty parameter C must be found through trial-and-error.

The objective of SVR is to find the best "street" that contains the maximum training points within the margin ε as illustrated in Fig. 7. Concretely, the cost function is constrained by the following equations:

$$\bar{w}\varphi(\bar{x}_i) + b - \bar{z}_i \le \varepsilon + \xi_i \qquad (4a)$$

$$\bar{z}_i - \bar{w}\varphi(\bar{x}_i) - b \le \varepsilon + \xi_i^* \qquad (4b)$$

$$\xi_i, \xi_i^* \ge 0, i = 1,2,\dots,l \qquad (4c)$$

The vector $\bar{w}$ shows the normal of "street" median. The vector $\bar{x}_i$ and $\bar{z}_i$ are the feature and output vectors, for all landmark (training) data l. Because the cost function is constrained by Eqn. (4); naturally, this can be solved with Lagrange multiplier method, refer to, Samui (2008) for more details.

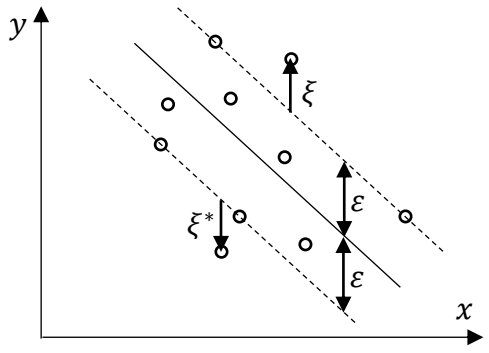

Fig. 7. Illustration of Slack Variable ξ and Margin/Tolerance Parameter ε in SVR Algorithm.

One key aspect in the shown constraints above is the transformed feature vector $\varphi(\bar{x}_i)$;

it represents a vector mapping in higher dimension. This mapping is required to find the hyperplane in higher dimension. Due to the neat formulation of SVR (and SVM in general), we can use a kernel trick to solve this transformed vector, making it computationally effective. In this study, we use the Radial Basis Function (RBF) kernel, formulated as follows:

$$K(\bar{x}, \bar{l}_i) = \exp\left(-\frac{\|\bar{x}-\bar{l}_i\|^2}{2\sigma^2}\right) \quad (5)$$

In summary, the following parameters shall be properly selected so that the SVR model accuracy can be maximized: (1) Penalty parameter, C; (2) Margin, ε; and (3) Kernel parameter, $\gamma = 1/2\sigma^2$.

The authors have used the grid search approach for finding the best parameters. The prediction is classified as accurate if it can predict the pile lateral capacity within +/-1 ton from the actual labelled capacity in the cross-validation data set; it is essentially the same prediction definition as the one used in logistic regression (see Section 3).

After several tries, we found that the best prediction can be obtained when using $\gamma = 2^{-5}$. Setting γ with that constant, contour from the grid-search SVR simulations with variation of c and ε is shown in Fig. 8. The prediction accuracy typically reaches 96%-98% (may vary for different shuffle); far above the prediction accuracy from the logistic regression algorithm.

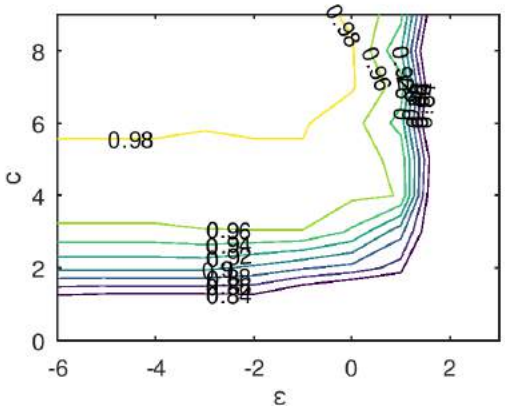

Fig. 8. Prediction Accuracy Contour for Variation of Penalty Parameter c and Margin ε with Constant $\gamma = 2^{-5}$. Note: Both Axes are in Log Base 2.

Now plugging these parameters ($\gamma = 2^{-5}$, $c = 2^{8}$, $\varepsilon = 2^{-4}$) into our data set and running it with three different random shuffles; it yields the following prediction accuracy (against cross validation data set): 95.02%, 99.10%, 97.29%. The corresponding squared correlation coefficients R^2 for these three cases are as follows: 0.9825, 0.9933, 0.9847.

These results show that the learning model (using SVR) can be generalized remarkably well for both clayey and sandy soils, with variations of PC Pile diameters.

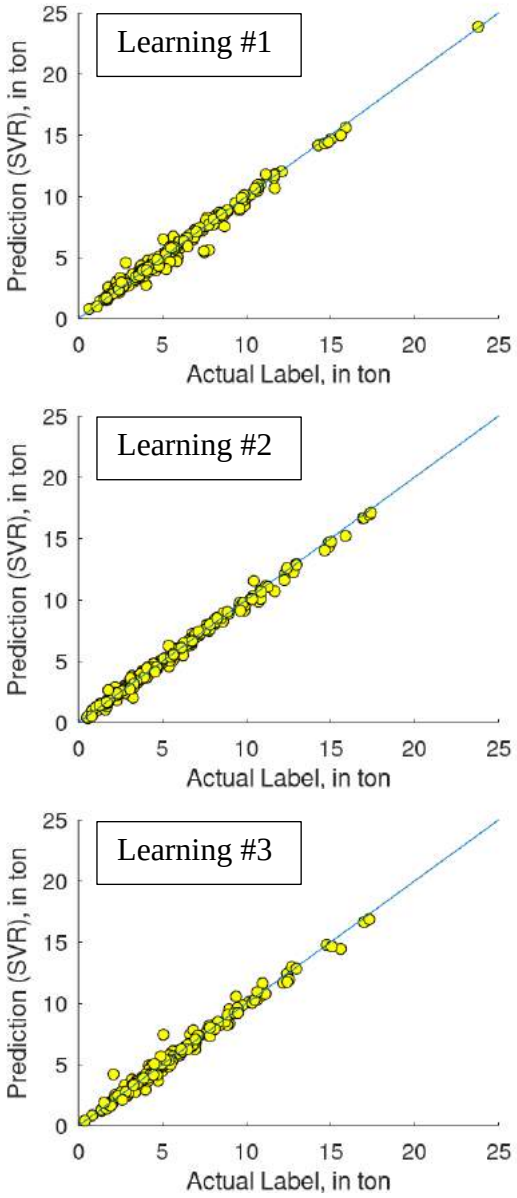

Fig. 9. Performance of SVR Model for Three Random Shuffles using $\gamma = 2^{-5}$, $c = 2^{8}$, $\varepsilon = 2^{-4}$ and RBF Kernel for Predicting Pile Lateral Capacities.

5 CONCLUSION AND DISCUSSION

In this study, the authors have collected 1104 data from p-y analyses with soil data variation and pile diameter variation. For the learning process and the generalization check, the data set have been divided into 80% training data and 20% cross validation data.

For the studied features, learning curve established with one-vs-all logistic regression indicates that the learning would yield qualitatively good generalization (low variance), when there are at least approximately 600 training data. To further illustrate this, using SVR algorithm with the selected parameters as discussed in Section 4, the prediction accuracy falls to 83%-93% with about 440 training data (40% of data set). It falls further to 67%-77% accuracy with about 220 training data (20% of data set); both against the same percentage of cross validation data (20%). This underlines the importance of data set sufficiency in machine learning study.

The diagnostic study shows that by using only four (4) meters of soil layer data; the learning model falls quickly into bias issue; hence it is not recommended to predict pile lateral capacity with only 4 m of soil data. Moreover, it also has been shown that among soil data features, SPT N-value is the least performing predictor.

The selection process of Support Vector Regression (SVR) parameters has been discussed in Section 4. Using the following SVR parameters: $\gamma = 2^{-5}$, $c = 2^{8}$, $\varepsilon = 2^{-4}$, more than 96% prediction accuracy is expected. In perspective, this machine learning model may be extended for further parametric analysis and/or sensitivity study.

REFERENCES

Broms, B.B. 1964a. Lateral Resistance of Piles in Cohesive Soils. *Journal of the Soil Mechanics and Foundations Division* 90(2).

Broms, B.B. 1964b. Lateral Resistance of Piles in Cohesionless Soils. *Journal of the Soil Mechanics and Foundations Division* 90(3).

Chang, C-C & Lin, C-J. 2011. LIBSVM : a Library for Support Vector Machines. *ACM Transactions on Intelligent Systems and Technology* 2(3).

Chang, Y.L. 1937. Discussion on "Lateral Pile Loading Tests by L.B. Feagin. *ASCE Transaction* 102.

CivilTech. 2007. *AllPile Version 7 User's Manual Volume 1 and 2.*

Das, S.K. & Basudhar, P.K. 2006. Undrained Lateral Load Capacity of Piles in Clay Using Artificial Neural Network. *Computer and Geotechnics* 33(8).

Das, S.K. & Suman S. 2015. Prediction of Lateral Load Capacity of Pile in Clay Using Multivariate Adaptive Regression Spline and Functional Network. *Arabian Journal for Science and Engineering* (40).

Eaton, J.W., Bateman D., Hauberg S., & Wehbring R. 2020. *GNU Octave version 6.1.0 Manual: a High-Level Interactive Language for Numerical Computations.*

Hansen, J.B. 1961. The Ultimate Resistance of Rigid Piles Against Transversal Forces. *Bulletin No. 12.* Copenhagen: Danish Geotechnical Institute.

Isenhower, W.M., Wang, S.T., & Vasquez, L.G. 2019. *LPILE 2019 – A Program for the Analysis of Deep Foundations Under Lateral Loading.*

JIS A5335. 1987. *Pretensioned Spun Concrete Piles.*

Matlock, H. 1970. Correlations for Design of Laterally Loaded Piles in Soft Clay. *Proceedings of the Offshore Technology Conference*. Houston, Texas, Paper OTC-1204.

Muduli, P.K., Das S.D., & Das M.R. 2013. Prediction Of Lateral Load Capacity of Piles Using Extreme Learning Machine. *International Journal of Geotechnical Engineering* 7(4).

Naval Facilities Engineer Command (NAVFAC). 1986. *Design Manual 7.02 – Foundations & Earth Structures.*

McNulty, J.F. 1956. Thrust Loading on Piles. *Journal of the Soil Mechanics and Foundations Division* 82(2).

OCDI. 2002. *Technical Standards and Commentaries for Port and Harbour Facilities in Japan.*

Poulos, H.G. & Davis, E.H. 1980. *Pile Foundation Analysis and Design.*

Rao, K.M & Kumar, V.S. 1996. Measured and Predicted Response of Laterally Loaded Piles. *Proceeding 6th International Conference and Exhibition on Piling and Deep Foundations*. India.

Rasmussen, C.E. 2013. *Function « fmincg »: Optimization Function for Continuous Differentiable Multivariate Function.*

Reese, L.C, Cox, W.R., & Koop, F.D. 1974. Analysis of Laterally Loaded Piles in Sand. *Proceedings of the Offshore Technology Conference*. Houston, Texas, Paper OTC-2080.

Reese, L.C. & Van Impe, W.F. 2011. *Single Piles and Pile Groups Under Lateral Loading 2nd Edition.*

Samuel, A. 1959. Some Studies in Machine Learning Using the Game of Checkers. *IBM Journal of Research and Development* 3(3).

Samui, P. 2008. Predicted Ultimate Capacity of Laterally Loaded Piles in Clay Using Support Vector Machine. *Geomechanics and Geoengineering: An International Journal* 3(2).

SNI 8460. 2017. *Persyaratan Perancangan Geoteknik.*

Vapnik, V.N. 1998. *Statistical Learning Theory*.

Wang, S.T. & Reese, L.C. 1993. *COM624P Laterally Loaded Pile Analysis Program for the Microcomputer Version 2.0 (FHWA-SA-91-048).*

APPENDIX: DATA SAMPLE

Parameters	Unit	Data Records												
		1	2	3	4	5	6	7	8	9	10	11	12	…
Pile Capacity (Label)	ton	2.142	3.880	2.470	4.741	1.453	2.738	2.124	3.686	0.789	1.344	1.357	2.368	…
GWL	m	0	0	0	0	0	0	0	0	0	0	0	0	…
Soil Type 0-1m	Clay/Silt/Sand	Clay	Clay	Clay	Clay	Clay	Clay	Clay	Clay	Clay	Clay	Clay	Clay	…
Soil Type 1-2m		Clay	Clay	Clay	Clay	Clay	Clay	Clay	Clay	Clay	Clay	Clay	Clay	…
Soil Type 2-3m		Clay	Clay	Clay	Clay	Clay	Clay	Clay	Clay	Clay	Clay	Clay	Clay	…
Soil Type 3-4m		Clay	Clay	Clay	Clay	Clay	Clay	Clay	Clay	Clay	Clay	Clay	Clay	…
Soil Type 4-5m		Clay	Clay	Clay	Clay	Clay	Clay	Clay	Clay	Clay	Clay	Clay	Clay	…
Soil Type 5-6m		Clay	Clay	Clay	Clay	Clay	Clay	Clay	Clay	Clay	Clay	Clay	Clay	…
Soil Type 6-7m		Clay	Clay	Clay	Clay	Clay	Clay	Clay	Clay	Clay	Clay	Clay	Clay	…
Soil Type 7-8m		Clay	Clay	Clay	Clay	Clay	Clay	Clay	Clay	Clay	Clay	Clay	Clay	…
Soil Type 8-9m		Clay	Clay	Clay	Clay	Clay	Clay	Clay	Clay	Clay	Clay	Clay	Clay	…
Soil Type 9-10m		Clay	Clay	Clay	Clay	Clay	Clay	Clay	Clay	Clay	Clay	Clay	Clay	…
SPT 0-1m	N/A	0	0	0	0	0	0	0	0	0	0	0	0	…
SPT 1-2m		0	0	0	0	0	0	2	2	0	0	0	0	…
SPT 2-3m		0	0	0	0	0	0	0	0	0	0	0	0	…
SPT 3-4m		0	0	0	0	0	0	0	0	0	0	0	0	…
SPT 4-5m		2	2	0	0	0	0	0	0	2	2	0	0	…
SPT 5-6m		2	2	50	50	0	0	0	0	2	2	0	0	…
SPT 6-7m		9	9	50	50	21	21	20	20	9	9	0	0	…
SPT 7-8m		9	9	50	50	50	50	37	37	9	9	27	27	…
SPT 8-9m		9	9	50	50	50	50	37	37	9	9	27	27	…
SPT 9-10m		17	17	50	50	50	50	50	50	17	17	40	40	…
Phi 0-1m	Degree	0	0	0	0	0	0	0	0	0	0	0	0	…
Phi 1-2m		0	0	0	0	0	0	0	0	0	0	0	0	…
Phi 2-3m		0	0	0	0	0	0	0	0	0	0	0	0	…
Phi 3-4m		0	0	0	0	0	0	0	0	0	0	0	0	…
Phi 4-5m		0	0	0	0	0	0	0	0	0	0	0	0	…
Phi 5-6m		0	0	0	0	0	0	0	0	0	0	0	0	…
Phi 6-7m		0	0	0	0	0	0	0	0	0	0	0	0	…
Phi 7-8m		0	0	0	0	0	0	0	0	0	0	0	0	…
Phi 8-9m		0	0	0	0	0	0	0	0	0	0	0	0	…
Phi 9-10m		0	0	0	0	0	0	0	0	0	0	0	0	…
Cohesion 0-1m	kN/m^2	1.8	1.8	1.8	1.8	1.8	1.8	1.8	1.8	1.8	1.8	1.8	1.8	…
Cohesion 1-2m		1.8	1.8	1.8	1.8	1.8	1.8	14.4	14.4	1.8	1.8	1.8	1.8	…
Cohesion 2-3m		1.8	1.8	1.8	1.8	1.8	1.8	1.8	1.8	1.8	1.8	1.8	1.8	…
Cohesion 3-4m		1.8	1.8	1.8	1.8	1.8	1.8	1.8	1.8	1.8	1.8	1.8	1.8	…
Cohesion 4-5m		12	12	1.8	1.8	1.8	1.8	1.8	1.8	12	12	1.8	1.8	…
Cohesion 5-6m		12	12	296.9	296.9	1.8	1.8	1.8	1.8	12	12	1.8	1.8	…
Cohesion 6-7m		51.5	51.5	296.9	296.9	126.9	126.9	119.7	119.7	51.5	51.5	1.8	1.8	…
Cohesion 7-8m		51.5	51.5	296.9	296.9	298.7	298.7	222	222	51.5	51.5	160.4	160.4	…
Cohesion 8-9m		51.5	51.5	296.9	296.9	298.7	298.7	222	222	51.5	51.5	160.4	160.4	…
Cohesion 9-10m		102.3	102.3	296.9	296.9	298.7	298.7	300.4	300.4	102.3	102.3	239.4	239.4	…
k 0-1m	MN/m3	1.1	1.1	1.1	1.1	1.1	1.1	1.1	1.1	1.1	1.1	1.1	1.1	…
k 1-2m		1.1	1.1	1.1	1.1	1.1	1.1	9	9	1.1	1.1	1.1	1.1	…
k 2-3m		1.1	1.1	1.1	1.1	1.1	1.1	1.1	1.1	1.1	1.1	1.1	1.1	…
k 3-4m		1.1	1.1	1.1	1.1	1.1	1.1	1.1	1.1	1.1	1.1	1.1	1.1	…
k 4-5m		7.5	7.5	1.1	1.1	1.1	1.1	1.1	1.1	7.5	7.5	1.1	1.1	…
k 5-6m		7.5	7.5	661.3	661.3	1.1	1.1	1.1	1.1	7.5	7.5	1.1	1.1	…
k 6-7m		67.7	67.7	661.3	661.3	238.5	238.5	221	221	67.7	67.7	1.1	1.1	…
k 7-8m		67.7	67.7	661.3	661.3	665.3	665.3	479.8	479.8	67.7	67.7	322.2	322.2	…
k 8-9m		67.7	67.7	661.3	661.3	665.3	665.3	479.8	479.8	67.7	67.7	322.2	322.2	…
k 9-10m		179.6	179.6	661.3	661.3	665.3	665.3	669.4	669.4	179.6	179.6	523.5	523.5	…
e_{50} 0-1m	%	5.38	5.38	5.38	5.38	5.38	5.38	5.38	5.38	5.38	5.38	5.38	5.38	…
e_{50} 1-2m		5.38	5.38	5.38	5.38	5.38	5.38	2.08	2.08	5.38	5.38	5.38	5.38	…
e_{50} 2-3m		5.38	5.38	5.38	5.38	5.38	5.38	5.38	5.38	5.38	5.38	5.38	5.38	…
e_{50} 3-4m		5.38	5.38	5.38	5.38	5.38	5.38	5.38	5.38	5.38	5.38	5.38	5.38	…
e_{50} 4-5m		2.32	2.32	5.38	5.38	5.38	5.38	5.38	5.38	2.32	2.32	5.38	5.38	…
e_{50} 5-6m		2.32	2.32	0.33	0.33	5.38	5.38	5.38	5.38	2.32	2.32	5.38	5.38	…
e_{50} 6-7m		0.96	0.96	0.33	0.33	0.55	0.55	0.57	0.57	0.96	0.96	5.38	5.38	…
e_{50} 7-8m		0.96	0.96	0.33	0.33	0.33	0.33	0.39	0.39	0.96	0.96	0.48	0.48	…
e_{50} 8-9m		0.96	0.96	0.33	0.33	0.33	0.33	0.39	0.39	0.96	0.96	0.48	0.48	…
e_{50} 9-10m		0.63	0.63	0.33	0.33	0.33	0.33	0.33	0.33	0.63	0.63	0.38	0.38	…
Pile Length	M	13	13	7	7	8	8	12	12	13	13	13	13	…
Pile Diameter	mm	600	600	600	600	600	600	600	600	400	400	600	600	…
Pile Fixity Head	Free / Fixed	Free	Fixed	Free	Fixed	Free	Fixed	Free	Fixed	Free	Fixed	Free	Fixed	…

Analisis Tekanan Air Pori Ekses Akibat Pemancangan dengan Metode Numerik untuk Prediksi Soil Setup pada Tanah Lempung

David Wibisono Setiabudi
Universitas Katolik Parahyangan

Paulus Pramono Rahardjo
Universitas Katolik Parahyangan

Budijanto Widjaja
Universitas Katolik Parahyanagan

ABSTRAK: Pemancangan tiang pada tanah lempung lunak akan menimbulkan peningkatan tekanan air pori ekses (Δ_u) yang menyebabkan tegangan vertikal efektif tanah (σ_v') akan berkurang. Seiring dengan bertambah waktu, Δ_u akan mengalami proses disipasi, lamanya proses disipasi bergantung pada permeabilitas suatu partikel tanah. Dalam proses disipasi, daya dukung tanah akan meningkat. Peristiwa peningkatan daya dukung tiang terhadap waktu dikenal sebagai fenomena *soil setup*. Penelitian ini dilakukan dengan mengambil sampel pada tanah lempung Cirebon, dimana tanah lempung konsistensi lunak ditemukan setebal 12 m. Pemancangan tiang dengan jenis tiang *concrete spun* sedalam 35 m, dilakukan uji dinamik (PDA) pada waktu *end of driving* (eod), 30 menit, 3 hari, dan 7 hari; kemudian pada waktu 30hari dilakukan uji statik tekan terinstrumentasi. Penelitian ini mengkaji secara numerik perubahan Δ_u dan prediksi *soil setup* dengan menggunakan pendekatan *cavity expansion* pada beberapa waktu yang ditentukan, yaitu eod, 30 menit, 1 hari, 3 hari, 7 hari, 30 hari, 60 hari, dan 365 hari. Hasil dari penelitian ini menunjukan bahwa perubahan Δ_u signifikan terjadi pada waktu 30 menit ke 1 hari, berbanding lurus dengan peningkatan daya dukung pada waktu tersebut. Penelitian ini kemudian dilanjutkan untuk memprediksi besarnya nilai *soil setup* (A) berdasarkan metode Skov & Denver, diperoleh bahwa dari hasil uji lapangan A = 0,13; sedangkan berdasarkan hasil numerik diperoleh nilai A = 0,13 – 0,19. Jadi, penelitian dengan model numerik dapat memberikan hasil yang cukup mendekati dengan hasil uji lapangan.

Kata Kunci: tekanan air pori ekses, soil setup, cavity expansion¸ PDA, uji beban statik terinstrumentasi

ABSTRACT: Excess pore pressure (Δ_u) arises as the result of pile driving in case of soft soil. Considerable excess pore pressure causes low pile capacity. As the soil surrounding the pile recovers from the installation disturbance, a time dependent increase in pile capacity often occurs, this phenomenon is referred to as "set-up". The objective of this research is to determine the excess pore pressure behavior and predict the soil setup with modelling pile driving using cavity expansion theory. This research is carried out with soil data from Cirebon soil, which found 12 m thickness of soft clay layer. The concrete spun pile with closed ended pipe was driven into 35 m depth; to determine the soil setup phenomena dynamic test (PDA) monitoring was performed during pile driving (eod), 30 min, 3 days, and 7 days; then 30 days instrumented static load test was performed. This research of Δ_u and soil setup was performed with numerical analysis with cavity expansion theory approach, with variation of time from eod, 30 mins, 1 days, 3 days, 7 days, 30 days, 60 days, and 365 days. Result shows the value of excess pore pressure is decrease as it increases time, proportional with increasing of pile resistance. To predict the soil setup value (A) is used Skov & Denver method, based on in-situ test using PDA and instrumented static load test shows the A = 0.13, while using numerical analysis obtained the A = 0.13 – 0.19. Thus, this research contributes to at least can explain the prediction of soil setup with result of numerical model is approach the in-situ test result.

Keywords: excess pore pressure, soil setup, cavity expansion, PDA, instrumented static load test

1 PENDAHULUAN

Perhitungan daya dukung fondasi tiang pancang, pada umumnya diestimasikan dengan formula statik berdasarkan data penyelidikan tanah. Penyelidikan tanah tersebut umumnya dilakukan sebelum proses pemancangan dilakukan. Perlu diketahui bahwa, akibat dari pemancangan akan memberikan dampak berupa perubahan kondisi tanah di sekitar selimut dan ujung tiang. De Mello (1969) mengklasifikasikan efek dari pemancangan pada tanah lempung menjadi empat kategori utama: (1) ketergangguan atau kerusakan pada tanah di sekeliling tiang, (2) alterasi kondisi tegangan tanah pada tiang, (3) disipasi tekanan air pori ekses, (4) fenomena jangka panjang terbentuknya kembali daya dukung atau tegangan tanah. Pemancangan tiang pada tanah lempung lunak akan menimbulkan adanya peningkatan tekanan air pori ekses (Δ_u), seiring proses disipasi dari tekanan air pori ekses (Δ_u) maka daya dukung tanah akan terbentuk kembali bahkan meningkat. Fenomena ini dikenal sebagai *soil setup*.

Pada makalah ini, dibahas mengenai studi kasus pada proyek yang berlokasi di Cirebon, Jawa Tengah, Indonesia. Digunakan fondasi tiang pancang (*spun pile*) diameter 600mm. Pemancangan dilakukan dengan menggunakan *diesel hammer* jenis PILECO D46-32. Selama pemancangan dilakukan *monitoring* secara kontinu menggunakan *Pile Driving Analyzer* (PDA). Untuk memprediksi nilai *soil setup*, dilakukan uji PDA pada waktu yang berbeda. Makalah ini juga membahas mengenai analisis secara numerik perubahan tekanan air pori ekses (Δ_u) dan *soil setup*.

2 DATA PROYEK

2.1 *Data Penyelidikan Tanah*

Data investigasi geoteknik yang dilakukan terdiri dari *drilling log* dan *Standard Penetration Test* (SPT). Lokasi titik penyelidikan tanah dan titik tiang uji (TP-1) ditunjukkan pada Gbr. 1. Stratifikasi tanah pada area ini ditampilkan pada potongan A-A' yang disajikan pada Gbr. 2. Dapat dilihat pada potongan A-A', kondisi tanah pada proyek ini didominasi oleh tanah lempung, di mana tanah lempung dengan konsistensi sangat lunak (*very soft clay*) ditemukan pada kedalaman 0 hingga 12 m, diikuti dengan tanah lempung dengan konsistensi medium hingga teguh pada kedalaman ±12-18 m. Kemudian, lensa pasir dengan konsistensi padat-sangat padat. Pada kedalaman 20 hingga 50 m kembali ditemukan lapisan tanah lempung dengan konsistensi sangat teguh.

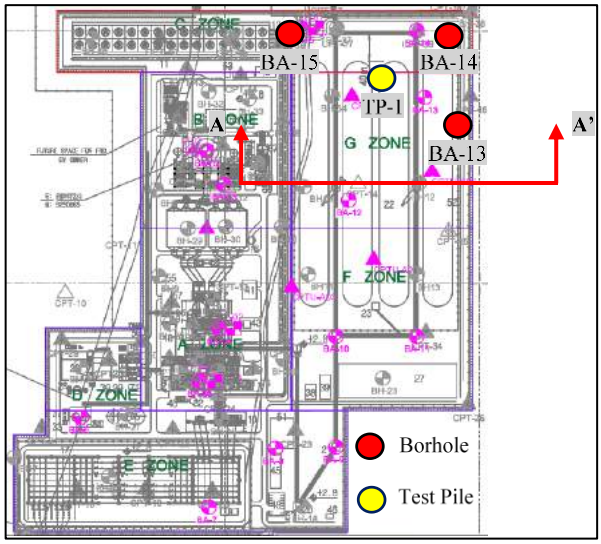

Gbr. 1. Lokasi Tiang Uji dan Titik Penyelidikan Tanah.

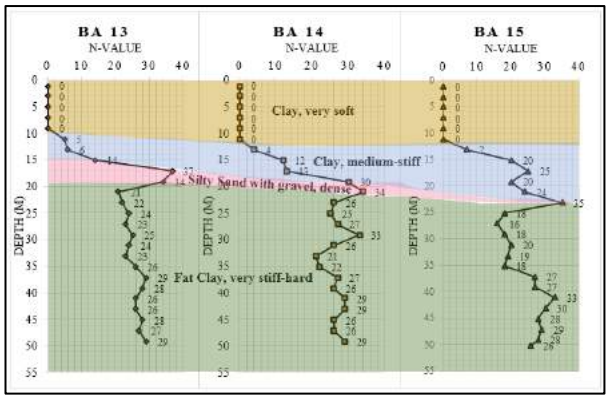

Gbr. 2. Stratifikasi Tanah pada Potongan A-A'.

2.2 *Data Tiang Uji*

Sistem fondasi tiang digunakan tiang pancang jenis *spun pile* dengan diameter 600 mm. Pemancangan dilakukan dengan sistem *diesel hammer* jenis PILECO D46-32, berat *hammer* adalah 46 kN dengan tinggi jatuh 2 m. Pemancangan tiang dilakukan hingga kedalaman penetrasi tiang mencapai 35 m. Selama proses pemancangan dilakukan *monitoring* secara kontinu menggunakan uji PDA sehingga perilaku tiang dan performa *hammer* di setiap kedalaman penetrasi tiang

dapat di *monitoring* secara aktual. Gbr. 3. menujukkan hasil daya dukung ultimit tiang (RMX) dan energi *hammer* (EMX) yang terukur pada setiap kedalaman penetrasi.

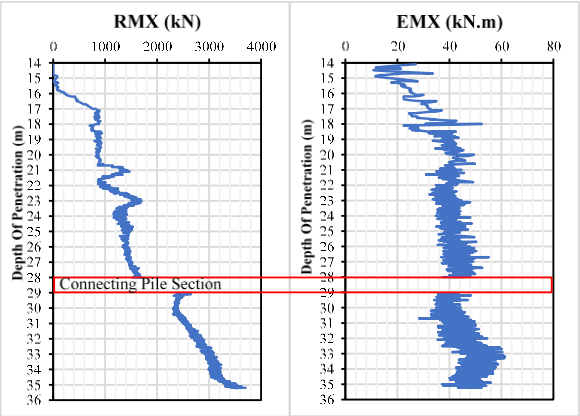

Gbr. 3. Hasil *Monitoring* Kontinu PDA.

Monitoring PDA mulai dilakukan pada *section* tiang *middle* dikarenakan *section* tiang *bottom* sepanjang ±12 m penetrasi ke dalam tanah tanpa adanya perlawanan dari tanah. Jumlah *blow* dan *final set* adalah 1905 *blow* dan 23 mm/10 *blow* secara berturut-turut. Melalui *monitoring* PDA dapat melihat konsistensi performa *gammer*, nilai EMX yang terukur cukup konsisten yaitu pada rentang 40 – 50 kN-m; dapat dikatakan bahwa *hammer* dalam performa yang baik. Pemancangan berhenti pada kedalaman 35 m, di mana ujung tiang berada pada tanah lempung sangat teguh berdasarkan data penyelidikan tanah dengan nilai daya dukung ultimit tiang (RMX) bernilai 3000 – 3500 kN pada akhir pemancangan (*end of driving*; EOD). Setelah akhir pemancangan (EOD), PDA kembali dilakukan (PDA *restrike*) dalam 3 waktu yang berbeda, yaitu: 30 menit, 3 hari, dan 7 hari. PDA *restrike* dilakukan salah satunya unruk mengetahui besarnya nilai *soil setup*. Hasil uji PDA pada beberapa waktu ditunjukkan pada Tabel 1.

Tabel 1. Hasil Daya Dukung Tiang dari Uji PDA.

Time	RMX (kN)	CAPWAP Analysis		
		Friction capacity (kN)	End Bearing capacity (kN)	Ultimate capacity (kN)
EOD	3220	2310,5	554,1	2864,8
30min	3570	2390,7	488,9	2879,6
3days	4230	3923,2	391,4	4314,6
7days	4290	3997,6	398,7	4396,6

Hasil uji PDA menunjukkan bahwa terjadi peningkatan daya dukung yang cukup signifikan pada waktu 30 menit dan 3 hari dari waktu EOD, sedangkan peningkatan daya dukung tiang pada waktu 3 hari ke 7 hari tidak signifikan. Lebih lanjut, dilakukan analisis CAPWAP guna melakukan proses *matching* kurva gelombang antara data aktual dengan data perhitungan; selain itu CAPWAP juga dapat memunculkan berapa nilai daya dukung friksi dan daya dukung ujung. Pada Tabel 1, terlihat peningkatan daya dukung tiang terjadi pada porsi daya dukung friksi. Sedangkan pada porsi daya dukung ujung tidak terlihat adanya peningkatan, hal ini kemungkinan dikarenakan energi *hammer* yang kurang besar sehingga energi tersebut tidak dapat memobilisasi daya dukung di sepanjang tiang.

3 TEKANAN AIR PORI EKSES AKIBAT PEMANCANGAN TIANG

Pemancangan tiang pada tanah lempung jenuh dapat menyebabkan munculnya tekanan air pori ekses (Δ_u). Besarnya nilai Δ_u dapat mencapai 1,5 hingga 2 kali terhadap nilai tegangan efektif tanah (σ_v'); nilai Δ_u akan lambat laun berkurang dan bernilai 0 ketika mencapai kembali pada kondisi tekanan hidrostatik pada jarak 30 – 40 diameter tiang. Beberapa metode telah dikembangkan untuk memprediksi distribusi dari peningkatan Δ_u pada tanah lempung jenuh di sekitar pemancangan tiang. Lo dan Stermac (1965) menurunkan persamaan untuk mengestimasi besarnya nilai Δ_u yang terjadi. Persamaan ini mempertimbangkan zonasi kerusakan radial dari tanah di sekitar tiang pancang, sebagai berikut:

$$\frac{\Delta u_m}{\sigma_{vo}'} = \left[(1 - K_o) + \frac{2S_u}{\sigma_{vo}'}\right] A_f \qquad (1)$$

di mana Δu_m adalah nilai tekanan air pori ekses maksimum, σ_{vo}' adalah nilai tegangan efektif tanah, K_o adalah koefisien tegangan tanah *at rest*, A_f adalah koefisien tekanan air pori saat gagal, dan S_u adalah kuat geser tanah tak teralir.

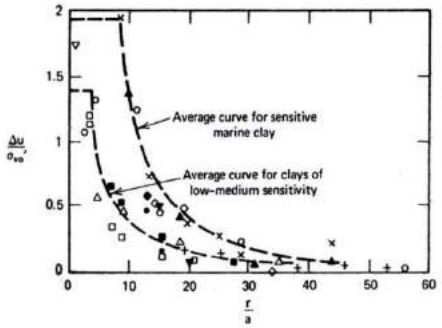

Gbr. 4. Hubungan Δ_u/σ_{vo}' dan r/a.

Airhart et al. (1969) menyatakan bahwa di daerah sekitar ujung tiang, Δ_u akan bernilai 3 hingga 4 kali dari σ_{vo}'. Pada r/a lebih besar dari 4 pada tanah lempung terkonsolidasi normal dan lebih besar 8 pada tanah lempung sensitif, maka Δ_u akan cepat terdisipasi, sedangkan jika r/a lebih besar dari 30 maka Δ_u dapat diabaikan.

4 STUDI *SOIL SETUP* DENGAN UJI DINAMIK

Mengukur perubahan daya dukung akibat *setup*, dibutuhkan minimal dua nilai daya dukung yang terukur dalam waktu yang berbeda. Pengukuran pertama dilakukan saat akhir pemancangan, dan pengukuran berikutnya dilakukan pada jeda waktu yang cukup panjang setelah akhir pemancangan, Komurka (2004). Tan et al. (2004) mengusulkan mengenai pengukuran kedua dilakukan setelah 24 jam pada jenis tanah pasiran, dengan pertimbangan bahwa pada tanah pasiran akan terjadi disipasi tekanan air pori ekses yang relatif cepat.

Terdapat beberapa persamaan empiris yang dapat digunakan untuk memprediksi perubahan daya dukung tiang terhadap waktu. Salah satu persamaan umum yang paling sering digunakan adalah persamaan empiris yang diusulkan oleh Skov dan Denver (1988), yaitu:

$$\frac{Q_{st}}{Q_{so}} = A.\log\left(\frac{t}{t_o}\right) + 1 = \left(\frac{m_s}{Q_{so}}\right) log\left(\frac{t}{t_o}\right) + 1 \quad (2)$$

di mana A adalah faktor *setup* tidak berdimensi, Q_{st} adalah daya dukung friksi tiang saat waktu t, Q_{so} adalah daya dukung friksi tiang saat waktu inisial t_o, t adalah waktu sejak EOD, t_o adalah waktu referensi, dan m_s adalah persamaan kemiringan semilog dari grafik Q_s terhadap waktu dalam skala log.

Bullock et al. (2005), Axelsson (1998a), dan Chow et al. (1998) menyimpulkan bahwa fenomena *soil setup* terjadi akibat peningkatan daya dukung friksi tiang, bukan *end bearing* tiang. Hal ini terjadi akibat penetrasi tiang yang mengakibatkan tanah bergerak keluar dan menjauhi tiang, terjadi destrukturisasi dan perubahan gaya geser tanah yang terjadi pada sisi selimut tiang lebih signifikan daripada ujung tiang. Analisis CAPWAP yang dilakukan pada kasus proyek ini menunjukkan bahwa terjadi peningkatan yang signifikan pada daya dukung friksi tiang, sedangkan daya dukung ujung tidak mengalami peningkatan. Gbr. 5 dan Gbr. 6 menunjukkan peningkatan daya dukung friksi terhadap waktu pada proyek ini.

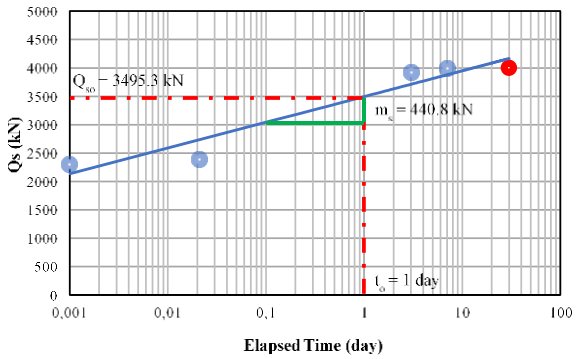

Gbr. 5. Penentuan nilai m_s dan Q_{so}.

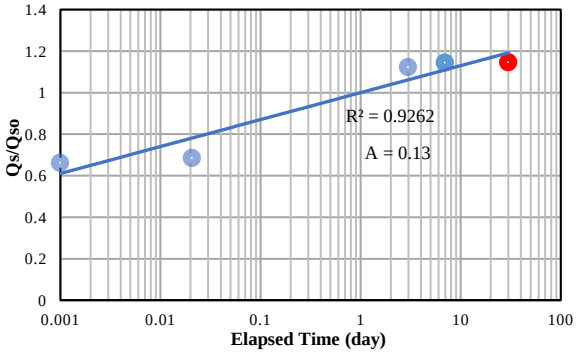

Gbr. 6. Penentuan Nilai *Soil Setup* (A).

Bullock et al. (2005) merekomendasikan nilai t_o = 1 hari untuk menghilangkan kesulitan dalam menentukan waktu mulai pada grafik semilog-linear *setup* dan nilai A mendeskripsikan daya dukung friksi saja bukan total daya dukung. Sebagai pendekatan, daya dukung saat waktu EOD diplot pada waktu 1 menit. Berdasarkan Gbr. 6, daya dukung tiang pada proyek ini meningkat 1,13 kali dari daya dukung tiang saat EOD.

5 CYLINDRICAL CAVITY EXPANSION

Teori *cavity expansion* dapat dibagi ke dalam zona elastis dan plastis. Asumsi mengenai *cylindrical cavity expansion* diuraikan sebagai berikut:

1. Memodelkan tegangan dalam kondisi simetri aksial (*axial symmetric*) pada tanah terkonsolidasi normal.
2. Terdapat partikel solid yang termampatkan, deformasi tanah terbentuk akibat adanya jarak antar partikel dari air atau air yang keluar.
3. Tanah memiliki daya lekat atau kohesi yang rendah.

4. Silinder dipertimbangkan memiliki lingkup yang tidak terbatas dan terkepung oleh massa tanah yang tidak terbatas.
5. Tegangan utama di sekeliling silinder, dinotasikan sebagai: $\sigma_r = \sigma_1$ dan $\sigma_t = \sigma_3$.

Gbr. 7. mengilustrasikan mengenai proses *cavity expansion* menggunakan kriteria kegagalan Mohr-Coulomb dan tegangan radial vs modulus deformasi.

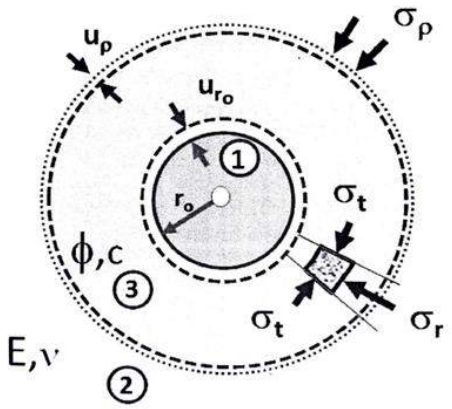

Gbr. 7. Ilustrasi *Cylindrical Cavity Expansion*, Mecsi (2013).

Mecsi menjelaskan bahwa terdapat tiga zona utama dalam teori *cavity expansion* ketika tanah mulai untuk mengembang.

- Zona 1 merupakan mulainya pengembangan volume rongga tanah.

$$(r_u^2 - r_o^2).\pi \quad (3)$$

- Zona 2 merupakan perpindahan tanah menuju zona elastis.

$$[\rho^2 - (\rho - u_p)^2].\pi \quad (4)$$

- Zona 3 merupakan perubahan volume tanah menuju zona plastis.

$$\Delta.(\rho^2 - r_u^2).\pi \quad (5)$$

Besarnya pengembangan tanah dapat dihitung sebagai total dari zona 2 ditambah dengan zona 3.

6 HASIL DAN ANALISIS MODEL

Analisis numerik dengan bantuan *software* Plaxis 2D dilakukan untuk mensimulasikan perubahan tekanan air pori ekses dan prediksi *soil setup*. Fondasi tiang pancang dimodelkan secara *axisymetry* dengan model material *linear-elastic* dan *non-porous*. Proses pemancangan dimodelkan dengan pendekatan teori *cavity expansion*, di mana tiang dimodelkan dengan kondisi awal diameter adalah 0,05 m; kemudian diberikan gaya *displacement* secara horizontal sebesar 0,25 m sehingga membentuk jari-jari (r) tiang adalah 0,30 m atau sama dengan diameter 0,60 m.

Untuk memodelkan perubahan tekanan air pori ekses, dilakukan analisis konsolidasi dengan variasi waktu, yaitu EOD, 30 menit, 1 hari, 3 hari, 7 hari, 14 hari, 30 hari, 60 hari, dan 365 hari. Gbr. 8. menunjukkan pemodelan analisis secara numerik. Analisis daya dukung tiang dilakukan dengan memberikan gaya *displacement* arah vertikal sebesar 25 mm. Nilai ini dipertimbangkan sebagai batasan *displacement* untuk memobilisasi daya dukung tiang.

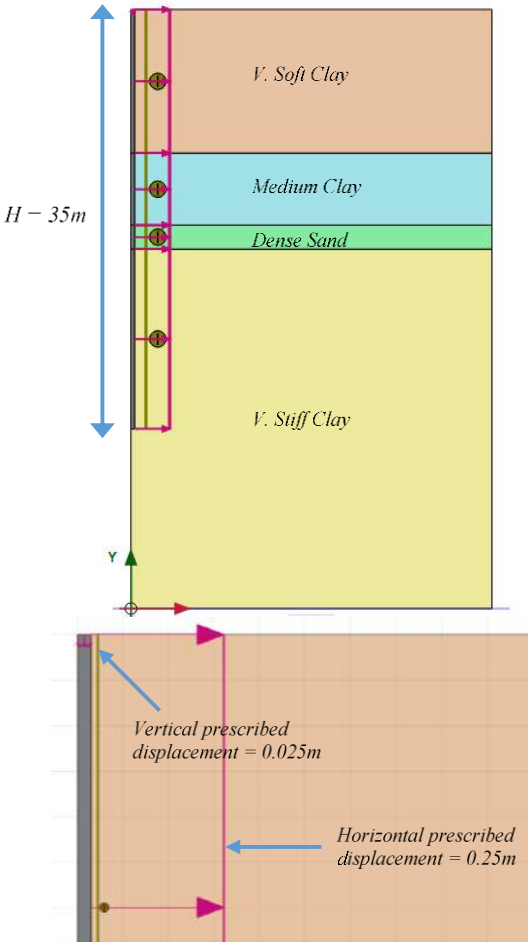

Gbr. 8. Model Numerik 2D.

Layer lempung lunak dimodelkan menggunakan model konstitutif yaitu *Soft Soil model* (SS), sedangkan layer lempung medium-teguh dan layer pasir padat dicoba dimodelkan dengan model konstitutif yang berbeda yaitu

Mohr Coulomb (MC) dan *Hardening Soil* (HS). Parameter tanah yang digunakan dalam analisis numerik ini ditampilkan pada Tabel 2 dan Tabel 3.

Tabel 2. Parameter Tanah Model SS-MC.

	Soft Clay	Medium Clay	Dense Sand	Stiff Clay
Model	Soft Soil	Mohr Coulomb		
Type	Undrained A	Undrained A	Drain	Undrained A
γ unsat	15,5	17,6	20	20
γ sat	14,5	16,6	19	19
λ*	0,098	-	-	-
κ*	9,84 x 10^{-3}	-	-	-
k	2 x 10^{-5}	7,4 x 10^{-5}	4,32	4,4 x 10^{-4}
$R_{interface}$	0,75	0,75	1,0	0,75

Tabel 3. Parameter Tanah Model SS-HS.

	Soft Clay	Medium Clay	Dense Sand	Stiff Clay
Model	Soft Soil	Hardening Soil		
Type	Undrained A	Undrained A	Drain	Undrained A
γ unsat	15,5	17,6	20	20
γ sat	14,5	16,6	19	19
λ*	0,098	-	-	-
κ*	9,84 x 10^{-3}	-	-	-
E_{50}^{ref}	-	5100	26300	6400
E_{oed}^{ref}	-	5100	26300	6400
E_{ur}^{ref}	-	10200	52600	12800
k	2 x 10^{-5}	7,4 x 10^{-5}	4,32	4,4 x 10^{-4}
$R_{interface}$	0,75	0,75	1,0	0,75

6.1 *Hasil Analisis Perubahan Tekanan Air Pori Ekses*

Hasil analisis dengan menggunakan dua pendekatan parameter tanah menunjukkan perilaku perubahan tekanan air pori ekses (Δ_u) yang mirip yang ditandai dengan terbentuknya kurva lengkung *isochrone* pada tanah lempung, sedangkan pada tanah pasir di kedalaman 18-20 m tidak terlihat terjadinya peningkatan Δ_u. Nilai Δ_u kemudian berangsur-angsur terdisipasi seiring bertambahnya waktu; disipasi Δ_u cukup signifikan terjadi pada waktu 30 menit ke 1 hari. Gbr. 9. menunjukkan analisis tren perubahan nilai Δ_u terhadap kedalaman pada waktu yang bervariasi. Nilai perubahan Δ_u ditampilkan pada Tabel 4 dan Tabel 5.

Analisis numerik kemudian dilanjutkan untuk menentukan distribusi Δ_u terhadap jarak pemancangan untuk mengetahui sejauh mana efek pemancangan terhadap kondisi tanah di sekitar khususnya pada tanah lempung lunak. Diambil beberapa jarak (r) dalam analisis, yaitu 0,5 m; 1 m; dan 1,5 m. Dengan model SS-MC diperoleh nilai Δ_u meningkat sebesar 1.,5 kali dari nilai σ_v'; sedangkan pada model SS-HS diperoleh nilai Δ_u meningkat sebesar 1,7 kali dari nilai σ_v'. Kemudian, rasio nilai Δ_u/σ_v' tersebut diplot terhadap r/a dan dibandingkan terhadap penelitian terpublikasi, ditunjukkan pada Gbr. 10.

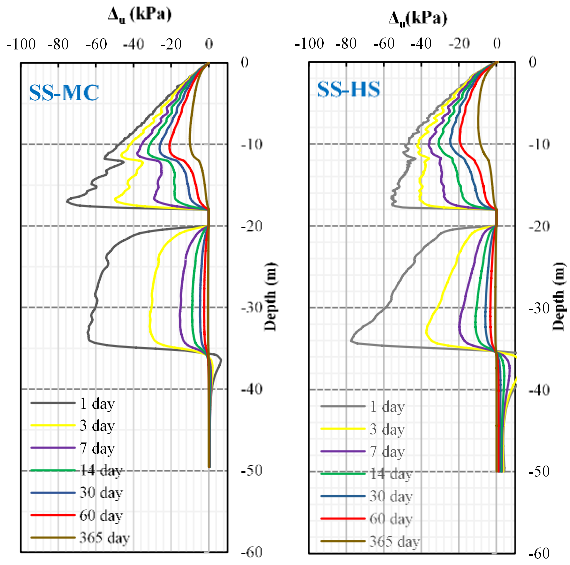

Gbr. 9. Hasil Perubahan Tekanan Air Pori Ekses Terhadap Waktu.

Perubahan nilai tekanan maksimum air pori terhadap waktu pada masing-masing layer tanah ditampilkan pada Tabel 4 dan Tabel 5.

Tabel 4. Perubahan Δ_u Model SS-MC.

Soil	Δu (kPa)								
	EOD	30 min	1 days	3 days	7 days	14 days	30 days	60 days	365 days
Soft Clay	107,8	76,7	55,4	46,6	38,0	32,3	26,0	20,9	10,1
Med Clay	146,5	113,7	75,2	49,8	29,1	21,3	16,5	12,8	4,9
Dense Sand	82,0	7,8	0,2	0,1	0,0	0,0	0,0	0,0	0,0
Stiff Clay	318,5	284,8	64,4	31,4	15,3	8,9	4,7	2,5	0,5

Tabel 5. Perubahan Δ_u Model SS-HS.

Soil	Δu (kPa)								
	EOD	30 min	1 days	3 days	7 days	14 days	30 days	60 days	365 days
Soft Clay	109,6	58,2	49,8	42,3	36,2	30,8	24,7	19,7	9,7

Soil	Δu (kPa)								
	EOD	30 min	1 days	3 days	7 days	14 days	30 days	60 days	365 days
Med Clay	165,8	78,5	56,1	41,1	30,4	23,4	16,7	11,8	4,2
Dense Sand	157,3	15,5	0,3	0,1	0,1	0,0	0,0	0,0	0,0
Stiff Clay	300,3	292,6	77,6	37,4	19,8	11,2	5,9	3,4	0,7

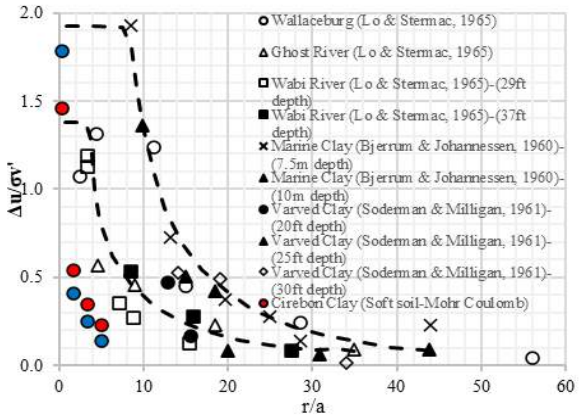

Gbr. 10. Perbandingan Hasil Analisis Numerik Terhadap Pengukuran Δ_u Terpublikasi.

Pada Gbr. 10. menunjukkan bahwa plot hasil analisis secara numerik sedikit lebih di bawah dari rentang penelitian yang terpublikasi. Namun demikian, pada jarak yang cukup dekat dengan pemancangan, peningkatan Δ_u terhadap σ_v' berada pada rentang 1,5 – 2,0 dari hasil Lo Stermac.

6.2 *Estimasi Daya Dukung Tiang*

Estimasi daya dukung tiang secara numerik dilakukan dengan memberikan beban *displacement* arah vertikal sebesar 25 mm. Untuk memprediksi *soil setup*, maka dilakukan analisis dengan variasi waktu yang disesuaikan dengan variasi waktu pada analisis tekanan air pori ekses. Kemudian melalui analisis numerik ditampilkan kurva transfer beban di sepanjang tiang terhadap variasi waktu yang ditinjau.

Hasil kurva transfer beban menunjukan bahwa nilai daya dukung berangsur-angsur meningkat seiring bertambahnya waktu. Peningkatan daya dukung ini seiring dengan berkurangnya tekanan air pori ekses sehingga hasil analisis numerik dapat terbukti sesuai dengan teori yang ada. Gbr. 11. menunjukkan peningkatan daya dukung terlihat signifikan pada waktu ke-30 menit menuju 1 hari.

Hasil analisis numerik ini kemudian dibandingkan dengan uji beban statik terinstrumentasi yang dilakukan pada waktu ke-30 hari. Uji beban statik terinstrumentasi dilakukan dengan beban 200% x 2000 kN. Terlihat bahwa tren kurva transfer beban yang dihasilkan secara numerik pada waktu ke-30 hari cukup menyerupai kurva transfer beban dari hasil uji beban statik terinstrumentasi. Terlihat bahwa dengan model SS-HS, nilai daya dukung secara numerik cukup mendekati hasil daya dukung aktual dari uji beban statik.

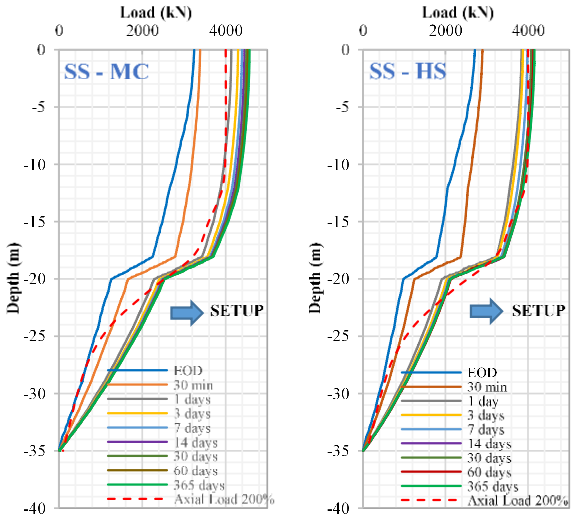

Gbr. 11. Kurva Transfer Beban Hasil Numerik dan Hasil Uji Beban Statik Terinstrumentasi.

Hasil daya dukung friksi dari hasil analisis numerik pada masing-masing layer tanah ditampilkan pada Tabel 6 dan Tabel 7.

Tabel 6. Daya Dukung Friksi Model SS-MC.

Soil	Friction Capacity (kN)						
	1 days	3 days	7 days	14 days	30 days	60 days	365 days
Soft Clay	163,4	170,4	174,3	175,7	181,6	188,6	198,0
Med Clay	329,0	358,8	385,7	404,9	420,7	429,8	439,0
Dense Sand	848,6	852,7	856,5	859,0	861,4	863,0	866,9
Stiff Clay	1698,1	1792,5	1836,2	1857,4	1870,9	1877,8	1881,8

Tabel 7. Daya Dukung Friksi Model SS-HS.

Soil	Friction Capacity (kN)						
	1 days	3 days	7 days	14 days	30 days	60 days	365 days
Soft Clay	159,8	166,9	170,4	175,9	182,3	190,3	204,5
Med Clay	225,0	253,9	277,9	295,9	307,9	316,5	323,4
Dense Sand	973,0	889,2	915,1	971,1	936,9	958,6	943,3
Stiff Clay	1365,1	1453,0	1490,1	1502,7	1516,6	1518,8	1512,4

6.3 *Hasil Numerik vs Hasil Uji Lapangan*

Penelitian ini kemudian dilengkapi dengan komparasi hasil *soil setup* yang diprediksi secara numerik dan hasil *soil setup* dari uji lapangan (uji PDA dan uji beban statik terinstrumentasi. Gbr. 12. menunjukan grafik peningkatan daya dukung ultimit (Q) terhadap waktu yang diplot dalam skala logaritma, hasil yang diperoleh secara numerik dengan model SS-HS cukup menyerupai hasil lapangan. Dilengkapi pula pola perubahan tekanan air pori ekses terhadap waktu pada masing-masing layer tanah lempung yang diprediksi melalui analisis numerik.

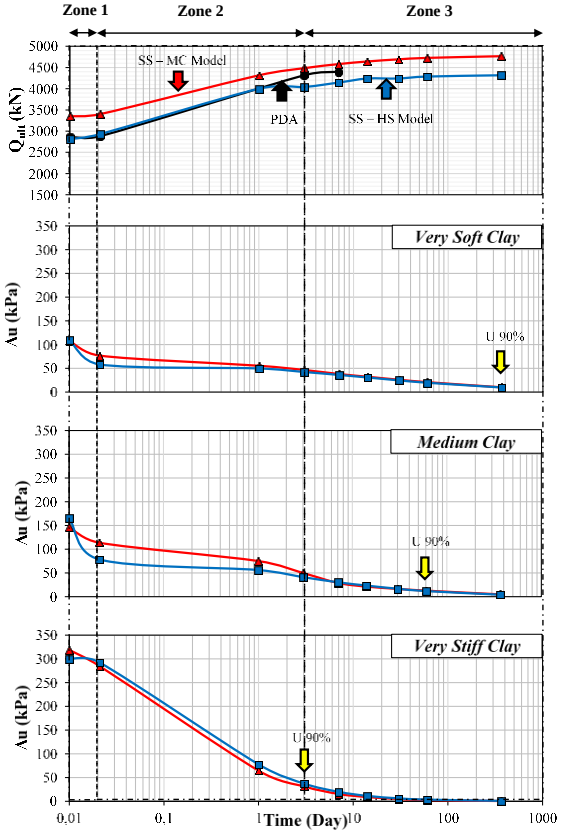

Gbr. 12. Pola Perilaku *Soil Setup* Terhadap Perubahan Tekanan Air Pori Ekses.

Hasil komparasi peningkatan daya dukung terhadap waktu (*soil setup*) dana perubahan tekanan air pori ekses, diusulkan untuk dibagi menjadi 3 zona, yaitu zona 1: waktu EOD hingga 30 menit, zona 2: waktu 30 menit hingga 7 hari; dan zona 3: waktu 7 hari hingga 365 hari. Dengan menggunakan metode Skov & Denver dapat ditentukan nilai A pada zona 1 diperoleh nilai 0,01 – 0,09 dengan waktu t_o = 0,015 hari; pada zona 2 diperoleh nilai A = 0,14 – 0,19 dengan waktu t_o = 0,3 hari; dan pada zona 3 diperoleh nilai A = 0,03 – 0,05 dengan waktu t_o = 5 hari. Pembagian zona tersebut kemudian dikomparasikan dengan perubahan disipasi tekanan air pori ekses (Δ_u) pada masing-masing layer tanah. Derajat konsolidasi 90% (U90) pada masing-masing layer tanah telah tercapai pada area zona 3, di mana U90 pada tanah lempung lunak (*soft clay*) tercapai dalam waktu 365 hari; tanah lempung medium (*medium clay*) tercapai dalam waktu 60 hari; tanah lempung teguh (*stiff clay*) tercapai dalam waktu 3 hari. Pada zona 3 ini pula, peningkatan daya dukung relatif tidak signifikan artinya dapat diprediksi bahwa ketika disipasi Δ_u mendekati U90 maka peningkatan daya dukung tiang pada layer tanah lempung yang terjadi tidak terlalu signifikan.

7 KESIMPULAN

Penelitian ini dilakukan mengambil studi kasus pemancangan tiang pada tanah lempung di daerah Cirebon, Jawa Barat untuk memprediksi fenomena perubahan tekanan air pori ekses (Δ_u) dan *soil setup* (A). Kondisi tanah pada proyek ini didominasi tanah lempung dengan lapisan lensa berupa pasir padat.

Dalam memprediksi perubahan Δ_u dan *soil setup* dilakukan kajian analisis secara numerik menggunakan program Plaxis 2D. Ide dari analisis ini adalah memodelkan pemancangan tiang menggunakan pendekatan teori *cavity expansion*; di mana kondisi awal diameter tiang dimodelkan 0,05 m kemudian diberikan gaya *displacement* horizontal 0,25 m, Kemudian prediksi perubahan daya dukung tiang dilakukan dengan memberikan gaya *displacement* vertikal sebesar 25 mm.

Kesimpulan dari penelitian ini menunjukan bahwa pola atau tren kurva transfer beban dari analisis numerik cukup mirip dengan tren kurva transfer beban dari hasil uji beban statik terinstrumentasi. Lebih lanjut kurva hubungan peningkatan daya dukung tiang terhadap waktu baik hasil numerik maupun lapangan juga menunjukan hasil yang kurang lebih sama. Pada akhirnya penelitian ini menyajikan mengenai zonasi *soil setup* dan Δ_u, terlihat bahwa zona 1 dan zona 2 masih terjadi peningkatan daya dukung tiang yang diiringi dengan masih terjadinya disipasi Δ_u, peningkatan daya dukung sudah berhenti/tidak signifikan diiringi dengan disipasi Δ_u sudah mendekati U90 ditunjukan pada zona 3. Zona 1 menghasilkan nilai A: 0,01 – 0,09; zona 2 menghasilkan nilai A: 0,14 – 0,19; dan zona 3 menghasilkan nilai A: 0,03 – 0,05.

DAFTAR PUSTAKA

C. S. Chen, S. S. Liew, and Y. C, Tan. Time Effects on The Bearing Capacity of Driven Piles. SSP Geotechnics Sdn Bhd, Malaysia.

B. Widjaja. Juni, 2007. Peningkatan Daya Dukung Pondasi Tiang Pancang pada Tanah Pasiran dan Kelempungan Studi Kasus Porto dan Jakarta. *Media Komunikasi Teknik Sipil* No. 2: 137-154.

H. G. Poulos, E. H. Davis. 1980. *Pile Foundation Analysis and Design*. University of Sidney: 6-8.

P. J. Bullock. 2008. The Easy Button for Driven Pile Setup: Dynamic Testing. *Research to Practice in Geotechnical Engineering Congress*: 471-488.

J. Mecsi. 2013. Geotechnical Engineering Examples and Solutions Using the Cavity Expanding Theory. *Hungarian Geotechnical Society*: 77-79.

MJ. Tomlinson. 1994. *Pile Design and Construction Practice*. 4th ed. London SE18HN, UK.

Study on Soil Spring Parameter for Rectangular Underground Structures

Indah Sri Wahyuningtyas
Shimizu Corporation

Masrur Abdull Hamid Ghani
Shimizu Corporation

Kenichi Ito
Shimizu Corporation

ABSTRAK: Struktur bawah tanah sudah umum digunakan untuk memenuhi kebutuhan infrastruktur. Pada pendesaianan struktur, terlebih untuk struktur bawah tanah, tanah memegang peran penting dalam menghasilkan respon struktur. Oleh karena itu, penting untuk mengetahui parameter dari interaksi tanah dan struktur agar dapat diaplikasikan dalam desain analisis. Parameter interaksi tanah dan struktur atau disebut dengan *soil spring* atau pegas dari tanah, belum banyak diaplikasikan dalam pendesainan struktur, karena umumnya interaksi tersebut diwakilkan dalam analisis FEM. Namun, parameter soil spring akan sangat berguna untuk membuat analisa lebih sederhana dan juga dapat mendukung dilakukannya model nonlinear pada analisis numerik. Dalam studi kali ini, akan dilakukan studi terhadap metode perhitungan *soil spring* parameter dari beberapa sumber literasi. Tujuan dari studi ini adalah untuk memberikan pemahaman kebutuhan penguasaan akan interaksi struktur dan tanah, dan juga untuk memberikan gambaran dalam metode penentuan *soil spring* yang dapat pembaca gunakan untuk melakukan analisis desain.

Kata Kunci: struktur bawah tanah, interaksi tanah dan struktur, soil spring

ABSTRACT: Underground structures has been commonly used to meet the needs of infrastructure. In the structural design, especially for underground structures, the soil has a significant impact on the response of the structure. Therefore, it is important to understand the parameters of the soil-structure interactions to be applied in the design analysis. The soil-structure interaction parameter as referred to be soil spring, has not been applied widely in structural design, as commonly the interaction is represented by FEM analysis. However, soil spring parameter will significantly become useful to simplify the analysis, also can comply with the nonlinear model in the numerical analysis. This paper carries out a study on the calculation method of soil spring parameter from several literature sources. The purpose of this study is to make an introduction on the importance to understand soil-structure interaction, and to give a picture of the method to determine soil spring in which readers can determine the most suitable approach to be used in the analysis.

Keywords: underground structure, soil-structure interaction, soil-spring

1 INTRODUCTION

In recent civil engineering practices, underground structures have been commonly designated to solve the problem of transportation, drainage system, piping, and other purposes in which area occupancy is the main issue. In Indonesia, large-scale underground structures have been introduced in recent years (i.e., Jakarta MRT project), and this may lead to other underground structure projects in the future.

During the design of upper ground structures, the structure is designed apart from its foundation. The structure base that connects to the foundation usually is assumed to be fixed support. Then, the foundation design will be carried out by considering the load governed from the upper structure analysis. However, for the underground station, the main structure itself will also act as the foundation, meaning transferring the load to the surrounding soil. Therefore, soil-structure interaction should be carefully considered in the analysis of the main

structures, especially in an earthquake-prone area. This due to soil imposes the seismic force on the structure.

Nowadays, the behavior of structure together with the surrounding soil is commonly analyzed by using a software geotechnical based. However, for simplified analysis, the soil-structure interaction is represented as soil spring.

Referring to building and bridge structure designs, in Indonesia, the standard has been established progressively with updates within some periodic of years to keep up with the current findings. However, currently, a dedicated standard to design underground structures has not been established yet. Therefore, in this paper, a literature study on soil spring parameters that are commonly used in other countries is carried out. The study will focus on the box type of underground structure. This paper will provide information on the obtaining methods of soil spring parameters in which readers can determine the most suitable approach of soil spring parameters to be used in the analysis.

2 SOIL SPRING PARAMETER

2.1 *General*

In a recent study, FEMA P-2091, A Practical Guide to Soil-Structure Interaction was developed by FEMA and ATC to help practicing engineers with the design guideline. Soil-structure interaction (SSI) can make a substantial difference in how buildings behave during earthquake shaking and how they should be designed, and yet there is relatively little implementation of SSI effects by practicing engineers, FEMA (2020). Soil-structure interaction is determined as the interrelationships between a structure, its foundation, and the soil.

PEER (2017) explained that for fixed foundation level of the basement of the building will result in biases computed structural response and provides no rational means to assess seismic pressures on basement walls. The level of bias can be difficult to assess a priori and may result in over or under-design conditions. Hence, PEER (2017) encouraged designers to consider SSI effects when developing analytical models for seismic evaluation of tall buildings. NIST (2012) earlier did a study and concluded that for the common case of buildings with relatively long periods on the descending portion of the spectrum, the use of a $\hat{S}_a$ (flexible base) instead of S_a (fixed base) typically results in reduced base shear demand. Conversely, inertial SSI can increase the base shear in relatively short-period structures. The illustration can be seen in Fig. 1.

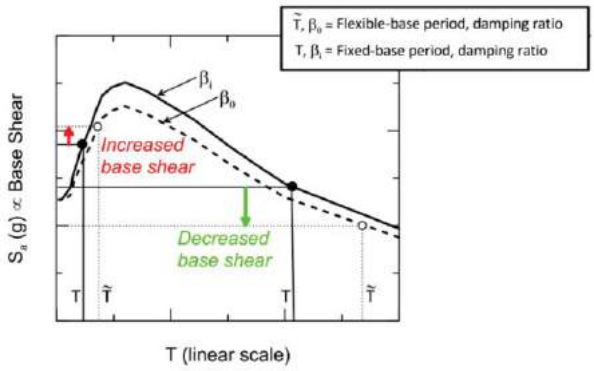

Fig. 1. Illustration of inertial SSI effects on spectral acceleration (base shear) associated with period lengthening and change in damping (Adapted from Fig. 2-3 in NIST, 2012).

These studies of soil-structure interaction, e.g. NIST (2012), PEER (2012), and FEMA (2020), mainly focused on building structures. On the other hand, the major guideline considering soil-structure interaction for underground structures is more limited. A few codes or major report studies that focused on the underground structure are Japanese Design Standard of Railway Structures and Commentary (Tunnel) or Japanese Standard Specifications for Tunneling, Wang (1993), and Hashash et al. (2001). In this paper, the soil-structure interaction of some references will be elaborated, with the focus on the box structure type.

2.2 *Wang (1993) – Seismic Design of Tunnels: A simple State-of-the-Art Design Approach*

The study conducted by Wang (1993) expedites the understanding of seismic design methodology for an underground structure. The underground structure has long been assumed to be resistant to earthquake damage. However, in several studies and actual events, the earthquake did damage the tunnel on some levels of damage.

Referring to Wang (1993), which has also been cited by Hashash et al. (2001), there are two main/common methods to quantify the effect due to design earthquake which can be seen in Table 1.

Table 1. Methods to Quantify the Effects of The Design Earthquake.

Free field deformation	Soil structure interaction approach
Stiff/rock soil	Soft Soil
There is no consideration of structure material properties	Considering the interaction between the underground structure and surrounding ground
Underground structure deformation is the same as the surrounding soil	The presence of an underground structure modifies the free-field ground deformations
Empirical formula, analyze the strain effect. The result will be compared to allowable strain to conclude that the tunnel is adequate or not.	Empirical formula, analyze the sectional forces; axial, bending moment, shear forces.

Wang (1993) developed the analytical solution to do the seismic analysis design of underground structures. The analytical solution of maximum axial force, bending moment, and shear force explicitly account for the tunnel-ground interaction, which is represented by spring coefficients and sectional modulus. Aside from the soil and structure properties, the wavelength is also considered in the analysis. The application of these analytical solutions is necessary only when tunnel structures are built-in soft ground. Furthermore, the study also shows that tunnel/underground structures located in soft soil conditions but not considering soil-structure interaction has an overestimated seismic design.

Wang (1993) did explain that St. John and Zahran (1987) suggested a maximization scheme that is similar to the JSCE (1987) approach except that the spring coefficients (K_a or K_t) are assumed to be functions of wavelength, L, in the maximization process, as follow:

$$K_a = K_t = \frac{16\pi G_m(1-\nu_m)}{(3-4\nu_m)}\frac{d}{L} \qquad (1)$$

where K_a and K_t = longitudinal and transversal spring coefficient of medium (force per unit deformation per unit length of the tunnel); G_m, ν_m = shear modulus (force per unit square of area) and Poisson's ratio of the medium, d = diameter of the circular tunnel (or height of rectangular structure). And working on Dobry et al. (1976) and Idriss and Seed (1968), *L* is the estimated wavelength equals *4h*, in which *h* is the thickness of the soil deposit.

Wang (1993) further explained that the derivations of these spring coefficients differ from those for the conventional beam on elastic foundation problems in that spring coefficients should be representative of the dynamic modulus of the ground under seismic loads, and derivations should consider the fact that loading felt by the surrounding soil (medium) is alternately positive and negative due to the assumed sinusoidal seismic wave. Therefore, the above spring coefficient equation (1) shall be limited to the related analytical solution developed by Wang (1993).

The other merit of Wang (1993) is for transversal behavior analysis, the relative stiffness between the tunnel and the medium is represented as flexibility ratio for both circular and rectangular (box) tunnel, also compressibility ratio for the circular tunnel.

2.3 *FEMA (2020) – FEMA P-2091: A practical Guide to Soil-Structure Interaction*

As mentioned earlier, this guideline report is mainly focused on building structures. However, as the basic concept of soil-structure interaction has similar consideration for underground structure, the soil spring considered in this guideline report will also be studied here.

FEMA (2020) classified two common modeling approaches of SSI, which are the substructure approach and the direct analysis approach, illustrated in Fig. 2. The first approach is representing the soil with springs, while the latter approach is modeling both soil and structure using finite elements. The direct analysis approach is commonly used on large, critical projects, which requires specialist expertise.

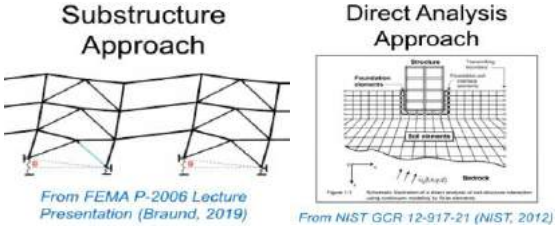

Fig. 2. Types of Soil-Structure Interaction Modeling and Scope.

FEMA (2020) provided methods to compute the flexibility of soil supporting building foundations, which must be incorporated in analyses when SSI is considered. The flexibility of soil in the model analysis is generally accounted to model the connection of structural elements to the support with the spring element. The spring can be a single point spring that represents each degree of freedom at the base or can be distributed springs representing the soil support as a discretized continuous medium, which is known as a Wrinkler foundation.

There are three types of springs: vertical, rotational, and horizontal springs. While the vertical and rotational springs affect the structure rocking through vertical or rotational movement, horizontal springs model the displacement relative to the free-field soil displacement or the resistance of the soil in the horizontal direction.

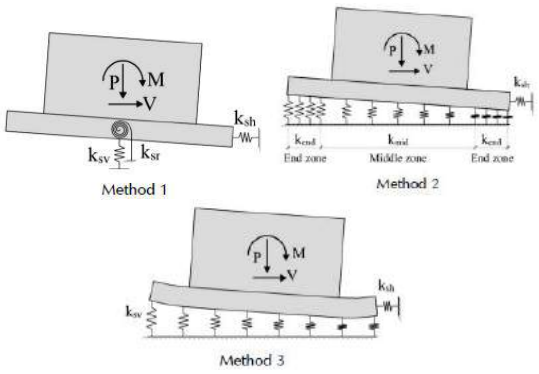

Fig. 3. Three Methods for Foundation Modeling Approaches with Springs, FEMA (2020).

Based on FEMA (2020), there are three methods to determine the vertical and/or rotational springs as shown in Fig. 3. The methods are based on the foundation and soil condition. Method 1 is for rigid foundation and flexible soil, represented by a point spring. Method 2 is for flexible foundation and nonlinear flexible soil, distributed as continuous with springs at each end of the footing increased in stiffness. Method 3 is for flexible foundation and linear flexible soil, distributed springs that representing the continuous soil support with a uniform value for the springs. The third method is the best practice when the flexibility of structural elements of the foundation are modeled explicitly as suggested by FEMA (2020). The vertical springs or unit subgrade spring coefficient (force per unit length cubed, or vertical stiffness per unit area) is represented by

$$k_{sv} = \frac{1.3G}{B_f(1-\nu)} \tag{2}$$

with G is the effective shear modulus, B_f is the full width of the foundation, and ν is Poisson's ratio of the soil. FEMA (2020) is correlated with ASCE 7-16 Chapter 19 about soil-structure interaction for seismic design (same with SNI 1726-2019 Chapter 14), therefore the effective shear modulus can refer to this code. However, it is suspected that the soil parameter can also refer to the other study method.

In the same case as vertical and rotational spring, ASCE 7-16 does not provide the guidance to develop the horizontal spring. Horizontal spring has a less significant effect on the structure if compared to vertical and rotational spring. However, all sources of flexibility must be considered. FEMA (2020) suggested three methods to develop horizontal spring: considering horizontal stiffness, considering resistance due to passive pressure, and considering resistance due to friction or cohesion. Method 1 has equations taken from NIST (2012), in which the horizontal spring is applied at the ground surface and working parallel to the length of the foundation. The equation for horizontal spring which is originated from Pais and Kausel (1988) is shown below:

$$K_x = K_{x,sur}\eta_x \tag{3}$$

$$K_{x,sur} = \frac{GB}{2-\upsilon}\left[6.8\left(\frac{L}{B}\right)^{0.65} + 2.4\right] \tag{4}$$

$$\eta_x = \left[1.0 + \left(0.33 + \frac{1.34}{1+L/B}\right)\left(\frac{D}{B}\right)^{0.8}\right] \tag{5}$$

with D is the depth of the foundation.

From the above vertical and horizontal springs equation we can understand that the soil springs correlate to the soil shear modulus, soil Poisson's ratio, and foundation dimension.

2.4 *RTRI (2001): Design Standard of Railway Structures and Commentary (Cut-and-Cover Tunnel)*

In Japan, underground structure or tunnel has been widely used to support their infrastructure needs. Therefore, there are many advanced studies on underground structure, and the design guideline for the tunnel has been established and applied in the engineering practice. The most commonly used standards or

codes for tunneling are Standard Specifications for Tunneling developed by Japan Society of Civil Engineers and Design Standard of Railway Structures and Commentary developed by Railway Technical Research Institute.

Referring to Standard Specification for Tunneling-2006: Cut-and-Cover Tunnels, the ground is modeled by using the method of representing the soil as a spring. Within this standard, it is explained that soil spring can be set as a linear spring for modeling elastic deformation. The coefficient of subgrade reaction is responsible not only for the soil deformation coefficient, but also for the function of shape, dimension, and rigidity of the loaded surface in which the deformation factor of the structure. Therefore, these factors shall be carefully considered to determine the soil spring coefficient.

For determining the subgrade reaction or soil spring, JSCE (2006) referred to the Design Standard of Railway Structures and Commentary (Cut-and-Cover Tunnel) by RTRI (2001). For the cut-and-cover tunnel, box underground structure, there are four types of springs that shall be considered in the analysis, as can be shown in Fig. 4.

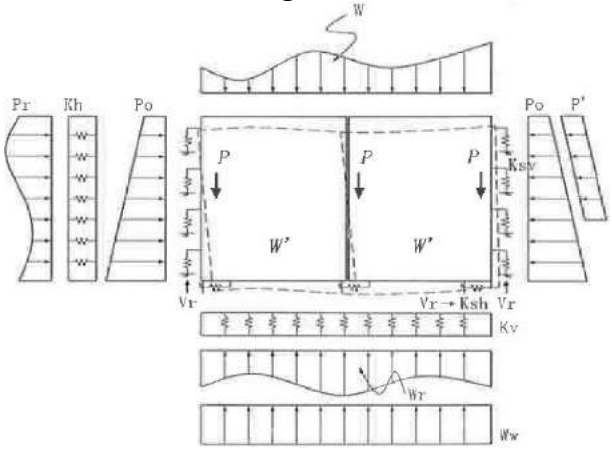

Fig. 4. Example of Structural Analysis, RTRI (2001).

2.4.1 *Vertical coefficient of subgrade reaction, k_v*

This subgrade reaction or soil spring is applied at the upper surface of top slab and the lower surface of lower slab, determined by

$$k_v = f_{rk}\left(1.7\alpha E_0 {B_v}^{-\frac{3}{4}}\right) \quad (6)$$

where, k_v : design coefficient of vertical subgrade reaction (kN/m^3); α : correction factor for E_0calculation method and loading condition (refer to Table 2); E_0 : subgrade deformation coefficient (kN/m^3); B_v : converted width of upper and lower slab (m), refer to Fig. 5; f_{rk} : ground resistance coefficient (generally, this is taken to be 1.0).

2.4.2 *Shear coefficient of subgrade reaction, k_{sv}*

This subgrade reaction or soil spring is applied at the upper surface of top slab and the lower surface of lower slab, determined by

$$k_{sv} = \lambda k_v \quad (7)$$

where, k_{sv} : design coefficient of shear subgrade reaction (kN/m^3); λ : conversion factor (generally, this may be taken as 1/3).

2.4.3 *Horizontal coefficient of subgrade reaction, k_h*

This subgrade reaction or soil spring is applied at the side of side wall, determined by

$$k_h = f_{rk}\left(1.7\alpha E_0 {B_h}^{-\frac{3}{4}}\right) \quad (8)$$

where, k_h : design coefficient of horizontal subgrade reaction (kN/m^3); α : refer to Table 2; B_h : converted width of side wall (m), refer to Fig. 5; f_{rk} : generally, this is taken to be 1.0.

2.4.4 *Shear coefficient of subgrade reaction, k_{sh}*

This subgrade reaction or soil spring is applied at the side of side wall, determined by

$$k_{sh} = \lambda k_h \quad (9)$$

where, k_{sh} : design coefficient of shear subgrade reaction (kN/m^3); λ : generally, this may be taken as 1/3.

Table 2. Correction factors for E_0 calculation method and loading condition, RTRI (2001).

Testing method	Correction factor α*1
Plate bearing test	1
Horizontal load test within a hole	4
Unconfined compression test	4
Triaxial compression test	4
Standard penetration test	1
Elastic wave velocity logging	0.125

*1 Multiply the value in the table by 2 to study loads other than permanent load

The converted width of the slab or side wall can be determined by the equation as follow:

$$B \geq L \rightarrow B_v = (B \times L)^{\frac{1}{2}} \; and \; if \; B < L \rightarrow B_v = B$$

$$H \geq L \rightarrow B_h = (H \times L)^{\frac{1}{2}} \; and \; if \; B < L \rightarrow B_h = H$$

Fig. 5 is intended to help the understanding of the converted width variable.

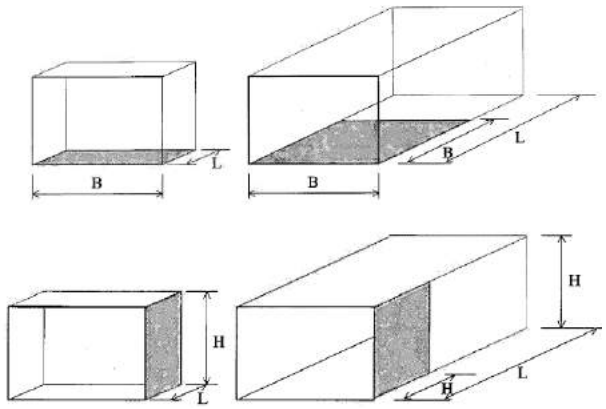

Fig. 5. Converted width of underground structure, RTRI (2001).

The soil springs determined by DSRSC method can be used both in the static and dynamic conditions of the structure.

3 CONCLUSIONS

The material described in this report describes the methods of determining soil-structure interaction in the form of soil spring. Not many codes or standards have incorporated the soil spring in the structural design. Hence, the number of applications of the soil spring to represent the soil-structure interaction in the structural design is still lacking. Furthermore, a lesser number of studies are conducted for determining soil springs for underground structures.

The soil spring is an important parameter to design the structure. Commonly, FEM is conducted to account for soil-structure interaction. However, if referring to load combination in SNI 1727, the load combination is quite complex in which sometimes it is difficult to do the soil FEM analysis. Furthermore, as the nonlinear FEM analysis of structure is progressing to be used in the performance-based design, considering the soil spring will be more beneficial in this analysis.

From the three main literatures studied in this paper, the first Wang (1993) soil springs is limited to combined with the provided analytical solution. The use of its spring coefficient to be applied directly to the structure numerical analysis shall be studied further. FEMA (2020), the recent guideline of considering soil-structure interaction for building, shows the practical guide to design a structure with the consideration of SSI. The implementation of this guideline to fully underground structure design shall be studied further.

The third literature is a code mainly used in Japan. This code has compulsively shown the method or formulas to determine the soil springs for the underground structure. For the current study, this code has the closest practice method for supplementing the design of the underground structure. However, further study is required to understand the structural behavior due to considering the soil spring calculated by this method and due to considering soil-structure interaction in FEM is widely used in current design practice. Furthermore, RTRI (2001) is focused on the rectangular tunnel, hence a further study to consider the applicability of the soil spring determination method for building with the embedded basement will be useful to understand the best practice for soil-structure interaction consideration.

REFERENCES

FEMA and ATC. 2020. FEMA P-2091: *A Practical Guide to Soil-Structure Interaction*. California.

Hashash, Y., Hook, J., Schmidt, B. and Yao, J. 2001. Seismic Design and Analysis of Underground structures. *Tunnelling and Underground Space Technology 16.*

Japan Society of Civil Engineers. 2007. Standard Specifications for Tunneling-2006: Cut-and-cover Tunnels. Tokyo: Tunnel Engineering Committee.

NIST. 2012. NIST GCR 12-917-21: *Soil-Structure Interaction for Building Structures.* Gaithersburg.

PEER. 2017. *Guidelines for Performance-Based Seismic Design of Tall Buildings*. Berkeley.

Railway Technical Research Institute. 2001. *Design Standard of Railway Structures and Commentary* (Cut-and-Cover Tunnel): 64-65.

Wang, J.N. 1993. *Seismic Design of Tunnels: A State-of-the-Art Approach.* New York: Jaw-Nan Wang and Parsons Brinckerhoff Inc.

Displacement Ratio untuk Mengestimasi Pergerakan Tanah akibat Pekerjaan Pemancangan – Studi Kasus di Bekasi dan Jakarta Utara

Kirana Rongsadi
Geotechnical Engineer – PT Geotechnical Engineering Consultant

Prieschila C. Tamsir
Geotechnical Engineer – PT Geotechnical Engineering Consultant

Bondan W. Anggoro
Senior Geotechnical Engineer – PT Geotechnical Engineering Consultant

Paulus P. Rahardjo
Professor of Geotechnical Engineering – Universitas Katolik Parahyangan

ABSTRAK: Konstruksi bangunan menggunakan sistem pondasi tiang pancang merupakan suatu hal yang umum dilakukan pada area dengan lapisan tanah seragam dengan konsistensi lunak hingga sedang di bagian permukaan.Dalam pelaksanaannya,pekerjaan pemancangan akan menyebabkan adanya perpindahan volume yang secara umum dapat menyebabkan adanya desakan tanah baik kearah horizontal maupun vertikal. Apabila pekerjaan pemancangan dilakukan dengan massal (dalam jumlah banyak) dan berdekatan dengan bangunan eksisting, maka desakan yang terjadi dapat menyebabkan deformasi yang berujung kerusakan pada bangunan tersebut. Untuk mengetahui efek desakan tanah tersebut, maka dilakukan pengamatan pergerakan horizontal tanah secara berkala pada saat pemancangan di area studi kasus Jakarta utara dan Bekasi dengan menggunakan Inklinometer. Untuk mengestimasi efek desakan tersebut pada banyaknya jumlah tiang pancang yang dipancang, maka kami menggunakan parameter "*displacement ratio"*, Rahardjo (2013), Maryono (2014) yang adalah rasio antara luas tiang dan luas area lingkaran dengan jarak antara tiang dan objek yang ditinjau sebagai jari-jarinya. *Displacement ratio* tersebut kemudian dapat dikaitkan dengan besarnya perpindahan objek yang ditinjau.

Kata Kunci: tiang pancang, desakan tanah, deformasi, displacement ratio, pemancangan massal, tanah lunak

ABSTRACT: High rise buildings on driven piles as foundation system is commonly used if there is soil layer with soft to medium consistency on the surface. In the construction process, the pile driving will displace the volume of the existing soil which will cause additional stresses of the existing soil. Especially if the pile is driving massively and there is existing buildings located nearby, the additional soil pressure can cause damage to those buildings. To estimate the effect of pile driving, we monitored the horizontal displacement in soil periodically during construction with Inclinometer for case study area in North Jakarta and Bekasi. To estimate the pressure effect to number of piles, we use a parameter called "displacement ratio", Rahardjo (2013), Maryono (2014) which is a ratio between area of pile and circular area of the distance between pile to the object as radius. The displacement ratio then can be related to displacement of the object.

Keywords: driven pile, soil pressure, deformation, displacement ratio, mass pile driving, soft soil

1 PENDAHULUAN

Konstruksi dengan menggunakan pondasi tiang pancang merupakan salah satu metode konstruksi yang digemari karena proses konstruksi yang cukup cepat dan lebih murah dibandingkan dengan menggunakan tiang bor. Hanya saja dalam pelaksanaannya, tidak jarang konstruksi tiang pancang mengakibatkan masalah baru, selain dikarenakan proses konstruksinya yang dapat menimbulkan getaran dan gangguan suara, proses penetrasi tiang pancang ke dalam tanah dapat menimbulkan pergerakan tanah lateral dan vertikal pada area sekitarnya.

Tanah dan air tanah di sekitar area pondasi tiang pancang di konstruksi "dipaksa" untuk mengalami perpindahan dan restrukturisasi butiran tanah secara radial yang tidak jarang

mengakibatkan kerusakan pada bangunan serta pondasi eksisting pada bangunan sekitar.

Pada tulisan ini, penulis mengumpulkan data-data mengenai pergerakan akibat konstruksi tiang pancang pada area studi kasus di kota Bekasi dan Jakarta Utara.

2 INFORMASI AREA STUDI

Kedua area studi merupakan area yang akan direncanakan untuk pembangunan bangunan tinggi untuk bangunan *Mixed-Use*. Kedua area studi memiliki lapisan lempung pada bagian atas yang cukup dalam, dengan jenis tanah pada bagian permukaan untuk area studi Bekasi adalah tanah lempung medium dengan nilai NSPT rata-rata 5*blows/ft* hingga kedalaman kurang lebih 16 m (Gbr. 1). Sedangkan area studi Jakarta Utara memiliki jenis tanah lempung lunak dengan NSPT rata-rata 1blows/ft hingga kedalaman 12 m.

Gbr. 1 merupakan sketsa pelapisan tanah tipikal pada daerah tinjauan.

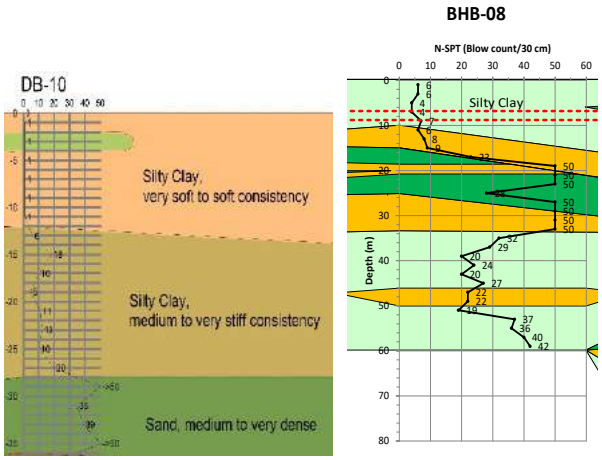

Gbr. 1. Tipikal Jenis Tanah Area Tinjauan Jakarta Utara (kiri) dan Bekasi (kanan).

Pondasi yang digunakan pada area studi merupakan pondasi tiang pancang spun pile dengan ukuran D60cm untuk kedua area studi. Metode pemancangan untuk area Bekasi menggunakan Jack-In Pile dengan panjang tiang rata-rata antara 18-21 m, dan metode pemancangan di area studi Jakarta Utara menggunakan Diesel Hammer (Tipe JW DD 63) dengan panjang tiang rata-rata antara 30-35 m.

Gbr. 2. Kondisi di lokasi studi, Jarak antara tiang pancang dan Inklinometer.

Pada saat konstruksi tiang pancang, dilakukan juga monitoring pergerakan horizontal secara kontinu di dalam tanah dengan menggunakan Inklinometer pada tanah sekitar. Jarak Inklinometer area studi Jakarta Utara ke titik pemancangan terdekat adalah sekitar 4 m dengan kedalaman pemasangan Inklinometer sedalam 45 m, sedangkan area Bekasi memiliki jarak Inklinometer dengan pancang terdekat 9 m dengan kedalaman pembacaan Inklinometer 25 m. Deformasi yang cukup besar berdasarkan data hasil inclinometer disebabkan karena kondisi tanah yang lunak pada bagian permukaan dan pemancangan massal.

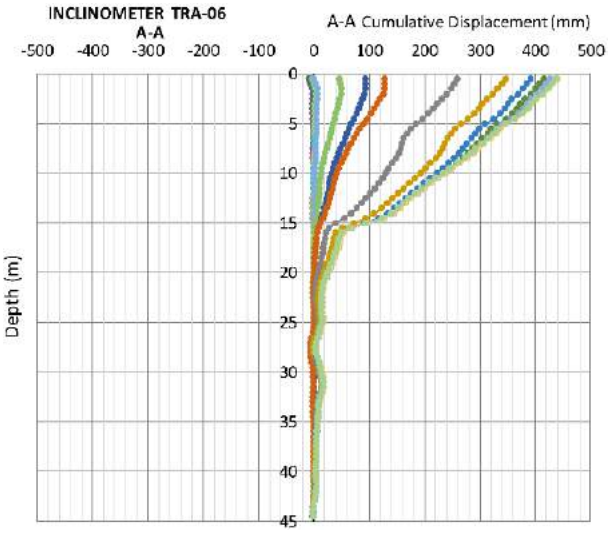

Gbr. 3. Tipikal Grafik Pembacaan Inklinometer dan Jenis Tanah di Area Studi Jakarta Utara.

Hasil pengamatan yang dilakukan pada area studi menunjukkan adanya hubungan antara jarak pemancangan terhadap titik pengukuran inclinometer, kecepatan pemancangan, serta deformasi yang terukur dari hasil monitoring inclinometer itu sendiri. Untuk menghubungkan beberapa parameter tersebut, maka digunakan suatu parameter yang merupakan perbandingan antara luas penampang dari tiang yang dipancang terhadap luas area dengan jari-jari lingkaran yang merupakan jarak antara tiang yang dipancang dengan lokasi titik inclinometer yang dikenal dengan istilah *displacement ratio.* Rahardjo et al. (2013), Maryono (2014).

Pembacaan Inklinometer di area Studi Jakarta Utara (Gbr. 3) menunjukkan pergerakan lateral pada permukaan Inklinometer dengan putaran sudut terbesar berada pada kedalaman ±15 m, hal ini sesuai dengan kedalaman tanah lunak pada area studi kasus dimana terdapat tanah lunak dan medium hingga kedalaman tanah 15 m (Gbr. 1). Selain itu arah deformasi yang terukur juga menjauhi area pemancangan (sudah sesuai dengan ekspektasi yaitu kearah arah A+).

Sedangkan di area studi Bekasi tampak bahwa pergerakan yang di hasilkan kearah A- karena fungsi utama dari inclinometer ini adalah mengukur pergerakan tanah akibat galian (rencana besmen bangunan) sehingga arah pergerakan dari pemancangan menjauhi arah galian, karena efek dorongan pemancangan dimana tanah lunak pada area studi berada hingga kedalaman ±20 m.

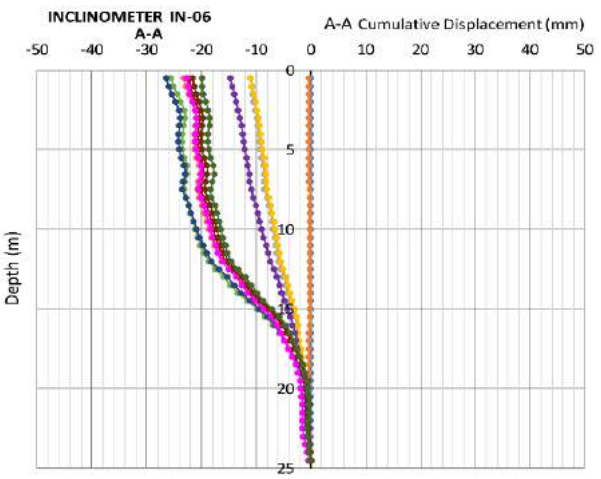

Gbr. 4. Tipikal Grafik Pembacaan Inklinometer di Area Studi Bekasi.

3 DISPLACEMENT *RATIO*

Untuk menjelaskan hubungan antara dimensi tiang yang dipancang, jarak pemancangan, kecepatan pemancangan, serta pergerakan yang terjadi pada tanah pada saat dilakukan pemancangan maka digunakan suatu parameter yang dinamakan *Displacement Ratio,* Rahardjo et al. (2013), Maryono (2014).

Displacement ratio didefinisikan sebagai luas area dari tiang pancang (A_{pile}) dibagi dengan luas area lingkaran dengan titik inklinometer sebagai titik pusatnya ($A_{distance}$) dan jarak tiang dengan titik tinjau inklinometer sebagai radius lingkaran (r_d) (persamaan 1 dan Gbr 5).

$$\frac{\sum A_{pile}}{\sum A_{distance}} = \frac{\sum \pi {r_p}^2}{\sum \pi {r_d}^2} = \frac{\pi {r_{p(1)}}^2 + \pi {r_{p(2)}}^2 + \pi {r_{p(3)}}^2 + \cdots + \pi {r_{p(n)}}^2}{\pi {r_{d(1)}}^2 + \pi {r_{d(2)}}^2 + \pi {r_{d(3)}}^2 + \cdots + \pi {r_{d(n)}}^2} \quad (1)$$

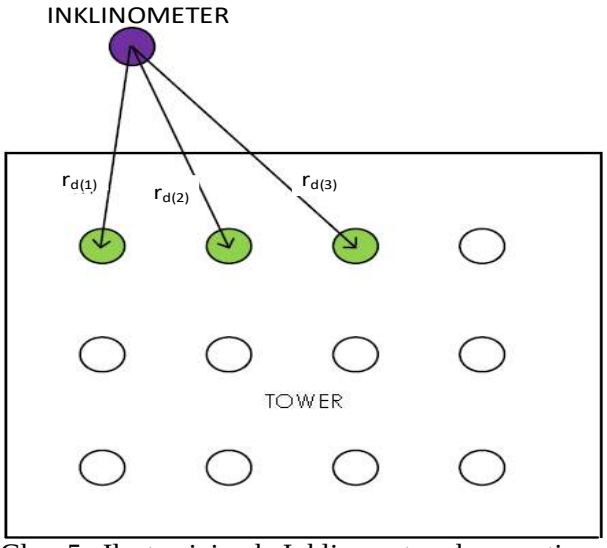

Gbr. 5. Ilustrasi jarak Inklinometer dengan tiang pancang untuk menghitung *Displacement Ratio*.

Semakin dekat tiang pancang dengan lokasi titik tinjau, maka nilai displacement ratio semakin tinggi, begitu juga sebaliknya. Nilai kumulatif dari *displacement ratio* dihitung berdasarkan tiang pancang yang di konstruksi serta jarak terhadap titik inklinometer pada satu periode monitoring tertentu dan di bandingkan dengan pergerakan yang terbaca di Inklinometer.

Data ini kemudian dapat digunakan untuk mengestimasi efek dari kecepatan pemancangan terhadap displacement yang dapat terjadi pada titik tinjauan tersebut.

4 HASIL PENGAMATAN *CUMMULATIVE DISPLACEMENT RATIO* PADA AREA STUDI KASUS

Pengamatan dilakukan berdasarkan data pembacaan inclinometer yang dilakukan di area studi kasus Jakarta Utara dan Bekasi. Metode estimasi dilakukan sebagai berikut:

a. Mengacu pada Gbr. 6 hubungan antara *displacement ratio* terhadap *horizontal displacement* ditunjukkan garis warna oranye pada gambar yang atas dengan slope y=48.69x. Sedangkan hubungan antara *displacement ratio* terhadap waktu ditunjukkan oleh grafik warna oranye pada gambar yang bawah y=1.3674x.
b. Dengan adanya rencana pemancangan dari kontraktor maka hubungan antara *displacement ratio* terhadap waktu dapat dibagi menjadi beberapa *sequence* dan dihitung slopenya.
c. Berdasarkan slope dari rencana pemancangan tersebut dapat dihitung estimasi *horizontal displacement* berdasarkan data korelasi pada poin a.

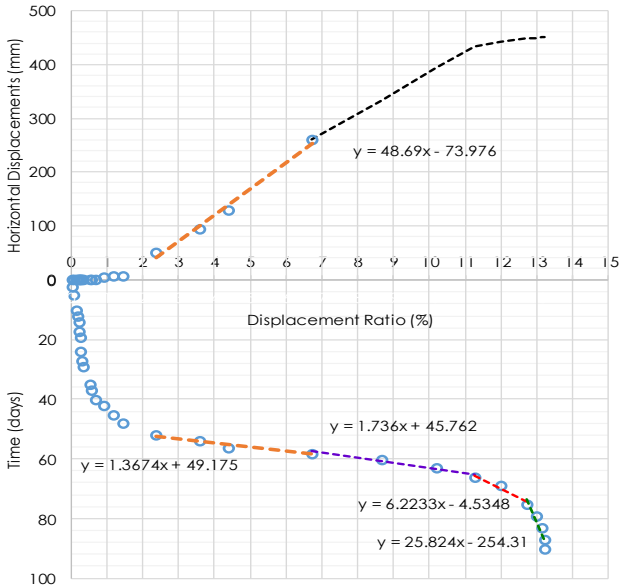

Gbr. 6. *Displacement Ratio vs Horizontal Displacements* dan *Time* pada Studi Kasus Jakarta Utara.

Selanjutnya berdasarkan data hasil monitoring didapatkan bahwa besarnya estimasi pergerakan memberikan hasil yang cukup konsisten dengan deformasi horizontal yang terukur seperti pada Gbr. 7 berikut ini.

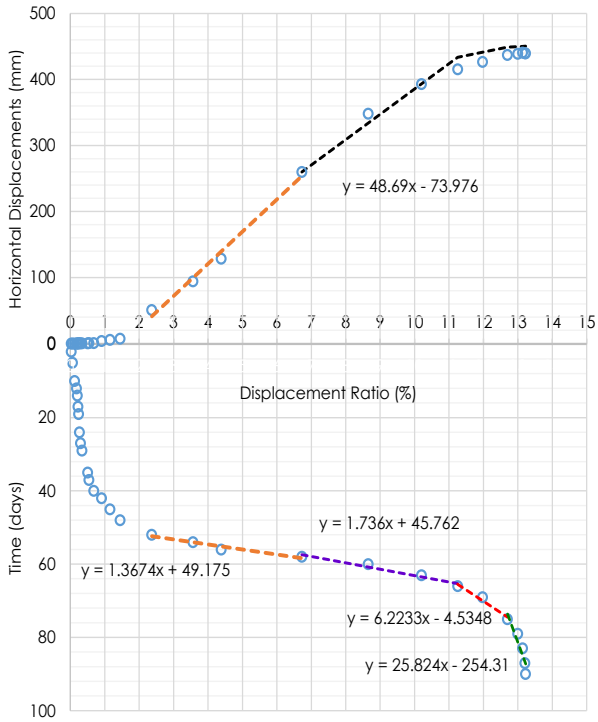

Gbr. 7. *Displacement Ratio vs Horizontal Displacements* (Estimasi dan Terukur) dan *Time* pada Studi Kasus Jakarta Utara.

Berdasarkan hasil pengamatan pergerakan akibat pemancangan, tampak bahwa nilai estimasi pergerakan *horizontal* cukup konsisten dengan nilai *horizontal displacement* yang terukur dalam inklinometer.

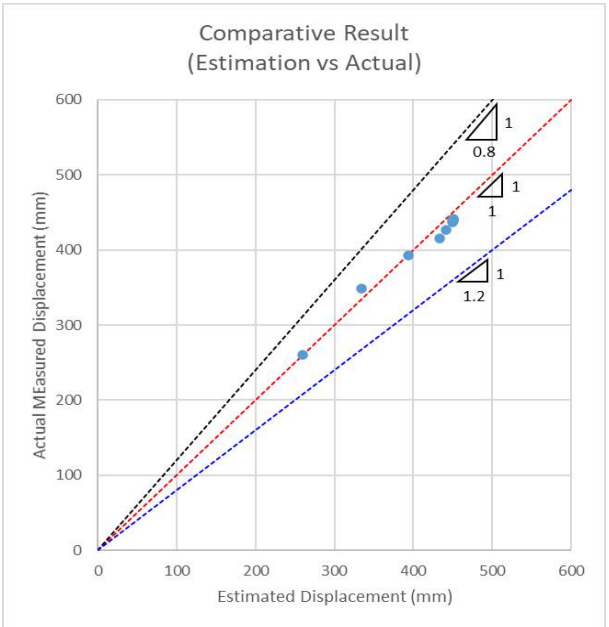

Gbr. 8. *Displacement Ratio vs Horizontal Displacements* dan *Time* pada Studi Kasus di Jakarta Utara.

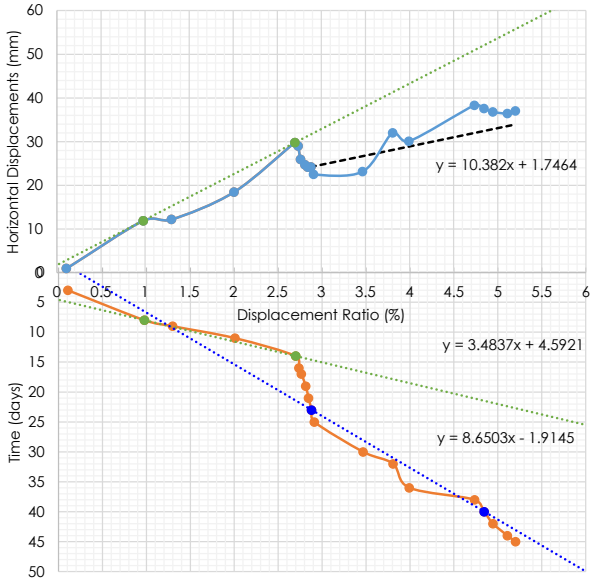

Gbr. 9. *Displacement Ratio vs Horizontal Displacements* dan Waktu pada Studi Kasus Bekasi.

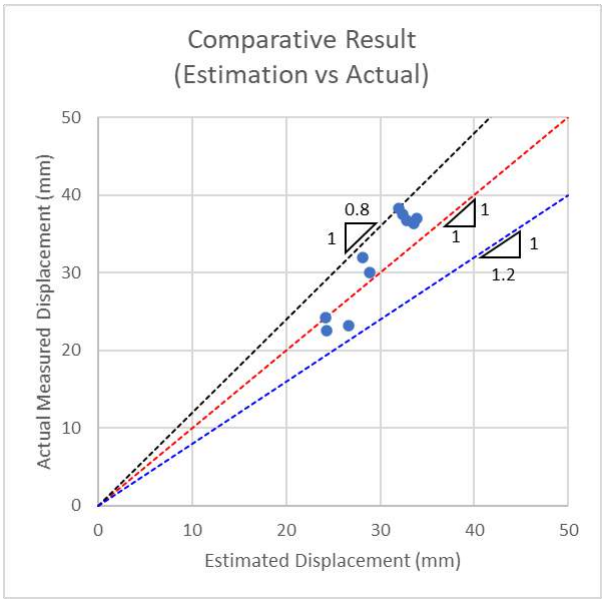

Gbr. 10. *Displacement Ratio vs Horizontal Displacements* dan Waktu pada Studi Kasus Bekasi.

Studi kasus area Bekasi memiliki kurva *Displacement Ratio vs Time* dengan urutan pemancangan yang tidak teratur diakibatkan karena adanya keterbatasan penggunaan lahan, sehingga pada saat pemancangan di lakukan terjadi penyesuaian urutan pemancangan yang mengharuskan pemancangan dilakukan secara massal pada area di dekat titik Inklinometer (Gbr 9).

5 KESIMPULAN

Berdasarkan hasil pengukuran deformasi dari data Inklinometer terlihat bahwa nilai estimasi dengan pergerakan yang terukur cukup konsisten dengan *error margin* ±20% (Gbr. 8 dan Gbr. 10).

Adanya perbedaan antara estimasi dengan data hasil pengukuran aktual merupakan hal yang sangat mungkin terjadi sehubungan dengan adanya beberapa parameter yang tidak diperhitungkan dalam kajian ini antara lain adanya tekanan air pori ekses yang muncul akibat pemancangan, dan/atau adanya "*barrier*" tiang pancang dengan pekerjaan pemancangan yang dilakukan menjauhi titik tinjau.

Dimana dalam penelitian lebih lanjut kedua hal tersebut dapat ikut diperhitungkan dan dapat memberikan nilai estimasi yang lebih akurat.

UCAPAN TERIMA KASIH

Ucapan terima kasih secara khusus disampaikan oleh penulis kepada PT Geotechnical Engineering Consultant yang telah memberikan data yang kami gunakan dalam penyusunan makalah ini.

DAFTAR PUSTAKA

Maryono. 2014. *Analisis Deformasi Tanah dan Sheet Pile Akibat Pemancangan Tiang pada Tanah Lunak.* Tesis. Universitas Katolik Parahyangan. Bandung.

Paulus P. Rahardjo, Adityaputera Wirawan, & Ricky Setiawan. 2014. Analytical and Empirical Study on Ground Movement and Excess Pore Pressures Generation due to Pile Driving in Soft Soils. *Proceedings of Soft Soils 2014* A8-1 to A8-13.

Ricky Setiawan. 2014. *Kajian Tekanan Air Pori Ekses Akibat Pemancangan dengan Metode Injeksi.* Skripsi. Universitas Katolik Parahyangan. Bandung.

Dynamic Bearing Capacity Exclusivity of Driven Pile with the Danish, Navy-McKay and Eytelwein Empirical Formulas by Using the Final Set Value

Munirwansyah
Professor, Department of Civil Engineering-Geotechnic – Universitas Syiah Kuala

Reza P. Munirwan
Lecturer, Department of Civil Engineering-Geotechnic – Universitas Syiah Kuala

Fauzan Mufid
Student, Department of Civil Engineering-Geotechnic – Universitas Syiah Kuala

ABSTRAK: Pondasi adalah sebuah sistem rekayasa yang bekerja dengan meneruskan dan menopang beban serta beratnya sendiri ke dalam tanah dasar (*bearing layer*) yang terletak di bawahnya. Objek yang menjadi kajian dalam penelitian ini adalah Proyek Pelebaran Jembatan Alue Lamteh. Jembatan Alue Lamteh merupakan jembatan yang berlokasi di Kecamatan Kuta Cot Glie, Kabupaten Aceh Besar dengan titik koordinat 5°23'42,4" LU dan 95°29'35,9" BT. Tujuan dari penelitian ini adalah untuk menganalisis daya dukung pondasi tiang pancang jembatan Alue Lamteh menggunakan metode formula dinamis. Nilai kapasitas daya dukung tiang pancang dihitung menggunakan metode Navy-McKay, Danish, dan Eytelwein. Berdasarkan hasil perhitungan daya dukung dinamis didapat daya dukung terbesar yaitu menggunakan metode Danish pada tiang P1.2 dan P3.2 dengan nilai final set (s) = 12 mm masing-masing sebesar 121,478 ton sedangkan daya dukung terkecil yaitu menggunakan metode Navy-McKay pada tiang P2.2 dengan nilai final set (s) = 24 mm sebesar 35,470 ton.

Kata Kunci: pondasi tiang pancang, formula dinamis, pengujian calendaring

ABSTRACT: The foundation is an engineering system that works by transmitting and supporting the load and its weight into the subgrade (bearing layer). The object of study in this research is the Alue Lamteh Bridge Widening Project. Alue Lamteh Bridge is located in Kuta Cot Glie District, Aceh Besar Regency, with coordinates of 5°23'42.4" N and 95°29'35.9"E. This study aims to analyze the Alue Lamteh bridge's pile foundation bearing capacity using the dynamic formula method. The bearing capacity values were calculated using the Navy-McKay, Danish, and Eytelwein methods. Based on the results of the dynamic bearing capacity calculation, the largest bearing capacity was obtained using the Danish method on the P1.2 and P3.2 piles with the final set value (s) = 12 mm each of 121.478 tons, while the smallest bearing capacity was using the Navy-McKay method on P2.2 pile with the final set value (s) = 24 mm of 35.470 tons.

Keywords: pile foundation, dynamic formula, calendaring test

1 INTRODUCTION

The bridge is a construction building, and the bridge consists of an upper structure and sub-structure. The bridge has a function as a liaison between the two roads due to lower obstacles. These obstacles can be in the form of river channels, traffic lanes, irrigation canals, etc.

The planner must plan a solid and safe foundation in designing a bridge. According to Hardiyatmo (1996), a foundation is a component of a structure that is capable of transmitting the building's load into the subgrade or rock beneath it.

The object of study in this research is the Alue Lamteh Bridge. Alue Lamteh Bridge is located in Kuta Cot Glie District, Aceh Besar Regency, with coordinates of 5°23'42.4" North Latitude and 95°29'35.9" East Longitude.

The Alue Lamteh Bridge's volume of traffic has increased, demanding significant expansion. There is a change in the dimensions of the building structure on the left and right sides of the bridge, with 12 additional points of concrete piles on each side. The bridge connecting the Banda Aceh-Medan National Road is near the Seulawah Volcanic Mountain and the Seulimum Fault in Aceh Province. The

bridge's condition that has experienced widening and is close to the source of the earthquake is the reason why the bearing capacity of the pile foundation needs to be analyzed. The purpose of this study is to determine the load-bearing capacity of the pile foundations used in the Alue Lamteh Bridge widening project using the dynamic approach.

2 LITERATURE REVIEW

2.1 *Overview*

According to Bowles (1997), there are two requirements that must be met in planning a building foundation. The first requirement is that the subgrade must be able to support the working load without experiencing shear failure. The second requirement is that the settlement that can occur must be within the allowable limit. According to Tobing et al. (2019), piles are one part of the construction of sub-structure buildings that can be made of concrete, wood, or steel, which functions to transmit the load to the subgrade with a greater bearing capacity. Piles distribute the load received from the top construction to the hard soil layer at a relatively deep location. Pratama (2019) states that piles are a type of foundation that is used if the soil at shallow depths cannot support the load originating from the superstructure with the hard soil layer located at a depth relatively far from the surface. According to Sardjono (1988), piles are a type of foundation that can be utilized when the hard soil lacks the bearing capacity needed to support construction loads.

2.2 *Types of Pile Foundation*

Based on the shape and material of its formation, pile foundations can be distinguished as follows.

Hardiyatmo (2018) categorizes piles into the following categories:

a. Large displacement piles, are hollow piles with a closed-end that are driven into the ground, which results in the displacement of a large enough volume of soil.
b. Small displacement piles, are hollow piles with closed-ends that are driven into the ground, but the volume transfer in the soil that occurs is relatively small.
c. Non-displacement piles, are a type of piles that are driven by the excavation process or by drilling the ground.

Tomlinson (1994) also describes several types of piles that are often used in construction, namely:

a. Driven piles
b. Driven and cast in places pile
c. Screw piles
d. Bore piles
e. Vibration piles driven
f. Hydraulic pile driven
g. Kneading

Hardiyatmo (2018) also categorizes piles based on the material that will be used as the building material, which is as follows:

a. Timber Piles

A timber pile is a type of pile that is made of wood, generally between 10-25 cm in diameter or between 8-10 cm and 4 meters in length. Timber pile is cheaper and has the advantage of being easy to handle. However, these types of piles are prone to decay and even damage by insects. This damage can be avoided by protecting the ends of the pile using iron shoes. The highest load that a single wooden pile can carry is 270-300 kN.

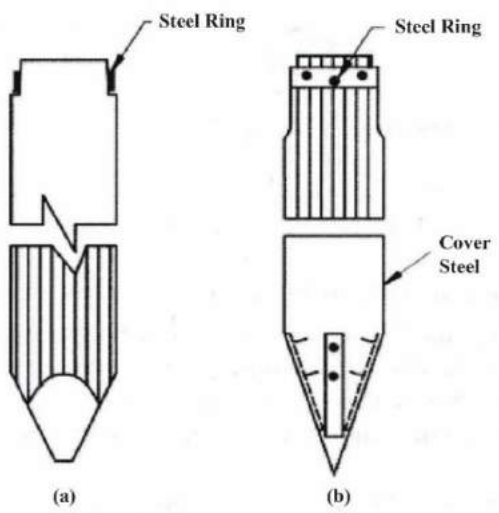

Fig 1. Timber Piles. (a) without Cover Steel, (b) with Cover Steel, Hardiyatmo (2018).

b. Precast Concrete Piles

This type of pile is made of concrete which is molded somewhere and then transported to the construction site. The diameter of the pile, which is generally used for non-perforated piles is 20-60 cm. The maximum load that can be carried on a small size range from 300 to 800 kN.

c. Cast-In-Place Concrete Piles

This type of concrete pile is divided into two types, the first is a pipe sheathed pile, and the second is a pile that is not sheathed with a pipe.

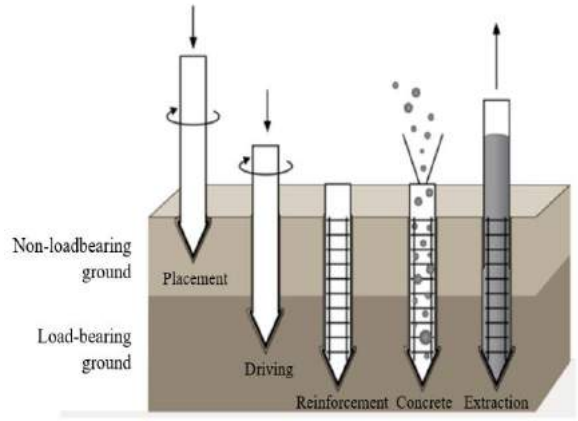

Fig. 2. Precast Concrete Pile, Hardiyatmo (2001).

d. Bored Piles

This form of pile is a pole that is installed into the ground via drilling, followed by the insertion of reinforcing bars that have been assembled and then cast with concrete.

e. Structural steel

According to Nurdiani (2013), this steel pile foundation has a shorter and easier duration for installation and implementation. The disadvantage is that steel piles will easily corrode and rust when used in areas with moist soil properties or near the coast.

f. Composite pile

Composite piles are those piles of two different materials driven one over the other to enable them to act together to perform the function of a single pile. This type of pile can be used to overcome certain soil problems, for example, the decay of wooden poles that are staked above the groundwater level. This problem can be overcome by erecting a composite pile in the form of a concrete pile at the top and connecting it to a wooden pile at the bottom of the groundwater table.

2.3 *Types of Pile Driving Methods Based on The Type of Hammer*

According to Pratama (2020), the selection of this pile driving method can be influenced by the number of piles, pile size, the impact of piling, project location and topography, soil characteristics, and the presence of piles at the project location.

Hardiyatmo (2018) divides the pile driving method using the following type of hammer:

a. Drop hammer

According to Sombah (2016), a Drop hammer is a tool for driving piles. This tool consists of a heavy steel hammer driven by steel cables. The hammer lifted by the steel cable is then dropped from the top of the pile foundation head.

b. Single-acting hammer

This driving tool has an elongated shape equipped with a ram that moves upward due to compressed air/steam. However, the downward movement of the ram is due to the weight of the ram itself; in this case, the energy generated in a single acting hammer is equal to the weight of the ram multiplied by the height of the fall.

c. Double-acting hammer

The double-acting hammer utilizes steam/air in lifting the ram, as well as in accelerating the downward motion of the ram. The speed of the hit and the amount of energy released is larger than those produced by a single action hammer.

d. Diesel hammer

According to Yulianto (2017), diesel hammer has high mobility, fuel efficiency, lightweight, and small dimensions. A diesel hammer can also be used on dense, cohesive soils but cannot be used on soft soils.

e. Vibratory hammer

This type of hammer uses high-frequency vibrations. The estimated bearing capacity of the pile obtained is usually based on the number of strokes required in the driving process in accordance with the previously determined penetration.

2.4 *Calculation of Pile Bearing Capacity with Dynamic Method*

Mayangsari (2018) stated that the bearing capacity of a pile refers to the pile's ability to support a load. Calculation of the pile bearing capacity can be done statically or dynamically. Meanwhile, Coduto (1994) divides into three things in calculating the bearing capacity of pile foundations, including the static method, the dynamic method, and the loading test.

According to Mulyono (2015), the bearing capacity of a pile must be sufficient to support the weight working on it (axial load). Thus, we require a method for determining whether a pile has sufficient bearing value in the field, one of which is by examining the amount of penetration per blow derived from field piling data. So, we need a way to calculate whether a

pile has sufficient bearing value, one of which is by looking at the penetration rate per blow obtained from the piling data at the project site. However, Olson (1967) argues that using the dynamic technique to determine the bearing capacity of a pile will result in an inaccurate value, necessitating the inclusion of a large number of safety parameters.

According to Bowles (1997), there are ten methods of dynamic formulas that can be used in calculating the bearing capacity of piles. The ten methods are as follows:

a. Navy-McKay Methods

The Navy-McKay method uses Eqn. (1) with a Safety Factor (SF) value of 6

$$Qu = \frac{e_h E_h}{s(1+0.3C_1)} \quad (1)$$

b. Danish Methods

The Danish method uses Eqn. (2) with a Safety Factor (SF) value of 3-6

$$Qu = \frac{e_h E_h}{s+ C_1} \quad (2)$$

c. Eytelwein Methods

The Eytelwein method uses Eqn. (3) with a Safety Factor (SF) value of 6

$$Qu = \frac{e_h E_h}{s + C(\frac{Wp}{Wr})} \quad (3)$$

3 RESEARCH METHODOLOGY

In this study, the data used is only secondary data. Secondary data is data obtained from existing sources. In calculations using this dynamic formula, supporting data are needed relating to the implementation of pile driving in the field.

The secondary data used in this study, in the form of Detail Engineering Design (DED) of the Alue Lamteh Bridge Widening Project, the final set value (s) of calendering test on the pile P1.2 = 12 mm, P2.2 = 24 mm, P3.2 = 12 mm, P4.2 = 17 mm, hammer weight = 3.5 tons, hammer drop height = 2.5 meters, pile weight = 5.13 tons, pile length = 17 meters, pile diameter = 50 cm, pile compressive strength (fc') = 30 MPa.

The pile bearing capacity calculation using a dynamic formula is obtained from the final set value (s). The equations used in this study are based on Bowles, namely the Navy-McKay method, the Danish method, and the Eytelwein method.

Furthermore, the results of the bearing capacity calculation using this dynamic formula will be divided by the safety factor number according to the method used so that it will produce a bearing capacity value with good considerations and safety factors.

4 RESULTS AND DISCUSSION

4.1 *Pile Bearing Capacity of The Navy-McKay Method*

Table 1. Recapitulation of The Dynamic Bearing Capacity of The Navy-McKay Method.

Piles number	s (mm)	Qall (ton)
P1.2	12.0	84.411
P2.2	24.0	42.206
P3.2	12.0	84.411
P4.2	17.0	59.584

Based on the results of calculations using Eqn. (1), the lowest bearing capacity value is obtained in the Navy-McKay method with a final set value (s) of 24 mm, namely on the P2.2 pole of Qall = 42.206 tons, while the highest bearing capacity value is the final set value (s) 12 mm, namely on the piles P1.2 and P3.2 each of Qall = 84.411 tons. The recapitulation of the dynamic bearing capacity of the Janbu method is shown in Table 1.

The graph showing the relationship between the final set (s) value and the pile bearing capacity of the Janbu method is shown in Fig. 3.

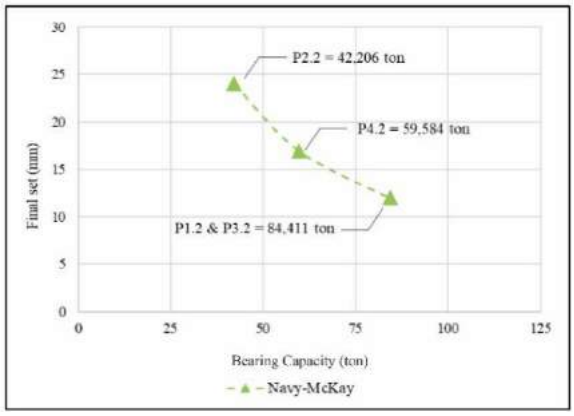

Fig. 3. Graph of The Relationship between The Final Set (s) Value and The Pile Bearing Capacity of The Navy-McKay Method.

4.2 *Pile bearing capacity of Danish method*

Based on the results of calculations using Eqn. (2), the lowest bearing capacity value is obtained in the Danish method with a final set value (s) of 24 mm, namely on the P2.2 pile of Qall = 80.997 tons, while the highest bearing capacity value is the final set value (s) 12 mm, namely on the piles P1.2 and P3.2 each of Qall = 121.478 tons. The recapitulation of the dynamic bearing capacity of the Janbu method is shown in Table 2.

Table 2. Recapitulation of The Dynamic Bearing Capacity Value of The Danish Method.

Piles number	s (mm)	Qall (ton)
P1.2	12.0	121.478
P2.2	24.0	100.541
P3.2	12.0	121.478
P4.2	17.0	80.997

The graph of the relationship between the final set (s) value and the bearing capacity of the Danish method of piles is shown in Fig. 4.

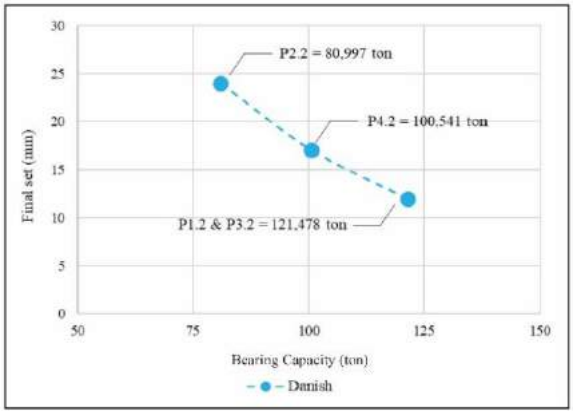

Fig. 4. Graph of The Relationship between The Final Set (s) Value and The Bearing Capacity of the Pile Using the Danish Method.

4.3 *Pile Bearing Capacity of Eytelwein Method*

Based on the results of calculations using Eqn. (3), the lowest bearing capacity value is obtained in the Eytelwein method with a final set value (s) of 24 mm, namely on the P2.2 pile of Qall = 80.997 tons, while the highest bearing capacity value is the final set value (s) 12 mm, namely on the piles P1.2 and P3.2 each of Qall = 121.478 tons. The recapitulation of the dynamic bearing capacity of the Janbu method is shown in Table 3.

Table 3. Recapitulation of The Dynamic Bearing Capacity Value of the Eytelwein Method.

Piles number	s (mm)	Qall (ton)
P1.2	12.0	92.752
P2.2	24.0	52.604
P3.2	12.0	92.752
P4.2	17.0	70.373

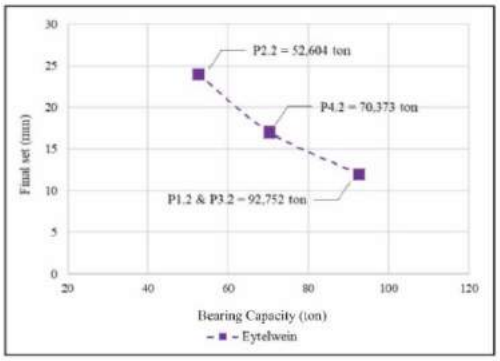

Fig. 5. Graph of the Relationship between The Final Set (s) Value and The Bearing Capacity of The Pile Using the Eytelwein Method.

The graph of the relationship between the final set (s) value and the bearing capacity of the Eytelwein method of piles is shown in Fig. 5.

4.4 *Relationship between pile bearing capacity and final set value(s)*

As illustrated in Fig. 6, the combined graph of the relationship between the final set (s) value and the pile bearing capacity using the Navy-McKay, Danish, and Eytelwein methods, the Danish method produces the highest dynamic bearing capacity value. In contrast, the Navy-McKay method has the lowest dynamic bearing capacity value.

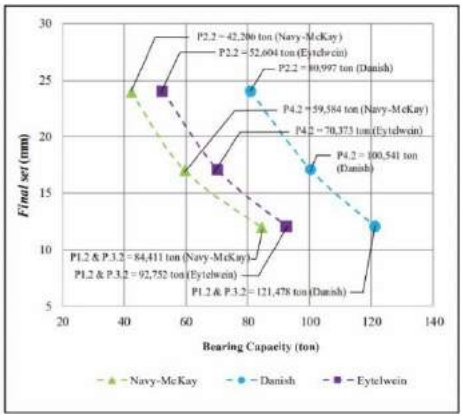

Fig. 6. The combined graph of the Relationship between the Final Set Value (s) and the Pile Bearing Capacity Using the Dynamic formula.

Fig. 6 also shows that the smaller the final set (s) value, the greater the dynamic bearing capacity value produced and vice versa if the larger the final set (s) value, the smaller the resulting bearing capacity value.

5 CONCLUSION AND SUGGESTION

Based on the results of calculations and analysis in Chapter IV, the following conclusions are obtained:

1. Based on the results of the calculation of the bearing capacity using the Navy-McKay method, the Danish method, and the Eytelwein method, it was found that the largest dynamic bearing capacity value is using the Danish method, namely on the P1.2 and P3.2 piles with the final set value = 12 mm each of 121,478 tons while the dynamic bearing capacity value is using the Navy-McKay method, namely on the P2.2 pile with the final set value = 24 mm, which is 42,206 tons.
2. The final set value of the calendering test results is very influential on the value of the bearing capacity that will be produced by a pile. The larger the final set (s) value, the smaller the bearing capacity value that will be produced, and if the final set (s) value is smaller, then the resulting bearing capacity value will be even greater.

Suggestions for further research is to get a more accurate value of dynamic bearing capacity that can be calculated using several other dynamic methods such as the Janbu, AASHTO, ENR-Modified, Gates, CNB, PCUBC, Hiley methods.

REFERENCES

Bowles, J.E. 1997. *Analisis dan Desain Pondasi Jilid 1*. Jakarta: PT. Erlangga.

Coduto, D.P., 1994. *Foundation Design: Principles and Practices.* Pretince Hall International Editions.

Hardiyatmo, H.C. 1996. *Teknik Fondasi I*. PT. Gramedia Pustaka Utama: Jakarta

Hardiyatmo, H.C. 2018. *Analisis dan Perancangan Fondasi II*. Gajah Mada University Press: Yogyakarta.

Mayangsari. 2018. Analisis Perbandingan Pondasi Tiang Pancang Dengan Pondasi Tiang Bor Pada Proyek Pebangunan Rumah Sakit Gigi Dan Mulut Universitas Brawijaya. *Naskah Publikasi Teknik Sipil Fakultas Teknik.* Malang: Universitas Brawijaya.

Mulyono, T. 2015. *Teknik Pondasi 2 Pondasi Dalam*. Jakarta: Universitas Negeri Jakarta.

Nurdiani, N. 2013. Pekerjaan Pondasi Tiang Pancang: Cara Pemancangan, Kendala dan Teknologi Terbaru. *Comtech* Vol. 4 (2): 776-784.

Olson, R.E., Flaate, K.S. 1967. Pile Driving Formulas for Friction Piles in Sand. *J. Soil Mech. Found. Eng. ASCE* Vol. 93, no. SM6: 270–296.

Pratama, M.I., Bhaskara, A. 2020. Komparasi Biaya dan Waktu Pekerjaan Tiang Pancang Metode Hydraulic Static Pile Driver dengan Drop Hammer. *Reviews in Civil Engineering* V.04, n.2: 62-68.

Pratama, R.R., Lukman, H., Rahmah, A. 2019. Analisa Daya Dukung Tiang Pancang Berdasarkan Hasil Data Kalendering Pada Proyek Icon City Delta Mas, Cikarang Pusat, Bekasi. *Jurnal Teknik Sipil Universitas Pakuan*: 1-7.

Sardjono, H.S. 1988. *Pondasi Tiang Pancang*. Surabaya: Sinar Wijaya.

Sombah, M.C., Dundu, A.K.T., Sibi, M. Studi Analisis Pelaksanaan Pekerjaan Pemancangan Dengan Metode Value Engineering Pada Proyek Interchange Maumbi – Manado. *Jurnal Ilmiah Media Engineering* Vol.6 No.1: 448-462.

Tobing, B.M.L., Munirwansyah. 2019. Perbandingan Kapasitas Penggunaan Formula Dinamis Pada Tiang Pancang Sebagai Kontrol Daya Dukung. *Journal of The Civil Engineering Student* Vol. 1 (3):43-49.

Tomlinson, M., Woodward, J. 1994. *Pile Design and Construction Practice*. London and Newyork: Francis and Taylor Group.

Yulianto, J. 2017. Pemilihan Alat Pancang Menggunakan Expert Choice. *Jurnal Riset Rekayasa Sipil Universitas Sebelas Maret*: 50-58.

Influence of Pile Spacing to Immediate Settlement of Short Piled Raft Foundation System on Peat Soil under Static Load

Sajiharjo Marto Suro
Institut Teknologi PLN

Dyah Pratiwi Kusumastuty
Institut Teknologi PLN

Kasbi Basri
Universiti Tun Hussein Onn Malaysia

Adnan Zainorabidin
Universiti Tun Hussein Onn Malaysia

ABSTRAK: Sistem pondasi rakit bertiang pendek adalah modifikasi dari pondasi rakit bertiang, yang panjang tiangnya relatif pendek. Jarak tiang merupakan parameter variabel yang penting, terkait dengan penurunan segera. Oleh karena itu pengaruh jarak tiang perlu dipelajari. Metode elemen hingga digunakan untuk mensimulasikan kinerja stabilitasnya. Sistem pondasi Rakit Bertiang Pendek dengan pelat beton 7,0 m x 7,0 m persegi dan tebal 0,15 m diasumsikan dibangun di atas lapisan tanah gambut 3,5 m. Diameter luar tiang adalah 0,32 m dan panjang tiang 3,00 m, sedangkan jarak tiang bervariasi dari 0,50 sampai 3,00 m. Beban titik bervariasi dari 0 sampai 100 kN diasumsikan sebagai beban statis, yang bekerja pada bagian tengah pelat beton. Dengan membandingkan setiap hasil simulasi numerik, dapat disimpulkan bahwa jarak tiang 1,00 m merupakan jarak yang optimal, menghasilkan penurunan segera sebesar 31,80 mm.

Kata Kunci: sistem pondasi rakit bertiang pendek, jarak tiang, penurunan segera

ABSTRACT: Short piled raft foundation system is a modified piled raft, which the pile length is relatively shorter. Pile spacing is an important variable parameter, related to immediate settlement. Therefore, the influence of pile spacing need to be studied. Finite element method was used to simulate the stability performance. Short Piled Raft foundation system with concrete slab of 7.0 m x 7.0 m square and thickness of 0.15 m was assumed to be built on 3.5 m peat layer. The outer diameter of pile was 0.32 m and pile length was 3.00 m, while the pile spacing varied from 0.50 to 3.00 m. Point load varied from 0 to 100 kN was considered as a static load, acted on the centre of the concrete slab. By comparing each numerical result of simulations, it could be concluded that 1.00 m pile spacing was an optimal one, produced immediate settlement of 31.80 mm.

Keywords: short piled raft foundation system, pile spacing, immediate settlement

1 INTRODUCTION

The last few decades, due to limited land available, many construction projects have penetrated into the problematic soil area, with some of the problems faced, Patil et al. (2013). Completion of construction by using a conventional foundation system such as pile foundation system is still considered to be quite expensive, Effendi (2013). To overcome these problems, several foundation systems have been developed, among others, is a piled raft

foundation, which the concept of this system has received considerable attention in recent years, Prakoso and Kulway (2001) and even proves to be more effective on such conditions, increasingly recognized as a foundation more economical and effective on problematic soil, Srilakshmi and Moudgalya (2013).

Moreover, especially at peat area, the construction method on peat is different for the different depth of peat, Bakar (2014). For peat with the depth less than 3 m, removal and replacement method are usually used. For the depth of 3 m to 10 m, engineers normally used sand drain, lightweight fills and stone column. While for the depth more than 10 m, the suitable method is deep stabilization techniques such as pile and dynamic compaction. This condition

motivates to develop a foundation system that can be directly implemented on peat with the depth of 3 m to 10 m, neither by using removal and replacement method nor soil stabilization.

2 SCOPE, LIMITATION AND OBJECTIVE

In this study, a Short Piled Raft (hereinafter abbreviated as SPR only) foundation system was introduced, built on peat which is known as problematic soil. SPR foundation system is a modified piled raft foundation system, which is a combination between pile foundation and raft foundation, which the pile length relatively shorter, with a ratio between the length and diameter of pile not more than 20, Das and Sivakugan (2019), and considered as a reinforced concrete slab resting on a number of piles. Typical of SPR foundation system can be seen in Fig. 1.

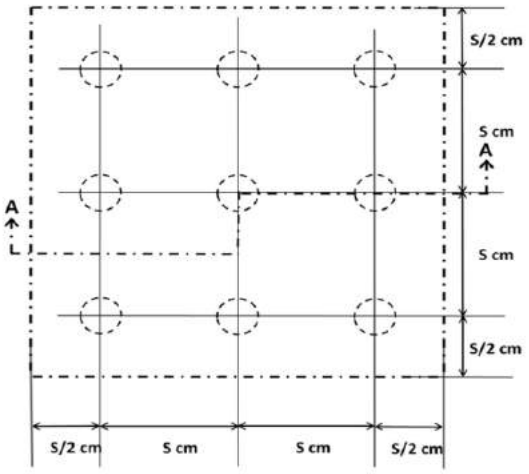

(a)

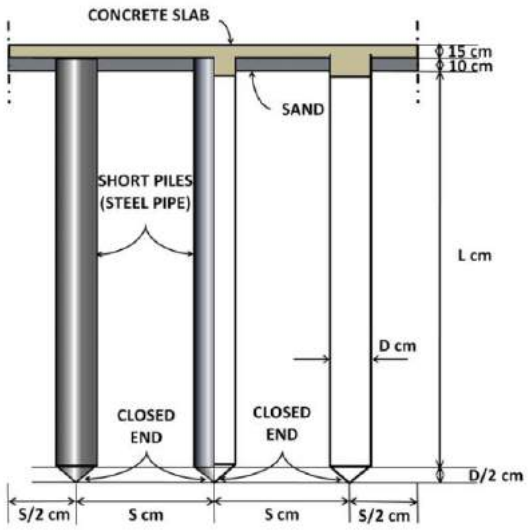

(b)

Fig. 1. SPR Foundation System; (a) General Plan; (b) Cross Section A-A.

The basic concept of SPR foundation system considers that the thin concrete slab floats on the supporting soil while the piles serve as stiffeners slab concrete and also to improve stability performance by reducing settlement of the foundation, Tandjiria (1999).

The scope of this study was to simulate behaviour of SPR foundation system, on peat soil with different pile spacing under static load, especially related to immediate settlement.

The limitation of this study was only conducted numerically, with a certain condition e.g., on peat with the layer thickness of 3.5 m, constant ground water level, consolidated drained, the thickness of concrete slab, length and diameter of pile assumed to be constant.

While the objective of this study was to investigate the influence of pile spacing to immediate settlement of SPR foundation system on peat soil under static load, by using finite element method program for simulation.

3 FINITE ELEMENT METHOD

A three-dimensional finite element method program, namely Plaxis 3D Foundation was used. Plaxis 3D Foundation is a special purpose three-dimensional finite element program used to perform deformation and stability analysis for various types of geotechnical applications. With Plaxis 3D Foundation, complex geometry of soil and structures can be defined in two different modes. These modes are specifically defined for soil or structural modeling.

The finite element method provides a valuable analytical tool for the analysis and design of foundations. Since the piled raft is typical example of soil - structure interaction, a special type of element at pile – soil interface, simulating the displacement discontinuity between the pile and the soil mass is needed. Hence, PLAXIS 3D Foundation, in which the pile is assumed as a slender beam element, Dao (2011).

The pile-soil interaction is governed by relative movements between the pile nodes and the soil nodes. The connection between these nodes is established by means of special – purposed non – linear spring representing the pile - soil contact at the base. Based on the materials, linear elastic material model is used for concrete and steel pile structure to simulate their stress – strain behavior, while the Soft Soil Creep model is used for peat, Brinkgreve (2007) and for soft clay under the peat layer, the

Mohr - Coulomb model is selected, Qaissy *et a*l. (2013).

4 METHODOLOGY

An SPR foundation system with the size of 7.0 m x 7.0 m was considered as a model simulation. Concrete slab was set as 0.15 m thickness. Pile outer diameter D was 0.32 m with the wall thickness of 0.003 m of galvanized steel pipe to be selected, by considering availability on the market.

Point load varied from 0 kN to 100 kN with increment of 20 kN were considered as a static load, acted on the centre of the concrete slab.

While the site of selected problematic soil area, as a model in this study was Parit Nipah Darat, Batu Pahat, Johor, Malaysia. Peat layer at Parit Nipah Darat has depth from 0.0 m to 3.0 m, while at depth 3.0 m – 3.5 m, peats have mixed clay and at depth of $\geq$ 3.5 m is completely soft clay, as illustrated in Fig. 2.

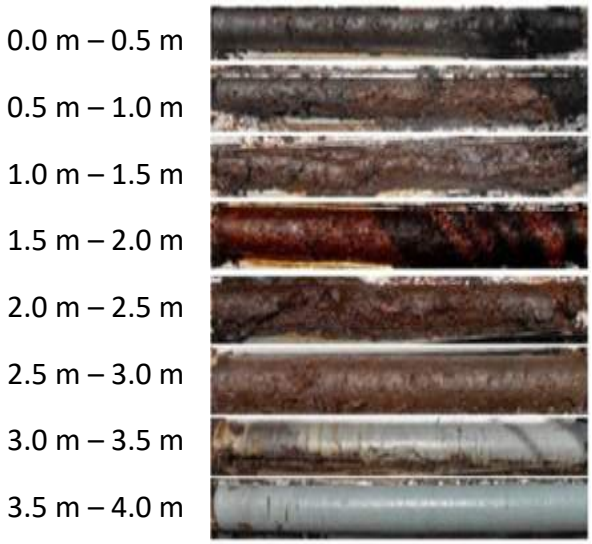

Fig. 2. Soil Profile of Parit Nipah Darat Using Peat Sampler, Said et al. (2014).

The simulations were conducted by applying pile spacing of 0.50 m, 0.75 m, 1.00 m, 1.50 m, 2.00 m and 3.00 m in each simulation series respectively. In order to obtain the best configuration of piles, some simulation series by applying varies load at the centre of raft should be conducted with the scenario as shown in Table 1.

Table 1. Variation of Pile Spacing for Simulation.

No.	Pile Spacing (m)	Number of Piles	Loading (kN)
1.	0.50	169	20, 40, 60, 80, 100
2.	0.75	81	20, 40, 60, 80, 100
3.	1.00	49	20, 40, 60, 80, 100
4.	1.50	25	20, 40, 60, 80, 100
5.	2.00	16	20, 40, 60, 80, 100
6.	3.00	9	20, 40, 60, 80, 100

Parameters used for simulating the SPR foundation system in this study as shown in Table 2.

5 RESULTS AND DISCUSSIONS

Illustration of SPR foundation system in numerical model is shown in Fig. 3.

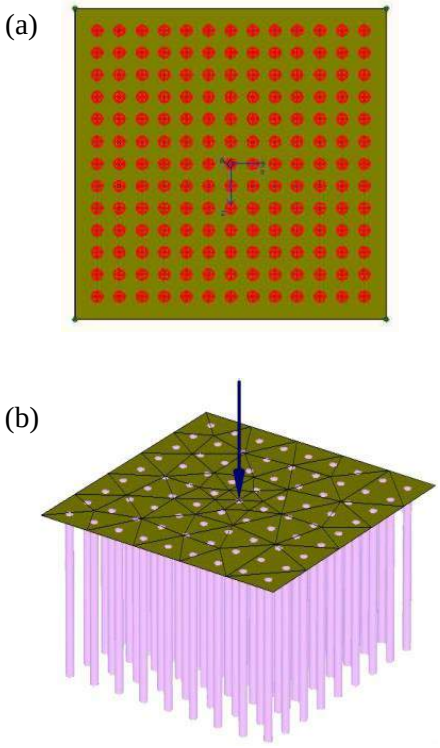

Fig. 3. Model of SPR Foundation System with 7.0 m x 7.0 m Concrete Slab, (a) Plan with Pile Spacing of 0.50 m; (b) Upper View with Pile Spacing of 0.75 m.

Table 2. Soil, Pile and Raft Parameters used for SPR Foundation System Simulation.

Soil properties (Peat)	Obtained from	Value
C	Laboratory test	4.0 (kN/m^2)
φ	Laboratory test	16 (^{0})
E_{ref}	Plaxis 3-D's suggestion	200 (kN/m^2)
γ_{unsat}	Plaxis 3-D's suggestion	10 (kN/m^3)
γ_{sat}	Plaxis 3-D's suggestion	11 (kN/m^3)
V	Plaxis 3-D's suggestion	0.12
Thickness of layer	Previous research	3.50 (m)
Soil Properties (Soft clay)	**Obtained from**	**Value**
C	Previous research	5.0 (kN/m^2)
φ	Previous research	25 (^{0})
E_{50}	Plaxis 3-D's suggestion	2000 (kN/m^2)
γ_{unsat}	Plaxis 3-D's suggestion	16 (kN/m^3)
γ_{sat}	Plaxis 3-D's suggestion	17(kN/m^3)
V	Plaxis 3-D's suggestion	0.3
Thickness of layer	Determined for numerical model simulation purposes	$\geq$ 16.50 (m)

While before calculating immediate settlement, generated 3-D mesh of SPR foundation system, automatically formed is shown in Fig. 4.

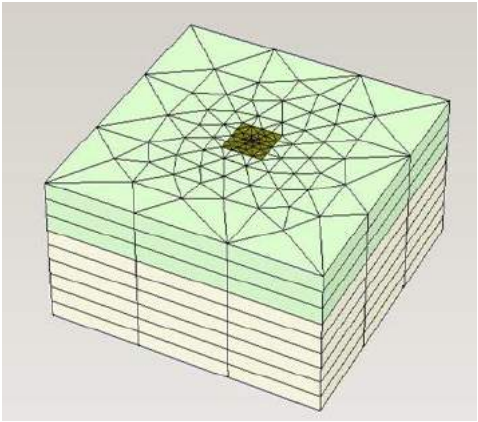

Fig. 4. Generated 3-D Mesh of SPR Foundation System Model.

Simulation by calculating of immediate settlement consist of several steps. Starting from initial condition, followed by activating piles, and then activating concrete slab, and finally activating point load from 0 kN up to 100 kN with increment of 20 kN. These steps were conducted for each pile spacing from 0.50 m, 0.75 m, 1.00 m, 1.50 m, 2.00 m and 3.00 m.

The results of these simulations are tabulated in Table 3a. and Table 3b. as follows.

Table 3.a. Relationship between Pile Spacing and Settlement Under the Load of 0 – 40 kN.

Spacing (m)	Load (kN)		
	0	20	40
	Settlement (mm)		
0.50	30.52	32.20	33.88
0.75	22.41	24.28	26.16
1.00	19.94	21.97	24.01
1.50	19.58	21.97	24.36
2.00	21.28	23.97	26.80
3.00	25.94	29.69	33.43

Table 3.b. Relationship between Pile Spacing and Settlement Under the Load of 60 – 100 kN.

Spacing (m)	Load (kN)		
	60	80	100
	Settlement (mm)		
0.50	35.56	37.23	38.91
0.75	28.03	29.91	31.78
1.00	26.04	28.08	30.11
1.50	26.76	29.22	31.80
2.00	29.73	32.65	35.57
3.00	37.19	40.95	44.74

These results of simulations can also be presented graphically as shown in Fig. 5. It can be seen, that in general if the spacing of pile increases (more than 1.0 m), the settlement will increase and so if the spacing of pile decreases (less than 1.0 m), the settlement will also increase. Das (2011) stated that ideally, the piles in a group should be spaced so the load-bearing capacity of the group is not less than the sum of the bearing capacity of the individual piles. In practice, the minimum centre-to-centre pile spacing is 2.5 D and, in ordinary situations, is actually about 3 to 3.5 D.

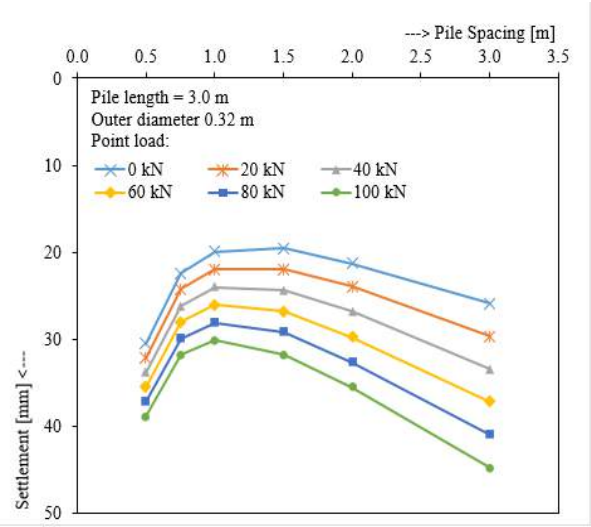

Fig. 5. Relationship between Pile Spacing and Settlement Under the Load of 0 – 100 kN.

While based on previous research, pile spacing is 2.08 D, Tandjiria (1999), 4D, Prakoso (2001), 5D – 13.3 D, Hardiyatmo (2011), 1.5D – 2D, Sönmez (2013) and 5 D, Waruwu (2017).

It means that when the piles are placed close to each other, a reasonable assumption is that the stresses transmitted by the piles to the soil will overlap, reducing the load-bearing capacity of the piles. Moreover, if pile spacing decreases (in this case less than 1.0 m), the total weight of foundation relatively heavier and leads to contribute larger settlement.

While for the piles are placed more than 1.00 m, the number of piles in a group will decrease, causes the load-bearing capacity of the group also decreases and leads to contribute larger settlement. It can be seen that in the case of SPR foundation system with 7.0 m x 7.0 m of concrete slab and vertical static load of 0, 20, 40, 60, 80 and 100 kN on it, at the center of concrete slab, then pile spacing of 1.0 m produces the minimum settlement. Therefore, the pile spacing influences on immediate settlement of SPR foundation system significantly. In this study, the optimum pile spacing was 1.00 m. In this case, 3 to 3.5 D is equal to 0.96 m to 1.12 m, it means that the optimum pile spacing 1.0 m is in that range.

6 CONCLUSION

Based on the results and discussions, it can be drawn some conclusions as follows. When the piles are placed too close to each other, it will cause reducing the load-bearing capacity of the piles. Moreover, if pile spacing decreases, the total weight of foundation relatively heavier and leads to contribute larger settlement. While for the piles are placed too far, the number of piles in a group will decrease, causes the load-bearing capacity of the group also decreases and leads to contribute larger settlement. In this study, pile spacing of 1.0 m was an optimum pile spacing and produced the minimum settlement. Therefore, it is obviously that the pile spacing influences to immediate settlement of SPR foundation system significantly.

ACKNOWLEDGEMENTS

The authors wish to express their gratitude to Research Centre for Soft Soil – Universiti Tun Hussein Onn Malaysia (RECESS – UTHM) for their supports and provision of excellent facilities during this study.

REFERENCES

Bakar, I. 2014. Challenges in Peat Soil Research - Malaysian Experiences. *South East Asia Conference on Soft Soils Engineering and Ground Improvement*. Bandung.

Brinkgreve, R.B.J. 2007. *Plaxis 3D Foundation, Version 2*. Delft University of Technology and Plaxis bv, The Netherlands.

Dao, T.P.T. 2011. *Validation of PLAXIS Embedded Piles for Lateral Loading*. Master of Science Thesis, Delft University of Technology, The Netherlands.

Das, B.M. 2011. *Principles of Foundation Engineering*. *Seventh Edition*. Boston: Cengage Learning.

Das, B.M., & Sivakugan N. 2019. *Principles of Foundation Engineering*. 9th Edition. Boston: Cengage Learning.

Effendi, S. 2013. Cakar Ayam Soft Foundation System Revisited. *Soft Soil Engineering International Conference*. Kuching, Sarawak.

Hardiyatmo, H. C. 2011. *Analisis dan Perancangan Fondasi II*. Edisi Kedua, Gadjah Mada University Press, Yogyakarta.

Patil, J. D., Vasanvala, S. A. & Solanki, C. H. 2013. *A* Study on Piled Raft Foundation: State of Art. *International Journal of Engineering Research & Technology* (IJERT).

Prakoso, W.A. & Kulway, F.H. 2001. Contribution To Piled Raft Foundation Design. *Journal of Geotechnical and Geoenvironmental Engineering*.

Qaissy, M.A., Karim, H.H. & Hameedi, M.K. 2013. Behavior of Experimental Model of Piled Raft Foundations on Clayey Soils. *1st International Conference for Geotechnical Engineering and Transportation ICGTE*.

Said, M. J. M., Zainorabidin, A. & Madun, A. 2014. Seismic Refraction on Peat Soils at Parit Nipah. *South*

East Asia Conference on Soft Soils Engineering and Ground Improvemnet. Bandung.

Sőnmez, N. 2013. *A Study on Design of Piled Raft Foundation Systems.* Middle East Technical University. MSc Thesis.

Srilakshmi, G. & Moudgalya, D. 2013. Analysis of Piled Raft Foundation Using Finite Element Method. *International Journal of Engineering Research and Science & Technology* Vol. 2, No. 3.

Tandjiria, V. 1999. Numerical Modelling of Chicken-Foot Foundation. *Dimensi Teknik Sipil* Volume 1, no. 1 Maret.

Waruwu, A., Hardiyatmo, H. C. & Rifa'i, A. 2017. Behaviour of Nailed-Slab System on Peat Soil Under Loading. *The 1st Warmadewa University International Conference on Architecture and Civil Engineering*. Bali, Indonesia.

Kajian Penentuan Parameter Viskositas Material Pasir Kelanauan Pada Kondisi Terlikuifaksi dengan Menggunakan Shake Table dan Melalui Tahanan Friksi dari Hasil Pembacaan CPTu

Albert Johan
Universitas Katolik Parahyangan – PT Geotechnical Engineering Consultant

Paulus P. Rahardjo
Universitas Katolik Parahyangan

Budijanto Widjaja
Universitas Katolik Parahyangan

ABSTRAK: Fenomena likuifaksi menjadi salah satu perhatian utama bagi Indonesia dan dunia, terutama pasca peristiwa likuifaksi di Palu akibat gempa Palu - Donggala pada 28 November 2018. Berangkat dari fenomena likuifaksi tersebut, diketahui bahwa *flow liquefaction* merupakan suatu peristiwa yang memerlukan perhatian khusus perihal peristiwa tersebut dapat mengakibatkan tingkat kerusakan yang tinggi, seperti Desa Sibalaya yang terletak di Palu. Untuk menunjang kajian aliran pada peristiwa *flow liquefaction* pada Desa Sibalaya yang didominasi oleh material pasir kelanauan, maka telah dilakukan pengambilan sampel tanah pada Desa Sibalaya. Penelitian ini difokuskan terhadap kajian penentuan parameter reologi berupa viskositas dari material pasir kelanauan pada kondisi terlikuifaksi dengan menggunakan instrumen *shake table, chamber, rod extruder,* dan CPTu. Pasir kelanauan dalam *chamber* dijenuhkan terlebih dahulu agar material pasir kelanauan dapat mengalami likuifaksi ketika diberikan beban dinamik. Parameter viskositas dapat diperoleh dari gesekan selimut dari penetrasi CPTu saat material pasir kelanauan masih berperilaku sebagai likuid. Besarnya gesekan selimut, kecepatan penetrasi CPTu, dan zona area terganggu akibat penetasi CPTu menjadi kunci utama dalam penentuan nilai viskositas.

Kata Kunci: likuifaksi, viskositas, pasir kelanauan, shake table, CPTu

ABSTRACT: The phenomenon of liquefaction has become one of the main concerns for Indonesia and the world, especially after the liquefaction event in Palu due to the Palu - Donggala earthquake in 28 November 2018. Departing from the liquefaction phenomenon, it is known that flow liquefaction is an event that requires special attention regarding the event that can lead to high levels of damage, such as Sibalaya Village that located in Palu. To support flow studies on flow liquefaction events in Sibalaya Village which is dominated by silty sand material, soil sampling has been carried out in Sibalaya Village. This research is focused on the study of determining rheological parameters in the form of viscosity of silty sand material in liquefied conditions using shake table, chamber, rod extruder, and CPTu instruments. The silty sand material in the chamber must be in saturated condition so that the silty sand material can experience liquefaction when given a dynamic load. The viscosity parameter can be obtained from the friction resistance of the CPTu penetration when the silty sand material still behaves as a liquid. The friction resistance, the speed of CPTu penetration, and the zone of disturbed area due to CPTu penetration are the main keys in determining the viscosity value.

Keywords: liquefaction, viscosity, silty sand, shake table, CPTu

1 PENDAHULUAN

Dewasa ini, likuifaksi menjadi salah satu sorotan bagi selintir masyarakat Indonesia maupun dunia khususnya setelah bencana Gempa Palu - Donggala 2018. Fenomena likuifaksi yang terjadi di Palu tersebut mendapatkan perhatian khusus karena telah berhasil memporak-porandakan inftrastruktur maupun perumahan dalam skala yang besar sehingga membuat kejutan terhadap masyarakat, khususnya masyarakat yang mengalami langsung atau melihat langsung kejadian tersebut. Terzaghi dan Peck (1967) mendiskripsikan likuifaksi sebagai hilangnya kuat geser tanah pasir yang memiliki kepadatan

lepas dan dapat mengakibatkan longsoran aliran jika diberi gangguan eksternal. Fenomena likuifaksi dapat dibagi menjadi 2 tipe yaitu *flow liquefaction* dan *cyclic mobility*. Pada umumnya *flow liquefaction* lebih jarang terjadi dibandingkan *cyclic mobility*, namun kerusakan yang diakibatkan oleh *flow liquefaction* dapat sangat fatal karena dapat mengakibatkan pergerakan tanah yang sangat cepat dengan volume tanah yang masif.

Ketika suatu material tanah mengalami likuifaksi, maka tanah tersebut dapat diasumsikan berbentuk seperti fluida (Hamada dan Wakamatsu, 1998). Berdasarkan hasil penelitian yang dilakukan oleh Sasaki et al. (1992) pada pengujian *shake table*, diketahui bahwa aliran yang terjadi pada tanah pasir yang terlikuifaksi mengalami kemiripan dengan fluida dan arah deformasi dikontrol oleh gradien hidrolik.

Menurut Chen et al. (2006), karakteristik aliran pada pasir yang mengalami likuifaksi akan bersifat aliran non-Newtonian (shear thinning) yang mana viskositas pasir dalam kondisi likuifaksi akan semakin menurun seiring dengan meningkatnya shear strain rate. Penelitian Hamada dan Takahashi (2004) menunjukkan bahwa perilaku aliran pada tanah yang terlikuifaksi akan mendapatkan kekakuan awalnya secara perlahan-lahan dan kembali ke bentuk solid. Dengan pemahaman demikian, maka peristiwa *flow liquefaction* memiliki kaitan yang sangat erat terhadap ilmu reologi yang mempelajari mengenai deformasi dan aliran suatu benda. Menurut Newton (1687), resistensi pada suatu fluida pada saat mengalir disebut juga sebagai viskositas (η) yang mana merupakan salah satu parameter reologi yang berperan penting dalam mempelajari perilaku suatu material fluida.

Sehubungan dengan pemahaman yang telah disampaikan di atas, maka parameter viskositas merupakan salah satu parameter pokok yang berperan penting dalam suatu pemodelan aliran *flow liquefaction*. Untuk menunjang hal tersebut, maka telah dilakukan penelitian untuk menentukan parameter viskositas pada material tanah yang terlikuifaksi sehingga parameter viskositas tersebut diharapkan dapat digunakan sebagai parameter input dalam pemodelan aliran *flow liquefaction* sehingga masyarakat dapat mengantisipasi area-area yang berpotensi terdampak oleh aliran *flow liquefaction* yang bersifat sangat destruktif pada masa mendatang.

2 LOKASI KAJIAN PENELITIAN

Kajian penentuan parameter reologi berupa viskositas dilakukan terhadap material sampel tanah yang diambil dari Desa Sibalaya, Kecamatan Tanambulava, Kabupaten Sigi, Sulawesi Tengah. Desa Sibalaya merupakan salah satu area yang terdampak likuifaksi yang diakibatkan oleh Gempa Palu - Donggala seperti yang dapat dilihat pada Gbr. 1. Berdasarkan peta geologi lembar Palu dan sekitarnya, diketahui bahwa Desa Sibalaya berada pada daerah yang didominasi oleh material alluvium (Q_{al}) seperti yang dapat dilihat pada Gbr. 2.

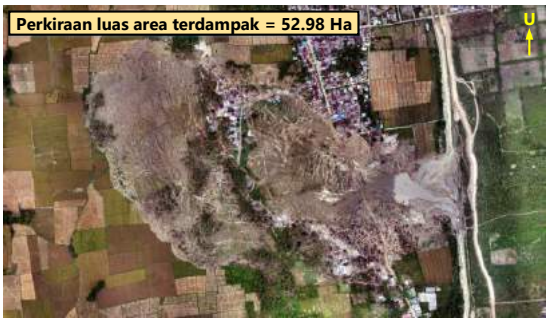

Gbr. 1. Tampak Atas Area Desa Sibalaya yang Terdampak Likuifaksi.

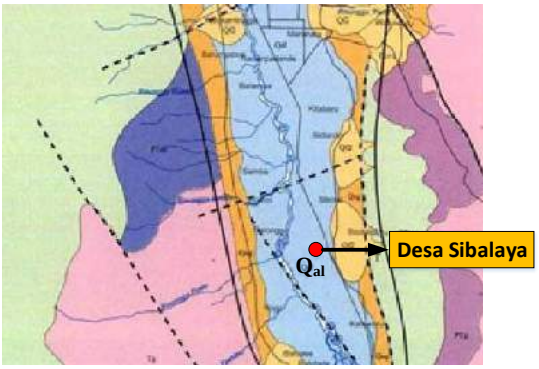

Gbr. 2. Kondisi Geologi Desa Sibalaya, Soehaimi et al. (2000).

Material sampel tanah (Gbr. 3) yang digunakan dalam penelitian ini ialah material sampel tanah Desa Sibalaya yang diambil pada sisi permukaan. Material sampel ini didominasi oleh material pasir kelanauan seperti yang dapat dilihat pada rekapitulasi persentase distribusi butiran tanah yang ditunjukkan pada Tabel 1.

Tabel 1. Persentase Distribusi Butiran Tanah.

Jenis Material	Distribusi Butiran Tanah (%)
Gravel	0,00
Coarse sand	0,00
Medium sand	39,71
Fine sand	46,49
Silt & clay	13,80

Gbr. 3. Kondisi Material Sampel Tanah pada Desa Sibalaya.

3 METODE PENENTUAN PARAMETER VISKOSITAS

Pada penelitian ini, penentuan viskositas mengacu kepada metode yang diusulkan oleh Mahajan dan Budhu (2006). Menurut Mahajan dan Budhu (2006), ketika suatu *rigid shaft* mengalami penetrasi pada suatu butiran tanah, maka tanah yang terletak pada area ujung konus akan mengalami tegangan yang tinggi dan akan berada dalam kondisi *failure* seperti yang dapat dilihat pada Gbr. 4, sehingga tanah tersebut akan mengalir melalui sekeliling permukaan shaft selama penetrasi berlangsung seperti yang dapat dilihat pada Gbr. 5.

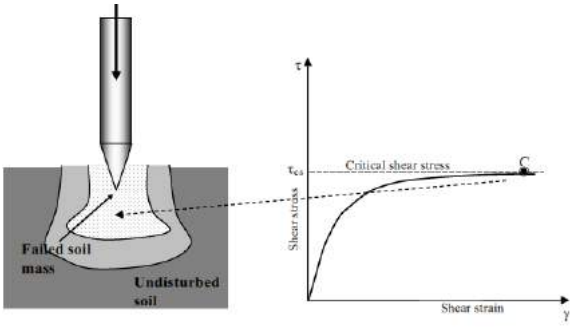

Gbr. 4. Kondisi Tanah yang Mengalami Failutre pada Area Ujung Konus , Mahajan dan Budhu (2006).

Pergerakan aksial dari suatu *shaft* dengan *radius*, r_0, dalam kondisi *viscous*, menghasilkan total tegangan resistensi selimut (τ) yang terdiri dari komponen statik / komponen CS *shear stress* (τ_{cs}) yang independen terhadap rate penetrasi dan komponen *viscous* (τ_v) yang bergantung terhadap rate penetrasi seperti yang dapat dilihat pada Pers. (1) dan Pers. (2).

$$\tau = \tau_{cs} + \tau_v \quad (1)$$

$$\tau = \tau_{cs} + \eta\,(du/dr) \quad (2)$$

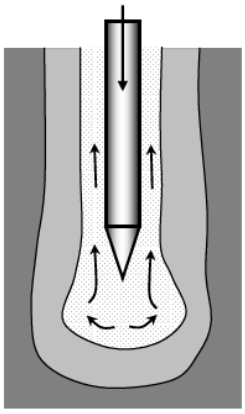

Gbr. 5. Tanah pada Area Ujung Konus Mengalir Melalui Sekeliling Permukaan *Shaft*, Mahajan dan Budhu (2006).

Komponen *viscous* sangat bergantung terhadap rate dari kecepatan penetrasi. Jika shaft berada dalam kondisi diam (rate penetrasi = 0), maka resistensi *viscous* akan tidak bekerja, sehingga praktis total resistensi selimut hanya terdiri dari komponen statik. Berdasarkan pemaparan di atas, maka gaya yang bekerja dan zona yang terpengaruh pada saat penetrasi *shaft* dapat dilihat pada Gbr. 6.

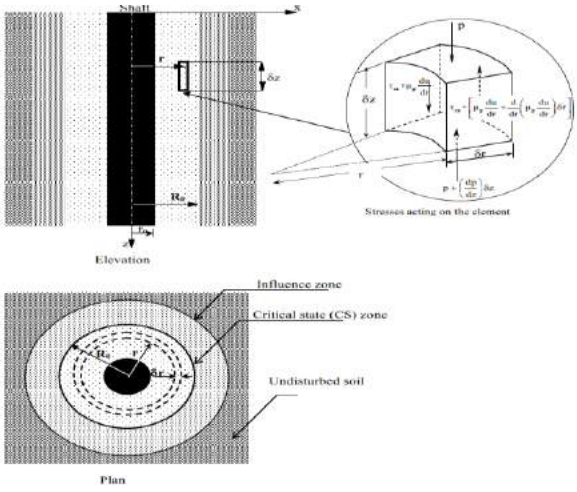

Gbr. 6. Gaya yang Bekerja pada Saat Penetrasi *Shaft*, Mahajan dan Budhu (2006).

Sehubungan dengan saat pengujian CPT, penetrasi konus akan mengakibatkan tanah yang berada di sekeliling konus akan berada dalam kondisi *viscous*, maka pendekatan nilai viskositas dapat didapatkan melalui pengujian CPTu tersebut. Menurut Mahajan dan Budhu (2006), friksi yang terjadi pada saat pengujian CPT terdiri dari friksi selimut dalam kondisi statik (f_{ss}) dan friksi selimut dalam kondisi *viscous* (f_{sv}) seperti yang dapat dilihat pada pada Pers. (3) (satuan dalam kPa).

$$f_s = f_{ss} + f_{sv} \quad (3)$$

Dikarenakan friksi selimut kondisi viscous sangat bergantung terhadap parameter viskositas (η), rate penetrasi (V_z), zona area critical state (β_0), dan keliling sondir (πD), maka parameter friksi selimut dalam kondisi viscous (f_{sv}) dapat dilihat pada Pers. (4) (satuan dalam kPa).

$$f_{sv} = \frac{2\,\pi\,\eta\,Vz\,\beta 0}{\pi\,D} \quad (4)$$

Pada perhitungan parameter friksi selimut dalam kondisi *viscous* (f_{sv}), peran dari ukuran dari zona *area critical state* sangat bergantung terhadap parameter λ_0 yang mana merupakan ratio dari jari-jari zona area terpengaruh terhadap jari-jari konus. Zona area *critical state* merupakan suatu area yang terletak di sekeliling shaft yang mengalami deformasi dengan kondisi volume dan *shear stress* yang konstan. Hubungan dari parameter λ_0 terhadap β_0 dapat dilihat pada Pers. (5) dan Pers. (6).

$$\lambda_0 = \frac{R_0}{r_0} \quad (5)$$

$$\beta_0 = \frac{{\lambda_0}^4 - 4\,{\lambda_0}^3 + 4\ln\lambda_0 + 3}{(1-{\lambda_0}^2)\,[(1-{\lambda_0}^2)(\ln\lambda_0 - 1) - 2\,ln\,\lambda_0)]} \quad (6)$$

Berdasarkan hubungan antara λ_0 dan β_0 diketahui bahwa $\lambda_0 < 4$ akan menghasilkan perubahan resistensi *viscous* yang signifikan perihal terjadi penurunan pada nilai β_0, sedangkan $\lambda_0 > 4$ tidak secara signifikan berdampak terhadap resistensi *viscous* perihal nilai β_0 cenderung berada dalam nilai konstan seperti yang dapat dilihat pada Gbr. 7.

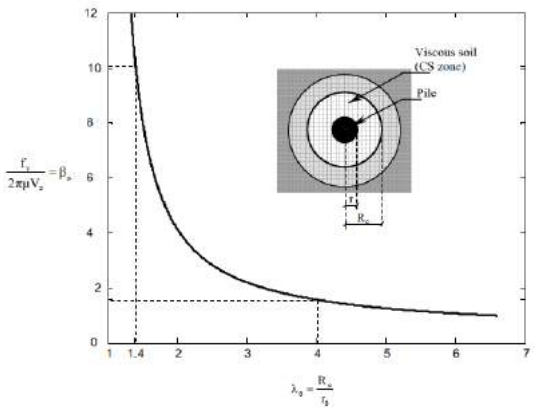

Gbr. 7. Hubungan Parameter λ_0 Terhadap Parameter β_0, Mahajan dan Budhu (2006).

Menurut Flaate (1972), berdasarkan hasil observasi terhadap *material driven timber shaft* dan hasil studi literatur, penetrasi *shaft* akan berdampak sebesar 2 – 2,5 kali dari *radius shaft*. Cooke dan Price (1973) melakukan pengujian *load test* dengan menggunakan *instrumented pile* pada material London Clay dan menemukan bahwa pergerakan tanah (yang diduga sebagai CS Zone) di sekeliling *shaft* terjadi sekitar 4 kali dari *radius shaft*. Randolph et al. (1979) mengasumsi bahwa instalasi atau penetrasi shaft dapat dimodelkan *plane strain* dalam kondisi *undrained expansion* dengan menggunakan model *Cam Clay*. Dari kajian tersebut, didapatkan bahwa zona *area critical state* ($\lambda 0$) bernilai 5 untuk tanah *normally consolidated* dan bernilai 4 untuk tanah *over consolidated* (OCR = 8).

4 METODE PENELITIAN

Pada penelitian ini, terdapat beberapa tahapan pekerjaan yang dilakukan yaitu sebagai berikut.

- *Persiapan Sampel Tanah Penelitian*

Sehubungan dengan sampel tanah Desa Sibalaya didominasi oleh pasir kelanauan seperti yang dapat dilihat pada Tabel 1, maka persiapan sampel material tanah pada *chamber* ditentukan menggunakan metode konsolidasi dengan menggunakan *slurry* seperti yang diusulkan oleh Rahardjo (1989) yaitu dengan cara mengkonsolidasikan material pasir kelanauan tersebut. Kondisi di alam, material tanah aluvial telah mengalami proses pengendapan dan telah terkonsolidasi selama beberapa tahun. Proses alami ini dapat disimulasikan di laboratorium dengan cara mengkonsolidasikan material pasir kelanauan tersebut dalam bentuk *slurry*. Metode *slurry* ini

juga dapat menghasilkan suatu material sampel tanah dengan tingkat saturasi yang tinggi (> 90%). Kekurangan dari metode *slurry* ialah metode pekerjaannya tidak dapat diotomatisasi seperti pluviator dan memerlukan waktu yang untuk proses konsolidasi. Pada tahapan ini, material sampel tanah ditargetkan memiliki nilai kepadatan relatif (Dr) sebesar 50%. Dokumentasi tahapan konsolidasi material sampal tanah pada *chamber* dapat dilihat pada Gbr. 8.

Gbr. 8. Dokumentasi Material Sampel Tanah pada Intrumen *Chamber* dan *Shake Table*.

- *Pemberian Beban Surcharge*

Untuk memodelkan kondisi lapangan, maka sampel tanah diberikan beban *surcharge* sebesar 3,8 kPa melalui pelat besi yang memiliki berat 30 kg pada suatu pelat kayu yang berukuran 60 cm yang terletak di atas material sampel tanah seperti yang dapat dilihat pada Gbr. 9. Pada tahapan ini, penetrasi konus CPTu dilakukan sedalam 20 cm terlebih dahulu sebelum pemberian beban *surcharge* diberikan. Hal tersebut bertujuan agar CPTu dapat digunakan untuk memantau efek peningkatan dan penurunan dari air pori ekses pasca pemberian beban *surcharge* seperti yang dapat dilihat pada Gbr 10.

Gbr. 9. Dokumentasi Pemberian Beban Surcharge pada Material Sampel Tanah.

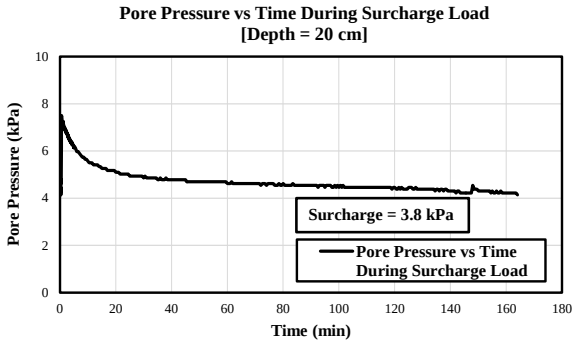

Gbr 10. Perilaku Tekanan Air Pori Terhadap Waktu pada Tahap Pemberian Beban *Surcharge*.

- *Pemberian Beban Dinamik*

Setelah air pori ekses yang muncul pasca pemberian beban *surcharge* telah terdisipasi seluruhnya, maka tahap selanjutnya ialah pemberian beban dinamik pada arah horizontal melalui *shake table*. Beban dinamik yang dihasilkan oleh penggetaran *shake table* diukur menggunakan akselerometer sehingga dapat diketahui input dari percepatan yang diberikan oleh *shake table* terhadap waktu seperti yang dapat dilihat pada Gbr. 11, Gbr. 12, Gbr. 13, dan Gbr. 14.

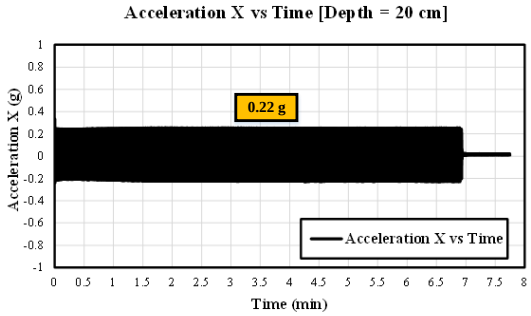

Gbr. 11. Input Beban Dinamik pada Arah X Terhadap Waktu.

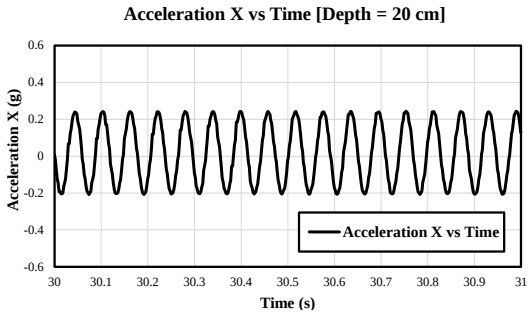

Gbr. 12. Detail dari Input Beban Dinamik pada Arah X Terhadap Waktu.

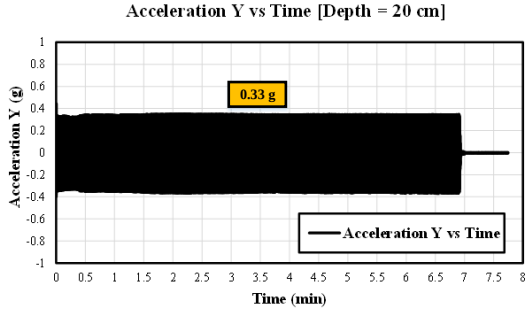

Gbr. 13. Input Beban Dinamik pada Arah Y Terhadap Waktu.

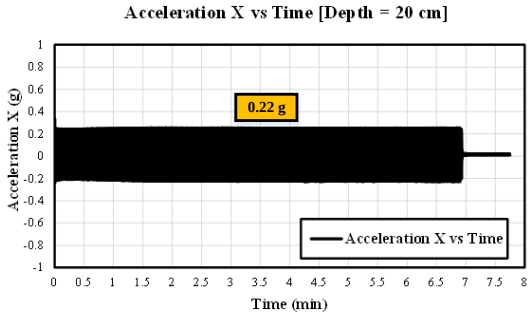

Gbr. 14. Detail dari Input Beban Dinamik pada Arah Y Terhadap Waktu.

Pada tahap ini, CPTu digunakan kembali untuk memantau peningkatan air pori ekses pasca beban dinamik diberikan sehingga dapat diketahui nilai ratio tekanan air pori ekses (r_u) yang terjadi selama beban dinamik diberikan seperti yang dapat dilihat pada Gbr. 15 dan Gbr. 16. Dari hasil pengamatan terhadap nilai ratio tekanan air pori ekses seperti yang dapat dilihat pada Gbr. 16, diketahui bahwa material sampel tanah Desa Sibalaya yang terdiri dari material pasir kelanauan mengalami likuifaksi dengan nilai ratio tekanan air pori ekses sebesar 0,94.

Gbr. 15. Dokumentasi Ketika Material Tanah Mengalami Likuifaksi.

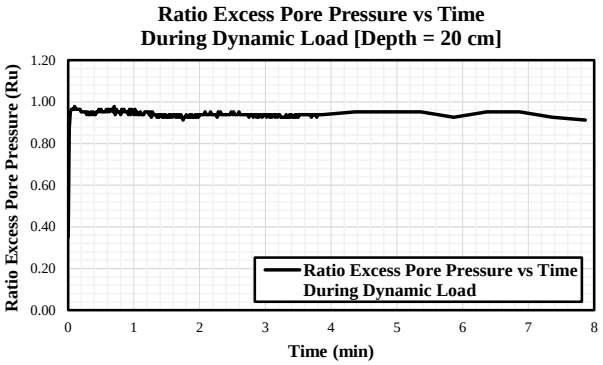

Gbr. 16. Perilaku Ratio Tekanan Air Pori Ekses Terhadap Waktu pada Tahap Pemberian Beban Dinamik.

- *Penetrasi CPTu pada Saat Material Sampel Tanah dalam Kondisi Terlikuifaksi*

Setelah sampel tanah mengalami likuifaksi dan beban dinamik tetap dibiarkan selama ± 6,9 menit, tahap selanjutnya ialah penghentian pemberian beban dinamik yang kemudian diikuti dengan penetrasi konus CPTu dengan menggunakan instrumen *rod extruder* hingga dasar *chamber* sehingga dapat didapatkan informasi dari tahanan ujung konus dan tahanan friksi dari sampel material tanah yang mengalami likuifaksi dengan kecepetan penetrasi sebesar 1,5 cm/s.

5 HASIL PENELITIAN

Mengacu kepada metode penelitian yang telah disampaikan di atas, diketahui bahwa nilai

tahanan ujung konus pada saat penusukan ialah berkisar antara 1,1 – 6,1 kg/cm^2, sedangkan untuk nilai friksi selimut ialah berkisar antara 1,2 – 4,8 kN/m^2 seperti yang dapat dilihat pada Gbr. 17 dan Gbr. 18.

Dari pengamatan yang dilakukan, terlihat bahwa hasil pengukuran pada kedalaman 20 - 28 cm dan 40 - 50 cm mengalami efek dari *boundary condition*, sehingga hasil pengukuran yang dianggap valid ialah yang terletak pada kedalaman 28 - 40 cm. Oleh karena itu, penentuan viskositas pada penelitian ini mengacu kepada hasil pengukuran friksi selimut pada kedalaman 28 - 40 cm tersebut dengan mengasumsikan efek friksi selimut dalam kondisi statik (f_{ss}) pada saat likuifaksi ialah sebesar 0, sehingga perhitungan viskositas hanya memperhitungkan efek friksi selimut dalam kondisi *viscous*. Selain itu, diasumsikan juga bahwa zona pengaruh pada saat penusukan konus diasumsikan sebesar 4 kali dari jari-jari konus. Mengacu kepada hasil pengukuran friksi selimut dan beberapa asumsi yang disampaikan di atas, maka didapatkan nilai viskositas rata-rata pada kedalaman 28 - 40 cm pada saat material tanah mengalami likuifaksi ialah sebesar 18 Pa-s seperti yang dapat dilihat pada Gbr. 19.

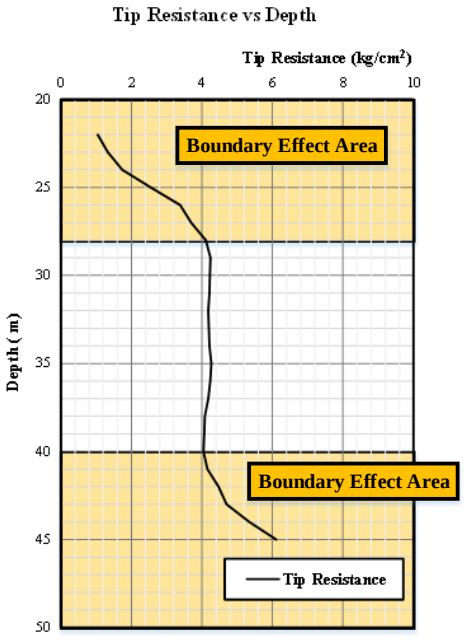

Gbr. 17. Nilai Tahanan Ujung Konus Terhadap Kedalaman Pasca Pemberian Beban Dinamik.

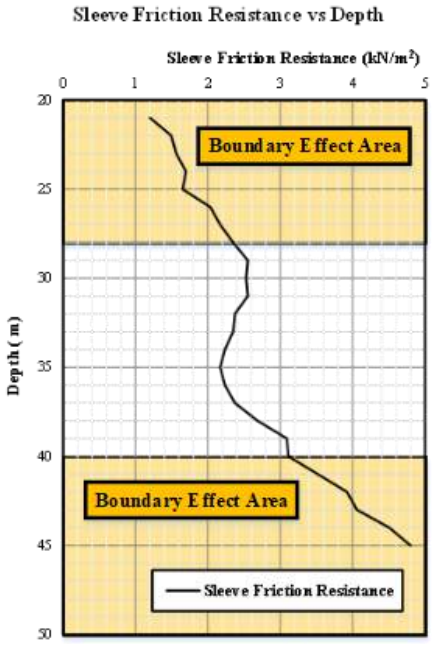

Gbr. 18. Nilai Tahanan Friksi Terhadap Kedalaman Pasca Pemberian Beban Dinamik.

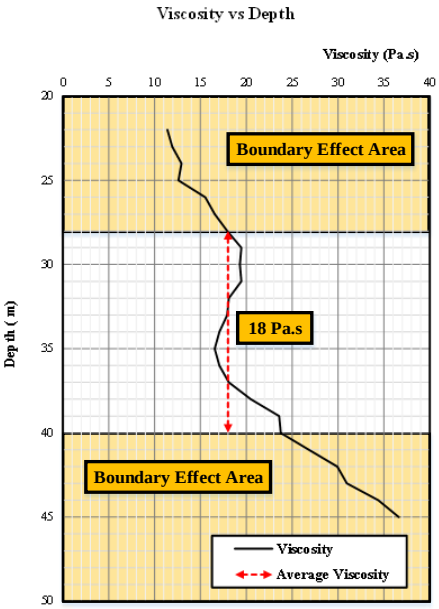

Gbr. 19. Nilai Viskositas Terhadap Kedalaman Pasca Pemberian Beban Dinamik.

6 KESIMPULAN

Berdasarkan kajian yang telah dilakukan, maka berikut di bawah ini ialah beberapa kesimpulan yang dapat disampaikan.

1. Aliran pada material tanah yang mengalami *flow liquefaction* dapat diasumsikan bersifat seperti fluida.
2. Parameter viskositas merupakan parameter reologi yang berperan penting dalam suatu pemodelan aliran *flow liquefaction*.

3. Material sampel tanah Desa Sibalaya didominasi oleh material tanah pasir kelanauan dan berdasarkan hasil pengujian, diketahui bahwa material sampel tanah mengalami likuifaksi dengan nilai ratio tekanan air pori ekses sebesar 0,94.
4. Nilai tahanan friksi yang terukur pada pengujian CPTu dapat digunakan untuk mendapatkan parameter nilai viskositas. Dari hasil pengujian, diketahui bahwa nilai viskositas sangat bergantung terhadap parameter rate penetrasi dan zona *area critical state* yang mana merupakan fungsi dari zona pengaruh akibat penusukan konus.
5. Berdasarkan nilai tahanan friksi yang terukur dan asumsi-asumsi terhadap nilai friksi selimut kondisi statik & zona pengaruh penusukan konus terhadap material sampel tanah Desa Sibalaya yang terdiri dari pasir kelanauan, diketahui bahwa nilai viskositas pada saat sampel tanah mengalami likuifaksi ialah sebesar 18 Pa-s.

UCAPAN TERIMA KASIH

Penulis ingin mengucapkan terima kasih sebesar-besarnya atas dukungan finansial dan fasilitas yang diberikan oleh Universitas Katolik Parahyangan dan PT Geotechnical Engineering Consultant khususnya kepada Prof. Paulus Pramono Rahardjo, Ph.D dalam rangka pembuatan dan pengembangan perangkat penelitian likuifaksi ini.

DAFTAR PUSTAKA

Chen, Y., Liu. H., dan Zhou, Y. 2006. Analysis on Flow Characteristics of Liquefied and Post-Liquefied Sand. *Chinese Journal of Geotechnical Engineering* Vol. 28: 1139-1143.

Cooke, R. W., dan Price, G. 1973. Strains and Displacements Around Friction Piles. *Proc. 8th International Conference on Soil Mechanics and Foundation Engineering*. Moscow Vol 2 (1): 53-60.

Flaate, K. 1972. Effects of Pile Driving in Clays. *Canadian Geotech. J*. 9: 81-88.

Hamada, M. dan Takahashi, Y. 2004. An Experimental Study on the Fluid Properties of Liquefied Sand During Its Flow. *Proceedings of 13th World Conference on Earthquake Engineering*. Vancouver. Paper no. 64.

Hamada, M. dan Wakamatsu, K. 1998. Liquefaction-Induced Ground Displacement Triggered by Quaywall Movement. *Soils and Foundation* Vol. 38: 85-95.

Mahajan, S. P. 2006. *Viscous Effects on Penetrating Shafts in Clay*. Ph.D. Dissertation, The University of Arizona.

Rahardjo, P. P. 1989. *Evaluation of Liquefaction Potential Silty Sand Based on Cone Penetration Test*. Ph.D. Dissertation. Virginia Polytechnic Institute and State University.

Randolph, M. F., Carter, J. O., dan Wroth, C. P. 1979. Driven Piles in Clay – The Effects of Installation and Subsequent Consolidation. *Geotechnique* Vol. 29, Issue. 4: 361-393.

Sasaki, Y., Towhata, I., Tokida, K., Yamada, K., Matsumoto, H., Tamari, Y., dan Saya, S. 1992. Mechanism of Permanent Displacement of Ground Caused by Seismic Liquefaction. *Soils and Foundations* Vol. 32, No. 3: 79–96.

Terzaghi, K. dan Peck, R. B. 1967. *Soil Mechanics in Engineering Practice*. 1st Ed. New York: Wiley.

Potensi Likuifaksi di Kota Padang Menggunakan Metode Empiris

Hendri Warman
Universitas Bung Hatta

Indra Farni
Universitas Bung Hatta

Monica Trinandi
Universitas Bung Hatta

Zufrimar
Universitas Bung Hatta

ABSTRAK: Peristiwa gempa bumi yang terjadi di Kota Padang dan sekitarnya pada 30 September 2009 dengan Mw 7,6 menyebabkan terjadinya kerusakan bangunan dan infrastruktur yang cukup parah, sehingga banyak bangunan yang amblas dan memakan banyak korban jiwa. Pakar geoteknik berpendapat bahwa fenomena amblas-nya bangunan tersebut adalah likuifaksi. Dalam analisisnya, data yang digunakan adalah data *Standard Penetration Test* (SPT) dan *Cone Penetration Test* (CPT). Analisis potensi likuifaksi ini bertujuan untuk mengetahui faktor keamanan likuifaksi, kekuatan gempa yang menyebabkan likuifaksi dan titik-titik berpotensi likuifaksi. Metode yang digunakan adalah metode empiris yang dihitung secara manual dan menggunakan program Liqit v.4.7.7.5. Hasil perhitungan manual, dari 25 titik pengujian terdapat 17 titik yang berpotensi likuifaksi pada magnitudo Mw 6,5. Sedangkan perhitungan menggunakan program, dari 25 titik pengujian terdapat 17 titik yang berpotensi likuifaksi pada magnitudo Mw 6,0. Wilayah yang memiliki potensi likuifaksi terbesar berada di Kecamatan Nanggalo, Kecamatan Padang Barat dan Kecamatan Padang Utara.

Kata Kunci: gempa bumi, likuifaksi, Liqit v.4.7.7.5

ABSTRACT: Earthquake that hit the city of Padang on September 30, 2009 with 7.6 Magnitude has caused seere building and infrastucture damage resulted in colapsed of buildings and casualties in such of massive quanty. Geotechnicexpert assumed the cause that make those buildings collapsed was due to liquefaction. During analysis, data were used is Standard Penetration Test (SPT) and Cone Penetration Test (CPT). This analysis of liquefaction potention aim to obtained liquefaction safety factor, earthquake magnitude that may caused liquefaction, the sites where liquefaction might potentially occur. Method used for the analysis is empirical method analysed manually by LiqIT v.4.7.7.5. The result of this manual analysis 17 sites out of 25 sites observed has potential to experience liquefaction under 6.5 moment magnitude earthquake. And than the result of program analysis 17 sites out of 25 sites observed has potential to experience liquefaction under 6.0 moment magnitude earthquake. The area that has the highest potention of liquefaction located in Nanggalo, West Padang, and North Padang Sub District.

Keywords: earthquake, liquefaction, Liqit v.4.7.7.5

1 PENDAHULUAN

Bencana alam adalah salah satu musibah yang tidak pernah diketahui kapan akan terjadinya dan kehadirannya tidak diharapkan. Salah satu bencana alam yang sering terjadi saat ini adalah gempa bumi. Kota Padang Provinsi Sumatera Barat merupakan salah satu daerah rawan gempa. Peristiwa gempa bumi yang terjadi di Kota Padang pada 30 September 2009 dengan Mw 7,6 menyebabkan terjadiny kerusakan bangunan dan infrastruktur yang cukup parah, sehingga menimbulkan korban jiwa yang tidak sedikit. Selain getaran yang kuat, fenomena likuifaksi yang terjadi di beberapa daerah pesisir dan pinggir sungai Kota Padang, terutama di Kecamatan Koto Tangah, Padang Utara, Padang Selatan dan Padang Barat, Tohari et al. (2011).

2 LANDASAN TEORI

2.1 *Pengertian Likuifaksi*

Likuifaksi adalah proses perubahan kondisi tanah pasir yang jenuh air menjadi cair akibat meningkatnya tekanan air pori yang harganya menjadi sama dengan tegangan total dikarenakan adanya beban dinamik atau beban bergerak, sehingga tegangan efektif tanah menjadi nol. Terzaghi (1923) merumuskan bahwa tegangan efektif adalah tegangan total dikurangi tekanan air pori, sehingga jika tekanan air pori meningkat tajam tegangan efektif akan menurun drastis sampai mendekati nol, maka berarti kuat dukung tanah pun menurun. Pada keadaan tanah dimana tegangan efektif sama dengan nol, maka tanah akan bersifat likuid seperti air dan terjadi likuifaksi Tekanan air pori bisa jadi melebihi tegangan total tanah, sehingga pasir yang bersifat likuid menyembur ke atas permukaan tanah dengan suhu panas karena gesekan yang dikenal sebagai sand boils, Hasmar (2013).

2.2 *Faktor-faktor Likuifaksi*

Menurut Pawirodikromo (2012), faktor-faktor yang menyebabkan likuifaksi adalah sebagai berikut:

- Karakteristik getaran
- Jenis tanah
- Muka air tanah
- Distribusi diameter butir
- Kepadatan awal

2.3 *Syarat Terjadinya Likuifaksi*

Menurut Pawirodikromo (2012), faktor-faktor yang menyebabkan likuifaksi adalah sebagai berikut:

- Intensitas gempa
- Jarak episenter
- Kedalaman air tanah maksimum
- Karakteristik butir-butir pasir
- Rentang lapis likuifaksi

2.4 *Bahaya yang Timbul Akibat Likuifaksi*

- *Sand boils*
- *Flow failures of slope*
- *Failure of retaining wall*
- *Buoyant rise of buried structure*
- *Lateral spreads*
- *Ground oscillation*
- *Loss of bearing capacity*
- *Ground settlement*

3 METODOLOGI ANALISIS

Dalam analisis ini terdapat dua perhitungan yaitu secara manual dan menggunakan program LiqIT v.4.7.7.5. Dalam penelitian ini menggunakan dua jenis data yaitu data *Cone Penetration Test* (CPT) dan *Standard Penetration Test* (SPT)yang dihitung secara empiris. Analisis likuifaksi ini menggunakan variasi magnitude gempa yaitu Mw 5,5; 6,0; 6,5; 7,0; 7,5; 8,0; 8,5; 9,0.

Untuk perhitungan manual, data CPT dianalisis menggunakan metode yang disepakati pada workshop mengenai CRR oleh NCEER pada tahun 1996 dan tahun 1998, yang dimuat dalam *Journal of Geotechnical and Geoenvironment Engineering*, volume 127, nomor 10, Oktober 2001 halaman 817-833. Workshop tersebut diketuai oleh Youd T.L. dan Idriss, I. M. Workshop tersebut pada dasarnya mengembangkan *simplified procedure* yang diusulkan oleh Seed dan Idriss (1971) yang memfokuskan pada analisis ketahanan tanah terhadap bahaya likuifaksi, Idriss dan Boulanger (2008) dalam jurnal milik Christian Vicky Delfis Lonteng. Untuk perhitungan manual menggunakan data SPT, metode yang digunakan adalah *Hyperbolic Function* yang disampaikan oleh Jin-Hung Hwang pada workshop geoteknik oleh NCEER pada tahun 2019 di Hotel Inna Muara Padang, Provinsi Sumatera Barat. Sedangkan pada perhitungan likuifaksi menggunakan program LiqIT v4.7.7.5, untuk data SPT metode yang digunakan adalah dari NCEER (1997) dan untuk data CPT metode yang digunakan adalah dari Robertson et al. (1998).

3.1 *Metode Pengumpulan Data Tanah*

Data hasil uji lapangan yaitu data bor (SPT) dan data sondir (CPT) yang ada di Kota Padang diperoleh dari UPTD Balai Pengujian Mutu Bahan dan Pekerjaan Propinsi Sumatera Barat dan *Geotechnical Engineering Consultant*. Data yang diperoleh tersebut menyebar di seluruh Kota Padang yang terdiri dari 10 lokasi proyek dengan jumlah keseluruhan titik bor atau sondir adalah 25 titik.

Tabel 1. Lokasi Data Analisis.

Lokasi	Kecamatan	Data	Jumlah Titik Bor/Sondir
Masjid Al-Hijrah	Nanggalo	CPT	4
Rumah Tinggal	Padang Barat	CPT	2
Gudang Sepeda Motor	Lubbuk Begalung	CPT	6
Prasjal Tarkim	Padang Utara	SPT	2
Hotel Inna Muara	Padang Barat	SPT	4
Hotel Kawana Padang	Padang Selatan	SPT	1
Dinas Peternakan	Padang Timur	SPT	1
Dinas Perkebunan	Padang Barat	SPT	1
Gedung Jl. Hang Tuah	Padang Barat	SPT	2
Hotel Jl. Bagindo	Padang Timur	SPT	2

3.2 *Metode Pengumpulan Koordinat Lokasi Penelitian*

Koordinat lokasi penelitian diperoleh dengan menggunakan website Google Earth. Koordinat ini berfungsi untuk menentukan jarak episenter yang mana akan digunakan pada analisis menentukan percepatan tanah maksimum. Berikut adalah data koordinat lokasi penelitian:

Tabel 2. Koordinat Lokasi Penelitian.

Lokasi	Koordinat
Masjid Al-Hijrah	0,91ºS dan 100,37ºE
Rumah Tinggal	0,96ºS dan 100,36ºE
Gudang Sepeda Motor	0,93ºS dan 100,40ºE
Prasjal Tarkim	0,93ºS dan 100,36ºE
Hotel Inna Muara	0,96ºS dan 100,36ºE
Hotel Kawana Padang	0,96ºS dan 100,37ºE
Dinas Peternakan	0,93ºS dan 100,36ºE
Dinas Perkebunan	0,93ºS dan 100,36ºE
Gedung Jl. Hang Tuah	0,95ºS dan 100,35ºE
Hotel Jl. Bagindo	0,95ºS dan 100,36ºE

3.3 *Menentukan Nilai Percepatan Tanah Maksimum (a_{max})*

Berikut ini adalah tahapan dalam menentukan nilai percepatan tanah maksimum, Marlisa et al. (2016):

1. Identifikasi sumber gempa
2. Mengubah magnitudo gelombang body (magnitudo awal) ke dalam bentuk gelombang permukaan

$$Ms = 1{,}78\ Mb - 5{,}17 \quad (1)$$

Dimana:
Ms = Magnitudo gelombang permukaan
Mb = Magnitudo gelombang body

3. Hitung jarak episenter

$$\Delta^2 = (x_2 - x_1)^2 + (y_2 - y_1)^2 \quad (2)$$

Dimana:
Δ = Jarak episenter (km); 1º = 111 km
x1 = Bujur lokasi penelitian (º)
x2 = Bujur episenter (º)
y1 = Lintang lokasi penelitian (º)
y2 = Lintang episenter (º)

4. Hitung jarak hiposenter

$$R^2 = \Delta^2 + h^2 \quad (3)$$

Dimana:
R = Jarak hiposenter (km)
Δ = Jarak episenter (km)
h = Kedalaman gempa (km)

5. Hitung percepatan tanah maksimum (a_{max})

$$a = \frac{472{,}3 * 10^{0.278Ms}}{(R+25)^{1.301}} \quad (4)$$

Dimana:
a = Percepatan tanah maksimum (gal)
1 gal = 0.001 g
R = Jarak hiposenter (km)
Ms = Magnitudo gelombang permukaan

3.4 *Menentukan Faktor Keamanan (Perhitungan Manual)*

Dalam suatu analisis potensi likuifaksi dibutuhkan suatu standar untuk mengetahui apakah likuifaksi berpotensi terjadi atau tidak. Satndar ini disebut dengan faktor kemanan (FK). Sebelum menentukan faktor keamanan, maka nilai dari CSR dan CRR harus dianalisis terlebih dahulu. Dengan demikian FK dapat ditentukan dengan persamaan berikut, Youd dan Idriss (2001):

$$FK = \frac{CRR\ 7{,}5}{CSR} . MSF \quad (5)$$

Dimana:
FK < 1 ⟶ Terjadi likuifaksi
FK = 1 ⟶ Kondisi kritis
FK > 1 ⟶ Tidak terjadi likuifaksi

$$CSR = \frac{\tau cyc}{\sigma'} = 0{,}65 \frac{amax}{g} \frac{\sigma}{\sigma'} r_d \quad (6)$$

Dimana:
a_{max} = Percepatan tanah maksimum (gal)
g = Percepatan gravitasi bumi (9.81 m/s^2)
σ' = Tegangan vertikal efektif
σ = Tegangan vertikal total
r_d = Faktor reduksi terhadap tegangan

a. Menentukan nilai *Cyclic Resistance Rasio* ($CRR_{7.5}$) untuk data SPT

Nilai Cyclic Resistance Ratio (CRR) akan dihitung berdasarkan gempa dengan magnitudo 7,5 SR yang mana gempa tersebut dijadikan sebagai referensi karena gempa dengan magnitudo 7,5 SR dianggap seolah-olah mempunyai resistance atau perlawanan yang lebih besar, sehingga diperlukan koreksi untuk gempa-gempa dengan magnitudo yang lain. HBF (2012) juga menyatakan bahwa tanah yang rentan likuifaksi adalah ketika nilai (N1)60cs < 39. Menentukan nilai *Cyclic Resistance Ratio* (CRR) pada besaran skala gempa M = 7,5 dan pasir murni dengan (N1)60cs < 39 dapat menggunakan persamaan dari HBF (2012) sebagai berikut, Hwang (2019) :

$$CRR_{7,5} = 0{,}08 + \frac{0{,}0035\ (\mathbf{N1})\mathbf{60cs}}{1 - \frac{(\mathbf{N1})\mathbf{60cs}}{39}} \quad (7)$$

b. Menentukan nilai *Cyclic Resistance Rasio* ($CRR_{7.5}$) untuk data CPT

Nilai CRR7.5 yang menggunakan data CPT dapat di analisis dengan persamaan dari Youd dan Idriss (2001) sebagai berikut:

- (Qc1N)cs < 50

$$CRR_{7,5} = 0{,}833 \left[\frac{(Qc1N)cs}{1000}\right] + 0{,}05$$

- 50 < (Qc1N)cs < 160

$$CRR_{7.5} = 93 \left[\frac{(Qc1N)cs}{1000}\right] + 0{,}08 \quad (8)$$

3. Menentukan nilai *Magnitude Scalling Factor* (MSF)

Magnitude Scaling Factor (MSF) adalah faktor skala magnitude gempa yang akan bernilai sama dengan 1 (satu) pada magnitude 7,5 SR. Seed dan Idriss mendapatkan nilai MSF untuk magnitudo lebih kecil dari 7.5 SR dan magnitudo lebih besar dari 7,5 SR sebagai berikut:

M < 7,5 ⟶ $MSF = \frac{10^{2,24}}{M^{2,56}}$ (9)

M = 7.5 ⟶ MSF = 1 (10)

M > 7,5 ⟶ $MSF = \left(\frac{M}{7,5}\right)^{-2,56}$ (11)

3.5 *Menentukan Faktor Keamanan (Perhitungan Proram Liqit v 4.7.7.5)*

Dalam perhitungan likuifaksi menggunakan program LiqIT v.4.7.7.5 tahapan-tahapan perhitungan antara data SPT dan data CPT hampir sama. Adapun yang membedakannya adalah pada penginputan data dan metode yang digunakan.

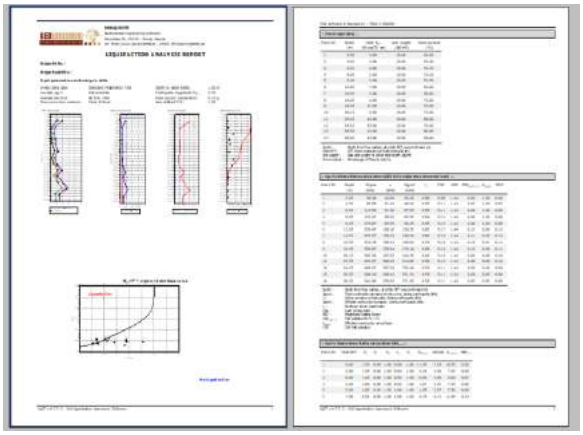

Gbr. 1. Contoh Report Potensial Likuifaksi Menggunakan Program LiqIT.

3.6 *Pemetaan Wilayah Potensi Likuifaksi*

Hasil dari analisis ini akan ditampilkan dalam bentuk titik-titik likuifaksi dengan menggunakan fitur yang ada di *google maps* yaitu *my maps.*

4 HASIL ANALISIS

4.1 *Hasil Perhitungan Analisis Potensi Likuifaksi*

a) Persentase Lapisan Tanah Terlikuifaksi (Perhitungan Manual)

Tabel 3. Persentase Lapisan Tanah Terlikuifaksi (Perhitungan Manual)

Lokasi		Titik Bor/Sondir	Persentasi Lapisan Tanah yang Teerlikuifaksi Berdasarkan Nilai Faktor Keamanan (FK) (%)							
			M5,5	M6,0	M6,5	M7,0	M7,5	M8,0	M8,5	M9,0
Masjid Al-Hijrah	Kel. Tebing Banda Gadang, Kec. Nanggalo	1	0	67	79	81	85	93	96	95
		2	0	58	78	81	87	88	96	97
		3	0	57	76	81	84	90	96	96
		4	0	57	79	88	94	96	97	99
Rumah Tinggal Guung Pangilun,	Jl. Kali Kecil II No.22 Kec. Padang Barat	1	0	0	2	12	26	37	53	56
		2	0	0	0	6	26	42	55	65
Gudang Sepeda Motor	Jl. By Pass Km 9 Kec. Lubuk Begalung, Kota Padang	1	0	0	0	35	54	62	65	65
		2	0	0	0	0	0	0	6	6
		3	0	0	0	0	0	0	0	0
		4	0	0	0	0	7	13	13	20
		5	0	0	0	0	0	0	0	6
		6	0	0	0	0	0	0	0	0
Gedung Dinas Prasjal Tarkim	Jl. Taman Siswa No. 1, Alai Parak Kopi Kec. Padang Utara	1	0	7	40	47	53	53	60	67
		2	0	0	27	33	40	47	47	53
Hotel Inna Muara	Jl. Khairil Anwar Kec. Padang Barat	1	0	0	20	60	70	80	80	80
		2	0	10	40	50	70	70	90	90
		3	0	0	40	50	60	60	80	80
		4	0	0	5	25	45	50	50	50
Hotel Aliga Padang	Jl. Thamrin Kec. Padang Selatan	1	0	0	0	29	29	29	29	43
Dinas Peternakan	Jl. Rasuna Said Kec. Padang Timur	1	0	0	13	40	40	53	60	80
Dinas Perkebunan	Jl. Jendral Sudirman Kec. Padang Timur	1	0	7	27	47	67	87	93	93
Gedung Jl. Hang Tuah	Jl. Hang Tuah No. 150 D-E Kec. Padang Barat	1	0	6	38	44	50	50	50	63
		2	7	27	47	47	47	47	53	53
Hotel Jl. Bagindo	Padang	1	0	5	30	40	45	45	50	65
		2	0	0	20	40	50	50	55	55

b) Persentase Lapisan Tanah Terlikuifaksi (Perhitungan Program LiqIT)

Tabel 4. Persentase Lapisan Tanah Terlikuifaksi (Perhitungan Program LiqIT)

Lokasi		Titik Bor/Sondir	Persentasi Lapisan Tanah yang Teerlikuifaksi Berdasarkan Nilai Faktor Keamanan (FK) (%)							
			M5,5	M6,0	M6,5	M7,0	M7,5	M8,0	M8,5	M9,0
Masjid Al-Hijrah	Kel. Tebing Banda Gadang, Kec. Nanggalo	1	7	30	33	36	37	39	39	39
		2	9	42	42	42	45	45	48	49
		3	0	21	22	22	22	24	26	28
		4	0	22	29	32	35	37	40	40
Rumah Tinggal Guung Pangilun,	Jl. Kali Kecil II No.22 Kec. Padang Barat	1	0	0	0	12	28	37	49	58
		2	0	0	0	6	16	10	61	68
Gudang Sepeda Motor	Jl. By Pass Km 9 Kec. Lubuk Begalung, Kota Padang	1	0	0	19	19	38	46	50	58
		2	0	0	0	0	0	0	0	6
		3	0	0	0	0	0	0	13	19
		4	0	0	0	0	20	27	53	53
		5	0	0	0	0	0	0	31	38
		6	0	0	0	0	0	0	24	24
Gedung Dinas Prasjal Tarkim	Jl. Taman Siswa No. 1, Alai Parak Kopi Kec. Padang Utara	1	20	27	53	53	80	80	80	80
		2	7	20	40	47	47	67	80	80
Hotel Inna Muara	Jl. Khairil Anwar Kec. Padang Barat	1	0	50	50	70	80	80	90	100
		2	10	40	50	50	90	90	100	100
		3	0	40	50	60	60	80	80	80
		4	0	10	35	45	50	50	50	55
Hotel Aliga Padang	Jl. Thamrin Kec. Padang Selatan	1	14	29	29	29	43	57	57	57
Dinas Peternakan	Jl. Rasuna Said Kec. Padang Timur	1	0	13	40	53	80	80	80	80
Dinas Perkebunan	Jl. Jendral Sudirman Kec. Padang Timur	1	0	40	67	93	93	93	100	100
Gedung Jl. Hang Tuah	Jl. Hang Tuah No. 150 D-E Kec. Padang Barat	1	0	19	44	50	56	56	63	63
		2	20	47	53	53	60	67	67	73
Hotel Jl. Bagindo	Padang	1	0	15	40	45	45	45	45	85
		2	10	25	50	50	60	60	60	75

4.2 *Peta Lokasi Analisis dan Potensi Likuifaksi*

a) Wilayah Potensi Likuifaksi (Perhitungan Manual)

Gbr. 4. Wilayah Potensi Likuifaksi (Perhitungan Manual).

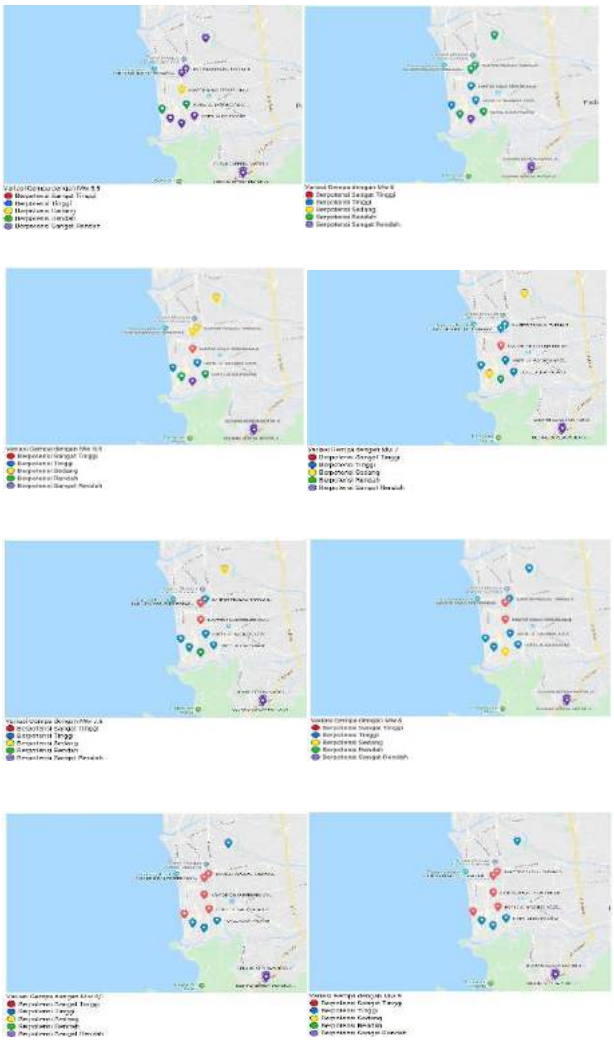

Gbr. 5. Wilayah Potensi Likuifaksi (Perhitungan Program LiqIT).

5 KESIMPULAN

Berdasarkan tabel hasil analisis, didapatkan hasil sebagai berikut:

1) Menurut perhitungan manual, dari 25 titik pengujian terdapat 17 titik yang berpotensi likuifaksi pada magnitudo Mw 6,5.
2) Menurut perhitungan menggunakan program LiqIT, dari 25 titik pengujian terdapat 17 titik yang berpotensi likuifaksi pada magnitudo Mw 6,0.
3) Dari perhitungan manual dan program didapatkan hasil yang tidak jauh berbeda
4) Wilayah yang memiliki potensi likuifaksi terbesar berada di Kecamatan Nanggalo, Kecamatan Padang Barat dan Kecamatan Padang Utara.

6 DAFTAR PUSTAKA

G. Zhang, P. R. R. B. 2002. Estimating Liquefaction – Induced Ground Settlements from CPT for level Ground. *Geotech Journal* 39:1168-1180. Canada.

G. Zhang, P. R. R. B. 2004. Estimating Liquefaction-Induced Lateral Displacement Using The Standard Penetration Test or Cone Penetration Test. *s.l.:Journal of Geotechnical and Geoenviromental Engineering* Vol. 130: 861- 871.

Hardiyatmo, H. C. 2014. *Analisis dan Perancangan Fondasi I dan II.* Yogyakarta: UGM Press.

Hasmar, H. H. 2013. *Dinamika Tanah dan Rekayasa Kegempaan.* Yogyakarta: UII Press.

Hwang, J. H. 2019. Soil Liquefaction Evaluation and Countermeasures. *The Workshop on Geotechnical Engineering Internasional Conference on Earthquake Engineering ad Disaster Mitigation*

(ICEEDM). Asosiasi Ahli Rekayasa Kegempaan Indonesia (AARGI). Padang.

Idriss, I.M., dan Boulanger, R. W. 2008. Soil Liquefaction During Earthquakes. *Earthquake Engineering Research Instituate (EERI)*. USA.

Kamawan, et al. 2004. *Peta Geomorfologi Lembar Padang, Sumatera.* Padang: Pusat Penelitian dan Pengembangan Geologi.

Kramer, S. 1996. *Geotechnical Earthquake Engineering*. New Jersey: Prentice Hall.

Luna, R. a. 1998. Spatial Liquefaction Analysis System. *Journal of Computing in Civil Engineering. s.l.:ASCE*.

Marlisa, Pujiastuti, D. & Billyanto, R. 2016. Analisis Percepatan Tanah Maksimum Wilayah Sumatera Barat (Studi Kasus Gempa Bumi 8 Maret 1997 dan 11 September 2014). s.l.:Fisika Unand.

Pawirodikromo, W. 2012. *Sesmologi Teknik & Rekayasa Kegempaan.* Yogyakarta: s.n.

Terzaghi, 1923. *Mekanika Tanah Jilid 1*. Institusi Teknologi 10 Nopember Surabaya: Penerbit Erlangga.

Tohari, A., Sugianti, K. & Soebowo, E. 2011. Liquefaction potential at Padang City: Acomparison of Predicted and Observed Liquefaction During the 2009 Padang Earthquake. *J. Riset dan Pertambangan, Puslit Geoteknologi-LIPI* 21(1): 7-19.

Youd, T.L., Idriss, I.M. 2001. Liquefaction Resistance of Soils: Summary Report from The 1996 NCEER and 1998 NCEER/NSF Workshop on Evaluation of Liquefaction Resistance of Soils. S.1.: J. Geotech Geoenvirom.

Bund Wall Stability Analysis in Open-pit Coal Mines Affected by Soft Soil Layers

Faizal Amru
Universitas Pertamina

Rangga Adiprima Sudisman
Universitas Pertamina

ABSTRAK: *Bund Wall* merupakan struktur timbunan tanah yang berfungsi untuk menampung tanah buangan tambang. *Bund wall* dikatakan stabil jika memenuhi nilai faktor keamanan minimum. Pada kasus ini, terdapat lapisan tanah lunak berupa lumpur di lokasi rencana pembangunan *bund wall* sehingga menjadi perhatian karena dapat mengganggu kestabilan *bund wall*. Penelitian ini dilakukan untuk menentukan rekomendasi skenario perkuatan *bund wall* dan tahapan penimbunannya. Metode yang dilakukan untuk analisis kestabilan lereng *bund wall* adalah dengan metode kesetimbangan batas Spencer dan metode elemen hingga. Lereng *bund wall* dapat dikatakan aman jika nilai faktor keamanan yang dihasilkan lebih dari 1,2 untuk kondisi statis dan 1,1 untuk kondisi pembebanan dinamis. Hasilnya adalah ditentukan jarak optimum pembersihan lapisan tanah lunak kaki *bund wall* rencana sebelum konstruksi dilakukan. Selain itu, ditentukan juga tinggi penimbunan konstruksi *bund wall* setiap lapisan saat konstruksi.

Kata Kunci: stabilitas lereng, waste dump, bendungan tanah

ABSTRACT: A bund wall is a soil structure that looks like a dam in a mine and is used to contain waste. In this case, there is a layer of soft soil in the form of mud at the planned bund wall construction site, which is a concern because it can disrupt the bund wall's stability. The purpose of this study was to develop recommendations for bund wall reinforcement scenarios and backfilling stages. The Spencer limit equilibrium method and the finite element method were used to analyze the stability of the bund wall slope. If the resulting safety factor is greater than 1.2 for static conditions and 1.1 for dynamic loading conditions, the bund wall slope is said to be safe. As a result, the optimum distance for cleaning the soft soil layer of the planned bund wall toe is determined prior to construction.

Keywords: slope stability, waste dump, earth dam

1 INTRODUCTION

Open-pit mining is a common method to extract coal beneath the ground. In general, open-pit coal mining stages include land clearing, stripping topsoil, stripping coal cover layers, and coal mining, Andriyan et al. (2018). The overburden layer must be relocated to a disposal area Kristyanto et al. (2015). And it must be properly planned so that the soil pile remains stable Prasetyo et al. (2011). Bund wall cells are a common method for dumping overburden by forming small cells in the mining area where the overburden material will be dumped.

This case study includes a disposal plan for an open-pit coal mine area in Kalimantan. A soft mud layer originating from the collapsed bund wall cell surrounds the planned dumping location. The soft mud layer is identified as fat clay, which is an inorganic clay with high plasticity, according to the Unified Soil Classification System (USCS). When compressed, the permeability of this material is watertight. This material has a low shear strength and a high compressibility under saturated conditions, and it is not suitable for use as a construction material, Wagner (1957).

As a result, it is necessary to investigate the cleaning of mudslides.

Slope stability analysis on the bund wall is required to ensure that the slope design of the bund wall is stable, preventing landslides from disrupting mining operations and ensuring soil stability around the bund wall. The analysis of the stability of the bund wall slope is concerned with determining the effect of the mud layer on the stability of the bund wall above it, so that it can be determined how far the mud layer must be cleaned for the bund wall to be stable.

2 DESIGN METHOD

The value of the safety factor is used to determine slope stability analysis. As expressed in Eqn. (1), the safety factor is the ratio of the resisting force to the driving force.

$$SF = \frac{\text{Resisting force}}{\text{Driving force}} = \frac{cA + W\cos\alpha\tan\phi}{W\sin\alpha} \quad (1)$$

The driving force can be generated by gravity and vibration loads, whereas the resisting force is determined by soil cohesion and the angle of internal friction, Oscar et al. (2016). The safety factor's value is proportional to the shear strength of the soil. The greater the soil's shear strength, the greater the safety factor produced, Das & Sobhan (2014). Table 1 shows a classification of safety factor values based on authority regulation. If the safety factor is greater than 1.2 for static conditions and 1.1 for dynamic conditions, the slope is said to be safe, Kementerian ESDM (2018).

Table 1 Classification of Safety Factors, Kementerian ESDM (2018).

Slope Type	Failure Rate	Criteria	
		SF static	SF dynamic
Single slope	Low to high	1,1	N/A
Inter-ramp	Low	1-1,5	1,0
	Middle	1,2-1,3	1,0
	High	1,2-1,3	1,1
Overall Slope	Low	1,2-1,3	1,0
	Middle	1,3	1,05
	High	1,3-1,5	1,1

The internal resistance per unit area that the soil mass can deal with to resist failure and sliding along any plane within it is referred to as the shear strength of the soil mass. Mohr-Coulomb is the failure criterion used to model the slope. As shown in Eqn. (2), the Mohr-Coulomb failure criterion estimates shear stress in the failure plane as a linear function of normal stress, Coulomb (1776).

$$\tau_f = c + \sigma\tan\phi \quad (2)$$

The Mohr-Coulomb failure criterion for the effective stress condition is written as follow,

$$\tau_f = c' + \sigma'\tan\phi' \quad (3)$$

The Limit Equilibrium Method and the Finite Element Method were used to analyze stability. The limit equilibrium method assumes the shape of the slope surfaces that occur, Aprilia et al. (2019). This method requires three equilibrium conditions to be met: vertical forces, horizontal forces, and moments. Spencer's limit equilibrium method was used in this study because it meets all three equilibrium limits, Duncan et al. (2014).

The finite element method divides the analyzed area into several small zones known as elements. These elements are linked together at several nodes. Based on the displacement at the nodes, the displacement at any point can be calculated. The Strength Reduction Method can be used to calculate safety factors. The shear strength of the material is gradually reduced until a failure mechanism forms on the slope, according to the principle. Material Shear Strength Reduction can be expressed using Eqn. (4) and Eqn. (5).

$$c_f = \frac{c}{SRF} \quad (4)$$

$$\phi_f = \tan^{-1}\left(\frac{\tan\phi}{SRF}\right) \quad (5)$$

An illustration of the strength reduction method process can be seen in Fig. 1.

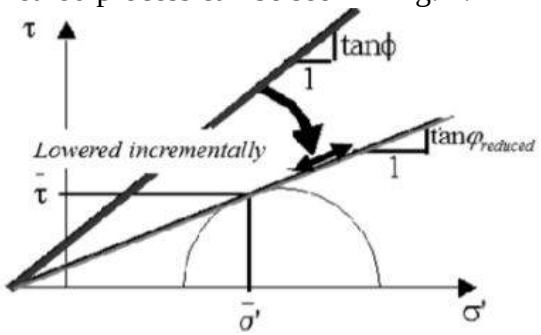

Fig. 1. Illustration of Shear Strength Reduction Calculation, Liong & Herman (2012).

Slope stability can be increased by reducing driving forces, increasing resisting forces, and protecting slopes, Hoek & Bray (1981). To determine how many material layers of mud must be cleaned for the slope to be stable, Rocscience Slide is used to assist calculations using the Limit Equilibrium Method, and Plaxis is used to assist calculations using the Finite Element Method. The slope geometry and soil strength parameters from laboratory test results are used as inputs in the slope modeling.

3 RESULTS

3.1 *Soil Profile*

A bund wall is planned to be built inside the pit. The northern part of the bund wall is a coal mining operation area that must be protected, and the southern part of the bund wall is a dump mud failure material plan Fig. 2 depicts a preliminary design of the bund wall cross-section geometry under the assumption that no mud/fat clay is cleaned. The design bund wall's top elevation is 30 meters from the existing road, and the mud thickness is 10 meters high with a length of 305 meters. The top of the bund wall is determined as a relative height level (RL) of 0 m, as a benchmark.

3.2 *Soil Data*

Laboratory tests were carried out to determine the properties and parameters of the soil. Based on laboratory test results, soil types are classified into four types: mud sediment, mud failure, overburden (OB), and hard soil material (in this case, called IB4). Soil shear strength parameters are derived from the Triaxial Unconsolidated Undrained results. The soil parameters used in this case study are listed in Table 2.

3.3 *Loading*

Two loads are considered in this bund wall stability analysis: static and dynamic loads. Static loads are caused by heavy equipment passing through the bund wall's top, whereas dynamic loads are caused by blasting activity around the bund wall. A heavy equipment load is evenly distributed derived from the vehicle's full weight at the largest axial distribution as wide as the heavy equipment of 42 kPa. The seismic load coefficient factor for horizontal and vertical directions is the dynamic load input into the Limit Equilibrium Method calculation. The value of the seismic load coefficient is half of the peak acceleration value. The peak acceleration value at the mine site is 0.05g, and the seismic load coefficient value is 0.025g, according to blasting measurements at the mine site.

An acceleration curve against time that generates cyclic loads (intervals of 0.01 seconds) with constant frequency or harmonic motion is used as the dynamic load input into the Finite Element Method calculation, Guler et al. (2012). The equation used to obtain an acceleration curve is Eqn. (6).

$$\ddot{U}(t) = \sqrt{\beta \cdot e^{-\alpha \cdot t} \cdot t^{\xi}} \sin(2 \cdot \pi \cdot f \cdot t) \quad (6)$$

α, β, and ξ are constant coefficients with values of 5.5, 55, and 15, respectively. f denotes frequency, and t denotes time. The frequency value is 7.5 Hz, and the time is 5 seconds, according to blast measurements taken at the mine site. Fig. 3 depicts an acceleration curve with time intervals ranging from 0.01 s to 5.00 s.

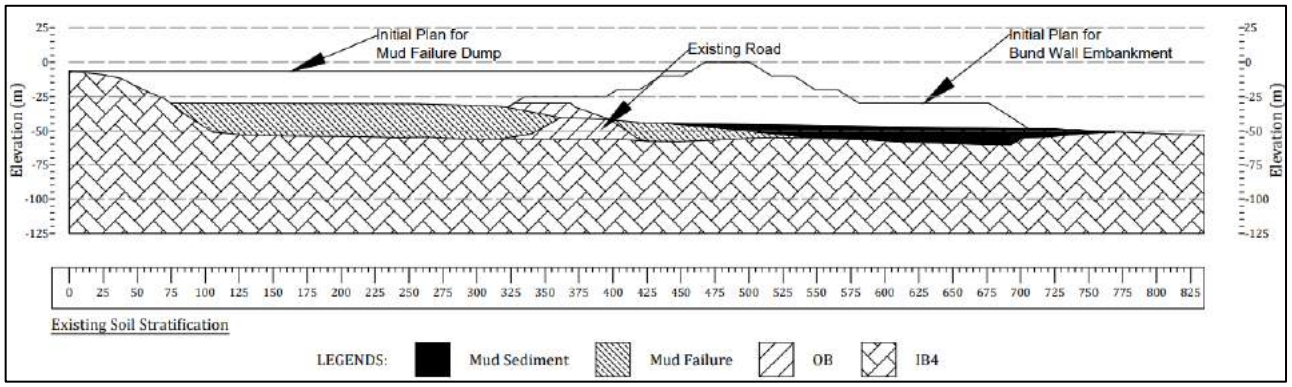

Fig. 2. Soil Stratification.

Table 2. Soil Parameters.

Material	γ (kN/m³)	ϕ (°)	c (kPa)	F depth (kPa/m)	E' (kPa)	ν'
Mud sediment	14.42	-	4.90	0.21	2458.80	0.35
Mud failure	14.94	-	6.00	0.26	2968.10	0.35
OB	17.00	28	6.00	-	50000	0.35
IB4	20.00	148	23.00	-	50000	0.30

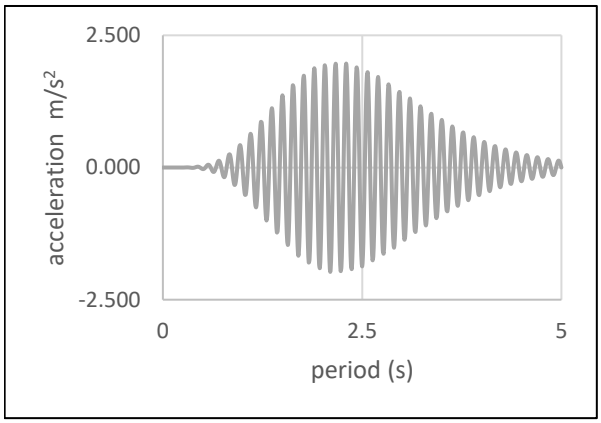

Fig. 3. Accelerogram Curve.

3.4 *Bund Wall Stability Analysis in Limit Equilibrium Method*

The Limit Equilibrium Method analysis is conducted by determining an optimum geometry design combined with optimum mud cleaning, so that the safety factor value meets the minimum criteria. For each analysis, two slip surface analyses were performed, namely circular and non-circular slip surfaces. These two methods are used to determine a critical surface in order to determine the slip surface with the lowest overall safety factor for a given slope. Geometry of the bund wall, c, ϕ, and γ, of the material are used as input models for the slope.

The results of the bund wall stability analysis using the original geometry design, as shown in Fig. 4, generated a safety factor value of 0.156 for circular slip surface and 0.305 for non-circular slip surface. Those values do not meet the minimum safety factor criteria. As a result, geometric iterations and mud cleaning are performed to determine the design that meets the minimum safety factor criteria. Table 3 summarizes the safety factor values obtained using the Limit Equilibrium Method.

Table 3. Recapitulation of Safety Factor Values using Limit Equilibrium Methods.

Model	Safety Factor	
	NC	C
1. Initial Design	0.156	0.305
2. Mud Cleaning 100 m	0.757	0.748
3. Mud Cleaning 125 m	0.921	0.871
4. Mud Cleaning 150 m	1.157	1.153
5. 155 m Mud Cleaning - *Berm* Modifications	1.235	1.246
6. 155 m Mud Cleaning - *Berm* Modifications	1.164	1.164

Note:
- Number 1 to 5 is a static loading condition.
- Number 6 is a dynamic loading condition.
- Berm Modifications to the bund wall are made to improve stability.

3.1 *Bund Wall Stability Analysis in Finite Element Method*

In the Finite Element Method, stability analysis is performed for the planning of the construction phase of the bund wall. The OB layer is backfilled every 10 m, and the mud failure layer on the south side of the bund wall is given a 2 m lower height difference from the top of the bund wall to ensure that the mud failure material does not overflow when it rains.

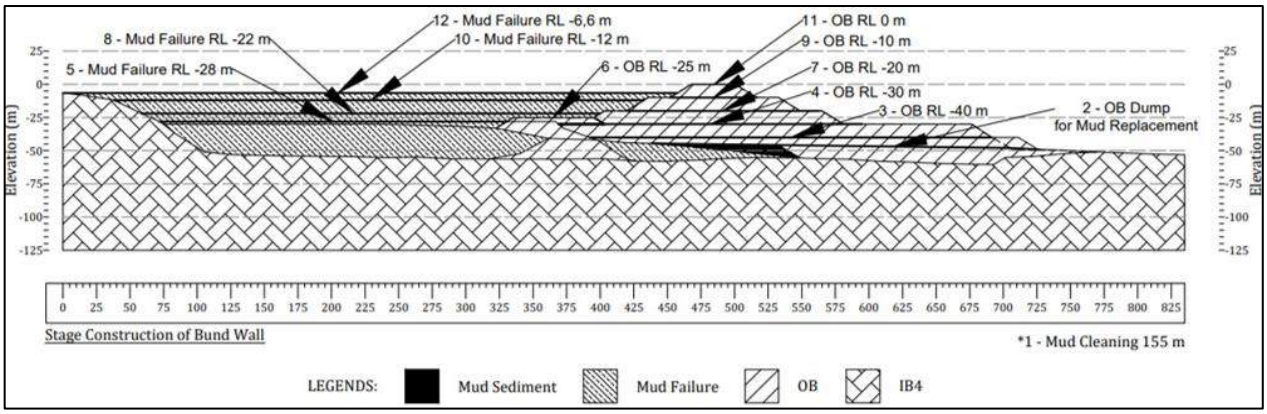

Fig. 4. Construction Stages of The Bund Wall.

Fig. 4 depicts the stages of construction of the bund wall. In the case of embankment construction, the most critical condition occurs immediately after the embankment is built before consolidation occurs. As a result, the analyzed stability is its short-term safety factor for static and dynamic loading conditions. Table 4 summarizes the values of security factors calculated using the Finite Element Method.

Table 4. Recapitulation of Safety Factor Values using Finite Element Method.

Stages	Safety Factor	
	Static	Dynamic
Mud cleaning	1,005	1,005
OB dump for mud replacement	1,238	1,197
OB dump RL -40 m	1,234	1,198
OB dump RL -30 m	1,234	1,197
Mud failure dump RL -28 m	1,454	1,449
OB dump RL -25 m	1,452	1,458
OB dump RL -20 m	1,457	1,453
Mud failure dump RL -22 m	1,461	1,462
OB dump RL -10 m	1,517	1,455
Mud failure dump RL -12 m	1,442	1,458
OB dump RL 0 m	1,465	1,461
Mud failure dump RL -6,5 m	1,454	1,469

4 CONCLUSION

4.1 *Conclusion*

According to the results of the slope stability analysis, the initial design was unstable since it did not meet the minimum safety factor criteria for static conditions (SF 1.2) and dynamic conditions (SF 1.1). Therefore, iteration is performed by cleaning the mud layer beneath the bund wall plan prior to construction to improve the slope's stability.

The analysis results show that the value of the safety factor increases with the number of soft mud materials cleaned. It was determined that the cleaned mud material was 155 m out of a total of 305 m, and the berm on the northern part of the bund wall was modified at heights of RL -10 m, RL -20 m, and RL -40 m to increase the resisting force.

The scenario for bund wall construction begins with cleaning mud, stockpiling OB instead of mud, stockpiling OB RL -40 m and OB material every 10 meters in addition to RL 0 m. Meanwhile, the mud waste is dumped at a lower height of about 2 m from the OB construction to prevent mud from overflowing towards the OB construction in the event of rain.

4.2 *Suggestion*

The cleaning of 155 m of mud met the safety factor criteria after iteration. However, there is still a soft mud layer along 150 m with a height of 10 m that must be considered because it may disrupt stability. As a result, it is advised to improve the soil by hastening the dissipation of excess pore pressure from the soft mud layer, allowing the effective soil stress to rise. The vertical drainage method is one method for soft soil improvement.

The OB material can be used as a preloading load against the mud material below. To maintain the stability of the bund wall slope during construction, OB material must be built in stages.

More research is needed to determine the best vertical drainage methods and their impact on soil carrying capacity and soil subsidence.

ACKNOWLEDGEMENT

We would like to thank Mr. Seto Wahyudi, Ph.D., from PT Zekon Indonesia as the company that has allowed the authors to obtain data and studies the problems that occur.

REFERENCES

Andriyan, S. H., Hirnawan, F., & Yuliadi. 2018. Stabilisasi Optimal Lereng Timbunan Overburden pada Area Disposal PT Insani Baraperkasa Tambang Loa Janan, Provinsi Kalimantan Timur dengan Rekayasa Geoteknik. *Prosiding Teknik Pertambangan* (hal. 391-397). Bandung: Fakultas Teknik Universitas Islam Bandung.

Aprilia, J., Muslim, D., Zakaria, Z., & Tedy, O. 2019. Evaluasi Kestabilan Lereng Tambang Batubara Pit 'XY' Menggunakan Metode Kesetimbangan Batas PT. Bukit Asam Tbk. *Padjajaran Geoscince Journal*: 175-181.

Coulomb, C. A. 1776. Essai sur une application des regles de Maximums et Minimis á quelques. *Memoires de Mathematique et de Physique* (p. 38). Paris: á l'Academie Royale des Sciences.

Das, B. M., & Sobhan, K. 2014. *Principles of Geotechnical Engineering.* Stamford: Cengage Learning.

Duncan, J. M., Wright, S. G., & Brandon, T. L. 2014. *Soil Strength and Slope Stability.* Hoboken: John Wiley & Sons, Inc.

Guler, E., Cicek, E., Demirkan, M. M., & Hamderi, M. 2012. Numerical Analysis of Reinforced Soil Walls with Granular and Cohesive Backfills Under Cyclic Loads. *Bull Eearthquake Engineering*: 793-811.

Hoek, & Bray. 1981. *Rock Slope Engineering 3rd Edition.* London: Institution of Mining and Metallurgy.

Kementerian ESDM. 2018. *Keputusan Menteri Energi dan Sumber Daya MIneral Nomor 1827 K/30/MEM/2018 tentang Pedoman Pelaksanaan Kaidah Teknik Pertambangan yang Baik.* Jakarta: Kementerian Energi dan Sumber Daya Mineral.

Kristyanto, T. H., Muslim, D., Zakaria, Z., Mendes, J. I., & Hirnawan, F. 2015. Determination of Dumping Area Based on Engineering Geological Study. *ACEAIT-3662*: 683-644.

Liong, G. T., & Herman, D. J. 2012. Analisa Stabilitas Lereng Limit Equilibrium vs Finite Element Method. *HATTI-PIT-XVI.* Jakarta: HATTI.

Oscar, A. W., Muslim, D., Sulaksana, N., & Hirnawan, F. 2016. Response of Stable Overall Slope Geometry of Open Pit Coal Mine in Warukin Formation to Dewatering and Peak Ground Seismic in South Kalimantan, Indonesia. *Buletin Sumber Daya Geologi*: 55-72.

Prasetyo, S. I., Hariyanto, & Cahyadi, T. A. 2011. Studi Kasus Analisa Kestabilan Lereng Disposal di Daerah Karuh Kec. Kintap, Kab. Tanah Laut, Kalimantan Selatan. *Seminar Nasional ke 6 Tahun 2011 STTNAS*: 381-387. Yogyakarta: UP Veteran Yogyakarta.

Wagner. 1957. The Use of The Unified Soil Classification System. *International Conference Soil Mechanics and Foundations Engineering 4th*: 125. London: Bureau of Reclamation.

Studi Perbandingan Hasil Perambatan Percepatan Gempa Terhadap Hasil Penyusunan *Modified Motion* Permukaan Tanah di Kota Bandung Berdasarkan Standar Nasional Indonesia (SNI) 1726 Tahun 2012 dan 2019

Bayu Wintoro
Mahasiswa Magister Program Studi Teknik Sipil – Institut Teknologi Bandung

Muhammad Asrurifak
Peneliti Pusat Studi Gempa Nasional – Institut Teknologi Bandung

Masyhur Irsyam
Profesor Program Studi Teknik Sipil – Institut Teknologi Bandung

ABSTRAK: *Modified ground motion* dibuat karena adanya keterbatasan informasi mengenai pencatatan percepatan gempa dalam bentuk *time history* yang dapat diakses secara bebas di wilayah Indonesia. Keterbatasan ini menjadi penyebab sulitnya akses untuk mendapatkan informasi gerak tanah yang diperlukan, meskipun peruntukannya dalam dunia akademis maupun penelitian. Penyusunan suatu *ground motion* dalam bentuk *time history* percepatan gempa di suatu lokasi yang tidak memiliki informasi *motion* perlu dilakukan, yang mana nantinya dapat digunakan sebagai *input*/masukan untuk analisis lanjutan dalam perencanaan suatu bangunan tahanan gempa. Analisis penskalaan gerak tanah dilakukan dengan menggunakan program Seismomatch dan Microsoft Excel, baik untuk penskalaan gerak tanah di batuan dasar maupun di permukaan. Hasil penskalaan di batuan dasar kemudian dirambatkan ke permukaan, dengan bantuan perangkat lunak Deepsoil, sehingga diperoleh nilai percepatan gempa di permukaan. Kemudian nilai ini akan dibandingkan dengan percepatan gempa hasil penskalaan gerak tanah terhadap target spektra permukaan tanah yang disusun berdasarkan SNI 1726: 2012 dan 2019.

Kata Kunci: penskalaan gerak tanah, perambatan gerak tanah, seed motion, spektra target, pembandingan percepatan

ABSTRACT: The modified ground motion was created due to limited information regarding recording earthquake acceleration that can be accessed freely in Indonesia. It is necessary to prepare a ground motion in the form of a time history of earthquake acceleration in a location that does not have motion information, which can later be used as input for further analysis in the planning of an earthquake resistant building. The motion scaling analysis was carried out using the Seismomatch and Microsoft Excel, both for scaling motion in bedrock and on the surface. The scaling results in the bedrock are then propagated using Deepsoil, so that the earthquake acceleration value on the surface is obtained. Then this value will be compared with the acceleration of the earthquake as a result of scaling the ground motion with the target ground surface spectra compiled based on SNI 1726: 2012 and 2019.

Keywords: ground motion scaling, ground motion propagation, seed motion, target spectra, acceleration comparison

1 PENDAHULUAN

Indonesia masuk ke dalam kawasan *Ring of Fire* atau cincin api Pasifik yang aktif akibat pergerakan lempeng–lempeng tektonik utama yang senantiasa bergerak dari waktu ke waktu. Sebagaimana yang diketahui, pergerakan ini yang menjadi pemicu terjadinya goncangan yang kemudian berdampak pada munculnya ancaman gangguan kehidupan serta kerusakan infrastruktur.

Kota Bandung merupakan salah satu kota besar di Indonesia. Sebagai ibukota Provinsi Jawa Barat, informasi mengenai tingkat resiko untuk kebutuhan mitigasi dan tindakan pencegahan kerusakan yang disebabkan oleh gempa, khususnya dalam hal pembangunan gedung maupun infrastruktur lainnya sangat diperlukan. Sebagai salah satu kota besar,

tingkat populasi dan infrastruktur yang tinggi menyebabkan resiko kerusakan yang terjadi akibat gempa semakin besar juga. Kerugian akibat terjadinya gempa bumi dapat diminimalisasi salah satunya dengan melakukan analisis potensi bahaya gempa pada suatu kawasan. Keluaran dari analisis potensi bahaya gempa ini menjadi masukan untuk tahap analisis selanjutnya, yakni mengenai tingkat ketahanan suatu struktur terhadap gempa.

Modified Ground motion dibuat karena adanya keterbatasan informasi mengenai pencatatan percepatan gempa dalam bentuk *time history* yang disebar secara bebas di wilayah Indonesia. Keterbatasan ini menjadi penyebab sulitnya akses untuk mendapatkan informasi yang diperlukan, meskipun peruntukannya digunakan dalam dunia akademis maupun penelitian. Maka dari itu, melalui tulisan ini, akan disusun suatu *motion* dalam bentuk *time history* percepatan gempa di permukaan yang nantinya dapat digunakan sebagai input/masukan untuk analisis lanjutan yang perlu dilakukan. Selain itu, melalui tulisan ini juga akan dilihat bagaimana hasil yang diperoleh berdasarkan analisis perambatan yang dilakukan, apabila dibandingkan dengan hasil perhitungan untuk percepatan gempa maksimum yang diperoleh dari penskalaan gerak tanah terhadap spektra target di permukaan yang disusun berdasarkan Standar Nasional Indonesia 1726: 2012 dan 2019 yang sudah beredar.

2 STUDI LITERATUR

2.1 *Penyusunan Modified Ground Motion*

Prosedur untuk menciptakan dan menstimulasi *ground motion* kuat secara umum dibagi menjadi beberapa klasifikasi utama: model *computational geophysical*, model *empirical attenuation*, dan model *empirical stochastic*, Dickinson (2011).

Metode yang sederhana dalam menentukan *modified ground motion* adalah dengan memodifikasi *ground motion* yang telah ada. Penskalaan ini dapat mengubah *ground motion* aktual ke tingkat goncangan yang lebih rendah atau lebih tinggi, sesuai dengan target spektra desain rencana di lokasi tinjauan. Prosedur ini dinamakan spectral *matching analysis*, Hutapea & Mangape (2009).

2.2 *Penskalaan Motion Gempa*

Penskalaan *motion* atau gerak tanah akibat gempa dilakukan untuk memperoleh *motion* gempa yang representatif untuk digunakan di suatu lokasi tinjauan studi. Dalam pemilihan jumlah komponen *motion* gempa, mengacu pada SNI 1726, sebanyak minimal 11 pasang *motion* horisontal dipilih untuk setiap target respons spektrum, dimana tiap *motion* ini terdiri dari 2 (dua) komponen *motion* horisontal yang saling tegak lurus. *Motion*/gerak tanah yang dipilih merupakan gerak tanah yang terjadi dan tercatat di stasiun/akibat gempa di lokasi lain, yang mana gerak tanah yang dipilih harus memiliki karakteristik sumber gempa (*magnitude* dan jarak) yang sama dengan lokasi tinjauan studi. Pada penskalaan gerak tanah, terdapat 2 metode yang dapat dilakukan, yakni *spectral matching* dan *amplitude scaling*.

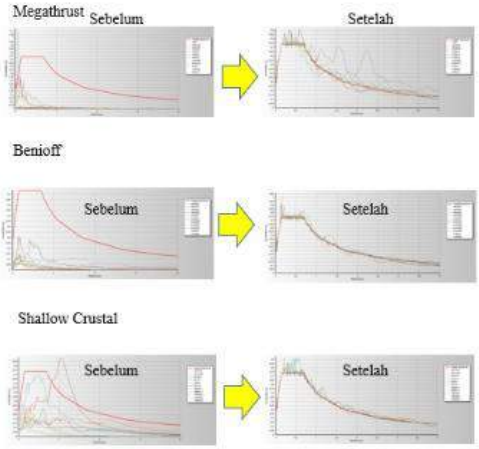

(a)

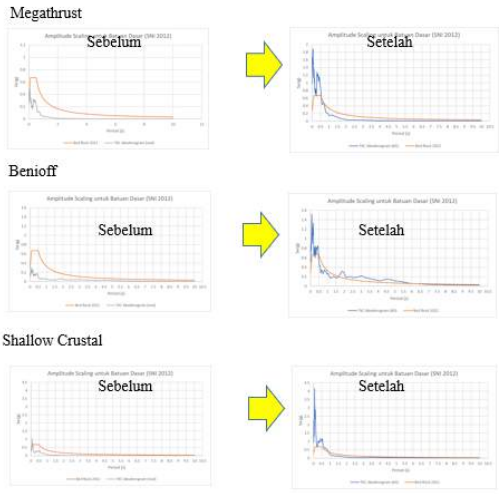

(b)

Gbr. 1. (a) Contoh hasil penskalaan dengan metode *spectral matching* (b) Contoh hasil penskalaan dengan metode *amplitude scaling.*

Berdasarkan analisis yang dilakukan, target spektral yang diperoleh tidak kurang dari 110% dari target respons spektrum yang dipilih.

2.3 *Efek Amplifikasi Lokasi Lokal*

Ground motion yang terjadi pada batuan dasar akan mengalami amplifikasi ketika melalui suatu media rambat tertentu, entah itu tanah keras maupun tanah lunak. Besarnya amplifikasi bergantung pada kondisi tanah lokal di sekitarnya. Ketika getaran mengalami amplifikasi, maka terjadi perubahan pada beberapa parameter getaran, yakni durasi getaran yang mungkin bertambah, selain itu frekuensi juga mungkin mengalami perubahan.

2.4 *Klasifikasi Kelas Situs*

Klasifikasi kelas situs akan menentukan seberapa besar faktor amplifikasi gempa di permukaan tanah. Pada dokumen SNI nomor 1726, klasifikasi kelas situs pada tanah mengacu kepada dokumen ASCE 07 Tahun 2010. Tanah diklasifikasi berdasarkan profil tanah sedalam 30 meter dari lapisan permukaan tanah. Klasifikasi tersebut disajikan pada Tabel berikut ini.

2.5 *Sintesis dan Kerangka Berpikir Analisis*

Berdasarkan kajian literatur yang telah dilakukan, kebutuhan analisis untuk penelitian maupun pekerjaan konstruksi untuk suatu bangunan tahan gempa membutuhkan informasi time history gempa, bukan hanya sekadar nilai percepatan yang terdapat pada buku gempa maupun SNI yang bisa diakses bebas.

Tidak terdapatnya *ground motion* yang bisa diakses bebas untuk keperluan penelitian maupun pekerjaan konstruksi, mengakibatkan perlunya disusun suatu *ground motion* tertentu, yang mampu menggambarkan nilai percepatan suatu gempa dalam suatu selang waktu tertentu.

Kondisi lapisan tanah spesifik di suatu lokasi tertentu, akan mempengaruhi besarnya hasil perambatan getaran akibat gempa dari batuan dasar. Maka pengaruh suatu sumber gempa pada suatu lokasi tertentu, akan berbeda apabila diamati di lokasi lain, yang tentunya memiliki karakteristik tanah dasar yang berbeda.

Untuk mengkonfirmasi hasil analisis, akan dilakukan perbandingan nilai dari percepatan gempa yang diperoleh berdasarkan analisis pada penelitian yang dilakukan (dalam bentuk *time history* percepatan gempa di batuan dasar maupun di permukaan tanah), dengan nilai percepatan gempa yang terdapat pada dokumen buku gempa maupun SNI yang beredar.

Tabel 1. Klasifikasi Kelas Situs pada Dokumen SNI 1726 yang Mengacu pada ASCE 07 Tahun 2010.

Kelas Situs	$\overline{V}_s$ (m/detik)	$\overline{N}$ atau $\overline{N}_{ch}$	$\overline{S}_u$ (kPa)
SA (batuan keras)	>1500	N/A	N/A
SB (batuan)	750 -1500	N/A	N/A
SC (tanah keras, sangat padat dan batuan lunak)	350 - 750	>50	$\geq$100
SD (tanah sedang)	175 – 350	15 – 50	50 – 100
	<175	<15	$\leq$50
SE (tanah lunak)	Atau setiap profil tanah yang mengandung lebih dari 3 m tanah dengan karakteristik sebagai berikut: 1. Indeks plastisitas, PI $\geq$ 20, 2. Kadar air, w $\geq$ 40%, 3. Kuat geser niralir $\overline{S}_u$ < 25 kPa		
SF (tanah khusus, yang membutuhkan investigasi geoteknik spesifik dan analisis respons spesifik situs yang mengikut 6.10.1	Setiap profil lapisan tanah yang memiliki salah satu atau lebih dari karakteristik berikut: 1. Rawan dan berpotensi gagal atau runtuh akibat beban gempa seperti mudah likuifaksi, lempung sangat sensitive, tanah tersementasi lemah 2. Lempung sangat organic dan/atau gambut (ketebalan H>3m) 3. Lempung berplastisitas sangat tinggi (ketebalan H>7,5 m dengan Indeks Plastisitas PI>75 4. Lapisan lempung lunak/setengah teguh dengan ketebalan H>35 m dengan $\overline{S}_u$ <50 kPa		

Catatan: N/A = tidak dapat dipakai

3 METODOLOGI ANALISIS

3.1 *Pengumpulan Data Sekunder*

Beberapa data yang diperlukan untuk analisis diantaranya:

- Nilai kecepatan rambat gelombang
- Data tanah dan nilai NSPT pada beberapa lokasi hingga kedalaman 30 meter

Pengukuran nilai kecepatan rambat gelombang dilakukan dengan pengukuran langsung di lapangan, yakni dengan metode mikrotremor. Hasil pengolahan data mikrotremor lapangan ini adalah berupa kecepatan gelombang geser yang terjadi di bawah permukaan tanah, yang nantinya akan digunakan untuk perambatan percepatan getaran gempa dari batuan dasar ke permukaan tanah. Dari nilai kecepatan geser yang dihasilkan oleh mikrotremor, dapat diketahui nilai kedalaman batuan dasar.

Sementara itu untuk data tanah, diperoleh dari data *boring log* berbagai proyek pembangunan di Kota Bandung yang telah dikumpulkan. Data tanah yang dimiliki kemudian divisualisasikan, yang mana tujuannya untuk memudahkan mengetahui kondisi tanah di Kota Bandung, sehingga pemilihan beberapa lokasi tinjauan lebih mudah dilakukan.

3.2 *Identifikasi Sumber Gempa*

- Hasil Deagregasi

Pada penelitian ini, nilai magnitude beserta jarak dominan dari gempa yang terjadi, digunakan data hasil deagregasi yang telah dilakukan pada penelitian dan studi sebelumnya, Asrurifak (2017). Hasil deagregasi yang telah dilakukan disajikan pada tabel dibawah ini.

Tabel 2. Hasil Deagregasi Gempa Wilayah Bandung Periode Ulang Gempa 2500 Tahunan, Untuk T=0 Detik, Asrurifak (2017).

No	Deag	Source	M	R (Km)
1	PGA, 2500 yr	Megathrust	8.69	134.99
2		Shallow crustal	6.30	25.83
3		Benioff	7.40	112.22

Mengacu pada SNI 8899: 2020 Tentang: Tata cara pemilihan dan modifikasi gerak tanah permukaan untuk perencanaan gedung tahan gempa, pemilihan gerak tanah dilakukan dengan mempertimbangkan mekanisme sumber gempa, besaran magnitudo, dan jarak terhadap sesar atau sumber gempa yang dapat merepresentasikan kondisi kegempaan pada lokasi yang ditinjau. Jika memungkinkan, gerak tanah harus diambil dari hasil rekaman akselerometer yang terpasang di permukaan tanah.

Pemilihan gerak tanah harus juga mengacu pada hasil analisis deagregasi sebagai bagian dari proses PSHA pada rentang periode struktur yang mendominasi perilaku struktur yang sedang dikaji.

Gambar berikut menyajikan kumpulan data akselelogram yang digunakan dalam penelitian, dan dipilih berdasarkan pertimbangan mekanisme sumber gempa, besaran magnitude, dan jarak terhadap sumber gempa di lokasi lain yang memiliki kemiripan karakteristik dengan lokasi tinjauan penelitian. Untuk tiap mekanisme sumber gempa, dipilih masing-masing 11 pasang akselelogram.

Tabel 3. Rekapitulasi Akselelogram yang Digunakan dalam Analisis.

Source	M	R (km)	Recorded Ground Motion (Actual GM)			
			CESMD & KIK-net	Station	M	R (km)
Megathrust/Subduksi	8,69	134,99	Tokachi-oki 2003-09-25 19:50:07 UTC	Memuro, Japan (TKCH06)	8,0	133,2
				Akkeshi, Japan (HKD076)	8,0	163,4
				Shizunai, Japan (HDKH06)	8,0	133,2
Shallow crustal	6,3	25,83	Southern Honshu 1997-06-25 09:50:12 UTC	Hagi, YMG002	6,1	31,8
				Ikumonaka, YMG003	6,1	20,0
				Masuda, SMN013	6,1	25,9
				Susa, YMG001	6,1	19,5
Benioff	7,4	112,2	Hokkaido 2004-11-28 18:32:14 UTC	Utoro, HKD061	7,0	126,8
				Kawayu, HKD081	7,0	100,9
				Chokubetsu, HKD086	7,0	110,1
				Akankohan, HKD082	7,0	104,1

Source	M	R (km)	Recorded Ground Motion (Actual GM)		
			PEER	M	R (km)
Megathrust/Subduksi	8,69	134,99	Chichi KAU062, TAP042, Denali (Alaska) Anchorage K205, K-06, NOAA weather facility, Police HG, Statefish and Game	8,4	392,0
Shallow crustal	6,3	25,83	Coalinga 1983 (Cantua Creek School, Parkfield – Fault Zone 14, Parkfield – Faultzone 7, Parkfield – Vineyard Cany), Chichi 1999 (CHY025, CHY101)	6,7	272,5
Benioff	7,4	112,2	Taba (Iran), Chichi (Taiwan) KAU011, KAU015, KAU058, KAU062, KAU064, TAP084	6,8	186,0

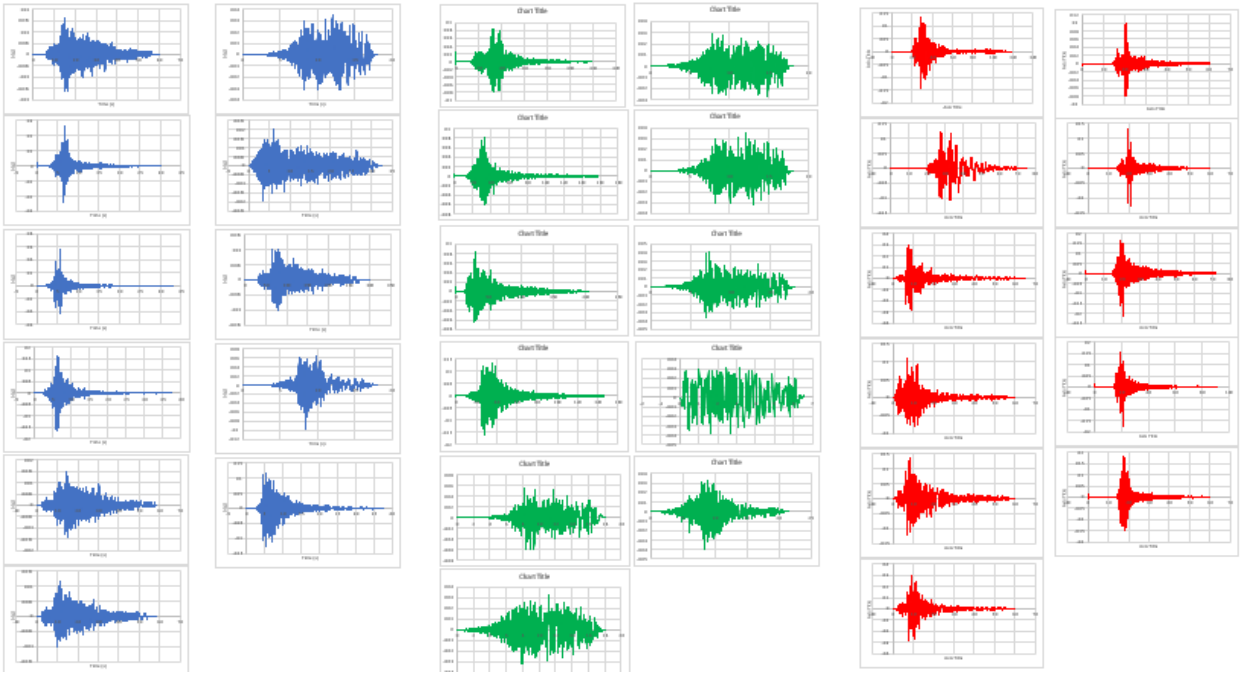

(a) (b) (c)

Gbr. 2. *Seed Motion* yang Digunakan untuk Masing-Masing Mekanisme Sumber Gempa (A) Megathrust, (B) Benioff, (C) Shallow Crustal.

3.3 *Input Parameter Tanah*

Berdasarkan beberapa data sekunder yang diperoleh dari studi literatur pada studi sebelumnya, gambar berikut menyajikan profil kondisi tanah yang digunakan dalam analisis perambatan gelombang dari batuan dasar ke permukaan.

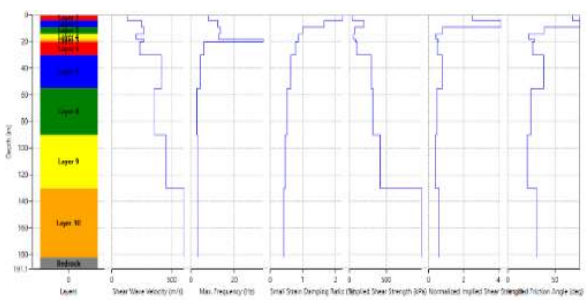

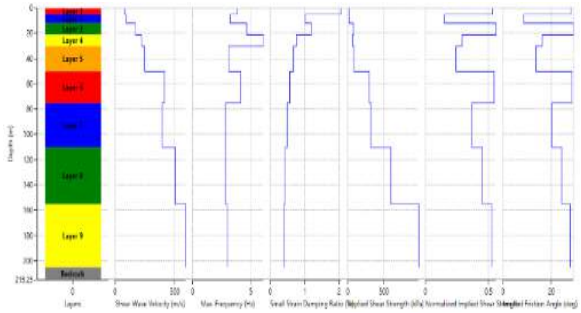

Gbr. 3. Profil Kondisi Tanah untuk Klasifikasi Kelas Situs SD dan SE di Kota Bandung.

4 HASIL ANALISIS

Setelah *motion* gempa dirambatkan, diperoleh motion baru yang merupakan gerak tanah di permukaan. Dari gerak tanah permukaan ini, ditentukan kembali respon spektra dari masing-masing gerak tanah. Dari kumpulan respon spektra ini, ditentukan rata-rata respon spektranya, dimana respon spektra rata-rata ini kemudian dijadikan respon spektra target untuk masing-masing gerak tanah yang telah dirambatkan sebelumnya.

Proses penskalaan dilakukan kembali pada gerak tanah yang sebelumnya telah dirambatkan. Pada akhirnya diperoleh gerak tanah yang sudah terskalakan dengan respon spektra target rata-rata dari hasil perambatan gerak tanah yang telah dilakukan. Gempa yang dipertimbangkan dalam tulisan ini adalah gempa dengan risiko tertarget (*Risk-targeted Maximum Considered Earthquake*), perioda ulang 2475 tahun dengan 1% probabilitas risiko keruntuhan terlampaui dalam 50 tahun.

Sehingga diperoleh gerak tanah baru, yang kemudian nilai dari percepatan maksimum dari tiap gerak tanah ini dikumpulkan dan dibandingkan nilainya dengan percepatan maksimum pada gerak tanah dari hasil penskalaan terhadap respon spektra target dari SNI untuk masing-masing kelas situs di permukaan tanah.

4.1 *Perbandingan hasil perambatan terhadap target spektra SNI 1726 2012*

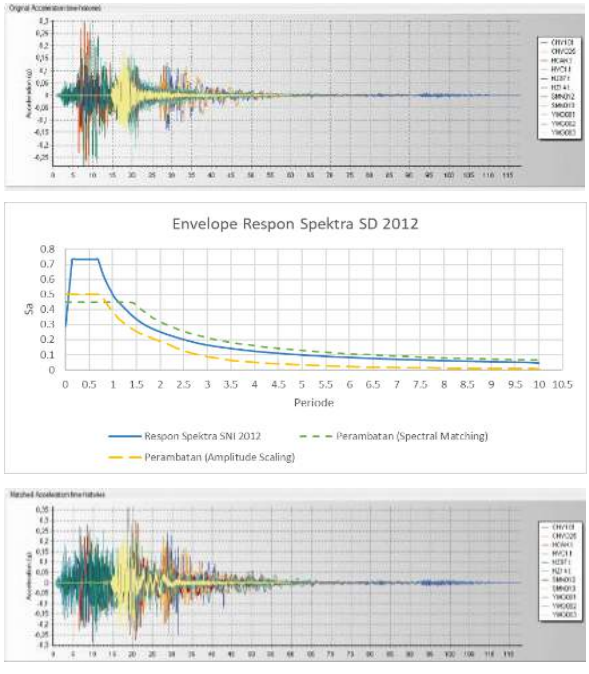

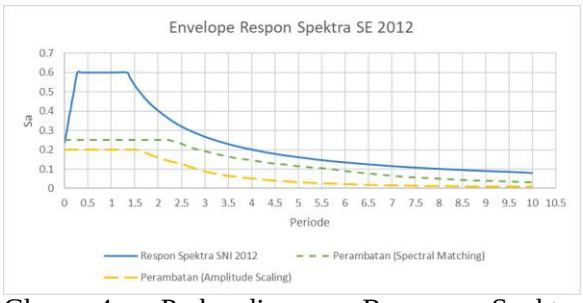

Gbr. 4. Perbandingan Respon Spektra Perambatan-Respon Spektra Target dan Contoh Grafik Percepatan Sebelum-Setelah Diskalakan Hasil Perambatan yang Disusun Berdasarkan SNI 1726 2012.

4.2 *Perbandingan hasil perambatan terhadap target spektra SNI 1726 2019*

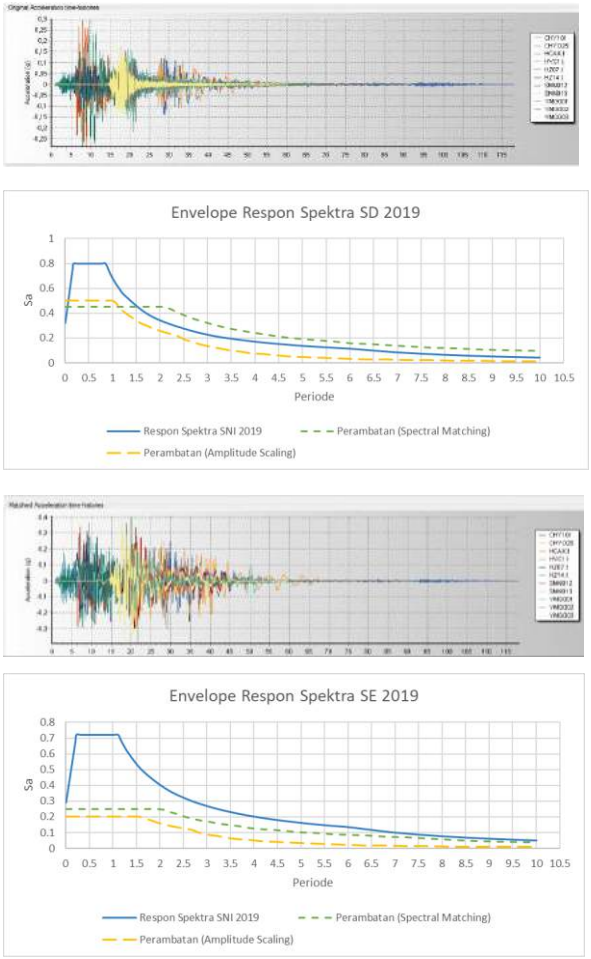

Gbr. 5. Perbandingan Respon Spektra Perambatan-Respon Spektra Target dan Contoh Grafik Percepatan Sebelum-Setelah Diskalakan Hasil Perambatan yang Disusun Berdasarkan SNI 1726 2019.

4.3 *Analisis*

Dari hasil analisis yang telah dilakukan, baik untuk analisis berdasarkan SNI 1726 2012 maupun 2019, didapatkan hasil bahwa percepatan spektral di permukaan tanah

cenderung menurun dengan bertambahnya kedalaman batuan dasar dan ketebalan lapisan.

Validasi lebih mendetail perlu dilakukan kembali dalam menskalakan *motion* gempa yang digunakan dalam analisis. Karena bagaimanapun, *motion* gempa yang diskalakan perlu diperiksa apakah memenuhi beberapa persyaratan yang diperlukan atau tidak untuk menggunakan suatu metode tertentu dalam melakukan penskalaan, untuk kemudian digunakan hasilnya.

Nilai percepatan hasil perambatan gelombang dengan melakukan input parameter maupun kondisi detail dari tanah untuk tiap lokasi tinjauan, secara konsisten memiliki nilai yg lebih kecil apabila dibandingkan dengan hasil percepatan di permukaan yang diperoleh dengan mengacu pada kondisi *site* yang tedapat pada SNI, baik itu untuk metode penskalaan dengan *spectral matching* maupun dengan *amplitude scaling*.

5 KESIMPULAN

Tidak terdapat perubahan signifikan yang terjadi antara nilai percepatan maksimum di batuan dasar, apabila dibandingkan dengan nilai percepatan maksimum yang diperoleh di permukaan tanah (nilai spektra target di permukaan tanah sesuai dengan SNI).

Percepatan tanah hasil perambatan yang dilakukan untuk beberapa sampling lokasi dan jenis lapisan tanah di Kota Bandung, mengalami penurunan nilai percepatan maksimum (percepatan tanah di batuan dasar, lebih besar dibanding percepatan tanah hasil perambatan di permukaan tanah), dimana dapat dilihat bahwa nilai percepatan untuk masing-masing hasil perambatan terhadap hasil penskalaan di permukaan, untuk SNI 2012 dan 2019 disajikan sebagai berikut:

Percepatan gravitasi, a (g) – SNI 2012				
di batuan dasar	di permukaan (SD)	di permukaan (hasil perambatan SD)	di permukaan (SE)	di permukaan (hasil perambatan SE)
Spectral Matching				
0,28	0,29	0,16	0,25	0,08
Amplitude Scaling				
0,25	0,24	0,14	0,22	0,07

Percepatan gravitasi, a (g) – SNI 2019				
di batuan dasar	di permukaan (SD)	di permukaan (hasil perambatan SD)	di permukaan (SE)	di permukaan (hasil perambatan SE)
Spectral Matching				
0,32	0,33	0,16	0,31	0,08
Amplitude Scaling				
0,27	0,26	0,15	0,25	0,07

Nilai percepatan hasil perambatan ke permukaan dengan sampling penskalaan menggunakan metode *amplitude scaling* menghasilkan nilai percepatan yang relatif lebih kecil apabila dibandingkan dengan metode penskalaan *spectral matching*. Namun demikian, berdasarkan kajian dan tinjauan pustaka, metode *spectral matching* menghilangkan karakteristik bawaan dari masing-masing *motion* gempa yang digunakan untuk analisis, sehingga dalam kondisi tertentu, metode *amplitude scaling* akan lebih menghasilkan hasil penskalaan yang lebih baik dibandingkan metode *spectral matching*. Selain itu juga, diperoleh hasil bahwa *motion* hasil penskalaan dengan *spectral matching* memiliki pola grafik respon spektra yang relatif tidak sama dengan grafik respon spektra di batuan dasar, lain halnya dengan metode *amplitude scaling* yang memberikan hasil pola respon spektra yang mirip dengan respon spektranya di batuan dasar. Hal ini diperkirakan terjadi akibat adanya modifikasi konten frekuensi pada penskalaan dengan metode *spectral matching*.

Terkait jarak terhadap sumber gempa dari akselelogram yang dipilih dalam tulisan ini, perlu dilakukan penyesuaian dan studi lebih lanjut kembali dikarenakan keterbatasan data yang ditemukan.

PENGHARGAAN

Penghargaan diberikan kepada Institut Teknologi Bandung, khususnya Program Studi Magister Teknik Sipil sebagai naungan utama penulisan dan penerbitan tulisan ini bisa dilakukan. *The Pacific Earthquake Engineering Research Center (PEER), Kiban Kyoshin Network (KIK NET), Center for Engineering Strong Motion Data (CESMD) USGS,* sebagai sumber utama pemilihan *seed motion* yang digunakan untuk analisis. Andhika Sahadewa, Dedi Apriadi, Sugeng Krisnanto, Nick Alexander, Mahdi Ibrahim Tanjung, dan Yuamar Imarrazan Basarah, sebagai *corrector* dan rekan diskusi/*brainstorming* serta pengarah penyusunan tulisan.

DAFTAR PUSTAKA

Asrurifak, M., Irsyam, M., & Budiono, B. 2010. Development of Spectral Hazard Map for Indonesia with A Return Period of 2500 Years using Probabilistic Method. *Civil Engineering Dimension*: 52-62.

Bardet, J., & Tobita, T. 2001. A Computer Program for Nonlinear Earthquake Site Response Analyses of Layered Soil Deposits. California.

Bhingarde, N. S., & Naik, a. N. 2016. Site-Specific Seismic Ground Response for Mormugao Port, Goa, India. *Geo-Chicago 2016 GSP*: 269.

Boore, D. M. 2002. Comments on Baseline Correction of Digital Strong-Motion Data: Examples from the 1999 Hector Mine, California, Earthquake. *Bulletin of the Seismological Society of America*: 1543–1560.

Boore, D. M. (2005). Processing of Strong-Motion accelerograms: needs, options and consequences. *Soil Dynamics and Earthquake Engineering* 25: 93-115.

Delfebriyadi. (2011). Deagregasi Hazard Kegempaan Provinsi Sumatera Barat. *Jurnal Teknik Sipil Volume* 18 *No.* 3.

Desai, S. S., & Choudhury, D. 2015. Site-Specific Seismic Ground Response Study for Nuclear Power Plants and Ports in Mumbai. *American Society of Civil Engineers*.

Han, S. W., & Seok, S. W. 2013. An Efficient Procedure for Selecting and Scaling Ground Motions for Response History Analysis. *Journal of Structural Engineering*.

Heo, Y., & Kunnath, S. K. 2011. Amplitude-Scaled versus Spectrum-Matched Ground Motions for Seismic Performance Assessment. *Journal of Structural Engineering*: 278-288.

Hines, E. M., Baise, L. G., & Swift, S. S. 2011. Ground-Motion Suite Selection for Eastern North America. *Journal of Structure Engineering*: 137:358-366.

Housner, G. (1946). *Characteristics of Strong-Motion Earthquakes*. Geoscience World.

Marihat, B., & Mangape, I. 2009. Analisis Hazard Gempa dan Usulan Ground Motion pada Batuan Dasar. *Jurnal Teknik Sipil Volume* 16 No. 3.

Misliniyati, R., Sahadewa, A., Hendriyawan, & Irsyam, M. 2019. Parametric Study of One-Dimensional Seismic Site Response Analyses Based on Local Soil Condition of Jakarta. *J. Eng. Technol. Sci*. 51, No. 3: 392-410.

Sengara, I., Irsyam, M., Hendriyawan, Asrurifak, M., Prakoso, W., Juniansyah, U., Jayasaputra, U. 2010. Laporan Akhir Pendayagunaan Peta Mikrozonasi Gempa di DKI Jakarta. Pusat Mitigasi Bencana ITB.

SNI, 1. 2012. Tata Cara Perencanaan Ketahanan Gempa untuk Bangunan Gedung dan Non-Gedung. *SNI-1726 2012*. Jakarta: Badan Standardisasi Nasional.

SNI, 1. 2019. Tata Cara Perencanaan Ketahanan Gempa untuk Bangunan Gedung dan Non-Gedung. *SNI-1726 2019*. Jakarta: Badan Standardisasi Nasional.

SNI, 8. 2020. Tata Cara Pemilihan dan Modifikasi Gerak Tanah Permukaan untuk Perencanaan Gedung Tahan Gempa. Jakarta: Badan Standardisasi Nasional.

Tjong, A. P. 2017. *Pembuatan Peta Mikrozonasi Gempa Wilayah Kota Bandung dengan Metode Deterministik Menggunakan Sumber Gempa Sesar Dangkal, Megathrust, dan Benioff Zone*. Bandung.

Evaluasi Stabilitas Sandaran Bendungan Bener Berdasarkan Korelasi Geomekanik Bawah Permukaan

Daru Jaka Sasangka
Politeknik Pekerjaan Umum

Pranu Arisanto
Politeknik Pekerjaan Umum

Wahyu Prasetyo
Politeknik Pekerjaan Umum

Dian Insani
BBWS Serayu Opak

ABSTRAK: Lapisan *top soil* Rencana Bendungan Bener cukup tipis antara 0 – 5 meter, sehingga faktor pengontrol utama untuk pondasi infrastuktur yang di bangun disini adalah batuan. Lithologi penyusun lokasi bendungan umumnya breksi vulkanik andesit yang baik untuk menompang mega infrastruktur yang dibangun disana namun perlu di dukung data kualitas massa batuan untuk memastikan kehandalan dari pondasi. Kualitas massa batuan sangat menentukan kestabilan infrastruktur terutama pada bagian lereng, terowongan dan bendungan inti. Korelasi bawah permukaan menunjukan sandaran bendungan secara umum tersusun oleh stratifikasi kualitas massa batuan sedang dibagian atas dan kualitas massa batuan baik di bagian bawah dari klasifikasi *Rock Mass Rating* (RMR). Kualitas massa batuan Sedang memiliki nilai Rata –Rata RMR 52,5 dan Kualitas Baik dengan nilai RMR 65,4. Data kualitas massa batuan diolah untuk mendapatkan nilai kestabilan sandaran bendungan. Lokasi rencana sandaran bendungan secara umum termasuk dalam kategori stabil berdasarkan klasifikasi *Slope Mass Rating* (SMR) dimana lapisan atas memiliki nilai SMR 60 -70 dan lapisan bawah 65 – 80.

Kata Kunci: RMR, SMR, bendungan

ABSTRACT: The top soil layer of the Bener Dam is quite thin between 0 – 5 meters, so the main controlling factor for the infrastructure foundation built here is rock. The lithology which composes the dam site is generally andesite volcanic breccia and it is good supporting the mega infrastructure which built there. The supporting rock needs to be supported by rock mass quality data to ensure the reliability of the foundation. The quality of the rock mass determines the stability of the infrastructure, especially on the slopes, tunnels and core of the dams. The subsurface correlation shows that the dam foundation is generally composed of moderate rock mass quality stratification at the top and good rock mass quality at the bottom based on the Rock Mass Rating (RMR) classification. The moderate rock mass quality which has an Average value of RMR 52.5 and Good Quality with an RMR value of 65.4. The dam layed on the stable foundation which has value of the Slope Mass Rating (SMR) 60 -70 on top layer and 65 – 85 on the lower layer.

Keywords: RMR, SMR, dam

1 PENDAHULUAN

Bendungan bener dibangun di wilayah administrasi Desa Guntur, Kecamatan Bener, Kabupaten Purworejo. Bendungan ini direncanakan memiliki 169 m, dan panjang 534 m dan menjadi salah satu yang tertinggi di Asia Tenggara. Pemanfaatan Bendungan ini antara lain untuk menjamin pemenuhan air irigasi untuk Daerah Irigasi (D.I.) Guntur dan Penungkulan (907 ha), suplesi ke D.I. Kedung Putri (4341 ha), D.I. Boro (5126 ha), D.I. Loning-Kragilan (2532 ha), dengan pola tanam padi-padi-palawija, Bendungan ini juga dibangun untuk menjamin kebutuhan air irigasi untuk pembukaan lahan sawah baru seluas 3000 Ha (2250 Ha di Kec. Gebang) dan memenuhi kebutuhan air baku (BBWS Serayu Opak, 2018).

Breksi vulkanik andesit dan Breksi Polimik menempati sebagian besar lokasi pembangunan bendungan, dan sandaran bendungan sendiri

berada pada satuan batuan breksi vulkanik andesit, Daru Jaka Sasangka et al. (2019). Breksi vulkanik andesit dan Breksi polimik memiliki daya dukung yang berbeda. Penyelidikan kekuatan batuan dengan *Uniaxial Compression Strenght (UCS)* sesuai yang dipersyaratan (SNl, 2017) telah dilakukan yang menunujukan bahwa Breksi Vulkanik Andesit dalam kondisi tidak lapuk memiliki nilai *point load Index* rata – rata 2.91 MPa, dan breksi polimik 0,65 MPa, Daru Jaka Sasangka (2021). Breksi vulkanik andesit dari pengujian UCS memiliki nilai kuat tekan 31.05 MPa sedangkan breksi polimik 15.39 MPa, Daru Jaka Sasangka et al. (2019).

Penilaian kestabilan berdasarkan kualitas massa batuan telah dilakukan pada portal terowongan namun dengan data permukaan dan bawah permukaan yang terbatas. Kestabilan lereng inlet terowongan pengelak memiliki nilai SMR 67.3 yang termasuk kedalam lereng yang stabil, D J Sasangka et al. (2019).

Adanya data pemboran bawah permukaan pada lokasi bendungan inti yang sesuai dengan standar perancangan geoteknik untuk penyelidikan lapangan dapat dioptimalkan dengan memetakan stabilitas sandaran bendungan berdasarkan data tersebut.

2 TINJAUAN PUSTAKA

Lapisan tanah yang tipis di lokasi pembangunan bendungan menjdikan faktor kontrol utama kestabilan pondasi bendungan adalah batuan. Penilaian kestabilan sandaran bendungan berdasarkan nilai SMR. Nilai SMR didapatkan dengan pengolahan data RMR dengan koreksi kondisi lapangan atau dari rumur empirik.

Nilai RMR menjadi salah satu parameter penentuan kualitas massa batuan yang paling tepat untuk batuan beku seperti yang ditemukan di lokasi penelitian. Nilai RMR dipengaruhi oleh beberapa faktor antara lain Kuat Tekan Batuan (UCS), nilai Rock Quality Designation (RQD), spasi antar bidang diskontinyuitas, kondisi bidang diskontinyuitas dan parameter air tanah, Bieniawski (1989) (Tabel 1).

Dengan melihat geometri sandaran bendungan, tinjuan kestabilan sandaran bendungan dapat didekati dengan analisis kestabilan lereng. Kondisi lereng dapat ditunjukan dengan nilai SMR yang dapatkan dari nilai RMR dengan melakukan penyesuaian kondisi lapangan (Tabel 2) atau penyerdahanaan dengan persamaan linear atau logaritmik.

Penyesuaian kondisi lapangan dari data RMR untuk mendapatkan nilai SMR dengan persamaan sebagai berikut:

$$SMR = RMR + (F1.F2.F3) + F4 \quad (1)$$

Diterangkan bahwa

- F1 nilainya tergantung selisih antara jurus dari bidang diskontinuitas dan bidang lereng. Nilainya berkisar dari 1,00 (saat kedua bidang hampir paralel) sampai 0,15 (saat sudut antara kedua jurus > 300°), kemudian F2 mengacu pada sudut kemiringan dari bidang diskontinuitas. Nilainya berkisar dari 1,00 (bidang diskontinuitas dengan kemiringan > 45°) hingga 0,15 (bidang diskontinuitas dengan kemiringan < 200°) dan F3 mencerminkan hubungan antara kemiringan lereng dengan kemiringan bidang diskontinuitas (Tabel 2), Romana et al. (2015).
- F4 merupakan faktor penyesuaian terhadap metode ekskavasi (Tabel 2), Romana et al. (2015).

Hubungan antara RMR dengan SMR secara empirik dengan hubungan linear dapat dilihat pada Pers. (2), Hall (1985); dalam, Zakaria & Muslim (2012), sedangkan hubungan secara logaritmik dapat dilihat dari persamaan (3), Orr (1992); dalam, Zakaria & Muslim (2012).

$$SMR = 0{,}65\,RMR + 25 \quad (2)$$

$$SMR = 35\,ln\,RMR - 71 \quad (3)$$

Pemboran dalam pada lokasi bendungan dilengkapi juga dengan pengujian lugeon. Data lugeon digunakan sebagai dasar penanganan pondasi yang harus dilakukan salah satunya yang sering dilakukan pada bendungan adalah dengan grouting, SDA PUPR (2005). Nilai lugeon menunjukan kemampuan pondasi dalam meloloskan air atau juga sebagai nilai petunjuk nilai permeabilitas batuan di lapangan.

Kualitas massa batuan mempengaruhi kestabilan batuan, dan tingkat permeabilitas batuan sebagai pondasi. Tingkat permeablitas batuan dapat dilihat dari nilai lugeon. Satu Lugeon unit (LU) didefinisikandebit air 1 liter per meter panjang uji per meter pada tekanan 10 bar (1000 kPa) dan sangat mendekati K=1,2 $x10^{-5}$.

Tabel 1. Rock Mass Rating Classification.

1	Strength of Intact Rock of Intact Rock	Point Load Strength Index	> 10 MPa	4 - 10 MPa	2 - 4 MPa	1 - 2 MPa	For this Range - Uniaxial Compresive is Prefered	
		Uniaxial Comp. Strength	> 250 MPa	100 - 250 MPa	50 - 100 MPa	25 - 50 MPa	5 - 25 MPa	1 - 5 MPa / < 1 MPa
	Rating		15	12	7	4	2	1 / 0
2	RQD		90 - 100%	75 - 90%	50 - 75%	25 - 50%	< 25%	
	Rating		20	17	13	8	3	
3	Spacing of Disc		> 2 m	0.6 - 2 m	20 - 60 cm	6 - 20 cm	< 6 cm	
	Rating		20	15	10	8	5	
4	Condition of Discontinuities		Very rough surface not continuos	Slightly rough surface separation < 1 mm	Slightly rough surface separation < 1 mm	Slickensided surface or Gauge < 5 mm thick		Soft gauge > 5 mm thick or Separation > 5 mm
			No separation	Slightly weathered walls	Highly weathered walls	or Separation 1 - 5 mm		Continous
	Rating		Unweathered Wall Rock 30	25	20	Continous 10		0
5	Groundwater		Completely dry	Damp	Wet	Dripping	Flowing	
			15	10	7	4	0	

Tabel 2. Penentuan Nilai SMR dengan Penyesuaian terhadap Data Lapangan.

Slope Failure Potential		Highly Favorable	Favorable	Fair	Unifavorable	Very Unfavorable
Planar Topling Wedges	I αj - αs I I αj - αs - 180° I I αi - αs I	> 30°	30 - 20°	20 - 10°	10 - 5°	< 5°
Planar/Wedges/Topling	F1	0.15	0.4	0.7	0.85	1
Planar Wedges	βj βi	< 20°	20 - 30°	30 - 35°	35 - 45°	> 45°
Planar/Wedges	F2	0.15	0.4	0.7	0.85	1
Topling	F2	1	1	1	1	1
Planar Wedges	I βj - Bs I I βi - Bs I	> 10°	10 - 0°	0°	0 - (-10)°	< 10°
Topling	I βj + Bs I	< 100°	< 110 - 120°	> 120°	-	-
Planar/Wedges/Topling	F3	0	-6	-25	-50	-60

Excavation Method	Value of F4
Natural Slope No Blasting No Excavation	+15
Blasting with Pre - Splitting	+10
Smooth Blasting	+8
Normal Blasting or Mechanical Excavation	0
Poor Blasting	-8

Class No.	V	IV	III	II	I
SMR Value	0 - 20	21 - 40	41 - 60	61 - 80	81 - 100
Rock Mass Description	Very Bad	Bad	Fair	Good	Very Good
Stability	Completely Unstable	Unstable	Partialy Stable		Completely Stable
Failure	Big Planar or Soil - Like or Circular	Planar or Big Wedges	Planar Along Some Joint and Many Wedges	Some Block Failure	No Failure
Probability of Failure	0.9	0.6	0.4	0.2	0

Hubungan antara nilai lugeon dan keperluan grouting sebagai berikut Nilai LU 1 menunjukan derajad permeabilitas pada pondasi yang ketat (tight) dan hampir tidak perlu di grout, Nilai LU 3 pondasi perlu sedikit digrouting, nilai LU 5 ponadi perlu dijamin dengan grouting yang ekstensif untuk bendungan beton dan grouting regional untuk bendungan urugan tanah atau batu, nilai LU 10 perlu dijamin dengan grouting untuk semua tipe bendungan, nilai LU 20 menunjukan bahwa pondasi memiliki banyak rekahan (kekar) dengan bukaan yang relatif kecil dan nilai LU 1000 menunjukan bahwa pondasi memiliki banyak rekahan (kekar) dengan bukaan yang relatif kasar.

3 PEMBAHASAN

3.1 *Kestabilan Sandaran Sayatan A*

Analisis stabilitas sandaran bendungan dilakukan pada kondisi tanpa adanya ekskavasi. Analisis dilakukan dengan dua sayatan yaitu sayatan A di lokasi inti bendungan dan sayatan B dibagian lebih hulu (Gbr. 1).

Data kualitas massa batuan (RMR) didapat dari analisis data pemboran bawah permukaan. RMR digunakan untuk menghitung nilai SMR dengan rumus empirik seperti yang dijelaskan pada bagian sebelumnya dan dengan mempertimbangkan orientasi bidang lemah utama, kemiringan lereng dan arah lereng. Nilai SMR menunjukan tingkat kestabilan lereng batuan (Tabel 2), SMR juga digunakan untuk memperkirakan sudut kemiringan lereng pengupasan yang aman berdasarkan parameter RMR, Zakaria & Muslim (2012).

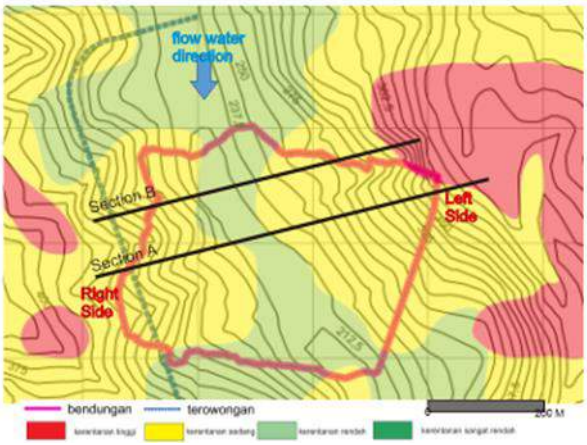

Gbr. 1. Letak Sayatan Lereng Sandaran Bendungan terhadap Proyek.

Secara umum sandaran bendungan pada sayatan A baik di sisi sandaran kanan dan sandaran kiri memiliki 2 region kualitas massa batuan yaitu bagian atas dan bagian bawah. Bagian atas memiliki kualitas massa batuan sedang (fair rock) dan bagian bawah memiliki kualitas massa batuan (good rock). Dari pengukuran lapangan didapat bahwa region atas memiliki nilai LU antara 18 – 32, sedangkan bagian bawah antara 12 – 20.

Pada as bendungan (sayatan A) sebelah kanan region kualitas massa batuan sedang yang berada dibagian atas memiliki pengaruh antara kedalaman 5 sampai kedalaman 23 meter di bawah permukaan tanah (Gbr. 2). Nilai RMR lapisan ini adalah 53,3 dan nilai SMR antara 59,64 (Persamaan Hall dengan hubungan Linear) hingga 68,16 (Persamaan Orr dengan hubungan logaritmik). Bagian bawah yang merupakan region kualitas massa batuan baik memiliki nilai RMR 67.57 dan nilai SMR antara 68.92 (Persamaan Hall dengan hubungan Linear) hingga 76.46 (Persamaan Orr dengan hubungan logaritmik) (Gbr. 2).

Pada inti bendungan (sayatan A) sebelah kiri region kualitas massa batuan sedang yang berada dibagian atas memiliki pengaruh antara kedalaman 14 sampai kedalaman 35 meter di bawah permukaan tanah (Gbr. 2). Nilai RMR rata rata lapisan ini adalah 54.21 dan nilai SMR antara 60,24 (Persamaan Hall dengan hubungan Linear) hingga 68,75 (Persamaan Orr dengan hubungan logaritmik). Bagian bawah yang merupakan region kualitas massa batuan baik memiliki nilai RMR rata-rata 66,08 dan nilai SMR antara 67,95 (Persamaan Hall dengan hubungan Linear) hingga 75.68 (Persamaan Orr dengan hubungan logaritmik) (Gbr. 2).

Secara umum terdapat 2 lapisan (region) yaitu region atas dengan kualitas massa batuan sedang di bagian atas dan kualitas massa batuan baik di bagian bawah. Berdasarkan pengamatan bawah permukaan tidak region bawah tidak hanya terdiri dari kualitas massa batuan baik namun ada cluster atau lensa dengan kualitas massa batuan sedang bahkan buruk yang interval kemunculannya tidak signifikan, kondisi tersebut dipengaruhi oleh patahan – patahan minor. Sedangkan kualitas massa batuan sedang di bagian atas selain dipengaruhi oleh struktur geologi pengaruh dari tektonik,

juga dipengaruhi oleh oksidasi atau tingkat pelapukan

Dari sayatan A dapat dilihat bahwa berdasarkan nilai SMR yang diperoleh maka lereng termasuk dalam kondisi yaNg stabil dan termasuk kelas lereng II, Romana et al. (2015), sehingga tidak membutuhkan penanganan yang signifikan hanya beberapa penanganan setempat jika kemudian dilakukan penggalian, Singh & Goel (2011).

3.2 *Kestabilan Sandaran Sayatan B*

Sayatan B berada dibagian hulu dibandingkan dengan sayatan A (Gbr. 1). Seperti halnya sayatan A, Sayatan B baik di sisi sandaran kanan dan sandaran kiri memiliki 2 region kualitas massa batuan yaitu bagian atas dan bagian bawah. Bagian atas memiliki kualitas massa batuan sedang (fair rock) dan bagian bawah memiliki kualitas massa batuan (good rock). Dari pengukuran lapangan didapat bahwa region atas memiliki nilai LU antara 12 – 32, sedangkan bagian bawah antara 2 – 15.

Pada inti bendungan (sayatan B) sebelah kanan region kualitas massa batuan sedang yang berada dibagian atas dijumpai antara kedalaman 7 sampai kedalaman 12 meter di bawah permukaan tanah (Gbr. 3). Nilai RMR lapisan ini adalah 50,17 dan nilai SMR antara 57,61 (Persamaan Hall dengan hubungan Linear) hingga 66,04 (Persamaan Orr dengan hubungan logaritmik). Bagian bawah yang merupakan region kualitas massa batuan baik memiliki nilai RMR 63,96 dan nilai SMR antara 66,57 (Persamaan Hall dengan hubungan Linear) hingga 74.54 (Persamaan Orr dengan hubungan logaritmik) (Gbr. 3).

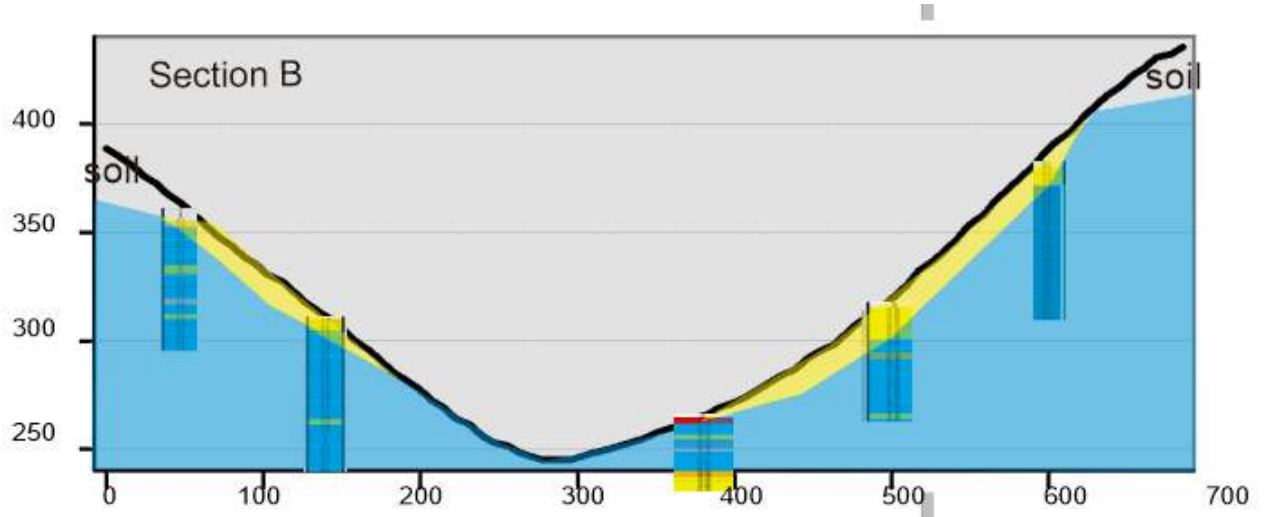

	Sandaran Kanan			Sandaran Kiri		
	RMR	SMR (Hall)	SMR (Orr)	RMR	SMR (Hall)	SMR (Orr)
Region (lapisan) Atas	50,17	57,61	66,04	52,26	58,97	67,47
Region (lapisan) Bawah	63,96	66,57	74,54	64,14	66,69	74,64

Gbr. 2. Sayatan B pada Inti Bendungan.

Pada sayatan B sebelah kiri region kualitas massa batuan sedang yang berada dibagian atas memiliki pengaruh antara kedalaman 15 sampai kedalaman 35 meter di bawah permukaan tanah (Gbr. 3). Nilai RMR rata rata lapisan ini adalah 52,26 dan nilai SMR antara 58,97 (Persamaan Hall dengan hubungan Linear) hingga 67,47 (Persamaan Orr dengan hubungan logaritmik). Bagian bawah yang merupakan region kualitas massa batuan baik memiliki nilai RMR rata-rata 64,14 dan nilai SMR antara 66,69 (Persamaan Hall dengan hubungan Linear) hingga 74.64 (Persamaan Orr dengan hubungan logaritmik) (Gbr. 3).

Seperti halnya sayatan A, region bawah tidak hanya terdiri dari lapisan dengan kualitas massa batuan yang baik namun terdapat lensa yang dikontrol oleh sesar minor sehingga turun kualitas massa batuannya menjadi kualitas massa batuan sedang (Fair Rock).

Dari sayatan B dapat dilihat bahwa berdasarkan nilai SMR yang diperoleh walaupun terdapat 1 nilai SMR yang menunjukan nilai dibawah 60 berarti termasuk

kelas lereng III yang berarti sebagian stabil namun secara umum lereng termasuk dalam kondisi yang stabil dan termasuk kelas lereng II baik region atas maupun bawah ((Romana et al., 2015). Dari kelas lereng tersebut sehingga lereng tanapa ekskavasi tidak membutuhkan penanganan yang signifikan hanya beberapa penanganan setempat jika kemudian dilakukan penggalian (Singh & Goel, 2011).

Tabel 3. Analisis Kinematik SMR.

REGION ATAS												
Location	RMR	Slope Data			Discontinyuity data of slope		WEIGHTING FACTORS (ROMANA 1985)				SMR
		(SLOPE DIRECTION) (A)	Main Strike of slope (B)	DIP of slope (C)	strike (D)	dip (E)	F1 (D-B)	F2 (E)	F3 (E-C)	F4	
Sandaran Kanan REGION ATAS		65	155	35	210	80	35	80	35	0	SMR = RMR + (F1.F2.F3) + F4
Score	53.30						0,4	1	0	0	53.3

REGION BAWAH											
Location	RMR	Slope Data			Discontinyuity data of slope		WEIGHTING FACTORS (ROMANA 1985)				SMR
		(SLOPE DIRECTION) (A)	Main Strike of slope (B)	DIP of slope (C)	strike (D)	dip (E)	F1 (D-B)	F2 (E)	F3 (E-C)	F4	
Sandaran Kanan REGION BAWAH		65	155	35	210	80	35	80	0	0	SMR = RMR + (F1.F2.F3) + F4
Score	67.6						0,4	1	-0	0	67.6

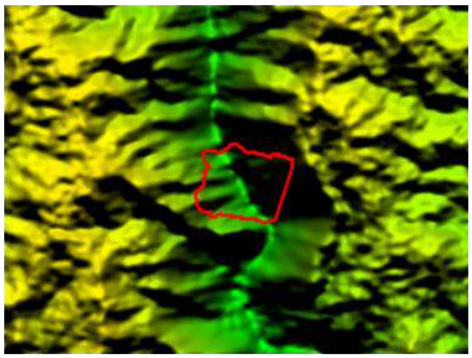

3.3 *Analisis Kinematic Sandaran Kanan As Bendungan*

Analisis Kinematik dilakukan pada lokasi Sayatan A pada sandaran kanan. Data kemenerusan slope lereng dan kemiringan lereng didapat dari survey lapangan dan dari data *DEM* sedangkan data bidang diskontinyuitas didapat dari survey lapangan dan ditentukan bahwa orientasi bidang diskontinyuitas yang digunakan dalam analisis adalah arah patahan minor yang merupakan kontrol ketidaksatabilan lereng utama dengan jenis longsoran kinematik adalah longsoran tipe planar (Tabel 3).

Analisis menunjukan bahwa SMR untuk region atas 53,3 dan region bawah 67,6. Nilai SMR tersebut menunjukan bahwa lereng bagian atas termasuk kedalam kelas lereng III yang berarti sebagian stabil (partialy stable) dan lereng bagian bawah termasuk kedalam kelas lereng II.

3.4 *Analisis Numerik*

Analisis Numerik dilakukan pada sayatan A sandaran kanan. Analisis numerik sebagai koreksi atas perhitungan dengan metode empirik. Analisis numerik mendapatkan kondisi lereng yang stabil. Nilai kestabilan terlihat dari nilai *Safety Reduction Factor* (SRF) sebesar 2,51. (Gbr. 4).

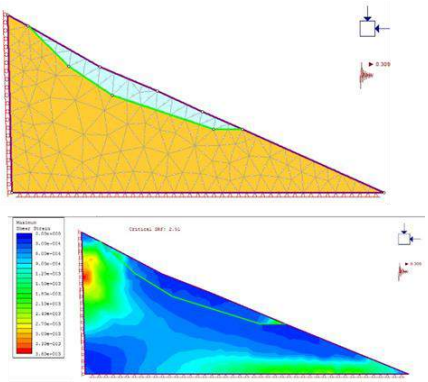

Gbr. 4. Analisis Numurik Sandaran Kanan.

4 KESIMPULAN

Secara umum lokasi sandaran bendungan terdiri dari dua kualitas massa batuan yang berbeda yaitu lapisan atas dengan kualitas massa batuan yang sedang dan bagian bawah terdiri dari kualitas massa batuan yang baik. Kualitas massa batuan dipengaruhi oleh menifestasi struktur geologi dan tingkat pelapulan terutama pada lapisan (region) atas. Nilai Lugeon semakin kecil untuk kualitas massa batuan yang baik, dan membesar ketika kualitas massa batuan turun (menjadi kualitas massa batuan sedang)

Kestabilan lereng eksisting (tanpa ekskavasi) dari analisis empirik maupun analisis numerik menunjukan kondisi yang stabil pada umumnya. Namun perlu sedikit perbaikan jika kemudian ada ekskavasi yang menyebabkan lereng terganggu.

Ekskavasi bendungan menyebabkan geometri lereng berubah namun memudahkan dalam akusisi data geomekanik bawah pernukaan maka penyelidikan kestabilan sandaran lanjutan perlu dilakukan dengan penambahan data geomekanaik permukaan sehingga analisis empirik dengan tipe keruntuhan kinematik dapat dilakukan dengan lebih detail

PENGHARGAAN

Ucapan terimkasih kami ucapkan kepada Politeknik Pekerjaan Umum yang telah memfasilitasi penelitian ini. Kami ucapkan terimaksih kepada Balai Besar Wilayah Sungai Serayu Opak dan seluruh direksi lapangan yang tidak dapat kami sebutkan satu persatu yang telah memberikan izin dan membantu dalam akusisi data permukaan maupun data sekunder.

DAFTAR PUSTAKA – REFERENCES

BBWS Serayu Opak. 2018. *Laporan geologi*. *September*.

Bieniawski, Z. T. 1989. *Engineering Rock Mass Classifications:* 251. New York: Wiley & Sons.. http://www.dot.ca.gov/hq/esc/geotech/references/Rockfall_References/05_Bieniawski_Eng_Rx_Mass_Classification.pdf

Romana, M., Tomás, R., & Serón, J. B. 2015. Slope Mass Rating (SMR) Geomechanics Classification: Thirty Years Review. *13th ISRM International Congress of Rock Mechanics* 2015-MAY(May): 1–10.

Sasangka, D J, Taufik, R., & Indrawan, I. G. B. 2019. Engineering Geology Investigation for Slope Geometry Design of Diversion Tunnel Portal In Bener Dam Purworejo. *Proceeding of SLOPE: 1–8.* https://www.researchgate.net/profile/Daru_Sasangka/publication/343788725_ENGINEERING_GEOLOGY_INVESTIGATION_FOR_SLOPE_GEOMETRY_DESIGN_OF_DIVERSION_TUNNEL_PORTAL_IN_BENER_DAM_PURWOREJO/links/5f3f9e13299bf13404da6adb/ENGINEERING-GEOLOGY-INVESTIGATION-FOR-SLO

Sasangka, Daru Jaka. 2021. *Analisis Metode Ekskavasi Terowongan Pengelak Bendungan Bener Berdasarkan Data Geologi Teknik*. *9*(85): 13–24.

Sasangka, Daru Jaka, Indrawan, I. G. B., Taufik, R., & Insani, D. 2019. *Modelling of Engineering Geology Condition of Bener Dam Diversion Tunnel Based on Surface and Subsurface Data Ministry of Public Works and Housing of the Republic of Indonesia , 2 Gadjah Mada University*. *JCY*: 1–6.

SDA PUPR. 2005. *Pedoman Grouting Untuk Bendungan* (p. 298). http://222.124.202.167/balai_bendungan/file/19) PEDOMAN. GROUTING UNTUK BENDUNGAN.pdf

Standar Nasional Indonesia 8460:2017. 2017. *Persyaratan Perancangan Geoteknik*.

Singh, B., & Goel, R. K. 2011. *Engineering Rock Mass Classification*. Elsevier. http://library1.nida.ac.th/termpaper6/sd/2554/19755.pdf

Zakaria, Z., & Muslim, D. 2012. Koreksi Smr Pada Desain Lereng Tambangterbuka Batubara Pada Formasi Balikpapan & Formasi Kampungbaru, Sangasanga, Kalimantan Timur. *Buletin Sumber Daya Geologi 7*(3): 147–157. https://doi.org/10.47599/bsdg.v7i3.115

Proposed Ground Motion Selection and Modification for Jakarta Site based on ASCE 7-16 and SNI 8899-2020

Det Komerdevi
PT WSP Engineering Consultant

I Wayan Sengara
PT WSP Engineering Consultant
Institut Teknologi Bandung

ABSTRACT: This paper present application of ground motion selection and modification as to satisfy requirements of SNI 8899-2020 and ASCE 7-16. This intended to generate an appropriate ground motion for high rise building in case for Jakarta site. The requirement consists of providing minimum 11-pairs of orthogonal horizontal ground motion components. The 11-pairs ground-motions have been selected, modified and spectrally matched with the recommended target spectrum resulted from site-specific response analysis for particularly site in Jakarta. Corresponding de-aggregation analysis has been considered to select events and their seed-motions within the same general tectonic regime, having generally consistent magnitudes and fault distances as those controlling the target spectrum, and have similar spectral shape to the target spectrum. It is indicated that, for selection of 11-pairs orthogonal horizontal for Jakarta site majority of ground -motion are from subduction sources. The paper also highlights maximum direction (RotD100), Arias intensity, and overall requirements as an integrated process in the pairs of ground-motions generation.

Keywords: de-aggregation, 11-pairs of ground motion, RotD100, arias intensity

1 INTRODUCTION

Although theory of performance-based design (PBD) and non-linear time-history analysis (NLTH) has long been developed in America and Europe, application of PBD and NLTH in particular is still relatively new and subject of interest of many Indonesian geotechnical and structural earthquake engineer. The new Indonesian seismic building code (SNI-1726-2019), as adopted from ASCE 7-16, provided alternative of NLTH for particular building structures to meet certain measurement or predictable performance requirements. The structure performance needs to be identified by evaluating damage of the structure when it is subjected by a design earthquake with a certain return period. Based on SNI 1726-2019, NLTA analysis is requires generation of minimum 11-pairs of seismic ground motions. This paper briefly presents case on generation process of this 11-pairs through selection and modification of ground-motions to satisfy requirements of SNI 8899-2020.

Target response spectral acceleration at ground surface could be referred from seismic building codes specifying its corresponding site class for pairs of ground-motion generation. Apart from this reference, this ground-motions generation is actually an integrated with target response spectral acceleration as the seismic wave propagate from reference base-rock to the ground surface, considering the shear waves velocity profile of the specific site. Therefore, this process would be better to incorporate site-specific response analysis (SSRA) for recommendation of target response spectra at ground surface. Furthermore, for selection of ground-motions at reference base-rock as input to the SSRA, probabilistic seismic hazard analysis (PSHA) involving de-aggregation analysis is needed to identify controlling seismic source ground motions in term of magnitude and epicentral distance associated with the periods of the ground motions as well as its hazard level or return period. This paper presents this integrated process for generation of pairs of ground motions of a site in Jakarta city.

2 TARGET SPECTRA AT BEDROCK

2.1 Probabilistic Seismic Hazard Analysis (PSHA)

To estimate response spectral acceleration at a site Jakarta, site-specific probabilistic seismic hazard analysis (PSHA) and response analysis (SSRA) have been conducted. The PSHA considered source zones and seismicity data within 500 km radius from the site. The PSHA has identified combination of subduction and shallow crustal sources from Java Megathrust, Cimandiri Fault, Sunda Fault, Lembang Fault, shallow, and deep background be considered. The seismicity data has been analyzed for the main shock (independent) data through distance and time-window analysis.

The PSHA methodology considers 3-dimensional seismic source zones. Total probability theorem assuming earthquake magnitudes (M), hypocenter distances (r) as continuous independent random variables that affected the intensity (I), in this case PGA or spectral acceleration, is adopted in this PSHA that implemented in EZ-FRISK computer program [Risk Engineering, Version 7.62, 2011]. The essential components of the PSHA should consist of seismic source zoning, earthquake recurrence, ground motion model, and logic tree formulation. **Error! Reference source not found.** 1 shows seismic source zones and seismicity data for Jakarta site adopted for the PSHA.

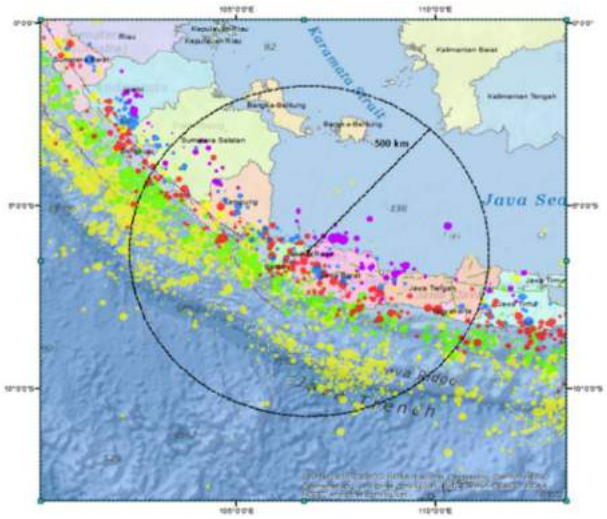

Fig. 1. Seismotectonic of Jakarta Radius 500 km.

2.2 Uniform Hazard Spectra (UHS)

Uniform Hazard Spectrum is developed for a given hazard level resulted from PSHA (for a given probability of exceedance).

Two hazard levels were calculated, that is representing 50% probability of exceedance (PE) in 30 years (43 years earthquake return period) and 2 % PE in 50 years (2,475 years earthquake return period) ground motions at reference base-rock with Vs=760 m/s (S_{BC}) of Jakarta site as presented in Fig. 2.

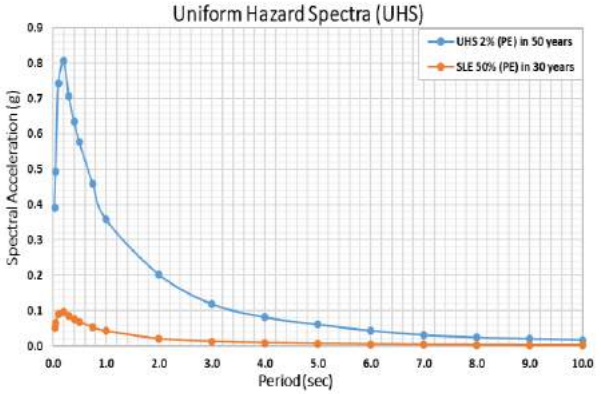

Fig. 2. Uniform Hazard Spectra at Jakarta Site.

2.3 Hazard Curve

Hazard curves result of seismic hazard analysis are show hazard curves with each seismic source contribution to the seismic hazard at certain period of interest. Fig. 3 shows that hazard curve for period T=7.0 second provides total hazard of annual frequency of exceedence and spectral acceleration at Jakarta site.

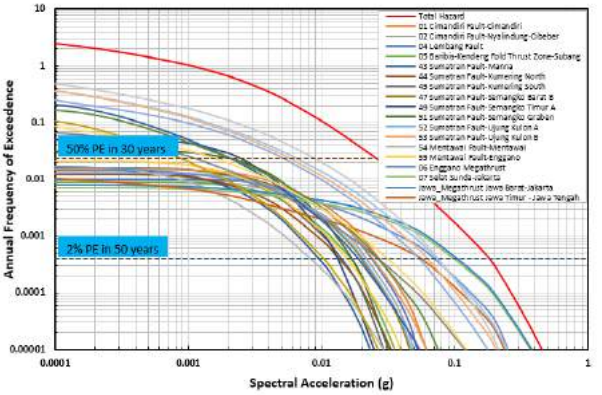

Fig. 3. Hazard Curve for T=7.0 sec at Jakarta Site.

2.4 Directionality Factor

To accomodate the maximum response, the spectra should be scaled by factor to increase the target spectra at bedrock. The scale factor is

1.1 for periods less than or equal to 0.2 s, 1.3 for a period of 1.0 s, and 1.5 for periods greater than or equal to 5.0 s, unless it can be shown that other scale factors more closely represent the maximum response, in the horizontal plane, to the geometric mean of the horizontal components. No factor is multiplied to the PGA value and scale factors between these periods should be obtained by linear interpolation.

2.5 Bedrock Risk-Targeted Ground-Motion (RTGM)

The analysis developed risk-targeted ground motion (RTGM) is based on MCE_R defined as 1% probability of collapse of the building in 50 years. The C_{RS} and C_{R1} values have been calculated used integrated hazard spectra combined with fragility building, meanwhile for period $T \geq 1.0$ the C_R value taken as C_{R1} , for period of $T \leq 0.2$ the C_R value taken as C_{RS} , for period of T between 0.2 – 1.0 sec the value of C_R used linear interpolation and for T=PGA the C_R value taken as 1.0. MCE_R target spectra are obtained by multiplying MCE with C_R values for each period of interest.

3 SSRA AND SURFACE TARGET SPECTRA

Ground response analyses are used to predict ground surface motions for development of design spectra, to evaluate dynamic stresses and strains and to determine the earthquake-induced forces that can lead to instability of earth and earth-retaining structures. The propagation of stress waves through the earth to the top of bedrock beneath a particular site is influenced by the soil lie above the bedrock. The influence of local soil conditions on the nature of earthquake damage by strong ground motion has been recognizes for many years. The rock-based earthquake motions can be amplified at soil layers and will be cause severe structural damages at ground surface.

Response spectra at bedrock should be modified to provide ground surface response. There are two methods usually used to determine response at ground surface, firstly multiply with the amplification factor F_a and F_v for S_s and S_1 respectively and second through wave propagation using site specific response analysis method.

Method 1 relatively simple to use while method 2 we need to have an extra effort to conduct waves propagation procedures. Through waves propagation process, the local site effect has to be considered in earthquake resistant design and must be accounted for on a case-by-case basis. This condition usually develops of one or more design ground motion that reflect certain levels of strong motion amplitude, frequency content, and duration that a structure or facility at a particular site should be design. In addition, shear waves velocity Vs=760 m/s should also determine as reference of bedrock layers.

The seismic wave propagate from base-rock to ground surface was conducted by using Computer Program NERA (Non-linear Earthquake Response Analysis, Bardet dan Tobita, 2001). Shear wave propagates vertically in a one-dimensional layered system, in which the soil layers are assumed to be horizontally homogeneous, infinite horizontal extent, and subjected only to horizontal motion from base-rock. Sengara & Komerdevi, 2020 have been conducted site-specific response at Jakarta site and provide recommendation response spectrum at ground surface for Jakarta as shown in Fig. 4.

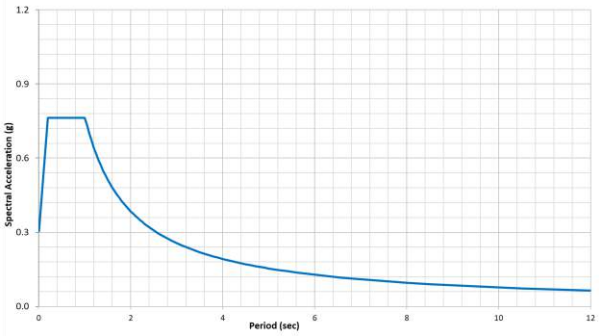

Fig. 4. Recommendation of Response Spectrum Target at Ground Surface for Jakarta Site.

4 SELECTION AND SCALING OF GROUND MOTION

4.1 De-aggregation Hazard

De-aggregation as integrated process of the PSHA illustrates the properties of ground motions that meet or exceed a given intensity at a particular location (mathematically, the probability distribution of properties such as earthquake magnitude and distance, conditional on exceedance of some ground motion intensity

level). Error! Reference source not found. shows chart bar distribution magnitude and distance that have contribution to the sesimic hazard at T=7.0 second of MCE. The height of the bars indicates the percentage contribution to exceedance of a given intensity level from of earthquakes from a particular magnitude and distance (indicated by the coordinates of the horizontal axes) and ε (indicated by the color of the bar). It is indicated that total hazard at T=7.0 second dominated by megathrust and benioff with magnitude 7.0 – 8.5 and distance 150 – 250 km.

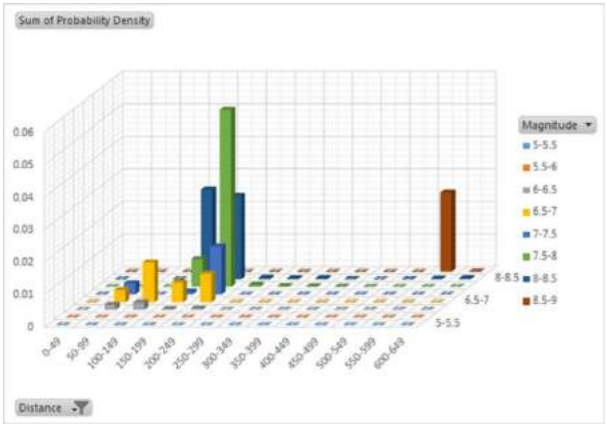

Fig. 5. Deaggregation Hazard for T=7 sec.

4.2 *Period of Scaling*

The upper-bound period of spectrum has accordingly been raised from 1.5T to 2.0T, where T is redefined as the *maximum* fundamental period of the building (i.e. the maximum of the fundamental periods in both translational directions and the fundamental torsional period). is made for consistency with the similar 90% mass requirement in the Modal Response Spectrum Analysis procedure.

The period of building is around 7.0 second, meaning that spectral scaling is within the range of period 0.2 x 7.0 sec = 1.4 second and 1.5 x 7.0 sec = 10.4 second. This period range of scaling is applied on response spectra modification.

4.3 *Ground Motion Selection*

Ground motion selection for building is associated with the de-aggregation as resulted from PSHA and presented in section 4.1, based on the contribution of earthquake to the hazard. The selection should consider the source mechanism, magnitude, soil condition, usable frequency of the ground motion, period/frequency sampling, and site-to-source distance. Eleven (11) pairs of ground motion are selected for the building, consisting of 4 (four) ground motions from shallow crustal sources within contribution 27.3% and 7 (seven) ground motions from subduction source within contribution 72.7% to the hazard curve. The selected ground motions are listed in Table 1.

4.3.1 *Ground Motion Catalog*

The open sources of ground-motion catalog include databases that could be downloaded from the Consortium of Organizations for Strong Motion Observation Systems (COSMOS) Virtual Data Center website (www.cosmos-eq.org), the Pacific Earthquake Engineering Research (PEER) Center Strong Motion Database website (https://ngawest2.berkeley.edu), and the U.S. National Center for Engineering Strong Motion Data (NCESMD) website (http://www.strongmotioncenter.org) etc. For this study the shallow crustal sources are downloaded for PEER NGA-West2 and also for subduction sources from NGA-Sub.

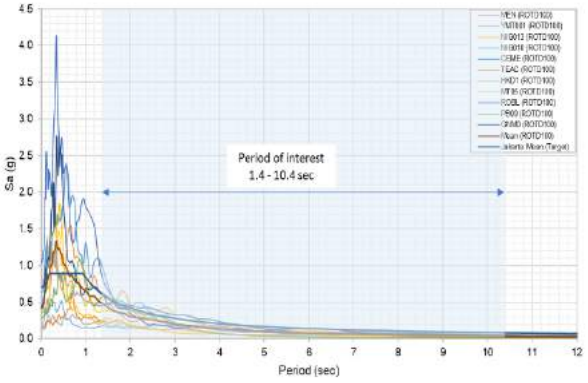

Fig. 6. Selected and Scaling 11-pairs of Ground Motions (Shallow Crustal & Subduction) at Jakarta Site.

Table 1. Eleven (11) Original Ground Motion Catalog

No	Event	Station	Title	RSN	Date	Mw	dRup (km)	Mechanism
1	Loma Prieta	Foster City - Menhaden	MEN	760	Wed Oct/18/1989 12:05 AM	6.93	45.58	Shallow Crustal
2	Iwate	YMT001	YMT001	5744	Fri Jun/13/2008 11:43 PM	6.90	77.06	
3	Niigata, Japan	NIG013	NIG013	4203	Sat Oct/23/2004 08:56 AM	6.63	40.59	
4	Chuetsu-oki	NIG010	NIG010	5256	Mon Jul/16/2007 10:13 AM	6.80	49.19	

No	Event	Station	Title	RSN	Date	Mw	dRup (km)	Mechanism
5	South.Peru	ARICA CEMENTERIO	CEME	6001021	Sat Jun/23/2001 08:33 PM	8.41	204.9	
6	Michoacan, Mexico	TEACALCO	TEAC	3001963	Thu Sep/19/1985 01:17 PM	7.99	180.54	
7	Tokachi-oki	OIWAKE	HKD1	4028605	Thu Sep/25/2003 07:50 PM	8.29	137.79	
8	Coastal.Chile	MT05	MT05	6002253	Wed Sep/16/2015 10:54 PM	8.31	169.62	Subduction
9	2844986	ROBL	ROBL	6001801	Sat Feb/27/2010 06:34 AM	8.81	141.99	
10	Iquique	PB09	PB09	6001383	Sat Jan/04/2014 11:46 PM	8.15	191.53	
11	Tohoku	TAKASAKI	GNM0	4000842	Thu Nov/03/2011 05:46 AM	9.12	160.94	

4.3.2 *Maximum Direction*

The term maximum direction (RotD100) is used to refer to the spectral response acceleration (Sa) of a bidirectional system subjected to two components of a ground motion record, measured along the direction that gives the maximum response, Hanchem et al. (2010).

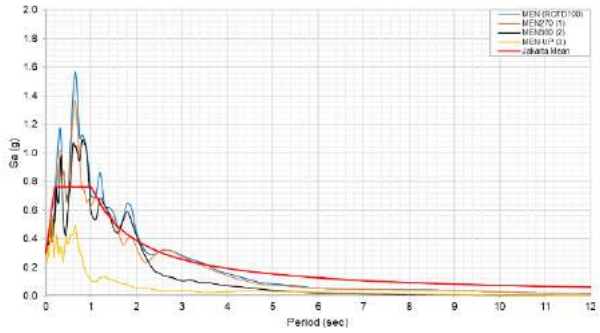

Fig. 7. RotD100 and Set of Triplet Spectra for Loma Prieta Earthquake, RSN 760.

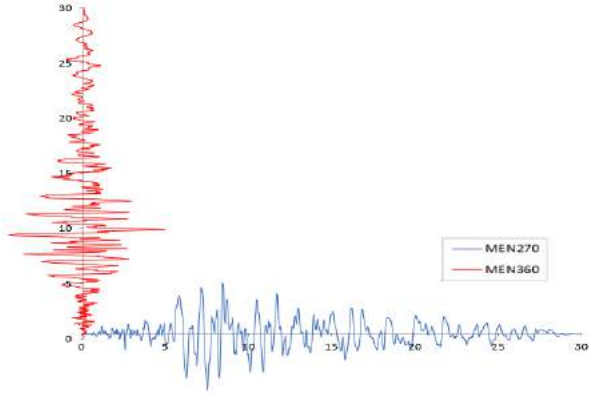

Fig. 8. Pairs of Original Ground Motion of Loma Prieta Earthquake, RSN 760.

Following ASCE 7-16 Chapter 21, it is mentioned that the probabilistic spectral response accelerations shall be taken as the spectral response accelerations in the direction of maximum horizontal response represented by a 5 percent damped acceleration response spectrum that is expected to achieve a 1 percent probability of collapse within a 50-year period, correspons to MCE_R (Risk-Targeted Maximum Considered Earthquake). Fig. 9 provides illustration on the maximum direction (RotD100) of case ground-motion record of Loma Prieta Earthquake.

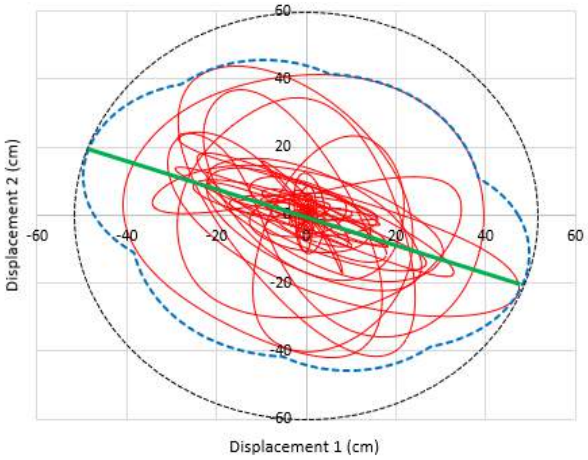

Fig. 9. RotD100 (Max direction) for Loma Prieta Earthquake, RSN 760.

5 SPECTRAL MATCHING AND GROUND-MOTION GENERATION PROCESS

5.1 Spectral Matching

Method of matching is conducted by iterative process using RSP-Match procedures developed by Linda Al Atik and Norman Abrahamson (2010). Results of the spectral matching is shown in Fig. 9, indicating the mean value (average) of 11 ground motions at maximum direction (RotD100) that have been matched to the target spectra or this method called mean matching method.

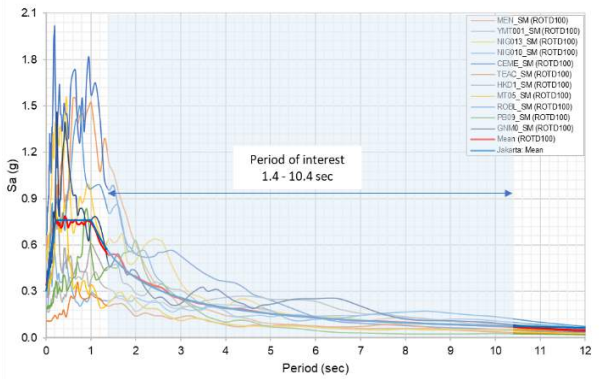

Fig. 9. Mean Spectral Matching of 11 selected Ground-Motion for Jakarta site

Even though mean spectral matching preserves the peak and valley, characteristic period, and energy content of each record compared to tight matching, but when the variation of spectra is very significant the tight matching spectra could be chosen. Therefore, tight matching spectra technique is adopted in this process. **Error! Reference source not found.** 10 shows tight spectral matching with target spectra exceeds 110% as ASCE 7-16 requirement. This tight matching relatively close to recommended spectra provide by Sengara and Komerdevi (2020) as shown in Fig. 11.

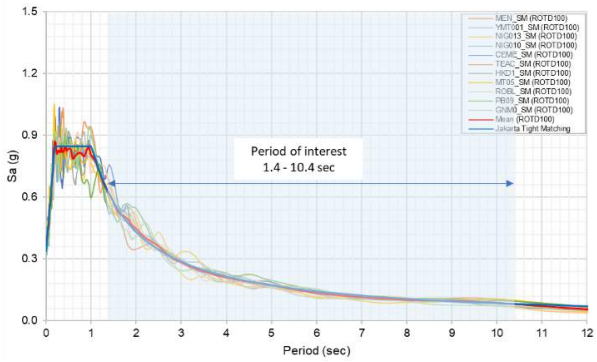

Fig. 10. Tight Spectral Matching of 11 Selected Ground Motion for Jakarta Site.

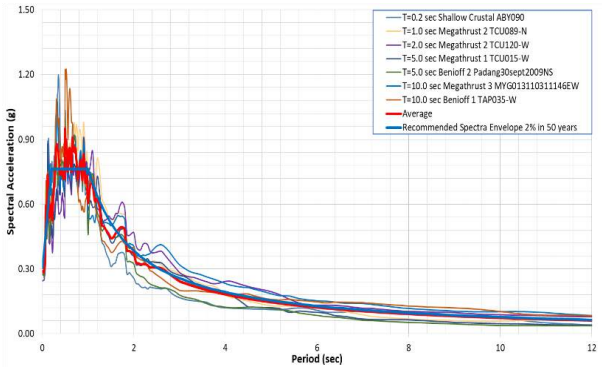

Fig. 11. Spectral Matching of 7 Ground Motion for Jakarta Site (Sengara & Komerdevi, 2020)

5.2 Arias Intensity

One of the requirements of matching criteria is the arias intensity from the original and matching relatively not much different. Fig. 12 shows the arias intensity for the original and matched spectra (mean & tight) for Loma Prieta Earthquake Station Foster City (MEN-RSN 760)

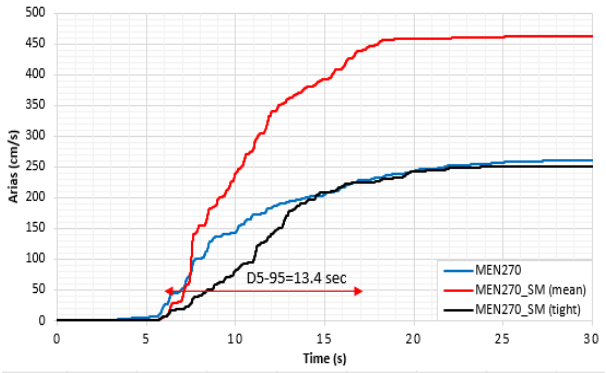

Fig. 12. Arias Intensity for Loma Prieta Earthquake, RSN 760.

5.3 Ground Motion Generation

As per SNI-1726-2019, NLTH of a building structure requires 11-pairs of ground-motion time-history generated at the ground surface. These ground motions have different combinations of moment magnitude, distance, amplitude, and duration. Fig. 13 shows comparison of original seed motion and spectrally matched time-history adopting mean and tight matching procedures.

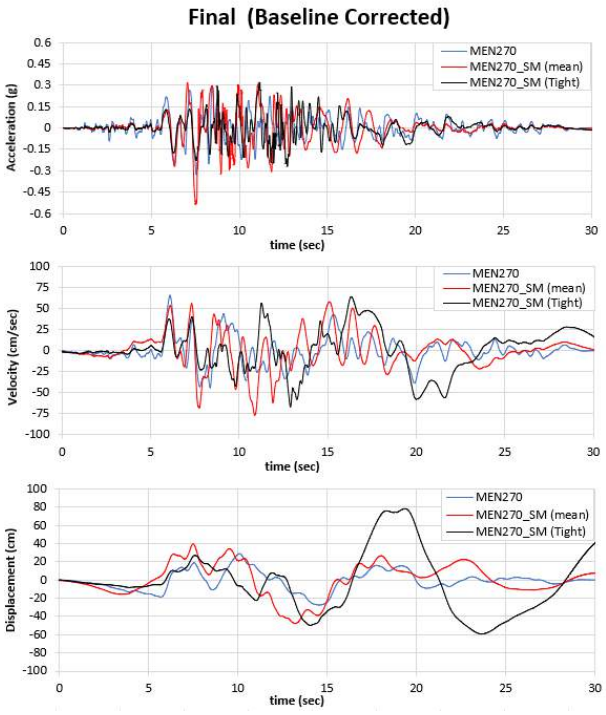

Fig. 13. Spectral original and matched record of Loma Prieta Earthquake, Station MEN270

6 CONCLUDING REMARKS

1. PSHA and SSRA have been conducted as an integrated process for generation of 11-pairs of ground-motions with identification of mainly subduction ground-motions hazard for Jakarta.
2. The ground motion scaling of the response spectrum has been made within period range of 0.2 T – 1.5 T (where T = the natural period of the structure).
3. The selection of ground motions has considered de-aggregation analysis, based on the contribution of each earthquake source. 4-pairs of ground motion from shallow crustal sources (27.3% contribution) and 7-pairs from Subduction sources (72.7% contribution) to hazard curve.
4. The ground motion modification process has adopted tight matching technique, resulted in more consistent arias intensity and shape of ground motion time history compared to mean matching.
5. Tight Spectral Matching technique has been chosen and applied for the 11-pairs ground-motions generation.
6. Maximum direction ground-motions requirements have been particularly considered

ACKNOWLEDGEMENTS

Authors appreciate numerous input and support provided by Mahmoud Hachem, Ph.D, discussion and input by Dr. Ramin Golesorkhi from California and Prof. Indrajati Sidi are also appreciated.

REFERENCES

American Society of Civil Engineers Standards, ASCE SEI-7-10. 2010. Minimum Design Loads for Buildings and Other Structures. *Structural Engineering Institute ASCE*. Virginia, USA.

American Society of Civil Engineers Standards, ASCE SEI-7-16. 2016. Minimum Design Loads for Buildings and Other Structures. *Structural Engineering Institute ASCE*. Virginia, USA.

Bardet J.P., Tobita T. 2001. *NERA, A Computer Program for Nonlinear Earthquake Site Response Analyses of layered Soil Deposits*. University of Southern California.

Walker Martin et. al. 2010. From Recording to Time History Analysis: A Primer on Maximum Direction Ground Motion. *SEAOC 2010 Convention Proceedings.*

NEHRP Recommended Seismic Provisions for New Buildings and Other Structures Volume I: Part 1 Provisions, Part 2 Commentary FEMA P-1050-1/2015 Edition, Building Seismic Safety Council. Washington D.C.

Pacific Earthquake Engineering Research Center. 2010. *Tall Building Initiative Guidelines for Performance Based Seismic Design of Tall Buildings*. Report N0. 2010/5.

Risk Engineering. 2011. *EZ-FRISK (*Software for in-depth Seismic Hazard Analysis) User's Manual. *Risk Engineering Inc*. Golden: Colorado, USA.

Sengara & Komerdevi. 2020. Site-Specific Response Analysis (SSRA) and pairs of ground motions time-history generation of a site in Jakarta. *4th International Conference on Earthquake Engineering and Disaster Mitigation* (4thICEEDM).

Sengara, IW., Irsyam M., Sidi, I.D., Mulia, A., Asrurifak, M. Hutabarat, D., and Partono, W. 2019. New 2019 Risk-Targeted Ground Motions for Spectral Design Criteria in Indonesian Seismic Building Code. *4th International Conference on Earthquake Engineering and Disaster Mitigation* (4thICEEDM).

Sengara, IW. 2009. Development of Earthquake Scenario for Three Different Sites within City of Jakarta. *Earthquake Geotechnical Engineering Satellite Conference XVIIth International Conference on Soil Mechanics & Geotechnical Engineering*. Alexandria, Egypt.

Sengara, IW., and Jayasaputra, U. 2010. Study of Empirical Correlations to Estimate Shear Wave Velocity based on MASW, Seismic Downhole, and Soil Investigation Data, Research Report. *Geotechnical Engineering Laboratory*. Inter

University Center for Engineering Science, Institut Teknologi Bandung.

Sengara, IW., Sumiartha, P., Handayani, G., and Yulman, M.A. 2012. *Report on Probabilistic Seismic Hazard and Site-Specifiv Response Analysis to Derive Seismic Design Criteria for Signature Tower – Jakarta, a Report submitted to PT. Grahamas Adisentosa*. PT Georeka Indonesia.

Stewart, J.P., Archuleta, R.J., and Power, M.S. 2008. *Earthquake Spectra, The Professional Journal of the* Earthquake Engineering Research Institute. *Special Issue on the Next Generation Attenuation Project*. Vol. 24, Number 1.

SNI-1726-2019. 2019. *Tata Cara Perencanaan Ketahanan Gempa untuk Struktur Bangunan Gedung dan Non Gedung.* Badan Standarisasi Nasional.

SNI-8899-2020. 2020. *Tata Cara Pemilihan dan Modifikasi Gerak Tanah Permukaan untuk Perencanaan Gedung Tahan Gempa*. Badan Standarisasi Nasional.

Youngs, R. R., Chiou, S. J., Silva, W. J., Humphrey, J. R. 1997. Strong Ground Motion Attenuation Relationship for Subduction Zone Earthquake. *Bulletin of Seismological Society of America* Vol. 68, No. 1.

Zhao, John X., Jian Zhang, Akihiro Asano, Yuki Ohno, Taishi Oouchi, Toshimasa Takahashi, Hiroshi Ogawa, Koijiro Irikura, Hong K. Thio, Paul G. Sommerville, Yasuhiro Fukushima, and Yoshimitsu Fukushima. 2006. Attenuation Relations of Strong ground Motion in Japan Using Site Classification Based on Predominant Period. *Bulletin of the Seismological Society of America* 96(3): 898-913.

Flexible Rockfall Barriers: Proposed Design Method and Indonesian Case Study

Rivai Sargawi
Geomandiri Adhi Pratama

Matteo Lelli
Maccaferri Malaysia

David Saputra
Maccaferri Indonesia

ABSTRACT: Several things in life are out of our control, for example, natural disasters. As climate change worsens, the frequency of rockfalls increases due to changes in temperature and extreme rainfalls that destabilize slopes. Rockfall events can bring about massive impacts including loss of lives, the least of which is the destruction of properties affecting access and transportation which, in turn, affect the economy as well. This paper describes some solutions to mitigate the effects of rockfall events and protect not only the properties but also lives. This work focuses on flexible rockfall barriers and proposes a design method according to the recently revised Italian design guideline UNI 11211-4:2018. A case study follows, showcasing one of Indonesia's first steps in rockfall protection, a flexible rockfall barrier with an energy absorption capacity of 3,000 kJ recently installed in West Java.

Keywords: rockfall, barrier, protection

1 INTRODUCTION

Rockfall barriers are commonly used to provide rockfall protection along roads, railways, in open-pit mines, for infrastructures and job sites to protect valuable assets and human lives. Rockfall barriers can be classified as passive mitigation systems because they do not affect the source of rockfall events, but they simply arrest the rock masses trajectories reducing their falling velocity and thus energy. Other rockfall passive mitigation systems include debris flow barriers, embankments, and attenuators. The purpose of this paper is to introduce the most comprehensive design method for rockfall barriers that suits Indonesia's geological condition and can be used by engineers in Indonesia.

Generally, for very high energy impacts, rockfall embankments are suggested, while flexible barriers are generally used events with medium-high energy levels (up to 9,000-10,000 kJ), thanks to their capacity to deform (Fig. 1).

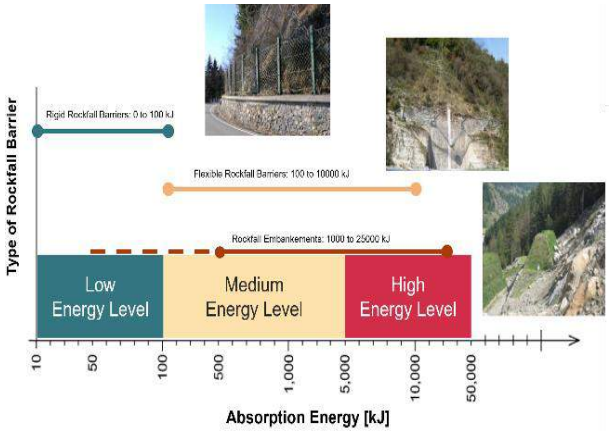

Fig. 1. Rockfall Barriers Classification based on Impact Energy.

The capacity to elongate and deform of the barrier, allows to increase the time required to arrest the block and consequently to reduce the forces acting on the barrier itself (Eqn. 1).

$$F = m \, \Delta v / \Delta t \quad (1)$$

Where F is the force acting against the fence at the moment of impact, m is the mass of the block, v is the velocity of the block, and Δt is the time required to arrest the block.

In agreement with the European Assessment Document (EAD) 340059-00-0106, subsequently referred to in this article as EAD and formerly known as ETAG 027, a rockfall barrier is a "kit" made up of a number of components, which must be able to stop an impacting block having certain energy. The kit is composed by (Fig. 2):

1. Interception structure: made up of principal net and optional additional layer.
2. Support structure: made up of metallic posts (for example, tubular or other sections) and base plates.
3. Connection components: may consist of metallic ropes, wires and/or bars of different types, junctions, wire rope grips, energy dissipating devices (elements which are able to dissipate energy and/or allow a controlled displacement when activated.

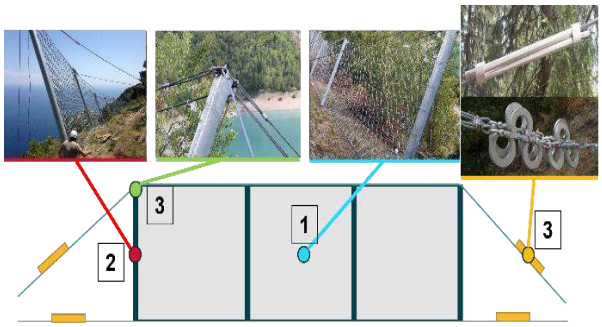

Fig. 2. Rockfall Barriers Components.

According to the EAD, the barrier foundation system is not considered part of the kit.

Due to the difficulties and uncertainties in modelling the dynamics of a rockfall event impacting a complex structure made up of several heterogeneous components, it is generally accepted that the performance of rockfall barriers, when impacted by rockfall events, is assessed through full-scale tests carried out per EAD (former ETAG 027) or other equivalent guidelines. Since full-scale crash tests are not able to describe the barrier behaviour for all the real impact conditions, the test must be considered as an index test. Therefore, the rated energy capacity of the fence must be considered nominal, Brunet et al. (2012). To study the real behaviour and define the technological limits of the barriers, some manufacturers perform full-scale crash tests, according to EAD or ETAG027, modifying some of the requirements described in the guideline. For example, tests with only 2 functional modules, or with multiple impacts, or impact on the posts, etc., have been carried out. Unfortunately, these tests are extremely costly, and it is almost impossible to simulate all the potential configurations that may happen in real cases. For the above reasons, in 2012 the Italian Standard Organization (UNI – Ente Nazionale di Unificazione) issued the UNI 11211-4:2012 standard, which describes the methodology to design passive rockfall fences using a Limit State Design (LSD) approach. Later in 2018, UNI issued a new version of the mentioned standard: the UNI 11211-4:2018, which supersedes the previous one.

2 EAD340059-00-0106 (FORMER ETAG 027)

To evaluate the performance of rockfall barriers and to be able to compare their behaviour, the European Organization for Technical Approval (EOTA) issued, in 2008, the ETAG 027 guideline for testing and assessment of the performance of rockfall protection kits with maximum energy absorption capacity above 100 kJ.

In 2018, EAD 340059-00-0106 superseded the ETAG 027 and standardized the detailed procedure to carry out full-scale crash tests on rockfall kits. EAD defines:

1. Shape, minimum dimensions, and density of the impacting block.
2. Dimension of the tested barrier: it must have at least 3 functional modules (3 spans).
3. Minimum impact velocity of the block: not lower than 25 m/s (approx. 90 km/h).
4. The test field has to be able to accelerate the impacting block to the minimum impact velocity; it can be either on a vertical or inclined slope.
5. Two tests be performed: the first one involving an impact at the barrier Maximum Energy Level (MEL), the second one consists in two subsequent impacts at the Serviceability Energy Level (SEL = 1/3 of

the MEL) of the tested barrier. These two tests must be carried out on 2 different barriers A and B, having the same geometrical and mechanical characteristics.

Fig. 3. Full-Scale Crash Test on A Flexible Rockfall Barrier.

For the kit to pass the MEL test (Fig.3), the barrier A must stop the block with MEL without the block touching the ground before the barrier reaches its maximum elongation. After the MEL test is completed, the kit is subjected to the SEL test. Two subsequent impacts are required for the SEL test, each with an energy equal to one third of the MEL. No repairs are allowed between the two consecutive tests. Moreover, the second impact can be carried out only if the residual height of the barrier, previously crashed by the first SEL impact, is at least the 70% of the nominal height of the tested fence (before the impact). During the second SEL impact the barrier simply has to withstand the falling block.

During the crash test the following parameters/performance are measured:

1. Maximum dynamic elongation of the interception screen (Fig. 4).
2. Residual height (h_R): minimum distance between the lower and the upper longitudinal cables, measured orthogonally to the reference slope after the test and without removing the block from the interception structure. The h_R is expressed as a certain percentage of the nominal height of the barrier (h_N), which is the distance between the upper longitudinal cable and the connection line between the base of the posts, before the impact, and measured perpendicular to the reference slope (Fig. 5).
3. Forces applied on the anchoring systems.
4. Photos and description of the damages occurred in the rockfall barrier.

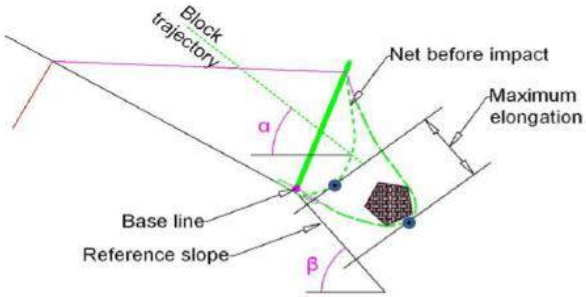

Fig. 4. Maximum Elongation of the Interception Screen After Crash Test.

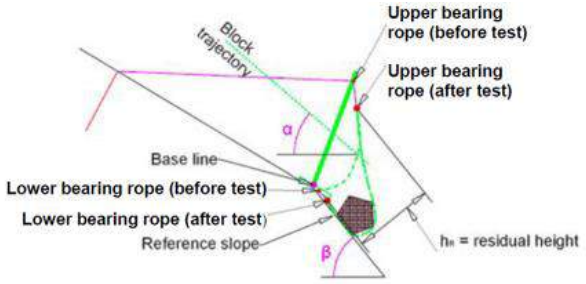

Fig. 5. Residual Height of the Barrier After Crash Test.

EAD classifies the barriers in three categories based on the residual height after MEL impact: when $hR \geq 50\%\ hN$, the fence is classified in Category A; if $30\%\ hN < hR < 50\%\ hN$ the barrier is in Category B; and if $hR \leq 30\%\ hN$ the barrier is in Category C.

3 PROPOSED DESIGN METHOD ACCORDING TO UNI11211-4:2018

At the base of passive rockfall protection with barriers, rockfall simulations should be carried out to identify define the trajectories of the potentially unstable blocks along the slope. The simulations aim to define the statistical distribution of energy, velocity, height of the bounces, and endpoints of the falling rocks. The input data necessary for the rockfall trajectories analysis are generally geo-mechanical surveys, to characterize the unstable slope areas and the number and the dimension of the potential falling blocks; geological surveys, to identify the different types of soils present on the slope; and finally, topography surveys, to identify the

geometry of the study area and the exact location of the unstable rocks.

Rockfall simulations are generally performed with the aid of commercial software such as RocFall, CRSP, Rock falls 3D, which may use different calculation approaches. For instance, Lumped Mass Analysis (LMA) has been used extensively. For a lumped mass model, the normal coefficient of restitution R_n (a parameter that depends on the material property of the ground) and tangential coefficient of friction resistance R_t (an experimental parameter that depends on the slope material and the vegetation). Moreover, the rock is considered a dimensionless point mass. Nowadays, new methods have been implemented to offer a more realistic behaviour of the falling blocks. For example, the Rigid Body Impact Mechanics (RBIM) model introduces the effect of the size and shape of the rock and its interaction with the slope. It uses the soil material parameters R_n, R_t, dynamic friction coefficient (μ: tangent of the friction angle, obtained with experimental data), and the rolling friction, Chai et al. (2013).

According to the UNI 11211-4:2018, the design of a rockfall barrier can be done considering an Ultimate Limit State (MEL) or a Serviceability Limit State (SEL) approach. In both cases, the Limit State Design (LSD) approach introduces some partial coefficients: load coefficients, which increase the unfavourable actions acting on the barrier, and reduction coefficients, which reduce the resistance of the structure.

The equation at the base of this new design approach is:

$$E_{sd} < E_{barrier} / \gamma_E \quad (2)$$

where E_{sd} is the design energy level developed by the block; $E_{barrier}$ is the energy capacity absorption of the barrier, as measured during the crash test carried out according to EAD (MEL or SEL); γ_E is a safety coefficient to be applied, equal to 1.2 in case of design following a MEL approach and equal to 1.0 in case of SEL approach. E_{sd} can be defined with the classic equation of kinetic energy:

$$E_{sd} = 1/2 \times m_d \times V_d^2 \quad (3)$$

The spin effect of the falling rock can be neglected because this generally contributes only 10-15% of the total kinetic energy; therefore, it can be compensated by the introduced partial safety coefficients. In Equation 3, m_d is the design mass of the block; V_d is the design velocity of the block; m_d and V_d are expressed respectively as:

$$m_d = Vol_b \times \gamma \times \gamma m \quad (4)$$

$$V_d = Vt \times \gamma F \quad (5)$$

In Eqn. 4, Vol_b is the volume of the design block; γ is the unit weight of the rock; γ_m is an amplification expressed as:

$$\gamma_m = \gamma_{VolF1} \times \gamma_\psi \quad (6)$$

where γ_ψ is a coefficient related to the uncertainties on the unit weight of the rock (generally equal to 1.0); γ_{VolF1} is a safety coefficient depending on the reliability of the rock volume estimation and equal to 1.02 in case of availability of accurate surveys, or equal to 1.1 in case of no site-specific surveys.

In Eqn. 5, V_t is the velocity resulting from rockfall trajectories analysis and taken as the 95th percentile of the normal distribution of velocities provided as output in the rockfall trajectories analysis; γF is expressed as:

$$\gamma F = \gamma TR \times \gamma DP \quad (7)$$

γ_{Tr} is a safety coefficient depending on the reliability of the simulation which is equal to 1.02 if ground restitution coefficients (R_n, R_t) are derived from back analysis or equal to 1.10 if restitution coefficients are taken from bibliography. γ_{Dp} is a safety coefficient introduced to reflect the quality of the topographic survey used in the rockfall trajectories analysis and equal to 1.02 if a good quality topographic survey is available and equal to 1.10 if a low-medium quality topographic survey is used instead.

UNI 11211-4:2018 also guides the choice of the height of the barrier to be selected: the total interception height of the barrier in the expected point of impact should be greater, with a certain factor of safety, than the falling rock trajectory height:

$$h_{tot} \geq h_d + f_{min} \quad (8)$$

where h_{tot} is the interception height of the barrier at the point of impact; h_d is the design interception height defined as per Eqn. 9, and f_{min} is a minimum freeboard. The freeboard is to be taken at the highest value between 0.5m or the radius of the design impacting block.

$$h_d = h_t \times g_F \quad (9)$$

where h_t is the trajectory height resulting from rockfall trajectories analysis and generally taken as the 95th percentile of the normal distribution of heights provided as output in the rockfall trajectories analysis; g_F is expressed as per Eqn. 7.

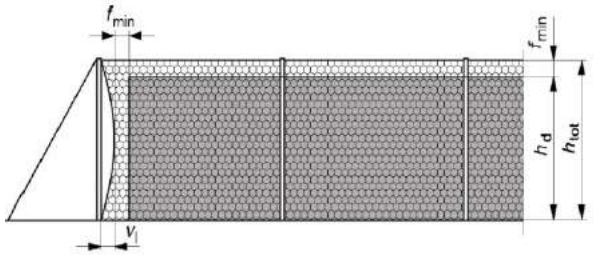

Fig. 6. Total Interception Height (Htot) of the Rockfall Barrier as Defined in UNI11211-4:2018.

UNI11211-4:2018 also prescribes the minimum distance (d_A) between the barrier and the asset to be protected:

$$dA = d_{barrier} \times \gamma D \quad (10)$$

where $d_{barrier}$ is the maximum deformation of the barrier kit measured during the full-scale crash test according to EAD. $d_{barrier}$ has to be taken equal to the maximum deformation during MEL or SEL test depending on whether the rockfall protection kit is designed to withstand a MEL or a SEL impact. g_D is a partial safety factor equal to 1.3.

4 INDONESIAN CASE STUDY

The Ministry of Public Works and Public Housing through PJN 2 PPK 2.5 West Java carried out the construction of a national road that connects Bandung and South Cianjur. The purpose of road construction is to establish better traffic and to improve the economy in the southern part of West Java.

A rockfall hazard was discovered along Bts. Bandung/Cianjur – Naringgul – Cidaun Road due to weathered conditions of the rock slope that endangers the lives of the road users. Thus, a solution to prevent the hazard was needed and should be obtained by considering the impact of the rockfall potential.

The key points to be considered in choosing the suitable solution and/or material for this project include:

1. The forces of falling rock
2. The capacity of the material to dissipate the forces
3. Impacted zones

The designated material had to withstand an estimated rockfall of 10 tons mass from 30m height and 4m^2 of volume.

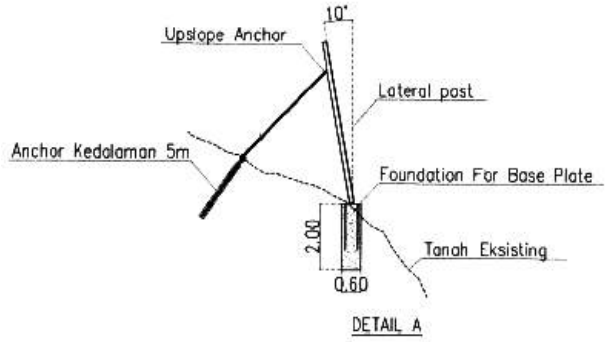

Fig. 7. Typical Section of the Rockfall Barrier.

To comply with the requirements of enduring the estimated falling rocks, a rockfall barrier (Maccaferri - model RB 3000) was selected as the solution to dissipate the energy of falling rocks of up to 3,000 kJ with 6 meters height and 25 meters total length.

The interception structure is made of ring nets as the principal and additional layer of double-twisted steel wires with smaller openings that enable it to catch smaller rocks as well. The ring nets and steel wires are coated with Galfan (ZnAl5% - Class A) for corrosion protection.

To withstand the large energy impact, the system is held in place with an array of support structures and connection components. These include steel posts, T-FAST (spiral rope anchor), concrete foundations, and an energy-dissipating device to absorb most of the energy from the rockfall.

Fig. 8. The Installed Rockfall Barrier Protecting the Infrastructure Below.

5 CONCLUSIONS

The need to expand our living space and the supporting infrastructure means it is unavoidable that we have to deal with potential rockfall events. The uncertainties and their potential impact on the livelihood and economy are large enough to warrant good prevention measures. Through this paper, the Authors have explained the definitions, tests, and a proposed design method for flexible rockfall barriers used as a passive protection method.

The full-scale test procedure described based on the prescription of EAD 340059-00-0106 is a very useful tool for Engineers and project owners to evaluate the performance of rockfall barriers in terms of maximum energy absorption capacity, maximum deformations, and forces transferred to the foundations. Combined with the design method presented, it allows for better research and the development of more effective rockfall barriers. The proposed design method based on UNI11211-4:2018 from Italy is general enough to be applied globally. Until Indonesia has its own design guidelines for rockfall barriers, this design method should be considered and observed.

REFERENCES

Brunet G., Giacchetti G., Grimod A., 2013. Rockfall Barrier Behavior Under Multiple Impact Events. *64th Highway Geology Symposium*, September 9-12, 2013. New Hampshire, USA.

Cerro, M, Giacchetti, G, Lelli, M, Grimod, A & Arul, A. 2016. ETAG certified rockfall barriers — new design approach according to UNI 11211:4/2012. *APSSIM 2016: Proceedings of the First Asia Pacific Slope Stability in Mining Conference*: 443-456. Perth: Australian Centre for Geomechanics.

ETAG 027. *Guideline for European Technical Approval of Falling Rock Protection Kits*. Brussels. www.eota.be.

EAD 340059-00-0106. 2018. *Falling Rock Protection Kits*.

UNI 11211-4. 2018. *Rockfall Protective Measures – Part 4*: *Definitive and Executive Design*.

Analysis of Wedge Failure Characteristic and Early Warning System in Open-Pit Mining from the Point of View of Slope Stability Radar Data

Irvan Rahmawan
Geotechncial Engineer – PT GroundProbe Indonesia

La Ode M. Shaleh
Senior Geotechnical Engineer – PT GroundProbe Indonesia

Rachmat Hamid Musa
Global Practice Lead, Remote Monitoring – PT GroundProbe Indonesia

ABSTRAK: Proses pergerakan massa lereng batuan dasar sangat tergantung pada orientasi diskontinuitas struktur dalam massa batuan. Bahaya terkait biasanya ditentukan oleh orientasi struktur dan mekanisme terkait kegagalan lereng yang salah satunya ialah longsoran baji. Paper ini akan membahas mengenai perilaku dan karakteristik longsor baji yang terjadi pada beberapa tambang terbuka ditinjau dari pemantauan lereng menggunakan *Slope Stability Radar* (SSR). Data geologi dan parameter geoteknik di lapangan diperoleh dari insinyur geoteknik lapangan dari masing-masing dimana data diperoleh. Perilaku lereng yang dianalisis adalah bagaimana respon lereng ketika akan terjadi longsor, dan karakteristik longsor yang dianalisis berdasarkan data deformasi, kecepatan, invers kecepatan, dan waktu menuju longsor (*warning time*). Rekomendasi operasional umum untuk pemantauan lereng yang efektif dan sistem peringatan dini dapat diaplikasikan untuk tambang dengan karakteristik struktur yang serupa di kemudian hari.

Kata Kunci: longsor baji, tambang terbuka, slope stability radar

ABSTRACT: Slope failure in the open pit mostly dependent on the orientations of structural discontinuities within the rock mass. The associated hazards are usually determined by the orientation of the structure and the mechanisms associated with slope failure, one of which is wedge failures. This paper will discuss the behaviour and characteristics of wedge failures that occur in several open pit mines in terms of slope monitoring using the Slope Stability Radar (SSR). Geological data and geotechnical parameters are acquired from site geotechnical engineers on each sample data was taken. The analysis of slope behaviour is how the response of the slope when a failure will occur, and the analysis of failure characteristics based by deformation data, velocity, inverse velocity, and time to failure (warning time). General operational recommendations for effective slope monitoring and early warning systems can be applied to mines with similar structural characteristics in the future.

Keywords: wedge failure, open pit mines, slope stability radar

1 INTRODUCTION

Slope instability is one of the most challenging problem in mining activity. There are a lot of things that may lead to slope instability occurrence such as slope design or slope geometry, geological structure, and also external factors such as rain event, blasting activity, etc. By the time the slope instability couldn't be resolved, then it may lead to the next stage, which is slope failure. Therefore, detecting slope deformation is very important aspect in the field of geotechnical engineering, especially in active mining area, considering the risks and mitigation to prevent any damage to employees and equipments.

Varnes (1978) defined a landslide as a downward movement and outward movement of slope forming materials which are affected by gravity. The landslide itself may be divided into four types based on its slippery plane, which is plane failure, wedge failure, toppling failure, and circular failure, Hoek and Bray (1981). Plane failure is a failure which occurred

when the rock mass moves downward the slope along its slippery plane Wedge failure is a slope failure that happen on the cross section of discontinuities over the structural area and in result the failure shape like a wedge. Toppling failure is a slope failure which happen when the rock mass fail and move through the air instead of its slippery plane. Circular failure is a slope failure that happen on the soft rock or highly weathered rock.

From these 4 types of slope failures, one of the most common failure that we may have seen in mining activity is wedge failure. Considering its high frequency occurrences, it is very important for us to learn characteristics of this wedge failure, so in the future we have a reference to face this wedge failure challenge. This research will discuss about the characteristic of a wedge failure by using the data from Slope Stability Radar (SSR) GroundProbe. Furthermore, this research will also discuss about the early warning system for wedge failure, using back analysis result from 15 cases of wedge failure, and provide new insights of precursor deformation leading to wedge failure in-particular.

2 METHODOLOGY

The research has been performed by using structural and systematic approach, which in general the stages are explained by flowchart below on Fig. 1.

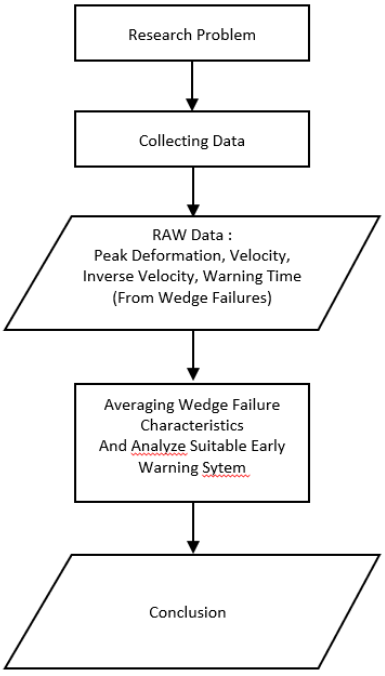

Fig 1. Research Methodology.

This paper will focus on using data from slope stability radar (SSR) GroundProbe XT-version. Slope stability radar has been arguably the most accurate instrument to detect slope deformation and standard procedure for active mining nowadays. Slope stability radar calculate deformation by using interferometry method (measuring different phases between the first signal data acquisition to the next signal data acquisition) with a very high accuracy from a very long range.

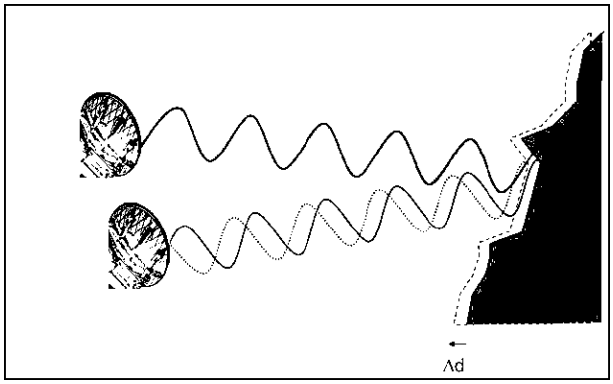

Fig 2. Interferometry method of Slope Stability Radar (SSR) GroundProbe.

After the deformation data is obtained by the radar by using interferometry method, then the data will be used to analyze the slope behavior. As the result, we will get the value of maximum velocity of deformation, minimum inverse velocity, and time to failure.

In order to understand slope behavior, in general Broadbent and Zavodni (1982) defined that there are three advanced stages of the slope movement, these are regressive deformation trend, linear/translation deformation trend, and progressive deformation trend. Meanwhile Mercer (2006) classified slope behavior into 2 stages, those are pre-collapse and post-collapse period.

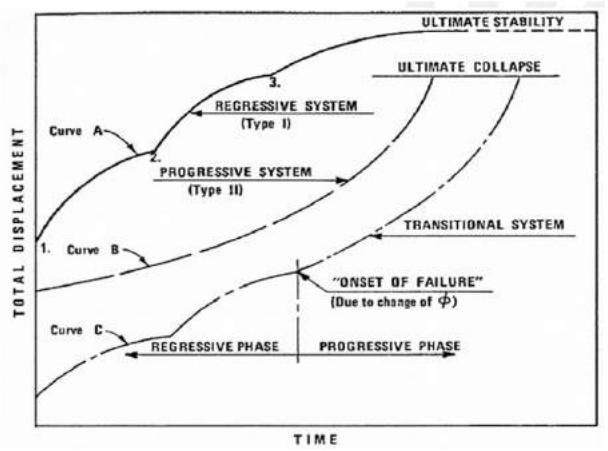

Fig 3. Three Stages of the Slope Movement, Broadbent dan Zavodni (1982).

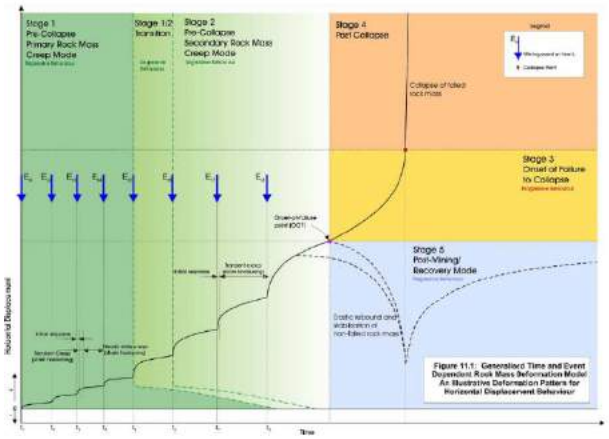

Fig. 4. Two Stages of the Slope Movement, Pre-Collapse and Post-Collapse, Mercer (2006).

3 DISCUSSION

Before we take a step into the main discussion about this research, we need to familiarize nomenclatures that are going to be used on this research. Table 1 below shows nomenclatures that need to understand before we go into further discussion.

Talk about slope failure, there are a lot of factors that may contribute either external factors like rain event, blasting, etc – or internal failure such as slope geometry, material properties, etc. However, displacement and velocity are both most considerable as the main indicators of slope behavior, Lacasse and Nadim (2009). Especially, when we're looking from SSR (Slope Stability Radar) user point of view, things that should be kept in mind is the value of deformation, maximum velocity, and minimum inverse velocity.

Tabel 1. Nomenclatures Related to Slope Deformation in This Research.

Term	Definition
Instability	Deformation movement or slope behavior that does not involve collapse or failure (Mercer, 2006)
Regressive Deformation	Decelerating behavior leading to a stable slope (Zavodni and Broadbent, 1980)
Linear Deformation	Constant acceleration of deformation movement
Progressive Deformation	Accelerating behavior leading to slope failure (Zavodni and Broadbent, 1982)
Failure Pattern	Final Stage of progressive deformation data stated as ambigu along with drop in coherence data
Collapse	Physical, complete overall loss of rock mass integrity and structure (Mercer, 2006)
On-set of Failure	Starting point where the deformation encounters an acceleration in rate of velocity

Tabel 2. SSR Data from 15 Wedge Failures.

Case	Site	Peak Velocity (Vf) mm/h	Min. Inverse Velocity (IV f) h/mm	Time to Failure (Tf)
#1	GP-NRA	13.4	0.074	3:44:00
#2	GP-NRA	13.3	0.075	1:54:00
#3	GP-NRA	20.5	0.049	2:48:00
#4	GP-JNG	6.93	0.169	2:15:00
#5	GP-JNG	312.5	0.003	0:54:00
#6	GP-JNG	8.8	0.11	1:59:00
#7	GP-JNG	17	0.16	2:39:00
#8	GP-KLM	12.5	0.08	3:29:00
#9	GP-REG	23.2	0.043	5:43:11
#10	GP-TLF	12.4	0.08	1:34:00
#11	GP-TLF	12.3	0.081	1:19:00
#12	GP-REG	16.7	0.06	2:58:56
#13	GP-REG	27.7	0.036	9:35:00
#14	GP-REG	19.7	0.051	3:13:00
#15	GP-REG	11.7	0.085	3:06:00

Table 2 summarizes the main characteristics of wedge failure case studies. These were all happens relatively fast, so we may consider them as rapid brittle failure with wedge mechanism, though there's one failure with time to failure up to 9 hours. Regardless this "anomaly", 14 other failures were captured with time of failure less than 5 hours. Even the duration of the progressive deformation trend leading to slope failure events were extremely short, and they were also associated with quite low velocity and inverse velocity.

The first step hypotheses should be tested in order to see how well the data observations that are being compared by using R2 statistical

method. The result is shown on Fig. 4 below, that R2 shows the value of 0.9169 close to 1 (R2= 0~1). This R2 value indicates that the data is well observed and corresponding to each other.

Fifteen slope failures captured by SSR GroundProbe were used in this research. One of cumulative slope deformation relative to the radar, velocity of the deformation, and also inverse velocity with calculation period using VCP 60 minutes. Cumulative slope deformation is the amount of slope deformation that has occurred since the radar was deployed.

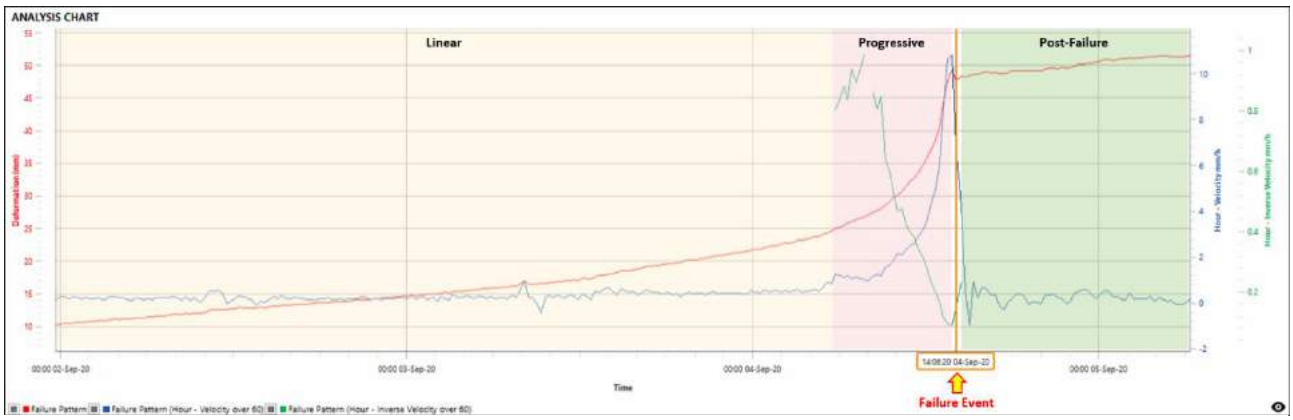

Fig. 6. Deformation to failure event record from the wedge failure case study #14. The first yellow zone is the first stage (linear deformation), the red zone is the second stage (progressive deformation), the orange line indicates the time of failure event, and green zone is the post-failure stage.

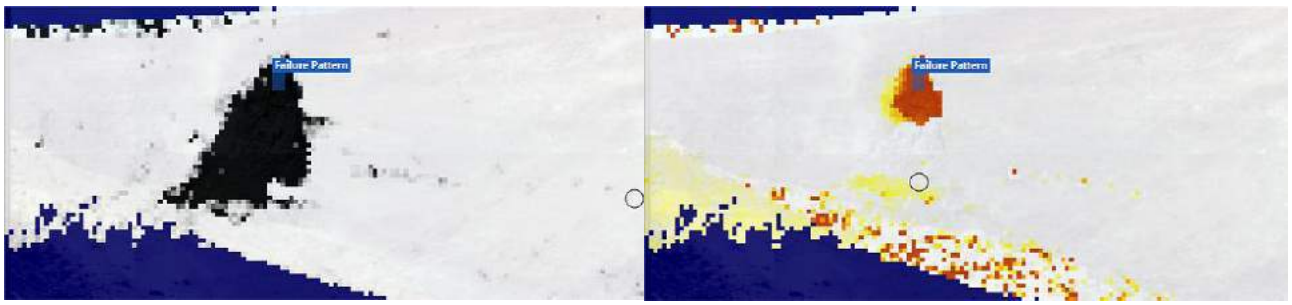

Fig. 7. Coherence image indicates the area of failure (left), meanwhile deformation image indicates the highest deformation occurred within the scan area (right). Coherence image is only available on SSR GroundProbe. Basically, coherence image shows that there's physical changes between the latest data compared to previous data on low coherence area (dark color).

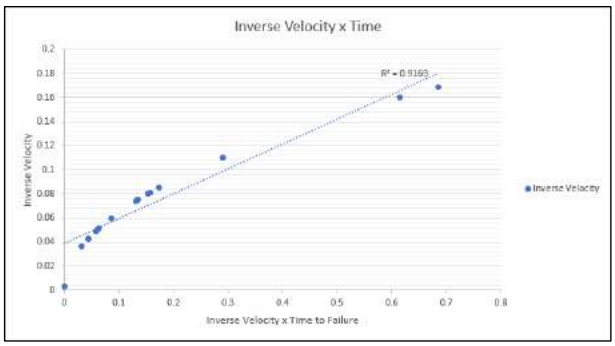

Fig. 5. Statistic R2 from Inverse Velocity and Time to Failure.

The examples is shown on Fig. 5 that present the result of SSR GroundProbe deformation measurements. The graph plot shows the

Velocity is the rate movement of slope deformation which calculated over a given time period, while inverse velocity is an alternative measure of the rate of wall movement, defined as the time it takes the wall to move a certain distance towards or away from the SSR. Equations for velocity and inverse velocity are following below:

$$V = \frac{d2-d1}{t2-t1} = \frac{d2-d1}{Velocity\ Calculation\ Period} \quad (1)$$

$$IV = \frac{1}{Velocity} = \frac{Velocity\ Calculation\ Period}{d2-d1} \quad (2)$$

From the deformation graph, we can define the slope behavior clearly, specifically in this case #14 on Fig. 5. The first stage is linear

deformation trend, where the slope moving within constant velocity relative to the radar.

The second stage is progressive deformation trend, it is the stage where the slope moving within accelerating velocity until the slope reach the peak velocity right before the failure occurred. The first point where the progressive deformation trend started is known as On-set of failure (OOF), Dick et al. (2014). Then, after OOF stated we may get the result of time to failure which is accumulative time from OOF to failure event (total period of progressive deformation trend until failure event).

After all, deformation analysis will get us results all the information related to deformation, peak velocity, minimum inverse velocity, and time to failure from every single failure event as shown on Table 2.

Plot distribution from Fig. 8 explain that wedge failure occurrences were dominated by inverse velocity somewhere in between 0.1 h/mm to 0.05 h/mm. Several anomalies have been observed with the value of inverse velocity below 0.05 h/mm and also more than 0.1 h/mm. These anomalies could be affected by any external factors such as blasting activity, extremely rain event, mining activity, etc – the exact reason is yet unknown.

Similarly, another parameter as main characteristic from failure to be evaluated is peak velocity as shown on Fig. 9. As we may also have seen on table 1, peak velocities on failure were distributed dominantly somewhere between 10 mm/h to 20 mm/h.

Taking a look on the results above, the average of time to failure for wedge failure is considered to be very quick. With range 1 hour to 4 hours, it is very important to setting up the SSR in optimal condition, with scan time optimized to less than 10 minutes at least for a single data acquisition. Thus, in 1 hour period we will get 6 data scans more or less with expectations we can capture precursor movement leading to failure.

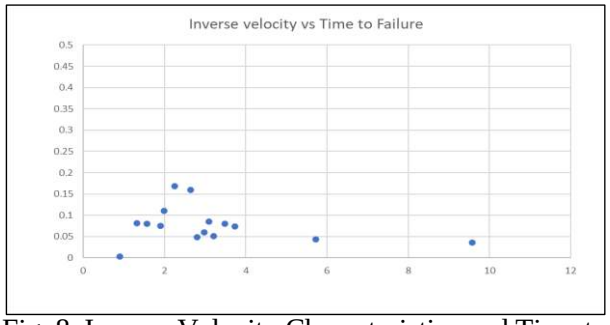

Fig. 8. Inverse Velocity Characteristics and Time to Failure from Fifteen Cases of Wedge Failure.

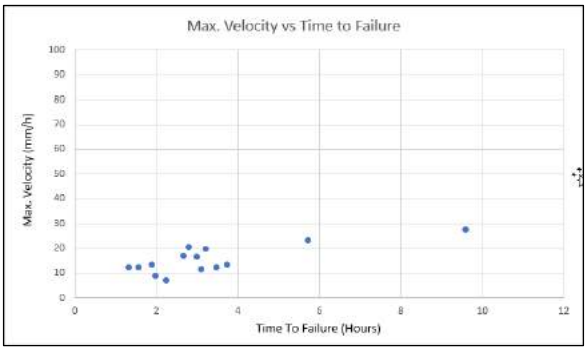

Fig. 9. Peak Velocity Characteristics and Time to Failure from Fifteen Cases of Wedge Failure.

Considering averaging time to failure within the range of 1 hour to 4 hours, setting up alarm for early warning system is very essential to prevent miss collapse. Based on the result of wedge failure characteristics, with the range of minimum inverse velocity 0.1 hr/mm to 0.05 hr/mm, and maximum velocity in the range of 10 mm/h to 20 mm/h, setting up alarm consisting of threshold sequences may be divided as 3 level below:

1. Alarm Level 1: Designed for the first stage of early warning system, alarm may be set by using velocity slightly above the velocity of linear trend (i.e., if we have a linear deformation trend consisting of velocity around 2 mm/hr, then we may set up the alarm in 2.5 mm/hr.
2. Alarm Level 2: The purpose of alarm level 2 is to get notified by the time alarm level 1 has been passed. Alarm level 2 will have a larger value than alarm level 1, so increasing velocity will be considered for threshold alarm level 2.
3. Alarm Level 3: This is the most critical alarm and the final stage of hierarchical alarms. Alarm level 3 is designed to give us final alert before collapse. Alarm level 3 may be set by using inverse velocity reaching to minimum value of inverse velocity right before collapse. From the result of this research, wedge failure may be occurred in the range of inverse velocity from 0.1 hr/mm to 0.05 hr/mm. Thus, it may propriate to setting up the inverse velocity alarm slightly above the inverse value on collapse (e.g. inverse threshold set for 0.3 hr/mm for failure that may expected to reach minimum inverse 0.1 hr/mm).

However, before alarming system created, several things should be considered as those may affect the results of radar measurement such as vector loss, scan time, etc. In particular,

early warning system would depend on its calibration based on-site slope characteristics. While the results of back analysis summarize on this research may give us general indications and took a crucial part for comparison to any wedge failure in the future. Also, additional wedge failure in the future need to be collected so this research may be reviewed as more cases collected.

4 CONCLUSION

Considering the frequency of occurrences wedge failure in mining activity, it is very important for us to understand the characteristics of wedge failure so we may prepare its mitigation plan in the future.

From the analysis of fifteen cases wedge failure from SSR GroundProbe monitoring data in various undisclosed open pit mine that have been explained, we get the details of characteristics subject to wedge failure. As the goal of this research is to define the characteristics of wedge failure in open pit mine and appropriate strategy, so this will allow us to have insights and assess the most suitable for early warning system to face wedge failure in open pit mine in the future.

As the results, it was observed that the characteristics of wedge failure as following below:

1. Minimum inverse velocity of wedge failure is dominated between 0.1 hr/mm to 0.05 hr/mm
2. Peak velocity of wedge failure is dominated between 10 mm/h to 20 mm/h.
3. Time to failure of wedge failure is in the range of 1 hour to 4 hours from on-set of failure.
4. Although, some anomalies have been captured out of range above. These may be caused by a lot of factors such as rain event, blasting, mining activity, etc.
5. Early warning system is essential as a part of mitigation plan for wedge failure. Considering time to failure of wedge failure in a very short period, alarming system consisting of threshold sequences will be very appropriate.

ACKNOWLEDGEMENTS

The authors would like to thank GroundProbe for their advance technology SSR that could make this research eventually possible to publish. Our gratitude is also addressed to PT. GroundProbe Indonesia who is funding this research.

REFERENCES

Dick, G.J. 2013. *Development of an Early Warning Time-of-Failure Analysis Methodology for Open Pit Mine Slopes Utilizing the Spatial Distribution of Ground-Based Radar Monitoring Data*. M.A.Sc Thesis. The University of British Columbia. Vancouver, BC.

GroundProbe Pty Ltd. 2012. SSRViewer 5.4 User Manual. Brisbane, Australia.

Hoek, E., Bray, J.W. 1981. Rock Slope Engineering. *Revised 3rd Edition, The Institution of Mining and Metallurgy:* 341-351. London.

Mercer, K.G. 2006. *Investigation Into the Time Dependent Deformation Behaviour and Failure Mechanisms of Unsupported Rock Slopes Based on the Interpretation of Observed Deformation Behaviour*. Ph.D. Thesis. University of Witwatersrand. Johannesburg, South Africa.

Varnes, D.J. 1978. Slope Movement Types and Processes. *Special Report 176: Landslides Analysis and Control: Transportation and Road Research Board:* 11-33. Washington D. C.: National Academy Press.

Zavodni, Z.M., Broadbent, C.D. 1980. Slope Failure Kinematics. *Bulletin, Canadian Institute of Mining:* 69-74.

Comparison of Material Point Method and Finite Element Method for Post-Failure Large Deformation Geotechnical Analysis

Arif Yunando Soen
Civil Engineering Dept. – Parahyangan Catholic University

Ezra Y.S. Tjung
Civil Engineering Dept. – Calvin Institute of Technology

Aswin Lim
Civil Engineering Dept. – Parahyangan Catholic University

ABSTRAK: Saat ini, metode yang umum digunakan untuk menganalisis stabilitas lereng adalah Limit Equilibrium Method (LEM) dan Finite Element Method (FEM). Sebagai metode berbasis gaya, LEM biasanya digunakan untuk menghitung faktor keamanan tanpa mempertimbangkan deformasi. Di lain sisi, FEM yang merupakan standar industry diketahui memiliki ketidak-akuratan dalam menyimulasikan permasalahan deformasi besar akibat distorsi mesh. Maka dari itu, sebuah metode campuran pendekatan Eularian dan Lagrangian bernama Material Point Method (MPM) diperkenalkan untuk menyelesaikan masalah deformasi besar. Dalam implementasinya, metode ini menggunakan material point yang bergerak diatas mesh komputasi. Artikel ini menunjukan perbandingan analisis stabilitas lereng dalam kasus buatan menggunakan FEM dan MPM. Setelah dilakukan simulasi, diketahui bahwa meski analisis FEM dapat menunjukan vektor deformasi setelah keruntuhan, hasil analisis MPM dapat mendemonstrasikan vektor tersebut menjadi gerakan yang sesungguhnya dan menghasilkan geometri tanah setelah runtuh. Simulasi ini juga menunjukan aliran tanah saat longsoran, profil tanah disekitar longsoran, dan distribusi regangan setelah longsor.

Kata Kunci: metode elemen hingga, metode material point, stabilitas lereng

ABSTRACT: Currently, some methods commonly used to analyze slope stability problem are Limit Equilibrium Method (LEM) and Finite Element Method (FEM). As a force-based method, LEM is usually used to estimate the safety factor with no deformation being considered. FEM, a state-of-the-art method, is known to have inaccuracies when simulating large-deformation problem due to mesh distortion. Hence, a hybrid Eularian - Lagrangian approach called Material Point Method (MPM) which utilized moving material points over computational mesh is used to tackle large deformation problems. This article presents a comparison of a hypothetical slope which is analyzed using Finite Element Method (FEM) and Material Point Method (MPM). The simulation shows that while FEM analysis is able to show post-failure displacement vector, MPM analysis can demonstrated those vectors into actual movements and present post-failure geometry. The simulation also shows how landslides affect neighboring soil profile after sliding, post-failure strain distribution, and soil flows during failure.

Keywords: finite element method, material point method, slope stability

Stability Design of Coal Mine Dumping Based on Analysis of Limit Equilibrium Method and Finite Element Method

Nuzulridha Rizki Ramadhani
Universitas Pertamina

Rangga Adiprima Sudisman
Universitas Pertamina

ABSTRAK: Kestabilan lereng dipengaruhi oleh beberapa faktor dan dikuantifikasikan dalam nilai angka keamanan (SF). Perancangan ini bertujuan untuk menyusun stabilitas lereng dan skenario geometri penimbunan secara bertahap pada lereng tanah buangan, studi kasus tambang batubara di Kalimantan Timur. Metode yang digunakan yaitu analisis kesetimbangan batas dengan irisan Spencer dibandingkan dengan analisis elemen hingga dengan diskritisasi segitiga 15 nodal. Hasil analisis menunjukkan selisih perbedaan SF dari kedua metode berkisar antara 0,00% - 5,29% untuk masing-masing tahapan penimbunan, dengan nilai SF diatas 1,2 pada pembebanan statik dan diatas 1,1 pada pembebanan dinamik. Penimbunan terdiri dari enam tahapan dengan tambahan *buttress*. Masing-masing timbunan bersudut 37^o, tinggi 10 meter dan lebar *crest* yang bervariasi, menghasilkan geometri akhir timbunan setinggi 69meter dan sudut 11^o yang dikalkulasikan mampu menampung volume timbunan sebanyak 2.364.575 BCM. Berdasarkan analisis elemen hingga didapatkan pula nilai deformasi penurunan lereng yang bertambah seiring peningkatan timbunan.

Kata Kunci: stabilitas lereng, tanah buangan, metode kestabilan batas, metode elemen hingga

ABSTRACT: Slope stability is governed by several factors and quantified in the safety factor value (SF). This design aims to develop slope stability and geometry scenarios of gradual backfilling at disposal slopes, a case study of coal mines in East Kalimantan. Analysis methods include Limit Equilibrium (LEM) based on Spencer compared to Finite Element (FEM) by discretizing 15 nodal triangles. The difference in SF ranges from 0.00%-5.29% for each stage, with SF greater than 1.2 under static conditions and larger than 1.1 under dynamic conditions. The dumping process consists of six stages with the addition of a buttress. Each embankment is angled 37o, 10 meters high, and has a varying crest width, resulting in a final geometry of 69 meters high and an 11o overall angle, accommodating a fill volume of 2,364,575 BCM. Based on FEM, we also found that the deformation value of slope reduction increases with an increasing embankment.

Keywords: slope stability, soil disposal, limit equilibrium method, finite element method

1 INTRODUCTION

Indonesia has a lot of natural resources, one of which is coal. Based on data released by the World Energy Council (2017), it states that Indonesia ranks 9th in the world with 2.2% of global coal reserves. Most of the national coal production is exported to foreign countries, with an average percentage during 2000-2009 of 74.3%, as stated by Bappenas (2016). It increases state income, but also raises concerns about decreasing coal stocks for domestic energy security.

Most coal mining companies push to increase production even more so that activities can be completed quickly and continuously. Often, mining activities are carried out without the support of design recommendations based on the results of previous geotechnical studies, as well as the process of uncontrolled stockpiling in the disposal area, which is usually a site that is planned to accommodate waste material or unused overburden. This area

is less profitable for the production process but becomes very detrimental if there is instability because it is associated with a potential hazard that does not control workers, production activities, and mining equipment, as well as the implications directly on the economics of the mining project.

2 DESIGN METHOD

2.1 *Soil Stress and Soil Collapse*

The normal stresses in the soil can be resisted by interparticle forces, whereas the shear stress can be resisted by soil particles using forces that emerge from particle contact, as describes by Craig & Soepandji (1991). Porewater pressure rises when the soil is entirely saturated because it helps the soil endure typical stresses.

The idea of the failure criterion for soils, commonly known as the Mohr-Coulomb theory, was introduced by Mohr in 1900, and argues that the collapse of a material is caused by a critical combination of normal and shear stresses illustrated on a linear failure curve. The Hoek-Brown theory, which is based on empirical evidence, can reflect other failure criteria for rock materials. The Hoek-Brown and Mohr-Coulomb equations are compared in Fig. 1.

2.2 *The Safety and Slope Stability Factor*

Slope stability is determined by two factors: resisting forces, or the slope's power to keep it stable, and driving forces, or the force that causes failure or slippage. A safety factor (SF) is required to determine the level of slope stability using the following Eqn. (1):

$$SF = \frac{Resisting\ Forces}{Driving\ Force} = \frac{cA+W\cos\alpha\tan\Phi}{W\sin\alpha} \qquad (1)$$

Where:
SF>1.0 the slope is declared stable.
SF=1.0 the slope is in equilibrium and may experience a landslide if there is a disturbance.
SF<1.0 the slope is considered unstable.

According to Abramsom et al. (2001), slope stability is influenced by a number of factors including technical constraints, site constraints, environmental constraints, time, and cost. Furthermore, according to Hoek and Bray (1981), the slope stability approach can be separated into three avalanche countermeasures: lowering thrust, increasing resistance, and protecting against loose material.

2.3 *LEM and FEM Slope Stability Analysis*

LEM is a well-known and widely used method for assessing slope stability in both translational and rotational landslides. According to Liong & Herman (2012), various researchers have used the slice approach, which involves doing calculations under static equilibrium conditions. Furthermore, assumptions must be established at the outset to determine the geometry of the collapsing plane, as described by Arif (2016).

Furthermore, as described by Hamdan and Pratiwi (2017), FEM is one of the numerical approaches that may be applied to complex slopes and generate representative results. This numerical method divides the region to be investigated into multiple elements by creating mathematical equations from several approach to algebraic equations with the values at the discrete points of the section being evaluated. Discretization, as defined by Wirjosoedirdjo (1986), is the selection of element configurations in the form of separating an object into numerous suitable little objects, which are referred to as finite elements.

2.4 *Analysis with The Slide and Plaxis*

Slide is a two-dimensional software that uses LEM to create SF values. With the probability input parameters, the analysis can be displayed. Based on the iteration results in the weakest plane (global minimum slip surfaces), the value of the SF, landslide area, and information between slices can be determined.

Plaxis is also a two-dimensional and three-dimensional FEM program. Plane strain and axisymmetric are two options for modeling. This program has the advantage of presenting the structure's deformation plane. There are 15 or 6 nodes in different with triangular elements. To get an elastic-plastic deformation evaluation, deformation analysis and plastic calculations are typically utilized. When evaluating pore water dissipation, consolidation might be chosen. The last step is Phi-c reduction to obtain SF, which leads to soil collapse. There is also a dynamic computation if the external load is a moving load, such as an earthquake or an explosion. Deformation, displacement, strain, stress, plastic point, pore pressure, degree of saturation, and water table

are some of the factors that can be determined from interpretation results.

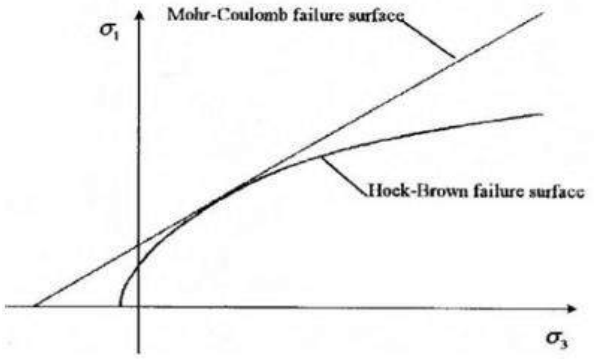

Fig. 1. Comparison of the Hoek-Brown and Mohr-Coulomb, Rockscience (2002).

3 SITE AND SOIL CONDITION

A disposal slope in one of the open-pit mines in East Kalimantan has experienced failure, which is identified by some cracks in the buttress. A geotechnical engineering solution is required to solve that problem. In this study, both the LEM and the FEM are expected to produce slope geometry for the best stockpiling scenario according to the field orientation.

The design form of this case consists of several stages such as: preliminary to identification problem, collection data of topographical situation and the laboratory data, data processing with LEM using Spencer because it considers all aspects in moment equilibrium, moment force, normal force between slices, shear force between slice, and the slope of the relationship and resultant, corresponds to Liong & Herman (2012). The analysis begins with the existing condition and the original design plan with a height of 59 meters.

In this case, the field assumptions are circular collapse, which has been modified to the field conditions. According to Hoek & Bray (1981), embankments of considerable dimensions in the stockpile region will collapse in the form of a circular arc. According to Wyllie and Mah (2004), the geological structural element has little effect on the embankment's stability, but the slope's stability is determined by the embankment's material properties, the slope's dimensions, and the slope's stability groundwater conditions and external influences. The most optimal stockpile scenario is then generated using FEM analysis utilizing plain strain 15 nodes with Phi-c reduction.

3.1 *Soil Data Analysis*

The results of the soil study around the disposal slope, which includes an SPT (Standard Penetration Test) bore log and data processing in the laboratory, are contained in the soil data analysis. The drilling data for the original soil, in this case, had six points (ABE 01, ABE 02, ABE 03, ABE 06, ABE 07, and ABE 08) with a point depth of 15 to 50 meters, based on the collection of a bore log that had been analyzed and categorized. The soil stratification in Fig. 2 is derived via data rectification and correlation with a cross-section on a topographic map. Buttress, embankment material, coal seam, and bedrock as the subgrade are all used in the stockpile area. The groundwater level was then monitored at a depth of 12 meters below the surface, according to the investigation's findings.

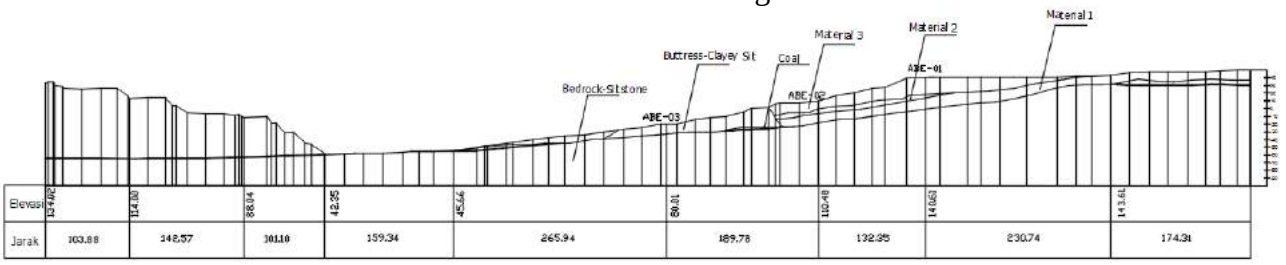

Fig. 2. Soil Stratification.

To get soil parameter values, laboratory analysis is performed. Sieve analysis (particle size and hydrometer analysis) on soil samples ABE 01–ABE 03 and ABE 06–ABE 08 revealed that more than 50% of the soil passed sieve no.200, indicating that the soils are fine-grained. Furthermore, the Atterberg Limit with the LL and PI values of each depth plotted on the Casagrande chart. Based on the result, a description and classification of soil samples in each drill point is obtained, notably non-organic clay with medium to high plasticity (soil types CL, CH, and ML). Apart from the direct shear test, the unconsolidated undrained (UU) Triaxial test also used to calculate cohesion and internal shear angle. In addition, direct shear and uniaxial compression experiments were performed on rocks. The characteristics for an embankment based on undrained shear strength (Su) are calculated using the SPT and Triaxial UU findings, as shown in Eqn. (2):

$$Su\ (kPa) = 4 \times N60 \quad (2)$$

Where N60 is the corrected value from SPT data. Then some additional inputs are needed such as the value of the modulus of elasticity (E) and Poisson's ratio obtained from Triaxial UU, where the value of (E) is used for a structural design using the value of E_{50} which is the value at stress 50%. In the laboratory, the value of (E) is from the Triaxial test stress-strain relationship defined as the secant's modulus obtained from the value $(\sigma 1 - \sigma 3)50/\varepsilon 50$. In addition, the value of (E) is also combined from literature references based on soil type correlation. Based on overall data, soil parameters are used for LEM and FEM following Table 1 and Table 2:

Table 1. Input Data LEM.

	Physical Properties		Total Strength	Effective Strength	
Description	γ (kN/m^3)	γ_{sat} (kN/m^3)	s_u (kPa)	C (kPa)	Φ (°)
Bedrock	20	22	300	-	-
Coal Seam	12.5	13	-	223	55
Buttress	17	17.5	70	-	-
Dump 1	16.5	17	T=50, F=4	-	-
Dump 2	16.5	17	T=120, F=0	-	-
Dump 3	16.5	17	T=50, F=4.78	-	-
New Waste	16.5	17	50	-	-
NewButtess	17	17.5	70	-	-

*Note: T = Top and F = Fdepth

Table 2. Input Data FEM.

Properties	Dumping	Buttress	Bedrock	Coal Seam	Unit
Model	MC	MC	MC	MC	-
Type	Und	Und	Und	Und	-
γ_{dry}	16.5	17	20	12.5	kN/m^3
γ_{sat}	17	17.5	22	13	kN/m^3
Kx	0	0	0	0	m/day
Ky	0	0	0	0	m/day
Eref	10954.02	11198.9	80000	1000	kN/m^2
v	0.35	0.35	0.35	0.35	-
Cref	50	70	300	223	kN/m^2
Φ	0	0	0	55	°
ψ	0	0	0	0	°

*Note: Und = Undrained

3.2 *Loading Condition*

Static loading conditions result from the added weight of heavy equipment, while dynamic loading conditions result from blasting. The static design surcharge is based on a permissible load of 163.78 tons, with the maximum weight distribution of 68.6% on the rear wheels and dispersed along the body of the dump truck, with a vehicle area of 1.995 tons/m^2 equivalent to 19.56 kPa, and a safe distance of 10 meters from the top. In dynamic, a coefficient factor of 0.025g was utilized in the vertical and horizontal axes, calculated according to Eqn. (3):

$$Blasting\ Coef = 0.5 \times Peak\ Acceleration \quad (3)$$

LEM accepts that value immediately, whereas FEM requires an accelerogram curve created by Guler et al. (2011) harmonic wave Eqn. (4):

$$\ddot{U}(t) = \sqrt{\beta . e^{-\alpha . t} . t^{\xi}} . sin\ (2.\pi . f . t) \quad (4)$$

Where: $\alpha = 5.5$, $\beta = 55$, dan $\xi = 12$ (constant - coefficient), f = frequency, and t = blasting time. The f value is set at 7.5 Hz and t at 5s. The curve is created by entering a multiple of 0.01s (5s / 500 steps) into the equation. The value of safety factor to be achieved from static loading is 1.2 and from blasting loading is 1.1. This refers to the Decree of ESDM (2018) No. 1827 K/30/MEM/2018 for the inter-ramp mine slope SF value.

4 RESULTS AND DISCUSSION

The initial analysis was performed on the existing geometry, which proved to be safe under both loading situations; following

analyses were performed on the original geometry, which proved to be unsafe under no-load conditions with SF below 1.2. Modifications to the original geometry are required, as well as the inclusion of a buttress at the slope's toe. The stages are completed in order from the first to the sixth, with the buttress added after the third. In addition to the opposing force against the driving force, the addition of embankment to the preceding stage is also carried out at stage 4. In this scenario, trial and error is used with not-too-steep angles, not-too-long crest widths, and the placement of a buttress as a counterweight to prioritize slope stability. Failure stockpiling is illustrated in Table 3.

In actual situations, the slope of the embankment must have a perimeter drain at its toe to drain runoff, as well as a bund wall at the end of the bench to serve as a safeguard. Furthermore, the addition of embankment soil might alter the breadth of the preceding crest; the width of this embankment's crest is also utilized as heavy equipment transportation lines, thus the width must be changed in accordance with standards such as AASHTO (1973) and ESDM (2018). The minimal width after the next embankment in this case is 24.0975 meters, making it a two-lane road. The final geometry values in Table 4, visualized in Fig. 3, compared with FEM according to Fig. 4 and resulted SF value in Table 5.

Table 3. Examples of the 4th Stockpiling Failure Analysis Results Without Paying Attention to the Geometry Design Parameters.

Consideration on the 4th stage	SF Static	SF Dynamic
-No buttress added.	1.132	1.014
-Steep angle (45º).	1.108	1.005
-The crest width is too long (following the original geometry) even though with the addition of the buttress.	1.143	1.007
-The addition of embankment is not gradual (directly in 20 meters) even though with the addition of buttress.	0.894	0.829

Table 4. Final Geometry.

A	B	C	D	E	F	G	H
Buttress	-49	-30	19	19	37	37	30.437
1	-30	-20	10	29	37	16	30.438
2	-20	-10	10	39	37	15	63.048
3	-10	0	10	49	37	13	30.437
4	0	+10	10	59	37	13	72.439
5	+10	+20	10	69	37	11	110.00

*Note: A=Stockpiling, B=Toe Elevation (m), C=top Elevation (m), D=Height (m), E=Total Height (m), F=Angle (º), G=Total Angle (º), H=Top Width (m)

Table 5. Differences in SF Values and Deformation Change.

Static Condition				
Stockpiling	SF LEM	SF FEM	Deviation (%)	FEM Deformation (cm)
1	1.29	1.262	2.69%	3.99
2	1.29	1.259	2.94%	19.5
3	1.30	1.265	2.92%	23.35
4	1.29	1.256	3.18%	28.84
5	1.22	1.25	2.16%	34.17
6	1.25	1.242	0.81%	181.66
Dynamic Condition				
Stockpiling	SF LEM	SF FEM	Deviation (%)	FEM Deformation (cm)
1	1.12	1.161	2.76%	2.59
2	1.12	1.155	2.25%	4.38
3	1.12	1.191	5.29%	14.4
4	1.13	1.157	2.07%	54.40
5	1.15	1.15	0.00%	65.63
6	1.15	1.144	1.31%	313.16

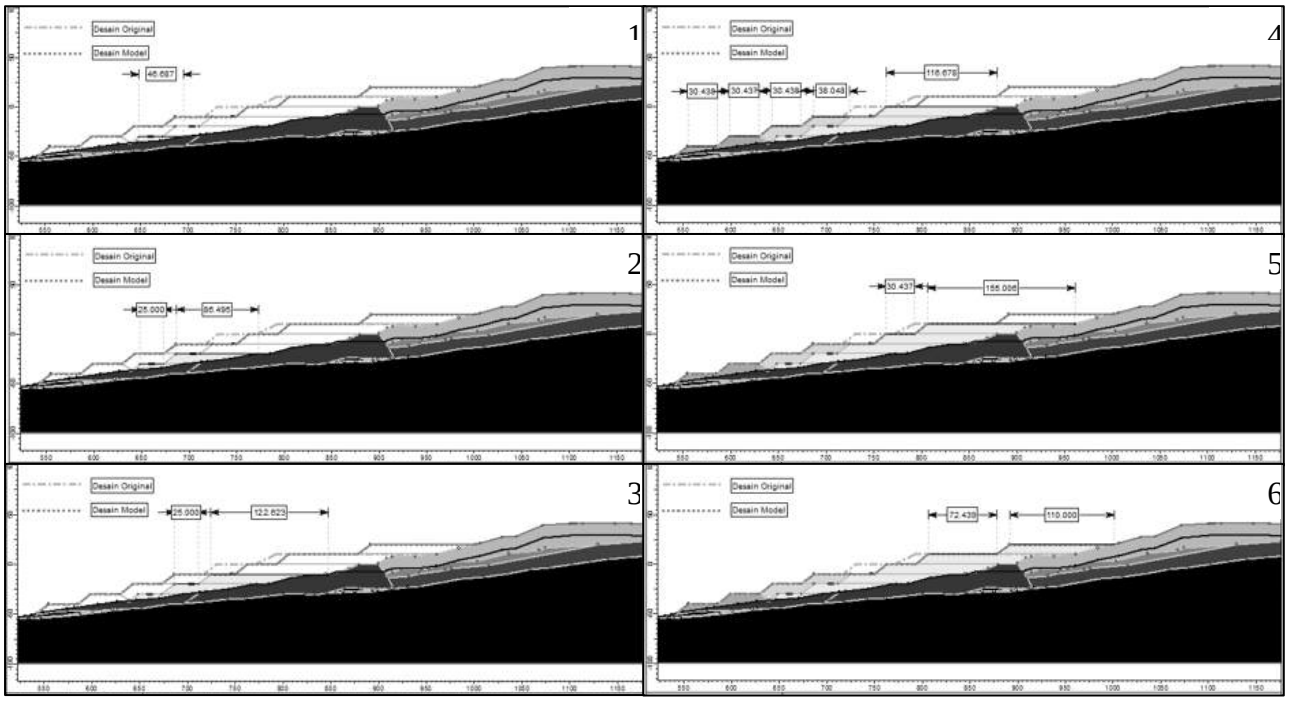

Fig. 3. Geometry Scenario of Stockpiling (1:2500).

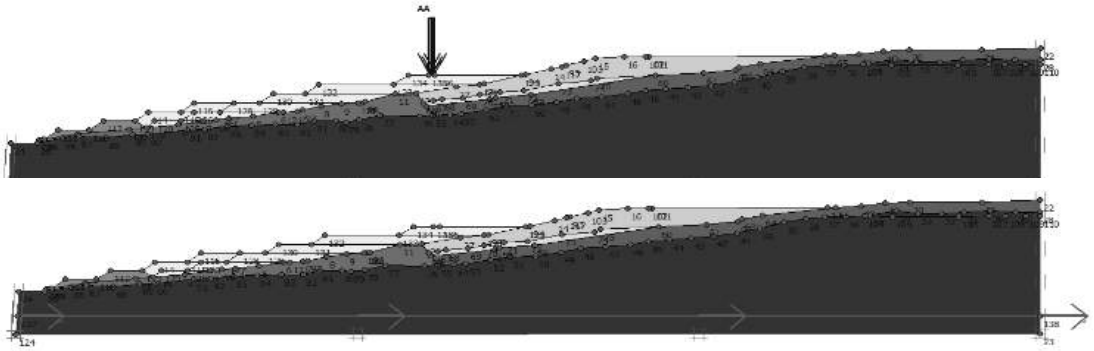

Fig. 4. FEM Model with Static and Dynamic Load.

Based on the findings of both applications, the embankment's SF is nearly same; nevertheless, based on modeling results, the difference in this situation ranges from 0.00%-5.29%. Furthermore, the failure findings from the two applications are identical. FEM also displays the total displacement value, which is the sum of the absolute values of horizontal and vertical displacement. Furthermore, with the addition of an embankment, deformation increases and is inversely related to a decrease in SF value.

Both LEM and FEM can be employed in geotechnical situations based on this. The discrepancy in the resultant SF value is attributable to a variety of reasons, including input differences in calculating the limits based on the application's restrictions and characteristics, differences in computation iterations, and parameter considerations. The volume of the storage capacity is computed using the technique of calculating the volume of a truncated pyramid, yielding a result of 2,364,575 BCM, which is different from the original design of 2,293,538 BCM. As a result, the revised shape created will be able to accommodate the projected overburden discharge.

5 CONCLUSION

The geometrical scenario appropriate for the case study was described in the preceding section, and the results of the analysis using FEM and LEM are very similar. Following that, due to the low permeability of the subgrade and embankment, it takes a long time for the water and air in the pores to escape, or the soil goes

through a dissipation process, and future SF will be higher than current SF since the soil is continuously squeezed and drained. Geotechnical tools such as a piezometer, an inclinometer, and a slope stability radar are essential for monitoring. A blastmate must be erected for general blasting to break up overburden. Then, in order to increase the value of the disposal area, a research on reclamation with revegetation or alternative land use is expected to be conducted.

ACKNOWLEDGEMENTS

We would like to thank Mr. Seto Wahyudi, Ph.D., Mr. Muhammad Addifa Yulman, M.T., and Mrs. Laura Fahmy, S.T. from PT Zekon Indonesia as the company that has allowed the authors to obtain data and studies the problems that occur. We also would like to thank Mr. Wirman Hidayat, M.T., and Mr. Teuku Mahlil, Ph.D. for fruitful discussions as well as their support and encouragement. With all humility, hopefully, it can be useful.

REFERENCES

AASHTO, A. A. 1973. *Way Design Planning.* AASHTO.

Abramsom, L. W., Lee, T. S., Sharma, S., & Boyce, G. M. 2001. *Slope Stability and Stabilization Methods 2nd Edition.* New York: A Wiley-Interscience.

Arif, I. 2016. *Geoteknik Tambang.* Jakarta: PT Gramedia Pustaka Utama.

Bappenas. 2016. *Coal Domestic Market Obligation*.

Craig, R. F., & Soepandji, B. S. 1991. *Soil Mechanic Ed.4.* Jakarta: Erlangga.

ESDM. 2018. *Keputusan Menteri Energi dan Sumber Daya Mineral Republik Indonesia Nomor 1827 K/30/MEM/2018 Tentang Pedoman Pelaksanaan Kaidah Teknik Pertambangan Yang Baik.*

Guler, E., Cicek, E., Demirkan, M. M., & Hamderi, M. 2011. Numerical Analysis of Reinforced Soil Walls with Granular and Cohesive Backfills Under Cyclic Loads. *Bull Earthquake Eng (2012) 10:793-811*, 803.

Hamdan, I. N., & Pratiwi, D. S. 2017. Analisis Stabilitas Lereng dalam Penangana Longsoran di Jalan Tol Cipularang Km. 91+200 dan Km. 92+600 Menggunakan Metode Elemen Hingga (FEM). *Jurnal Rekayasa Hijau No.1 Vol.1 Juli 2017 ISSN 2550-1070*, 103.

Hoek, E., & Bray, J. 1981. *Rock Slope Engineering 3rd Edition.* London: Institution of Mining and Metallurgy.

Liong, I. G., & Herman, D. J. 2012. Analisa Stabilitas Lereng Limit Equilibrium Method vs Finite Element Method. *HATTI-PIT-XVI.* Jakarta.

Rockscience. 2002. *Rockscience*. Retrieved from https://www.rocscience.com/help/rocdata/rocdata/Generalized_Hoek-Brown_Criterion.htm

Wirjosoedirdjo, S. J. 1986. *Dasar-Dasar Metode Elemen Hingga.* Jakarta: Erlangga.

World Energy Council. 2017. Retrieved from https://www.worldenergy.org/

Wyllie, D. C., & Mah, C. W. 2004. *Rock Slope Engineering Civil and Mining 4th Edition.* London: Spon Press.

Analysis of Interface Slope Stability Using Thin Soil Materials in Finite Element Software

Fathiyah Hakim Sagitaningrum
Universiti Teknologi Malaysia

Samira Albati Kamaruddin
Universiti Teknologi Malaysia

Idrus Muhammad Alatas
Institut Sains dan Teknologi Nasional

ABSTRAK: Kelongsoran pada tanah *clayshale* merupakan kasus yang sering terjadi di Indonesia. Selain dikarenakan properti *clayshale*, pelemahan batas antarmuka antara dua tanah dengan kekuatan yang berbeda juga dapat terjadi. Penelitian ini bertujuan untuk mengetahui kondisi kuat geser antarmuka dari *clayshale* berdasarkan kasus kelongsoran di tol Semarang-Bawen. Kondisi antarmuka digambarkan sebagai sebuah material tanah tipis yang berada dalam perbatasan material timbunan dan *clayshale* di bawahnya. Nilai kohesi dan sudut geser pada antarmuka tersebut dicari sampai mendapatkan nilai faktor keamanan kritis. Kemudian, nilai tersebut dicocokkan dengan hasil laboratorium yang sudah dilakukan. Ditemukan bahwa sebagian besar kondisi antarmuka pada laboratorium berada di atas garis kritis faktor keamanan. Hal ini menunjukkan bahwa antarmuka *clayshale* dengan timbunan cukup lemah walaupun nilai sudut gesernya cukup besar. Dari hasil tersebut, dapat disimpulkan bahwa diperlukan kehati-hatian dalam melakukan desain atau analisis apabila melakukan konstruksi pada tanah *clayshale*.

Kata Kunci: clay shale, finite element, kuat geser, antarmuka

ABSTRACT: Landslide in clay shale soil is one of the most occurring cases in Indonesia. Besides the clay shale property, the weak interface between two different strengths of soil was analyzed as the cause of a landslide. This research examined the shear strength condition at the interface of clay shale at a landslide at Semarang-Bawen toll-road. The interface condition was modelled as a thin soil material between the underlying clay shale and its overburden. The interface cohesion and friction angle were determined using iteration from several combinations to find the critical safety factor. Afterwards, the values were compared to laboratory results. It was found that most of the laboratory shear strength was above the critical safety factor line. The results showed that the interface was quite weak although it had great friction angle values. Thus, it could be concluded that caution is needed when designing and analyzing for clay shale interface.

Keywords: clay shale, finite element, shear strength, interface

1 INTRODUCTION

Slope stability had been an important issue in geotechnical engineering. Not only that, the existence of problematic soil such as clay shale also complicates the problems. One of the intriguing failures is the Semarang-Bawen toll road slope failure. As stated by Alatas et al. (2015), the failure was due to the weathering of clay shale and there was an indication that it happened at the interface of clay shale with its overburdened soil.

Clay shale is known to be in between the characterization as soil and rock. Clay shale was sensitive to wetting and drying due to water and air. When faced with this cyclic condition, clay shale would weather and degrade. The weathering would then lead to a degradation of shear strength, Alatas et al. (2016).

Studies were done in understanding the properties of clay shale, however, only several studies specifically discussed the interface behavior of clay shale with other soil. One of the research was done by Pellet and Keshavarz

(2014) which studied the interface between steel and clay shale rock.

As experiments of the interface shear strength were developed, the modeling of this interface shear strength mostly used a simple model of shearing, Frikha and Jellali (2018) or the predetermined interface function. However, these interfaces were usually done on soil-solid interfaces.

In the Semarang-Bawen toll road failure, the interface was between two different soils. Thus, the predetermined and developed finite element analysis might not describe the cohesion and friction angle of the interface.

This research would like to give an overview of using a thin material as the interface of two different strengths of soil. The analysis would also add a prior laboratory test of the interface, which would help to understand the slope failure condition.

2 RESEARCH METHODOLOGY

2.1 *Research Flowchart*

The research summary can be seen in Fig. 1 as follows.

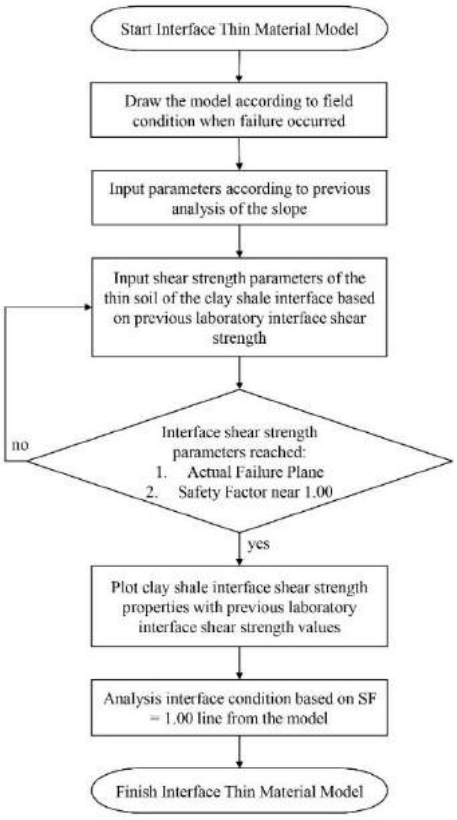

Fig. 1. Research Flowchart for Interface Thin Material Model.

From Fig. 1, it could be seen that first the slope was modeled according to the field condition. The model was adopted from previous research on the same location. Alatas (2017). However, to determine the exact interface shear strength of the clay shale with overburden material, a thin soil material was used instead of the interface function. The thin soil material used the interface direct shear test results which were previously done in the laboratory.

The previous interface direct shear test was conducted on undisturbed clay shale with weathered clay shale and sand combinations. The weathered clay shale (WCS): Sand (S) combinations were divided into: 100% S, 75% S: 25% WCS, 50% S: 50% WCS, 25% S: 75% WCS, and 100% WCS. Throughout the interface direct shear test, water was added to the top of the overburdened soil. It was assumed that the water would seep to the interface. The test was done on different water content conditions of the overburdened soil until its 100% soaked condition.

2.2 *Finite Element Model*

The finite element program used in this research is Plaxis 8.6. The model was based on previous research of the same location, Alatas (2017). The finite element model could be seen in Fig. **2** below.

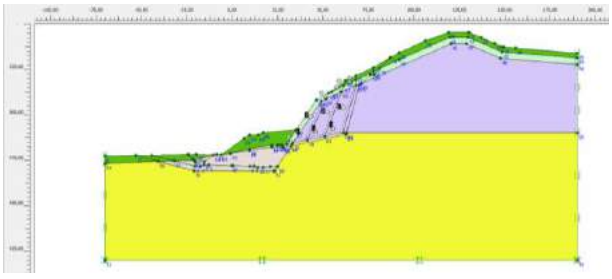

Fig. 2. Plaxis 8.6 Model of Thin Material Model

The thin material was placed under the weathered tuff breccia soil. It was modeled with a height of 1 meter. Whereas the length was from the bottom of the tuff breccia-tuff breccia interface until the silty clay overburden at the feet of the slope.

In the laboratory, tuff breccia was modeled as the weathered clay shale and sand combinations. The model assumed that the clay fraction of tuff breccia was replaced with a low shear strength of clay shale (WCS).

The soils in Plaxis 8.6 were modeled as a Mohr-Coulomb model analysis. The properties for each soil could be seen in Table 1 below. It should be noted that the (*) for the interface cohesion and friction angle would be the combinations used in this study.

Table 1. Material Properties.

Soil Properties	Tuff Breccia	Weathered Tuff Breccia	Silty Clay	Fresh Clay Shale	Interface Clay Shale
Color	Purple	Slight Green	Dark Green	Slight Brown, Dark Yellow	Light Yellow
Unsaturated Unit Weight (kN/m^3)	17	17	15	18	18
Saturated Unit Weight (kN/m^3)	18	18	17	18	18
Elastic Modulus (kN/m^2)	150000	60000	10000	100000	100000
Poisson Ratio	0.25	0.25	0.30	0.30	0.30
Shear Modulus (kN/m^2)	60000	24000	3846	38460	38460
Cohesion (kN/m^2)	100	50	15	250	*
Friction Angle (^{o})	38	30	30	41	*

Lastly, the groundwater table for the slope used the natural groundwater table provided by the previous research, Alatas (2017) which can be seen in Fig. 3 below.

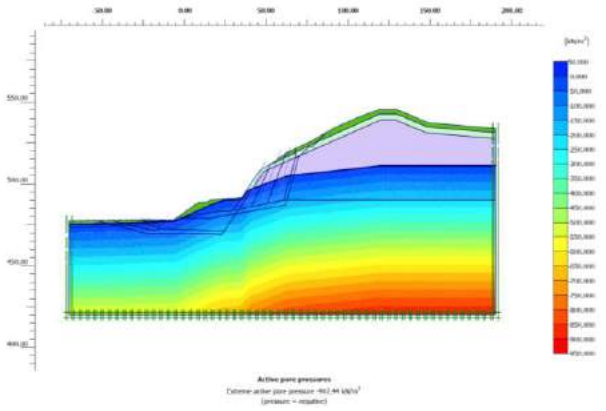

Fig. 3. Groundwater Table Condition of the Slope.

The calculation used the Total Multipliers which determine the slope's condition according to its weight and the Phi-c reduction to determine the Safety Factor for the shear strength combinations of the clay shale interface. According to the previous research, the failure plane was from the interface of tuff breccia with the weathered tuff breccia to the interface of clay shale with the overburdened soil. The close-to-real failure plane can be seen in Fig. 4 below.

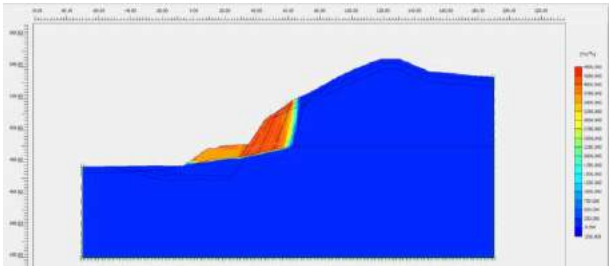

Fig. 4. Failure Plane of the Slope According to the Close-to-Real Condition.

The shear strength parameters of the interface material resulted in a value of Safety Factor = 1.00 were recorded. The shear strength parameter values were plotted with the interface direct shear test results. Thus, the interface conditions which resulted in shearing could be predicted.

3 RESULTS AND ANALYSIS

3.1 *Cohesion and Friction Angle Results at the Thin Material Interface*

From the results of the estimated safety factor procedure, the break-off point of 1.010 was taken. Thus, the results of around eight points could be seen in Table 2 below.

Table 2. Cohesion, Friction Angle, and Safety Factor at the Clay Shale Interface Layer.

Combination	Cohesion (kPa)	Friction Angle (^{o})	Safety Factor
1	15	20	1.062
2	13	21	1.056
3	10.5	22	1.053
4	7	23	1.061
5	3.5	24	1.029
6	3	25	1.029
7	2	26	1.043
8	1	26.5	1.006

It can be seen that with a higher interface friction angle, the result would give lower interface cohesion. Although the target was to have the same failure plane throughout the entire sequence, it was found that from

combination 5, the failure plane shifted, which can be seen in Fig. 5 below.

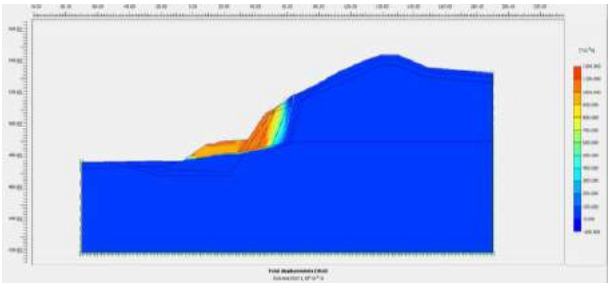

Fig. 5. Shifting Failure Plane.

As seen in the image above, although the failure plane shifted, the entire soil mass that failed was still the same as in the field. Thus, it is still reasonable and acceptable.

3.2 *Thin Soil Material Plot Against Laboratory Results*

To understand the slope condition at failure, the interface laboratory shear strength parameters were plotted against this study's results. The interface laboratory results were plotted as points, whereas this study's results were plotted as a line. The graph can be seen in Fig. 6 below.

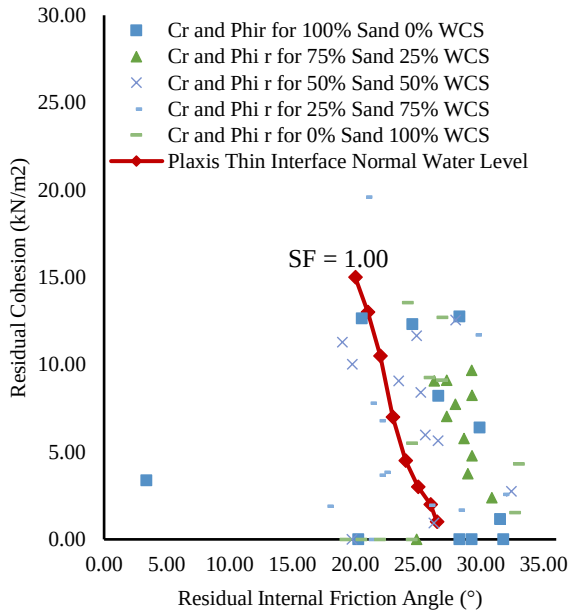

Fig. 6. Interface Cohesion and Friction Angle for Thin Material Model and Laboratory Results.

From Fig. 6, it could be seen that the line from this study represented the safety line. Data under the safety factor line would indicate failure. Thus, the laboratory results under this line would indicate the interface condition at failure. Whereas data above the line indicated the situation where the slope was safe.

From the plot, several conditions of the degree of saturation at the interface of clay shale with its overburdened material initiate failure. The value could be seen in Table 3 below.

Table 3. Interface and Overburden Condition at Failure

Overburden Combinations	Degree of Saturations
100% Sand	12.28%, 17%, 100%
75% S: 25% WCS	100%
50% S: 50% WCS	28.98%, 35.48%, 42.31%, 100%
25% S: 75% WCS	27.71%, 33.74%, 37.39%, 40.80%, 43.55%, 47.22%, 100%
100% WCS	51.78%, 54.95%, 58.1%, 100%

From the results, the weathered clay shale had a great role in determining the failure at the interface. It was known that weathered clay shale had a lower initial shear strength due to the deteriorating condition of the material. The weathering clay shale itself was known to be a significant factor in a landslide. Thus, the results were acceptable, Oktaviani et al. (2018), Sadisun et al. (2005), Alatas et al. (2015).

The thin material model could describe the phenomenon adequately. However, the limitation of cohesion of 1 kPa in the program and the limit set for this study might limit the safety factor line on the graph. The materials in this study were set as a controlled variable, whereas only the thin clay shale interface material was used as the free variable. Thus, there may be several other conditions that were not depicted in this study. Further investigations may be needed to have a throughout analysis for the model in the future.

4 CONCLUSIONS

The study aims to give an overview of the usage of thin soil material to model a soil interface on a slope stability case with a finite element method software. The slope was modeled based on Semarang-Bawen toll road failure which happened at the interface between clay shale and its overburdened material. All of the soil properties were based on previous research of the same slope, with only the thin soil material model as the free variable. Using the failure plane as this study's criterion, several interface shear strength parameters could be acquired.

The results gave eight combination points with high friction angle values customized according to the laboratory results. It was known that all of the overburden combinations of sand and weathered clay shale had several degrees of saturation that fell under the safety line from this study. The laboratory results and finite element model results were in line with the low shear strength of weathered clay shale. The low shear strength gave a lower interface shear strength. Thus, it resulted in a lower safety factor for the slope.

Lastly, this study was limited to the controlled variable of the soil materials and the software limitation. Thus, there may be some conditions that could not be depicted in this study. Further investigations might be needed to confirm the model assumptions and the laboratory results.

ACKNOWLEDGEMENTS

The authors would like to thank Prof. Ramli Nazir and Prof. Budi Susilo Soepandji for the input for this research.

DAFTAR PUSTAKA - REFERENCES

Alatas, I. M. 2017. *Kesan Luluhawa terhadap Kekuatan Ricih Syal Lempung dalam Penentuan Parameter Kestabilan Cerun*. Malaysia: Universiti Teknologi Malaysia.

Alatas, I. M., Kamaruddin, S.A., Nazir, R. & Irysam, M. 2016. Effect of Weathering on Disintegration and Shear Strength Reduction of Clay Shale. *Jurnal Teknologi* 78: 93-99.

Alatas, I. M., Kamaruddin, S.A., Nazir, R., Irysam, M. & Himawan, A. 2015. Shear Strength Degradation of Semarang Bawen Clay Shale due to Weathering Process. *Jurnal Teknologi* 77: 109-118.

Frikha, W. & Jellali, B. 2018. Numerical and Experimental Studies of Sand-Clay Interface. Ground Improvement and Earth Structure. Sustainable Civil Infrastuctures.

Oktaviani, R., Rahardjo, P. P. & Sadisun, I. A. 2018. Landslides Induced by Slaking of Geomaterial. *International Conference on Disaster Management* (ICDM 2018). MATEC Web of Conferences. 03011.

Pellet, F. L. & Keshavarz, M. 2014. Shear Behavior of the Interface between Drilling Equipment and Shale Rocks. *Journal of Petroleum Exploration and Production Technology* 2014(10).

Sadisun, I. A., Shimada, H., Ichinose, M. & Matsui, K. 2005. Study on the Physical Disintegration Characteristics of Subang Claystone Subjected to a Modified Slaking Index Test. *Geotechnical and Geological Engineering* 23: 199-218.

Perencanaan Perbaikan Kelongsoran Lereng pada TPA Melonguane, Kabupaten Kepulauan Talaud

Musta'in Arif
Dosen Teknik Sipil – ITS

Herman Wahyudi
Dosen Teknik Sipil – ITS

Yudhi Lastiasih
Dosen Teknik Sipil – ITS

ABSTRAK: TPA Melonguane beroperasi di Kabupaten Kepulauan Talaud, terletak di Pulau Karakelang. Lokasi TPA tersebut di daerah perbukitan dengan elevasi ketinggian bervariasi antara +70,00 hingga +86,00 dikelilingi lahan terbuka. Awal tahun 2019, TPA Melonguane mengalami kerusakan berupa tanah longsor. Kelongsoran terjadi di jalan tanah yang difungsikan sebagai jalan menuju IPL, pada bulan Agustus 2019 terjadi longsor susulan di lereng dekat bangunan workshop IPLT. Oleh karena itu, perlu dilakukan evaluasi penyebab kelongsoran dan perbaikannya sehingga kelongsoran tidak terjadi lagi. Pada perencanaan perbaikan, analisa stabilitas lereng existing dilakukan dengan 2 pendekatan, yaitu lereng dengan tinggi terbatas (finite slope) dan lereng menerus (infinite slope). Sulawesi merupakan daerah rawan gempa karena merupakan lokasi pertemuan tiga lempeng tektonik. Maka dari itu, dari 2 pendekatan tersebut, analisa stabilitas lereng dilakukan dengan 2 kondisi, yaitu tanpa gempa dan dengan gempa. Ada beberapa perbaikan lereng antara lain ialah perkuatan dengan turap, geotextile+subdrain, dan gabion+geotextile.

Kata Kunci: gabion, geotextile, longsor, subdrain, turap

ABSTRACT: TPA Melonguane operates in the Talaud Islands Regency, located on Karakelang Island. The location of the *landfill* is in a hilly area with elevations varying from +70.00 to +86.00 surrounded by open land. At the beginning of 2019, the Melonguane *Landfill* was damaged in the form of a landslide. The landslide occurred on a dirt road that functions as a road to IPL, in August 2019 there was another landslide on the slope near the IPLT workshop building. Therefore, it is necessary to evaluate the causes of landslides and repair them so that landslides do not occur again. In the improvement planning, the existing slope stability analysis is carried out with 2 approaches, namely slopes with limited height (finite slope) and continuous slope (infinite slope). Sulawesi is an earthquake-prone area because it is the meeting point of three tectonic plates. Therefore, from these 2 approaches, slope stability analysis was carried out under 2 conditions, namely without an earthquake and with an earthquake. There are several slope improvements, including reinforcement with sheet piles, geotextile + subdrain, and gabion + geotextile.

Keywords: gabion, geotextile, landslide, subdrain, sheet pile

1 PENDAHULUAN

Kabupaten Kepulauan Talaud merupakan salah satu Kabupaten yang ada di Provinsi Sulawesi Utara dengan ibu kota Melonguane. Wilayah ini merupakan kawasan paling utara di Indonesia Timur, berbatasan dengan Filipina. Kepulauan Talaud terdiri dari 3 pulau utama, yaitu Pulau Karakelang, Pulau Salibabu, dan Pulau Kabaruan serta ada pulau-pulau kecil lainnya.

Dalam hal pengelolaan sampah, Kabupaten Kepulauan Talaud hanya memiliki satu fasilitas Tempat Pembuangan Akhir (TPA) yaitu TPA Melonguane yang terletak di Pulau Karakelang. Lokasi dari TPA tersebut di daerah perbukitan dengan kontur bervariasi antara +70,00 hingga +86,00 yang dikelilingi lahan terbuka. TPA mulai beroperasi pada tahun 2017 dan menggunakan sistem pembuangan *controlled landfill*. Jenis tanah dasar di TPA Melonguane didominasi oleh *clay* (lempung) dan

mengandung plastik dengan nilai N-SPT antara 4-50 dan tanah keras terletak pada kedalaman rata-rata 11,5 m. Karena TPA terletak di perbukitan, maka *landfill* dan Instalasi Pengolahan Lindi (IPL) berada di pinggir lereng. Selain itu, terdapat jalan tanah pada sisi lereng yang difungsikan sebagai jalan menuju kolam IPL.

Pada awal tahun 2019, TPA Melonguane mengalami kerusakan karena adanya bencana alam berupa tanah longsor. Kelongsoran terjadi di jalan tanah yang difungsikan sebagai jalan menuju IPL (Gbr. 1) sehingga jalan tersebut saat ini membentuk tebing di sisi sampingnya. Lalu, pada bulan Agustus 2019 terjadi longsor susulan di lereng dekat bangunan *workshop* IPLT. Kerusakan semakin bertambah sampai pada pipa lindi dari *landfill* ke kolam IPL terputus sehingga mengganggu pengoperasian TPA karena lindi tidak terolah di IPL.

Gbr. 1. Kelongsoran di Jalan Menuju Kolam IPL.

Karena TPA ini penting, kelongsoran yang terjadi perlu ditangani secepatnya supaya kerusakan tidak menjadi semakin parah. Upaya ini juga merupakan tindakan penting untuk mencegah kerusakan pada beberapa lokasi yang berpotensi mengalami kelongsoran sehingga TPA dapat berfungsi kembali dan dapat menampung sampah dalam 50 tahun ke depan. Oleh karena itu, perlu direncanakan perbaikan lereng untuk mengatasi kelongsoran di TPA Melonguane.

2 METODOLOGI

Tahapan perencanaan dapat dilihat pada Gbr. 2.

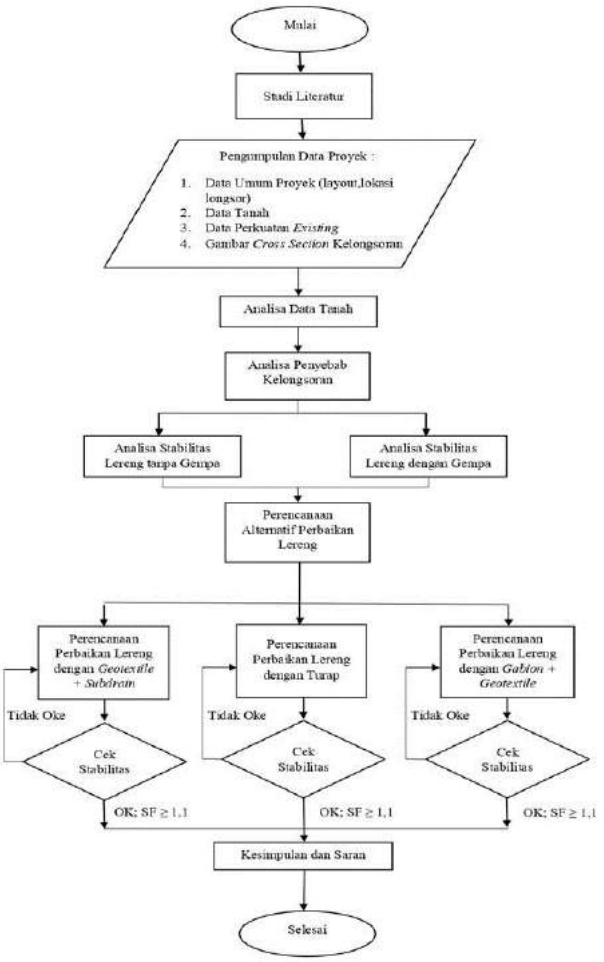

Gbr. 2. Diagram Alir Perencanaan.

3 ANALISA DATA TANAH

Data yang didapatkan dalam perencanaan ini adalah data N-SPT serta data laboratorium. Data hasil N-SPT perlu dilakukan korelasi untuk mencari nilai parameter-parameter tanah yang dibutuhkan dalam perencanaan. Korelasi menggunakan Tabel Bowless dan Tabel Burt Look. Lalu, hasil korelasi dan data laboratorium akan dibandingkan. Dari hasil analisa perbandingan tersebut, parameter tanah yang digunakan untuk analisa selanjutnya adalah data hasil korelasi karena sesuai dengan kondisi asli di lapangan (Tabel 1). Adapun statigrafi pada potongan kelongsoran (P5) dapat dilihat pada Gbr. 3.

Tabel 1. Parameter Tanah Hasil Korelasi.

Depth m		Jenis Tanah	N_{SPT}	γsat t/m³	Cu t/m²	ϕ o
0	-6	Clay Boulder	14	1,77	5,56	16,7
-6	-13	Clay Silt	10	1,68	3,95	14,4
-13	-20	Clay Sand	43	1,95	9,19	21,8

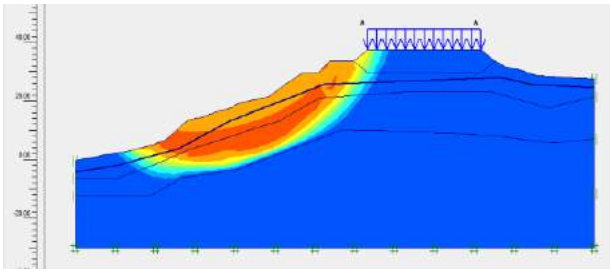

Gbr. 3. Stratigrafi pada Geometri P5.

4 ANALISA STABILITAS LERENG

4.1 *Analisa Stabilitas Lereng*

Analisa stabilitas lereng *existing* dilakukan dengan 2 pendekatan, yaitu lereng dengan tinggi terbatas (*finite slope*) dan lereng menerus (*infinite slope*). Sulawesi merupakan daerah rawan gempa karena merupakan lokasi pertemuan tiga lempeng tektonik. Pada tahun 2019 terjadi 4 kali gempa bumi pada bulan Januari, Maret, September dan Desember. Maka dari itu, dari 2 pendekatan tersebut, analisa stabilitas lereng dilakukan dengan 2 kondisi, yaitu tanpa gempa dan dengan gempa.

4.1.1 *Analisa Lereng dengan Tinggi Terbatas (Finite Slope)*

Analisa stabilitas lereng tanpa gempa dilakukan dengan program bantu GeoStudio menggunakan metode irisan Bishop. Muka air tanah diasumsikan pada kondisi tinggi yaitu 1,5 m dibawah permukaan tanah. Permodelan menggunakan beban *surcharge* 10 kPa sesuai dengan SNI 8460:2017 pasal 7.5.1. Dari hasil analisa lereng, didapatkan SF sebesar 0,874. Dikarenakan SF<1, maka lereng tersebut longsor dan tidak aman terhadap keruntuhan global (*overall*). Kondisi ini sudah sesuai dengan kondisi asli dilapangan dimana kelongsoran terjadi sampai lereng yang ada di bawahnya. Analisa stabilitas lereng dengan gempa yang digunakan adalah metode pseudostatic dengan menggunakan Pers. (1) dan (2) berdasarkan analisis Newmark dalam Hoek and Bray (1981), didapatkan nilai Kv = 0,128 dan Kh = 0,255. Setelah dianalisa, didapatkan SF 0,856 yang berarti lereng tersebut longsor (Gbr. 4).

$$K_h = 0{,}5\ \frac{PGAM}{g} \quad (1)$$

$$K_v = 0{,}5\ K_h \quad (2)$$

Dimana:
K_h = Koefisien gempa horizontal
K_v = Koefisien gempa vertikal
PGAM = Percepatan puncak di permukaan tanah (g)
g = Percepatan gravitasi

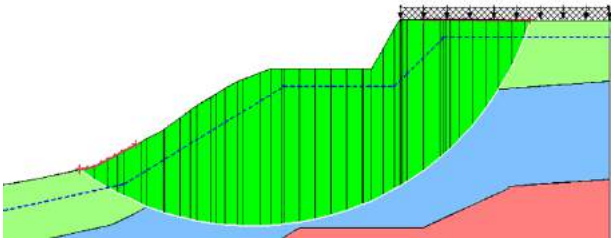

Gbr. 4. Bidang Longsor Lereng (SF = 0,856).

4.1.2 *Analisa Lereng dengan Tinggi Menerus (Infinite Slope)*

Analisa lereng menerus tanpa gempa dilakukan dengan menggunakan Pers. 3 yaitu analisa lereng menerus dengan rembesan. Sementara analisa lereng menerus dengan gempa dilakukan dengan menggunakan Pers. 4 yaitu analisa lereng menerus dengan koefisien seismik gempa.

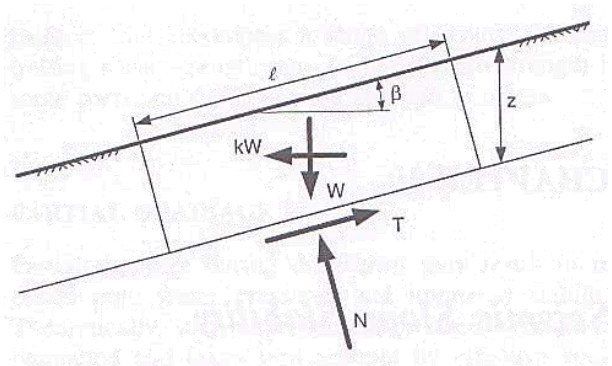

Gbr. 4. Geometri Lereng Menerus.

$$SF = \frac{c}{\gamma_{sat}\ H\ cos^2\beta \tan\beta} + \frac{\gamma'}{\gamma_{sat}} \frac{\tan\phi}{\tan\beta} \quad (3)$$

$$SF = \frac{c + \gamma z\ cos^2\ \beta\ - k\gamma z \cos\beta \sin\beta \tan\phi}{\gamma z \cos\beta \sin\beta + k\gamma z\ cos^2\ \beta} \quad (4)$$

Dimana:
SF = Faktor keamanan
c = Kohesi
$\emptyset$ = Sudut geser tanah
γ' = Berat volume efektif
γsat = Berat volume jenuh
β = Kemiringan lereng terhadap bidang horisontal
H = Tinggi lereng
k = Koefisien gempa horizontal

Hasil rekapitulasi SF kondisi lereng sebelum longsor dapat dilihat pada Tabel 2.

Tabel 2. Rekapitulasi SF Lereng.

Kondisi	Tipe Lereng	SF	Cek
Tanpa Gempa	Infinite Slope	0,874	LONGSOR
	Finite Slope	0,885	LONGSOR
Dengan Gempa	Infinite Slope	0,856	LONGSOR
	Finite Slope	0,832	LONGSOR

4.2 *Penyebab Kelongsoran Lereng*

Dapat disimpulkan bahwa penyebab kelongsoran ada beberapa hal, sebagai berikut:

- Geometri lereng tidak aman (curam). Sebelum terjadi kelongsoran, kemiringan lereng bagian atas ± 60^0. Setelah terjadi longsor, kemiringan lereng bagian atas menjadi ± 30^0.
- Tingginya curah hujan. Adanya kondisi ini menyebabkan lereng dalam kondisi jenuh atau setengah jenuh sehingga memperbesar kemungkinan terjadi longsor.
- Gaya luar berupa faktor getaran yang disebabkan oleh gempa. Gempa dapat menimbulkan retak-retak (*cracks*) yang dapat mereduksi kuat geser tanah.

5 PERENCANAAN PERBAIKAN LERENG

5.1 *Perencanaan Sheet Pile*

Turap (*sheet pile*) yang direncanakan adalah turap yang berfungsi sebagai cerucuk dan harus direncanakan memotong bidang longsor. Turap yang digunakan adalah CPC *Sheet Piles* tipe W-400 Class A dengan spesifikasi sebagai berikut:

f'c = 62 Mpa
W = 400 kg/m
A = 1598 cm^2
I = 248,691 cm^4
Mcr = 20,1 tm

Direncanakan turap ditempatkan pada 2 titik (Gbr. 5) dengan panjang turap ditancapkan sampai tanah keras sedalam 15 m dan 17 m. Berdasarkan hasil analisis dengan program bantu Geostudio, untuk analisa dengan gempa pseudostatik didapatkan *safety factor* sebesar 1,395 sehingga lereng tersebut dapat dikatakan stabil dan aman terhadap kelongsoran.

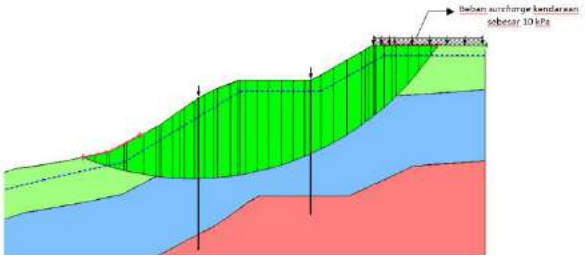

Gbr. 5. Perkuatan Lereng dengan Turap (SF = 1.395).

5.2 *Perencanaan Geotekstile + Subdrain*

Subdrain yang direncanakan terbuat dari susunan batu pecah dan kerikil yang dibungkus dengan *geotextile non-woven* dan dipasang dari bagian atas hingga kaki lereng, sehingga lereng tetap dalam kondisi kering. Untuk dimensi *subdrain* direncanakan menggunakan 20 cm × 20 cm. Ilustrasi pemasangan dapat dilihat pada Gbr. 6.

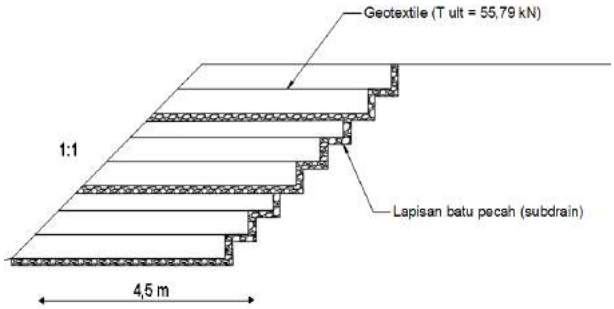

Gbr. 6. Ilustrasi *Geotextile + Subdrain.*

Pada perencanaan perkuatan lereng dengan geotextile, perlu dilakukan perubahan geometri lereng berupa pembuatan lereng bertingkat (teras lereng) dengan slope 1:1 dan dibuat 3 tingkat. Adapun data tanah timbunan adalah sebagai berikut:

γ = 19 kN/m^3
ϕ = 30^o
c = 0 kPa

Perhitungan kebutuhan geotextile dilakukan dengan meninjau bidang longsor lereng secara local. Setelah didapat jumlah kebutuhan geotextile tiap lereng, maka ditinjau stabilitas nya secara keseluruhan (overall) dengan software Geostudio.

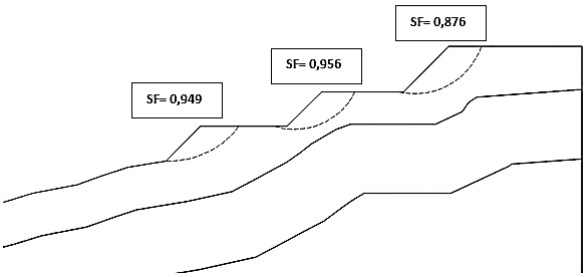

Gbr. 7. Bidang longsor lereng

Sebelum menghitung kebutuhan *geotextile*, maka perlu dilakuka perhitungan ΔM_R dengan menggunakan persamaan:

$$M_D = \frac{M_R}{SF_{existing}} \quad (5)$$

$$M_{R\ Butuh} = M_D \times SF_{rencana} \quad (6)$$

$$\Delta M_R = M_{R\ Butuh} - M_{R\ Aktual} \quad (7)$$

Pada perencanaan ini digunakan *geotextile woven* type 25 dengan $T_{ultimate}$ sebesar 55,79 kN/m dan jarak pemasangan (Sv) sebesar 0,5 m. Perhitungan tegangan izin dapat dilakukan dengan menggunakan persamaan:

$$T_{allow} = \frac{T_{ult}}{FS_{id} \times FS_{cr} \times FS_{cd} \times FS_{bd}} \quad (8)$$

Dimana:
T_{allow} = Kekuatan *geotextile* yang tersedia
T_{ult} = Kekuatan *ultimate geotextile*
FS_{ID} = Faktor reduksi akibat kesalahan pemasangan
FS_{CR} = Faktor reduksi akibat rangkak
FS_{CD} = Faktor reduksi akibat pengaruh kimia
FS_{BD} = Faktor reduksi akibat pengaruh biologi

Selanjutnya, untuk menghitung panjang *geotextile* yang diperlukan adalah dengan menggunakan persamaan:

$$L_{TOTAL} = L_o + L_e + L_R \quad (9)$$

Dimana:
L_{TOTAL} = Panjang total *geotextile*
L_o = Panjang lipatan *geotextile*
L_e = Panjang *geotextile* di belakang bidang longsor (minimal 1 meter)
$L_e = \frac{Tallow \times SF}{(\tau_{atas} + \tau_{bawah}) \times E}$
τ_{atas} = Tegangan geser antara tanah asli dengan *geotextile* = c + σ_v tan ϕ
τ_{bawah} = Tegangan geser antara tanah timbunan dengan *geotextile* = c + σ_v tan ϕ
E = Efisiensi (80%)
SF = Faktor keamanan
L_R = Panjang *geotextile* di depan bidang longsor

Setelah mengitung kebutuhan *geotextile* selanjutnya adalah mengitung kontrol stabitilitas eksternal *geotextile* sebagai berikut:

a) SF Guling

$$FS_{OT} = \sum \frac{\text{Momen Penahan}}{\text{Momen Penggerak}} \quad (10)$$

$$= \frac{W_i X_i + P_a \sin\delta\ (L)}{P_a \cos\delta\ (\frac{H}{3})} > 2$$

b) SF Geser

$$FS_S = \sum \frac{\text{Gaya Penahan}}{\text{Gaya Penggerak}} \quad (11)$$

$$= \frac{[c + \left(\frac{W_i + P_a \sin\delta}{L}\right) \tan\delta\ ]L}{P_a \cos\delta} > 1{,}5$$

c) SF Daya Dukung

$$FS_b = \frac{Qu}{Q\ max} > 3 \quad (12)$$

Dimana:
FS_{OT} = Angka keamanan lereng terhadap guling
Wi = Berat dinding tanah
Xi = Jarak ke titik berat
Pa = Tekanan tanah aktif
δ = Sudut geser antara tanah dan *geotextile*
L = Panjang *geotextile*

Berdasarkan hasil analisis dengan program bantu Geostudio, untuk analisa dengan gempa pseudostatik didapatkan *safety factor* sebesar 1,405 sehingga lereng tersebut dapat dikatakan stabil dan aman terhadap kelongsoran (Gbr. 8).

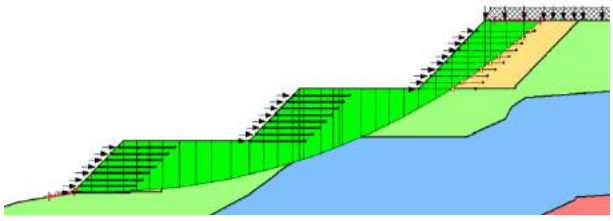

Gbr. 8. Perkuatan Lereng dengan *Geotextile+Subrain* (SF=1,405).

5.3 *Perencanaan Gabion + Geotekstile*

Gabion (bronjong) dengan ukuran 50x100 cm dan panjang 200 cm. Gabion dipasang pada permukaan miring lereng 1:1 dan ditarik oleh *reinforcement* berupa *geotextile*. Pada perencanaan ini, perlu dilakukan perubahan geometri lereng berupa pembuatan lereng bertingkat (teras lereng) dengan *slope* 1:1 dan dibuat 3 tingkat. Perhitungan gabion hanya berupa kontrol terhadap guling dan geser karena gabion berfungsi sebagai penahan timbunan lereng agar tidak tergerus oleh air sementara *geotextile* berfungsi sebagai perkuatan gabion agar tidak longsor.

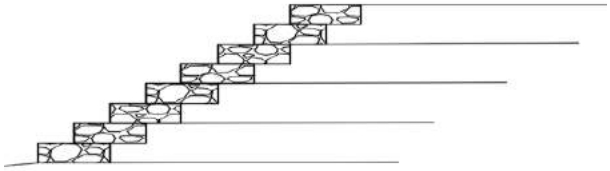

Gbr. 9. Geometri Ilustrasi + Gabion.

Adapun perhitungan gabion adalah sebagai berikut:

a) Menghitung koefisien tekanan tanah aktif

Koefisien tekanan tanah aktif akibat gempa dihitung dengan menggunakan persamaan sebagai berikut:

$$K_{AE} = \frac{cos^2(\phi-\theta-\beta)}{\cos\theta cos^2\beta \cos(\delta+\theta+\beta)\left[1+\left(\frac{\sin(\delta+\phi)\sin(\phi-\theta-t)}{\cos(\delta+\beta+\theta)\cos(t-\beta)}\right)\right]^2} \quad (13)$$

$$\theta = tan^{-1}\left[\frac{kh}{(1-kv)}\right] \quad (14)$$

Dimana:
ϕ = Sudut geser tanah
β = Kemiringan dinding terhadap bidang vertikal,
δ = Sudut geser dinding, dan
t = Kemiringan dinding terhadap bidang horizontal.

b) Menghitung σ_v dan σ_h

$$\sigma_v = q + (\gamma \times h) \quad (15)$$

$$\sigma_h = (\sigma_v \times Ka) - (2 \times c \times \sqrt{Ka}) \quad (16)$$

Dimana:
σ_v = Tegangan vertikal
σ_h = Tegangan horizontal
Ka = Koefisien tekanan tanah aktif
h = Tebal lapisan tanah

c) Mengitung momen penahan gabion (Mr)

$$Mr = dg \times Wg \quad (17)$$

$$dg = \frac{\sum A_x}{\sum A} \quad (18)$$

$$W_g = A \times \gamma_t \quad (19)$$

Dimana:
Wg = Berat gabion
γt = Berat jenis batu pengisi = 18 kN/m^3
A = Luas gabion
dg = Jarak horizontal gabion terhadap titik 0
∑A = Luasan total gabion
x = Jarak titik berat tiap elemen gabion terhadap titik 0

d) Menghitung faktor keamanan

Faktor keamanan terhadap guling

$$SF_o = \frac{\sum Mr}{\sum Mo} = \frac{162}{119{,}2} = 1{,}358 < 2 \text{ (NOT OK)}$$

Faktor keamanan terhadap geser

$$SF_s = \frac{\mu Wg}{Ph} = \frac{\tan\phi \; x \; Wg}{Ph} = \frac{\tan 30 \; x \; 72}{81{,}024} = 0{,}513 < 1{,}5$$

(NOT OK)

Karena nilai faktor keamanan terhadap geser tidak memenuhi persyaratan, maka perlu adanya tambahan berupa *geotextile*. *Geotextile* yang digunakan adalah *geotextile woven* type 25 dengan $T_{ultimate}$ sebesar 55,79 kN/m dan jarak pemasangan (Sv) sebesar 1 m.

Berdasarkan hasil analisis dengan program bantu Geostudio, untuk analisa dengan gempa pseudostatik didapatkan *safety factor* sebesar 1,465 sehingga lereng tersebut dapat dikatakan stabil dan aman terhadap kelongsoran (Gbr. 10).

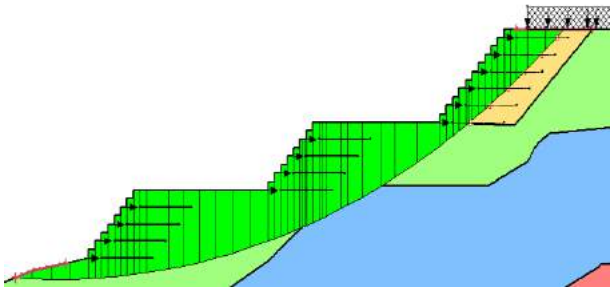

Gbr. 10. Perkuatan Lereng dengan *Geotextile+Gabion* (SF=1,465).

6 KESIMPULAN

1. Dari hasil analisa pada potongan lereng, stabilitas lereng kondisi tinggi terbatas (*finite slope*) dengan menggunakan program Geostudio, diperoleh SF= 0,874, sedangkan kondisi menerus (*infinite slope*) dengan menggunakan rumus diperoleh SF= 0,885.
2. Analisa stabilitas lereng dengan gempa yang digunakan adalah dengan metode *pseudostatic*, dimana untuk daerah Kabupaten Kepulauan Talaud, Kh = 0,255 dan Kv = 0,128. Hasil analisa stabilitas lereng kondisi tinggi terbatas (*finite slope*), diperoleh SF= 0,856, sedangkan kondisi menerus (*infinite slope*) dengan menggunakan rumus diperoleh SF= 0,832.
3. Perencanaan *sheet pile* terdiri dari 2 buah sheet pile tipe CPC Sheet Pile W-400 Class A dengan kedalaman 15 m dan 17 m serta dipasang 20 m sepanjang daerah kelongsoran.
4. Perencanaan *geotextile* + *subdrain*, geometri lereng diubah menjadi teras lereng (3 tingkat). Untuk lereng bawah dan tengah (H=4m), digunakan 8layer *geotextile* dengan panjang 5 m dan Tult sebesar 55,79 kN/m. Untuk lereng atas (H=5,3m), digunakan 11layer *geotextile* dengan panjang 5 m. *Subdrain* dipasang secara terasering, dibuat untuk mengalirkan air tanah dari balik lereng. Dimensi subdrain yang digunakan 20 x 20 cm. Namun, opsi perkuatan ini tidak disarankan karena pelaksanaannya yang susah di lapangan.
5. Perencanaan *gabion* + *geotextile*, geometri lereng diubah menjadi teras lereng (3 tingkat). Dimensi bronjong yang digunakan yaitu 50 x 100 x 200 cm yang diisi dengan batu kali pecah. Untuk lereng bawah dan tengah (H=4m), digunakan 4layer *geotextile* dengan panjang 4 m dan Tult sebesar 55,79 kN/m. Untuk lereng atas (H=5,3m). digunakan 6-*layer geotextile* dengan panjang 4 m. Namun, opsi perkuatan ini tidak disarankan karena pelaksanaannya yang susah di lapangan.

DAFTAR PUSTAKA

B. G. 2007. *Look, Handbook of Geotechnical Investigation and Design Tables, 1st ed*. London: Taylor & Francis Group.

Das, Braja M. 2011. (translated by Mochtar N.E, and Mochtar I.B.). *Mekanika Tanah (Prinsip-prinsip Rekayasa Geoteknik) Jilid II*. Jakarta: Erlangga.

Duncan, J. M., & Wright, S. G. 2005. *Soil Strength and Slope Stability*. New Jersey: Jwiley & Sons, inc.

Hoek, E and Bray, J.W. 1981. *Rock Slope Engineering 3rd Ed*. London: The Institution of Mining and Metallurgy.

J. E. Bowless. 1984. *Sifat-sifat Fisis dan Geoteknis Tanah (Mekanika Tanah)*, 2nd ed. Jakarta: Erlangga.

Standar Nasional Indonesia. 2017. *SNI 8460 Perancangan Geoteknik*. Jakarta: Standar Nasional Indonesia.

Efek Cracks Lereng Tanah terhadap Design Bored Pile Beton untuk Penanggulangan Gejala Longsor pada Fasilitas Dermaga Penyebrangan Sei Kapitan Tebing Sungai Kumai Kabupaten Kotawaringin Barat

Stephanus Alexsander
Dosen Teknik Sipil – Universitas Palangka Raya

ABSTRAK: Penanganan gejala longsor pada daerah penelitian dilakukan dengan 2 pendekatan yaitu analisa Geofisika dan Geoteknik. Pendekatan Geofisika digunakan geolistrik resistivitas 2 dimensi. Hasil geolistrik menunjukan adanya bidang-bidang yang diprediksi sebagai *cracks* yang didapatkan melalui hasil survey Geolistrik 2 dimensi yang memiliki kedalaman bidang longsor 8 meter lebih dengan nilai reisitivitas 0,24 – 6,5 ohm meter dan memiliki bukaan bidang longsor lebih dari 18 meter yang terjadi pada tebing sungai. Untuk pendekatan geoteknik dilakukan dengan bantuan *software* Plaxis ver 8,6 dengan model tanah *Hardening Soil Model* yang dilakukan melalui 2 pendekatan, yaitu model tebing sungai dengan *cracks* yang terjadi di dalam tebing yang didapatkan dari hasil survey Geolistrik 2 dimensi dan model tebing sungai tanpa adanya bidang longsor. Penanganan longsor digunakan *bored pile* beton diameter 30 cm yang didesain dengan panjang 18 meter. Hasil penanggulangan didapatkan untuk model tebing dengan adanya *cracks, bored pile* momen lentur *bored pile* sebesar 38,03 kNm/m dan untuk model tebing tanpa adanya *cracks*, didapatkan momen lentur 16,47 kNm/m

Kata Kunci: geolistrik 2 dimensi, cracks, momen bored pile

1 PENDAHULUAN

Longsor merupakan fenomena alam yang terjadi di seluruh dunia. Longsor merupakan pergerakan massa tanah dan batuan dari tempat yang tinggi ke tempat yang rendah. Longsor dapat terjadi pada saat hujan lebat ataupun sesaat setelah hujan lebat terjadi ataupun adanya peristiwa *rapid-drawdown*. Peristiwa *rapid-drawdown* yang menyebabkan longsor sering terjadi pada daerah tebing sungai besar yang diakibatkan adanya perbedaan muka air yang terjadi di sungai dan di dalam tebing. Menurut Mochtar (2010, 2011), pemicu kelongsoran yang terjadi umumnya terjadi akibat adanya *cracks* yang telah terjadi di dalam tebing yang telah terisi oleh material kasar seperti pasir dan kerikil yang terbawa oleh air hujan masuk ke dalam tebing melalui *cracks* yang terdapat di dalam tebing. Banyaknya *cracks* yang terisi oleh pasir yang menyebabkan suatu tebing ataupun lereng mengalami kelongsoran yang menyerupai kelongsoran seperti pasir, sehingga dapat disebut sebagai "*Behaving Like Sand*". Banyaknya *cracks* yang terjadi di dalam tebing dapat menjawab hal yang mendasar bahwa suatu bentang lereng tertentu dan memiliki material tanah yang hampir sama serta mengalami intensitas hujan yang sama harusnya mengalami longsor secara bersamaan tetapi faktanya kelongsoran yang terjadi pada tempat-tempat tertentu saja. Selain Mochtar peneliti lain yang meneliti tetang *cracks* adalah Zhang (2012) yang melakukan penilitian yang menunjukan adanya pengaruh *cracks* arah vertikal maupun horisontal yang memiliki sudut inklinasi yang terjadi di dalam tebing. *Cracks* yang ada dapat memberikan pengaruh yang besar terhadap stabilitas lereng terutama pada saat terjadi hujan sangat lebat, yang dapat menyebabkan pertambahan *cracks* bahkan kelongsoran.

Penelitian ini dilakukan pada daerah Sei Kapitan, Kabupaten Kotawaringin Barat Kecamatan Kumai untuk mengamankan pembangunan fasilitas dermaga dan dermaga penyebrangan yang ada pada lokasi penelitian. Kegiatan pengukuran gejala longsor dengan menggunakan resisitivitas tomografi untuk memprediksi *cracks* yang terjadi di dalam

lereng. Pengukuran hasil geolistrik Geolistrik 2 dimensi kemudian dilakukan validasi dengan menggunakan pendekatan geoteknik untuk melihat deformasi bahkan momen yang terjadi pada *bore pile* yang dapat berpengaruh terhadap design *bore pile* yang menahan beban horisontal.

Selama ini hasil penanganan kelongsoran umumnya memodelkan berdasarkan hasil bor geoteknik berupa log bor tanpa melihat adanya posisi letak bidang longsor yang telah terjadi di dalam lereng. Penelitian dilakukan dengan 2 pendekatan yang berbeda dalam memodelkan penanganan terhadap kelongsoran. Model pertama digunakan tanpa melihat adanya bidang longsor, sehingga model tanahnya dianalisa berdasarkan hasil log bor dan model kedua dilakukan kombinasi antara hasil bor log dan hasil dari tomografi resistivitas. Hasil kedua model tersebut kemudian dapat disimpulkan apakah dengan adanya *cracks* yang telah ada di dalam tebing dapat memberikan efek yang berarti terhadap design *bored pile.*

Alexsander (2018) menjelaskan bahwa pada daerah tebing sungai maupun lereng yang memiliki kadar air yang tinggi dan mengalami siklus bergantian antara jenuh dan kering maka daerah tersebut ditemukan adanya *cracks* yang terbentuk di dalam lereng. *Cracks* yang terbentuk lama kelamaan akan membentuk suatu pola yang menyerupai bidang longsor

2 LOKASI PENELITIAN DAN HASIL SURVEY DAN PENGAMBILAN DATA TANAH

Penelitian ini dilakukan di daerah tebing Sungai Kumai yang akan dibangun dermaga dan fasilitas dermaga penyebrangan yang terdapat pada wilayah Kecamatan Kumai tepatnya pada koordinat 02^{o} 45’ 22.7” LS dan 111^{o} 43’ 01.5” BT yang dapat dilihat pada Gbr. 1.

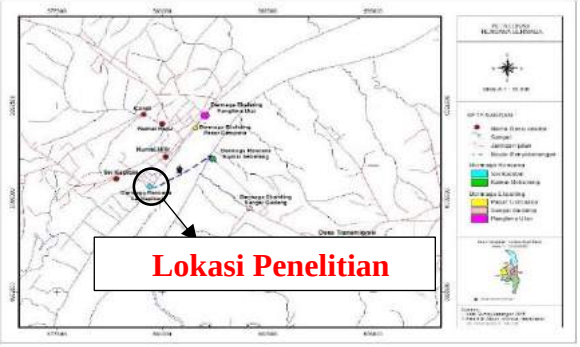

Gbr. 1. Lokasi Penelitian Lokasi Sei Kapitan.

Untuk survey dan pengambilan data yang dilakukan untuk penanganan kelongsoran adalah survey bathimetri dan topografi, geolistrik, sondir dan pengeboran geoteknik. Untuk hasil setiap survey yang dilakukan dapat dilihat pada Gbr. 2 – Gbr. 6.

Hasil penyelidikan tanah dan hasil geolistrik pada Gbr. 3, 4, 5 dan 6, memperlihatkan dari hasil sondir dan bor didapatkan adanya korelasi yang kuat dengan hasil geolistrik 2 dimensi yang menunjukan dari permukaan tanah hingga kedalaman 8 meter merupakan tanah lepas dengan tekanan konus dan nilai SPT yang rendah serta hasil geolistrik 2 dimensi memprediksi pada kedalaman hingga 8 meter akan mengalami kelongsoran. Selain menunjukan adanya bidang kelongsoran pada kedalaman 8 meter hasil geolistrik 2 dimensi juga menunjukan adanya intrusi air laut yang terjadi pada lokasi penenlitian dengan nilai resisitivitas ≤ 0.2 ohm meter. Untuk daerah penelitian terdapat pada potangan warna hijau dan biru dengan jarak setiap potongan 50 meter yang dapat dilihat pada Gbr. 2.

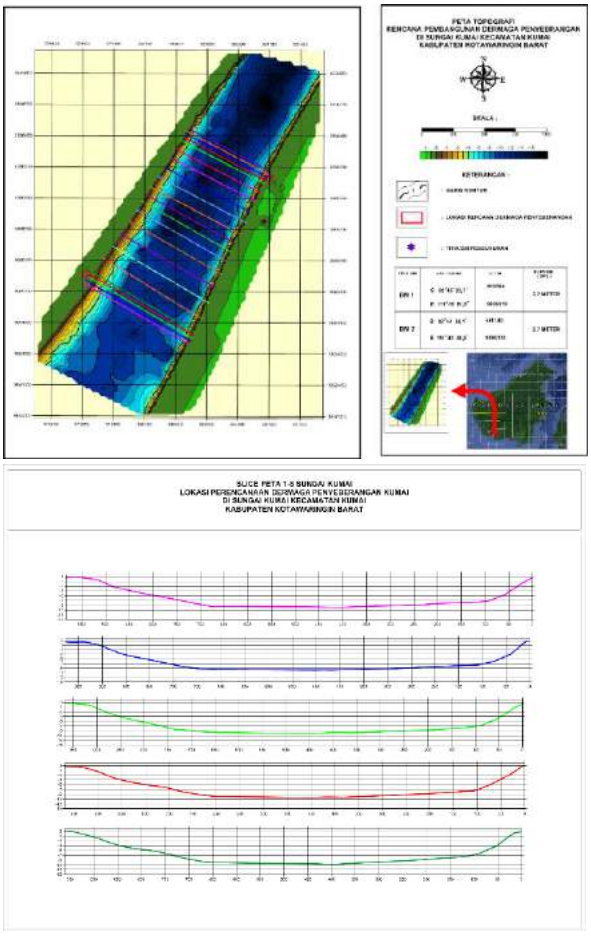

Gbr. 2. Hasil Survey Topografi, Bahimeteri dan Potongan di Daerah Penelitian.

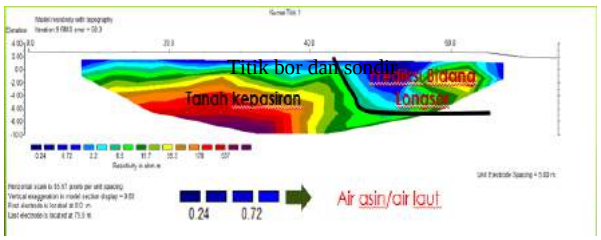

Gbr. 3. Hasil Geolistrik 2 Dimensi Tegak Lurus dengan Sungai Kumai.

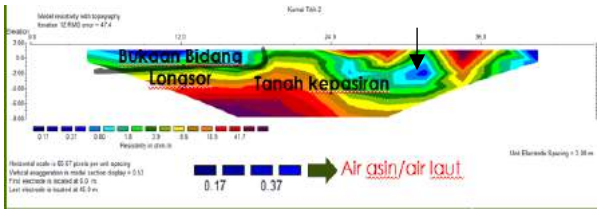

Gbr. 4. Hasil Survey Geolistrik 2 Dimensi Sejajar dengan Sungai Kumai.

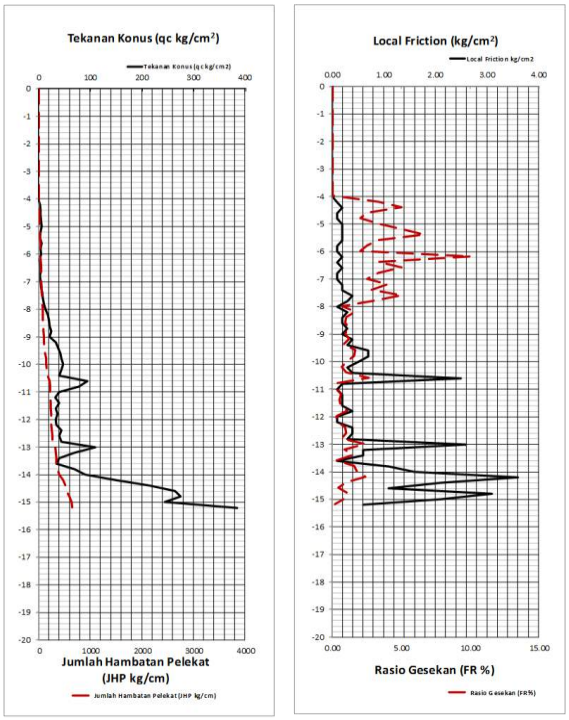

Gbr. 5. Hasil Sondir Daerah Penelitian.

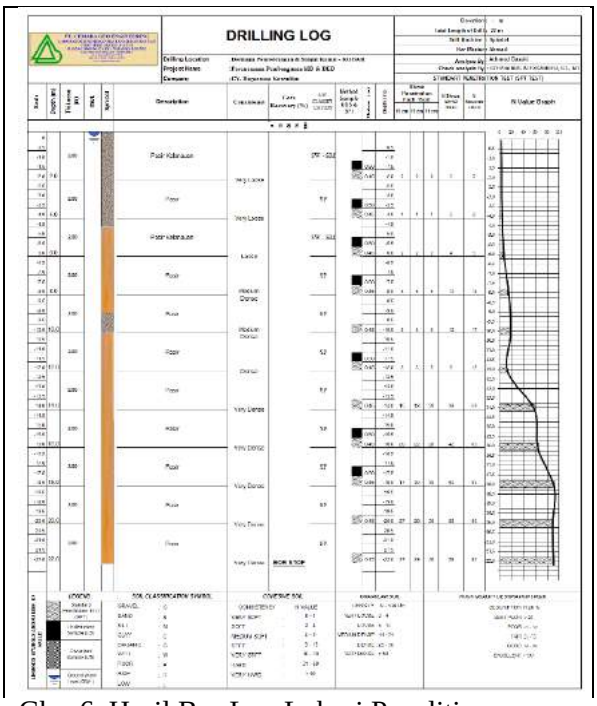

Gbr. 6. Hasil Bor Log Lokasi Penelitian.

3 PEMILIHAN MODEL TANAH DALAM ANALISA LONGSOR DENGAN MENGGUNAKAN PLAXIS

Pada penelitian ini digunakan software Plaxis 8.6 dengan pemodelan tanah menggunakan *Hardening Soil* model, pemilihan pemodelan tanah ini dikarenakan model ini sangat *reasonable* untuk menganalisa kasus longsor, di sisi lain dalam manual plaxis 2011 didapatkan dalam bentuk tabel dari setiap model tanah dan bentuk kasus yang dapat dilakukan oleh setiap model dengan *output* hasil yang baik oleh *software* plaxis yang dapat dilihat pada Tabel 1.

Tabel 1. Model Tanah dan Kasusnya yang Dapat Dikerjakan dengan Baik oleh Software Plaxis.

Soil Constitutive Model (Application of Soil Model – Type of Cases)								
Considering different types of applications (consider also type of soil)								
Model	Foundation	Excavation	Tunnel	Embankment	Slope	Dam	Offshore	Other
Linear Elastic			C					
Mohr-Coulomb	C	C	C	C	C	C	C	C
Hardening Soil	B	B	B	B	B	B	B	B
HS Small	A	A	A	A	A	A	A	A
Soft Soil Creep	B	B	B	A	A	B	B	B
Soft Soil	B	B	B	A	A	B	B	B
Jointed Rock	B	B	B	B	B	B	B	B
Modified Cam-Clay	B	B	B	B	B	B	B	B
NGI-ADP	B	B	B	A	A	B	A	B

Soil Constitutive Model (Application of Soil Model – Type of Cases)								
Hoek-Brown	B	B	B	B	B	B	B	B

Source : Plaxis Manual 2D 2011

A : The best standard model in PLAXIS for this application
B : Reasonable modelling
C : First order (crude) approximation

3.1 Hardening Soil Model

Model Hardening Soil merupakan model tingkat lanjut untuk memodelkan perilaku dari tanah. Seperti pada model Mohr-Coulomb, kondisi tegangan batas dideskripsikan oleh sudut geser, φ, kohesi, *c* dan sudut dilatansi, ψ. Namun demikian, kekakuan tanah dideskripsikan secara lebih akurat dengan menggunakan tiga masukan kekakuan yang berbeda: kekakuan pembebanan triaksial, E_{50}, kekakuan pengurangan beban (*unloading*) triaksial, E_{ur} dan kekakuan pembebanan satu arah, E_{oed}. Untuk nilai tipikal dari berbagai jenis tanah, dapat digunakan $Eur \approx 3 \cdot E_{50}$ dan $Eoed \approx E_{50}$, tetapi tanah yang sangat lunak dan tanah yang sangat kaku cenderung memberikan rasio E_{oed}/E_{50} yang berbeda. Berbeda dengan model Mohr-Coulomb, model Hardening Soil telah mengikutsertakan modulus kekakuan yang bergantung pada tegangan. Hal ini berarti bahwa kekakuan akan semakin meningkat terhadap tegangan. Karena itu, ketiga masukan kekakuan merupakan nilai yang berhubungan dengan sebuah tegangan acuan, yang umumnya diambil sebesar 100 kPa.

3.2 Keterbatasan Hardening Soil Model

Model ini merupakan model *hardening* yang tidak mengikutsertakan pelunakan tanah akibat dilatansi dan efek lepasnya ikatan antar butir. Pada faktanya, model ini merupakan model *hardening* isotropis sehingga tidak memodelkan efek histeresis, pembebanan siklik maupun mobilitas siklik (*cyclic mobility*).

4 HASIL ANALISA LONGSOR

Lokasi pengambilan data tanah berupa sondir dan boring terdapat pada bentang katoda geolistrik 47 meter pada survey geolistrik 2 dimensi yang dilihat pada Gbr. 3. Pada Gbr. 3 diperlihatkan bahwa adanya bidang longsor yang didalamnya diprediksi adanya *cracks* yang telah terjadi di dalam tebing sungai. Untuk tanah kerasnya pada hasil sondir dan boring didapatkan pada kedalaman lebih dari 14 meter, sedangkan dari hasil Geolistrik 2 dimensi pada Gbr. 3. memperlihatkan adanya pendangkalan tanah keras yang menjauhi tebing sungai, di mana pada bentang 0 – 40 meter pada survey geolistrik 2 dimensi didapatkan tanah keras mulai pada kedalaman 8 meter dengan nilai resistivitas ≥ 537 ohm meter. Sehingga model tanah yang terdapat adanya *cracks* dapat digambarkan pada program plaxis sesuai dengan kondisi lapangan dengan mengikuti hasil dari geolistrik 2 dimensi atau biasa disebut sebagai tomografi resistivitas.

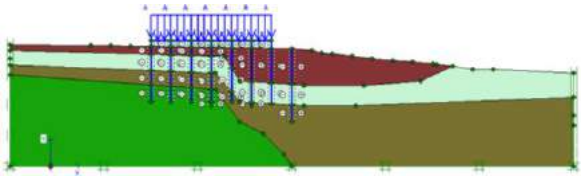

Gbr. 7. Model Tanah yang Disesuaikan dengan Hasil Geolistrik 2 Dimensi.

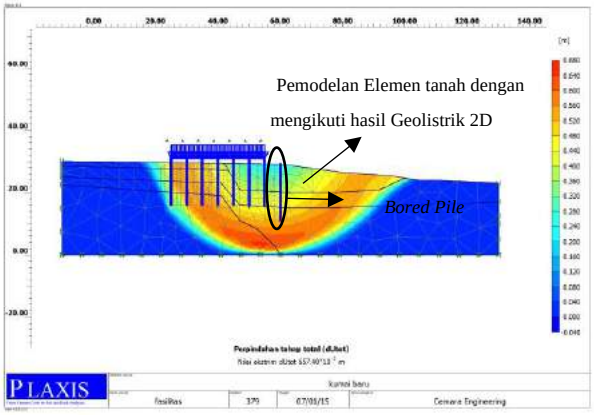

Gbr. 8. Model Longsoran yang Terjadi pada Model Tanah.

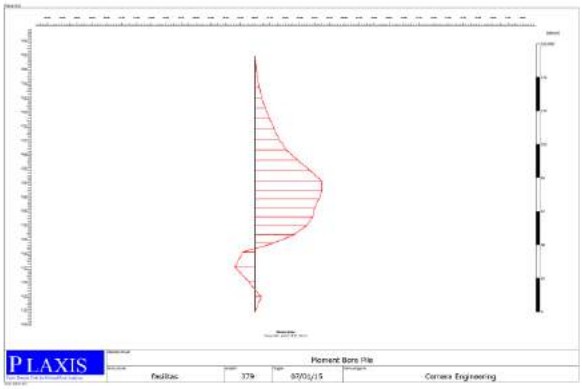

Gbr. 9. Moment Bore Pile 38,03 kNm/m.

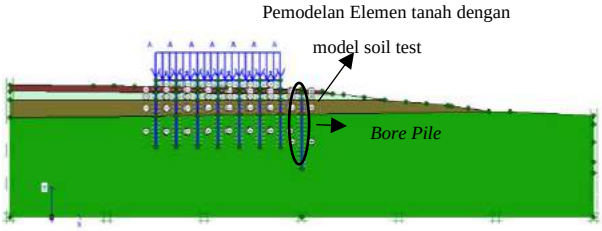

Gbr. 10. Model Tanah yang Disesuaikan dengan Model Tanah yang Diinterpresi dari Hasil *Bore*

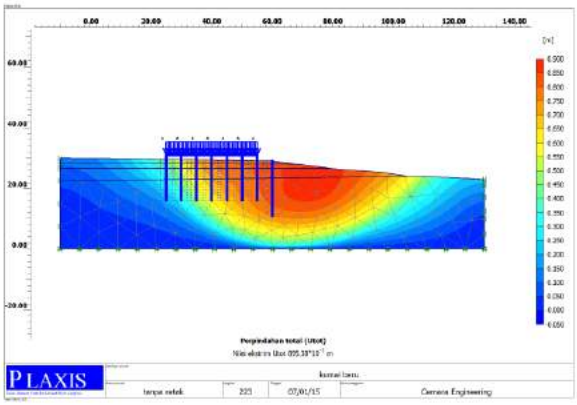

Gbr. 11. Model Longsoran yang Terjadi pada Model Tanah

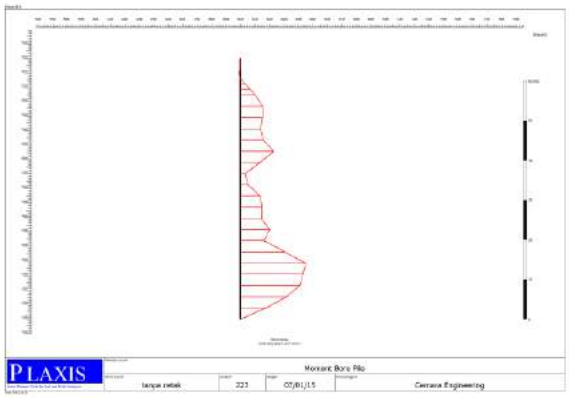

Gbr. 9. Moment Bore Pile 16,47 kNm/m

Berdasarkan hasil analisa dengan menggunakan plaxis versi 8.6 didapatkan hasil yang cukup signifikan antara model tanah dengan menggunakan *cracks* berdasarkan hasil geolistrik 2 dimensi dan hasil hanya mengandalkan interpretasi dari hasil *bor log*. Untuk perbedaan mendasar yang terjadi pada *bored pile* adalah besarnya nilai *moment* yang terjadi pada *bored pile* adalah sebesar 38.03 kNm/m untuk model berdarsarkan hasil geolistrik 2 dimensi dan 16.47 kNm/m untuk model interpretasi berdasarkan hasil bor log.

5 KESIMPULAN DAN SARAN

5.1 *Kesimpulan*

Berdasarkan hasil uraian dan kajian di lapangan maka didapatkan :

1. Besarnya momen yang terjadi dari hasil interpretasi bersadasarkan hasil *bor log* dan hasil geolistrik 2 dimensi memiliki perbedaan yang *significant.* Untuk model tanah yang dimodelkan berdasarkan hasil interpresi geolistrik 2 dimensi memiliki nilai yang lebih besar dengan nilai maksimum momen *bore pile* sebasar 38.03 kNm/m dan 16.47 kNm/m berdasarkan hasil intepretasi *bore log.*
2. *Cracks* yang terdapat di dalam lereng dapat memberikan konstribusi yang besar terhadap moment design perkuatan tebing dalam kasus ini adalah *bored pile* hal tersebut dapat terlihat dari hasil analisis pada daerah yang memiliki tingkat kejenuhan yang tinggi berdasarkan hasil tomography resistivity

5.2 Saran

1. Dalam analisis longsor hendaknya tidak mengandalkan data bor saja, tetapi harus dikombinasikan dengan survey geofisika dalam hal ini menggunakan geolistrik 2 dimensi.
2. Kita tahu bahwa bor yang ada belum tentu mampu menggambarkan bawah permukaan dengan baik. Sehingga bepengaruh terhadap penggambaran model stratifikasi tanah.
3. Untuk tanah dengan kondisi sering mengalami perubahan siklus penjenuhan dan pengeringan umumnya telah terbentuk cracks. *Cracks* yang terbentuk lama kelamaan membentuk pola bidang longsor.

DAFTAR PUSTAKA

Alexsander Stephanus. 2011. *Analisa Longsor daerah Gang Mandau Kota Palangka Raya*. Final Report Penelitian Departemen Pekerjaaun Umum Kota Palangka Raya.

Alexsander Stephanus. 2018. Identifikasi Keberadaan dan Perubahan Cracks di Dalam Lereng Tanah Melalui Pengujian Tomographic Resistivity dan Induced Polarization Sebagai Upaya Pembuktian Hipotesa "The Concept of Cracked Soil".

Anonim. 2015. Laporan Penyelidikan Tanah Laboratorium Mekanika Tanah dan Batuan Cemara Engineering.

----------. 2012. Geotechnical Engineering from Theories to Practices. *Short Course on Geotechnical Engineering*. ITB. Bandung.

----------. 2004. Catatan Kuliah Pengujian Tanah Lanjut Program Pascasarjana Teknik Sipil Bidang Keahlian Geoteknik ITS Surabaya.

Gouw T.L. 2010. Computational Geotechnic Course Geotomo Software. July 2011. Manual Res2dinv Ver 3.71. Malaysia.

Mochtar Indrasurya.B. 2000. *Teknologi Perbaikan Tanah dan Alternatif Perencanaan Pada Tanah Bermasalah*. ITS Surabaya.

Mochtar,B Indrasurya. 2012 Kenyataan Lapangan Sebagai Dasar Untuk Usulan Konsep Baru Tentang Analisa Kuat Geser Tanah dan Kestabilan Lereng. *Pertemuan Ilmiah Tahunan Himpunan Ahli Teknik Tanah Indonesia*. PIT HATTI 2012.

Plaxis BV. 2007. Manual Plaxis Versi 8.6 Bahasa Indonesia.

Plaxis BV.2011. Manual Plaxis versi 2011. Netherlands: Balkema Publisher.

Zhang, Ga, Wang, Rui, Qian, Jiyun, Zang, Jian-Min, dan Qian, Jiangu. 2012. Effect Study of Crack on Behavior of Soil Slope under Rainfall Conditions. *Soils and Foundations*: 634-643.

Zhou, Y. D., Cheuk, C. Y., Tham, L. G. 2009. Deformation and Crack Development of a Nailed Loose Fill Slope Subjected to Water Infiltration. *Landslides* Vol 6: 299-308.

Zhou, Y. F., Tham, L. G. dan Yan, R. W. M. et al. 2014. *The Mechanism of Soil Failures Along Crack Subjected to Water Infiltration*. Elsavier: 330-341.

Linear Shrinkage and its Correlation to the Shrinkage Limit and Index Properties of Kaolinite, Bentonite, and Eight Bandung Fine-Grained Soils

Ignatius Tommy Pratama
Department of Civil Engineering – Parahyangan Catholic University

Ana Yelina Arif
Department of Civil Engineering – Parahyangan Catholic University

Budijanto Widjaja
Department of Civil Engineering – Parahyangan Catholic University

ABSTRACT: Linear shrinkage test is a laboratory test for measuring the linear shrinkage ratio of a soil sample that passes a 0.425 mm sieve. Linear shrinkage can also be determined from the shrinkage limit using correlations. Thus, this paper aims to study the relationships between linear shrinkage ratio and shrinkage limit determined by the wax and mercury methods, and also the activity, plasticity index, and the clay content of kaolinite, bentonite, and also eight fine-grained soils obtained from eight different places in Greater Bandung. The results indicate there was an inconsistent relationship between the linear shrinkage ratio and soil activity. Then, the shrinkage limits from the mercury and the wax methods could produce a good estimate of the linear shrinkage ratio. It was also found that the linear shrinkage ratio was directly proportional to the plasticity index and clay content of the soils and inversely proportional to the shrinkage limit values.

Keywords: linear shrinkage, shrinkage limit, plasticity index, clay content

1 INTRODUCTION

Moisture content plays a significant role in determining the state of soil (i.e., liquid state, plastic state, semi-solid state, and solid-state). As the moisture content decrease due to evaporation, the volume of clay-rich soil will reduce and the soil state will change. Soil shrinkage is a phenomenon where the soil state changes from semi-solid state to solid-state and the moisture content at this phase transition is called shrinkage limit (Hazarika and Ishibashi, 2015). Under such conditions, no further volume change will occur. It is also worth noting that soil shrinkage will result in cracks in the soil. The cracks make the soil more permeable to water and may damage the geotechnical structures (Stirk, 1954; Peron et al., 2009). Thus, it is necessary to understand the soil shrinkage behavior and its properties, such as shrinkage limit.

The two common methods to estimate the shrinkage limit of soil are the mercury (ASTM D427:2004) and the wax (ASTM D4943:2008) shrinkage limit tests. In addition, the shrinkage limit of soil can also be determined from the linear shrinkage ratio obtained from the linear shrinkage test (BS 1377-2:1990). According to Altmeyer (1956), a linear shrinkage test could also be used to observe the soil shrinkage behavior and its expansive tendencies. In the linear shrinkage test, the initial length of the soil sample at which the moisture content is at the liquid limit and the oven-dried length are measured to obtain the ratio of the shrinkage length to the initial length. This ratio is later called the linear shrinkage ratio.

Cerato and Lutenegger (2006) showed that both the linear shrinkage test and the mercury shrinkage limit test could produce similar shrinkage curves (i.e., the volume of soil to the moisture content curve) and suggested that the linear shrinkage test could be a surrogate test to the mercury shrinkage limit test. This also signifies that both tests could produce a similar shrinkage limit value. However, the wax shrinkage limit test could be carried out to extend and confirm the results of Cerato and Lutenegger's (2006) study. Later, Widjaja and Chriswandi (2020) studied the correlation between the linear shrinkage ratio and the shrinkage limits obtained from various previous studies. They found that the linear shrinkage ratio was inversely proportional to the shrinkage limit.

Furthermore, some researchers proposed empirical correlations between either linear shrinkage ratio or shrinkage limit and soil plasticity index and/or soil liquid limit. Whitlow (1995) recommended an empirical equation to estimate the plasticity index of soil from the linear shrinkage ratio. Budhu (2011) suggested an empirical equation to estimate shrinkage limit from liquid limit and plasticity index. This may signify that the shrinkage behavior of a soil correlated to soil liquid limit and plasticity index. However, Sridharan and Prakash (1998) and Izdebska-Mucha and Wójcik (2013) showed that no satisfactory correlation was exhibited between the soil shrinkage limit and soil plasticity. Sridharan and Prakash (1998) suggested that the shrinkage limit of soil was primarily controlled by the relative grain size distribution of the soil, not the soil plasticity characteristics.

The above findings from many researchers may indicate that although many studies had been conducted, further studies are still required to confirm and to understand the shrinkage behavior of soil. Thus, this paper aims to study the relationship between the linear shrinkage ratio obtained from the linear shrinkage test and shrinkage limits produced by the mercury and the wax shrinkage limit tests. In addition, the relationships between the linear shrinkage ratio and the soil activity, percentage of clay particles, and the soil plasticity index were also investigated. The laboratory shrinkage tests were carried out on kaolinite, bentonite, and eight fine-grained soils obtained from eight different places in Greater Bandung. The results will then be discussed in the following chapters.

2 SHRINKAGE TEST METHODS

2.1 *Linear Shrinkage Test*

The testing procedure for the linear shrinkage test is based on BS 1377-2:1990. The linear shrinkage test used a 150 g soil sample that particle sizes smaller than a 425-μm sieve. The testing procedure was started by remolding the soil samples with distilled water to form soil paste until the moisture content was at about the liquid limit of the soils. Next, the sample was put and leveled on the shrinkage mold (as shown in Fig. 1). In this phase, the initial moisture content and its weight were measured before being dried at room temperature for about 24 hours. The drying was continued in the oven at a temperature not greater than 65 °C until shrinkage has largely ceased, and then at about 105 °C to 100 °C for 24 hours to complete the drying. Eventually, the length and weight of the oven-dried soil samples were measured. The percentage of linear shrinkage was calculated as:

$$LS_T = \left(1 - \frac{L_D}{L_0}\right) 100 \quad (1)$$

where LS_T is the linear shrinkage percentage, L_0 is the initial length of the soil sample (mold length), and L_D is the dried sample length. Later, in this paper, the LS_T was obtained from Eqn. (1) is also regarded as the tested linear shrinkage ratio.

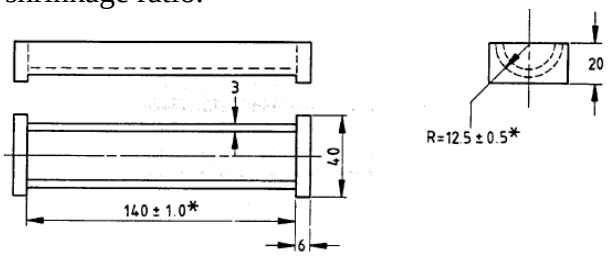

Fig. 1. Mold Dimension in Millimeters for Linear Shrinkage Test (BS 1377-2:1990).

2.2 *Mercury and Wax Methods Correlation*

Linear shrinkage ratio can also be calculated by using correlation from shrinkage limit. Meanwhile, shrinkage limits can be obtained from two methods, which are the mercury method (ASTM D427:2004) and the wax method (ASTM D4943:2008). Similarly, those tests used soil samples that passed the 425-μm sieve. In the shrinkage limit tests, the soil sample was firstly remolded with distilled water to form the soil paste until its consistency was at about the liquid limit. Then, the samples were oven-dried at about 110 °C for 24 hours. For the wax shrinkage limit test, the oven-dried soil samples should be firstly coated with wax to prevent water absorption. Next, for the mercury method, the oven-dried samples were immersed into the mercury, and then the displaced mercury was weighted. Similarly, for the wax method, the wax-coated samples were immersed into water and the displaced water was weighted. Eventually, the shrinkage limit (*SL*) can be calculated as follows:

$$SL = w_1 - \left[\frac{(V - V_d)\rho_w}{m_s}\right] \times 100 \quad (2)$$

where w_1 is initial water content, V is initial sample volume, V_d is dried sample volume, m_s is dried soil mass, and ρ_w is water density.

To determine the linear shrinkage ratio (*LS*), the shrinkage ratio (*R*) and the volumetric shrinkage (V_s) should be firstly computed by using the following equations:

$$R = \frac{m_s}{V_d \times \rho_w} \quad (3)$$

$$V_s = R(w_1 - SL) \quad (4)$$

The *LS* value can then be expressed as follows:

$$LS = 100\left[1 - \left(\frac{100}{V_s + 100}\right)^{\frac{1}{3}}\right] \quad (5)$$

3 RESULTS AND DISCUSSIONS

The shrinkage limit tests and the linear shrinkage tests were carried out on ten fine-grained soil samples. The samples consist of eight samples obtained from fields in the Greater Bandung area, kaolinite soil, and bentonite soil. In addition, the index properties and Atterberg's limits tests, such as water content (*w*), plastic limit (*PL*), and liquid limit (*LL*) tests, and also the sieve and hydrometer tests were also conducted to know the physical properties, clay content (%Clay), and the classification of the soils. The laboratory test results of index properties and clay content are shown in Table 1. In Table 1, *PI* means plasticity index which is equal to *LL* – *PL*.

Table 1. Index Properties and Clay Content Laboratory Test Results.

Soil Samples	w_1 (%)	*PL*	*PI*	% Clay	USCS[a]
Kaolinite	1.5	34	38	49.6	CH
Bentonite	21.0	44	52	39.9	MH
Lembang	46.6	43	21	11.1	MH
Loc. 1	45.1	40	18	30.3	MH
Loc. 2	61.0	33	30	39.5	MH
Loc. 3	65.8	47	17	17.4	MH
Loc. 4	66.5	44	14	26.1	MH
Setiabudi	34.6	37	21	30.5	MH
Punclut	49.6	42	36	68.6	MH
Buah Batu	41.6	28	36	29.0	CH

Note: [a]USCS is a Unified Soil Classification System.

3.1 *Linear Shrinkage Test and Soil Activity*

Table 2 shows the results of the linear shrinkage test. The L_0 and L_D values in Table 2 were used to obtain LS_T by using Eqn. (1). The LS_T value shown in Table 2 (except kaolinite and bentonite) ranges from 6.4% to 18.7%. Meanwhile, the LS_T value for the kaolinite and bentonite samples is 8.9% and 23.9%, respectively. These results signify that the bentonite sample had the highest volume change due to soil shrinkage, whereas the Loc. 1 sample had the lowest volume change.

Table 2. Linear Shrinkage Test Results.

Soil Samples	L_0 (cm)	L_D (cm)	LS_T (%)
Kaolinite	14.1	12.8	8.9
Bentonite	14.1	10.7	23.9
Lembang	14.0	13.1	6.4
Loc. 1	14.1	12.6	10.4
Loc. 2	14.0	12.1	14.1
Loc. 3	14.1	12.9	8.4
Loc. 4	14.1	12.7	10.3
Setiabudi	14.0	12.2	13.4
Punclut	14.1	11.4	18.7
Buah Batu	14.0	11.8	16.2

Table 3. Soil Activities (A).

Soil Samples	*A*	Soil Sample	*A*
Kaolinite	0.77	Loc. 3	0.96
Bentonite	1.30	Loc. 4	0.54
Lembang	1.90	Setiabudi	1.01
Loc. 1	1.35	Punclut	0.52
Loc. 2	0.76	Buah Batu	1.24

Soil activity (*A*) is a parameter that is commonly used to characterize the swelling and shrinkage potential of clay-rich soils, Hazarika and Ishibashi (2015). The *A* value is expressed by the ratio between *PI* and %Clay, Skempton (1953). The higher the *A* value, the higher the potential of the soil to shrink and swell. However, according to the results of this study, there was no clear relationship between the *A* and the LS_T values. As shown by Table 3 where it shows the *A* values for all soil samples and Table 2, although the bentonite soil and Loc. 1 soil samples were both classified as active soils according to Budhu (2011), the bentonite soil sample with *A* = 1.3 had the highest LS_T value whereas the Loc. 1 sample with *A* = 1.9 had the lowest LS_T value. Furthermore, the inactive soil samples with A <

0.75, Budhu (2017) such as Loc .4 soil and Punclut soil samples showed a higher LS_T value than the LS_T value of the normal soil samples with A value ranging from 0.75 to 1.25, Budhu (2011) such as the kaolinite soil and Loc. 3 soil samples. These show that the A and the LS_T values had an inconsistent relationship. This might be caused by the shrinkage mechanism of soil which was not controlled by the soil plasticity characteristics such as PI value, Sridharan and Prakash (1998).

3.2 *Shrinkage Limit Test and Correlation to Linear Shrinkage*

The comparison of the shrinkage limits obtained from wax (SL_W) and mercury (SL_M) methods are shown in Fig. 2. Fig. 2 indicates that the wax and mercury methods could produce similar shrinkage limits since the shrinkage limit values were close to the $SL_M = SL_W$ line.

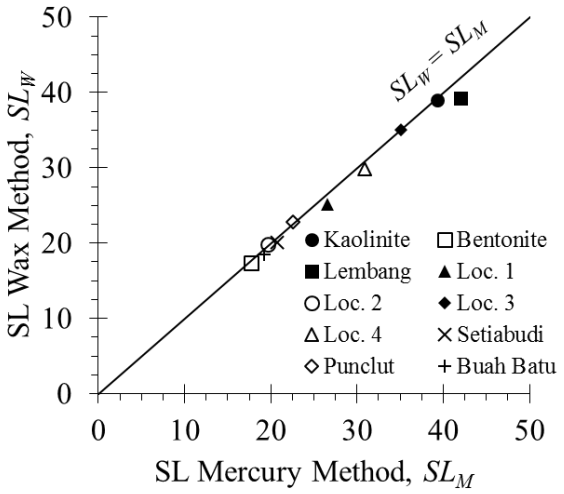

Fig. 2. Shrinkage Limit Comparison of Wax and Mercury Methods.

After obtaining the shrinkage limit, Eqns. 3 to 5 were then used to calculate the correlated linear shrinkage. Later, the linear shrinkage ratio obtained from SL_W is denoted as LS_W, whereas the linear shrinkage ratio obtained from SL_M is denoted as LS_M. The comparison between LS_T and LS_M is shown in Fig. 3, whereas for LS_T vs. LS_W is exhibited in Fig. 4. Figs. 3 and 4 show that the linear shrinkage obtained from mercury and wax methods was close to the linear shrinkage ratio obtained from the linear shrinkage test. This was signified by the data points which are located close to the $LS_M = LS_T$ or $LS_W = LS_T$ line. This may also indicate that either the mercury or wax shrinkage limit tests could be used to estimate the linear shrinkage ratio.

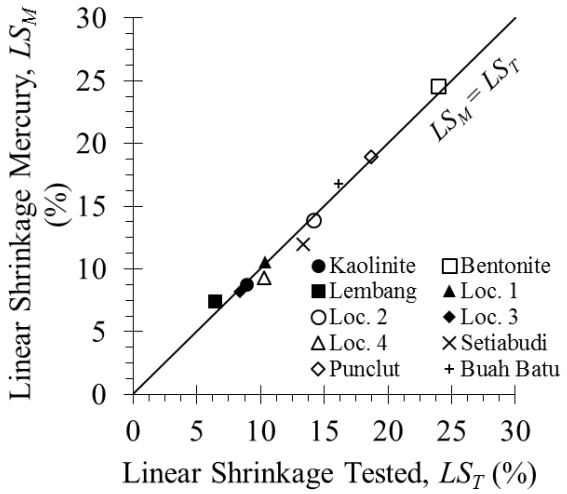

Fig. 3 Comparison between LS_T and LS_M.

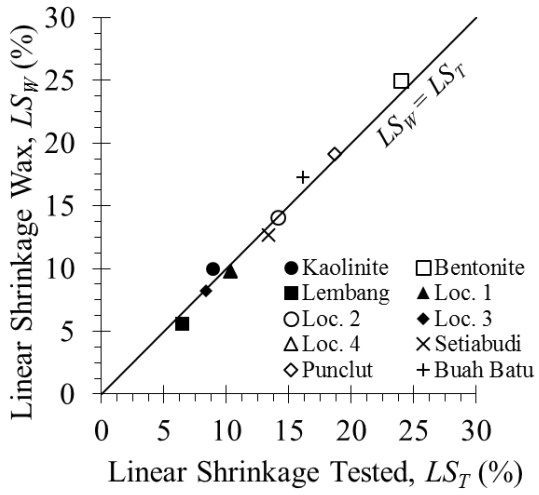

Fig. 4 Comparison between LS_T and LS_W.

3.3 *Correlation with Plasticity Index and Clay Content*

The correlation between plasticity index (PI) and clay content (%Clay) with the tested linear shrinkage (LS_T) was also studied in this paper. Fig. 5. and Fig. 6 show the relationship between LS_T and PI and LS_T and the clay content, respectively. The figures show that a larger PI value and the clay content could produce higher LS_T. However, the results (Figs. 5 and 6) signify that based on the R^2 values, the correlation between LS_T and PI and LS_T and the clay content showed no satisfactory relationship, since the criteria for R^2 value of 0.8 could not be achieved. Therefore, the correlations that were derived from Fig. 5 and Fig. 6 could only be interpreted as both properties are directly proportional with linear shrinkage and

inversely proportional with shrinkage limit. The previous research by Earl (2005) indicated that the equation for *PI* needs to be adjusted for the clay and silt content in the soil sample to achieve the minimum R^2 value of 0.8. Additional sampling is also required to minimize the possible outliers and result in a more accurate estimating equation.

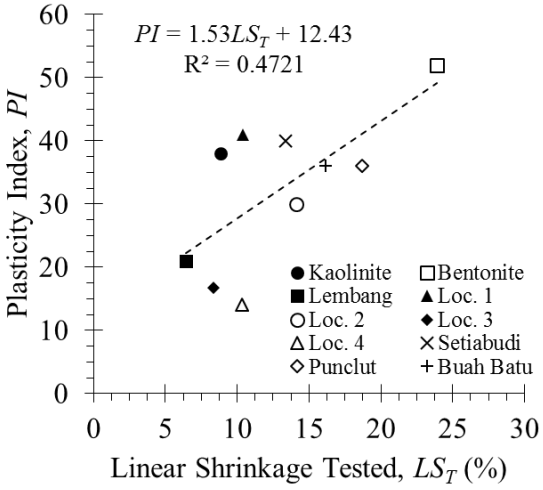

Fig. 5 Correlation between LS_T and PI.

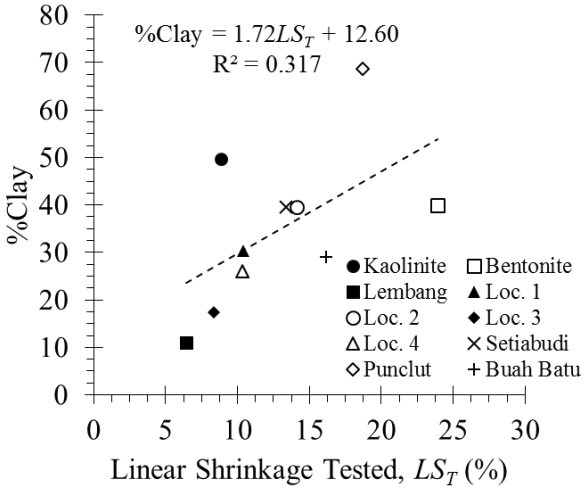

Fig. 6 Correlation between LS_T and clay content.

4 CONCLUSION

This paper studies relationship between shrinkage limit and linear shrinkage ratio of eight Bandung fine-grained soil samples together with the kaolinite and bentonite soils samples. In addition, the relationships between linear shrinkage ratio and soil activity, plasticity index, and clay content were also investigated. It was found that there was no consistent relationship between the linear shrinkage ratio and soil activity. It was hypothesized for the reason that the shrinkage mechanism of soils was not controlled by the soil plasticity characteristics. Thus, further investigation on clay mineralogy with a higher number of samples was suggested to obtain a comprehensive result. Furthermore, the linear shrinkage ratio could be estimated by using the shrinkage limit obtained from either the mercury or the wax methods. Considering the similar results obtained from both mercury and wax methods, it was worth noting that the wax method was more preferable to be adopted for further studies because mercury was highly toxic to the environment. As for the relationship between plasticity index and clay content and linear shrinkage ratio, it was found that plasticity index and clay content were directly proportional with linear shrinkage and inversely proportional with shrinkage limit. More samples were required to validate the results of this study. Furthermore, some modifications on the percentage silt and clay contents might be required to obtain a more accurate estimation of the relationship between linear shrinkage and plasticity index, and clay content.

ACKNOWLEDGEMENTS

Special thanks to Viqbalias Thifaldi, Cecilia Andriana, and Derry Triady for providing their research data for this paper.

REFERENCES

Albrecht, Brian A. & Craig H. Benson. 2001. Effect of Desiccation on Compacted Natural Clays. *Journal of Geotechnical and Geo-environmental Engineering* 127(1): 67-75.

Altmeyer, W.T. 1956. Discussion following paper by Holtz and Gibbs. *Transactions of the American Society of Civil Engineers* 2(1): 666-669

ASTM D427. 2004. *Standard Test Method for Shrinkage Factors of Soils by the Mercury Method*. ASTM International.

ASTM D4943. 2008. *Standard Test Method for Shrinkage Factors of Soils by the Wax Method*. ASTM International.

Budhu, M (3rd ed.). 2011. *Soil Mechanics and Foundations.* Hoboken: John Wiley & Sons.

BS 1377-2. 1990. *British Standard Methods of Test for Soils for Civil Engineering Purposes: Part 2. Classification Tests.* British Standards Institution.

Peron, H., Hueckel, T., Laloui, L. & Hu, L. 2009. Fundamentals of Desiccation Cracking of Fine-Grained Soils: Experimental Characterisation and

Mechanisms Identification. *Canadian Geotechnical Journal* 46(10): 1177-1201.

Cerato, A.B. & Lutenegger, A.J. 2006. Shrinkage of Clays. *Unsaturated Soils 2006:* 1097-1108.

Das, B.M (7th ed.). 2010. *Principles of Geotechnical Engineering.* Stamford: Cengage Learning.

Earl, D. 2005. To Determine if There is a Correlation Between the Shrink Swell Index and Atterberg Limits for Soils within the Shepparton Formation. University of Southern Queensland.

Ishibashi, I. & Hazarika, H (2nd ed.). 2015. *Soil Mechanics Fundamentals and Applications*. Boca Raton: CRC Press.

Izdebska-Mucha, D. & Wójcik, E. 2013. Testing Shrinkage Factors: Comparison of Methods and Correlation with Index Properties of Soils. *Bulletin of Engineering Geology and the Environment 72*(1): 15-24.

Ledesma, A. 2016. Cracking in Desiccation Soils, E3S Web of Conferences. *3rd European Conference on Unsaturated Soils* – "E-UNSAT 2016" 9(2016): 03005.

Sánchez, M., Wang, D., Briaud, J.L. & Douglas, C. 2014. Typical Geomechanical Problems Associated with Railroads on Shrink-Swell Soils. *Transportation Geotechnics* 1(4): 257–274.

Skempton, A.W. 1953. The Colloidal Activity of Clays. *the Third International Conference of Soil Mechanics and Foundation Engineering* (1):57-61.

SNI 4144:2012. *Metode Uji Penentuan Faktor-Faktor Susut Tanah*. Jakarta: Badan Standardisasi Nasional.

Stirk, G.B. 1954. Some Aspects of Soil Shrinkage and the Effect of Cracking upon Water Entry into the Soil. *Australian Journal of Agricultural Research* 5(2): 279-296.

Widjaja, B. & Chriswandi, C. 2020. New Relationship between Linear Shrinkage and Shrinkage Limit for Expansive Soils. *IOP Conference Series: Materials Science and Engineering* 1007(1): 012187.

Whitlow, R (3rd ed.). 1995. *Basic Soil Mechanics*. Harlow: Addison Wesley Longman Limited.

Evaluasi Korelasi Indeks Kompresi Tanah Lempung Indonesia

Erza Rismantojo
Program Studi Teknik Sipil, Fakultas Teknik Sipil dan Lingkungan – Institut Teknologi Bandung

Rizal Maulana
Program Magister, Program Studi Teknik Sipil, Fakultas Teknik Sipil dan Lingkungan – Institut Teknologi Bandung

Fadlli Ash-Shidiqqy
Program Magister, Program Studi Teknik Sipil, Fakultas Teknik Sipil dan Lingkungan – Institut Teknologi Bandung

ABSTRAK: Tulisan ini membahas berbagai model korelasi terpublikasi untuk memprediksi indeks kompresi C_c dan kesesuaiannya untuk tanah lempung Indonesia. Data tanah yang digunakan di dalam penelitian ini berasal dari berbagai lokasi di Pulau Jawa, Sumatera, Kalimantan, dan Papua. Banyak hasil penelitian yang menemukan hubungan antara C_c tanah lempung dengan properti indeksnya seperti kadar air, batas cair, dan angka pori. C_c tanah yang digunakan untuk penelitian ini memiliki korelasi yang kuat dengan kadar airnya sehingga digunakan sebagai prediktor utama. Kesesuaian beberapa persamaan regresi terpublikasi yang menggunakan kadar air sebagai prediktor dievaluasi dan diperoleh beberapa persamaan regresi yang mampu memprediksi C_c tanah lempung Indonesia terutama untuk tanah dengan C_c kurang dari 0,8.

Kata Kunci: indeks kompresi, korelasi, regresi, tanah lempung

ABSTRACT: This paper discusses various published correlation models for predicting compression index C_c and their applicability for Indonesian clay soils. The soil data used in this study is collected from various locations in Indonesia including Java, Sumatra, Kalimantan, and Papua. Many researchers have reported various relations between C_c of clays with their index properties such as moisture content, liquid limit, and void ratio. C_c of soil usedin this study have been found to strongly correlate with their water content. The applicability of selected correlation models with water content as their predictor is evaluated and this study found that several of the regression models may be used to predict C_c of Indonesia clays especially for soils with C_c of less than 0.8.

Keywords: compression index, correlation, regression, clay

1 PENDAHULUAN

Compression index (C_c) adalah salah satu parameterkompresibilitas tanah lempung yang digunakan untuk menentukan besarnya penurunan konsolidasi. Parameter C_c biasanya tidak segera tersedia pada tahap awal desain karena parameter ini ditentukan dengan uji oedometer yang memerlukan waktu pengerjaan sekitar sepuluh sampai empat belas haribahkan lebih jika pengujian melibatkan proses siklus *unloading-reloading* di sekitar beban tegangan prakonsolidasi untuk mendapatkan indeks rekompresi (C_r) yang akurat.

Banyak penelitian yang menemukan hubungan antara C_c dengan parameter tanah lainnya, seperti di antaranya kadar air, batas cair, dan angka pori, dengan tujuan untuk mendapatkan perkiraan awal harga C_c karena parameter kadar air dan batas cair dapat diperoleh dengan cepat. Permasalahan muncul karena korelasi yang terpublikasi tergantung pada karakteristik tanah lokal dan tidak selalu dapat digunakan di lokasi yang berbeda. Hal ini terlihat dari jenis prediktor yang digunakan di dalam persamaan regresi yang dihasilkan dan lokasidi mana persamaan tersebut dihasilkan. Misalnya Skempton (1944) menemukan bahwa batas cair adalah prediktor yang baik untuk *remolded clays* sedangkan Peck dan Reed (1954), Cozzolino (1961), Nishida (1956), dan Hough (1957) menemukan angka pori sebagai prediktor yang baik untuk tanah asli yang berasal dari lokasi tempat mereka melakukan

penelitian. Peneliti lain seperti Moran et al. (1958) dan Peck dan Reed (1954)menemukan kadar air sebagai prediktor yang baik sedangkan Cherubini (1991) dan Al-Khafaji dan Andersland (1992) menggunakan angka pori bersama dengan batas cair sebagai dua prediktor di dalam persamaan regresinya. Azzouz et al. (1976), menggunakan tanah lempung dari Yunani dan Amerika, juga menemukan angka pori sebagai prediktor yang baik dan keakuratan prediksinya tidak bertambah signifikan jika prediktornya ditambah dengan kadar air, dan/atau batas cair tetapiAzzouz et al. (1976) menemukan bahwa kadar air sebagai prediktor kedua terbaik setelah angka pori. Korelasi-korelasi yang dihasilkan oleh para peneliti ini umumnya berbentuk persamaan regresi linear dengan satu atau dua variabel.

Berdasarkan hasil penelitian terdahulu maka dapat dipastikan bahwa pemilihan predictor menjadi tahapan yang paling penting dan hal ini dilakukan tidak saja berdasarkan analisis statistik tetapi juga berdasarkan pemahaman geoteknik terkait pengaruh dari karakteristik tanah terhadap perilaku kompresibiltasnya. Secara umum penelitian-penelitian ini melaporkan angka pori, kadar air, dan batas cair sebagai prediktor yang memiliki pengaruh paling signifikan terhadap *compression index* tanah lempung dan lanau. Dari ketiga prediktor tersebut kadar air adalah parameteryang paling mudah dan cepat diperoleh dan juga memiliki metode pengujian dengan tingkat kesalahan yang rendah.

Tulisan ini berisi hasil penelitian untuk data tanah yang berasal dari beberapa lokasi di Sumatera,Jawa, Kalimantan, dan Papua. Pada saat tulisan ini dibuat tersedia 347 data yang digunakan untuk mengevaluasi kesesuaian beberapa korelasi empiristerpublikasi terhadap tanah Indonesia.

2 KARAKTERISTIK TANAH

Tabel 1 menampilkan karakteristik statistik *index properties* dan C_c dari data tanah yang digunakan di dalam penelitian ini. Sebanyak 25% memiliki derajat saturasi kurang dari 91% dengan kandungan lolos saringan No. 200 kurang dari 87%. Berdasarkan *Unified Soil Classification System* (USCS) tanah-tanah ini terdiri atas 257 CH, 22 CL, 43 MH, 6 ML, 10 SC, dan 9 SM. Klasifikasi kandungan butiran halus, yaitu material lolos saringan No. 40, berdasarkan batas cair dan indeks plastisitasnya dapat dilihat pada Gbr. 1. Benda uji dari semua tanah ini dapat dibentuk, termasuk tanah yang mengandung pasir (SC dan SM), dan diuji dengan oedometer beban bertahap.

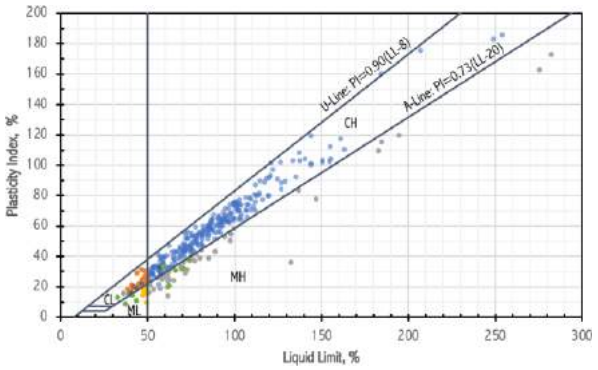

Gbr. 1. *Plasticity Chart*.

Tanah yang digunakan untuk penelitian ini, berdasarkan Kulhawy dan Mayne (1990), terdiri dari 55% memiliki kompresibilitas tinggi dengan harga Cc > 0.4, 43% kompresiblitas sedang dengan $0.2 \leq Cc \leq 0.4$ dan 2% kompresibilitas rendah dengan Cc < 0.2.

3 KORELASI ANTAR PARAMETER

Seperti sudah dijelaskan sebelumnya bahwa banyak penelitian terpublikasi menemukan kadar air, batas cair, dan angka pori sebagai parameter yang paling sering terdeteksi memiliki korelasi yang baik dengan *compression index*.

Korelasi di antara ketiga parameter ini termasuk dengan compression index dapat dilihat pada Gbr. 2 dalam bentuk matriks korelasi. Di dalam masing-masing gambar tertera juga harga koefisien korelasi di antara parameter-parameter tersebut. Hubungan antara Cc dengan kadar air yang memiliki koefisien korelasi terbesar, r = 0.82, menunjukkan adanya hubungan yang kuat di antara kedua parameter tersebut. Terlihat juga hubungan yang cukup kuat di antara Cc dengan angka pori dengan koefisien korelasi r = 0.78. Berdasarkan koefisien korelasi ini maka kadar air dan angka pori dapat menjadi kandidat yang baik sebagai prediktor Cc. Perlu diperhatikan bahwa kadar air dan angka pori memiliki korelasi yang kuat dengan r = 0.96 sehingga kedua parameter tersebut tidak dianjurkan berada di dalam satu persamaan regresi.

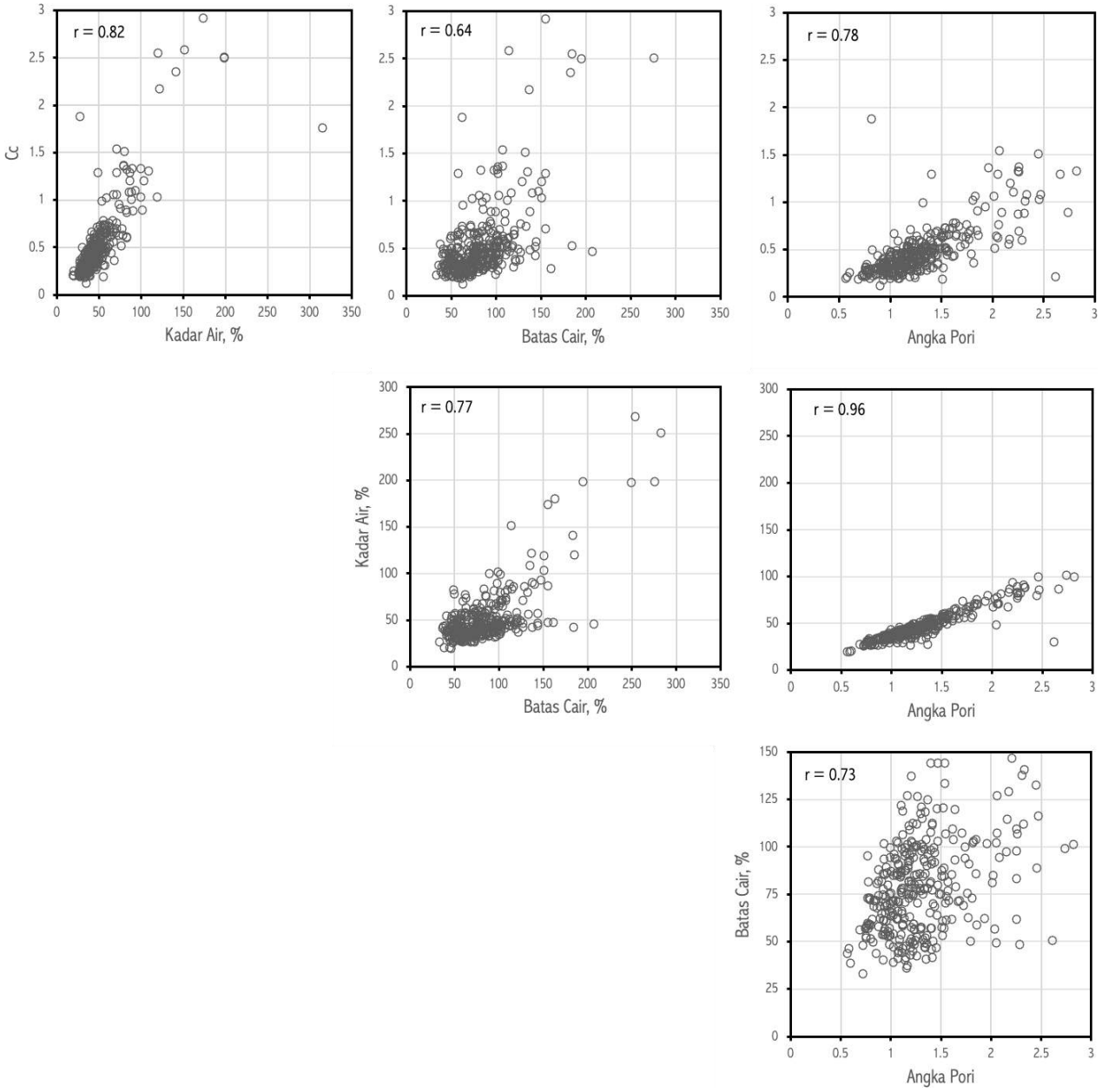

Gbr. 2. Matriks Korelasi.

4 EVALUASI PERSAMAAN REGRESI

Berdasarkan adanya korelasi yang kuat antara C_c dan kadar air dari tanah-tanah ini maka kami melanjutkan dengan melakukan evaluasi terhadap persamaan-persamaan regresi terpublikasi yang menggunakan kadar air sebagai prediktor dari beberapa peneliti seperti yang tertera di Tabel 2, Bogireddy et al. (2017). Kesesuaian persamaan regresi ini untuk tanah yang kami miliki dievaluasi dengan cara membandingkan bias, RMSE (*root mean squared error*), dan *coefficient of variance* (COV) dari error. Bias, *b*, adalah perbandingan antara harga aktual dengan harga perkiraan. Harga bias rata-rata, $\bar{b}$, untuk masing-masing persamaan regresi adalah jumlah harga bias masing-masing data dibagi dengan jumlah data. Persamaan regresi yang memiliki harga $\bar{b}$ sama dengan satu artinya persamaan tersebut tidak memiliki bias terhadap data pengamatan. RMSE menunjukkan tingkat keakuratan persamaan regresi sedangkan COV dari eror memperlihatkan variasi penyebaran eror terhadap harga rata-rata eror.

Hasil perhitungan harga $\bar{b}$, eror rata-rata, standar deviasi eror, COV eror, dan RMSE untuk masing- masing persamaan regresi terhadap data yang kami miliki dapat dilihat di Tabel 3. Beberapa persamaan regresi yang memiliki harga $\bar{b}$ hampir satu, dengan RMSE

yang relatif kecil di antara persamaan- persamaan yang ada, adalah persamaan regresi dari Moran & Rutledge (1958) dan Bowles (1989). Plot yang memperlihatkan hubungan antara harga Cc aktual dengan harga perkiraan dari masing-masing persamaan regresi tersebut dapat dilihat pada Gbr. 3 dan 4.

Table 1. Karakteristik Statistik Data.

Parameter	n	*Min*	25%(1)	50%(2)	75%(3)	*Max*	*Mean*	*Standard Deviasi*	COV
w_n	347	20	37	43	54	315	52	33	0,64
e_0	347	0,56	1,04	1,22	1,51	8,92	1,45	0,89	0,62
Sr	347	49	91	96	99	100	94	7	0,07
F_{200}	347	20	87	97	99	100	89	17	0,19
LL	347	33	59	78	99	402	85	39	0,46
PL	347	15	24	28	33	118	31	12	0,40
PI	347	9	32	49	67	284	54	31	0,58
C_c	347	0,12	0,32	0,44	0,59	5,73	0,58	0,59	1,02

Catatan: (1) 25% data berada di bawah nilai yang tertera
(2) Median
(3) 75% data berada di atas nilai yang tertera

Tabel 2. Persamaan Regresi.

Persamaan Regresi	Referensi	Lokasi
$C_c = 0.000176w^2 + 0.00593w - 0.135$	Peck and Reed (1954)	Chicago subsoils
$C_c = 0.0054(2.6w_n - 35)$	Nishida (1956)	Undisturbed clays
$C_c = 0.0102(w_n - 9.15)$	Hough (1957)	Inorganic cohesive soil: silt, silty clay
$C_c = 0.0115w_n$	Moran & Rutledge (1958)	Soft clays
$C_c = 0.01w_n$	Osterberg (1972)	Chicago clay, (Normally consolidated, St<1.5)
$C_c = 0.01(w_n - 5)$	Azzouz et. al. (1976)	USA and Greece Clay
$C_c = 0.01(w_n - 7.549)$	Herrero (1980)	All clays
$C_c = 0.01w_n$	Koppula (1981)	Chicago and Alberta clays, (Normally consolidated, St < 1.5)
$C_c = 0.0102(w_n - 9.15)$	Serajuddin (1987)	Alluvial clay and silt inBangladesh
$C_c = 0.0115w_n$	Bowles (1989)	Organic silt and clays (Normally consolidated, St < 1.5)
$C_c = 0.0066w_n$	Abdrabbo & Mahmoud(1990)	Egyptian clays with (20% < w_n < 140%)
$C_c = 0.012w_n - 0.1$	Lav & Ansal (2001)	Soil in Turkey
$C_c = 0.01(w_n + 2.83)$	Yoon et al. (2004)	Busan clay
$C_c = 0.0091w_n + 0.0522$	Solanki and Desai (2008)	Alluvial deposits, Surat, India
$C_c = 0.0072(w_n - 12.625)$	Vinod and Bindu (2010)	Remoulded, highly plastic,marine clays, Kerala, Ind
$C_c = 0.013w_n - 0.115$	Park and Lee (2011)	Soils in Korea
$C_c = 0.0074w_n - 0.007$	Kalantary & Afshin (2012)	Clayey soils, Mazandaran, Iran
$C_c = 0.014(w_n - 22.7)$	Bryan et al. (2014)	Irish soft soils
$C_c = 0.0102(w_n + 11.57)$	Widodo & Abdelazim (2012)	Pontianak soft clay, Indonesia
$C_c = 0.0136w_n + 0.0156$	Sari & Firmansyah (2013) (1)	Surabaya soft soil, Indonesia (w_n = 0 - 150%; PI = 0 - 70%)

Persamaan Regresi	Referensi	Lokasi
$C_c = 0.0141w_n + 0.0078$	Sari & Firmansyah (2013) (2)	Surabaya soft soil, Indonesia (w_n = 0 - 150%; PI = 0 - 120%)
$C_c = 0.0143w_n - 0.0165$	Sari & Firmansyah (2013) (3)	Surabaya soft soil, Indonesia (w_n = 0 - 100%; PI = 0 - 70%)
$C_c = 0.0327w_n - 0.3819$	Sari & Firmansyah (2013) (4)	Surabaya soft soil, Indonesia (w_n = 0% - 30%)
$C_c = 0.0179w_n - 0.1005$	Sari & Firmansyah (2013) (5)	Surabaya soft soil, Indonesia (w_n = 30% - 50%)
$C_c = 0.0137w_n + 0.0034$	Sari & Firmansyah (2013) (6)	Surabaya soft soil, Indonesia (w_n = 50% - 70%)

Tabel 3. Hasil Evaluasi Beberapa Persamaan Regresi Terpublikasi untuk Semua Tipe Tanah yang Tersedia.

Persamaan Regresi	*Mean Bias*	*Mean Error*	*Standard Deviation*	*Absolute COV Error*	*RMSE*
Nishida (1956)	1,12	0,04	0,34	7,61	0,34
Park and Lee (2011)	1,04	0,02	0,34	14,12	0,34
Moran & Rutledge (1958)	0,93	-0,01	0,35	26,82	0,35
Bowles (1989)	0,93	-0,01	0,35	26,82	0,35
Lav & Ansal (2001)	1,10	0,06	0,35	5,75	0,36
Sari & Firmansyah (2013) (6)	0,78	-0,13	0,34	2,61	0,36
Sari & Firmansyah (2013) (3)	0,77	-0,14	0,34	2,40	0,37
Sari & Firmansyah (2013) (1)	0,77	-0,14	0,34	2,48	0,37
Sari & Firmansyah (2013) (2)	0,75	-0,16	0,34	2,19	0,37
Yoon et al. (2004)	1,01	0,04	0,37	10,38	0,37
Widodo & Abdelazim (2012)	0,84	-0,06	0,37	5,77	0,37
Osterberg (1972)	1,07	0,06	0,37	5,80	0,38
Koppula (1981)	1,07	0,06	0,37	5,80	0,38
Bryan et al. (2014)	1,73	0,18	0,34	1,93	0,38
Azzouz et. al. (1976)	1,21	0,11	0,37	3,26	0,39
Solanki and Desai (2008)	1,04	0,06	0,39	6,60	0,39
Herrero (1980)	1,29	0,14	0,37	2,67	0,40
Hough (1957)	1,33	0,15	0,37	2,51	0,40
Serajuddin (1987)	1,33	0,15	0,37	2,51	0,40
Sari & Firmansyah (2013) (5)	0,69	-0,24	0,35	1,46	0,43
Kalantary & Afshin (2012)	1,48	0,21	0,42	2,02	0,46
Abdrabbo&Mahmoud (1990)	1,62	0,24	0,43	1,80	0,49
Vinod and Bindu (2010)	2,12	0,30	0,42	1,40	0,51
Sari & Firmansyah (2013) (4)	0,45	-0,73	0,68	0,94	1,00
Peck and Reed (1954)	1,05	-0,25	1,30	5,22	1,33

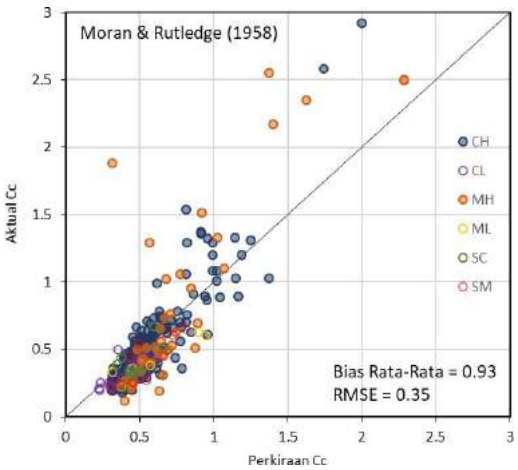

Gbr. 3. Aktual vs Perkiraan Cc, Moran & Rutledge (1958).

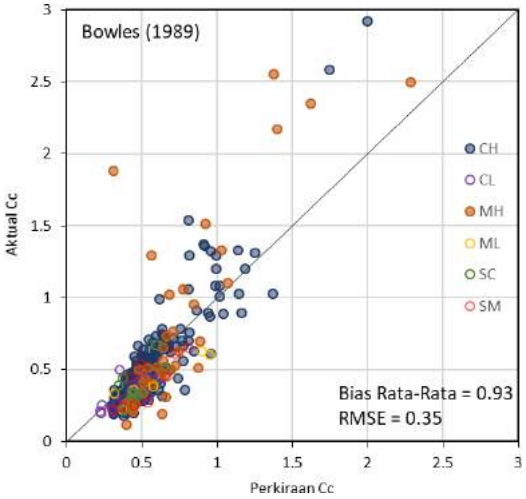

Gbr. 4. Aktual vs Perkiraan Cc, Bowles (1989).

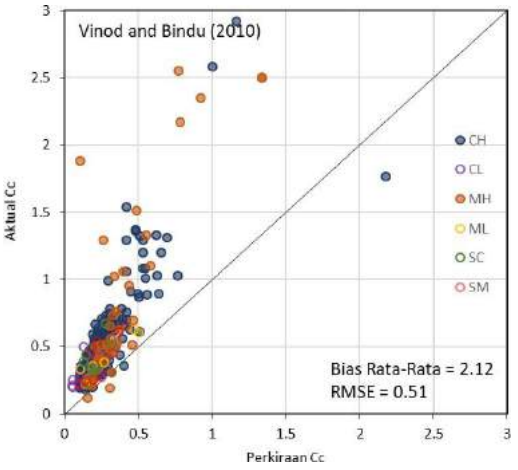

Gbr. 5. Aktual vs Perkiraan $C_{c,}$ Vinod & Bindu (2010).

Salah satu contoh persamaan regresi yang memiliki bias yang besar, seperti yang dimiliki oleh persamaan Vinod & Bindu (2010) dengan $\bar{b}$ sekitar 2,12 dapat dilihat pada Gbr. 6.

Penelitian ini menemukan bahwa persamaan-persamaan regresi yang memiliki harga $\bar{b}$ mendekati satu umumnya dapat memprediksi harga C_c, yang harganya kurang dari sekitar 0,8 dengan RMSE yang relatif kecil. Untuk harga C_c yang lebih besar dari 0,8 hasil perkiraan dari persamaan-persamaan regresi linear orde satu ini cenderung lebih kecil dari aktual dan menghasilkan deviasi kesalahan yang lebih besar. Salah satu penyebabnya adalah kemungkinan adanya faktor-faktor lain yang mempengaruhi perilaku kompresibilitas tanah lempung terutama untuk kondisi kadar air yang tinggi. Persamaan regresi Peck & Reed (1954) berusaha menangkap perilaku tersebut dengan menggunakan persamaan polinomial derajat dua walaupun hasil perkiraan yang diperoleh, untuk harga C_c di atas 0,8 masih terlalu besar dengan $\bar{b}$ =1,05 dan RMSE = 1,33 (Gbr. 6).

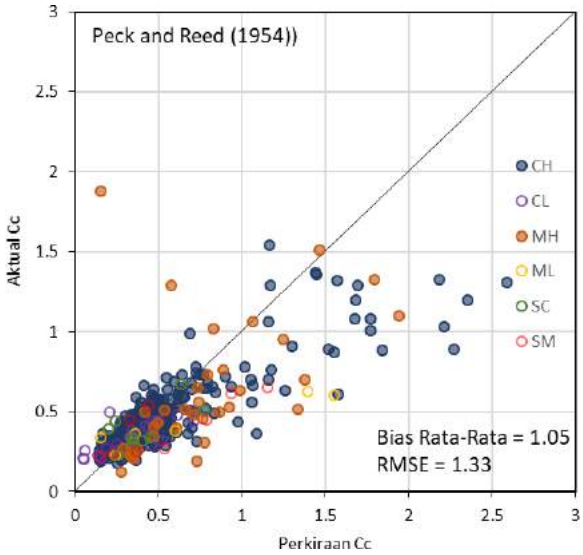

Gbr. 6. Aktual vs Perkiraan Cc (Peck & Reed 1954).

Tanah yang digunakan penelitian ini didominasi oleh lempung berplastisitas tinggi CH, yaitu sekitar 74 persen dari tanah yang tersedia, mengindikasikan bahwa lempung CH memiliki kemungkinan lebih sering untuk ditemukan. Oleh karena itu kami juga mengevaluasi persamaan-persamaan regresi ini untuk tanah CH saja di mana pada Tabel 4 dapat dilihat bahwa tidak ada perubahan yang signifikan pada harga $\bar{b}$, RMSE dan COV tetapi menunjukkan hasil yang sedikit lebih baik sehingga dapat disimpulkan bahwa persamaan-persamaan regresi ini, terutama yang berbentuk linear orde satu dengan harga $\bar{b}$ sekitar 1, sesuai untuk tanah lempung CH. Karakteristik statistik dari 257 tanah CH dapat dilihat pada Tabel 5.

Tabel 4. Hasil Evaluasi Beberapa Persamaan Regresi Terpublikasi untuk Tanah CH Saja.

Persamaan Regresi	*Mean Bias*	*Mean Error*	*Standard Deviation*	*Absolute COV Error*	*RMSE*
Park and Lee (2011)	1,03	0,02	0,32	17,03	0,32
Moran & Rutledge (1958)	0,93	-0,02	0,33	15,92	0,33
Bowles (1989)	0,93	-0,02	0,33	15,92	0,33
Nishida (1956)	1,11	0,04	0,33	8,01	0,33
Lav & Ansal (2001)	1,10	0,05	0,32	5,97	0,33
Yoon et al. (2004)	1,00	0,03	0,34	12,54	0,34
Osterberg (1972)	1,07	0,06	0,34	6,10	0,34
Koppula (1981)	1,07	0,06	0,34	6,10	0,34
Widodo & Abdelazim (2012)	0,83	-0,07	0,33	4,58	0,34
Solanki and Desai (2008)	1,04	0,05	0,34	7,15	0,35
Sari & Firmansyah (2013) (6)	0,77	-0,13	0,32	2,41	0,35
Azzouz et. al. (1976)	1,21	0,11	0,34	3,20	0,35
Sari & Firmansyah (2013) (1)	0,77	-0,14	0,32	2,28	0,35
Sari & Firmansyah (2013) (3)	0,77	-0,14	0,33	2,25	0,36
Herrero (1980)	1,29	0,13	0,34	2,57	0,36
Hough (1957)	1,33	0,14	0,33	2,42	0,36
Serajuddin (1987)	1,33	0,14	0,33	2,42	0,36
Sari & Firmansyah (2013) (2)	0,75	-0,16	0,33	2,04	0,36
Bryan et al. (2014)	1,76	0,17	0,32	1,90	0,37
Kalantary & Afshin (2012)	1,47	0,19	0,37	1,90	0,41
Sari & Firmansyah (2013) (5)	0,68	-0,24	0,36	1,48	0,43
Abdrabbo&Mahmoud (1990)	1,62	0,23	0,38	1,67	0,44
Vinod and Bindu (2010)	2,10	0,29	0,37	1,29	0,47
Sari & Firmansyah (2013) (4)	0,45	-0,71	0,70	0,99	0,99
Peck and Reed (1954)	1,03	-0,22	1,37	6,13	1,38

Tabel 5. Karakteristik Statistik Tanah CH.

Parameter	n	*Min*	25%(1)	50%(2)	75%(3)	*Max*	*Mean*	*Standard Deviation*	*COV*
w_n	257	27	37	43	51	315	50	31	0,62
e_0	257	0,69	1,01	1,20	1,44	8,92	1,40	0,84	0,60
Sr	257	71	92	96	99	100	95	6	0,06
F_{200}	257	50	91	98	99	100	93	11	0,11
LL	257	42	70	85	102	402	90	36	0,40
PL	257	15	24	28	32	118	29	9	0,31
PI	257	20	43	57	71	284	61	29	0,47
C_c	257	0,18	0,33	0,44	0,58	3,94	0,56	0,52	0,92

Catatan: (1) 25% data berada di bawah nilai yang tertera.
(2) Median.
(3) 75% data berada di atas nilai yang tertera.

Salah satu contoh hasil evaluasi ini adalah persamaan regresi dari Yoon et al. (2004) yang semula memiliki harga $\bar{b}$=1,01 dan RMSE=0,37 untuk semua tipe tanah menjadi $\bar{b}$=1,00 dan RMSE=0,34 untuk tanah CH saja. Plot yang memperlihatkan hubungan antara harga C_c aktual dengan harga perkiraan dari persamaan regresi Yoon et al. (2004) tersebut dapat dilihat pada Gbr. 7. Kami juga menemukan bahwa umumnya persamaan-persamaan regresi linear orde satu yang dievaluasi menghasilkan prediksi yang lebih besar dari harga aktual jika harga aktual C_c kurang dari 0,5 dan menghasilkan prediksi yang lebih kecil jika harga aktual C_c lebih dari 0,5.

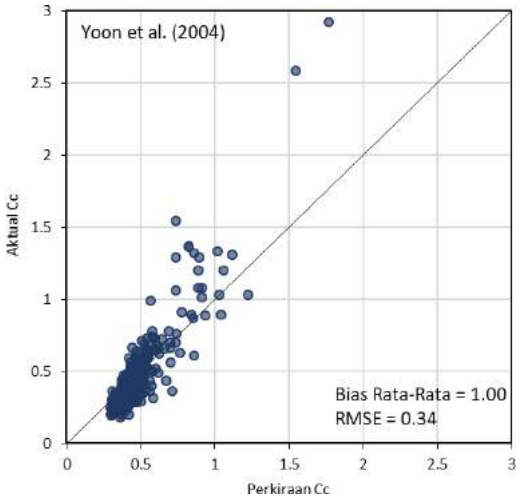

Gbr. 7. Aktual vs Perkiraan Cc, Yoon et al. (2004) Tanah CH.

Hasil penelitian yang dilaporkan dalam tulisan ini adalah bagian dari penelitian yang akan mengevaluasi lebih dalam, dengan metode *machine learning*, bagaimana faktor-faktor karakteristik tanah lainnya mempengaruhi perilaku kompresibilitas tanah lempung atau lanau Indonesia yang hasilnya akan disampaikan dalam laporan terpisah.

5 KESIMPULAN

Beberapa kesimpulan yang dapat ditarik dari hasil evaluasi persamaan-persamaan regresi ini adalah:

1. Beberapa persamaan regresi terpublikasi, seperti Moran & Rutledge (1958), Bowles (1989), dan Yoon et al. (2004), yang berbentuk persamaan linear orde satu dapat digunakan untuk memprediksi C_c tanah lempung dan lanau Indonesia berdasarkan kadar airnya terutama untuk tanah dengan C_c kurang dari 0,8. Persamaan-persamaan regresi ini cenderung lebih sesuai untuk tanah CH dengan catatan perkiraan yang dihasilkan cenderung lebih besardari harga aktual jika harga aktual C_c kurang dari 0,5 dan menghasilkan perkiraan yang lebih kecil untuk harga aktual C_c lebih besar dari 0,5.
2. Perilaku tanah lempung dan lanau yang memiliki kompresibilitas tinggi dengan harga C_c lebih besar dari 0,8 kelihatannya dipengaruhi oleh faktor lain selain kadar air. Perilaku tersebut dapat dimodelkan dengan persamaan regresi nonlinear seperti yang diperlihatkan oleh persamaan regresi polinomial orde dua Peck & Reed (1954) tetapi hasil perkiraannya menjadi lebih besar dari aktualnya.
3. Penelitian lebih lanjut akan dilakukan di mana metode machine learning akan digunakan untuk mengevaluasi mekanisme pengaruh faktor-faktor lainnya terhadap perilaku kompresibilitas tanah lempung dan lanau Indonesia.

PENGHARGAAN

Kami mengucapkan terima kasih kepada program Penelitian dan Pengabdian kepada Masyarakat(P2MI) Institut Teknologi Bandung tahun 2021 atas terselenggaranya penelitian ini.

DAFTAR PUSTAKA

Abdrabbo FM., Mahmoud MA. 1990. Correlations Between Index Tests and Compressibility of Egyptian Clays. *Soils and Foundations* 30(2):128-32.

Al-Khafiji, A. W.N., and Andersland, O.B. 1992. Equations for Compression Indeks Approximation. *Journal of Geotechnical Engineering ASCE* Vol. 118 (1): 148-153.

Azzouz, A. S., Krizek, R. J., & Corotis, R. B. 1976. Regression Analysis of Soil Compressibility. *Soils and Foundations* 16(2): 19-29.

Bogireddy Chandra, Ganesh Sutar, Solanki CH, and Vasanwala SA. 2017. Regional Normalized Empirical Correlations for The Compression Index (Cc) of Soil – Acritical Overview. *International Journal of Civil Engineering and Technology* (IJCIET). Volume 8.

Bowles J., E. 1989. Physical and Geotechnical Properties of Soils. New York: McGraw-Hill.

Bryan A. McCabe, Brian B. Sheil, Michael M. Long, Fintan J. Buggy, Eric R. Farrell. 2014. Empirical Correlations for The Compression Index of Irish Soft Soils. *Proceedings of ICE Geotechnical Engineering*

Volume 167 Issue GE6: 510–517 http://dx.doi.org/10.1680/geng.13.00116.

Cherubini C. 1991. Compressibility Characteristics of The Matera Blue Clays as Determined by Means of Statistical Correlations. *Proc 10th Europan Conf. on Soil Mechanics and Foundation Engineering (AGI)*: 59-62. Firenze.

Cozzolino, V. M. 1961. Statistical Forecasting of Compression Index. *Proc. 5th Int. Conf. on Soil Mech. and Found. Eng.* Vol. 1: 51-53. France.

Herrero Oswald Rendon. 1980. Universal Compression Indeks Equation. *Journal of Geotechnical and Geoenvironmental Engineering* 106.ASCE 15829.

Hough BK. 1957. *Basic Soils Engineering*: 114-115. New York: The Ronald Press Company.

Kalantary Farzin, and Afshin Kordnaeij. 2012. Prediction of Compression Index Using Artificial Neural Network. *Scientific Research and Essays* 7.31.

Koppula, S. D. 1981. Statistical Estimation of Compression Index. *Geotechnical Testing Journal GTJODJ* Vol.4(2): 68-73.

Kulhawy FH, Mayne PW. 1990. Manual on Estimating Soil Properties for Foundation Design. *Report EL-6800*. Electric Power Research Institute. Palo Alto, California, USA.

Lav, M. A., and Ansal, A. M. 2001. Regression Analysis of Soil Compressibility. *Turkish Journal of Engineering and Environmental Sciences* 25(2): 101-109.

Lotman Monica, Leena KT. 2021. Transformation Models for The Compressibility Properties of Finnish Clays Using a Multivariate Database. *Georisk Assessment and Management of Risk for Engineered Systems and Geohazards*.

Moran P. 1958. Mueser and Rutledge., Study of Deep Soil Stabilization by Vertical Sand Drains. *Bureau of Yards and Docks*. New York: Department of the Navy.

Nishida Y. A. 1956. Brief Note on Compression Index of Soil. *Journal of the Soil Mechanics and Foundations Division* 82(3):1-4

Park, H. I., and Lee, S. R. 2011. Evaluation of The Compression Index of Soils Using an Artificial Neural Network. *Computers and Geotechnics* 38(4):472-81.

Peck RB, Reed WC. 1954. Engineering Properties of Chicago Subsoils. University of Illinois at Urbana Champaign, College of Engineering. Engineering Experiment Station.

Sari PT, Firmansyah YK. 2013. The Empirical Correlation Using Linear Regression of Compression Index for Surabaya Soft Soil. *ASEM13* Sept.8-12, Korea.

Serajuddin M. 1987. Universal Compression Index Equation and Bangladesh Soils. *In Proceedings of the Ninth Southeast Asian Geotechnical Conference*: 61-72.

Skempton, A. W. 1944. Notes on The Compressibility of Clays. *Quarterly J. Geological Society of London* 100(Part 2): 119-135. London.

Solanki, C. H., and J. A. Desai. 2008. Significance of Atterberg Limits on Compressibility Parameters of Alluvial Deposits New Correlations. *Proceedings of Indian Geotechnical Conference* Vol. 23: 20. Bangalore, India.

Vinod, P., and Bindu. J. 2010. Compression Index of Highly Plastic Clays an Empirical Correlation. *Indian Geotechnical Journal* 40(3): 174-180.

Widodo Slamet, and Abdelazim Ibrahim. 2012. Estimation of Primary Compression Index (Cc) Using Physical Properties of Pontianak Soft Clay. *International Journal of Engineering Research and Applications (IJERA)* 2.5.

Yoon GL, Kim BT, Jeon SS. 2004. Empirical Correlations of Compression Index for Marine Clay from Regression Analysis. *Canadian Geotechnical Journal* 41 (6):1213-21.

Effect of Variation in Concentration of Dispersing Agent Solution on Atterberg Limits and Soil Gradation

Budijanto Widjaja
Parahyangan Catholic University

Fendy
Parahyangan Catholic University

ABSTRACT: The function of a dispersing agent in a hydrometer test is to release electrochemical bonds from clay minerals. Hence, the clay particles can be separated and obtain the sedimentation rate of the fine-grained soil particle size. This study aims to determine the influence of variations in the dispersing agent concentration on the liquid limit, plastic limit, and soil gradation. The type of dispersing agent used is sodium hexametaphosphate. The molarity concentrations used varied from 0 M, 0.05 M, 0.065 M, 0.1 M, and 0.2 M for bentonite, kaolin, and Garut soil. The results showed that adding a dispersing agent reduces the liquid and plastic limit value, followed by an increase in the density and clay content. Therefore, one should take the right concentration, especially when considering reliable hydrometer test results.

Keywords: dispersing agent, hydrometer test, sodium hexametaphosphate, gradation

ABSTRAK: Fungsi dari dispersing agent pada uji hydrometer adalah untuk melepaskan ikatan elektrokimia pada mineral lempung. Jadi, partikel lempung dapat dipisahkan sehingga dapat ditentukan laju sedimentasi dari ukuran partikel tanah butir halus. Studi ini bertujuan untuk menentukan pengaruh dari variasi konsentrasi terhadap nilai batas cair, batas plastis, dan gradasi tanah. Jenis dispersing agent yang digunakan adalah sodium hexametafosfat. Konsentrasi molaritas memiliki variasi dari 0 M, 005 M, 0.065 M, 0,1 M, dan 0.2 M untuk bentonite, kaolin, dan tanah Garut. Hasil analisis menunjukkan bahwa penambahan dispersing agent memberikan pengaruh berupa reduksi nilai batas cair dan batas plastis, diikuti oleh peningkatan berat isi dan kadar lempung. Oleh karena itu, pemilihan konsentrasi yang baik perlu diperhatikan agar dapat diperoleh hasil uji hidrometer yang representatif.

Kata Kunci: dispersing agent, uji hidrometer, sodium hexametafosfat, gradasi

1 INTRODUCTION

Several applications in the field use dispersing agents to solve problems due to fine-grained soil, such as hydrometer tests and tunnelling. In the hydrometer test, chemicals are used in dispersing agents to destroy lumps of fine-grained soil so the gradation curve of the soil can be accurate. Due to the nature of the dispersing agent, in overcoming the problem of clay clogging that occurs when tunnelling is often used to reduce the stickiness of clay. The stickiness of clay is related to its plasticity, which the Atterberg limit can determine. One type of dispersing agent that is often used is sodium hexametaphosphate $(NaPO_3)_6$ or commonly called Calgon. This research will examine the effect of sodium hexametaphosphate solution on Liquid Limit (LL), Plastic Limit (PL), Plasticity Index (PI), and gradation of soil samples.

2 MATERIALS AND METHODS

Three soil samples were used in this study, including Garut clay, Betonite, and kaolin. The soil samples studied were poly-mineral and mono-mineral clays. The Garut clay (poly-mineral clay) samples were from Sirnagalih Village, Cigalontang District, Tasikmalaya Regency.

Bentonite and kaolin samples are a type of mono-mineral clay which both show extreme behavior of clay. Kaolin and bentonite are the dominant soil formed by kaolinite (mineral 1:1) and montmorillonite (mineral 2:1), respectively. Bentonite has a different activity, plasticity, swelling, and shrinkage behavior than kaolin. Bentonite is very susceptible to considerable shrinkage and tends to have higher plasticity than kaolin. Not surprisingly, bentonite LL, PL, and PI are higher than Kaolin, Mitchell and Soga (2005); Ishibasi and Hazarika (2015); Holtz et al. (2011); Yong et al. (2012).

All three soil samples must adjust their particle size before testing. Pieces of Garut clay samples must be mashed with a rubber hammer into smaller sizes to pass the #40 sieve (for the fall cone penetrometer test and Casagrande's method) and #200 sieve (for the hydrometer test) (ASTM D 4318; ASTM D 422). Bentonite and kaolin obtained from chemical stores have already passed the #200 sieve to be used directly.

Sodium hexametaphosphate solution is made in several concentrations, including 0 M, 0.001 M, 0.002 M, and 0.004 M. It is used in the Atterberg limit test. Sodium hexametaphosphate powder will be dissolved into 500 mL of distilled water to form a solution for each concentration. The LL and PL with various concentrations of the dispersing agent were tested by the Casagrande Cup test and fall cone penetrometer test. In addition, two tests were conducted to check the consistency of laboratory test results. PI is the difference between the PL and LL of the soil.

3 RESULTS AND DISCUSSION

Garut clay occurred a substantial decrease in LL with increasing the solution's concentration in both tests. The liquid limit differences between 0 M and 0.004 M concentrations reached 16 % in the fall cone penetrometer test and 25 % in the Casagrande cup test (Fig. 1). The reduction of bentonite's LL from 0 M to 0.004 M solution's concentration in both tests was insignificant. The LL differences reached 4 % in both the fall cone penetrometer and Casagrande cup test. Graphically, the trend of bentonite's liquid limit is relatively flat compared to the other soil samples. Kaolin significantly decreases LL by increasing the solution's concentration in the fall cone penetrometer test, whereas the Casagrande cup test result shows a significant decrease.

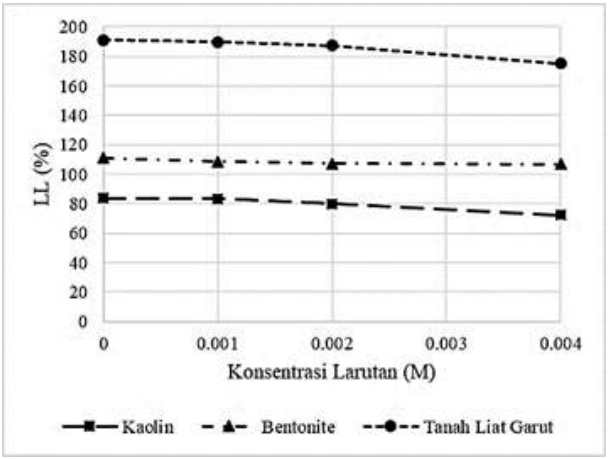

(a)

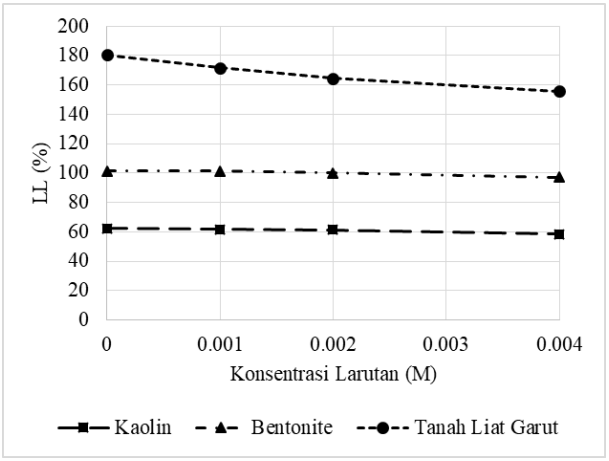

(b)

Fig. 1. Liquid Limit Test Results of Soil Samples Using Fall Cone Penetrometer (a) and Casagrande Cup Test (b).

The changes in Garut clay's PL became the most striking from the other soil samples. The reduction in PL from 0 M to 0.004 M concentrations can reach 25 % in the fall cone penetrometer test and 15 % in the Casagrande Cup test. An increase in the concentration of the solution follows the decrease of PL in bentonite and kaolin. The results show that it is more striking in the fall cone penetrometer test than the Casagrande method. For solution concentrations smaller than 0.001 M, the change in Kaolin's PL tends to be very small, close to zero.

Two different tests generate different Garut clay's PI trends which; the fall cone penetrometer test generates an upward trend, and the Casagrande method generates a fluctuating trend as the concentration of the solution increases. Bentonite's PI trends tend to increase with increasing solution concentration

in both tests (Fig. 3). On the other hand, Kaolin's PI trends tend to reverse from Garut clay. The fall cone penetrometer test produces a fluctuating trend, and the Casagrande method has an upward trend with increasing the solution's concentration.

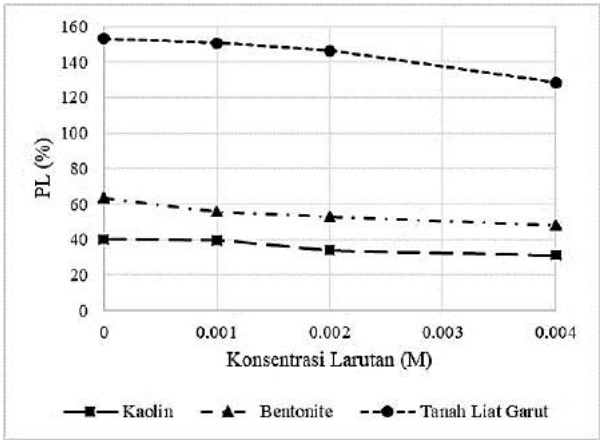

(a)

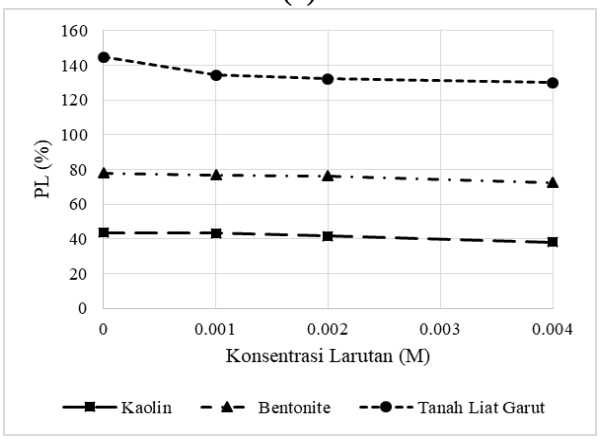

(b)

Fig. 2. Plastic Limit Test Results of Soil Samples Using Fall Cone Penetrometer and Casagrande's Method.

Grain size distribution of the three soil samples experiences a very significant increase in clay content when the solution concentration is increased from 0 to 0.05 M. Bentonite is the most considerable gradation changes soil compared to the other one. When the solution concentration increased from 0 to 0.05 M, the clay content increased from 18 % to 66 %, and silt content decreased from 82 % to 34 %. Increasing clay content and decreasing silt content of Garut clay and kaolin shows insignificant compared to bentonite. Kaolin undergoes gradation changes that tend to be more significant than Garut clay. As the solution's concentration increases from 0 to 0.05 M, clay content increases from 7 % to 45 %, and silt content decrease from 93 % to 55 %. For Garut clay, its clay content increased from 7 % to 30 %, and silt content decreased from 86 % to 64% when the concentration of the solution was increased from 0 to 0.05 M. For the solution's concentration greater than 0.05 M, gradations of the three soil samples did not experience a significant change in clay and silt content.

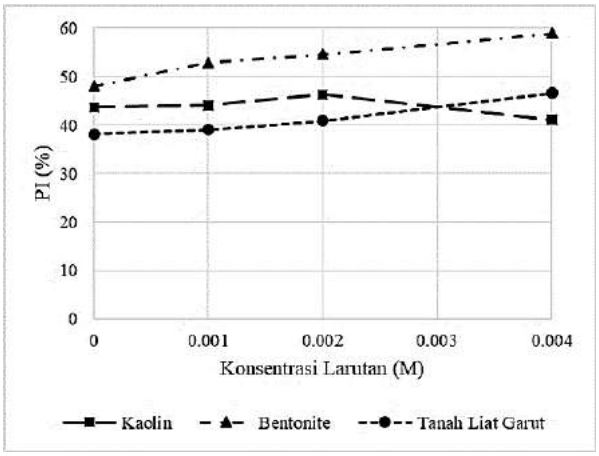

(a)

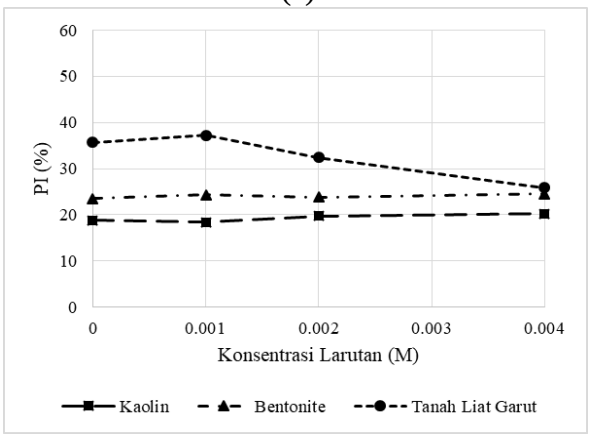

(b)

Fig. 3. Plasticity Index Test Results of Soil Samples Using Fall Cone Penetrometer and Casagrande's Method.

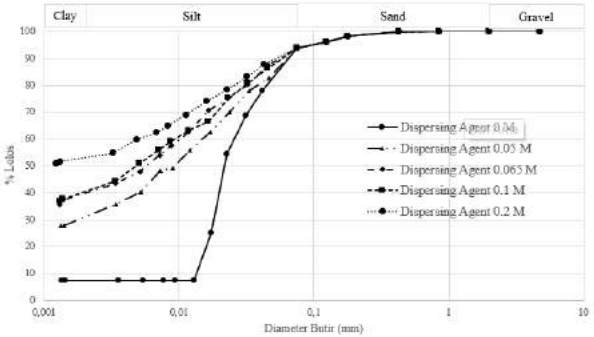

Fig. 4. Grain Size Distribution of Garut Clay.

A diffuse double layer is one of the causes of LL, PL, and PI changes. The diffuse double layer consists of 2 layers: the cation's surface and the cation's diffuse layer. One can obtain the thickness of this layer using Gouy Chapman's theory.

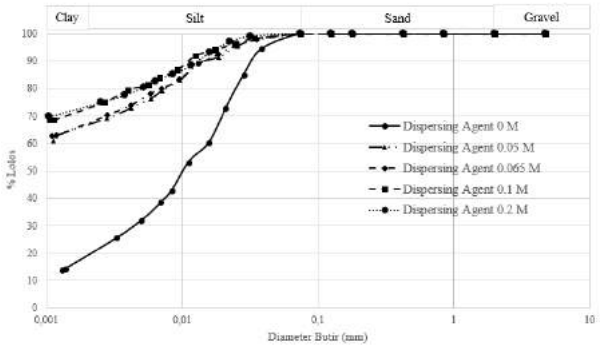

Fig. 5. Grain Size Distribution of Bentonite.

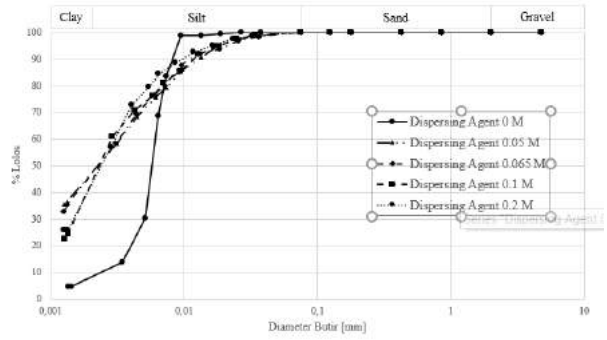

Fig. 6. Grain Size Distribution of Kaolin.

The LL will increase if the diffused double layer between the clay crystals gets thicker. Conversely, the liquid limit will decrease if the diffuse double layer between the clay crystals gets thinner, Sridharan and Rao (1975). The diffuse double layer is related to electrical potential, which is associated with the electrolyte concentration. The most significant electrical potential occurs on the surface of clay crystals which are usually called surface potentials, Mitchell and Soga (2005). If the concentration of electrolytes increases, the electrical potential (surface potential) will decrease. Therefore, the thickness of the diffuse double layer will reduce, and the liquid and plastic limit of the soil will decrease.

On the contrary, the electrolyte concentration decreases, electrical potential increases, diffuse double layer gets thicker, and liquid and plastic limit of the soil increase, Mitchell and Soga (2005); Holtz et al. (2011); Yong et al. (2007). When the diffuse double layer gets thicker, the distance between clay particles will get farther and vice versa. In addition, when the electrolyte concentration increases, the reduction in electrical potential and increasing distance will be faster, and the distance between clay particles will get closer. Hence, the traction force between clay particles will be stronger, Mitchell and Soga (2005). When a pair of clay crystals are close together, their diffuse double layer's thickness determines the distance between them.

The dielectric constant is the ratio between electrical energy in a material due to potential and electrical energy in the same material in vacuum conditions. This constant is one factor that influences the electrical potential (surface potential) and the thickness of the diffuse double layer. Therefore, the potential surface decreases and the diffuse double layer becomes thinner as the dielectric constant decreases, Mitchell and Soga (2005); Holtz et al. (2011). According to Gadani et al. (2012), the more concentrated the solution, the smaller the dielectric constant. Therefore, the liquid and plastic limit of the soil will decrease when the dielectric consistency decreases.

Based on Liu et al. (2018), as the concentration of sodium hexametaphosphate solution increases, the liquid and plastic limit of the soil samples decreases, its plasticity index should also decrease. However, the results of this research still show that the PI's trend of each soil sample is ascending or fluctuating as the concentration of the solution increases. A study conducted by Liu et al. (2018) states that mixing various concentrations of sodium hexametaphosphate solution with soil samples can influence changes in the plasticity index. Atterberg limit test results of several soil samples showed that the plasticity index's trend fluctuates at zero hour mixing time. The plasticity index's trend tends to decrease when the mixing time reaches five hours. It shows the importance of mixing time in reducing the plasticity index of the soil samples. Therefore, researchers interested in this study's topic can do further research related to the time of mixing various concentrations of sodium hexametaphosphate solution with soil samples and can be compared with Liu et al. (2018).

The bonding type in the minerals, adsorbed water, Cation Exchange Capacity (CEC), and other factors will influence changes in the liquid and plastic limit of the soil.

Kaolin is dominantly composed of Kaolinite mineral, a 1:1 mineral in the form of a bond between one sheet of silica and one sheet of strong alumina. This bond is primary (hydrogen bond). It is stronger than the van der Waals bond that presents in the Montmorillonite mineral, and it will remain stable with the presence of water [4] [5] [6]. In addition, this bond prevents hydration and allows silica-alumina sheets to accumulate and form clay crystals [6].

Unlike kaolin, bentonite is dominantly composed of montmorillonite minerals in a bond between two silica sheets and one alumina sheet. This bond is secondary (van der Waals bond). The bond between the silica sheets is relatively weak, and there is a negative charge on the alumina sheet. Hence, water and cations can quickly enter the gap between the sheets and separate them. As a result, bentonite is very susceptible to significant shrinkage and tends to have high plasticity, Mitchell and Soga (2005); Holtz et al. (2011); Yong et al. (2007). Not surprisingly, bentonite's liquid limit, plastic limit, and plasticity index are higher than kaolin.

The adsorbed water layer is a layer of water molecules surrounding each clay crystal, causing clay particles in nature to always be hydrated. The attraction between water molecules and the surface of clay crystal is powerful (occurred right on the particle surface). It will decrease with increasing the distance from the particle surface. The thickness of the adsorbed water layer is almost the same in all types of clay. The adsorbed water layer is the factor of differences in liquid and plastic limit and plasticity index of Kaolin and Bentonite. The size of the clay crystal influences it. Bentonite crystal is smaller than kaolin, so it tends to have greater activity, plasticity, shrinkage, and volume changes than kaolin [6].

Each clay crystal always wants to reach electrically neutral. Therefore, the cations contained in water will be strongly attracted to the surface of the clay crystal depending on the amount of negative charge on its surface. Each type of clay has a different charge deficiency so that the tendency to pull cations from water is also distinct. Attracted cations are called exchangeable cations. One cation is easily exchanged for one other cation with the same valence or two other cations that have half the valence of the original cation. Cations with the more significant valence can easily substitute the smaller ones, Holtz et al. (2011).

Montmorillonite mineral has a greater charge deficiency so that the attraction of cations (exchangeable cations) is greater than Kaolinite mineral, Holtz et al. (2011). This reflects that the changes in liquid and plastic limit and plasticity index of kaolin are more significant than bentonite when the sodium hexametaphosphate solution is mixed into it. It should be noted that the cation exchange reaction on kaolin is instantaneous, faster than Bentonite, Mitchell and Soga (2005). Therefore, bentonite takes more time than kaolin for the liquid and plastic limit, and the plasticity index changes even more significantly.

4 CONCLUSIONS

From this study, several conclusions can be drawn as follows. As the concentration of sodium hexametaphosphate solution increases, the liquid limit and plastic limit of the soil samples decreases. Garut clay showed the most significant decreases in liquid limit and plastic limit compared to Kaolin and Bentonite.

The plastic limit of the soil samples changes more prominently than its liquid limit as the sodium hexametaphosphate solution increases. In this case, bentonite gives a more precise visualization than the other soil samples.

Plasticity index's trends of the soil samples tend to be opposite from its plastic limit's trends but follow its liquid limit as the sodium hexametaphosphate solution increases. In this case, Garut clay gives a more clear visualization than the other soil samples.

As the sodium hexametaphosphate solution increases, the clay content of the soil samples increases, and the silt content of the soil samples decreases. In this case, Garut clay gives a more clear visualization than the other soil samples. Meanwhile, bentonite was the most significant change in clay and silt content.

REFERENCES

ASTM designation: D 4318 – 00. Standard Test Method for Liquid Limit, Plastic Limit, and Plasticity Index of Soils. *American Standard Testing and Material*. Barr Harbor Drive, West Conshohocken Pa. 19428-2959.

ASTM designation: D 422 – 63. Standard Test Method for Particle-Size Analysis of Soils. *American Standard Testing and Material*. Barr Harbor Drive, West Conshohocken Pa. 19428-2959.

British Standard designation: BS 1377-2:1990 Methods of Test for Soils for Civil Engineering Purpose Part 2: Classification Tests. 1998. *Board of the BSI*. London W4 4AL.

Gadani, D.H., Rana, V.A., Bhatnagar, S.P., Prajapati, A.N., dan Vyas, A.D. 2012. Effect of Salinity on the Dielectric Properties of Water. *Indian Journal of Pure & Applied Physics* Vol. 50: 405-410.

Holtz, R.D., Kovacs, W.D., Sheahan, T.C. 2011. *An Introduction to Geotechnical Engineering Engineering.* United States of America: Pearson Education Pearson.

Ishibashi, I., and Hazarika, H. 2015. *Soil Mechanics Fundamentals and Applications.* CRC Press, Boca Raton.

Liu, P., Wang, S., Ge, L., Thewes, M., Yang, J., Xia, Y. 2018. Changes of Atterberg limits And Electrochemical Behaviors of Clays with Dispersants as Conditioning Agents for EPB Shield Tunneling.

Mitchell, J.K., and Soga, K. 2005. *Fundamentals of Soil Behavior*. New Jersey: John Wiley & Sons.

O'Kelly, B. C. et al. 2018. Use of Fall Cones to Determine Atterberg Limits: A Review. *Géotechnique* 68, No. 10: 843–856.

Sridharan, A. 1998. Liquid Limit of Kaolinitic Soils. Geotechnique 38, No. 2: 191-198

Sridharan, A., and Rao, G. V. 1975. Mechanisms Controlling the Liquid Limit of Clays. *Proceedings of Istanbul Conference on SM and FE* Vol. 1: 75-84.

Sridharan, A., Rao, S.M., dan Murthy, N.S. 1986. Liquid Limit of Montmorillonite Soils. *Geotechnical Testing Journal, GTJODJ* Vol 9, No. 3:156-159.

Yong, R.N., Nakano, M., Pusch, R. 2012. *Environmental Soil Properties and Behavior.* CRC Press, Boca Raton.

Effectiveness of Using Cellulolytic and Lignocellulolytic Bacteria in Decomposing Fibers of Fibrous Peat

Noor Endah Mochtar
Department of Civil Engineering – ITS

Enny Zulaika
Department of Biology – ITS

Dwiaji Ari Yogyanta
Indonesia Public Works – BP2JK

ABSTRAK: Daya dukung tanah gambut berserat yang distabilisasi dengan kapur dapat berkurang secara drastik bilamana dekomposisi/kerusakan serat terjadi. Untuk menghindari hal itu, serat gambut harus dihancurkan sebelum stabilisasi dengan kapur dilakukan. Bakteri *endogenous aerobic decomposer*, yaitu bakteri *cellulolytic* dan *lignocellulolytic*, dapat dipergunakan untuk mempercepat proses dekomposisi. Dalam studi ini, sebanyak 10% (dari berat gambut basah) untuk masing-masing jenis bakteri dicampur dengan gambut berserat dan kemudian diperam selama 0, 14, dan 28 hari. Hasil tes menunjukkan bahwa karena percepatan proses dekomposisi serat oleh bakteria *endogenous aerobic decomposer*, prosentase dari serat kasar dan serat ukuran medium berkurang tapi serat halus bertambah. Selain itu, adanya dekomposisi serat juga mempengaruhi sifat fisik dan sifat teknis gambut berserat: penurunan kandungan serat, berat volume, *specific gravity*, dan sudut geser dalam; serta sedikit kenaikan kadar air, angka pori, dan kompressibilitasnya. Secara umum, penggunaaan bakteri *lignocellulolytic* lebih efektif dalam menghancurkan serat dalam gambut berserat dari pada bakteri *cellulolytic*.

Kata Kunci: bakteri cellulolytic, bakteri lignocellulolytic, dekomposisi, gambut berserat, serat

ABSTRACT: Bearing capacity of lime stabilized fibrous peat dropped significantly when the fiber decomposition occurs. To avoid that, its fibers have to be decomposed before lime stabilization carried out. Endogenous aerobic decomposer bacteria, cellulolytic and lignocellulolytic bacteria, were adopted to accelerate the fibers decomposition process. In this study, about 10% (by peat wet weight) for each bacteria was mixed with the fibrous peat and then cured for 0, 14, and 28 days. Test results show that due to acceleration of fiber decomposition process caused by the endogenous aerobic decomposer bacteria, the percentage of coarse and medium fibers decrease but the fine fibers increase. Besides, it affects the Physical and Engineering characteristics of fibrous peat: decrement of fiber content, unit weight, specific gravity, and internal friction angle; also slightly increment of water content, void ratio, its compression. In general, the use of lignocellulolytic bacteria is more effective in decomposing fibers than cellulolytic bacteria.

Keywords: cellulolytic bacteria, decomposition, fibers, fibrous peat, lignocellulolytic bacteria

Shear Strength Ratio of Marine Siltation

Hanif Audina Rahmawati
PT Hydrocore

Mifrokhah Haniffa
PT Taka Hydrocore Indonesia

Syukri Fitrialdi
PT Taka Hydrocore Indonesia
PT Hydrocore

ABSTRACT: Marine siltation is type of a very soft soil sediment that exist at the coastal and offshore area. Application of fill materials on very soft soils for nearshore pipeline design and reclamation works requires this shear strength ratio. In this research, various surcharge loads (p) were applied until primary consolidation was completed and then the shear strength (c) was measured by miniature laboratory vane shear to obtain the shear strength ratio (Δc/Δp). The results showed that the shear strength (c) of marine siltation is linearly increase with an increase in the surcharge load (p).

Keywords: marine siltation, shear strength ratio, consolidation

1 INTRODUCTION

Marine siltation is type of a very soft soil sediment that exist at the coastal and offshore area. In general, marine siltation has very high moisture content, high compressibility, and low shear strength.

According to Lambe & Whitman (1969), consolidation is the process in which reduction in volume takes place by the gradual expulsion or absorption of water under long-term static loads. If a surcharged load is applied on saturated clay or silt soils, thus will create the excess pore water pressures. As the excess pore pressure dissipates, the new compressive stress is transferred to soil grains and increasing the effective stress.

Suzuki and Yasuhara (2007) studied increase in shear strength of soft clay with regard to rate of consolidation in two soft marine clay deposits.

Putro (2010) conducted research to determine the value of secondary compression parameters obtained from the soft soil test results in Marunda with moisture content of about 50%. In the study, the parameters were obtained from standard oedometer test with small diameter and modified oedometer with large diameter by using CBR mold. The modified oedometer test was adopted for this paper.

In this research, consolidation was conducted with various surcharge loads (p) and then continued with miniature laboratory vane shear test to obtain shear strength (c). The result of these tests is shear strength ratio (Δc/Δp) which can be used to determine siltation strength when fill materials is applied on the soft clay.

2 METHOD OF RESEARCH

Marine siltation was sampled at the coastal area of Batang, Central Java. Physical properties are given in Table 1. Initial undrained shear strength is 0.11 – 0.44 kPa.

Table 1. Physical Properties of Soils Tested.

Soil Parameter	Unit	Range
Unit Weight	kN/m^3	11.33 - 14.29
Moisture Content	%	159.6 - 202.4
Initial Void Ratio		3.81 – 5.94
Liquid Limit	%	66 - 98

Soil Parameter	Unit	Range
Plastic Limit	%	28 - 38
Plasticity Index		34 - 61
Gravel	%	0.00
Sand	%	0.3 - 6.7
Silt	%	46.9 - 65.8
Clay	%	35.7 - 49.9

For preparation, the sample was mixed until homogeneous. Mass of mold and top cap was measured before the sample was placed into the mold. In this stage, the initial settlement will occur because of the mass of top cap. The mold was then placed into water bath to maintain soil saturation and applied the surcharge load as normal stress of soil (p) as illustrated by Fig.1.

The load as presented in Table 2 was applied onto each sample during five days (120 hours) to complete the primary consolidation (Fig.2). For the maximum stress (17 kPa), two loading stages were carried out to avoid the failure of soil. The loading stage was recorded by displacement transducer with time interval of 0.1, 0.25, 0.5, 1, 2, 4, 8, 15, and 30 minutes and 1, 2, 4, 8, 12, 24, 36, 48, 72, 84, 96, 108, and 120 hours. After the loading stage was completed, the final height of specimen was measured with calipers because the initial settlement by top cap was not recorded by transducer.

After consolidation test, miniature laboratory vane was used to determine undrained shear strength of the soil (c) in accordance with ASTM D4648. The VJTech laboratory vane with the smallest vane of 12.7x2.7mm was used (Fig.3). The final unit weight and moisture content of the soil were then measured.

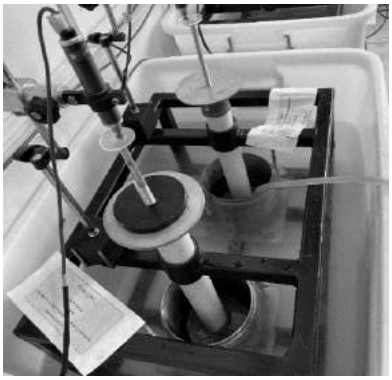

Fig. 1. Incremental Loading Consolidation Test Set Up Using CBR Mold.

Table 2. Applied Load.

	Load (kPa)
1	1.11 - 1.13
2	2.17 - 2.38
3	4.24 - 4.29
4	8.70 - 9.80
5	17.25 - 17.40

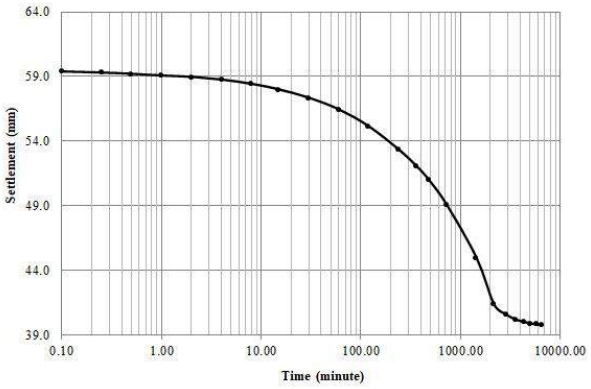

Fig. 2. Typical Consolidation Graph in This Experiment.

Fig. 3. Miniature Laboratory Vane Shear Test.

3 RESULT AND ANALYSIS

Final soil properties are summarized in Table 3. The unit weight increases and moisture content and void ratio decrease after loading.

Table 3. Summary Laboratory Test Result.

Parameter		Load 1	Load 2	Load 3	Load 4	Load 5
Unit Weight	kN/m^3	13.32 - 13.97	13.77 - 14.48	13.67 - 15.70	15.80 - 16.17	14.45 - 15.16
Moisture Content	%	126 - 150	116 - 131	97 - 115	98 - 108	92 - 102
Void Ratio		3.21 - 3.65	3.07 - 3.33	2.27 - 2.05	2.19 - 2.42	2.37 - 2.46
Shear Strength	kPa	0.51 - 0.89	0.95 - 1.24	1.33 - 1.88	1.68 - 2.17	4.34 - 5.85

Normal stress vs shear strength graph was then plotted to determine the relationship between normal stress and shear strength (Fig.4). Shear strength linearly increases as normal stress increases follows the below equation:

$$c = 0.2578\ p + 0.3722 \quad (1)$$

in which c is undrained shear strength in kPa and p is normal stress in kPa.

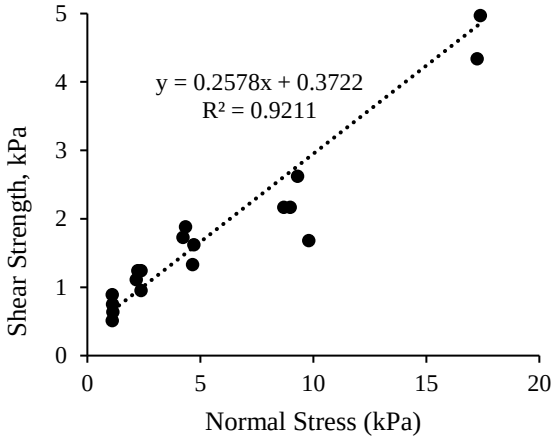

Fig. 4. Normal Stress (p) Versus Shear Strength (c) Graph.

The shear strength incremental ratio (Δc/Δp) is summarized in Table 4.

Table 4. Shear Strength Incremental Ratio.

Load	p	c	Δc/Δp
1	1.11 - 1.13	0.51 - 0.89	
			0.28 - 0.45
2	2.17 - 2.38	0.95 - 1.24	
			0.04 - 0.35
3	4.24 - 4.29	1.33 - 1.88	
			0.07 - 0.14
4	8.70 - 9.80	1.68 - 2.17	
			0.30 - 0.36
5	17.25 - 17.40	4.34 - 5.85	

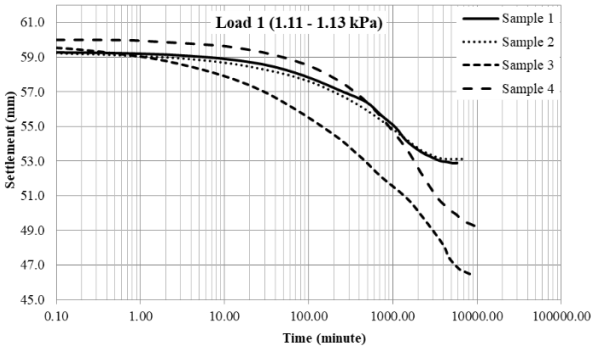

Fig. 5. Time (minute) Versus Settlement (mm) Graph for Load 1 (1.11-1.13 kPa).

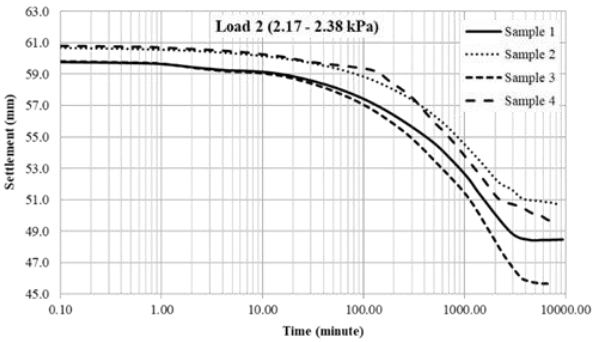

Fig. 6. Time (minute) Versus Settlement (mm) Graph for Load 2 (2.17-2.38 kPa).

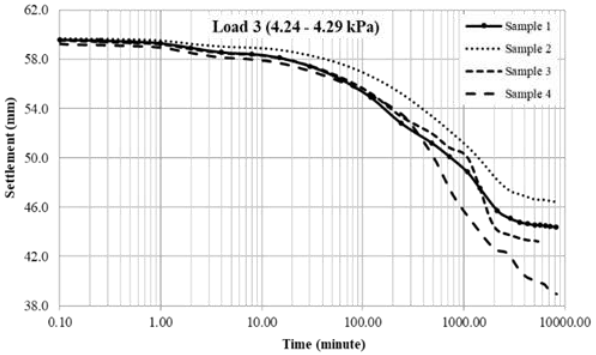

Fig. 7. Time (minute) Versus Settlement (mm) Graph for Load 3 (4.24-4.29 kPa).

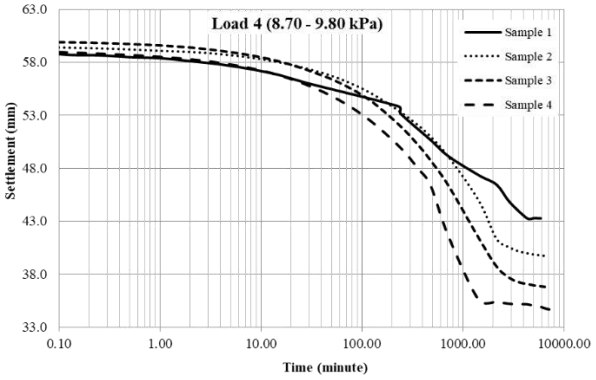

Fig. 8. Time (minute) Versus Settlement (mm) Graph for Load 4 (8.70-9.80 kPa).

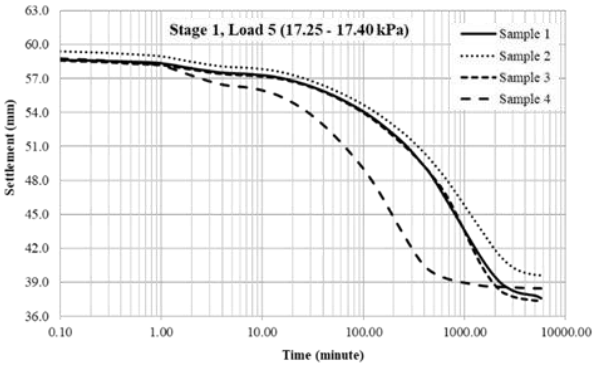

Fig. 9. Time (minute) Versus Settlement (mm) Graph for Stage 1, Load 5 (17.25-17.40 kPa).

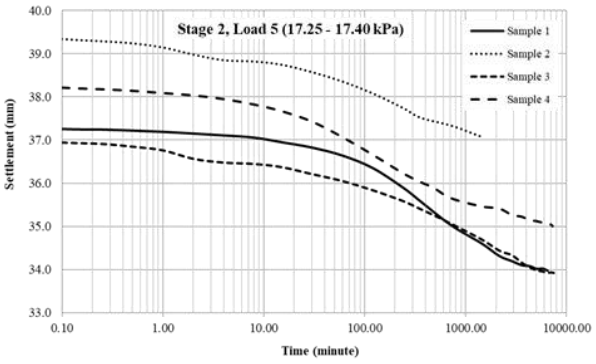

Fig. 10. Time (minute) Versus Settlement (mm) Graph for Stage 2, Load 5 (17.25-17.40 kPa).

4 CONCLUSION

This experiment is a miniature of when preloading or backfilling to increase undrained shear strength in marine siltation. Preloading should be carried out to complete primary consolidation.

The results show that the shear strength of marine siltation is linearly increase with an increase in the normal stress.

REFERENCES

ASTM. 2016. *ASTM D4648-Standard Test Methods for Laboratory Minivane Shear Test for Saturated Fine-Grained Soils.*

Lambe, T. W., & Whitman, R. V. 1969. *Soil Mechanics.* New York: John Wiley & Sons.

Putro, E. S. 2010. *Studi Parameter Kompresi Sekunder pada Tanah Lunak di Marunda.* Depok: Universitas Indonesia.

Suzuki, K., & Yasuhara, K. 2007. Increase in Undrained Shear Strength of Clay with Respect to Rate of Consolidation. *Soils and Foundations* Vol.47, No.2: 303-318.

Interface Shear Strength Progressive between Weathered and Fresh Clay Shale

Idrus M. Alatas
Program Studi Teknik Sipil – ISTN
HATTI PUSAT

Pintor T. Simatupang
Program Studi Teknik Sipil – Universitas Mercu Buana
HATTI PUSAT

ABSTRACT: The interface shear strength between weathered and fresh clay shale is very important to know for an analysis of slope stability in fresh clay shale soil with an overburden layer (OBL) on it. Progressive interface shear strength is a behavior of interface shear strength whose magnitude decreases because it is influenced by the addition of the water content of the OBL layer which is weathered clay shale (WCS) caused by rainfall. Through laboratory studies the progressive interface shear strength between weathered and fresh clay shale was obtained using the Multistage Reversal Progressive Shear Test (MRPST) method. The interface shear strength between weathered and fresh clay shale will be affected by the density and moisture content of the WCS. In the WCS at the optimum water content with a density of 100% maximum dry density (MDD), the ratio of maximum interface shear strength (□/□n) is 1.89. The interface shear strength ratio will decrease until it reaches 0.56 or the remaining 29% due to the increase in water content until the WCS becomes saturated (Sr=100%). If the WCS density decreases to 85% MDD, then the interface shear strength ratio will decrease until the remaining 10% due to an increase in content to result in Sr 100% (fully saturated).

Keywords: clay shale, weathered, interface, progressive, interface shear strength ratio, MRPST

The Effect of Diatomaceous Earth Addition to CBR Values of Glee Geunteng Soil Aceh Besar

Banta Chairullah
Lecturer, Department of Civil Engineering – University of Syiah Kuala

Munira Sungkar
Lecturer, Department of Civil Engineering – University of Syiah Kuala

Muhammad Ghiffari Ritonga
Alumni, Department of Civil Engineering – University of Syiah Kuala

ABSTRAK: Tanah sebagai tempat berdirinya konstruksi harus memiliki kekuatan yang stabil dalam menahan beban. Tanah yang tersedia di alam kadangkala memiliki sifat fisis dan mekanis yang terbatas sehingga diperlukan perbaikan tanah (stabilisasi). Dalam penelitian ini bahan tambahan yang digunakan adalah tanah Diatomae yang merupakan bahan pozzolan alami yang termasuk tipe SCM (*Suplementary Cementing Materials*). Stabilisasi kimiawi dilakukan dengan cara mencampurkan tanah dengan bahan stabilisasi seperti semen, kapur, abu terbang (*fly ash*), atau bahan lainnya yang bersifat dapat merubah komposisi kimiawi dan kombinasi tanah dengan bahan campuran. Tanah *diatomae* memiliki sifat pozzolan yang mirip dengan bahan pozzolan lainnya seperti *fly ash* dan metakaolin, sehingga diperkirakan dapat menjadi bahan stabilisasi tanah, yang dapat memperbaiki sifat-sifat tanah. Tanah yang digunakan berasal dari Glee Geunteng, Peukan Bada, sedangkan tanah diatomae berasal dari Desa Lambeureunut, Aceh Besar. Tujuan penelitian ini adalah untuk mendapatkan nilai CBR (*California Bearing Ratio*) pada tanah Glee Geunteng dengan mencampurkan tanah diatomae pada variasi 5%, 10%, 15% dan 20% dari berat kering tanah. Pengujian CBR terdiri dari pengujian CBR tanpa rendaman, pengujian CBR pada rendaman 4 hari serta sifat pengembangan (*swelling*) pada CBR dengan variasi campuran tanah *diatomae*. Tanah Glee Geunteng menurut klasifikasi AASHTO merupakan kelompok A-6(3) dan menurut klasifikasi USCS merupakan golongan SC *(silty clay)*. Hasil penelitian memperlihatkan bahwa pada tanah Glee Geunteng alami hingga campuran tanah diatomae 20% untuk pengujian CBR tanpa rendaman mengalami penurunan nilai CBR dari 35,96% menjadi 31,65%. Nilai pengujian CBR rendaman juga mengalami penurunan nilai CBR dari 15,57% menjadi 6,98%.

Kata Kunci: stabilisasi, tanah diatomae, CBR terendam dan CBR tidak terendam

ABSTRACT: Soil as a place for construction must have a strength to resist the load. Soil sometimes in nature has limited physical and mechanical properties so that soil improvement (stabilization) is needed. In this study, the additive used was Diatomaceous earth, which is a natural pozzolanic material as known as type of SCM (Supplementary Cementing Materials). Chemical stabilization is conducted by mixing the soil with stabilizing materials such as cement, lime, fly ash, or other materials that can change the chemical composition and combination of soil with mixed materials. Diatomaceous earth has similar pozzolanic properties with other pozzolanic materials such as fly ash and metakaolin powder, so it is expected to be a soil stabilizing agent, which can improve soil properties.The object of this study is soil from Glee Geunteng, Peukan Bada while the diatomaceous earth from Lambeureunut Village, Aceh Besar Regency. The purpose of this study was to obtain the CBR (California Bearing Ratio) value on Glee Geunteng soil by mixing diatomaceous earth at 5%, 10%, 15% and 20% from the dry weight of the soil. CBR testing consisted of unsoaked CBR, soaked CBR testing at 4 days and swelling properties of CBR with a variety of diatomaceous earth mixtures. Glee Geunteng soil was classified as A-6 Group Index 3 by the AASHTO soil classification and according to the USCS classification is the SC (silty clay) soil. The results showed that the natural Glee Geunteng soil to 20% diatomaceous earth for unsoaked CBR decrease in the value of CBR from 35.96% to 31.65%. The value of soaked CBR also decrease in the value of CBR from 15.57% to 6.98%.

Keywords: stabilization, diatomaceous earth, soaked CBR and unsoaked CBR

Consolidation Parameters of Marine Siltation

Nina Yuliana
PT Hydrocore

Eko Sumanto Putro
PT Hydrocore

Safrijhon Bastanta Tarigan
PT Hydrocore

ABSTRACT: In this paper, the consolidation test experiments were carried out to determine the compressibility parameters such as compression index (cc), recompression index (cr) and pre-consolidation pressure (p'c) of very soft soils taken from seabed sediments in Central Java. Four (4) types of consolidation test were adapted and developed for this study; standard constant rate of strain consolidation (CRS), CRS close loop system using CBR mold, CRS open loop system using CBR mold, and incremental loading consolidation test using CBR mold. The clayey soils used for the consolidation tests have high moisture content (more than 100%) and shear strength of less than 1 kPa. In addition, the correlations between compressibility characteristics of soils (cc and cr) and index properties (void ratio and water content) have been statistically calculated to obtain the empirical relations based on experimental test results and comparing with empirical relation from other researches.

Keywords: consolidation, very soft soils, marine siltation, constant rate of strain

1 INTRODUCTION

The consolidation parameters of marine siltation were required to calculate the consolidation settlement for example the settlement due to backfilling material. The marine siltation is generally very soft material dominated by fines soils (silt or clay) and having very low shear strength. Thus, it is difficult to measure the consolidation parameters by conventional laboratory testing due to its condition.

Umehara (1980) suggested that the constant rate of strain (CRS) test is applicable to determine the consolidation parameters of very soft soil with high water content. In this paper, four (4) types of consolidation test method were adapted and developed for this study; standard constant rate of strain consolidation (CRS), CRS close loop system using CBR mold, CRS open loop system using CBR mold, and incremental loading consolidation test using CBR mold. The CBR mold having larger diameter than conventional mold or ring was used in order to produce very small pressure on the specimen.

2 CHARACTERISTICS OF MARINE SILTATION

The samples of marine siltation or marine sediment for the experimental test were taken from seabed in Batang, Central Java. The soil conditions of the samples in this report are very soft silty clay/silt with high water content (more than 100%) and low shear strength (less than 1 kPa). Tests performed on the samples consisted of moisture contents and density (unit weight) tests. Additional tests such as Atterberg's limits, specific gravity, sieve analysis and hydrometer tests were also conducted. The characteristics of marine siltation are summarised in the following tables.

Table 1. Initial Condition of Marine Siltation.

Sample ID	Initial Void Ratio	Initial Moisture Content (%)
Spec. 1	5.512	189.4
Spec. 2	4.517	171.6
Spec. 3	4.652	172.6
Spec. 4	4.789	188.2
Spec. 5	10.018	349.2
Spec. 6	3.966	150.0

Sample ID	Initial Void Ratio	Initial Moisture Content (%)
Spec. 7	8.787	327.0
Spec. 8	5.214	199.7
Spec. 9	3.768	133.7
Spec. 10	6.195	248.1
Spec. 11	4.959	181.9
Spec. 12	5.084	194.0
Spec. 13	5.040	189.9
Spec. 14	7.677	287.1
Spec. 15	3.262	109.3
Spec. 16	5.719	215.3
Spec. 17	3.306	125.9
Spec. 18	3.020	116.9
Spec. 19	7.212	279.8
Spec. 20	6.190	228.2
Spec. 21	4.330	138.9
Spec. 22	4.205	153.9
Spec. 23	6.047	224.7

Table 2. Soil Properties of Marine Siltation.

Soil Properties	Unit	Average
Specific gravity	-	2.677
Liquid limit	%	75
Plastic limit	%	31
Plasticity index	-	44
Sand fraction	%	0.6
Silt fraction	%	51.6
Clay fraction	%	47.7
Shear strength, S_u	kPa	0.09

3 EXPERIMENTAL TEST APPARATUS AND METHODOLOGY

3.1 *Specimen Preparation*

The marine siltation is extremely soft with high water content (more than 100%) thus the samples were stirred using hand mixer to obtain the uniformity of soil specimen before commence the consolidation test.

3.2 *Constant Rate of Strain (CRS) Consolidation Test*

The constant rate of strain (CRS) consolidation tests were conducted using three methods; standard CRS, open loop system of CRS using CBR mold and close loop system of CRS using CBR mold in accordance with ASTM D4186. Drainage was permitted at the top of specimen. For open loop CRS, the drainage was uncontrolled and the excess pore pressure is disregarded. A base pressure or back pressure of 100 kPa was applied to saturate the specimen except in open loop system. A continuously increasing load was applied to the top of specimen so as to produce a constant rate of compressive strain. Strain rate of CRS tests was controlled using triaxial load frame that give constant speed rate of axial strain and load to the specimen. The rate of deformation was 1%/hour during the loading phase.

An overview of the arrangement of components for each CRS equipment is presented in the following figures.

Fig. 1. Standard CRS Consolidation Test System.

Fig. 2. Open Loop CRS Consolidation Test System Using CBR Mold.

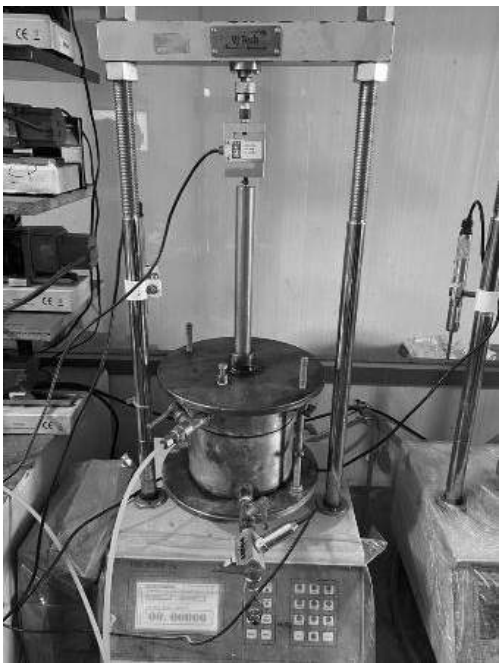

Fig. 3. Close Loop CRS Test System Using CBR Mold.

3.3 *Incremental Load Consolidation Test using CBR Mold*

Time intervals of approximately 0.1, 0.25, 0.5, 1, 2, 4, 8, 15 and 30min, and 1, 2, 4, 12, 24, 36, 48, 60, 72, 84, 96, 108 and 120h was recorded. During consolidation, measurements were made of change in height of specimen. The measurements were used to determine the relationship between void ratio or strain and effective stress. The effective stress was doubled for each increment with the initial effective pressure was resulted from the load of piston and top cap's weight.

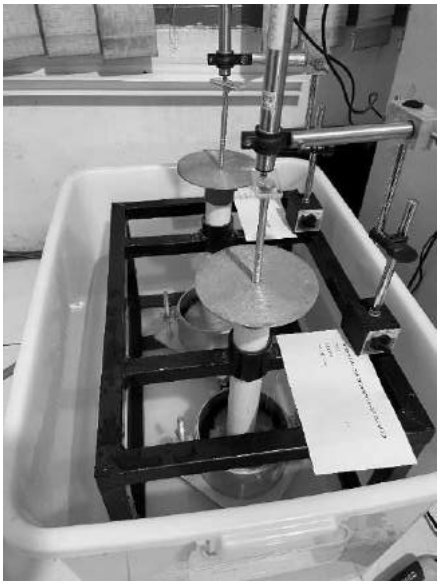

Fig. 4. Incremental Loading Consolidation Test System using CBR Mold.

4 TEST RESULTS

The experimental test results comprised 23 (twenty-three) specimens using four methods: 7 (seven) tests of standard CRS; 3 (three) tests of open loop CRS; 10 (ten) tests of close loop CRS and 3 (three) tests of incremental loading consolidation. The compressibility parameters such as compression index (c_c), recompression index (c_r) and pre-consolidation pressure (p'_c) of the tested marine siltation is tabulated in Table 3 as below:

Table 3. Compressibility Parameters of Marine Siltation.

Sample ID	c_c	c_r	p'_c (kPa)
Spec. 1	0.929	0.376	2.14
Spec. 2	0.890	0.189	1.15
Spec. 3	0.980	0.195	1.87
Spec. 4	0.914	0.389	0.33
Spec. 5	2.007	0.385	2.55
Spec. 6	0.754	0.204	6.35
Spec. 7	2.166	0.378	2.27
Spec. 8	1.391	0.290	0.73
Spec. 9	1.091	0.192	1.05
Spec. 10	1.642	0.665	0.30
Spec. 11	1.055	0.179	0.88
Spec. 12	1.311	0.214	1.73
Spec. 13	1.022	0.341	0.65
Spec. 14	1.899	0.294	1.38
Spec. 15	0.541	0.132	2.93
Spec. 16	1.329	0.238	1.51
Spec. 17	0.617	0.091	3.70
Spec. 18	0.462	0.076	4.45
Spec. 19	1.646	0.442	0.61
Spec. 20	1.468	0.470	0.48
Spec. 21	0.670	0.156	0.52
Spec. 22	0.730	0.361	0.80
Spec. 23	1.384	0.591	1.20

All the experimental test results of void ratio (e) versus consolidation pressure (p) are plotted in the Fig. 5.

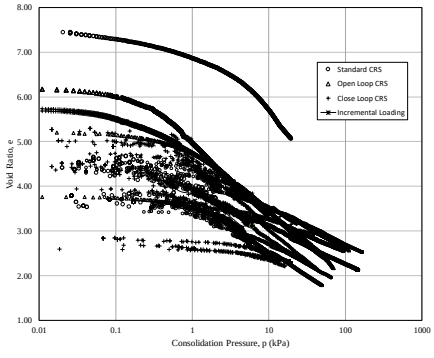

Fig. 5. e log p Curves of Consolidation Test Results on Marine Siltation.

The compression index (c_c) and its correlation to initial void ratio (e_0) and water content (W_n) were also plotted to determine the empirical calculations using linear regression and compared with the existing empirical equation from researcher that presented in the Table 4.

Table 4. Correlations of Compression Index (Cc).

References	Equation
Azzouz et al. (1976)	$C_c = 0.01 (W_n – 5)$
Serajuddin (1987)	$C_c = 0.013 (W_n – 8)$
Aminaton et al. (2002)	$C_c = 0.0026W_n + 0.1886$
Azzouz et al. (1976)	$C_c = 0.4 (e_0 – 0.25)$
Bowles (1979)	$C_c = 0.156e_0 + 0.0107$
Rendon-Herrero (1980)	$C_c = 0.3 (e_0 – 0.27)$

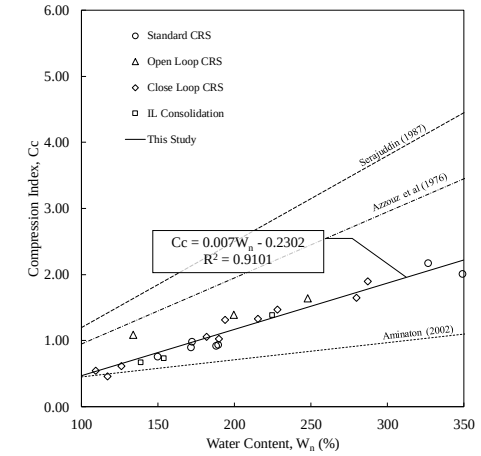

(a)

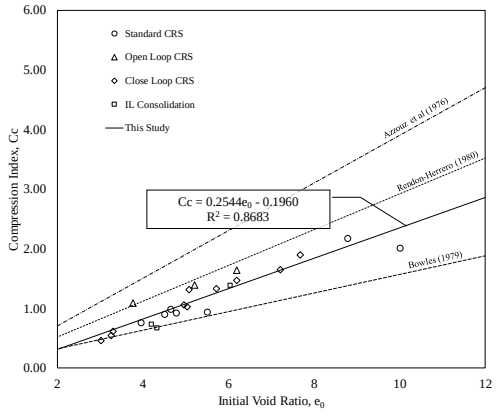

(b)

Fig. 6. Correlation between Compression Index (cc) and Index Parameters of the Samples: (a) Water Content; and (b) Initial Void Ratio.

The figure 6 shows an increasing trend for the compression index c_c while increasing the water content (W_n) or void ratio (e_0). The derived statistically correlation is stated in following equations

$$Cc = 0.007W_n – 0.2302 \quad : R^2 = 0.9101 \quad (1)$$

$$Cc = 0.2544e_0 – 0.1960 \quad : R^2 = 0.8683 \quad (2)$$

Furthermore, recompression index (c_r) and compression index (c_c) correlation are varied and the c_c value is in between 2 times and 10 times c_r as shown in Fig. 7.

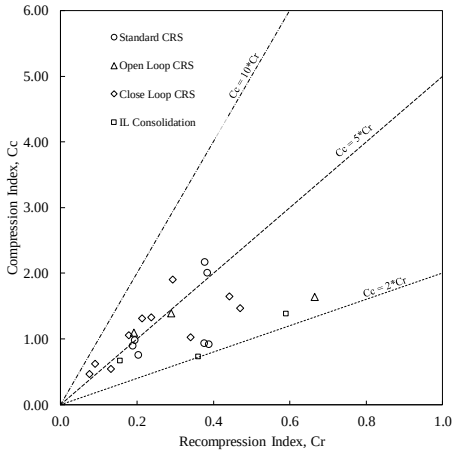

Fig. 7. Correlation between Compression Index (cr) and Recompression Index (cr)

5 CONCLUSION

The constant rate of strain (CRS) consolidation is more applicable for marine siltation. The correlation between compressibility parameters (Cc and Cr) and index parameters (initial moisture content and void ratio) show that the research is empirically relatively close to the research done by Azzouz et al. (1976), Aminaton (2002), Bowles (1979) and Rendon-Herrero (1980).

The consolidation of marine siltation due to self-weight need to be observed in the future.

REFERENCES

Ag, Ajoykumar. 1994. *Consolidation and Permeability Behavior of High Porosity Baltic Seabed Sediments*. Open Access Master's Theses. 916.

Budhu, M. 2000. *Soil Mechanics and Foundations*. New York: Wiley.

Umehara, Yasufumi and Kouki Zen. 1980. Constant Rate of Strain Consolidation for very Soft Clayey Soils. *Japanese Society of Soil Mechanics and Foundation Engineering Vol. 20, No. 2*: 80-95.

Umehara, Yasufumi and Kouki Zen. 1982. Consolidation Characteristics of Dredged Marine Bottom Sediments with High Water Content. *Japanese Society of Soil Mechanics and Foundation Engineering* Vol. 22, No. 2: 40-54.

Compaction Characteristics of Fine-grained Soil from Several Locations in Indonesia Controlled by Degree of Saturation and Plasticity Index

Hasbullah Nawir
Institute Technology Bandung

Laras Dipa Pramudita
Institute Technology Bandung

Tita Kartika Dewi
Institute Technology Bandung

ABSTRACT: Compaction test is done by giving certain mechanical energy to obtain maximum dry density $(\rho_d)_{max}$ and the optimum moisture content $(w)_{opt}$ which used for controlling field compaction. However, compaction energy level (CEL) and soil type in field are varied result in difficulty of accurate evaluation. Optimum degree of saturation $(Sr)_{opt}$ is the degree of saturation when $(\rho_d)_{max}$ obtained during compaction. The value of $(Sr)_{opt}$ is independent of both CEL and soil type thus expected to become control parameter that could describe the level of compaction better than conventional way. $(Sr)_{opt}$ of Indonesia's soil is unique which is different from soil in subtropical country. California Bearing Ratio (CBR) as one of physical properties of compacted soil and Plasticity Index (PI) at various CEL (supported by Unconfined Compression Test result) can be correlated with $(\rho_d)_{max}$ and $(Sr)_{opt}$. These findings may lead to new compaction control method which include design requirement as consideration.

Keywords: compaction, maximum dry density, degree of saturation, optimum degree of saturation, moisture content, CBR, plasticity index, index properties, unconfined compression test, Indonesia's soil

ABSTRAK: Pemadatan tanah dilakukan dengan memberikan energi mekanis yang berasal dari palu dengan berat dan tinggi jatuh tertentu. Secara konvensional, kontrol kepadatan menggunakan parameter kepadatan kering maksimum $(\rho_d)_{max}$ dan kadar air optimum $(w)_{opt}$. Di lapangan, energi dan jenis tanah akan bervariasi sehingga sulit dilakukan evaluasi kepadatan tanah secara akurat. Derajat saturasi optimum $(Sr)_{opt}$ merupakan derajat saturasi tanah saat nilai $(\rho_d)_{max}$ diperoleh. Dalam hal ini, $(Sr)_{opt}$ merupakan besaran yang tidak bergantung terhadap nilai tingkat energi kompaksi (CEL) maupun jenis tanah sehingga dapat digunakan sebagai kontrol yang lebih baik dalam menggambarkan kondisi kepadatan tanah dibandingkan dengan cara konvensional. Nilai $(Sr)_{opt}$ untuk tanah di Indonesia menghasilkan rentang tertentu yang unik. Nilai California Bearing Ratio (CBR) yang merupakan salah satu sifat fisis tanah terkompaksi dan nilai plasticity index (PI) pada berbagai tingkatan energi (didukung dengan hasil Unconfined Compression Test) dapat dihubungkan dengan nilai $(\rho_d)_{max}$ dan $(Sr)_{opt}$, sehingga diperoleh korelasi praktis yang dapat diterapkan di lapangan.

Kata Kunci: kompaksi, pemadatan tanah, berat isi kering maksimum, derajat saturasi, kadar air, CBR, plasticity index, index properties, unconfined compression test, compressive strength, tanah Indonesia

Compressive Strength Characteristics of Trass Stabilized Dredged Soil

Komang Arya Utama
Doctoral student, Department of Civil Engineering – Hasanuddin University

Tri Harianto
Department of Civil Engineering – Hasanuddin University

Achmad Bakri Muhiddin
Department of Civil Engineering – Hasanuddin University

Ardy Arsyad
Department of Civil Engineering – Hasanuddin University

ABSTRAK: Longsor besar yang terjadi pada kaldera Gunung Bawakaraeng memicu terjadinya endapan sedimen di daerah hilir Sungai Je'neberang. Salah satunya adalah pengendapan material sedimen di Bendungan Bilibili. Beberapa pengujian terhadap sifat dasar geoteknik material endapan sedimen yang dikeruk di Bendungan Bilibili menunjukkan bahwa material ini memiliki karakteristik yang buruk untuk aplikasi timbunan. Penelitian ini bertujuan untuk menganalisis sifat mekanik tanah kerukan sedimen yang distabilisasi dengan Tras. Tras sebagai bahan stabilisasi diberikan dengan komposisi 3%-12% terhadap berat kering tanah kerukan sedimen. Lebih lanjut, untuk melihat respon pemeraman pada tanah kerukan stabilisasi Tras ini, dilakukan beberapa masa pemeraman yaitu 3, 7 dan 14 hari. Uji pemadatan dan uji kuat tekan bebas (UCS) dilakukan pada sampel uji tanah stabilisasi. Hasil penelitian menunjukkan bahwa terjadi peningkatan nilai kepadatan kering maksimum (MDD) dari 14,06 kN/m3 menjadi 14,56 kN/m^3 dengan kadar air optimum (OMC) sebesar 24,36%. Selanjutnya, nilai UCS meningkat dari 235,19 kN/m^2 untuk tanah tanpa stabilisai menjadi 1149,81 kN/m^2 untuk tanah kerukan dengan stabilisasi Tras dengan masa pemeraman 14 hari.

Kata Kunci: tras, tanah kerukan, timbunan

ABSTRACT: A large landslide that occurred in the caldera of Mount Bawakaraeng triggered sediment deposits in the downstream area of the Je'neberang river. One of them is the deposition of sediment material at the Bilibili Dam. Several testing to the geotechnical basic properties of the dredged sedimentary material at the Bilibili Dam showed that this material has poor characteristics for embankment applications. This research aims to analyze the mechanical properties of sedimentary dredged soil stabilized with Trass. Trass as stabilizing agent was given with a composition of 3%-12% by dry weight. Furthermore, to see the curing response of this Trass stabilized dredged soil, several curing period of 3, 7 and 14 days were applied to the testing samples. Compaction test and unconfined compressive strength (UCS) tests were applied. The results showed that there is an increase in the maximum dry density (MDD) from 14.06 kN/m^3 to 14.56 kN/m^3 with optimum moisture content (OMC) is 24.36%. Furthermore, the UCS value was increased from 235.19 kN/m^2 for the untreated soil to 1149.81 kN/m^2 for the stabilized dredged soil with a curing period of 14 days.

Keywords*:* trass, dredged soil, embankment

Studi Pengaruh Pecampuran Senyawa *Synthetic Polyacrylamide* (PAM) pada Tanah Kohesif

Reza Rahman Syafei
Mahasiswa Magister Program Studi Teknik Sipil – Institut Teknologi Bandung

Masyhur Irsyam
Dosen Program Studi Teknik Sipil – Institut Teknologi Bandung

KM Abuhuroyroh
Tim Peneliti Geoteknik – Institut Teknologi Bandung

ABSTRAK: Dalam upaya mengoptimalisasi penggunaan material tanah disuatu lokasi pekerjaan, khusunya pada pekerjaan perbaikan tanah, penelitian ini akan membahas pengaruh penggunaan senyawa synthetic polyacrylamide (PAM) pada campuran tanah kohesif melalui uji laborarotium, pemodelan 3D, dan studi komeperatif terhadap data praktisi di lapangan, penelitian dilakukan guna mengetahui pengaruh dari penggunaan PAM terhadap nilai parameter kekuatan tanah, distribusi beban dan penurunan yang terjadi pada sistem CMC dengan LTP, Hasilnya menunjukan, nilai MDD berkurang 0,26 % pada IP tinggi dan meningkat 0,63 % pada IP rendah, nilai permeabilitas menurun dalam rentang 44,15-61,96 %, nilai kohesi meningkat dalam rentang 13,3-100% nilai awal, sudut geser dalam berkurang 5% pada IP tinggi, dan bertambah 13,5% pada IP rendah, dari distribusi tekanan terlihat peningkatan tegangan efektif, penurunan nilai regangan dan punching pada lapisan LTP dengan material yang ditambahkan PAM

Kata Kunci: perbaikan tanah, control modulus column, load transfer platform, synthetic polyacrylamide

ABSTRACT: In an effort to optimize the use of soil materials in a project location, especially in soil improvement work, this study will discuss the effect of the use of synthetic polyacrylamide (PAM) compounds on cohesive soil mixtures through laboratory tests, 3D modeling, and comparative studies of practitioner data in the field. in order to determine the effect of the use of PAM on the value of soil strength parameters, load distribution and settlement that occurs in the CMC system with LTP, the results show, the MDD value decreases by 0.26% at high IP and increases by 0.63% at low IP, the permeability value decreases. in the range of 44.15-61.96%, the value of cohesion increases in the range of 13.3-100% of the initial value, the friction angle decreases by 5% at high IP, and increases by 13.5% at low IP. The load distribution it is seen an increase on effective stress, a decrease in the value of strain and punching in the LTP layer with PAM added material.

Keywords: soil improvement, control modulus column, load transfer platform, synthetic polyacrylamide

1 PENDAHULUAN

Indonesia adalah negara berkembang yang sangat luas dengan begitu banyak pekerjaan pembangunan diseluruh wilayahnya. Pekerjaan pembangunan tersebut tidak terlepas dari dokumen-dokumen pekerjaan yang harus dipatuhi, walaupun tidak jarang permasalahan muncul di lapangan sehingga pemenuhan salah satu spesifikasi material sulit dicapai, seperti contohnya keterbatasan material dilapangan, sehingga harus mendatangkan material dari luar area pekerjaan yang akan berdampak pada biaya pekerjaan.

Pada Kasus pekerjaan perbaikan tanah menggunakan metode *Controlled Modulus Columns* (CMC) dengan *Load Transfer Platform* (LTP), permasalahan yang sering dialami adalah keterbatasan material granular penyusun LTP yang memenuhi spesifikasi teknis (*fine grained* <15%) dan apabila menggunakan material kohesif akan mengakibatkan LTP memiliki tebal lapisan yang jauh lebih besar dibandingkan penggunaan material granular, hal ini guna menghindari timbulnya *mushroom effect* pada permukaan LTP, akibat kekuatan geser yang tidak dapat dicapai.

Dalam upaya mengoptimalisasi material dilapangan khususnya area-area pekerjaan yang memlikik keterbatasan akses mobilisasi dan menekan biaya tambahan yang mungkin harus dibayarkan akibat proses pendatangan material dari luar area. Penggunaan senyawa *synthetic polyacrylamide* (PAM) pada campuran material sembarang khususnya tanah kohesif sebagai upaya peningkatan kekuatan tanah patut untuk diperhitungkan.

PAM merupakan konsentrat bubuk dari akrilamida, surfaktan, dan pengikat yang bila dicampur dengan air membentuk ko-polimer cair, fungsi utama dari penggunaan material ini adalah untuk meningkatan kekuatan tanah dalam kondisi basah dan kering pada tanah juga mereduksi nilai permeabilitas tanah.

Pada tulisan ini akan dilakukan studi penggunaan PAM pada tanah residual permukaan yang diambil dari daerah Subang, Jawa Barat. Studi diawili dari serangkaian pengujian sample material di laboratorium yang terdiri dari uji *Atteberg Limit*, uji kompaksi, uji permeabilitas, dan uji triaxial pada campuran tanah dengan dan tanpa PAM, data hasil pengujian yang didapatkan digunakan pada pemodelan 3D menggunakan Plaxis pada analisis pemodelan CMC dengan LTP untuk 2 variasi parameter LTP dengan material campuran dan tanpa campuran PAM untuk dibandingkan efek distribusi beban yang dihasilkan, terkahir pada tulisan ini dilakukan studi komperatif data laboratorium yang didapatkan dengan data-data prakitisi maupun literatur terkait lainnya.

2 STUDI LITERATUR

2.1 *Load Transfer Platform*

Load transfer platform adalah suatuh lapisan yang terletak dibagian atas dari CMC, lapisan ini bertujuan untuk menyalurkan beban merata keseluruh bagian ujung atas dari kolom. Asiri (2012) menunjukkan hasil dari pengujian terhadap model CMC, LTP yang terletak pada bagian bawah timbunan dimodelkan dengan memberi beban merata pada platform. Hasil kalkulasi mengindikasikan adanya beban geser yang terkonsentrasi pada bagian tepi dari platform dan membentuk zona yang mengerucut ke bagian kepala dari kolom inklusi seperti yang Gbr.1.

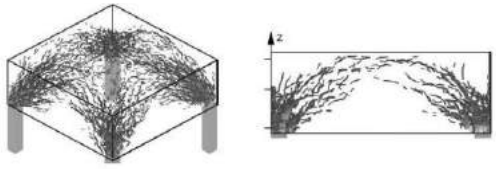

Gbr. 1. Mekanisme Distribusi Beban yang Terjadi di dalam LTP, Asiri (2012).

2.2 *Interaksi PAM dengan Tanah*

Synthetic polyacrylamide (PAM) merupakan senyawa polimer, menurut Romel N Georgees (2015) pada jurnalnya menjelaskan bahwa polimer adalah zat yang tersusun dari rantai molekul panjang (monomer), yang terikat oleh kovalen. Polimer, yang bisa ditemukan dalam bentuk alami dan sintetis, diklasifikasikan secara fungsional untuk stabilisasi tanah menjadi kationik, nonionik, dan anionik polimer.

Interaksi PAM dengan partikel tanah dijelaskan oleh B.K.G Theng (2012), pada bukunya yang mengatakan bahwa interaksi PAM dengan partikel tanah sangat dipengaruhi oleh besarnya penyerapan yang terjadi pada permukaan luar partikel tanah. Besarnya penyerapan ini bergantung pada muatan PAM dan jenis tanah (kandungan mineral) yang terkandung pada tanah terkait. Penyerapan PAM bermuatan positif relatif lebih banyak dibandingkan dengan PAM dengan kandungan ion negatif, hal ini disebabkan adanya tolakan dari kandungan molekul negatif yang berada pada permukaan lempung (lihat Gbr.2)

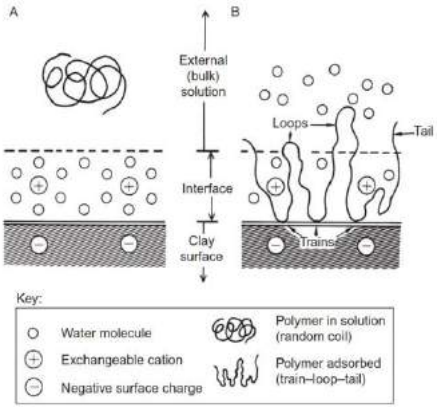

Gbr. 2. Ilustrasi Penyerapan PAM pada Permukaan Luar Partikel Tanah, B.K.G Theng (2012).

Pada proses penyerapan PAM oleh partikel tanah, untaian PAM menggantikan molekul air yang ada di permukaan eksternal partikel tanah dengan kata lain mendorong molekul air keluar dari permukaan luar partikel tanah. Gill dan

Herrington (1986) mengatakan bahwa ikatan yang terbentuk dikarenakan adanya PAM lebih kuat dibandingkan ikatan alamiah pada umumnya.

2.3 *Efek Penggunaan PAM pada Tanah*

Efek penggunaan polimer pada tanah ini sudah dianalisis oleh beberapa peneliti yang umumnya menyimpulkan bahwa pencampuran polimer dengan tanah akan meningkatan nilai kuat tekan tanah itu sendiri.

Georgees RN (2015), menyimpulkan bahwa penggunaan *synthetic polyacrylamide* (PAM) sebagai zat aditif penstabil tanah terbukti meningkatkan kepadatan tanah, dengan peningkatan yang tercatat sebesar 0,8% hingga 1,3% dibandingkan dengan sampel yang tidak dicampur PAM, Tanah yang ditambahkan PAM menghasilkan nilai UCS yang lebih besar, bergantung pada tingkat usaha pemadatan, dengan peningkatan yang tercatat sebesar 22,9% hingga 95,2% dibandingkan dengan sampel yang tidak dicampur PAM.

Pada penilitian lain Jin Liu (2010) melakukan penelitan pada tanah lempung dengan melakukan pengujian tekan (UCS) dan uji geser (*shear test*). Hasilnya memperlihatkan semakin besar konsentrasi PAM yang digunakan semakin tinggi nilai UCS yang dihasilkan, pada penelitiannya pun memperlihatkan bahwa diperlukan waktu untuk campuran material tanah dengan PAM mencapai kekuatan maksimumnya.

2.4 *Kadar Pencampuran PAM*

Pada pengaplikasiaanya PAM perlu dicampurkan dengan air, terdapat beberapa referensi kadara campuran PAM dengan tanah yang didapat dari berbegai literatur, secara garis besar merujuk pada nilai kadar yang sama.

Kadar pencampuran PAM yang direkomendasikan menurut Seal Group (2010) ialah sebesar 2 kg PAM untuk 50 m^3 tanah atau sekitar 0,002% dari berat material yang akan dicampur.

Georgees RN (2015), pada penelitiannya menggunakan rasio kandungan PAM sebesar 2gr/5liter air, dijelaskan pula bahwa rasio ini sudah memperhitungkan kadar yang disarankan oleh produsen, bahkan lebih yaitu sebesar 0,004% berat material yang akan dicampurkan.

PT Rekakarya Geoteknik dalam panduang pengujian menyarankan penggunaan PAM dengan rasio sebesar 3 gr PAM untuk 10 liter air, setara 2 kg/50 m^3.

3 METODOLOGI PENELITIAN

Alur penelitian yang dilakukan dapat dilihat pada Gbr. 3

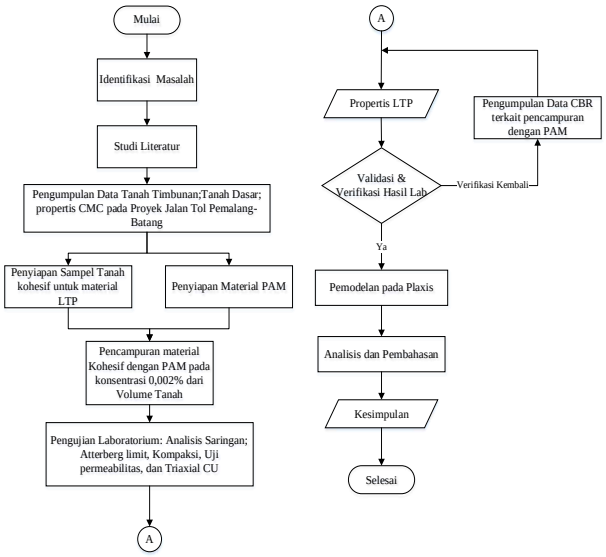

Gbr. 3. Bagan Alir Penelitian.

Secara umum penelitian ini dimulai dari pengujian laboratorium yang sampel tanah nya diambil secara acak dari daerah Subang, Jawa Barat, sekema pengujian dibagi menjadi 2 kategori, yaitu material tanah dengan campuran PAM dan tanpa campuran PAM, dari serangkaian pengujian laboratorium yang dilakukan (uji atteberg limit, kompaksi, permeabilitas, dan triaxial CU) didapatkan sebuah data nilai sudut geser dalam, kohesi, modulus elastisitas yang dijadikan parameter pemodelan LTP pada program Plaxis 3D. Data pemodelan lainnya seperti data sratigrafi tanah, propertis CMC dan geometri timbunan diambil dari data pekerjaan tol Pemalang-Batang.

Proses validasi data laboratorium dan data pemodelan dilakukan dengan cara diskusi dan komparasi hasil terhadap literatur dan data Pengujian CBR lapangan yang didapat dari proses trial oleh praktisi dilapangan.

Referensi pada penulisan ini adalah Georgees RN (2015), pada karyanya Georgess banyak menjelaskan penggunaan PAM dan juga menyatakan bahwa hasil penggunaan senyawa PAM dilapangan menghasilkan performa yang baik namun tidak tergambarkan dari hasil pengujian laboratorium.

4 HASIL ANALISIS

4.1 *Klasifikasi Sampel Tanah*

Pada penulisan ini terdapat dua jenis sampel tanah dengan data sebagai berikut:

Tabel 1. Propertis Tanah.

Propertis	Sampel	
	A1	A2
Distribusi Ukuran		
Pasir, %	8,36	50
Lanau, %	68,92	37,69
Lempung, %	22,71	12,31
Max. Dia (mm)	4,75	4,75
D60% (mm)	0,03	0,12
Atterberg Limit		
LL, %	67,7	31,39
PL, %	31,66	18,59
PI, %	36,11	12,80
Klasifikasi	CH	CL

Sampel A1 merupakan sampel dengan plastisitas tinggi sedangkan A2 merupakan sampel dengan plasitisitas rendah dengan 50% distribusi partikel didominasi oleh pasir.

4.2 *Hasil Pengujian Laboratorium*

Pengujian laboratorium menggunakan kadar PAM sebesar 3gr per 10 liter air hal ini sudah mengikuti standar pengujian dari produsen PAM atau setara dengan 2 kg untuk 50m^3 material yang akan dicampurkan.

4.2.1 Pengujian Kompkasi

Jenis pengujian yang dilakukan adalah *modified proctore* dengan masing-masing lapisan ditumbuk sebanyak 35 kali Hasil pengujian kompaksi memperlihatkan Dari 4 sampel pengujian yang dilakukan yang terdiri dari 2 sampel dengan PAM dan 2 sampel tanpa PAM didapatkan hasil bahwa pada nilai indeks plastisitas (IP) rendah nilai OMC menurun dari 13,9% menjadi 12,6 % dengan nilai MDD yang meningkat dari 1,898 kN/m^3 menjadi 1,91 kN/m^3 sedangkan pada nilai IP tinggi sebaliknya, nilai OMC meningkat dari 27,8% menjadi 28,2% dan MDD mengalami penurunan dari 1,513 kN/m^3 menjadi 1,509 kN/m^3.

Tabel 2. Hasil Pengujian Kompaksi.

Propertis	Sampel	
	A1	A2
Dengan PAM		
OMC, %	28,2	12,6
MDD, %	1,509	1,910
Tanpa PAM		
OMC, %	27,8	13,9
MDD, %	1,513	1,898

Data pada Tabel 2 dibandingkan dengan hasil pengujian Georgees RN (2015) sebagai validasi hasil, komparasinya dapat dilihat pada Gbr.4 dan Gbr. 5.

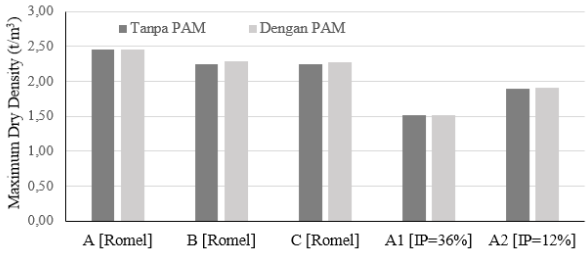

Gbr. 4. Perbandingan Hasil MDD dengan Hasil Georgees RN.

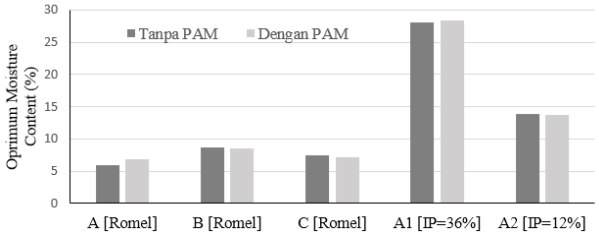

Gbr. 5. Perbandingan Hasil OMC dengan Hasil Georgees RN.

Pada penelitian ini persentasi perubahan nilai MDD dan OMC dapat dikatakan serupa atau dalam rentang nilai yang sama dengan yang dihasilkan oleh Georgees RN (2015) pada penelitiannya.

4.2.2 Pengujian Permeabilitas

Dari pengujian permeabilitas penggunaan PAM mereduksi nilai permeabilitas, pada sampel A1 dan A2 nilai permeabilitas menurun dengan rata-rata penurunan sebesar 53,06%, lebih rinci data pengujian permeabilitas dapat dilihat pada Tabel. 3.

Tabel 3. Hasil Pengujian Permeabilitas.

Propertis	Sampel	
	A1	A2
Dengan PAM	4,24E-05	5,67E-4
Tanpa PAM	1,12E-04	1,02E-03

4.2.3 Pengujian Triaxial

Secara umum penggunaan PAM dapat meningkatkan nilai parameter kekuatan tanah, dari pengujian Triaxial CU pada *sampel high plasticty* (A1) dan *low plasticity* (A2) mengindikasikan bahwa PAM cenderung meningkatkan nilai kohesi tanah terkait, hal ini memperkuat pernyataan bahwa PAM efisien digunakan pada tanah kohesif yang dipengaruhi mineral yang terkandung pada tanah tersebut. Data hasil pengujian triaxial secara rinci dapat dilihat pada Tabel 4.

Tabel 4. Hasil Pengujian Triaxial.

Propertis	Sampel	
	A1	A2
Dengan PAM		
Kohesi (kPa)	34	12
Friksi (˚)	21	32,7
Tanpa PAM		
Kohesi (kPa)	30	6
Friksi (˚)	22,2	28,8

Pada sampel A1 parameter kohesi mengalami peningkatan 13,3% dan untuk parameter sudut geser dalam mengalami penurunan sebesar 5,71 %, Pada sampel A2 parameter kohesi mengalami peningkatan 200 % dan untuk parameter sudut geser dalam mengalami peningkatan sebesar 13,54 %.

4.3 *Pengumpulan data CBR Laboratorium dan Lapangan*

Data hasil pengujian CBR material dengan PAM dikumpulkan dari beberapa praktisi yang telah melakukan pengujian pencampuran PAM dengan tanah, dari data yang didapatkan terlihat bahwa pencampuran PAM dengan tanah pada ruas tol Pekanbaru-Bangkinan mampu meningkatkan nilai CBR dengan peningkatan berkisar antara 9,4% - 134 % dari nilai CBR awal. Hal ini mengindikasikan bahwa penggunaan PAM pada tanah memperlihatkan pengaruh yang sangat baik.

Penerapan PAM pada proyek lain pun memperlihatkan performa yang baik, pada proyek di area Pama Adaro CBR meningkat sebesar 178,65 % dari nilai awal 6,3% menjadi 17,55%, pada proyek Bolaang mongondow CBR meningkat 141,6% dari nilai awal 16,55% menjadi 39,985%, pada proyek Tambang Mifa peningkatan terjadi sebesar 14,54% dari 24,55% menjadi 28,125 %.

4.4 *Hasil Pemodelan 3D menggunakan Plaxis 3D.*

Analisis pemodelan 3D dilakukan dengan membandingkan dua kondisi tipe material LTP yang berbeda, yaitu pada kondisi material LTP dengan PAM (sampel A1) dan material LTP dengan material granular. Analisis dilakukan pada nilai tegangan air pori, regangan, tegangan efektif pada LTP, dan penurunan yang terjadi.

4.4.1 Tegangan Air Pori

Tegangan air pori yang terjadi dari 2 pemodelan tidak jauh berbeda, tegangan air pori meningkat dan mencapai puncaknya pada tahap timbunan ke-7 dan berangsur-angsur nilainya mendekati nol pada hari ke 82. Dapat dikatakan perilaku yang terjadi pada tegangan air pori dipemodelan LTP treated menyerupai perilaku yang terjadi pada LTP rencana.

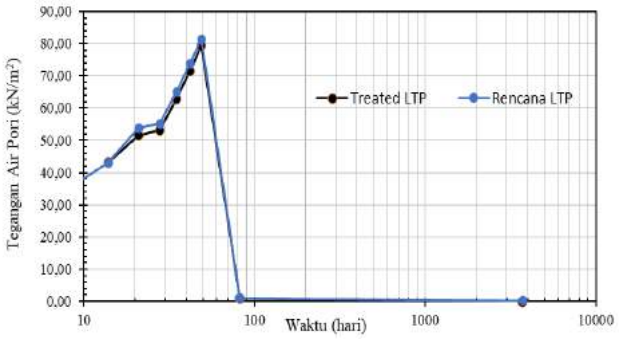

Gbr. 6 Perbandingan Nilai Tegangan Air Pori pada 2 Kondisi.

4.4.2 Regangan

Besar regangan yang terjadi pada 2 pemodelan, yaitu pada kondisi LTP dengan PAM dan LTP rencana dengan granular memperlihatkan hasil penurunan regangan akibat penambahan PAM. Nilai regangan dilihat pada lapisan permukaan LTP dengan hasil regangan pada kedua pemodelan dapat dilihat pada Tabel 5.

Tabel 5. Regangan pada Setiap Pemodelan LTP.

Elevasi	ε_{zz} Tanpa PAM	ε_{zz} Dengan PAM
0+00	0,08209	0,06927

4.4.3 Tegangan

Tegangan Efektif yang terjadi pada analisis LTP dengan material granular tanpa PAM dan LTP dengan PAM, memperlihatkan bahwa nilai-nilai tegangan efektif pada kedua analisis berturut-turut adalah (σ_1') 3100 kN/m^2 dan (σ_1') 1875 kN/m^2.

4.4.4 Penurunan Tanah

Besar penurunan pada U.90% adalah 0,53 meter pada LTP dengan PAM dan 0,50 pada LTP dengan material granular tanpa PAM, material residual yang dicampur dengan polycom memiliki besar penurunan total yang lebih besar dari material LTP yang direncanakan namun dengan selisih perbedanaan penurunan rata-rata adalah 0,014 meter atau 1,4cm, dengan nilai penurunan yang tidak signifikan perbedaannya, LTP treated dengan tanah residual memiliki performa yang cukup baik.

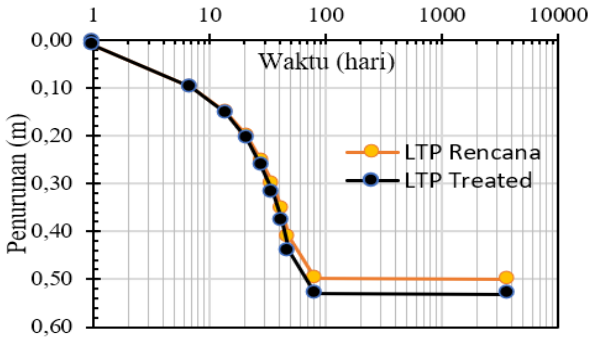

Gbr. 7. Perbandingan Hasil Penurunan Tanah.

5 KESIMPULAN

Hasilnya menunjukan, nilai MDD berkurang 0,26 % pada IP tinggi dan meningkat 0,63 % pada IP rendah, nilai permeabilitas menurun dalam rentang 44,15-61,96 %, nilai kohesi meningkat dalam rentang 13,3-100% nilai awal, sudut geser dalam berkurang 5% pada IP tinggi, dan bertambah 13,5% pada IP rendah, dari distribusi tekanan terlihat peningkatan tegangan efektif, penurunan nilai regangan dan punching pada lapisan LTP dengan material yang ditambahkan PAM.

PENGHARGAAN

Penghargaan diberikan kepada Institut Teknologi Bandung, khususnya program studi Magister Teknik Sipil sebagai sarana pengembangan ilmu pengetahuan, PT Rekakarya Geoteknik yang memberikan sampel PAM untuk penelitian ini, Turyadi selaku pemilik laboratorium yang memfasilitasi penelitian ini.

DAFTAR PUSTAKA

Georgees, R.N 2015. Effect of the Use of a Polymeric Stabilizing Additive on Unconfined Compressive Strength of Soils. *Transportation Research Board of the National Academies*. Washington.

Han, J. 2014. *Principle and Practice of Ground Improvement*. New Jersey: JohnWiley & Sons, Inc.

Liu, J. 2011. Research on the Stabilization Treatment of Clay Slope Topsoil by Organic Polymer Soil Stabilizer. *Engineering Geology*.

Theng, B.K.G. 2012. *Formation and Properties of Clay Polymer Complexes*.

Project, Asiri National. 2011. *Recomendations for the Desain, Contruction and Control of Rigid Inclusion Ground Improvements*.

Mapping Expansive Soil Characteristics on The National Road Segment in Java Island

Diah Affandi
Direktorat Bina Teknik Jalan dan Jembatan

ABSTRACT: Civil structures which are built causes on problematic soil causes many losses. The problem of construction erected on expansive soil causes a lot of losses. This is related to the condition of expansive soil that has high shrinkage. Damage that is often found especially on roads is longitudinal cracks, cracks in the shape of crocodile skin, wavy and landslides. To overcome potential problems the expansive soil, it is necessary to make an information about the spread of the expansive soil in the form of a map. To support the policy of the Ministry of Public Works in the field of roads and bridges, information on the distribution of expansive land can be used as an early indication in the design, construction, and maintenance of roads. In order to support this policy, the Road and Bridge Research and Development Center (Directorate of Road and Bridge Engineering) has carried out an activity of Mapping the Distribution of Expansive Soil Characteristics on National Roads in Java Island in 2019. Maps are a two-dimensional visualization or depiction of an area or region. With a map, a two-dimensional picture related to the location, position, or spatial relationship of an object to other objects. The method for making this mapping distribution uses descriptive qualitative with semi-quantitative weighting. The main data used to determine the level of soil expansivity is data from laboratory measurements. From the parameters of laboratory results, it can be included in the assessment of very high, high, medium, and low expansive degrees based on the Van De Merwe method.

Keywords: expansive soil degree, physical properties test, geological conditions, mapping

1 INTRODUCTION

1.1 *Background*

To support the policy of The Ministry of Public Works in the field of public works, especially in the field of roads and bridges, information on the distribution of problematic soils, especially the distribution of expansive soil characteristics, can be used as one of the initial indications in planning a construction to be built on it. The Reasearch and Development Agency through the Road and Bridge Research Development Center conducts research to obtain applied technology and guidelines and road constructions planning according to transportation condition and challenges in Indonesia.

A map is a two-dimensional visualization or depiction of an area or region. With a map, a two-dimensional picture related to the location, position, or spatial relationship of an object to other objects. Thus, human understanding of a space from an area or region will be better so that the activities to be carried out or allocated to a space can be planned. Likewise, in relation to the road construction, information about the area is needed, one of which is information on problematic soil, in this case, expansive soil.

1.2 *Purpose and Objectives*

The purpose of this activity is to provide an initial information on the vulnerability of expansive soils and create a distribution map that can be used as an initial reference for road improvement and maintenance facilities.

2 OVERVIEW

2.1 *Definition of Expansive Soil*

Expansive soil is soil that has changes in volume because of changes in water content in the soil. In general, expansive soil contain clay minerals consisting of smectite and montmorillonite which can absorb water. This change in volume was able to damage the strength of the structure of the building above the land. Expansive subgrade will expand and be able to cause damage to buildings or other structures that occupy the soil because of decreasing shear strength. The characteristics of damage due to expansive soil include cracked foundations, floors, and walls in a building. Such damage can occur if there is significant movement in the soil structure.

2.2 *Formation of Expanive Soil*

Types of source rock that undergo weathering have the potential to produce expansive soil, including basalt, mafic/intermediate intrusive rock, mudstone, shale, and alluvium, each of which previously comes from weathered rocks. (Table 1)

2.3 *Characteristic of Expansive Soil*

2.3.1 Geology

G.W Donaldson (1969) classifies the originating rock forming expansive soils into two groups. The first group is igneous basalt, Delorite, Sill, Dykes, and Norites. This group produces the mineral montmorillonite which is formed because of the decomposition of feldspar and pyroxine minerals. The second group is sedimentary rocks containing the mineral montmorillonite because of physical weathering.

2.3.2 Soil Menarology

Mineralogy of the clay affects its development properties, capacity of the ion exchange and the mineral structure of the clay.

2.3.3 Chemical Composition

The composition and chemical composition of expansive soil depend on the type of clay minerals contained in the soil. These clay minerals include Kaolinite, Montmorillonite and Ilite.

2.3.4 The Atterberg Limit

The potential for soil development will be greater if the soil has a high plasticity index and liquid limit value.

2.3.5 Identification of Expansive Soil

2.3.5.1 Direct Identification

Direct identification is carried out through direct development measurements, both for disturbed and undisturbed soil samples.

The following tests can be conducted for direct identification:

a. Potential of Volume Changes
b. Development Index Test

2.3.6 Indirect Identification

a) Level of Activity

According to the 2010 general specification (Revised 3), a highly expansive soil is a soil which has active value greater than 1.25 or a degree of development classified by AASHTO T258 as "very high" or "extra high". The following equation is used to determine the level of activity of a soil:

$$A_c = \frac{PI}{CF} \quad (1)$$

Where:
A_c = The level of activity (without units)
PI = The plastic index (%)
CF = The percentage of clay fraction (%)

If it is correlated with potentiality of the development, then the clay is divided into three classes based on the level of activity, as shown in Table 3.

Table 1. Expansive Soil Forming Rocks

Rock group	Rock types	Expansive property	Residual Soil	
			Colour	Expansive Property
Sedimentary Rocks	Claystone	Medium-high	Brown – black brown	Medium-high
	Clayshale	High-very high	Brown – black brown	High-very high
	Mudstone	Medium-high	Brown – black brown	Medium-high
	Limestone, Marl	-	Dark brown-black	Low-high
Volcanic Rock	Volcanic Breccia	-	Brown – Reddish brown	Low-high
	Coarse Grained Tuff	-	Brown – Reddish brown	Low-high
	Fine Grained Tuff	Low-high	Brownish yellow – reddish brown	Low-high
	Coarse Grained Alluvium	-	-	-
Alluvium	Fine Grained Alluvium	Low-high	Brown	Low-high
Ultrabasic rocks	Peridotite	-	Brown	Low-high

Table 2. Correlation of Swelling with Swelling Potential, Nelson and Miller (1992).

Swelling Indeks (EI)	Swelling Potential
0-20	Very low
21-50	low
51-90	medium
91-130	high
>130	very high

Table 3. Correlation of Activity Level with Swelling Potential, Skempton (1953), Nelson and Miller (1992).

Activity	Swelling Potential
<0.75	Non active
0.75-1.25	Normal
> 1.25	Active

b) Swelling Potential

Based on the general specification 2010 (Revised 3), the potential for expansive soil is classified as low, medium, high, and very high based on Van Der Merwe with the characteristics of longitudinal cracks parallel to the edge of the pavement.

Fig. 1. The Potential for Expansive Soil, Van der Merwe (1964).

2.3.7 Mineralogy Test

Clay minerals are the main factors controlling the expansive soil behavior. There are several methods that can be used to determine the mineralogy content of the soil, namely X-ray diffraction method, thermal differential analysis, chemical analysis, electron microscopy analysis and dye adsorption.

2.4 *Overview of Mapping Methods (Spatial Method)*

There are several methods that can be used to perform spatial interpolation. According to Demers (2000), spatial interpolation can be classified into three, namely global and local interpolation, exact interpolation and inexact interpolation, deterministic and stochastic interpolation.

2.4.1 Global and Local Interpolation

Global interpolation using all available control points. The estimation obtained are more general. An example of using global interpolation with a first-order trend surface (polynomial):

Local interpolation uses sample of control points only. This method is suitable for fields that exhibit complex variations. The assumption of this method is good spatial autocorrelation at local scale. Estimated values are more local. The general procedure for identifying points for destinations includes steps (1). A search region (neighboring) is defined around the point; (2). Sample points within the research area are identified; (3). A mathematical function is chosen to model the local variation between points; (4). The data value for the point is estimated from the function.

2.4.2 Exact Interpolation and Inexact Interpolation

Exact interpolation is a way of predicting the value at the control point that is the same as the observed value. Interpolation produces a surface that passes through the control points (see Fig. 3a). While inexact interpolation is used to predict values for control points that are different from the observed values (see Fig. 3).

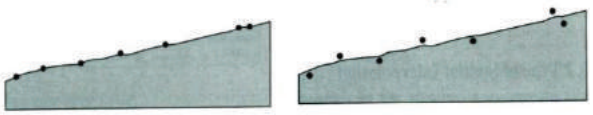

(a) (b)

Fig. 2. Control Points for Exact (a) and Inexact (b) Interpolation.

2.4.3 Deterministic and Stochastic Interpolation

Esri (2004) has a different classification of interpolation methods with the above classification. According to him, deterministic interpolation techniques can be divided into two groups, global and local. Global techniques perform calculations for predictions using the entire dataset. Local techniques calculate predictions from measured points (samples) in the environment, which are spatially smaller in size within a larger study area.

Among the popular deterministic methods are Trend, Spline, Inverse Distance Weighted (IDW) and Krigging. Each of these methods has different characteristics, so that if applied to the same area, different interpolation results will be obtained. The IDW method can be grouped into determenistic estimation, namely the interpolation is done based on mathematical calculations. While the Kriging method can be classified into stochastic estimation, where statistical calculations are used to produce interpolations, Pramono (2008).

2.5 *Geotechnical Investigation*

2.5.1 Field Investigation

Field investigations were carried out to obtain soil samples which were then carried out for laboratory testing. Sampling was used with a hand drill which was first peeled to a depth of 60 cm.

2.5.2 Laboratory Testing

The purpose of laboratory testing is to obtain data on the physical and technical properties of the soil in question. The types of soil testing in the laboratory are shown in Table 5.

Table 5. The Types of Soil Testing.

Test Type	Reference Standard
Specific gravity	SNI 03-1964-1990
Water content	SNI 03-1965-1990
Attereberg limits	SNI 03-1967-1990
	SNI 03-1966-1990
	SNI 03-3422-1990
Grain size distribution	SNI 03-1965-1990

3 METHODOLOGIES

The method used is descriptive qualitative with semi-quantitative weighting. The main data used to determine the level of soil expansiveness is data from laboratory measurements.

3.1 *Qualitative Approach*

A qualitative approach is carried out based on information on geological conditions and rock types at the research site. Rock types that are assumed to be expansive include:

1. Ultramafic rock, in the form of weathered soil Insitu.
2. Clay stone.
3. Limestone, in the form of insitu weathered soil mixed with other materials.
4. Alluvial.

With a very large scale of research, the types of rock units in geological formations at a scale of 1:100,000 the type of soil layers cannot be identified in detail. The approach taken from these conditions is to use primary data as the main parameter.

The approach taken in this quantitative analysis is divided into 2. That is based on the type of rock and based on the process of formation.

The first approach is to identify the rock type. Identification of rock types is only carried out if there is no primary data from field and laboratory observations.

The second approach is carried out by identifying the process of occurrence or the formation of soil and or rock. This process-based approach is also based on the type of lithology and formation.

3.2 *Quantitative Approach*

This process-based approach is based on the results of laboratory tests. Data obtained from the field is taken with a resolution of every 10 km to 20 km per sample. Data with quantitative parameters is then made in the form of simple weighting. This quantitative data was obtained by laboratory tests and resulted in 4 parameters, namely:

1. Ultra High Expansive
2. High Expansive
3. Medium Expansive
4. Low Expansion

With the expansive level, then grouping and weighting is carried out by entering high and very high expansive levels into one value, then the medium expansive level becomes one value and low expansive becomes one value. With these values, then identification and grouping of colors on the map is carried out.

3.3 *Grouping and Coloring*

The grouping and coloring of the two approaches above is based on the results of laboratory and qualitative tests. The qualitative approach then becomes the basic data in a simple weighting classification and is adjusted to the quantitative approach. As explained earlier that the quantitative approach is carried out for 4 parameters which is simplified to:

1. Very high and high expansive (red)
2. Medium Expansive (yellow)
3. Low Expansive (green)

3.4 *Primary and Secondary Data Collection*

Primary data collection is in the form of sampling laboratory tests, as well as secondary data that already exists from previous research.

3.5 *Field Data Testing*

Field data testing includes sampling using a hand drill and a test pit.

3.6 *Data Analysis (Primary and Secondary)*

Analyzing laboratory test data in the form of Properties Index and Engineering Properties test results. The results of this analysis are used to make criteria for the degree of expansiveness of each region which will be used as a reference for creating maps of the distribution of expansive soil characteristics.

3.7 *Determination of Expansive Soil Characteristic*

From the test results of primary and secondary data, the criteria for expansive soil

characteristics are determined, which consist of the following criteria: very high, high, medium, and low.

3.8 *Mapping*

The process of creating a characteristic of distribution map is by compiling spatial data and expansive soil attribute data in a GIS database system. Spatial data provides information on the location of expansive soil sampling, while attribute data is information on laboratory test results. Plotting of the data was carried out using GIS software overlaid with maps of the national road network as well as geological maps, topographic maps, and geotechnical maps. The layout of the map is adjusted to the standard provisions of map making.

4 ANALYSIS AND DISCUSSION

4.1 *Banten Province*

Study of Regional Geological Maps, the area of Banten Province is occupied by rock units as follows:

- (Qa) Alluvium, consisting of gravel, sand, silt, and mud.
- (Qc) coastal step deposits consisting of gravel, sand, clay, limestone debris, gravel, or mollusk shells.
- Qpvb Banten tuff consisting of tuff, limestone tuff, tuffaceous sandstone.
- Qvk consisting of coral volcanic products consisting of breccia, lava, and inseparable lava.
- Tmb bojongmanik formation alternating sandstone and shale claystone, inserting marl, conglomerate, limestone, tuff, and lignite.

Based on primary data on National roads in Banten Province, with location data consisting of 24 samples. The results of laboratory tests obtained:

- LL: 59,60 % - 118,48%
- PI: 24,61% -67,81%
- Clay content: 26,47 %-67,81%

From the results of the analysis using the Van de Merwe method, it gives the following potential swelling results:

- very high degree of expansive 68.20%,
- high expansive degree 18.52%,
- moderate degree of expansiveness, 9.10%.

From the results of a field survey on road conditions, it was found that the types of damage were longitudinal cracks, crocodile skin cracks and subsidence in some parts.

From the results mentioned above, the condition of the national road in Banten Province is located on expansive soil that has very high and high degrees. The condition of road damage is caused by several factors, among others:

- located on the land that is expansive high to very high,
- inadequate road drainage,
- heavy traffic load.

In some locations where you do not have enough data, the approach is done by means of descriptive analysis.

From the geological aspect, the Cilegon – Pasauran road section is dominated by fine-grained tuff of Banten. This road segment is categorized as soil that has a high degree of expansiveness. In addition, at several observation points, there are volcanic deposits in the form of breccia and lava. These deposits are generally not expansive, but location identification cannot determine locations that have a low degree of expansiveness because the scale used is relatively small. However, at this location, it consists of weathered volcanic deposits which are likely to be expansive so that they have a high level of vulnerability.

From the results of the potential swelling of the combined data, the condition of the national road in Banten province includes the condition of the national road which is located on expansive soil which has a very high degree and a fairly large percentage. to very high, inadequate road drainage conditions, coupled with the presence of several roads where the left and right of the road body have irrigation canals that are quite wide. These things add to the influence on the shrinkage of expansive soil which has an impact on road damage.

The results of the analysis can be seen on the Cilegon – Pasauran crossroad which does not have sufficient data. Along the road, it is dominated by banten tufa which generally has

fine grains and is generally in the form of weathered soil resulting from volcanic destruction. This road segment is categorized as soil that has a high degree of expansiveness. In addition, at several observation points along the Cilegon-Pasauran road, there are volcanic deposits in the form of breccia and lava. These deposits are generally not expansive, but site identification cannot determine locations that have a low degree of expansiveness because the scale used today is quite large. However, at the location of the deposit, it consists of weathered volcanic activity which has the possibility of expansive soil or soil in the form of sand grains, so it also has a high level of vulnerability.

Likewise, for the Cilegon Serang section, on this road section, there is not sufficient data so that the approach is carried out with analytical descriptive using samples taken in Serang and Cilegon. The similarity of soil and rock types is the basis for determining the expansive level of soil on this road segment. The type of rock that makes up this road section consists of tuff and the result of volcanic activity so that it is categorized as an expansive soil type.

The Cilegon-Merak road section has a high expansive rate. Although there are volcanic units in the northern part of Cilegon, the roads and soil samples obtained show a high expansive rate. For this segment, an analysis was carried out using non-linear interpolation modeling.

In the Pandegelang area, from the Pasauran to Cikeusik road, the dominant rock and soil types are alluvial deposits, sandstones, intercalated claystones and young volcanic deposits. In this section the data obtained are sufficient so that the identification of soil types can be carried out quite well. The type of expansive soil is high on this road segment and the modeling is carried out using a non-linear interpolation method.

On the Cibaliung to Binaungen road section, the dominant rock types are sandstone, claystone, limestone and tuff as well as alluvial deposits. In this road section, it is identified as soil with a high expansive level, because in addition to the soil type from laboratory results, it includes expansive soil and identification of regional geological maps. Through the results of this road section, identification of other roads that do not have laboratory test data with similar lithology types can be carried out.

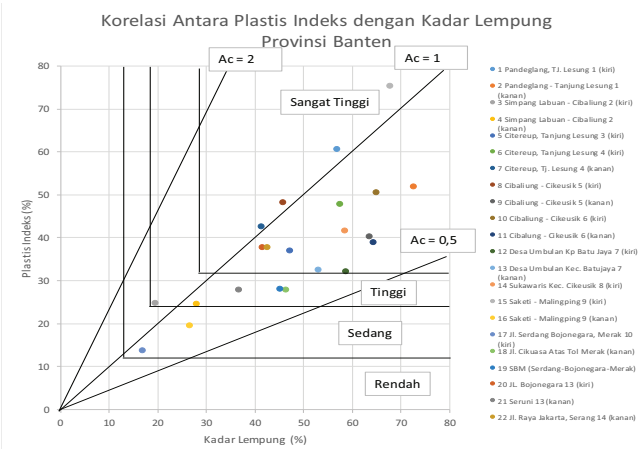

Fig. 3. Graph of Plastic Correlation Index and Clay Content in Banten Province, based on the Van De Merwe Method.

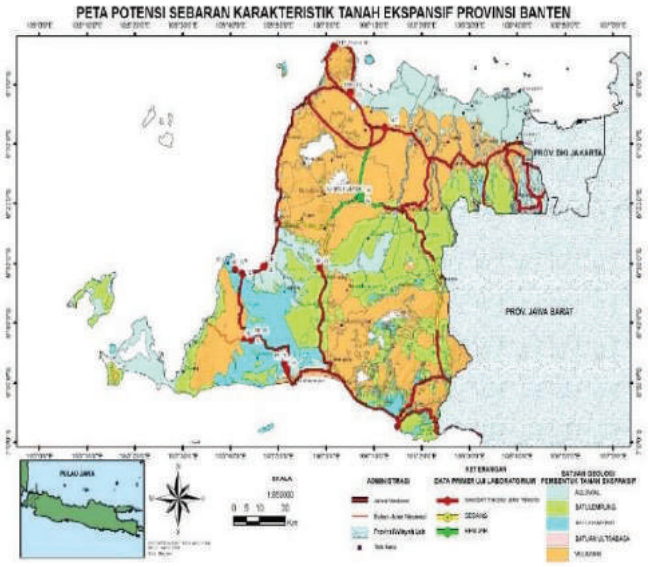

Fig. 4. Distribution of Expansive Soil Characteristics in Banten Province.

4.2 *West Java Province*

From the results of the study of geological conditions that have the potential to form expansive soils in the province of West Java, consisting of geological units

- (Tms) of claystone from the Subang formation where the claystone contains layers of dark gray napala limestone, limestone.
- - (Qa) Alluvium consisting of clay, silt, sand, gravel,
- (Qaf) floodplain sediment in the form of loamy sand, sandy loam, humus clay,
- Qav unit of Tufan sandstone and conglomerate and - (Qyu) which is rock

from young volcanic products that cannot be decomposed in the form of andesite and basalt lava breccias, tuffaceous sand, lapilli, derived from G. Tampomas and G Careme.

Based on the combined data between primary data and secondary data on National roads in West Java Province, 45 locations were obtained consisting of 33 primary data locations and 12 locations obtained from secondary data. The results of laboratory tests obtained the liquid limit value (LL) 56.67 - 115.83 %, the plasticity index ranged from 23.80 - 70.83% and the clay content (33.81 - 75.43) %.

From the results of the analysis using the van de Merwe method, the development potential is obtained as follows:

- very high degree of expansiveness: 54.17%.
- high expansive degree: 33,33 %
- moderate degree of expansiveness: 8.33%.
- Low grade: 4.17%

From the results of a field survey on the condition of road damage, it was found that the types of damage were longitudinal cracks, crocodile skin cracks and subsidence in some parts.

From the results of the potential swelling of the combined data of 45 locations, the condition of the national roads in West Java province and only 2 locations which include medium and low development potential conditions, namely Pangalengan and Cianjur. Meanwhile, from secondary data which includes the condition of national roads which are located on expansive land which has a very high and high degree, namely on the Gentong, Cibodas and Kedaton ring roads, the percentage of which is quite large. to very high, the lack of fulfillment of road drainage conditions, coupled with the existence of several roads where the left and right of the road body have irrigation channels that are quite wide. These things add to the influence on the shrinkage of expansive soil which has an impact on road damage. The condition of the rock that the road passes through lies in 75% claystone and 25% lies in clayey sand

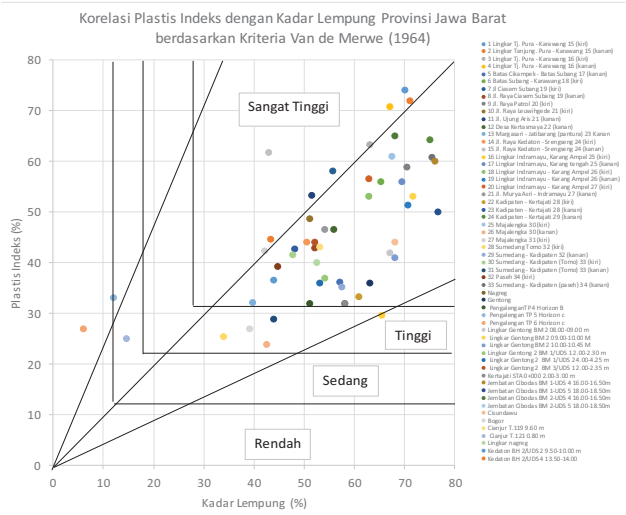

Fig. 5. Graph of Plastic Correlation Index and Clay Content in West Java based on the Van De Merwe Method.

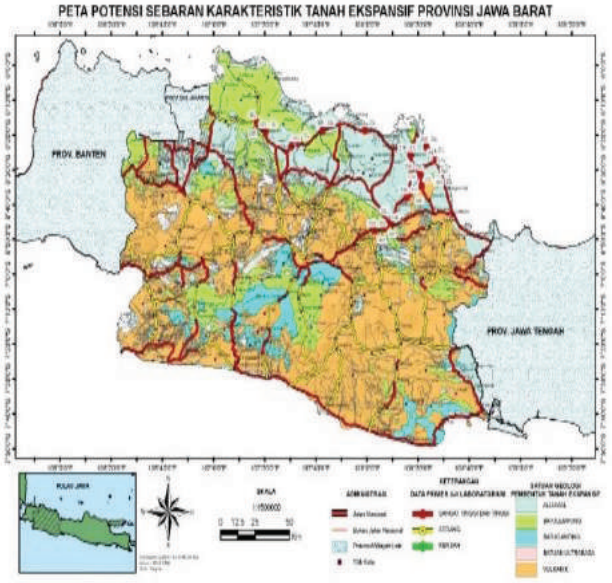

Fig. 6. Distribution of Expansive Soil Characteristics in West Java Province.

4.3 *Province of Central Java*

From the results of the study of geological conditions that have the potential to form expansive soils in Central Java province consisting of,

- Qa (alluvial) consisting of sediment, clastic and alluvium,
- Tmk (Ledok formation consisting of sediment, clastic, and sand,
- Tml1 (hoist formation,

- Tmpm1 (Mundu formation which consists of sediment, clastic, Fine, Marine,
- Tmpk1 (Kalibeng Formation) which consists of sediment, clastic, Fine, marine.

Based on the combined data between primary data and secondary data on National roads in Central Java Province, with location data consisting of 24 locations were obtained consisting of 21 locations of primary data and 3 locations obtained from secondary data.

The results of laboratory tests obtained the liquid limit value (LL) 56.67 - 115.83 %, the plasticity index ranged from 23.80 - 70.83% and the clay content (33.81 - 75.43) %.

From the results of a field survey on the condition of road damage, it was found that the road was damaged with longitudinal cracks, transverse cracks, crocodile skin cracks and subsidence in some parts.

From this swelling potential, there is only 1 location (Karangnongko-Purworejo) which has swelling potential while other areas have high to very high potential. The condition of road damage is caused by several factors including:

- the road segment is located on high to very high expansive soil,
- inadequate road drainage,
- there is a drainage channel beside the road which affects the condition of the road

These things add to the influence on the shrinkage of expansive soil so that it has an impact on road damage.

From the evaluation of the classification and type of soil, mostly including silty clay with clay with high plasticity (CH). The rock condition that the road passes through is 80 % alluvium and 20 % is marl.

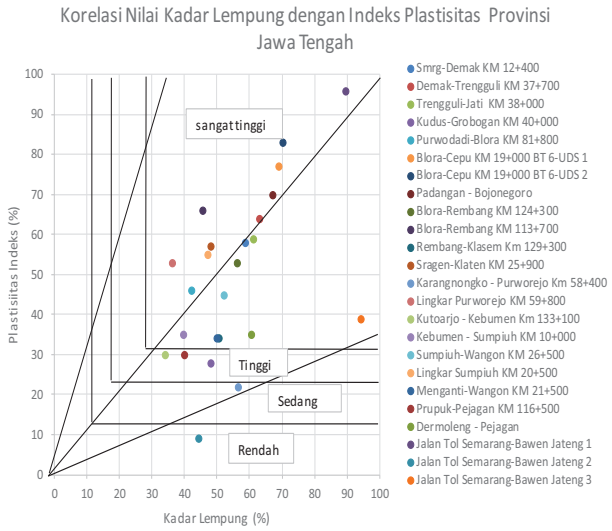

Fig. 7. Graph of Plastic Correlation Index and Clay Content in Central Java based on the Van De Merwe Method.

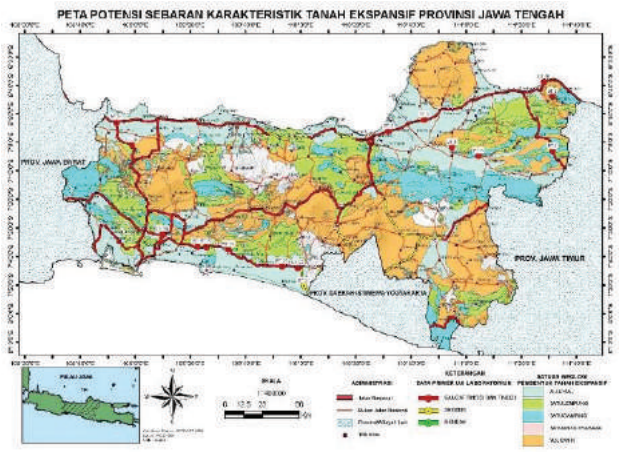

Fig. 8. Distribution of Expansive Soil Characteristics in West Java Province.

4.4 *Yogyakarta Province*

From the results of the study of geological conditions that have the potential to form expansive soil in the province of Jogyakarta consisting of

- Qa (aluvial) which consists of sediment, clastic and alluvium,
- Qvu3 volcanic rock, which is inseparable in the form of extrusive, intermediate and Polymic,
- Tmss (Sembipitu formation) which consists of of sediment, clastic, and sand,
- Tmw1, wonosari formation consisting of sediment, clastic, medium and limes.

Based on the combined data between primary and secondary data on National roads in Yogyakarta Province, 15 locations were obtained consisting of 11 primary data locations and 4 secondary data locations. The results of laboratory tests obtained liquid limit value (LL) 36% - 110%, plasticity index (PI) ranged from 14%-72% and clay content (11 – 75) %.

From the results of the analysis using the van de Merwe method, the development potential is obtained as follows:

- very high degree of expansiveness: 17%
- high degree of expansiveness: 39%
- moderate expansive degree: 33.33%.
- Low grade: 11.67%

From the results of a field survey on the condition of road damage, it is found that road damage with longitudinal cracks and crocodile skin cracks

From this swelling potential, there are only 2 locations (Karangnongko and some Piyungan) which have low swelling potential, other areas have high potential to very high. The condition of road damage is caused by several factors including:

- the road segment is located on high to very high expansive soil,
- inadequate road drainage
- coupled with indications of limestone, especially those located on several roads Piyungan –Gunung Kidul Boundary and Milir Sentolo –Gunung Kidul Boundary.

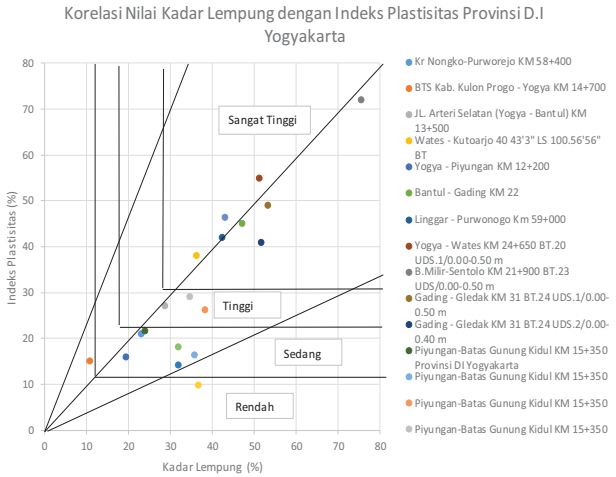

Fig. 9. Graph of Plastic Correlation Index and Clay Content in Yogyakarta Province based on the Van De Merwe Method.

From the evaluation of the classification and type of soil, mostly including silty clay sandy high plasticity (CH). The condition of the rocks that the road segment passes is located in limestone, marl and shale.

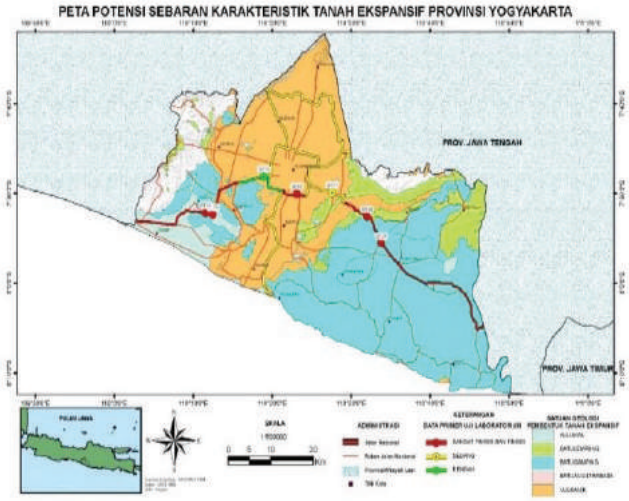

Fig. 10. Distribution of Expansive Soil Characteristics in Yogyakarta Province.

4.5 *East Java Province*

From the results of the study of geological conditions that have the potential to form expansive soils in East Java province, consisting of

- Qa (alluvial) consisting of sediment, clastic and alluvium,
- Qss1 (sedudo morphonite) consisting of extrusive, intermediate and lava sediments, and
- QTpt (tambakromo formation).

Based on the combined data between primary data and secondary data on National roads in East Java Province, 54 locations were obtained consisting of 38 primary data locations and 16 secondary data locations. The results of laboratory tests obtained liquid limit value (LL) 47% - 141%, plasticity index (PI) ranged from 14%-97% and clay content (14 – 76) %.

From the results of the analysis using the van de Merwe method, the development potential is obtained as follows:

- very high degree of expansiveness: 37.5%
- high degree of expansiveness: 42.50%

From the results of a field survey on the condition of road damage, it was found that road damage with longitudinal crack conditions, cracked crocodile skin.

From the results of a field survey on the condition of road damage, it was found that the road was damaged with longitudinal cracks, transverse cracks, crocodile skin cracks and subsidence in some parts.

From the results of the evaluation of the swelling potential, there are only 4 locations (Tulungagung-Kediri, Kediri statsiun Blitar, Banyuwangi-Jember and Jember-Lumajang) that have low swelling potential, other areas have high to very high potential. The condition of road damage is caused by several factors including:

- the road segment is located on high to very high expansive soil,
- inadequate road drainage

These things add to the effect on the shrinkage of expansive soil so that it has an impact on road damage. From the evaluation of the classification and type of soil, mostly including silty clay sandy high plasticity (CH). Conditions that the road segment passes are located in tuff, alluvium and breccia.

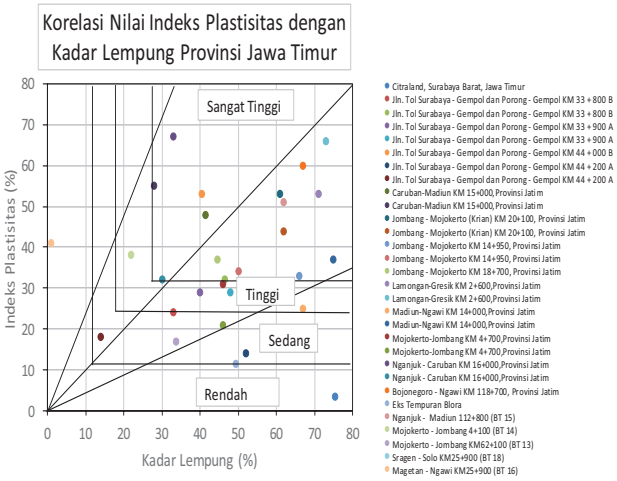

Fig. 11. Graph of Plastic Correlation Index and Clay Content in East Java Province based on the Van De Merwe Method.

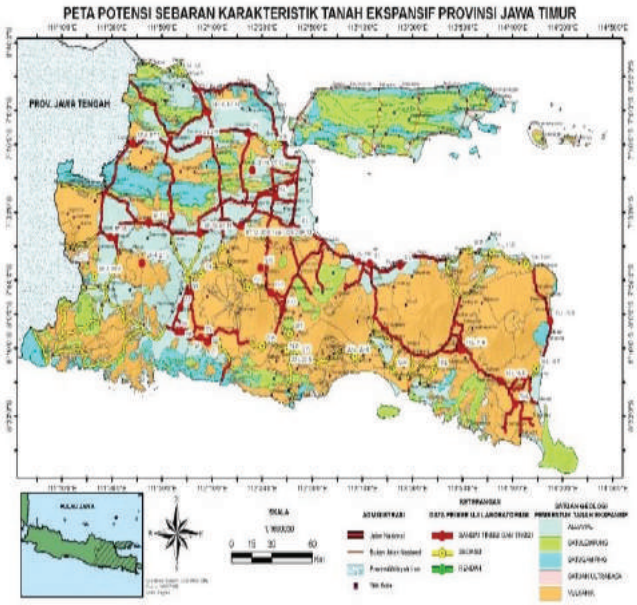

Fig. 12. Distribution of Expansive Soil Characteristics in East Java Province.

5 CONCLUSIONS AND SUGGESTIONS

5.1 *Conclusion*

Based on survey results and primary data analysis, most of the damage on national roads in all provinces in Java Island is due to passing through expansive soil-forming rocks, namely alluvium, claystone, marl and limestone.

Types of damage are generally crocodile skin cracks, longitudinal cracks and poor road drainage systems.

Based on analysis of laboratory test data and analysis of geological conditions on the damaged national roads, Java the degree of expansiveness is dominant from high to very high.

5.2 *Suggestion*

Additional data is still needed for the map that has been made so the map can provide more complete and accurate information.

REFERENCES

Affandi, D. 2005. *Karakteristik Tanah Lempung Ekspansif Bobonaro*. Bandung.

Cressie, Noel A. 1993. *Statistics for Spatial Data*. New York: John Wiley & Sons, Inc.

Hengl, T. 2007. *A Practical Guide to Geostatistical Mapping of Environmental Variables*. Luxembourg: JRC European Commision.

Isaaks, E.H. and R.M. Srivastava. 1989. *Applied Geostatistics*. NewYork: Oxford University Press.

Kitanidis, P. K. 1997. *Introduction to Geostatistics*. Applications in Hydrogeology XX: 249. Cambridge, New York

Laksana, E. A. 2010. *Analisis Data Geostatistika dengan Universal Kriging*. Universitas Negeri Yogyakarta.

Sudjianto, A. T. 2015. *Tanah Ekspansif Karakteristik & Pengukuran Perubahan Volume*. Yogyakarta: Graha Ilmu.

Suherman, M. (t.thn.). *Potensi Sifat Ekspansif Tanah Kelempungan*.

Umum, D. P. 2005. *Penanganan Tanah Ekspansif untuk Konstruksi Jalan* (PdT-10-2005-B).

Wibowo, Y., Anwar, H. Z., & Kumoro, Y. 2011. Studi Potensi Mengembang Dan Kekuatan Tanah Ekspansif Di Daerah Kebumen Dan Majenang, Jawa Tengah A. *Prosiding Pemaparan Hasil Penelitian Puslit Geoteknologi* – LIPI: 205 - 211. Bandung.

The Performance Of $Ca(OH)_2$ to Reduce The Plasticity Index and Increase The Shear Strength Parameter for Expansive Soil

Mila K.Wardani
Civil Engineering Department – Institute Technology Adhi Tama

Putu Tantri K.Sari
Civil Engineering Department – Institute Technology of Sepuluh Nopember

Mafrita Refionasari
Civil Engineering Department – Institute Technology Adhi Tama

ABSTRAK: Penelitian ini fokus pada penambahan kapur padam ($Ca(OH)_2$) pada tanah ekspansif di Lakarsantri, Surabaya. Penggunaan bahan stabilisasi dimaksudkan agar dapat membentuk ikatan pozzolan dalam tanah lempung sehingga dapat meningkatkan daya dukung. Parameter daya dukung yang diamati adalah perubahan kekuatan geser. Tanah diambil pada 2 titik kadar air tanah A 48,57% dan kadar air tanah B 35,12%, dengan nilai indeks plastitas tinggi > 50%. Prosentase ($Ca(OH)_2$) yang digunakan 6% - 24% pada usia peram tertentu. Nilai kekuatan geser tanah yang optimum pada ($Ca(OH)_2$) 6% usia 30 hari pada tanah A nilai kohesi 0,02 kg/cm^2 dan sudut geser 36°. Pada tanah B kekuatan geser optimum diperoleh ($Ca(OH)_2$) 6% pada usia 10 hari dengan nilai kohesi 0,14 kg/cm^2 dan sudut geser 23,80°.

Kata Kunci: tanah ekspansif, $Ca(OH)_2$, kuat geser, indeks plastisitas

ABSTRACT: This study focused on the addition of slaked lime (Ca(OH)2) to expansive soil in Lakarsantri, Surabaya. The use of stabilizing materials to form pozzolan in the clay increase the bearing capacity. the bearing capacity parameter to analysis is the change in shear strength. The soil was taken at 2 points of soil moisture content A 48.57% and soil water content B 35.12%, with a high plasticity index value > 50%. The percentage (Ca(OH)2) used is 6% - 24% at a certain ripening age. The optimum value of soil shear strength is (Ca(OH)2) 6% at 30 days of age in soil A, the cohesion value is 0.02 kg/cm^2 and internal shear angle 36°. In soil B the optimum shear strength was obtained (Ca(OH)2) 6% at the age of 10 days with a cohesion value of 0.14 kg/cm^2 and a internal shear angle of 23.80°.

Keywords: expansive soil, $Ca(OH)_2$, shear strength, plasticity index

Large Penetration Test (LPT) in Gravelly Soils

Syukri Fitrialdi
PT Hydrocore
PT Taka Hydrocore Indonesia

Sigit Prasetyo
PT Hydrocore

Nina Yuliana
PT Hydrocore

ABSTRACT: The standard penetration test (SPT) split-spoon sampler is too small for investigations in gravelly soils. SPT is considered inappropriate because the gravel particles can be large relative to the effective size of SPT sampler and the input energy of the SPT often would be insufficient to penetrate the gravelly strata efficiently. In addition, direct empirical correlation between gravel parameters and SPT blow counts are seldom encountered. The LPT having a larger size sampler and a larger energy would overcome these SPT limitation. The North America Large Penetration Testing (NALPT) is adapted for this paper. The purpose of this paper is to study the correlation between LPT's blow count and N60 SPT by using measuring hammer energy of LPT and SPT in gravel formation. The actual energy of SPT and NALPT is affected by the hammer weight, drop height, drill rod size, and the anvil diameter. The NALPT energy is measured using SPTMAN hammer energy measuring equipment.

Keywords: standard penetration test, large penetration test, North America large penetration test

1 INTRODUCTION

Standard Penetration Test (SPT) is used to determine the soil characteristics in geotechnical investigation. However, the application of SPT in gravelly soils is very limited because the size of the gravel can be larger than the diameter of the split-spoon sampler of the SPT (2"). To overcome the limitations related to the size of the gravel, a Large Penetration Test (LPT) with a split-spoon sampler size larger than the SPT, 3" in diameter, can be carried out as an alternative. Therefore, the application of LPT in the gravelly soil layer produces greater energy than SPT. In this paper, the LPT test was carried out by adapting the North America Large Penetration Test (NALPT) equipment to study the correlation between SPT and LPT based on hammer energy measurements.

2 STANDARD PENETRATION TEST (SPT) AND LARGE PENETRATION TEST (LPT)

LPT is a modified SPT dimensions which is enlarged in split-spoon sampler and hammer size so that the energy produced by LPT is greater than SPT. The procedure for implementing the LPT is the same as the SPT procedure in general.

On gravelly soils, the Standard Penetration Test (SPT) using a standard split-spoon sampler with an outer diameter of 2" (5.08cm) and a hammer weight of 140 lb (63.5kg) with a drop height of 30" (76.2cm) is considered inappropriate because: (a) the gravel particles can be relatively larger than the inside diameter of the SPT sampler's shoe of 1.375" (3.5 cm); and (b) the SPT input energy is sometime insufficient to penetrate the gravelly layer efficiently. In addition, a direct empirical correlation between the gravel characteristics and the number of SPT is very limited. The LPT which has a larger sampler size and energy will overcome the limitations of the SPT. One of the LPT's method in the geotechnical field is North

America Large Penetration Testing (NALPT). NALPT uses a standard split-spoon sampler with outside diameter of 3" (7.62cm) and a 300 lb (136.1kg) hammer with a 30" (76.2cm) drop height. The NALPT test was adapted in this paper with the specification and comparison with the SPT is summarized in the table below

Table 1. LPT and SPT Specification.

Detail	Units	LPT	SPT
Hammer weight	Lb	300	140
	Kg	136	63.5
Drop Height	inch	30	30
	cm	76.2	76.2
Sampler OD	inch	3	2
	cm	7.62	5.08
Sampler ID of	inch	2.40	1.375
opening shoe	cm	6.1	3.5
Sample Length	inch	18	18
	m	45.7	45.7
Maximum	Ft-lb	750	350
Potential Energy	Joule	1016.9	474.5

There are several correlations between NALPT and SPT from some study results including Daniel et al. (2003) that proposed the correlation by measuring the energy and correction on both tip and side resistance of sampler for both SPT and LPT.

Since the actual energies of SPT and LPT are affected not only by hammer weight and drop height, but also the drill rod size and anvil diameter. Thus, PT Hydrocore was carried out the LPT energy measurements on each borehole to measure the actual LPT energy then derived the N60 SPT which will be required for engineering calculations by applying overburden & hole diameter corrections. LPT and SPT energy were measured using SPTMAN equipment.

3 TEST METHOD

The correlation between LPT and SPT in this paper was based on the hammer energy measurement test results using SPTMAN Hammer Energy Analyzer. The SPTMAN was measured the actual energy transferred from the drive hammer to the drive rods. The BW rod having 54 mm outer diameter and 38 mm inner diameter was used for the LPT. The AW rod having 42 mm outer diameter and 30 mm inner diameter was used for the SPT.

Two holes of 6" (15.24 cm) in diameter with a distance of 3 m were prepared for the test. Each hole was filled with gravels and compacted using same method to obtain uniformity of gravel layer. The gravel properties is tabulated as Table 2 below.

Table 2. Gravel Properties.

Properties	Units	Value
Gravel Fraction	%	87.6
Sand Fraction	%	7.5
Fines Fraction	%	4.9
D10	mm	2.325
D30	mm	11.256
D50	mm	16.393
D60	mm	17.54
Cu	-	7.54
Cc	-	3.11

Energy measurements were carried out in accordance with BSEN ISO 22476-3:2005 during SPT and LPT within the gravel layer at the test hole locations to record the energy transfer ratio from the hammer to the drill rods. Actual energy measurements of hammer in each hole were measured at 1.5 m intervals and at the same depth.

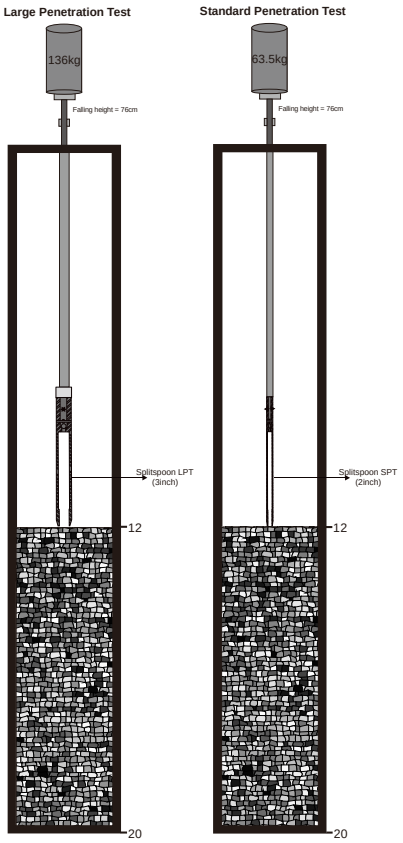

Fig. 1. Illustrated Test Method for Hammer Energy Measurement Test.

(a) (b)

Fig. 2. Hammer Energy Measurement Test of LPT (a) and SPT (b).

4 TEST RESULT

The results of the SPT and LPT energy measurements are presented in the appendix and summarized in the Table 3 and Table 4., Fig. 3 shows the ratio of LPT actual energy to SPT actual energy at the test depths.

The measured N_{SPT} and N_{LPT} with calculated $N60_{SPT}$ and N_{LPT} are tabulated in Table 5 and graphically presented in Fig. 4.

Table 3. Energy Measurements of LPT in Joule.

Depth	E1	E2	E3	E4	E5
12.00			608	639	607
12.15	626	592	643	535	511
12.30	553	550		541	510
16.50		601	708		827
18.00	950	848	792	914	779
18.15	855	881	910	1007	987
19.50		800	792	847	820
19.65		813	864	875	881

Table 4. Energy Measurements of SPT in Joule.

Depth	E1	E2	E3	E4	E5
12.00	183	202	175	191	185
	231	209	213	207	220
12.15	191	198	218	223	200
	233				
12.30	212	209	209	206	225
16.50	234	239	241	242	231
18.00	244	247	258	254	261
	268	251	273	273	260
18.15	263	272	271	273	275
	257	258	263	262	261
19.50	251	268	275	276	281
	284	260	274	267	274
19.65	278	267	268	269	274
	282	274	278	271	271

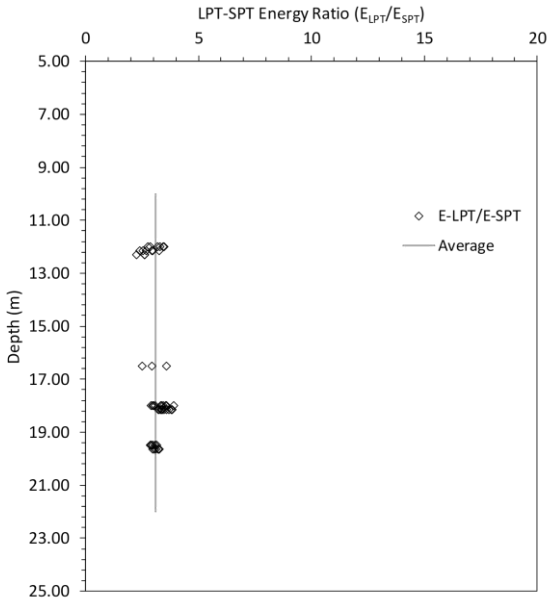

Fig. 3. LPT and SPT Energy Ratio Based on SPTMAN Hammer Energy Analyzer.

Table 5. Measured of N_{LPT} & N_{SPT}.

Depth (m)	NLPT	NSPT
12.00-12.45	13	21
13.50-13.95	10	22
15.00-15.45	14	22
16.50-16.95	14	23
18.00-18.45	11	24
19.50-19.95	8	17

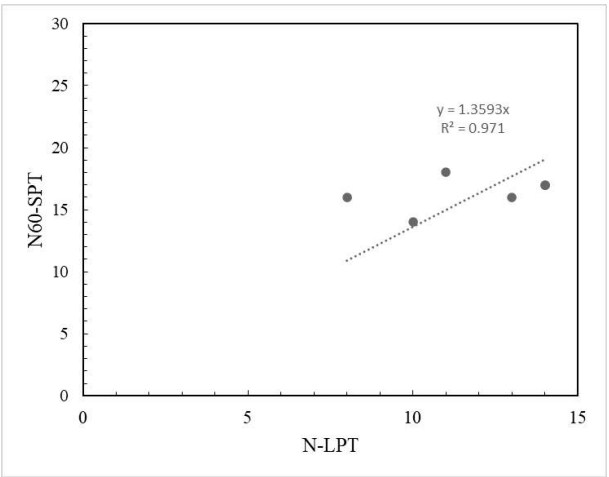

Fig. 4. Relation Between Measured $N60_{SPT}$ of N_{LPT}.

Based on the results on energy measurements, the derived statistically formula between SPT blows count (N_{SPT}) and LPT blows count (N_{LPT}) of gravel layer is as follow:

$$N_{SPT} = 3.1 \times N_{LPT} \quad (1)$$

The actual energy ratio (E_r) of the SPT hammer during the test was 50% in average. Hence, the correlation based on the Er of the LPT blow counts and N60 SPT can be described as the following equation:

$$N60_{SPT} = 2.6 \times N_{LPT} \quad (2)$$

The equation (1) and (2) are only based on the energy measurement without applying correction on both tip and side resistance of sampler. Daniel et al (2003) proposed SPT-LPT correlation with correction on both tip and side resistance of sampler (A_{TE} = bearing area factor) as the following equation:

$$N60_{SPT} = (E_{LPT}/E_{SPT})\ (A_{TE\text{-}SPT}/A_{TE\text{-}LPT})\ N_{LPT} \quad (3)$$

Where,

$$A_{TE} = C_1\ (D_o^2 - D_i^2)\ \pi/4 + C_2\ (D_i + D_o)\ \pi\ L\ R_f \quad (4)$$

in which A_{TE} is bearing area factor, $N60_{SPT}$ is SPT N value corrected for rod energy ratio to ER = 60%, E_{LPT} is stress wave energy passing a measurement point on the drill rod for LPT, E_{SPT} is stress wave energy passing a measurement point on the drill rod for SPT, N_{LPT} is LPT N value corrected to selected rod energy ratio.

C_1 and C_2 are SPT-CPT tip and side correlation factors, D_o and D_i are outer diameter and inner diameter of LPT or SPT samplers, L is sampler embedment length, and R_f is ratio of measured CPT side friction (fs) to tip resistance (qc).

By applying the Eqn. (3) and (4), the following SPT-LPT correlation can be derived.

$$N60_{SPT} = 1.33 \times N_{LPT} \quad (5)$$

The C_1=1, C_2=1 and R_f = 50% were used for typical values of granular deposits.

The empirical equation (5) shows a good correlation with ratio of measured $N60_{SPT}$ with measured N_{LPT} in Fig. 4.

5 CONCLUSION

Based on this study, the large penetration test (LPT) can be applied on gravelly soil as an alternative soil investigation method beside standard penetration test (SPT). From the hammer energy measurement test results using SPTMAN, it is confirmed that hammer energy of LPT is relatively constant in each depth. The LPT-SPT correlation based on energy measurement with correction on both tip and side resistance of sampler shows good correlation with actual measured N value of LPT and SPT.

REFERENCES

Daniel, Chris & Howie, John & Sy, Alex. 2003. A Method for Correlating Large Penetration Test (LPT) to Standard Penetration Test (SPT) Blow Counts. *Canadian Geotechnical Journal* 40: 66-77.

Daniel, Christopher. 2000. *Split Spoon Penetration Testing in Gravels.*

Dejong, Jason & Ghafghazi, Mason & Sturm, Alexander & Wilson, Daniel & Dulk, Joel & Armstrong, Richard & Perez, Adam & Davis, Craig. 2017. Instrumented Becker Penetration Test. I: Equipment, Operation, and Performance. *Journal of Geotechnical and Geoenvironmental Engineering*: 143.

Kulhawy, FH & Chen, Jie-Ru. 2005. Evaluation of Penetration Tests and Their Correlations in Gravelly Soils. *Proceedings of the 16th International Conference on Soil Mechanics and Geotechnical Engineering*: 707-710

Yoshida, Y., Motonori, I., and Kokusho, T. 1988. Empirical Formulas of SPT Blow-Counts for Gravelly Soils. *Proceedings of the 1st International Symposium on Penetration Testing* (ISOPT-1, 1988): 381–387. Orlando, Fla: A.A. Balkema, Rotterdam.

APPENDIX

1. SPT and LPT at 12.00m depth

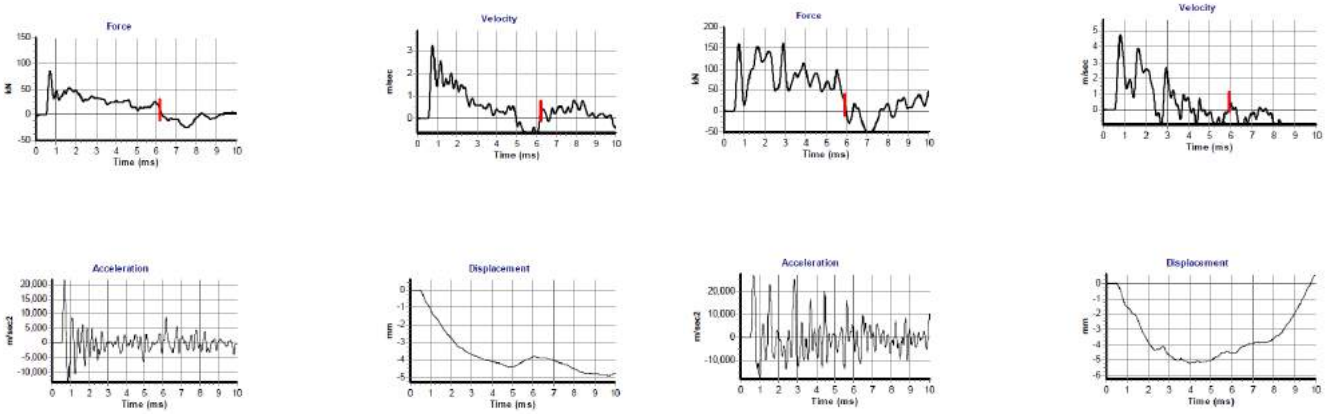

(a) SPT (b) LPT

2. SPT and LPT at 12.15m depth

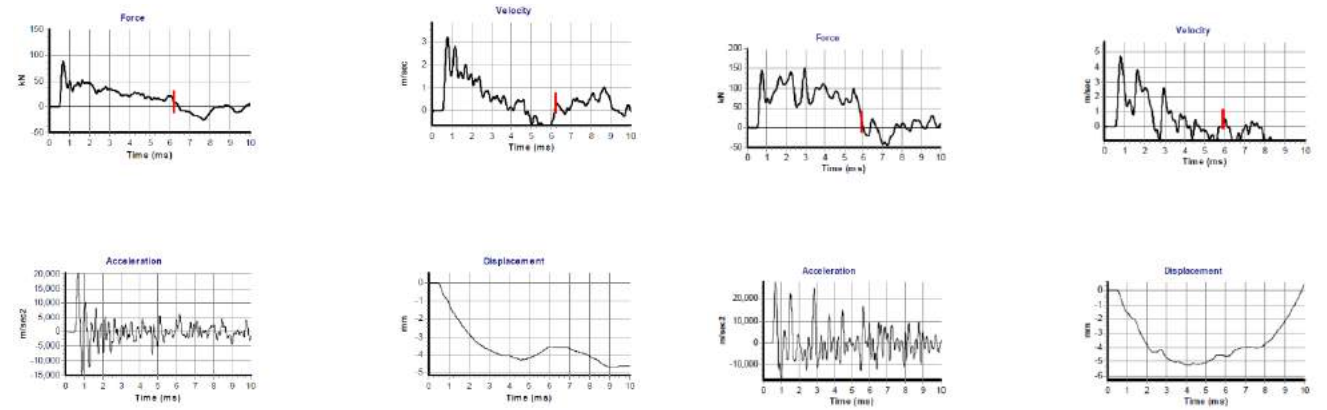

(a) SPT (b) LPT

3. SPT and LPT at 12.30m depth

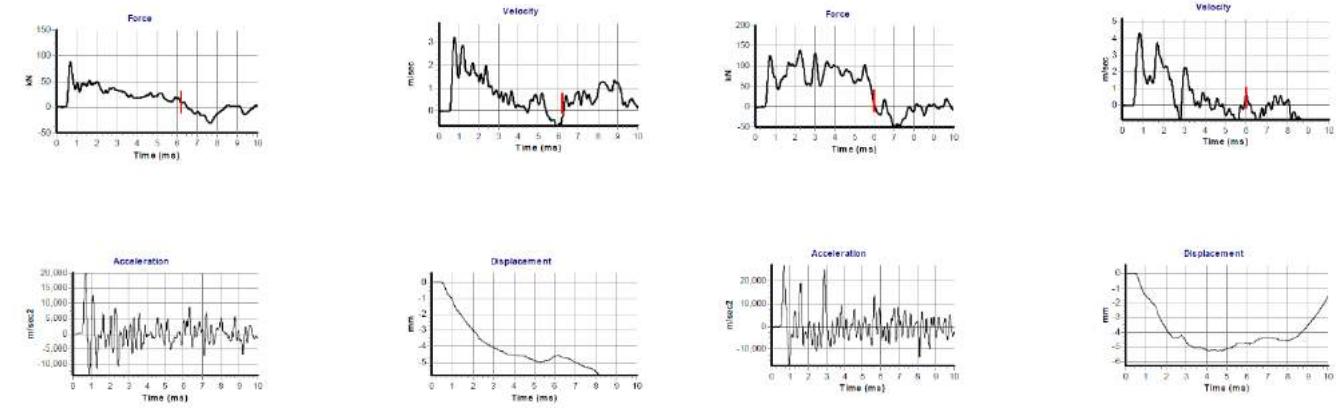

(a) SPT (b) LPT

4. SPT and LPT at 16.50m depth

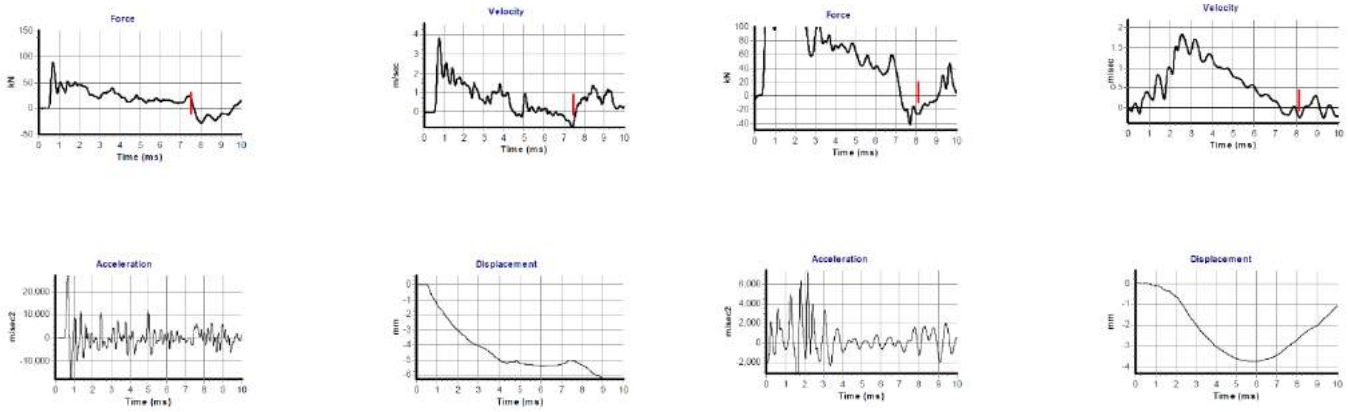

(a) SPT (b) LPT

5. SPT and LPT at 18.00m depth

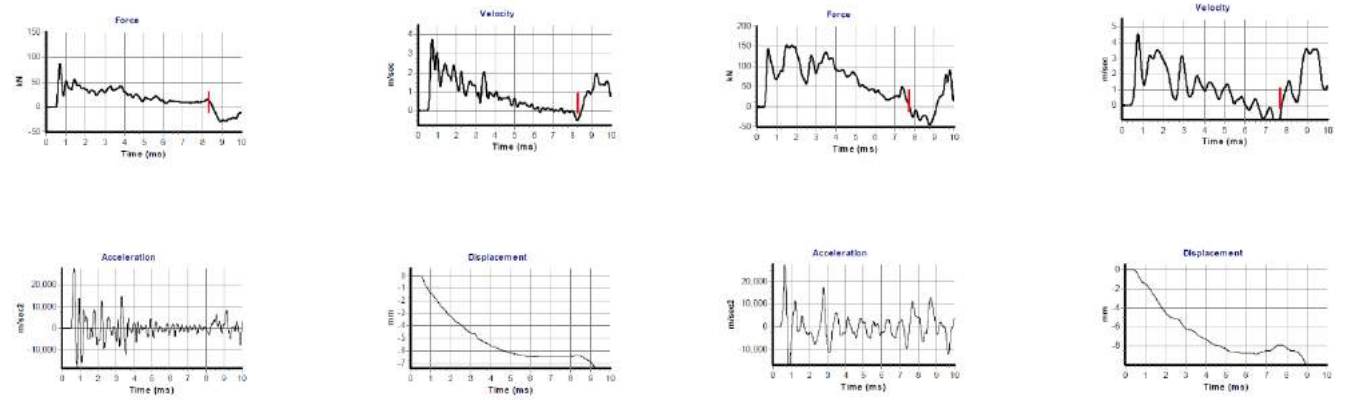

(a) SPT (b) LPT

6. SPT and LPT at 18.15m depth

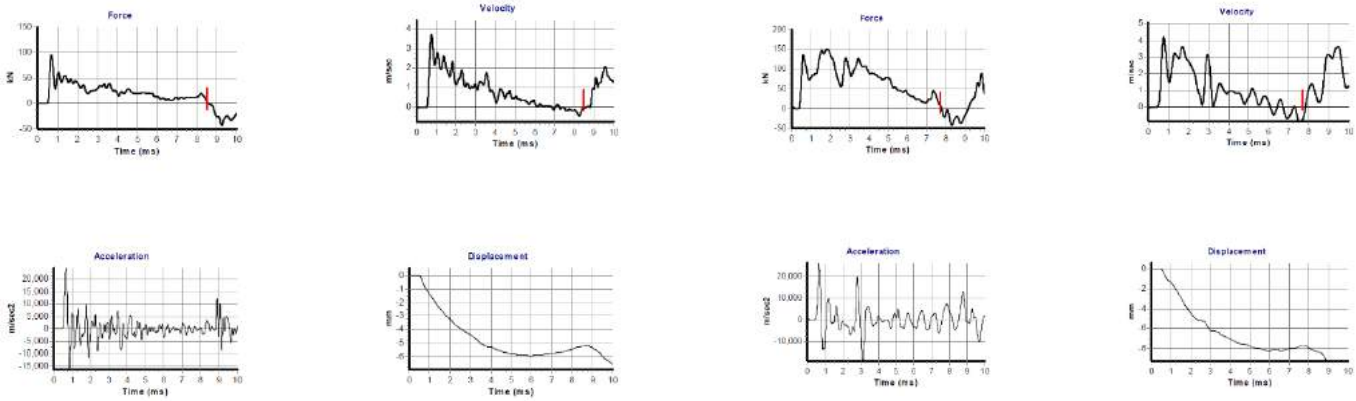

(a) SPT (b) LPT

7. SPT and LPT at 19.50m depth

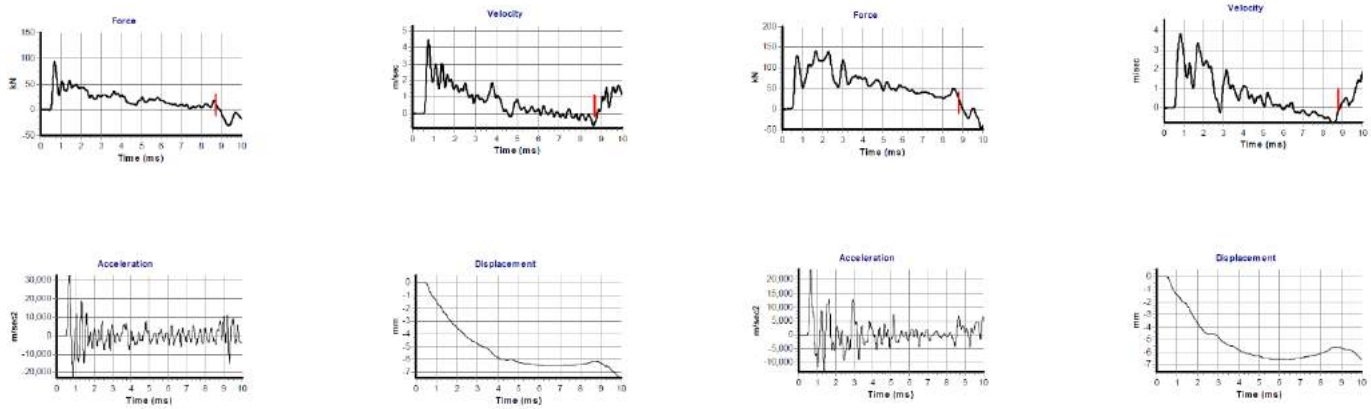

(a) SPT (b) LPT

8. SPT and LPT at 19.65m depth

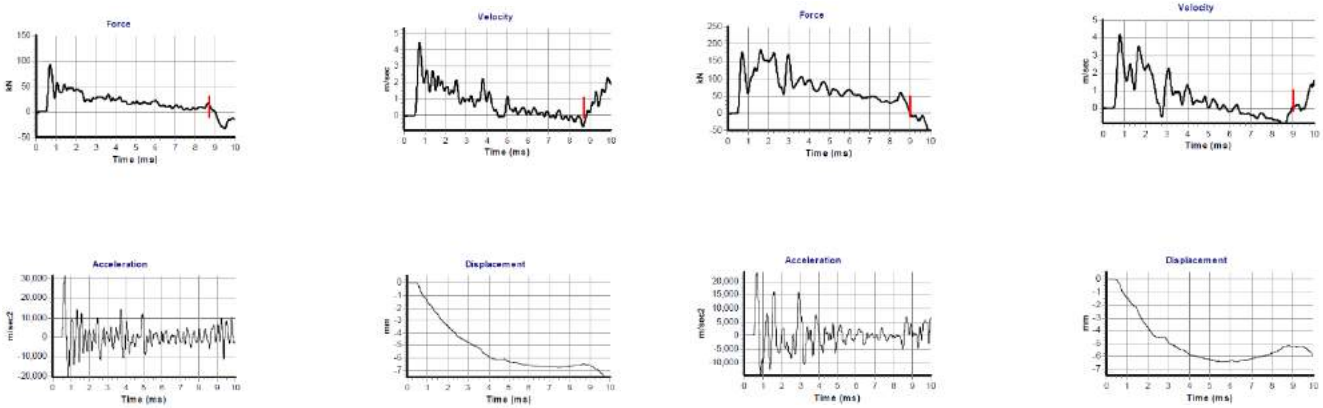

(a) SPT (b) LPT

9. Hammer

(a) LPT (b) SPT

Good Practice of Instrumentation and Monitoring of Deep Excavations

Agus Setianto Samingan
Mott MacDonald Singapore Pte Ltd

Kenneth Phua
Mott MacDonald Singapore Pte Ltd

Yudha Adi Prima
PT Mott MacDonald Indonesia

Andreas Putra
PT Mott MacDonald Indonesia

ABSTRAK: Instrumentasi dan *monitoring* merupakan suatu element penting dalam perkerjaan-pekerjaan konstruksi beresiko tinggi seperti galian dalam. Penggunaan bermacam instrumen, dalam hal ini didisain berdasarkan kebutuhan dari pekerjaan *monitoring* itu sendiri, dan setiap instrumen memiliki kelebihan dan kekurangan masing-masing. Makalah ini mendiskusikan sistem instrumentasi dan *monitoring* yang umumnya digunakan untuk pekerjaan galian dalam berdasarkan penerapan yang baik dan sesuai, dan juga pengalaman proyek di beberapa negara. Beberapa studi kasus ditampilkan juga di makalah ini termasuk contoh-contoh masalah yang umumnya ditemui dalam pekerjaan instrumensi dan *monitoring*. Diskusi yang dibawakan di sini terutama mengenai pengunaan instrumentasi dan *monitoring* untuk mitigasi resiko dan juga dalam evaluasi performa pekerjaan galian secara umum. Pentingnya pembacaan yang akurat dijelaskan di sini terutama berkenaan dengan peninjauan yang perlu dilakukan untuk menentukan apakah performa yang dicapai sesuai dengan disain. Rencana respon darurat yang baik juga diterangkan di makalah ini, yang mendasari pelaksanaan tidakan-tindakan darurat yang diperlukan.

Kata Kunci: instrumentasi dan monitoring, galian dalam pembacaan yang akurat, analisa balik, mitigasi resiko, rencana respon darurat

ABSTRACT: Instrumentation and monitoring (IM) is an important element in high-risk construction activities such as deep excavations. The use of various instruments is designed based on the purpose of the IM and each has advantages and disadvantages. This paper discusses typical IM system, which is commonly used for monitoring the deep excavation works based on the good practice and past project experience in different countries. Case studies are also presented together with samples of issues that are commonly encountered in the IM works. The discussion brought up is mainly on the purpose of IM for risk mitigation and also for evaluating the performance of the deep excavations in general. The importance of obtaining reliable instrumentation readings is hence described as assessment needs to be carried out to determine if the performance is as expected in the design. Good emergency response plan is described, based on which emergency actions shall be carried out.

Keywords: instrumentation and monitoring, deep excavations, reliable readings, back-analysis, risk mitigation, emergency response plan

1 INTRODUCTION

Due to land scarcity, underground development is getting momentum in the developing countries. Deep excavation is inevitable in the development of underground infrastructure such as for rapid transit facilities. The work is by nature high risk with many contributing factors such as uncertainty in ground conditions, impact to adjacent structures, facilities and services, interfacing parties and many others that warrant good mitigation measures to be required when dealing with it.

Instrumentation and monitoring (IM) is imperative in this high-risk construction work. The use of various instruments is designed based on its purpose. Land Transport Authority (LTA) of Singapore produced guideline in the

design of their facilities including the IM aspects of underground structure. Reference is made to LTA Civil Design Criteria or LTA CDC (LTA, 2019). In this guideline, the IM should be designed for the following purposes:

1) Verify the design assumptions
2) Confirm the predicted behavior during construction
3) Enable the assessment of impact on the adjacent structures and services to be made
4) Provide performance record
5) Enable safe construction to be carried out
6) Enable timely application of appropriate contingency measures

The IM work is designed typical to the work to be monitored. It is therefore important for engineers to first understand the behavior expected for the soils and also the retaining system utilized. For the case of deep excavations, as the excavation proceeds, its retaining wall will deflect and when struts are used, the struts will pick up load as a result of predominantly lateral soil and groundwater pressures. As water on the near face is removed during excavation, the unbalanced water pressure creates a waterflow from the far face, which may create groundwater drawdown. An excessive groundwater drawdown shall be avoided as it results in an excessive ground settlement that may adversely impact the adjacent structures and services.

This paper brings up good practice of typical IM system, which is commonly used for monitoring the deep excavation works based on the past project experience in different countries. Case studies are also presented together with samples of issues that are commonly encountered in the IM works. These include the importance of obtaining reliable instrumentation readings that are important when back-analysis is to be carried out for risk mitigation purpose. Good emergency response plan is also described, based on which emergency actions shall be carried out.

2 INSTRUMENTATION FOR DEEP EXCAVATION

2.1 *Typical Instrumentation*

Typical instrumentation required for deep excavations can be divided into the following categories:

2.1.1 *Geotechnical Instrumentation*

Planning and selection of geotechnical instruments for deep excavation involves stepped processes commencing with defining its objective and ending with the data interpretation. In certain circumstances, statutory requirement governs, which may dictate the zone of influence to be monitored.

From the explanation on the expected behavior during excavations given in the preceding section, the following typical geotechnical instruments are required:

a) Inclinometers
b) Ground settlement markers
c) Piezometers and water standpipes
d) Heave stakes and extensometers

Inclinometers are used to measure the soil deformation, normally in the lateral direction or perpendicular to the pipe, which is installed for measurement. When installed in the retaining wall (e.g., diaphragm wall, secant bored pile wall, etc.), wall deflection is measured.

Two inclinometers may be installed nearby, one in the wall (wall inclinometer) and the other in the soil (soil inclinometer). While in the medium stiff to very stiff soils readings of both inclinometers more or less tally, it may not be the case for soft soils, where the soil inclinometer may initially move lesser than that in the wall but at the end shows greater movement.

Several ground settlement markers may be installed in a line together with or close to inclinometers on both side of a deep excavation. Generally, the wall deflection shape is reflected in the shape of ground settlement – a concave shaped wall deflection results in a concave shaped ground settlement and similarly for the spandrel shape. This has been illustrated in the following figure by Clough and O'Rourke (1990). Hsieh and Ou (1998) shows that the zone of influence extends to 4 times the excavation depth (H) with the maximum settlement located at a distance of 0.5H from the wall for the spandrel shaped movement.

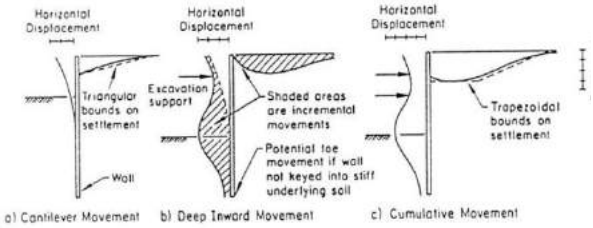

Fig. 1. Typical Wall Deflection and Ground Movement of Excavation, Clough & O'Rourke (1990).

Puller (2003) describes the behavior of soil during excavation and elaborates the change in pore-water pressure in the soil. At a point immediately behind the wall (the soil side), the pore-water pressure decreases as a result of wall movement towards the excavation side. As water flows under the hydraulic gradient, the long-term pore-water pressure is less than the initial hydrostatic value but may be greater than the value immediately after excavation. Groundwater drawdown may be observed depending on the coefficients of permeability of the soil layers encountered. A significant reduction in the pore-water pressure takes place at a point immediately in front of the wall (the excavation side) during excavation.

Piezometers are used to measure pore-water pressure while water standpipe provides indication of the position of groundwater table. At hydrostatic conditions, both measure the same value. A drop in the piezometric reading may not be straightaway followed by a drop in the groundwater table, thus both may not measure the same readings in response to the pore-water pressure alteration.

Heave is expected to occur within the excavation as a result of unloading, while settlement is observed behind the wall due to soil movement (mainly laterally) as the wall deflects. Heave stakes and extensometers can be used to monitor the heave during excavation. Heave stake is not popular nowadays due to its inaccuracy as it relies on a steel rebar (heave stake) to take measurement. Since the heave measurement is carried out within the excavation area, the measurement (either using heave stakes or extensometers) is frequently disrupted by the excavation works making the heave measurement always inaccurate.

Nonetheless, extensometers have been used to measure ground deformation at different depth e.g., using either rod or magnetic extensometers. The instruments are placed in a borehole and subsurface deformation at several points along the borehole can be determined.

2.1.2 *Temporary Work Instrumentation*

In many cases, struts are used to laterally support the earth retaining walls during excavation. As excavation progresses, the wall deforms, and struts pick up loads to resist the lateral earth pressure transferred from the wall. The measurement of strut loads is therefore critical to ensure that the excavation works can be carried out safely.

Load cells and strain gauges are normally utilized for the strut load measurement. A load cell is normally installed in line and closed to one end of a strut in such a way, so the strut load is directly transferred to it (Fig. 2). It is also used to monitor strut preloading. There may be mismatch between the load measured by the load cell and that applied by hydraulic jack during strut preloading, which is normally due to bending of the bearing plate since the load cell and jack are mostly not of the same diameter. This can be resolved by using a thicker bearing plate. Vibrating wire load cells are widely used and considered to be more superior compared to other types.

Fig. 2. Load Cell Installation.

Strain gauges are normally welded to the struts with a strain gauge sensor mounted on top. Strut load is measured by measuring the member strain, which can then be converted to load. Vibrating wire strain gauges normally come with temperature sensor to provide temperature compensation for the readings. McGough (2007) describes that despite the vibrating wire temperature compensation, readings are still significantly affected by temperature fluctuations (Fig. 3). A method has been proposed to calibrate onsite and correct the readings of vibrating wire strain gauges for accurate strut force measurement.

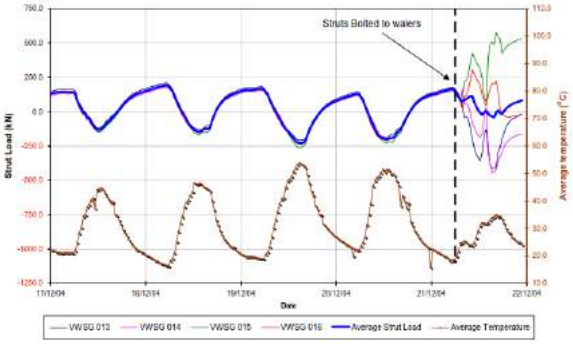

Fig. 3. Effects of Temperature on Strut Loads, McGough (2007).

2.1.3 *Instrumentation for Adjacent Structures and Services*

Assessment of the impact of deep excavation to the adjacent structures and services is of paramount importance in the risk evaluation. Not only safety and technical aspects, but it also has commercial and legal implication as it provides evidence if damage is in reality caused by the works.

The instruments listen in Table 1 are commonly used to monitor the impact of deep excavation on the adjacent structures and services.

2.1.4 *Use of InSAR and LiDAR Technologies in Monitoring Deep Excavation*

Interferometric Synthetic Aperture Radar (InSAR) technology is a radar image processing technique, which was initially introduced for military purposes. It was first used for measurement of ground movement about 20 years ago, mainly in mining industry. The radar images can be acquired using satellite, aerial or terrestrial platforms.

In Indonesia, the technology has been used to monitor land subsidence – many publications have been written on the use of this technique e.g., Abidin et al. (2005). In Italy, InSAR has been adopted for monitoring of building settlements as affected by the construction of underground infrastructures in the city of Rome, Paolo and Ivan (2012). It was reported that the measurements are affected by environment and moving vehicles within the city. Nonetheless, the data obtained using this technique agree well with those from the conventional monitoring system (optical prisms) indicating its promising application (Fig.4). Despite its current applications, it exhibits several challenges for measuring ground settlement covered by thick vegetations or snow.

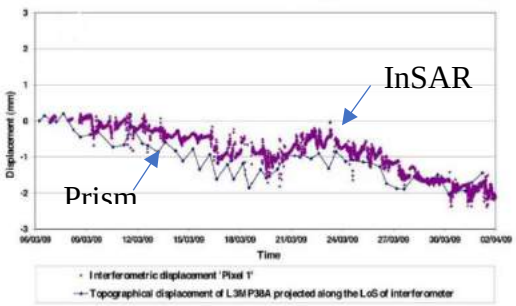

Fig. 4. Comparison of InSAR and Prism Building Settlement Measurements, Paolo and Ivan (2012)

Light detection and ranging or LiDAR uses laser to rapidly scan and record images. The scanning process can be undertaken either ground-based (using tripod) or aerial-based (using drone). The technique was first used in meteorological fields, while in the geotechnical fields, its application is mainly on ground movement monitoring for landslide study. Although, this technique is promising to be used to monitor ground movement due to excavation, its accuracy makes it only suitable to measure large movement and thus it is so far adopted mostly to monitor the excavation progress instead of its impact. Su et al., (2006) monitored the progress of excavation of a building with 2 basements (8m deep). No attempt so far to use the technique for settlement monitoring since the value was not large.

Table 1. Various Instruments for Monitoring Impact on Adjacent Structures and Services.

Instrument	Description
Building settlement marker	Sometimes also called building settlement points or precise levelling. Usually installed at corners of structures
Tilt meter	Measures tilt of existing structures such as buildings, retaining walls, viaducts, etc.
Optical prism	Used together with surveying theodolite similar to building settlement markers
Crack meter	Placed at existing cracks to monitor if these cracks widen
Utility settlement monitoring	Placed either on or just above utilities. Extensometers can be used for the purpose.
Vibration monitoring	Measures vibration due to construction activities. Provides indication if limits for structure integrity and comfort-related human response exceeded.

2.2 *Monitoring Inaccuracy and Errors*

All measurements involve inaccuracy and errors. Dunnicliff (1988) describes errors as a deviation of the measured from true value. Gross errors are normally related to human factor such as inexperience and carelessness, while systemic errors are caused by improper calibration and inherent instrument characteristics such as non-linearity and hysteresis. There are also errors induced by the environment, where the monitoring is conducted e.g., temperature effects, humidity, vibration, etc.

A typical acceptable accuracy of inclinometer is ±6 mm per 25 m casing length. It is imperative to ensure that the inclinometer casing is installed to a depth of 3 to 6 m into a stable ground, failing which the casing toe moves resulting in erroneous readings taken. Placing an optical prism at the top of inclinometer casing can provide possible correction to the errors.

Vibrating wire piezometers are generally more accurate than the pneumatic type and open type (Casagrande). Response time is also more rapid. Generally, an accuracy of 1% of the actual pore-water pressure is acceptable and can be achieved with the vibrating wire piezometers.

2.3 *Minimum Deep Excavation Instrumentation and Monitoring*

In general, the minimum requirements of instrumentation and monitoring for deep excavation should mainly be governed by its purpose. As minimum, instruments for measuring ground deformation (lateral movement and settlement), groundwater level and pore-water pressure, and impact to adjacent structures and services shall be provided.

The ground settlement measurement should cover an area wider than the zone of influence. It is recommended to cover at least 5 to 6 times the excavation depth (D) (versus the zone of influence of 4D). Near to the wall, at least six ground settlement markers should be installed every 0.25D. Fig. 5 shows a typical instrumentation array referenced to LTA CDC ,LTA (2019), which is considered to be a good practice of the instrumentation for monitoring deep excavation. It is important to note that while the zone of influence extends to 4 times the excavation depth, groundwater drawdown may stretch much longer that that. Hence, it is crucial to carry out pre-construction survey of structures and services within a wider area to establish the baseline conditions before the works commence.

It must also be noted that for a long deep excavation e.g., deep excavation for a cut-and-cover tunnel or an underground station, a more simplified arrays (Types A and B) can be mixed with that shown in Fig. 5. Details can be found in LTA CDC, LTA (2019).

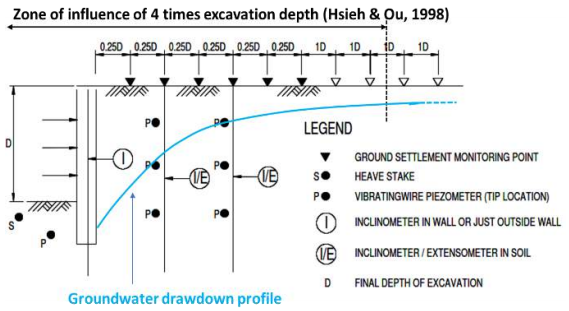

Fig. 5. Instrumentation Array (Type C), Modified from LTA (2019).

2.4 *Threshold or Review Levels*

Threshold or review levels shall be assigned to each instrument, which are based on the design. Traffic light colors are sometimes used – green represents the acceptable limit, yellow cautious and requires attention and red signifies a situation where destabilizing works are to be halted. Usually, the red limit is the predicted value of response derived using a conservative approach or conservative geotechnical parameters. The traffic-light-color system is generally adopted in America and some European countries.

In Singapore, Building and Construction Authority provides control strategy guides for monitoring deep excavation, Table 2. Zone 1 refers to an area, where the location of buildings, structures, and critical utilities (x) is less than the excavation depth (H) or $x/H<1$, Zone 2 and Zone 3 is for $1 \leq x/H \leq 2$ and $x/H>2$, respectively, BCA (2009).

Table 2. Control Strategy Guide for Deep Excavation.

Zone 1	Allowable Limits		
	Alert Level		Work Suspension Level
	70% WSL		Allowable wall deflection limit
Zone 2 and 3	Allowable Limits		
	Check Level	Alert Level	Work Suspension Level
	50% WSL	70% WSL	Allowable wall deflection limit

Indonesia National Standard or Standar Nasional Indonesia (SNI) on geotechnical design requirement i.e., SNI 8460: 2017 (SNI, 2017) provides requirements on the maximum wall deflection for deep excavation similar to BCA Advisory Note 1/09, BCA (2009). While the maximum movement of mechanically stabilized soil (MSE) walls is stipulated, no guideline on review levels has been provided.

2.5 *Realtime Instrumentation System*

From the risk management perspective, it is important to relay the instrumentation readings as quickly as possible to enable an assessment to be carried out so that necessary measures can be implemented in time. It is therefore imperative to employ a real time monitoring system for some critical instruments.

An Instrumentation Data Management System (IDMS) was adopted in a utility project in Singapore involving deep excavation, Maxwell et al. (2015). Real time settlement monitoring was undertaken, from which settlement contours could be generated and compared with the prediction.

It is possible to carry out real time monitoring for inclinometers. However, in-place or stationary inclinometers must be used. Building settlement and tilt can also be monitored real time similar to strut force monitoring using strain gauges and load cells.

InSAR and LiDAR require image processing to be conducted before arriving at the measured ground or structure settlements. Depending on how fast this can be carried out, pseudo real time measurement can be expected.

3 CASE STUDIES

3.1 *Deep Excavation for A Cut-and-Cover Tunnel Structure – Singapore Case*

A cut-and-cover tunnel had been constructed in the Southern part of Singapore with a deep excavation of more than 17m deep. A good presentation of a cross section from the cut-and-cover tunnel excavation with the instruments installed around it is shown in Fig. 6, from which one can visualize the measured data compared with the design prediction. It is important to highlight that the inclinometer tube was inserted sufficiently long into the hard stratum (in this case, Old Alluvium), which allows for accurate measurements to be undertaken.

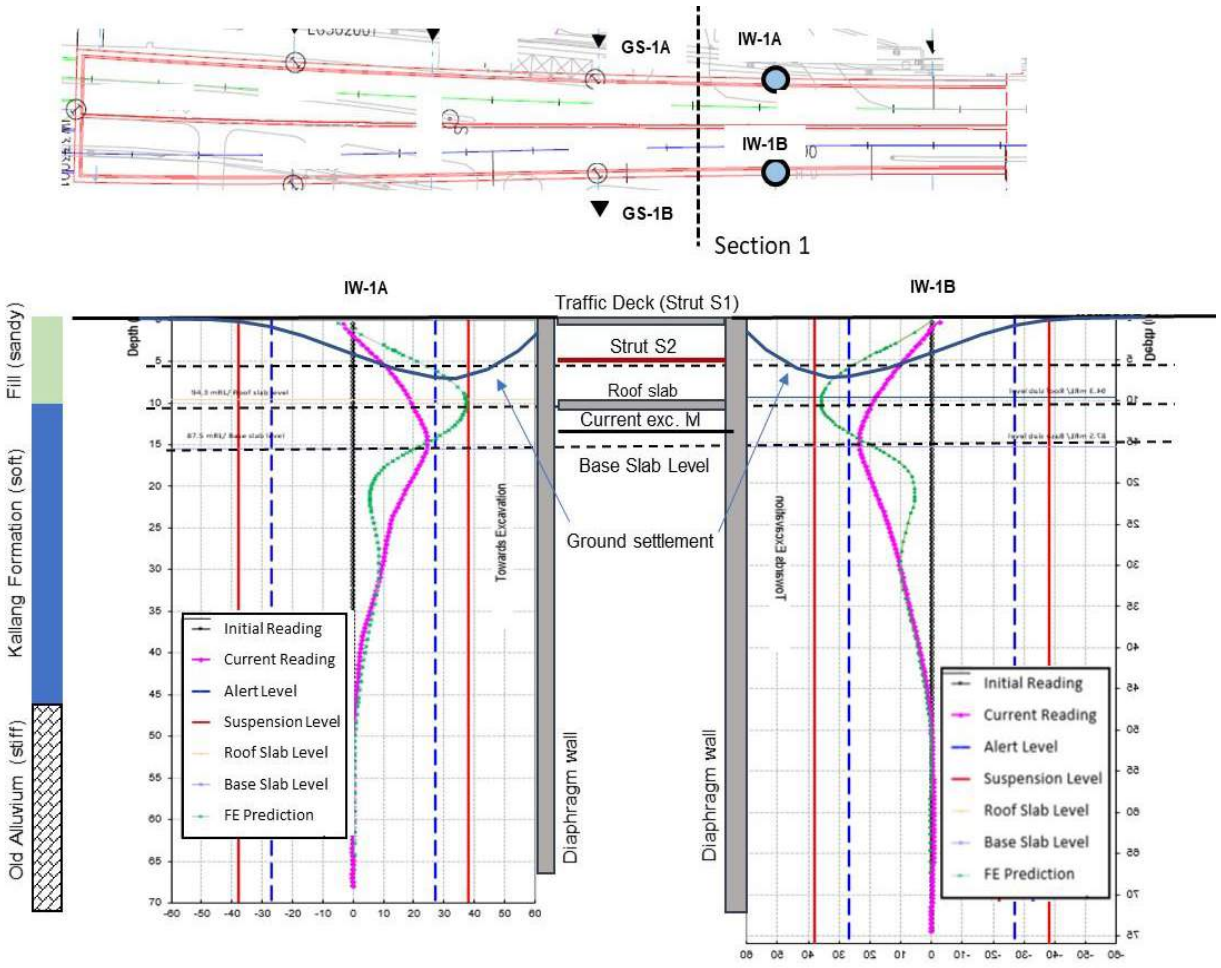

Fig. 6. Comparison of Retaining Wall Deflection from Prediction and Measurement – Singapore Case.

The review levels following the guide in Table 2 is also shown in the figure to indicate if various measures according to Emergency Response Plan (refer to Section 4) should be carried out. One can easily appreciate that while the measured wall deflection agrees well in terms of magnitude with the prediction at this excavation stage, its value is well below the overall alert level (AL). The curvature of wall deflection is also less for the case of measured data compared with the design estimate. Hence, it is unlikely that the wall bending moment and shear capacity are exceeded, Table 1.

3.2 *Deep Excavation for An Underground Facility – Jakarta Case*

The second case study is from a deep excavation for an underground facility, which was constructed in Jakarta, Indonesia (**Error! Reference source not found.**). The geology generally comprises of soft to medium stiff clays. The structure has three levels of slab with each stage of excavation show in the figure refers to the excavation carried out to construct each slab.

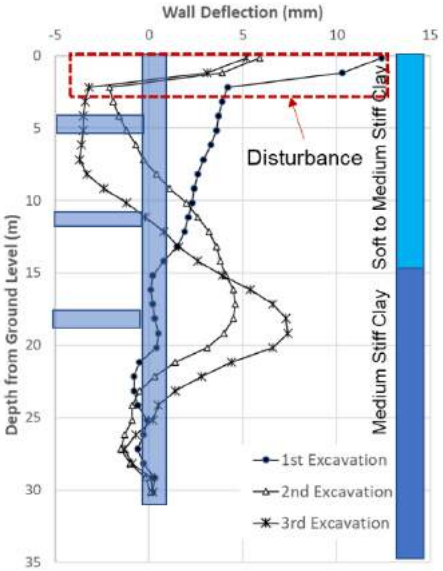

Fig. 7. Inclinometer Readings from an Underground Facility – Jakarta Case.

One would easily recognize that the readings for the first two meters from the ground level are peculiar, which were later found out to be caused by disturbance from the construction vehicles damaging the inclinometer pipe.

The wall deflection from the inclinometer readings appears to be too small for the excavation deeper than 19 m in such ground conditions. The wall deflection for the 1st excavation stage shows a movement towards the soil side, which is abnormal. Similar trends are also displayed for the other two excavation stages. This can be due to the inclinometer pipe toe was not extended deep enough at a level, where zero or insignificant lateral soil movement is expected. Since the inclinometer measurement uses its pipe toe as the reference point, the wall toe movement was not captured in this particular case. This was later confirmed by ground settlement monitoring, which showed settlement well in excess of the maximum wall deflection recorded by the inclinometer. A good practice is to embed the pipe 2m into a good (stiff) stratum.

Corrections could have been given to the readings by installing an optical prism at the top of inclinometer pipe. The measurement using prism is normally undertaken with theodolite, thus it is independent of the inclinometer reference point. The movement obtained from the prism readings can be compared to that measured by the inclinometer and the difference can be considered to signify the wall toe movement. Assuming that the wall toe moved 15 mm, 20 mm and 25 mm for the three stages, respectively, corrected inclinometer readings shown in Fig. 6 are obtained and compared with the uncorrected ones.

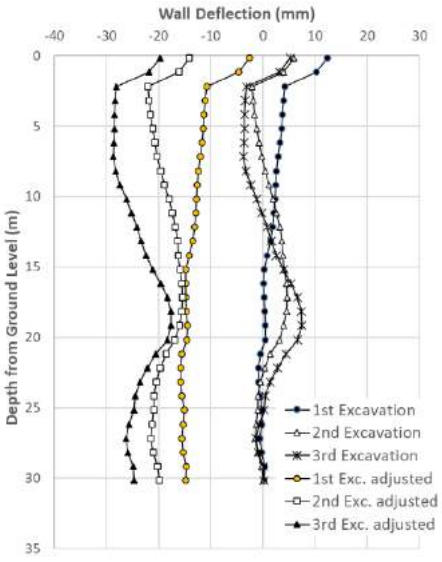

Fig. 8. Comparison between Uncorrected and Corrected Inclinometer Readings.

4 EMERGENCY RESPONSE PLAN

Emergency responses shall be activated when the threshold/review levels have been breached. The responses should ideally be agreed at the onset of the project, which also depends on the project setup, role and responsibility of different parties involved and the local

regulations. Below describes in general what has been adopted in Singapore's major infrastructure projects involving deep excavations, where the instrumentation and monitoring contractor (IMC) is under the ultimate client, not under the civil contractor.

1) When review levels are breached, the IMC shall first verify that the readings are correct.
2) **If the alert level (AL) is breached** the IMC shall notify all the parties, including the authority ideally within 24 hours, which will be followed by site inspection attended by the IMC, the civil contractor, designer and supervision team.
3) An assessment will need to be carried out including review of the reading trend – cause and effect should be established, and if necessary, the designer may recommend contingency measures, which will be activated when the readings exceed certain values, not necessarily the work suspension level (WSL).
4) **If the WSL is breached**, upon notifying all the parties and authority (No. 2 above), the work shall ideally be suspended.
5) Stabilization work shall immediately be carried out to arrest the movement (e.g., backfilling the excavation, etc.) followed by site inspection.
6) An assessment shall be carried out and resumption of the works can only proceed upon approval by the authority with sufficient and appropriate remedial and contingency measures in place.

The processes are different in other countries since the IMC may be under the civil contractor.

5 CONCLUSIONS

The following can be concluded from the above description of good practice of instrumentation and monitoring (IM) for deep excavation:

1. The IM is important in deep excavation as the works involve high risk activities.
2. When designing the IM, it is important to understand its purpose and the ground mechanisms envisaged so that appropriate and sufficient IM plan can be assigned.
3. Typical instrumentation for deep excavations includes geotechnical instrumentation such as inclinometers, ground settlement markers, piezometers and water standpipes, heave stakes and extensometers; strut monitoring using strain gauges and load cells; and also instrumentation for measuring the impact on the adjacent structures and services such as building settlement markers, tilt meters, etc. as shown in Table 1.
4. InSAR offers good potentials for measuring the ground and structure deformation but is not widely used at present.
5. The paper emphasizes on the importance of obtaining reliable IM data to enable assessment to be carried out accurately.

REFERENCES

Abidin, H.Z., Andreas, H., Gamal, M. Djaja, R., Subarya, C., Hirose, K., Maruyama, Y., Murdohardono, D. & Rajiyowiryono, H. 2005. Monitoring Land Subsidence of Jakarta (Indonesia) Using Leveling, GPS Survey and InSAR Techniques. In: Sansò F. (eds) A Window on the Future of Geodesy. *International Association of Geodesy Symposia* 128: 561-566.

Building and Construction Authority. 2009. *Advisory Note 1/09 on Earth Retaining or Stabilizing Structure (ERSS)*.

Clough, G.W. & O'Rourke, T.D. 1990. Construction Induced Movements of In Situ Walls. *Specialty Conference of Earth Retaining Structures*: 439-470.

Dunnicliff, J. 1988. *Geotechnical Instrumentation for Monitoring Field Performance*. John Wiley & Sons.

Hsieh, P.G. & Ou, C.Y. 1998. Shape of Ground Surface Settlement Profiles Caused by Excavation. *Canadian Geotechnical Journal* 35(6): 1004-1017.

Land Transport Authority (LTA). 2019. *Civil Design Criteria for Road and Rail Transit Systems*.

Maxwell, A., Chong, P.T. & Chin, M.Y.K. 2015. Thrusting in the Same Direction – Client-contractor collaboration for integrated TBM process and geotechnical control – Powergrid Cable Tunnels Singapore. *Proceedings of International Conference and Exhibition of Tunnelling and Underground Space*. IEM Kuala Lumpur.

McGough, P. 2007. Thermal Calibration of Strain Gauges for High Quality Strut Load Measurement. *Common Ground Proceedings of 10th Australia-New Zealand Conference on Geomechanics*: 348-353. Brisbane.

Paolo, M. & Ivan, C. 2012. Terrestrial SAR Interferometry Monitoring of a Civil Building in The City of Rome. *Proceedings of 'Fringe 2011 Workshop 2011*. Italy.

Puller, M. 2003. *Deep Excavations: a Practice Manual*. 2nd Edition. Thomas Telford.

Standar Nasional Indonesia (SNI). 2017. *Persyaratan Perancangan Geoteknik*. Badan Standardisasi Nasional (BSN).

Su, Y.Y., Hashash, Y.M.A. & Liu, L.Y. 2006. Integration of Construction As-Built Data via Laser Scanning with Geotechnical Monitoring of Urban Excavation. *Journal of Construction Engineering and Management* 132(12): 1234-1241.

Bearing Capacity of Land as Main Factor of Environmental Carrying Capacity in Regional Spatial Planning (A Study in Semarang)

Pribadi Agung Wahyudi
Engineering Faculty – Pekalongan University

ABSTRAK: Daya dukung lahan untuk pemanfaatan ruang selama ini kriterianya berdasar untuk pertanian dan fisik lahan. Indikator penting belum masuk dalam kriteria, yakni tijauan karakteristik geologi teknik. Gejala nyata dan belum terukur, bahwa lahan akibat alami maupun rekayasa mengalami amblesan, penyebab gagalnya daya dukung lingkungan. Gejala ini lebih pada persoalan karakteristik geologi teknik. Penelitian daya dukung lahan berbasis karakteristik geologi teknik dilakukan di Kota Semarang-Jawa Tengah-Indonesia, dengan 122 bor dalam, 109 bor dangkal dan 205 sondir. Sampel tanah dianalisis karakteristiknya dilaboratorium. Analisis uji lapangan dan laboratorium mendapatkan sebaran nilai daya dukung lahan dan zonasi material, selanjutnya disusun Peta Daya Dukung Lahan Kota Semarang kedalaman 2.50 dan 5.00 m. Kisaran daya dukung lahan : 0,201–14,248 kg/cm^2. Kajian ini dimaksutkan memberi kontribusi indikator daya dukung lahan berbasis karakteristik geologi teknik, sebagai penentu kemampuan lahan yang terukur, dalam daya dukung lingkungan hidup diwilayah Kota Semarang.

Kata Kunci: daya dukung lahan, peta daya dukung lahan, daya dukung lingkungan hidup

ABSTRACT: The bearing capacity of land (BCL) for spatial use has been based on the criteria for agriculture and physical land. Important indicators have not been included in the criteria, namely a review of engineering geological characteristics, because the general phenomenon is more a matter of engineering geological characteristics. The research was carried out with 122 deep drills, 109 shallow drills and 205 DCP. Soil samples were analyzed in the laboratory. Field and laboratory analysis obtained the distribution of the value of BCL and the zonation of the material, then a Map of the Land Bearing Capacity was compiled with a depth of 2.50 and 5.00 m. Land bearing capacity range is 0.201–14.248 kg/cm^2. This study is intended to contribute indicators of land bearing capacity based on engineering geological characteristics, as a determinant of the measured land capability, in the environmental bearing capacity of the Semarang City area.

Keywords: bearing capacity of land, map of bearing capacity of land, environmental bearing capacity

1 INTRODUCTION

Land capability for spatial use has so far been based on land capability for agriculture and from the physical aspect of the land (Regulation of the State Minister for the Environment No. 17 of 2009). There are important indicators of carrying capacity not included in the guidelines, namely those related to land capability in terms of engineering geological characteristics *Kementerian Lingkungan Hidup*, (2009).

The ability of the mass of soil material that forms a stretch of land does not only include the ability for agriculture or physical aspects, but rather the stratigraphy of the subsurface soil mass, namely the characteristics of engineering geology.

One of the environmental damage phenomena related to engineering geological characteristics is land subsidence. The subsidence rate in Semarang–Demak City at the Mixed Room designation location is 13.00 cm/year, the Industrial Space allotment location is 7.80 cm to 9.30 cm/year, Irsyam (2018). Land subsidence is a process that occurs in soils that experience stress and strain. The integration of

strain or deformation per unit length along the depth of stress effect is a decrease.

Semarang as a coastal area is geographically located between 6°50'–7°10' South Latitude and 109°50' – 110°35'East longitude, with an area = 373.70 km^2. From the geological aspect, the Semarang plain is composed of alluvial deposits of rivers, delta plains and tidal flats, consisting of alternating layers of sand, silt sand and soft clay, with lens inserts of gravel and volcanic sand (Marsudi, 2001).

The Semarang area is topographically different in height, so it has an upper area (in the form of hilly areas with a slope of 15–40% and 40% and above) and a lower area (lowlands with a slope of 2–5%).

Semarang needs areas that are ready to build city facilities and infrastructure, Pemerintah Kota Semarang (2011). Dewi et al. (2016) stated that the availability of land within the city is fixed and not limited to meet the needs of the population, and it causes changes in land use in suburban areas, Dewi et al. (2016).

In the analysis of the bearing capacity of land (BCL) focused on the depth of -2.50 m and -5.0 m from the ground surface. With consideration based on the area of spatial land use in the Part of City Area (PCA), the need for information on BCL for environmental engineering and consideration of building substructure analysis.

Field and laboratory test studies obtained the distribution of the value of the BCL and the zoning of the material, compiled the BCL Map. The final result is an indicator of the stability of the BCL, as a determinant of the measurable capacity of the land for determining the environmental carrying capacity.

2 METHODOLOGY

2.1 *Location and Methods*

The research was conducted in Semarang City which is geographically located between 6°50' – 7°10' S 109°50' – 110°35' E, located in the coastal area of the Java island with the northern boundary of the Java Sea, the southern boundary of Semarang Regency, the western boundary of the Kendal Regency area, the eastern boundary of the Demak Regency area, with an area = 373.70 km^2 , Statistic Center Agency of Semarang City (2018). Field test points were carried out randomly spread over the area of Semarang City consisting of 122 deep drills, 109 shallow drills and 205 DCP test with a capacity of 2.50 tons.

The design used in this research is exploratory-descriptive-analytical-experimental. Drilling to obtain representative native soil samples, at various depths, totaled 239 samples. As a follow-up, samples were analyzed in the soil mechanics laboratory to determine the values of geotechnical parameters, both physical properties and engineering properties, hydraulic properties and settlement parameters. In some laboratory tests, the experimental method is used with the saturation treatment. Analysis of BCL was carried out using Microsoft Excel software, Ozcep (2010).

2.2 *Analysis of The Bearing Capacity of Land (BCL)*

The BCL was calculated using following Meyerhof's equation, Verhoef (2017).

$$Q_{all} = N/F(K_d)(K_m) \quad (1)$$

Eqn. (1) is a formula used to calculate BCL in Qall (kg/cm^2). Where Kd is a depth factor defined as 1+0.33Df/B < 1.33, Km is a safety factor that has been set at 1.5, with N/F determined using Terzaghi and Peck's graphs (Fig. 1.), Craig (1989). B is one unit contact area < 1.2 meters. Df is a contact area for vertical distance.

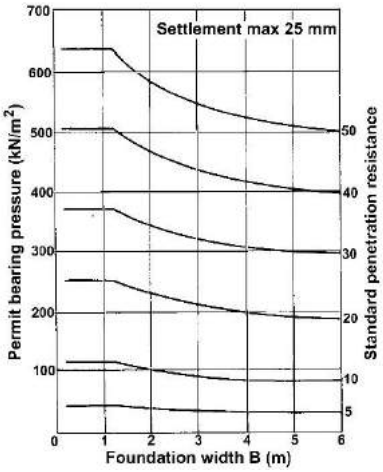

Fig. 1. Graph of Relationship between Permit Bearing Capacity and SPT Value.

Mapping of field data and laboratory data into the form of map images or in the form of simulation models using ArcGIS 10.3 software, Price (2010).

The research points are plotted according to their coordinates on the Semarang city map. The zonation of depth is determined at 2 depth levels namely 2.5 m and 5.0 m and material zones are plotted based on field data i.e., drill and DCP profiles. Interpolation in the transition zone between two different types of material is determined by overlapping the geological map, the material zonation map from the previous study, and the topographic map of the Semarang city. The map legend includes material types with different consistency at 2 predetermined depth levels along with data on BCL. For studies related to the administrative area, it is overlapped with the map of the PCA in the spatial layout of the Semarang city.

3 RESULTS AND DISCUSSION

3.1 *General*

The results of field testing with hand drills, sondir and deep drills,Incision of the soil layer is carried out in several sectors so that it is obtained cross-sectional profile of the soil layer stratification in the land of the city of Semarang which is represented in Fig. 2. By projecting the entire profile of the drilling results on the cutting plane as depicted in the Fence Diagram, it shows a 3-dimensional geological section of the land of the Semarang city in Fig. 3.

This subsurface stratification cross-section if exposed to the earth following the slope of the boundary layer by layer by intersecting the layer plane with the topography of the earth's surface will get zoning lines for the type of land material characteristics in the city of Semarang as shown in Fig. 4. which is zoned clay, silt, silt - sand, sand, and gravel.

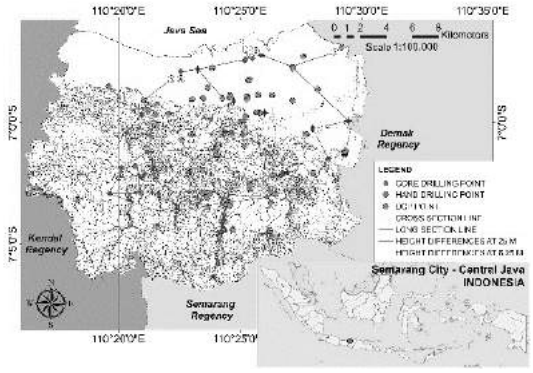

Fig. 2. Soil Section of Semarang City.

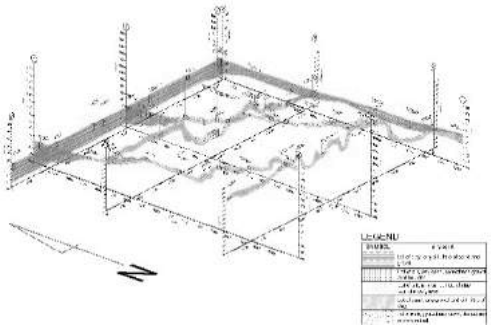

Fig. 3. Fence Diagram of Soil Layer.

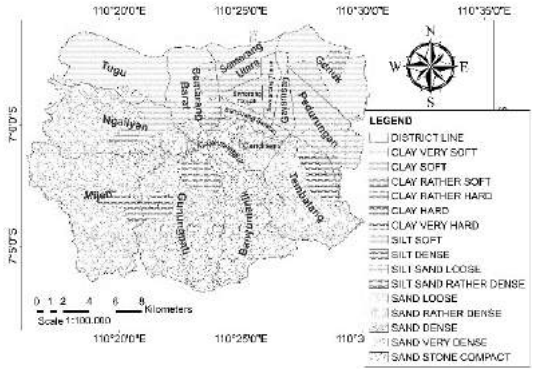

Fig. 4. Infographics of Soil Type at 5 Meters Depth.

3.2 *The BCL in Spatial Planning*

The definition of land is a land area whose characteristics include all signs regarding the biosphere, atmosphere, soil, geology, relief, hydrology, plant and animal populations, as well as the results of past and present human activities that are steady or cyclical, Kementerian Lingkungan Hidup (2009).

Land arrangement is one of the sides that becomes the unity of the three sides of spatial planning, namely land space, ocean space and air space. The preparation of spatial plans must always be based on thinking towards the desired future state, starting from data, information on science and technology that can be used, and paying attention to the diversity of perspectives on activities of each sector.

The provincial government, regency or municipal government in accordance with the order of the law must prepare a regional spatial plan according to the level by taking into account the environmental carrying capacity, Pemerintah Republik Indonesia (2007), Pemerintah Republik Indonesia (2010).

Determination of the environmental carrying capacity is measured by knowing the capacity of the natural environment and resources to support human life in that space for their existence. The size of the capacity is influenced

by the conditions and characteristics of the resources in the space including: a) the BCL for the allocation of spatial use, b) the comparison between the availability and the need for land, c) the comparison between the availability and the need for water.

The current BCL is based on land capability for agriculture and is reviewed based on categories: a) land capability classification, b) land capability at the class level, c) land capability at the sub-class level, d) soil capability at the management unit level, Kementerian Lingkungan Hidup (2009). The BCL is not enough to only be measured from the 4 aspects above, but there are main factors of land capability, namely the engineering geological characteristics of the soil mass forming the stretch of land.

The BCL becomes very important in determining the environmental carrying capacity, because 2 other factors, namely the comparison between the availability and demand for land and water will never materialize if the BCL is unstable.

The results of the analysis of material zoning and geological characteristics of the subsurface soil of Semarang City as well as the calculation of the BCL are described in the BCL Map of the Sematang city, with a depth of -2.50 m.(Fig. 5.) and depth - 5.00 m from ground level (Fig. 6.).

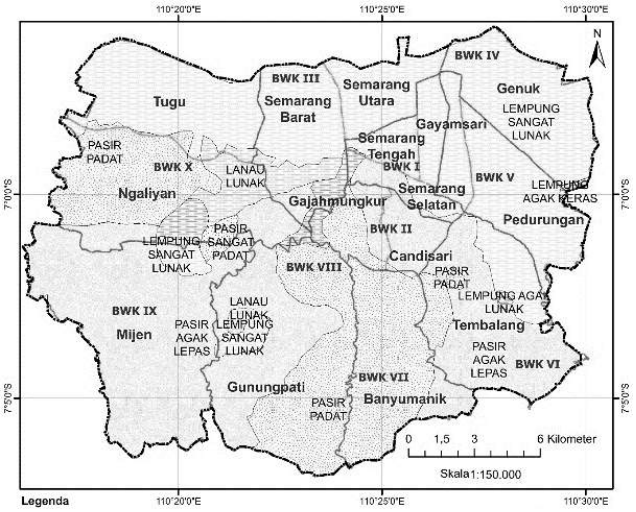

Fig. 5. BCL Map at 2.50 Meters Depth.

Table 1. Distribution of BCL at 2.50 m Depth.

District / PCA	Material Type	BCL (Q) (kg/cm^2)
Semarang Tengah (01) PCA I	Very soft clay	0.201 – 0.608
	Rather soft clay	1.218 – 1.320
	Rather loose sand	0.404 – 1.829
Semarang Utara (02) PCA III	Very soft clay	0.201 – 0.608
Semarang Timur (03) PCA I	Very soft clay	0.201 – 0.608
Gayamsari (04) PCA V	Very soft clay	0.201 – 0.608
Genuk (05) PCA IV	Very soft clay	0.201 – 0.608
	Rather hard clay	1.320 – 4.576
Pedurungan (06) PCA V	Very soft clay	0.201 - 0.608
	Rather hard clay	1.320 - 4.576
Semarang Selatan (07) PCA I	Very soft clay	0.201 - 0.608
	Rather soft clay	1.218 - 1.320
	Rather loose sand	0.404 - 1.829
	Dense sand	2.032 - 7.120
Candisari (08) PCA II	Rather loose sand	0.404 - 1.829
	Dense sand	2.032 - 7.120
Gajahmungkur (09) PCA II	Rather soft clay	1.218 - 1.320
	Rather loose sand	0.404 - 1.829
	Dense sand	2.032 - 7.120
Tembalang (10) PCA VI	Very soft clay	0.201 - 0.608
	Rather hard clay	1.320 - 4.576
	Rather loose sand	0.404 - 1.829
	Dense sand	2.032 - 7.120
Banyumanik (11) PCA VII	Rather loose sand	0.404 - 1.829
	Dense sand	2.032 - 7.120
Gunungpati (12) PCA VIII	Very soft clay	0.201 - 0.608
	Rather soft clay	1.218 - 1.320
	Soft silt	0.313 - 0.710
	Rather loose sand	0.404 - 1.829
	Dense sand	2.032 - 7.120
Semarang Barat (13) PCA III	Very soft clay	0.201 - 0.608
	Rather soft clay	1.218 - 1.320
	Soft silt	0.313 - 0.710
	Rather loose sand	0.404 - 1.829
Mijen (14) PCA IX	Very soft clay	0.201 - 0.608
	Rather soft clay	1.218 - 1.320
	Rather loose sand	0.404 - 1.829
	Very dense sand	11.696 - 14.248
Ngaliyan (15) PCA X	Very soft clay	0.201 - 0.608
	Rather soft clay	1.218 - 1.320
	Soft silt	0.313 - 0.710
	Rather loose sand	0.404 - 1.829
	Dense sand	2.032 - 7.120
	Very dense sand	11.696 - 14.248
Tugu (16) PCA X	Very soft clay	0.201 - 0.608
	Soft silt	0.313 - 0.710
	Dense sand	2.032 - 7.120

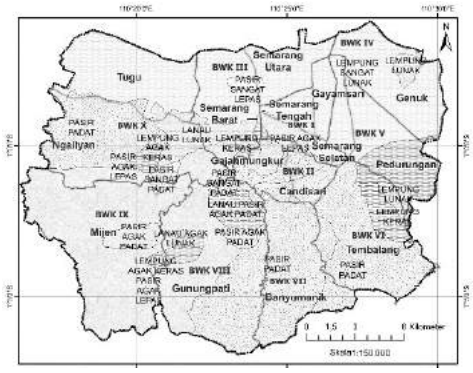

Fig. 6. BCL Map at 5.00 Meters Depth.

Table 2. Distribution of BCL at 5.00 m Depth.

District / PCA	Material Type	BCL (Q) (kg/cm^2)
Semarang Tengah (01) PCA I	Very soft clay	0.201 - 0.404
	Rather loose sand	2.338 - 5.085
Semarang Utara (02) PCA III	Very soft clay	0.201 - 0.404
	Rather loose sand	0.404 - 2.439
Semarang Timur (03) PCA I	Very soft clay	0.201 - 0.404
Gayamsari (04) PCA V	Very soft clay	0.201 - 0.404
Genuk (05) PCA IV	Very soft clay	0.201 - 0.404
	Soft clay	0.710 - 0.811
Pedurungan (06) PCA V	Very soft clay	0.201 - 0.404
	Soft clay	0.710 - 0.811
	Rather soft clay	0.506 - 0.811
Semarang Selatan (07) PCA I	Very soft clay	0.201 - 0.404
	Rather hard clay	1.931 - 4.678
	Rather loose sand	2.338 - 5.085
	Dense sand	6.916 - 12.408
	Very dense sand	13.731 - 14.036
Candisari (08) PCA II	Rather loose sand	2.338 - 5.085
	Dense sand	6.916 - 12.408
	Very dense sand	13.731 - 14.036
	Rather hard clay	1.931 - 4.678
	Hard clay	4.373 - 10.577
Gajahmungkur (09) PCA II	Rather loose sand	2.338 - 5.085
	Rather dense sand	2.338 - 12.408
	Dense sand	6.916 - 12.408
	Very dense sand	13.731 - 14.036
Tembalang (10) PCA VI	Very soft clay	0.201 - 0.404
	Soft clay	0.710 - 0.811
	Rather soft clay	0.506 - 0.811
	Hard clay	4.373 - 10.577
	Dense sand	6.916 - 12.408
Banyumanik (11) PCA VII	Dense sand	6.916 - 12.408
Gunungpati (12) PCA VIII	Rather hard clay	1.931 - 4.678
	Rather soft silt	0.710 - 0.913
	Very dense silt sand	2.833 - 3.050
Semarang Barat (13) PCA III	Rather loose sand	2.338 - 5.085
	Rather dense sand	2.338 - 12.408
	Dense sand	6.916 - 12.408
	Very dense sand	13.731 - 14.036
	Very soft clay	0.201 - 0.404
	Rather hard clay	1.931 - 4.678
	Hard clay	4.373 - 10.577
	Soft silt	0.313 - 0.710
	Rather loose sand	0.404 - 2.439
Mijen (14) PCA IX	Rather loose sand	2.338 - 5.085
	Rather dense sand	2.338 - 12.408
	Very dense sand	13.731 - 14.036
	Rather hard clay	1.931 - 4.678
Ngaliyan (15) PCA X	Rather loose sand	2.338 - 5.085
	Rather dense sand	2.338 - 12.408
	Very dense sand	13.731 - 14.036
	Very soft clay	0.201 - 0.404
	Rather hard clay	1.931 - 4.678
	Soft silt	0.313 - 0.710
	Rather loose sand	2.338 - 5.085
	Dense sand	6.916 - 12.408
	Very dense sand	13.731 - 14.036
Tugu (16) PCA X	Very soft clay	0.201 - 0.404
	Soft silt	0.313 - 0.710
	Dense sand	13.731 - 14.036

3.3 *The Significance of BCL in Environmental Carrying Capacity*

In research Abidin et al. (2013) explained that land subsidence in Semarang has been widely reported and its impact can be seen in everyday life. Based on estimates from Leveling survey methods, Interferometric Synthetic Aperture Radar (InSAR), Microgravity and Global Positioning System (GPS), land subsidence at a rate of up to about 19 cm/year was observed during the period 1999 to 2011. Results derived from GPS from 2008 to 2011 shows that land subsidence in Semarang has spatial and temporal variations, with a spatial average rate of about 6 to 7 cm/year and a maximum rate that can reach 14–19 cm/year at certain locations. This subsidence is believed to be due to a combination of natural consolidation of young alluvium soils, extraction of groundwater and building and construction loads, Abidin et al. (2013).

The BCL as a result of this study is very useful for early mitigation instruments for engineering the BCL in determining the construction used so that there is no

construction failure, especially subsidence. The effectiveness of the preparation of planning guidelines for design activities, preparation of building licensing documents can be carried out efficiently considering that information from the BCL map can be used as an initial guide.

From a social and economic point of view, the results of this paper study are measured by the benefits of supporting planning performance aspects in anticipating the failure of the BCL with all its implications, especially subsidence, which means it can reduce infrastructure or construction failures, loss of investment value from failed construction does not occur, inundation of the area due to the tidal wave that affects community activity or mobility and economic activity can also be avoided.

Sarah et al. (2012) concluded in the study of the Preliminary Study of Estimating Physical Losses Due to Land Subsidence in the City of Semarang. The magnitude of the loss is related to the rate of subsidence, in general the greater at rate of subsidence, implicate the greater at losses incurred. The study concluded that the total loss due to physical damage to roads, bridges, houses and buildings could reach 3.5 trillion rupiah, Sarah et al. (2012).

The negative aspects of the failure of the BCL in the form of deformation or subsidence, the impact of disturbing peace in life due to loss of living space, psychologically affecting the social role as a member of the community, while on a communal scale land subsidence on a regional scale will cause the loss of function of space as a community area that can degrades human functions as social beings, which means that there is a disturbance in the ability of the environment to support life and means that the environmental carrying capacity is degraded.

The effect of failure of land engineering and construction as a result of the failure of the BCL that is not in accordance with the use of space and has a negative impact on the economic, social or community and environmental aspects can be avoided by utilizing the BCL for spatial planning mitigation.

The benefit of the BCL map from the cultural dimension is that it can be a source of knowledge or information for humans as social beings that can be used to understand the environment and improve their experiences and become behavioral guidelines, especially in human efforts in the field of environmental engineering.

This paper examines the condition of natural resources with specific BCL or land capability of subsurface soil properties or engineering geological characteristics as an indicator of the ability of the soil to form a stretch of land. This study resulted in a standard value of land capability for the allocation of land use from the aspect of carrying capacity to a safe load, without deformation damage.

4 CONCLUSION

From the study, it can be concluded that:

1. The BCL Map of Semarang City clearly provides information on the classification of soil material zones, strata of BCL, and subsidence size. BCL = 0.201 kg/cm^2 – 14.248 kg/cm^2.
2. The BCL is the main factor in the environmental carrying capacity in spatial planning.
3. The value of the BCL can be used as a supplement to the Regulation of the Minister of the Environment N0. 17 of 2009 concerning Guidelines for Determining Environmental Carrying Capacity in Regional Spatial Planning in the City of Semarang.

REFERENCES

Abidin, H.Z., Andreas, H., Gumilar, I., Sidiq, T.P., Fukuda, Y. 2013. Land subsidence in coastal city of Semarang (Indonesia): characteristics, impacts and causes. Geomatics, Nat. Hazards Risk 4, 226–240. https://doi.org/10.1080/19475705.2012.692336

Craig, R.F. 1989. *Mekanika Tanah, edisi I*. Jakarta, Indonesia: Erlangga.

Dewi, D.I.K., Ratnasari, R.A., Pangi. 2016. Land Use Change in Sub District Mranggen Because of Residential Development. *Procedia - Soc. Behav. Sci*. 227:210–215. https://doi.org/https://doi.org/10.1016/j.sbspro.2016.06.064

Irsyam, M. 2018. Land Subsidence dan Settlement Tanah di Semarang. *Seminar Dampak dan Antisipasi Land Subsidence dan Settlement di Semarang.*

Kementerian Lingkungan Hidup. 2009. Peraturan Menteri Negara Lingkungan Hidup Nomor 17 Tahun 2009 Tentang Pedoman Penentuan Daya Dukung Lingkungan Hidup Dalam Penataan Ruang Wilayah. Jakarta KLH 27.

Marsudi, M. 2001. Prediksi Laju Amblesan Tanah di Dataran Alluvial Semarang Propinsi Jawa Tengah. Disertasi Progr. Pascasarj. ITB.

Ozcep, F. 2010. Soil Engineering: A Microsoft Excel® spreadsheet© Program for Geotechnical and

Geophysical Analysis of Soils. Comput. *Geosci* 36: 1355–1361. https://doi.org/https://doi.org/10.1016/j.cageo.2010.01.015

Pemerintah Kota Semarang. 2011. Peraturan Daerah Kota Semarang no 14 tahun 2011 Tentang Rencana Tata Ruang Wilayah Kota Semarang Tahun 2011-2031 [WWW Document]. BAPPEDA Kota Semarang. https://doi.org/10.16194/j.cnki.31-1059/g4.2011.07.016.

Pemerintah Republik Indonesia. 2010. Peraturan Pemerintah Nomor 15 Tahun 2010 Tentang Penyelenggaraan Penataan Ruang. Lembaran Negara Republik Indonesia Nomor 5103 [WWW Document]. Jakarta. Indonesia. URL https://peraturan.bpk.go.id/Home/Details/5023/pp-no-15-tahun-2010.

Pemerintah Republik Indonesia. 2007. Undang Undang Republik Indonesia Nomor 26 Tahun 2007 Tentang Penataan Ruang [WWW Document]. BPN. URL https://peraturan.bpk.go.id/Home/Details/39908/uu-no-26-tahun-2007.

Price, M.H. 2010. *Mastering ArcGIS*. McGraw-Hill.

Sarah, D., Soebowo, E., Syahbana, A.J., Murdohardono, D., Setiawan, T., Mulyono, A., Satrio, N.A. 2012. Perhitungan Penurunan Tanah Lintasan Bandarharjo-Poncol, Kota Semarang Berdasarkan Permodelan 2 Dimensi. *Pros. GEOTEKNOLOGI LIPI*: 199–208.

Statistic Center Agency of Semarang City. 2018. Semarang Municipality in Numbers 2018. 33740.1805. https://doi.org/1102001.3374.

Verhoef, P.N.W. 2017. Wear of Rock Cutting Tools: Implications for the Site Investigation of Rock Dredging Projects. Routledge.

Wesley, L.D. 1989. *Mekanika Tanah*, *Edisi I*. Jakarta: Badan Penerbit Pekerjaan Umum.

Determining Yield Stress Ratio and Constrained Modulus of Volcanic Soil in Kediri by Using SPT

Prayoga Jeremia Pangaribuan
Student – Universitas Katolik Parahyangan

Martin Wijaya
Lecturer – Universitas Katolik Parahyangan

Siska Rustiani
Assistant professor – Universitas Katolik Parahyangan

Paulus Pramono Rahardjo
Professor of Geotechnical Engineering – Universitas Katolik Parahyangan

ABSTRAK: Tekanan Pra-konsolidasi sudah umum di pergunakan untuk menggambarakan tegangan maksimum yang pernah dialamai oleh tanah dan sudah dengan sukses di implementasikan untuk tanah-tanah sedimen. Namum, banyak penelitian yang menunjukan bahwa istilah tekanan pra-konsolidasi kurang cocok dipergunakan untuk tanah residu dan menyarankan untuk mempergunakan istilah tegangan leleh sebagai istilah yang lebih umum. Tegangan leleh tidak hanya di akibatkan oleh tegangan maksimum yang pernah dialami oleh tanah tapi juga oleh ikatan dan perubahan struktur yang mungkin terjadi akibat proses pelapukan yang dialami oleh tanah residu. Didalam penelitian ini, data dari oedometer dan uji penetrasi standar yang di lakukan di tanah residu yang di dapatkan di Kediri dikumpulkan dan korelasi antara nilai SPT-N, tegangan leleh, dan modulus terkekang akan di ajukan.

Kata Kunci: tanah residu, tanah vulkanik, oedometer, SPT, tegangan leleh, modulus terkekang

ABSTRACT: Pre-consolidation pressure has been commonly used to describe the maximum stress that has been experienced by the soil and has been successfully implemented for sedimentary soils. However, a number of researched have shown that the term pre-consolidation pressure is not appropriate for residual soils and another term such as yield stress is coined as a more generic term. Yield stress is not only affected by the maximum stress that has been experienced by the soil but also by the bonding and structural alteration that might occur due to the weathering process. Hence, the value of yield stress depends on the origin and the weathering process that is experienced by the residual soil. In this research, data from oedometer and standard penetration test conducted at Kediri's residual soil are collected and correlation between SPT-N value, yield stress and constrained modulus are proposed.

Keywords: residual soil, volcanic soil, oedometer, SPT, yield stress, constrained modulus

1 INTRODUCTION

The city of Kediri has been subjected to enormous development in Indonesia, started with the development of Dhoho airport. Based on the geological map which is shown in Fig. 1, the project geological formation is volcanic rocks of Quarternary Pleistocene Period (Pawonsewu Morphocet – Qp) which consists of volcanic breccia with pyroxene andesite fragments, tuff, agglomerate, and pyroxene andesite lava. Hence, most of the soil in this area are residual soil from the volcanic rocks which is commonly referred as volcanic soil.

Pre-consolidation pressure (P_c) has long been used to describe the maximum stress that has been applied to the soil, Holtz et al. (2011) and has been proven to be very important when dealing with shear strength and compressibility issues in geotechnical engineering.

Fig. 1. Geological Map of the Madiun Quadrangle and Google Earth TM.

While sedimentary soil is formed systematically when there is a deposition of materials, residual soil is formed due to physical and chemical weathering of parent rock, Wesley (2010). As a result, the concept of pre-consolidation pressure and over consolidation ratio (OCR) are no longer applicable as the soil has never been consolidated. However, residual soil subjected to consolidation test shows compression curve similar with the one in sedimentary soils as shown in Fig. 2 where the soil behaves elastically at the beginning of the test until it yield after specific stress (and hence referred as yield stress, P_y) which has the same function as P_c, Wesley (2010). The term OCR is replaced with yield stress ratio (YSR) which is defined as:

$$YSR = \frac{P_y}{\sigma_{v'}} \tag{1}$$

In Fig. 2, the value of P_y is 361 kPa which is quite high for soil sampled at depth of 3.00m. Hence, the YSR is approximately 8. However, it is important to note that yield stress is affected by diagenesis, bonding, fabric and intrinsic structural alterations that occurs during the weathering process, Mayne (2014), Wesley (2010), Mayne (2013). Hence, very high and irregular yield stress and YSR pattern with depth are expected.

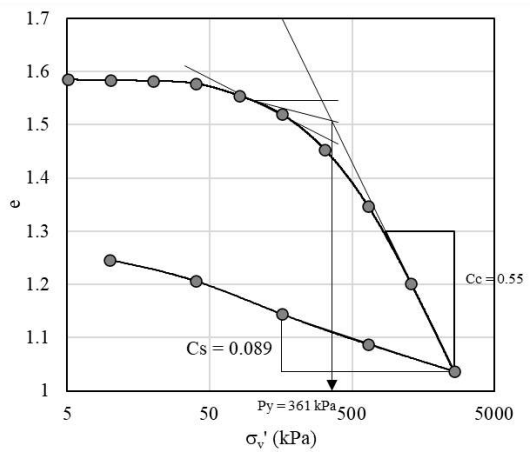

Fig. 2. Compression Curve of Volcanic Soil at Kediri.

Irregularity in YSR pattern with depth makes determination of such values difficult as it will be costly to conduct oedometer test at very short interval. Standard Penetration Test (SPT) is commonly used in Indonesia to determine soil properties due to its low cost and it is usually conducted in very short interval. Hence, using SPT to determine YSR value will be very cost effective.

Mayne and Kemper (1988) collects data from more than 50 sites (110 data points) from all over the world without distinction whether the soil is from sedimentary soil or residual soils. The data are shown in Fig. 3. Mayne and Kemper (1988) proposed to determine with the equation is shown in Eqn. (2):

$$OCR = 0.193\left[\frac{N}{\sigma_v'(MPa)}\right]^{0.689} \tag{2}$$

With alternative equation where the exponent is forced as 1 is given in Eqn. (3)

$$OCR = 0.05\left[\frac{N}{\sigma_v'(MPa)}\right] \tag{3}$$

The problem with Eqn. (2) and (3) are that the unit are not normalized. Hence, Mayne and Kemper (1988) proposed the third form of equation which is given as follow:

$$OCR = k_s\left(\frac{N}{\sigma_v'}\right)P_a \tag{4}$$

Where P_a is atmospheric pressure (100 kPa) and k_s is empirical parameter which is varied between 0.2 to 1 as shown in Fig. 3. It is difficult to evaluate proper k_s value especially for volcanic soil in Kediri. It is therefore worth to evaluate whether the equations proposed by Mayne and Kemper (1988) are suitable for volcanic soils in Kediri and any necessary adjustment which is required to better estimate the YSR value of volcanic soils in Kediri by using SPT test.

It is also important to note that constrained modulus (E_{Oed}) is also an important parameter especially for settlement analysis. Thus, it is also of interest to determine the E_{Oed} by using SPT test for vulcanic soils.

In this paper, correlation between 65 oedometer test result and SPT-N value will be conducted. Oedometer test will be used to determine the YSR value and E_{Oed} determined at the effective vertical stress. Nearest SPT-N value will then be used to represent both YSR and E_{Oed} in order to establish suitable correlation.

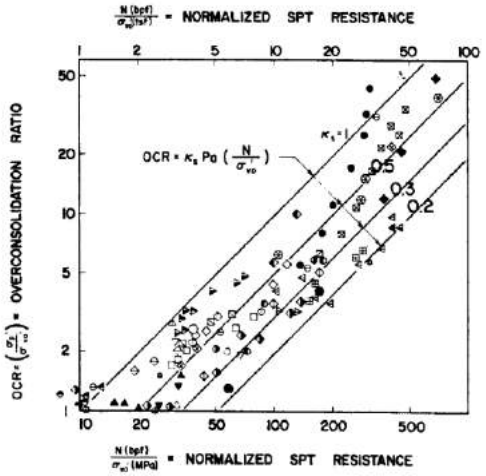

Fig. 3. Correlation between SPT-N, Effective Stress and OCR, Mayne and Kemper (1988).

2 METHODS

Oedometer tests data and SPT values from all over Kediri are collected for the analysis. Yield stress is constructed by using Casagrande (1936) construction method as illustrated in Fig. 2 while E_{Oed} are determined by conducting regression analysis on the strain-stress curve which is shown in

Fig. 4. Regression of Stress-Strain Curve from Oedometer Test Data.

.

Regression curve between stress-strain curve is differentiated to obtain soil's modulus of volume compressibility (m_v) at the respective effective stress which can then be converted easily into constrained modulus (E_{Oed}) through the following equation:

$$E_{Oed} = \frac{1}{m_v} \quad (5)$$

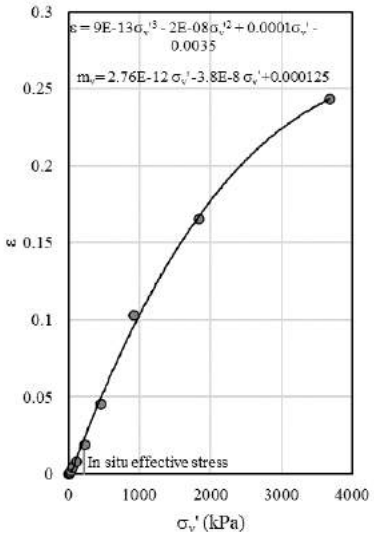

Fig. 4. Regression of Stress-Strain Curve from Oedometer Test Data.

Oedometer test result and SPT test with similar depth are then plotted together and data with the nearest depth are correlated as shown in Fig. 5.

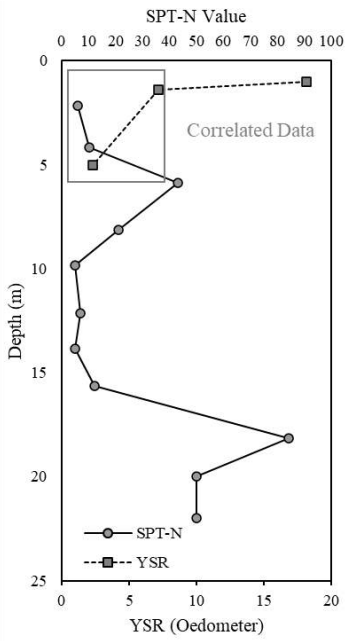

Fig. 5. Correlation Procedure for SPT-N and YSR Value.

3 PROPOSED CORRELATION

Fig. 6 shows the collected data points compare with the equations proposed by Mayne and Kemper (1988). As shown in Fig. 6, Eqn. (2) tend to overestimate YSR at low N/σ_v'. Eqn. (3) is the upper bound line and hence tend over-estimate YSR value. Eq (4) with $k_s = 0.2$ seems to give rather low estimate of the YSR when N/σ_v' is low but over estimate YSR when N/σ_v' is high.

In order to appropriately determined the YSR value of volcanic soil in Kediri, two equations are proposed:

$$YSR = 19.029\left(\frac{N}{\sigma_v'(kPa)}\right)^{0.731} \quad (6)$$

$$YSR = 12\left(\frac{N}{\sigma_v'(kPa)}\right)^{0.85} \quad (7)$$

Eqn. (6) is best fit equations which represent the median of most data points while

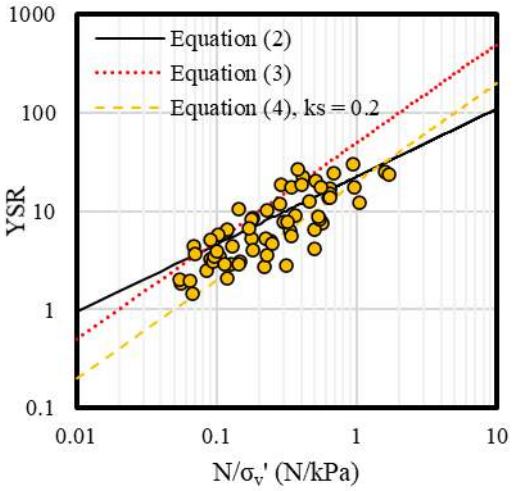

Fig. 6. Comparison between Mayne and Kemper (1988) Equation and Data Points.

Eqn. (7) is the lower bound equations which gives more conservative estimate for YSR value. Fig. 7 shows the comparison between Eqn. (6) and (7) with the data points. Correlation between E_{oed} and SPT-N value are shown in Fig. 8. It is proposed that E_{Oed} can be estimated through the following equation:

$$E_{Oed} = A.N^{0.2} \quad (8)$$

Where A is empirical parameters that can be either 3000 for lower bound estimate, 6000 for the best fit and 12000 for the upper bound value.

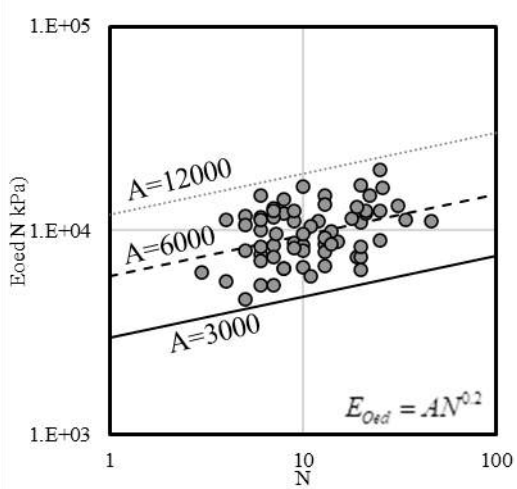

Fig. 7. Comparison between Proposed Correlation and Data Points.

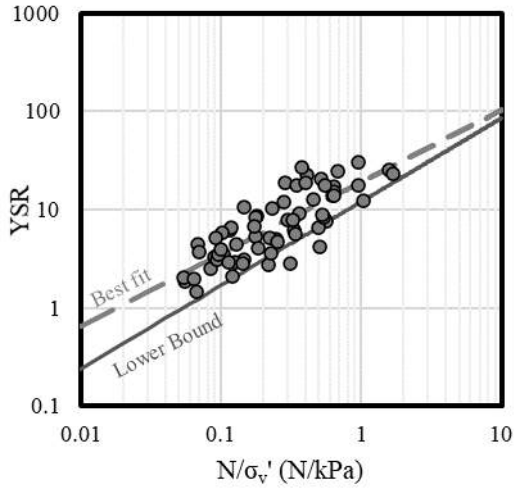

Fig. 8. Correlation between SPT-N Value and $E_{Oed.}$

4 CONCLUSION

In this paper, correlation between SPT-N value, yield stress ratio and constrained modulus have been carried. Two equations have been proposed to correlate SPT-N value and yield stress value where the first equation fits the median of the data very well while the second equation serves as lower bound estimate. Another correlation has also been proposed to estimate constrained modulus and SPT-N value. Different empirical parameters can be adopted in order to obtain lower bound, best fit and upper bound of the constrained modulus.

ACKNOWLEDGEMENTS

The authors would like to express their gratitude to Parahyangan Catholic University (UNPAR) and P.T. Geotechnical Engineering Consultant (GEC) for all of the supports which have been provided to complete this research.

REFERENCES

Casagrande, A. 1936. The Determination of the Pre-Consolidation Load and Its practical significance. *Proceedings of the First International Conference on Soil Mechanics and Foundation Engineering* 3:60-64.

Holtz, R. D., Kovacs, W. D. & Sheahan, T. C. 2011. *An Introduction to Geotechnical Engineering. 2nd Edn.* Pearson Education, Inc.

Mayne, P. & Kemper, J. B. 1988. Profiling OCR in Stiff Clays by CPT and SPT. *Geotechnical Testing Journal - GEOTECH TESTING J* 11.

Mayne, P. W. 2013. Evaluating Yield Stress of Soils from Laboratory Consolidation and in-Situ Cone Penetration Tests. *In Sound Geotechnical Research to Practice*: 405-419.

Mayne, P. W. 2014. Generalized CPT Method for Evaluating Yield Stress in Soils. *In Geo-Congress 2014 Technical Papers*: 1336-1346.

Wesley, L. D. 2010. *Geotechnical Engineering in Residual Soils.*

Evaluasi Penurunan Akhir Akibat Jeda Penimbunan dengan Pendekatan Analisis Balik Data *Settlement Plate*

Yogina Lestari Ayu
Departemen Teknik Pertanian dan Biosistem – Universitas Padjadjaran

Josua Adrianov
Maratama Cipta Mandiri

Benny Beckham Marbun
Maratama Cipta Mandiri

ABSTRAK: Pembangunan Jalan Tol merupakan prioritas pembangunan di Indonesia sehingga pelaksanaannya tidak terpungkiri akan bertemu kondisi lahan bermasalah, salah satunya adalah tanah lunak terkompresibel. Penurunan tanah dihitung dari pendekatan 1 dimensi Terzaghi menggunakan parameter uji laboratorium konsolidasi. Penurunan aktual di lapangan sering kali menunjukkan perbedaan dibandingkan pendekatan Terzaghi. Pada salah satu pembangunan jalan tol digunakan perbaikan tanah PVD (*Prefabricated Vertical Drain*) dan penimbunan (*preloading)*. Pekerjaan sempat terhenti saat proses penimbunan selama 8 (delapan) bulan, kemudian dilanjutkan kembali. Sehingga perhitungan balik terhadap pembacaan *settlement plate* perlu dilakukan untuk mendapatkan perkiraan penurunan akhir ketika penimbunan dilanjutkan kembali. Koefisien hasil analisis balik digunakan untuk analisis penurunan 1 dimensi Terzaghi dan pendekatan elemen hingga. Peningkatan kekuatan tanah lunak terkompresibel selama penimbunan berhenti menjadi parameter tambahan dalam analisis. Analisis balik menujukkan nilai koefisien penurunan (Cc) lebih besar 50% dibandingkan data laboratorium. Nilai penurunan konsolidasi terkoreksi memberikan penurunan akhir dengan metode elemen hingga mmeberikan hasil lebih kecil dibandingkan dengan pendekatan 1 dimensi Terzaghi.

Kata Kunci: tanah lunak terkompresibel, PVD (Prefabricated Vertical Drain), settlement plate

ABSTRACT: Highway construction, which is a priority in developing Indonesia, makes constructing in a problematic soil an inevitable condition, especially in soft compressible soil layer. Consolidation settlements are calculated using 1-D Terzaghi using laboratory soil test parameters. Actual consolidation settlement mostly gave bigger value than 1-D Terzaghi analysis. In one of highway construction which used PVD Preloading as soil improvement method, the construction came to a halt for 8 (eight) months. To have an actual total consolidation settlement after construction resumes, a back calculation analysis was done using 1-D Terzaghi and finite element method. A gain strength value was obtained for the soft soil compressible layer from momentary pause of the preloading construction which became an added parameters value in analysis. Back calculation analysis gave a consolidation coefficient (Cc) 50% bigger than Cc from soil laboratory tests. Corrected consolidation settlement values in finite element method gave smaller settlement than 1-D Terzaghi.

Keywords: soft soil compressible layer, PVD (Prefabricated Vertical Drain), settlement plate

1 PENDAHULUAN - INTRODUCTION

Indonesia, khususnya Jawa Barat, mayoritas terbentuk dari lapisan alluvium, lapisan ini merupakan endapan, sehingga bersifat lunak dan *compressible*. Jawa barat merupakan daerah yang memiliki laju pertumbuhan dan pembangunan yang signifikan. Hal ini mendorong kebutuhan akan jalan penghubung yang baik. Di sisi lain, pembangunan penduduk yang pesat menghasilkan keterbatasan lahan yang baik. Lahan yang tersisa adalah lahan dengan kondisi tanah kurang baik.

Pembangunan jalan Tol merupakan salah satu prioritas pembangunan di Indonesia dan menjadi solusi akan kebutuhan jalan koneksi yang baik. Pembangunan jalan tol membutuhkan area yang cukup luas, dengan keterbatasan lahan, maka kondisi tanah yang kurang baik tidak dapat dihindari.

Tanah lunak memiliki daya dukung yang kurang baik dan berpotensi mengalami penurunan dalam jangka waktu tertentu. Pembangunan di atas tanah lunak memerlukan penanganan tanah terlebih dahulu. Metode penanganan tanah yang dipakai dalam kasus tanah lunak ini adalah *Prefabricated Vertical Drain* dengan *Preloading*.

Keberhasilan pekerjaan *Prefabricated Vertical Drain* dengan *Preloading* dimonitor dengan instrumentasi lapangan berupa *settlement plate* dan *piezometer*. Besar penurunan dihitung dengan *settlement plate*. Pada pekerjaan jalan tol ini sempat terhenti saat proses penimbunan selama 8 bulan, kemudian dilanjutkan kembali.

2 KONDISI UMUM PROYEK

Tebal tanah lunak di lokasi pekerjaan 10meter dengan rencana tinggi timbunan 6,5 meter. Beban perkesarasan yang diaplikasikan sebesar 9 kPa dan beban lalu lintas sebesar 15 kPa. Nilai *Coefficient of Consolidation (CC)* dari tanah lunak tersebut 0,377. Tanah timbunan berupa lempung kelananuan dengan berat isi 13 kN/m^3.

Penimbunan berlangsung dari tanggal 26 Juni 2020 hingga 20 Desember 2020. Tinggi penimbunan saat itu 5,8 meter dengan penurunan sekitar 80 cm. Penimbunan direncanakan dilanjutkan pada bulan Agustus 2021 dimana sudah terjadi penurunan total 160 cm. PVD yang digunakan pola segitiga dengan spasi 1 m.

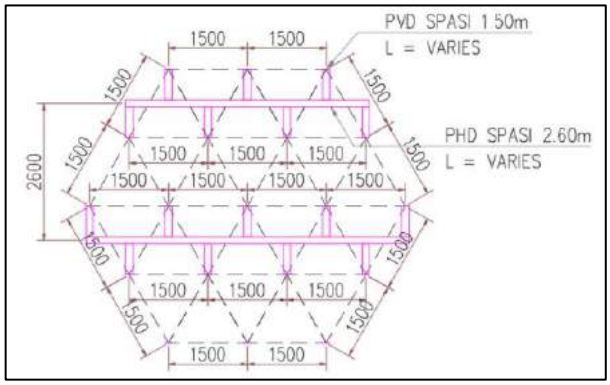

Gbr. 1. Pola PVD Segitiga dengan Spasi 1 m.

3 METODOLOGI

Penurunan dihitung dengan pendekatan 1D-Terzaghi dengan nilai CC hasil uji laboratorium. Penurunan ID – Terzaghi dibandingkan dengan penurunan aktual di lapangan. Perbandingan hasil penurunan memberikan nilai CC aktual.

Nilai CC aktual dipakai untuk memprediksi nilai penurunan akhir saat penimbunan selesai. Penurunan dilakukan juga dengan metode elememn hingga dengan memperhitungkan kenaikan kuat geser tanah.

4 HASIL DAN PEMBAHASAN

Grafik penimbunan dan penurunan sampai dengan timbunan 5.8 meter dapat dilihat pada gambar berikut.

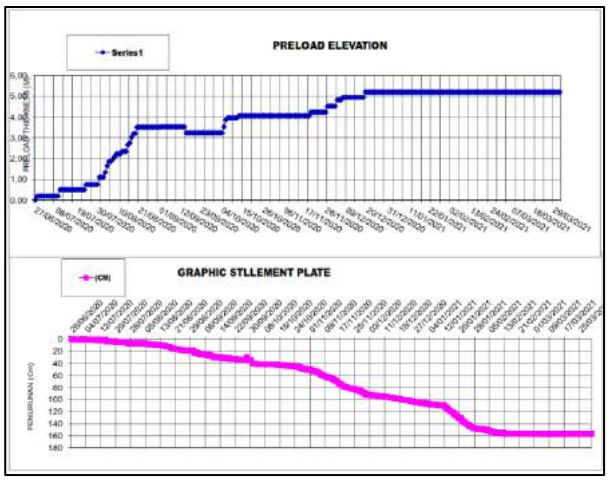

Gbr. 2. Grafik Penurunan vs Penimbunan.

Grafik perbandingan penurunan berdasarkan nilai CC laboratorium, aktual, dan metode elemen hingga untuk tinggi timbunan 5.8 meter dapat dilihat pada gambar berikut.

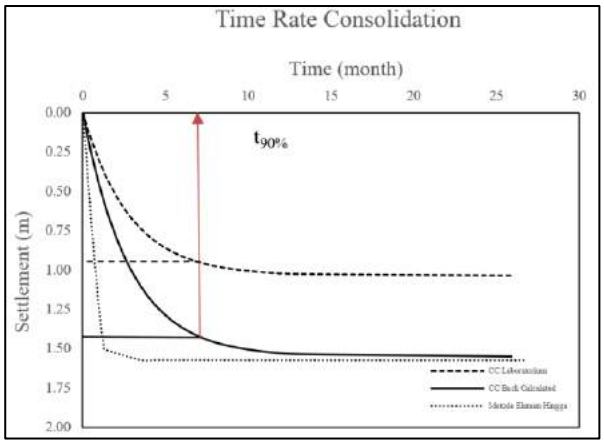

Gbr. 3. Perbandingan Penurunan Berdasarkan CC Laboratorium, Aktual, dan pendekatan Metode Elemen Hingga.

Berdasarkan perbandingan di atas penurunan aktual memberikan nilai 1.5 kali lebih besar dibandingkan perhitungan berdasarkan nilai CC laboratorium.

Berdasarkan nilai CC yang terkoreksi, dilakukan analisis penurunan untuk timbunan akhir, beban perkerasan, dan beban jalan. Hasil analisis penurunan berdasarkan 1D-Terzaghi dan pendekatan elemen hingga dapat dilihat pada gambar dibawah.

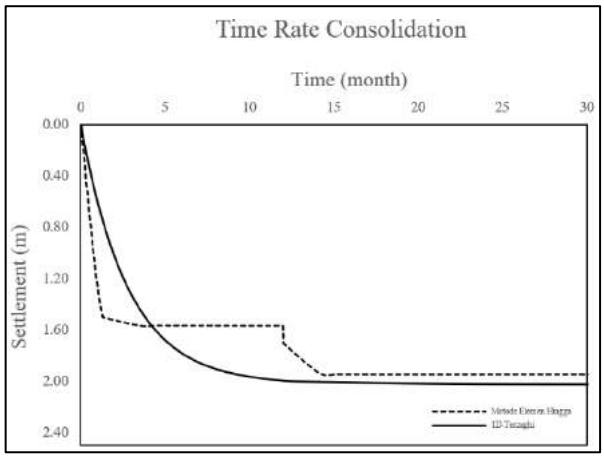

Gbr. 4. Perbandingan Penurunan 1 D Terzaghi dan Metode Elemen Hingga.

Penurunan berdasarkan elemen hingga (1,94 m) lebih kecil dibandingkan pendekatan 1 D Terzaghi (2,02 m).

5 KESIMPULAN

Penurunan aktual memberikan nilai 1,5 kali lebih besar dibandingkan perhitungan berdasarkan nilai CC laboratorium. Nilai CC terkoreksi akan digunakan untuk analisis selanjutnya.

Penurunan akhir dianalisis berdasarkan nilai CC terkoreksi. Penurunan berdasarkan metode elemen hingga lebih kecil 5 % dibandingkan pendekatan 1D-Terzaghi. Hal ini terjadi karena adanya peningkatan kuat geser tanah saat jeda penimbunan.

DAFTAR PUSTAKA - REFERENCES

Asaoka, A. 1978. Observational Procedure of Settlement Prediction. *Soils and Foundations* 18(4): 87–101.

Bergado, D.T. & Daria, P.M. 1991. Prediction of Embankment Settlement by In-Situ Tests. *Geotechnical Testing Journal* 14(4): 425–39.

Briaud, J. -L. 2013. *Introduction to Geotechnical Engineering: Unsaturated and Saturated Soils*. Canada: John Wiley & Sons Ltd.

Carter, M. & Bentley, P. S. 2016. *Soil Properties and Their Correlations*. London: John Wiley & Sons Ltd.

Look, G. B. 2014. *Handbook of Geotechnical Investigation and Design Tables.* Australia: CRC Press/Balkema.

Mikasa, M. 1965. *The Consolidation of Soft Clay—A New Consolidation Theory and Its Application*. *Japan Society of Civil Engineering*: 21–6. Tokyo.

Terzaghi K. Settlement and Consolidation of Clay. *Principles of Soil Mechanics. IV*. Engineering News-Record 1925; 95:874–8.

CPT-SPT Correlation of Volcanic Soils in Kediri, East Java

Aflizal Arafianto
Universitas Katolik Parahyangan

Gregorius Rayhan
Universitas Katolik Parahyangan

Martin Wijaya
Universitas Katolik Parahyangan

ABSTRAK: Korelasi CPT-SPT merupakan salah satu korelasi yang paling umum dibuat dalam praktek geoteknik. Peneliti-peneliti telah mengusulkan korelasi tersebut untuk tanah kohesif maupun tanah granular. Namun demikian, korelasi untuk tanah khusus, misalnya tanah vulkanik, masih terbetas. Artikel ini membahas tentang korelasi CPT-SPT pada tanah vulkanik di Kediri, Jawa Timur. Uji Penetrasi Konus (CPT), yaitu dalam hal ini uji *piezocone* (CPTu), dilakukan secara berdampingan dengan Uji Penetrasi Standar (SPT). Tujuh belas pasang data CPTu dan SPT digunakan untuk membuat korelasi $q_t - N$ dan $f_s - N$. Korelasi $q_t - N$ memberikan hasil rasio q_t/N = 2,15 (q_t dalam satuan kg/cm^2) dengan koefisien determinasi R^2 sebesar 0,92. Korelasi ini cenderung mirip dengan korelasi untuk material lempung dan lempung kelanauan. Korelasi yang baik juga diperoleh untuk hubungan $f_s - N$, dimana dihasilkan rasio f_s/N = 9 (f_s dalam satuan kPa) dengan R^2 sebesar 0,88. Sebagai tambahan, nilai *N*-SPT terstandardisasi (N_{60}) diestimasi menggunakan korelasi antara indeks perilaku tanah (I_c) dari pengukuran CPTu dan nilai *N*-SPT yang diusulkan Lunne dkk. (1997) dan Robertson (2012). Hasil estimasi menunjukkan bahwa kedua korelasi memberikan nilai N_{60} terprediksi lebih rendah 20 hingga 49 persen daripada nilai N_{60} yang terukur di lapangan. Dengan demikian, sebuah korelasi baru diusulkan untuk jenis tanah spesifik ini dan didapati korelasi yang lebih baik.

Kata Kunci: uji penetrasi konus (CPT), uji penetrasi standar (SPT), korelasi, tanah vulkanik

ABSTRACT: CPT-SPT correlation is one of the most common correlations made in geotechnical practice. Researchers have been proposed such correlations for both cohesive and granular soils. However, correlations for a particular soil, for instance, volcanic soils, are still limited. This paper presents CPT-SPT correlations of volcanic soils in Kediri, East Java. Cone penetration tests, namely piezocone test (CPTu), were conducted side-by-side with Standard Penetration Test (SPT). Seventeen CPTu and SPT data pairs were mainly used to develop $q_t - N$ and $f_s - N$ correlations. The $q_t - N$ correlation results q_t/N = 2.15 (q_t in kg/cm^2) with a coefficient of determination R^2 of 0.92. This relationship tends to be similar to the same correlation for clay and silty clay materials. A good agreement is also obtained for the $f_s - N$ correlation, which resulted in f_s/N = 9 (f_s in kPa) with an R^2 of 0.88. Additionally, a standardized SPT *N*-value (N_{60}) is estimated using a relationship between soil behavior index (I_c) from the CPTu measurement and SPT *N*-value, suggested by Lunne et al. (1997) and Robertson (2012). Results show that both relationships give 22 to 49 percent lower predicted values of N_{60} compared to in-situ N_{60} values. A new correlation, thus, is proposed for this particular soil type, and a better agreement is obtained.

Keywords: cone penetration test (CPT), standard penetration test (SPT), correlation, volcanic soils

1 INTRODUCTION

Cone Penetration Test (CPT) and Standard Penetration Test (SPT) are two in-situ tests most used globally, including Indonesia. Their application in projects has become more common since they were required by Indonesian National Standard (SNI), specifically SNI 8460:2017 (SNI, 2017) about Geotechnical Design Requirements. Additionally, many future projects, both scaled

locally and nationally, promote the usage of these tests even more.

The abundance of CPT and SPT data encourages researchers and practitioners to study and correlate these two test results for practical use. Many empirical CPT-SPT correlations for numerous soils have been proposed, including non-textbook materials, for example, residual and volcanic soils. In fact, in Indonesia, both practitioners and academicians often encounter these unique materials in projects. Nonetheless, it appears that even though the CPT and SPT data are plentiful, such correlations on these materials are still limited.

This paper attempts to provide reliable local CPT-SPT correlations for volcanic soils in Kediri. The relationship between the two tests was developed using high-quality field data. Therefore, the proposed correlations can be utilized maximally by practical engineers to evaluate and design various geotechnical works. Moreover, this study was also intended to suggest a new CPT-SPT correlation between $(q_t/p_a)/N_{60}$ and CPT-based SBT Index (I_c) for this specific soil type. The suggested correlation can then be used for predicting standardized N_{60} values using piezocone (CPTu) soundings.

2 PREVIOUS STUDIES OF CPT-SPT CORRELATION

Zhao and Cai (2013) noted that the study of CPT-SPT correlations could be broadly delineated into three categories:

2.1. *Ratio method*

In this method, the cone resistance of the CPT and the SPT *N*-value was assumed to have a simple linear relationship. Many researchers have proposed the ratio of q_c /*N* for various types of soils, including other materials such as volcanic soils. Table 1 and Table 2 recap some available q_c – *N* correlations from the 1950s to 2000s. This method is prevalent because of its practicability and convenience since many geotechnical designs often use empirical correlations based on CPT and SPT. For instance, if the q_c data are present, they can be converted easily to SPT *N*-value or vice versa. The converted values are then can be used for the evaluation or design of geotechnical works. Nevertheless, it should be noted that every soil type has different q_c/N ratios, and other materials may have unique ratios.

Table 1. Some Published q_c – *N* Correlations.

Soil Type	q_c/N (kg/cm^2)	References
Silts, sandy silts, slightly cohesive silt-sand mixtures	2	Schmertmann (1970)
Clay, silty clay, clayey silt	3.5	Velloso (1959)
	3	Sanglerat (1972)
	1.3	Kruizinga (1982)
Sandy clay and silty sand	2	Velloso (1959)
Sandy clay	4	Sanglerat (1972)
Sandy silt	3.5	Velloso (1959)
Clean, fine to medium sands and slightly silty sands	3 – 4	Schmertmann (1970)
Silty sand	5	Sanglerat (1972)
Coarse sands and sands with little gravel	5 – 6	Schmertmann (1970)
Clayey sand	6	Sanglerat (1972)
(Silty) fine sand	4	Meigh and Nixon (1961)
Fine sand	4	Meyerhof (1956)
	6	Velloso (1959)
Medium and coarse sand	8	Meigh and Nixon (1961)
Sand	10	Velloso (1959)
	4.5	Kruizinga (1982)
Sandy gravels and gravel	8 – 10	Schmertmann (1970)
Gravelly sand	12	Meigh and Nixon (1961)
Sandy gravel	12 – 16	Meigh and Nixon (1961)

Table 2. Available q_c – *N* Correlations for Other Materials.

Soil Type	q_c/N (kg/cm^2)	References
Pumice, volcanic ash, loam	8	Miura et al. (2003)
Alluvium silty sand, silt (volcanic soil deposits)	8.5	Takesue et al. (1996)
Silty sand (residual soil)	3.9	Costa et al. (2016)

Soil Type	q_c/N (kg/cm^2)	References
Sandy estuarine sediment	2.2	Kantey (1965)
Chalk	3 – 7	Power (1982)

2.2. *Function method*

This method considers that the relation between q_c and SPT N-values is not linear. Some researchers suggested a more complicated function of these two parameters to increase the accuracy, Akca (2003), Kara and Gunduz (2010), Zhao and Cai (2013). This approach, however, did not consider the soil properties which may affect the CPT-SPT correlation. Moreover, a complicated mathematical expression is often less preferable to engineers because it includes time-consuming math operations.

2.3. *Soil parameter method*

One of the first CPT-SPT correlation studies that included soil properties was Robertson et al. (1983), which suggested the q_c/N ratio as a function of mean grain size (D_{50}). Ten years later, Jefferies and Davies (1993) discovered a new relationship between the q_c/N ratio and Soil Behavior Type (SBT) Index, I_c. They suggested that the most reliable way to obtain SPT N-values was to perform a CPT and convert them to an equivalent SPT. They proposed a method to convert the CPT cone resistance, q_t, to an equivalent SPT N-value at 60% energy, N_{60}, using Jefferies and Davies's Soil Behavior Type (SBT) index, I_{cJD}.

Jefferies and Davies (1993) method was then modified by Lunne et al. (1997), in which they used the I_c formulation from Robertson and Wride (1990) as follows:

$$I_c = [(3.47 - \log Q_t)^2 + (\log F_r + 1.22)^2]^{0.5} \qquad (1)$$

Where:
Q_t = Normalized cone resistance
$= (q_t - \sigma_{vo})/\sigma'_v$
F_r = Normalized friction ratio
$= f_s/(q_t - \sigma_{vo})$
q_t = Corrected cone resistance
$= q_c + (1 - a)\, u_2$;
a = Area ratio of the cone
σ_{vo}= Overburden pressure (total)
σ_v'= Overburden pressure (effective)

Then, the CPT-SPT relationship they proposed can be expressed as:

$$(q_t/p_a)/N_{60} = 8.5\,[1 - (I_c/4.6)] \qquad (2)$$

Robertson (2012) reported that the above method had been shown to work effectively in a wide range of soils. However, recent experience in North America has shown that Eqn. (1) tends to underpredict the N_{60} values in some clays. Hence, Robertson (2012) recommended an updated relationship that can be defined by an equation as follows:

$$(q_t/p_a)/N_{60} = 10^{(1.1268 - 0.2817\, I_c)} \qquad (3)$$

He added that the above equation produced a slightly larger N_{60} in fine-grained soils than the Jefferies and Davies (1993) method. In fine-grained soils with high sensitivity, Eqn. (3) may overestimate the N_{60}.

3 CPT AND SPT METHODOLOGY

CPT and SPT data used in this research were collected from an airport project at Kediri, East Java. All test was carried out by the same company, and the same procedure was applied to all locations. The following subsection outlines the CPT and SPT methodology utilized for each testing point.

3.1 *Cone Penetration Testing*

The Cone Penetration Test (CPT) is a versatile and widely used method for geotechnical investigation. In the research site, the CPT conducted were all piezocone (CPTu) tests. In principle, the test is performed by pushing a piezocone into the soil with a constant pushing rate, following ASTM D5778 (ASTM, 2020). Fig. 1 shows the overview of CPT.

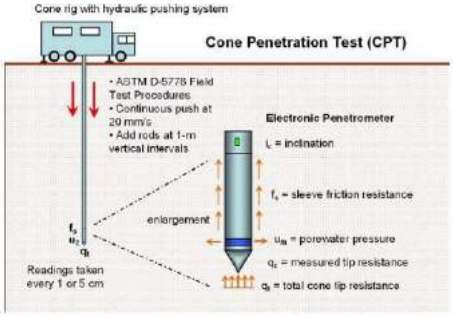

Fig. 1. Overview of the Cone Penetration Test (CPT) Per ASTM D 5778 Procedures, Mayne, (2007).

3.2 *Standard Penetration Testing*

The Standard Penetration Test (SPT) was performed following the ASTM D1586, ASTM (2018). The test drives a standard split spoon sampler into the soil/rock at a certain depth in a borehole. An automatic hammer of 63.5 kg weight falling freely from a height of 75 cm (30 inches) on the drill rod is used to drive the sampler. The number of hammer blows to drive the second and the third 15 cm of penetration is called the SPT *N*-value, representing the number of blows per 30 cm of penetration.

In order to calculate the standardized SPT *N*-value (N_{60}), the following equation is used:

$$N_{60} = N \times \left(\frac{ER}{60}\right) \times C_B \times C_s \times C_R \qquad (4)$$

Where:
N = Field-measured blow count
ER = SPT hammer efficiency as determined by energy measurements in accordance with ASTM D4633 (ASTM, 2016)
C_B = Correction factor for borehole diameter
C_S = Correction factor for sampler geometry
C_R = Correction factor for rod length

In this study, since the test was performed using the automatic hammer, the *ER* was taken 75. Other SPT correction factors such as borehole diameter, sampler geometry, and rod length were assumed to be 1.0.

4 DATA PROCESSING AND DEVELOPED CORRELATIONS

4.1 *Data Processing*

It is well known that the mechanism of CPT and SPT is different from one to another, especially regarding the measurement of resistance of the soils. In the CPT, the soil resistance is measured due to quasi-static penetration of the cone. On the other hand, SPT measures soil resistance based on dynamic force from a free-fall hammer transferred to the rod at a certain depth. Thus, to provide a comparable CPT and SPT measurement, the mean of each CPT variable (q_c, f_s, and I_c) was determined over the 300 mm length of each SPT. Averaging on the seating drive was excluded since the soil experienced high disturbance from the hammer blows. Fig. 2 visualizes the averaging method of the CPT variable.

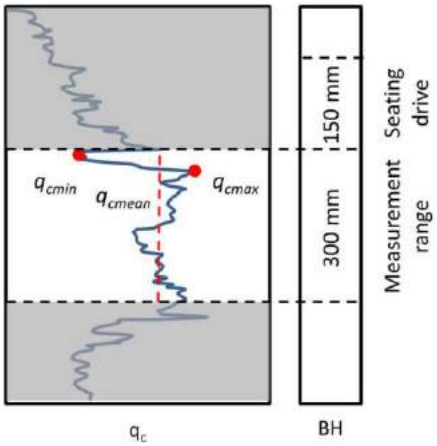

Fig. 2. Calculation of CPT Parameters based on SPT Location (Wotherspoon et al. 2015).

There were more than 100 CPT and boreholes available on the research site, and these data undoubtedly provide valuable information for local correlations. However, not all of them can be utilized because there were differences in testing elevation and the distance between the tests was too far apart. Hence, to refine the datasets, the following filters were applied:

1. CPT and SPT soundings used are only spaced equals or less than 10 m apart and with the same test elevations. The reason behind this is to reduce the effect of inhomogeneity.
2. All incomplete SPT drive lengths were removed (i.e., those with less than 450 mm total penetration).
3. SPT *N*-values higher than 20 were excluded since the specific CPT apparatus used in the field hardly penetrates this stratum.

Based on the above filters, a total of six CPT and SPT soundings were evaluated, resulting in 17 data pairs for correlations. The location of the tests is shown in Fig. 3. The majority of the testing points were located in the north area except for the CPT PCPT1-15 and borehole BH2-11.

The observed depths range from 1 to 14 m below the existing ground, with 12 data located above the groundwater level (GWL). As for the soil types, the identification was determined using the Unified Soil Classification System (USCS). Table 3 summarizes the filtered data used for developing correlations. It is clearly shown that silts are the most common soil type found on site.

Fig. 3. Borehole and Piezocone (CPTu) Locations.

Table 3. Filtered Data for Correlations.

BH No.	CPT No.	Depth (m)	Sample Location	Soil Type
BH6-37	PCPT1-32	6	Above GWL	ML
BH6-37	PCPT1-32	8	Above GWL	ML
BH6-36	PCPT2-48	2	Above GWL	SM
BH7-2	C2-8	2	Above GWL	MH
BH7-2	C2-8	4	Above GWL	MH
BH7-2	C2-8	6	Above GWL	ML
BH7-2	C2-8	12	Above GWL	CL
BH7-2	C2-8	14	Below GWL	CL
BH8-57	C2-9	7	Above GWL	ML
BH8-57	C2-9	9	Above GWL	ML
BH5-24	S-26	2	Above GWL	CH
BH5-24	S-26	4	Above GWL	MH
BH5-24	S-26	8	Below GWL	MH
BH2-11	PCPT1-15	1	Above GWL	ML
BH2-11	PCPT1-15	3	Above GWL	ML
BH2-11	PCPT1-15	5	Above GWL	CH
BH2-11	PCPT1-15	7	Above GWL	ML

4.2 *Developed Correlations*

As mentioned earlier in section 2, the study of CPT-SPT correlations can be divided into three categories: ratio method, function method, and soil parameter method. In this study, the proposed correlations focus on the first and the third method, considering the more practical application. The ratio of cone resistance and SPT N-value (q_t/N) was developed based on a simple linear relationship with zero intercept. This approach is very logical and widely accepted by engineers and academicians. In addition to q_t/N, the same approach was applied to develop the ratio of sleeve friction to SPT *N*-value (f_s/N).

Furthermore, the CPT-SPT relationship in terms of Soil Behavior Type (SBT) Index, I_c, formulated by Robertson and Wride (1990), was suggested. Previous correlations from Lunne et al. (1997) and Robertson (2012) are used to evaluate their reliability to estimate N_{60} values of Kediri volcanic soils. Finally, this study aims to provide a local relationship between $(q_t/p_a)/N_{60}$ and I_c for this specific soil type.

5 SOIL AND GEOLOGICAL CONDITION

The ground condition can be assessed using in-situ test data and information from a local geological map. Rather than contradicting each other, these two pieces of information are more likely to complement. The CPT and SPT provide measured data and actual condition of the ground, while a geological map gives an idea of what geological layer is beneath the project location.

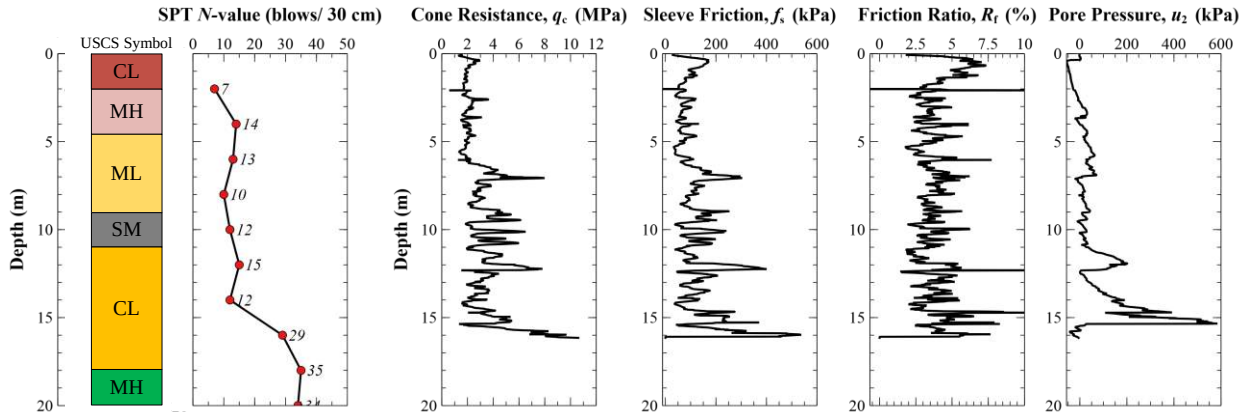

Fig. 4. Soil Condition from SPT and CPT Soundings.

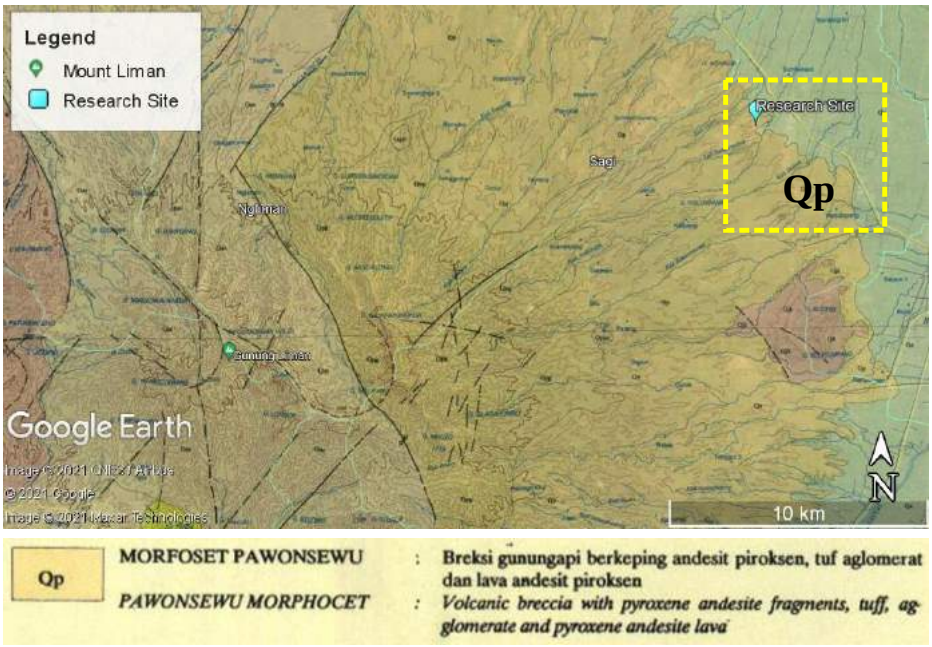

Fig. 5. Research Site on Geological Map of Madiun Quadrangle, Java (Map Data: Google, © 2021 Maxar Technologies; Geological Map Reprinted from Hartono et al. 1992).

Drilling and SPT identified the surface layer as a cohesive stratum of clays and silts with medium to stiff consistency and a thickness of 2 to 3 meters. A hard layer was found at a depth of about 16 m below the existing ground level. This condition was also consistent with the CPT soundings. In addition, based on the collected samples, the cementation of materials was not present except for the hard consistency of the volcanic breccia layer. Fig. 4 depicts the typical soil stratification at the research site based on the CPT and SPT. The volcanic breccia stratum in this figure is not visible because it is located 30 m below the ground surface.

Information contained in the geological map is also beneficial for identifying the soil condition. Based on the geological map of Madiun Quadrangle, Hartono et al. (1992), the research site is located on the geological layer of *Qp*, which consists of volcanic breccia, tuff, agglomerate, and lava. Therefore, it can be expected that the soils were volcanic soils and the weathering products of volcanic rocks.

6 ANALYSIS AND RESULTS

6.1 $q_t - N$ and $f_s - N$ Correlations

As presented earlier in the introduction section, numerous researchers have proposed q_c/N ratios for many soils, but only some researchers suggested f_s/N correlation, Kruizinga (1982), Takesue et al. (1996). In fact, for most soils, the SPT *N*-value is dominated by sampler side friction. Therefore, this study presents both correlations to provide options to geotechnical engineers for design. Fig. 6 shows the obtained correlations for Kediri volcanic soils.

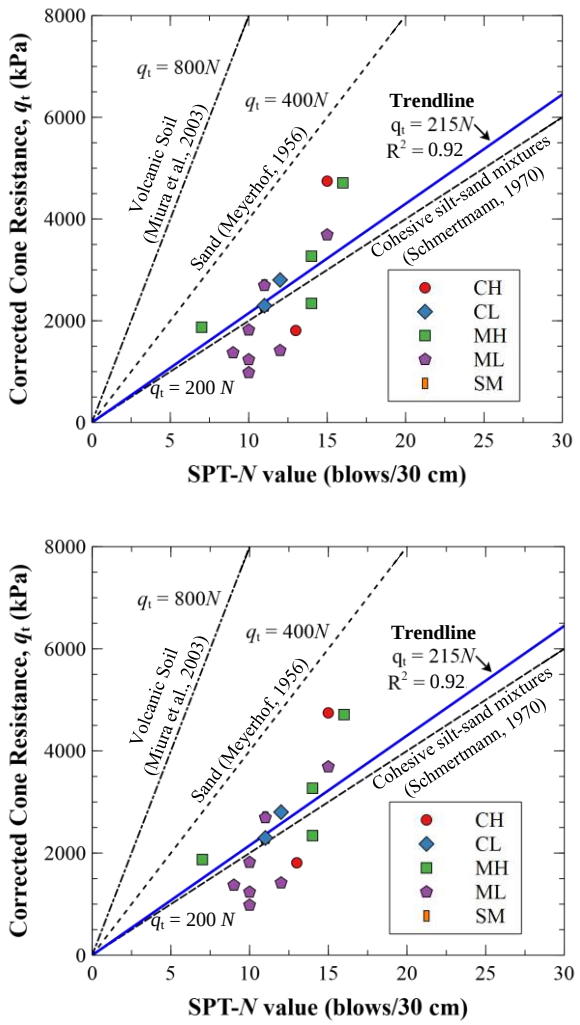

Fig. 6. $q_t - N$ and $f_s - N$ Correlations for Volcanic Soils in Kediri.

Results show that a good agreement is obtained for both $q_t - N$, and $f_s - N$ correlations, in which the coefficient of determination (R^2) are 0.92 and 0.88, respectively. The q_t/N (in kg/cm^2) ratio is approximately 2.15, close to the ratio for cohesive silt-sand mixtures proposed by Schmertmann (1970). This correlation, however, is significantly different from the results obtained by Miura et al. (2003). The reason is that the Kediri volcanic soils are not cemented, and thus, the effect of particle crushing during SPT is not present. Moreover, the ratio of f_s/N (in kPa) is about 9, higher than quartz sands and alluvium silty sands and silts. These results were obtained since the soils are dominated by cohesive soils (clays and silts).

6.2 *Estimation of N_{60} from CPTu*

Based on the previous studies of Lunne et al. (1997) and Robertson (2012), this study examines whether their proposed correlations can be used for Kediri volcanic soils. Equivalent N_{60} values were predicted using both methods to evaluate their reliability. Fig. 7 shows the comparison between measured N_{60} and N_{60} estimated by the two equations.

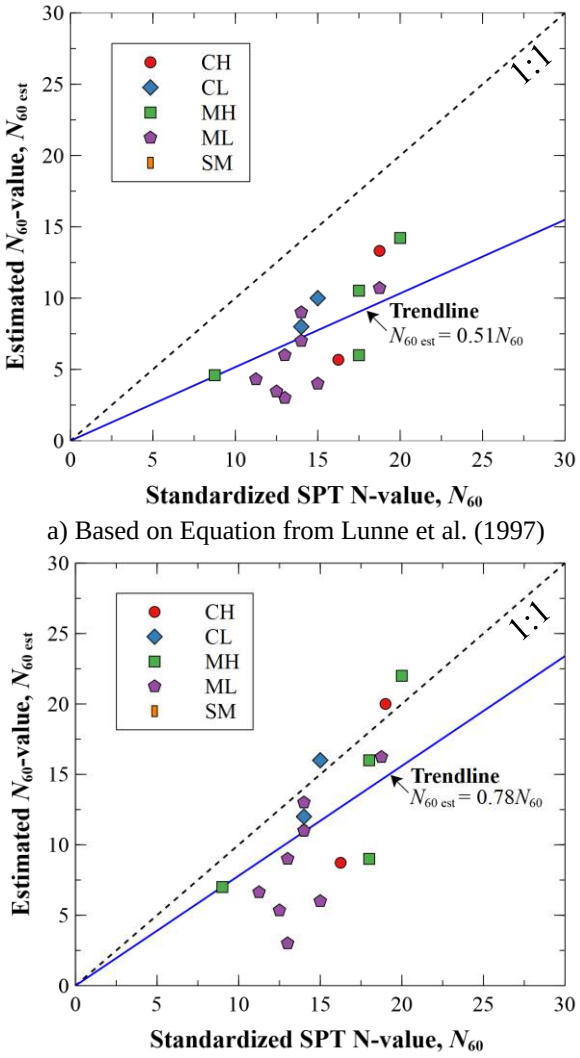

a) Based on Equation from Lunne et al. (1997)

b) Based on Equation from Robertson (2012)

Fig. 7. Prediction of N_{60} from CPT.

The graphs show that the two equations underpredict the N_{60} by 49% for the Lunne et al. (1997) method and 22% for the Robertson (2012) method. Although it is better than the Lunne et al. (1997) method, estimation based on Robertson's method still depicts a scattered data, with most of them produces lower values of N_{60}. This result shows that the existing equations are less suitable for Kediri volcanic soils.

A graph was made with SBT Index (I_c) in the x-axis and the ratio of $(q_t/p_a)/N_{60}$ in the y-axis to develop a more accurate prediction of N_{60}. Measured data were then plotted into the graph, and a trendline was proposed. The suggested relationship is slightly modified from

Robertson (2012), and it can be written as follows:

$$(q_t/p_a)/N_{60} = 10^{(1.1 - 0.32\, I_c)} \quad (5)$$

Fig. 8 shows the proposed and previous CPT-SPT correlations, along with the Kediri volcanic soils data. Some ML soil type data points seem to be out of the flock because their $(q_t/p_a)/N_{60}$ equals or less than unity. Nevertheless, the above relationship represents the best fit line to the data.

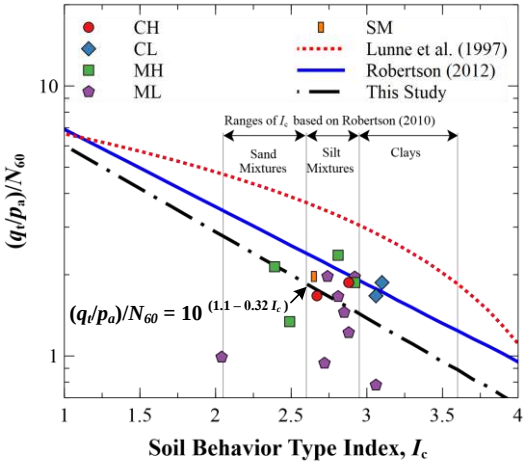

Fig. 8. Proposed and Previous SPT-CPT Correlations in terms of $(q_t/p_a)/N_{60}$ and CPT-based SBT Index I_c.

Estimation of N_{60} was performed once again using the proposed equation. The comparison of the predicted and the measured N_{60} can be seen in Fig. 9. The result showed that a good agreement was met, in which the estimated N_{60} was 7% higher than the measured data. Though scatters can still be recognized, for Kediri volcanic soils, the proposed relationship better predicts N_{60} values than two previous correlations.

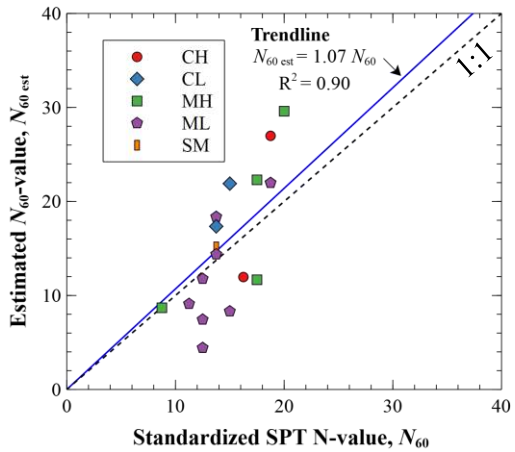

Fig. 9. Prediction of N_{60} from CPT Based on the Proposed Equation.

7 CONCLUSION SUMMARY

CPT – SPT correlation for volcanic soils of Kediri has been proposed, namely q_t – N and f_s – N correlation. Estimation of N_{60} from CPTu was also performed based on existing equations, and a specific equation for Kediri volcanic soils was suggested. The results of this study can be summarized as follows:

1. From 17 data pairs of CPT and SPT results, the ratio of q_t/N for Kediri volcanic soils is about 2.15 (in kg/cm^2), which is similar to clays and silt-like materials rather than volcanic-cemented soils in Japan (as reported by Miura et al. 2003). The reason is that the observed volcanic soils in Kediri are mainly uncemented silts and clays.
2. The f_s/N ratio (in kPa) was found around 9, higher than those of quartz sands and alluvium silty sand and silt reported by Takesue et al. (1996). Again, this finding is because those Kediri volcanic soils are predominantly clays and silts, and therefore, the sleeve resistance (f_s) is higher than those in sands.
3. Estimation of N_{60} from CPTu using existing equations from Lunne et al. (1997) and Robertson (2012) resulted in lower values of N_{60} compared to measured N_{60}, and thus, less suitable for practical application on Kediri volcanic soils. A new equation was suggested in a simpler expression, and it resulted in a better estimation of N_{60} with only 7% higher than the in-situ N_{60} values.

ACKNOWLEDGMENTS

The authors are grateful to PT Geotechnical Engineering Consultant for allowing and sharing the geotechnical investigation data to be used in this study. Also, the authors express their gratitude to the Geotechnical Engineering Division of Universitas Katolik Parahyangan for their comments and suggestions to improve this research.

REFERENCES

Akca, N. 2003. Correlation of SPT–CPT data from the United Arab Emirates. *Engineering Geology 67*(3): 219-231.

ASTM. 2016. Standard Test Method for Energy Measurement for Dynamic Penetrometers. *ASTM D4633-18*. West Conshohocken, PA: ASTM.

ASTM. 2018. Standard Test Method for Standard Penetration Test (SPT) and Split-Barrel Sampling of Soils. *ASTM D1586-18.* West Conshohocken, PA: ASTM.

ASTM. 2020. Standard Test Method for Electronic Friction Cone and Piezocone Penetration Testing of Soils. *ASTM D5778-20*. West Conshohocken, PA: ASTM.

Costa, Y. D., Cunha, E. S., Costa, C. L., and Pereira, A. C. 2016. Correlations between SPT and CPT data for a sedimentary tropical silty sand deposit in Brazil. *Proceedings of the 5th International Conference on Geotechnical and Geophysical Site Characterization*. Gold Coast, Australia.

Hartono, U., Baharuddin, and Brata, K. 1992. Geologic Map of the Madiun Quadrangle, Java. Bandung, Indonesia: Pusat Penelitian dan Pengembangan Geologi.

Jefferies, M. G., and Davies, M. P. 1993. Use of CPTu to Estimate Equivalent SPT N_{60}. *Geotechnical Testing Journal* 16(4): 458-468.

Kantey, B.A. 1965. Discussion on Shallow Foundations and Pavements. *Proceedings of the 6th International Conference on Soil Mechanics and Foundation Engineering*. Montréal, Canada.

Kara, O., and Gündüz, Z. 2010. Correlation between CPT and SPT in Adapazari, Turkey. *Proceedings of the 2nd International Symposium on Cone Penetration Testing*. Huntington Beach, CA.

Kruizinga, J. 1982. SPT – CPT Correlations. *Proceedings of the 2nd European Symposium on Penetration Testing*. Amsterdam, The Netherlands.

Lunne, T., Powell, J. J. M., and Robertson, P. K. 1997. *Cone Penetration Testing in Geotechnical Practice*. London: CRC Press.

Mayne, P. W. 2007. *Cone Penetration Testing State-of-Practice (NCHRP Project 20-05).* Washington: Transportation Research Board.

Meigh, A. C., and Nixon, I. K. 1961. Comparison of In Situ Tests for Granular Soils. *Proceedings of the 5th International Conference on Soil Mechanics and Foundation Engineering*. Paris, France.

Meyerhof, G. G. 1956. Penetration Tests and Bearing Capacity of Cohesionless Soils. *Journal of the Soil Mechanics and Foundations Division* 82(1): 866-1-866-19.

Miura, S., Yagi, K., and Asonuma, T. 2003. Deformation-Strength Evaluation of Crushable Volcanic Soils by Laboratory and In-situ Testing. *Soils and Foundations* 43(4): 47-57.

Power, P. T. 1982. The Use of the Electric Static Cone Penetrometer in the Determination of the Engineering Properties of Chalk. *Proceedings of the 2nd European Symposium on Penetration Testing*. Amsterdam, The Netherlands.

Robertson, P. K. 2010. Soil Behaviour Type from the CPT: an Update. *Proceedings of the 2nd International Symposium on Cone Penetration Testing*. Huntington Beach, CA.

Robertson, P. K. 2012. Interpretation of In-Situ Tests – Some Insights. *Proceedings of the 4th International Conference on Geotechnical and Geophysical Site Characterization.* Recife, Brazil.

Robertson, P. K., Campanella, R. G., and Wightman, A. 1983. SPT-CPT Correlations. *Journal of Geotechnical Engineering* 109(11): 1449-1459.

Robertson, P. K., and Wride, C. E. 1998. Evaluating Cyclic Liquefaction Potential Using the Cone Penetration Test. *Canadian Geotechnical Journal* 35(3): 442-459.

SNI. 2017. *Persyaratan Perancangan Geoteknik*. SNI 8460:2017. Jakarta: Badan Standarisasi Nasional

Sanglerat, G. 1972. *The Penetrometer and Soil Exploration*: *Interpretation of Penetration Diagrams - Theory and Practice*. Amsterdam: Elsevier Publishing Company.

Schmertmann, J. H. 1970. Static Cone to Compute Static Settlement Over Sand. *Journal of the Soil Mechanics and Foundations Division* 96(3): 1011-1043.

Takesue, K., Sasao, H., and Makihara, Y. 1996. Cone Penetration Testing in Volcanic Soil Deposits. *Proceedings of the International Conference on Advances in Site Investigation Practice.* London, United Kingdom.

Velloso, D. A. 1959. *O Ensaio De Diepsondering E A Determinaçao Da Capacidade De Carga Do Solo [Cone Penetration Test and the Determination of Soil Bearing Capacity].* Revista Rodovia No 29.

Wotherspoon, L. M., Li, Z., and Haycock, I. 2015. Assessment of SPT - CPT Correlations Using Canterbury Site Database. *Proceedings of the 12th Australia New Zealand Conference on Geomechanics.* Wellington, New Zealand.

Zhao, X., and Cai, G. 2015. SPT-CPT Correlation and Its Application for Liquefaction Evaluation in China. *Marine Georesources & Geotechnology* 33(3): 272-281.

SPT and CPT Correlation of Expansive Clay in Cikarang, Indonesia

Eddy Triyanto Sudjatmiko
President Universty

ABSTRAK: Korelasi CPT-SPT telah banyak dikembangkan dari berbagai belahan dunia untuk memperkirakan parameter tanah dari data yang tersedia. Korelasi tersebut umumnya untuk tanah-tanah lanau dan pasiran. Hanya sedikit informasi yang ditemukan apakah korelasi tersebut sesuai dengan kondisi tanah di Indonesia. Paper ini bertujuan untuk memverifikasi dan memodifikasi korelasi SPT-CPT yang telah digeneralisir tersebut untuk khususnya untuk kondisi tanah di Indonesia guna meningkatkan akurasi dan tingkat kepercayaannya. Tanah yang distudi adalah lempung kelanauan yang banyak dijumpai di sepanjang pantai utara Jawa Barat. Tanah jenis ini memiliki kecenderungan mengembang dan menyusut dengan perubahan kadar air. Pengumpulkan data dilakukan di 8 (delapan) titik uji yang didedikasi untuk studi ini, dengan jarak 2meter untuk setiap pasang data SPT dan CPT. Melalui analisa regresi statistik, didapatkan persamaan korelasi yang cukup meyakinkan yakni $n = q_c/N_{SPT} = 0.225$ (Mpa) dengan nilai n terdistribusi pada rentang antara 0.14 hingga 0.34 (Mpa). Hasil ini juga menunjukan nilai n yang lebih rendah dibandingkan berbagai korelasi yang dipublikasikan sebelumnya.

Kata Kunci: SPT, CPT, korelasi, lempung kelanauan, tanah ekspansif

ABSTRACT:

Many CPT-SPT correlation relationships have been proposed worldwide to enable estimation soil parameters from available data to the other. While most of correlations are for silty and sandy soils, limited information are found whether this correlation are fit to Indonesia soils conditions. This paper aims to verify and modifying the generalized CPT-SPT correlation published, especially for Indonesia soils condition with the intention to improve its prediction accuracy and reliability. The soils studied is silty clay soil deposits covers majority of Northen parts of West Java, which is recognize having tendency to undergo volume change due to change in water content with seasonal variation. Data collection consisted of 8 (eight) pairs of dedicated SPT and CPT tests at 2 (two) m distance between each other. A high correlation of $n = q_c/N_{SPT} = 0.225$ (Mpa) was obtained based on statistical regression analysis, with data distribution of n ranges from 0.14 to 0.34 (Mpa). This result shows much lower n values compared to various correlation have been published.

Keywords: SPT, CPT, correlations, silty clay, expansive soils

Duck Feet System Foundation (DFSF) for Building on Soft Soil

Syahirman Suriadi
Ph.D Kandidat Teknik Sipil, Fakultas Teknik – Undip Semarang
Dosen, Fakultas Teknik, Jurusan Teknik Sipil – Unihaz Bengkulu

Prabandiyani RW
Dosen, Fakultas Teknik, Jurusan Teknik Sipil – Undip Semarang

Endra Susila
Dosen, Fakultas Teknik Sipil dan Lingkungan – Institut Teknologi Bandung

Windu Partono
Dosen, Fakultas Teknik, Jurusan Teknik Sipil – Undip Semarang

ABSTRAK: Untuk membangun bangunan di atas tanah lunak, masalah yang dipertimbangkan daya dukung rendah dan penurunan besar. Pondasi bangunan di atas tanah ini beberapa sudah ada diantaranya: pondasi sistem cakar ayam, pondasi konstruksi sarang laba-laba. Pondasi yang mengadopsi sistem kerja tapak bebek belum ada yang mengusulkan. Penelitian ini mencari ukuran struktur pondasi sistem tapak bebek (PSTB) terbaik dengan Plaxis. Tujuan penelitian membuktikan PSTB dapat diusulkan untuk bangunan di atas tanah lunak. Untuk mengkalibrasi hasil uji dengan Plaxis dilakukan uji pembebanan langsung PSTB skala penuh. Hasil penelitian struktur PSTB terbaik: panjang tiang 50 cm, diameter tiang 13 cm, spasi tiang 50 cm, tebal plat 9 cm, dan daya dukung ultimate PSTB = 70 kN.

Kata Kunci: tanah lunak, PSTB, plaxis, daya dukung ultimate

ABSTRACT: To construct a building on soft soil, the problems considered are low bearing capacity and large settlement. Some of the building foundations on this land already exist, including chicken claw system foundation, cobweb construction foundation. The foundation that adopts the duck tread work system has not yet been proposed. This study is looking for the best size of the foundation structure of the tread duck system (PSTB) using Plaxis. The research objective is to prove that PSTB can be proposed for buildings on soft soil. To calibrate the test results with Plaxis, a full-scale PSTB direct loading test was performed. The results showed that the best PSTB structure: length of pile 50 cm, diameter of pile 13 cm, spacing of pile 50 cm, plate thickness 9 cm, and ultimate bearing capacity of PSTB = 70 kN.

Keywords: soft soil, PSTB, plaxis, ultimate bearing capacity

1 INTRODUCTION

The area of soft-land in Indonesia reaches 14,905 million hectares1 Sari (2012). Soft clay soil is a layer of soil that contains organic and inorganic soil with consistency very soft, cone resistance value ≤ 50 kPa and CBR value ≤ 3%, Djaranto (2015). Naturally, soft soil has a high water content, the groundwater is shallow and less of loading, so the mechanical properties are not able to carry the load, the nature of there will be an undrained failure to build buildings on soft soil layers, technical issues that is underneath, if the soil layer is hard, the bearing capacity of the soil is strong enough to withstand the failure, to build buildings on soft soil layers, technical issues considered are the bearing capacity is small and the potential for a large decline, Hardiyatmo (2008). Determination of the type and shape of the foundation depends on the layer of soil beneath it, if the soil layer is hard, the soil bearing capacity is strong enough to withstand the existing load, if the soil is soft, it needs special handling so that it has a large bearing capacity, Martini (2009). If the building is built on soft soil, it will experience some common problems, such as bearing capacity low, excessive downside, and long-running consolidation time, Buisman (1936). Many studies have been carried out to increase the bearing capacity of foundations on soft soil, including research mixing soft soil with better material, Sutikno and Yatmadi (2010); mixing with cement,

research on cement and combination alcove, Soeteddi et al. (2005); reinforcement with bamboo groves, Suroso et el. (2008); soft soil reinforcement method with bamboo grids, Ratna et el. (2013); with a combination of recesses and bamboo grids, Suroso et al. (2008); with geotextiles, Subianto dan Harry (2002); with geotextile combination bamboo grids1 Soewignjo, dan Nugroho (2011). Soft soil with bamboo mat, Irsyam (2008), and soil improvement method using vertical drain, Basu et al (2006). Several foundations for buildings on soft soil have existed, including in 1961 Sedijatmo proposed the foundation of the chicken claw system (FCCS), Ardiansyah (2016), foundation adopts chicken claw work system used for buildings that support temporary loads such as airport foundations, Setiawan et al. (2013). In 1976 Ryantori and Soecipto created the foundation for the construction of cobwebs (FCC), Djajaputra et al. (2009) which mimicked the cobweb construction work system used for buildings that support fixed loads such as buildings, Djaranto (2015). There are no practical economic foundations for Hardiyatmo created the foundation of the riveted plate pavement system (FP2S) in 2008 to imitate the work system of nailed plates, Puri et al. (2015), residential buildings, irrigation canals, etc. to be built on soft land. No one proposes a foundation that mimics the working system of duck treads, considering that duck treads have fins between their fingers, as shown in Fig. 1.

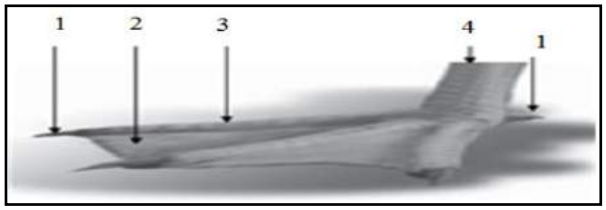

1. Duck’s Toenail
2. Duck's Web
3. Duck’s Toe
4. Duck's Leg

Fig.1. Duck’s Feet.

Fig.1 which is a distinct advantage of ducks. The philosophy of the duck footwork system is shown in Fig. 2.

As a result of the rotation of the force as:

1. The more the surface area of the fins due to fin deflection due to pressure from the fingers supporting the load from the foot, the greater the friction force (3).
2. Loads that press on soft soil will result in soil sticking to fingers and fingers, which causes friction (3).
3. The greater the load will cause the soft soil into the fins between the two nails the greater, which causes the compressive force laterally (8) the soft soil to the fins is greater which causes greater friction (3).
4. The greater the load will cause the soft soil into the fins between the two nails (4), the greater that causes the compressive force of the soft soil due to the outside, which causes greater carrying capacity (7).
5. The softer the soil, the easier it will be to enter the fins between the two nails, which causes greater bearing capacity and friction.
6. If the force (8) has been maximized due to load (4), it will cause the force (6) to be immobile again (the ground has become solid, the air cannot get out again), which causes the air trapped in the fin pouches between two fingers to behold the duck leg down, as shown in Fig. 2.

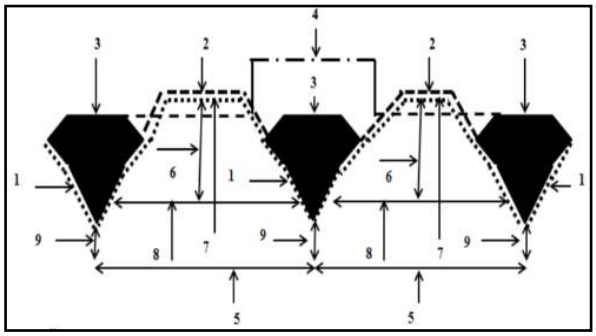

1. Duck's Toenail
2. Duck’s Web
3. Duck’s Toe
4. Duck's Leg
5. Spaces between Duck’s Toe
6. The Soft Soil Moves Up and Down within The Web’s Deflection, Deflection
7. Friction Revolving Around Web-Toe-Nail
8. The Nail’S Horizontal Pinching Force That Moves Left-Right
9. 9. The Nail’S Horizontal Pinching Force That Moves Left- Right

Fig. 2. The Philosophy of Duck's Feet Working System.

From the philosophy of the duck tread work system (DFSF) above, it can be concluded that it is suitable to be used for building foundations on soft. Duck tread is not single, between two duck treads there is always a distance, and the

width of the duck tread is always smaller than the body area of a duck. Based on this philosophy, the size of the foundation of the duck tread system is proposed to be small, ie between 100 cm^2 to 200 cm^2. To support heavier loads it is proposed to use several foundations of the duck tread system which are arranged so that it resembles the ceramic arrangement on the tiled floor. This research intends to find the best DFSF structure size, which has the greatest ultimate bearing capacity, to be proposed as a foundation for simple buildings such as houses, irrigation channels, drainage channels, embankments and others, which must be built on soft soil. While the purpose of this study is to prove that the DFSF can be proposed for building foundations in accordance with the research objectives. To determine the ultimate carrying capacity of DFSF is based on the theory, which states that the pile has collapsed if the test graph VS load decreases have started to level off, or start to decrease, Bell dan Robinson (2012).

2 METHOD, MODEL, AND MATERIALS

This research is an experimental study using an inductive approach, which is an approach that draws conclusions from the general one (Plaxis program model test results) to be more specific (full-scale loading test results in the field so that it can be applied to building foundation planning on soft soil. The research scenario is as follows: Start, Preparation: Literature study, a survey of research sites, procurement of soft soil samples, and testing of soft soils in the laboratory, soft soil data obtained, If yes, continued: Analysis looking for the best DFSF structure size using plaids, requirements accepted a practical, economical, and safe DFSF structural model that supports a load of ≥50 kN/m^2, If yes, continued: Making the DFSF model with the best model, making 1 unit of DFSF model loading test equipment, and the best DFSF structure test with Plaxis, the test equipment can provide a load of ton 12 tons, the practical, economical and safe DFSF structural model supports a load of ≥ 50 kN/m^2. If yes, go on: Test the loading of the DFSF model in full-scale in the field, the practical, economical, safe DFSF structural model supports static loads ≥ 5 t/m^2, if yes, continue: Conclusions, complete.

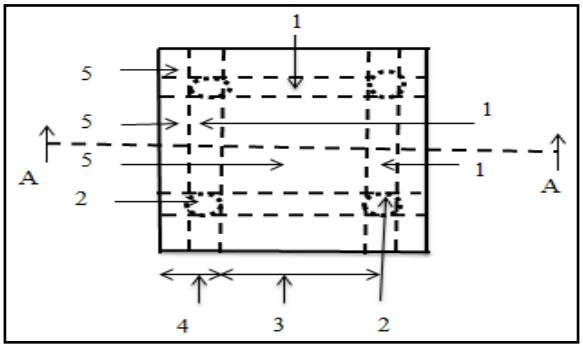

1. 10 x 19 cm concrete beam as the duck's toe
2. Ø 12-15 cm concrete mini pile as the duck's toenail
3. A space of 0.5-1m between each toe
4. 0.5 x Space, as the duck's outer web
5. 5. Concrete plate 8-10 cm thick, as fins for duck feet

Fig.3. DFSF Test Model Top Vie.

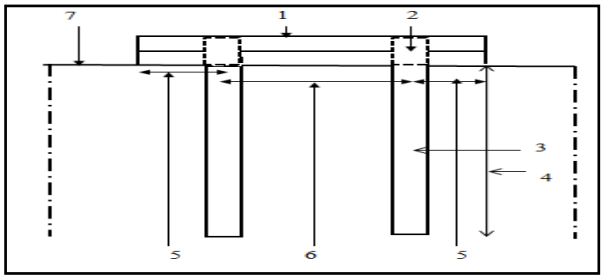

1. 8-10 cm thick concrete slab as the duck's web
2. 10 x 19 cm concrete block as the duck's toe
3. Ø 12-15 cm concrete mini pile as the duck's toenail
4. 0-100 cm-long mini pile as the duck's toenail
5. 0.5 x Space, as the duck's outer web
6. A space of 50-100 cm between each toe
7. Soft-soil surface.

Fig.4. A-A Cut of DFSF Test

Making DFSF models for Plaxis test, and for full-Scale loading tests in the field using the best DFSF structural model measurement results with Plaxis, as shown in Fig. 3, and Fig. 4. while the material used to make the DFSF test model is f'c quality concrete -15, and concrete steel used in U-24. One unit of test equipment (Load Frame) loading of the best full-size structure DFSF model as shown in Fig. 5.

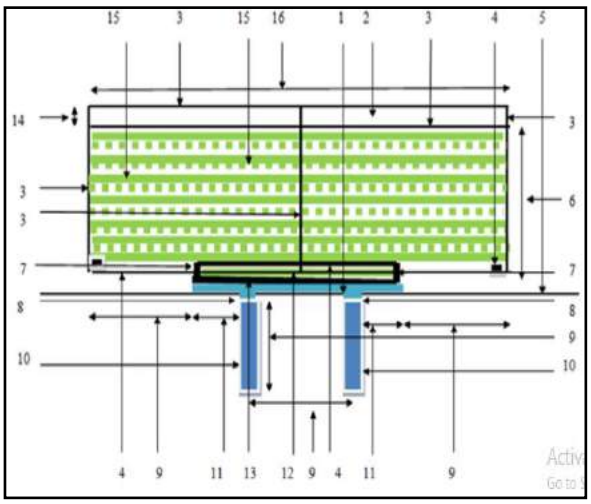

1. 9 cm thick PSTB Slab
2. Space provided for additional load /sand sack, if necessary
3. 6 x 6 cm wood block,
4. 6 x 12 cm wood block
5. Soft-soil surface
6. 130 cm
7. 6 x 12 wood column with 20 cm high
8. 10 x10 cm concrete block
9. 50 cm
10. 13 cm diameter mini pile
11. 25 cm
12. 13x10x100 cm concrete block, a weight of ± 25 kg/bt, 10 bt/layer, installed in parallel ways U->S for odd layer, T->B for even layer
13. 6x100x100 cm plank, above PSTB slab
14. 20 cm
15. 13x10x200 cm concrete block, a weight of ± 50 kg/bt, 20 bt/layer,installed in parallel ways U->S for odd layer, T->B for even layer
16. 16. 200 cm.

Fig. 5. Load Frame Side View Over The.

This study took place in Gemulak village, Sayung District, Demak Regency, Central Java, Indonesia. In order to obtain physical and mechanical properties of the soft soil to support DFSF, Sondering test, Boring test, and laboratory test using ASTM were done.

3 RESULT AND DISCUSSION

3.1 *Afield Research and Soil Testing in The Laboratory*

The field research is stripping and drilling, hatching results (CPT) as shown in Fig. 6, soil test results in the laboratory Table 1, and Plaxis data input Table 2 as follows:

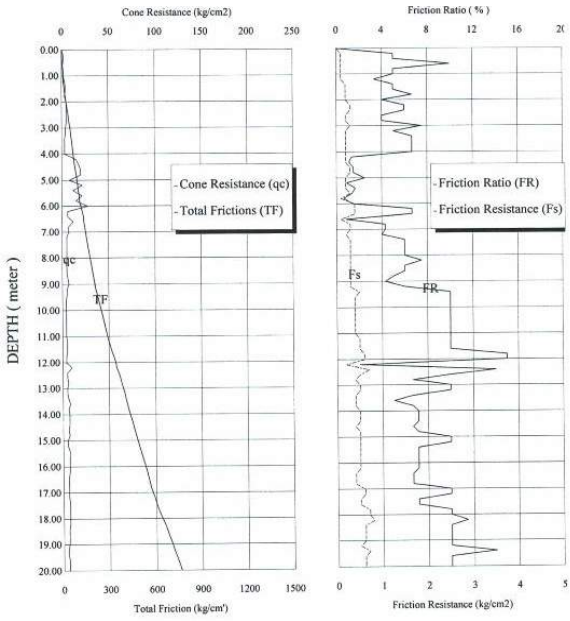

Fig.6. Dutch Cone Penetrometer Result Graph (CPT).

Table 1. The Results of Soil Tests in the Laboratory.

Parameter	Symbol	Unit	Value
Water content	w	%	67.67
Specific gravity of solid	Gs	-	26.14
Unit weight	γ_{sat}	kN/m^3	16.153
Dry unit weight	γ_{unsat}	kN/m^3	9.671
Porosity	n	%	2.992
Void ratio	e	%	1.712
Liquid limit	LL	%	66.58
Plastic limit	PL	%	32.15
Plastic index	PI	%	54.03
Permeability	k	cm/sec	$6xE^{-07}$
Cohesion	c	kN/m^2	10.25
Friction angle	ø	°	1

Table 2. Soft Soil Parameter for Plaxis (Soft Soil Creep Model).

Parameter	Symbol	Unit	Value
Water content	w	%	67.67
Specific gravity of solid	Gs	-	26.14
Unit weight	γ_{sat}	kN/m^3	16.153
Dry unit weight	γ_{unsat}	kN/m^3	9.671
Dilatancy angle	Ψ	[°]	0
Modified compression index	λ*	[-]	0.0713
Modified swelling index	K*	[-]	0.0087

Parameter	Symbol	Unit	Value
Modified creep index	μ	[-]	0.0036
Permeability	k	cm/sec	$6xE^{-07}$
Cohesion	c	kN/m^2	10.25
Friction angle	ø	°	1

3.2 *Analysis of DFSF Structure Dimension*

Analysis to obtain the best mini pile length for DFSF. This analysis was done on mini piles with 0 cm, 50 cm, and 100 cm length, the result showed that the mini pile with 50 cm length had the largest bearing capacity, as shown in Fig.7.

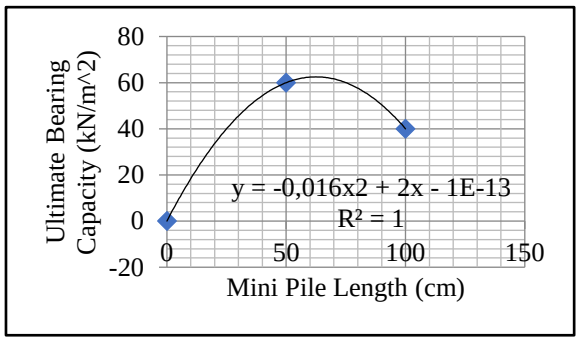

Fig.7. Graphic the effect of Length of Mini Pile vs Ultimate Bearing Capacity.

Analysis to obtain the best mini pile diameter for DFSF structure. This analysis was done on mini piles with 12 cm, 13 cm, and 15 cm diameter, the result showed that the mini pile with 13 cm diameter had the largest bearing capacity, as shown in Fig.8.

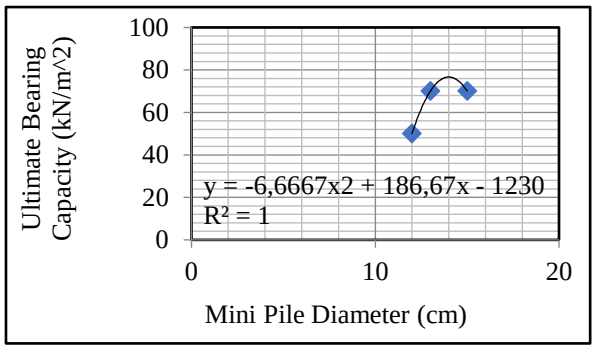

Fig. 8. Graphic the Effect of Diameter of Mini Pile vs Ultimate Bearing Capacity.

Analysis to obtain the best mini pile space for DFSF structure. This analysis was done on mini piles with 50 cm, 75 cm, and 100 cm space, the result showed that the mini pile with 50 cm length had the largest bearing capacity, as shown in Fig. 9.

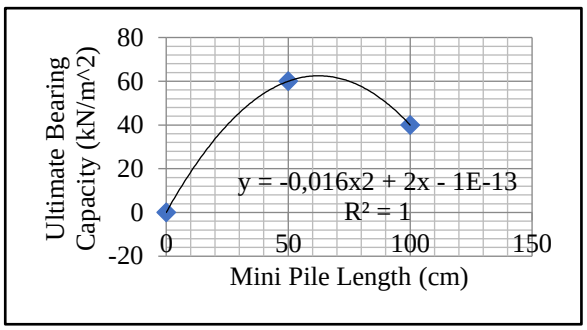

Fig. 9. Graphic the Effect of Mini Pile Space vs Ultimate Bearing Capacity.

Analysis for obtaining the best slab thickness for DFSF structure. The analysis was done on slabs with 8 cm, 9 cm, and 10 cm thick, the result showed that 9 cm thick- slab exhibited the largest bearing capacity, as shown in Fig.10.

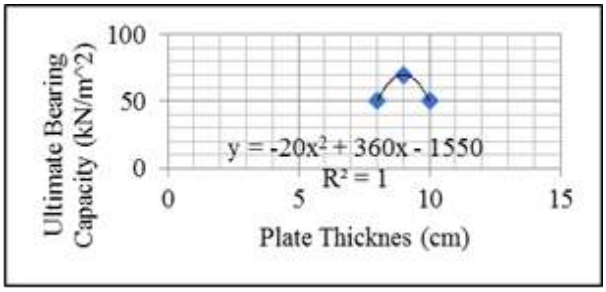

Fig.10. Graphic Effect of Slab Thickness vs Ultimate Bearing Capacity.

3.3 *Determining the Best DFSF Structure Dimension*

After the analysis and discussion on the DFSF structure dimension, the next step was to determine the best DFSF structure, as shown in Table 3 below

Table 3. The Best DFSF Structure Dimension.

Description	Unit	Value		
Mini pile length	cm	0	50	100
Ultimate bearing capacity	kN/m^2	0	60	40
Mini pile diameter	cm	12	13	15
Ultimate bearing capacity	kN/m^2	50	70	70
Mini pile space	cm	50	75	100
Ultimate bearing capacity	kN/m^2	50	40	22.5
Slab thickness	cm	8	9	10
Ultimate bearing capacity	kN/m^2	50	70	50

DFSF structure dimension in **bold** represents the best DFSF structure dimension

3.4 *Testing The Best DFSF Structure Model Using Plaxis*

Before conducting loading test on the full-scale DFSF a test using Plaxis was conducted. The result is shown in Fig.11 and Fig. 14.

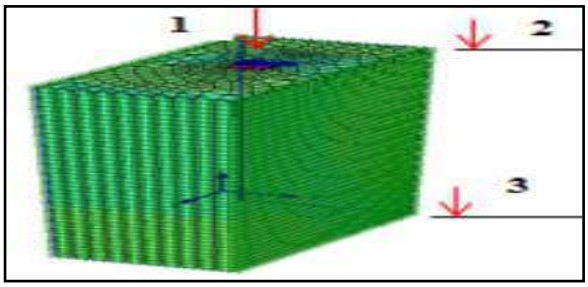

1. FDFS 1m x 1m
2. Depth ± 0,00 m
3. Depth -20m

Fig.11. Vertical Displacement of DFSF on Soft Soil.

3.5 *Loading Test of The Full-Scale DFSF*

This test aimed to calibrate the test result with numerical method (Plaxis), Fig.12, Fig.13, and Fig. 14 as well as table 4 below show the test and the result.

Fig.12. FDFS Model Top View Dimension 1m x1m on Soft Soil.

1.LVDV, total load 120 kN

Fig.13. Implementation of Loading Test of DFSF on Soft Soil.

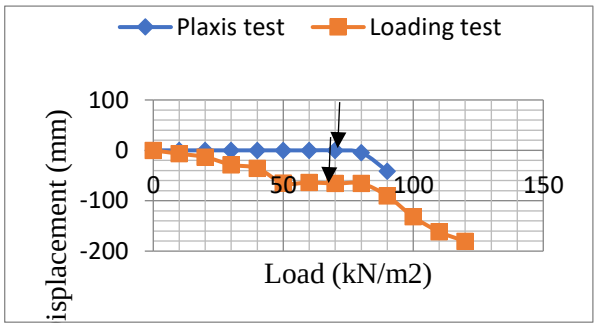

Qult=70 kN/m^2

Fig.14.Load Graph VS Displacement in Loading Test Results in the Best Full -Scale FSF Structure Model on Soft Soil.

Table 4. Plaxis Test Result vs Loading Test Result.

Description	Unit	Value	
Minipile			
Length	(cm)	50	
Diameter	(cm)	13	
Space	(cm)	50	
Slab thickness	(cm)	9	
Test Type		Plaxis	Loading Test
$Q_{ultimate}$ bearing capacity	(kN/m^2)	70	70
$Q_{planned}$ bearing capacity	(kN/m^2)	50	50
Safety factor		1.4	1.4

$Q_{planned}$; $Q_{ultimate}$ of DFSF agreed in Dissertation proposal, and SF = $Q_{ultimate}$ divided by $Q_{planned}$

From Table 4. show the results of the PSTB test with the finite element (Plaxis) method of known bearing capacity= 70 kN with Safety Factor = 1.4, and the results of the PSTB loading test are known to be bearing capacity = 70 kN with Safety Factor = 1.4, from this analysis, the test results are with the finite method element (Plaxis) calibrated with the results of the loading test is the same (valid), namely Qultimate = 70 kN, with Safety Factor = 1,4> 1 (Safe), this means that the PSTB uses the best structure size can be proposed for the foundation of residential buildings, irrigation channels, drainage channels, embankments and others to be built on soft soil.

4 CONCLUSION

Based on the laboratory test and finite element model and loading test a full-scale model, this study manages to model and reveal the load transfer mechanism of DFSF. This study concludes that:

Based on the laboratory test and finite element model and loading test a full-scale model, this study manages to model and reveal the load transfer mechanism of DFSF. This study concludes that:

1. The best structure dimension of DFSF is as follow:
2. Mini pile length of 50 cm, diameter of 13 cm, space of 50 cm, and slab thickness of 9 cm.
3. PSTB that uses the best full-scale structure size has an ultimate bearing capacity of 70 kN, and SF =1.4 then the PSTB of the best structure size can be used for residential buildings, irrigation canals, drainage channels, embankments, etc. to be built on soft soil.

REFERENCES

Subianto T., Harry P. 2002. The Modelling of Shallow Foundation using Three Layers of Geotextile on Soft Soil. *Dimensi Teknik Sipil* Vol. 4. No. 1. Petra Christian University. Surabaya.

Soeteddi, D.,Suherman, M., Prabudi, S. 2005. *The Stabilization of Shallow Soft Soil for Road Pile with Cement and Pile.*

Basu, P., Basu, B., P., Prezzi, M. 2006. Analytical Solutions for Consolidation Aided by Vertical Drains. *Geomechanics and Geoengineering: An International Journal* Vol. 1. No. 1: 63-71. USA.

Suroso, Munawir, A., Indrawahyuni, H. 2008. *The Effect of Using Cerucuk and Bamboo Matting on The Carrying Capacity of Soft Clay Soil*. Accessed on 21 April 2014 at http://rekayasasipil.ub.ac.id/ index .php / rs /article o. 1, April 2011. ITB. Bandung. Indonesia.

Irsyam, M., Krisnanto, S. 2008. *Full CPFS Testing and Analysis of Bamboo Mattress Pile Strength for Road Body Stack on Soft Soil at Tambak Oso Surabaya*. Accessed on Maret 2013. http://puslit2.petra.

Hardiyatmo, H. C. 2008. The Nailed Slab System for Concrete Slab Reinforcement on Rigid Pavement. *Proceedings of The National Seminar on Appropriate Technology in Handling Infrastructure*. MPSP JTSL FT. UGM. Pp. M-1-M-7.

Martini. 2009. Soil Bearing Capacity Analysis on Shallow Foundation. *Mektek* Vol. XI (2): 75-87. Department of Civil Engineering, Faculty of Engineering. Tadulako University. Palu-Indonesia.

Djajaputra, A.,Sofwan, A.,Rahardian, H.,Pane, I.,Taufik, R., Rukmono, A. 2009. *The Application of Spiderweb Construction Technology on Runway, Taxiway, and Container Yard*. Research Grant-Incentive Program Capacity Building for Science and Technology Production System.

Sutikno & Yatmadi, D. 2010. A Study on Expansive Soil Stabilization with Sand Addition for Subgrade of Road Construction. *Poli Teknologi* Vol. 9 (1). Department of Civil Engineering. Jakarta State Polytechnic.

Soewignjo, & Nugroho, A. 2011. The Study on Soil Bearing Capacity of Shallow Foundation on Peat Soil with Combination of Geotextile and Bamboo Grid. *Jurnal Teknik Sipil* Vol. 18 (N).

Sari, E. N. N. 2012. *Facts on Peat Soil*. Accessed on 26 Maret 2014,. http://peatland.

Bell, A. and Robinson, C. 2012. Single Pile in Burland. J., Chapman, T., Skiner, H. and Brown, M. ICE Manual of Geotechnical Engineering. *Vol II. Geotechnical Design, Construction and Verification. ICE Publishing*. London E14 9TP - UK.

Ratna, D., Sutejo, Yulindasari, Hanafiah. 2013. Increasing Soil Supporting Capacity with Strengthening Plaits and Bamboo Grids. *Proceedings of The 17th Annual Scientific Meeting. Geotechnical Solutions in Indonesia to Respond to The Challenges Of Urban, Industry, Infrastructure and Mining Development*. Borobudur Hotel. Jakarta – Indonesia.

Setiawan, B., Hardiyatmo, HC, Suhendro, B. 2013. Full-Scale Individual Test on Modification of Duck Foot System in Expansive Soil in the Field. *Proceedings PIT HATI XII*. Jakarta-Indonesia.

Djaranto, H. 2015. *The Mechanism of Load Transfer on Foundation Using Spiderweb Construction by Full – Scale Vertical Static Load Test and 3D Numerical Analysis*. Unpublished Dissertation. Civil Engineering Doctoral Program. Faculty of Engineering. Diponegoro University. Semarang.

Puri,A.,Hardiyatmo,H.C.,Suhendro,B.,Rifa'i,A. 2015. The Behavior of Nailed Slab Pavement System on Silty Soil. *Proceedings of the 2015 CPFS Bachelor of Civil Engineering*. (KNPTS) National Conference. ITB. Bandungc- Indonesia.

Ardiansyah, R. 2016. Duck Feet System Foundation. *Science and Civil Structure Media*. Diakses 26 September 2016. Chicken-Paw-Foundation-Needs- to Be Considered Program. Faculty of Engineering. Diponegoro University. Semarang – Indonesia.

Buisman, K. 1936. Results of Long Duration Settlement Tests. *Proceeding's 1st International Conference on Soil Mechanics and Foundation Engineering. Cambridge*. Mass. Vol. 1: 103-107.

Three-Dimensional Effects of Deep Excavation in Soft Soils

Ferawati Hariyanto
Mott MacDonald Singapore Pte Ltd
Keng Hwa Lee
Mott MacDonald Singapore Pte Ltd
Arlingga Putra
PT Mott Macdonald Indonesia
Irawan Tani
PT Mott Macdonald Indonesia

ABSTRAK: Sebuah *shaft* dibangun untuk pembangunan infrastruktur bawah tanah masa akan datang dengan metode top-down. Dalam pembangunan tersebut, pekerjaan galian dalam dianalisa dengan metode elemen hingga. Dalam makalah ini, aspek-aspek yang berkenaan dengan desain dari penggalian dalam ini dipaparkan. Masalah-masalah yang berkaitan dengan defleksi dinding dan penurunan tanah didiskusikan. Aplikasi efek sudut digambarkan untuk mencegah overestimasi hasil analisa elemen hingga 2D. Studi sensitivitas juga dilakukan untuk membandingkan hasil analisa elemen hingga 2D dan 3D untuk menjustifikasi prinsip penurunan tanah.

Kata Kunci: galian dalam, launch shaft, struktur bawah tanah, defleksi dinding, penurunan tanah, efek sudut, studi sensitivitas

ABSTRACT: A shaft is constructed for a future underground infrastructure development using top-down construction methodology. For this development, design of its deep excavation works is carried out using finite element analysis. In this paper, aspects related to the design of this deep excavation are presented. Issues related to wall deflection and ground movement are discussed. Application of corner effect is described with an objective to avoid overestimation from the 2D finite element analysis. Sensitivity study has also been carried out to compare the results from the 2D and 3D finite element in 2D and 3D analysis and to justify the approach in deriving the ground movement.

Keywords: deep excavation, shaft, underground structure, wall deflection, ground movement, corner effect, sensitivity study

1 INTRODUCTION

A launch shaft is to be constructed to facilitate construction of an underground facility. Wall deflection and ground movement due to excavation impact is inevitable and impractical to be ignored. Impact assessment is caried out based on the predicted retaining wall deflection and vertical ground movement, ground settlement.

This shaft is constructed in a rectangular shape. Conventionally, a two-dimension (2D) plane strain finite element modelling (FEM) would be adopted in most of the excavation analyses. The wall deflections and ground settlements from 2D analysis are often overestimated due to the ignorance of three-dimension (3D) corner effect and the stiffness restrain effect of the wall and the slab which is constructed as excavation progresses.

The objective of this paper is to demonstrate that 3D FEM can obtain a more realistic wall and ground deformation for a rectangular shaft excavation works in soft soil.

This paper presents sensitivity study that has been carried out related with wall deflection and ground movement in the design phase. The study does not present wall forces comparison (bending moments and shear forces).

2 THE BACKGROUND

2.1 *Project Description*

This project is located in Jakarta, capital city of Indonesia. The proposed launch shaft will be part of a future underground facility. The proposed underground structure footprint is at the middle of the road and near to the existing buildings. The nearest adjacent building is approximately 17m away from the edge of excavation. Most of the nearby existing buildings are high rise buildings with more than 20m in height, notably can be assumed supported by pile foundation. The layout of the proposed shaft and nearby buildings shown in Fig. 1. A cut-and-cover tunnel structure is to be built after the completion of launch shaft construction.

This paper presents the study the wall and ground movement due to the excavation of the launch shaft and its impacts to the adjacent buildings. Top-down construction method is adopted with 0.8m thick diaphragm wall as earth retaining structures (ERS) and kingpost acting as temporary column to support roof slab and concourse slab during construction.

The excavation depth is 19.52m and diaphragm wall toe level is terminated at 10m below the final excavation level (FEL). Three-meter thickness of Jet Grout Pile (JGP) ground improvement is provided below FEL to increase excavation performance.

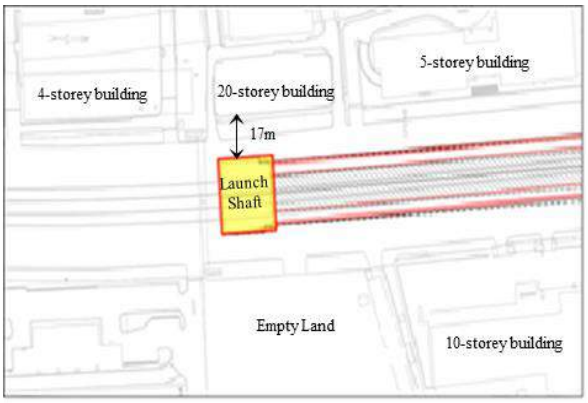

Fig. 1. The Proposed Launch Shaft Layout.

2.2 *Geological Conditions*

The ground condition at this area is dominated by very soft to hard silty clay layer with some organic content mixed. The geological profile consists of fill sandy materials, underlain by very soft silty clay, followed by soft to firm silty clay, medium stiff to very stiff clay and very stiff to hard silty clay. The proposed launch shaft geological profile is shown in Fig. 2.

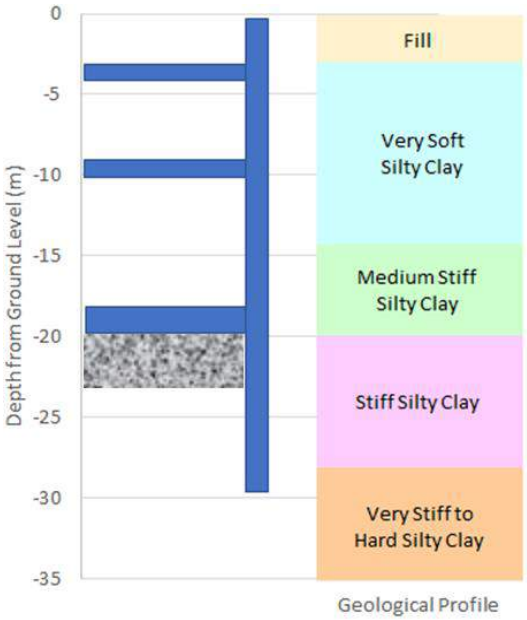

Fig. 2. Geological Profile Section.

2.3 *Geotechnical Design Parameters*

The moderately conservative soil parameters used in the design refer to geotechnical interpretation report for this project. This report provides critical appraisal of the ground and groundwater conditions beneath the site based on factual geotechnical data and establishes general recommendations for soil parameters and the ground model, hardening soil model is adopted in the design. The extracted soil parameters are tabulated in Table 1.

3 2D AND 3D FEM ANALYSIS

Ou et al (1996) and Wu CH. et al (2010) observed wall deflection behavior of a rectangular shaft excavation using 3D FEM. From this study, plane strain ratio (PSR) can be obtained from the relation between site aspect ratio of the excavation and the distance to the corner as shown in Fig.3.

Table 1. Soil Parameters.

Soil Type	γ kN/m^3	Su kPa	c' kPa	ϕ' degree	E_{50} MPa	E_{oed} MPa	E_{ur} MPa	m	k_0	kx m/s	ky m/s
Fill	16.0	-	1	35	15	-	-	-	0.43	2.0E-05	2.0E-05
Very soft silty clay	15.0	25	8	29	3	1	15	1.00	0.72	7.0E-08	2.3E-08
Medium stiff silty clay	16.0	42	16	26	8.3	3.8	29.8	0.70	0.82	7.0E-08	2.3E-08
Stiff silty clay	16.5	85	18	26	34	20.4	102	0.50	0.79	2.0E-07	6.7E-08
Very stiff to hard silty clay	16.5	150	27	29	60	36	180	0.50	0.59	2.0E-07	6.7E-08

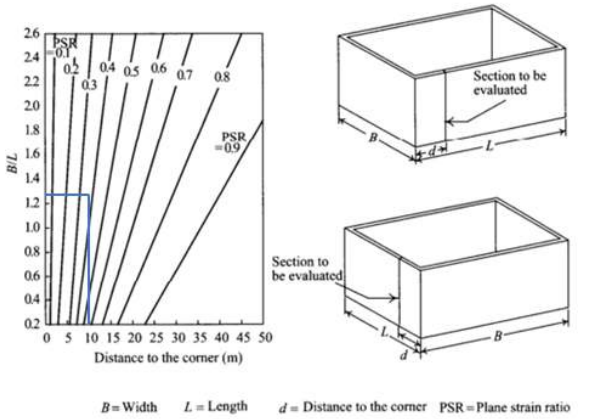

Fig. 3. Relation between PSR, Site Aspect Ratio (B/L) and Distance to Corner, Ou et al. (1996).

The proposed launch shaft dimension is 25.2m width and 20m long. The finite element software, Plaxis 2D, is used to analyze a section located 10m from the corner. Refer to chart in Fig.3, PSR value obtained is 0.35. The reduction of wall deflection is applied by using PSR factor of 0.35. The cross section view from 2D modeling is shown in Fig. 4.

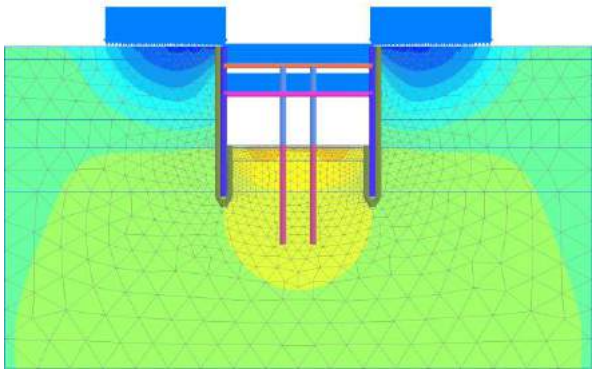

Fig. 4. Cross Section View in 2D Modelling.

To demonstrate a more realistic result, further study was carried out by using Plaxis 3D software. There are two 3D geometry models are presented in this paper, 3D plane strain model and rectangular shaft model. The section view of 3D plane strain model is shown in Fig. 5. There are 3 sections are indicated in this model, section A is located at the middle of the wall, section B is located at 10m distance from the corner and section C is located at 80m distance from the corner.

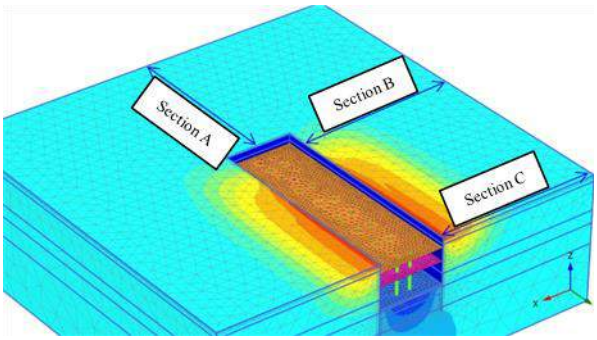

Fig. 5. 3D Plane Strain Model Section View.

The section view of 3D rectangular shaft model is shown in Fig.6. This model indicated the actual dimension of the proposed launch shaft, section A and B is located at the middle of the wall.

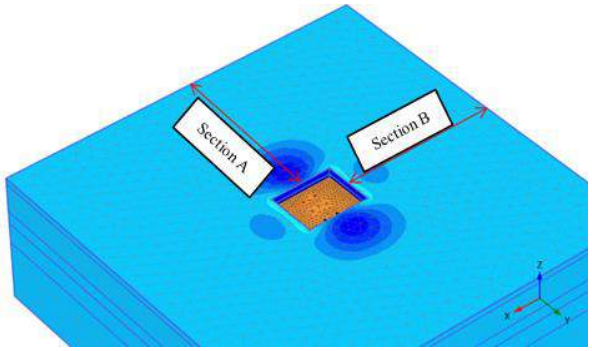

Fig. 6. 3D Rectangular Shaft Model Section View.

3.1 *Case 1: 2D and 3D Plane Strain*

The proposed launch shaft is modelled as infinite long section in 3D to demonstrate the plane strain behavior. The result of 3D plane strain model section C is compared with 2D result in term of wall deflection and ground settlement at excavation to FEL stage. The comparison of wall deflection and ground settlement results are shown in Fig. 7 and Fig. 8 respectively.

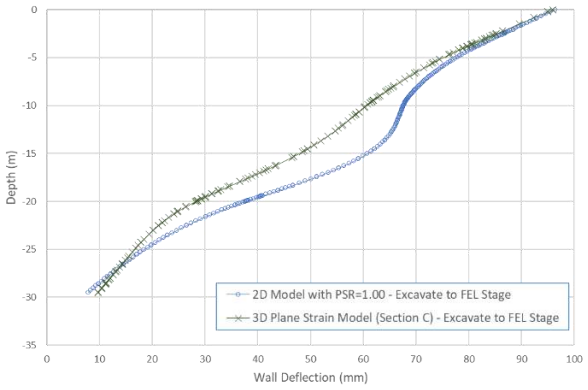

Fig. 7. 2D and 3D Plane Strain (Section C) Wall Deflection Comparison.

Refer to Fig. 7, the maximum wall deflection obtained from 2D model has the same value with 3D plane strain section C result, 96mm. The wall deflection behavior from these two models indicated similar deformation shape. PSR value of 1 is obtained from case 1 study.

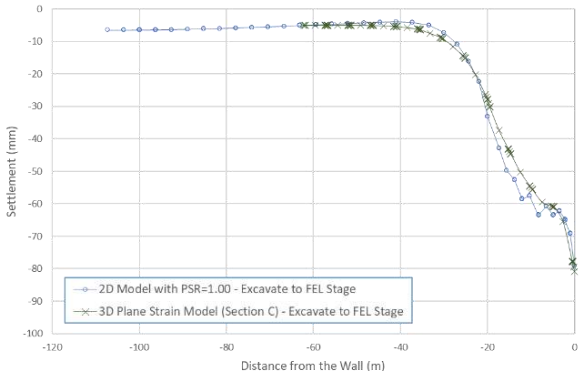

Fig. 8. 2D and 3D Plane Strain (Section C) Ground Settlement Comparison.

Refer to Fig. 8, the maximum ground settlement obtained from 2D model is 79mm, similar with 3D plane strain section C result, 81mm. The ground settlement behavior has similar deformation shape as well.

3.2 *Case 2: 3D Plane Strain and 3D Rectangular Shaft*

An actual dimension of rectangular launch shaft is modeled in 3D to demonstrate the actual behavior of the wall due to the impact of excavation works in soft soil. The result from 3D rectangular shaft model is compared with the result from the 3D plane strain model. The comparison result of wall deflection and ground settlement for section A is shown in Fig.9 and Fig. 10, section B comparison result is shown in Fig.11 and Fig. 12 respectively.

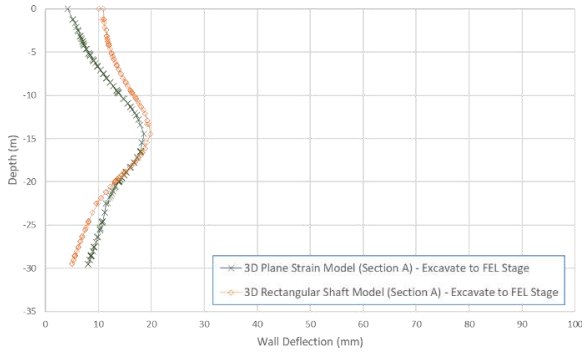

Fig. 9. 3D Rectangular Shaft and 3D Plane Strain (Section A) Wall Deflection Comparison.

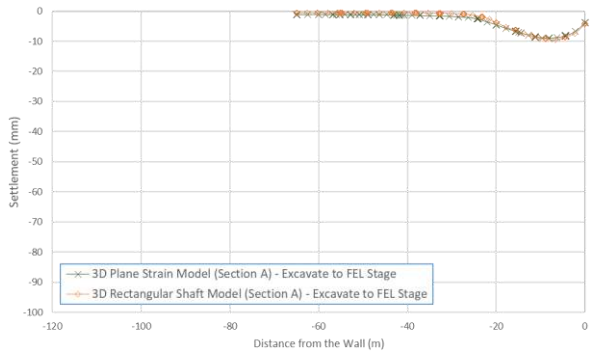

Fig. 10. 3D Rectangular Shaft and 3D Plane Strain (Section A) Ground Settlement Comparison.

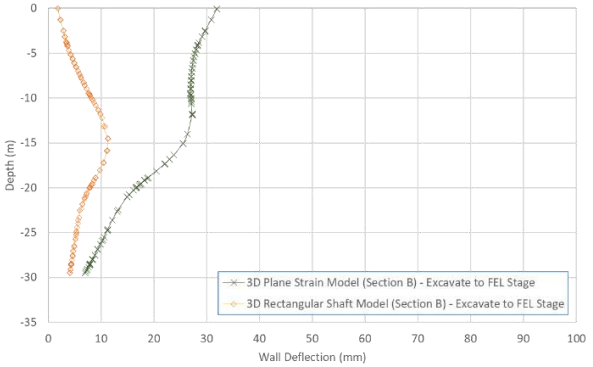

Fig.11. 3D Rectangular Shaft and 3D Plane Strain (Section B) Wall Deflection Comparison.

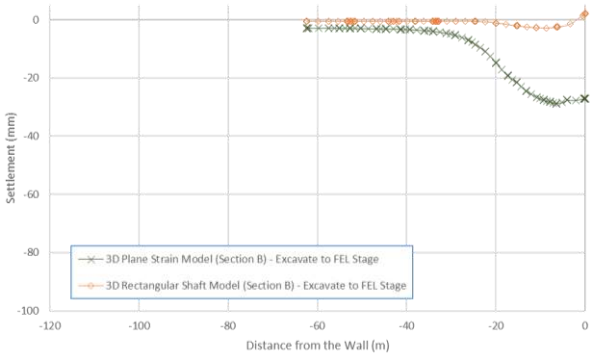

Fig.12. 3D Rectangular Shaft and 3D Plane Strain (Section B) Ground Settlement Comparison.

Refer to Fig. 9 and Fig. 10, the wall deflection and ground settlement behaviour from two models indicated similar maximum value and deformation shape. It proves that there is no plane strain effect in section A and corner effect considered in the analysis. The maximum wall deflection of section B is 32mm for 3D plane strain model and 11.3mm for 3D rectangular shaft model shown in Fig. 11. There are big difference in term of magnitude and deformation shape that proves two sides corner effect, reflect actual condition of the shaft, considered in 3D rectangular shaft model. PSR ratio of 0.35 is obtained from comparison 3D rectangular shaft model with two sides corner effect and 3D plane strain with one side corner effect. Similarly for ground settlement of section B, the big difference of maximum ground settlement shown in Fig. 12.

Large wall deflection and ground settlement were observed from 2D model. A further sensitivity study is carried out to demonstrate the relation between PSR and 2D result behavior. PSR factor of 0.35 is applied into 2D wall deflection, reflected in Fig,13 and Fig. 14. The result is compared with 3D plane strain section B.

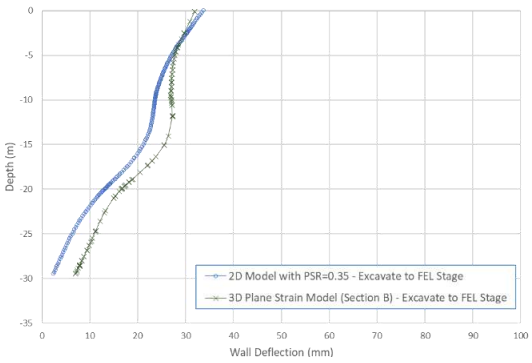

Fig.13. 2D with PSR and 3D Plane Strain (Section B) Wall Deflection Comparison.

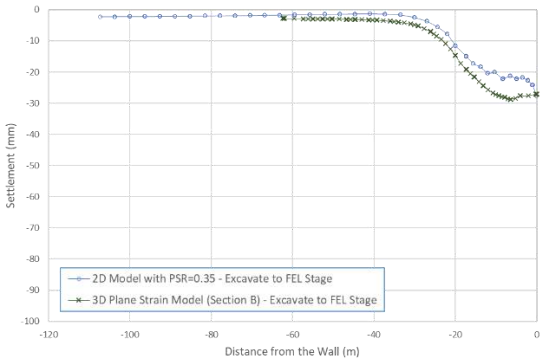

Fig. 14. 2D with PSR and 3D Plane Strain (Section B) Ground Settlement Comparison.

The result indicated the wall deflection and ground settlement have similar value and behaviour.

The wall deflection limit, 0.5% of excavation depth, is applied for this project. Although 2D wall deflection result still within the allowable limit, ERS system for rectangular shaft excavation should expect a smaller wall deflection value that proves from 3D rectangular shaft result. This is reflected the result from 2D is overestimate the wall deflection and ground settlement. The deformation shape in 2D model is unable to present the actual behavior of rectangular shaft excavation. PSR factor obtained from this study is summarized in Table 2.

Table 2. Maximum Wall Deflection and PSR Summary.

Wall Deflection (mm)				Plane Strain Ratio (PSR) in Comparison with 2D			
2D	3D PS Sect. B	3D PS Sect. C	3D RS Sect. B	3D PS Sect. B	3D PS Sect. C	3D RS Sect. B	Ou et al (1996)
96	32	96	11.3	0.33	1	0.12	0.35

Note: PS (Plane Strain) and RS (Rectangular Shaft)

The excavation modelled in 2D and 3D plane strain section C produced the same result in term of maximum wall deflection value and deformation behaviour. It proves there is no corner effect if the section is located far away, 80m distance in this study, from corner. When the section is located nearer to corner, 3D plane strain section B, maximum wall deflection has similar value to 2D model with PSR of 0.33 applied. It proves that the smaller distance to corner will reduce the maximum wall deflection value. 2D model is unable to capture this condition unless PSR value applied as reduction

factor to the wall deflection result. However, this simplification is unable to obtain the actual deformation shape. Further, this study concluded that PSR value obtained has similar value with PSR chart shown in Fig. 3. The result is aligned with the reference from Ou et al. (1996).

PSR value obtained is 0.12 in 3D rectangular shaft model that represent actual dimension of the shaft. This value is lesser than 0.35, PSR value from Ou et al. (1996) in Fig.3. The result is off because the presence of corner effect from two direction or both sides.

4 EMPIRICAL STUDY AND FEM ANALYSIS

There are many past studies have been proven FEM analysis can give better prediction for wall deflection than ground settlement when using Mohr-Coulomb model. Clough and O'Rourke (1990), Hsieh and Ou (1998) presented a moderately good prediction for ground settlement at the final excavation stage. The excavation works induced ground settlement that is usually correlated to the horizontal wall deflection. Refer to empirical data from past study, the maximum ground settlement caused by excavation is equal to the maximum wall deflection predicted from FEM analysis. This is reasonably conservative to use 1:1 correlation between maximum wall deflection and maximum ground settlement.

In this study, 2D and 3D FEM models with hardening soil were carried out to analyze the ground settlement. The results are compared with empirical method from Hsieh and Ou. The ground settlement comparison result reflected in Fig. 15 and Fig. 16.

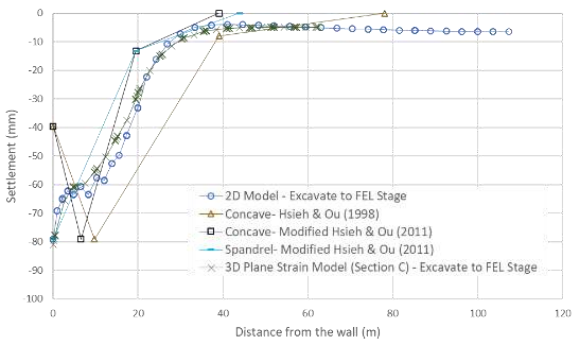

Fig. 15. 2D, 3D Plane Strain (Section C) and Empirical Methods Ground Settlement Comparison.

Refer to Fig.15, the ground settlement result from 2D and 3D plane strain section C models are directly extracted from FEM. Both models indicated that there is no 0mm ground settlement after 60m distance from the wall. It is not practical if launch shaft excavation works cause infinite zone of influence. These results are then compared with empirical data from Hsieh and Ou (1998) and modified Hsieh and Ou (2011). The ground settlement value from FEM models is aligned with empirical data at primary influence zone, two times of excavation depth. The ground settlement profile from FEM models is reflected by spandrel shapes that is aligned with modified Hsieh and Ou (2011). However, the ground settlement result from FEM models is off at secondary influence zone (distance after two times of excavation depth) in comparison with empirical method.

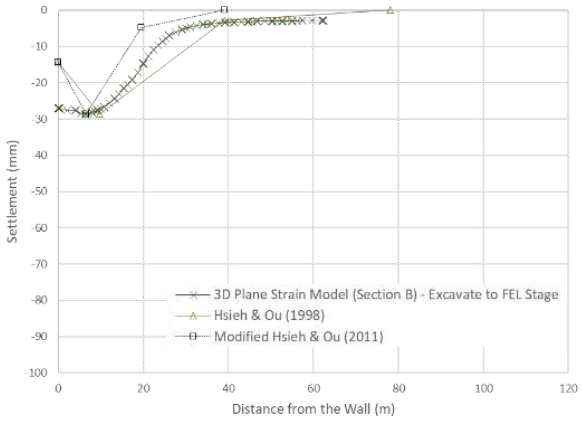

Fig. 16. 3D Rectangular Shaft (Section A) and Empirical Methods Ground Settlement Comparison.

In 3D rectangular shaft model, the ground settlement value is lesser than plane strain models, but the profile or behaviour is similar. It proves that not only wall deflection but also ground settlement value is subjected to the presence of corner effect. The result then compared with empirical method as shown in Fig. 16. Similar with Fig.15, FEM results at the primary influence zone is aligned with empirical method but it is off at secondary influence zone.

5 CONCLUSION

The prediction of wall deflections due to proposed launch shaft excavation works are captured from 2D model analysis. Sensitivity study has been carried out, 2D result produced higher wall deflection in comparison with 3D models. PSR value can be applied to reduce

wall deflection from 2D model. However, the wall deflection behavior is different because 2D model unable to capture corner effect.

The impact of ground settlement due to excavation works are significant to determine zone of influence to assess the existing buildings nearby. The ground settlement result extracted from FEM models are not practical to adopt at secondary influence zone. However, FEM results at primary influence zone are aligned with empirical data in term of value and behavior. Therefore, empirical method with wall deflection correlation is often used to plot ground settlement profile. With this correlation, PSR value can be applied to determine ground settlement profile of the proposed launch shaft excavation from 2D model.

ACKNOWLEDGEMENTS

The authors acknowledge contribution from the geotechnical team members of this project (Agus Samingan, Yudha Adi, Victoria Prijadi and Andreas Putra).

REFERENCES

Clough, G.W. & O'Rourke, T.D. 1990. Construction-Induced Movements of In Situ Walls. In: Proceedings of The Design and Performance of Earth Retaining Structures. *ASCE Special Conference*: 439–70. Ithaca, New York.

Hsieh, P.G. & Ou, C.Y. 1998. Shape Of Ground Surface Settlement Profiles Caused by Excavation. *Can Geotech J* 35(6): 1004–17.

Hsieh, P.G. & Ou, C.Y. 2011. A Simplified Method for Predicting Ground Settlement Profiles Induced by Excavation in Soft Clay. *Computers and Geotechnics* 38(8): 987–997.

Ou, C.Y., Chiou, D.C. & Wu, T.S. 1996. Three-Dimensional Finite Element Analysis of Deep Excavations. *Journal of Geotechnical Engineering ASCE* Vol. 122 (5): 337-345.

Wu, C.H., Ou, C.Y. & Tung N. 2010. Corner Effects in Deep Excavations-Establishment of A Forecast Model for Taipei Basin T2 Zone. *Journal of Marine Science and Technology* 18(1).

Seismic Finite Element Response of Soil-Pile Kinematic Interaction Behavior on Interface of Soft and Medium Clay Soil

Dedi Apriadi
Civil Engineering Department – Institute Teknologi Bandung

Zaitun Andarwan
Civil Engineering Department, Former Master Student – Institute Teknologi Bandung

Suched Likitlersuang
Civil Engineering Department – Chulalongkorn University of Thailand

Thirapong Pipatpongsa
Department of Managemnet – Kyoto University

ABSTRACT: Foundation design so far only considers the effect of inertia and ignores the kinematic effect. Even though the maximum response that occurs on the foundation can be caused by the inertia interaction or kinematic interaction. In this study, evaluation of pile kinematic response due to seismic load was carried out by three-dimensional (3D) finite element method using ABAQUS software. Validation of modeling techniques is done by comparing the results of soil responses and pile foundations responses from the centrifugal test. This parametric study was carried out using 30 m of Bandung clay consisting of two layers. The upper layer is soft clay and the lower layer is medium clay. The soil constitutive model used is nonlinear Extended Cam Clay. Evaluation of the moment and shear force responses that occur on the interfaces of the two soil layers are reviewed based on the effect of increasing Peak Ground Acceleration (PGA), the ratio of embedded pile length (Ld) to pile diameter (D), the ratio of soft soil thickness (La) to the embedded pile length (Ld), earthquake predominant period and pile group effect. The representation of the upper structure is modeled as axial and lateral loads acting on pile cap according to the static allowable capacity of a single pile. Based on the results of the analysis, the maximum moment and the shear force of the pile occur around the interface of the two soil layers. The increase in the maximum moment and shear values is proportional to the increase in the Magnitude of PGA, inversely proportional to the increase in the Ld/D ratio, proportional to the increase in the La/Ld ratio, proportional to the approaching natural soil period and the earthquake predominant period and inversely proportional to the increase in the number of pile groups.

Keywords: soil-pile interaction, finite element method, soil interface

CMC Application and Performance Under High Rise Building with Combined Raft Footing System Case Study: Pelleting Structure with 140 M Height

Yudhistira Rian Nugraha
Program Magister, Faculty of Civil and Environmental Engineering – Institute Technology Bandung

K.M. Abuhuroyroh
Geotechnic Research Group, Faculty of Civil and Environmental Engineering – Institute Technology Bandung

Masyhur Irsyam
Professor, Faculty of Civil and Environmental Engineering – Institute Technology Bandung

ABSTRACT: In the case of high building foundations on soft soil, drill pile foundations are often chosen as the solution. But on the other hand, this drill foundation solution also requires a lot of material consumption in the form of concrete or reinforcing steel. Along with the development of soil improvement technology, there are considerations for using Controlled Modulus Column (CMC) is one option among several existing solutions. CMC can be a more efficient solution than drill piles because the penetration depth is relatively shallower so as to reduce consumption of concrete and reinforcing steel. However, this combined raft foundation system (footing overlying on reinforced soil) still needs a more comprehensive study, especially in terms of its ability to carry dominant seismic load. The interaction between the soil surrounding and the column itself should be ensured to remain in a single rigid body condition, so that when subjected to seismic waves both column and soil move together without any resistance in both elements. The 140 m tall industrial building which was designed as a silo for processing plastic raw materials in Cilegon uses a combined raft system with CMC, and so far, it has been recorded and still achieving required settlement based on instrumentation in the field. The raft foundation system with CMC is designed based on an analytical method that refers to ASIRI National Project, 2012 design framework. The difference between displacement of the column and the soil surrounding is set to be less than 0.01. Column and soil interactions are separated into inertial and kinematic effects. Lateral displacement due to inertial effects is the magnitude of the reaction on footing due to seismic vibrations on superstructure which one value of the highest load combination reaction. Meanwhile, the lateral displacement of the kinematic effect is obtained through numerical iteration of one-dimensional wave propagation equation for first eigenmode solution (resonant conditions) which is viewed as a free field motion model, because the column and the soil are considered as one system. Then, the results of the lateral displacement of the inertial and kinematic effects are summed and used as the basis for calculating response to the column in the form of bending moments, shears, and reaction curves obtained based on the derivation of beam on elastic support theory. ASIRI MV2 model is used for vertical load analysis which includes aspects of deformation, and determination of load proportionality. Meanwhile, the ASIRI MH2 model is used to calculate lateral deformation and the response in the column as described previously. Comparative analysis shows that CMC elements need additional reinforcing steel to anticipate bending load because the eccentricity requirement that must be less than Dc/8 has not been met. In addition, further review is needed regarding the movement of soil on the surface due to wave propagation (dg), where the calculation results of Eurocode 8 recommendation are different from SNI 1726:2019, this is presumably due to differences in earthquake mechanism in the European and Indonesian regions.

Keywords: footing, CMC, rigid body, free-field motion, beam on elastic support.

Perencanaan dan Pelaksanan Konstruksi Geoteknik di Mandalika International Street Circuit Lombok

Hari Nugraha Nurjaman
Persada Indonesia University

Dwianto Winaryo
Indonesian Tourism Development Corporation

ABSTRAK: Mandalika International Street Circuit adalah konstruksi yang digunakan untuk balap motor internasional dan jalan raya biasa. Pembangunan konstruksi sirkuit dimulai 15 Juli 2020, perkerasan lintas utama selesai 15 Agustus 2021, dan seluruh konstruksi pada 30 September 2021. Balapan pertama World Superbike rencana dilakukan pada bulan November 2021 dan balapan pertama MotoGP pada bulan April 2022. Konstruksi dengan fungsi ganda ini mempunyai spesifikasi teknis yang lebih tinggi dari jalan raya biasa, sehingga membutuhkan dukungan konstruksi geoteknik yang baik. Sirkuit sepanjang 4,301 km ini terletak di area pantai Mandalika Lombok, yang mempunyai variasi kondisi geoteknik sepanjang sirkuit, seperti tanah pasir lepas dengan potensi likuifaksi, tanah lempung lunak dengan potensi penurunan yang besar, dan struktur geologi lokal. Makalah menyampaikan usaha untuk menghasilkan konstruksi geoteknik yang dapat mendukung pemenuhan spesifikasi teknis sirkuit, mulai dari proses penyelidikan geoteknik, perencanaan konstruksi geoteknik yang efisien, pelaksanaan konstruksi dan kontrol kualitas yang dilakukan untuk memastikan konstruksi sesuai spesifikasi.

Kata Kunci: street circuit, likuifaksi, struktur geologi

ABSTRACT: The Mandalika International Street Circuit is a construction used both for international motorcycle racing and regular highways. Construction of the circuit began on July 15,2020, maintrack pavement finished August 15,2021, and all construction at September 30,2021. This dual-function construction has a higher technical specification than ordinary road, so it requires good geotechnical construction support. This 4.3 km circuit is located in the coastal area of Mandalika Lombok, which has a variety of geotechnical conditions along the circuit, such as loose sand with liquefaction potential, soft clay with large settlement potential, and local geological structures. The paper explains effort to produce geotechnical construction that fulfill circuit technical specification, starting for geotechnical investigation process, designing efficient geotechnical construction, construction and quality control that carried out to ensure the construction meets to all specification.

Keywords: street circuit, liquifaction, geological structure

1 PENDAHULUAN

Sirkut Mandalika direncanakan untuk fungsi sirkuit dengan Grade A untuk melaksanakan pagelaran event MotoGP. Lintasan sirkuit direncanakan oleh MRK1 Consulting dengan panjang 4,301 km dengan jumlah tikungan 11 ke kanan dan 6 tikungan ke kiri, dan ada dua terowongan dibawah Sirkuit. Salah satu spesifikasi khusus circuit adalah syarat Polished Stone Value (PSV) dari aggregate lapis aspal atas adalah lebih besar dari 50 dan delta elevasi lapis atas aspal adalah ± 2 mm dengan menggunakan Straight Edge panjang 4 meter, hal ini disyaratkan untuk menjamin keselamatan event balap motor. Proses desain dan pelaksanaan dimulai dari studi data geologi, penyelidikan tanah serta desain layout track yang secara pararel dilakukan pembahasan dengan pihak Federation International Motorcycles (FIM). Desain yang dihasilkan harus mendapatkan homologasi dari

FIM sebelum dilaksanakan pekerjaan konstruksi di lapangan.

Gbr. 1. Pembangunan Sirkuit Mandalika.

Secara umum pelaksanaan pekerjaan seperti pelaksanaan pekerjaan jalan perkerasaan lentur, pekerjaan sub base, pemasangan drainase Hauraton, di lanjutkan dengan aspal lapis pertama jenis (AC-Base 8 cm), aspal lapis kedua (AC-Binder 6cm) dan terakhir aspal lapis ketiga lapis atas (SMA Surface 4 cm).

Penyelidikan geoteknik yang dilakukan adalah penyelidikan tanah standar dan pengukuran geolistrik untuk melihat secara menyeluruh kondisi tanah dibawah lintasan sirkuit. Hasil dari kedua data ini lalu diinterpretasi secara integratif untuk menentukan konstruksi geoteknik yang diperlukan untuk mendukung pemenuhan persyaratan teknis sirkuit. Hasil penyelidikan menunjukkan adanya variasi kondisi tanah di sepanjang lintasan sirkuit. Kondisi tanah tanah dasar sebagian besar adalah tanah pasir padat yang dapat mendukung struktur perkerasan sirkuit. Pada beberapa lokasi terbatas ditemukan beberapa kondisi khusus seperti tanah pasir lepas, lempung lunak dan struktur geologi yang membutuhkan konstruksi geoteknik khusus.

Konstruksi geoteknik khusus yang digunakan adalah Controlled Modulus Columns (CMC) untuk mengatasi potensi liquifaksi tanah pasir lepas dan kombinasi CMC dan matras beton untuk mengatasi potensi penurunan berlebihan pada tanah lempung lunak dan struktur geologi. Konstruksi terowongan direncanakan agar tidak memberikan potensi beda penurunan pada lintasan.

2 SURVEY GEOLOGI DAN GEOTEKNIK

2.1 *Survey Geologi*

Sirkuit direncanakan berada pada Kawasan Pariwisata Mandalika dengan luas ± 1250 Ha. Review dilakukan pada tiga (3) lokasi, yaitu:

a. Sta. 3+250 sampai Sta. 4+200
b. Sta. 3+050 sampai Sta. 3+250
c. Sta. 2+500 sampai Sta. 3+050

Gbr. 2. Peta Geologi Lembar Lombok, Pusat Penelitian dan Pengembangan Geologi (1994).

2.2 *Penyelidikan Tanah*

Penyelidikan tanah pada proyek ini dilakukan oleh PT Comsindo dan Geo-Engineering Research Group (2018). Penyelidikan tanah yang dilakukan meliputi penyelidikan lapangan dan pengujian laboratorium.

Pada lokasi proyek dilakukan pengujian lapangan yang meliputi:

a. Pemboran teknik sebanyak dua belas (12) titik dengan kedalaman 30 m.
b. Lima puluh (50) titik uji sondir kapasitas 2.5 ton.
c. Standard Penetration Test (SPT) pada setiap titik bor dengan interval pengujian antara 1.5 m.

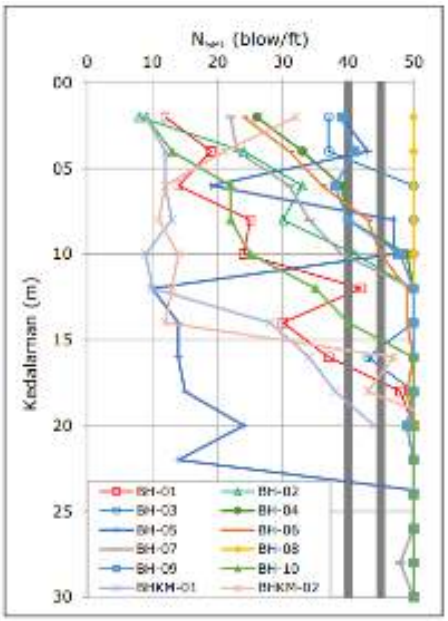

Gbr. 3 Kurva NSPT terhadap Kedalaman pada Masing-masing Titik Pemboran Teknik.

Berdasarkan komposisi butiran tanah hasil penyelidikan tanah terdapat potensi likuifaksi.

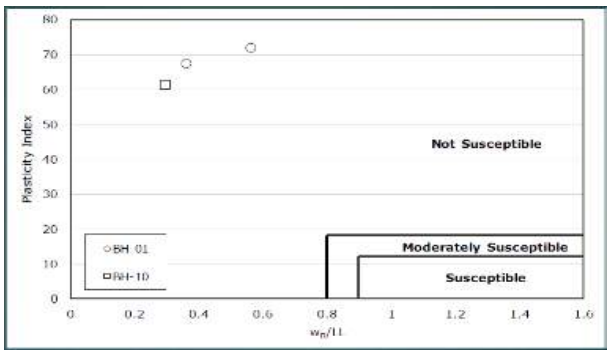

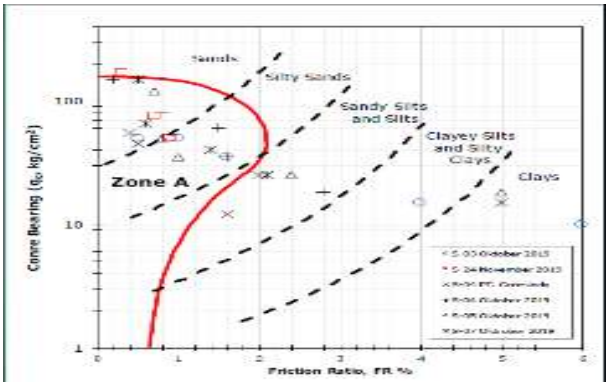

Gbr. 4. Potensi Likuifaksi berdasarkan Data Boring dan Sondir.

Dari hasil analisa likuifaksi didapat potensi likuifaksi pada area di beberapa titik yakni antara STA 3+050 sampai STA 3+150, STA 0+400 sampai STA 9+600 dan STA 3+800 samapai STA 4+100.

2.3 *Pengujian Geolistrik*

Penelitian ini dimaksudkan untuk memberikan gambaran kondisi geologi dibawah permukaan dalam rangka mendukung pembuatan jalur sirkuit Mandalika (BPPT,2020). Area survei adalah sepanjang koridor lintasan sirkuit sepanjang 4,32 km. Dalam pelaksanaan survei ini mengikuti jalur trek sirkuit yang direncanakan sepanjang 4,301 km, dibagi menjadi 38 lintasan pengukuran.

Survei dilakukan dengan pengukuran dua dimensi (multy channels geoelectrical survey) dengan konfigurasi Wenner-Schlumberger array. Digunakan jumlah elektrode sebanyak 16 yang disusun dalam formasi garis lurus dengan jarak antar elektrode besarnya sama (a = 10 m).

Gbr. 4. Lokasi Pengukuran Geolistrik Pias 12,13,14,37.

Data DEMNAS area sirkuit ini diperleh dari instansi BIG (Badan Informasi Geospasial) yang sudah dipublish pada portal BIG. Dengan menggunakan software Arc GIS dan Global Mapper data DEMNAS ini dapat diolah sehingga menghasilkan nilai elevasi, kontur, penampang melintang, dan 3 dimensinya.

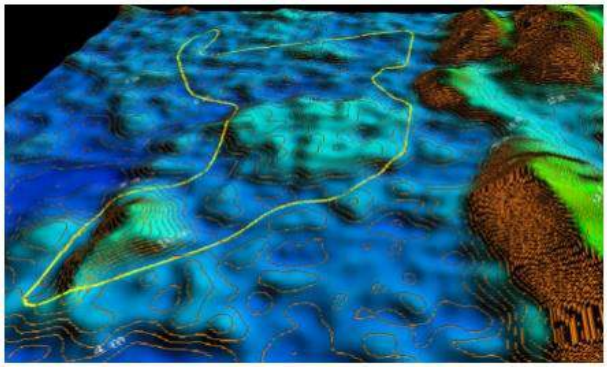

Gbr. 5. Profil 3D dan Kontur Interval 2 meter di Area Sirkuit.

Profil penampang melintang area kajian dari data DEMNAS, menampakkan ada area sedikit bergelombang dibeberapa bagian. Ini hanya indikasi awal penampakan permukaan bumi melalui data DEMNAS yang sangat perlu diverifikasi dengan data geolistrik.

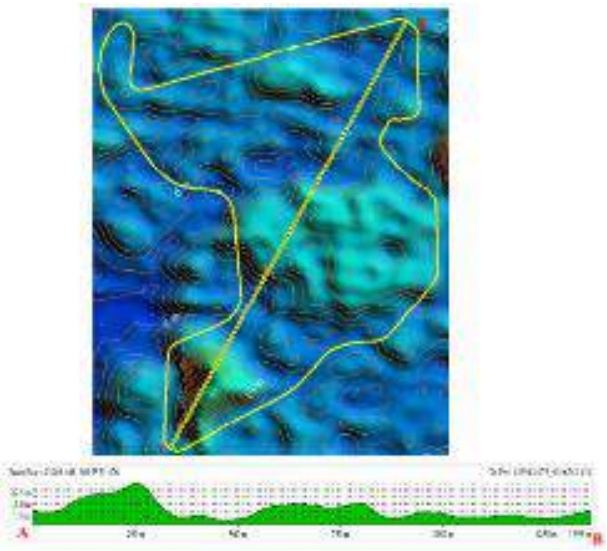

Gbr. 6. Profil Penampang Melintang A-B dan Kontur Interval 2 meter di Area Sirkuit.

Data geolistrik ini akan dicocokkan atau dikalibrasi dengan data-data sampel tanah dan batuan yang sudah diambil sebelumnya.

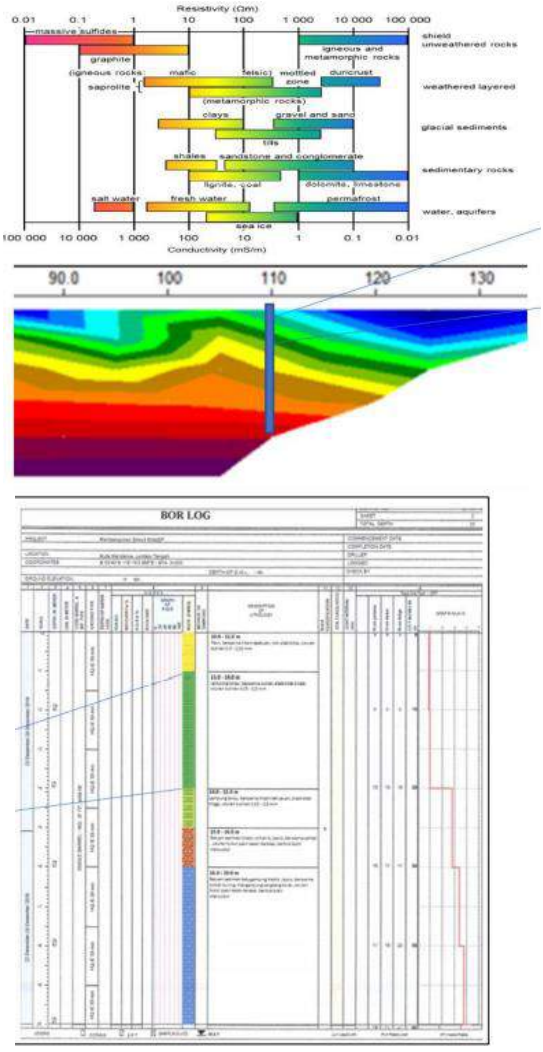

Gbr. 7. Metode Kalibrasi Data Modelling dengan Bor Log dan Geologi Regional.

3 PERENCANAAN KONSTRUKSI GEOTEKNIK KHUSUS

3.1 *Tata Letak Konstruksi Geoteknik pada Lintasan*

Berdasarkan kajian secara teknik penanganan likuifaksi menggunakan metode Controlled Modolus Column (CMC) ditinjau aspek waktu pelaksanaan dan metode kerja (mudah, praktis, dan efektif), PT Wijaya Karya (2020).

Gbr. 8. Layout Pemasangan CMC pada Zone 1.

Gbr. 9. Area Pemasangan CMC pada Zone 1 yaitu STA 0+400 sampai STA 0+600.

Untuk menjaga stabilitas lereng pada area sirkut Zone 2 dilakukan perkuatan dengan bronjong batu kali.

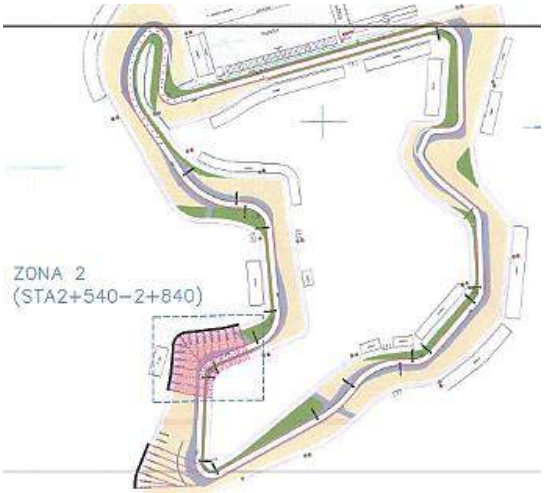

Gbr. 10. Layout Perkuatan Lereng pada Zone 2.

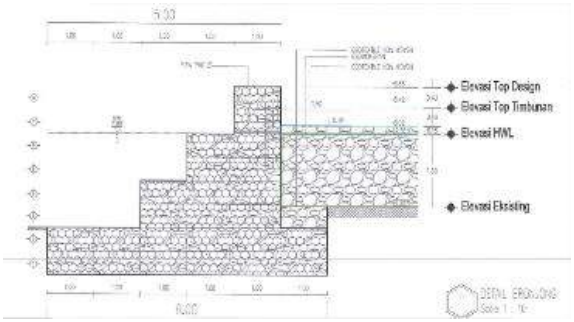

Gbr. 11. Detail Perkuatan Lereng dengan Bronjong Batu Kali pada Zone.

Pada Zone 3 dilakukan penanganan lempung lunak dimana dilakukan pemasangan CMC dengan plate matras beton.

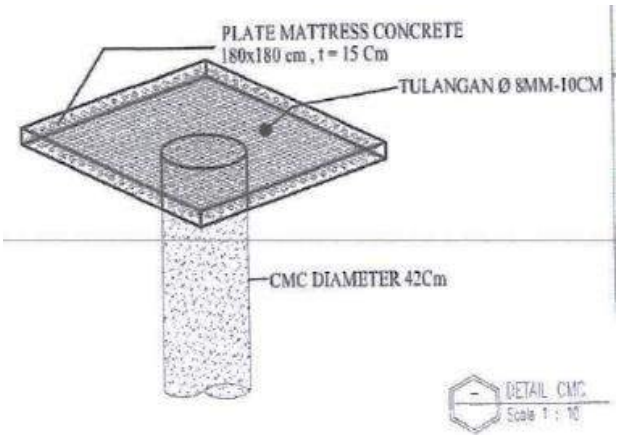

Gbr. 12. Gambar detail CMC dengan Plate Matras Beton.

Gbr. 13. Layout Pemasangan CMC pada Zone 3.

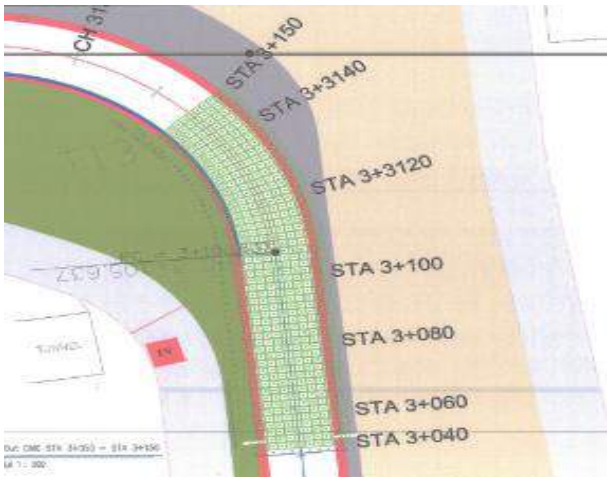

Gbr. 14. Area pemasangan CMC pada Zone 3 yaitu STA 3+040 sampai STA 3+150.

Pada Zone 4 STA 3+800 sampai STA 4+100 dilakukan penanganan likuifaksi dan struktur geologi dengan metode CMC.

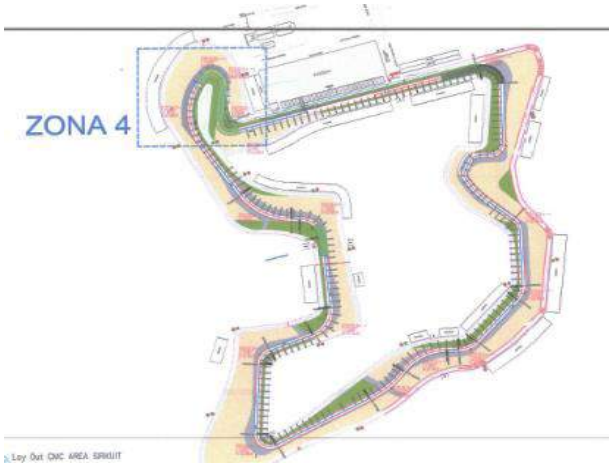

Gbr. 15. Layout Pemasangan CMC pada Zone 4.

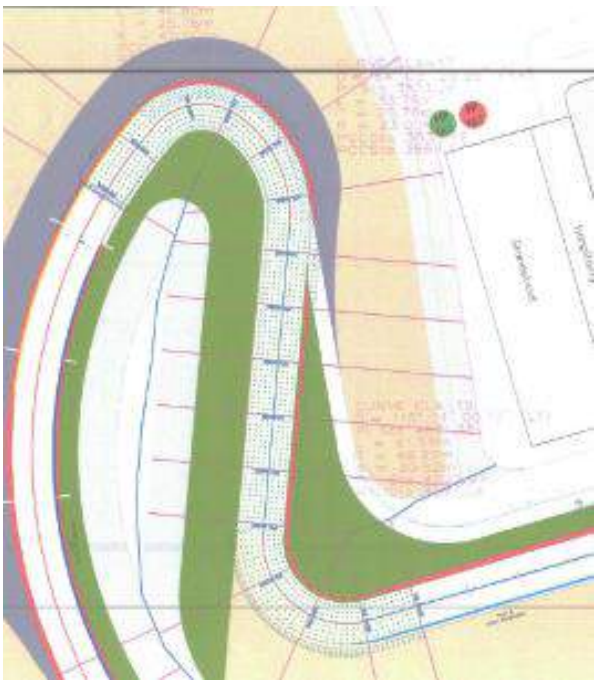

Gbr. 16. Area Pemasangan CMC pada Zone 4.

3.2 *Perencanaan Konstruksi untuk Mengatasi Potensi Likuifaksi dan Mengatasi Penurunan Lempung Lunak*

Pada Analisa Potensial Liquifaksi ini perhitungan Liquifaksi dengan menggunakan data Sondir STA 0+600 dan STA 4+000, ERKA (2018).

Perhitungan potensial liquifaksi dengan menggunakan Peta Gempa Berdasarkan USGS dengan percepatan gempa (PGA) sebesar 0,3g (500 tahun) dan 0,4g (1000 tahun).

Dari hasil analisa pada Tabel 1 maka dapat disimpulkan sebagai berikut:

a. Berdasarkan metode Nceer pada STA 0+600 kedalaman 0 – 7,8 m dan 14 – 16,6 m berpotensi terjadi Liquifaksi
b. Berdasarkan metode Nceer pada STA 1+400 kedalaman 0 – 13,8 m dan 15 – 19,4 m berpotensi terjadi Liquifaksi
c. Berdasarkan metode Nceer pada STA 4+000 kedalaman 0 – 7,4 m dan 10,8 – 17,4 m berpotensi terjadi Liquifaksi

Pada teknik penanganan likuifaksi menggunakan metode Controlled Modulus Columns (CMC). Dimana pada metode CMC terdapat kelebihan yakni dapat membuat lubang dan memasukan beton dengan waktu dan instalasi cepat dan tidak membuang material disposal. Modulus column dapat dikontrol sehingga material bisa lebih menyatu dengan tanah perkuatan (tidak sekaku tiang bor atau tiang pancang), sehingga mengurangi potensi likuifaksi. Pada Zone 3 dimana ditemukan lapisan lunak yang cukup tebal, metoda CMC dikombinasikan dengan matras beton untuk meratakan beban, sehingga settlement pada track kecil dan tidak bergelombang. Kombinasi ini juga diterapkan subbagian Zona 4 yang ditemukan adanya struktur geologi dari pengukuran geolistrik.

Tabel 1. Hasil Perhitungan Potensial Liquifaksi Metode NCEER STA 0+600.

τave/σv'	Cq	qC1N	fs	Q	F	Ic	Kc	(qc1N) cs	MSF	τave/σv'	FK	Keterangan
0,675	1,815	104,38	0,55	1041,70	0,01	0,918	1,00	104,38	1,00	0,19	0,28	Potensi Liquifaksi
0,633	5,400	121,50	1,55	119,53	0,07	1,394	1,00	121,50	1,00	0,25	0,39	Tidak Potensi Liquifaksi
0,640	2,900	118,60	2,55	116,58	0,06	1,404	1,00	118,60	1,00	0,24	0,37	Potensi Liquifaksi
0,653	2,020	129,82	3,55	127,75	0,06	1,364	1,00	129,82	1,00	0,28	0,43	Potensi Liquifaksi
0,660	1,614	49,29	4,55	47,18	0,16	1,843	1,14	56,16	1,00	0,08	0,12	Potensi Liquifaksi
0,66	1,399	27,98	5,55	25,85	0,30	2,173	1,60	44,83	1,00	0,08	0,12	Tidak Potensi Liquifaksi
0,637	1,133	27,19	6,55	25,12	0,30	2,182	1,62	44,15	1,00	0,07	0,11	Tidak Potensi Liquifaksi
0,612	0,888	19,24	7,55	17,24	0,39	2,376	2,22	42,65	1,00	0,07	0,11	Tidak Potensi Liquifaksi
0,594	0,735	19,18	8,55	17,22	0,36	2,367	2,18	41,86	1,00	0,07	0,11	Tidak Potensi Liquifaksi
0,582	0,622	39,95	9,55	38,00	0,16	1,935	1,22	48,89	1,00	0,08	0,14	Potensi Liquifaksi
0,575	0,539	87,33	10,55	85,38	0,07	1,539	1,00	87,33	1,00	0,14	0,25	Tidak Potensi Liquifaksi

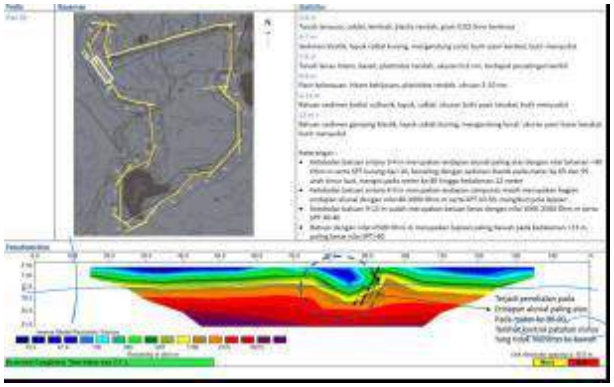

Gbr. 17 Struktur Geologi dari Pengukuran Geolistrik.

3.3 *Perencanaan Terowongan/Tunnel*

Pada area track circuit MotoGP terdapat beberapa tunnel dimana tunnel tersebut di pergunakan untuk jalan kawasan agar fungsi layanan kawasan tetap berjalan dengan baik saat race maupun saat non race sesuai dengan standardisasi event MotoGP.

Lokasi tunnel berada di bawah track circuit MotoGP, dimana terdapat 2 lokasi tunnel yaitu berada pada area selatan dan utara track circuit. Tunnel berada pada kedalaman ± 7 s/d 8 m dibawah track circuit.

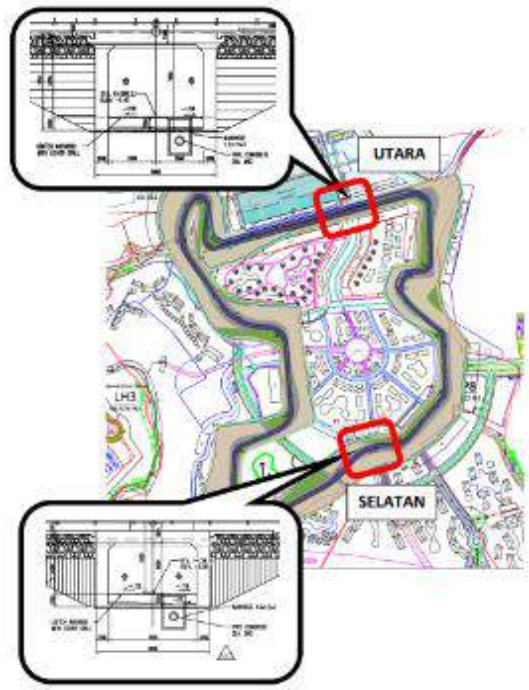

Gbr. 18. Layout Lokasi Area Perkuatan Tunnel Sisi Utara dan Sisi Selatan.

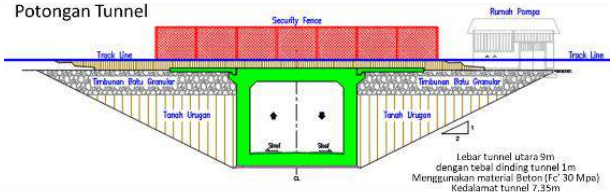

Gbr. 19. Potongan Tunnel dibawah Track Sirkuit.

Pada analisa terdapat beban yang diterima oleh tunnel dalam Analisa.

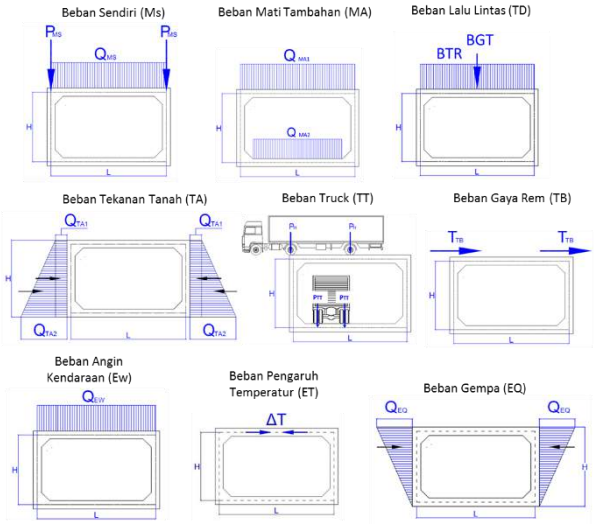

Gbr. 20. Beban yang diterima Tunnel dalam Analisa.

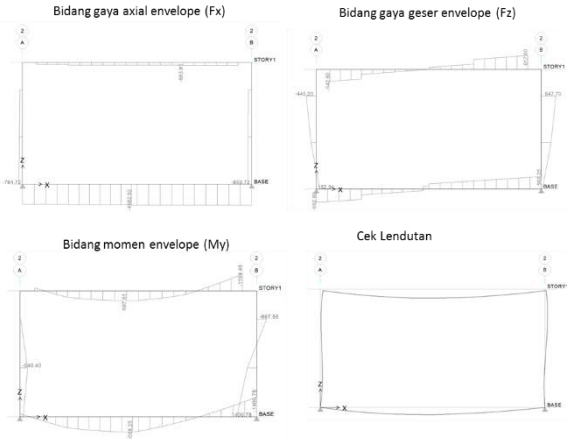

Gbr. 21. Gaya-gaya dalam pada Tunnel Menggunakan Program ETABS.

4 PELAKSANAAN DAN KONTROL KUALITAS

Sebelum pelaksanaan lapis perkerasan lentur, dilaksanakan pekerjaan perbaikan tanah dasar dengan metode CMC di beberapa lokasi, pekerjaan sub grade dan pekerjaan tunnel serta box drainase dan box utilitas, PT Wijaya Karya (2018).

Gbr. 22. Pelaksanaan Pekerjaan Perbaikan Tanah Dasar dengan Metode CMC.

Gbr. 23. Pelaksanaan Pekerjaan Box Tunnel atau Terowongan dibawah Track Sirkuit.

Kontrol kualitas dilakukan dengan sangat ketat, hampir keseluruhan uji kualitas dapat dilakukan di site proyek, kecuali beberapa uji kualitas khusus, seperti test Wheel Tracking tes dilakukan di Balai Jalan Cikampek dan tes PSV dilakukan di London dengan mengirim sampel material secara periodik dalam masa produksi material ke laboratorium di London.

5 PENUTUP

Mandalika International Street Circuit adalah konstruksi berfungsi ganda yang mempunyai spesifikasi teknis khusus yang lebih tinggi dari jalan raya biasa. Untuk menjamin terpenuhinya fungsi tersebut diperlukan suatu rekayasa geoteknik sesuai dengan kondisi lingkungan. Rekayasa dilakukan mulai dari proses survey geologi, penyelidikan tanah baik yang standar maupun dengan teknologi geolistrik, sehingga dapat ditentukan konstruksi geoteknik untuk mendukung perkerasan sirkuit. Pada beberapa lokasi ditemukan kondisi yang membutuhkan konstruksi geoteknik khusus: likuifaksi, penurunan akibat lempung lunak, serta struktur geologi lokal.

Konstruksi khusus yang digunakan adalah sistem Control Modulus Column (CMC) untuk mengatasi potensi likuifaksi, sebagai sistem yang lebih efisien, lebih cepat, lebih bersih dan menyatu dengan tanah dibanding sistem pondasi dalam konvensional. Sistem CMC dikombinasikan dengan matras beton untuk mengatasi kondisi lempung lunak dan struktur geologi, sehingga beban terdistribusi lebih merata sehingga dapat mengontrol penurunan perkerasan. Konstruksi terowongan direncanakan terutama untuk menjaga kerataan lintasan tetap sesuai persyaratan.

Pembangunan sirkuit berkelas internasional memanfaatkan secara maksimal sumber daya konstruksi dalam negeri yang dikombinasikan dengan teknologi dan tenaga konstruksi mancanegara termaju. Pengalaman

pembangunan sirkuit ini akan memperkaya kemampuan teknis para pelaku konstruksi nasional untuk bisa melakukan secara mandiri melakukan rekayasa konstruksi sirkuit semacam ini di masa datang.

PENGHARGAAN

Penghargaan kepada Indonesian Tourism Development Corporation sebagai pemilik proyek, MRK 1 – Amsecon Berlian Sejahtera sebagai konsultan perencana, PT Wika BRL sebagai kontraktor design & build konstruksi geoteknik, dan PT Pembangunan Perumahan sebagai kontraktor perkerasan dan terowongan.

DAFTAR PUSTAKA

BPPT. 2020. *Pengujian Geoloistrik pada Ruas Sirkuit*. PT Wijaya Karya (Persero) Tbk-PT Bunga Raya Lestari. Mataram: Indonesia.

ERKA. 2018. *Report Hasil Perhitungan Potensial Liquifaksi Proyek Sirkuit Mandalika*. PT Wijaya Karya (Persero) Tbk-PT Bunga Raya Lestari. Mataram: Indonesia

Geo-Engineering Research Group. 2018. *Laporan Penyelidikan Tanah*. ITDC, Mataram: Indonesia.

PT Wijaya Karya (Persero) Tbk-PT Bunga Raya Lestari, KSO. 2018. *Gambar Design sesuai Metoda Pilihan*. ITDC. Mataram: Indonesia.

PT Wijaya Karya (Persero) Tbk-PT Bunga Raya Lestari, KSO. 2018. *Metoda Kerja Ground Improvement Sirkuit MotoGP Mandalika*. ITDC, Mataram: Indonesia.

The Influence of Portland Cement to Shear Strength and Durability in Mixing Weathered Clay Shale

Pintor T. Simatupang
Civil Engineering – Universitas Mercu Buana

Idrus M. Alatas
Civil Engineering – Institut Sains dan Teknologi Nasional

Ayu Kartika Redyananda
Civil Engineering – Institut Sains dan Teknologi Nasional

Eko Arif Purnomo
Civil Engineering – Institut Sains dan Teknologi Nasional

ABSTRACT: Weathered clay shale used as embankment material is reported to have suffered a lot of failure. In this study, weathered clay shale was mixed with Portland cement (PC) to increase the shear strength and durability. It is hoped that if weathered clay shale is used as embankment material the mixing with PC can meet the embankment requirements. The mixed material of weathered clay shale and PC is compacted according to Proctor Standard procedure. The percentage of PC in the mixed material is limited to only 20%. Tests for shear strength and durability index on mixed materials are carried out at optimum moisture content. Tests are also conducted at less than and more than optimum moisture content. The highest normalization shear strength is obtained in the mixed material with a PC percentage of 10% and a moisture content of 8% above the optimum moisture content, which is 265% when compared to the original weathered clay shale. While the durability index increased to 24%.

Keywords: weathered clay shale, shear strength ratio, durability index

Analysis of the Axial Foundation Bearing Capacity for Bridge Construction in the Mantuil Region, Muara Harus District, Tabalong Regency, South Kalimantan Province

Muhammad Tobiby Pratama Pohan
Fresh Graduate, Faculty of Geological Engineering – Universitas Padjadjaran

Bekti Djatmiko
Wiratman Cipta Manggala

Nur Khoirullah
Department of Applied Geology, Faculty of Geological Engineering – Universitas Padjadjaran

ABSTRAK: Keamanan dan stabilitas struktur jembatan baru sangat tergantung pada keamanan dan kesesuaian pondasi itu sendiri, seperti untuk pembangunan jembatan baru di salah satu sungai di Desa Mantuil, Kalimantan Selatan. Metode yang digunakan untuk analisis daya dukung dilakukan dengan menggunakan *Standard Penetration Test* (SPT) yang diperoleh dari 3 lubang bor. Daya dukung dihitung menggunakan metode Meyerhof dan metode *American Association of State Highway and Transportation Officials* (AASHTO). Berdasarkan hasil analisa, dengan perkiraan diameter pondasi tiang 0,4 m, lapisan litologi dengan daya dukung terkuat terdapat pada lapisan konglomerat dengan daya dukung tiang tunggal 62 – 536 ton/m^2, dan lapisan batubara dengan nilai daya dukung tiang tunggal sebesar 136 hingga 643 ton/m^2, dan konfigurasi pondasi dengan tiang pancang 3 kali 5 atau tiang pancang 3 kali 4 sudah sesuai untuk pondasi.

Kata kunci: pondasi, daya dukung aksial, group pile effect, konstruksi jembatan, standard penetration test

ABSTRACT: The safety and stability of a new bridge structure are dependent on the safety and the compatibility of the foundation itself, like for constructing a new bridge in one of the rivers in Mantuil Village, South Kalimantan. The method used for bearing capacity analysis is conducted using the Standard Penetration Test (SPT) obtained from 3 boreholes. The bearing capacity was calculated using the Meyerhof method and the American Association of State Highway and Transportation Officials (AASHTO) method. Based on the analysis, with the diameter of pile foundation 0.4 m, the lithological layer with the strongest bearing capacity was found in the conglomerate layer with a single-pole bearing capacity of 62 to 536 ton/m^2, and coal layers with a single-pole bearing capacity value of 136 to 643 ton/m^2, and the configuration of the foundation with 3 by 5 piles or 3 by 4 piles was appropriate for the foundation.

Keywords: foundation, axial bearing capacity, group pile effect, bridge construction, standard penetration test

1 INTRODUCTION

Since a long time ago, human life has not been separated from activities that rely on land as a medium to support the burdens it carries, such as for housing, planting, and transportation. One of the means of transportation used for human activities is a bridge, Brunning (2001), Brunning et al. (2012).

The safety and stability of a bridge structure are highly dependent on the foundation it uses, Baban (2016), Das (2015). Therefore, a quite crucial step in starting to design a bridge structure is to know the design of the foundation the building is going to use, which should be powerful enough to withstand stress from both its weight and the things on it.

To know how much stress a bridge can withstand, one must know the bearing capacity of both its foundation and the soil. The value of bearing capacity in question is the limit to the value of the force per unit area that can be applied to a soil material before the soil fails, Zakaria (2006). The value of the bearing capacity of the foundation is known from the value of the bearing capacity of the soil, which is calculated according to the geometry of

the foundation itself, Meyerhof (1976) in Das, 2015.

This bearing capacity calculation is carried out preferably before building construction begins, in order to anticipate failure during construction and after the building has been completed, and to ensure the safety and stability of the foundation itself , SNI 8460 (2017).

That is why, before constructing a new bridge to replace a broken one on one of the rivers in Mantuil Village, Muara Harus District, Tabalong Regency, South Kalimantan Province, the design of the foundation must be ensured to be able to withstand the target load of its building and things that will go over it.

2 METHODOLOGY

The Standard Penetration Test (SPT) is used to collect the N-SPT data and samples from 3 drilling points across the river in Mantuil Village (Fig. 2.1). SPT is used to know the strength of a material, by using normal force that is blown by the hammer from the SPT to the material, and counting the number of blows to drive the hammer until it reaches 300 mm to get the N number, Bowles (1997). To get a more accurate N value, the measured N values must be corrected using Eqn. (1), SNI 4153 (2008).

$$N_{60} = N_M \times C_N \times C_E \times C_B \times C_R \times C_S \quad (1)$$

With:

N_{60} = Corrected N-SPT value for 60% efficiency

N_M = N-SPT value collected from the test

C_N = Adjustment for effective overburden pressure = $\frac{2,2}{(1,2+\left(\frac{\sigma v}{100}\right))}$

σv = Effective overburden pressure

C_E, C_B, C_R, C_S = Adjustment factors from Table 1

Table 1. Correction of SPT N Value against Different Types of SPT Equipment, Youd & Idriss in SNI 4153 (2008).

Faktor	Jenis Alat	Parameter	Koreksi
Tegangan vertikal efektif		C_N	2,2 / (1,2+(σ'_{v_o}/Pa))
Tegangan vertikal efektif		C_N	$C_N \leq 1,7$
Rasio tenaga	Palu donat (Donut hammer)	C_E	0,5 s.d 1,0
Rasio tenaga	Palu pengaman (Safety hammer)	C_E	0,7 s.d 1,2
Rasio tenaga	Palu otomatik (Automatic-trip Donut-type hammer)	C_E	0,8 s.d 1,3
Diameter bor	65 s.d 115 mm	C_B	1,0
Diameter bor	150 mm	C_B	1,05
Diameter bor	200 mm	C_B	1,15
Panjang batang	< 3 m	C_R	0,75
Panjang batang	3 s.d 4 m	C_R	0,8
Panjang batang	4 s.d 6 m	C_R	0,85
Panjang batang	6 s.d 10 m	C_R	0,95
Panjang batang	10 s.d 30 m	C_R	1,0
Pengambilan contoh	Tabung standar	C_S	1,0
Pengambilan contoh	Tabung dengan pelapis (liner)	C_S	1,1 s.d 1,3

To know the bearing capacity of the material from the corrected N value, Meyerhof's (1976) in Das, 2015) equations, which are Eqn. (2), (3), (4), (5), and (6), for pile foundation, are used. For cohesive soils, the Meyerhof formula does not really use N values, instead, it uses cohesion as its dominant shear strength, Husain (2015), Hakam (2010). To get cohesion property from N value, we use the N value of soil through the undrained shear strength correlation graph Terzaghi & Peck (1967), Sowers (1979) in Vidayanti, 2013 (Fig. 1.).

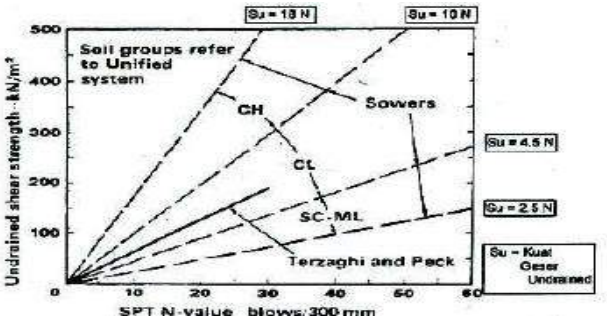

Fig. 1. Correlation between N-SPT Value and Undrained Shear Strength, Terzaghi & Peck (1967), Sowers (1979).

$$Q_{ult} = Qb \times Qs \quad (2)$$

For non-cohesive soil:

$$Q_p = A_p(40\ NL/D) \leq 400\ N \quad (3)$$

$$Qs = \Sigma p f_{av}\ \Delta L \quad (4)$$

For cohesive soil:

$$Q_p = 9 c_u A_p \quad (5)$$

$$Qs = \Sigma p \alpha c_u \Delta L \quad (6)$$

With:
Q_{ult} = Ultimate bearing capacity
Qb = Bearing capacity of the pile point
Qs = Frictional resistance from the soil-pile interface
L = Depth
D = Pile diameter
Ap = The cross-sectional area of the pile
N = Value from SPT = (N2 + N3)/3
p = Circumference of the pile
fav = Average shear strength = Average N-SPT
α = Adhesion factor (Table 2)
cu = Undrained cohesion (Figure 1)

Table 2. Correlation between Undrained Cohesion and Adhesion Factor, Terzaghi, Peck, and Mesri, (1996) in Das, 2015.

C_u / P_a	α
≤ 0,1	1
0,2	0,92
0,3	0,82
0,4	0,74
0,6	0,62
0,8	0,54
1	0,48
1,2	0,42
1,4	0,4
1,6	0,38
1,8	0,36
2	0,35
2,4	0,34
2,8	0,34

Pa = atmospheric Pressure ≈ 100 kN/m^2

For the foundation to be able to hold the target stress that we aimed for, we need multiple piles for one foundation. Since the Meyerhof formula only measures the bearing capacity for a single pile, we need another formula for multiple piles to know the configuration of the piles themselves, therefore we use Eqn. (7) and (8) from the American Association of State Highway and Transport Officials (AASHTO) from their Bridge Specification (2017) for group pile effect analysis.

$$E_g = 1 - \Theta \frac{(n-1)m+(m-1)n}{90 \times m \times n} \quad (7)$$

$$Q_{(group)} = Q \times n' \times E_g \quad (8)$$

With:
Eg = Pile group efficiency
Θ = $\tan^{-1}$ D/s
D = Pile diameter
s = Distance between piles
= 2,5×D+0,02×L (Fellenius, 2017)
m = Number of pile columns
n = Number of pile rows
$Q_{(group)}$ = Pile group bearing capacity
Q = Single pile bearing capacity
n' = Number of piles

3 DISCUSSION

The Analysis of bore log data from three (3) drilling sites were conducted then calculated to get the bearing capacity value for each seam in every drilling site. First, we must know the single-pile bearing capacity of each seam using the Meyerhof method, by using Eqn. (1), with

the pile diameter of 0,4 m. The results of these calculations are shown in table 3 for drill site BH-01, table 4 for drill site BH-02, and table 5 for drill site BH-05.

The N-SPT values shown in this analysis have already been corrected using Eqn. (1), with the assumption of it using NQ drilling type (7.5 mm) with the drill length the same as the depth of the drill hole, and with standard tube and donut hammer.

Table 3. Bearing Capacity of BH-01.

Depth (m)	N60	Q_p (kN/m^2)	Q_s (kN/m^2)	Q_{ult} (kN/m^2)	Q_{all} (Ton)
1,5	6,20	83,63	75,27	158,91	6,36
3	10,40	141,10	197,55	338,65	13,50
4,5	12,40	167,78	335,55	503,33	20,10
6	8,90	120,91	386,93	507,85	20,30
7,5	1,90	25,20	193,22	218,42	8,74
9	2,60	35,08	287,66	322,75	12,90
10,5	2,40	32,72	313,06	345,79	13,80
12	4,40	59,97	495,75	555,72	22,20
13,5	2,70	37,06	455,84	492,90	19,70
15	4,40	659,73	106,05	765,78	30,60
16,5	7,00	1244,07	119,28	1363,35	54,50
18	8,70	1809,56	135,71	1945,27	77,80
19,5	13,70	3308,10	161,49	3469,58	139,00
21	23,50	13194,70	205,85	13400,50	536,00
22	5	67,71	1026,30	1093,97	43,80
23,5	6,90	93,13	1313,10	1406,23	56,20
25	5,30	71,76	1235,80	1307,57	52,30

The results of the single-pile bearing capacity for each seam in BH-01 can be seen on the table 3. The description of the single-pile bearing capacity value for each layer from the top to the bottom are: The top layer is described as silty clay with a bearing capacity of 6.36 to 22.2 ton/m^2, and the next lower layer is described as clayey sand with a bearing capacity of 30.6 to 54.5 ton/m^2, and then the next layer described as coarse sand with a bearing capacity value of 77.8 to 139 ton/m^2, and the next layer of this borehole described as conglomerate with a bearing capacity value of 536 ton/m^2, and at the deepest of this borehole described as silty clay with a bearing capacity of 43.8 to 56.2 ton/m^2. The layer with the highest single-pile bearing capacity value in this bore hole is found at a depth of 21 meters, which is the conglomerate layer.

Table 4. Bearing Capacity of BH-02.

Depth (m)	N60	Q_p (kN/m^2)	Q_s (kN/m^2)	Q_{ult} (kN/m^2)	Q_{all} (Ton)
1,5	23,91	324,51	183,89	508,40	20,3
3	2,64	35,90	98,13	134,03	5,36
4,5	1,22	16,63	83,13	99,76	3,99
6	2,22	30,16	164,90	195,07	7,80
7,5	6,95	94,36	424,62	518,97	20,80
9	3,60	48,89	361,76	410,65	16,40
10,5	4,94	66,99	484,61	551,61	22,10
12	3,03	24,01	294,49	318,50	12,70
13,5	9,03	71,50	664,95	736,45	48,00
15	7,07	1036,73	121,82	1158,54	46,30
16,5	8,95	1555,09	138,68	1693,77	67,80
18	27,37	11309,7	190,27	11500,00	460,00
19	25,95	11938,1	233,05	12171,10	487,00
20	12,40	3141,59	250,05	3391,64	136,00
21	6,20	84,16	1060,40	1144,59	45,80
22,5	7,21	97,93	1322,10	1419,98	56,80
24	5,56	75,47	1247,80	1323,27	52,90
25,5	6,15	83,43	1276,40	1359,86	54,40
27	6,59	89,49	1449,70	1539,18	61,60
28,5	11,17	126,38	1680,90	1807,28	72,30
30	6,02	68,07	1406,80	1474,86	59

The results of the single-pile bearing capacity for each seam in BH-02 can be seen on the table 4. The description of the single-pile bearing capacity value for each layer from the top to the bottom are: The top layer is described as silty clay with a bearing capacity of 3.9 to 22.1 ton/m^2, and the next lower layer is described as coarse sand with a bearing capacity of 29.5 to 46.3 ton/m^2, and then the next layer described as conglomerate with a bearing capacity value of 67.8 ton/m^2, and the next layer of this borehole described as coal seam with a bearing capacity value of 136 to 487 ton/m^{2,} and the next lower layer is described as silty clay again with a bearing capacity of 45.8 to 61.6 ton/m^2 and at the deepest of this borehole described as alternating layers of silt clay and silt sandstone with a bearing capacity value of 59 to 72.3 ton/m^2. The layer with the highest single-pile bearing capacity value in this bore hole is found at the depth of 19 meters, which is the coal layer.

Table 5. Bearing Capacity of BH-05.

Depth (m)	N60	Q_p (kN/m^2)	Q_s (kN/m^2)	Q_{ult} (kN/m^2)	Q_{all} (Ton)
1,5	14,90	117,72	94,178	211,901	8,48
3	17,40	235,67	251,38	487,05	19,50
4,5	12,90	175,13	332,75	507,89	20,30
6	2,00	75,40	88,82	164,22	6,57
7,5	1,80	94,25	92,26	186,51	7,46
9	3,30	45,34	335,50	380,84	15,20
10,5	6,10	82,82	521,73	604,55	24,20
12	4,90	66,37	548,66	615,03	24,60
13,5	9,00	1187,52	112,96	1300,48	52,00
15	10,70	1696,46	156,39	1852,85	74,10
16,5	14,30	2695,49	183,28	2878,76	115,00
18	6,20	1357,17	194,90	1552,07	62,10
19,5	23,90	12252,20	239,86	12492,10	500,00
20,5	13,00	3735,35	258,00	39930,36	160,00
22	21,40	13823,00	297,86	14120,90	565,00
23,5	20,10	14765,50	335,39	15100,90	604,00
25	19,00	15708,00	370,85	16078,80	643,00

The results of the single-pile bearing capacity for each seam in BH-05 can be seen on the table 5. The description of the single-pile bearing capacity value for each layer from the top to the bottom are: The top layer is described as silty clay with a bearing capacity from 8.48 to 20.3 ton/m^2, and the next lower layer is described as clayey sand with a bearing capacity ranging from 6.57 to 7.46 ton/m^2, and then the next layer described as silty clay with a bearing capacity value of 15.2 to 24.6 ton/m^2, and the next layer of this borehole described as clayey sand again with a bearing capacity value from 52 to 74.1 ton/m^2, and then the layer under that is described as alternation between clayey sand with coal with a bearing capacity value of 115 ton/m^2, and then the next layer described as conglomerate with bearing capacity value of 62m1 to 500 ton/m^2, and then the next layer described as coal with bearing capacity value of 565 to 643 ton/m^2, and at the deepest of this borehole described as silty clay again with bearing capacity of 43.8 to 56.2 ton/m^2. The layer with the highest single-pile bearing capacity value in this bore hole is found at the depth of 25 meters, which is the coal layer.

Based on the data of tables 3 to 5, it can be analyzed that the value of the bearing capacity tends to increase with increasing depth. Apart from the fact that the deeper it is the higher the N-SPT value, there is also higher pile friction the deeper the pole is. The highest bearing capacity value is found in the coal layer and at the conglomerate seam at drill point BH-01 with an SPT value above 50 and an allowed carrying capacity value of around 500 to 600 ton/m^2 per pile.

The calculated foundation bearing capacity is the bearing capacity for only a single pile for every hole, where to fulfill the load plan to be placed above this ground, which is planned at 3858 ton/m^2, requires more than only one pile, because the bearing capacity value for a single pile of the coal seam is only about 500 to 600 ton/m^2.

To calculate the bearing capacity for the group piles, Eqn. (7) and (8) are used. The layer that is calculated for its group pile bearing capacity is only the layer that is selected to later be used as the bottom end of the pile for this foundation, where the criteria that must be met are not only that the layer is very strong compared to other layers, but also the one closest to the ground surface.

Table 6. Bearing Capacity of BH-05.

Drill Site	Depth	S (m)	m	n	E_g	Q (ton/m^2)	Qgroup (ton/m^2)
BH-01	21	1	3	4	0,657	536,02	422,90
BH-02	18	1	3	5	0,645	460,00	4448,55
BH-05	19,5	1	3	5	0,641	499,68	4710,17

Based on the foundation analysis summarized on table 6, at the BH-01 site, the most optimal layer to support the foundation is the conglomerate layer at a depth of 21 meters, with a single pile bearing capacity of 536.02 ton/m^2, and with a 3-column and 4-row pile configuration having a bearing capacity of 4224.9 ton/m^2. At BH-02 site, the most optimal layer is the coal seam at a depth of 18 meters, with a single pile bearing capacity of 460 ton/m^2, and with a 3-column and 4-row pile configuration having a carrying capacity of 4448.55 ton/m^2. At BH-05 site, the most optimal layer is the conglomerate layer at a depth of 19.5 meters with a single pile bearing capacity of 499.68 ton/m^2, and with a 3 column and 4-row pile configuration having a bearing capacity of 4710.17 ton/m^2.

4 CONCLUSION

It can be concluded that the value of the bearing capacity of the research area for each layer for the N-SPT data, with pile foundation diameter of 0,4 m, the deeper it is, the higher bearing capacity tends to be, with the highest bearing capacity values with N-SPT data ranging from 460 to 643 ton/m^2 at a depth of 18 to 25 meters, namely in the conglomerate on the BH-01, and coal seams on BH-03 and BH-05.

Based the bearing capacity analysis using the N-SPT data, it is found that the design of the pile group foundation is different at each drill point, namely at the BH-01 site on the conglomerate layer that as deep as 21 meters with 3 columns and 4 rows of piles, at the BH-02 site on the coal seam as deep as 18 meters with 3 columns and 5 rows of piles, and at the BH-05 site on the conglomerate layer as deep as 19.5 meters with 3 columns and 5 rows of piles.

REFERENCES

AASHTO (2017) LRFD Highway Bridge Design Specifications 8th Edition. *American Association of State Highway and Transportation Officials*. Washington, D.C.

Anonymous. (2008). SNI 4153: 2008 *Cara Uji Penetrasi Lapangan dengan SPT.* Jakarta: Badan Standardisasi Nasional.

Anonymous. (2017). SNI 8460: 2017 *Persyaratan Perancangan Geoteknik.* Jakarta: Badan Standardisasi Nasional.

Baban, T. M. 2016. *Shallow Foundations*. John Wiley & Sons.

Bowles, L. E. 1997. *Foundation Analysis and Design*. McGraw-Hill.

Brunning, R. 2001. The Somerset Levels. *Current Archaeology* 15(4), 139-143.

Brunning, R., Bronk Ramsey, C., Cameron, N., Cook, G. T., Davies, P., Gale, R., & Kenward, H. 2012. Somerset's Peatland Archaeology: Managing and Investigating a Fragile Resource. Oxbow.

Das, B. M. 2015. *Principles of Foundation Engineering*. Cengage learning.

Fellenius, B. 2017. *Basics of Foundation Design*. Pile Buck International, Sidney, Canada.

Hakam, A., Yuliet, R., & Donal, R. 2010. Studi Pengaruh Penambahan Tanah Lempung pada Tanah Pasir Pantai Terhadap Kekuatan Geser Tanah. *Jurnal Rekayasa Sipil (JRS-Unand)* 6(1): 11-22.

Husain, R. 2015. *Geokimia Mineral Lempung dan Implikasinta terhadap Gerakan Tanah.* Program Pasca Sarjana Universitas Hasanuddin. Makassar.

Meyerhof. GG. 1976. Bearing Capacity and Settlement of Pile Foundations. *Journal of Geotech*. Eng. ASCE, Vol. 102, No. 3: 1–19.

Sowers, G. F. 1979. *Introductory Soil Mechanics and Foundations 4th Edition*:621. New York: Macmillan.

Terzaghi, K. and Peck, R.B. 1967. *Soil Mechanics in Engineering Practice*: 729. New York: John Wiley.

Vidayanti, D., Simatupang, P. T., & Silalahi, S. 2013. Korelasi Nilai N-SPT Dengan Parameter Kuat Geser Tanah Untuk Wilayah Jakarta dan Sekitarnya (133G). *Konferensi Nasional Teknik Sipil* 7:99-107.

Zakaria, Z. 2006. *Daya Dukung Tanah Fondasi Dangkal.* Bandung Laboratorium Geologi Teknik, Jurusan Geologi. *FMIPA UNPAD.*

Pengaruh Getaran Akibat Proses Pemancangan pada Tanah terhadap Bangunan Sekitar

Mochammad Rahadian Yunush
Department of Civil Engineering, Faculty of Civil Engineering and Planning – University of Trisakti
Aksan Kawanda
Department of Civil Engineering, Faculty of Civil Engineering and Planning – University of Trisakti

ABSTRAK: Dalam membangun infrastruktur, pemakaian fondasi tiang pancang sering dilakukan karena memiliki kelebihan. Permasalahan yang dapat ditimbulkan meliputi getaran dan suara bising yang mengakibatkan kerusakan dan menganggu kenyamanan lingkungan disekitar area pemancangan. Getaran yang ditimbulkan akibat pemancangan dapat ditinjau oleh beberapa faktor, yaitu: jarak dan intensitas sumber getaran. Pengukuran getaran diperlukan untuk mengetahui besar sebuah getaran dengan jarak tertentu akibat pemancangan yang merambat melalui tanah terhadap bangunan disekitar. Metode pengukuran getaran yang dilakukan adalah metode Attewel dan Farmer, metode Hechman dan Hagerty, dan J.M. Ko et al. Serta pengukuran menggunakan alat *Vibration Measurement Test*. Hasil pengukuran menunjukkan batas getaran yang dapat diterima oleh bangunan struktur sesuai batas getaran yang ditetapkan.

Kata Kunci: getaran, fondasi tiang pancang, vibration measuring test (VMT), diesel hammer

ABSTRACT: In building the infrastructure, the use of pile foundations are often conducted because it has advantages, but there are also problems in the installation. Problems that can be posed include vibration and noise resulting in damage and disturbing the comfort of the environment around the area of the erection. Vibration caused by the erection can be reviewed by several factors, namely: the distance and the intensity of the vibration source. Vibration measurement is required in order to determine a vibration with a certain distance due to the erection that propagate through the ground to the buildings around. The method of vibration measurement is done Attewel and Farmer, method Hechman and Hagerty, and J.M. Ko et al. As well as the measurement using the tool Vibration Measurement Test. The measurement results show the limits of vibration that can be accepted by the building structure within the limits of the vibration set.

Keywords: vibration, pile foundations, vibration measurement test (VMT), diesel hammer

1 PENDAHULUAN

Konstruksi ialah sebuah aktivitas membangun sarana dan prasarana. Dalam membangun suatu prasarana, diperlukan fondasi yang kuat untuk menopang beban yang ada diatas bangunan tersebut. Jenis fondasi yang umum dipakai di Indonesia ialah fondasi tiang pancang. Fondasi tiang pancang memiliki banyak kelebihan, seperti pengerjaannya yang mudah, kualitas dan mutu terjamin serta waktu pelaksanaannya relatif cepat dibandingkan pelaksanaan jenis fondasi lain. Tetapi dalam pelaksanaannya banyak dapat menimbulkan permasalahan apabila dilakukan dilokasi pemukiman padat penduduk.

Permasalahan yang dapat ditimbulkan meliputi getaran dan suara bising yang mengakibatkan kerusakan dan menganggu kenyamanan lingkungan disekitar area pemancangan. Getaran yang ditimbulkan akibat pemancangan dapat ditinjau oleh beberapa faktor, yaitu: jarak dan intensitas sumber getaran. Sehingga getaran dapat menyebabkan dampak yang berbeda tergantungjenis tanah dan kedalaman tanah area pemancangan serta jarak titik lokasi pemancangan yang menjadi sumber getaran terhadap bangunan disekitarnya.

2 TINJAUAN PUSTAKA

2.1 *Getaran*

Getaran merupakan sebuah gerakan yang berulang-ulang pada jarak waktu tertentu. Getaran berhubungan dengan gerak osilasi dari sebuah barang dan gaya yang berkaitan dengan gerak barangnya. Tiap barang mempunyai massa dan nilai elastisitas akan terjadi getaran ketika diimplementasikan pada sebuah gaya, contohnya dalam konstruksi mesin dan struktur rekayasa kerap kali terjadi fenomena getaran hingga derajat tertentu.

2.2 *Gelombang*

Gelombang merupakan getaran yang merambat. Diantara gelombang yang terdapat dalam sebuah kejadian yakni gelombang mekanik, gelombang mekanik ialah gelombang yang dalam perpindahannya memerlukan perantara. Perantara bisa berbentuk benda padat, cair dan gas. Besaran yang dipergunakan untuk mendeskripsikan gelombang yakni panjang gelombang (λ) yaitu jarak antara dua puncak yang urut, frekuensi (f) ialah jumlag gelombang yang melalui sebuah titik tiap satuan waktu, periode (T) ialah waktu yang dibutuhkan oleh gelombang melalui sebuah titik, amplitudo (A) ialah simpangan maksimum dari titik setimbang, kecepatan gelombang (v) ialah kecepatan yang mana puncak gelombangnya bergerak.

2.3 *Getaran Tanah*

Getaran tanah dapat dihasilkan oleh adanya kegiatan konstruksi. Kegiatan konstruksi seperti pemasangan fondasi tiang pancang menjadi salah satu yang dapat menimbulkan getaran. Getaran merambat dari peralatan konstruksi melalui tanah ke penerima sensor getaran jarak yang jauh terutama melalui gelombang permukaan dan yang kedua oleh gelombang benda (Amick & Gendreau, 2000). Amplitudo gelombang berkurang dengan jarak dari sumber getarannya. Redaman ini disebabkan oleh dua faktor: perluasan muka gelombang (redaman geometris) dan disipasi energi di dalam tanah (redaman material).

2.4 *Fondasi Tiang Pancang*

Fondasi tiang pancang merupakan bagian dari struktur yang berguna untuk menyalurkan dan menerima beban dari struktur atas ke tanah degan tertentu. Fondasi tiang pancang memiliki bahan utama yang terdiri dari kayu, baja dan beton, Bowles (2005). Seperti tipe fondasi lain, tujuannya fondasi tiang ialah untuk mendistribusikan fondasi ke tanah keras, dan sebagai penahan beban vertikal, lateral, uplift.

2.4.1 Alat Tiang Pancang

Menurut Rohmanhadi (1992), terdapat beberapa tipe alat pancang yang bisa dipergunakan untuk memancang tiang pancang, seperti *drop hammer, single acting hammer, double acting hammer, differential hammer* dan *diesel hammer*. Tipe pancang *drop hammer* mempunyai kecepatan pukulan yang rendah maka jarang dipergunakan kecuali untuk jumlah tiangnya tidak banyak. Pada pemancangan tiang beton umumnya menggunakan *diesel hammer* dikarenakan kinerja paling sederhana diantara alat pancang lainnya.

2.4.2 Diesel Hammer

Diesel Hammer ialah alat pancang yang sangat simpel dari alat pancang lainnya. Yakni berbentuk silinder dengan piston atau ram yang fungsinya untuk memberi tekanan pada tiang pancang. Disamping itu, ada 2 mesin diesel yang menjadi penggerak piston ini. Sewaktu bekerja, mesin diesel akan menekan udara dalam silinder. Penambahan tekanan udara ini akan menggerakan piston sehingga memukul tiang pancangnya.

2.5 *Uji Vibrasi*

Uji vibrasi dilakukan dengan menggunakan *Nomis Mini Supergraph II* ialah pengukur getaran atau alat analisis perangkat elektronik yang bisa memproses sinyal getaran. Pengujian ini memperoleh data seperti kecepatan, percepatan dan simpangan pada getaran.

Peralatan uji vibrasi, *Vibration Measurement Test* (VMT) ini mencakup beberapa komponen, yaitu:

1. Terdiri dari satu monitor LCD.
2. Satu kabel pendeteksi suara
3. Satu kabel pendeteksi suara yang dihubungkan ke *triaxial geophone*.

Peralatan tambahan seperti meteran rol dan cangkul.

2.6 *Analisis Getaran Akibat Pemancangan Dengan Metode Empiris*, Rahardjo (2017)

2.6.1 Metode Attewel dan Farmer (1973)

$$V = K\sqrt{\frac{W_b}{R}} \quad (1)$$

Dengan,
V = Kecepatan partikel (mm/s)
K = Suatu Konstanta (0,25 – 1,50), sering diambil = 0,75
W_b = Energi (joules)
R = Jarak (m)

2.6.2 Metode Hechman dan Hagerty (1978)

$$V = K\sqrt{\frac{W_b}{R}} \quad (2)$$

Dengan,
V = Kecepatan partikel (mm/s)
K = Suatu Konstanta dimana nilai K tergantung dari besaran ($\frac{E.A}{C}$)
E = Modulus elastis
A = Luas Penampang
W_b = Energi (joules)

2.6.3 Metode J.M Ko et al (1990)

$$V = 70\sqrt{\frac{1}{R}\cdot exp[-\mathrm{a}\cdot(R-1)]} \quad (3)$$

Dengan,
V = Kecepatan partikel (mm/s)
a = Koefisien Atenuasi
R = Jarak (m)

2.7 *Standar Uji Getaran*

Pada sejumlah negara sudah mempunyai standar bangunan untuk menghindari kerusakan karena getaran dari pemancangan misalnya DIN 4150 (Jerman). Berikut merupakan tabel standar uji getar DIN 4150- 3:

Tabel 1. Standar Uji Getaran DIN 4150-3(Deutsches Institut fur Normung, 1999).

Line	Type of structure	Guideline values for velocity, v_i , in mm/s			
		Vibration at the foundation at a frequency of			Vibration at horizontal plane of highest floor at all frequencies
		1 Hz to 10 Hz	10 Hz to 50 Hz	50 Hz to 100 Hz *)	
1	Buildings used for commercial purposes, Industrial buildings, and buildings of similar design	20	20 to 40	40 to 50	40
2	Dwellings and buildings of similar design and/or occupancy	5	5 to 15	15 to 20	15
3	Structures that, because of their sensitivity to vibration, cannot be classified under lines 1 and 2 and are of great intrinsic value (e.g., listed buildings under preservation order)	3	3 to 8	8 to 10	8

*) At frequencies above 100 Hz, the values given in this column may be used as minimum values.

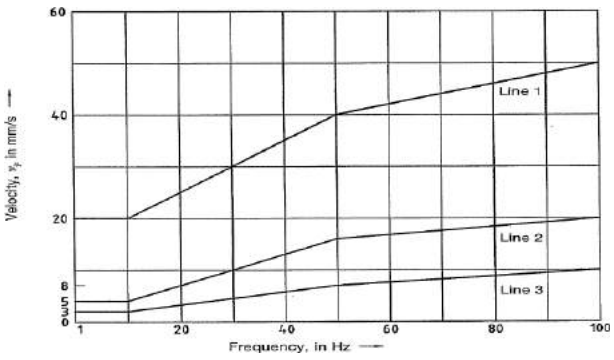

Gbr. 1. Kurva Standar Uji Getaran pada Tabel 1 (Deutsches Institut fur Normung, 1999).

3 METODE

Dalam pengujian ini, proses yang dilakukan terlebih dahulu adalah dengan melakukan pengujian getaran akibat pemancangan di lapangan dengan jarak tertentu. Pada pengujian dilapangan didapat juga data pendukung seperti, data *hammer*. Data pengujian getaran dilapangan kemudian di bandingkan dengan perhitungan metode empiris, yaitu Metode Attewel dan Farmer, Metode Hechman dan Hagerty dan Metode J.M Ko et al. Setelah dilakukan perhitungan, hasil perbandingan

antara perhitungan menggunakan metode empiris dengan pengujian getaran di lapangan untuk menentukan hasil pengujian mana yang lebih efisien.

4 PEMBAHASAN

4.1 *Analisis Data Tanah*

Dalam melakukan penelitian ini, dibutuhkan data dari hasil pengujian tanah. pengujian yang didapat berupa data *Standard Penetration Test* (SPT). Data SPT dapat digunakan dalam menentukan klasifikasi jenis tanah.

Tabel 2. Data N-SPT.

Depth (m)	N-SPT	Depth (m)	N-SPT	Depth (m)	N-SPT
2	4	24	13	48	27
4	3	26	15	50	25
6	0	28	16	52	26
8	0	30	14	54	31
10	0	32	26	56	29
12	0	34	27	58	31
14	1	36	32	60	38
16	13	38	60	62	44
18	12	40	60	64	46
20	9	42	60	66	47
22	14	44	32	68	41
		46	28	70	45

4.2 *Data Hammer*

Dalam pengukuran getaran di lapangan, mesin pancang yang digunakan yaitu *diesel hammer*. Tipe alat pancang *diesel hammer* tersebut memiliki spesifikasi seperti di Tabel 3.

Tabel 3. Spesifikasi Tipe *Hammer*.

Hammer Type	Ram Weight (kN)	Maximum Stroke (m)	Maximum Energy (kNm)	Pressure (kPa)	Effici-ency
Juwei DD65	63,73	2,97	189,274	10	0,7

Tabel 4. Hasil Perhitungan PPV dengan Variasi Kedalaman menggunakan Metode Empiris.

Jarak dari Sumber Getar (m)	PPV (mm/s)		
	Attewel & Farmer (1973)	Heckman &Hagerty (1978)	J.M.Ko et al. (1990)
4	10,318	18,160	26,006
8	7,296	12,841	12,376
16	5,159	9,080	3,964

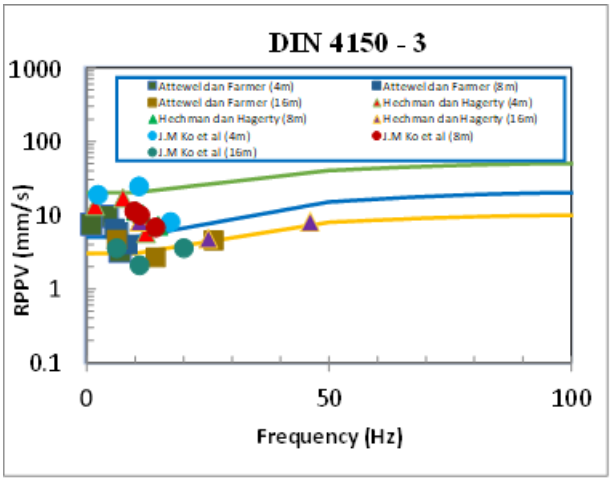

Gbr. 2. Kurva PPV menggunakan Metode Empiris.

4.3 *Pengumpulan Data Vibration Measurement Test (VMT)*

Dalam penetlitian ini, peneliti menggunakan alat pengukur *Vibration Meter Test* (VMT) untuk kecepatan getaran yang di hasilkan dalam kegiatan pemancangan. Hasil pengukuran disajikan sebagai *Particle Peak Velocity* (mm/s) *Frequency* (Hz). Berdasarkan DIN 4150-3, nilai-nilai ini dapat ditoleransi yang disebabkan oleh sumber yang mempengaruhi struktur yang ada. Batas toleransi ditunjukkan seperti pada Tabel 4.

Tabel 5. Hasil Monitoring Getaran.

Lokasi	Sumber Getaran	Jarak (m)	Maks. RPPV (mm/s)
J8A1 No.8	P1	4	22,295
		8	10,167
		16	2,999
J8A1 No.7	P2	4	17,729
		8	6,483
		16	3,262
J8A1 No.12	P3	4	18,194
		8	9,353
		16	3,536
J8A1 No.11	P4	4	12,399
		8	9,484

Lokasi	Sumber Getaran	Jarak (m)	Maks. RPPV (mm/s)
		16	3,066
J8A1 No.15	P5	4	13,383
		8	5,812
		16	3,999
J8A1 No.10	P6	4	17,366
		8	5,64
		16	3,055
J8A1 No.14	P7	4	19,16
		8	9,175
		16	2,826
J8A1 No.18	P8	4	23,205
		8	5,384
		16	2,276
J8A1 No.13	P9	4	25,852
		8	8,857
		16	3,978
J8A1 No.17	P10	4	20,524
		8	9,749
		16	2,814
J8A1 No.21	P11	4	28,634
		8	12,262
		16	3,506
J8A1 No.16	P12	4	14,191
		8	9,759
		16	3,383
J8A1 No.20	P13	4	14,664
		8	7,967
		16	3,793
J8A1 No.26	P21	4	10,274
		8	6,862
		16	2,963
J8A1 No.22	P22	4	39,897
		8	13,529
		16	4,539
J8A1 No.29	P23	4	32,317
		8	13,919
		16	4,928
	P24	4	23,139
J8A1 No.25		8	6,025
		16	5,172
J8A1 No.35	P25	4	23,268
		8	12,242
		16	4,564
J8A1 No.32	P26	4	28,651
		8	7,564
		16	5,828
J8A1 No.34	P27	4	34,097
		8	10,052
		16	5,551
J8A1 No.31	P28	4	36,158
		8	12,623
		16	5,472

Pengukuran getaran dilakukan pada 28 titik pemancangan. Jarak pengukuran yang diuji dilakukan pada jarak 4 m, 8 m dan 16 m.

Pada monitoring getaran di jarak 4 m, besar getaran berada diantara batas atas garis jingga (bangunan industri) dan batas bawah garis abu-abu (bangunan perumahan). Hal tersebut dapat dilihat pada Gbr. 3.

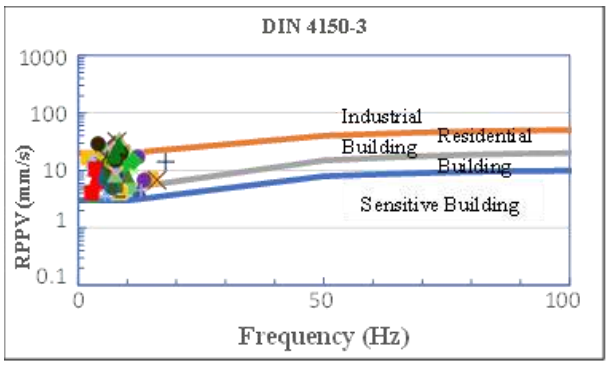

Gbr. 3. Kurva Monitoring Getaran dengan Jarak 4 m.

Pada monitoring getaran di jarak 8 m, besar getaran melebihi batas getaran yang dapat diterima bangunan perumahan (garis abu-abu) tetapi tidak melebih batas getaran yang dapat diterima bangunan industri (garis jingga). Hal tersebut dapat dilihat pada Gbr. 4.

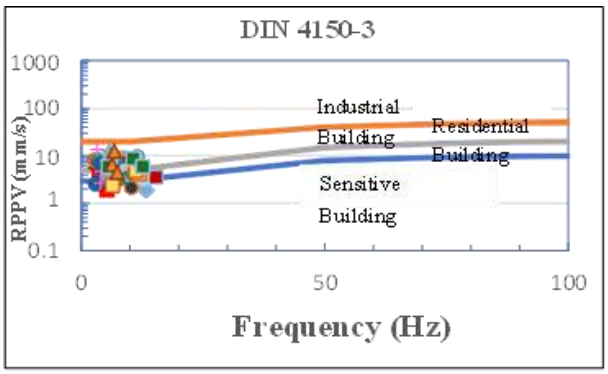

Gbr. 4. Kurva Monitoring Getaran dengan Jarak 8 m.

Pada monitoring di jarak 16 m, Sebagian getaran berada di batas bawah garis biru (bangunan sensitif). Seperti yang dilihat pada Gbr. 5.

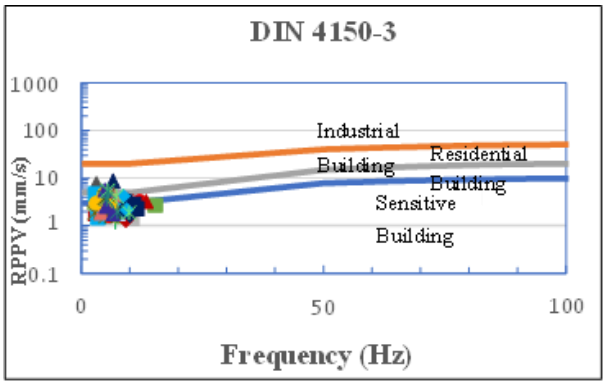

Gbr. 5. Kurva Monitoring Getaran dengan Jarak 16 m.

5 KESIMPULAN

1. Pada Metode Attewel dan Farmer serta metode Hechman dan Hagerty terjadi penurunan masing masing 29,29 % dari jarak 4 m ke 8 m dan jarak 8 m ke 16 m. Sedangkan metode J.M Ko et al terjadi penurunan kecepatan getaran sebesar 52,41% dari jarak 4 m ke 8 m dan dari jarak 8 m ke 16 m sebesar 67,97%.
2. Pada jarak 16 m, berdasarkan metode analisis sebagian besar getaran berada dibawah batas bangunan sensitive hingga batas bangunan perumahan. Kecuali metode Hechman dan Hagerty. Sedangkan menurut pengujian dilapangan, Sebagian besar getaran pada jarak 16 m berada diantara Batasan bawah bangunan sensitif hingga dibawah Batasan bangunan perumahan berdasarkan standar uji getaran DIN 4150-3.
3. Pada pengukuran getaran di lapangan, penurunan maksimum terjadi pada jarak 4 m ke jarak 8 m sebesar 76,80%. Dan penurunan getaran minimum sebesar 6,71% pada jarak 8 m ke jarak 16 m.

DAFTAR PUSTAKA

Amick, H., & Gendreau, M. 2000. *Construction Vibrations and Their Impact on Vibration- Sensitive Facilities*. Proceedings of Construction Congress VI: Building Together for a Better Tomorrow in an Increasingly Complex World, 278(Asce): 758–767. https://doi.org/10.1061/40475(278)80

Bowles, J. E. 2005. *Analisis Dan Desain Pondasi II*. Jakarta: Erlangga 2: 474.

Deutsches Institut fur Normung. 1999. DIN 4150- 3:1999 *Structural Vibration - Part 3: Effects of Vibration on Structures*.

Rahardjo, P. P. 2017. *Manual Pondasi Tiang 5th Ed*. Deep Foundation Research Institute (DFRI).

Rohmanhadi. 1992. *Alat Berat dan Penggunaannya*. 40.

Perancangan *Secant Pile* dengan Perkuatan *Ground Anchor*

Farhan Azfiansyah Yazid
Department of Civil Engineering, Faculty of Civil Engineering and Planning – University of Trisakti
Aksan Kawanda
Department of Civil Engineering, Faculty of Civil Engineering and Planning – University of Trisakti

ABSTRAK: Maraknya pembangunan gedung di kondisi lahan yang sempit membuat basement menjadi salah satu solusi terbaik agar para pengunjung tetap merasa nyaman. Oleh karena itu, dinding penahan tanah diperuntukan agar tanah di sekitar gedung terutama di bagian basement tidak tergelincir atau longsor. Metode ground anchor merupakan metode yang paling umum digunakan untuk dijadikan perkuatan dinding penahan tanah. Tahap pertama yang harus dilakukan adalah menganalisis data tanah yang didapat agar mendapatkan nilai-nilai yang dibutuhkan dalam proses perhitungan. Setelahnya, dilanjutkan dengan tahap perhitungan dengan teori free earth method. Lalu dilanjutkan perancangan menggunakan aplikasi GEO5 slope stability dan GEO5 sheeting check. Hasil perancangan menunjukan bahwa pengunaan secant pile sebagai dinding penahan tanah dan ground anchor sebagai perkuatan dinding penahan tanah efektif meningkatkan nilai faktor keamanan.

Kata kunci: dinding penahan tanah, ground anchor, geo5

ABSTRACT: The rise of building construction in a narrow land condition makes basement as one of the best solutions so that visitors still feel comfortable. Therefore, the retaining wall is intended so that the soil around the building, especially in the basement does not slip or slide. Ground anchor method is the primary method where people use it as retaining wall excitation. First thing in design of retaining wall is analyze the soil data so we can get the data for the designing phase by using free earth method theory. Then, we use GEO5 slope stability and GEO5 sheeting check after designing manually. The result of the design will show that using secant pile as a retaining wall and ground anchor as excitation effectively increasing the safety factor of the area.

Keywords: retaining wall, ground anchor, geo5

1 PENDAHULUAN

Perkembangan pembangunan semakin berkembang setiap tahunnya. Di lahan Jakarta yang kecil dengan pembangunan yang semakin meningkat dari tahun ke tahunnya membuat *basement* menjadi salah satu solusi terbaik agar pengunjung tetap merasa nyaman. *Basement* memiliki fungsi yang beragam. Namun, di penelitian ini penulis akan membahas *basement* yang diperuntukan sebagai tempat parkir. Dikarenakan *basement* terletak di bawah tanah suatu bangunan sehingga dibutuhkan suatu konstruksi yang dapat menahan tanah disekitarnya, maka dari itu menggunakan dinding penahan tanah merupakan solusi dari hal-hal tersebut. Pada proyek gedung bertingkat banyak menggunakan jenis dinding penahan tanah *secant pile*, alasan menggunakan *secant pile* dikarenakan *secant pile* adalah dinding penahan tanah yang kedap air. Sedangkan sistem perkuatan *secant pile* sudah banyak pilihan, tetapi sistem perkuatan yang sering digunakan yaitu *ground anchor*. Sehingga pada perancangan ini digunakan *secant pile* sebagai dinding penahan tanah dan *ground anchor* sebagai sistem perkuatan.

Perancangan ini ditujukan untuk merancang *secant pile* dengan sistem perkuatan *ground anchor*. Ruang lingkup pembahasan dalam perancangan ini adalah:

1. Pembahasan difokuskan pada perancangan *secant pile* dengan sistem perkuatan *ground anchor*.
2. Tidak memperhitungkan beban gempa.
3. Tidak memperhitungkan biaya.

2 TINJAUAN PUSTAKA

2.1 *Dinding Penahan Tanah*

Dinding Penahan Tanah adalah sebuah konstruksi yang digunakan untuk menahan tekanan tanah lateral dan memberikan kestabilitasan pada suatu lereng yang disebabkan oleh tanah urug atau tanah asli. Dinding penahan tanah memiliki banyak jenis, tetapi pada perancangan kali ini dinding penahan tanah yang digunakan adalah dinding penahan tanah yang diperuntukan untuk galian dalam. Jenis dari dinding penahan tanah untuk galian dalam pun beragam tetapi *secant pile* merupakan dinding penahan tanah yang paling cocok untuk perancangan ini. Alasan *secant pile* adalah dinding penahan tanah yang paling cocok karena *secant pile* adalah dinding penahan tanah yang kedap air dan pemasangan *secant pile* tidak menganggu lingkungan sekitar.

2.2 *Sistem Perkuatan*

Agar fungsi dari dinding penahan tanah bekerja secara optimal, diberikanlah sistem perkuatan. Sistem perkuatan dinding penahan tanah memiliki banyak jenis tetapi yang paling sering digunakan adalah *ground anchor*. *Ground anchor* adalah suatu elemen struktur yang digunakan untuk membantu dinding penahan tanah dalam menahan beban dan gaya yang ditahannya, elemen batu dan pasir yang berada di *ground anchor* berfungsi untuk mentransmisikan beban tarik yang diterapkan ke dalam tanah dan dapat menahan beban lateral dari timbunan tanah di belakang dinding penahan tanah. Alasan digunakannya *ground anchor* yaitu karena dapat mempercepat proses konstruksi.

2.3 *Analisis Stabilitas Galian Dalam*

Sebelum proses galian dalam dimulai, SNI 8460:2017 menyarankan bahwa tanah yang akan digunakan untuk galian dalam harus terbebas dari 3 bahaya. Bahaya tersebut berupa:

- *Basal Heave*

Basal Heave termasuk analisis keruntuhan geser menyeluruh pada suatu dinding penahan tanah. Bahaya basal heave terjadi karena mengalirnya tanah ke dalam galian sebagai akibat terganggunya kesetimbangan daya dukung tanah pada level ujung bawah dinding penahan tanah. Terdapat beberapa rumus dalam memeriksa bahaya basal heave, tetapi untuk perancangan kali ini, perancang menggunakan rumus dari Terzaghi. Berikut adalah rumusnya:

$$F_b = \frac{1}{He} \times \frac{5{,}7 \times S_u}{\gamma - (\frac{S_u}{D})} \geq 1.25 \qquad (1)$$

- Pergolakan atau *Upheaval*

Pergolakan atau upheavel adalah suatu kejadian yang dimana lapisan tanah memiliki perbedaan jenis seperti tanah permeabilitas berada dibawah tanah tidak permeabilitas, tanah tidak permeabilitas mempunyai kecenderungan untuk terangkat karen tekanan air dari tanah permeabilitas. Oleh karena itu, diperlukannya pemeriksaan akan bahaya ini. Rumus dari pemeriksaan bahaya ini adalah:

$$F_{up} = \frac{\Sigma \gamma ti.hi}{Hw.\gamma w} \geq 1.25 \qquad (2)$$

- *Sand boiling*

Sand Boiling merupakan suatu kejadian dimana aliran air naik keatas dan menyebabkan tekanan efektif ditengah lapisan tanah menjadi 0 dan tidak mampu menahan beban. Biasanya kejadian ini terjdai di zona pasif. Menurut Terzaghi (1922), mengatakan bahwa bedasarkan beberapa test jarak biasanya kejadian ini terjadi di jarak Hp/2 dari dasar dinding penahan tanah. Rumus dari pemeriksaan bahaya ini adalah:

$$F_s = \frac{\gamma' (He.\ 2Hp\text{-}di\text{-}dj)}{\gamma w \Delta Hw} \qquad (3)$$

2.4 *GEO5*

GEO5 adalah suatu aplikasi geoteknik yang sangat mudah dimengerti untuk menyelesaikan permasalahan geoteknik. GEO5 memiliki banyak macam. GEO5 yang dipakai oleh perancangan kali ini adalah GEO5 *slope stability* dan GEO5 *sheeting check*.

3 RENCANA PERANCANGAN

Pada perancangan ini akan direncanakan sebuah *basement* 2 lantai dengan ketinggian masing-masing lantai setinggi 3 m. *Basement* ini direncanakan akan memiliki lebar sebesar 30 m dan panjang 30 m pada setiap lantainya. Titik *ground anchor* akan direncanakan 2 m dibawah permukaan tanah. Lalu rencana *basement* ini Perancangan *basement* ini mencakup 2 titik *boring hole* yang memiliki lapisan tanah yang berbeda. Titik *boring hole* yang digunakan sebagai acuan adalah *boring hole* 10 dan *boring hole* 11. Pada saat perancangan ditambahkan beban diatas permukaan tanah sebebsar 10kN/m beban itu dianggap beban konstruksi yang sedang bekerja diatas permukaan tanah.

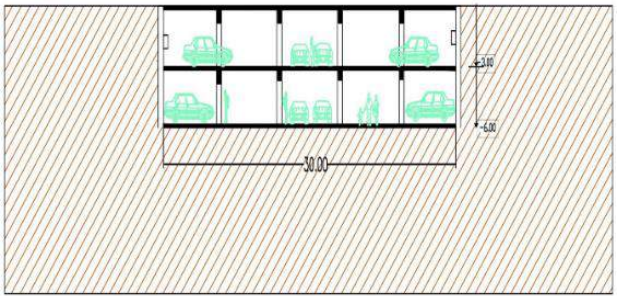

Gbr. 1. Rencana *Basement.*

4 PROSES PERANCANGAN

4.1 *Pengumpulan Parameter Tanah*

4.1.1 Pengumpulan data tanah

Pengumpulan data tanah ini bertujuan agar mempermudah saat perancangan. Data tanah biasanya didapatkan dari hasil uji lapangan. Data yang didapatkan biasanya nilai N-SPT perlapisan tanah.

- Titik BH10

Tabel 1. Data nilai N-SPT titik BH10.

Jenis Tanah	Kedalaman	N-SPT
Lanau Berpasir	0 – 1,5 m	1
Lanau Kelempungan	1,5 – 4,5 m	4
Pasir Berlanau	4,5 – 7,5 m	15
Lanau Kelempungan	7,5 – 10,5 m	24

- Titik BH11

Tabel 2. Data nilai N-SPT titik BH11

Jenis Tanah	Kedalaman	N-SPT
Lanau Kelempungan	0 – 3 m	8
Lanau Berpasir	3 – 4,5 m	8
Pasir Berlanau	4,5 – 6 m	2
Lanau Kelempungan	7,5 – 10,5 m	34

- Parameter Tanah yang Digunakan
  - Berat Jenis Tanah (γ)
  - Berat Jenis Tanah Jenuh (γSAT)
  - Nilai Sudut Geser (ϕ^*)
  - Nilai Kohesi (c)
  - Nilai Kuat Geser pada Tegangan Efektif (C')
  - Nilai Friksi (δ)
  - Nilai Poisson's ratio
  - Nilai Eodometric modulus (E_{eoff})

- Cara Menginput parameter tanah pada perhitungan

  a. Pada Perhitungan Manual
  Pada perhitungan manual, parameter tanah diinput menyesuaikan dengan rumusan perhitungan yang digunakan.

  b. Pada GEO5
  Menginput parameter data tanah sangat penting pada penggunaan aplikasi GEO5. Untuk memasukan parameter data tanah, penulis menggunakan fitur *soils*. Pada fitur tersebut diminta beberapa parameter yang bertujuan untuk membantu perancangan.

4.1.2 Stratigrafi Tanah

Stratigrafi merupakan gambaran yang mencakup lapisan-lapisan tanah yang tersusun sedemikian rupa, data yang digunakan umumnya berupa data N-SPT melalui *boring log* atau memakai pendekatan statistik sederhana.

4.1.3 Melengkapi Data Tanah

Sebelum perancangan dimulai, data tanah yang dibutuhkan harus dilengkapi terlebih dahulu. Untuk data tanah yang tidak didapati dari uji lapangan dapat menggunakan beberapa tabel korelasi.

4.2 *Perhitungan Manual*

Perhitungan manual ini menggunakan teori *free earth support method*. *Free earth support method* atau metode tanah bebas adalah metode yang mengasumsikan bahwa kedalaman turap tidak mencapai tanah keras sehingga ujung bawah turap tidak cukup kaku dan dapat berotasi. Kedalaman turap dibawah dasar galian dianggap tidak cukup untuk menahan tekanan tanah yang terjadi pada bagian atas dinding turap. Langkah-langkah perhitungan manual seperti berikut:

a. Menentukan nilai Ka dan Kp.
b. Menentukan nilai tegangan perlapisan tanah.
c. Menentukan panjang dari tegangan aktif dibawah galian.
d. Mencari nilai P dan nilai momen di titik D.
e. Mencari panjang dari tegangan aktif dibawah galian ke nilai P.
f. Mencari panjang dari tegangan pasif dibawah galian.
g. Mencari kedalaman dinding penahan tanah.
h. Mencari nilai gaya tarik angkur.
i. Mencari panjang free length dan fixed length.
j. Mencari jarak momen maksimum pada gaya geser = 0
k. Mencari nilai momen maksimum

4.3 *Perancangan menggunakan aplikasi GEO5*

4.3.1 GEO5 *Slope Stability*

GEO5 *slope stability* digunakan untuk mendapatkan faktor keamaan galian tanpa adanya dinding penahan tanah dan perkuatannya.

4.3.2 GEO5 *Sheeting Check*

GEO5 *sheeting check* digunakan untuk memeriksa apakah hasil perancangan sebelumnya sudah layak digunakan atau belum.

5 HASIL PERANCANGAN

5.1 *Titik BH10*

5.1.1 Analisis stabilitas galian

- *Basal Heave*
  $F_b = 5.2615 > 1.25$
- *Upheavel*
  $F_{up} = 1.5939 > 1.25$
- *Sand boiling*
  $F_s = 6.81 > 1.5$

5.1.2 Kedalaman dan dimensi

Setelah dilakukan perancangan menggunakan perhitungan manual dan pemeriksaan menggunakan aplikasi dan GEO5 *sheeting check* didapati kedalaman dinding penahan tanah pada titik BH10 sedalam 12 m dengan dimaeter dinding penahan tanah sebesar 0,8 m dan tulangan 8D19 dengan tebal selimut 75 mm.

5.1.3 Data angkur

- Kekuatan angkur = 90 kN
- Kemiringan angkur = 30°
- Panjang free length = 8,5 m
- Panjang fixed length = 3 m
- Diameter lubang = 200 mm

5.1.4 Nilai faktor keamanan galian

Dengan menggunakan aplikasi GEO5 *slope stability* didapati nilai faktor keamanan titik BH10 sebesar 0,47.

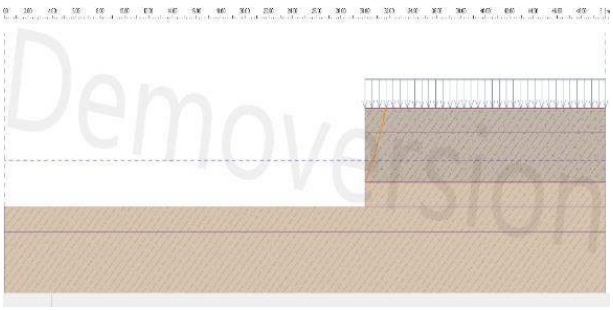

Gbr. 2. Galian dalam di Titik BH10 tanpa DPT dan Angkur.

5.1.5 Nilai faktor keamanan galian dengan dinding penahan tanah dan sistem perkuatan

Dengan menggunakan aplikasi GEO5 *sheeting check* lalu memasukan data-data tanah dan dinding penahan tanah sebelumnya, lalu didapati beberapa nilai seperti *bending moment, shear force, displacement* dan faktor keamanan. Berikut adalah nilai-nilai pada titik BH10:

- *Bending Moment*

Nilai *Bending moment* maksimum sebesar 102,52 kN/m

- *Shear force*

Nilai *shear force* maksimum sebesar 67,09 kN/m

- *Displacement*

Nilai *displacement* maksimum sebesar 16.5 mm. Menurut Chang Yu Ou (2006), displacement bisa di estimasi dengan rumus:

$$\delta_{hm} = (0{,}2 - 0{,}5\%)\ He \quad (4)$$

$$= \frac{0.5}{100} \times 6\ \text{m}$$

$$= 0{,}03\ \text{m} \approx 30\ \text{mm}$$

Sehingga *displacement* yang dihasilkan memenuhi estimasi yang diperkirakan.

- Faktor keamanan

Nilai faktor keamanan meningkat menjadi 1.94

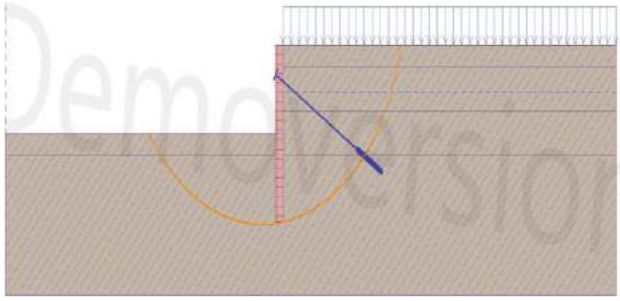

Gbr. 3. Galian dalam setelah Adanya DPT dan Angkur.

5.2 *Titik BH11*

5.2.1 Analisis stabilitas galian

- *Basal Heave*
  Fb = 6,6827 > 1,25
- *Upheaval*
  Fup = 2,4658 > 1,25
- *Sand boiling*
  Fs = 4,4169 > 1,5

5.2.2 Kedalaman dan dimensi

Untuk titik BH11 didapati kedalaman turap sedalam 10,5 m dengan diameter dinding penahan tanah sebesar 0,8 m dan tulangan 8D19 dengan tebal selimut 75 mm.

5.2.3 Data angkur

- Kekuatan angkur = 90 kN
- Kemiringan angkur = 30°
- Panjang *free length* = 8,5 m
- Panjang *fixed length* = 3 m
- Diameter lubang = 200 mm

5.2.4 Nilai faktor keamanan galian

Untuk faktor keamanan galian di titik BH11 didapat sebesar 0,59 dengan menggunakan aplikasi GEO5 *slope stability*.

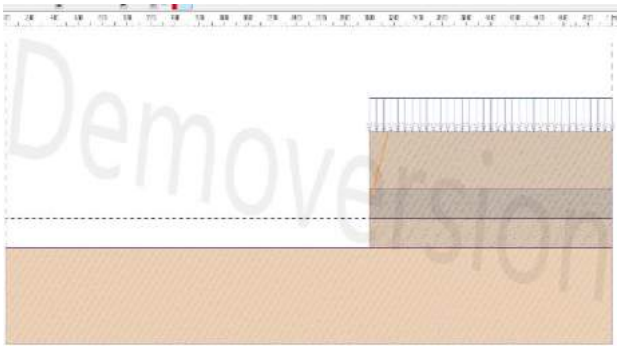

Gbr. 4. Galian dalam di Titik BH11 Tanpa DPT dan Angkur.

5.2.5 Nilai faktor keamanan galian dengan dinding penahan tanah dan sistem perkuatan

Untuk titik BH11 faktor keamanan yang didapati setelah menggunakan dinding penahan tanah dan sistem perkuatan yang diguanakan meningkat. Dengan menggunakan GEO5 *sheeting check* didapati nilai *bending moment*, *shear force*, *displacement* dan faktor keamanan. Berikut adalah nilai-nilai pada titik BH11:

- *Bending Moment*

Nilai *Bending moment* maksimum sebesar 102,52 kN/m

- *Shear force*

Nilai *shear force* maksimum sebesar 67,09 kN/m

- *Displacement*

Nilai *displacement* maksimum sebesar 16,5 mm. Menurut Chang Yu Ou (2006), *displacement* bisa di estimasi dengan rumus:

$$\delta_{hm} = (0{,}2 - 0{,}5\%)\ He \quad (5)$$

$$= \frac{0.5}{100} \times 6\ \text{m}$$

$$= 0{,}03\ \text{m} \approx 30\ \text{mm}$$

Sehingga *displacement* yang dihasilkan memenuhi estimasi yang diperkirakan.

- Faktor keamanan

Nilai faktor keamanan meningkat menjadi 1,85

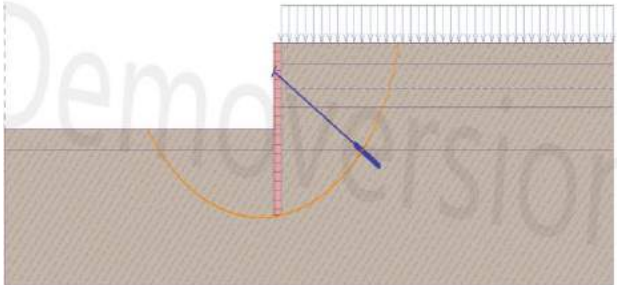

Gbr. 5. Galian dalam di Titik BH11 setelah Adanya DPT dan Angkur.

6 KESIMPULAN

1. Kedua titik telah terbebas dari 3 bahaya yang disebutkan pada SNI 8460:2017 yaitu *basal heave*, *upheaval* dan *sand boiling*. Sehingga kedua titik tersebut bisa dilakukan galian untuk *basement*.
2. Faktor keamanan di kedua titik meningkat. Untuk titik BH10 meningkat dari 0,47 ke 1,94 dan untuk titik BH11 meningkat dari 0,59 ke 1,85.

DAFTAR PUSTAKA

Badan Penelitian dan Pengembangan, Kementrian Pekerjaan Umum dan Perumahan Rakyat, Himpunan Ahli Teknik Tanah Indonesia. 2017. *Persyaratan Perancangan Geoteknik*. Jakarta: Badan Standarisasi Nasional.

Hardiyatmo, H. C. 2011. *Analisis dan Perancangan Fondasi Bagian 1*. Yogyakarta: Universitas Gajah Mada.

Ou, C. Y. 2006. *Deep Excavation Theory and Practice*. London: Taylor and Fracis Group.

Sabatini, P., Pass, D., & Bachus, R. C. 1999. *Geotechincal Engineering Circular No.4, Ground Anchors and Anchored Systems.* Washington, D.C.: Federal Highway Administration.

Tan, Y. 2008. Design of Retaining Wall and Support Systems for Deep Basement Construction–A Malaysian Experience. *Design of Retaining Wall and Support Systems for Deep Basement Construction–A Malaysian Experience*: 28.

Abidin, M. 2003. P*erencanaan Secant Pile Sebagai Dinding Penahan Basement Dengan Menggunakan Program Plaxis v8.2*. Tugas Akhir Universitas Mercu Buana Fakultas Teknik Perencanaan Desain Program Studi Teknik Sipil.

Hardiyatmo, Hary Christady, 2002. *Mekanika Tanah II*. Jakarta: PT. Gramedia Pusaka Utama.

ltd, Fine. "GEO5 User's Guide." *GEO5-Software.bg*, 2018. GEO5-software.bg/support_files/rykovodstvo_na_potrebitelia/GEO5-ug-02-user-s-guide-1.pdf.

Planning and Static and Dynamic Analysis of Operating Basis and Maximum Design Earthquake of Embankment Dam

Alvin Tjahjadi
Department of Civil Engineering – Universitas Pertamina

Wirman Hidayat
Department of Civil Engineering – Universitas Pertamina

Jevania Simanjuntak
Department of Civil Engineering – Universitas Pertamina

ABSTRAK: Kerusakan bendungan akibat gempa bumi merupakan resiko yang dapat terjadi akibat gaya gaya gempa dan kondisi perancangan bendungan yang tidak memenuhi syarat. Wilayah Indonesia yang mempunyai potensi gempa yang tinggi, menjadi faktor yang harus dipertimbangkan dalam perencanaan bendungan. Parameter beban gempa yang digunakan meliputi kondisi *Operating Basis Earthquake* (OBE) untuk menganalisis kemanan bendungan selama umur layan dan *Maximum Design Earthquake* (MDE) untuk menganalisis keamanan bendungan terhadap beban gempa maksimum yang mungkin terjadi. Perhitungan perancangan dan analisis bendungan urugan dilakukan menggunakan metode kesetimbangan batas dengan perangkat lunak GeoStudio dan metode elemen hingga menggunakan perangkat lunak Plaxis 2D dan 3D. Tahap perancangan menghasilkan bendungan tipe urugan 4 zona dengan tinggi dan lebar bendungan sebesar 77 dan 561 meter. Angka keamanan kritis stabilitas lereng yang dihasilkan pada kondisi MDE sebesar 1.055 dari hasil perhitungan GeoStudio, 1.172 dari hasil perhitungan Plaxis 2D, dan 1.449 dari hasil perhitungan Plaxis 3D.

Kata Kunci: bendungan, operating basis earthquake, maximum design earthquake, stabilitas statis, stabilitas dinamis

ABSTRACT: Dam damage due to earthquakes is a risk that can occur due to earthquake forces and dam design conditions that do not meet the requirements. The territory of Indonesia which has a high earthquake potential, is a factor that must be considered in dam planning. The earthquake load parameters used include Operating Basis Earthquake (OBE) conditions to analyze the safety of the dam during its service life and Maximum Design Earthquake (MDE) to analyze the safety of the dam against the maximum earthquake load that may occur. Calculation of the design and analysis of the embankment dam was carried out using the boundary equilibrium method with GeoStudio software and the finite element method using Plaxis 2D and 3D software. The design phase resulted in a 4 zones embankment dam with a height and width of 77 and 561 meters respectively. The critical number of safety for slope stability under MDE conditions is 1,055 by GeoStudio calculation, 1,172 by Plaxis 2D calculation, and 1,449 by Plaxis 3D calculation.

Keywords: dam, operating basis earthquake, maximum design earthquake, static stability, dynamic stability

1 INTRODUCTION

The territory of Indonesia which is located between active tectonic plates has a high earthquake potential, this is a factor that must be considered in dam design. The dam design carried out in this paper is the type of earth embankment or earth fill with criteria including stability and deformation that satisfy the safety requirements in static and dynamic conditions when an earthquake occurs. Basudhar (2010) arguments that the design of the dam as an earth structure, the analysis be made considering the possibility that these may experience severe

seismic acceleration during its service period, so that adequate safety certainty can be made for better performance when an earthquake occurs.

This paper presents the design of the embankment dam which is satisfy the safety requirement when an operating basis earthquake condition and maximum design earthquake condition occur. Operating Basis Earthquake (OBE) condition to analyze the safety of the dam during its service life, and Maximum Design Earthquake (MDE) to analyze the safety of the dam against the maximum earthquake load that may occur. The selection of the dam material refers to Indonesian National Standard, SNI 8064:2016 and the slope safety requirements also refers to Indonesian National Standard, SNI 8062:2015.

This paper also presents the result of a parametric study analysis to determine the number of slope dam safety by investigate the effects of system geometry of the embankment dam, shear strength of the embankment dam material, and the pseudo-static coefficient. Pseudo-static coefficient refers to Stability Analysis of Embankment Dam Type Due to Earthquake Indonesia Guideline, Pd T-14-2004-A by using the 2017 seismic probability maps by various of return of period.

The planned embankment dam located in North Sumatera, Deli Serdang, Percut River with 4.8 m^3/s and 1.4 m^3/s of stream debit in rainy season and dry season.

2 DATA

The technical data of the reservoir could see as below,

Table 1. Technical Data of Reservoir of The Dam.

Technical Data Reservoir	
Elevation bottom of stream	+ 184.50 m
Elevation flood water level	+ 251.78 m
Elevation normal water level	+ 246.80 m
Elevation minimum water level	+ 224.20 m

The embankment planned with 4 zones: (1) Core Zone, (2) Filter Zone, (3) Transition Zone, and (4) Water pass Zone. All the specification of the dam material refers to SNI 8064:2016. The soil material data could see as below,

Table 2. Specification Embankment Material.

Zone / Specific Data	Core Zone	Filter
γd (kN/m3)	12.91	12.92
γ (kN/m3)	17.01	17.02
γsat (kN/m3)	17.90	17.90
K (cm/s)	$3.29\ 10^{-7}$	$2.19\ 10^{-5}$
E (kN/m2)	14,000	28,000
v	0.383	0.370
c' (kPa)	27.57	24.03
ϕ' (°)	21,11	23,19

Zone / Specific Data	Transition	Water pass Zone
γd (kN/m3)	13.89	15.79
γ (kN/m3)	17.41	17.56
γsat (kN/m3)	18.46	22.90
K (cm/s)	$1.28\ 10^{-3}$	$3.50\ 10^{-1}$
E (kN/m2)	35,000	63,000
v	0.370	0.278
c' (kPa)	24.33	38.26
ϕ' (°)	23,48	41,20

Geotechnical conditions under the dam were dominated by andesite stone and sandstone with the number of RQD above 50% and the number of SPT above 60.

3 FAILURE OF EARTH DAMS DUE TO EARTHQUAKES

Tosun (2007) states the safety concerns for embankment dams subjected to earthquakes involve either the loss of stability due to a loss strength of the embankment and foundation materials or excessive deformations such as slumping, settlement, cracking and planer or rotational slope failures. Sherard *et al*. (1963) states the possible ways of the failure of earth dams due to earthquakes as follows: (1) Failure due to disruption of the dam by major fault movement in the foundation. (2) Slope failure induced by ground motions. (3) Loss of freeboard due to differential tectonic ground movement. (4) Loss of freeboard due to slope failure or soil compaction induced by ground shocks. (5) Piping failure through cracks due to ground movements. (6) Overtopping of dams due to slides or rock-falls into the reservoir. (7) Sliding of the dams on weak foundation materials.

Vernes (1978) states several failures of the slope as follows: (1) Rotational landslide, (2) Translational landslide, (3) Block slide, (4) Rockfail, (5) Topple, (6) Lateral slide, (7) Debris, (8) Earthflow, and (9) Creep. Basudhar (2010) mentions that adequate design precautions should be adopted to preclude any possibility of failure due to the above causes and often simply involve the exercise of good planning and judgment along with the incorporation of the features such as (a) Avoidance of active faults in the foundation, (b) Provision of ample freeboard to allow for some loss due to subsidence of slope slumping, (c) Provision of wide transition section of filter materials that are not vulnerable to cracking, (d) Use of such materials in wider core that are capable of self-healing if there be any eventual development of cracking, (e) Careful examination of the stability of slopes adjoining the reservoir, and (f) Provision of appropriate crest details to minimize erosion in the event of overtopping. In this study, provision of the freeboard, the width of the dam crest, every embankment zone thickness, have followed the Indonesian standard.

4 PSEUDO-STATIC ANALYSIS

If the peak ground motion acceleration is known by using the seismic hazard probability maps and do corrections with local ground soil conditions, the inertial force on the soil element can be obtained by multiplying the mass of the element with the seismic acceleration coefficient. Kramer (1996) defines the equation as follows:

$$F_h = \frac{a_h W}{g} = K_h W \quad (1)$$

$$F_v = \frac{a_v W}{g} = K_v W \quad (2)$$

Where F_h and F_v is horizontal and vertical seismic force, a_h and a_v is horizontal and vertical pseudo-static acceleration, W is weight of the element, and K_h and K_v is horizontal and vertical pseudo-static coefficient.

Pseudo-static is the dynamic effect of the seismic is replaced by a pseudo-static force, and the equilibrium is maintained inclusive of this force. As shown on Pd T-14-2004-A, the seismic load analysis is carried out in two seismic level: (1) no damage requirements or operating basis earthquake (OBE), and (2) allowed damage without collapse or maximum design earthquake (MDE). OBE using short seismic return period, and the number in range 50-200 years depend on risk class of the embankment dam. MDE using long seismic return period, and the number in range 1,000-10,000 years also depend on risk class of the embankment dam. Considering the flexibility of the embankment dam, an acceleration of seismic increase with the height of the dam, so that to define the coefficient of the seismic, need some modifying. The number of coefficients depend on the number of return period of the dam and also various with the depth of Y from the crest of the dam. For stability analysis, points observation carried out on Y=0.25H; Y=0.50H; Y=0.75H where H is height of the dam.

By considering location, soil or rock class site, and risk class of the dam, the return period of the dam for OBE and MDE requirement of 100 years and 5,000 years. The result seismic coefficient could see as below,

Table 3. Pseudo-Static Coefficient.

Y/H	K	
	T = 100 years	T = 5,000 years
0.25	0.1665	0.3668
0.5	0.1389	0.3060
0.75	0.1267	0.2790

5 LIMIT EQUILIBRIUM AND FINITE ELEMENT ANALYSIS

The initial design process by using limit equilibrium method resulting the preliminary design of the dam and then the 3D finite element method is used as the final detail for the design stage to obtain the optimum condition. Because an appropriate soil constitutive model, accurate geometry, and proper interaction parameters can be incorporated into the analysis to cover all aspects of dam material behavior, the 3D finite-element analysis may be superior to the simplified method. Bhartiya (2019).

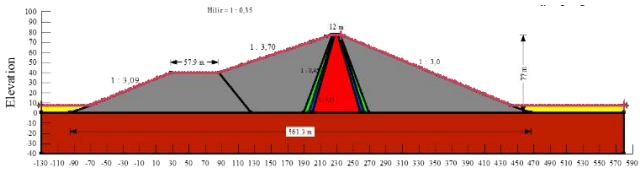

Fig. 1. Model of The Embankment Dam.

Limit equilibrium analysis using GeoStudio software and using Fellenius method. The number of increments of slip surface configuration is set by 100, number of increments of radius circular slip surface is set by 4, number of slices of plane is set by 30, and maximum number of iterations is set by 100. By considering loading conditions such as (1) After Construction (AC), (2) Minimum Water Level (MWL), (3) Normal Water Level (NWL), (4) Flood Water Level (FWL), (5) Instantaneous Rapid Drawdown (IRD), and (6) Gradually Rapid Drawdown (GRD), and considering seismic forces either OBE or MDE, the model of the dam was obtained as shown in Fig. 1. The model of the embankment dam fulfils all the requirements with the results could see as following table:

Table 4. SF of Slope Stability without Earthquake.

No	Conditions	Safety Factor	
		Req.	SF
1	AC (upstream)	1.3	4.067
2	AC (downstream)	1.3	3.078
3	MWL (upstream)	1.5	3.280
4	MWL (downstream)	1.5	2.843
5	NWL (upstream)	1.5	4.069
6	NWL (downstream)	1.5	3.078
7	FWL (upstream)	1.5	4.349
8	FWL (downstream)	1.5	3.078
9	IRD (upstream)	1.3	4.067
10	IRD (downstream)	1.5	3.079
11	GRD (upstream)	1.3	3.280
12	GRD (downstream)	1.3	3.078

Table 5. SF of OBE Slope Stability.

No	Conditions		Safety Factor (SF)		
	Y/H	Req.	0.25	0.5	0.75
	Seismic Coeff.		0.167	0.139	0.127
1	AC (upstream)	1.2	2.351	2.532	2.620
2	AC (downstream)	1.2	1.941	2.077	2.141
3	MWL (upstream)	1.2	1.853	2.037	2.122
4	MWL (downstream)	1.2	1.941	2.077	2.141
5	NWL (upstream)	1.2	1.892	2.094	2.194
6	NWL (downstream)	1.2	1.940	2.077	2.141
7	FWL (upstream)	1.2	1.964	2.174	2.279
8	FWL (downstream)	1.2	1.931	2.069	2.134
9	IRD (upstream)	1.1	1.882	2.084	2.183
10	IRD (downstream)	1.1	1.931	2.069	2.134
11	GRD (upstream)	1.1	1.844	2.024	2.060
12	GRD (downstream)	1.1	1.939	2.077	2.141

Table 6. SF of MDE Slope Stability.

No	Conditions		Safety Factor (SF)		
	Y/H	Req.	0.25	0.5	0.75
	Seismic Coeff.		0.367	0.306	0.279
1	AC (upstream)	1.2	1.522	1.713	1.811
2	AC (downstream)	1.2	1.296	1.415	1.528
3	MWL (upstream)	1.2	1.055	1.248	1.336
4	MWL (downstream)	1.2	1.296	1.451	1.528
5	NWL (upstream)	1.2	1.070	1.247	1.343
6	NWL (downstream)	1.2	1.288	1.446	1.525
7	FWL (upstream)	1.2	1.081	1.262	1.360
8	FWL (downstream)	1.2	1.259	1.425	1.505
9	IRD (upstream)	1.1	1.068	1.245	1.340
10	IRD (downstream)	1.1	1.259	1.425	1.505
11	GRD (upstream)	1.1	1.059	1.226	1.315
12	GRD (downstream)	1.1	1.266	1.446	1.525

The 77 meters dam height and 12 meters and 561 meters of width crest and dam foundation is resulted. The model is need additional dam toe to reduce the upstream side slope failure. Height of the dam toe is 40 meters and 57.9 meters of width. The slope detail for each zone as follow:

1) DS/US of core zone = 1:0.35
2) DS/US of filter zone = 1:0.40
3) DS/US of transition zone = 1:0.45
4) DS of the water pass zone = 1:2.70
5) US of the water pass zone = 1:3.70
6) US of the water pass toe zone = 1:3.09

*DS and US is downstream side and upstream side.

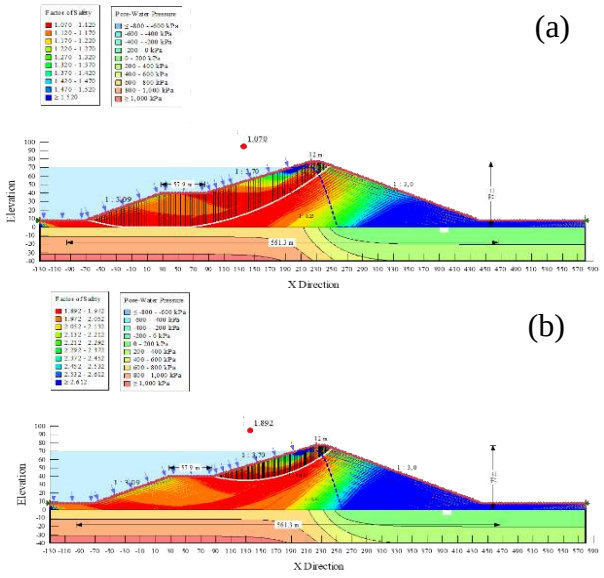

Fig. 2. SF of (a) NWL with MDE; (b) NWL with OBE Slope Stability.

For cases instantaneous rapid drawdown and gradually rapid drawdown, need to be more analyzed to get the safety factor. In rapid drawdown conditions, the pore water pressure changes over time so that need to see the resulted safety factor over time. The change of safety factor to time could see as Fig. 3 to Fig. 6.

For IRD downstream side condition, the resulted safety factor for downstream side increase over time and stable constant at 1.285. For IRD upstream condition, the resulted safety factor for upstream side decrease over time and stable constant at 1.0678. For GRD downstream condition, the most critical safety factor at 1.288 after 1.2 hour of drawdown and after the SF increase and stable constant at 1.295. For GRD upstream condition, the SF decrease reach the most critical number at 1.059 after 40 hour of drawdown and the SF increase reach 1.076.

This proves that the value of the safety value changes with time and reaches the lowest value at any time during the rapid drawdown condition. In the upstream side of gradually rapid drawdown conditions, it is necessary to pay attention to the condition of the reservoir in the 40th to 50th hours, because the upstream slope of the dam has the most critical condition in the early hour.

The rapid drawdown on the normal water level to minimum water level conditions is more common and certain to occur than the instantaneous rapid drawdown on floodwater level to normal water level, so this condition is a critical condition for the design dam. This

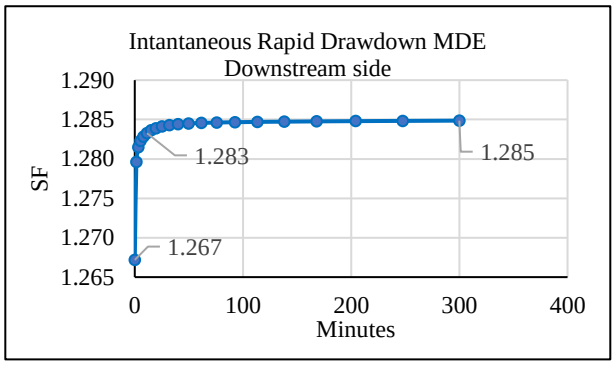

Fig. 3. SF of IRD Downstream Side over Time.

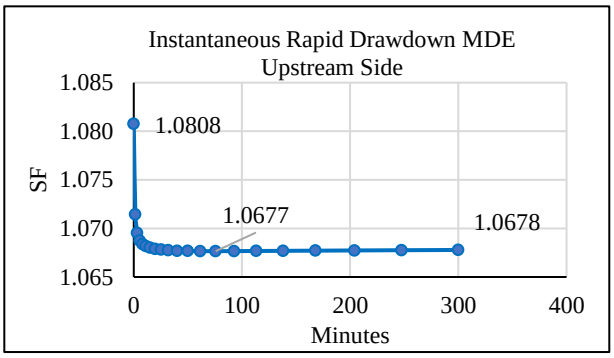

Fig. 4. SF of IRD Upstream Side over Time.

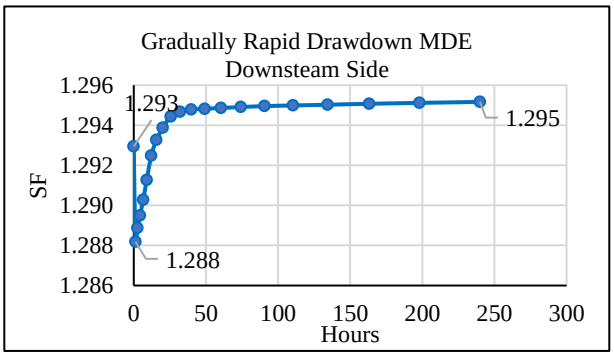

Fig. 5. SF of GRD Downstream Side over Time.

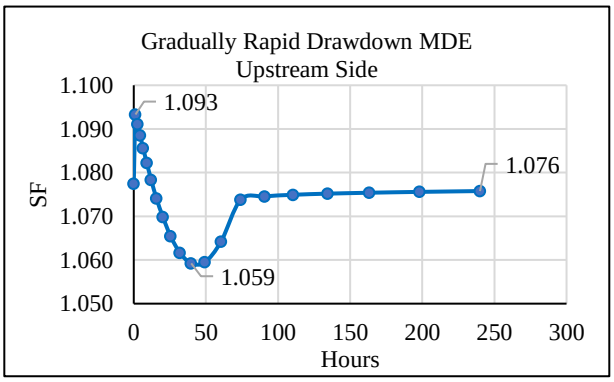

Fig. 6. SF of GRD Upstream Side over Time.

condition takes 3 days to lower the reservoir water level from NWL to MWL which may not be as fast as 3 days as in this plan. This 3-day time limit can be used as a guideline for reducing the reservoir water level, longer than

3 days is better, while faster than 3 days requires further analysis and consideration.

Three-dimensional finite element analysis of the embankment dam was performed using the software PLAXIS 3D. The finite element analysis was run in 4 steps every condition: (1) Applying the water level conditions to the initial phase (the initial dam geometry), (2) Determining the safety factor of static condition by safety calculation, (3) Adding pseudo-static force, and (4) Determining the safety factor of dynamic condition by safety calculation. The conditions were run by finite element are AC, MWL, NWL, and FWL.

In this study, three-dimensional finite element is made in two forms: (1) the real condition three-dimensional (3D) and (2) the two-dimensional with 10 meters of dam-length (2D). The resulted number of safety by using two-dimensional and three-dimensional finite element method could see as following table:

Table 7. SF of 2D and 3D Finite Element.

Condition	FE 2D	FE 3D
	Static	
AC =	2,835	3,191
MWL =	2,769	3,143
NWL =	2,380	2,776
FWL =	2,269	2,645
	OBE	
AC =	2,020	2,309
MWL =	2,150	2,368
NWL =	2,238	2,432
FWL =	2,260	2,455
	MDE	
AC =	1,172	1,449
MWL =	1,222	1,455
NWL =	1,264	1,476
FWL =	1,278	1,483
	lowest SF	

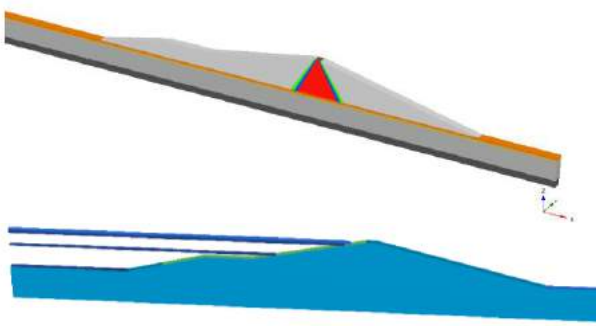

Fig. 7. 2D Finite Element Model.

Using assumed 2D finite element model, results lower values for the factors of safety than using 3D finite element model. The difference computed factors of safety between two form of finite element were about in range 8.6% – 23.6%. In compare with the limit equilibrium, SF number of LE lower than FE. Richards (2005) also studied that the limit equilibrium method yielded lower values for the factor of safety, which could result in more conservative designs based on the limit equilibrium method for a given shear strength.

In static condition, in all water level and empty reservoir, the slope failure occurred to the downstream side. Whereas in dynamic condition, in all water level and empty reservoir, the slope failure occurred to the upstream side.

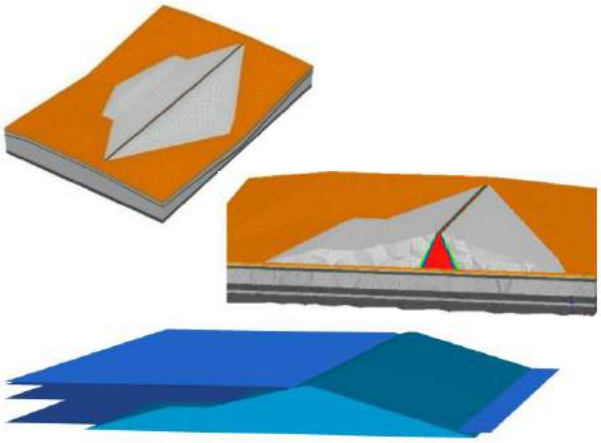

Fig. 8. 3D Finite Element Model.

6 PARAMETRIC STUDY OF SLOPE STABILITY

The main concern addressed in the present study is the number of slope safety by varying the slope of the dam, the shear strength (cohesion and angle of friction) of the water pass zone material, and the pseudo-static coefficient. The water pass zone is the most significantly contribute the slope failure, thus in this parametric study focusing on water pass zone, while core zone significantly contributes in impermeability and reducing the flow discharge. For the parametric study, the finite element model using assumed 2D finite element. The use 3D finite element requires large computational resources and times, and have to be carefully performed, paying proper attention to minute modelling details to obtain reliable resources.

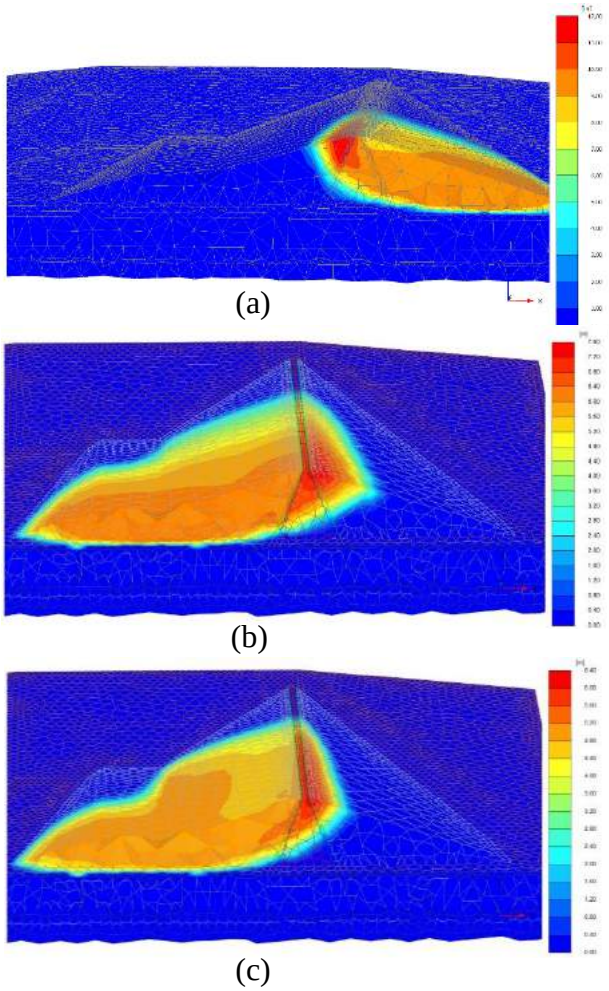

Fig. 9. Slope Failure (a) NWL Static; (b) NWL MDE; (c) NWL OBE.

6.1 *Pseudo-Static Coefficient to Safety Factor of Slope Stability.*

Pseudo-static coefficient in range 0.1 – 0.4 shown in following figure:

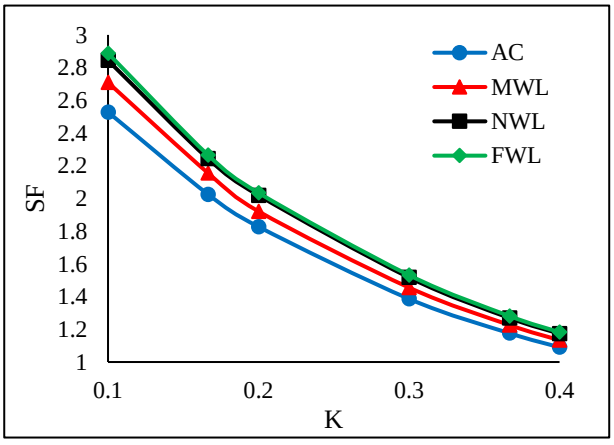

Fig. 10. Safety Factor to Pseudo-Static Coefficient.

In above result, water level affects the safety of the slope stability. The flood water level which highest water level results more good safety than the other water level even than the empty reservoir. As the water level decreases, the factors of safety decreases.

The number Pseudo-static coefficient of 0 means the condition is in the static condition which the result of SF not always bigger than in dynamic condition as shown in Fig. 11. In static condition, the water level also affect the factors of safety. Otherwise, empty reservoir has SF higher than MWL, NWL, and FWL. As water level increases, the SF decreases. Refers to obtained result, in static condition, the slope failure occurred to downstream side while in dynamic condition occurred to upstream side, so that the SF between static and dynamic condition is independent.

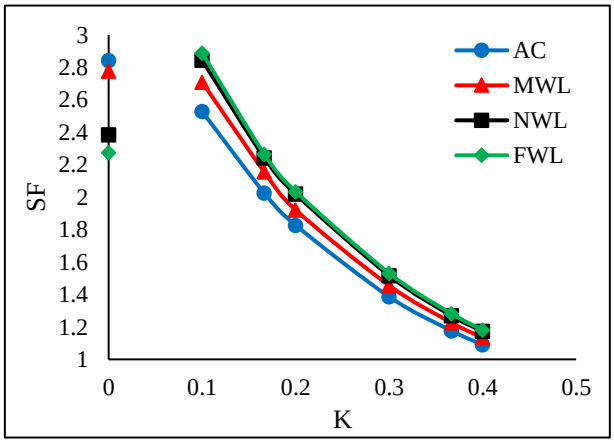

Fig. 11. SF in Static and Dynamic Condition.

6.2 *Variation of Slope to Increment of Safety Factor of Slope Stability*

Seven side slopes were modeled for the geometry and the effect of the downstream and upstream slope magnitudes shown in following figure:

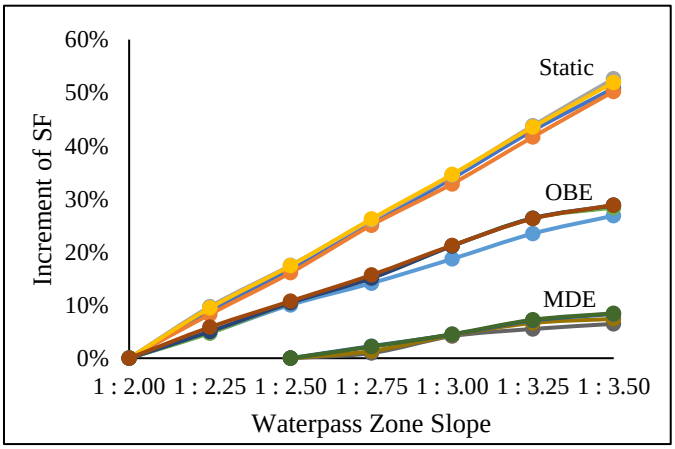

Fig. 12 Variation of Water Pass Zone Slope to Increment of SF.

The increment of SF is the different between SF of observed slope and SF reference, in this case is the obtained SF of 1:2 of slope for the

static and OBE condition, while the obtained SF of 1:2.5 of slope for the MDE condition. The increment of the slope in static condition, increases the SF linearly. Increasing 0.25 of the slope (upstream and downstream), the SF increases 8.9% - 9.7% for all water level. The increment of SF in OBE condition lower than static by 4.8% - 5.8% for all water level.

In MDE condition, using 1:2.5 slope is the most critical with the lowest SF value is 1.036. And the increment of 0.25 of slope to the SF in MDE condition is the lowest by 1% - 2.3% for all water level. In this parameter study also results for the static condition, as increasing water level, the SF decreases. Otherwise, in dynamic conditions, the SF increases as the water level increases.

6.3 *Variation of Shear Strength to Increment of Safety Factor of Slope Stability*

In this study the variations are cohesion (c) number and angle of friction (ϕ) number. Cohesion added linearly of 5 kPa and ϕ added linearly of 5° for every model. From Fig. 13 to Fig. 15, increasing the cohesion number not significantly increasing the SF. Increasing 20 kPa of cohesion, just increases the SF of 0.9% - 1.2% for any water level and seismic conditions. Using the 3D finite element, the resulted SF has more increasing than using 2D finite element form by up to 0.79% from the resulted 2D SF, but in MDE condition, decreases down to 0.85%

Otherwise, from Fig. 16 to Fig. 18, increasing the angle of friction, significantly increasing the SF. In static condition, increasing 20° of ϕ, increase the SF of 5.7% - 15.8% with the lowest number of SF increment by normal water level. In OBE condition, increasing 20° of ϕ, increases the SF of 8.6% - 14.6% with the lowest number of SF increment by empty reservoir. In MDE condition, increasing 20° of ϕ, increases the SF of 4% - 6.2% with the lowest number of SF increment by AC condition.

Using the 3D finite element, the resulted SF has more increasing than using 2D finite element form by up to 7% - 12.7% from the resulted 2D SF as shown in Fig. 19.

7 CONCLUSION

Limit equilibrium and finite element method have been the most common methods employed by engineers to estimate the stability of slopes.

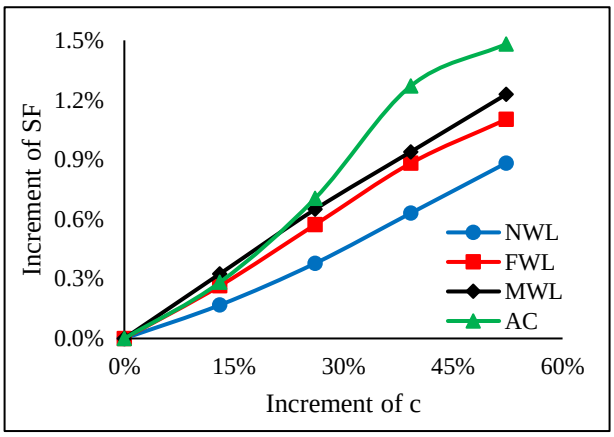

Fig. 13. Variation of Cohesion to Increment of SF for Static Condition.

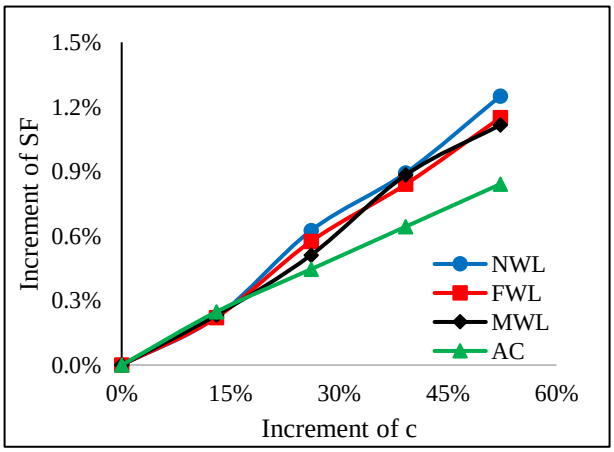

Fig. 14. Variation of Cohesion to Increment of SF for OBE Condition.

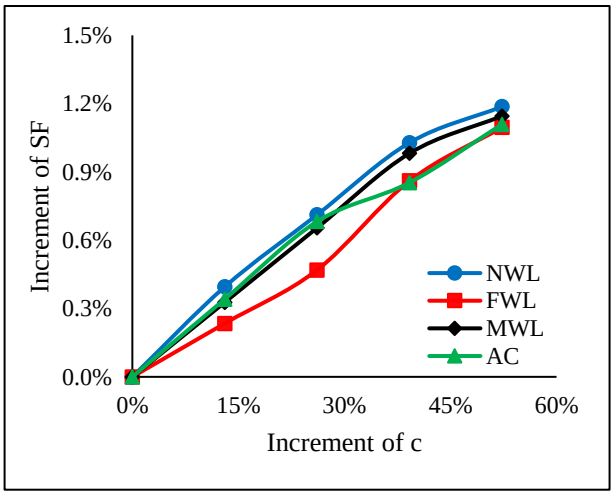

Fig. 15 Variation of Cohesion to Increment of SF for MDE Condition.

The 4 zones embankment dam design which considering the safety factor of slope stability has 77 meters of dam height, 12 meters of width crest dam, 561 and 976 meters of foundation width and length of the dam. The critical SF by limit equilibrium calculation which the most

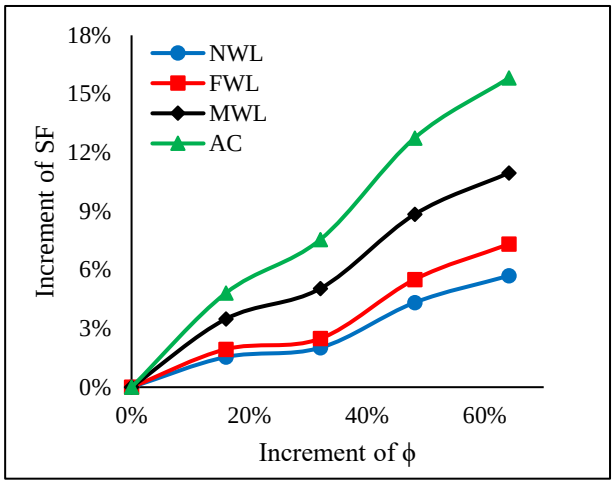

Fig. 16. Variation of ϕ to Increment of SF For Static Condition.

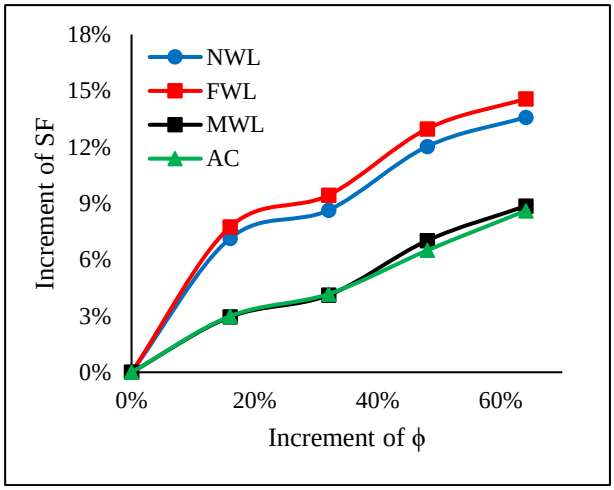

Fig. 17. Variation of ϕ to Increment of SF for OBE Condition.

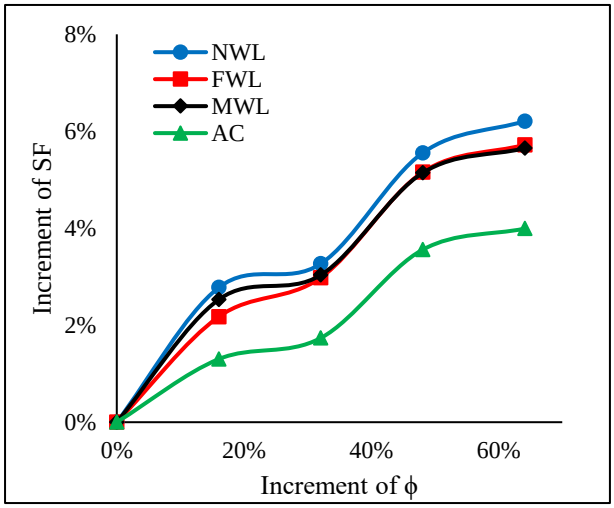

Fig. 18. Variation of ϕ to Increment of SF for MDE Condition.

conservative result by 1.055, by assumed 2D finite element method is 1.172 and by 3D finite element method is 1.449. The used of 3D FE results higher resulted SF than 2D FE by 8.6% - 23.6%.

The parametric study results that increasing the slope, upstream and downstream of 0.25, could increases the SF up to 8.9% - 9.7% in static condition, 4.8% - 5.8% in OBE condition, and 1% - 2.3% in MDE condition. Increasing the ϕ of water pass zone material is the most significantly increasing the SF in MDE condition rather than adding the slope. Increasing the 20° could increases the SF up to 5.7% - 15.8% in static condition, 8.6% - 14.6% in OBE condition, and 4% - 6.2% in MDE condition.

Refers to this dam design, in static condition, the slope failure occurred to the downstream side while in dynamic condition, the slope failure occurred to the upstream side. This could be a consideration to adding the slope or increasing the shear strength material of water pass zone by considering the direction of the failure.

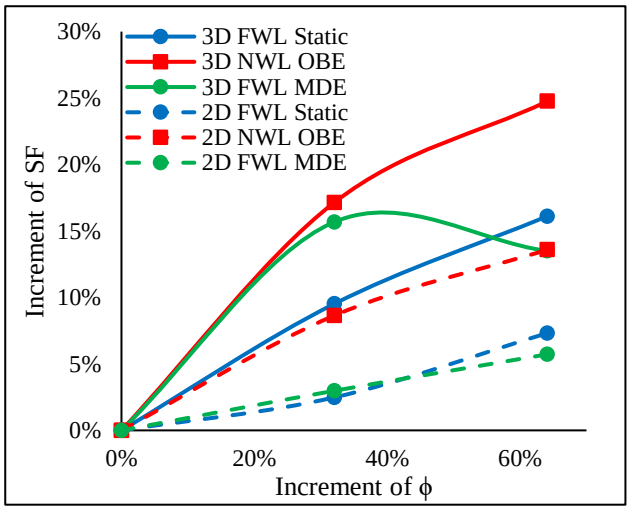

Fig. 19. Variation of ϕ to Increment of SF 2D vs 3D Form.

REFERENCES

Badan Standardisasi Nasional. 2015. Tata Cara Desain Tubuh Bendungan Tipe Urugan. SNI 8062.

Badan Standardisasi Nasional. 2016. Metode Analisis Stabilitas Lereng Statik Bendungan Tipe Urugan. SNI 8064.

Basudhar, Prabir K., et al 2010. 2D FEM Analysis of Earth and Rockfills Dams Under Seismic Condition. *Recent Advances in Geotechnical Earthquake Engineering and Soil Dynamics: Fifth International Conference*. Paper No. 4.28b.

Bhartiya. P. 2019. Settlement Estimation of Piled Rafts for Initial Design. *Journal of Geotechnical. Geoenvironment. Engineering* 146(2): 04019127.

Departemen Permukiman dan Prasarana Wilayah. 2004. Analisis Stabilitas Bendungan Tipe Urugan Akibat Beban Gempa. *Pedoman Konstruksi dan Bangunan*. Pd-T-2004-A.

Kramer, S.L. 1996. *Geotechnical Earthquake Engineering.* New Jersey: Upper Saddle River: Prentice-Hall, Inc.

Richards, K.S. and Reddy, K.R. 2005. Slope Failure of Embankment Dam under Extreme Flooding Conditions: Comparison of Limit Equilibrium and Continuum Models. *GSP140 Slopes and Retaining Structures Under Seismic and Static Conditions.*

Sherard, J.L., Woodward, R.J., Gizienski, S.J. and Clevenger, W.A. 1963. *Earth and Earth-Rock Dams*. New York: John-Wiley and Sons.

Tosun, H., Zorluer, İ., Orhan, A., Seyrek, E., Savaş, H. and Türköz, M. 2007. Seismic Hazard and Total Risk Analyses for Large Dams in Euphrates Basin, Turkey. *Engineering Geology* 89: 155-170.

Laboratory Study of Compressibility Characteristics of Compacted Volcanic Soils (AMM)

Charles Maxwelliem
Student – Universitas Katolik Parahyangan

Stefanus Diaz Alvi
Deputy Head Division – PT Geotechnical Engineering Consultant

Paulus P. Rahardjo
Professor of Geotechnical Engineering – Universitas Katolik Parahyangan

ABSTRACT: Compressibility characteristics of the compacted volcanic soil are normally used for embankment construction. This research observes differences in soil compressibility behaviors, by conditioning the soil through compaction using a standard proctor. The soil used in this research is collected from a soil embankment in Batang, Central Java. The test conducted in this research consists of index properties test and consolidation test using the oedometer instrument. Oedometer test results show that compacted volcanic soil embankment's settlement on saturated and unsaturated conditions does not consist primarily of immediate settlement, but also time-dependent settlement as well. The reliability of the time rate (c_v) parameter can be obtained by plot the time vs settlement curve using the c_v value taken from the standard methods such as the square root fitting method and the log fitting method. Compacted volcanic soil embankment's coefficient of consolidation (c_v) has better accuracy when obtained using the matching method, rather than square-root fitting, log fitting, and beta methods. Based on The Oedometer test conducted on compacted volcanic soil embankment through various applied pressure, the test needs to be observed for more than 24 hours. Since it has secondary consolidation and slows down only after 7 days.

Keywords: compressibility, compacted volcanic soil, oedometer test

1 INTRODUCTION

Volcanic soils are formed from the activity of volcanoes. They only cover one percent of the earth but are commonly found in countries that are surrounded by the 'ring of fire' or the rim of the Pacific Ocean, including Indonesia. Volcanic soils are often used for compacted fill in Indonesia. The main issue of soil embankment is the compressibility of the underlying layer (below the embankment). As for the compressibility behavior of the embankment's material is very rarely, if ever observed. Most of the practitioners assume the compressibility of the embankment is the immediate settlement during compaction only.

The compression of compacted volcanic soil is time-dependent and able to cause many problems, including differential settlements that can affect the performance of the construction upper the fill.

The compressibility behavior of volcanic soil is different from alluvial soils. However, soil mechanics theory only discusses the compressibility behavior for alluvial soils.

2 RESEARCH METHODS

Soils that are used in this research are collected from Batang, Central Java. The test consists of index properties test, grand-size analysis, and consolidation using the Oedometer test. This paper discusses compressibility characteristics of compacted volcanic soils under saturated conditions and unsaturated conditions.

The soil sample used is fine-grained soils by sieve analysis to obtain the soil size finer than 4.75 mm. Index properties test to acquire the specific gravity, unit weight, and Atterberg Limit. Moreover, the use of the standard proctor for compaction is considered to simulate the desired density of compacted soils. For the standard proctor that consists of 3 layers, the soil sample is compacted 25 times for each layer (75 in total). The soil is compacted

without adding water to achieve the same soil condition as they are on site. For the Oedometer test, 2 samples are tested for both unsaturated and saturated conditions. For the saturated condition, the soil sample is soaked for three days to achieve full saturation. The applied pressure to the sample ranging from 0.25 to 8 kg/cm^2. Refer to the standard procedure of The Oedometer Test, the deformation measurement is observed for 24 hours (1440 minutes) for each applied pressure. For this research, the measurement is extended to 3 days for 1 kg/cm^2 of applied pressure.

3 INDEX PROPERTIES OF VOLCANIC SOIL IN BATANG

The results of the index properties test are shown in Tabel 1. From Table 1, it is shown that Batang soil is nearly saturated (Sr = 78%) and it has a specific gravity of about 2,6.

Table 1. Index Properties of Batang Soil.

Index Properties (Batang)				
γ (gr/cm^3)	γ_{dry} (gr/cm^3)	w	Sr	Gs
1.64	1.19	50.9%	78%	2.6

4 COMPRESSIBILITY CHARACTERISTICS OF COMPACTED VOLCANIC SOILS IN BATANG

4.1 *Oedometer Test Results (Unsaturated)*

The following figures are the sample height versus time for various applied pressure in unsaturated condition.

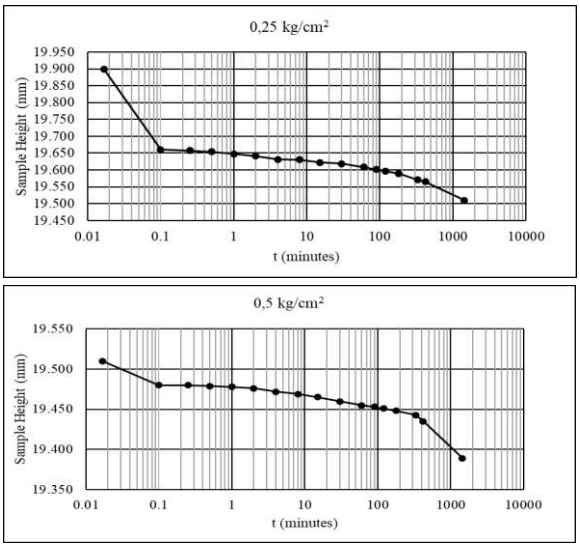

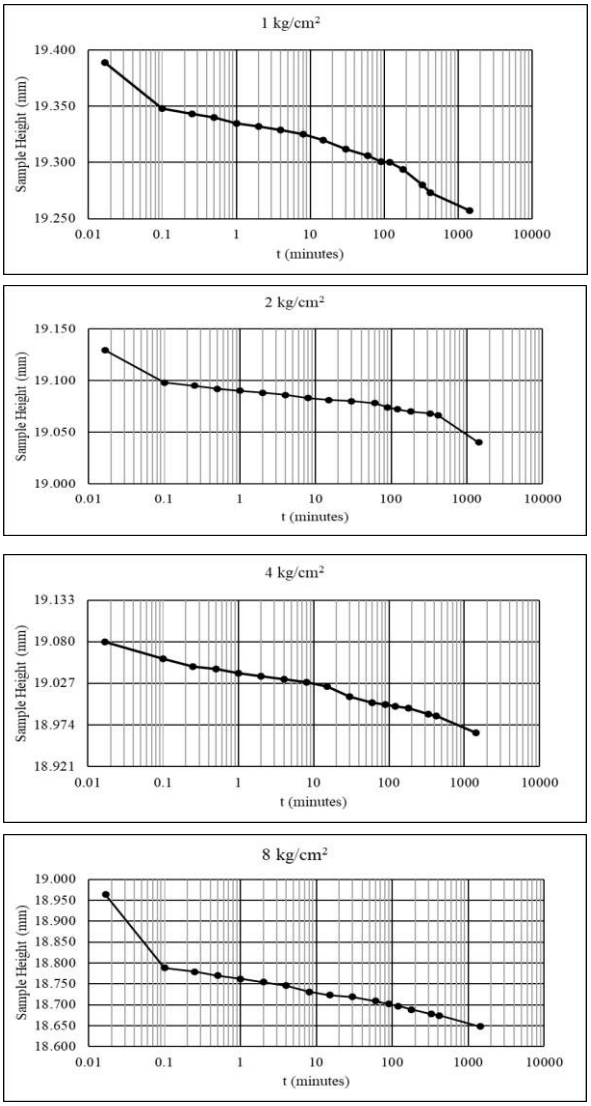

Fig. 1. Test Results: Unsaturated Sample 1.

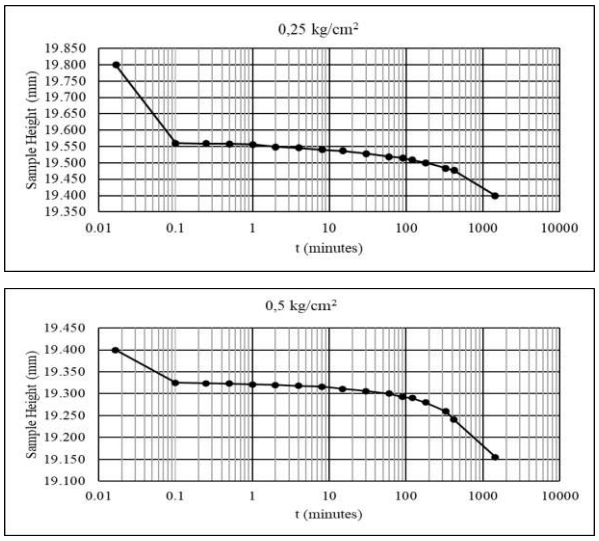

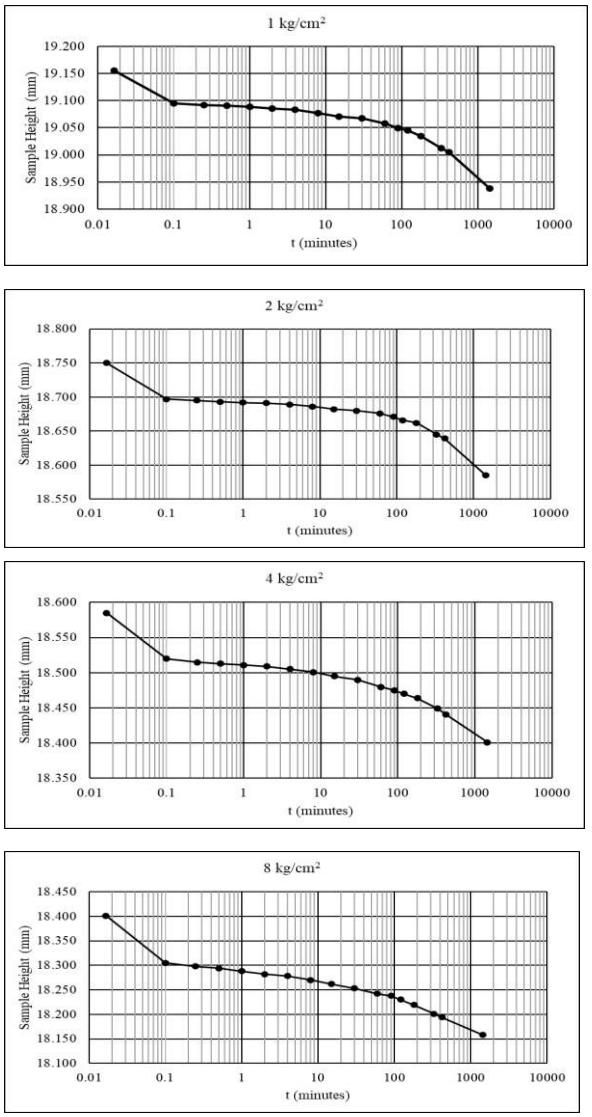

Fig. 2. Test Results: Unsaturated Sample 2.

According to Fig. 1 and Fig. 2, it is shown that compacted volcanic soil has a unique behavior of compressibility. From both tests, it can be obtained that for each applied pressure, the compacted sample has a large immediate settlement from 1 s to 6 s. After 6 s, the sample continues to experience time-dependent settlement. The applied pressure itself also affects how much the sample settles, if the applied pressure increases (for example from 0.25 to 0.5 kg/cm^2) the immediate settlement and the primary consolidation settlement proportion will decrease.

The tests show that the sample height still decreases after 24 hrs. Different from sediment soil in general, usually after 24 hrs its settlement will slow down because it will reach 90% degree of consolidation (U%). This is primarily the reason why consolidation tests using the oedometer instrument are limited to only 24 hrs. Based on this result, it is evident that further duration in observation is required to see exactly when the settlement slows down.

4.2 *Oedometer Test Results (Saturated)*

The following figures are the sample height versus time for various applied pressure in a saturated condition.

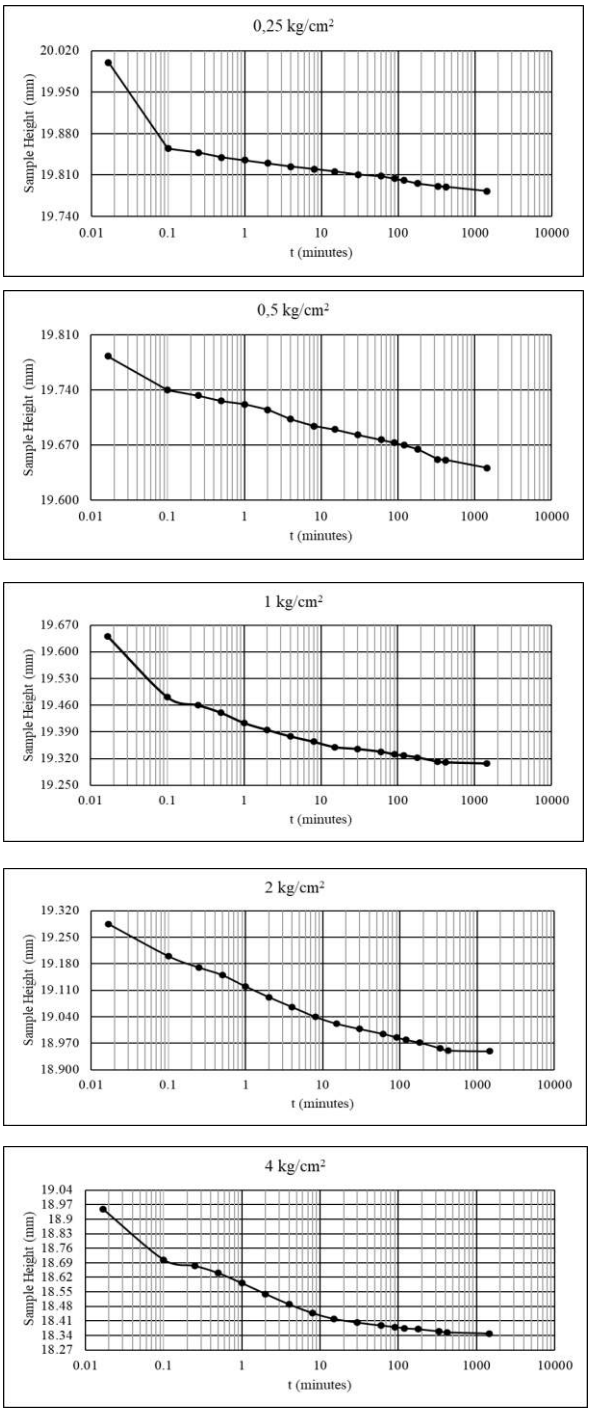

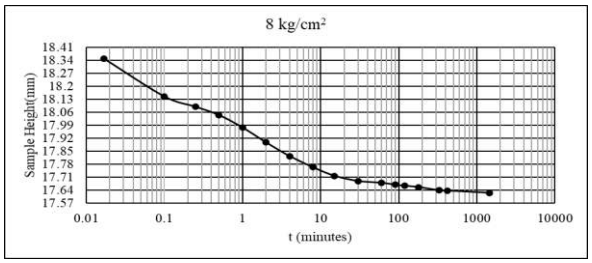

Fig. 3. Test Results: Saturated Sample 1.

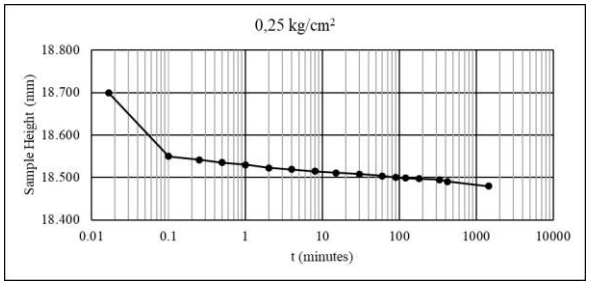

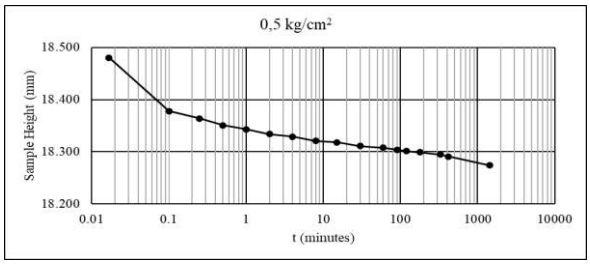

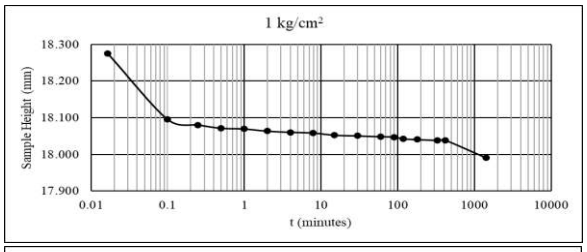

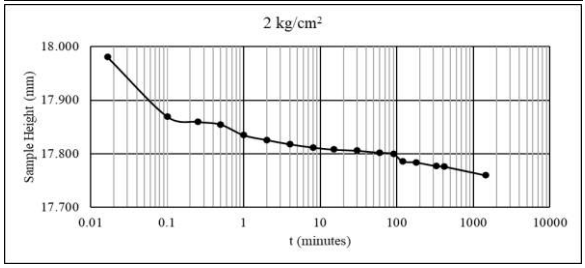

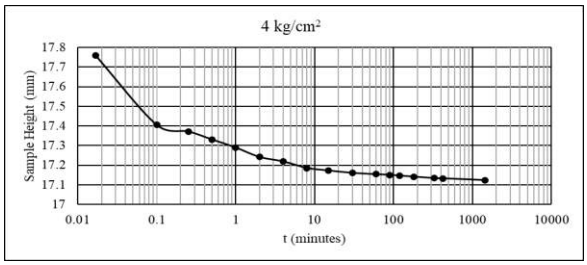

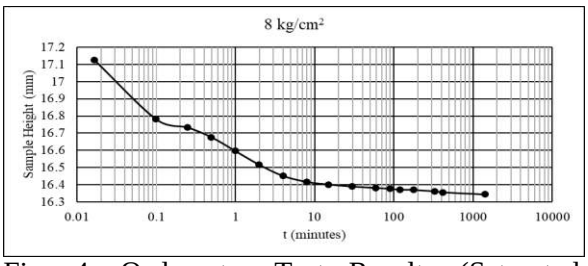

Fig. 4. Oedometer Test Results (Saturated Sample 2).

Based on Fig. 3 and Fig. 4 shows that in saturated conditions, sample height in the Oedometer test also decreases with time. Similar to the unsaturated conditions, the sample also has a large immediate settlement and time-dependent settlement, albeit with the settlement showing signs of slowing down after 24 hrs.

Terzaghi's one-dimensional consolidation theory, which assumes that if soils are fully saturated, their strain will relatively be small. It is evident that with the increase of applied pressure, the soil sample will also be more compact, this is also the reason why the settlement curve of 8 kg/cm^2 resembles Terzaghi's fully saturated alluvial soil settlement curve more than it is lower applied pressures.

An extended duration of observation during the Oedometer test is required to see precisely when Batang compacted volcanic soil settlement starts to slow down. The observation both in unsaturated conditions are extended at 1 kg/cm^2 applied pressure for 45 days. The result for the extended observation at unsaturated conditions is shown in Fig. 5.

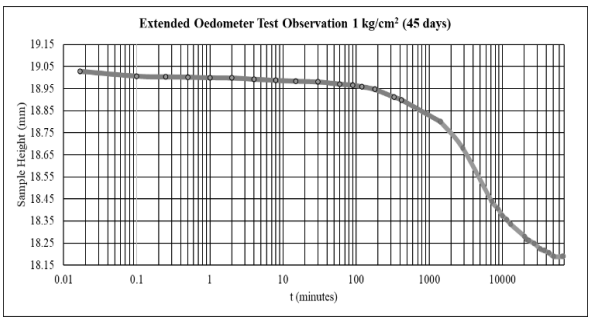

Fig. 5. Extended Unsaturated Oedometer Test 45 Days Observation (1 kg/cm^2).

From Fig.5, extended observation for the Oedometer test in unsaturated condition goes to show that after 10.000 minutes of observation, the settlement curve starts to slow down. The value of the secondary compression index (c_α) only is obtained after an extended period of observation. Based on the results, the soil has a

unique and different characteristic of compressibility compared to sediment or alluvial soils.

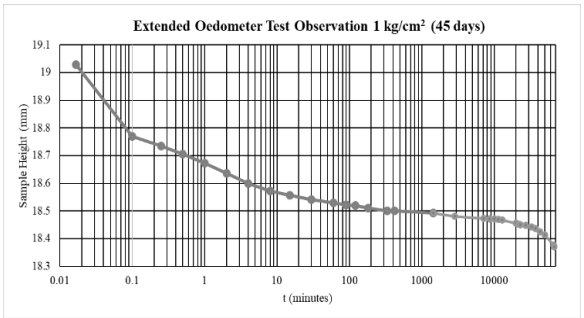

Fig. 6. Extended Saturated Oedometer Test 45 Days Observation (1 kg/cm^2).

Fig. 6 shows the result for the settlement curve in saturated condition for 45 days. The final settlement as shown in the picture has not been reached after an extended period of observation. Instead, the soil sample continues to settle even after 45 days, showing signs of tertiary consolidation.

4.3 *Coefficient of Consolidation*

The coefficient of consolidation, or commonly known as the c_v is the rate at which the consolidation process occurs in area per unit time. Oedometer tests are required to determine the c_v of soils. For the coefficient of consolidation's value, the followings are a few methods or correlations that are typically used, especially in soil mechanics:

1. Square-Root Method by Taylor (1948)

$$cv = \frac{0.197 \text{ x } Hdr^2}{t50} \quad (1)$$

2. Log-Fitting Method by Casagrande (1940)

$$cv = \frac{0.848 \text{ x } Hdr^2}{\sqrt{t90}} \quad (2)$$

3. Beta Method by Edil (1991)

$$\beta 1 = \frac{-6 \text{ x } cv}{H^2} \ (Double\ Drainage) \quad (3)$$

4.4 *Coefficient of Consolidation Value For Batang Compacted Volcanic Soil*

Using Terzaghi's value of time factor and c_v obtained with Square-Root, Log-Fitting, and Beta Method, compression versus time curve can be generated. Corrected compression is required to generate the compression versus time curve. The compression is corrected by eliminating the immediate settlement so that the compression versus time curve will consist only of primary and secondary compression.

Fig.7 shows the comparison of compression vs time from three methods and the Oedometer test results of 0.25 kg/cm^2 applied pressure.

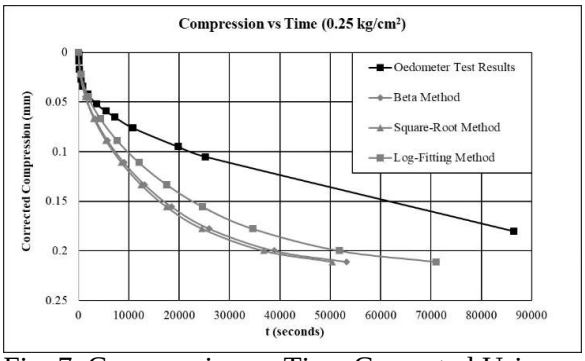

Fig. 7. Compression vs Time Generated Using c_v Values (0.25 kg/cm^2).

From Fig.7, it is shown that by using c_v obtained from Square-Root, Log-Fitting, and Beta Method, the compression versus time curve does not match the curve obtained from the Oedometer test results. Meaning that through those three methods, none can represent the time rate of settlement of Batang's soil settlement, and thus the c_v values cannot be used for compacted volcanic soils.

As an alternative, the Matching method is proposed to obtain the correct value of c_v. The matching method conducts trial-and-error of c_v value until the curve quite matches the oedometer test results. As an example, the curve of compression versus time at 0.25 kg/cm^2 from soil sample 1 (unsaturated condition) is used.

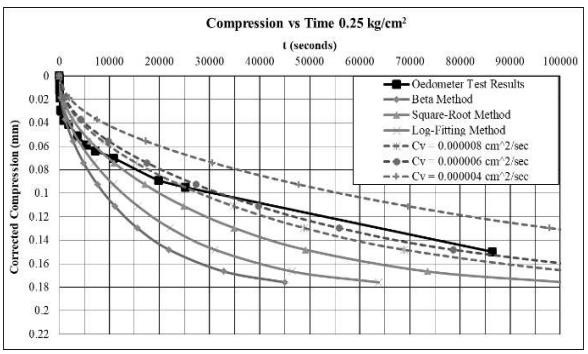

Fig. 8. Compression Versus Time Generated From Matching Method's c_v (0.25 kg/cm^2).

By using the Matching method (trial-and-error), it is shown in Fig. 8 that the settlement curve generated from the Matching method's c_v value matches the Oedometer's settlement curve better than Square-Root, Log-Fitting, and Beta methods. It shows that the Matching method is a more reliable method than the others. The results for the Matching method from the 0.5, 1, 2, 4, and 8 kg/cm^2 Batang soil in unsaturated condition sample 1 are as follows:

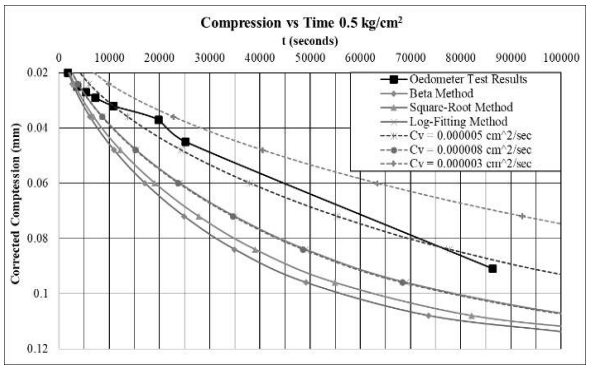

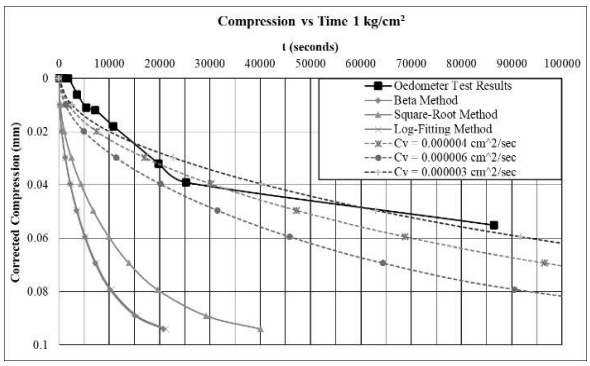

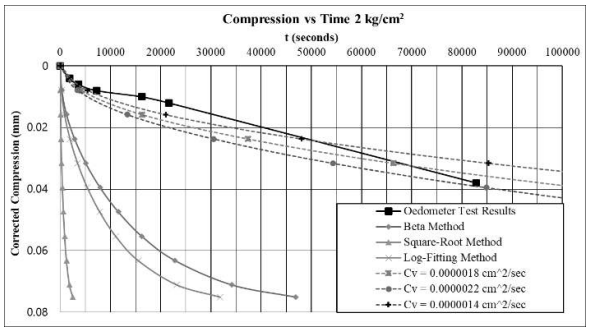

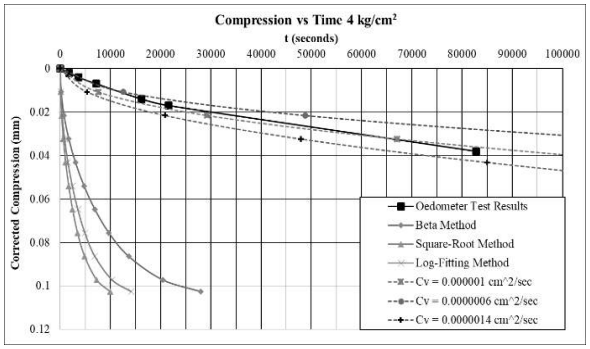

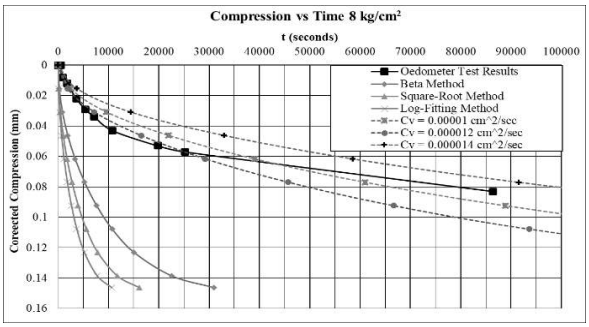

Fig. 9. Compression vs Time Generated Using Matching Method's (0.5, 1, 2, 4, 8 kg/cm^2).

However, one of the limitations on this matching method still uses the time factor (Tv) proposed by Terzaghi, whereas the time factor for compacted volcanic soil is different from alluvial soils. Hence, the time factor (Tv) for compacted volcanic soil should be developed for further research.

4.5 *Strain Vs Time of Batang Compacted Volcanic Soil*

Using the value of deformation (ΔH) in soil sample on Oedometer test, the strain for each applied pressure can be calculated by using the equation below:

$$\varepsilon = \frac{\Delta H}{H} \tag{4}$$

Where H is the initial height before applied pressure is added, and the results are as follows:

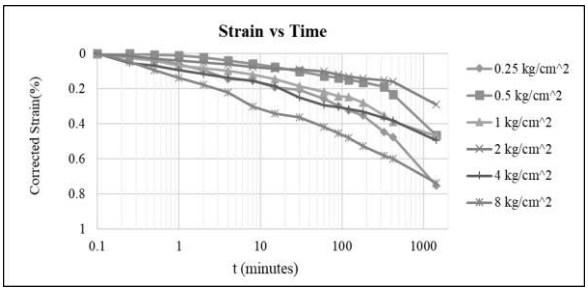

Fig. 10. Strain vs Time: Unsaturated Sample 1.

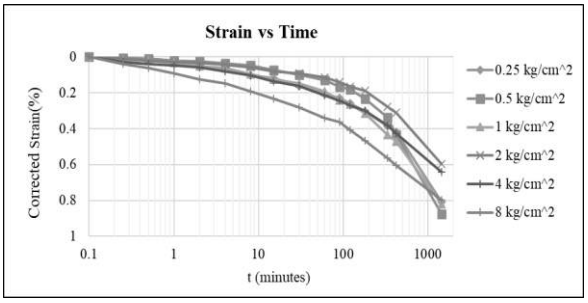

Fig. 11. Strain vs Time: Unsaturated Sample 2.

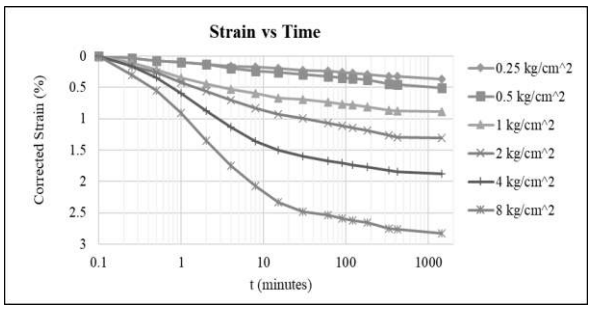

Fig. 12. Strain vs Time: Saturated Sample 1.

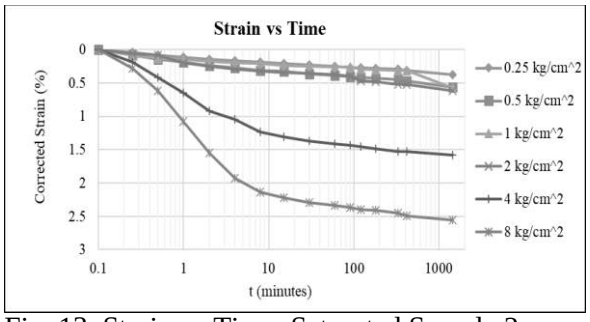

Fig. 13. Strain vs Time: Saturated Sample 2.

From Fig. 10, and Fig. 11, the strain versus time curve from both unsaturated samples tested shows that the largest applied pressure (8 kg/cm^2) also has the largest strain after 24 hours of observation, followed by 4 kg/cm^2, and 1 kg/cm^2. However, instead of the lowest applied pressure (0.25 kg/cm^2) that has the lowest strain, it's 2 kg/cm^2 of applied pressure that has the lowest strain. This result is consistent in both unsaturated samples.

From Fig. 12, and Fig. 13, the strain versus time curve for the saturated condition sample shows different characteristics than the unsaturated ones. The strain from the saturated sample increases along with its applied pressure. σ = 0.25 kg/cm^2 applied pressure has the lowest strain against time, followed by 0.5 kg/cm^2, 1 kg/cm^2, 2 kg/cm^2, 4 kg/cm^2, and 8 kg/cm^2. From both unsaturated and saturated conditions, the largest applied pressure will also have the largest strain.

4.6 *Ck* vs Time for Batang Compacted Volcanic Soil*

Generally, the time rate of soil settlement is assumed to be constant. In reality, the permeability of soil changes in the same applied pressure to the soil during consolidation, making it a non-constant variable. Because of this, a new parameter to represent the change of soil strain with time is proposed (Ck*), the equation for Ck* are as follows:

$$Ck^* = \frac{\Delta\varepsilon}{\Delta t}$$

By using the strain versus time curve, its gradient can be used to calculate Ck*. Then the values of Ck* are plotted against time to make a Ck* versus time curve, which is shown in the figures below:

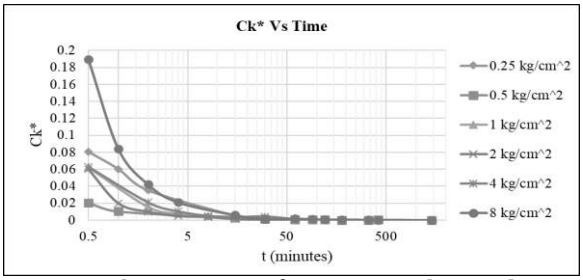

Fig. 14. Ck* vs Time of Unsaturated Sample 1.

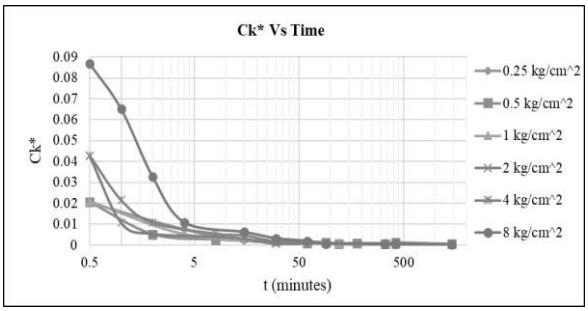

Fig. 15. Ck* vs Time of Unsaturated Sample 2.

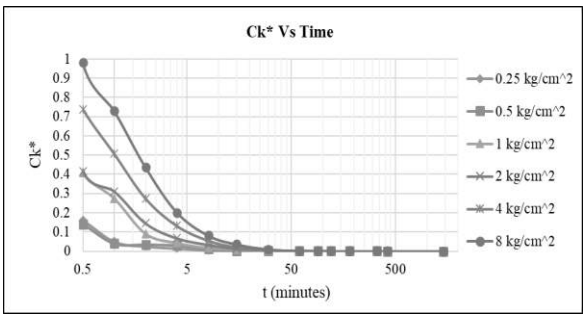

Fig. 16. Ck* vs Time of Saturated Sample 1.

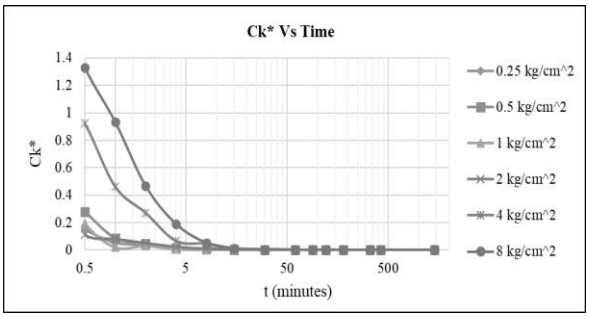

Fig. 17. Ck* vs Time of Saturated Sample 2.

As shown from Fig. 14, and Fig. 15, Ck* values for the unsaturated condition in both sample 1 and sample 2 shows that in 8 kg/cm^2 of applied pressure, the Ck* value is also the

highest with the maximum Ck* versus time value of sample 1 and 2, is 1.9 and 0.086 respectively. The 0.5 kg/cm^2 of applied pressure has the lowest Ck* value with sample 1 and sample 2 both have a maximum value of 0.02. As the order of the applied pressure that generates the highest to lowest Ck* value are as follows: 8 kg/cm^2, 4 kg/cm^2, 0.25 kg/cm^2, 1 kg/cm^2, 2 kg/cm^2, and 0.5 kg/cm^2.

Fig. 16 and Fig. 17 in saturated conditions shows that Ck* versus time value increases along with the applied pressure. Meaning that 0.25 kg/cm^2 has the lowest Ck* value with it's maximum value reaching 0.15, addition of applied pressure in 0.5 kg/cm^2, 1 kg/cm^2, 2 kg/cm^2, 4 kg/cm^2, 8 kg/cm^2 the Ck* value also gets higher, meaning that in Oedometer test conducted in saturated conditions, the highest Ck* value is at 8 kg/cm^2 of applied pressure (with a value of 0.98 and 1.33 for sample 1 and 2 respectively).

5 CONCLUSION

Based on the results from the consolidation or oedometer test, conclusions are acquired as follows:

1. That settlement from compacted volcanic soil is not mainly governed only by immediate settlement but is followed by time-dependent settlement for both unsaturated and saturated conditions.
2. The Oedometer test observation for both unsaturated and saturated conditions needs to be done for more than 24 hours because none reaches the final settlement.
3. Batang compacted volcanic soil has a unique and different characteristic on compressibility compared to sediment or alluvial soils.
4. The matching method proves to be a better alternative to obtain c_v value than Square-Root Fitting, Log-Fitting, and Beta methods. Although the matching method has a limitation where the Tv used is still proposed by Terzaghi, whereas the Tv for compacted volcanic soils is different from alluvial soils.
5. In unsaturated and saturated conditions, both samples show that the largest strain is caused by the largest applied pressure (8 kg/cm^2). The lowest strain is caused by 0.25 kg/cm^2 in the saturated condition, and 2 kg/cm^2 in the unsaturated condition.
6. Ck* is proposed as a new parameter to represent the change of strain against the change of time (in minutes). Based on the results, it can be concluded that in unsaturated and saturated conditions, the highest Ck* is also caused by the larger applied pressure. As for the lowest Ck* value is from 0.5 kg/cm^2 for unsaturated conditions, and 0.25 kg/cm^2 (the lowest applied pressure) for saturated conditions.

ACKNOWLEDGEMENTS

The authors acknowledge and appreciate Universitas Katolik Parahyangan (UNPAR) for providing the opportunity to research in the laboratory and PT. Geotechnical Engineering Consultant (PT GEC) for providing the soil sample needed and the necessary inputs to conduct the tests needed for this paper study.

REFERENCES

Casagrande, A. and Fadum, R.E. 1940. Notes on Soil Testing for Engineering Purposes. *Soil Mechanics Series* No. 8, Pub. No. 268: 37. Harvard University, Cambridge.

Das, Braja M. 1995. *Mekanika Tanah (Prinsip-Prinsip Rekayasa Geoteknis) Jilid 1*. Jakarta: Penerbit Erlangga.

Edil, T.B. 1991. Observational Procedure for Settlement of Peat. *GEO COAST '91*: 166. Yokohama

Fredlund. 1990. *Soil Mechanics for Unsaturated Soils*. University of Saskatchewan, Saskatoon, Canada. p.1

Taylor, D.W. 1948. *Fundamentals of Soil Mechanics*. New York : John Wiley and Sons, Inc.

Terzaghi, K. 1943. *Theoretical Soil Mechanics*. New York: John Wiley and Sons, Inc.

UNPAR, KBI Geoteknik. 2017. *Manual Praktikum Penyelidikan Tanah*. Bandung: Universitas Katolik Parahyangan.

Wesley, Laurence D. 2010. *Geotechnical Engineering in Residual Soils*. Hoboken, N.J.: John Wiley & Sons.

Studi Numerik Distribusi Beban dan Penurunan pada Fondasi Tiang-Rakit (Studi Kasus: Proyek Pembangunan Apartemen di Fatmawati, Jakarta Selatan)

Angela Dewi Maharani Susiyanti
Jurusan Teknik Sipil, Fakultas Teknik – Universitas Katolik Parahyangan

Ignatius Tommy Pratama
Jurusan Teknik Sipil, Fakultas Teknik – Universitas Katolik Parahyangan

Aswin Lim
Jurusan Teknik Sipil, Fakultas Teknik – Universitas Katolik Parahyangan

ABSTRAK: Studi ini bertujuan untuk mengevaluasi distribusi beban pada fondasi tiang-rakit pada proyek pembangunan apartemen di Fatmawati, Jakarta, dan pada tanah pasir dan lempung homogen. Selain itu, studi parametrik juga dilakukan pada fondasi tiang-rakit dengan memvariasikan beban kerja dan jarak antar tiang fondasi tiang-rakit. Hal ini dilakukan untuk membandingkan nilai distribusi beban dan penurunan yang terjadi. Studi dilakukan dengan menggunakan program berbasis metode elemen hingga tiga dimensi dengan model perilaku tegangan-regangan tanah Mohr-Coulomb untuk menyimulasikan pembebanan pada fondasi tiang-rakit. Hasil analisis menunjukkan bahwa fondasi tiang pada fondasi tiang-rakit di tanah pasir homogen menerima beban yang lebih besar dibandingkan dengan fondasi tiang di tanah lempung homogen dan pada kondisi tanah eksisting. Selain itu, penggunaan fondasi tiang pada fondasi tiang-rakit memiliki efek reduksi penurunan pada fondasi tiang-rakit yang relatif serupa baik pada tanah homogen maupun pada kondisi tanah eksisting.

Kata Kunci: fondasi tiang-rakit, distribusi beban, metode elemen hingga, penurunan

ABSTRACT: This study aims to evaluate the load distribution on a pile-raft foundation in an apartment construction project in Fatmawati, Jakarta, and in the homogeneous sand and clay soils. In addition, parametric studies were also carried out on the pile-raft foundations by varying the workload and the pile spacing on the pile-raft foundations to compare the load distribution and settlement of the pile-raft foundations. The analyses were executed by using a three-dimensional finite element method-based program with the Mohr-Coulomb soil stress-strain model to simulate the loading on the pile-raft foundations. The results indicate that the piles on the pile-raft foundations in the homogeneous sand soil carried a larger load than those were in the homogeneous clay soil and the existing soil conditions. Moreover, the piles had a relatively similar effect on reducing the settlement of the pile-raft foundations either in the homogeneous soil or in the existing soil stratum conditions.

Keywords: pile-raft foundation, load distribution, finite element method, settlement

1 PENDAHULUAN

Pada sistem fondasi tiang-rakit, fondasi tiang dapat digunakan untuk menambah daya dukung atau untuk mengurangi penurunan atau beda penurunan ke nilai yang diizinkan, Burland (1995). Disamping itu, penggunaan tiang pada fondasi tiang-rakit juga akan mengubah distribusi beban kerja pada fondasi. Fondasi rakit diasumsikan tidak memberikan kontribusi dalam memikul beban dalam fondasi tiang-rakit sehingga berdampak dalam jumlah fondasi tiang yang dibutuhkan, Clancy dan Randolph (1993). Namun, Katzenbach (2017) mengindikasikan bahwa fondasi tiang memikul 80% dari total beban yang bekerja. Pada kasus lain, Liang et al. (2003), Lee et al. (2010), dan Long et al. (2010) menunjukkan bahwa fondasi rakit dapat menahan 15% sampai 70% beban total struktur berdasarkan *full scale pile group test*. Kemudian, SNI 8460:2017 memberikan rekomendasi bahwa di dalam perancangan sebuah fondasi tiang-rakit, beban yang diizinkan untuk dipikul oleh fondasi rakit

adalah 25%, sedangkan sisanya dipikul oleh fondasi tiang.

Namun, rasio beban yang dipikul oleh fondasi tiang dan rakit terpublikasi hanya berlaku untuk kondisi tertentu seperti tanah pasir Berlin, Nguyen et al. (2013) dan tanah lempung Frankfurt, Lee et al. (2010). Maka, studi ini bertujuan untuk mengetahui mekanisme penyaluran beban yang diterima pada tiang dan rakit pada fondasi tiang-rakit, memperoleh rasio penurunan antara fondasi rakit dan fondasi tiang-rakit, dan mendapatkan distribusi beban yang dipikul oleh tiang dan rakit. Pertama-tama, analisis balik dilakukan untuk memperoleh parameter tanah di lokasi proyek berdasarkan uji pembebanan aksial tekan tiang bor. Kemudian, studi parametrik dilakukan pada fondasi tiang-rakit dengan beban kerja dan jarak antar tiang bervariasi untuk mengetahui pengaruh perubahan beban kerja dan jarak antar tiang terhadap rasio beban dan penurunan. Untuk mengetahui aplikasi nilai rasio beban dan penurunan pada jenis tanah yang berbeda, analisis numerik dengan metode elemen hingga tiga dimensi dilakukan pada fondasi tiang-rakit yang berada di tanah asli dan di tanah pasir dan lempung homogen dengan parameter yang ditentukan berdasarkan hasil analisis balik.

2 STUDI KASUS

2.1 *Deskripsi Proyek*

Proyek pembangunan apartemen terletak di Fatmawati, Jakarta Selatan. Gedung apartemen terdiri dari 4 buah tower di mana setiap tower terdiri dari 35 lantai (termasuk lantai atap), 1 lantai dasar, 1 lantai *semi-basement*, dan 3 lantai *basement*. Pada penelitian ini, hanya 1 tower, yaitu Tower 1 yang dianalisis karena struktur lantai dan pembebanan yang relatif tipikal.

Fondasi yang digunakan pada apartemen ini adalah fondasi tiang-rakit. Panjang dan lebar rakit yang digunakan secara berturut-turut adalah 42 m dan 32,4 m dengan tebal rakit sebesar 2,2 m. Fondasi tiang menggunakan fondasi tiang bor dengan diameter (D) 1,2 m, panjang tiang (L) 17 m, dan jarak antar tiang 3 m untuk arah X (S_h) dan 3,3 m untuk arah Y (S_v). Fondasi tiang rakit direncanakan untuk memikul beban terdistribusi merata ekuivalen sebesar 500 kN/m^2. Gbr. 1 menujukkan bahwa terdapat 143 tiang bor yang digunakan di dalam sistem fondasi tiang-rakit di proyek ini. Lokasi *cut off level* (COL) fondasi tiang-rakit adalah 15 m di bawah permukaan tanah eksisting.

2.2 *Simulasi Numerik dan Analisis Balik*

Analisis balik atau *back analysis* pertama-tama dilakukan dengan membandingkan kurva beban vs. penurunan hasil uji *loading test* di lapangan dengan hasil simulasi numerik pada program berbasis metode elemen hingga. Hal ini dilakukan untuk memperoleh parameter tanah yang sesuai dengan kondisi lapangan. Tiang uji *loading test* memiliki L = 17, D = 1,2 m dan dimodelkan sebagai *embedded beam*.

Berbagai korelasi empiris, Whilliam et al. (1962), Terzaghi dan Peck (1967), Peck (1974), Duncan dan Buchignani (1976), Das (1995), Shen (2011) digunakan untuk menentukan parameter tanah berdasarkan nilai N_{SPT} rata-rata pada suatu lapis tanah. Kemudian, model material Mohr-Coulomb digunakan untuk menyimulasikan perilaku tegangan dan regangan yang terjadi pada tanah. Tipe drainase pada tanah lempung atau lanau yang digunakan adalah *Undrained* B, sedangkan pada tanah pasir adalah *Drained* dengan lokasi muka air tanah pada kedalaman 5,2 m. Nilai angka Poisson efektif (υ') yang digunakan pada tanah lempung atau lanau, yaitu sebesar 0,3 dan pada tanah pasir sebesar 0,35. Profil tanah dan parameter tanah yang digunakan di dalam analisis numerik berdasarkan hasil analisis balik secara berturut-turut ditunjukkan oleh Gbr. 1 dan Tabel 1.

Pemodelan fondasi rakit di dalam studi ini menggunakan elemen *plate*, sedangkan pemodelan tiang menggunakan *embedded beam*. Untuk memodelkan interaksi antara tanah dengan struktur, parameter *interface* R_{inter} sebesar 0,8 digunakan. Pemodelan fondasi tiang-rakit dilakukan pada area *boundary* 200 m × 200 m × 90 m dengan posisi fondasi-tiang rakit berada di tengah *boundary*. Kemudian, distribusi elemen 10 nodal sangat halus digunakan di dalam proses diskretisasi domain (*meshing*) elemen tanah. Gbr. 1 menunjukkan model fondasi dan disribusi elemen yang digunakan.

Perlu diperhatikan bahwa kepala fondasi tiang berada di elevasi COL, sehingga proses galian perlu disimulasikan untuk memperoleh perilaku tegangan-regangan tanah yang mendekati kondisi di lapangan. Di dalam simulasi, galian hingga ke elevasi COL dilakukan pada keseluruhan model.

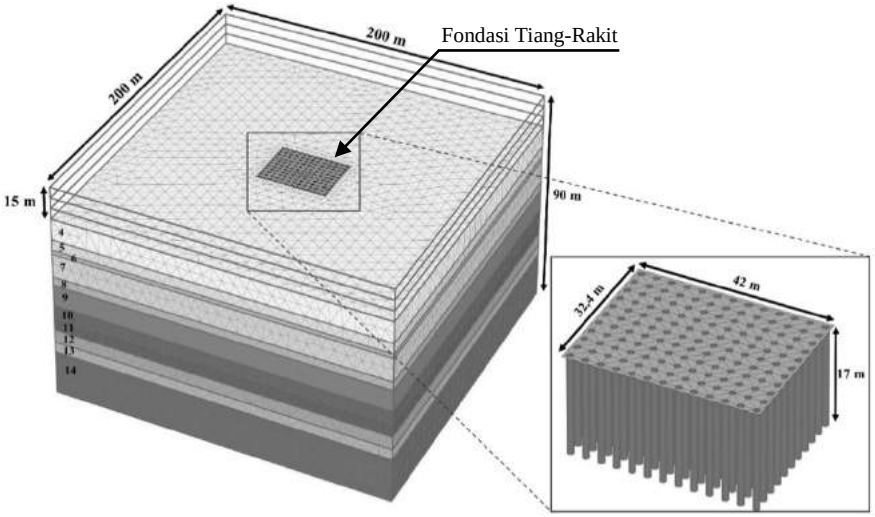

Gbr 1. Pemodelan Elemen Hingga Fondasi Tiang-Rakit.

Tabel 1. Parameter Tanah pada Pemodelan.

No	Kedalaman (m)	N_{SPT} Desain	Jenis Tanah	γ (kN/m^3)	γ_{sat} (kN/m^3)	s_u (kN/m^2)	ϕ' (°)	E' (kN/m^2)	K_0
1	0 – 5	6	Lempung	17	19	60		24.960	0,95
2	5 – 10	8	Lempung	17	19	80		33.280	0,95
3	10 – 15	11	Lempung	18	20	110		45.760	0,82
4	15 – 25	35	Lempung	20	22	350		145.600	0,82
5	25 – 30	60	Pasir	20	22		47	240.000	0,27
6	30 – 32	45	Lempung	20	22	450		187.200	0,82
7	32 – 43	58	Pasir	20	22		46	232.000	0,28
8	43 – 47	30	Lempung	20	22	300		60.000	0,82
9	47 – 57	58	Pasir	20	22		46	232.000	0,28
10	57 – 63	60	Lanau	20	22	600		120.000	0,74
11	63 – 69	30	Lempung	20	22	300		60.000	0,74
12	69 – 75	60	Pasir	20	22		47	240.000	0,27
13	75 – 80	60	Lanau	20	22	600		120.000	0,74
14	80 – 90	60	Pasir	20	22		47	240.000	0,27

Keterangan: berat isi tanah (γ), berat isi tanah jenuh (γ_{sat}), kuat geser tanah kohesif tak teralir (s_u), sudut geser tanah efektif (ϕ'), modulus elastisitas tanah (E'), koefisien tekanan tanah dalam keadaan diam (K_0).

2.3 *Studi Parametrik*

Studi parametrik dilakukan di dalam studi ini dengan memvariasikan jarak antar tiang dan jumlah tiang. Jarak antar tiang yang digunakan berkisar antara 2,5D hingga 5D. Perlu diperhatikan bahwa dimensi fondasi rakit dipertahankan, yaitu 42 m × 32,4 m di dalam analisis, sehingga hal ini akan mengakibatkan perubahan jumlah fondasi tiang pada fondasi tiang-rakit. Skema variasi jarak antar tiang di dalam studi ini dapat dilihat pada Tabel 2 di mana S_{tepi} merupakan jarak dari as fondasi tiang ke tepi fondasi rakit sebagai *pile cap*.

Variasi beban yang digunakan adalah 50, 250, 500, dan 1000 kN/m^2. Selain itu, studi parametrik juga dilakukan pada kondisi tanah yang berbeda-beda, yaitu pada kondisi tanah asli dan tanah lempung dan pasir homogen. Hal ini bertujuan untuk mengetahui perbedaan distribusi beban yang diterima oleh tiang dan rakit pada tanah asli, serta pada tanah lempung dan pasir homogen. Parameter tanah untuk tanah lempung dan untuk tanah pasir ditentukan berdasarkan hasil analisis balik parameter tanah lapis 4 untuk tanah lempung dan lapis 5 untuk tanah pasir yang dapat dilihat pada Tabel 1.

2.4 *Koefisien Tiang-Rakit (α_{pr})*

Distribusi beban yang dipikul oleh fondasi tiang dan rakit direpresentasikan oleh koefisien tiang-rakit (α_{pr}). Nilai α_{pr} menunjukkan perbandingan antara beban yang dipikul oleh fondasi tiang dengan beban keseluruhan dan dapat dinyatakan oleh Pers. (1).

$$\alpha_{pr} = \frac{\sum_{i=1}^{n} R_{tiang}}{R_{total}} = \frac{\sum_{i=1}^{n} R_{tiang}}{\sum_{i=1}^{n} R_{tiang} + R_{rakit}} \qquad (1)$$

di mana R_{tiang} adalah gaya perlawanan fondasi tiang terhadap gaya aksial yang terjadi dan R_{rakit}

adalah resistensi fondasi rakit yang diperoleh dari pengurangan beban yang diterima oleh fondasi tiang-rakit dengan resistensi seluruh tiang. Berdasarkan Pers. (1), ketika nilai α_{pr} = 0, maka fondasi rakit memikul seluruh beban yang diberikan. Sebaliknya, jika seluruh beban dipikul oleh fondasi tiang maka nilai α_{pr} = 1. Menurut Katzenbach et al. (2017), nilai α_{pr} antara 0,5 sampai 0,7 dapat dianggap optimum dari aspek teknis maupun ekonomi.

2.5 *Rasio Penurunan Fondasi Tiang-Rakit (β)*

Rasio penurunan fondasi tiang-rakit (β) adalah perbandingan antara penurunan fondasi tiang-rakit (s_{pr}) dan penurunan fondasi rakit (s_{sf}) dengan luas tapak yang sama dan beban yang sama. Pers. (2) menyatakan rasio β.

$$\beta = \frac{s_{pr}}{s_{sf}} \tag{2}$$

Apabila nilai β mendekati 0, hal ini mengindikasikan bahwa penambahan fondasi tiang dapat mengurangi penurunan keseluruhan dari sistem fondasi tiang-rakit dan β = 1 mengartikan penambahan fondasi tiang pada rakit tidak mengurangi penurunan yang terjadi.

Tabel 2. Skema Studi Parametrik.

Spasi	2,5D	3D	4D	5D
D (m)	1,2	1,2	1,2	1,2
L (m)	17	17	17	17
n	143	108	63	42
S_h (m)	3,3	3,6	4,8	6,6
S_v (m)	3	3,75	4,8	6
S_{tepi} (m)	1,2	1,2	1,2	1,2

3 HASIL DAN PEMBAHASAN

3.1 *Analisis Koefisien Tiang-Rakit (α_{pr})*

Berdasarkan hasil analisis pengaruh variasi beban kerja dan jarak antar tiang pada tanah lempung, secara umum, nilai α_{pr} pada tanah lempung berkisar antara 0,38 hingga 0,64. Kemudian, hasil analisis juga menunjukkan bahwa penurunan nilai α_{pr} terjadi seiring dengan bertambahnya beban yang diberikan pada fondasi tiang-rakit. Namun, penurunan menjadi relatif tidak signifikan ketika beban total yang diberikan melebihi 700.000 kN atau setara dengan beban merata 500 kN/m^2. Hal ini mengindikasikan bahwa fondasi tiang akan menopang sebagian besar beban yang terjadi pada saat beban kerja masih relatif kecil.

Kemudian, pada saat daya dukung tiang telah melampaui kapasitasnya, fondasi rakit akan menopang beban kerja yang terjadi hingga mencapai kapasitasnya dan nilai α_{pr} menjadi relatif konstan. Hasil serupa juga ditunjukkan oleh Horikoshi dan Randolph (1998) dimana kapasitas tiang total, yaitu 40-60% dari total beban rakit. Kemudian, untuk pemodelan fondasi tiang rakit dengan beban kerja sama, beban kerja yang diterima oleh tiang akan semakin kecil seiring dengan meningkatnya jarak antar tiang. Hal ini dapat disebabkan oleh pengurangan jumlah tiang, sehingga semakin sedikit jumlah tiang, maka semakin besar beban yang diterima oleh fondasi rakit. Gbr. 2 menunjukkan perubahan nilai α_{pr} terhadap perubahan beban kerja dan spasi antar tiang pada fondasi tiang-rakit di tanah lempung dan pasir homogen.

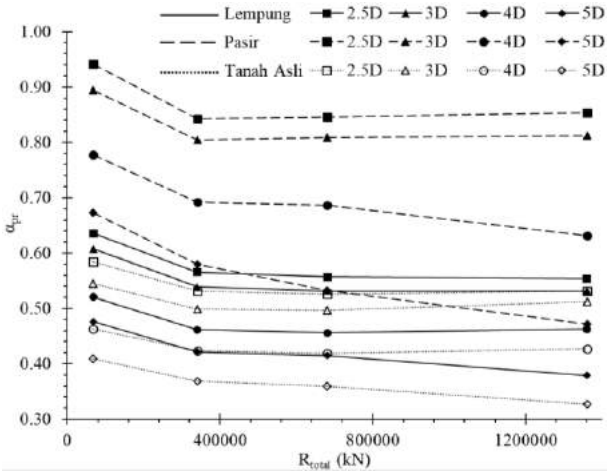

Gbr 2. Grafik α_{pr} terhadap Resistensi Tiang-Rakit (R_{total}).

Gbr. 2 menunjukkan bahwa pada pemodelan fondasi tiang-rakit dengan jarak antar tiang 5D, distribusi beban yang diterima oleh tiang masih mengalami penurunan. Hal ini dapat diakibatkan oleh jarak antar tiang yang relatif jauh dan jumlah tiang yang relatif sedikit, sehingga fondasi tiang tidak berperan dominan dalam menopang beban kerja dan kapasitas tiang belum mencapai batas ultimitnya.

Pada pemodelan fondasi tiang-rakit di tanah pasir, nilai α_{pr} secara umum memiliki rentang berkisar antara 0,5 hingga 0,81. Selain itu, nilai α_{pr} pada tanah pasir juga memiliki kecenderungan serupa dengan perubahan nilai α_{pr} pada fondasi tiang-rakit di tanah lempung. Nilai α_{pr} menurun seiring meningkatnya beban dan menjadi relatif konstan pada saat beban kerja melebihi 600.000 kN. Selain itu, pada

beban kerja yang sama, nilai α_{pr} akan menurun seiring dengan meningkatnya jarak antar tiang. Namun, di dalam pemodelan fondasi tiang-rakit di tanah pasir, peran fondasi tiang menjadi relatif dominan di dalam memikul beban. Hal ini ditunjukkan dengan nilai nilai α_{pr} yang mendekati satu (1) pada fondasi tiang-rakit dengan jarak antar tiang 2,5D. Maka, dapat diindikasikan bahwa fondasi tiang-rakit menjadi kurang efektif di tanah pasir karena fondasi rakit memiliki peran yang relatif tidak signifikan di dalam menopang beban kerja.

Kemudian, untuk kondisi tanah asli, nilai α_{pr} memiliki tren yang relatif serupa dengan tren nilai α_{pr} pada tanah lempung. Nilai α_{pr} pada tanah asli yang diperoleh berkisar antara 0,33 hingga 0,58 dan nilai tersebut cenderung serupa dengan nilai α_{pr} pada tanah lempung (α_{pr} = 0,38 – 0,64). Hal ini mengindikasikan bahwa distribusi beban yang terjadi pada fondasi tiang-rakit di tanah asli serupa dengan yang terjadi pada fondasi tiang-rakit di tanah lempung dan perilaku fondasi tiang-rakit di lokasi proyek di kontrol oleh lapisan tanah lempung.

Nilai α_{pr} juga dipengaruhi oleh parameter tanah, yaitu nilai modulus tanah (E), s_u, dan ϕ'. Ketika nilai E dan ϕ' semakin besar maka α_{pr} akan semakin kecil. Sementara itu, nilai s_u tidak terlalu mempengaruhi nilai α_{pr} (hasil tidak ditampilkan pada makalah ini).

3.2 *Analisis Rasio Penurunan Fondasi Tiang-Rakit (β)*

Gbr. 3 merupakan grafik perubahan rasio β terhadap beban yang diberikan pada fondasi tiang-rakit di tanah lempung dengan variasi beban dan berbagai nilai jarak antar tiang. Untuk fondasi tiang-rakit pada tanah lempung, rasio β berkisar antara 0,74 hingga 0,91.

Selain itu, hasil analisis pada Gbr. 3 juga mengindikasikan bahwa pada mulanya, fondasi tiang dapat secara efektif menurunkan penurunan fondasi tiang rakit. Namun, ketika beban kerja meningkat, rasio β meningkat menuju nilai β = 1. Hal ini mengindikasikan bahwa fondasi tiang tidak lagi efektif dalam mengurangi penurunan fondasi tiang-rakit. Namun, pada pemodelan fondasi tiang-rakit dengan jarak antar tiang 2,5D dan 3D di tanah lempung, rasio β relatif konstan pada saat beban kerja ditingkatkan.

Kemudian, pada beban kerja yang sama (Gbr. 3), fondasi tiang-rakit dengan nilai jarak antar tiang yang lebih besar akan memiliki rasio β yang juga lebih besar. Hal ini mengindikasikan bahwa fondasi tiang akan semakin tidak efektif dalam mengurangi nilai penurunan fondasi tiang-rakit apabila jarak antar tiang semakin besar dan jumlah tiang semakin sedikit. Hasil serupa ditunjukkan oleh Cho et al. (2012) di mana rasio β menurun sampai titik belok tertentu dan meningkat seiring dengan beban yang semakin besar, meskipun penurunan pada tiang-rakit meningkat dengan meningkatnya beban yang diberikan. Lee dan Chung (2005) menyarankan penggunaan konfigurasi jarak antar tiang di bawah 4D–5D pada pemodelan fondasi tiang-rakit untuk menurunkan penurunan maksimum yang disebabkan oleh rakit secara optimal.

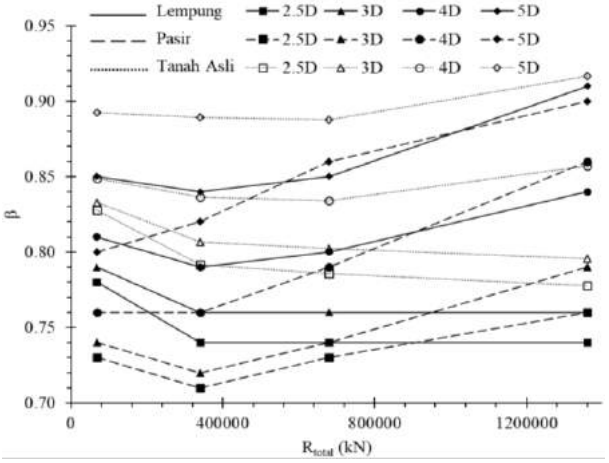

Gbr 3. Grafik β terhadap Resistensi Tiang-Rakit (R_{total}).

Secara umum, rasio β pada tanah pasir di dalam studi ini memiliki rentang antara 0,71 hingga 0,92. Hasil analisis pada tanah pasir menunjukkan tren rasio β yang serupa dengan rasio β pada pemodelan fondasi tiang-rakit di tanah lempung. Nilai β pada tanah pasir akan cenderung meningkat seiring dengan peningkatan beban kerja. Selain itu, pada beban kerja yang sama, nilai β juga akan meningkat seiring dengan bertambahnya jarak antar tiang pada fondasi tiang-rakit.

Untuk fondasi tiang-rakit pada tanah asli, Gbr. 3 menunjukkan bahwa perubahan rasio β pada tanah asli juga memiliki tren yang serupa dengan perubahan rasio β pada tanah lempung. Pada tanah asli, rasio β yang memiliki rentang nilai antara 0,79 – 0,92. Namun, nilai β yang diperoleh pada tanah asli dengan jarak antar tiang yang sama lebih besar dibandingkan yang diperoleh pada tanah lempung maupun pasir. Hal ini dapat terjadi akibat kombinasi kekakuan dan perilaku tanah lempung dan pasir di sepanjang tiang. Nilai rasio β juga dipengaruhi oleh nilai s_u di mana semakin besar nilai s_u, maka semakin kecil rasio β. Semetara itu, untuk

variasi terhadap nilai E, rasio β semakin besar seiring dengan semakin besarnya nilai E. Namun, rasio β tidak menunjukkan tren khusus untuk variasi terhadap nilai ϕ' (hasil tidak ditampilkan pada makalah ini).

4 KESIMPULAN

Penelitian ini menyajikan hasil studi parametrik fondasi tiang-rakit dengan berbagai nilai jarak antar tiang dan beban kerja, serta pada kondisi tanah yang berbeda-beda, yaitu pada kondisi tanah asli berdasarkan studi kasus proyek pembangunan apartemen di Fatmawati, Jakarta, kemudian pada tanah lempung, dan tanah pasir homogen.

Berdasarkan hasil analisis dengan menggunakan program elemen hingga tiga dimensi, persentase beban yang dipikul oleh tiang pada sistem tiang-rakit di tanah lempung homogen sebesar 38–64% dan pada tanah pasir homogen sebesar 47–94% dengan nilai rasio penurunan yang didapatkan pada tanah lempung homogen sebesar 0,91–0,74 dan pada tanah pasir homogen sebesar 0,90–0,71. Pada tanah asli, didapatkan persentase beban yang dipikul oleh tiang sebesar 33-58% dan rasio penurunan yang didapatkan sebesar 0,92–0,79.

Dalam studi parametrik, ditemukan bahwa mekanisme distribusi beban pada fondasi tiang-rakit adalah tiang menerima beban yang diberikan sampai mencapai batas maksimum kemudian dilanjutkan dengan rakit yang menerima beban kerja. Maka, pemodelan fondasi tiang sangat penting pada sistem fondasi tiang-rakit. Didapatkan bahwa jarak antar tiang di bawah konfigurasi empat (4) hingga lima (5) kali diameter tiang dapat memberikan nilai koefisien tiang-rakit (α_{pr}) dan rasio penurunan (β) yang lebih optimal.

DAFTAR PUSTAKA

Badan Standardisasi Nasional. 2017. *Standar Nasional Indonesia SNI 8460:2017 Tentang Persyaratan Perancangan Geoteknik*. Jakarta: Badan Standardisasi Nasional.

Brinkgreve, R.B. & Shen, R.F. 2011. *Structural Elements & Modelling Excavations in PLAXIS*. Delf, the Netherlands.

Burland, J.B. 1995. Piles as Settlement Reducers. *Proceeding's 19th National Italian Geotechnical Conference:*21-34. Pavia, Italy.

Cho, J., et al. 2012. The Settlement Behavior of Piled Raft In Clay Soils. *Ocean Engineering 53*, 153-163.

Clancy, P. & Randolph, M.F. 1993. An Approximate Analysis Procedure for Piled Raft Foundations. *International Journal for Numerical and Analytical Methods in Geomechanics* 17: 849-869.

Das, Braja M. 1995. *Mekanika Tanah Jilid 1 Terjemahan*. Jakarta: Erlangga.

Duncan, J.M., & Buchignani, A.L. 1976. *An Engineering Manual for Settlement Studies.* University of California, Department of Civil Engineering.

Horikoshi, K., & Randolph, M. F. 1998. A Contribution to Optimum Design of Piled Rafts. *Geotechnique* 48(3): 301-317.

Katzenbach, R., Leppla, S., & Choudhury, D. 2016. *Foundation Systems for High-Rise Structures. CRC* Press.

Lee, S. H., and Chung, C. K. 2005. An Experimental Study of The Interaction of Vertically Loaded Pile Groups in Sand. *Canadian Geotechnical Journal* 42(5): 1485-1493.

Lee, S. W., Cheang, W. W. L., Swolfs, W. M., & Brinkgreve, R. B. J. 2010. Modelling of Piled Rafts with Different Pile Models. *In Proceedings of the 7th European Conference on Numerical Methods in Geotechnical Engineering*: 637-642. Trondheim, Norway: CRC Press.

Liang, F. Y., Chen, L. Z., & Shi, X. G. 2003. Numerical Analysis of Composite Piled Raft with Cushion Subjected to Vertical Load. *Computers and Geotechnics* 30(6): 443-453.

Long, P.D. & Vietnam, V.W. 2010. Piled Raft—A Cost-Effective Foundation Method for High-Rises. *Geotechnical Engineering* 41(1): 149.

Nguyen, D. D. C., Jo, S. B., & Kim, D. S. 2013. Design Method of Piled-Raft Foundations Under Vertical Load Considering Interaction Effects. *Computers and Geotechnics* 47: 16-27.

Peck, Ralph B., Hanson, Walter E., & Thornburn, Thomas H. 1974. *Foundation Engineering, 2nd ed*. New York, NY: John Wiley and Sons, Inc.

Terzaghi, K. & Peck, R. 1967. *Soil Mechanics in Engineering Practice, 2nd Edn*. New York: Wiley.

William, T. & Whitman, Robert V. 1962. *Soil Mechanics.* New York, NY: John Wiley and Sons, Inc.

The Geological and Geotechnical Studies for Road Construction Site Planning by Spatial Analysis and Slope Stability Modeling (Case Study: Penggaron-Mluweh Road, Semarang Regency, Central Java)

M. Hajjrol Dava
Geological Engineering – Diponegoro University

Lia Suryani
Geological Engineering – Diponegoro University

ABSTRACT: Landslide is one of the natural disasters that have many impacts on various sectors in society, such as damage to public facilities and infrastructure, even causing many casualties, so a planning step is needed to minimize these impacts. The research location on the street of Penggaron-Mluweh has complex geological conditions. The methods used in this study are remote sensing and shear strength reduction (SSR) using phase2 software. The results of the analysis show that the research location is in an area that is prone to landslides. Slope stability analysis shows that of the 7 slopes, 2 slopes are in an unstable condition with an SRF value < 1. The results of field investigations found a shear fault zone near the L2 location. Based on the results of the study, it was interpreted that the landslide of the road was closely influenced by the presence of unfavorable rock mass conditions and shear faults zone that caused the slope to become unstable. It is hoped that this study can assist in the planning of road infrastructure development.

Keywords: slope stability, shear strength reduction, study of geology and geotechnical, spatial analysis

1 INTRODUCTION

Roads are land transportation infrastructure that is very important to facilitate community activities between one region and another. The good road conditions will facilitate community mobility, while damaged road conditions will have an impact on economic, social activities, and can even result in accidents that take lives. Thus, at the road planning stage, geological and geotechnical studies are needed to minimize road damage and the impacts that will occur.

The Penggaron – Mluweh road which is located in the East Ungaran area, Semarang Regency is the only alternative road that connects the Mluweh area Penggaron. The existence of this road facilitates community mobilization so that it becomes more efficient than having to go through the main road which is quite far away. However, with the existing geological and morphological conditions, at some points on the road, it is often damaged and even experienced landslides. This landslide has also caused Mluweh's access to Penggaron to be cut off.

Therefore, the role of geological and geotechnical studies at the planning stage is necessary to minimize damage, loss, and even fatalities.

2 REGIONAL GEOLOGY

The research area is in the Mluweh-Penggaron Street, Kabupaten Semarang, Central Java Province. The location of reaserch has several types of lithology, slope, and geomorphology. Based on the Geological Map of Indonesia, Magelang – Semarang Sheet, Thanden, et al. (1996), the research area is composed of stratigraphy in the form of:

2.1 *Kerek Formation (Tmk)*

The lithology in the form of alternating claystone, marl, tuffaceous sandstone, conglomerate, volcanic breccia, limestone, and there is light gray claystone containing fossil forams, mollusks, and coral colonies. Thin layers of conglomerate lithology are found in claystone at Kripik River and in sandstones. In

general, the limestone is layered, crystalline, and sandy, and has a total thickness of more than 400 meters.

2.2 *Kalibeng Formation (Tmkb)*

The lithology is composed of marl, marl with tuffaceous sandstone inserts, and limestone. Marble is greenish-grey-black in color, contains clay minerals, and is at the top of the carbonized area. Limestone nodules are 3 – 200 cm in size and have a diameter. The tuffaceous sandstone is yellow-black, while the limestone is grayish-white.

2.3 *Kaligetas Formation (Qpkg)*

The rock consists of breccias and lahars with lava inserts and fine to coarse tuff, locally found at the bottom of the claystone containing molluscs and tuffaceous sandstone. Generally, it has undergone quite intensive weathering to produce reddish-brown soil material, exposed at Kali Putih, Mount Sambi, Mount Cerme, Sukorejo and Singorojo.

2.4 *Volcanic Gajahmungkur Formation (Qhg)*

The rock is andesite lava, gray-black in color, fine-grained, holocrystalline, the composition consists of feldspar, hornblende and augite, hard and compact.

3 METHODOLOGY

Data analysis using two methods, namely spatial analysis and slope stability. The following is a description of each analysis:

3.1 *Spatial Analysis*

This analysis is carried out by processing lithological data, land cover, elevation, slope, distance to road, distance to stream, and distance to straightness. The data is then weighted using the AHP (Analytical Hierarchy Process) method to obtain a landslide-prone map zoning.

3.2 *Slope Stability*

In this analysis using the Finite element method by shear strength reduction, this method is considered to be able to provide detailed results. The parameters used in this analysis are rock geomechanics, dynamic loads, and joint conditions, all data obtained directly from observations in the field. This analysis uses phase2 software to get the Strength Reduction Factor (SRF) value.

4 RESULT AND DISCUSSION

4.1 *Spatial Data Analysis*

Based on the lithological data, it is processed into a lithological map (see Fig. 1) in the study area in the form of claystone from the Kerek formation which is the most dominant lithology in the study area, sandstone from the Kalibeng formation, breccias from the Kaligetas formation, and andesite from the Gajahmungkur Volcanic formation. The land cover data was processed into a land cover map (see Fig. 2) which shows the existence of 3 land covers, namely settlements, mixed dryland agriculture which is the dominant land cover in the study area, and open land. Elevation data is made from DEM data which is extracted into an elevation map (see Fig. 3) which is then classified into 5 zones, namely elevation 58 – 115 m, 115 – 160 m, 160 – 211 m, 211 – 279 m, and 279 – 420 m. Slope data is made from DEM data which is extracted into a slope map (see Fig. 4) which is then classified into 5 zones, namely very gentle slopes, gentle slopes, moderate slopes, steep slopes, and very steep slopes. Distance maps to roads, streams, and lineaments (see Fig. 5, 6, 7) were made from data on road networks, river networks, and lineament distributions which were then processed using Euclidean distance and obtained 5 zones, namely at a distance of 0 – 250 m, 250 – 500 m, 500 – 750 m, 750 – 1000 m, and >1000 m.

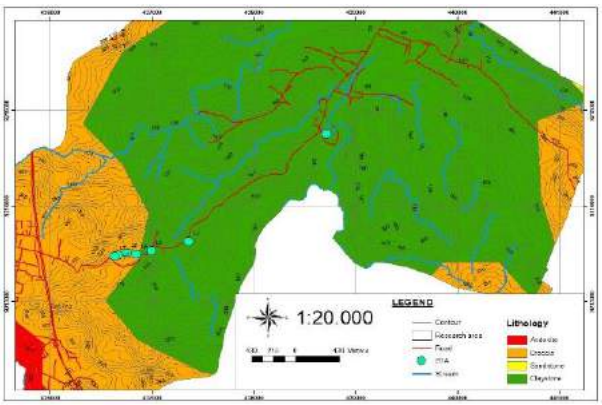

Fig. 1. The Map of Lithology.

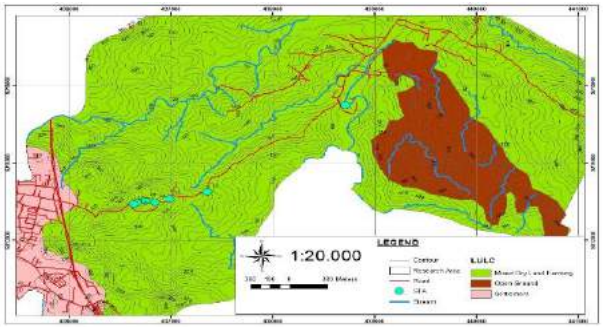

Fig. 2. The Map of LULC (Land Use and Land Cover).

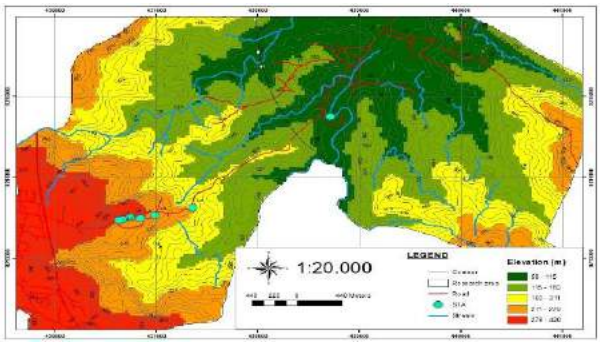

Fig. 3. The Map of Elevation.

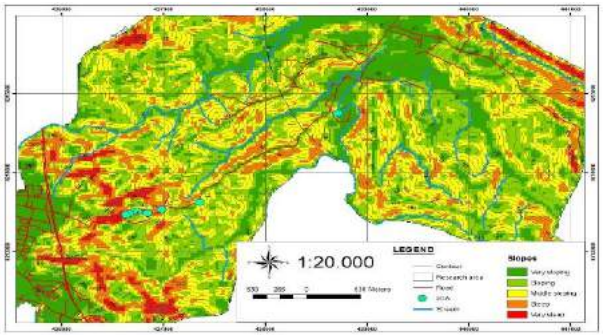

Fig. 4. The Map of Slopes.

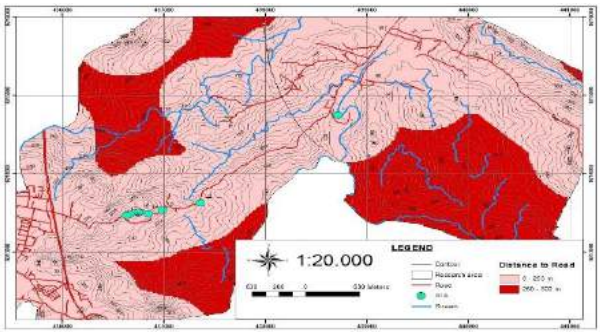

Fig. 5. The Map of Distance to Road.

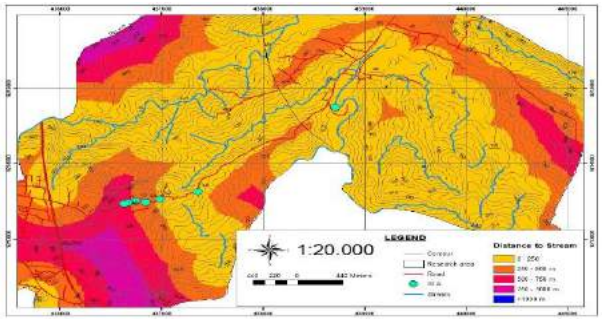

Fig. 6. The Map of Distance to Stream.

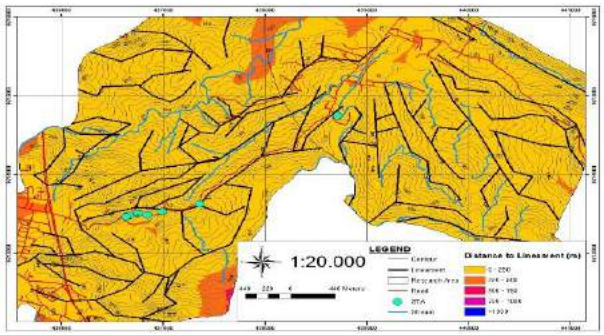

Fig. 7. The Map of Distance to Lineament.

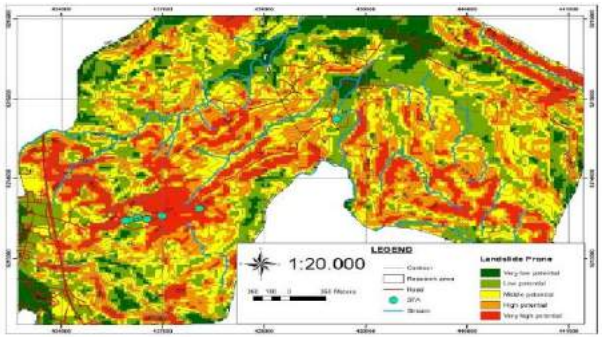

Fig. 8. The Map of Landslides Hazard.

A landslide hazard map (see Fig. 8) was created by weighting the data on lithology, land cover, elevation, slope, distance to road, distance to streams, and distance to straightness using the AHP method, Saaty (1980). Based on the weighting (see Table 1), there are 5 landslide-prone zones, namely very low potential, low potential, medium potential, high potential, and very high potential. Based on the results and discussion, it was found that the research area is in a landslide-prone zone with moderate to very high potential, this is supported by the unstable claystone lithology. Land use and land cover (LULC) is located on mixed dry agricultural land so that there is a lack of vegetation to bind soil/rock material. The elevation and slope at the study site are at a moderate to very steep level. The existence of a road network affects the load and vibration received. The existence of a stream network indicates a weak zone in the area, and a large number of lineament networks causes the geological structure to also affect landslides in the study area.

4.2 *Slope Stability Analysis*

In the study area, 7 locations with the highest landslide rates were selected (Fig. 9). All of geotechnical data such as joint conditions, Schmidt hammer reflection values , and GSI from the lithology of each slope, the UCS value was obtained through the results of empirical

calculations given by Saptono et al. (2013), as well as the value of the young modulus obtained from the empirical calculations given by Yagiz (2009). The results of field observations can be seen in Table 2.

Table 1. The Weighting of AHP (Analitical Hierarchy Process), Saaty (1980).

	Lithology	LULC	Elevation	Slopes	Distance to Road	Distance to Stream	Distance to Lineament	Weighting
Lithology	1	5	5/4	1	5/2	5/3	5/4	20%
LULC	1/5	1	1/4	1/5	1/2	1/3	1/4	4%
Elevation	4/5	4	1	4/5	2	4/3	1	16%
Slopes	1	5	5/4	1	5/2	5/3	5/4	23%
Distance to Road	2/5	2	2	2/5	1	2/3	1/2	8%
Distance to Stream	3/5	3	3/4	3/5	3/2	1	3/4	12%
Distance to Lineament	4/5	4	1	4/5	2	4/3	1	16%

Fig. 9. Collection and Assessment of Geotechnical Data in Field.

Table 2. The Geotechnical Parameters for Slope Assessment

Slope	Schmidt Hardness	UCS	Young Modulus (Mpa)	GSI
L1	9.2	5.8545	31083.1719	43
L2	10.1	6.6265	35936.4132	53
L3	14.6	10.8055	63724.0936	53
L4	12.6	8.8867	50680.7653	53
L5	16.8	13.0177	79261.1613	57
L6	18.3	14.5822	90531.0112	53
L7	15.6	11.7985	70636.5274	53

In making slope modeling, there are several parameters needed including geometry, geomechanics, and joint conditions. The joint distribution modeling in 2-dimensional slope stability analysis is assumed by several models while in this analysis the researcher uses 2 models, namely the Voronoi model and the beacher model. The Voronoi model is used on slopes that have joint conditions that tend to be random and have a net pattern, while the beacher model is used on slopes that have a clear joint orientation.

The joint condition itself is also carried out by data collection, while the data needed to model the joint condition are Normal Stiffness (Kn) and Shear Stiffness (Ks). To get the values of Kn and Ks in this study, the empirical calculations given by Barton (1972). Parameters of joint conditions of slope stability modeling in this study can be seen in Table 3.

Table 3. Parameters of Joint Condition Slope Stability Model.

Slope	Joint	Schmidt's Rebound	UCS	Ei (Mpa)	Erm (Mpa)	L (m)	Kn	Ks	Model
L1	JS1	17.6	13.847	85205.297	2360.410	1,000	2427.663	242,766	Voronoi
L2	JS1	9.5	6.109	32672.961	2392.070	1,000	2581.034	258,103	Voronoi
L3					Massive				
L4	JS1	16.0	12.202	73471.967	1984.550	2,000	1019.821	101,982	Beacher
L4	JS2	14.6	10.806	63724.094	1984.550	2,000	1024.171	102,417	Beacher
L5	JS1	18.7	15.007	93625.668	1984.550	1,000	2027.527	202,753	Voronoi
L6	JS1	10.4	6.889	37609.320	1984.550	1,500	1396.736	139,674	Voronoi
L7	JS1	16.7	12.915	78528.971	1984.550	2,000	1018.001	101,800	Beacher

After analyzing the stability of the slopes using the shear strength reduction (SSR) method with the software phase2, it is found that the Shear Strength Reduction (SRF) values are varied. There are 2 out of 7 slopes that are in an unstable condition and the remaining 5 slopes are in a stable condition.

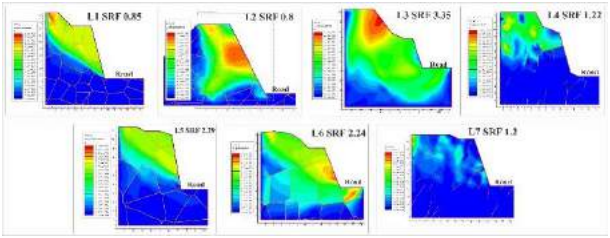

Fig 10. Slope Stability Analysis by SSR Each Slope.

Table 4. Stability Grades Each Slope Investigation.

Slope	SRF	Stability Grade (Kepmen, ESDM 2018)
L1	0,85	Unstable
L2	0.8	Unstable
L3	3.35	Stable
L4	1.22	Stable
L5	2.29	Stable
L6	2.24	Stable
L7	1.2	Stable

The results of the analysis show that there are 2 slopes, namely the L1 and L2 slopes which are in an unstable condition. This is supported by the finding of landslides at both locations (Fig 11). The results of field observations found that there was a destruction zone in the southern part of the former L2 landslide (Fig 11). It is interpreted that this destruction zone occurs due to reactivation of shear faults in the study area, as it is known from regional geological studies that this area is indeed flanked by 3 shear faults. In addition to faults, external factors such as weathering that is quite intense on rocks, dynamic loads and high rainfall are also some of the main triggering factors for landslides in this area.

Fig. 11. The Landslide Area.

CONCLUSION

Based on the results of the analysis, it can be concluded that:

1. Road construction planning must take into account the geological conditions of the area and its engineering geology.
2. Geological studies using spatial analysis can be carried out to determine the potential for landslide disasters.
3. Technical geological assessment can be carried out periodically if the area being built is in an area prone to landslides.

ACKNOWLEDGEMENTS

The author is grateful to the Laboratory of Soil and Rock Mechanics, Vocational School of Civil Engineering, Diponegoro University for allowing the author to use the Schmidt Hammer Test tool.

REFERENCES

Barton, N. R. 1972. 1993. A Model Study of Rock-Joint Deformation. *International Journal of Rock Mechanics and Mining Sciences & Geomechanics Abstracts* Vol. 9. No. 5. Pergamon.

Menteri Energi dan Sumber Daya Mineral. 2018. *Pedoman Pelaksanaan Kaidah Teknik Pertambangan yang Baik*. Indonesia.

Saaty TL. 1980. *Analytic Hierarchy Process*. New York: McGraw Hill.

Saptono, S., Kramadibrata, S. and Sulistianto, B., 2013. Using the Schmidt Hammer on Rock Mass Characteristic in Sedimentary Rock at Tutupan Coal Mine. *Procedia Earth and Planetary Science*, *6*: 390395.

Thanden, R.E., Sumadirdja, H., Richards, P.W., Sutisna, K. dan Amin, T.C. 1996. *Peta Geologi Regional Lembar Magelang dan Semarang Skala 1:100.000*. Pusat Penelitian dan Pengembangan Geologi, Bandung.

Yagiz, S., 2009. Predicting Uniaxial Compressive Strength, Modulus of Elasticity and Index Properties of Rocks Using the Schmidt Hammer. *Bulletin of Engineering Geology and the Environment 68*(1): 55-63.

Studi Parametrik Kondisi Batas Melalui Simulasi Numerik Uji Pembebanan Tiang Tunggal

Kyrie Eleisia
Program Studi Teknik Sipil, Fakultas Teknik – Universitas Katolik Parahyangan

Ignatius Tommy Pratama
Program Studi Teknik Sipil, Fakultas Teknik – Universitas Katolik Parahyangan

Aswin Lim
Program Studi Teknik Sipil, Fakultas Teknik – Universitas Katolik Parahyangan

ABSTRAK: Di dalam pemodelan struktur geoteknik, seperti fondasi tiang dengan menggunakan pendekatan numerik, kondisi batas perlu ditentukan dengan tepat untuk menghindari efek batas. Namun, studi terkait penentuan kondisi batas khususnya pada kasus fondasi tiang masih relatif terbatas. Studi ini bertujuan untuk memperoleh nilai kondisi batas yang diperlukan melalui simulasi uji pembebanan fondasi tiang tunggal dengan menggunakan program Plaxis 2D. Analisis dengan variasi pada panjang dan diameter fondasi tiang, serta kondisi batas dalam arah horizontal maupun vertikal, dilakukan untuk mengetahui pengaruh geometri tiang terhadap kondisi batas. Hasil analisis menunjukkan bahwa diperlukan jarak horizontal minimum sebesar 25 kali diameter tiang dan jarak vertikal minimum sebesar 3 kali panjang tiang. Selain itu, studi pada titik-titk keruntuhan yang terjadi menunjukkan bahwa titik-titik keruntuhan yang bertepatan dengan batas model akan menghasilkan daya dukung ultimit yang tidak konsisten.

Kata Kunci: Plaxis 2D, fondasi tiang, kondisi batas, daya dukung ultimit

ABSTRACT: In modeling geotechnical structures, such as pile foundations using a numerical approach, boundary conditions need to be determined precisely to avoid boundary effects. However, the studies related to the estimation of boundary conditions, especially in the case of pile foundations, are still relatively limited. Thus, this study aims to obtain the required boundary conditions through a single pile foundation loading test simulation by using Plaxis 2D. Analyses with various lengths and diameters of the pile foundation, as well as boundary conditions in the horizontal and vertical directions, were performed to observe the effects of pile geometry on boundary conditions. The results show that the required horizontal and vertical boundaries were 25 times the pile diameter and 3 times the pile length, respectively. Furthermore, the study on the occurred failure points indicates that the coincided failure points with the model boundaries would result in an inconsistent ultimate bearing capacity.

Keywords: Plaxis 2D, pile foundation, boundary conditions, ultimate bearing capacity

1 PENDAHULUAN

Pemodelan struktur geoteknik seperti uji pembebanan pada fondasi tiang dengan menggunakan pendekatan numerik telah banyak dilakukan untuk memperkirakan nilai daya dukung tiang. Permasalahan yang umumnya terjadi pada simulasi numerik uji pembebanan tiang adalah adanya perbedaan antara daya dukung tiang hasil simulasi numerik dengan daya dukung tiang hasil estimasi kurva beban terhadap penurunan hasil uji pembebanan di lapangan. Hal ini dapat disebabkan oleh adanya efek batas di dalam pemodelan fondasi tiang secara numerik.

Kondisi batas, baik dalam arah vertikal maupun horizontal perlu diperhatikan di dalam pemodelan fondasi tiang secara numerik. Menurut Vermeer et al. (2005), batas vertikal harus diletakkan pada kedalaman di mana perubahan tegangan akibat penambahan beban ($\Delta\sigma$) kurang dari 10%. Dong et al. (2017) menjelaskan bahwa batas-batas yang dimodelkan dapat mendistorsi tegangan dan regangan, sehingga mengakibatkan nilai daya dukung tiang yang terlalu tinggi.

Bowles (1997) mengestimasi zona tegangan yang terjadi pada fondasi tiang sebesar 6-10D dari ujung tiang ke atas dan sebesar 2-4D dari ujung tiang ke bawah dimana D adalah

diameter dari fondasi tiang. Gbr.1 mengilustrasikan zona pengaruh yang direkomendasikan oleh Bowles (1997). Namun, studi lebih lanjut diperlukan untuk memverifikasi aplikasi estimasi zona tegangan oleh Bowles (1997) pada berbagai kondisi tanah dan geometri tiang, serta kondisi batas.

Menurut Dong (2017), batas horizontal memiliki pengaruh yang signifikan terhadap daya dukung tiang di tanah lempung homogen, sehingga diperlukan jarak horizontal lebih dari 15 kali diameter tiang untuk meminimalkan pengaruh batas. Namun, studi yang dilakukan oleh Dong (2017) hanya berfokus pada studi parametrik berbasis metode elemen hingga pada tiang tunggal yang diberikan beban lateral. Sehingga, pemodelan numerik dengan berbagai kondisi batas masih perlu dilakukan berulang kali untuk mendapatkan jarak yang memadai agar meminimalisir efek batas, khususnya pada kondisi beban aksial tekan.

Pada studi ini, dilakukan simulasi uji pembebanan aksial tekan fondasi tiang tunggal pada tanah lempung homogen dengan menggunakan program berbasis elemen hingga dua dimensi yaitu Plaxis 2D. Analisis dilakukan dengan memvariasikan panjang tiang, diameter tiang, dan jarak kondisi batas untuk memperoleh jarak horizontal dan jarak vertikal yang optimal.

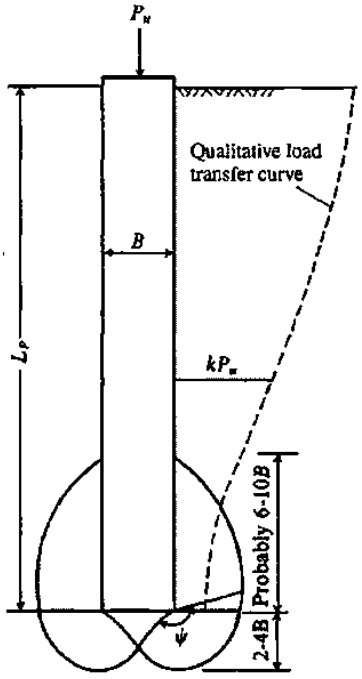

Gbr. 1. Zona Pengaruh Fondasi Tiang, Bowles (1997).

2 METODE

2.1 *Parameter Tanah dan Tiang*

Pada studi ini, tanah yang digunakan adalah tanah lempung homogen dengan konsistensi sedang atau setara dengan nilai N_{SPT} = 5. Pemodelan perilaku tegangan dan regangan pada tanah dilakukan dengan menggunakan model material *Mohr-Coulomb* dan tipe drainase *Undrained C*. Dengan kondisi tipe *Undrained C*, analisis tegangan total (*total stress*) dengan parameter *undrained* diadopsi di dalam studi ini. Selain itu, pada kondisi ini, elevasi muka air tidak dimodelkan di dalam analisis.

Parameter berat isi tanah natural (γ_{unsat}) dan berat isi tanah jenuh (γ_{sat}) yang digunakan ditentukan berdasarkan data terpublikasi oleh Coduto (2001). Berdasarkan Briaud (2013), nilai modulus elastisitas tanah lempung tak teralir (E_u) untuk tanah lempung sensitif yang terkonsolidasi normal adalah sebesar 200–500S_u, di mana S_u merupakan nilai kuat geser tanah kohesif tak alir. Menurut Terzaghi & Peck (1967), nilai S_u untuk nilai N_{SPT} = 4-8 berkisar antara 25-50 kN/m^2, dan pada studi ini nilai S_u diasumsikan sebesar 30 kN/m^2. Nilai angka Poisson pada kondisi tak teralir (υ_u) adalah sebesar 0,495. Untuk memodelkan interaksi antara fondasi dengan tanah, digunakan interface pada selimut dan ujung tiang dengan parameter R_{inter} sebesar satu (1). Untuk tipe drainase *Undrained C* pada analisis ini, nilai koefisien tekanan *at-rest* (K_0) adalah satu (1). Tabel 1 menunjukkan parameter tanah yang digunakan di dalam studi ini.

Tabel 1. Parameter Tanah.

Parameter	Nilai	Satuan
γ_{unsat}	16	kN/m^3
γ_{sat}	16	kN/m^3
E_u	12000	kN/m^2
S_u	30	kN/m^2
ϕ_u	0	°
υ_u	0,495	-
R_{inter}	1	-
$K_{0,x} = K_{0,y}$	1	-

Pada studi ini, fondasi tiang dimodelkan sebagai *soil volume*. Kemudian, untuk memodelkan perilaku tegangan dan regangan pada tiang, model material *linear elastic* digunakan dengan tipe drainase *non-porous*. Tipe drainase *non-porous* digunakan karena

material tiang fondasi diasumsikan sebagai material beton yang kedap, sehingga tekanan air pori tidak dapat terjadi di dalam fondasi tiang. Material beton diasumsikan tidak memiliki berat sendiri sehingga nilai berat isi beton (γ_c) adalah nol (0). Nilai modulus Young beton (E_c) dan angka Poisson beton (υ_c) yang digunakan secara berturut-turut adalah 2,5 × 10^7 kN/m^2 dan 0,15. Parameter tiang yang digunakan dapat dilihat pada Tabel 2.

Tabel 2. Parameter Tiang.

Parameter	Nilai	Satuan
γ_c	0	kN/m^3
E_c	2,5x10^7	kN/m^2
υ_c	0,15	-
R_{inter}	1	-

2.2 *Skema Penelitian*

Variasi pemodelan di dalam studi parametrik dilakukan pada panjang tiang (L), diameter tiang (D), batas horizontal yang dinyatakan dalam rasio antara jarak batas horizontal dan diameter tiang (x/D), dan batas vertikal yang dinyatakan dalam rasio antara batas vertikal terhadap panjang tiang (y/L). Skema penelitian yang dilakukan dapat dilihat pada Tabel 3.

Tabel 3. Skema Penelitian.

L (m)	D (m)	x/D	y/L	Tujuan
5 7,5 10 12,5 15 17,5	0,5 0,8 1,0 1,2 1,5	10 15 25 40 80 100	2	Mengidentifikasi pengaruh batas horizontal
5 7,5 10 12,5 15 17,5	0,5 0,8 1,0 1,2 1,5	25	1,2 2 3 4	Mengidentifikasi pengaruh batas vertikal

2.3 *Pemodelan Tiang dan Simulasi Pembebanan Aksial Tekan*

Pada studi ini, model yang digunakan adalah *axisymmetry*. Distribusi elemen segitiga 15 nodal yang digunakan dalam tahap diskretisasi klaster tanah dan tiang (*meshing*) adalah sangat halus (*very fine*). Gbr. 2 menunjukkan pemodelan tiang yang digunakan di dalam studi ini.

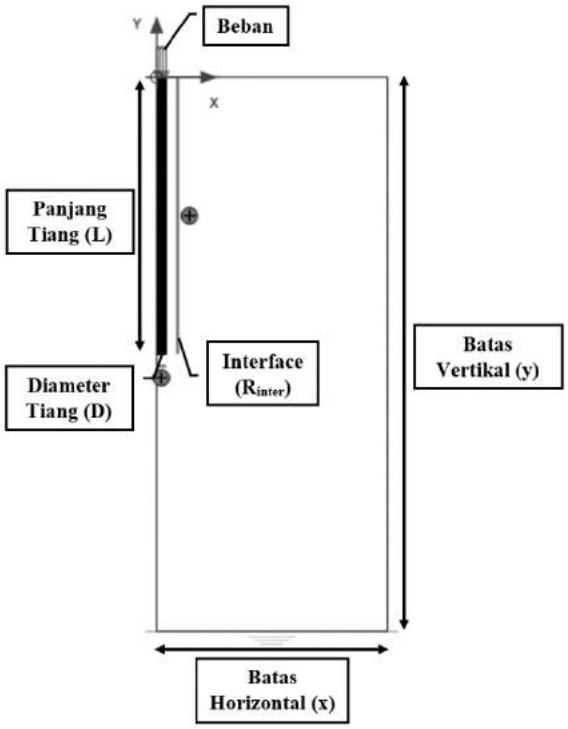

Gbr. 2. Pemodelan Tiang.

Tahapan konstruksi pada simulasi Plaxis 2D dibagi menjadi 3 yaitu, tahap *initial phase*, *construction*, dan *loading*. Tahap *initial phase* merupakan tahapan di mana tegangan-tegangan awal tanah akan dihitung, sehingga fondasi tiang tidak aktif atau belum di konstruksi pada tahap ini. Pada tahap *construction*, instalasi tiang di dalam tanah disimulasikan. Tahap *loading* merupakan tahap terakhir pada pemodelan di mana tiang diberikan beban permukaan (*surface load*) di kepala tiang hingga tanah mengalami kegagalan. Pada penelitian ini, beban merata yang diberikan adalah 5.000 kN/m^2 untuk setiap simulasi. Hasil dari simulasi uji pembebanan adalah kurva beban vs. penurunan tiang.

2.4 *Interpretasi Hasil Uji dengan Kurva Beban vs. Penurunan*

Kurva beban vs. penurunan yang telah diperoleh kemudian dinormalisasi menjadi kurva P/P_{max} vs. δ_v/δ_{vmax}. P/P_{max} merupakan nilai beban aksial (P) yang dinormalisasi terhadap nilai beban aksial maksimum (P_{max}) yang ditentukan berdasarkan nilai beban aksial terbesar dari *output* pemodelan Plaxis 2D, sedangkan δ_v/δ_{vmax} adalah penurunan vertikal pada saat beban P bekerja (δ_v) yang dinormalisasi terhadap nilai penurunan yang terjadi pada saat P_{max} (δ_{vmax}). Hal ini bertujuan

untuk memvisualisasikan perubahan dan pengaruh kondisi batas terhadap kurva beban vs. penurunan tiang. Gbr. 3 dan Gbr. 4 merupakan contoh kurva P/P_{max} vs. δ_v/δ_{vmax} untuk contoh kasus L = 15 m dengan D = 1 m untuk berbagai nilai x/D dan y/L secara berturut-turut.

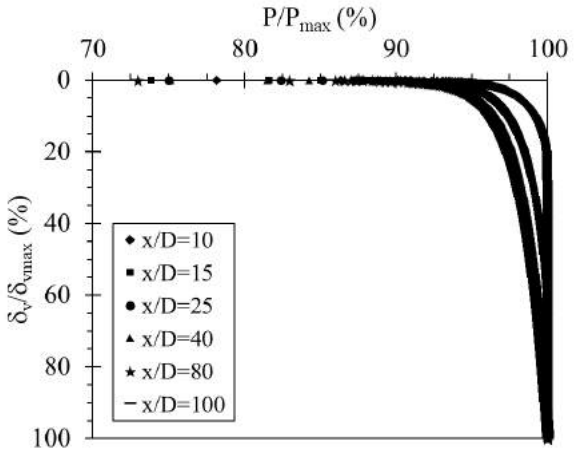

Gbr. 3. Kurva P/Pmax vs. δv/δvmax untuk Kasus L = 15 m dengan D = 1 m pada y/L = 2.

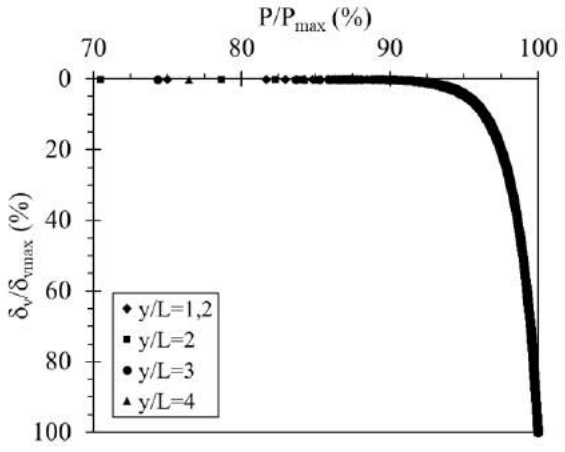

Gbr. 4. Kurva P/Pmax vs. δv/δvmax untuk Kasus L = 15 m dengan D = 1 m pada x/D = 25.

2.5 *Interpretasi Hasil Uji Berdasarkan Titik-Titk Keruntuhan*

Titik-titik keruntuhan (*failure points*) pada *output* Plaxis 2D yang disimbolkan dengan titik merah pada Gbr. 5 menunjukkan lokasi di mana tegangan yang terjadi berada dalam keadaan plastis. Titik-titik merah ini kemudian diinterpretasikan sebagai zona pengaruh dari pemodelan. Kondisi batas dapat dikatakan mencukupi apabila titik-titik keruntuhan tidak berimpit dengan batas horizontal maupun batas vertikal.

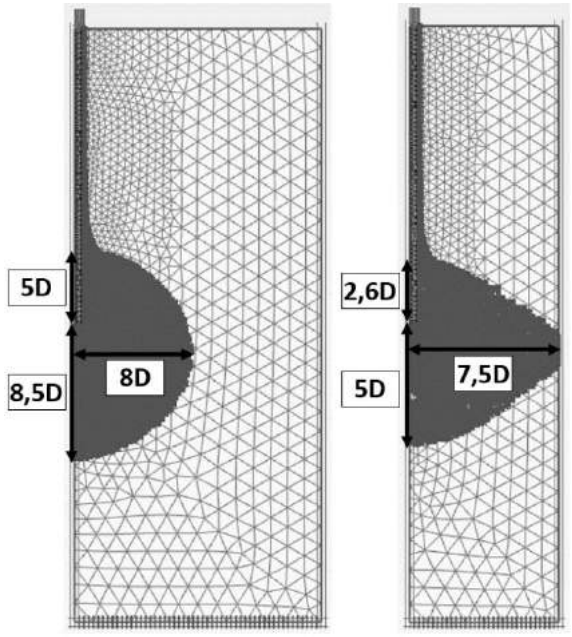

Gbr. 5. Titik-Titik Keruntuhan untuk Kasus L = 15 m dengan D = 1 m (a) x/D = 25 dan y/L = 2. (b) x/D = 15 dan y/L = 2.

2.6 *Interpretasi Daya Dukung Ultimit Hasil Uji dengan Metode Chin*

Chin (1970) mengasumsikan bahwa kurva beban vs. penurunan berbentuk hiperbolik. Untuk membuat kurva menggunakan metode Chin dapat dilakukan dengan menggambarkan nilai penurunan yang dinormalisasi terhadap beban pada sumbu x dan nilai penurunan pada sumbu y. Kemudian, kurva linear dapat dibentuk seperti pada Gbr. 6 dan Gbr. 7 yang dinyatakan dalam Pers. (1).

$$S / Q = c_1 S + c_2 \quad (1)$$

Dimana:
S = Penurunan yang terjadi pada tiang
Q = Beban kerja yang diberikan pada tiang
c_1 = Kemiringan pada kurva
c_2 = Perpotongan y pada bagian lurus kurva

Daya dukung ultimit tiang (Q_u) menurut metode Chin dapat ditentukan dengan menggunakan Pers. (2).

$$Q_u = \frac{1}{c_1} \quad (2)$$

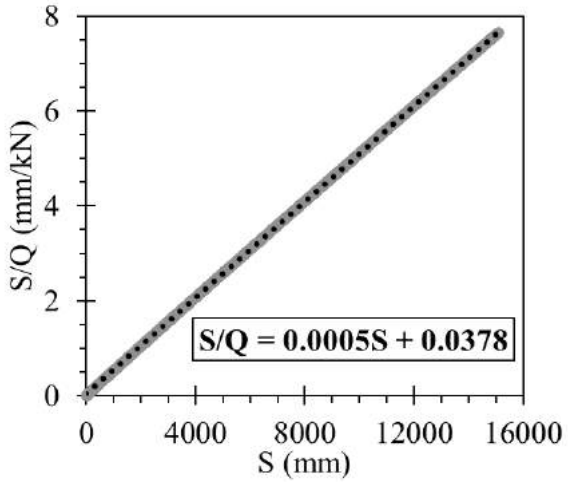

Gbr. 6. Kurva S/Q vs. S untuk Kasus L = 15 m dengan D = 1 m pada x/D = 25 dan y/L = 2.

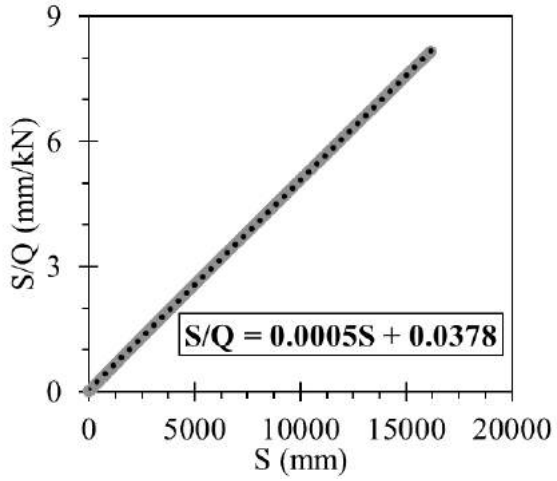

Gbr. 7. Kurva S/Q vs. S untuk Kasus L = 15 m dengan D = 1 m pada x/D = 25 dan y/L = 3.

3 HASIL DAN PEMBAHASAN

3.1 *Evaluasi Kondisi Batas Berdasarkan Kurva Normalisasi Beban vs. Penurunan*

Hasil berupa kurva P/P_{max} vs. δ_v/δ_{vmax} pada studi ini kemudian dievaluasi dengan meninjau kekonvergenannya. Kurva P/P_{max} vs. δ_v/δ_{vmax} dapat dikatakan konvergen apabila kurva berimpit satu sama lain dan menuju ke titik akhir yang sama. Sebagai contoh, pada Gbr. 3, kurva P/P_{max} vs. δ_v/δ_{vmax} untuk x/D = 10 dan x/D = 15 merupakan kurva yang tidak konvergen karena kedua kurva saling berjauhan atau tidak berimpit. Hal ini dapat disebabkan oleh batas horizontal yang disimulasikan tidak memadai. Sedangkan kurva P/P_{max} vs. δ_v/δ_{vmax} untuk x/D = 25 hingga x/D = 100 merupakan kurva yang konvergen. Sedangkan untuk batas vertikal seperti yang ditunjukkan pada Gbr. 4, kurva P/P_{max} vs. δ_v/δ_{vmax} untuk y/L = 1,2 hingga y/L = 4 saling berimpit satu sama lain, sehingga kurva dapat dikatakan konvergen.

Hasil kurva P/P_{max} vs. δ_v/δ_{vmax} yang konvergen mengindikasikan bahwa nilai daya dukung yang tidak jauh berbeda antara variasi batas pemodelan satu dengan yang lain. Ketidak konvergenan kurva P/P_{max} vs. δ_v/δ_{vmax} dapat terjadi akibat ada tegangan-tegangan ataupun pergerakan pada tanah yang tidak diperhitungkan dan titik-titik keruntuhan yang berimpit dengan batas horizontal maupun batas vertikal. Berdasarkan hasil evaluasi terhadap kurva P/P_{max} vs. δ_v/δ_{vmax}, batas horizontal yang diperlukan untuk mencapai kekonvergenan adalah x/D = 25, sedangkan untuk batas vertikal adalah y/L = 1,2.

3.2 *Evaluasi Kondisi Batas Berdasarkan Distribusi Titik-Titk Keruntuhan*

Evaluasi kondisi batas juga dilakukan dengan meninjau distribusi titik-titik keruntuhan (*failure points*). Hal ini bertujuan untuk menentukan batas horizontal dan vertikal yang memadai dan tidak berimpit dengan titik-titik keruntuhan. Titik-titik keruntuhan yang berimpit dengan batas pemodelan dapat berdampak pada nilai daya dukung yang dihasilkan dari simulasi numerik.

Titik-titik keruntuhan yang berimpit dengan batas adalah seperti yang diilustrasikan pada Gbr. 5b. Sementara itu, titik-titik keruntuhan yang ideal ditunjukkan oleh Gbr. 5a di mana titik-titik keruntuhan tidak berimpit pada batas horizontal maupun batas vertikal. Kemudian, Gbr. 5 juga menampilkan besarnya titik-titik keruntuhan yang melebihi estimasi dari Bowles (1997) (Gbr. 1). Hal ini dapat terjadi karena adanya perbedaan kondisi tanah dan geometri tiang yang menyebabkan distribusi tegangan yang terjadi pada ujung fondasi berbeda. Hasil evaluasi berdasarkan distribusi titik-titik keruntuhan menunjukkan bahwa nilai yang memadai untuk batas horizontal adalah x/D = 25 dan untuk batas vertikal adalah y/L = 3.

3.3 *Evaluasi Kondisi Batas Berdasarkan Nilai Q_u*

Evaluasi ini dilakukan untuk melihat pengaruh batas horizontal dan vertikal terhadap nilai Q_u. Gbr. 8 menunjukkan perubahan nilai Q_u terhadap rasio x/D untuk contoh kasus L = 15

m. Berdasarkan hasil pada Gbr. 8, nilai Q_u mulai relatif konstan pada saat rasio x/D = 25. Nilai Q_u yang relatif konstan mengindikasikan bahwa tidak adanya perubahan pada tegangan dan regangan yang terjadi akibat pembebanan. Kemudian, Gbr. 9 menunjukkan perubahan nilai Q_u terhadap rasio y/L untuk contoh kasus L = 15 m pada analisis batas vertikal. Nilai Q_u konstan pada saat y/L = 1.2 hingga y/L = 4. Maka dari itu, batas horizontal x/D = 25 dan batas vertikal y/L = 1,2 merupakan batas yang mencukupi untuk menyimulasikan uji pembebanan aksial tiang tunggal.

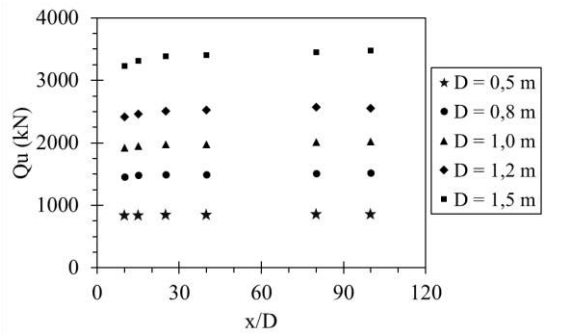

Gbr. 8. Kurva Qu - x/D untuk Kasus L = 15 m pada y/L = 2.

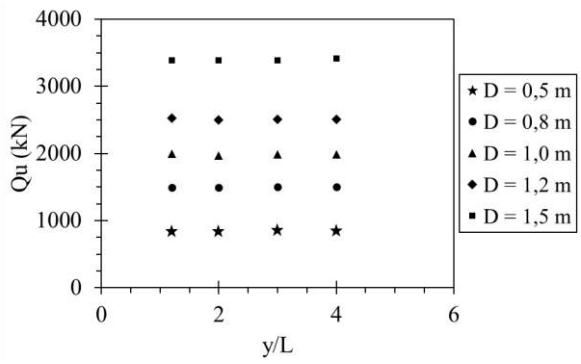

Gbr. 9. Kurva Qu - x/D untuk Kasus L = 15 m pada y/L = 1,2.

3.4 *Hasil Evaluasi*

Berdasarkan hasil evaluasi terhadap kekonvergenan batas horizontal dan vertikal berdasarkan kurva normalisasi beban vs. penurunan, distribusi titik-titik keruntuhan, dan evaluasi nilai daya dukung ultimit tiang, maka dapat disimpulkan bahwa jarak horizontal yang memadai adalah sebesar 25 kali diameter tiang dan jarak vertikal sebesar 3 kali panjang tiang untuk simulasi uji pembebanan aksial tekan fondasi tiang tunggal pada tanah lempung homogen.

4 KESIMPULAN

Studi ini menyampaikan hasil studi parametrik dengan menggunakan Plaxis 2D untuk menyimulasikan uji pembebanan aksial tekan pada fondasi tiang tunggal di tanah lempung homogen. Studi parametrik dilakukan dengan memvariasikan panjang dan diameter fondasi tiang, serta kondisi batas dalam arah horizontal maupun vertikal pada tanah lempung homogen. Evaluasi efek batas dilakukan berdasarkan kurva normalisasi beban vs. penurunan, distribusi titik-titik keruntuhan, dan perubahan nilai daya dukung ultimit. Berdasarkan evaluasi hasil analisis, diperoleh beberapa kesimpulan, sebagai berikut:

1. Kurva normalisasi beban vs. penurunan mulai konvergen pada saat jarak horizontal sebesar 25 kali diameter tiang dan jarak vertikal sebesar 1,2 kali panjang tiang.
2. Jarak memadai berdasarkan distribusi titik-titik keruntuhan adalah sebesar 25 kali diameter tiang untuk batas horizontal dan sebesar 3 kali panjang tiang jarak vertikal.
3. Daya dukung ultimit mulai relatif konstan ketika jarak horizontal bernilai 25 kali diameter tiang dan jarak vertikal bernilai 1,2 kali panjang tiang.
4. Jarak horizontal minimum yang diperlukan dalam pemodelan numerik untuk menghindari efek batas adalah 25 kali diameter tiang dan jarak vertikal sebesar 3 kali panjang tiang.

DAFTAR PUSTAKA

Bowles, J.E. 1997. *Foundation Analysis and Design Second Edition*. New York: McGraw-Hill Book Company.

Briaud, J.L. 2013. *Geotechnical Engineering: Unsaturated and Saturated Soils*. USA: John Wiley & Sons.

Brinkgreve, R.B.J. 2020. *PLAXIS 2D Reference Manual CONNECT Edition V20*. The Netherlands: PLAXIS.

Chin, F. K. 1970. Estimation of the Ultimate Loaf of Piles not carried to Failure. *Proceedings, 2nd Southeast Asian Conference on Soil Engineering, Singapor*e: 81–90.

Coduto, D.P. 2001. *Foundation Design Principle and Practices Second Edition*. New Jersey: Prentice-Hall Inc.

Das, M.B. 2011. *Principles of Foundation Engineering Seventh Edition*. USA: Global Engineering.

Dong, J., Chen, F., Zhou, M. & Zhou, X. 2017. Numerical analysis of the boundary effect in model

tests for single pile under lateral load. *Bulletin of Engineering Geology and the Environment* 77 (3): 1057–1068.

Vermeer, P.A. & Wehnert, M. 2005. *Beispiele von FE-Anwendungen – Man lernt nie aus. In: FEM in der Geotechnik (ed. Grabe et.al.)*. Harburg: Technische Universität Hamburg.

Terzaghi, K., Peck, R.B. & Mesri, G. 1996. *Soil Mechanics in Engineering Practice Third Edition*. USA: John Wiley & Sons, Inc.

Analisis Efektivitas Penggunaan Geotekstil untuk Perkerasan Lentur Jalan pada Tanah Lempung Lunak

Rangga Wishnu Wardhana
Department of Civil Engineering, Faculty of Civil Engineering and Planning – University of Trisakti
Aksan Kawanda
Department of Civil Engineering, Faculty of Civil Engineering and Planning – University of Trisakti

ABSTRAK: Meningkatnya pembangunan infrastruktur jalan di Indonesia sejatinya tidak terlepas dari aspek-aspek geoteknik. Banyak aspek dalam perencanaan geoteknik yang harus diperhatikan, salah satunya adalah lokasi pembangunannya. Tidak semua lokasi pembangunan jalan memiliki tanah yang baik, ada juga yang memiliki tanah yang buruk. Pada kondisi tanah yang buruk seperti tanah lempung lunak perlu dilakukan perkuatan menggunakan geotekstil. Untuk menggunakan geotekstil sebagai perkuatan tanah perlu dilakukannya analisis perhitungan untuk dapat memilih kelas geotekstil yang efektivitasnya paling baik terutama pada perencanaan perkerasan jalan lentur. Penelitian ini akan menganalisis 2 metode yaitu modifikasi AASHTO-Polyfelt dan metode Steward et al. yang akan dibandingkan mana yang efektif untuk perkerasan lentur jalan. Hasil Penelitian ini menunjukkan bahwa dari 2 metode tersebut menghasilkan kelas geotekstil yang sama tetapi untuk efektivitas dalam tebal urugan dan daya dukung, hasil Steward et al. menunjukkan hasil yang lebih rendah dibanding modifikasi AASHTO-Polyfelt.

Kata Kunci: geotekstil, daya dukung, perkerasan lentur, tanah lempung

ABSTRACT: Road infrastructure development in Indonesia cannot be separated from the geotechnical aspects. There are many aspects that affect geotechnical planning, and construction site is one aspect that needs to be noticed. Some road construction sites have good soil, while others have poor soil. In poor soil conditions like soft clay requires soil reinforcement with the geotextile method. A calculation is needed to utilize the geotextile method as soil reinforcement to classify the geotextile class with the best effectiveness, especially in flexible pavement design. This research was designed to analyze two methods, namely the AASHTO-Polyfelt modified and the Steward et al., then compared them to obtain the most effective method for flexible pavement design. This research indicates that the two methods generate the same geotextile class but differ in the effectiveness of fill soil thickness and soil bearing capacity. The Steward et al. method showed lower results than the AASHTO-Polyfelt modified.

Keywords: geotextile, bearing capacity, flexible pavement, soft clay soil

1 PENDAHULUAN

Pembangunan infrastruktur Indonesia saat ini semakin berkembang pesat, terutama dalam pembangunan infrastruktur jalan. Dalam pembangunan infrastruktur jalan sejatinya tidak bisa terlepas dari aspek-aspek geoteknik. Banyak aspek dalam perencanaan geoteknik yang perlu diperhatikan, salah satunya adalah lokasi pembangunannya. Tidak semua lokasi pembangunan jalan memiliki tanah yang baik, ada juga yang memiliki tanah yang kurang baik.

Dalam pelaksanaan konstruksi jalan yang terdapat tanah lempung yang lunak, sering sekali ditemui permasalahan yang berhubungan dengan kemampuan daya dukung tanah serta stabilitas tanahnya. Maka untuk mengantisipasi masalah tersebut perlu adanya upaya yang harus dilakukan salah satunya dengan metode perkuatan tanah menggunakan geotekstil. Penulisan ini bertujuan untuk menganalisis dua metode pemilihan kelas geotekstil yang efisien pada perencanaan jalan dengan perkerasan lentur di atas permukaan tanah lempung lunak.

2 TINJAUAN PUSTAKA

2.1 *Penggunaan Geotekstil Untuk Perencanaan Jalan*

Geotekstil merupakan lembaran kain berbahan polymer yang bersifat lolos air, yang berbentuk bahan tidak teranyam, rajutan atau anyaman dari kumpulan benang-benang sintetis. Geotekstil banyak digunakan untuk perkuatan tanah dasar pada perencanaan struktur perkerasan jalan. Geotekstil pada lokasi yang terdapat tanah lempung lunak, geotekstil dapat mencegah naiknya tanah ke sistem perkerasan jalan yang mengakibatkan rusaknya lapisan perkerasan jalan. Geotekstil dibagi dalam 3 kelas. Standard yang menjadi acuan telah dikeluarkan Departemen PU adalah berdasarkan kekuatan yang dapat ditahan oleh geotekstil tersebut yang juga disarankan oleh AASHTHO (1977) dalam FHWA (1998), kekuatan geotekstil harus sama atau melebihi nilai-nilai yang telah ditentukan.

Tabel 1. Kelas Ketahanan Pelaksanaan, FHWA (1998).

CBR Tanah di Lokasi Saat Pemasangan	< 1		1 sampai 2		> 3	
Tekanan Kontak Alat Berat ke Tanah (kN/m^2)	> 350	< 350	> 350	< 350	> 350	< 350
Tebal Material Penutup2 (Padat) (mm)						
100[3,4]	NR[5]	NR	1[5]	1	2[5]	2
150	NR	NR	1	1	2	2
300	NR	1	2	2	2	2
>450	1	2	2	2	2	2

Catatan:
1. Ambil CBR jenuh, kecuali jika jadwal pelaksanaan dapat dikendalikan
2. Ukuran agregat maksimum tidak melebihi separuh tebal penutup yang dipadatkan
3. Untuk volume rendah, jalan tanpa perkerasan (ADT<200 kendaraan)
4. PEnutup minimum 100 mm terbatas pada lapis fondasi eksisting dan tidak dimaksudkan untuk pembangunan baru
5. NR = tidak disarankan, ketahanan tinggi terkait dengan geotekstil Kelas 1 dan ketahanan sedang terkait dengan geotekstil Kelas 2, AASHTO (1997)

2.2 *Beban Sumbu*

Dalam desain perencanaan jalan menggunakan geotekstil, beban Sumbu digunakan untuk mencari tebal urugan yang dibutuhkan. Untuk perkiraan lalu lintas dan beban sumbu pada lalu lintas rendah yang memiliki tipe jalan lokal.

2.3 *Susunan Lapis Perkerasan*

Perancangan jalan dengan perkerasan umumnya terdiri dari beberapa jenis lapisan yang tersusun. Untuk perencanaan jalan yang memiliki volume lalu lintas rendah sususan lapis perkerasannya, menurut Wulansari (2018) menggunakan beberapa susunan jenis lapisan yang dibuat berdasarkan (SNI 03-1732-1989) adalah sebagai berikut:

- Lapis permukaan menggunakan Laston MS 340 kg
- Lapis fondasi atas menggunakan Batu Pecah Kelas C
- Lapis fondasi bawah menggunakan Pasir Batu Kelas C
- Tebal D1 minimumnya 5 cm
- Tebal D2 minimumnya 20 cm

2.4 *Metode modifikasi AASHTO-Polyfelt*

Merupakan metode hitungan yang didasarkan pada AASHTO (1972) berdasar pengalaman lapangan dan uji laboratorium dari pabrik geotekstil *Polyfelt*. Persamaan angka struktural diberikan dalam:

$$SN=a_1D_1+a_2\ D_2+a_3\ D_3 \quad (2)$$

Angka struktural (SN) yang dibutuhkan di atas tanah dasar jalan untuk volume jalan yang rendah dapat dihitung sebagai fungsi dari daya dukungan tanah (S), standar beban berulang (W_{80KN}), faktor regional (R) dan Kemampuan Pelayanan Sambungan (p_t) dengan menggunakan gambar nomogram dibawah ini.

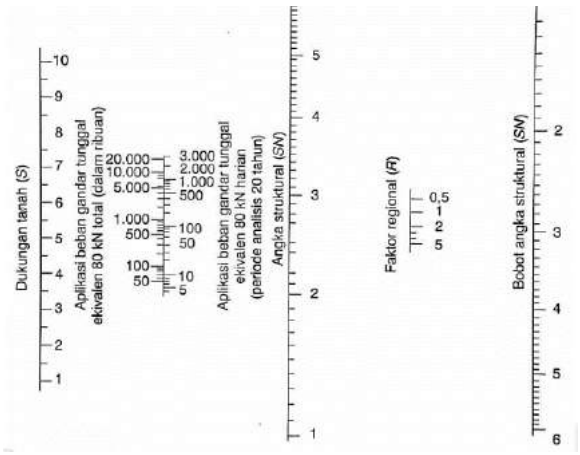

Gbr. 1. Nomogram Perancangan Nilai SN untuk pt = 2,0 (Volume Lalu Lintas Rendah), AASHTO (1972).

Dalam metode modifikasi AASHTO-*Polyfelt*, korelasi daya dukungan tanah (S) dan CBR dipakai hubungan empirik yang diusulkan oleh Utah State Department of Highways (1966).

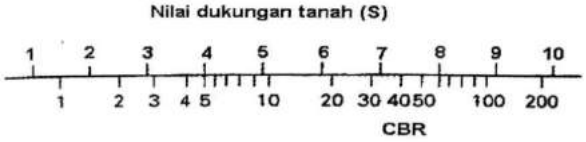

Gbr. 2. Hubungan Daya Dukungan Tanah (S) dan CBR, Utah Department of Highway (1966).

Pengaruh geotekstil *polyfelt* TS terhadap kenaikan kekuatan daya dukung tanah dasar dinyatakan oleh:

$$S_g = F_1 S \quad (3)$$

Dengan :

S_g = Daya dukungan tanah termodifikasi oleh geotekstil
S = Daya dukungan tanah tanpa geotekstil
F_1 = Faktor pengaruh geotekstil *polyfelt*

Dengan pemasangan geotekstil maka akan menambah umur pelayanan jalan. pengaruh geotekstil *polyfelt* TS terhadap penambahan umur rancangan, untuk CBR ≤ 3 dan kedalaman alur r ≤ 150 mm, dinyatakan oleh:

$$W_{80g} = \frac{W_{80}}{T_g} \quad (4)$$

Dengan:

W_{80g} = Standar beban berulang 80 kN setelah dipakai geotekstil
W_{80} = Standar beban berulang 80 kN sebelum dipakai geotekstil
Tg = Faktor pengaruh umur rancangan

Hubungan Pengaruh geotekstil *polyfelt* terhadap daya dukung tanah dasar jalan ditunjukkan dalam Gambar berikut.

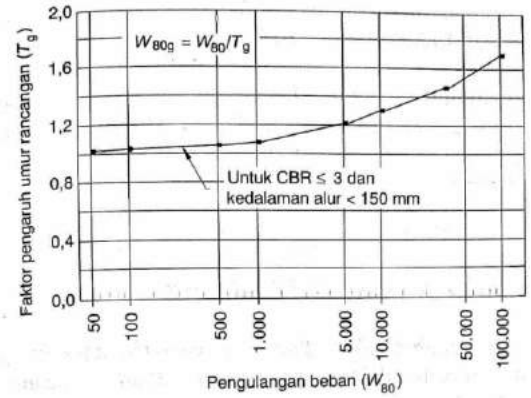

Gbr.3. Pengaruh Geotekstil Polyfelt terhadap Daya Dukung Tanah Dasar Jalan, *Polyfelt* (1994).

Hubungan faktor pengaruh umur rancangan dan pengulangan beban W_{80} ditunjukkan dalam gambar berikut.

Gbr. 4. Pengaruh Geotekstil Polyfelt terhadap Faktor Pengaruh Umur Rancangan, *Polyfelt* (1994).

Angka struktural (SN) termodifikasi dapat diperoleh dari Nomogram Untuk perancangan perkerasan dengan p_t = 2,0 , AASHTO (1972). Dari sini, dengan koefisien lapis material (ai), maka tebal urugan dengan menggunakan geotekstil dapat ditentukan.

2.5 *Metode Steward et al. 1977*

Metode yang dikembangkan oleh Steward et al. (1977) ini awalnya untuk *U.S Forest Service* (USFS). Metode ini memperhitungkan jumlah jejak bekas roda yang akan terjadi pada tanah dasar akibat beban lalu lintas, kedalaman jejak bekas roda, faktor kapasitas daya dukung (Nc) dan jenis beban roda yang bisa diantisipasi selama penerapan, ketebalan agregat yang

diperlukan dengan dan tanpa geotekstil dapat diperoleh dari Tabel 3.

Tabel 2. Hubungan Kedalaman Bekas Roda, Jumlah Lintasan dan Faktor Kapasitas Daya Dukung Nc, Memakai Geotekstil dan Tanpa Geotekstil, Steward et al. (1977)

Geotekstil	Kedalaman bekas roda, r (mm)	Jumlah berulang beban gandar 80 kN (ESAL)	Faktor kapasitas daya dukung, Nc
Tanpa geotekstil	<50 >100	>1000 <100	2,8 3,3
Memakai geotekstil	<50 >100	>1000 <100	5,0 6,0

Selain penggunaan tabel, Steward et al. (1977) juga memperkenalkan metode grafik seperti yang diperlihatkan pada Gbr. 5. guna mendesain tebal lapis fondasi yang dibutuhkan. Steward et al. memperlihatkan derajat tegangan yang bekerja pada tanah dasar dalam kaitanya dengan faktor kapasitas daya dukung. Kapasitas daya dukung tanah dapat dihitung menggunakan persamaan:

$$q_u = c_u N_c \quad (6)$$

Dengan :
q_u = Kapasitas daya dukung ultimit (kN/m^2)
c_u = Kohesi tak terdrainase (kN/m^2)
Nc = Faktor kapasitas daya dukung

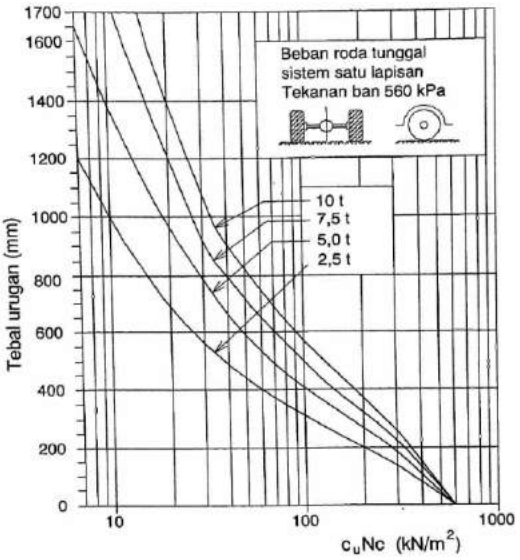

Gbr.5. Kurva Penentuan Tebal Agregat untuk Beban Roda Tunggal, Steward et al. (1977).

3 METODE

Proses awal yang perlu dilakukan adalah dengan melakukan korelasi parameter tanah untuk melengkapi data tanah yang akan dibutuhkan. Dalam perencanaan jalan dengan perkerasan lentur menggunakan geotekstil yang efisien pada permukaan tanah lempung, selain dengan perhitungan menggunakan metode modifikasi AASHTO-*Polyfelt* penulis juga akan menggunakan perhitungan perencanaan jalan dengan perkerasan lentur menggunakan Metode Steward et al. dengan atau tanpa geotekstil. Setelah melakukan pehitungan menggunakan dua metode tersebut, penulis juga akan melakukan perbandingan hasil klasifikasi ketahanan minimum geotekstil yang sesuai secara efektif.

4 PEMBAHASAN

4.1 *Klasifikasi Jenis Tanah*

Dalam melakukan perancangan perkerasan jalan lentur menggunakan geotekstil yang memiliki kondisi tanah lempung lunak maka akan dilakukan pengelompokan klasifikasi tanahnya untuk mengetahui apakah terdapat tanah lempung lunak.

4.2 *Analisa Nilai CBR Tanah*

Dalam melakukan perancangan perkerasan lentur jalan menggunakan geotekstil, diperlukan nilai CBR tanah. Penulis akan menggunakan korelasi menggunakan Pers. (1). Perlu dicari nilai CBR yang paling mewakilkan untuk digunakan selanjutnya dalam perhitungan. Untuk itu akan digunakan metode yang terdapat pada SNI 1732 (1989). Penulis membatasi kedalaman yang ditinjau hanya sedalam 4 meter saja untuk mendapat nilai CBR.

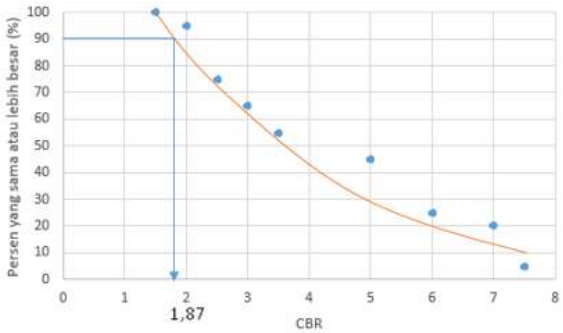

Gbr.6. Grafik CBR yang Mewakili pada Titik 1.

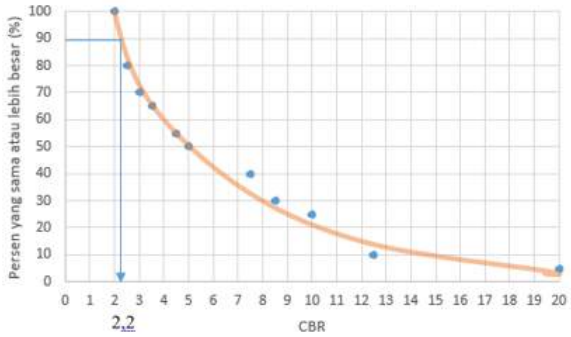

Gbr.7. Grafik CBR yang Mewakili pada Titik 2.

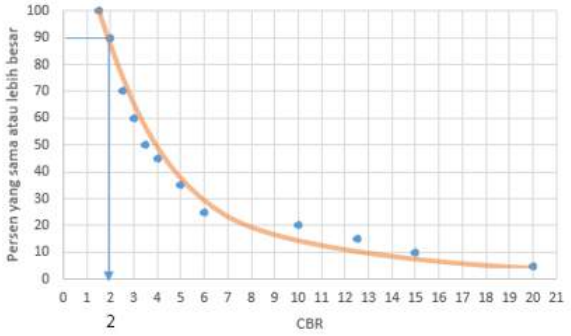

Gbr.8. Grafik CBR yang Mewakili pada Titik 3.

4.3 *Analisa Data Lalu Lintas*

Dalam melakukan perancangan perkerasan lentur jalan menggunakan *geotekstil*, diperlukan data lalu lintas rencana untuk mengetahui beban rencana kendaran yang akan melintas pada jalan. Penulis akan menggunakan data sekunder dari jurnal yang disusun oleh Wulansari (2018) pada Tabel 4.

4.4 *Analisis Klasifikasi Ketahanan Minimum Kelas Geotekstil*

Pada Modifikasi AASHTO dengan adanya geotekstil menunjukkan efektifitas seperti naiknya nilai daya dukung tanah sebesar 20% dimasing-masing titik tinjau.

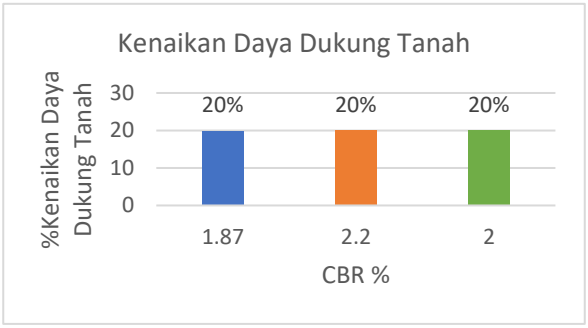

Gbr.9. Grafik Persentase Kenaikan Daya Dukung Tanah Modifikasi AASHTO-*Polyfelt.*

Tabel 3. Pehitunggan Standar Beban Berulang w80 kN.

Tipe Kendaraan	Jumlah Kendaraan	Faktor Ekivalen	Faktor Pertumbuhan	Beban Berulang
Mobil Penumpang, 2 ton	171.550	0,0004	22,019	1510,944
Truk 2 as 10 ton	10.950	0,3116	22,019	75.129,268
Standar beban berulang w80 kN				76.640,212

Tabel 4. Hasil Kelas Geotekstil yang Akan Digunakan di 3 Titik Tinjau.

	Metoda Modifikasi AASHTHO 1	Metoda Steward 1	Metoda Modifikasi AASHTHO 2	Metoda Steward 2	Metoda Modifikasi AASHTHO 3	Metoda Steward 3	Satuan
CBR	1,87%		2,20%		2,00%		
Tanpa geotekstil							
Daya dukung	600	157,08	675	184,8	625	168	kN/m^3
Tebal lapisan penutup	984,73	320	892,36	280	938,55	310	mm
Dengan geotekstil							
Daya dukung	720	280,5	806,6	330	746,9	300	kN/m^3
Tebal lapisan penutup	915,45	210	823,09	180	869,27	200	mm
Kelas geotekstil	2	2	2	2	2	2	

Tebal lapis penutup fondasi juga mengalami efektifitas dalam hal penurunan tebalnya. Seperti yang dilihat pada Gbr. 10.

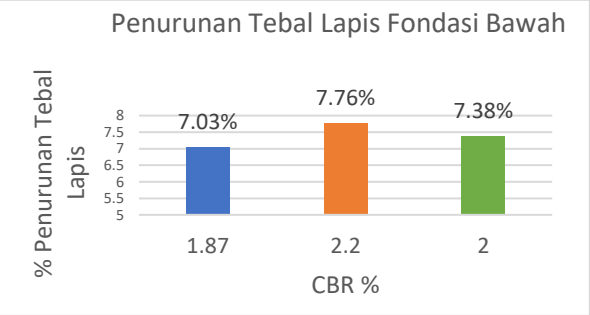

Gbr. 10. Grafik Persentase Penurunan Tebal Lapis Fondasi Modifikasi AASHTO-*Polyfelt*.

Sedangkan pada metode Steward et al. dengan adanya geotekstil juga menunjukan efektifitas yang lebih tinggi pada kenaikan daya dukungnya. Hal tersebut dapat dilihat pada Gbr.11.

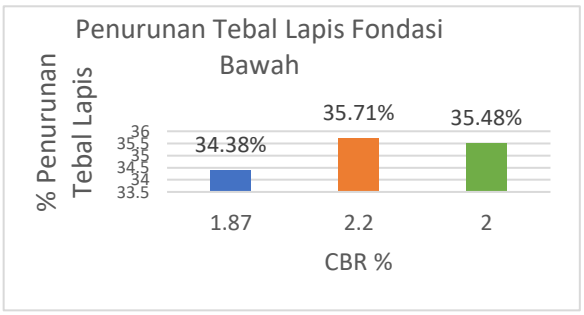

Gbr. 11. Grafik Persentase Kenaikan Daya Dukung Tanah Metode Steward et al.

Tebal lapis penutup fondasi juga mengalami efektifitas yang lebih tinggi dalam hal penurunan tebalnya. Seperti yang dilihat pada Gbr. 12.

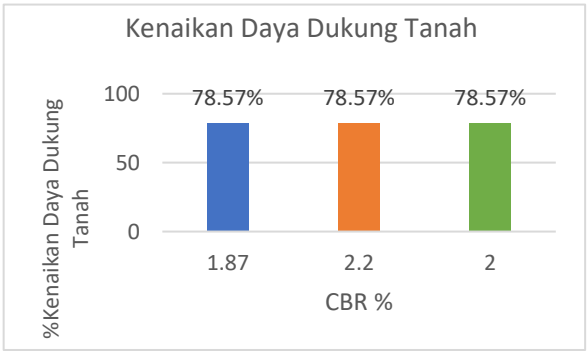

Gbr. 12. Grafik Persentase Penurunan Tebal Lapis Fondasi Metode Steward et al.

Pada metode modifikasi AASHTO memiliki perbedaan nilai CBR yang hanya kurang lebih sekitar 0,4 saja, daya dukung tanahnya dapat naik hingga 12% dan tebal lapis penutupnya dapat turun hingga 10%. Pada metode steward et. al. perbedaan nilai CBR sekitar 0,4 daya dukung tanahnya juga mengalami hal yang sama, tetapi persentasenya berbeda yaitu mendapat kenaikan hingga 18% dan tebal lapis penutupnya dapat turun hingga 14%.

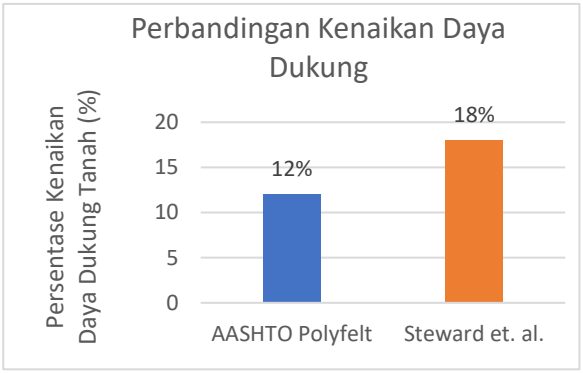

Gbr. 13. Grafik Persentase Perbandingan Kenaikan Daya Dukung antara Metode AASHTO Polyfelt dengan Metode Steward et al.

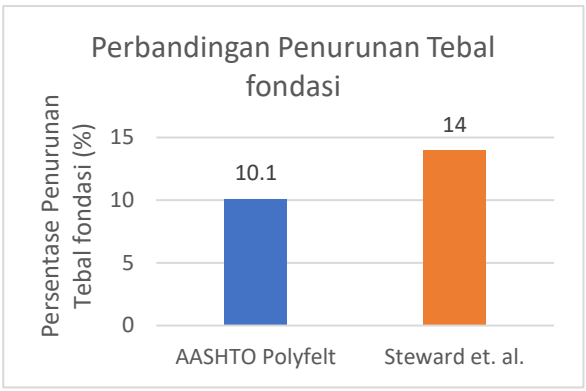

Gbr. 14. Grafik Persentase Perbandingan Penurunan Tebal Fondasi antara Metode AASHTO *Polyfelt* dengan Metode Steward et al.

5 KESIMPULAN

1. Perbandingan efektivitas penggunaan geotekstil antara perhitungan metode AASHTO *Polyfelt* dan Steward et al. jika CBR ditinjau tidak terlalu besar perbedaannya dapat menghasilkan hasil kelas geotekstil yang sama yaitu kelas geotekstil 2. Tetapi dengan perhitungan metode Steward et al. memiliki hasil yang lebih baik dalam kenaikan daya dukung tanahnya dan juga penurunan tebal lapis fondasi bawah yang masing masing mendapat perbedaan 2% dan 4%.
2. Beban lalu lintas harian rencana yang sama juga menjadi faktor yang mempengaruhi hasil klasifikasi kelas geotekstil sehingga mendapat hasil yang sama antara metode AASHTO *Polyfelt* dan Steward et al.

DAFTAR PUSTAKA

AASHTO. 1972. *Interim Guide for Design of Pavement Structures*.

FHWA. 1998. *Geosynthetic Design and Construction Guidelines*.

Polyfelt. 1994. *Perancangan Stabilisasi untuk Struktur Berbahan Tanah (Earth Structure) dengan Geotekstil di atas Tanah Lunak*.

Steward, J., Williamson, R., & Mohney, J. 1977. *Guidelines for Use of Fabrics in Construction and Maintenance of Low-Volume Roads*.

Utah State Department of Highways. 1966. Manual of Instruction.

Wulansari, D. N. 2018. Analisis Tebal Perkerasan Lentur Menggunakan Metode Analisa Komponen dan Metode Aashto pada Ruas Jalan Nagrak Kabupaten Bogor. *Jurnal Kajian Teknik Sipil* Vol. 3 No. 1, 10, 3 : 22–31.

Upaya Stabilisasi Tanah Berpotensi Likuifaksi Menggunakan *Stone Column*

Mardianti Alvionita
Department of Civil Engineering, Faculty of Civil Engineering and Planning – Trisakti University
Aksan Kawanda
Department of Civil Engineering, Faculty of Civil Engineering and Planning – Trisakti University

ABSTRAK: Perencanaan konstruksi bangunan di lahan dengan kondisi tanah yang buruk sangat umum dijumpai dan tidak dapat dipungkiri akan adanya kerusakan besar pada kontruksi diatasnya saat terjadi gempa bumi. Gempa bumi dapat menyebabkan peristiwa lain sesuai dengan karakteristik tanah asli, seperti likuifaksi. Likuifaksi dapat dicegah dengan upaya stabilisasi tanah menggunakan stone column. Tahap pertama yang dilakukan adalah menganalisis potensi likuifaksi pada tanah menggunakan teori Idriss dan Boulanger. Setelahnya, melakukan perancangan stone column dengan acuan FHWA yang dibuat dengan beberapa diameter, spasi pemasangan, dan kedalaman yang berbeda. Hasil penelitian menunjukkan bahwa penggunaan stone column berdiameter 1 m yang ditanam sedalam 10 m dengan spasi pemasangan 1,2 m dapat bekerja secara efektif karena memiliki nilai rasio pergantian luas dan nilai konsetrasi tegangan yang sudah mencukupi.

Kata kunci: likuifaksi, stabilisasi tanah, stone column.

ABSTRACT: Construction planning of buildings on land with poor ground conditions is very common, and it cannot be denied that there will be great damage to the construction above it during an earthquake. Earthquakes can cause other events according to the characteristics of the original soil, such as liquefaction. Liquefaction can be prevented by stabilizing the soil using stone columns. The first step is to analyze the liquefaction potential of the soil using the Idriss and Boulanger's theory. After that, the stone column design with the FHWA reference was made with different diameters, installation spaces, and depths. The results showed that the use of stone columns with a diameter of 1 m planted with a depth of 10 m with an installation space of 1.2 m can work effectively because it has the highest area replacement ratio and an adequate stress concentration value.

Keywords: liquefaction, soil stabilization, stone column.

1 PENDAHULUAN

Perkembangan dunia konstruksi di Indonesia semakin bertumbuh pesat dari waktu ke waktu, seiring dengan meningkatnya kesulitan dalam menemukan lahan dengan kondisi tanah yang baik. Sehingga perencanaan konstruksi bangunan di lahan dengan kondisi tanah yang buruk sangat umum dijumpai dan tidak dapat dipungkiri akan adanya kerusakan besar pada kontruksi diatasnya apabila terjadi bencana alam, seperti gempa bumi. Gempa bumi dapat menyebabkan peristiwa lain sesuai dengan karakteristik tanah asli, salah satunya adalah peristiwa likuifaksi. Tanah berpotensi likuifaksi dapat dicegah dengan melakukan upaya stabilisasi tanah menggunakan *stone column*. Penelitian ini bertujuan untuk mengetahui analisis potensi likuifaksi pada suatu daerah dan merencanakan hingga merancang *stone column* sebagai upaya stabilisasi tanah.

2 TINJAUAN PUSTAKA

2.1 *Likuifaksi*

Likuifaksi merupakan fenomena hilangnya kekuatan lapisan tanah akibat tegangan air pori yang timbul akibat beban siklik (getaran).

Getaran yang dimaksud dapat berupa getaran yang berasal dari gempa bumi maupun yang berasal dari aktifitas konstruksi seperti pondasi mesin.

Syarat Terjadinya Likuifaksi

Suatu daerah dapat dikatakan berpotensi likuifaksi apabila memenuhi syarat-syarat tertentu. yaitu:

1. Keberadaan tanah berbutir kasar (granular soils) yang seragam serta dominan
2. Kondisi lapisan tanah jenuh air
3. Lapisan tanah tidak padat (lepas)
4. Terjadi gempa dengan intensitas dan durasi yang cukup besar (Magnitudo > 5,0 dan kecepatan gempa > 0,1 g)

Parameter Indeks Tanah

Karakteristik likuifaksi tanah dapat dikorelasikan dengan berbagai macam parameter indeks tanah, seperti *Standard Penetration Test* (SPT) dan *Cone Penetration Test* (CPT). Data SPT dan CPT dapat digunakan secara bersamaan pula dalam proses analisis potensi likuifaksi. Dengan cara ini, keuntungan penuh dapat diambil dari keuntungan prosedur uji CPT dan data ekstensif berdasarkan korelasi SPT dengan karakteristik likuifaksi lapangan.

2.2 *Metode Evaluasi Zona Berpotensi Likuifaksi*

Menganalisis potensi likuifaksi pada suatu tanah dapat dilakukan dengan cara pendekatan perhitungan dari tes uji lapangan yaitu dengan data CPT dan SPT. Pendekatan ini dilakukan berdasarkan teori Idriss dan Boluanger (2008) yang bertujuan untuk mencari dua parameter utama, yaitu: nilai *Cyclic Resistance Ratio* (CRR) yang merupakan ketahanan untuk menahan likuifaksi dan *Cyclic Stress Ratio* (CSR) yang merupakan nilai tegangan yang disebabkan oleh gempa bumi.

***Cyclic Stress Ratio* (CSR)**

Idriss dan Boulanger (2008) menggunakan formulasi persamaan sama seperti yang diusulkan oleh Seed dan Idriss (1971) dalam mencari nilai rasio tegangan siklik. Persamaan tersebut adalah sebagai berikut:

$$CSR = \frac{\tau_{av}}{\sigma'_{vo}} = 0{,}65 \left(\frac{a_{max}}{g}\right)\left(\frac{\sigma_{vo}}{\sigma'_{vo}}\right) \mathrm{r}_d \qquad (1)$$

Dimana:
a_{max} = Percepatan gempa
g = Gravitasi
σ_{vo} = Tegangan overburden vertikal
σ'_{vo} = Tegangan overburden vertikal efektif
r_d = Faktor reduksi

Nilai r_d dapat diperoleh menggunakan persamaan:

$$\mathrm{r}_d = \frac{(1-0{,}4113z^{0{,}5}+0{,}04052z+0{,}0017353z^{1{,}5})}{(1-0{,}4177z^{0{,}5}+0{,}057279z-0{,}006205z^{1{,}5}+0{,}001210z^{2})} \qquad (2)$$

***Cyclic Resistance Ratio* (CRR)**

Metode evaluasi *Cyclic Resistance Ratio* (CRR) dapat dilakukan dengan evaluasi berdasarkan data SPT dan CPT.

- Berdasarkan SPT

Ada beberapa tahapan untuk memperoleh nilai CRR menggunakan data SPT, yaitu mencari nilai $(\mathrm{N}_1)_{60}$ dan $(\mathrm{N}_1)_{60cs}$. Menurut Idriss dan Boulanger (2008) ada beberapa faktor koreksi yang dibutuhkan untuk memperoleh nilai $(\mathrm{N}_1)_{60}$ adalah sebagai berikut:

$$(N_1)_{60} = N_M C_N C_E C_B C_R C_S \qquad (3)$$

Dimana:
N_M = Nilai tahanan penetrasi standar
C_N = Faktor normalisasi Nm terhadap tegangan overburden pada umumnya
C_E = Koreksi ratio energy hammer (ER)
C_B = Koreksi untuk diameter lubang bor
C_R = Faktor koreksi dari panjang batang
C_S = Koreksi untuk sampel

Nilai faktor koreksi tegangan overburden (C_N) yang digunakan tidak boleh lebih dari 1,7. C_N diperoleh menggunakan persamaan:

$$C_N = \frac{2{,}2}{(1{,}2+\frac{\sigma'_0}{P_a})} \qquad (4)$$

Sedangkan faktor lainnya selain C_N, dapat diperoleh dari tabel faktor koreksi untuk nilai N-SPT milik teori Idriss dan Boulanger (2008).

Idriss dan Boulanger (2008) juga mengembangkan sebuah persamaan untuk faktor koreksi nilai $(\mathrm{N}_1)_{60}$ penyetaraan pasir bersih (*clean sand*), yaitu:

$$(N_1)_{60cs} = \alpha + \beta(N_1)_{60} \quad (5)$$

Dimana α dan β adalah koefisien yang didapat bergantung pada *fines content* (FC) yaitu:

a. Jika FC < 5%, maka nilai α = 0 dan β = 1,0
b. Jika 5% < FC < 35%, maka nilai α = exp [1.76 – (190/FC2)] dan β = [0.99 + (FC1.5/1,00)]
c. Jika FC > 35%, maka nilai α = 5,0 dan β = 1,2

Nilai $CRR_{7.5}$ merupakan nilai CRR pada saat magnitudo gempa mencapai nilai 7,5 M_w dan dapat didapatkan menggunakan persamaan sebagai berikut:

$$CRR_{7.5} = exp\left[\frac{(N_1)_{60cs}}{14{,}1} + \left(\frac{(N_1)_{60cs}}{126}\right)^2 - \left(\frac{(N_1)_{60cs}}{23{,}6}\right)^3 + \left(\frac{(N_1)_{60cs}}{25{,}4}\right)^4 - 2{,}8\right] \quad (6)$$

- Berdasarkan CPT

Idriss dan Boulanger (2008) mengatakan bahwa nilai $CRR_{7.5}$ diperoleh menggunakan rumus:

$$CRR_{7.5} = exp\left[\frac{q_{c_1N_{cs}}}{540} + \left(\frac{q_{c_1N_{cs}}}{67}\right)^2 - \left(\frac{q_{c_1N_{cs}}}{80}\right)^3 + \left(\frac{q_{c_1N_{cs}}}{114}\right)^2 - 3\right] \quad (7)$$

Jika $q_{c_1N_{cs}}$ < 211.
Jika nilai $q_{c_1N_{cs}}$ > 211, maka $CRR_{7.5}$ adalah 2.
Dimana perhitungan nilai ekuivalen normalisasi CPT $q_{c_1N_{cs}}$ dapat ditentukan menggunakan persamaan berikut:

$$q_{c_1N_{cs}} = q_{c1N} + \Delta q_{c1N} \quad (8)$$

$$q_{c1N} = C_N \frac{qc}{P_a} \quad (9)$$

$$C_N = \left(\frac{P_a}{\sigma'v}\right)^n \quad (10)$$

$$\Delta q_{c1N} = \left(5{,}4 + \frac{q_{c1N}}{16}\right) . exp\left(1{,}63 + \frac{9{,}7}{FC+0{,}01} - \left(\frac{15{,}7}{FC+0{,}01}\right)^2\right) \quad (11)$$

$$FC = 2{,}8\, Ic^{2.6} \quad (12)$$

$$Ic = [(3{,}47 - \text{Log Q})^2 + (1{,}22 + \text{Log F})^2]^{0.5} \quad (13)$$

$$Q = \left(\frac{qc - \sigma_{vc}}{Pa}\right)\left(\frac{Pa}{\sigma'_{vc}}\right)^n \quad (14)$$

$$F = \left(\frac{fs}{qc - \sigma_{vc}}\right) . 100\% \quad (15)$$

Magnitude Scalling Factor (MSF)

Jika perencanaan menggunakan magnitudo gempa selain dari 7,5, baik lebih besar atau lebih kecil, maka diperlukan faktor koreksi *Magnitude Scaling Factor* (MSF) yaitu suatu faktor pengali magnitudo gempa dalam skala momen agar setara dengan CRR saat M_w = 7,5. Menurut Idriss dan Boulanger (2008) syarat nilai MSF yang digunakan adalah kurang dari atau sama dengan 1,8 dan nilai tersebut dapat diperoleh menggunakan persamaan:

$$MSF = 6.9\, exp\left(\frac{-M_w}{4}\right) - 0.058 \quad (16)$$

Faktor Keamanan (FS)

Faktor keamanan (FS) merupakan suatu nilai perlu diketahui saat mengevaluasi zona berpotensi likuifaksi.

$$FS = \frac{CRR}{CSR} \quad (17)$$

Dimana:
Jika FS > 1, maka tidak terjadi likuifaksi
Jika FS = 1, maka kondisi kritis
Jika FS < 1, maka terjadi likuifaksi

2.3 *Stone Column*

Perancangan *stone column* yang dilakukan dalam penelitian ini menggunakan rumusan-rumusan berdasarkan FHWA (*Federal Highway Administration Office of Engineering and Highway Operations Research and Development Washington, D.C.*).

Pola dan Tipe *Stone Column*

Pola yang digunakan saat perancangan *stone column* adalah pola segitiga. Selain itu, penelitian ini menggunakan tipe pemasangan *floating type* yang dimana *stone column* dipasang secara mengambang di tanah lunak.

Diameter Ekuivalen (D_e)

Dalam penggunaan pola segitiga sama sisi ini, maka persamaan yang dibutuhkan dalam mencari diameter ekuivalen (D_e) yang dipengaruhi oleh 1 *stone column* adalah sebagai berikut:

$$D_e = 1{,}05\ s \tag{18}$$

Dimana:
s = spasi pemasangan *stone column*.

Rasio Pergantian Luas (a_s)

Dalam menghitung jumlah pergantian tanah yang dibutuhkan *stone column* ditetapkan nilai rasio pergantian luas (a_s), dengan persamaan sebagai berikut:

$$a_s = \frac{A_S}{A} \tag{19}$$

$$a_c = \frac{A - A_S}{A} \tag{20}$$

Dimana untuk mencari nilai luas *stone column* (A_s) pada pola pemasangan segitiga sama sisi menggunakan rumusan sebagai berikut:

$$A_s = 0{,}907 \left(\frac{D}{s}\right)^2 \tag{21}$$

atau dengan persamaan:

$$A_c = \frac{1}{4}\pi(D)^2 \tag{22}$$

$$A = \frac{1}{4}\pi(D_e)^2 \tag{23}$$

Dimana:
A = Luas total *unit cell*
D = Diameter *stone column*

Konsentrasi Tegangan (σ_u)

Saat di lapangan diasumsikan bahwa penurunan yang terjadi, baik pada *stone column* maupun tanah yang diperkuatnya, dianggap sama besar dan terjadi dalam waktu bersamaan sehingga terjadi penumpukan tegangan yang diterima keduanya. Berdasarkan metode FHWA, besar nilai faktor penumpukan tegangan (n) berkisar antara 2 – 5. Dengan adanya faktor penumpukan ini, maka dapat dilhat nilai rasio tegangan yang diterima oleh tanah yang diperkuatnya menggunakan persamaan sebagai berikut:

$$\sigma_u = \sigma_s \,.\, a_s + \sigma_c(1 - a_s) \tag{24}$$

$$\sigma_c = \frac{\sigma}{[1+(n-1)a_s]} = \mu_c \sigma \tag{25}$$

$$\sigma_s = \frac{n\sigma}{[1+(n-1)a_s]} = \mu_s \sigma \tag{26}$$

$$\mu_c = \frac{1}{[1+(n-1)a_c]} \tag{27}$$

$$\mu_s = \frac{n}{[1+(n-1)a_s]} \tag{28}$$

Dimana:
n = Faktor konsentrasi tegangan
μ_c = Rasio tegangan pada *stone column* terhadap tegangan rata-rata pada daerah pengaruh
μ_s = Rasio tegangan pada tanah yang diperbaiki terhadap tegangan rata-rata pada daerah pengaruh
σ_s = Tegangan yang terjadi pada *stone column*
σ_c = Tegangan yang terjadi pada tanah yang diperbaiki.

3 PEMBAHASAN

3.1 *Analisis Potensi Likuifaksi*

Pada penelitian ini analisis potensi likuifaksi dilakukan berdasarkan hasil 2 (dua) data uji SPT dan 2 (dua) data uji CPT. Keadaan tanah dibawah permukaan didominasi oleh tanah non kohesif (tanah pasir) yang dapat dilihat pada Gbr. 1. Kekuatan gempa bumi yang digunakan untuk perhitungan analisis potensi likuifaksi pada peneltian ini adalah 7.5 M_w dengan data percepatan gempa (PGA) sebesar 0.506 g yang diperoleh dari Pusat Litbang Perumahan dan Pemukiman (Puskim) seperti yang terlihat pada Tabel 1.

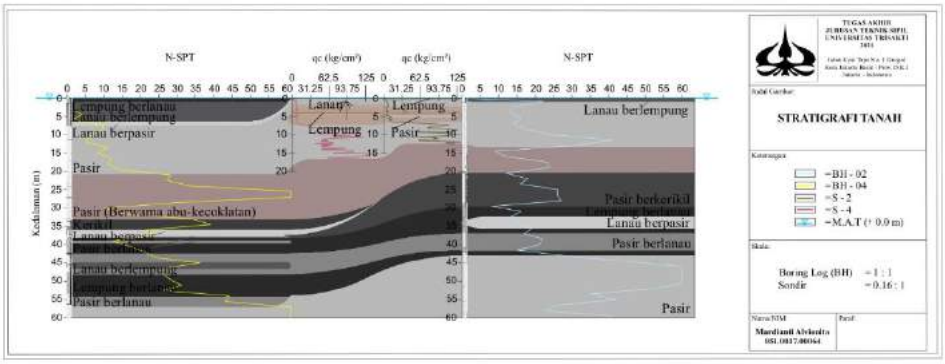

Gbr. 1. Stratigrafi Tanah.

Tabel 1. Data Percepatan Gempa (puskim.pu.go.id).

Variabel	Nilai
PGA (g)	0.506
S_S (g)	1.343
S_1 (g)	0.599
C_{RS}	1.068
C_{R1}	0.952
F_{PGA}	1.000

Berdasarkan Data SPT

Pada perhitungan analisis potensi likuifaksi berdasarkan data SPT ini menggunakan data tanah dari *bore log* nomor 02 dan 04. Masing-masing pemboran dilakukan hingga mencapai kedalaman 59.5 m dan 60 m dengan muka air tanah (M.A.T) berada tepat di permukaan tanah atau + 0 m.

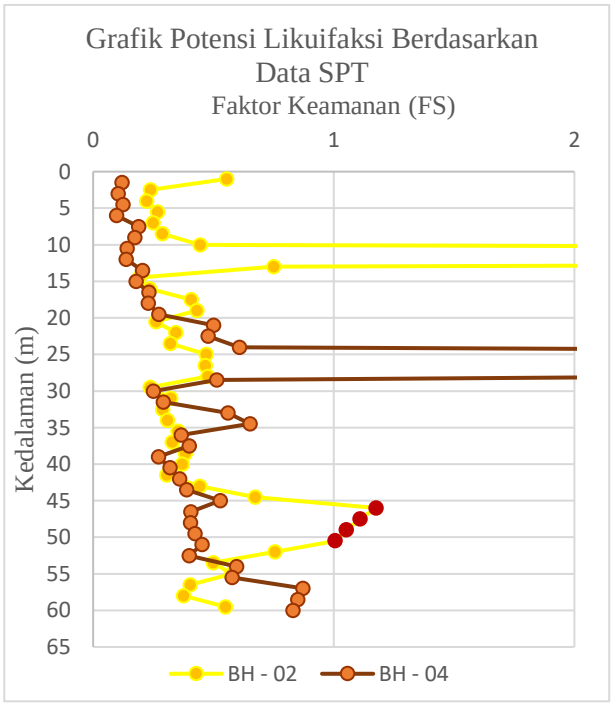

Gbr. 2. Grafik Potensi Likuifaksi Berdasarkan Data SPT.

Pada Gambar 2. terlihat bahwa baik hasil analisis dari data BH – 02 maupun BH – 04 terdapat lapisan tanah non-likuifaksi (nilai FS > 1) yang berada di antara lapisan-lapisan tanah yang berpotensi likuifaksi (nilai FS < 1). Lapisan tanah yang berada diatas dan/atau diantara lapisan tanah berpotensi likuifaksi akan terkena dampak likuifaksi tersebut. Maka, dapat dikatakan bahwa semua lapisan tanah pada data BH - 02 dan BH - 04 berpotensi serta terdampak likuifaksi.

Berdasarkan Data CPT

Pada perhitungan analisis potensi likuifaksi berdasarkan data CPT ini menggunakan data tanah dari sondir nomor 02 dan 04. Masing-masing pengujian dilakukan hingga mencapai kedalaman 12.6 m dan 16.8 m dengan muka air tanah (M.A.T) berada tepat di permukaan tanah atau + 0 m. Analisis potensi likuifaksi berdasarkan data CPT dilakukan setiap kedalaman 0,2 m dari permukaan tanah.

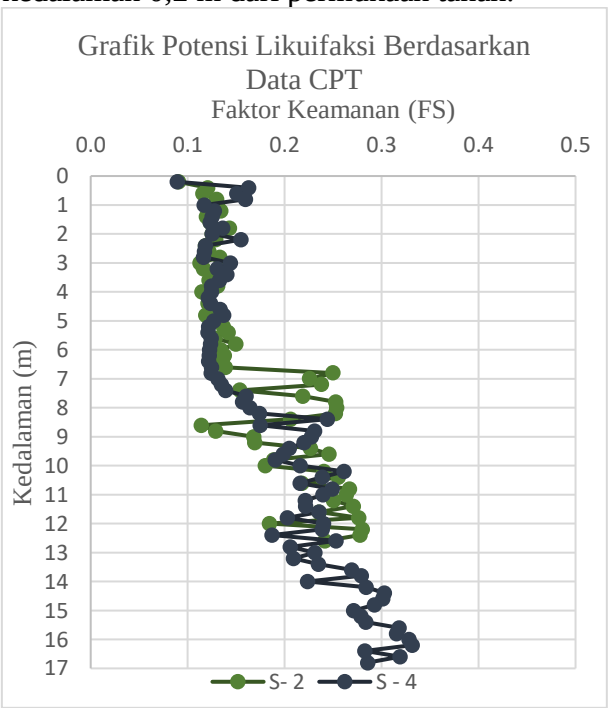

Gbr. 3. Grafik Potensi Likuifaksi Berdasarkan Data CPT.

Berdasarkan hasil analisis yang terlihat pada Gbr. 3 maka dapat dinyatakan bahwa, baik hasil analisis dari data S – 02 maupun S – 04, semua lapisan tanah berpotensi untuk terjadi likuifaksi karena memiliki nilai FS < 1 dari permukaan tanah hingga titik terdalam pengujian.

3.2 *Perancangan Stone Column*

Pada penelitian ini, perancangan *stone column* dilakukan menggunakan beberapa acuan kedalaman, yaitu 10 m, 20 m, 30 m, dan 40 m.

Diameter *Stone Column*

Diameter *stone column* yang digunakan dalam perancangan ada beberapa, yaitu 0,6 m, 0,8 m, dan 1 m.

Jarak Pengaruh *Stone Column*

Jarak pengaruh *stone column* biasa disebut juga dengan diameter ekuivalen (D_e). Dalam perancangannya, diameter ekuivalen bergantung dengan spasi pemasangan setiap *stone column*. Maka dari itu, dalam penelitian ini penulis menggunakan tiga asumsi spasi pemasangan yaitu 1,2 m, 1,6 m, dan 2 m. Berdasarkan hasil perhitungan pada Tabel 2 maka dapat disimpulkan bahwa diameter ekuivalen berbanding lurus dengan spasi pemasangan *stone column*. Artinya, semakin besar spasi pemasangan antar *stone column*, maka semakin besar pula diameter ekuivalennya.

Tabel 2. Hasil Perhitungan Diameter Ekuivalen (De).

s (m)	D_e (m)
1.2	1.260
1.6	1.680
2	2.100

Rasio Pergantian Luas

Rasio pergantian luas menentukan besarnya kenaikan atau perbaikan yang terjadi pada tanah yang diperbaiki. Pada Gbr. 4 dapat dilihat bahwa nilai rasio pergantian luas saat menggunakan *stone column* berdiameter 1 m dengan spasi 1,2 m adalah nilai yang paling mendekati nilai 1. Hal itu terjadi dikarenakan parameter spasi dan diameter juga menentukan besarnya nilai rasio pergantian luas yang diberikan oleh 1 *stone column*.

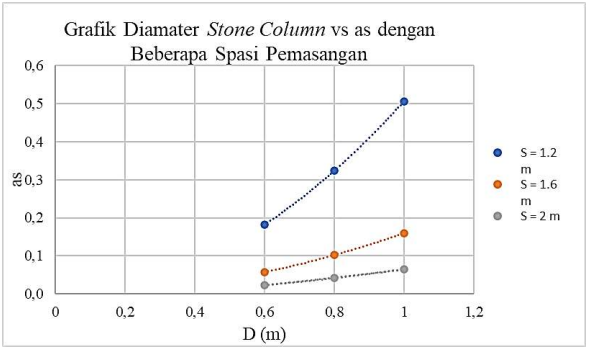

Gbr. 1. Grafik Diameter *Stone Column* vs as dengan Beberapa Spasi Pemasangan.

Konsentrasi Tegangan

Pada penelitian ini nilai n diasumsikan sebesar n=2. Nilai tegangan untuk menghitung konsentrasi tegangan menggunakan tegangan total vertikal dalam perhitungan analisis potensi likuifaksi, diambil sesuai dengan kedalaman yang dibutuhkan. Gbr. 5 menunjukkan bahwa semakin dalam perancangan dan semakin besar diameter *stone column* yang digunakan maka semakin besar pula nilai konsentrasi tegangan. Sebaliknya, semakin besar spasi pemasangan *stone column* maka semakin kecil nilai konsentrasi tegangan. Selain itu juga, bila dibandingkan dengan nilai tegangan vertikal total yang digunakan, terlihat bahwa *stone column* berdiameter 1 m dengan spasi pemasangan 1,2 m disetiap asumsi kedalaman sudah mencukupi.

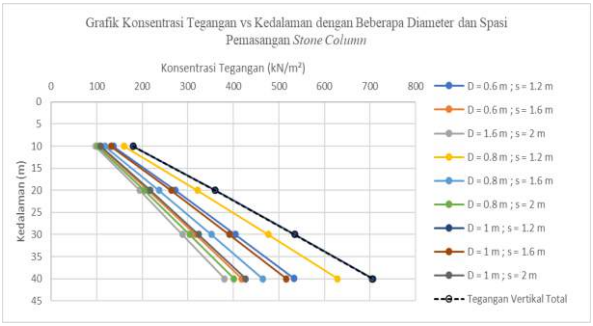

Gbr. 2. Grafik Konsentrasi Tegangan vs Kedalaman dengan Beberapa Diameter dan Spasi Pemasangan *Stone Column.*

4 KESIMPULAN

Berdasarkan hasil perhitungan perancangan *stone column* sebagai metode yang digunakan dalam upaya stabilisasi tanah berpotensi likuifaksi, maka dapat disimpulkan bahwa:

1. Setelah dilakukannya perhitungan analisis potensi likuifaksi berdasarkan data uji SPT dan CPT menggunakan teori Idriss dan Boulanger (2008) diperoleh bahwa hingga mencapai titik terdalam pengujian (BH-02 59,5 m, BH-04 60 m, S-2 12,6 m, dan S-4 16,8 m) yang telah dilakukan berpotensi untuk terjadinya likuifaksi.
2. *Stone column* yang dirancang menggunakan diameter 1 m dengan spasi pemasangan sejauh 1,2 m dan ditanam sedalam 10 m dapat dikatakan efektif karena memiliki nilai rasio pergantian luas tertinggi dan nilai konsentrasi tegangan yang diperoleh sudah mencukupi.

DAFTAR PUSTAKA

FHWA/RD-83/026 *Design and Construction of Stone column* Vol. I (1983)

FHWA/RD-83/027 *Design and Construction of Stone column* Vol. II (1983)

Idriss, I.M., and Boulanger, R.W. 2008. *Soil Liquefaction During Earthquakes*. Earthquake Engineering Research Institute (EERI).

Pusat Litbang Perumahan dan Pemukiman. 2011. *Desain Spektra Indonesia*. Jakarta: Kementrian Pekerjaan Umum dan Perumahan Rakyat.

Towhata, I. 2008. *Geotechnical Earthquake Engineering*. Springer.

Shear Strength Characteristics of Volcanic Soils Mixed with Cement (AMM)

Richo Brian
Student – Universitas Katolik Parahyangan

Paulus P. Rahardjo
Professor of Geotechnical Engineering – Universitas Katolik Parahyangan

Stefanus Diaz Alvi
Deputy Head Division – PT Geotechnical Engineering Consultant

ABSTRACT: Volcanic soils are frequently used as embankment material in Indonesia. In nature, volcanic soil has medium to high shear strength and durable in its original state. However, it is not the case when they are used for embankment. This research uses volcanic soil sample retrieved from Batang, Central Java where UU triaxial test, crumb test and CBR test are carried out to investigate its shear strength and durability when mixed with cement. Crumb test results displayed the soil having very sensitive reaction when exposed to water. However, this situation no longer applies after the volcanic soil is mixed with cement. CBR test result indicates that 8% cement is the optimum cement percentage to be mixed since mixing more than 8% cement to the soil displayed insignificant increase to the soil CBR value. UU triaxial test also showed that mixing 8% cement to the volcanic soil actually increases its shear strength 4 times its original.

Keywords: shear strength, durability, volcanic soil, cement, compacted soil

1 INTRODUCTION

Volcanic soils are formed through the weathering of volcanic materials such as lava, pyroclastic flows and volcanic ash and are commonly found throughout Indonesia. In nature, volcanic soils have medium to high shear strength and is durable in its original state since it is chemically bonded, this condition however no longer applies when they are used for embankment, as the bond perishes when the volcanic soil was excavated causing the soil to have low shear strength and sensitive when exposed to water. As such, volcanic soil imposes problem during embankment in construction projects.

An alternative often used by engineer in construction projects to increase shear strength of volcanic soils is mixing cement, since replacing the entire soil would require more budget and time. Although mixing cement to volcanic soils is a common solution to solve the problems volcanic soils impose, actual laboratory research to provide concrete evidence as to the optimum cement percentage to be added is seldom discussed.

This paper uses volcanic soils retrieved from Batang, Central Java and discusses the results investigated through shear strength and durability tests such as UU triaxial test, dispersion test and CBR test in compacted condition using the standard proctor method. Index properties are also provided in this paper to give information about the characteristics of volcanic soils. The data displayed is from both original and cemented volcanic soils to provide clear insight on the effect cement mixture has on volcanic soils.

2 RESEARCH METHOD

2.1 *Soil Cement Mixing*

The amount of cement to be mixed to the volcanic soil is calculated using the following equation.

$$Ws=1/(1+w) \quad (1)$$

$$Wc=\%Cement(Ws) \quad (2)$$

The amount of cement to be mixed to the volcanic soil is 4%, 6%, 8%, 10% dan 12%. The volcanic soil is mixed inside a container with the cement and then mixed.

2.2 *Shear Strength Characteristics*

The shear strength of the volcanic soil is investigated using the UU triaxial test. The parameters investigated using the UU triaxial test is the c dan ϕ using the Mohr – Coulomb graph in total stress condition. A volcanic soil sample of 3.8 cm diameter and 7.6 cm height is restricted using a rubber membrane and applied confining pressure of 0.25 kg/cm^2, 0.5 kg/cm^2 and 1 kg/cm^2. Axial stress is then applied to the soil sample using the UU triaxial machine.

2.3 *Soil Dispersive Characteristics*

The dispersive characteristic of the volcanic soil is investigated using the crumb test. The parameters investigated using the crumb test is the dispersive grade of the soil when exposed to water. The dispersive grade of the soil for crumb test is taken from ASTM 6572 in which the grade are as follows.

1. Grade 1 (Nondispersive): No reaction, the soil has no reaction when exposed to water.
2. Grade 2 (Intermediate): Slight reaction, the soil has slight reaction when exposed to water.
3. Grade 3 (Dispersive): Moderate reaction, the soil has a moderate reaction when exposed to water.
4. Grade 4 (Highly Dispersive): Strong reaction, the soil has strong reaction when exposed to water.

The grades of the soils are purely dependent on the judgement of the researcher.

2.4 *Optimum Cement Percentage*

The optimum cement percentage of the volcanic soil is investigated using the CBR test. The parameters investigated using the CBR test is the CBR design value where the required CBR design value is 10%.

3 PHYSICAL PROPERTIES OF ORIGINAL VOLCANIC SOIL

3.1 *Soil Retrieval Location*

The volcanic soil investigated is retrieved from Batang, Central Java where an ongoing project is being constructed. The volcanic soil in the location is used as embankment material. The soil is retrieved and transported to laboratory to investigate its shear strength characteristic in original condition and mixed with cement. Picture of the retrieval location can be seen in Fig. 1.

Fig. 1. Volcanic Soil from Batang, Central Java.

3.2 *Index Properties*

Index properties provided in this paper includes the natural water content, unit weight, degree of saturation, void ratio, porosity and specific gravity of the soil. The index properties investigated are as follows.

Table 1. Batang Volcanic Soil Index Properties.

Batang Volcanic Soil Index Properties	
w (%)	42 - 51
γ (gr/cm^3)	1.64
Sr (%)	78.54
e	1.34
n	0.57
Gs	2.62

3.3 *Atterberg Limits*

The Atterberg limits of the volcanic soil are also investigated to provide better depiction of the volcanic soil characteristics. As the plastic limit, liquid limit and plasticity index of the soil can be used to determine the classification of a soil. The Atterberg limits of the soil investigated are as follows.

Table 2. Batang Volcanic Soil Atterberg Limits.

Batang Volcanic Soil Atterberg Limits	
PL (%)	37
LL (%)	53
LL_{Oven} (%)	40.5
PI	16

Casagrande plasticity chart also shows that the soil classifies as MH shown in Fig. 2. Wesley plasticity chart is also included to show that the soil follows the volcanic soil research trend investigated by Wesley (2010) shown in Fig. 3.

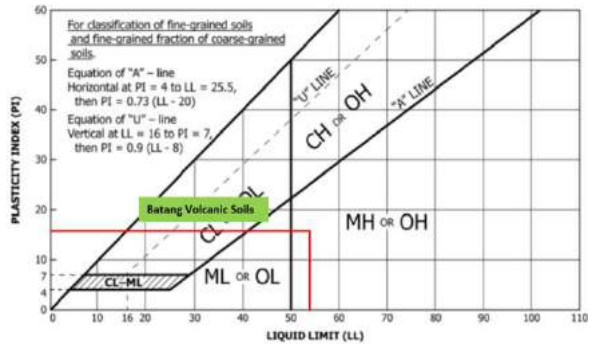

Fig. 2. Casagrande Plasticity Chart for Batang Volcanic Soils.

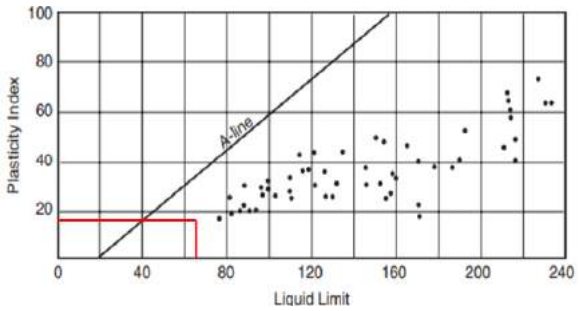

Fig. 3. Wesley Plasticity Chart for Batang Volcanic Soils.

3.4 *Maximum dry unit weight and optimum water content*

The maximum dry unit weight and optimum water content of the volcanic soil is investigated using standard proctor compaction method. The maximum dry unit weight and optimum water content is used as standard to determine the optimum cement percentage to be added to the volcanic soil using the CBR test as medium. The maximum dry unit weight and optimum water content investigated are as follows.

Table 3. Batang Volcanic Soil Maximum Dry Unit Weight and Optimum Water Content.

Batang Volcanic Soil Maximum Dry Unit Weight and Optimum Water Content	
$\gamma dry_{maximum}$ (gr/cm^3)	1.3
$w_{optimum}$ (%)	39.8

3.5 *Grain Size Distribution*

The soil grain size distribution is investigated to provide information on the content of the volcanic soil. Information on the content of the volcanic soil may provide further insight about how the content of the soil corresponds to the soil characteristics. The soil grain size distribution of the soil investigated are as follows.

Table 4. Grain Size Distribution of Batang Volcanic Soil.

Batang Volcanic Soil Grain Size Distribution	
Gravel (%)	0
Coarse to Medium Sand (%)	6.1
Fine Sand (%)	11.27
Silt (%)	48.86
Clay (%)	33.76

The soil grain size distribution graph can be seen in Fig. 4.

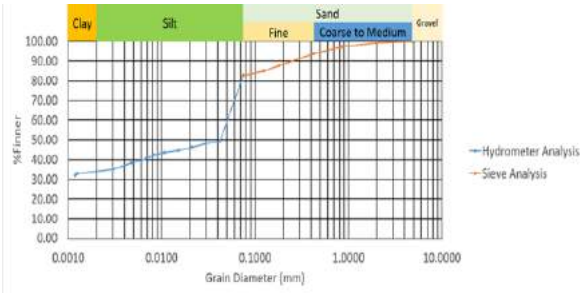

Fig. 4. Soil Grain Size Distribution for Batang Volcanic soils.

4 SHEAR STRENGTH CHARACTERISTICS OF VOLCANIC SOILS MIXED WITH CEMENT

4.1 *Volcanic soil shear strength*

Volcanic soils retrieved from Batang, Central Java is tested using the UU triaxial test to investigate the shear strength characteristic of the soil in two conditions original and cemented. Test in two different conditions of the soil can provide comparison where this comparison can help better perceive the increase in shear strength after cement is mixed to the volcanic soil. The data investigated in accordance to this test are as follows.

Table 4. Batang Volcanic Soil Shear Strength Summary

Batang Volcanic Soil Shear Strength Summary			
Sample	Cohesion	Internal Friction Angle	E50
	(kPa)	(°)	(kPa)
Original	16	22	2,255
8% Cemented	68	31	16,620
10% Cemented	72	34	27,500
12% Cemented	86	38	35,714

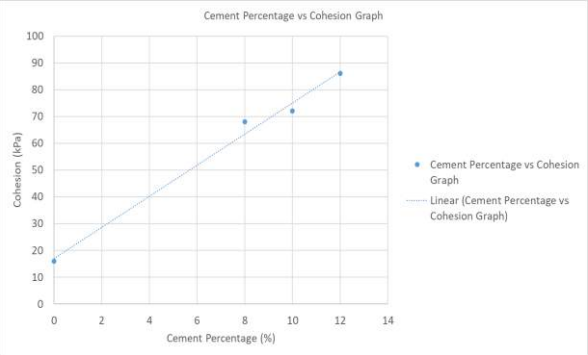

Fig. 5. Batang Volcanic Soil Cement Percentage vs Cohesion Graph.

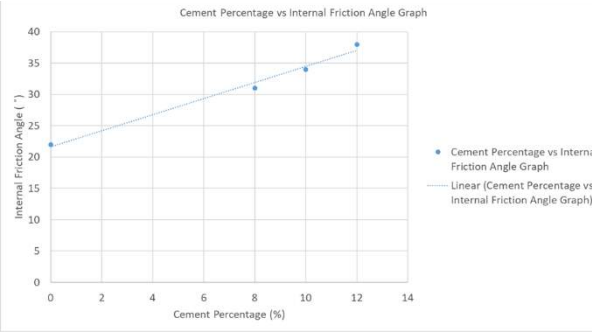

Fig. 6. Batang Volcanic Soil Cement Percentage vs Internal Friction Angle Graph.

From the data investigated above it could be seen that adding cement mixture to volcanic displays increasing trend corresponding to its shear strength characteristics. Fig. 5. proves that mixing cement to volcanic soils increases the volcanic soil cohesion significantly. Fig. 6. also displays increase in the volcanic soil internal friction angle, however not as significant as the increase in its cohesion.

4.2 *Volcanic soil durability*

Volcanic soils retrieved from Batang, Central Java is tested using crumb test to investigate the durability of the soil when exposed to water in its original condition and when mixed with cement to provide clear evidence on how cement affects the durability of volcanic soils. Crumb test is conducted on volcanic soils mixed with varying cement percentage. The data investigated in accordance to this test are as follows.

Table 5. Batang Volcanic Soil Crumb Test.

Batang Volcanic Soil Crumb Test Grading			
Sample	Grade		
	2 min	1 hour	6 hours
Original	2	4	Failure
4% Cemented	1	1	1
6% Cemented	1	1	1
8% Cemented	1	1	1
10% Cemented	1	1	1
12% Cemented	1	1	1

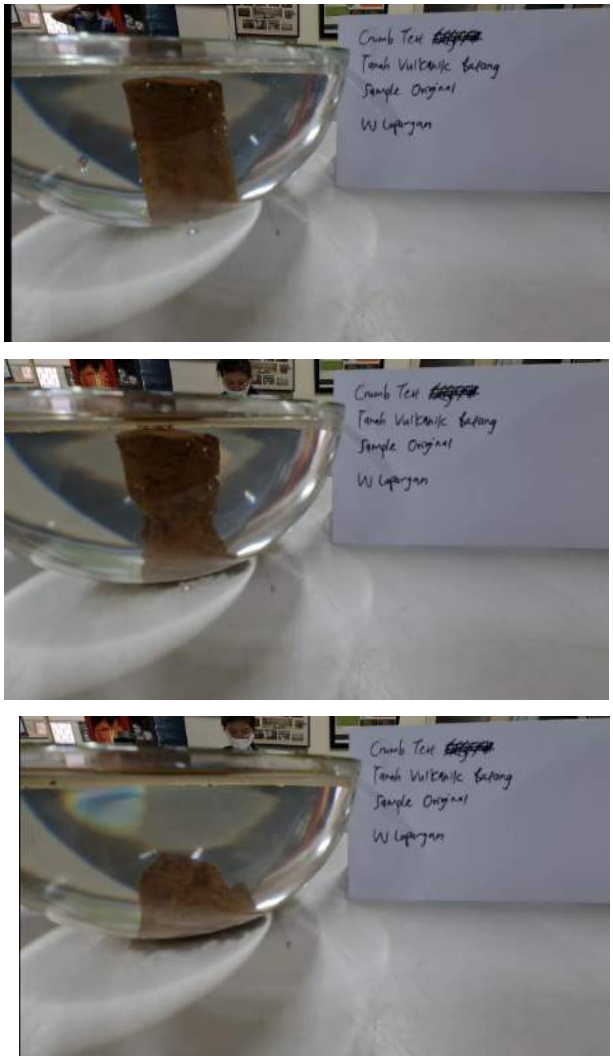

Fig. 7. Batang Original Volcanic Soil Crumb Test After 2 Minutes, 1 Hour and 3 Hours 13 Minutes.

Fig. 8. Batang 4% Cemented Volcanic Soil Crumb Test After 2 Minutes, 1 Hour and 6 Hours.

From the data investigated above in Fig. 7. it could be seen that volcanic soils are sensitive when exposed to water resulting it to crumble before the allocated 6 hours for the crumb test. However, in Fig. 8. after cement is mixed to the volcanic soils it could be seen that the volcanic soils are no longer affected by water resulting in a nondispersive state even after 6 hours passed for the crumb test of the volcanic soils.

4.3 *Optimum cement percentage for volcanic soils*

Volcanic soils retrieved from Batang, Central Java is tested using the CBR test to investigate the optimum cement percentage to be added to the volcanic soils. The CBR value for this particular volcanic soil is set to be reached at 10%, as such the optimum cement percentage to be added to the volcanic soils can be determined upon reaching 10% CBR value in the CBR test. The data investigated in accordance to this test are as follows.

Table 6. Batang Volcanic Soil CBR Test.

Batang Volcanic Soil Optimum Cement Percentage Summary				
Sample	CBR Value (%)			
	CBR 10 Blows	CBR 25 Blows	CBR 56 Blows	CBR Value
Original	0.89	1.53	4.38	2.7
4% Cemented	1.27	1.58	1.76	2.8
6% Cemented	2.2	4.33	6.89	6.9
8% Cemented	3.45	4.55	11.38	11.4
10% Cemented	7.77	14.41	16.87	11.9
12% Cemented	9.76	16.78	17.44	13

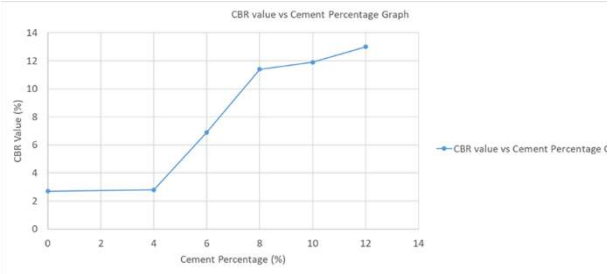

Fig. 9. Batang Volcanic Soil CBR Value vs Cement Percentage Graph.

From the result investigated above from Fig. 9. it could be seen that 8% cement mixture is the optimum amount of cement mixture to be added to volcanic soils to increase its shear strength and durability. From Fig. 9. It could also be seen that mixing 4% cement to volcanic soils gives little to no effect to the volcanic soils as seen from its CBR value. However, when 6% - 8% of cement mixture is added to the volcanic soils the CBR value increases significantly. Until 10% of cement mixture is added to the volcanic soils, the CBR value still increases however as seen from Fig. 9. the increase in the CBR value is no longer as significant. This result shows and proves that the assumption of adding 8% cement mixture to problematic volcanic soils proves very effective in improving the soil quality in terms of shear strength and durability, as replacing the soil entirely is for most cases is economically and practically harder to implement adding cement mixture to volcanic soils is considered a very practical and cost-efficient solution for soil improvement also proven by the results of this investigation.

5 CONCLUSION

From the results investigated corresponding to mixing cement mixture to volcanic soils there are some conclusions that could be made.

1. From the Casagrande Plasticity Chart it could be concluded that the Batang volcanic soils classifies as MH.
2. From the cement percentage vs cohesion and cement percentage vs internal friction angle graphs it could be seen that the increase in cohesion is more significant in contrast to the increase in the internal friction angle. This result implies that cement mixtures affect the cohesion of volcanic soils more than it affects the internal friction angle of volcanic soils.
3. From the CBR tests it could be concluded that mixing 4% cement mixture to volcanic soils does not provide significant effect as the amount of cement mixture mixed may be too little to impose any effects on the volcanic soils.
4. Mixing 8% cement to volcanic soil satisfies the minimum design requirement in construction projects which is a minimum of 10% CBR design value. As such, mixing cement mixture to volcanic soils could be a practically viable and cost-effective soil improvement method.

ACKNOWLEDGEMENTS

Writer wishes to show appreciation to Universitas Katolik Parahyangan Geotechnical Laboratory for allowing writer to conduct experiment corresponding to investigating volcanic soils. Also, writer wishes to show appreciation to PT. Geotechnical Engineering Consultant for allowing writer to conduct experiment in relation to the construction project in Batang, Central Java.

REFERENCES

Alvi, Stefanus Diaz, Bryan Marcus Sila, and Paulus P. Rahardjo. 2020. *Karakterisasi Tanah Lempung Vulkanik di Bogor Dengan Uji Cptu Dan Uji Dilatometer*. Universitas Katolik Parahyangan, Bandung.

ASTM. n.d. Standard Test Methods for Determining Dispersive Characteristics of Clayey Soils by the Crumb Test. N.p.: ASTM.

D. Wesley, Laurence. 2010. *Geotechnical Engineering in Residual Soils.* New Jersey: John Wiley & Sons, Inc.

Head, K.H. 1986. *Manual of Soil Laboratory Testing Volume 3 Effective Stress Tests*. New York: Halsted Press.

Knodel, Paul C. 1991. *Characteristics and Problems of Dispersive Clay Soils*. Denver: United States Department of The Interior.

M. Das, Braja, and Nagaratman Sivakugan. 2010. *Geotechnical Engineering a Practical Problem-Solving Approach*. Fort Lauderdale: J. Ross Publishing, Inc.

UNPAR, KBI Geoteknik. 2017. *Manual Praktikum Penyelidikan Tanah*. Bandung: Universitas Katolik Parahyangan.

Raft Pile Foundation Application for A 20-Story Building on Dense Sand Soil

Alvin Tjahjadi
Civil Engineering – Universitas Pertamina

Jeffry Arnold Panggabean
Civil Engineering – Universitas Pertamina

Rangga Adiprima Sudisman
Civil Engineering – Universitas Pertamina

Arif Salman Dabigi
Geotechnical Engineer – Ministry of Public Works and Housing

ABSTRAK: Sebuah bangunan 20 lantai yang dibangun di atas tanah berpasir padat memerlukan desain fondasi yang memenuhi syarat daya dukung dan juga deformasi. Fondasi dangkal memberikan daya dukung yang cukup pada kondisi tanah berpasir padat, akan tetapi berpotensi mengalami penurunan fondasi yang besar. Penggunaan tambahan fondasi tiang atau fondasi *raft pile* dapat mengurangi penurunan berlebih. Perancangan dan perhitungan fondasi *raft pile* dilakukan menggunakan *Poulos-Davis-Randolph Simplified Design Method* dengan prinsip interaksi tiga arah antara *raft*, *pile*, dan tanah, dan Metode Elemen Hingga 3D. Perancangan fondasi *raft pile* menghasilkan dimensi *raft* sebesar 80 x 24 x 2,6 m dengan tambahan 252 tiang berdiameter 0,7 m dan panjang 30 m. Desain menghasilkan penurunan sebesar 0,2937 m, daya dukung aksial sebesar 12.544 MN dan daya dukung lateral sebesar 411,7 MN yang kesemuanya memenuhi persyaratan izin.
Kata Kunci: interaksi raft-pile-soil, daya dukung, penurunan tanah

ABSTRACT: A 20-story building built on dense sandy soil requires a foundation design that meets the requirements for bearing capacity as well as deformation. Shallow foundations may provide sufficient bearing capacity on dense soil but have the potential for considerable settlement. The use of additional pile foundations or raft pile foundations can reduce excessive settlement. The design and calculation of the raft pile foundation are carried out using the Poulos-Davis-Randolph Simplified Design Method with the principle of the three-way interaction between raft, pile, and soil, and the 3D Finite Element Method. The design of the raft pile foundation resulted in a raft dimension of 80 x 24 x 2.6 m with additional 252 piles with 0.7 m of diameter and 30 m of length. The design has 0.2937 m settlement, 12,544 MN axial bearing capacity, and 411.7 MN lateral bearing capacity which satisfied all requirements.
Keywords: raft-pile-soil interaction, bearing capacity, settlement

1 INTRODUCTION

Local soil conditions must be taken into account in foundation design to ensure adequate bearing capacity and serviceability. On dense sandy soil conditions, a 20-story building is planned. A large dimensional raft foundation is suitable for use on dense sandy soils by providing a significant soil bearing capacity. The use of a raft foundation, on the other hand, has the potential to cause significant soil settlement for the structure.

Based on the preliminary calculation, the use of the raft foundation itself can provide sufficient bearing capacity to withstand the load of the structure but not with the requirement of settlement. Adding some piles to the raft foundation system can avoid excessive settlement. Prakoso (2001) reported that the main purpose for adding these piles is to minimize or control the settlement and/or differential displacements. Dafalla (2020) assumed that piles and the raft share the load and reduce the overall settlement. The raft bearing capacity is generally sufficient, but the settlement is often larger than the allowable value. Therefore, piles are used as settlement reducers (Russo and Viggiani, 1998).

Bhartiya (2019) reported that the analysis and design of pile raft foundation (PRF) must consider the complex three-way interaction, raft-pile-soil interaction, in response to the variations of load, structural configuration, and soil properties. The simplified method from Poulos and Davis (1980) and Randolph (1994) were used to analyze and design for the

preliminary design stage. The 3D finite element method is used as the final detail for the design stage to obtain the optimum number, location, and configuration of the piles, as well as to compute the detailed settlement distributions. Because an appropriate soil constitutive model, accurate geometry, and proper interaction parameters can be incorporated into the analysis to cover all aspects of PRF behavior, the 3D finite-element analysis may be superior to the simplified method.

The main objective of this study is to reduce the settlement by adding several piles in any scenario to consider selecting the optimum design. The scenarios are varying the number of piles, varying the diameter of piles, and the thickness of the raft to obtain the settlement and differential displacement.

2 BUILDING AND SOIL CONDITIONS

The 20-story building with a 4-story underground basement has 24 m width and 80 m length of floor dimension. The raft will be placed at a depth of 16 meters and will be laid on an 18-meter layer of dense sandy soil. Table.1 displays the total forces on the building, while Table.2 displays the soil properties.

Table 1. Total Forces on Building.

Reaction Forces Direction	Magnitude
Vertical (z dir.)	453.39 kPa
Horizontal (x dir.)	17,113.98 kN
Horizontal (y dir.)	17,359.17 kN

Table 2. Soil Data Properties for Preliminary Design.

Depth	Type of Soil	γ_d	γ_{sat}	c	ϕ
0-7.5	Soft Silty Clay	13.47	14.93	50	3.0
7.5-12	Dense Sand	18.00	20.02	16	31.0
12-15	Soft Silty Clay	13.47	14.93	50	3.0
15-33	Dense Sand	18.00	20.02	16	31.0
33-36	Silty Clay	13.47	14.93	50	3.0
36 - 39	Dense Sand	18.00	20.02	16	31.0
39-40.5	Silty Clay	13.47	14.93	50	3.0
40.5-51	Very Hard Sand	16.00	18.00	16	34.2
51-54	Hard Silty Clay	14.99	16.60	135	3.6
54-60	Very Hard Sand	16.00	18.00	16	34.2

3 PRELIMINARY DESIGN

In the preliminary stage, it is necessary first to evaluate the vertical and lateral bearing capacity performance of a raft foundation itself without piles, and settlement is estimated by conventional method or simplified standard calculation, Poulos (2001). The general bearing capacity calculation estimates 6,368.21 kPa which is adequate to withstand 453.39 kPa of structural load and able to retain the tilt failure by assumed the raft is rigid. Using force equilibrium and taking the shear strength of the soil into account, the lateral capacity to retain sliding of 314.6 MN is obtained, which is also sufficient to withstand the lateral load of the structure of 17.36 MN.

Raft foundation has good performance in bearing capacity, which is indicated by a high safety factor. However, it does not meet the requirement for a settlement of 0.310 m due to elastic settlement. The estimated settlement without considering the weight of the raft is 0.434 m. The weight of the raft is a variable, which depends on the thickness and stiffness based on the structural design.

The raft-pile capacity design refers to Poulos (2001). It is necessary to consider the stiffness interaction raft-pile as outlined by Randolph (1994) when estimating the load distribution and settlement between raft and piles. The stiffness of the piled raft system can be estimated with the following equation:

$$K_{pr} = \frac{K_p + K_r\,(1 - \alpha_{cp})}{1 - \alpha^2_{cp}\,K_r\,K_p} \quad (1)$$

K_{pr}, K_p, K_r, α_{cp} the raft-pile stiffness, pile stiffness in the form of pile group, raft stiffness, and raft-pile interaction factor, respectively.

The pile stiffness can be estimated using the following equation, Randolph and Wroth (1978):

$$\frac{P_t}{w_t d G_L} = \frac{\frac{2\eta}{(1-\nu)\xi} + \frac{2\pi\rho}{\zeta}\frac{\tanh(\mu L)}{\mu L}\frac{L}{d}}{1 + \frac{8\eta}{\pi\lambda(1-\nu)\xi}\frac{\tanh(\mu L)}{\mu L}\frac{L}{d}} \quad (2)$$

P_t/w_t is stiffness of the pile; d and L are the diameter and length of the pile; G_L is the shear modulus of soil at the tip of the pile; $\eta = 1$; ν is the Poisson ratio of the soil; $\xi = G_L/G_b$ and G_b is the shear modulus of soil at the bottom of the pile; $\rho = G_{ave}/G_L$ and G_{ave} is the average shear modulus of soil along with the pile; $\lambda = E_p/G_L$ and E_p is the modulus of elasticity of the pile; ζ

= ln(2rm/d) and rm is the influenced maximum radius = {0.25+ξ[2.5ρ(1-μ_s)–0.25]}L; and μL_p = 2sqrt(2/ζλ)(L_p/d).

The stiffness of the raft can be estimated with the following equation, Fraser and Wardle (1976):

$$K_r = k_r \frac{2.25\ G\ B}{(1-\nu)} \quad (3)$$

k_r is the stiffness coefficient based on the dimension of the raft. The equation is as follows:

$$k_r = \frac{4\ E_r\ (1-\nu_s^2)\ t^3}{3\ E_s\ (1-\nu_r^2)\ B^3} \quad (4)$$

E_r and E_s is the elasticity moduli of raft and soil. ν_r and ν_s are the Poisson ratio of raft and soil. t and B are the thickness and width of the raft.

The following equation can be used to calculate pile-raft interaction:

$$\alpha_{cp} = 1 - \frac{\ln(r_c/r_o)}{\zeta} \quad (5)$$

$r_c = A_{raft}/n$; A_{raft} is raft area, n is the number of piles, and r_o is the radius of the pile. The load-settlement relationship is presented in Fig. 1.

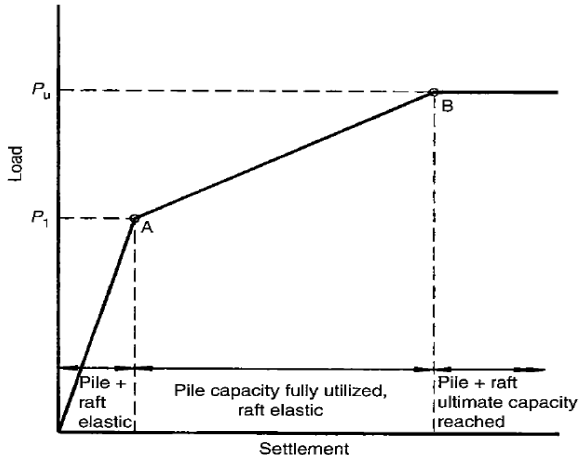

Fig. 1. Simplified Load-Settlement Curve for Preliminary Analysis, Poulos (1980).

By varying the thickness of the raft and the pile diameter, a minimum settlement of 0.304 m is estimated when the thickness of the raft and the pile diameter is 2.1 and 0.6 meters, respectively. The required number of piles is 320, with a pile group to raft width ratio (B_g/B_r) of 1.0, which indicates a fully rafted pile. The entire results were evaluated with 3D finite element analysis to provide a more precise calculation.

4 FINITE-ELEMENT ANALYSIS

PLAXIS 3D was used to perform three-dimensional finite element analysis of rafts, pile groups, and pile rafts. The analysis was carried out in four steps as illustrated in Fig.2: (a) basement excavation to a depth of 16 meters, (b) using the raft as a plate by adjusting the thickness, (c) assigning load, in which the vertical distributed load was applied on the raft surface to see the settlement that occurred without the addition of piles, and (d) adding piles and assigning the load to evaluate the piles' contribution to reduplication. The raft's weight accounts for the distributed load by multiplying the plate's unit weight by 0. The reset displacement to zero option box was selected to account for zero displacements that occurred during the excavation phase and when adding the raft plate.

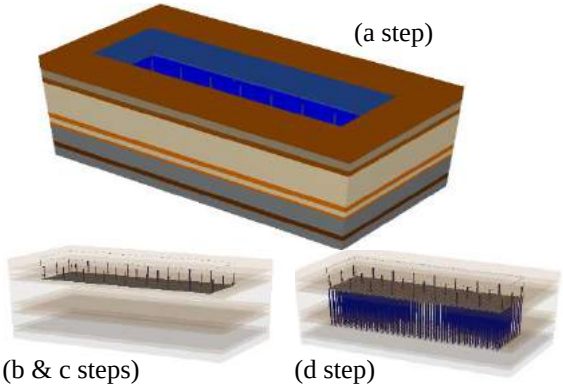

Fig. 2. The steps of FE Calculation and Analysis.

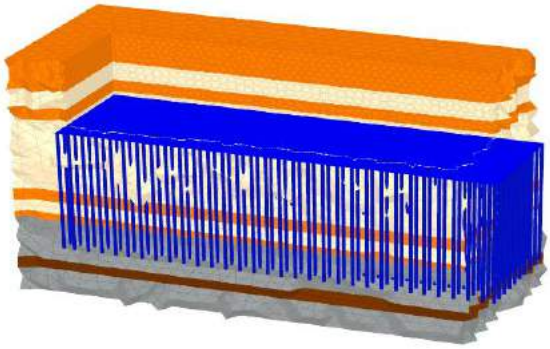

Fig. 3. Finite Element Model Meshing.

Table 3. Soil Data Properties for FE Analysis.

Depth	Type of Soil	Modulus Elasticity, E (kPa)	Poisson Ratio, v
0 - 7.5	Soft Silty Clay	26,060	0.35
7.5 - 12	Dense Sand	24,440	0.3
12 - 15	Soft Silty Clay	26,060	0.35
15 - 33	Dense Sand	24,440	0.3
33 - 36	Silty Clay	26,060	0.35
36 - 39	Dense Sand	24,440	0.3
39 - 40.5	Silty Clay	26,060	0.35
40.5 - 51	Very Hard Sand	10,890	0.3
51 - 54	Hard Silty Clay	71,550	0.35
54 - 60	Very Hard Sand	10,890	0.3

5 PARAMETRIC STUDY – ELASTIC

The main concern addressed in this study is the soil settlement beneath the foundation. The pile group system geometry must be optimized. A parametric study was carried out to investigate the effects of system geometry elements such as pile number (n), pile diameter (D), and raft thickness (t_r) on the performance of piled rafts such as reference settlement (Se_{ref}) and differential displacement (ΔSe). The settlement of the raft foundation without piles by using 2.6 m of thickness is 0.465 m, which does not meet the requirement. According to Prakoso's (2001) parametric study, a pile group to raft width ratio (B_g/B_r) of 1 is more effective in reducing settlement; thus, B_g/B_r is used at a value of 1 in this study.

5.1 *Reference Settlement*

The reference settlement normalized by that of the corresponding raft, Se_{ref} (=Change Se for piled raft to raft/Se for raft), for piled rafts with different numbers of piles is shown in Fig.4. The reduced settlement increases as the number of piles increases and decreases when passing over the optimum condition. In that case, it shows that adding the piles does not always increase the reduced settlement. The optimum or maximum reduced settlement is 41.02% by using 0.6 m of diameter and a 9 x 28 configuration of the group piles (252 piles). All diameter variables have the optimum reduced settlement by using 252 piles. This means that for this building and soil condition, the 9 x 28 configuration of the group pile has the most optimum efficiency in reducing the settlement. The pile spacing in this configuration is 2.9 m.

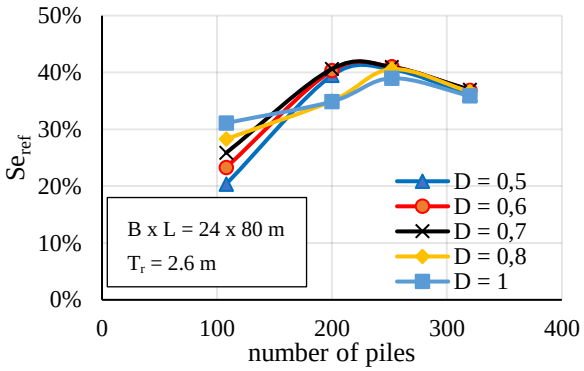

Fig. 4. Reference Settlement vs Number of Piles.

According to the Prakoso study, increasing the inverse pile spacing (either the pile spacing or the number of piles) reduces the displacement ratio between the piled raft and the raft. However, the inverse spacing of the pile varies between 0 and 0.25 in Prakoso's pile spacing parameter. That means the piles' minimum spacing is 4 meters, whereas, in this study, the spacing ranged from 2.4 to 4.6 meters.

The effect of pile diameter, D, as shown in Fig. 5, is that increasing the pile diameter does not significantly increase the reduced settlement, with the exception of a small number of piles, which can increase the reduced settlement by 10%. In another set of piles, the maximum Se_{ref} was calculated by taking 0.6 and 0.7 of the pile's diameter and gradually decreasing as the diameter increased.

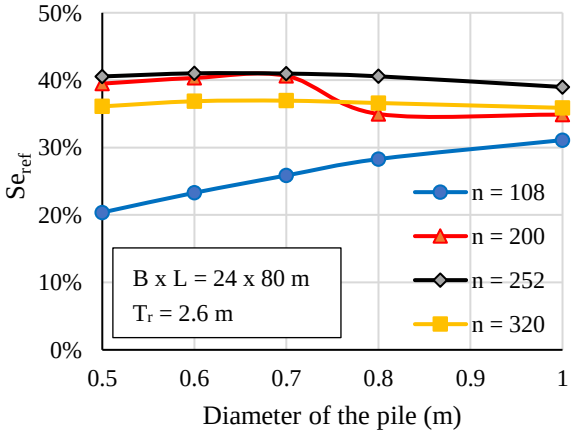

Fig. 5. Reference Settlement vs Pile Diameter.

5.2 *Center-Edge Differential Displacement*

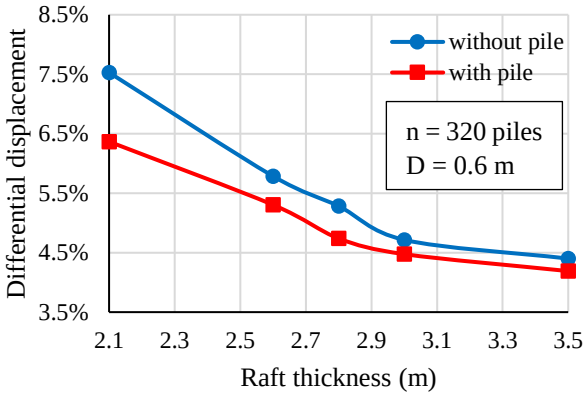

Fig. 6. Differential Displacement vs Raft Thickness.

The differential displacement accounts for displacement changes at the bottom raft surface's center and edge ($\Delta Se = (Se_{center} - Se_{edge})/(L_r/2)$).

The effect of raft rigidity, in terms of raft thickness, t_r, on the differential displacement, ΔSe is shown in Fig.6. In the study by Prakoso (2001), by varying the B_g/B_r into the raft thickness versus the differential displacement, the fully piled raft has a more significant effect on reducing the differential displacement. In this study, B_g/B_r of 1 is taken into account, and as shown by the graphic, the differential displacement decreases as the raft thickness increases. By adding the piles, the decrease in differential displacement by a various number of raft thicknesses from 2.1 to 3.5 m, 2%, and without adding the piles, 3%.

Fig. 7 depicts the effect of the number of piles on the differential displacement Se. By adding more piles, the differential displacement decreases until it reaches its optimum value, at which point it increases. The optimal number of piles to achieve the smallest differential settlement is 252, or 9 x 28 of group pile configuration with a 2,9-meter spacing.

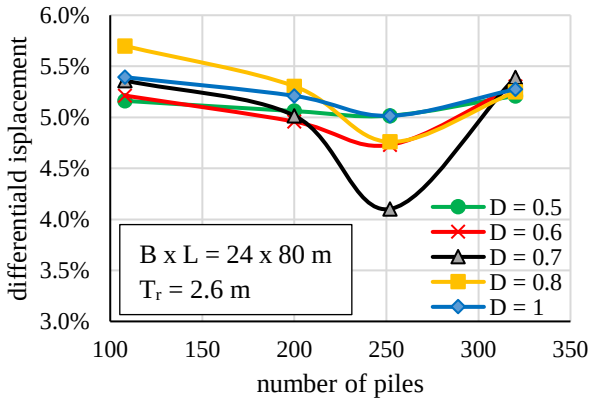

Fig. 7. Number of Piles vs Differential Displacement.

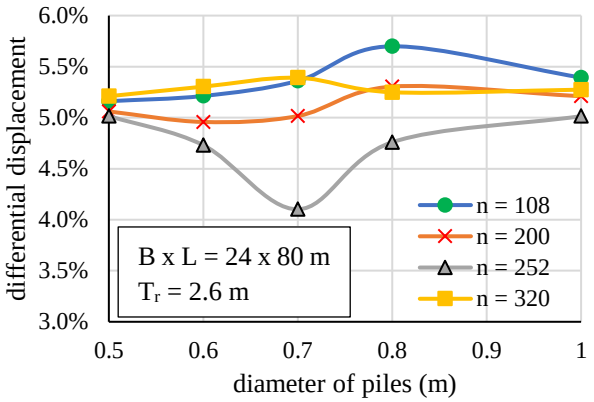

Fig. 8. Diameter of Piles vs Differential Displacement.

As the diameter of the pile increases, it seems not to have an effect on ΔSe. Fig. 8 shows that increasing the diameter of the piles by 0.7 m and adding 252 piles results in the fewest differential displacements.

5.3 *Reduce Bending Moment*

Reduced bending moment is calculated in percentage form by subtracting the bending moment of the raft without a pile from the bending moment of the raft with the additional pile. The raft bending moment is reduced by adding piles. As shown in Fig. 9, increasing the number of piles causes the reduced bending moment to increase until it reaches its optimum value, at which point it begins to decrease. The application of 0.5, 0.6, and 0.7 m of the piles have the optimum reduced bending moment at a number of piles of 200, and 0.8 and 1 m of the piles have the optimum reduced bending moment at a number of piles of 252. The optimization of the design has to consider reinforcing requirements, which are indicated by the moment bending value.

According to Prakoso (2001), as the thickness of the raft increases, the raft bending stresses generally decrease, even though the

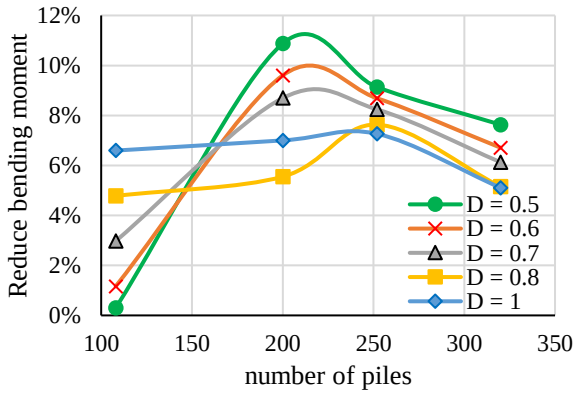

Fig. 9. Number of Piles vs Reduce Bending Moment.

thickness increase has a negligible effect on the differential displacement. A decrease in stresses with an increase in raft thickness could imply a reduction in the required reinforcing steel with an increase in the required concrete volume, implying that the required raft thickness should be determined based on the optimum volume of both materials.

6. CONCLUSION

The raft pile foundation needs to be applied to a 20-story building on the dense sandy soil to reduce the elastic settlement. The parametric study of the raft pile foundation using the 3D finite element method yields the best options designs. It is necessary to consider the number of piles or pile spacing since increasing the number of piles or decreasing the pile spacing does not always reduce the settlement; there is an optimum number to be reached. The requirement of the settlement is met by using pile spacing of 2.9 meters (9 x 28 group piles configuration) and group pile and raft width ratio of 1 by varying the diameter of the pile from 0.5 to 1 meter, even though using 3.3 meters pile spacing with 0.5, 0.6, and 0.7 also meets the requirement. By taking into account the differential displacement, using 0.7 diameter piles and 2.9 meters of pile spacing, the maximum differential displacement is reduced. Additionally, increase the raft thickness by reducing the differential displacement, while the optimum volume of reinforcement steel and concrete materials must be considered for optimization.

REFERENCES

Bhartiya. P. 2019. Settlement Estimation of Piled Rafts for Initial Design. *Journal of Geotechnical. Geoenvironment. Engineering* 146(2): 04019127.

Dafalla, M. et al. 2020. Efficient Pile Distribution for Piled-Raft Foundations for Tall Buildings. *Geo-Congress 2020*.

Fraser, R.A. and Wardle, L. J. 1976. Numerical Analysis of Rectangular Rafts on Layered Foundation. *Geotechnique* 26 No. 4: 613-630.

Meyerhof, G. G. 1963. Some Recent Research on the Bearing Capacity of Foundations. *Canadian Geotechnical Journal* Vol. 1, No. 1:16–26.

Poulos, H. G., and e. H. Davis. 1980. *Pile Foundation Analysis and Design.* New York: Wiley.

Prakoso, W. A., Kulhawy, F. H. 2001. Contribution To Piled Raft Foundation Design. *Journal of Geotechnical Geoenvironment Engineering* 127: 17-24.

Randolph, M. F. 1994. Design Methods for Pile Groups and Piled Rafts. *Proc., XIII ICSMFE:* 61-82. Rotterdam, Netherlands: A.A.Balkema.

Randolph, M. F., and Wroth. C. P. 1978. Analysis of Deformation of Vertically Loaded Piles. *Journal of Geotechnical Engineering Division ASCE*. Vol. 104. GT12: 1465-1488.

Russo, G., and C. Viggiani. 1998. Factors Controlling Soil-Structure Interaction for Piled Rafts. *Darmstadt Geotech*. 2 (4): 297-321.

Korelasi Hasil Uji Lapangan dengan Parameter Kuat Geser *Undrained* pada Tanah Lunak Kendal

Salma Aulia Andari
Departemen Teknik Sipil, Fakultas Teknik – Universitas Indonesia, Kampus Baru UI

Nastiti Tiasundari
PT Geoforce Indonesia

ABSTRAK: Tanah lunak merupakan tanah yang memiliki kompresibilitas tinggi, kuat geser serta permeabilitas yang rendah sehingga dapat menimbulkan masalah pada saat maupun pasca konstruksi seperti timbunan jalan dan bangunan. Persebaran tanah lunak di Indonesia cukup luas, di mana salah satu daerahnya adalah Kendal. Investigasi tanah berupa Cone Penetration Test (CPT) dan Standard Penetration Test (SPT) dilakukan di lapangan, di mana sampel yang diambil dari pengujian SPT diuji dengan triaksial *unconsolidated-undrained* dan triaksial *consolidated-undrained*. Korelasi antara pengujian lapangan dan kuat geser *undrained* dievaluasi. Hasil studi menunjukkan bahwa terlihat adanya korelasi sedang antara tahanan konus dengan kohesi, korelasi lemah antara *friction ratio* dengan sudut geser dalam, korelasi sedang antara nilai N-SPT dengan kohesi, dan korelasi lemah antara nilai N-SPT dengan sudut geser dalam.

Kata Kunci: tanah lunak, korelasi, investigasi tanah, kuat geser undrained

ABSTRACT: Soft soil is a soil which has high compressibility, low shear strength and permeability where this condition could lead into problems during and after construction such as highway embankment and building. This type of soil is distributed quite a lot all over Indonesia, where one of the places is in Kendal. Soil investigation, Cone Penetration Test (CPT) and Standard Penetration Test (SPT), was done on the site. The samples taken during SPT were tested by unconsolidated-undrained triaxial and consolidated-undrained triaxial compression tests. Correlation between field tests and undrained shear strength was evaluated. This study shows that there is a moderate correlation between tip resistance and cohesion, weak correlation between friction ratio and friction angle, moderate correlation between N-SPT and cohesion, also weak correlation between N-SPT with friction angle.

Keywords: soft soil, correlation, soil investigation, undrained shear strength

1 PENDAHULUAN

Indonesia memiliki tanah lunak sebanyak 10% dari luas total daratannya, di mana tanah lunak ini terdiri dari dua jenis, yaitu tanah lempung lunak dan tanah gambut. Persebaran tanah lempung lunak salah satunya berada di Kabupaten Kendal. Tanah lempung lunak memiliki kadar air tinggi, kuat geser rendah dan kompresibilitas tinggi. Pemampatan jenis tanah ini relatif lama dikarenakan jalur keluar air yang rapat, sehingga tanah lempung lunak dapat menyebabkan masalah ketidakstabilan dan penurunan jangka panjang.

Dalam desain, dibutuhkan estimasi dari kekuatan tanah. Pada kasus tanah kohesif, kondisi *undrained* merupakan kondisi yang kritis, sehingga kuat tanah *undrained* digunakan dalam menghitung *bearing capacity*, Remai (2013). Berbagai metode telah ada untuk mengestimasi parameter kuat geser, akan tetapi belum ada informasi yang cukup mengenai parameter kuat geser *undrained* dari tanah lempung lunak Kendal. Data dari 2 lokasi di Kabupaten Kendal dievaluasi korelasi uji lapangan dan parameter kuat geser *undrained* dalam *paper* ini.

2 TANAH LEMPUNG LUNAK

Tanah merupakan material yang terdiri dari agregat mineral padat yang tidak terikat secara kimia dengan satu sama lain dari bahan bahan organic yang telah melapuk, serta disertai dengan zat cair dan gas yang mengisi ruang kosong diantara partikel padat, Das & Sobhan (2012). Struktur tanah lunak sebagian besar terdiri dari butiran lanau dan lempung, di mana karakteristiknya adalah sebagai berikut:

- Kadar air tinggi
- Angka pori tinggi
- Kuat geser rendah
- Kompresibilitas tinggi

3 PENGUJIAN LAPANGAN

3.1 *Standard Penetration Test (SPT)*

Standard Penetration Test dilakukan dengan memasukkan *split spoon sampler* dengan jatuhan *hammer* secara berulang, di mana nilai jumlah pukulan (N-SPT) yang dibutuhkan untuk masuk sedalam 30 cm dihitung, Budhu (2011). Dengan adanya *split spoon sampler*, sampel tanah dapat diambil dan diangkat ke permukaan tanah, sehingga tidak terjadi pemadatan tanah dan sampel dalam keadaan undisturbed.

Berdasarkan pengujian SPT, dapat ditentukan stratifikasi tanah, lokasi tanah keras dan juga didapatkan sampel tanah yang dapat diuji di laboratorium. Dalam pelaksanaannya, dapat terjadi ketidakakuratan hasil pengujian akibat keadaan dan kebersihan alat, serta kekeliruan metode yang dilakukan saat pengujian. Terdapat korelasi nilai N-SPT yang dikoreksi terhadap *undrained shear strength* pada tanah lempung tersaturasi.

Tabel 1. Korelasi Nilai N_{60} dan Su pada Tanah Lempung Tersaturasi, Budhu (2011).

N_{60}	Deskripsi	s_u (kPa)
0-2	Sangat lunak	< 10
3-5	Lunak	10-25
6-9	Sedang	25-50
10-15	Kaku	50-100
15-30	Sangat kaku	100-200
>30	Sangat kaku sekali	>200

3.2 *Cone Penetration Test (CPT)*

Cone Penetration Test dilakukan dengan melakukan penetrasi konus yang tersambung batang ke dalam tanah. Hasil yang didapatkan dari pengujian ini berupa tahanan konus dan tahanan friksi. Tanahan konus dipengaruhi oleh tegangan tanah, kepadatan tanah, stratigrafi, mineral tanah, tipe tanah dan geometri butiran tanah Budhu (2011). Dalam pengujian CPT, tidak diperlukan *borehole*, namun sampel tanah *undisturbed* tidak dapat diambil dari metode ini.

Kekurangan dari metode ini ialah jika konus bertemu dengan benda keras, maka akan terdeteksi sebagai tanah keras. Hasil pengolahan data dari pengujian CPT dapat diinterpretasi melalui *Soil Behavior Type* berdasarkan tahanan konus (q_c) dan *friction ratio* (FR).

4 PENGUJIAN LABORATORIUM

4.1 *Triaxial Unconsolidated Undrained (UU)*

Pengujian *triaxial* merupakan salah satu metode dalam menentukan parameter kuat geser tanah. Tujuan dari triaxial UU adalah menentukan parameter kuat geser *undrained* dari tanah tersaturasi. Pengujian ini dilakukan dengan mengaplikasikan beban konstan dan dilakukan dalam waktu singkat, di mana *excess porewater pressure* tidak diperbolehkan untuk keluar.

4.2 *Triaxial Consolidated Undrained (CU)*

Pengujian *triaxial* CU dilakukan untuk mendapatkan parameter kuat geser *drained* dan *undrained*, di mana *excess porewater pressure* diukur. Sampel dikonsolidasi terlebih dahulu dan pengukuran *excess porewater pressure* dilakukan sehingga parameter kuat geser *drained* dapat diestimasi.

5 KONDISI TANAH DAN PENGUJIAN SAMPEL

Investigasi tanah dilakukan pada dua lokasi di Kendal, yaitu di Jl. Pelabuhan dan Kaliwungu. Di mana kedua lokasi studi merupakan bekas tambak. Pengujian lapangan yang dilakukan ialah SPT dan CPT, dengan pengujian laboratorium *triaxial UU* dan *triaxial* CU untuk

mengetahui parameter kuat geser undrained pada tanah lunak Kendal.

Lokasi studi memiliki elevasi tanah dasar -1,5 MSL. Tanah dasar memiliki karakteristik seperti pada umumnya di daerah pantai utara jawa, yaitu endapan alluvium, dengan warna keabu-abuan dengan konsistensi sangat lunak. Pada kedua lokasi, nilai N-SPT kurang dari 10 hingga kedalaman 20 m, dan setelahnya meningkat hingga nilai N-SPT 14. Muka air tanah pada lokasi ini berada pada permukaan tanah, di mana ketika dibebani, beban tersebut akan menimbulkan deformasi pada tanah. Berdasarkan nilai tahanan ujung dan *friction ratio* yang diplot pada *Soil Behavior Type Chart*, Robertson (2010), tanah lunak memiliki perilaku seperti tanah organik, lempung dan campuran lanau.

Pengujian Triaxial UU dan Triaxial CU dilakukan pada dua lokasi, di mana hasil pengujiannya dapat disimpulkan dalam tabel berikut:

Tabel 2. Hasil Pengujian Triaxial UU dan CU di Jl. Pelabuhan, Kendal, Geoforce (2020)

Jl. Pelabuhan				
Kedalaman	Triaxial UU		Triaxial CU	
(m)	φ (°)	c (kPa)	φ (°)	c (kPa)
3,5 – 4,0		-	4,74	7,20
5,5 – 6,0		-	5,69	7,56
7,5 – 8,0	9,28	3,93		-
9,5 – 10,0	7,41	3,51		-
11,5 – 12,0		-	7,43	13,91
13,5 – 14,0		-	13,00	7,36
15,5 – 16,0	10,04	3,95		-
17,5 – 18,0	7,89	8,94		-
19,5 – 20,0		-	10,62	10,50
21,5 – 22,0		-	11,23	22,28
23,5 – 24,0	11,37	21,67		-
25,5 – 26,0	12,79	21,91		-

Tabel 3. Hasil Pengujian Triaxial UU dan CU di Kaliwungu, Kendal, Geoforce (2018)

Kaliwungu				
Kedalaman	Triaxial UU		Triaxial CU	
(m)	φ (°)	c (kPa)	φ (°)	c (kPa)
2,0 – 2,5	2	6		
2,5 – 3,0	2	2,4		
4,0 – 4,5			4,1	7
4,5 – 5,0			5,9	2,48
6,0 – 6,5	1,8	5		
6,5 – 7,0	1	3		
8,0 – 8,5			3,9	7
8,5 – 9,0			6,2	16
10,0 – 10,5			-	
10,5 – 11,0			2	2,1
12,0 – 12,5	1,6	3		
12,5 – 13,0	2,8	5		
14,0 – 14,5			3,6	4
14,5 – 15,0			-	
16,0 – 16,5	2,1	7		
16,5 – 17,0	1,6	4		
18,0 – 18,5			2,8	9
20,5 – 21,0	3,6	15		
22,5 – 23,0	3,4	9		

6 KORELASI PARAMETER KUAT GESER UNDRAINED DENGAN HASIL PENGUJIAN LAPANGAN

Nilai N-SPT, tahanan konus (q_c) dan *friction ratio* (FR) dibandingkan terhadap parameter kuat geser pada kedalaman yang sama, di mana nilai tahanan konus dan *friction ratio* dirata-ratakan pada kedalaman yang dimaksud.

Korelasi dilakukan dengan menggabungkan data yang ada dalam satu analisis yang kemudian diregresi secara linear. Nilai R berada diantara +1 dan -1, di mana jika nilainya mendekati satu menggambarkan hubungan linier antara kedua data yang dimaksud Schober, Boer & Schwarte (2018). Skala berikut digunakan dalam *paper* ini.

Tabel 4. Skala Interpretasi Koefisien Korelasi, Schober, Boer & Schwarte (2018).

Besaran Absolut dari Koefisien Korelasi	Interpretasi
0.00-0.10	Tidak memiliki korelasi
0.10-0.39	Korelasi lemah
0.40-0.69	Kolerasi sedang
0.70-0.89	Kolerasi kuat
0.90-1.00	Kolerasi sangat kuat

6.1 *Korelasi Hasil Uji CPT dengan Parameter Kuat Geser Undrained*

Korelasi dilakukan untuk tahanan konus dan *friction ratio* terhadap sudut geser dalam dan kohesi. Tahanan konus memiliki korelasi sedang terhadap kohesi, dan *friction ratio* memiliki korelasi lemah terhadap sudut geser dalam. Hubungan positif terjadi antara tahanan konus dan kohesi, di mana terjadi hubungan negatif antara friction ratio dan sudut geser dalam. Hasil korelasi ditampilkan dan diringkas dalam gambar dan tabel berikut:

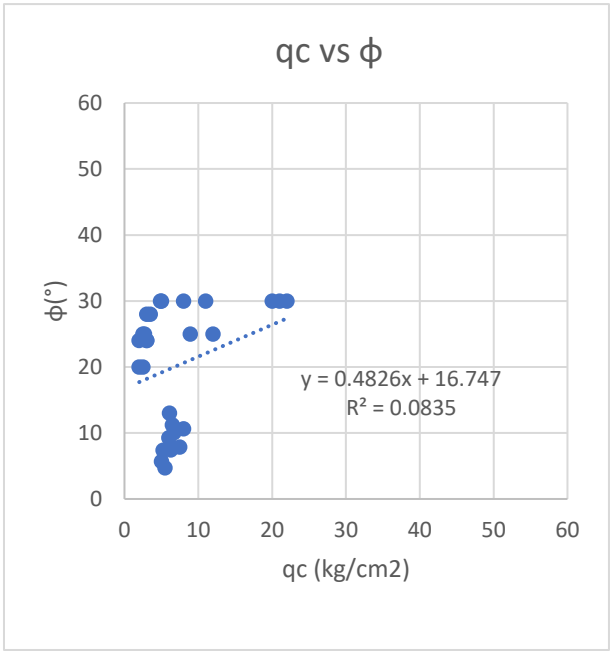

Gbr. 1. Korelasi q_c dengan Sudut Geser Dalam.

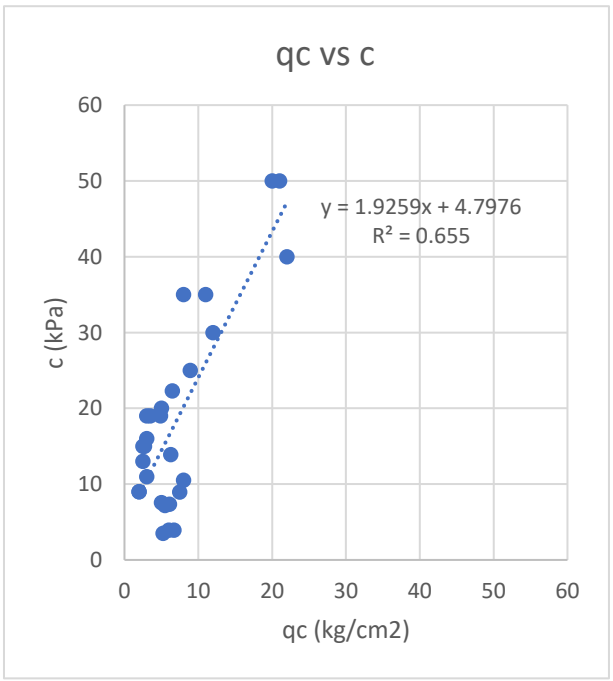

Gbr. 2. Korelasi q_c dengan Kohesi.

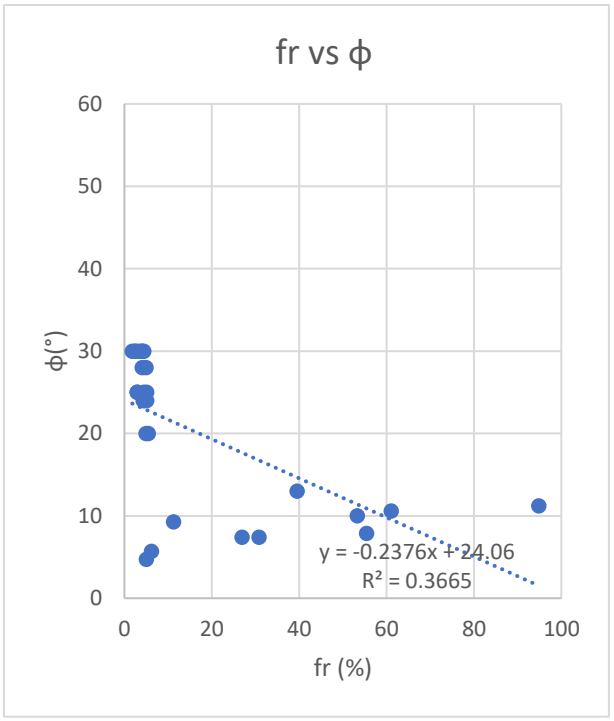

Gbr. 3. Korelasi *Friction Ratio* dengan Sudut Geser Dalam.

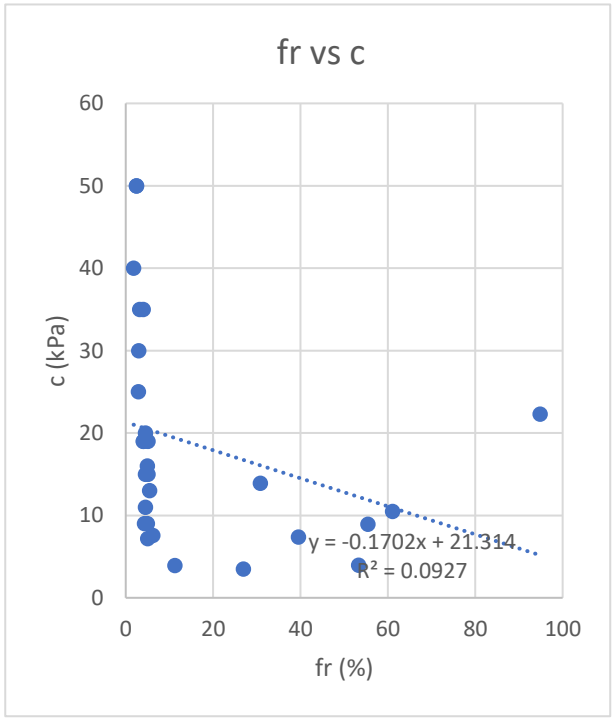

Gbr. 4. Korelasi Friction Ratio dengan Kohesi.

Tabel 5. Kesimpulan Korelasi Hasil Uji SPT dengan Parameter Kuat Geser Undrained.

Persamaan Korelasi	Koefisien Korelasi	Interpretasi Korelasi
$\varphi = 0{,}4826\ q_c + 16{,}747$	0,0835	Tidak memiliki korelasi
$c = 1{,}9259\ q_c + 4{,}7976$	0,655	Korelasi Sedang
$\varphi = -0{,}2376\ FR + 24{,}08$	0,3665	Korelasi Lemah
$c = -\ 0{,}1702\ FR + 21{,}314$	0,0927	Tidak memiliki korelasi

6.2 *Korelasi Hasil Uji SPT dengan Parameter Kuat Geser Undrained*

Korelasi dilakukan untuk nilai N-SPT terhadap sudut geser dalam dan kohesi. Nilai N-SPT memiliki korelasi lemah terhadap sudut geser dalam dan korelasi sedang terhadap kohesi. Hasil korelasi ditampilkan dan diringkas dalam gambar dan tabel berikut:

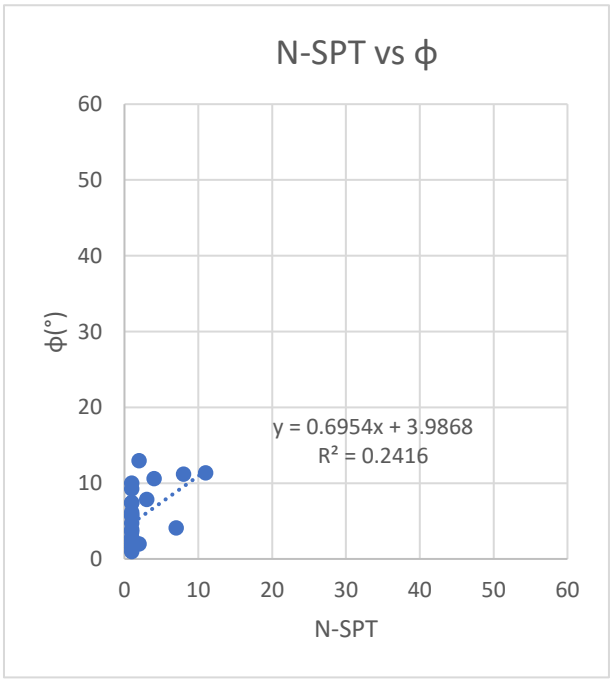

Gbr. 5. Korelasi N-SPT dengan Sudut Geser Dalam

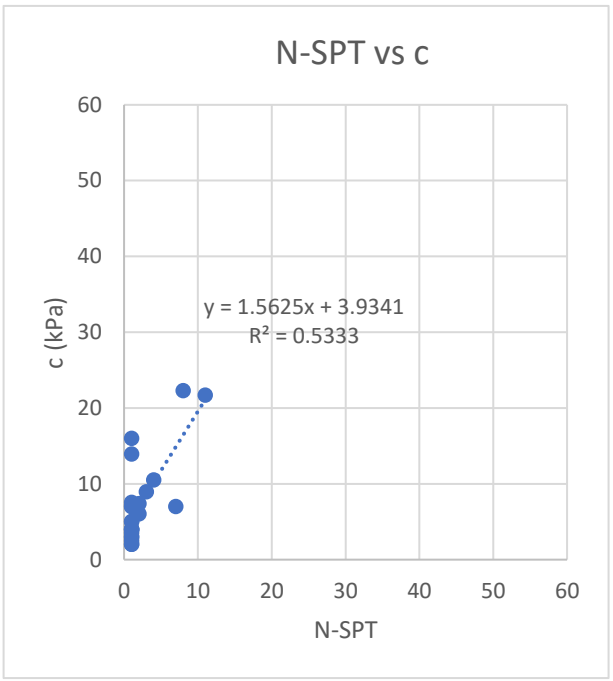

Gbr. 6. Korelasi N-SPT dengan Kohesi

Tabel 6. Kesimpulan Korelasi Hasil Uji SPT dengan Parameter Kuat Geser Undrained.

Persamaan Korelasi	Koefisien Korelasi	Interpretasi Korelasi
$\varphi = 0.6954$ N-SPT +3.9868	0.2416	Korelasi lemah
$c = 1.5626$ N-SPT + 3.9341	0.5333	Korelasi Sedang

7 KESIMPULAN

Korelasi hasil uji lapangan dan parameter kuat geser *undrained* tanah lunak Kendal dianalisis dari dua tempat. Korelasi dari milai N-SPT, tahanan konus (q_c) dan *friction ratio* (FR) dibandingkan terhadap parameter kuat geser pada kedalaman yang sama dilakukan. Terdapat korelasi antara hasil uji lapangan dengan parameter kuat geser *undrained* pada tanah lunak Kendal, di mana terdapat korelasi sedang antara tahanan konus dengan kohesi, korelasi lemah antara *friction ratio* dengan sudut geser dalam, korelasi sedang antara nilai N-SPT dengan kohesi, dan korelasi lemah antara nilai N-SPT dengan sudut geser dalam.

DAFTAR PUSTAKA

Budhu, M. 2011. *Soil Mechanics and Foundations, Third Edition.* USA: John Wiley & Sons, Inc.

Das, B. M., & Sobhan, K. 2012. *Principles of Geotechnical Engineering, Eighth Edition, SI.* Stamford, USA: CENGAGE Learning.

Remai, Z. 2013. Correlation of undrained shear strength and CPT Resistance. *Periodica Polytechnica*: 39-44.

Robertson, P. K. 2010. *Guide to Cone Penetration Testing for Geo-Environmental Engineering: 2nd Edition.* California: Gregg Drilling & Testing Inc.

Schober, P., Boer, C., & Schwarte, L. A. 2018. Correlation Coefficients: Appropriate Use and Interpretation. *Anesthesia & Analgesia*: 1763-1768.

The Use of Jack Bean Meal as A Biocatalyst in Enzyme Mediated Calcite Precipitation for Soil Improvement Technique

Alfaris Baqir Arrazzaq
IPB University

Zayyaan Nabiila Khairunnisa
IPB University

Heriansyah Putra
IPB University

ABSTRAK: *Enzyme mediated calcite precipitation* (EMCP) merupakan salah satu metode baru yang sedang dikembangkan untuk perbaikan tanah. Enzim urease digunakan sebagai biokatalis dimana enzim urease membentuk kalsit dari hidrolisis urea kemudian berikatan dengan ion kalsium (Ca). Pada penelitian ini, dilakukan evaluasi terhadap penggunaan *Jack Bean Meal* sebagai biokatalis dalam larutan EMCP dan pengaruhnya terhadap perbaikan tanah pasir dengan dilakukannya pengujian kecepatan hidrolisis, uji pengendapan, dan kuat tekan (UCS). Pengujian kecepatan hidrolisis dilakukan untuk mengetahui pengaruh perlakuan sampel terhadap laju hidrolisis urea dalam pembentukan kalsit. Pengujian UCS dilakukan untuk mengevaluasi efektivitas perkuatan tanah pasir. Hasil pengujian UCS menunjukkan bahwa tanah pasir yang telah diinjeksi satu kali memiliki nilai UCS 210 kPa. Berdasarkan hasil pengamatan kuat tekan dan juga laju hidrolisis kalsit yang terbentuk, *Jack Bean Meal* berpotensi sebagai bahan biokatalis pada metode EMCP.

Kata Kunci: EMCP, enzyme, kalsit, pasir, perbaikan tanah

ABSTRACT: Enzyme mediated calcite precipitation (EMCP) is one of the new methods being developed for soil improvement. The urease enzyme is used as a biocatalyst where the urease enzyme forms calcite from the hydrolysis of urea and then binds to calcium ions (Ca). In this study, an evaluation was carried out on the use of Jack Bean Meal as a biocatalyst in EMCP solution and its effect on the improvement of sandy soil by testing the speed of hydrolysis, precipitation test, and compressive strength (UCS). The hydrolysis speed test was conducted to determine the effect of sample treatment on the rate of urea hydrolysis in the formation of calcite. UCS testing was carried out to evaluate the effectiveness of sandy soil reinforcement. The results of the UCS test showed that the sand soil that had been injected once had a UCS value of 210 kPa. Based on observations of compressive strength and the rate of hydrolysis of calcite formed, Jack Bean Meal has the potential as a biocatalyst material in the EMCP method.

Keywords: EMCP, enzyme, calcite, sand, soil improvement

1 INTRODUCTION

Every single soil has a different bearing capacity. Poor bearing capacity can occur subsidence on building foundations. Area around the coast has low to medium soil density, which makes the soil bearing capacity low, Fahrian and Apriyani (2015). Soil bearing capacity functions as a resistance force against the pressure that is given by the weight on it, if the weight is bigger, the soil will encounter subsidence. Soil bearing capacity affected by soil properties such as soil texture, weight, dan structures, Suparding et al. (2018). A lot of methods for soil improvement have been applied.

Grouting is one of the common methods for soil improvement. This method is usually used in mining, tunnel, landfill, and basement. Cement is the material that is used for grouting, so it requires some parameters such as water-cement ratio, grouting pressure, and processing time, Ren et al. (2021). Not only limited by cement, Anagtopolous et al. (2020) added a superplasticizer based on polycarboxylate ether and polynaphthalene so it can increase grouting

injectability. However, cement utilization is not environmentally friendly. Naemi and Haddad (2018) compared environmental impact results between grouting and other method that used microbes or known as Microbially Induced Calcite Precipitation (MICP).

MICP is an improvement method through calcite precipitation in the form of calcium carbonate ($CaCO_3$). The carbonate is obtained from urea's breakdown by urease enzyme. Bacteria is the agent that creates the urease enzyme, that is the reason why this method is named as MICP. Soil improvement using MICP is proven more environmentally friendly than the conventional methods. However, because bacteria are an organism and sensitive to its environmental conditions, bacteria performance is uncontrollable and needs special treatment such as bacteria cultivation, Mujah et al. (2016). Furthermore, bacteria life in the soil is difficult to know, so there is a need for other alternatives.

The other method is *Enzyme Mediated Calcite Precipitation* (EMCP) which utilizes calcite precipitation from biological materials, namely biocatalysts as a soil strengthening material. The use of biocatalysts in the formation of calcite can be directly produced from plant enzymes, there are several plants that have the potential to extract urease enzymes such as soybeans, Zulfikar et al. (2021), Pratama et al. (2021) and watermelon seeds, Al Imran et al. (2020). Based on Baiq et al. (2020) the best urease enzyme comes from jack beans with maximum catalyst activity at pH 6-7 with a temperature of 65°C. The results of calcite deposits produced by MICP and EMCP are the same, only different from the urea breaker material. This method has a better potential in soil improvement because it is more environmentally friendly and more cost-effective than other conventional methods, Putra et al. (2020), Growthaman et al. (2021).

The mineralization results from the enzymes produced by EMCP are higher than using microbes because in the MICP process, the nutrients transported into the microbes are limited by the outer layers of bacteria and will also be limited if there is damage to the cell membrane, Krajewska (2018). Even so, in terms of efficiency, MICP is still superior to EMCP because the carbonate crystals produced are better in terms of size, morphology, and structure so that further innovation or alternatives to EMCP are needed, Yuan et al. (2020).

Based on the need for innovation in EMCP, this study evaluates the use of Jack Bean Meal as a biocatalyst in EMCP solution and its effect on sand soil improvement by testing the hydrolysis rate, precipitation test, and compressive strength/UCS (Unconfined Compressive Strength).

2 MATERIALS AND METHODS

2.1 *Materials*

The materials used in this research are sand and EMCP solution. The EMCP solution consisted of reagents and jack bean meal as a biocatalyst. Urea ($CO(NH_2)_2$) and calcium chloride ($CaCl_2$) were used as reagents with a concentration of 1 mol/L. Hydrochloric acid (HCl) as an acid leaching material

2.2 *Hydrolysis Rate*

This test was used to determine the speed of Jack Bean Meal as a biocatalyst to hydrolyze urea. The procedure for testing the hydrolysis speed followed the method reported by Putra et al. (2021). The procedure for testing the hydrolysis speed followed the method reported by Putra et al. (2021). The calculation of conductivity with time was determined using the Hanna Edge Multiparameter 230. The concentration of Jack Bean Meal used was 1 g/L, 5 g/L, 10 g/L, 15 g/L, and 20 g/L. The hydrolysis rate is measured by calculating the change in the conductivity gradient with time according to the following equation:

$$\text{Hydrolysis rate (u/g)} = \frac{\theta_{ms}}{\theta_{ms}} \,.\, v.N \qquad (1)$$

θ_{ms} is the sample gradient, θ_{sc} is the standard curve gradient, v is the sample volume (L), and N is the final ammonia concentration (mmol/L).

2.3 *Precipitation Test*

The amount of calcite formed was evaluated using the precipitation test. Tests were carried out to determine the optimum content of the Jack Bean Meal composition used with the reagent composition (urea and $CaCl_2$) of 1 mol/L. The precipitation test was carried out on a transparent polypropylene (PP) tube with varying concentrations of Jack Bean Meal, namely 1 g/L, 5 g/L, 10 g/L, 15g/L, and 20 g/L.

2.4 *Unconfined Compressive Strength (UCS) Test*

The soil bearing capacity test was carried out on soil samples injected with EMCP solution. The sample was printed with a cylindrical mold with a diameter of 5 cm and a height of 10 cm. The sample curing time varied, namely 3, 7, and 14 days. The reagent (urea and NaOH) used is 1 mol/L. Jack Bean Meal biocatalyst was used with a maximum concentration of 5 g/L and 10g/L as precipitation test results. The composition of the solution is shown in Table 1.

Table 1. Proportion of EMCP Solution.

Jack Bean Meal /Urease Concentration (g/L)	Urea (mol/L)	$CaCl_2$ (mol/L)
5	1	1
10	1	1

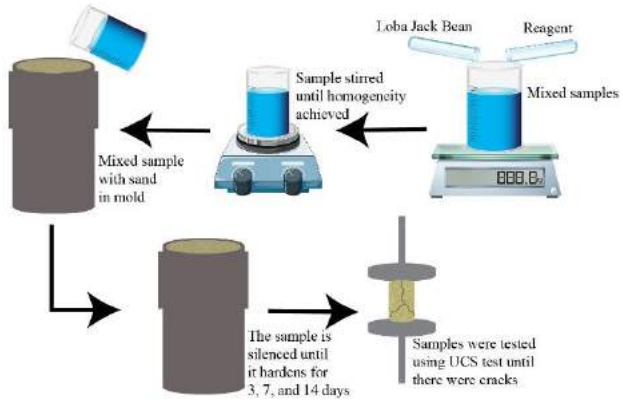

Fig. 1. UCS Test.

2.5 *Acid Leaching`*

Acid leaching test was carried out to determine the amount of calcite formed. The test uses UCS compressive strength sample data of 50 g. The test sample was removed by removing calcite by immersing it in HCl solution, stirring until no bubbles remained. The sample was rinsed using distilled water and then the sample was baked in an oven to dry and reweighed. The difference between the initial weight and the final weight is the weight of calcite formed.

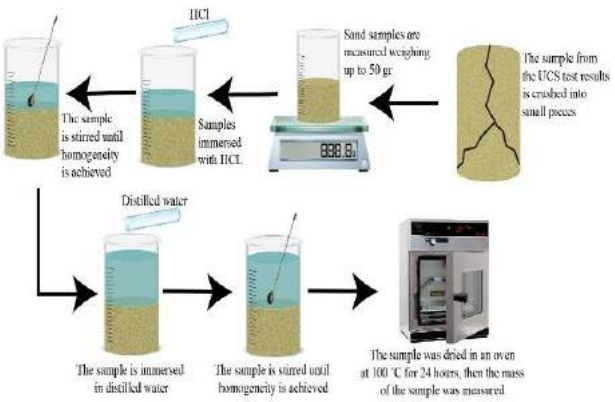

Fig. 2. Acid Leaching Process.

3 RESULTS AND DISCUSSION

3.1 *Hydrolysis Rate*

Hydrolysis test was conducted to evaluate the effect of Jack Bean Meal in hydrolyzing urea. The better the hydrolyzed urea, the better the effect of EMCP. Evaluation is done by linking time with conductance and Jack Bean Meal concentration with the level of hydrolysis. In this test, two treatments were carried out, namely filtered coded "UF" and centrifuged coded "UC". Changes in the conductance value due to differences in the treatment of the solution can be seen in Fig. 3 and 4.

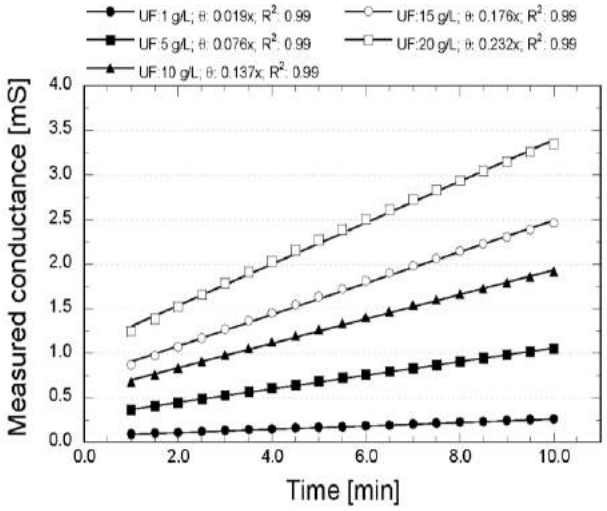

Fig. 3. Changes in Conductance with Time and Variations in Concentration Jack Bean Meal (Filtered).

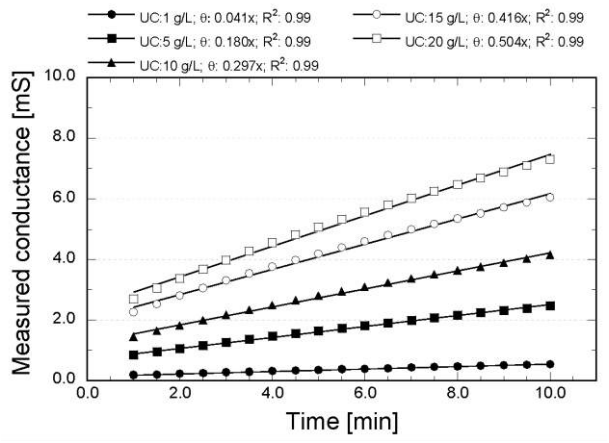

Fig. 4. Changes in Conductance with Time and Variations in Concentration Jack Bean Meal (Centrifuged).

The results of the hydrolysis level test can be seen in Fig. 5. The test results show that the centrifuged treatment can hydrolyze urea better than the filtered treatment. Jack Bean Meal with centrifuged yields a hydrolysis value of 100 - 1200 u/g. Meanwhile, filtered Jack Bean Meal produces a hydrolysis value of 50 - 500 u/g. The value of urea hydrolysis will affect the effectiveness of the EMCP solution. The more urea is hydrolyzed, the more carbonate is formed so that more calcite is formed. The greater the concentration of Jack Bean Meal, the higher the level of hydrolysis. This happens because more and more urease are produced to break down urea so that hydrolysis is faster, Sigurdarson et al. *(*2018).

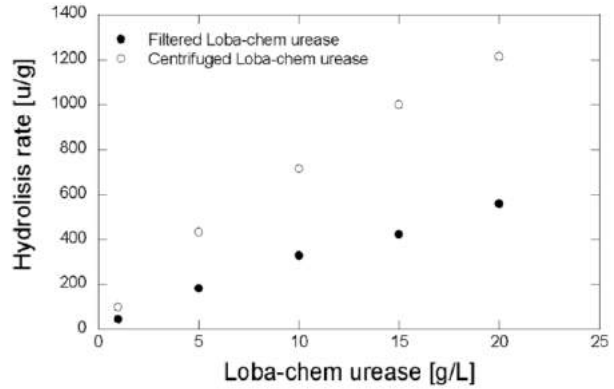

Fig. 5. Hydrolysis Rate Test Results.

Based on the results of conductance measurements and hydrolysis rate, the best solution for urea hydrolysis is the one that has a high hydrolysis rate with a fast time. This can be seen by the slope of the line on the graph. The more vertical the line, the better the hydrolysis rate. The test results on UF and UC samples showed that the greater the concentration of Jack Bean Meal, the more upright the conductance line. If the two treatments were compared, the UC sample was better at hydrolyzing urea. One of the factors that influence this value is the ability of centrifuged to separate the urease enzyme better than just filtering, as according to Gimbert et al. (2005), centrifugation is more efficient to produce a fraction with a section size closer to the required value than filtration.

3.2 *Calcite Precipitation*

Calcite precipitation test was carried out for calcite produced. Variations carried out in this test include using Jack Bean Meal concentrations of 1 g/L, 5 g/L, 10 g/L, 15 g/L, and 20 g/L with two treatments using filter paper and centrifuge. The test results can be seen in Fig. 6. Based on the test results, the centrifugation treatment had better precipitation results than the filter at Jack Bean Meal urease concentration of 10 g/L. The centrifugation treatment resulted in 95% precipitation while the filter treatment resulted in 90% precipitation. However, at concentrations of 15 g/L and 20 g/L, the precipitation results were the same, which was around 95%. This indicates that the centrifugation treatment did not experience a significant change above 10 g/L so that the optimal condition was obtained at a concentration of 10 g/L.

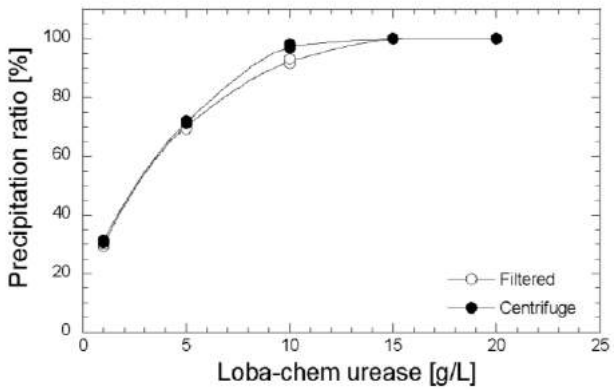

Fig. 6. Calcite Precipitation Test Results with Variations in Concentration of Jack Bean Meal.

3.3 *Soil Strength*

The compressive strength of the soil was tested through the Unconfined Compression Strength (UCS) test. Variations carried out in this test include using Jack Bean Meal concentrations of 5 g/L and 10 g/L with measurements of 3, 7, and 14 days.

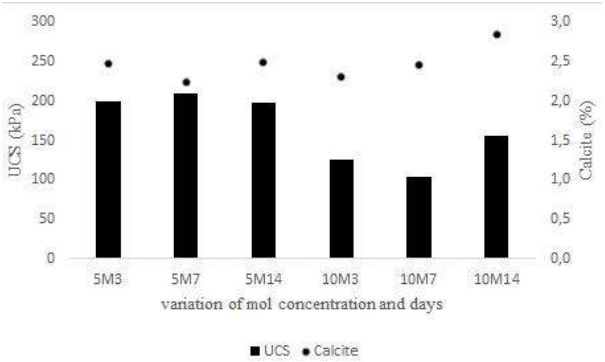

Fig. 7. UCS Test Results with Variations in Jack Bean Meal Concentration and Percentage of Calcite Formed.

The results of the UCS test can be seen in Fig. 7. From the Figure, the compressive strength of the soil treated with EMCP solution watering ranged from 100-210 kPa. The highest compressive strength was obtained at a concentration of 5 g/L of 210 kPa. Meanwhile, at a concentration of 10 g/L, the maximum compressive strength was 156 kPa. In fact, the compressive strength value will be directly proportional to the amount of calcite produced. However, in the test, the UCS value of a concentration of 10 g/L was smaller than that of a concentration of 5 g/L. This is because there is a possibility that the filtration process is not good and the distribution of the solution to the sample is not evenly distributed so that the resulting calcite is not spread well and does not reach the bottom soil. Gowthaman et al. (2021) explained that the deeper or longer the soil to be tested, the smaller the compressive strength value. In addition, more calcite is produced along with increasing levels of reagents and urease enzymes (Putra et al., 2021).

Choi et al. (2016) carried out soil improvement through the MICP method using eggshells and vinegar and Pratama et al. (2021) through the EMCP method with soybeans. In the MICP conducted by Choi et al. (2016) obtained the optimum value of 400 kPa, while the EMCP conducted by Pratama et al. (2021) the compressive strength value is 64.71- 623.18 kPa. When compared with soil improvement using the previous MICP and EMCP methods, the test results are smaller. This can occur because the distribution of calcite is not evenly distributed throughout the soil. This can be overcome by injecting several times the EMCP solution as in Pratama et al. (2021).

4 CONCLUSIONS

Jack Bean Meal has the potential to be used as a biocatalyst in EMCP. The results of the hydrolysis rate test show that the hydrolysis value is 100 - 1200 u/g in the centrifuge treatment and 50 - 500 u/g in the filter treatment where the higher the hydrolysis value, the more calcite that can be formed. Calcite precipitation test obtained optimum results at a concentration of 10 g/L with centrifuge treatment. The highest compressive strength or UCS value was owned by the sample with a Jack Bean Meal concentration of 5 g/L, which was 210 kPa. The compressive strength of the sample with a concentration of 10 g/L has a smaller value than the concentration of 5 g/L, this is most likely due to the poor filtration process and the uneven distribution of the solution in the sample.

ACKNOWLEDGEMENTS

We thank you profusely for the funding assistance from the Ministry of Research, Technology and Higher Education with application number 1/E1/KP.PTNBH/2021.

REFERENCES

Ahmad, I. 2007. Analisa Metode Perbaikan Tanah Lunak dan Kohesif. *Menara J Tek Sipil* 2(2): 45-52.

Baiq, HS., Yasuhara, H., Kinoshita, N., Putra, H., & Johan, E. 2020. Examination of calcite precipitation using plant-derived urease enzyme for soil improvement. *Int J GEOMATE* 19(72): 231–237.

Choi, SG., Wu, S. & Chu, J. 2016. Biocementation for Sand Using an Eggshell as Calcium Source. *Journal of Geotechnical and Geoenvironmental Engineering* 142(10): 1-4.

Fahriani, F. & Apriyanti, Y. 2015. Analisis Daya Dukung Tanah Dan Penurunan Pondasi Pada Daerah Pesisir Pantai Utara Kabupaten Bangka. *Journal Fropil* 3(2): 89–95.

Gimbert, LJ., Maygarth, PM., Beckett, R., & Worsfold, PJ. 2005. Comparison of Centrifugation and Filtration Techniques for the Size Fractionation of Colloidal Material in Soil Suspensions Using Sedimentation Field-Flow Fractionation. *Environ. Sci. Technol* 39(6): 1731-1735.

Growthaman, S., Yamamoto, M., Nakashima, K., Ivanov, V., & Kawasaki, S. 2021. Calcium phosphate biocement using bone meal and acid urease: An eco-friendly approach for soil improvement. *Journal of Cleaner Production* 319: 1-13.

Imran, A., Nakashima, K., Evelpidou, N. & Kawasaki, S. 2021. Improvement of Using Crude Extract Urease from Watermelon Seeds for Biocementation Technology. *Int J GEOMATE* 20(78):142–147.

Krajewska B. 2018. Urease-aided calcium carbonate mineralization for engineering applications: A review. *J Adv Res* 13: 59–67.

Mujah, D., Shahin, M.A., & Cheng, L. 2016. State-of-the-art review of biocementation by microbially induced calcite precipitation (MICP) for soil stabilization. *Geomicrobiology Journal* 34(6): 524-537.

Naeimi, M. & Haddad, A. 2018. Investigation on the Environmental Impact of Soil Improvement Techniques: Comparison of Cement Grouting and Biocement. *Proceedings of GeoShanghai 2018 International Conference: Geoenvironment and Geohazard* 2: 483-490.

Pratama, G.B.S., Yasuhara H., Kinoshita, N. & Putra H. 2021. Application of soybean powder as urease enzyme replacement on EICP method for soil improvement technique. *IOP Conf Ser Earth Environ Sc*i 622: 1-7.

Putra, H., Erizal, Sutoyo, Simatupang, M., & Yanto, DHY. 2021. Improvement of Organic Soil Shear Strength through Calcite Precipitation Method Using Soybeans as Bio-Catalyst. *Crystals* 11(9): 1-14.

Putra, H., Erizal, Sutoyo, Simatupang, M., & Yanto, D.H.Y. 2021. Improvement of Organic Soil Shear Strength through Calcite Precipitation Method Using Soybeans as Bio-Catalyst. *Crystals* 11: 1-14.

Putra, H., Yasuhara, H., Erizal, Sutoyo, Fauzan, M. 2020. Review of Enzyme-Induced Calcite Precipitation as a Ground-Improvement Technique. *Infrastructure* 5(6): 1-14.

Ren B., Wang L., Fan H., Ding K., Wang K., & Jiang C. 2021. Unsteady approximate model of grouting in fractures channel based on bingham fluid. *Geofluid* 2021: 1 -13.

Sigurdarson, JJ., Svane, S., & Karring, H. 2018. The Molecular Processes of Urea Hydrolysis in Relation to Ammonia Emission from Agriculture. *Rev Environ Sci Biotechnol* 17: 241-258.

Suparding, Suhardi, & Suhartono. 2018. Daya Dukung Tanah Pada Lahan Sawah Siap Tanam. *Journal AgriTechno* 11(1): 67-80.

Yuan, H., Ren, G, Liu, K., Zheng, W., & Zhao, Z. 2020. Experimental Study of EICP Combined with Organic Materials for Silt Improvement in the Yellow River Flood Area. *Applied Science* 10(21): 1-19.

Analisis Ledakan pada Struktur Basement dengan Dinding Diafragma

Kenny Erick
Universitas Tarumanagara

Alfred Jonathan Susilo
Universitas Tarumanagara

Aniek Prihatiningsih
Universitas Tarumanagara

Gregorius Sandjaja Sentosa
Universitas Tarumanagara

ABSTRAK: Sebagai salah satu beban dinamik yang dapat terjadi pada struktur *basement*, beban ledakan memiliki periode beban yang sangat singkat. Akibatnya, beban ledakan memberikan respons strukur *basement* yang berbeda jika dibandingkan dengan beban dinamik lainnya seperti beban gempa. Salah satu bentuk respons dari *basement* akibat beban ledakan adalah peningkatan deformasi dari dinding penahan tanah. Pada penelitian ini akan dianalisis apakah deformasi yang terjadi pada dinding penahan tanah akibat beban ledakan tetap memenuhi deformasi izin. Penelitian ini akan dilakukan dengan bantuan program Midas GTS NX dalam memodelkan struktur *basement* bangunan dan tanah disekitarnya dengan metode elemen hingga. Struktur *basement* yang dianalisa terdiri dari pelat tipe *flat slab*, dinding diafragma, *king post*, *raft*, dan fondasi tiang. Beban ledakan dianalisa dengan metode riwayat waktu dan merupakan beban ledakan permukaan yang terjadi di luar *basement*.

Kata Kunci: basement, dinding diafragma, beban ledakan, beban dinamik, riwayat waktu

ABSTRACT: As one of the dynamic loads that can occur in basement structures, blast loads have very short load period. As the result, the explosion load gives different response to the basement structure when compared to other dynamic loads such as earthquakes load. One form of response from the basement due to blast load is the increased deformation of the retaining wall. In this study, it will be analyzed whether the deformation that occurs in the retaining wall due to blast load still satisfies the allowable deformation. This research will be using Midas GTS NX program in modelling the basement structure of the building and the surrounding soil with the finite element method. Analyzed basement structure consists of flat slab, diaphragm wall, king post, raft, and pile foundation. The blast load analyzed is the surface blast load that occurs outside the basement by time history method.

Keywords: basement, diaphragm wall, blast loading, dynamic loading, time history

1 PENDAHULUAN

Ledakan terhadap struktur bangunan dapat terjadi akibat beberapa kejadian, misalnya serangan bom teroris, ledakan pom bensin, ledakan akibat kegiatan pertambangan, dan lain sebagainya. Salah satu kejadian ledakan terbaru di Indonesia adalah ledakan tangki minyak PT Pertamina (Persero) RU VI Balongan Indramayu yang terjadi pada 29 Maret 2021. Ledakan merupakan proses peningkatan tekanan dan pelepasan energi secara tiba-tiba yang bersifat destruktif akibat reaksi kimia dan umumnya mengeluarkan gas dan suhu panas.

Ledakan dapat sangat bersifat merusak jika ledakannya berada dekat dengan sebuah bangunan, karena tekanan yang dihasilkan sangat besar. Pada ledakan di permukaan tanah, sebagian energi dilepaskan sebagai energi panas, sedangkan sebagian lainnya dilepaskan ke udara sebagai ledakan udara dan ke dalam tanah sebagai gelombang kejut. Penggambaran ukuran besar kecilnya ledakan dapat menggunakan satuan setara TNT (Trinitrotoluene). Beban ledakan adalah beban

dinamis yang memiliki periode pendek. Dengan demikian, respons struktur akibat beban ledakan bisa berbeda dengan respons struktur terhadap beban dinamik lain seperti gempa.

Meskipun terletak di bawah tanah, *basement* tidak terlepas dari kemungkinan rusak akibat adanya beban dinamis seperti ledakan. Oleh karena itu perlu dianalisis respons struktur *basement* tersebut akibat beban yang terjadi. Struktur *basement* yang dianalisis terdiri dari dinding penahan tanah, pelat, *king post*, *raft*, dan fondasi. Dinding penahan tanah berfungsi untuk menahan beban lateral dari galian *basement*, sedangkan *king post* berfungsi sebagai kolom sementara untuk menahan beban dari struktur atas dan pelat dapat berfungsi sebagai *strut*. Penelitian ini akan berfokus pada analisa deformasi dinding diafragma tanpa dan dengan beban ledakan permukaan yang terjadi di luar *basement*, sehingga dapat diketahui apakah deformasi dinding diafragma tetap memenuhi deformasi izin jika dikenai ledakan. Selain itu, penelitian ini juga melihat respons struktur *basement* akibat beban ledakan yang terjadi.

2 TINJAUAN PUSTAKA

2.1 *Basement*

Basement merupakan bagian dari komponen struktur bangunan yang terletak di bawah tanah. *Basement* adalah bagian dari sarana sebuah gedung bertingkat tinggi. Adanya *basement* tentunya akan ada penggalian tanah. Bagian ini yang biasa terjadi dan merupakan langkah awal berdirinya sebuah gedung tinggi, Mistra (2012).

Menurut Mistra (2012), lantai *basement* biasanya dimanfaatkan untuk:

1. *Balancing* gedung di atasnya,
2. Ruang parkir kendaraan,
3. Ruang pengelola,
4. Pendukung utilitas gedung seperti penempatan ruang panel, reservoir, dan kebutuhan lain.

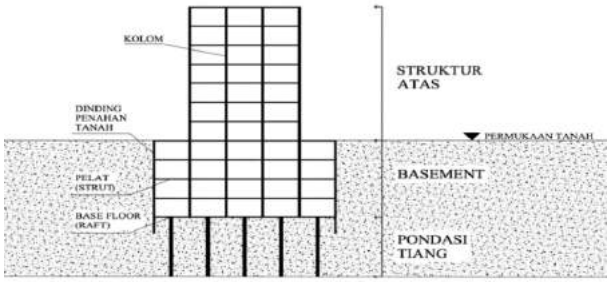

Gbr. 1. Gambaran Struktur Bangunan dengan *Basement.*

2.2 *Gelombang Ledakan*

Karakteristik dari detonasi sebuah ledakan diawali dengan peningkatan tekanan atmosfer secara instan ke tekanan puncaknya yang biasa disebut dengan *peak incident pressure*. Setelah gelombang kejut tersebut menyebar, tekanannya berkurang hingga mencapai tekanan awal di sekelilingnya. Secara teoritis, tekanan tersebut menurun secara eksponensial. Fase dari tekanan tersebut naik hingga turun ke tekanan atmosfer disebut dengan fase positif. Setelah tekanan mencapai tekanan ambien, tekanan tersebut berubah menjadi tekanan hisap yang dinamakan fase negatif seperti yang ditunjukkan pada Gbr. 2. Selama fase negatif akan terjadi gaya hisap seperti vakum. Hal ini juga disertai dengan angin hisap yang kuat dan membawa puing-puing (*debris*) jauh dari sumber ledakan. Fase negatif memiliki durasi yang lebih lama dibandingkan dengan fase positif, Figuli; Kavický; Boc; Vidriková & Jangl (2008).

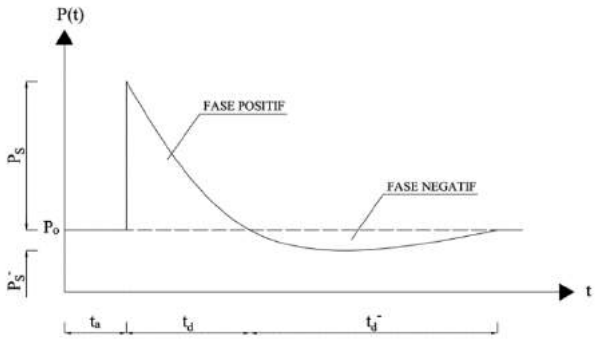

Gbr. 2. Fase Ledakan.

Persamaan tekanan yang dihasilkan akibat ledakan tersebut dapat diformulasikan dengan:

$$P(t) = P_o - P_S^- \left(\frac{t}{t_d^-}\right)\left(1 - \frac{t}{t_d^-}\right) e^{-4\frac{t}{t_d^-}} \qquad (1)$$

Untuk memudahkan perhitungan, fase negatif biasanya diabaikan dalam desain struktur dan tekanan dapat diasumsikan menurun secara linier seperti pada Gbr. 3.

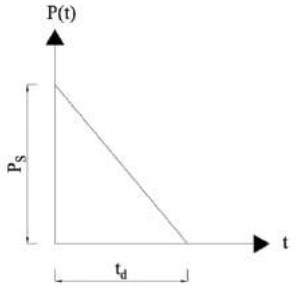

Gbr. 3. Simplifikasi Perhitungan Beban Ledakan.

Persamaan beban ledakan yang lebih sederhana dapat dinyatakan sebagai berikut:

$$P(t) = P_0 + P_s\left(1 - \frac{t}{t_d}\right) \quad (2)$$

Keterangan:
P_o = Tekanan ambien (MPa)
P_s = Tekanan puncak (MPa)
t = Waktu setelah gelombang datang (s)
t_d = Durasi tekanan pada fase positif (s)
t_d^- = Durasi tekanan pada fase negatif (s)
β = Koefisien parameter penurunan/*decay*

2.3 *Tipe Ledakan*

Ledakan eksternal dapat dibedakan menjadi 3 tipe dasar berdasarkan posisi relatif sumber ledakan terhadap struktur bangunan, Karlos & Solomos (2013) yaitu:

1. *Free-air bursts*

Ledakan terjadi di udara, gelombang ledakan merambat secara *spherical* dan langsung mengenai struktur tanpa berinteraksi dengan hambatan seperti tanah.

2. *Air bursts*

Ledakan terjadi di udara, gelombang ledakan merambat secara *spherical* dan mengenai struktur setelah mengalami interaksi dengan hambatan misalnya dengan tanah.

3. *Surface bursts*

Ledakan terjadi di permukaan tanah, gelombang ledakan langsung berinteraksi dengan tanah dan selanjutnya menyebar secara hemispherical dan mengenai struktur.

2.4 *Jarak Ledakan*

Jarak ledakan merupakan parameter yang sangat penting dalam menentukan besarnya gelombang ledakan yang timbul akibat suatu ledakan. Jarak tersebut dinamakan jarak antara atau *stand-off distance*. Energi yang dihasilkan dari ledakan akan berkurang apabila jarak sumber ledakan ke struktur bangunan semakin jauh. Dengan demikian, jarak ledakan yang semakin jauh membuat struktur menerima tekanan yang lebih kecil.

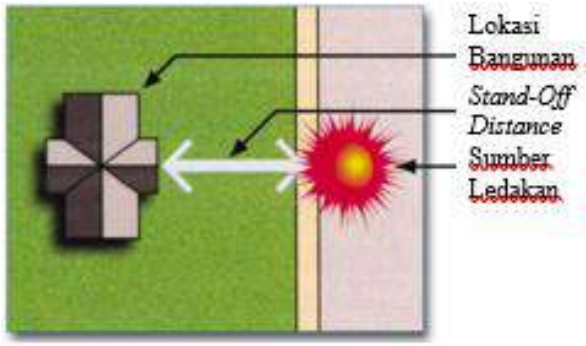

Gbr. 4. Jarak Ledakan/*Stand-Off Distance* (FEMA 420).

3 METODOLOGI PENELITIAN

3.1 *Data Tanah*

Data tanah pada penelitian ini diperoleh dari data pengujian laboratorium dan data dari pengujian SPT (*Standard Penetration Test*). Dari data tersebut, nilai parameter tanah yang akan digunakan diperoleh dari hasil rata-rata nilai parameter tanah pada tiap kedalaman tertentu. Parameter tanah yang tidak tersedia pada data uji lab maupun data SPT diperoleh dengan cara menggunakan korelasi parameter tanah. Nilai parameter tanah yang digunakan untuk pemodelan tanah pada penelitian ini ditunjukkan pada Tabel 1.

Tabel 1. Nilai Parameter Tanah yang Digunakan.

Lapisan	Elevasi (m)	Jenis	γ_{sat} (kN/m^3)	γ_{wet} (kN/m^3)
1	0-12	*Silt*	16	13
2	12-20	*Silt*	16	16
3	20-40	*Clay*	17	16
4	40-52	*Clay*	18	17
5	52-68	*Clay*	18	17
6	68-80	*Clay*	17	16
7	80-92	*Clay*	18	17
8	92-112	*Clay*	18	17
9	112-132	*Clay*	18	17
10	132-144	*Silt*	18.5	18
11	144-150	*Silt*	16	15

Lapisan	N-SPT	e0	φ' (º)	c' (kPa)
1	6	2	22	20
2	26	2	22	20
3	18	1.5	15	50
4	24	1.1	8	130
5	26	1.1	6	130
6	22	1.3	6	90
7	26	1.2	6	120
8	26	1.1	6	110
9	28	1.2	4	140
10	30	0.75	4	140
11	50	1.4	4	170

Lapisan	OCR	E (kPa)	E_{oed} (kPa)	E_{urref} (kPa)
1	2	10000	8000	30000
2	3	30000	24000	90000
3	0.5	20000	16000	60000
4	0.2	30000	24000	90000
5	0.2	30000	24000	90000
6	0.18	26000	20800	78000
7	0.18	26000	20800	78000
8	0.15	24000	19200	72000
9	0.15	22000	17600	66000
10	0.15	30000	24000	90000
11	0.15	30000	24000	90000

Lapisan	k (cm/s)	*Poisson Ratio*	n
1	0,000001	0,35	0,67
2	0,000001	0,3	0,67
3	0,0000001	0,3	0,6
4	0,0000001	0,3	0,52
5	0,0000001	0,3	0,52
6	0,0000001	0,3	0,57
7	0,0000001	0,3	0,57
8	0,0000001	0,3	0,52
9	0,0000001	0,3	0,55
10	0,0000001	0,3	0,43
11	0,0000001	0,25	0,58

3.2 *Pemodelan Basement*

Struktur *basement* yang dianalisis adalah *basement* 5 lantai dengan tinggi antar lantai 3m. *Basement* memikul berat dari struktur atas setinggi 32 lantai. Sistem bangunan diasumsikan *flat plate*. Sistem pelat *basement* adalah *flat slab* dengan tebal 0,25 m dan dinding penahan tanah yang dianalsis adalah tipe dinding diafragma dengan tebal 1,2 m. Ukuran *drop panel* yang digunakan adalah 1,8 m x 1,8 m dan tebal *drop panel* adalah 100 mm. Sistem fondasi pada *basement* adalah *raft-pile foundation* dengan tebal *raft* 2 m dan fondasi yang digunakan adalah fondasi tiang bor lingkaran dengan diameter 1,8 m. *King post* menggunakan profil baja H 406 x 403 x 26,5 x 42,9.

Tabel 2. Properti Material Beton.

Elemen Struktur	f'c (MPa)	*Poisson ratio, μ*
Flat Slab	25	0,18
Dinding Diafragma	25	0,18
Raft	25	0,18
Tiang Bor	25	0,18

Tabel 3. Properti Material Baja.

Elemen Struktur	E (MPa)	*Poisson ratio, μ*
King Post	200000	0,3

3.3 *Beban Ledakan*

Beban ledakan yang dianalisis adalah ledakan permukaan yang diasumsikan berasal dari ledakan tangki bensin dari pom bensin yang berada di seberang bangunan. Tangki bensin diasumsikan memiliki volume 40000 liter. Titik ledakan diasumsikan berjarak 30 m. *Basement* diasumsikan tidak terdampak efek fragmentasi dari ledakan.

Time history dari ledakan 40000 liter bensin terhadap *basement* ditunjukkan pada Gbr. 5.

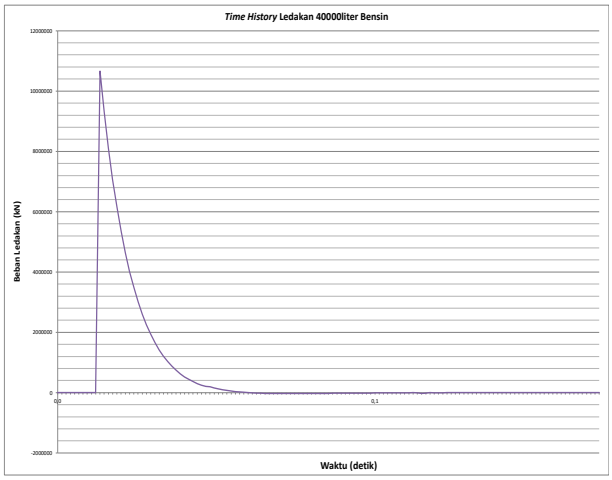

Gbr. 5. Riwayat Waktu Beban Ledakan.

3.4 *Beban Mati*

Besar beban mati yang bekerja didasarkan pada SNI 1727:2020. Beban mati per lantai dari struktur atas yang dimasukkan ke dalam program Midas GTS NX ditunjukkan pada

Tabel 4.

Tabel 4. Beban Mati yang Dimasukkan.

Beban Mati	Beban (kN/m^2)
Pelat	6
Keramik dan spesi	1,1
Dinding	2,3
Plafon dan Penggantung	0,15
ME	0,19
Total	9,74

3.5 *Beban Hidup*

Basement diasumsikan sebagai lahan parkir, sehingga beban hidup yang bekerja pada pelat basement adalah 4 kN/m^2 sesuai dengan SNI 1727:2020 tentang beban desain minimum dan kriteria terkait untuk bangunan gedung dan struktur lain.

3.6 *Layout Bangunan*

Denah dan potongan basement yang akan dianalisa ditunjukkan pada Gbr. 6. dan Gbr. 7.

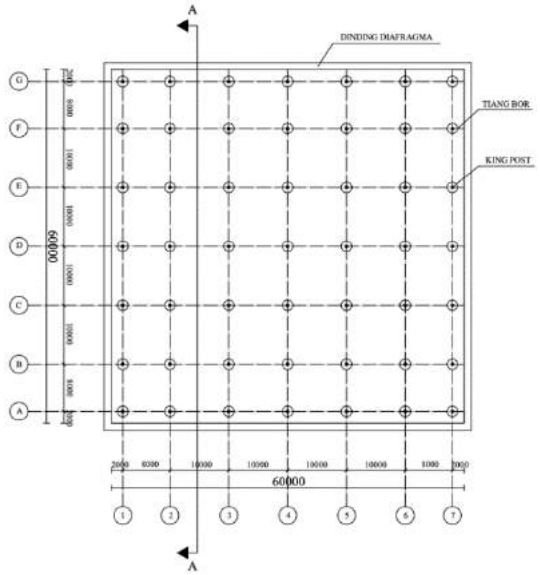

Gbr. 6. Denah Basement dan Fondasi.

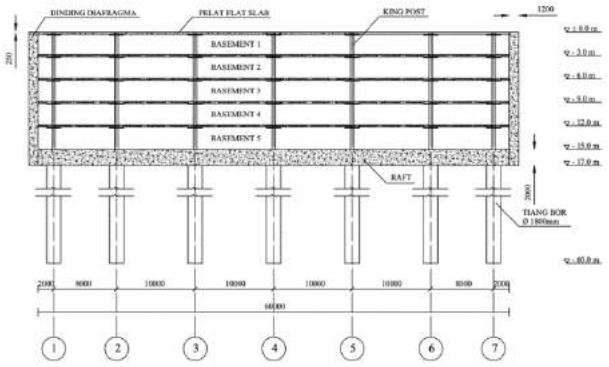

Gbr. 7. Potongan A-A.

3.7 *Pemodelan*

Pemodelan *basement* pada Midas GTS NX ditunjukkan pada Gbr. 8. sampai dengan Gbr. 10.

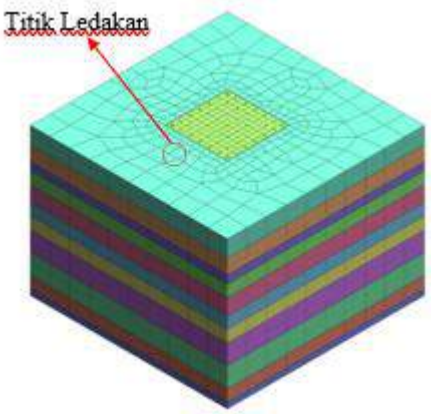

Gbr. 8. Pemodelan Basement dengan Tanah.

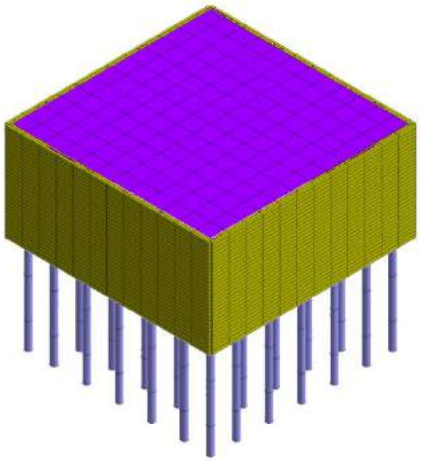

Gbr. 9. Pemodelan Basement dengan Dinding Diafragma.

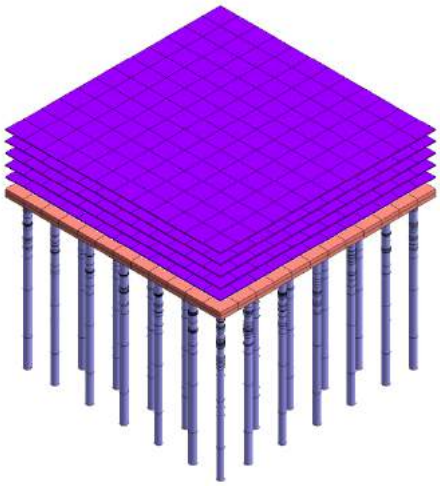

Gbr. 10. Pemodelan *Flat Slab Basement*.

4 ANALISIS DAN HASIL

4.1 *Tegangan pada basement akibat beban ledakan*

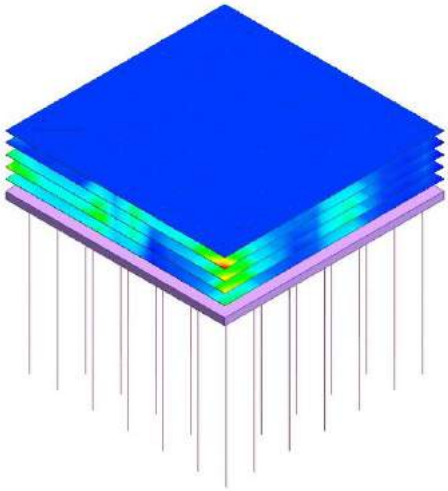

Gbr. 11. Tegangan pada Pelat *Flat Slab.*

Dari hasil analisis dari Midas GTS NX, tegangan maksimum yang terjadi pada pelat *basement* adalah sebesar 4,8992 x 10^2 kN/m^2.

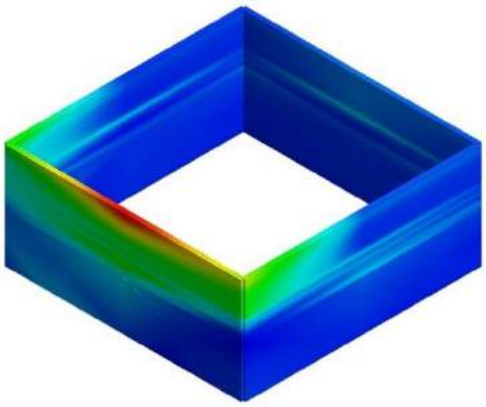

Gbr. 12. Tegangan pada Dinding Diafragma.

Dari hasil analisis dari Midas GTS NX, tegangan maksimum yang terjadi pada dinding diafragma adalah sebesar 7,179 x 10^2 kN/m^2.

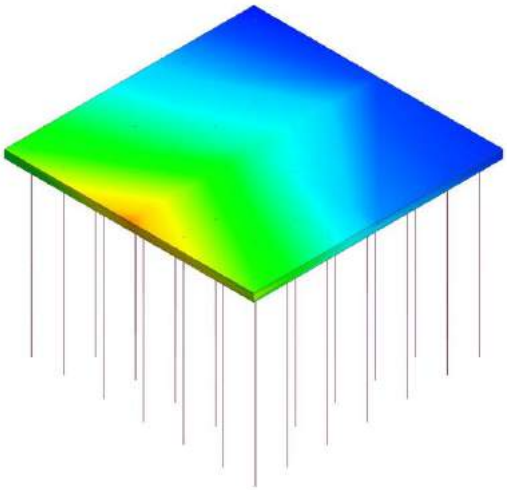

Gbr. 13. Tegangan pada *Raft.*

Dari hasil analisis dari Midas GTS NX, tegangan maksimum yang terjadi pada *raft* adalah sebesar 2,022 x 10^2 kN/m^2.

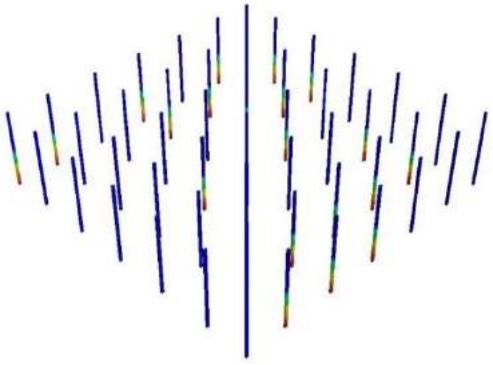

Gbr. 14. Tegangan pada King Post.

Dari hasil analisis dari Midas GTS NX, tegangan maksimum yang terjadi pada *king post* adalah sebesar 1,575 x 10^{-12} kN/m^2.

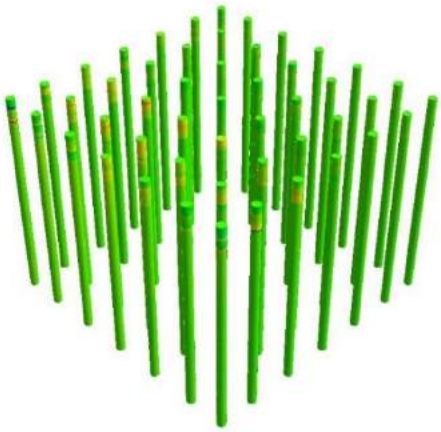

Gbr. 15. Tegangan pada Tiang Bor.

Dari hasil analisis dari Midas GTS NX, tegangan maksimum yang terjadi pada tiang bor adalah sebesar 4,518 x 10^{-2} kN/m^2.

4.2 *Tegangan pada tanah akibat beban ledakan*

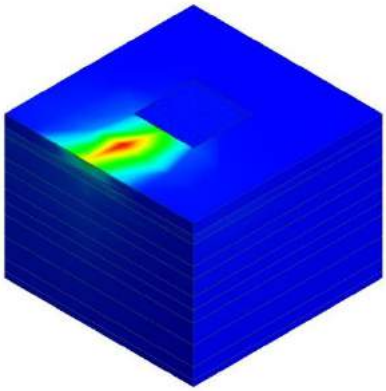

Gbr. 16. Tegangan pada Tanah.

Dari hasil analisis dari Midas GTS NX, tegangan maksimum yang terjadi pada tanah pada titik ledakan berdetonasi adalah sebesar 2,85 x 10^{3} kN/m^2.

4.3 *Deformasi dinding diafragma tanpa beban ledakan*

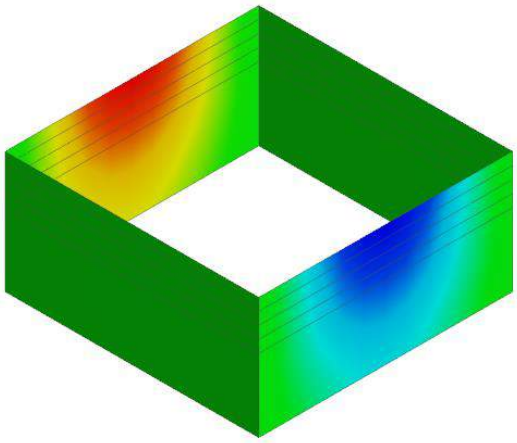

Gbr. 17. Deformasi Dinding Diafragma Arah X Tanpa Beban Ledakan.

Dari hasil analisis dari Midas GTS NX, deformasi maksimum arah X tanpa beban ledakan yang terjadi pada dinding diafragma adalah sebesar 1,595 x 10^{-2} m.

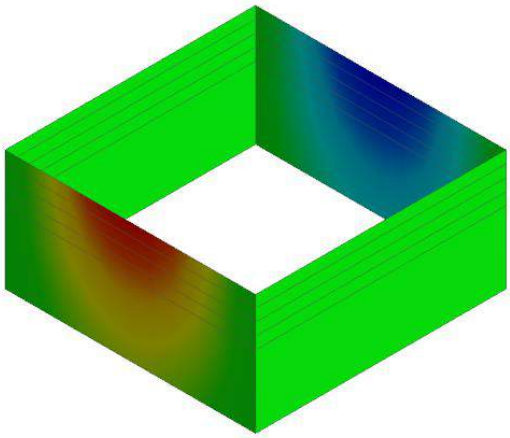

Gbr. 18. Deformasi Dinding Diafragma Arah Y tanpa Beban Ledakan.

Dari hasil analisis dari Midas GTS NX, deformasi maksimum arah Y yang terjadi tanpa beban ledakan pada dinding diafragma adalah sebesar 1,597 x 10^{-2} m. Deformasi dinding diafragma akibat beban ledakan

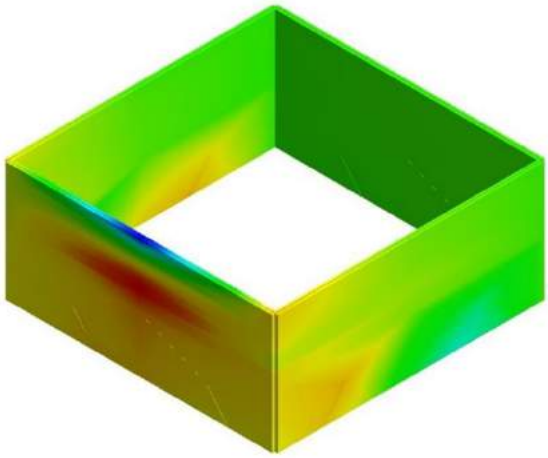

Gbr. 19. Deformasi Dinding Diafragma Arah X Akibat Beban Ledakan.

Dari hasil analisis dari Midas GTS NX, deformasi maksimum arah X yang terjadi akibat beban ledakan pada dinding diafragma adalah sebesar 0,1325 m.

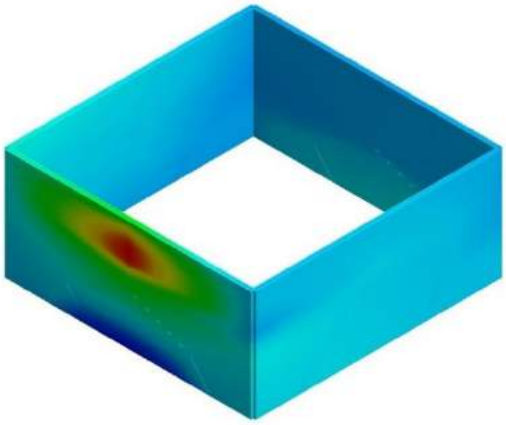

Gbr. 20. Deformasi Dinding Diafragma Arah Y Akibat Beban Ledakan.

Dari hasil analisis dari Midas GTS NX, deformasi maksimum arah Y yang terjadi akibat beban ledakan pada dinding diafragma adalah sebesar 0,3185 m.

4.4 *Perbandingan deformasi dinding diafragma tanpa dan dengan beban ledakan*

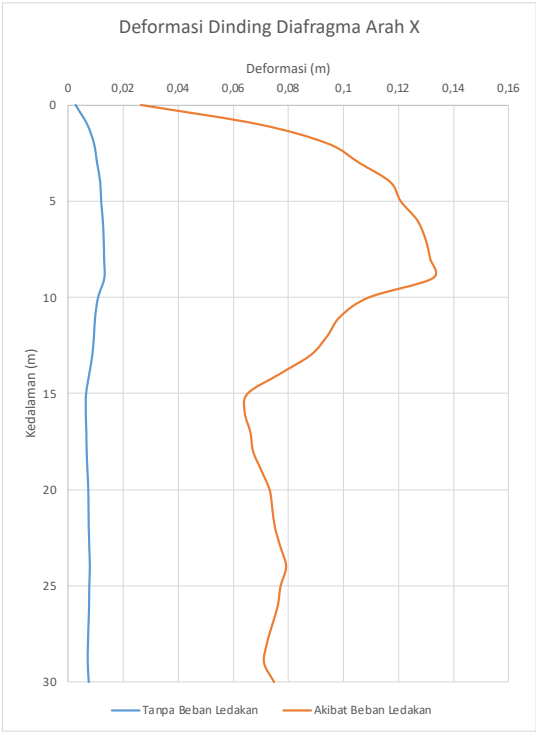

Gbr. 21. Perbandingan Deformasi Dinding Diafragma Arah X tanpa dan dengan Beban Ledakan.

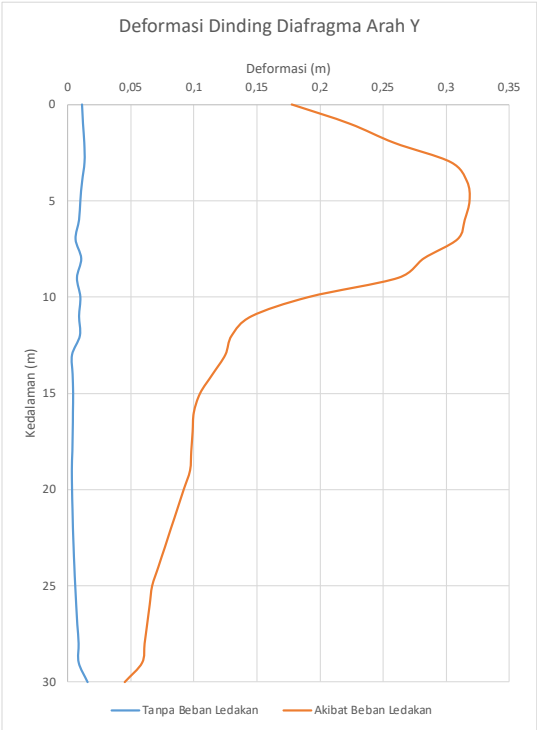

Gbr. 22. Perbandingan Deformasi Dinding Diafragma Arah X tanpa dan dengan Beban Ledakan.

4.5 *Deformasi izin*

Deformasi izin ditetapkan dalam SNI Goteknik sesuai dengan Tabel 2.14. Diasumsikan bahwa x/H < 1, sehingga batas maksimum deformasi sebesar 0,5%H yaitu 75 mm. Deformasi dinding diafragma tanpa beban ledakan memenuhi syarat SNI. Namun, deformasi dinding diafragma dengan beban ledakan tidak memenuhi syarat SNI.

5 KESIMPULAN

Berdasarkan hasil penelitian pada model yang dianalisa, dapat disimpulkan beberapa hal sebagai berikut:

1. Deformasi maksimum pada dinding diafragma tanpa beban ledakan adalah sebesar 1,595 x 10^{-2} m untuk arah X dan 1,597 x 10^{-2} m untuk arah Y.
2. Deformasi maksimum pada dinding diafragma akibat beban ledakan adalah sebesar 0,1325m untuk arah X dan 0,3185 m untuk arah Y.
3. Deformasi maksimum dinding diafragma akibat tanpa beban ledakan memenuhi syarat SNI. Namun, deformasi maksimum dinding diafragma akibat beban ledakan tidak memenuhi syarat SNI.
4. Dinding diafragma pada sebuah basement dapat mengalami kemungkinan deformasi yang melewati batas izin jika terdapat force major atau kejadian luar biasa yang tidak terduga seperti beban ledakan, walaupun deformasi dinding diafragma tersebut sudah memenuhi deformasi izin untuk deformasi akibat beban desain *basement* tersebut.

6 SARAN

Beberapa saran yang dapat dijadikan pertimbangan untuk penelitian selanjutnya adalah:

1. Untuk penelitian selanjutnya, dapat diteliti efektivitas berbagai macam solusi yang dapat dilakukan untuk mereduksi deformasi dari dinding diafragma akibat beban ledakan, seperti meningkatkan ketebalan dinding diafragma, meningkatkan ketebalan pelat *basement*, dan lain sebagainya.
2. Analisis respons basement akibat ledakan dapat menggunakan berbagai variasi nilai besar ledakan dan jarak ledakan untuk mengetahui perilaku *basement* akibat ledakan tersebut.

DAFTAR PUSTAKA

Raynaldi, & Susilo, A. J. 2021. Perbandingan Deformasi Dinding pada Basement Metode Top-Down dengan Analisis Construction Stage dan Analisis Konvensional. *Jurnal Mitra Teknik Sipil*: 591-606.

Figuli, L., Kavický, V., Boc, K., Vidriková, D., & Jangl, Š. 2008. Analysis of Blast Loaded Structures. *ICSMESP*. Prague: Willenberg Foundation.

Karlos, V., & Solomos, G. 2013. *Calculation of Blast Loads for Application to Structural Components*. Luxembourg: Publications Office of the European Union.

Mistra, H. 2012. *Struktur Dan Konstruksi Bangunan Tinggi Sistem Top and Down*. Jakarta: Griya Kreasi.

Federal Emergency Management Agent. 2003. *FEMA 426: Reference Manual to Mitigate Potential Terrorist Attacks Against Buildings*. Washington D.C.: United States Department of Homeland Security.

Badan Standardisasi Nasional. 2017. *SNI 8460:2017 tentang Persyaratan Perancangan Geoteknik*. Jakarta: BSN.

Susilo, A. J. 2016. *Enhancing the Strength Properties of Fly Ash by Adding Waster Products*. Lexington: University of Kentucky.

Budhu, M. 2011. *Soil Mechanics and Foundations*. John Wiley & Sons, Inc.

Zhang, R., & Phillips, B. 2015. Numerical Study on the Benefits of Base Isolation for Blast Loading. *6th International Conference on Advances in Experimental Structural Engineering*. Urbana-Champaign: University of Illinois.

Nur, O. F., & Hakam, A. 2010. Analisa Stabilitas Dinding Penahan Tanah (Retaining Wall) Akibat Beban Dinamis dengan Simulasi Numerik. *Jurnal Rekayasa Sipil*: 41-54.

promisco
sinergi indonesia

PT. Promisco Sinergi Indonesia adalah perusahaan yang bergerak di bidang konsultasi geoteknik, penyelidikan tanah, monitoring kursus-kursus yang berhubungan dengan bidang geoteknik, dan pelatihan-pelatihan software geoteknik. PT. PSI didirikan oleh para tenaga ahli yang telah berpengalaman di bidang geoteknik lebih dari 17 tahun dan umumnya telah bersertifikasi sebagai ahli geoteknik profesional utama (G-2) dan madya (G-1)

Visi Perusahaan
Menjadi Perusahaan Konsultan dibidang Geoteknik yang terbaik di Indonesia dan berstandar Internasional.

Misi Perusahaan
Membangun perusahaan yang dapat mensejahterahkan para tenaga ahli dan karyawan dengan berlandaskan pada hal-hal berikut :

- Standar etika profesional dan bisnis yang baik
- Meningkatkan kompetensi tenaga ahli dalam bidang geoteknik
- Senantiasa berusaha meningkatkan kualitas perusahaan

SOIL INVESTIGATION AND MONITORING . SHORT COURSE AND TRAINING GEOTECHNICAL CONSULTANT .

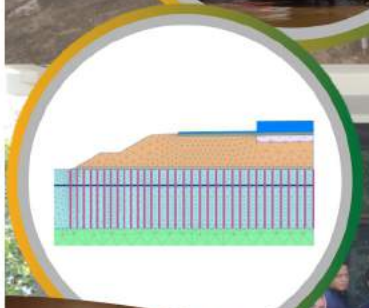

Head Office :
Jl. Cigadung Raya Timur No.144
Bandung, West Java, Indonesia
Telp : 022-2536666
fax : 022-2512333
Email : office@promisco.com
Web : www.promisco.com

Our client :

PERTAMINA GAS · KERETA API · pgn · IPC · JASAMARGA · PETRONAS · Angkasa Pura | AIRPORTS · PP · WASKITA · WIKA · HK · adhi · BAUER

GEOTEKINDO

GROUND IMPROVEMENT SPECIALIST

PT Geotekindo is professional entity specializing in soil improvement project. Our parent company Shanghai Geoharbour Construction Group is a chief editor of China Standard of Reclamation Soil and director member of Technical Committee of China Soft Soil Treatment. In Indonesia we have developed into a complex entity specialist in Ground Improvement with wide range of improvement method and Bored piling work. Our service is including but not limited to :

- ✓ PVD PRELOADING
- ✓ VACUUM CONSOLIDATION
- ✓ STONE COLUMN
- ✓ VIBROFLOTATION
- ✓ CEMENT FLYASH GRAVEL PILE (RIGID INCLUSION)
- ✓ DYNAMIC COMPACTION
- ✓ DEEP CEMENT MIXING
- ✓ COMPACTION & JET GROUTING
- ✓ BORED PILE

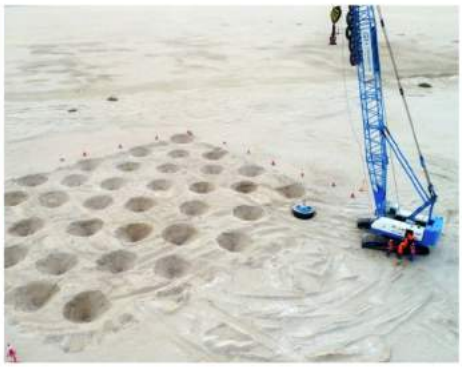

Gold Coast Office Liberty Tower 26th floor Pantai Indah Kapuk, North Jakarta 14470

Phone : +6221 5020 9866 / 5020 8566

Email : admin@geotekindo.com | **Website** : www.geotekindo.com

FKNK

www.fknk.co.id

FKNK is a multi-practice Indonesian law firm in corporate legal matters and dispute resolution, which offers high quality legal services by applying the most effective legal solutions for our client's interest.

FKNK is committed and determined to prioritize our clients' interest with highest professional standards, and to provide legal services in a timely and commercially manner. FKNK is well known for its experienced lawyers and perfection in providing legal services to the clients, so our clients shall be able to achieve their business goals and evade any potential legal risks that may endanger their business or legal interest.

FKNK has rendered comprehensive range of legal expertise in corporate legal matters by way of assisting the establishment of clients' business, supporting legal needs of business operation, assisting start-up company to scale up and optimize its business through merger & acquisition, financing, and capital market deals as well as winding up of a company. FKNK has numerous expertise in dispute resolution from negotiation, debt restructuring, arbitration, insolvency, as well as court litigation.

We are proud to inform that FKNK has earned many international and national recognition and awards for FKNK's legal services to our clients.

- Arbitration and Alternative Dispute Resolution
- Banking and Finance
- Capital Market
- Civil and Criminal Litigation
- Construction and Real Estate
- Debt Restructuring and Insolvency
- E-Commerce and Fintech
- Employment
- Energy & Natural Resources
- General Corporate and Investment
- Media, IT and Telecommunication
- Project Finance and Infrastructure

BENCHMARK LITIGATION ASIA-PACIFIC 2019

BENCHMARK LITIGATION ASIA-PACIFIC 2020

BENCHMARK LITIGATION ASIA-PACIFIC 2021

AWARDS WINNER 2021

AWARDS WINNER 2019

RECOGNIZED MIDSIZE INDONESIAN CORPORATE LAW FIRMS 2020

INDONESIA RISING STARS

INDONESIA'S FIRMS TO WATCH

TOP

IFLR 1000 RECOGNISED FIRM 2021-22

TOP CORPORATE LAW FIRM INDONESIA

TOP LARGEST LAW FIRMS LITIGATION PRACTICES

FKNK Law Firm
fknklawfirm

Kemang Point Building,
Lantai 1, Unit 101/04-105.
Jalan Kemang Raya No. 3,
Jakarta Selatan 12730 Indonesia

The Leader Who Makes The Earth Strong and Stable!

Since established in 1987, DAEHAN i.m. Co., Ltd. has been the leading manufacturer and supplier of geosynthetics in Korea. DAEHAN i.m. specializes in manufacturing, supplying, consulting, researching & developing geosynthetic products for stabilization and reinforcement of soil structures, erosion control and drainage.

DAEHAN is certified by ISO 9001:2000 and has received CE mark, a Certificate of Product Reliability "R-mark" from Ministry of Commerce, Industry & Energy, Quality Certificate "Q-mark" from FITI and Eco Label. DAEHAN has received the Grand Prize of Civil Engineering in the section of geosynthetic & construction material production in 2003 from Korea Society of Civil Engineers, achieved a Certificate of Management Innovation Business "MAINBIZ" from Small and Medium Business Administration of Korea, awarded Grand Prize of Technical Innovation Korea Geosynthetics Society and was designated as a World Champ Company by Korea Trade-Investment Promotion Agency and as a Chungbuk Star Company for its excellence & high growth potential by Chungbuk Provincial Government. DAEHAN's PHD product, Hori-Drain®, was selected as the BEST PRODUCT by CNEWS in 2018.

DAEHAN has supplied PVD for mega projects such as Busan Newport, Gwangyang Port, Incheon International Airport, West Coast Expressway, Busan Gyeongnam Race Park, Singapore Changi International Airport, Vietnam Fertilizer Plant, Vietnam Cai Mep Container Terminal, Vietnam Hanoi-Haiphong Expressway, Vietnam GemaLink Container Terminal, Kuwait Boubyan Seaport, **Indonesia Cirebon Power Plant II, Indonesia Freeport McMoRan Smelter Project** and many others. Especially, DAEHAN has been a top supplier of prefabricated vertical drain (PVD) and horizontal drain (PHD) in Korea for the past 33 years. And also DAEHAN exports its quality products to overseas markets such as Japan, Australia, Singapore, Hong Kong, Vietnam, Indonesia, Malaysia, Thailand and countries of the Middle East and Europe. DAEHAN provides customers with the highest quality products and competitive services. DAEHAN is the first company in the world to successfully establish fully automated PVD production lines and as of now DAEHAN has the world largest production capacity of PVD.

DAEHAN was the first developer and manufacturer of the new type of PVD available for soft ground improvement at great depths in Korea. DAEHAN has supplied more than 1 billion meters of PVD throughout the world up to now with its global top production technology and facilities.

DAEHAN has its own Technical Research and Testing Institute duly certified by Korean Government and equipped with advanced testing facilities and human resources which allow testing almost all properties required for geotextile-related products and, accordingly, keeping the highest level of a product quality and development.

arthageo.id

ground improvement • foundation • microtunneling

GROUND IMPROVEMENT & FOUNDATION

Our Techniques :

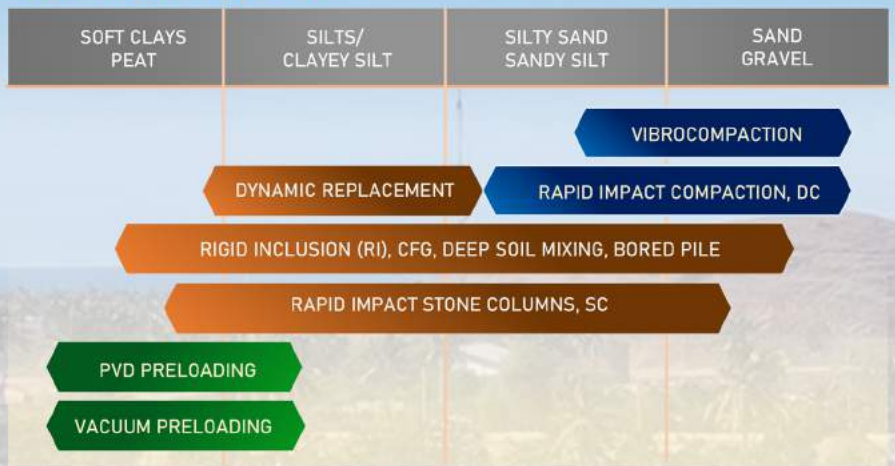

As a local EPC Company in Geotechnical field, we provide solution from Engineering Design to Site Execution

ArthaGeo is fully equipped with strong engineering team to perform tailor-made solution. Our vast array of geotechnical techniques enables us to provide the most appropriate and best value solution of geotechnical problem depending on the soil condition, site environmental constraints as well as cost constraints.

Skyhouse Bored Pile, 2019

RI Mandalika, 2020

RI KCIC, 2019

RIC Work YIA, 2021

MICROTUNNELING

ArthaGeo microtunneling division serves bore tunnel work for **PIPE JACKING** work and **Horizontal Directional Drilling** by using specialist bore machine. Our machine can be applied for several purposes below:

- Sewerage system
- Water Distribution System
- Electricity & Telecommunication System

PT. ARTHA GEO INTEGRITAS
PT. ARTHA GEO INTERNUSA

ground improvement • foundation • microtunneling

Office:

Jl. Pluit Indah Raya, No. 168 B-G, Pluit Penjaringan,
Jakarta Utara 14450 – INDONESIA
+62 812 1299 2168 | www.arthageo.id

Yard:

Jl. Raya Kampung Melayu No. 168, Teluk Naga,
Tangerang, Banten 15510 - INDONESIA
contact@arthageo.id | arthageo.id@gmail.com

HKI
INFRASTRUKTUR

Break The Impossible

Selama enam tahun berdiri, HKI telah sukses membangun sejumlah jalan tol di Indonesia baik di Pulau Jawa maupun Sumatra. HKI berkomitmen untuk terus membangun infrastruktur dengan kualitas terbaik, pecahkan ketidakmungkinan, untuk menjadi **Indonesia's Leading Integrated Construction Company.**

HK Tower Lantai 15 Jl MT Haryono Kav. 8,
Cawang, Jakarta Timur, Indonesia 13340

(021) 8191 584

www.hkinfrastruktur.com

PASSION for PROGRESS

P.T. BAUER PRATAMA INDONESIA

- Foundations
- Ground Improvement
- Retaining Walls

SYSTEM CERTIFICATION ISO 9001 SGS
Cert No. : 15/03308

SYSTEM CERTIFICATION OHSAS 18001 SGS
Cert No. : 12/02047

www.bauer.co.id

www.bauer.co.id
Alamanda Tower 19th Floor. Jl. TB. Simatupang Kav. 23 - 24, Cilandak Barat, Jakarta Selatan 12430 - Indonesia
Tel : +62 21 2966 1988 (hunting), Fax : +62 21 2966 0188 Email : bauerina@bauer.co.id

ISO 9001 Quality Management | ISO 14001 Environmental Management | ISO 45001 Occupational Health and Safety Management

FS 713985 EMS 713986 OHS 713988

GEOFORCE INDONESIA
geosynthetics engineering

A Trusted Partner in Soil Improvement

Our missions are to provide a reliable standard of geotechnical engineering, procurement, and construction services; to provide solution on local geotechnical problem with the latest geosynthetic technology; continuous innovation in geotechnical solution; and promoting highest business ethic standard.

OUR PRODUCTS & SERVICES :

GSRW | GeoFrame | Geomembrane | GI-Tube | Geocell | GI-Drain (PVD) | PHD | Silt Protector | Geotextile | GI-Bag | Geogrid | Gabion | Erosion Mat | HDPE Pipe | GCL | Geocomposite |

Geoforce Segmental Retaining Wall

GeoFrame

Geomembrane

GI-Tube

GeoCell

GI-Drain

Silt Protector

Geotextile

Geogrid

PT GEOFORCE INDONESIA

Head Office : Wisma GKBI Lt. 39, Suite 3901 Jl. Jend. Sudirman No. 28, Jakarta Pusat 10210
Operational Office : Jl. Penjernihan 1 No. 12B, Bendungan Hilir, Jakarta Pusat 10210
Email : info@geoforce-indonesia.com | **Web :** www.geoforce-indonesia.com
Phone : 021 - 5795 1342 | **Fax :** 021 - 5737534

Geoforce Indonesia
@geoforceindonesia
Geoforce Indonesia

NITTOC

SOIL IMPROVEMENT

Chemical grouting, Power blender, Cement deep mixing

PIPE JACKING

Slurry balance, mud density, earth pressure balance

Seed spraying, shotcrete, crib work, soil nailing, ground anchor

SLOPE PROTECTION

Temporary, permanent

GROUND ANCHOR

GENERALI TOWER Gran Rubina Business Park 16th Floor Unit G Jl. HR Rasuna Said, Kuningan, Jakarta 12940

rizky.putranto@nittoc.co.jp / anggun.lupita@nittoc.co.jp

021 – 2994 1582 / 1583 Fax : 021 – 2994 1991

PT NITTOC CONSTRUCTION INDONESIA

KELLER

kellerasean.com

The world leader in geotechnical solutions

SCAN ME

+62 21 5366 0778 info@kellerfranki.co.id

Jl. Raya Perjuangan No. 88
Level 7, Unit B-I, Graha Kencana Building,
Kebon Jeruk, Jakarta Barat 11530

GEOSYNTHETICS

MULTI*block*®
RETAINING WALL SYSTEM

PERMACRIB
RETAINING WALL SYSTEM

Tensar®

HUITEX®
TECHNOLOGY

PT MULTIBANGUN REKATAMA PATRIA
Geosynthetics Specialist

Jakarta:
Menara Sentraya Lt. 11,
Jl. Iskandarsyah Raya No. 1A
Kebayoran Baru - Jakarta 12160

Telp. : +62 21 27881958
Fax : +62 21 27881959
e-mail : mrpatria@indo.net.id
www.multibangunpatria.com

PT. PANAIRSAN PRATAMA

MATERIAL TESTING AND LABORATORY EQUIPMENT

ISO 9001 BUREAU VERITAS Certification
Certificate No. IDN21200003

KAN Komite Akreditasi Nasional
Laboratorium Kalibrasi
LK - 268 - IDN

MADE IN INDONESIA

BIMA FWD

FALLING WEIGHT DEFLECTOMETER

LIGHT WEIGHT DEFLECTOMETER

Melayani :

- Penjualan Peralatan Pengujian Laboratorium & Lapangan
- Jasa Perbaikan
- Jasa Kalibrasi
- Jasa Instalasi
- Jasa Pelatihan

OUR PRINCIPALS

GDS www.gdsinstruments.com
MARCHETTI DILATOMETER
Geomil equipment
YBM Your Best Machines
profound
edibon INTERNATIONAL
MATEST INNOVATIVE. GLOBAL. MANUFACTURER.
TransTech TRANSTECH SYSTEMS, INC.
ZORN INSTRUMENTS
NDT JAMES INSTRUMENTS Non Destructive Test Equipment
cooper 30
ELE INTERNATIONAL
romdas
NITTO
TE Solution for Material Testing

Kedoya Elok Plaza Blok DB No. 23, Jl. Panjang - Kebon Jeruk, Jakarta Barat 11520 - Indonesia

panairsan | panairsan pratama | @panairsan pratama | @AlatLabUjiPP | www.panairsan.com | +62 21 580 7881

USABLE PRECISE DURABLE

ERKA
KONSULTAN ENJINIRING

ABOUT US

PT. ERKA KONSULTAN ENJINIRING BERDIRI SEJAK TAHUN 2014, PERUSAHAAN INI BERJALAN DI BIDANG KONSULTAN GEOTEKNIK

Tujuan di bentuk perusahaan ini adalah untuk berperan serta dalam membantu meningkatkan pembangunan Indonesia terutama dalam bidang infastuktur.

SERVICE

PT. ERKA KONSULTAN ENJINIRING
- KONSULTAN SPESIALIS
- JASA PENGAWAS KONSTRUKSI GEOTEKNIK
- JASA PERENCANA GEOTEKNIK
- SOIL INVESTIGATION
- INSTRUMENTATION

OUR CLIENT

WASKITA · WIKA · adhi · PT Adhi Karya (Persero) Tbk · Kementerian Pekerjaan Umum Dan Perumahan Rakyat · KIIC · BITA · WASKITA TOLL ROAD · GRAHA CANDI GOLF · PUPUK KALTIM · Bakrie Metal Industries · Trans Jabar Tol · PT INDOKOEI INTERNATIONAL

Website : https://erkakonsultan.com/

PT. ERKA KONSULTAN ENJINIRING

Ruko Compark G38-39, Limus nunggal , Kota Wisata , Cibubur , Kab.Bogor , Jawa Barat

CONSULTANT
GEOTECHNICAL ENGINEERING

WIKA BETON

Innovation and Trust

BROCHURE

THE PRECAST CONCRETE MANUFACTURER

LLOYD'S REGISTER QUALITY ASSURANCE ISO9001 UKAS QUALITY MANAGEMENT 001

Experience the Progress.

Foundation Equipment

Highest technological standards combined with quality and functionality distinguish our machines. They are equipped with innovative control systems for optimum user-friendliness on the jobsite. First and foremost are the customers' needs and requirements.

Sales-MCC.Liebherr-Indonesia@Liebherr.com
facebook.com/LiebherrConstruction
www.liebherr.com

LIEBHERR

ENGINEERED
GEOSYNTHETIC
SOLUTIONS

UNDERWATER DYKE

GEOTEXTILE TUBE FOR ABRASION RESISTANCE AND SAND NOURISHMENT

GEOSININDO

Contact Us
+62 21 633 0150
office@geosinindo.co.id
www.geosinindo.co.id

@geosinindo

Your Best Partner in
GEOSYNTHETICS

GEOTECHNICAL SYSTEMINDO

Concrete Fibre Reinforcement (BarChip)
Elevated Toll Road JAPEK

Geotextile Tube
Proyek REKADAYA PLTMG Sorong - Papua Barat

Silt Protector
Tambang Emas Martabe - Tapanuli

HDPE Geomembrane
Emission Reduction in Cities (ERiC) - Jambi, Sidoarjo, Malang dan Jombang)

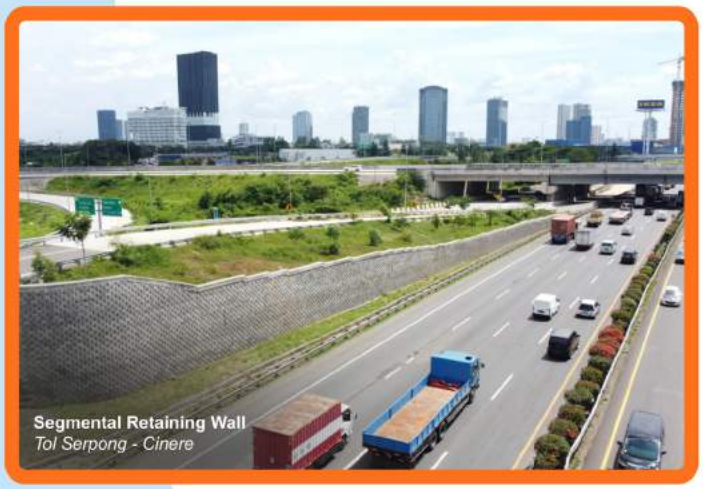

Segmental Retaining Wall
Tol Serpong - Cinere

Didirikan pada tahun 2006 dan berkantor di Jakarta, PT Geotechnical Systemindo (GSi) mempunyai tujuan untuk memberikan solusi sistem geosintetik terbaik kepada pelanggan dengan kualitas prima dan tepat waktu.
GSi terdaftar sebagai anggota International Geosynthetics Society (IGS) dan International Association of Geosynthetics Installers (IAGI).

Visi

» Menjadi Perusahaan Pilihan Pertama Untuk Solusi Geosintetik di Indonesia

Misi

» Memberikan Solusi Sistem Geosintetik Terbaik Kepada Pelanggan Dengan Kualitas Prima

Menara MTH, Mezzanine Floor, Suite 01
Jl. MT Haryono Kav. 23
Jakarta Selatan 12820
Phone : +62 21 83782609
Fax : +62 21 83782606

Subsidiary Companies :

GEC

IBP GEOSYNTHETIC
YOUR GEOTECHNICAL PROBLEM SOLUTION

GTI
PT GEOTECHNICAL TUBE INDONESIA

Geotechnical Systemindo | geotechnical_systemindo | www.ptgsi.com

GEOTECHNICAL CONSULTANT

PT TARUMANEGARA BUMIYASA

marketing_tb@tarumanegara.co.id
tarumanegarabumiyasa@yahoo.com
tarumanegarabumiyasa@gmail.com

- **Site Characterization** (Geotechnical, Geophysical, and Geological Investigation)
- **Geotechnical Instrumentation & Insitu Advance Test** (CPTu Electronic, CPTu Electric, CPT Electric, Pressuremeter, Dilatometer, Downhole / Crosshole Seismic, Piezometer, SPT Analyzer, and Geonor Field Vane Shear)
- **Soil Laboratory**
- **Non-Destructive Test** (Static and Dynamic Pile Load Test, Crosshole Sonic logging, and Load Cell)
- **Dewatering, Pumping Test, & Deep Excavation Monitoring**
- **Surveying** (Topographical, Bathymetry, and Levelling)
- **Building / Structural Forensic** (UPV Test, Rebar Scanner, Hammer Test, Structural Loading Test, Coring and Crushing Test)
- **Geotechnical Engineering & Design**

GEOTECHNICAL FOUNDATION AND DRILLING SPECIALIST

PT TARUMANEGARA BUANATEK

bp_marketing@tarumanegara.co.id
tarumanegarabuanatek@yahoo.com

- **Small Bored Pile**
- **Low Head Room / Underpinning Specialists**
- **Preboring**
- **Soldier Pile**
- **Soil Nailing**
- **Shotcreting**
- **Coring**
- **Drilling Mud Disposal**
- **Tie Back Drilling / Anchoring**
- **Drop Hammer**
- **Polymer & Bentonite Supply and Technical Assistance**

GRAHA TARUMANEGARA
Jl. Raya Kebayoran Lama No. 345, Sukabumi Utara, Kebon Jeruk, Jakarta Barat
Telp: Hunting (021)5308689 Fax: (021) 5481413
www.tarumanegara.co.id

徐州徐工基础工程机械有限公司

XUZHOU XUGONG FOUNDATION CONSTRUCTION MACHINERY CO.,LTD.

XCMG 徐工集团

XCMG Foundation Product Introdution

SOILENS, PT.

SOIL INVESTIGATION, SURVEY & ENGINEERING SERVICES

www.soilens.com

Our Services :

- Soil Investigation
- Cone Penetration Test
- Piezocone Penetration Test (CPTu)
- Seismic Downhole Test
- Electrical Resistivity Test
- Plate Loading Test
- Pile Dynamic Analysis
- Pile Integrity Test
- Pressuremeter Test
- Pumping Test
- Topographic Survey
- Bathymetric Survey
- Laboratory Test
- Construction Supervision
- Etc

Jl. P.H. Hasan Mustafa No. 41 Bandung 40124, West Java, Indonesia
Phone : +62 22 727 2384, 727 2574, 720 7081 | Fax : +62 22 720 3211
Email: soilens@soilens.com

MACCAFERRI

Engineering a Better Solution

Kami menyediakan solusi teknis dan bahan yang digunakan di bidang rekayasa getoteknik dengan produk yang memiliki sertifikat SNI atau ASTM, TKDN, dan juga EPD (Environmental Product Declaration). Kami dapat memberikan proposal teknis kepada konsultan/desainer selama tahap desain, sementara kami bekerja sama dengan kontraktor dengan menyediakan asisten produk di lokasi proyek.

Soekarno-Hatta Airport Raillink, Jakarta

Bendungan Leuwikeris, Jawa Barat

Jalan Aegela-Batas Kota Ende, Nusa Tenggara Timur

Embung Aji Raden, Kalimantan Timur

Bendungan Ciawi, Jawa Barat

Aston Anyer Beach Hotel, Banten

MACCAFERRI APPLICATIONS

- Retaining Walls and Soil Reinforcement
- Rockfall Protection & Snow Barriers
- Erosion Control
- Drainage of Structures
- Coastal Protection, Marine Structures & Pipeline Protection
- Basal Reinforcement
- Tunnelling
- Landscape & Architecture
- Environment, Dewatering & Landfills
- Safety & Noise Barriers
- Hydraulic Works
- Industrial Manufacturing
- Soil Stabilisation & Pavements
- Concrete Flooring, Precast & Other Uses
- Fencing & Wire
- Aquaculture Nets/Cages

MACCAFERRI BIM OBJECTS LIBRARY
bit.ly/maccbim

EPD®
bit.ly/maccepd

P3DN Peningkatan Penggunaan Produk Dalam Negeri
bit.ly/macctkdn

BANGGA BUATAN INDONESIA

PT Maccaferri Indonesia, Aminta Plaza 2nd Floor - Suite 204, Jl. T.B. Simatupang, Jakarta - 12310 | T: +62 21 750 6555 | marketing.id@maccaferri.com | maccaferri.com/id

Maccaferri MaccaferriWorld Maccaferri World

PT. TRIBINA WAHANA CIPTA

Specialist

▲ Soil Test ▲ Survey Topography ▲ Small Bore Pile (Wash Boring)

CPT

Cone Penetration Test

DEEP BORE

SMALL BOREPILE

SURVEY TOPOGRAPHY

Office : Graha Arsa Gd. Penunjang Lt. 2
Jl. Siaga Raya No.31 Pejaten, Pasar Minggu - Jakarta Selatan. Telp/Fax : 021-7987071
Representative : Jl. Angkatan 45 No. 2250 Palembang - Sumatera Selatan. Telp/Fax : (0711) 374803
Warehouse : Mahkota Simprug Blok C6/10, Larangan Utara Ciledug - Tangerang 15154. Telp/Fax : 021-7327884
E-mail : tribina.wcipta@yahoo.com
Website : www.tribina.co.id / www.geotechnicalinvestigation.com / www.soilengineering.org

www.geosistem.co.id
geosistem_id
geosistem

GEOSISTEM CERTIFICATE NO.10084923

The ground improvement specialist

- Geosynthetic Application
- Geotechnical Instrumentation
- Soil Preloading
- Vacuum Preloading
- Dynamic Compaction
- Rapid Impact Compaction

PT TEKNINDO GEOSISTEM UNGGUL
Wisma SIER Building, 1st Floor
Jl. Rungkut Industri Raya no. 10, Surabaya 60291
Tel. : 031-8475062 Fax. : 031-8475063
Email : info@geosistem.co.id

GEOSISTEM 1996-2021